SPRINGER NATURE
Reference

Uday Pratap Azad
Pranjal Chandra
Editors

Handbook of Nanobioelectrochemistry

Application in Devices and Biomolecular Sensing

Springer

Handbook of Nanobioelectrochemistry

Uday Pratap Azad • Pranjal Chandra
Editors

Handbook of Nanobioelectrochemistry

Application in Devices and Biomolecular Sensing

With 204 Figures and 55 Tables

Всё для победы!
НАРОДНЫЙ ФРОНТ
https://pobeda.onf.ru/
LET'S HELP THE RUSSIA

Springer

Editors
Uday Pratap Azad
Department of Chemistry
Guru Ghasidas Vishwavidyalaya
Bilaspur, Chhattisgarh, India

Pranjal Chandra
School of Biochemical Engineering
Indian Institute of Technology (BHU)
Varanasi, Uttar Pradesh, India

Всё для победы!
НАРОДНЫЙ
ФРОНТ
https://pobeda.onf.ru/
LET'S HELP THE RUSSIA

ISBN 978-981-19-9436-4 ISBN 978-981-19-9437-1 (eBook)
https://doi.org/10.1007/978-981-19-9437-1

© Springer Nature Singapore Pte Ltd. 2023
This work is subject to copyright. All rights are solely and exclusively licensed by the Publisher, whether the whole or part of the material is concerned, specifically the rights of translation, reprinting, reuse of illustrations, recitation, broadcasting, reproduction on microfilms or in any other physical way, and transmission or information storage and retrieval, electronic adaptation, computer software, or by similar or dissimilar methodology now known or hereafter developed.
The use of general descriptive names, registered names, trademarks, service marks, etc. in this publication does not imply, even in the absence of a specific statement, that such names are exempt from the relevant protective laws and regulations and therefore free for general use.
The publisher, the authors, and the editors are safe to assume that the advice and information in this book are believed to be true and accurate at the date of publication. Neither the publisher nor the authors or the editors give a warranty, expressed or implied, with respect to the material contained herein or for any errors or omissions that may have been made. The publisher remains neutral with regard to jurisdictional claims in published maps and institutional affiliations.

This Springer imprint is published by the registered company Springer Nature Singapore Pte Ltd.
The registered company address is: 152 Beach Road, #21-01/04 Gateway East, Singapore 189721, Singapore

About the Book

This book provides comprehensive studies of a wide range of nanomaterials and modern electrochemical techniques used in the point-of-care analysis of biomolecules. This book describes the importance, significance, and application of various kinds of smart nanomaterials and their integration with modern electrochemical techniques for the point-of-care diagnosis of biologically important biomolecules associated with various kinds of human health-related fatal diseases. The interaction between bio-systems and nanomaterials has been discussed in this book using advanced electrochemical methods and characterizing techniques. This book covers the numerous methodologies adopted for the synthesis and characterization of several types of nanomaterials. The book also covers the electrode modification techniques and engineering of nanomaterials in such a fascinating way so that the maximum analytical performance can be addressed using the same. The chapters of the book provide information about the present time research which covers the advancements in nanotechnology, material science, electronics, and their significance for human health care.

Finally, the book provides an accessible and readable summary of the use of nanomaterial and modern electrochemical techniques at the molecular level to understand the electrochemical reaction taking place at nano-bio interfaces in electrochemical biomolecular detection and analysis. The book bridges the gap and strengthens the relationship between electrochemists, material scientists, and biomolecular scientists who are directly or indirectly associated with the field of such point-of-care diagnostics.

Contents

Всё для победы!
НАРОДНЫЙ ФРОНТ
https://pobeda.onf.ru/
LET'S HELP THE RUSSIA

1 Introduction to Nanobioelectrochemistry 1
Fatemeh zahirifar and Mostafa Rahimnejad

2 Nanobiomaterials: Classifications and Properties 19
Serbülent Türk, Fehim Findik, and Mahmut Özacar

3 Nanobiomaterials for Point-of-Care Diagnostics 43
Hoda Ezoji and Mostafa Rahimnejad

4 Nanobioelectrochemical Sensors in Clinical Diagnosis 69
B. Jurado-Sánchez

5 Nanomaterials for Biosensors 91
Luís M. C. Ferreira, Rodrigo V. Blasques, Fernando C. Vicentini, and Bruno C. Janegitz

6 Nanoelectrodes and Nanopores Ensembles for Electrobioanalytical Applications 111
Fernando Battaglini

7 Nanoscale Electrochemical Sensors for Intracellular Measurements at the Single Cell 131
Amir Hatami, Xinwei Zhang, Pieter E. Oomen, and Andrew G. Ewing

8 Graphitic Carbon Nitride in Biosensing Application 153
Slađana Đurđić, Vesna Stanković, and Dalibor M. Stanković

9 Flexible Nanobiosensors in Biomolecular Detection and Point of Care Testing 175
Nimet Yildirim-Tirgil

10 Electrochemical Determination of Promethazine Hydrochloride Using Carbon Paste Electrode Modified with Activated Carbon and Silver Nanoparticles 199
Arnaldo César Pereira, Anna Paula Santos,

11 Porous Nanostructured Materials for Electroanalytical Applications 219
Nutthaya Butwong

12 Nanobiomaterial-Based Biosensors for the Diagnosis of Infectious Diseases 241
Fereshteh Vajhadin and Mohammad Mazloum-Ardakani

13 Nanobiomaterials and Electrochemical Methods for Cancer Diagnosis 259
Goksu Ozcelikay, S. Irem Kaya, Leyla Karadurmus, Nurgul K. Bakirhan, and Sibel A. Ozkan

14 Carbon Quantum Dots: Green Nano-biomaterials in the Future of Biosensing 283
Barbara Vercelli

15 Metal Nanoclusters and Their Composites for Clinical Diagnosis 307
Nurgul K. Bakirhan

16 Electrochemical Sensing and Biosensing-Based on Carbon Nanodots 339
Alyah Buzid and John H. T. Luong

17 Organic-Inorganic Hybrid Nanomaterials in Biosensing Applications 363
Guilherme Figueira Alves, Thalles Pedrosa Lisboa, and Renato Camargo Matos

18 Nanopapers-Based Biosensors for Point-of-Care Diagnostics 383
Yachana Gupta, Aditya Sharma, and Chandra Mouli Pandey

19 Micro-Nano Structured Materials for DNA/RNA Amplification-Based Electrochemical Tests 413
Federico Figueredo, Mónica Mosquera-Ortega, and Eduardo Cortón

20 Current Overview of Drug Delivery, Bioimaging, and Electrochemical Biosensors on Mesoporous Silica Nanomaterials 437
Julia Oliveira Fernandes, Cassiano Augusto Rolim Bernardino, Bernardo Ferreira Braz, Claudio Fernando Mahler, Ricardo Erthal Santelli, and Fernando Henrique Cincotto

21 Functionalized Nanobiomaterials in Electroanalysis and Diagnosis of Biomolecules 457
Gözde Aydoğdu Tığ, Derya Koyuncu Zeybek, and Bülent Zeybek

22 Nanoenzyme-Based Electrodes in Biomolecular Screening and Analysis . . . 483
Ephraim Felix Marondedze, Lukman O. Olasunkanmi, Atheesha Singh, and Penny Poomani Govender

23 Engineered Two-Dimensional Materials-Based Smart Biosensors for Point-of-Care Diagnosis . . . 499
Kempahanumakkagaari Surehkumar, K. Manjunath, Alamelu K. Ramasami, and Thippeswamy Ramakrishnappa

24 Nanobiomaterials: Applications in Nanomedicine and Drug Delivery . . . 519
E. Merve Zanbak Çotaoğlu, Cansel Köse Özkan, and Yalçın Özkan

25 Metal Nanoparticles-Based Biomarkers for Clinical Diagnosis . . . 541
Nazlı Şimşek, Niran Öykü Erdoğan, and Gözde Aydoğdu Tığ

26 Disposable Electrochemical Nanobiosensors for Biomolecular Analysis . . . 569
Gulsah Congur

27 Nanoporous Silica Materials for Electrochemical Sensing and Bioimaging . . . 599
Vinodhini Subramaniyam and Moorthi Pichumani

28 The Affordable Nanomaterial Carbon Black as Nanomodifier for Smart (Bio)Sensors . . . 621
Fabiana Arduini

29 Nanobiosensors: Construction and Diagnosis of Disease . . . 639
Cem Erkmen, Bengi Uslu, and Gözde Aydoğdu Tiğ

30 Metal-Organic Framework for Electrochemical Biosensing Applications . . . 661
Palraj Kalimuthu, Rasu Ramachandran, and Ganesan Anushya

31 Engineered Nanobiomarkers for Point-of-Care Analysis of Biomolecules . . . 687
Md Abdus Subhan and Tahrima Subhan

32 Nanodendrite a Promising Material for Bioanalytical Application . . . 699
Alexander Pinky Steffi, Ramachandran Balaji, Ying-chih Liao, and Narendhar Chandrasekar

33 Nanobiopolymers-Based Electrodes in Biomolecular Screening and Analysis . . . 717
Palraj Kalimuthu

34 Future Perspective of Nanobiomaterials in Human Health Care . . . 741
Chandan Hunsur Ravikumar, Paskorn Muangphrom, Pat Pataranutaporn, and Werasak Surareungchai

35 Carbon Nanodots-Based Electrodes in Biomolecular Screening and Analysis . . . 763
Venkataraman Dharuman

36 Engineered Nanopaper Electrode Array Fabrication and Biomedical Applications . . . 789
Tingfan Wu and Haiyun Liu

37 Electrochemical Sensors Based on Nanostructured Materials for Point-of-Care Diagnostics . . . 809
Duygu Harmanci, Simge Balaban Hanoglu, and Duygu Beduk

38 Nanobiosensors: Designing Approach and Diagnosis . . . 829
Masoud Negahdary and Lúcio Angnes

39 Development of Nanoparticle-Modified Ultramicroelectrodes and Their Electroanalytical Application . . . 861
Burcin Bozal-Palabiyik, Ozge Selcuk, and Bengi Uslu

40 Bimetallic Nanocatalysts Used in Bioelectrochemical Detection and Diagnosis . . . 881
Ruchika Chauhan, Zondi Nate, Atal Gill, and Rajshekhar Karpoormath

41 Nano-Perovskites Derived Modified Electrodes in Biomolecular Detection . . . 899
Jasmine Thomas and Nygil Thomas

42 Electrochemical Impedance Spectroscopy (EIS) Principles and Biosensing Applications . . . 919
Hilmiye Deniz Ertuğrul Uygun and Zihni Onur Uygun

Index . . . 933

About the Editors

Prof. Uday Pratap Azad is currently working as an Assistant Professor at the School of Physical Sciences, Department of Chemistry, Guru Ghasidas Vishwavidyalaya (GGV), Bilaspur, Chhattisgarh, India. He received his B.Sc. M.Sc., and Ph.D. degree from Banaras Hindu University, Varanasi, India. Before joining GGV as Assistant Professor, he worked as Post-Doctoral Fellow at Pusan National University and Yonsei University, respectively, for over 3 years. He has also worked as National Post-Doctoral Fellow at IIT(BHU) Varanasi, India. He is the recipient of several prestigious fellowships, e.g., President Fellowship (South-Korea), Brain Korean Fellowship (BK-21) South-Korea, and National Post-Doctoral Fellowship (SERB, India). He has expertise in electrochemical sensors, biosensors, fuel cells, energy storage, electrochemical water splitting, etc. His research interests include various kinds of nanomaterials, metal complexes, metal oxides, and nanocomposites-based modified electrodes for various electroanalytical applications. He has a better understanding of nano-electrochemistry and associated as a reviewer in more than 30 peer-reviewed international journals. He has more than 2 years of teaching experience and more than 5 years of research experience excluding the experience gained during Ph.D. tenure. He has also published more than 45 research articles in peer-reviewed international journals.

Prof. Pranjal Chandra is an Associate Professor at the School of Biochemical Engineering, Indian Institute of Technology (BHU), Varanasi, India. He earned his Ph.D. from Pusan National University, South Korea, and did post-doctoral training at Technion-Israel Institute of Technology, Israel. His research focus is highly interdisciplinary, spanning a wide range in biotechnology, nanobiosensors, material engineering, and nanomedicine. He has designed several commercially viable biosensing prototypes that can be operated for onsite analysis for biomedical diagnostics. He is an associate editor/editorial board member of various international journals, including *Scientific Reports*, *Sensors International*, *Frontiers in Bioengineering and Biotechnology*, *Molecules*, *Frontiers in Sensors*, and *Green Analytical Chemistry.* He is an expert member/reviewer of various national and international funding agencies. He has also been appointed as Advisor for the Biomedical Sensors Domain and Sensor Networks Systems at the Institution of Engineering and Technology (IET), Michael Faraday House, London, United Kingdom. Prof. Chandra has authored over 150 high-impact publications, including research/review papers and invited book chapters, and published 15 books on biosensors/medical diagnostics/material engineering. He has guided 5 Ph.D. and currently supervising 8 Ph. D. students. Prof. Chandra received many prestigious awards, coveted honors, and fellowships, such as Fellow of the Indian Chemical Society; Shakuntala Amirchand Award 2020 by the Indian Council of Medical Research; NASI-Prof. B.K. Bachhawat Memorial Young Scientist Lecture Award (2022); FSSAI Eat Right Award-2022 (Government of India); DST Ramanujan fellowship (Government of India); Early Career Research Award (ECRA) (DST, Government of India); BK-21 and NRF fellowship, South Korea; Technion Post-Doctoral Fellowship, Israel; Nano Molecular Society India Young Scientist Award; Biotech Research Society India Young Scientist Award; Young Engineers Award 2018; Highly Cited Corresponding authors in The Royal Society of Chemistry (RSC), Cambridge, London; Top 10% cited article in the General Chemistry Section RSC Journal, Cambridge, London; Gandhian Young Technology Innovation Award (GYTI) 2020; etc. Prof. Chandra is also listed among the world's top 2% scientists in 2020 and 2021 by Stanford University, USA.

Contributors

Guilherme Figueira Alves Chemistry Department, Institute of Exact Science, Federal University of Juiz de Fora, Juiz de Fora, Brazil

Lúcio Angnes Department of Fundamental Chemistry, Institute of Chemistry, University of São Paulo, São Paulo, Brazil

Ganesan Anushya Department of Physics, St. Joseph College of Engineering, Chennai, India

Fabiana Arduini Department of Chemical Science and Technologies, University of Rome "Tor Vergata", Rome, Italy

SENSE4MED, Rome, Italy

Nurgul K. Bakirhan University of Health Sciences, Gulhane Faculty of Pharmacy, Department of Analytical Chemistry, Ankara, Turkey

Nurgul K. Bakirhan Department of Analytical Chemistry, Gulhane Faculty of Pharmacy, University of Health Sciences, Ankara, Turkey

Ramachandran Balaji Department of Chemical Engineering, National Taiwan University, Taipei, Taiwan

Fernando Battaglini INQUIMAE (CONICET), Departamento de Química Inorgánica, Analítica y Química Física, Facultad de Ciencias Exactas y Naturales, Universidad de Buenos Aires, Buenos Aires, Argentina

Duygu Beduk Department of Biotechnology, Graduate School of Natural and Applied Sciences, Ege University, Izmir, Turkey

Cassiano Augusto Rolim Bernardino Department of Civil Engineering, COPPE, Federal University of Rio de Janeiro, Rio de Janeiro, Brazil

Rodrigo V. Blasques Department of Nature Sciences, Mathematics and Education, Federal University of São Carlos, São Carlos, Brazil

Burcin Bozal-Palabiyik Department of Analytical Chemistry, Faculty of Pharmacy, Ankara University, Ankara, Turkey

Bernardo Ferreira Braz Department of Analytical Chemistry, Institute of Chemistry, Federal University of Rio de Janeiro, Rio de Janeiro, Brazil

Nutthaya Butwong Applied Chemistry Department, Faculty of Sciences and Liberal Arts, Rajamangala University of Technology Isan, Nakhon Ratchasima, Thailand

Alyah Buzid Department of Chemistry, College of Science, King Faisal University, Al-Ahsa, Saudi Arabia

Narendhar Chandrasekar Department of Nanoscience and Technology, Sri Ramakrishna Engineering College, Coimbatore, India

Ruchika Chauhan Department of Pharmaceutical Chemistry, College of Health Sciences, University of KwaZulu-Natal, Durban, South Africa

Fernando Henrique Cincotto Department of Analytical Chemistry, Institute of Chemistry, Federal University of Rio de Janeiro, Rio de Janeiro, Brazil

National Institute of Science & Technology of Bioanalytics (INCTBio), São Paulo, Brazil

Gulsah Congur Vocational School of Health Services, Bilecik Seyh Edebali University, Bilecik, Turkey

Eduardo Cortón Laboratory of Biosensors and Bioanalysis (LABB), Biological Chemistry Department and IQUIBICEN-CONICET, Science School, University of Buenos Aires, Buenos Aires, Argentina

E. Merve Zanbak Çotaoğlu Department of Pharmaceutical Technology, Gulhane Faculty of Pharmacy, University of Health Sciences, Ankara, Turkey

Ana Elisa Ferreira de Oliveira Department of Natural Sciences, Federal University of São João del-Rei, São João del-Rei, Brazil

Venkataraman Dharuman Department of Bioelectronics and Biosensors, Alagappa University, Karaikudi, India

Slađana Đurđić University of Belgrade, Faculty of Chemistry, Belgrade, Serbia

Niran Öykü Erdoğan Ankara University, Graduate School of Natural and Applied Sciences, Department of Chemistry, Ankara, Turkey

Cem Erkmen Faculty of Pharmacy, Department of Analytical Chemistry, Ankara University, Ankara, Turkey

The Graduate School of Health Sciences, Ankara University, Ankara, Turkey

Hilmiye Deniz Ertuğrul Uygun Center for Fabrication and Application of Electronic Materials, Dokuz Eylül University, İzmir, Turkey

Andrew G. Ewing Department of Chemistry and Molecular Biology, University of Gothenburg, Gothenburg, Sweden

Hoda Ezoji Biofuel and Renewable Energy Research Center, Department of Chemical Engineering, Babol Noshirvani University of Technology, Babol, Iran

Julia Oliveira Fernandes Department of Analytical Chemistry, Institute of Chemistry, Federal University of Rio de Janeiro, Rio de Janeiro, Brazil

Luís M. C. Ferreira Center of Nature Sciences, Federal University of São Carlos, São Carlos, Brazil

Lucas Franco Ferreira Institute of Science and Technology, Federal University of the Jequitinhonha and Mucuri Valleys, Diamantina, Brazil

Federico Figueredo Laboratory of Biosensors and Bioanalysis (LABB), Biological Chemistry Department and IQUIBICEN-CONICET, Science School, University of Buenos Aires, Buenos Aires, Argentina

Fehim Findik Sakarya University, Biomaterials, Energy, Photocatalysis, Enzyme Technology, Nano & Advanced Materials, Additive Manufacturing, Environmental Applications and Sustainability Research & Development Group (BIOE ℕ AMS R & D Group), Sakarya, Turkey

Sakarya Applied Sciences University, Faculty of Technology, Metallurgical and Materials Engineering Department, Sakarya, Turkey

Atal Gill Department of Pharmaceutical Chemistry, College of Health Sciences, University of KwaZulu-Natal, Durban, South Africa

Penny Poomani Govender Department of Chemical Sciences, University of Johannesburg, Johannesburg, South Africa

Research Capacity Development, Postgraduate School: Research and Innovation, University of Johannesburg, Johannesburg, South Africa

Yachana Gupta Applied Science Department, The NorthCap University, Gurugram, Haryana, India

Simge Balaban Hanoglu Department of Biotechnology, Graduate School of Natural and Applied Sciences, Ege University, Izmir, Turkey

Duygu Harmanci Central Research Test and Analysis Laboratory Application and Research Center, Ege University, Izmir, Turkey

Amir Hatami Department of Chemistry and Molecular Biology, University of Gothenburg, Gothenburg, Sweden

Bruno C. Janegitz Department of Nature Sciences, Mathematics and Education, Federal University of São Carlos, São Carlos, Brazil

B. Jurado-Sánchez Department of Analytical Chemistry, Physical Chemistry, and Chemical Engineering, Universidad de Alcala, Alcala de Henares, Spain

Palraj Kalimuthu School of Chemistry and Molecular Biosciences, University of Queensland, Brisbane, QLD, Australia

Leyla Karadurmus Ankara University, Faculty of Pharmacy, Department of Analytical Chemistry, Ankara, Turkey

Department of Analytical Chemistry, Faculty of Pharmacy, Adıyaman University, Adıyaman, Turkey

Rajshekhar Karpoormath Department of Pharmaceutical Chemistry, College of Health Sciences, University of KwaZulu-Natal, Durban, South Africa

S. Irem Kaya Ankara University, Faculty of Pharmacy, Department of Analytical Chemistry, Ankara, Turkey

University of Health Sciences, Gulhane Faculty of Pharmacy, Department of Analytical Chemistry, Ankara, Turkey

Ying-chih Liao Department of Chemical Engineering, National Taiwan University, Taipei, Taiwan

Thalles Pedrosa Lisboa Chemistry Department, Institute of Exact Science, Federal University of Juiz de Fora, Juiz de Fora, Brazil

Haiyun Liu Institute for Advanced Interdisciplinary Research, University of Jinan, Jinan, Shandong, China

John H. T. Luong Innovative Chromatography Group, Irish Separation Science Cluster (ISSC), School of Chemistry and Analytical & Biological Chemistry Research Facility (ABCRF), University College Cork, Cork, Ireland

Claudio Fernando Mahler Department of Civil Engineering, COPPE, Federal University of Rio de Janeiro, Rio de Janeiro, Brazil

K. Manjunath Centre for Nano and Soft Matter Sciences (CeNS), Bangalore, Karnataka, India

Ephraim Felix Marondedze Department of Chemical Sciences, University of Johannesburg, Johannesburg, South Africa

Renato Camargo Matos Chemistry Department, Institute of Exact Science, Federal University of Juiz de Fora, Juiz de Fora, Brazil

Mohammad Mazloum-Ardakani Department of Chemistry, Faculty of Science, Yazd University, Yazd, Iran

Mónica Mosquera-Ortega Laboratory of Biosensors and Bioanalysis (LABB), Biological Chemistry Department and IQUIBICEN-CONICET, Science School, University of Buenos Aires, Buenos Aires, Argentina

Paskorn Muangphrom Sensor Technology Laboratory, Pilot Plant Development and Training Institute, King Mongkut's University of Technology Thonburi, Bangkok, Thailand

Nanoscience and Nanotechnology Graduate Program, Faculty of Science, King Mongkut's University of Technology Thonburi, Bangkok, Thailand

Zondi Nate Department of Pharmaceutical Chemistry, College of Health Sciences, University of KwaZulu-Natal, Durban, South Africa

Masoud Negahdary Department of Fundamental Chemistry, Institute of Chemistry, University of São Paulo, São Paulo, Brazil

Lukman O. Olasunkanmi Department of Chemical Sciences, University of Johannesburg, Johannesburg, South Africa

Department of Chemistry, Faculty of Science, Obafemi Awolowo University, Ile-Ife, Nigeria

Pieter E. Oomen Department of Chemistry and Molecular Biology, University of Gothenburg, Gothenburg, Sweden

ParaMedir B.V, Groningen, The Netherlands

Mahmut Özacar Sakarya University, Biomaterials, Energy, Photocatalysis, Enzyme Technology, Nano & Advanced Materials, Additive Manufacturing, Environmental Applications and Sustainability Research & Development Group (BIOE ℕ AMS R & D Group), Sakarya, Turkey

Sakarya University, Science & Arts Faculty, Department of Chemistry, Sakarya, Turkey

Goksu Ozcelikay Ankara University, Faculty of Pharmacy, Department of Analytical Chemistry, Ankara, Turkey

Cansel Köse Özkan Department of Pharmaceutical Technology, Gulhane Faculty of Pharmacy, University of Health Sciences, Ankara, Turkey

Sibel A. Ozkan Ankara University, Faculty of Pharmacy, Department of Analytical Chemistry, Ankara, Turkey

Yalçın Özkan Department of Pharmaceutical Technology, Gulhane Faculty of Pharmacy, University of Health Sciences, Ankara, Turkey

Chandra Mouli Pandey Department of Chemistry, Faculty of Science, Shree Guru Gobind Singh Tricentenary University, Gurugram, Haryana, India

Pat Pataranutaporn MIT Media Lab, Massachusetts Institute of Technology, Cambridge, MA, USA

Arnaldo César Pereira Department of Natural Sciences, Federal University of São João del-Rei, São João del-Rei, Brazil

Moorthi Pichumani Department of Nanoscience and Technology, Sri Ramakrishna Engineering College, Coimbatore, India

Mostafa Rahimnejad Biofuel and Renewable Energy Research Center, Department of Chemical Engineering, Babol Noshirvani University of Technology, Babol, Iran

Rasu Ramachandran Department of Chemistry, The Madura College, Madurai, India

Thippeswamy Ramakrishnappa Department of Chemistry, BAM Institute of Technology and Management, Bengaluru, Karnataka, India

Alamelu K. Ramasami Sri Sathya Sai University for Human Excellence, Kalaburagi, Karnataka, India

Chandan Hunsur Ravikumar Sensor Technology Laboratory, Pilot Plant Development and Training Institute, King Mongkut's University of Technology Thonburi, Bangkok, Thailand

Centre for Nano and Material Sciences, Jain Global Campus, Jain (Deemed-to-be-University), Bengaluru, India

Ricardo Erthal Santelli Department of Analytical Chemistry, Institute of Chemistry, Federal University of Rio de Janeiro, Rio de Janeiro, Brazil

National Institute of Science & Technology of Bioanalytics (INCTBio), São Paulo, Brazil

Anna Paula Santos Department of Natural Sciences, Federal University of São João del-Rei, São João del-Rei, Brazil

Ozge Selcuk Department of Analytical Chemistry, Faculty of Pharmacy, Ankara University, Ankara, Turkey

Aditya Sharma Applied Science Department, The NorthCap University, Gurugram, Haryana, India

Nazlı Şimşek Ankara University, Graduate School of Natural and Applied Sciences, Department of Chemistry, Ankara, Turkey

Atheesha Singh Water and Health Research Centre, University of Johannesburg, Johannesburg, South Africa

Dalibor M. Stanković University of Belgrade, Faculty of Chemistry, Belgrade, Serbia

The "Vinča" Institute of Nuclear Sciences, University of Belgrade, Belgrade, Serbia

Vesna Stanković Scientific Institution, Institute of Chemistry, Technology and Metallurgy, National Institute University of Belgrade, Belgrade, Serbia

Alexander Pinky Steffi Department of Nanoscience and Technology, Sri Ramakrishna Engineering College, Coimbatore, India

Md Abdus Subhan Department of Chemistry, ShahJalal University of Science and Technology, Sylhet, Bangladesh

Tahrima Subhan Khajanchibari International School and College, Sylhet, Bangladesh

Department of Social Work, ShahJalal University of Science and Technology, Sylhet, Bangladesh

Vinodhini Subramaniyam Department of Nanoscience and Technology, Sri Ramakrishna Engineering College, Coimbatore, India

Werasak Surareungchai Sensor Technology Laboratory, Pilot Plant Development and Training Institute, King Mongkut's University of Technology Thonburi, Bangkok, Thailand

Nanoscience and Nanotechnology Graduate Program, Faculty of Science, King Mongkut's University of Technology Thonburi, Bangkok, Thailand

School of Bioresources and Technology, King Mongkut's University of Technology Thonburi, Bangkok, Thailand

Kempahanumakkagaari Surehkumar Department of Chemistry, BAM Institute of Technology and Management, Bengaluru, Karnataka, India

Jasmine Thomas St. Joseph's HSS Vayattuparamba, Kannur, Kerala, India

Nygil Thomas Department of Chemistry, Nirmalagiri College, Kannur, Kerala, India

Gözde Aydoğdu Tiğ Faculty of Science, Department of Chemistry, Ankara University, Ankara, Turkey

Gözde Aydoğdu Tığ Department of Chemistry, Faculty of Science, Ankara University, Ankara, Turkey

Gözde Aydoğdu Tığ Ankara University, Faculty of Science, Department of Chemistry, Biochemistry Division, Ankara, Turkey

Serbülent Türk Sakarya University, Biomaterials, Energy, Photocatalysis, Enzyme Technology, Nano & Advanced Materials, Additive Manufacturing, Environmental Applications and Sustainability Research & Development Group (BIOE ℕ AMS R & D Group), Sakarya, Turkey

Sakarya University, Biomedical, Magnetic and Semiconductor Materials Application & Research Center (BIMAS-RC), Sakarya, Turkey

Bengi Uslu Faculty of Pharmacy, Department of Analytical Chemistry, Ankara University, Ankara, Turkey

Bengi Uslu Department of Analytical Chemistry, Faculty of Pharmacy, Ankara University, Ankara, Turkey

Zihni Onur Uygun Faculty of Medicine Medical Biochemistry Department, Kafkas University, Kars, Turkey

Center of Translational Medicine Research Center, Koç University, İstanbul, Turkey

Fereshteh Vajhadin Department of Chemistry, Faculty of Science, Yazd University, Yazd, Iran

Barbara Vercelli Istituto di Chimica della Materia Condensata e di Tecnologie per l'Energia, ICMATE-CNR, Milan, Italy

Fernando C. Vicentini Center of Nature Sciences, Federal University of São Carlos, São Carlos, Brazil

Tingfan Wu Institute for Advanced Interdisciplinary Research, University of Jinan, Jinan, Shandong, China

Nimet Yildirim-Tirgil Biomedical Engineering, Faculty of Engineering and Natural Sciences, Ankara Yildirim Beyazit University, Ankara, Turkey

Fatemeh zahirifar Biofuel and Renewable Energy Research Center, Department of Chemical Engineering, Babol Noshirvani University of Technology, Babol, Iran

Derya Koyuncu Zeybek Department of Biochemistry, Faculty of Arts and Science, Kütahya Dumlupınar University, Kütahya, Turkey

Bülent Zeybek Department of Chemistry, Faculty of Arts and Science, Kütahya Dumlupınar University, Kütahya, Turkey

Xinwei Zhang Department of Chemistry and Molecular Biology, University of Gothenburg, Gothenburg, Sweden

Introduction to Nanobioelectrochemistry

1

Fatemeh zahirifar and Mostafa Rahimnejad

Contents

1 Introduction 2
2 Electrochemistry 2
  2.1 Electrochemical Systems 3
  2.2 Basic Axioms of Electrochemical Characterization 4
3 Biotechnology 8
  3.1 Scope and Significance of Biotechnology 8
4 Bioelectrochemistry 9
  4.1 Bioelectrochemical Systems (BESs) 9
5 Nanotechnology 11
6 Nanoelectrochemistry 13
7 Nanobioelectrochemistry 13
8 Conclusions 16
References 16

Abstract

Biotechnology, as a novel field, incorporates biotechnology into electrochemistry. In contrast, nanotechnology aims to open new directions for research area in this field. Nanostructures (such as nanotubes, nanoparticles, etc.) are similar in dimensions to biomolecules such as DNA and proteins. The mixture of biomolecules and nanostructures leads to functional biointerfaces at the nanoscale with synergistic functions and characteristics. The aim of this chapter is to describe the terms and concepts used in nanobioelectrochemistry. More specifically, we will explain the components of nanobioelectrochemistry, namely electrochemistry, biotechnology, nanotechnology, nanoelectrochemistry, and bioelectrochemistry.

F. zahirifar · M. Rahimnejad (✉)
Biofuel and Renewable Energy Research Center, Department of Chemical Engineering, Babol Noshirvani University of Technology, Babol, Iran
e-mail: rahimnejad@nit.ac.ir

© Springer Nature Singapore Pte Ltd. 2023

U. P. Azad, P. Chandra (eds.), *Handbook of Nanobioelectrochemistry*,
https://doi.org/10.1007/978-981-19-9437-1_1

Keywords

Nanotechnology · Nanomaterial · Bioelectrochemical system (BES) · Electrode · Nanoelectrochemistry

1 Introduction

Nanobioelectrochemistry includes the novel fields of bioelectrochemistry, materials science, and nanoscience. The mixture of biological molecules with nanoscale structures and materials allows the development of biodevices with the ability to determine particular matters. Moreover, by applying bioelectrochemistry, the interaction that occurs between the biosystems and nanostructured materials can be investigated at the molecular level, in which numerous molecular behavior mechanisms are classified as oxidation–reduction reactions. The mixture of novel nanomaterial ingredients and biological molecules is crucial to developing modern systems at the nanoscale for electronic, medical, and biological applications.

Nanotechnology has improved sensing phenomena. Nanomaterials such as nanorods, nanotubes, nanowires, and nanoparticles have improved determination times and streamlined the reproducibility procedure. Nanomaterials have exceptional features, such as improved shock-bearing capability and high electrical conductivity, and they improve multipurpose color-based determination mechanisms. Piezoelectric materials are the only outcomes of a group of nanomaterial attributes, and the bioelectrochemical system (BES) is the microbial system that can directly manufacture electricity from organic waste by using chemicals to produce butyrate, medium-chain fatty acids, alcohols, and acetates. Nanotechnology involves monitoring substances with dimensions in the range of 1–100 nanometers, where unique phenomena lead to modern applications. Encompassing engineering, nanoscale science, and technology, nanotechnology involves modeling, imaging, manipulating, and measuring matter at the nanoscale. Materials in gaseous, solid, and liquid states can show eccentric biological, chemical, and physical features when nanosize, features that are different in vital ways from those of such materials in their bulk forms. A number of nanostructured substances are more powerful or possess more-diverse magnetic attributes compared with the other sizes or forms of the same substances. However, at conducting electricity or heat, for example, the other sizes are better. After altering a material's structure or size, it may change color, reflect light in a finer way, become more chemically reactive. Biotechnology modifies, uses, or upgrades a part of or the entirety of a biological system for industrial and human purposes.

2 Electrochemistry

Electrochemistry connects chemical and electrical phenomena in an interdisciplinary field of research and activity (Maier 2007; Bard and Murray 2012; Bard 2014). An electrochemical system is heterogeneous (Bouffier and Sojic 2020). This field is gaining significance thanks to its increasing performance and dependable energy systems (Maier 2007; Nnamchi and Obayi 2018). Electrochemistry uses electrical currents and chemical systems to make chemical changes thanks to the passage of an electric current that generates electrical energy through chemical reactions, in which phenomena such as electrophoresis take place and devices such as electroanalytical sensors are made (Maier 2007; Nnamchi and Obayi 2018).

Electrochemistry also refers to physical and chemical changes. Basic electrochemistry and chemical energy storage are relevant in reducing constraints on the efficiency of electrochemical devices. Innovative coverage of all the phenomena in a chemical conversion is the outcome of using electric power, and this electric power is produced via chemical processes. It contains the behavior and properties of electrolysis in solid and liquid forms. In addition, new electrochemistry can be grouped into bulk and interfacial electrochemistry. By contrast, interfacial electrochemistry varies from bulk electrochemistry in that it is used in electrode–electrolytic interphases and in that the kinetics and thermodynamics of reactions happen during the mass-transport effects (Bueno and Gabrielli 2009). Electrochemical determination is particularly appropriate to merge with analytical system-based properties because such a mixture can increase analyte measurements, resulting in increased sensitivity and reduced detection limits for characteristics such as miniaturization, ease of use, cost-effectiveness, and portability (Beitollahi et al. 2019).

The broad field of electrochemistry includes (a) electroanalysis, (b) sensors, (c) energy storage and conversion devices, (d) corrosion, (e) electrosynthesis, and (f) metal electroplating (Bouffier and Sojic 2020). For a variety of reasons, scientists perform electrochemical measurements on chemical systems. They aim to acquire thermodynamic information about a reaction. They might produce an unsteady average to assess its rate of deterioration or its spectroscopic attributes. They may seek to analyze a solution of small quantities of organic material or metal ions. In these instances, electrochemical procedures are used for instauration in the study of chemical devices, in the same way that spectroscopic procedures are often practical. There are also studies on the electrochemical characteristics of systems, such as the electrosynthesis of some manufactured items. Their utilization requires an understanding of the basic elements of electrode reactions and the electrical attributes of electrode–solution interfaces (Maier 2007). On the contrary, bulk electrochemistry deals with ion–ion and ion–solvent interactions, activity factors, and so on. Bulk electrochemistry optimizes the efficiency of electrolytes and is the key to future improvements in electrochemical elements used as membranes and ionic sources in solar energy systems for, for example, electric force generation and storing energy and in advancements in electroanalytical sensor apparatuses (Bueno and Gabrielli 2009).

2.1 Electrochemical Systems

Electrochemical methods include a set of instruments that are beneficial in neuroscience (Troyer et al. 2002). In these procedures is an electrode that prepares a surface or interface where a charge-transfer process takes place. This charge-transfer process produces currents or potentials that can be measured and linked via calibration to the material's concentration in the solution. These methods can be divided into two broad classes: (1) potentiometry for currents and measurements, which include currents at an electrode under potential check, and (2) voltammetry or amperometry, depending upon the uniqueness of the experimental plan. In electrochemical systems, important factors include the operations and elements that influence the transport of a charge across the interface of chemical phases, such as between an electrode and an electrolyte (Maier 2007). The significance of the electrochemical processes, the function of the processes in living organisms, and the inimitable specifications of their empirical group have resulted in the creation of electrochemistry as an independent discipline. This modern science concentrates on electrochemical kinetics, which is the study of the laws and mechanisms of the electrochemical reactions.

2.2 Basic Axioms of Electrochemical Characterization

Since the substrates of the working electrodes (WEs) can forcefully affect a reaction's performance, their features and ionic materials are crucial electrochemical characteristics. So the electrode surface reaction is the basis of electrochemical research. Electrochemical characterization is performed to study the electrochemical behavior of the materials under various electrochemical conditions. In an electrochemical cell, there are three kinds of electrode systems available, the two-electrode system, three-electrode system, and four-electrode system. Electrochemical characterizations can be performed using any of these electrode systems. The electrochemical cell consists of a working electrode and a counter electrode. The potential of the working electrode is sensitive to the analyte's concentration. The counter electrode closes the circuit. The potential of the working electrode should be calculated with respect to the counter electrode, as it acts as a reference potential. Hence, the potential of the counter electrode should remain constant. If the potential of the counter electrode is not constant, then two electrodes replace the counter electrode, a reference electrode whose potential remains constant and an auxiliary electrode to complete the electrical circuit. The area of the auxiliary electrode should be sufficient to support the current available in the circuit.

Electrochemical characterization of an electrochemical cell depends on various factors such as the condition of the working electrode and the counter electrode, the ions of the analyte in the electrolyte, and the current, charge, and voltage. All these things will be directly or indirectly connected to the redox reactions and will be responsible for the changes in the electrochemical properties of the materials.

2.2.1 The Potential of an Electrode Specifies the Analyte's Form at the Area of the Electrode

The electrode potential is the experimental basis for assessing the potential of a relationship with a specified reference electrode (RE). In electrochemical kinetics, the potential of the electrode is the more important variable, and the current is generally calculated as the rate of this variable. The conventional electropotential is a way to predict how a change in a solution's conditions impacts the position of an equilibrium reaction. The cell potential disparity, E, is determined by the free energy variation within the chemical reaction. The electrode potential, then, results from an arbitrary separation of E into two forms, each allocated to one of the two electrodes on the base of the standard electrode potential formed by the REs. In an oxidation–reduction reaction, the potential specifies the position of the reaction: A negative potential means that the cell provides electrons a lot more readily, and using a positive cell potential and a standard hydrogen electrode shows that the cell shares electrons so much more easily than the conventional hydrogen electrode does (Bueno and Gabrielli 2009).

2.2.2 Electrochemical Cell

Chemical reactions use an electrochemical cell to produce current and voltage. The three-electrode system is the most commonly used system in this field. It consists of an electrode where the reaction happens (WE), an auxiliary electrode (AE), and an RE. A diagram of this device is shown in Fig. 1.1. The WE connects with the analyte as its surface, the position where the reaction happens. After the WE has been used with an analyte, the change in the electrons among the electrodes and a valid potential begin. The current at the electrode will move away from the AE to maintain equilibrium. Usually, to make an AE, inert conducting substances such as platinum or graphite are used. No current passes from the RE. It only acts as a reference when determining the potential of the WE. A silver/silver chloride electrode, a standard hydrogen electrode (SHE), and a calomel electrode are the common REs used in three-electrode systems. To prevent contaminating the specimen solution, the RE can be separated from the specimen reaction by using a mid bridge. An RE includes the anode and its temperature, and an RE refers to an electrode whose potential is independent of the analyte's concentration of ions in a solution. The perfect RE needs to be simple to fabricate and apply. It is placed as close as possible to the WE to decrease drop inducement via cell resistance (iR). The perfect RE produces a stable, predictable potential so that any change in an electrochemical cell is incurred as a result of the effect of the analyte on the potential of the electrode indicator (Bueno and Gabrielli 2009) (Fig. 1.2).

2.2.3 Nanomaterial Concentrations May Not Be Identical to Bulk Concentrations

The concentration of the reacting nanomaterials at the interface varies from that of bulk variants because the former is depleted and cumulates during the reaction. The difference between the concentration of the bulk materials and that at the surface is important because of the interfacial concentrations of the species. There are two ways of doing this. One of variables, usually the current or the potential, is kept variable or stable while other objectives are measured. The concentration of the analyte at the surface of the electrode is computed by solving the transport equations of the conditions used. For the easiest type, the overpotential and the current are

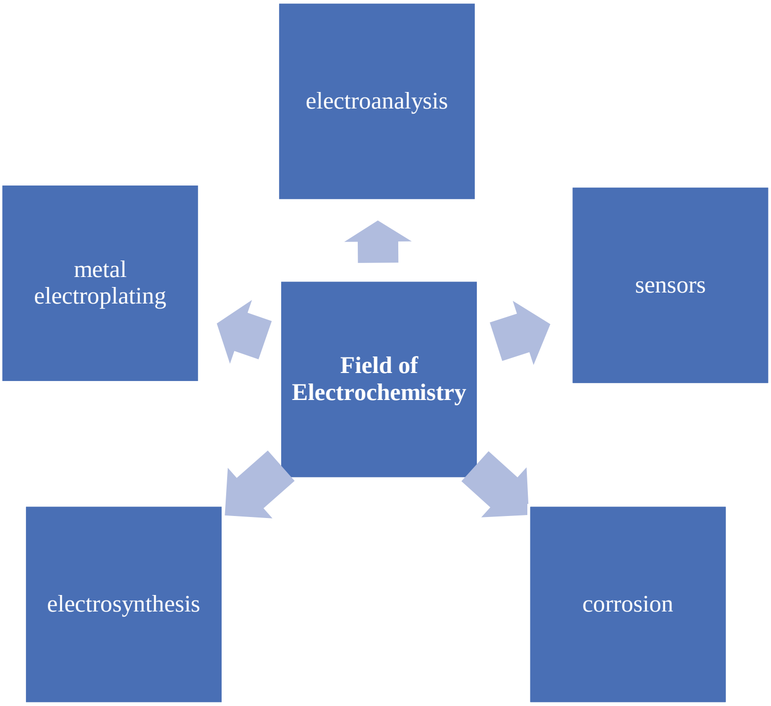
electroanalysis
metal electroplating
sensors
Field of Electrochemistry
electrosynthesis
corrosion

Fig. 1.1 Broad field of electrochemistry

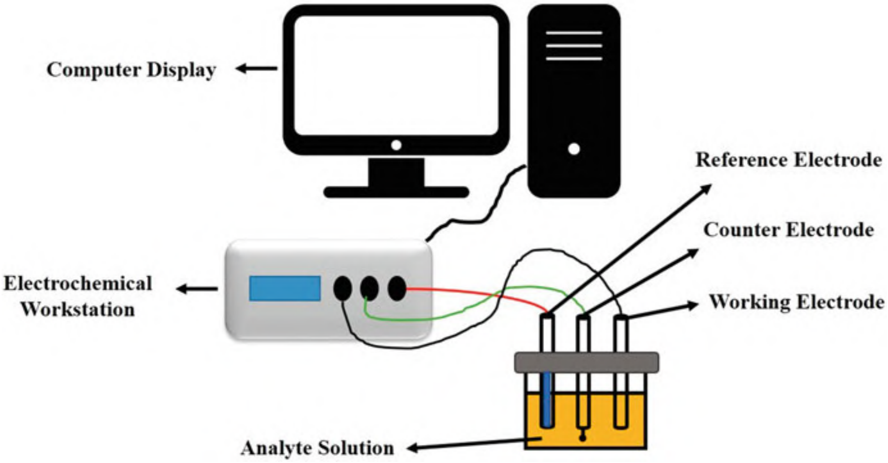
Computer Display
Reference Electrode
Counter Electrode
Electrochemical Workstation
Working Electrode
Analyte Solution

Fig. 1.2 A three-electrode electrochemical cell system

increased from zero to a constant amount. The transition of the other variable is registered and extrapolated back to the time when the step was taken – when the interfacial concentration had not yet been discharged, generally because of the mathematical relationship between the potential of the electrode and the concentrations of an analyte's oxidized and reduced forms in a solution. The reacting sample is boosted by convection if the geometry of the system is simple enough, whereas the equations of the mass transport and the concentrations of the surface are computed to measure the interfacial concentrations (Bueno and Gabrielli 2009).

2.2.4 The Analyte May Not Be Restricted from Participating in Other Reactions

In addition to the electrode potential, which relies on the ion's presence in the solution and whose concentration can be computed by using the Nernst equation, it may not be the only reaction affecting the concentration at the surface of the electrode or in a bulk solution. Many other reactions, including adsorption at the surface of the electrode, can also affect the concentration and the establishment of a metal–ligand complex in a bulk solution (Bueno and Gabrielli 2009).

2.2.5 Current Is Used as a Measure of Rate

The reduction of specimens into ions (for example Fe^{3+} to Fe^{2+}) uses an electron, which is taken from the electrode. The oxidation of other samples, maybe the solvent, at a second electrode is used as a source of this electron. The flow of electrons among the electrodes determines the rate of the current and the reduction reaction. Reaction speed and flow are directly related. In fact, the consequence of this justifies the zero current at equilibrium. However, current is influenced to varying degrees by distinct polarization, which is why it is used to measure the rate. For instance, the current in an electrochemical cell is limited by the rate at which reactants are removed from or brought to one or both of the electrode's surfaces, and its current is further limited by the rate at which electrons are moved among the reactants in a solution and at the electrode's surfaces. In both instances, the current is not fully relevant to the cell potential (Bueno and Gabrielli 2009).

2.2.6 Current and Potential Cannot Be Simultaneously Controlled

In an electrochemical test, one or more of these parameters – namely current (i), charge (Q), time (t), and potential (E) – can be measured. As mentioned, the reduction of samples into ions (from Fe^{3+} to Fe^{2+}) expends an electron until system equilibrium is reached – i.e., when the current becomes zero. Analogously, if we vary the potential from the equilibrium position, the current passes as the system transitions to a new balanced position. This mean that although the primary current is full, it declines over time, attaining zero when the reaction achieves equilibrium. The current therefore varies in response to the potential. As an alternative, we can pass a stabilized current through the electrochemical cell, squeezing the reduction. Because of the permanent change in the concentrations, the potential changes over time. Therefore, if we decide to rein in the potential, we ought to accept the contrariwise and resultant current, along with the resulting potential (Bueno and Gabrielli 2009).

3 Biotechnology

Biotechnology is a combination of biology and technology. Each technological application of biotechnology utilizes biological systems – living organisms or derivatives (especially cells and bacteria) – to make or modify products and processes for specific uses. In fact, it is the use of technology to modify or improve a part or the entirety of a biological system for industrial profits (Thieman 2009). It is a combination of diverse technologies, applied together to living cells, containing not only biology but also disciplines such as chemistry, mathematics, physics and engineering. Bioprocessing, enzyme, waste, and environmental technology; animal husbandry and agriculture; healthcare; and renewable resources are the major fields of biotechnology applications. Its applications range from agriculture to industry (food, pharmaceutical), medicine, environmental conservation, and cell biology, making it one of the fastest-growing fields. Biotechnology also modifies genetic structures in animals and plants to produce advantageous properties. It combines engineering sciences, biochemistry, and microbiology to use the properties of microorganisms, specifically those of their cultured tissue cells. Although the term *biotechnology* is rather new, the discipline itself is very old. In fact, biotechnology can be divided into two parts: traditional biotechnology and new biotechnology, which are briefly described below.

Traditional biotechnology: Biotechnology has long been used by humans. The ability of microorganisms to generate acids and gasses as outcomes of their normal cell metabolism has been used to make new foods for generations, such as in the production of cheese or bread.

New biotechnology: Recent advances in molecular biology have given biotechnology new meaning and potential via use of recombinant DNA technology. New biotechnology modifies the genetic material of living cells to generate new substances or perform new functions. Gene technology – or genetic engineering – allows a biologist to take a gene from one cell and attach it to another cell, which may be that of a plant, an animal, a bacterium, or a fungus, to produce new compositions of genes. There are two fundamental techniques utilized in biotechnology, namely tissue cultures and genetic engineering (Thieman 2009).

3.1 Scope and Significance of Biotechnology

Biotechnology has rapidly emerged as a field of activity that has important impacts on all aspects of human life, including food processing, environmental protection, and human health. Consequently, it now plays significant roles in improving productivity, manufacturing, commerce, human health, and quality of life all over the world. This is reflected in the growing number of biotechnology companies in the world. The total volume of commerce from biotechnology is gaining sharply every year, and it will soon become an important factor in global commerce. Some experts believe that the twenty-first century will be the century of biotechnology, just as the twentieth century was the age of electronics (Naz 2015).

4 Bioelectrochemistry

Bioelectrochemistry, as a modern interdisciplinary field, combines biotechnology and electrochemistry and concentrates on the structural formation and electron transfer (ET) operations of biointerfaces at the surfaces of electrodes. In addition, nanotechnology opens up new pathways for studies in this field. During the past twenty years, bioelectrochemistry has been demonstrated as a beneficial tool for understanding the electrochemical features of biomolecules as well as their principles. Also, it is a powerful approach to using the abovementioned biomolecules in the biointerfaces of biosensing devices. The design of the biointerfaces at the surfaces of electrodes has resulted in attractive developments in this field that generate sensitive and controlled biolayers by engineering the surfaces of electrodes. Biomolecules, or mixtures of them with biocompatible elements, provide modern bioelectrochemical systems and improve our understanding of the interaction between biomolecules and electrodes (Chen et al. 2007).

4.1 Bioelectrochemical Systems (BESs)

Bioelectrochemical systems (BESs) are described as mixtures of electrochemical and biological processes, containing electrochemically active bacteria that degrade organic substances from different sources, such as industrial biomass and effluent (Khoo et al. 2020). Over the past few years, BESs have been used for various purposes, such as for electrosynthesis, wastewater treatment, desalination, and energy production. These are exceptional, more-compatible, and sustainable processes that can vary the chemical energy captured from lignocellulosic biomass or effluent to produce electrical energy, by adding hydrogen to biochemicals through redox-reaction processes using biocatalysts (Kumar et al. 2017). The final outputs gained are hydrogen, electricity, or another precious combination, such as H_2O_2 (hydrogen peroxide), ethanol, etc. BESs are, broadly, simultaneously used for wastewater treatment and the manufacture of bioenergy. Therefore, BESs constitute a promising technology for the global energy crisis and managing water contamination. Photosynthetic microbial fuel cells (MFCs), basic MFCs, plant MFCs, and photosynthetic MFCs are various examples of BESs (Khoo et al. 2020). BESs are transdisciplinary hybrid devices that operate with inputs from several fields, such as electrochemistry, molecular research, fermentation, material science, environmental science, chemical engineering, etc. BESs can be perform considerable alterations in wastewater treatment to produce renewable energy. In BESs, electrochemically active microorganisms can shift the electrons from a reduced electron donating an electrode to an oxidized electron receiver, producing force.

Broadly, BES applications can be divided into three categories: force producers, devices for the recovery of value-added products, and wastewater treatment uses. These multifarious uses for BESs have piqued the interest of many researchers across the globe who want to expand stable waste treatment processes. BESs have been divided according to their uses into the following groups: microbial electrolysis cells (MEC) for electrolytic biofuel generation, MFCs for power production, microbial electrosynthesis (MES) for synthesizing the chemicals or fuels, microbial desalination cells (MDCs) for desalination and force generation, and BESs that carry out waste bioremediation. The major benefits of BESs are as follows: (a) low net-positive energy or energy input gain, (b) biological interposition, (c) the compatibility of microbes for generating various products/energy, (d) cost-effective design and function, (e) reaction under ambient conditions, (f) the selectivity of reactions, (g) the possibility of high value in the market, and (h) its self-regeneration of a biocatalyst. The feasibility of integrating chemical, biological, and physical parts during BES operation provides a chance to start different bioelectrochemical reactions, such as biochemical, electrochemical, and bioelectrochemical ones, among others. BESs are used for either producing electricity through spontaneous redox reactions or applying electrical power to generate value-added products to start nonspontaneous reactions. The most common reduction reactions of BESs are oxygen reductions to produce peroxide and proton reductions to produce hydrogen. The formation of oxidants and reactive specimens is an added benefit of BESs over other treatment systems for the treatment of complex wastewater flows. Sometimes, the polluters/parts of wastewater work as mediators in electron transfer. The usage of BES was also expanded to treat solid waste and toxic aromatic hydrocarbons under in situ biopotential. Studies on the mechanism of contaminant reduction and its role in electron transfer show the functional possibility of using this technology in the sustained removal of pollutants (Srikanth et al. 2018) (Fig. 1.3).

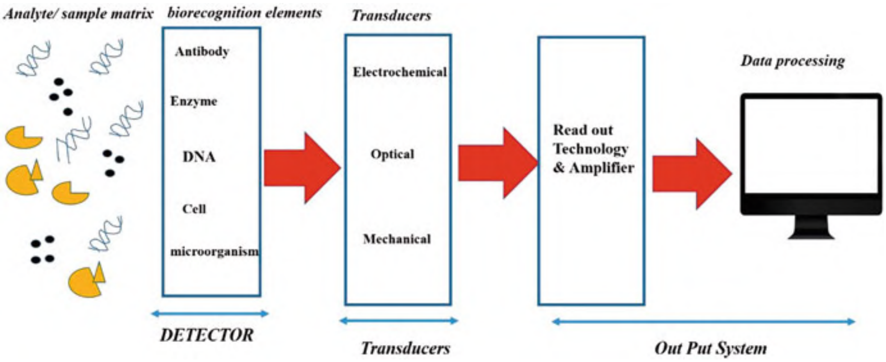

Fig. 1.3 Schematic of biosensor components

5 Nanotechnology

The simplest definition of *nanotechnology* is a type of technology that acts on the nanoscale and has applications in the real world. That is, it utilizes single molecules or atoms to form functional structures. No definition of *nanotechnology* would be complete without defining *nanoscale*: substances whose dimensions are within 1–100 nm. Nanotechnology, which started nearly 50 years ago, is one of the most active areas of investigation with both beneficial and new science uses, and it has gained in prominence over the past two decades (Pavlovic et al. 2013). Nanotechnology is an "atomically precise technology" or is "engineering with atomic precision." The dictionary definition of nanotechnology is "the design, characterization, manufacture and shape and size-controlled application of matters in the nanoscale." A substitute definition from the same dictionary is "the careful and controlled manipulation, precision placement, modeling, measurement, and production of materials at the nanoscale in order to make matters, systems, and devices by fundamentally novel properties and functions." Nanotechnology is a branch of knowledge, within a subclassification of technology in colloidal science, chemistry, physics, biology, and other scientific fields, encompassing the study of phenomena at the nanoscale. Finally, nanotechnology is a technology-based subclass in physics, chemistry, biology, colloidal science, and other fields of science for the investigation of nanoscale phenomena.

Nanotechnology is associated with materials and devices, the structures and elements of which show new, remarkably improved physical, biological, and chemical features, phenomena, and processes thanks to their nanoscale dimensions. The nanotechnology field includes the fabrication and use of biological, physical, and chemical devices that have structural properties from individual atoms or molecules in submicron dimensions and includes the integration of these created nanostructures into larger devices (Nasrollahzadeh et al. 2019). Nanotechnology is able to overcome challenges related to the sources of biomass via their specific active sites for different processes and reactions. Nanomaterials are the core ingredients of nanotechnology and nanoscience applications. Nanoscience and nanotechnology applications involve a broad interdisciplinary area of research and development (R&D) that has rapidly increased. Nanoscale substances are those that have at least one dimension that is 100 nm or smaller. This significantly small size results in a high surface-to-volume ratio and enhances the number of active sites for different processes and reactions. Moreover, nanomaterials have higher reaction rates with various molecules compared to their bulk variants. Nanomaterials have remarkable commercial impacts too. Awareness of nanomaterials will only increase thanks to their inimitable optical scale characteristics, which are effective in a wide variety of fields, such as polymers, electronics, bioenergy, mechatronics, ionic liquids, pharmaceuticals, medicine, etc. (Khoo et al. 2020). From the 1990s onward, much attention has been paid to nanotechnology in various applications, with a special focus on nanostructured materials demonstrating chemical and physical features that are different from their conventional bulk properties.

There are two main reasons for these diverse characteristics: (1) the large surface area of nanomaterials and (2) new quantum effects (Nnamchi and Obayi 2018). Nanoscience studies stimulating areas of science whose produced substances feature new size-dependent attributes. Nanoscale and single-molecule devices also hold various technological prospects in the electronics industry for data storage and sensors. Nanoscience has infiltrated many areas of research, such as the biological, physical and chemical sciences, especially electrochemistry (Zhang et al. 2005). The distinguished properties of these materials at the nanoscale are their rather large surface areas, whose value can be best understood through the new theory of quantum affects. Nanomaterials supply a far greater surface-to-volume ratio compared with their standard forms, and this area is effective in promoting better chemical reactivity. Given the fact that the reaction occurs on a nanoscale level, the specifications and characteristics of materials containing modern magnetized, optical, and electrical properties can be all the more indispensable thanks to quantum efficacy.

The usual types of nanomaterials include fullerenes, nanotubes, and quantum dots, and they have different chemical and physical specifications than their bulk variants (Khoo et al. 2020). The fundamental parts in nanostructure manufacturing are nanoparticles (NPs). NPs of different morphologies and sizes can be made in numerous synthetic ways, which produce premier-quality NPs, but the methods of biosynthesis are still being improved. Modern organic NPs include polymer constructs, liposomes, micelles, and polymersomes, all of which are used for genetic and drug-delivery purposes. Nanotechnology finds applications in analytical chemistry and environmental chemistry, and the life sciences change our imagination about its applications in chemical technology. Another use of nanotechnology can be found in electrochemistry. In electrochemistry, nanotechnology is used in sensors and in power sources such as accumulators and fuel cells. These substances are enhancing the sensitivity of sensors and the efficiency of power sources over those made of common bulk electrodes (Filanovsky). Meanwhile, inorganic nanoparticles, such as polymer-based or lipid nanoparticles, have also attracted attention in recent years thanks to their unmatched size-dependent physicochemical properties. Inorganic nanoparticles are remarkable because of their physical properties – such as their magnetism and size – and their chemical attributes – such as their stability, inactivity, and smooth functionalization. Thus, inorganic nanoparticles such as magnetized quantum dots, carbon nanotubes, and gold have broad potential in various novel applications. For example, metal oxide carbon nanotubes and magnetized nanoparticles (MNPs) are used for bioenergy generation. MNPs, which contain a magnetized core, are some of the most important inorganic nanomaterials. MNPs are used more often than any of the other tested nanoparticles for bioenergy generation because their magnetic attributes confer simple recoverability (Khoo et al. 2020). As the surface area per mass of a substance increases, a higher abundance of the substance comes into contact with circumambient materials, thus affecting reactivity. Also, samples at the nanoscale appear as nonaqueous and aqueous solutions of solvated and complexed molecules, which improves chemical reactivity, which itself affects NPs' attributes. In this way, electrochemical characterization is fundamental to nanomaterial research (Rusling et al. 2013).

6 Nanoelectrochemistry

The compound word *nanoelectrochemistry* contains the prefix *nano-* and the noun *electrochemistry*. Each of these terms encompasses a wide variety of meanings and features in various areas of scientific enquiry (Singh et al. 2012). Nanoelectrochemistry refers to the dimensional scale of electrodes and electrochemical occurrences, as opposed to volume, mass, or time. Nanoscale electrochemistry is significant for new electrochemical science and for many other key research areas, such as energy transformation, catalysis, sensor development, and environmental science. New electrochemical phenomena, attributes, and technological abilities indispensable to decreasing the dimensions of an electrochemical probe to the nanometer scale and the electrochemical attributes of new nanoscale electrode substances are the frontiers of nanoelectrochemistry. Conventional descriptions of the nanoscale refer to lengths between 1 and 100 nm. Nanoscale electrochemical studies have provided unique information unattainable via standard procedures. For instance, nanoelectrodes can measure very fast electron-transfer kinetics that are frequently too fast to study with study electrodes. Nanoscale electrochemical substances, such as metal nanoparticles, have unrivaled physical and chemical attributes, and nanoscale electrochemical procedures can be applied to produce advanced electrocatalytic substances. Further, the use of nanoscale electrodes has realized electrochemical imaging with nanoscale spatial resolutions, generating data that improve our understanding of heterogeneous electrode–solution interfaces (Palit and Hussain 2020). Nanoscale electrochemistry has played a crucial role in increasing our understanding of electron-transfer processes at the electrolyte or electrode interface and spurs on applied, fundamental, and basic electrochemical investigations. Nanoscale electrodes are important in nearly all aspects of nanoscale electrochemistry, including catalytic nanoparticles, nanoscale electrochemical descriptions, and electron-transfer kinetics. The key challenges and targeted domains in nanoscale electrochemistry have included the lack of structural control in nanoelectrode preparation and the necessity for advanced methods for structural characterization. This can be largely solved via the use of nanofabrication and nanocharacterization procedures. Nanopore-based electrochemical procedures have attracted global interest in research and will continue to rapidly grow in the future (Palit and Hussain 2020). Currently areas of nanoelectrochemistry include (a) the extraordinary properties of electrodes, (b) nanoelectrode fabrication, and (c) nanoelectrodes.

7 Nanobioelectrochemistry

Nanobioelectrochemistry covers the novel aspects of bioelectrochemistry, material science, and nanoscience. The combination of nanostructured substances and biological molecules enables the development of biodevices able to detect particular materials. In addition, by taking the bioelectrochemical approach, the interaction between a biosystem and nanostructured materials can be investigated at the molecular level, where many molecular mechanisms are elicited through redox reactions.

The combination of new nanomaterial components and biological molecules develops new nanoscale systems for future medical, biological, and electronic applications (Crespilho 2012). A biological event such as an antibody–antigen binding reaction and the transformation of a substrate via an enzyme or electron-transfer reaction of a redox protein using electrochemical procedures can lead to the development of new sensors (Murphy 2006). A biosensor can be defined as a sensing device or a measurement system that approximates the amount of a substance by assessing biological interactions and then translating these interactions into readable data with the help of transduction and electromechanical clarification (Purohit et al. 2020; Roy et al. 2019).

The basic components of biosensors include a detector, a transducer, and a bioreceptor. That is, a biosensor contains a bioreceptor mixed with a transducer and an electronic system that detects analytes. These analytes include great number of disease markers, biomolecules, etc. (Prajapati et al. 2020).

The principal function or goal of a biosensor is to sense a specific biological substance. Often, these substances are antibodies, proteins, enzymes, etc. (Malik et al. 2013). Developments in the field of nanotechnology propel the progression of biosensors. These biosensors gain selectivity, stability, sensitivity, linearity, and reproducibility thanks to their new properties. The research on biosensors is multidisciplinary, which means that it combines various scientific disciplines, such as electronics, food processing, nanotechnology, medical sciences, etc. In fact, biosensor technology has provided a strong platform for improving quality of life. In addition, the incorporation of nanotechnology into biosensor research has brought it more research interest and more high-quality production (Prajapati et al. 2020). A variety of nanoparticles containing nanowires and nanotubes, based on metals, semiconductors, polymeric species, or carbon, have been broadly studied for their ability to increase biosensor responses. Nanoparticles can be used to complete various tasks, such as modifying electrode surfaces and improving biological receptor molecules like enzymes, antibodies, and oligonucleotides (Murphy 2006). The classification of nanobiosensors varies depending on the nature of the nanomaterials that are combined in the biosensing operation (Mahato et al. 2020; Kumar et al. 2019; Mahato et al. 2018).

In addition, we categorize biosensors on the basis of two criteria, namely the type of substance to be analyzed and the signal transduction mechanism used. Biosensors follow the convention of being named after the nature of the analyte; for instance, they are named antigen biosensors when they sense antigens and enzyme biosensors when they sense enzymes. Similarly, biosensors can be divided according to their sensing mechanism into the following four types: (a) optical, (b) calorimetric, (c) electrochemical, and (d) acoustic. Each of these groups of sensors is based on the transduction mechanism and includes a series of overlapping sensors subsumed under it. For example, electrochemical sensors have potentiometric and amperometric biosensors, and optical biosensors carry optical fiber–based sensors. By studying various nanobiosensors, we can learn which characteristics of nanomaterials improve various sensing mechanisms. In fact, nanoparticle-based biosensors use metallic nanoparticles as amplifiers of biochemical signals. Further, nanobiosensors that use carbon nanotubes as amplifiers of the reaction are nanotube-based sensors, while biosensors that use nanowires for charge transportation and as charge carriers are nanowire-based biosensors. There are also quantum dots–based sensors, which use quantum dots as the contrast factors to improve optical responses. The major classes of nanobiosensors are as follows: (a) nanoparticle-based sensors, (b) magnetic biosensors, (c) electrochemical biosensors, (d) nanotube-based sensors, and (e) nanowire-based sensors (Malik et al. 2013). Electrochemical biosensors simplify or analyze biochemical reactions by using electricity.

These devices are often based on metallic nanoparticles. The chemical reactions among biomolecules can be easily and efficiently carried out with the help of metallic nanoparticles, which are crucial in immobilizing one of the reactants. This ability makes these reactions very material specific and eliminates the possibility of generating undesirable side products. Table 1.1 shows an overview of the nanomaterials that are used for improving biosensor technology. Nanobiosensors have biomedical, diagnostic, environmental, and other applications (Malik et al. 2013).

Nanomaterials are special candidates in many biofuel systems thanks to their large surface areas and specific characteristics: durability, efficient storage, high catalytic activity, crystallinity, stability, and adsorption capacity. The effects on the metabolic reactions of bioprocesses generating biofuel are increased with nanomaterials such as nanotubes, metallic nanoparticles, and nanofibers. Nanoparticles, which are commonly used to reduce inhibitory compounds and as catalytic agents, help increase the activity of anaerobic consortia and transmit electrons in order to increase the process efficiency. Nanomaterials such as nanocrystals, nanodroplets, and nanomagnets are also utilizing such nanoadmixtures to increase the mixing performance of biofuel with diesel and petrol/gasoline (Nasrollahzadeh et al. 2019).

Table 1.1 Overview of nanomaterials that are used for sensing technology

Nanomaterial	Benefits	References
Carbon nanotubes	Superior electrical communication, improved enzyme charging, and superior aspect ratios	Malik et al. (2013) and Zhao et al. (2002)
Nanoparticles	Excellent bioanalyte charging, improved immobilization, and fine catalytic attributes	Luo et al. (2006) and Merkoçi et al. (2005)
Quantum dots	Size-adjustable band energy, high fluorescence, quantum confinement for the charge bearer	Wang et al. (2002) and Huang et al. (2005)
Nanowires	Strong electrical and sensing attributes for chemical sensing and biosensing, better charge conduction, high versatility	Malik et al. (2013) and Mackenzie et al. (2009)
Nanorods	Excellent at finding specific answers, good plasmonic substances that can combine with sensing and size-adjustable energy regulation, compatible with Microelectromechanical systems (MEMS)	Malik et al. (2013) and Ramanathan et al. (2006)

8 Conclusions

Nanobioelectrochemistry shows a lot of promise in modeling new forms of matter by collecting molecules from biological structures, substances, and systems. Using nanosize substances brings a substantial increase in surface area and possible benefits from their unique properties at that size. At the nanoscale, life is a complex nanotechnological system containing a series of self-assembling processes. Nanobioelectrochemistry promises to make medical advances such as early detection, fast analysis by using a lab-on-a-chip, tissue regeneration, and new medicines. Nanomedicine requires carrying out repairs at the cellular level inside the human body, where the minute size of nanostructures can work well with the cell surfaces of biomolecules.

References

Bard AJ (2014) A life in electrochemistry. Annu Rev Anal Chem 7:1–21

Bard AJ, Murray RW (2012) Electrochemistry. Proc Natl Acad Sci 109:11484–11486

Beitollahi H, Safaei M, Tajik S (2019) Screen-printed electrode modified with ZnFe2O4 nanoparticles for detection of acetylcholine. Electroanalysis 31:1135–1140

Bouffier L, Sojic N (2020) Chapter 1 Introduction and overview of electrogenerated chemiluminescence. In: Analytical electrogenerated chemiluminescence: from fundamentals to bioassays. The Royal Society of Chemistry

Bueno PR, Gabrielli C (2009) Electrochemistry, nanomaterials, and nanostructures. In: Nanostructured materials for electrochemical energy production and storage. Springer

Chen D, Wang G, Li J (2007) Interfacial bioelectrochemistry: fabrication, properties and applications of functional nanostructured biointerfaces. J Phys Chem C 111:2351–2367

Crespilho FN (2012) Nanobioelectrochemistry: from implantable biosensors to green power generation. Springer

Filanovsky B (2017) Nanotechnology in electrochemistry. Nanotechnology letters 1(1):1

Huang Y, Zhang W, Xiao H, Li G (2005) An electrochemical investigation of glucose oxidase at a CdS nanoparticles modified electrode. Biosens Bioelectron 21:817–821

Khoo KS, Chia WY, Tang DYY, Show PL, Chew KW, Chen W-H (2020) Nanomaterials utilization in biomass for biofuel and bioenergy production. Energies 13:892

Kumar G, Saratale RG, Kadier A, Sivagurunathan P, Zhen G, Kim S-H, Saratale GD (2017) A review on bio-electrochemical systems (BESs) for the syngas and value added biochemicals production. Chemosphere 177:84–92

Kumar A, Purohit B, Maurya PK, Pandey LM, Chandra P (2019) Engineered nanomaterial assisted signal-amplification strategies for enhancing analytical performance of electrochemical biosensors. Electroanalysis 31:1615–1629

Luo X, Morrin A, Killard AJ, Smyth MR (2006) Application of nanoparticles in electrochemical sensors and biosensors. Electroanalysis 18:319–326

Mackenzie R, Auzelyte V, Olliges S, Spolenak R, Solak HH, Vörös J (2009) Nanowire development and characterization for applications in biosensing. In: Nanosystems design and technology. Springer

Mahato K, Maurya PK, Chandra P (2018) Fundamentals and commercial aspects of nanobiosensors in point-of-care clinical diagnostics. 3 Biotech 8:1–14

Mahato K, Kumar A, Purohit B, Mahapatra S, Srivastava A, Chandra P (2020) Nanomaterial functionalization strategies in bio-interface development for modern diagnostic devices. In: Biointerface engineering: prospects in medical diagnostics and drug delivery. Springer

Maier SA (2007) Plasmonics: fundamentals and applications. Springer Science & Business Media

Malik P, Katyal V, Malik V, Asatkar A, Inwati G, Mukherjee TK (2013) Nanobiosensors: concepts and variations. Int Sch Res Not

Merkoçi A, Aldavert M, Marın S, Alegret S (2005) New materials for electrochemical sensing V: nanoparticles for DNA labeling. TrAC Trends Anal Chem 24:341–349

Murphy L (2006) Biosensors and bioelectrochemistry. Curr Opin Chem Biol 10:177–184

Nasrollahzadeh M, Sajadi SM, Sajjadi M, Issaabadi Z (2019) An introduction to nanotechnology. In: Interface science and technology. Elsevier

Naz Z (2015) Introduction to biotechnology. https://doi.org/10.13140/RG.2.1.3517.8968

Nnamchi PS, Obayi CS (2018) Electrochemical characterization of nanomaterials. In: Characterization of nanomaterials. Elsevier

Palit S, Hussain CM (2020) Modern manufacturing and nanomaterial perspective. In: Handbook of nanomaterials for manufacturing applications. Elsevier

Pavlovic M, Mayfield J, Balint B (2013) Nanotechnology and its application in medicine. In: Handbook of medical and healthcare technologies. Springer

Prajapati S, Padhan B, Amulyasai B, Sarkar A (2020) Nanotechnology-based sensors. In: Biopolymer-based formulations. Elsevier

Purohit B, Vernekar PR, Shetti NP, Chandra P (2020) Biosensor nanoengineering: design, operation, and implementation for biomolecular analysis. Sens Int:100040

Ramanathan S, Patibandla S, Bandyopadhyay S, Edwards JD, Anderson J (2006) Fluorescence and infrared spectroscopy of electrochemically self assembled ZnO nanowires: evidence of the quantum confined Stark effect. J Mater Sci Mater Electron 17:651–655

Roy S, Malode SJ, Shetti NP, Chandra P (2019) Modernization of biosensing strategies for the development of lab-on-Chip integrated systems. Bioelectrochem Interface Eng:325–342

Rusling JF, Munge B, Sardesai NP, Malhotra R, Chikkaveeraiah BV (2013) Nanoscience-based electrochemical sensors and arrays for detection of cancer biomarker proteins. Nanobioelectrochemistry:1–26

Singh PS, Goluch ED, Heering HA, Lemay SG (2012) 1 Nanoelectrochemistry: fundamentals and applications in biology and medicine. In: Applications of electrochemistry and nanotechnology in biology and medicine II. Springer

Srikanth S, Kumar M, Puri S (2018) Bio-electrochemical system (BES) as an innovative approach for sustainable waste management in petroleum industry. Bioresour Technol 265:506–518

Thieman WJ (2009) Introduction to biotechnology. Pearson Education India

Troyer KP, Heien ML, Venton BJ, Wightman RM (2002) Neurochemistry and electroanalytical probes. Curr Opin Chem Biol 6:696–703

Wang J, Liu G, Polsky R, Merkoçi A (2002) Electrochemical stripping detection of DNA hybridization based on cadmium sulfide nanoparticle tags. Electrochem Commun 4:722–726

Zhang J, Chi Q, Albrecht T, Kuznetsov AM, Grubb M, Hansen AG, Wackerbarth H, Welinder AC, Ulstrup J (2005) Electrochemistry and bioelectrochemistry towards the single-molecule level: theoretical notions and systems. Electrochim Acta 50:3143–3159

Zhao Y-D, Zhang W-D, Chen H, Luo Q-M, Li SFY (2002) Direct electrochemistry of horseradish peroxidase at carbon nanotube powder microelectrode. Sensors Actuators B Chem 87:168–172

Всё для победы! НАРОДНЫЙ ФРОНТ
https://pobeda.onf.ru/
LET'S HELP THE RUSSIA

2

Nanobiomaterials: Classifications and Properties

Serbülent Türk, Fehim Findik, and Mahmut Özacar

Contents

1 Introduction 21
2 Material-Essenced Classification of Nanobiomaterials 22
  2.1 Natural Biomaterials 22
  2.2 Synthetic Biomaterials 24
3 Properties of Nanobiomaterials 27
  3.1 Toxicity Properties 27
  3.2 Mechanical Properties 28
  3.3 Electrical Properties 28
  3.4 Magnetic Properties 28
  3.5 Thermal Properties 29

S. Türk
Sakarya University, Biomaterials, Energy, Photocatalysis, Enzyme Technology, Nano & Advanced Materials, Additive Manufacturing, Environmental Applications and Sustainability Research & Development Group (BIOENAMS R & D Group), Sakarya, Turkey

Sakarya University, Biomedical, Magnetic and Semiconductor Materials Application & Research Center (BIMAS-RC), Sakarya, Turkey

F. Findik
Sakarya University, Biomaterials, Energy, Photocatalysis, Enzyme Technology, Nano & Advanced Materials, Additive Manufacturing, Environmental Applications and Sustainability Research & Development Group (BIOENAMS R & D Group), Sakarya, Turkey

Sakarya Applied Sciences University, Faculty of Technology, Metallurgical and Materials Engineering Department, Sakarya, Turkey

M. Özacar (✉)
Sakarya University, Biomaterials, Energy, Photocatalysis, Enzyme Technology, Nano & Advanced Materials, Additive Manufacturing, Environmental Applications and Sustainability Research & Development Group (BIOENAMS R & D Group), Sakarya, Turkey

Sakarya University, Faculty of Science, Department of Chemistry, Sakarya, Turkey
e-mail: mozacar@sakarya.edu.tr

© Springer Nature Singapore Pte Ltd. 2023

U. P. Azad, P. Chandra (eds.), *Handbook of Nanobioelectrochemistry*,
https://doi.org/10.1007/978-981-19-9437-1_2

  3.6 Optical Properties 30
  3.7 Smart Biomaterial Properties 31
4 Applications of Nanobiomaterials 32
  4.1 Drug Delivery 32
  4.2 Antibacterial Applications 33
  4.3 Bioimaging 34
  4.4 Tissue Engineering 35
  4.5 Infection 35
5 Functionalization of Nanobiomaterials 37
6 Conclusion and Future Perspectives 38
References 40

Abstract

Various organs or tissues of living things can be damaged by diseases or biological, physical, and chemical damages. Their treatment has led to the development of numerous new biomaterials that enable the regeneration of many living things. Biomaterials constitute an important part of the materials consumed in the health sector today, and their market shares in the world are increasing day by day. When materials are reduced to nano-dimensions, their biological, physical, and chemical properties and functions change significantly and show improvements in the desired direction for many applications. Biomaterials have helped millions of people achieve a better quality of life in almost every corner of the world. Nanobiomaterials (NBMs) are used in many fields, and their most critical applications can be summarized as drug delivery, antibacterial applications, and bioimaging. Nanomaterials have significant toxicity values due to their high surface area and activity. In this chapter, a classification of NBMs has been made, and various properties have been reviewed. First, NBMs were divided into natural and synthetic. Two classes of natural biomaterials, protein-based and polysaccharide-based, were investigated. Synthetic biomaterials are divided into six groups as metallic, ceramic, polymeric, carbon-based, composite, and combined, and the general structures of the materials in this subgroup are reviewed. Then, the toxic, mechanical, electrical, magnetic, thermal, optical, and smart properties of NBMs were investigated. Also, drug delivery, antibacterial, bioimaging, tissue engineering, and infection properties of NBMs were discussed. Finally, after focusing on the functionalization of NBMs, the study's general findings are summarized in the conclusion section, and a perspective on the future of these materials is given.

Keywords

Nanobiomaterials · Smart biomaterials · Drug delivery · Tissue-engineering · Functionalization

1 Introduction

Many acceptable definitions have been made for the biomaterial to date. Some of these definitions are as follows; “it is a pharmacologically and systemically inert material fabricated to be combined with or placed within living systems” or “an inanimate material used in any device that will interact with the biological systems” or as stated by the US National Institute of Health, “biomaterial is any substance other than drugs that can be utilized for any time to maintain or improve the quality of life of the individuals, and to perform any tissue, organ or body function partially or completely” (Thomas et al. 2018).

Various tissues or organs of living things can be damaged by diseases or biological, physical, and chemical destructions, and their treatment, regardless of tissue or organ transplantation, has led to the improvement of a large number of novel materials that allow the regeneration of many tissues and serve as scaffolds or implants. Great efforts are being made worldwide to develop novel biomaterials to improve human living standards by restoring tissue with scaffolds or replacing dysfunctional organs. Due to the exponential growth of the population and the increasing life expectancy, the need for a wide variety of biomaterials that can repair, regenerate, or replace hard and soft tissues like cartilage, bone, skin, and blood vessels is increasing day by day (Thomas et al. 2018). The global biomaterials market, which was USD 70.90 billion in 2016, is estimated to reach USD 149.17 billion in 2021 (Seifalian 2019). Today, many biomaterials made from organic and inorganic nature materials are widely used in therapeutic medicine, especially for device-essenced treatments, porous scaffolds in tissue regenerations, drug delivery systems, and bioimaging for diagnosis.

The most widely used metal implants in biomedical implementations were developed after the invention of stainless steel in 1913. The most important properties of first-generation metal implants developed in the 1960s and 1970s were biologically inertness. Second-generation biomaterials produced from bioactive materials with resorbable or bioactive properties were developed in the mid-1980s. Third-generation biomaterials currently being studied are combined with the multiple biological functions to activate genes and cells to stimulate the regeneration, heal, or repair of living tissues after implantation (Yang et al. 2017).

Tissue engineering (TE) aims to regenerate, reproduce, and repair tissues or improve regeneration rates in cases where tissue damage or dysfunction occurs and these tissues cannot heal themselves. Biomaterials help tissues to regain their natural functions by interacting between natural healing processes and medicines. Thus, biomaterials must be able to mimic the molecular structure of tissues and provide a protective extracellular medium. To achieve excellent results in TE implementations, biomaterials must have impressive biocompatibility, not cause any adverse reactions, and be enormously porous structures with interconnected channels for cell growth and metabolism. Also, their bioabsorbability or biodegradability rates should be suitable for use in real clinical implementations. Apart from these, they must have good mechanical features to withstand any stress, an appropriate surface structure for cellular adhesion, and the ability to be easily machined into three-dimensional shapes and sizes for a wide variety of implementations (Lin et al. 2019).

2 Material-Essenced Classification of Nanobiomaterials

Biocompatibility is the acceptance of implanted materials by surrounding tissue or organ in living things. Biomaterials can be primarily classified according to their biocompatibility as bioinert, bioactive, and bioabsorbable (Thomas et al. 2018):

Bioinert biomaterials refer to materials that produce a minimum adverse response to tissues or organs in the living things after contact with biological systems. Titanium, stainless steel, zirconia, alumina, and polyethylene used in dental implantation can be given as examples of this class. But bioinert biomaterials coated with fibrous capsules for their functionalities provide to tissue combination via implantation.

Bioactive biomaterials interact with the soft tissue of living things via stimulating mechanisms, initiating repair and regeneration processes. Synthetic hydroxyapatite, bioglass, glass-ceramic, and bioabsorbable tricalcium phosphate are the finest examples of this group. They are often coated on the surface of metal implants to increase their biocompatibility.

Bioabsorbable biomaterials generally interact with physiological fluids after implantation into the living things, dissolve in the biological environment, and then reabsorb into the human body through multiple metabolic processes and are gradually replaced by lately formed tissues like skin and bones. Polylactic-polyglycolic acid copolymers, gypsum, tricalcium phosphate, calcium carbonate, and calcium oxide are biomaterials widely used in the past three decades.

Furthermore, biomaterials can be categorized as synthetic and natural biomaterials depending on available sources. Additionally, natural biomaterials are split into protein-essenced and carbohydrate-essenced biomaterials. Synthetical materials are studied as metals, ceramics, polymers, composites, and combined biomaterials (Thomas et al. 2018).

2.1 Natural Biomaterials

Natural biomaterials are substances used to produce scaffolding or other implants obtained from natural resources or consisting of their forms modified with certain chemicals. Natural biomaterials can be split into two major groups as polysaccharide and protein-structured due to the nature of their origin (Barua et al. 2018).

2.1.1 Protein-Essenced Natural Biomaterials

Protein-based biomaterials consist of amino acids as the main component and certain recombinant proteins. They contain some biological and mechanical patterns obtained from natural proteins that ensured constructional brace and direct tissue or cell behavior. Fibrin, collagen (Col), and silk are the veriest studied protein-essenced natural biomaterials.

Silk is a protein-essenced polymer transformed into fiber by certain *Lepidoptera larvae*, including silkworm, spider, scorpion, mite, and fly. Along with water and some organic solvent-soluble gelatin materials, silk protein has been broadly utilized to produce composite scaffolds with 3D porous for renewal of skin, bone, and ligament tissues.

Collagen is a protein that ensures structural stability and strength in tissues, including tendons, cartilage, skin, bone, and blood vessels in the body. Col cross-linked with chitosan fibers, Hap, and mesenchymal stem cells has been utilized to fabricate porous scaffolds to repair bone tissues.

Fibrin, a natural polymer, is derived from fibrinogen protein that provides cell attachment by inducing angiogenesis, supporting many living tissues and wound healing. Fibrin-essenced hydrogel scaffolds are commonly utilized in treating cartilage and bone tissue as examples of TE implementation.

2.1.2 Polysaccharide-Essenced Natural Biomaterials

Natural polymers mimic the natural macromolecular environment of cells and exhibit exceptional biocompatibility with favorable mechanical properties and the ability to be loaded with growth elements essential for bone formation. Polysaccharide-essenced biomaterials are native polymers derived from polysaccharides containing various sugar monomers. Polysaccharides, highly bioactive for TE implementations, are attained from animal or plant sources. Polysaccharide biomaterials like hyaluronic acid, chitosan, alginate, and agarose have been widely utilized to develop scaffolds in TE.

Chitosan is a significant linear structured polysaccharide attained by the partial deacetylation of chitin, which is found as an essential constituent in the cell walls of yeast and fungi or exoskeleton of arthropods, and some parts in fish, jellyfish, crab, lobster, shrimp, coral, ladybug, butterfly, and invertebrates. Chitosan has proven to be a biomaterial that can be used to fabricate various poriferous composite scaffolds (Azmana et al. 2021).

Alginate, which is sodium, magnesium, or calcium salt of alginic acid, is a biopolymer formed of unbranched exopolysaccharides obtained from particular seaweed, brown algae, and bacteria. Alginate is used widely in biomedical implementations as oral transporting templates for protein drugs, scaffolds for wound healing and TE, and microencapsulation of cells and other nanobiomaterials (NBMs) (Wang et al. 2021).

Hyaluronic acid is a polysaccharide found in the extracellular matrices of tissues and supports early inflammation, crucial for wound heal. Hyaluronic acid is commonly used in the fabrication of composite bone skeletons. It has good biodegradability, biocompatibility, the capability to sustain a hydrated medium useful for cell percolation, and unique viscoelastic properties (Dovedytis et al. 2020).

Agarose is a seaweed polysaccharide attained via the extraction of red algae and particular seaweeds. Agarose-essenced hydrogel and composite scaffolds prepared from agarose with HAp find their implementations in the engineering for bone tissue (Zarrintaj et al. 2018).

Gellan Gum (GG) and Derivatives, fabricated via fermenting the *Sphingomonas elodea* bacteria that live on *Elodea Canadensis* algae, are extracellular, anionic, and high molecular weight polysaccharides. GG has been used in various cellular and acellular TE implementations like the regeneration of intervertebral discs to enhance their mechanical features, checking the blood vessel growth and endothelial cells percolation (Pina et al. 2015).

2.2 Synthetic Biomaterials

Synthetical biomaterials are generally made from artificial ingredients. It is likely to divide synthetic biomaterials into five main categories: metallic, ceramic, polymeric, carbon, and composite~~s~~.

2.2.1 Metallic Biomaterials

Metals are one of the furthermost commonly utilized scaffolding materials to produce implants for load-bearing situations. For example, metallic implants are generally preferred in many of the most widespread orthopedic surgeries. These implants include screws, simple wires, joint prostheses for shoulders, hips, knees, ankles, etc. Furthermore, metal implants are widely preferred in cardiovascular surgery, dental materials, and maxillofacial surgery, as well as orthopedics. The most frequently used metals and their alloys in medical device implementations are stainless steel, iron and titanium alloys, magnesium and zinc alloys, cobalt-essenced alloys, and zirconium alloys (Ping 2014).

2.2.2 Ceramic Biomaterials

Ceramic materials have usually been utilized to restore teeth in dentistry. These materials are used to produce various biomaterials such as dental crowns, cements, and prostheses. Certain ceramic scaffolds have been employed in joint replacement expansion and bone reparation. But, their use in load-bearing implementations is quite limited due to their weak fracture toughness. This group includes HAp, biphasic CaP, and β-tricalcium phosphate (HAp and β-tricalcium phosphate mixture) and apatite/wollastonite. These glass-type ceramics can be suitable matrices in bone renewal applications because of their micro/nanostructures and advanced mechanical features, for example, they can be used as intramedullary plugs to replace the total hip. The cytocompatibility of glass-ceramics functionalized by lysine has increased (Long et al. 2014).

2.2.3 Polymeric Biomaterials

Various polymers have been broadly utilized as biomaterials in many medical applications. Their implementations cover various areas from facial prostheses to tracheal tubes, heart components, liver parts, kidneys, prostheses, knee, and hip joints. Apart from these, polymeric biomaterials are widely used to prepare sealants, medical adhesives, and coatings for various functions such as imparting hydrophilic/hydrophobic properties or increasing biocompatibility. The physical features of the polymers used as biomaterials are very similar to soft tissue and are highly beneficial for repairing vascular walls, cartilage, tendon, and skin, as well as drug delivery and the like. While polyethylene is utilized instead of joint prostheses, polycaprolactone is used for absorbable screws, sutures, and plates to straighten the fractures (Teo et al. 2016).

2.2.4 Carbon-Essenced Biomaterials

Carbon-essenced nanomaterials (NMs) comprise carbon-essenced quantum dots, graphene oxide, graphene and its derivatives, carbon nanotubes, fullerenes, and nano-diamonds. These NMs have received significant attention in a variety of fields, inclusive of biomedical implementations, because of their matchless structural sizes and outstanding mechanical, optical, thermal, electrical, and chemical properties. Among the many applications, capacious studies have recently been performed on the cells and tissues imaging and the delivery of the therapeutic molecules for the reparation of tissue injuries and disease treatment. Carbon-essenced NMs have become nominee-imaging agents for tumor diagnosis due to their biocompatibility, wide-range single-photon properties, and easy functionalization (Patel et al. 2019).

2.2.5 Composite Biomaterials

The most efficient composite NBMs used in dentistry are dental cements and restoration materials. Carbon-strengthened polymers, and various carbon-carbon composites are widely preferred for joint implantation and bone reparation due to their low elastic modulus. In addition, composite biomaterials are widely used for prostheses limbs. Their low density/weight and high strength properties made nanocomposites the superior scaffolding for such implementations (Ebara et al. 2014).

2.2.6 Combined Biomaterials

In recent years, research has focused on improved structure and dimensionally stable biomaterials. Col/functionalized multiwalled carbon nanotube/chitosan/HAp composite scaffolds have been extensively studied as an example of a natural/synthetic biomaterial combination (Türk et al. 2018). Aliphatic polyesters such as polylactic acid, polyglycolic acid, and their copolymers are widely utilized in surgery stitches, drug-delivery systems, and TE. Furthermore, various copolymers are utilized as biodegradable matrices for cell microencapsulation and drug delivery systems (Ali et al. 2013).

Properties of fabricated biomaterials can be varied via blending, chemical modification, and copolymerization. Natural/natural combinations of biomaterials consisting of wood, bone, cartilage, dentin, collagen, and skin are used as absorbable biomaterials such as spongy wound dressings, drug delivery microspheres, and polyamino acids (Lakes 2000).

A smart drug delivery system consisting of NCQDs-based Dox and HA can be given as another combined biomaterial (Fig. 2.1). In this study (Türk et al. 2021), the synthesized combined biomaterial is an injectable hydrogel formed by in situ self-crosslinking, and it was observed that it is pH sensitive and the combined

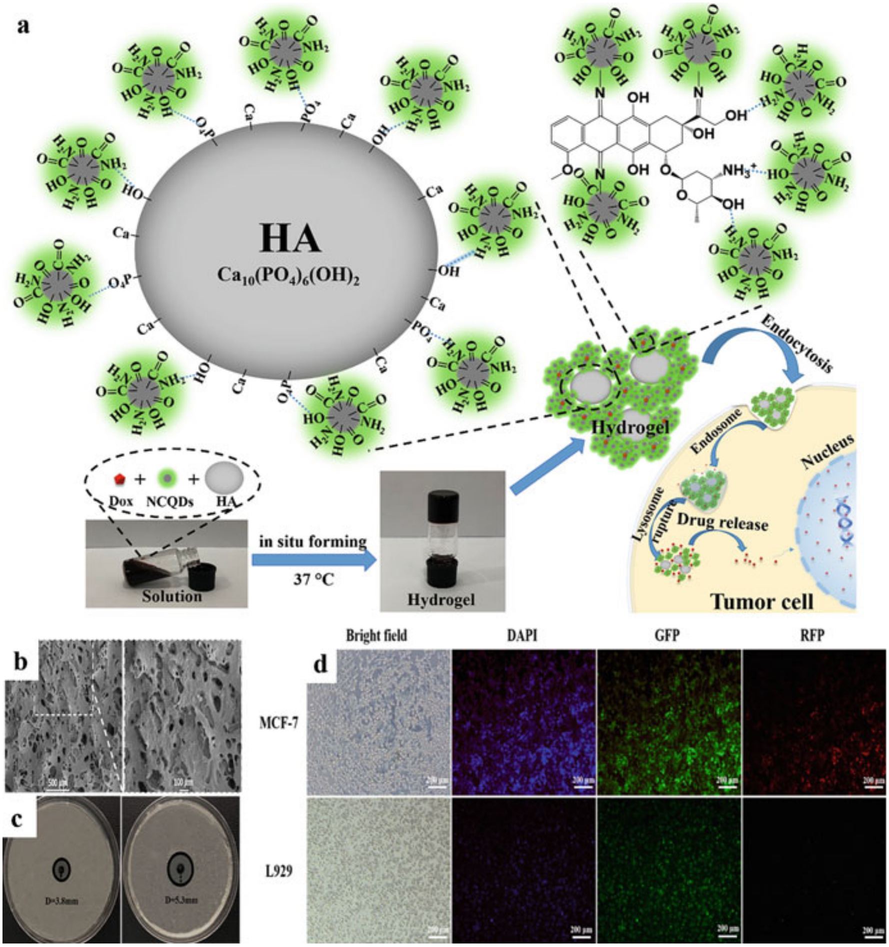
a
HA
$Ca_{10}(PO_4)_6(OH)_2$
Hydrogel
Endocytosis
Endosome
Nucleus
Lysosome rupture
Drug release
Tumor cell
Dox NCQDs HA
Solution
in situ forming
37 °C
Hydrogel
b
c
D=3.8mm
D=5.3mm
d
Bright field
DAPI
GFP
RFP
MCF-7
L929

Fig. 2.1 (**a**) Schematic illustration of tumor cell-triggered release mechanism of NCQDs-essenced injectable self-cross-linking and in situ producing hydrogel as a combined biomaterial; (**b**) morphology of NCQDs/HA/Dox (0.6/0.2/0.2 wt/vol) combined hydrogel; (**c**) antibacterial activity of NCQDs/Dox (left, 0.6/0.2 wt.) and NCQDs/HA/Dox (right, 0.6/0.2/0.2 wt) versus *S. aureus* bacteria on agar medium; and (**d**) the multicolor bioimaging potency of NCQDs (1 μg/mL) cultured in MCF-7 and L929 cell lines shows DAPI (Blue), GFP (Green), and RFP (Red). (From Türk et al. (2021), with permission) biomaterial. It has increased antibacterial properties and also can be used in the field of multicolor bioimagination.

3 Properties of Nanobiomaterials

For the selection of NBMs to be used in any biomedical application, it is essential to know their properties such as toxicity, mechanical, electrical, magnetic, thermal, optical, and smartness.

3.1 Toxicity Properties

Nanomaterials (NMs) are regarded destructive as they can pass through the cell dermis. NMs can have considerable toxicity values because of their large surface areas and superior reactivities. While NMs cause irritation and carcinogenic effects when in contact, if inhaled, they are entrapped in the lungs because of their extremely low mass and cannot be excreted. The toxicity of NMs depends on several factors such as duration of exposure and dose, aggregation and concentration, particle size and shape, surface area, crystal structure, surface functionality, and pre-exposure effect (Jeevanandam et al. 2018). Figure 2.2 shows the nanoparticles (NPs) species, experimental models, and toxic properties of NPs.

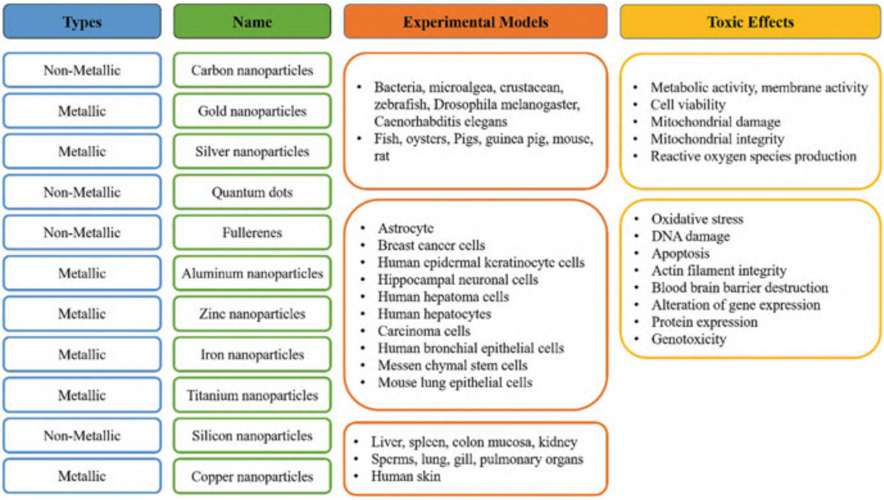

Types	Name
Non-Metallic	Carbon nanoparticles
Metallic	Gold nanoparticles
Metallic	Silver nanoparticles
Non-Metallic	Quantum dots
Non-Metallic	Fullerenes
Metallic	Aluminum nanoparticles
Metallic	Zinc nanoparticles
Metallic	Iron nanoparticles
Metallic	Titanium nanoparticles
Non-Metallic	Silicon nanoparticles
Metallic	Copper nanoparticles

Experimental Models

- Bacteria, microalgea, crustacean, zebrafish, Drosophila melanogaster, Caenorhabditis elegans
- Fish, oysters, Pigs, guinea pig, mouse, rat

- Astrocyte
- Breast cancer cells
- Human epidermal keratinocyte cells
- Hippocampal neuronal cells
- Human hepatoma cells
- Human hepatocytes
- Carcinoma cells
- Human bronchial epithelial cells
- Messen chymal stem cells
- Mouse lung epithelial cells

- Liver, spleen, colon mucosa, kidney
- Sperms, lung, gill, pulmonary organs
- Human skin

Toxic Effects

- Metabolic activity, membrane activity
- Cell viability
- Mitochondrial damage
- Mitochondrial integrity
- Reactive oxygen species production

- Oxidative stress
- DNA damage
- Apoptosis
- Actin filament integrity
- Blood brain barrier destruction
- Alteration of gene expression
- Protein expression
- Genotoxicity

Fig. 2.2 Kinds of NPs, experimental models, and toxic properties of NPs. (The figure was adopted and reproduced with permission from Kumar et al. (2017); Tynga and Abrahamse (2018))

3.2 Mechanical Properties

The mechanical properties of a material are defined by its reaction to physical forces it is exposed to. The mechanical properties of biomaterials are examined in two parts: elastic and viscoelastic properties and final properties such as plasticity, fatigue damage, fracture, and so on (Capurro and Barberis 2014). It is vital to know the biomaterials' mechanical features to be used in different biomedical applications. For example, by adjusting the elastic modulus of the biomaterial used as an implant between 4 and 30 GPa, the bone can be protected from stress. Furthermore, the biomaterial should be of high strength and low modulus in order to extend the life of the implant and avert loosening and not require revision (Hussein et al. 2015). Because NMs have higher surface tension values due to their higher tensile strength than bulk materials, they allow more robust connections between different clusters of particles. Thus, NMs can tolerate higher tensile or stretching forces without deterioration (Hakkani 2020).

3.3 Electrical Properties

Electroactive biomaterials are new posterity smart materials that enabled electrical signals' direct transmission through controlling electrical potential. Electroactive biomaterials can adapt their physical, chemical, and electrical features to the requirements of the implementation area. Conductive polymers, photovoltaic and piezoelectric materials, and electrets are biomaterials with electroactive properties (Tandon et al. 2018).

Electrical stimulation and controlled drug delivery are candidates for promising treatment methods for enhanced wound healing in damaged tissues with electroactive biomaterials. Conductive polymers and piezoelectrics as electroactive biomaterials have shown encouraging results in treating injuries to tissues such as skin, nerves, and bones. Electroactive matrices, especially piezoelectric ones that exhibit electrical and electromechanical properties, have a strong potential to build active or smart scaffolds that properly regenerate certain tissues, and especially increase the functionality of tissues in such as muscle and bone tissues (Ribeiro et al. 2015; Tandon et al. 2018).

3.4 Magnetic Properties

Among various functional NMs, magnetic nanoparticles (MNPs) have been expansively studied for different biomedical implementations, including medical imaging, therapy, drug delivery, magnetic separation, and biosensors. In particular, biocoherent iron oxide-essenced MNPs have been used as cancer imaging and therapy, magnetic resonance contrast agents, and iron supplementations and are ratified by the FDA for clinical implementations. The dimension, shape, and size distribution of MNPs greatly affect their magnetic properties (Kang et al. 2017).

Instead of choosing between natural or synthetic materials, it is often an excellent alternative to use them together. Combinations of MNPs with natural polymers are widely used to prepare advanced magnetic scaffolds in TE applications (Li et al. 2012). These magnetic scaffolds provide some extra advantages other than their using purpose: (i) Due to the ferromagnetic properties of magnetic scaffolds, the regions where they are located can be followed in vivo via magnetic resonance imaging; (ii) cell adhesion, proliferation, and differentiation to MNPs in scaffolds can easily occur during in vitro studies; and (iii) one of the most important features of this type of magnetic scaffold is that they gain magnetic momentum with an exterior magnetic field and act like magnets. Thus, they attract functionalized MNPs that are injected imminent to their implanted area. This situation allows MNPs loaded with drugs, cells, and growth factors to be directed and accumulated into the area to be treated after being injected (Li et al. 2012; Ziv-Polat et al. 2012).

3.5 Thermal Properties

Polymeric, metallic, ceramic, and composite NBMs, separately or together, are widely used in the biomedical field. These NBMs have different thermal properties such as expansion and contraction with temperature change, for example, polymeric materials expand more than metallic and ceramic materials. Due to the lowest thermal expansion coefficient, ceramic NBMs used in biomedical applications may hardly expand at all. The matrix that makes up the composite NBMs and the expansion of other materials that act as reinforcements must be compatible with each other. The possible cracking problem in interfaces of the composites could be solved by using the coating materials having the properties in between matrix and reinforcement.

It is vital to know the thermal features of biomaterials to solve many critical medical problems. Temperature changes occurring in organs are a native result of any heat exchange process. Hence, it is necessary to use ceramic, polymeric materials, or their composites with low-heat conduction coefficients to provide cryopreservation of the organs. Safe, simple, hemostatic, fast, and at the same time limiting cryosurgery has been used successfully in extreme cold surgeries for almost 100 years to prevent or destroy tissues. Another advantage of cryosurgery is that relatively difficult accessible parts of the organs can be approached without much interruption in the upper structures. Stainless steel, titanium alloys, and ceramic biomaterials are widely used in cryosurgery.

Thermal stress exhibits detrimental effects causing numerous physiological deviations of medical importance. Notable examples are heat stroke, burn injury, heat fatigue, dip injury, frostbite, and accidental hypothermia. Irreversible tissue damage caused by thermal injuries are challenging problems to solve.

Surgical hypothermia has regained attention in the last 10 years, as many studies to repair complex cardiac lesions have been conducted under conditions of hypothermic cardiac arrest. When working under hypothermia conditions, stainless steel and titanium alloys resistant to these conditions are used (Frederick Bowman et al. 1975).

3.6 Optical Properties

The optical features of NMs are one of their most charming and valuable properties enabling them to find many application areas. Optical detectors, sensors, laser, imaging, screen, phosphorescence, photoelectrochemistry, photocatalysis, solar cell, and biomedicine are implementations based on the optical features of NMs. The optical features of NMs are particularly dependent upon variables like shape, size, and surface properties, as well as further parameters such as doping material, quantity, and nearby microenvironment or interaction with other nanostructures. Similarly, their shape can have an important effect on the optical features of metal nanostructures. While the optical features of metal NPs alter very little as the nanoparticle grows, when anisotropy is adjoined to the nanoparticle, for example, the growth of nanorods, their optical properties vary meaningfully. Quantum dots (QDs) are colloidal luminescent NMs with advanced optical features such as wide excitation and narrow emission spectra, and high photoluminescence. Because of these properties, QDs are widely used in light-emitting diodes, sensors, solar cells, and biomedical diagnostics. The most critical parameters for using QDs in biological implementations are luminescence intensity, water solubility, and toxicity time against cells. As shown in Fig. 2.3, fluorescent carbon QDs attract attention as easy-to-synthesis NBMs used in bioimagining, optoelectronic, biomedicine, and biosensing applications due to their multicolor emission properties (Mazrad et al. 2018).

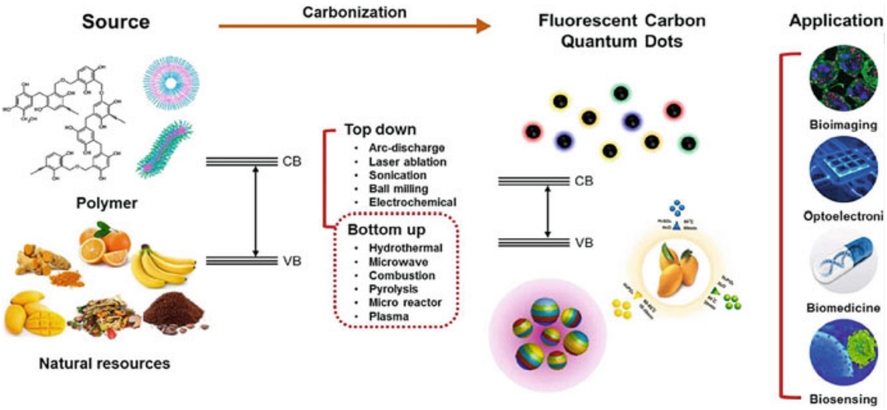
Source
Carbonization
Fluorescent Carbon Quantum Dots
Application
Polymer
Natural resources
CB
VB
Top down
Arc-discharge
Laser ablation
Sonication
Ball milling
Electrochemical
Bottom up
Hydrothermal
Microwave
Combustion
Pyrolysis
Micro reactor
Plasma
CB
VB
Bioimaging
Optoelectroni
Biomedicine
Biosensing

Fig. 2.3 Survey of the resources, fabrication methods, and implementations of fluorescent carbon QDs. (Reproduced from Mazrad et al. (2018) with permission from The Royal Society of Chemistry)

3.7 Smart Biomaterial Properties

Smart drug transport systems (Fig. 2.4) utilizing liposomes as nanocarriers contain (i) smart nanocarriers carrying anticancer drugs to the cancer area, (ii) targeting structures to find the cancered area, and (iii) stimulating methods to release pre-accommodated loads in the cancer cell area (Hossen et al. 2019).

Particles with sizes of 1–100 nm are commonly recognized as NPs. Presently, NPs are described as volume-specific surface areas. Naturally, particles with a volume-specific surface area identical to or more than 60 m^2/cm^3 are described as NPs. NPs are named nanocarriers when they function as transport for further substances. Traditional nanocarriers do not have the capability to transport and release drugs at the correct dose in the specified area under internal or external excitations. Thus, archetypal nanocarriers are not smart drug transport systems, but they can be made smart by modification or functionalization. Smart nanocarriers should have the following features. First, smart nanocarriers must evade the purging process of the immune system of the body. Second, they must only be amassed at the targeted area. Third, the smart nanocarrier should deliver the drug at the targeted area to correct concentrations under internal or external excitations (Peer et al. 2007).

In the last decade, as well as nano-/micro-sized fibrous structures, more importance has been given to mono fibers structures due to the features of nanoscale structures such as more porosity, a large number of pores, and high specific surface area. Fibrous structures are widely utilized in cell culture scaffolds for wound dressing and TE applications, especially due to the similarity of nanofibers to the extracellular matrix, which is a biomimetic possession. The use of smart fibers as biomaterials is fairly new; though, they have been utilized in this manner for less

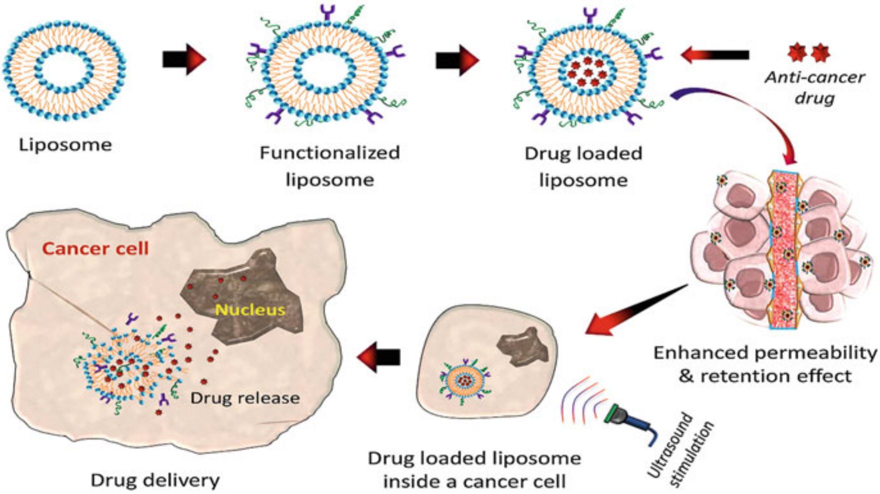

Fig. 2.4 Anticancer drug loading and releasing mechanisms of liposome-essenced smart drug transport systems used in cancer therapies. (From Hossen et al. (2019), with permission)

than a decade due to the instability of fibrous structures in aqueous solutions both above and below the lower critical solution temperature. Smart fibers, which are generally produced from heat-sensitive polymers, dissolve rapidly, and their structure is degraded during biomedical implementations as they have high water solubility; therefore, they must be bonded with strong cross-links in order to maintain their structure (Kim and Matsunaga 2017).

4 Applications of Nanobiomaterials

Applications of NBMs are constantly increasing. The most critical applications of NBMs can be summarized as topics such as TE, drug delivery, antibacterial applications, bioimaging, and infection field.

4.1 Drug Delivery

Developments in biomaterials used in drug delivery systems provide considerable advances in pharmacy, medicine, and biology. Multidisciplinary partnerships betwixt biologists, physicists, chemists, clinicians, and engineers fabricate innovatory materials and strategies to treat various diseases. Incredibly, last progress contains significant advancements in materials using for autoimmune diseases, cancer immunotherapy, and genome editing (Fenton et al. 2018).

Traditional drug delivery systems used for chemotherapeutic agents encompass numerous critical topics correlated with poor specificity, sensitive toxicity, and induction of drug resistance, which cause the therapeutical efficacy of most drug systems to diminish delicately. Nano-carrier-essenced systems are specialized platforms for the delivery of chemotherapeutically effective drugs, usually constituted of colloidal NPs of nano-sizes (generally <100 nm) characterized via greater surface/volume ratios. These prototypical nanosized systems have made possible active (inclusion of anticancer) drugs to be effectively delivered to diseased tissues. The general purpose of nanocarrier employment in drug transport implementations is to effectively cure a disease by minimal side influence, thus benefiting from the (patho-) physiology of the diseased tissue micromedium to improve therapeutic outcomes sensitively.

Novel smart nanostructured drug delivery systems can be separated into inorganic and organic nanocarriers by nature, while their physiochemical features can be adjusted by changing their compositions (inorganic, organic, hybrid, or composite), shapes (hyperbranched, rod, cube, sphere, and multilayered or multilamellar structures), sizes (great or small sizes), and surface features (surface charge, surface modification by functional groups, various coating processes, PEGylation, or bonding of targeting components). Although some nanocarrier-essenced systems have been ratified for the therapy of different diseases (inclusive of tumors), other studies are ongoing at various stages of clinical trials (Ventola 2017).

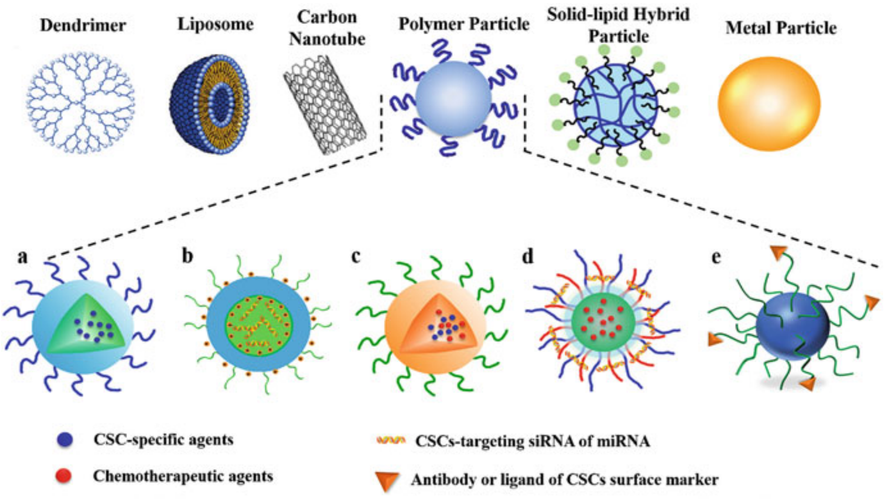
Dendrimer
Liposome
Carbon Nanotube
Polymer Particle
Solid-lipid Hybrid Particle
Metal Particle
a
b
c
d
e
● CSC-specific agents
● Chemotherapeutic agents
CSCs-targeting siRNA of miRNA
▼ Antibody or ligand of CSCs surface marker

Fig. 2.5 Various approaches to target cancer stem cells using different anticancer therapeutics, whose efficacy has increased with the advancement of drug delivery systems. Four groups of NPs delivery systems are used for cancer stem cells-essenced therapy; (**a**) Transport of chemical agents specific to cancer stem cells; (**b**) transport of nucleic acid drugs specific to cancer stem cells; (**c**) combination application of customary anticancer drugs and chemical agents specific to cancer stem cells; (**d**) combination application of customary anticancer drugs and nucleic acid drugs specific to cancer stem cells; and (**e**) use of some NPs modified with ligands or antibodies for specific targeting to cancer stem cells. (From Shen et al. (2016), with permission)

With growing awareness of cancer stem (like) cell biology and the advent of nanotechnology, the past decade has seen a large array of engineered systems forming to reach the goal of cancer stem (like) cell-targeting. Recorded nano-types introduced and tested to degrade cancer stem (like) cells by alteration of transported cargo and nanocarriers are summarized in Fig. 2.5 (Shen et al. 2016).

4.2 Antibacterial Applications

Antimicrobial NMs have attracted great attention in both academic research and daily practice. Instead of using active antimicrobial polymers that kill microbes directly, it would be a better choice to use nonactive antimicrobial polymers that prevent bacterial attachment and growth. The biocide release system of three bonded or leach polymers among the biocide releasing polymers, biocidal polymers, and polymeric biocides shows the most potential due to their controlled release properties. In spite of the significant advances in the developments of antimicrobial polymers, further studies are needed to elucidate the mechanisms that precisely explain antimicrobial interactions with microbes. Especially, elucidating the mechanisms associated with biofilm requires an intense effort to develop promising antimicrobial materials. A polymer that combines various antimicrobial mechanisms in its structure can contribute to the emergence of a more effective antimicrobial material (Huang et al. 2016).

Hydrogels can be used as alternative and suitable antibacterial biomaterials instead of conventional antibiotic treatments. Local application, enhanced biocompatibility, controlled and longtime release, stimulated on-off release, and increased mechanical toughness are prominent features that a spacious variety of hydrogels can ensure, and this is accurately what antibacterial biomaterials need. Hydrogels with antibacterial properties can be broadly used in urinary tract coatings, gastrointestinal infections, catheter-related infections, osteomyelitis, wound dressings, and contact lenses. Considering the current investigations on the enhancement and implementation of antibacterial hydrogels, many researchers are investigating combinations of hydrogels made of PEG, polysaccharides, or other hydrophilic polymers with various bactericidal agents. Biodegradability and biocompatibility are extremely significant necessities for the therapeutic use of hydrogels. Also, hydrogels used as a drug carrier should have high drug loading efficiency. As for the side effects, once hydrogels are biodegraded, they should not cause inflammation at the adjacent connective tissues. Given the aforementioned factors, smart hydrogel systems should be benefited to overwhelm the difficulties caused by local antibacterial drugs (Lin et al. 2019).

4.3 Bioimaging

The advantages of MNPs offer the potential to be used in many medical implementations like diagnosis, bioimaging, drug delivery systems, and therapy. MNPs, particularly superparamagnetic iron oxide NPs, developed with various formulations for use in medical and clinical applications such as imaging and therapeutics, have been extensively researched in the last decade. The biocompatibility and targeting-ability of MNPs can be evolved via the surface coating, which allows modification of surface properties, inclusive of chemical functionalities and physical features. But the covering material should be selected extremely carefully to provide the expected surface properties for a particular biomedical implementation. Usage of biocompatible polymers as coating material possesses unique advantages, such as boosting colloidal stability, hindering aggregation, avoiding the uptake of NPs by the reticuloendothelial system, and supplying a large surface for ligands conjugation like biomolecules and peptides with great affinity to targeted cells. More investigation is required to better figure out the physicochemical features of MNPs and how they act in vivo in order to gain broader acceptance of their potential in clinical implementations. Due to the difficulties encountered in using MNPs in vivo, their optimal safety and efficiency have not been wholly reached. But these shortcomings can be eliminated by improving magnetic targeted carriers through preclinical experiments and ongoing studies (Mohammed et al. 2017).

Graphene-essenced NMs have been widely used as imaging contrast components in various bioimaging implementations. Dyes, photosensitizers, QDs, gold nanoclusters, or up-conversion NPs, functionalized graphene oxide (GO)/reduced GO (rGO), are commonly utilized for fluorescence imaging. GQDs and their derivatives have also been used in fluorescence imaging and two-photon fluorescence imaging applications due to inherently photoluminescence. GOs were utilized for Raman imaging, which can be more improved by participating Ag, Au, or Pt NPs due to the inherent potent Raman signals of the D and G bands. Radionuclide-labeled GOs were investigated for single-photon emission-/positron emission-computed tomography imaging. For magnetic resonance imaging, paramagnetic metal ions or GO/rGO modified with iron oxide NPs have been developed. rGOs or photosensitizers-/dyes-modified GOs with potent optical absorption in the near-infrared region are appropriate for photoacoustic imaging. Multiple imaging can be performed with a combination of other materials with certain features on GOs. Graphene-essenced NMs will continue to play important roles in various bioimaging applications (Lin et al. 2018).

4.4 Tissue Engineering

Regenerative medicine and TE are increasingly developing fields because of numerous new tissue replacement and application approaches. Extension of information, including manufacturing biomaterials with developed biological and physicochemical properties, the prosperous extraction and preparation of stem cells, proliferation and division parameters, and biomimetic mediums, offer us matchless occasions to enhance diverse scaffold forms for TE. Advances in soft tissue regeneration or reconstruction show that new regenerative treatments are crucial in situations of serious soft tissue forfeit, trauma, diseases, congenital defects, and aging. Among the diverse scaffolds and biomaterials verified for soft tissue regeneration or reconstruction, artificial material sorts have attracted countless interest because of their adjustability, high versatility, and easy functional ability properties to provide better biocompatibility (Janoušková 2018).

On the other hand, treating critical-sized bone defects using biomaterials is a very important alternative to conventional treatments, including metal implants, allografts, and surgical reconstructions. Chitosan, a natural biopolymer with adjustable biological and chemical features, has been widely investigated for its use in bone regeneration implementations. But, the properties of chitosan, such as water-insolubility, hemo-incompatibility, faster in vivo depolymerization, and poor antimicrobial, significantly limit its potential for repair bone defects. Modifying the chitosan structure with different chemically functional groups offers solutions to such limitations (Logithkumar et al. 2016). Some examples of biomaterials used in the TE discipline are given in Table 2.1.

4.5 Infection

The body is protected from many exterior factors such as chemicals, pathogens, irritants, and harmful substances through the skin. When the skin is damaged or

Table 2.1 Some biomaterials instances utilized in TE discipline

Biomaterials	Biomedical applications				References
	Orthopedic devices	Drug delivery	Dental devices	Others	
Hydrogels		√		Ophthalmological	Banigo et al. (2019)
Silk fibroin	√	√			Sitarski et al. (2018)
Hyaluronic acid	√	√			Sitarski et al. (2018)
Polyethylene glycol	√	√			Sitarski et al. (2018)
Poly ε-caprolactone	√	√			Sitarski et al. (2018); Kress et al. (2012)
Polylactic acid	√	√			Kress et al. (2012)
Gelatine	√	√			Kress et al. (2012)
Hydroxyapatite	√	√	√		Banigo et al. (2019); Kress et al. (2012)
β-tricalcium phosphate	√		√		Kress et al. (2012)
Glass ceramic	√		√		Kress et al. (2012)
Alumina	√		√		Banigo et al. (2019)
Magnesium alloys	√		√		Kress et al. (2012)
Titanium	√		√		Banigo et al. (2019)
Stainless steel	√			Stents	Banigo et al. (2019)
Dacron				Vascular grafts	Banigo et al. (2019)
Silicone rubber				Catheters, tubing	Banigo et al. (2019)
Poly(methyl methacrylate)				Intraocular lenses, bone cement	Banigo et al. (2019)
Cellulose				Dialysis membranes	Banigo et al. (2019)
Polyurethanes				Catheters, pacemaker leads	Banigo et al. (2019); Kress et al. (2012)
Collagen				Ophthalmologic, wound dressings	Banigo et al. (2019); Sitarski et al. (2018); Kress et al. (2012)
Poly(lactic-co-glycolic acid)				Liver and ligament tissue	Sitarski et al. (2018); Kress et al. (2012)

worn, due to the fact that the body becomes sensitive to wound infection and microbial invasion, the formed wound healing is delayed and in some cases, life can be endangered. It is necessary to cover the wound with a suitable material to ensure effective healing of wounds and prevent infections. In the past, animal fats, honey pastes, plant fibers, and various biopolymers have been widely used as wound dressings. No wound dressing is perfect but should meet the minimum necessities such as esthetics, cost-effectiveness, quickly healing, and infection prevention, during treating wounds. Natural polymers have long been used as wound dressing and skin replacement materials because of their biodegradability, excellent biocompatibility, good mechanical strength, and other physical features. Moreover, biological dressings have better air and water permeabilities, as well as the ability to resist bacterial invasion and prevent infection. Bioactive compounds such as antibacterial agents, vitamins, growth factors, and the like can be added to biological dressings, and then through the leisurely and controlled release of bioactive components in the dressing, both infection formation is prevented, and tissue regeneration and wound healing accelerate. Considering that the expectations for skin regeneration and the care of various wounds are increasing day by day, biological dressings with very superior properties to conventional natural wound dressings can be developed using NMs (Wang et al. 2020).

Wounds types vary widely depending on the reasons they occur, and they have their own discriminating healing times and needs. Due to this awareness, many wound dressings with various properties have been developed. While developing different wound dressings, different NMs such as hydrogels, hydrocolloids, silk, and collagen-based dressings, foam dressings, alginate dressings, and synthetic polymer films were used, considering the wound healing properties and mechanisms of each. Recently, research on the development of wound dressings with superior properties by coating natural and synthetic polymers to ultrathin films and nanofibers using the electrospinning method has intensified (Mir et al. 2018; Wang et al. 2020).

5 Functionalization of Nanobiomaterials

Biocompatibility and surface features of biomaterials are extremely important in their applications in biological systems. Hence, there is serious requirement to change the surface of the biomaterial to improve their performances in such systems. The surface possessions of the biomaterial can be changed by modifying its surface without altering itself. To change the surface properties of NBMs, various physical or chemical processes are generally applied to atoms, molecules, or functional compounds on their surfaces, or their surfaces are coated by a thin film of diverse materials. Surface modification processes applied to NBMs can develop their biocompatibility, adhesion, corrosion resistance, energy, deterioration, and tribological features (Uwais et al. 2017).

The physicochemical properties of biomaterial surfaces, such as functional groups, hardness, topographic properties, and interfacial free energy, can significantly affect the biochemical reaction mechanisms in the biological environments in which these materials are used (Fig. 2.6). Also, widely used chemical processes and physical techniques for the modification of surface features can affect the interactions between biomaterials and cells (Rahmati and Silva 2020).

When the literature on coatings utilized to alter the surface properties of biomaterials is examined, in studies using carbon nanotube/HAp biocomposite coatings prepared by growing HAp on carbon nanotubes, improved fracture toughness and strength with osteoblast cell proliferation features were observed (Devgan and Sidhu 2019).

Biomaterials with superior properties can be obtained by combining the advantages of carbon nanotubes and different proteins to treat many diseases. Proteins can make carbon nanotubes soluble, arrange them concerning their size and steric properties, coat their surfaces, and make them biocompatible. In contrast, carbon

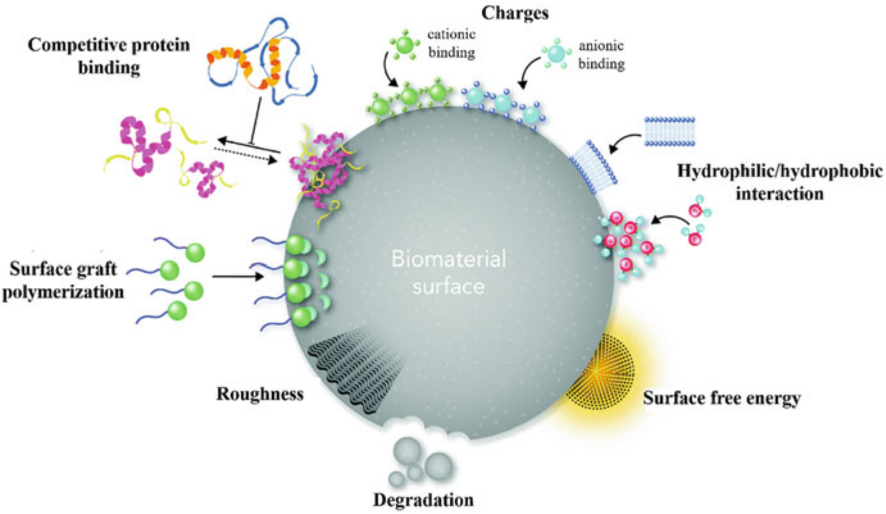

Fig. 2.6 Explanation of the role of physicochemical features of the surface in guiding the responses of biological systems against biomaterials. Physicochemical characteristics resulting from various functional groups on the surface of biomaterials can direct signal ways between cells and molecules. (Published by The Royal Society of Chemistry (Rahmati and Silva 2020))

nanotubes can immobilize enzymes, forming functional biomaterials used in a variety of implementations (Nagaraju et al. 2015).

The formation of surfaces to which cells can adhere by coating biomaterials can form advantages or disadvantages in accordance with conditions. In some applications, the adhesion, spread, and division of cells to the surface of the biomaterials used will be extremely important. In contrast, in other cases, such biological activities on the biomaterial will cause the failure of the biomaterial and consequently the need for replacement or removal. The adhesion of bacteria to the surface of biomaterials is an example of undesired cell adhesion and causes the biomaterials used to fail (Ferreira et al. 2015). Appropriate biocompatible materials for surface modification of metallic biomaterials are comparatively given in Table 2.2.

6 Conclusion and Future Perspectives

Although we consider biomaterials a relatively young field, their origins date back thousands of years. However, the development of the field of biomaterials took place after the Second World War. Also, in the first few decades after World War II, many national and international standards have been developed that require rigorous testing prior to implantation. Biomaterials constitute an important part of the materials consumed in the health sector today, and their market share in the world is increasing day by day. Some of the most common medical devices with a significant biomaterial component include replacement heart valves, synthetic vascular grafts,

Table 2.2 Some biocompatible materials for surface coating of metallic biomaterials

Coating biomaterials	Advantages	Disadvantages	References
Hydroxyapatite	High bioactivity High biocompatibility	Low strength Very brittle Low load-bearing capacity	Chocholata et al. (2019); Uwais et al. (2017); Tarun et al. (2011)
Tricalcium phosphate	Supports in vivo osteogenic differentiation	Incompressible nature Slow degradation	Chocholata et al. (2019); Tarun et al. (2011)
Bioactive glasses	Improve osteogenesis and differentiation	Low brittleness and strength	Chocholata et al. (2019); Uwais et al. (2017)
Tantalum	High bioactivity High corrosion resistance	Low elasticity modulus High affinity to oxygen	Uwais et al. (2017)
Agarose	No need cross-linking agents Little inflammatory response in vivo Wide range of gelling and melting temperatures	Poor cell attachment	Chocholata et al. (2019)
Collagen	Enzymatically biodegradable	Complex structure	Chocholata et al. (2019); Tarun et al. (2011)
Gelatin	Enzymatically biodegradable	Poor mechanical properties	Chocholata et al. (2019); Tarun et al. (2011)
Fibrin	Induce improved cellular interaction High biocompatibility	Rapid degradation in vivo Difficult to maintain structural integrity	Tarun et al. (2011)
Poly(ethylene glycol)	Biocompatible Hydrophilic	Poor cell adhesion	Sitarski et al. (2018)
Polyurethanes	High biocompatibility Excellent mechanical properties	Toxicity of degradation products (from aromatic diisocyanate component)	Chocholata et al. (2019); Uwais et al. (2017);
Poly(α-hydroxy acids)	Degradation products can be excluded from the body	Degradation by bulk erosion Hydrophobicity of the polymer surface Relatively poor mechanical properties	Chocholata et al. (2019)
Poly(ε-caprolactone)	A low melting point Nontoxic Biodegradable	Hydrophobicity Slow degradation	Chocholata et al. (2019)
UHMWPE	High abrasive resistance High-impact strength Low coefficient of friction	Low load-bearing capacity Thermal instability	Uwais et al. (2017)

hip and knee prostheses, heart-lung machines, and kidney dialysis equipment. When materials decrease to nanoscale sizes, their biological, physical, and chemical features and functionalities change significantly, and they show improvements in the desired direction for many applications. NMs possess a long history; however, major advances in nanoscience and nanotechnology have only been in the last two decades. The application of nanotechnology to biomaterials has become widespread after these advances.

Biomaterials have helped millions of people in almost every corner of the world achieve a better quality of life. Although the use of biomaterials has been widespread for thousands of years, developments in this area are still ongoing. Nanomaterial manufacturing methods can be used to produce biomaterials that will interact with biological systems in the body from natural biocompatible materials.

NBMs are used in many fields, and their most critical applications can be summarized as drug delivery, antibacterial applications, bioimaging, TE, and infection fields. NMs have significant toxicity values due to their high surface areas and activities. NMs can cause irritation, and show carcinogenic effects. If inhaled, they are trapped in the lungs due to their low mass and cannot be expelled. The toxicity of NMs depends upon numerous influences like concentration, exposure time and dose, particle size, surface area, crystal structure, and surface functionality. The biocompatibility and surface features play an important role in the responses of the biomaterials. Therefore, there are serious requirements to adapt the surface of the biomaterials to improve their performances in biological systems. Devoid of altering the bulk materials, their surface features can be changed by surface modifications. Why and how the toxic effects of NBMs on the body of human occur have been known, but more research is needed on their influences on health before they can be applied to human subjects.

The design and fabrication of new generation personalized NBMs will be carried out using advanced methods such as nanotechnological processes, computational and mathematical models, and 3D printers. Thus, the use of computer-aided design and manufacturing techniques in developing and producing novel NBMs will lead to promising advances.

References

Ali SHR, Almaatoq MMA, Mohamed ASA (2013) Classifications, surface characterization and standardization of nanobiomaterials. Int J Eng Technol 2:187–199

Azmana M, Mahmood S, Hilles AR, Rahman A, Arifin MAB, Ahmed S (2021) A review on chitosan and chitosan-based bionanocomposites: promising material for combatting global issues and its applications. Int JBiol Macromol 185:832–848

Banigo AT, Iwuji SC, Iheaturu NC (2019) Application of biomaterials in tissue engineering: a review. J Chem Pharm Res 11(4):1–16

Barua E, Deoghare AB, Deb P, Das LS (2018) Naturally derived biomaterials for development of composite bone scaffold: a review. IOP Conf Ser Mater Sci Eng 377:1–8

Capurro M, Barberis F (2014) Evaluating the mechanical properties of biomaterials. In: biomaterials for bone regeneration: novel techniques and applications. Woodhead Publishing Limited, Cambridge, UK pp 270–323

Chocholata P, Kulda V, Babuska V (2019) Fabrication of scaffolds for bone-tissue regeneration. Materials (Basel) 12:1–25

Devgan S, Sidhu SS (2019) Evolution of surface modification trends in bone related biomaterials: a review. Mater Chem Phys 233:68–78

Dovedytis M, Liu JL, Bartlett S (2020) Hyaluronic acid and its biomedical applications: a review. Engineered Regeneration 1:102–113

Ebara M, Kotsuchibashi Y, Narain R, et al (2014) Smart biomaterials. Springer, Tokyo. https://doi.org/10.1007/978-4-431-54400-5

Fenton OS, Olafson KN, Pillai PS et al (2018) Advances in biomaterials for drug delivery. Adv Mater 30:1–29

Ferreira P, Alves P, Coimbra P, Gil MH (2015) Improving polymeric surfaces for biomedical applications: a review. J Coatings Technol Res 12:463–475

Frederick Bowman H, Cravalho EG, Woods M (1975) Theory, measurement, and application of thermal properties of biomaterials. Annu Rev Biophys Bioeng 1975:43–80

Hakkani MFA (2020) Biogenic copper nanoparticles and their applications: a review. SN Appl Sci 2:1–20

Hossen S, Hossain MK, Basher MK et al (2019) Smart nanocarrier-based drug delivery systems for cancer therapy and toxicity studies: a review. J Adv Res 15:1–18

Huang KS, Yang CH, Huang SL et al (2016) Recent advances in antimicrobial polymers: a mini-review. Int J Mol Sci 17:1–14

Hussein MA, Mohammed AS, Al-Aqeeli N (2015) Wear characteristics of metallic biomaterials: a review. Materials (Basel) 8:2749–2768

Janoušková O (2018) Synthetic polymer scaffolds for soft tissue engineering. Physiol Res 67: 335–348

Jeevanandam J, Barhoum A, Chan YS et al (2018) Review on nanoparticles and nanostructured materials: history, sources, toxicity and regulations. Beilstein J Nanotechnol 9:1050–1074

Kang T, Li F, Baik S et al (2017) Surface design of magnetic nanoparticles for stimuliresponsive cancer imaging and therapy. Biomaterials 136:98–114

Kim YJ, Matsunaga YT (2017) Thermo-responsive polymers and their application as smart biomaterials. J Mater Chem B 5:4307–4321

Kress S, Neumann A, Weyand B, Kasper C (2012) Stem cell differentiation depending on different surfaces. Adv Biochem Engin/Biotechnol 126:263–283

Kumar V, Sharma N, Maitra SS (2017) In vitro and in vivo toxicity assessment of nanoparticles. Int Nano Lett 7:243–256

Lakes R (2000) Composite biomaterials. In: The biomedical engineering handbook. CRC Press, Boca Raton, pp 688–716

Li Y, Huang G, Zhang X et al (2012) Magnetic hydrogels and their potential biomedical applications. Adv Funct Mater 23:1–13

Lin J, Huang Y, Huang P (2018) Graphene-based nanomaterials in bioimaging. In: Micro and nano technologies, biomedical applications of functionalized nanomaterials. Elsevier, pp 247–287. https://doi.org/10.1016/B978-0-323-50878-0.00009-4

Lin K, Zhang D, Macedo MH et al (2019) Advanced collagen-based biomaterials for regenerative biomedicine. Adv Funct Mater 29:1–16

Logithkumar R, Keshavnarayan A, Dhivya S et al (2016) A review of chitosan and its derivatives in bone tissue engineering. Carbohydr Polym 151:172–188

Long Q, Zhou DL, Zhang X, Zhou JB (2014) Surface modification of apatite-wollastonite glass ceramic by synthetic coupling agent. Front Mater Sci 8:157–164

Mazrad ZAI, Lee K, Chae A et al (2018) Progress in internal/external stimuli responsive fluorescent carbon nanoparticles for theranostic and sensing applications. J Mater Chem B 6:1149–1178

Mir M, Ali MN, Barakullah A et al (2018) Synthetic polymeric biomaterials for wound healing: a review. Prog Biomater 7:1–21

Mohammed L, Gomaa HG, Ragab D, Zhu J (2017) Magnetic nanoparticles for environmental and biomedical applications: a review. Particuology 30:1–14

Nagaraju K, Reddy R, Reddy N (2015) A review on protein functionalized carbon nanotubes. J Appl Biomater Funct Mater 13:301–312

Patel KD, Singh RK, Kim HW (2019) Carbon-based nanomaterials as an emerging platform for theranostics. Mater Horizons 6:434–469

Peer D, Karp JM, Hong S et al (2007) Nanocarriers as an emerging platform for cancer therapy. Nat Nanotechnol 2:751–760

Pina S, Oliveira JM, Reis RL (2015) Natural-based nanocomposites for bone tissue engineering and regenerative medicine: a review. Adv Mater 27:1143–1169

Ping D (2014) Review on w phase in body-centered cubic metals and alloys. Acta Met Sin (Engl Lett) 27:1–11

Rahmati M, Silva EA (2020) Biological responses to physicochemical properties of biomaterial surface. Chem Soc Rev 49:5178–5224

Ribeiro C, Sencadas V, Correia DM, Lanceros-méndez S (2015) Piezoelectric polymers as biomaterials for tissue engineering applications. Colloids Surfaces B Biointerfaces 136:46–55

Seifalian A (2019) Market analysis on biomaterials and biomedical engineering. Insights Biomed 4:1–4

Shen S, Xia J, Wang J (2016) Biomaterials nanomedicine-mediated cancer stem cell therapy. Biomaterials 74:1–18

Sitarski AM, Fairfield H, Falank C, Reagan MR (2018) 3D tissue engineered in vitro models of cancer in bone. ACS Biomater Sci Eng 4:324–336

Tandon B, Magaz A, Balint R et al (2018) Electroactive biomaterials: vehicles for controlled delivery of therapeutic agents for drug delivery and tissue regeneration. Adv Drug Deliv Rev 129:148–168

Tarun G, Ajay B, Bhawna K et al (2011) Scaffold: tissue engineering and regenerative medicine. Int Res J Pharm 2:37–42

Teo A, Mishra A, Park I et al (2016) Polymeric biomaterials for medical implants and devices. ACS Biomater Sci Eng 2:454–472

Thomas S, Balakrishnan P, MSS (2018) Fundamental biomaterials: polymers. Woodhead Publishing, Oxford, UK

Türk S, Altınsoy I, Çelebi Efe G et al (2018) 3D porous collagen/functionalized multiwalled carbon nanotube/chitosan/hydroxyapatite composite scaffolds for bone tissue engineering. Mater Sci Eng C 92:757–768

Türk S, Altınsoy I, Çelebi Efe G et al (2021) A novel multifunctional NCQDs-based injectable self-crosslinking and in situ forming hydrogel as an innovative stimuli responsive smart drug delivery system for cancer therapy. Mater Sci Eng C 121:111829

Tynga IM, Abrahamse H (2018) Nano-mediated photodynamic therapy for cancer: enhancement of cancer specificity and therapeutic effects. Nano 8:1–14

Uwais ZA, Hussein MA, Samad MA, Al-Aqeeli N (2017) Surface modification of metallic biomaterials for better tribological properties: a review. Arab J Sci Eng 42:4493–4512

Ventola CL (2017) Progress in nanomedicine: approved and investigational Nanodrugs. Pharm Ther 42:742–755

Wang F, Hu S, Jia Q, Zhang L (2020) Advances in electrospinning of natural biomaterials for wound dressing. J Nanomater 2020:8719859

Wang M, Chen L, Zhang Z (2021) Potential applications of alginate oligosaccharides for biomedicine – a mini review. Carbohydr Polym 271:118408

Yang K, Zhou C, Fan H, Fan Y, Jiang Q, Song P, Fan H, Chen Y, Zhang X (2017) Bio-functional design, application and trends in metallic biomaterials. Int J Mol Sci 19(1):24. https://doi.org/10.3390/ijms19010024. PMID: 29271916; PMCID: PMC5795975.

Zarrintaj P, Manouchehri S, Ahmadi Z, Saeb MR, Urbanska AM, Kaplan DL, Mozafari M (2018) Agarose-based biomaterials for tissue engineering. Carbohydr Polym 187:66–84

Ziv-Polat O, Skaat H, Shahar A, Margel S (2012) Novel magnetic fibrin hydrogel scaffolds containing thrombin and growth factors conjugated iron oxide nanoparticles for tissue engineering. Int J Nanomedicine 7:1259–1274

Nanobiomaterials for Point-of-Care Diagnostics

3

Hoda Ezoji and Mostafa Rahimnejad

Contents

1 Introduction 44
2 Nanobiotechnology 45
3 Nanobiotechnology Applications 46
  3.1 Diagnosis 46
  3.2 Drug Delivery 46
  3.3 Agriculture 47
  3.4 Food 47
  3.5 Tissue Engineering 47
4 Nanobiomaterials 48
  4.1 Nanobiomaterials Classification 49
5 Nanobiomaterials Applications 54
  5.1 Tissue Engineering 55
  5.2 Drug Delivery 55
  5.3 Biomimetics 56
  5.4 Bioimaging 56
  5.5 Biofunctionalized Nanoelectromechanical Systems (BioNEMs) 56
  5.6 Point-of-Care (POC) Diagnostics 57
  5.7 Strip-Based Tests: Capillary Flow Assays 58
6 POC Assay Based on Printed Electrodes 61
7 POC Assays Based on Nanomaterials 62
  7.1 Nanoparticles 63
8 Conclusions 64
References 65

Abstract

Today, health care is recognized as a combination of prevention, diagnosis, and treatment of any human diseases that is persistently evolving with efficacious, rapid, and useful technologies. High standard systems of health care management

---

H. Ezoji · M. Rahimnejad (✉)
Biofuel and Renewable Energy Research Center, Department of Chemical Engineering, Babol Noshirvani University of Technology, Babol, Iran
e-mail: Rahimnejad@nit.ac.ir

© Springer Nature Singapore Pte Ltd. 2023

U. P. Azad, P. Chandra (eds.), *Handbook of Nanobioelectrochemistry*,
https://doi.org/10.1007/978-981-19-9437-1_3

that are gained by making decisions at the right time and on the basis of fast diagnostics, informatics analyses, and smart data analyses are of great significance to provide health care with better quality. In this regard, point-of-care (POC) technologies ensure rapid detection of various analytes next to the patients and simplify better diagnosis, monitoring, and management of diseases. In this way, rapid development of nanobiotechnology that is known as the unique integration of nanotechnology and biotechnology offers considerable improvements in POC evaluations. Although nanobiotechnology is still in its initial stages, this multidisciplinary field is leading the science of POC devices more and more closer to a wider range of applications. Nowadays, nanomaterials are important components in this field since they clearly increase the efficiency of POC devices. It seems that in the near future, these developments will affect almost all fields of medicine, so that POC devices based on nanomaterials will be available in such a perfect format that presents trustworthy clinical analyses everywhere.

Keywords

POC · Nanobiomaterials · Diagnosis · Biosensors · Drug delivery

1 Introduction

In 1959, the modern nanotechnology father, Richard Feyman, explained a process that permits manipulation and control of molecules and atoms via extremely accurate apparatus. The procedure can be used to design and fabricate systems atom by atom, at the nanoscale level. Several years later, in 1974, Norio Taniguchi defined and introduced the term "Nanotechnology" in a scientific conference (Wu and Yang 2001; Wu et al. 2002). Nanotechnology, the basic technology of the twenty-first century industrial revolution, refers to a leading multidisciplinary field of knowledge which combines various sciences, namely, engineering, biology, chemistry, physics, informatics, and medicine. It is a promising technological area of knowledge with excellent potential to conduct significant advancements in real life. Today, new nanomaterials, nanodevices, and biomaterials are produced and monitored using nanotechnology methods to study and adjust the responses, operations, and features of different living and nonliving substances with sizes less than 100 nanometers (Fiiipponi and Sutherland 2012; Baranwal et al. 2018). Nowadays, the broad application of nanomaterials in different mechanical and electronic systems, tissue engineering, magnetic and optical elements, quantum computing, and a variety of biotechnologies with dimensions below 100 nanometers and the tiniest characteristics, from economical point of view, is the most important aspect of nanotechnology. Due to the increasing production of nanomaterials, the fabrication of nanoproducts is also enhancing rapidly. Fabrication of the aforementioned nanomaterials with significant properties will lead to considerable changes in human beings lives, environment, health, etc. Nanotechnology, the novel frontier of twenty-first century, has

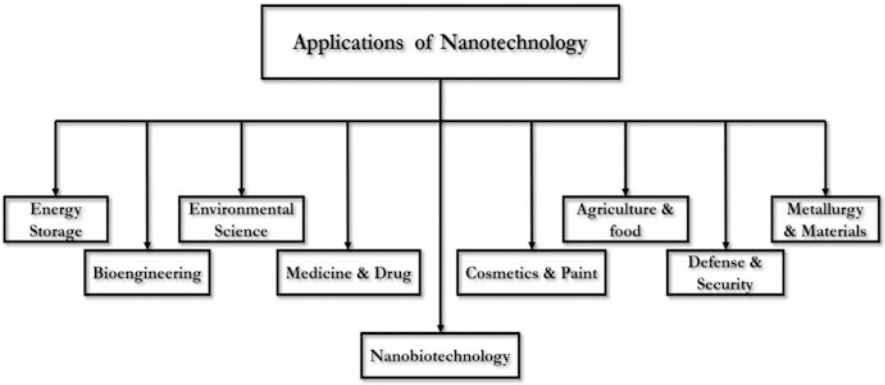

Fig. 3.1 Different applications of nanotechnology in human life

appeared as a flexible platform that could present eco-friendly, cost-effective, and efficacious answers for the sustainable problems and challenges that human beings will face. Materials, at the nanoscale, have new characteristics such as enhanced strength, electrical conductivity, and resiliency. Based on these features, nanotechnology and nanomaterials provide us the latest potential applications in various kinds of industries. They are used in the field of health and medicine for treating or diagnosing different kinds of diseases, in electronics and space exploration, protecting and monitoring the environment, energy generation and storage, improving food quality and crop production, and so on (Fakruddin et al. 2012; Nouailhat 2010). Some of the outstanding applications of nanotechnology are demonstrated in Fig. 3.1.

2 Nanobiotechnology

Biotechnology, as well as nanotechnology, is of utmost importance in the recent century. It is involved with the physiological processes such as metabolisms of microorganisms and other kinds of biological substances. Meanwhile, as mentioned before, in nanotechnology, the aim is to develop devices, materials, or other kinds of structures with at least one dimension below 100 nanometers. Therefore, by linking these technologies, nanobiotechnology, as a nanotechnology area which concentrated on the biological fields, emerged. As a matter of fact, nanobiotechnology is a unique integration of nanotechnology and biotechnology that can lead to the fusion of classical microtechnology and molecular biology in real. Using this approach and through combining or imitating biological systems or via fabrication of tiny tools to investigate or modulate various attributes of biological systems based on molecules, machines of atomic/molecular grade can be constructed. Accordingly, nanobiotechnology, by merging advanced applications of nanotechnology and information technology into current biological matters, can facilitate diverse paths of life science. Moreover, it has the potential to eliminate the apparent borders among chemistry, physics, and biology and form our opinions and knowledge. It is believed that integration of engineering and molecular biology will lead to a new group of multifunctional systems for chemical and biological analyses with much better specificity, sensitivity, and higher rates of detection versus the current devices (Maheshwari et al. 2019b; Thirumavalavan et al. 2016; Gartland and Gartland 2018).

3 Nanobiotechnology Applications

3.1 Diagnosis

Heath and medicine are two of the most promising and interesting fields of nanobiotechnology. This field of science presents potential advancements in cancer treatment, medical diagnosis and treatments, pharmaceuticals, tissue regeneration, implantable materials, and multifunctional devices, which combine multiple of the abovementioned operations. Such developed applications will surely convert the basis of prevention, diagnosis, and treatment of diseases in the near future. Today, for most diseases, the diagnostic methods depend on the appearance of visible symptoms. On the other hand, over time, the chances of treatments being effective may be reduced. Thus, early detection of diseases increases the likelihood of cure. As a consequence, it is better to diagnose and treat diseases before the onset of symptoms. One of the most essential aims of nanobiotechnology is the development of novel approaches to diagnose diseases with cheaper materials at the early stage (Suh et al. 2009).

3.2 Drug Delivery

Monitored drug delivery systems are applied to better the therapeutic effectiveness and drugs safety. In this respect, nanobiotechnology products can make drug delivery better via the targeted method by accumulating the nanoproducts on the site of diseased tissue at a rate determined on the basis of the environment's distinct pathophysiology. To this end, as the therapeutics, nanoparticles can be transferred to the targeted sites where are not easily reachable for standard drugs. For example, if a drug can be chemically bound to nanoparticles, then it can be led to the infection or disease site through magnetic or radio signals. Also, they can be designed in such a way to release at certain times when external stimulants are provided or particular molecules are available. Meanwhile, adverse effects of potent therapeutics can be prevented via decreasing the effective dosage for treatment (Patra et al. 2018). Drugs encapsulation in nanoscale materials (like nanoshells, organic dendrimers, and hollow capsules based on polymers) lead to their controlled release much more accurately than before. They are designed with the aim of carrying a therapeutic payload (gene therapy or chemotherapy and radiation) and for imaging usages. In this way, several agents that cannot be taken orally by cause of their insignificant bioavailability can now be applied in therapy using nanotechnology. Nanosized drug formulations extend drugs' half-lives by increasing their formulation retention via bioadhesion. Also, for agents which are prone to denaturation or degradation when exposed to excessive pH, they propose protection. Delivery of antigens in vaccination is another example of broad nanobiotechnology applications. Moreover, current developments in encapsulation and advancement of appropriate animal models displayed that nanoparticles and microparticles have the capability of increasing immunization (Amna et al. 2020; Shi et al. 2010).

3.3 Agriculture

Nanobiotechnology is a new field of science in agriculture that offers modern facilities to attain high levels of productivity at a controllable cost in the course of production and marketing of crops. Moreover, it has the capability to making fundamental changes to agriculture through the replacement of traditional farming; zerovalent nanoparticles can remediate soils that are contaminated with pesticides and heavy metals. Furthermore, delivery systems for pesticides using bioactive nanoencapsulation are being processed. Also, using nanofabricated materials that are designed based on plant nutrients, more nutrients can be transmitted to the soil. Moreover, more productive products are produced through genetic manipulation, decreasing the need for irrigation, fertilizers, and pesticides, and increasing resistance against various diseases (Jampílek and Kráľová 2015; Sekhon 2014).

3.4 Food

Nanobiotechnology research in food results in stopping food spoilage and poisoning. They contain changes in the composition of foods, organic combinations, and other food chemicals; detection and measuring pathogens using biosensors; and preservation of fruits using edible films. In recent years, nanobiotechnology has received a lot of attention in the food packaging sector. This research mainly involves the addition of biosensors, antimicrobial agents, antioxidants, and other nanomaterials to this section. Also, the potential capabilities of bio-nanocomposites and bio-based materials for food packaging are under consideration. Additionally, with the aim of improving the product's properties, food-based nanoparticles have been used in the pharmaceutical, medical, and cosmetic industries (Duncan 2011; Purohit et al. 2020; Bajpai et al. 2018). Numerous types of biosensors used in food quality assessment have been shown in Fig. 3.2.

3.5 Tissue Engineering

In recent years, tissue engineering is of great importance due to in vitro creation of new tissues using cells or their combinations. After that, the as-prepared tissue can

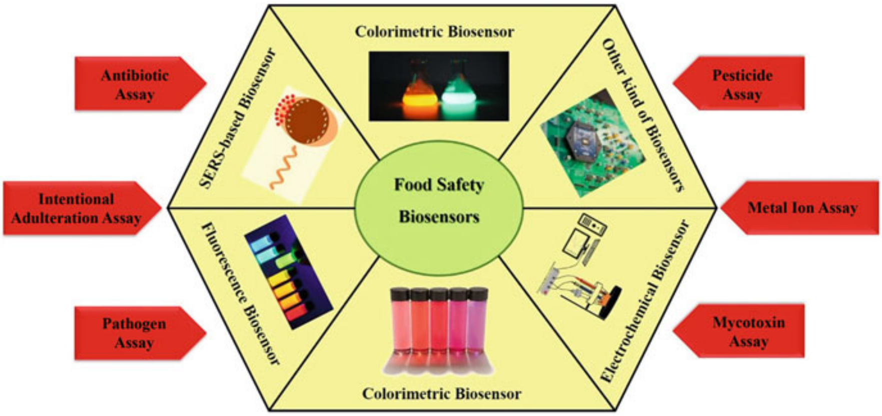
Colorimetric Biosensor
Antibiotic Assay
SERS-based Biosensor
Other kind of Biosensors
Pesticide Assay
Food Safety Biosensors
Intentional Adulteration Assay
Metal Ion Assay
Fluorescence Biosensor
Electrochemical Biosensor
Pathogen Assay
Mycotoxin Assay
Colorimetric Biosensor

Fig. 3.2 Various kinds of biosensors for food safety assessments

be replaced in the body via surgery. Also, tissue engineering stimulates regeneration through the insertion of implants, bionanoconstructs, and bio-mimicked scaffolds next to the damaged tissues (Maheshwari et al. 2019a). It is principally interested in materials that mimic the native issues in the body or are similar to them, either from patients or other persons or from the sources of other mammals. Nanobiotechnology in the field of tissue engineering results in the creation of biosynthetic tissues, nanoscale bio-mimicked scaffolds, and prosthetic implantable devices that provide a more viable and biocompatible microenvironment for cell growth in an end-stage diseased organ such as an ear, eye, joint, or heart, or for growing artificial organs. Moreover, nanoscale biomaterials have the ability to bio-mimic the native tissues like bone marrow, cardiac tissues, extracellular fluids, etc. Additionally, nanobiotechnology has transformed tissue engineering in the case of skin regeneration via applying biomaterials, cell therapy, injectable biopolymers, and growth factors, especially in chronic wounds, bruises, and severe burns, in which the current treatments cannot prevent scars. Figure 3.3 demonstrated some of the biomedical applications of nanobiotechnology (Atala 2005; Wheeldon et al. 2011).

4 Nanobiomaterials

The term “biomaterials” mainly refers to the group of materials that are utilized for biomedical usages and can be applied for treatment, strengthening, or replacement of any organ, tissue, or function in the body. In fact, the purpose of the development of these nonviable materials is to interact with the body’s biological system. Over the recent decade, the entry of biomaterials development into the era of nanotechnology has been obvious. One of the most interesting developments in biomaterials science and engineering is the possibility of designing novel materials for different biological applications at the level of nanoscale. These nanoscale materials are of the most importance among the nanotechnology products. They can present specific

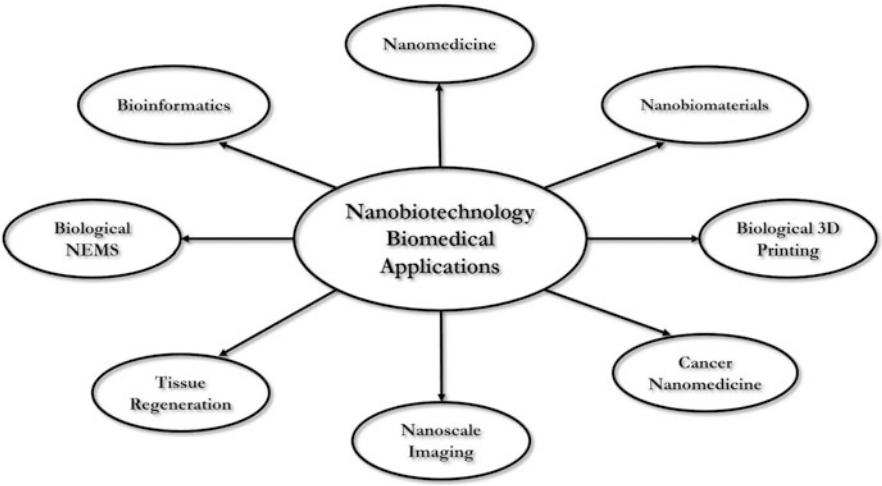

Fig. 3.3 Biomedical applications of nanobiotechnology

electrical, mechanical, and optical characteristics versus the other macroscopic or microscopic structures. Nanotechnology-derived biomaterials, which are commonly known as nanobiomaterials, specifically are materials in nanometer size with structures and components that exhibit new and remarkably changed characteristics. More importantly, they have important effects on medical science and the treatment of diseases. They are broadly employed in a wide spectrum of biomedical and biological applications, such as drug delivery, artificial implants, and medical imaging. Modern self-assembled materials, such as hydrogels, ceramics, polymers, and metals, are examples of nanobiomaterials. Undoubtedly, rapid advancements in nanotechnology and considerable developments in nanobiomaterials not only resulted in the creation of novel materials and instrumentation for biomedical usage but also changed the way of applying them in science and technology. Actually, it created a novel multidisciplinary area including nanotechnology, materials science, and biology (Singh et al. 2016).

4.1 Nanobiomaterials Classification

The engineering of nanobiomaterials for diverse biological uses is an emerging area in nanotechnology. It provides phenomenal materials with unique properties and structures to solve conventional biomedical puzzles. Aiming to avoid the negative effects of nanobiomaterials on the body, it is necessary to check their categories before applying them in medical applications. Nanobiomaterials include a broad range of biomaterials, comprising natural and artificial ones, employed for different applications. Accordingly, they can be categorized into three major classes: the first class is based on natural biomaterials; the second class is based on artificially

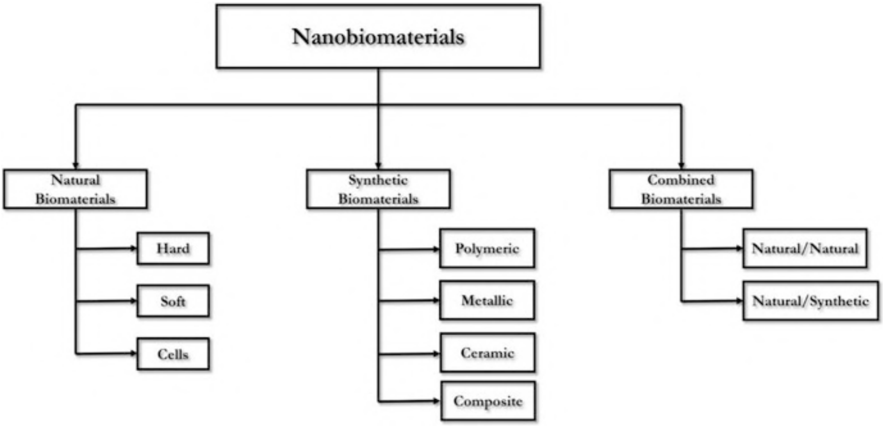

Fig. 3.4 Nanobiomaterials classification

engineered biomaterials; and the third class is created as a result of advanced biomaterials engineering technology. This category, which plays between the first two ones, is named combined biomaterials. Based on the foregoing, Fig. 3.4 exhibits the nanobiomaterials classification block diagram.

4.1.1 Natural Biomaterials

This group is made up of materials that have similar structures to the native ones and are used with the intention of substituting, repairing, or augmenting body organs or tissues. In the human body, natural biomaterials can be classified into hard, soft, and cell types. By virtue of their advantages, especially shape and mechanical compatibility, natural biomaterials find extensive applications versus synthetic ones (Ige et al. 2012).

4.1.2 Synthetic Biomaterials

Synthetic biomaterials are man-made materials employed to substitute organs or restore body function. They are used continuously in direct or indirect connection with body fluids. These artificial materials can be categorized into four major groups: metallic, ceramic, polymeric, and composite biomaterials. Nowadays, some of them are commercialized and used in clinical applications, namely, intraocular lenses, Dacron, and metal hips. Nevertheless, they suffer from a number of disadvantages, including their composition and structure, which are not the same as the native ones. Also, their ability to remodel and their biocompatibility are poor. Thus, in order to overcome these disadvantages, other kinds of biomaterials were developed. In this context, naturally derived types have attracted the wide attention of scientists all over the world (Wieling 2008).

4.1.3 Combined Biomaterials

Over the past decades, scientists, using natural/natural or natural/synthetic combinations of biomaterials, have developed the advanced forms of them, which are stable in terms of dimensions. A number of advantages and disadvantages of this type of biomaterials are listed in Table 3.1.

As mentioned before, nanobiomaterials consist of a broad spectrum of nanoscale devices and particles that are produced with the aim of biomedical and biological applications such as nanopharmaceutics, drug delivery, and multiple therapeutic applications. In fact, they have very broad and diverse potential applications. Generally, they are eminently employed in bioimaging and biosensors, as biomarkers for diagnosis, as nanocarriers, nanobots, and biocatalysts, in drug and gene delivery, preclinical diagnosis, molecular imaging for CT scanning and MRI, in cancer therapy, and so on. Accordingly, another way to classify nanobiomaterials is on the basis of their nature and potential applications. Figure 3.5 displays the major categories of nanobiomaterials based on their applications (Park and Bronzino 2002).

Some kinds of nanobiomaterials are described below.

4.1.4 Metallic Nanobiomaterials

Metallic nanobiomaterials are a group of nanobiomaterials that have attracted the attention of a great number of researchers to develop methods for their synthesis,

Table 3.1 Combined biomaterial characterizations

Advantages	Disadvantages
Outstanding biocompatibility	Having xenografts and allografts associated inflammation and infection and perceived ethical
Easy degradation and resorption	Morbidity and inadequate supply

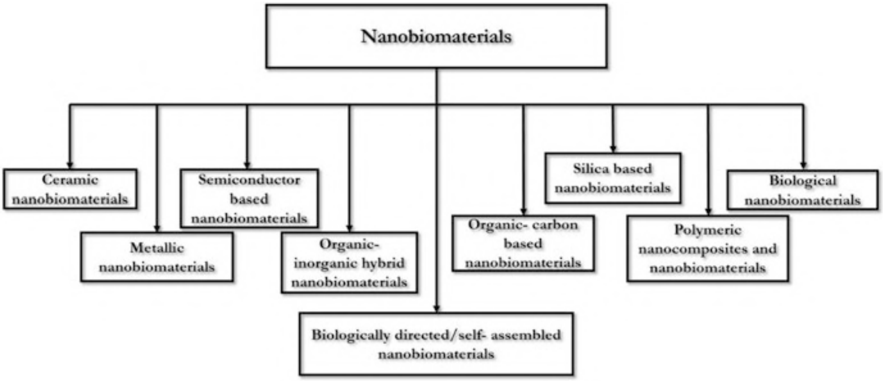
Nanobiomaterials
Ceramic nanobiomaterials
Semiconductor based nanobiomaterials
Silica based nanobiomaterials
Biological nanobiomaterials
Metallic nanobiomaterials
Organic-inorganic hybrid nanobiomaterials
Organic- carbon based nanobiomaterials
Polymeric nanocomposites and nanobiomaterials
Biologically directed/self- assembled nanobiomaterials

Fig. 3.5 Main classifications of nanobiomaterials

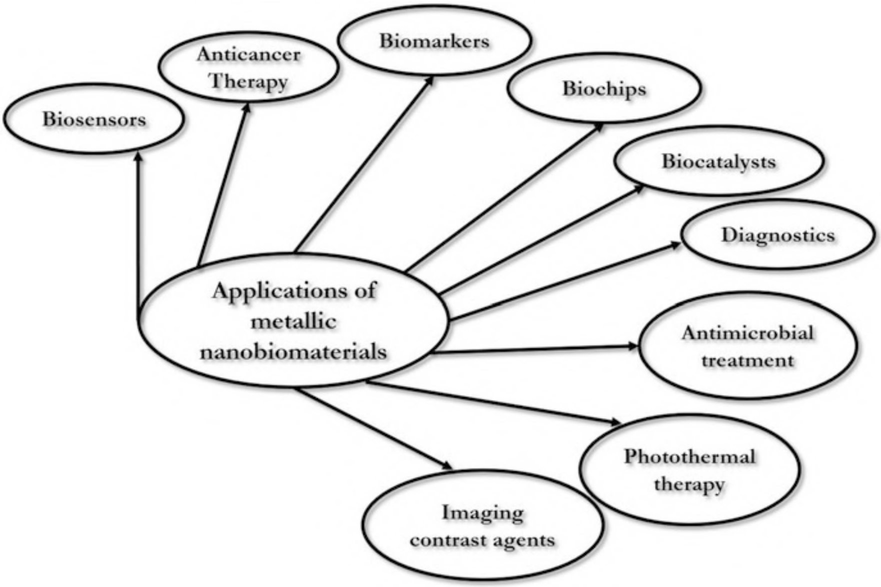
Biosensors
Anticancer Therapy
Biomarkers
Biochips
Biocatalysts
Diagnostics
Applications of metallic nanobiomaterials
Antimicrobial treatment
Photothermal therapy
Imaging contrast agents

Fig. 3.6 Main application areas of metallic nanobiomaterials

characterization, and application. They are metals in nanosize that have at least one dimension less than 100 nanometers. These kinds of nanomaterials are widely categorized into four main classes: nanoparticles (0D); nanorods, nanowires, and nanotubes (1D); nanoplatelets, sheets, and layers (2D); and nanoshells and other kinds of nanostructures (3D). The initial usage of these nanomaterials was their application in the medieval period in the production of stained glasses that were applied to decorate porcelain ware and cathedral windows. However, the earliest report of the scientific discovery of metallic nanomaterials was in 1857, by Michael Faraday. Up until now, scientists have paid lots of attention to these materials thanks to their desirable attributes for essential needs and commercial productions. At the moment, among the industrial sections, biomedical engineering is strongly focused on the use of different nanomaterials. Gold (Au), copper (Cu), silver (Ag), zinc oxide (ZnO), iron oxide (Fe_2O_3), titanium dioxide (TiO_2), selenium (Se), platinum (Pt), palladium (Pd), and gadolinium (Gd) are the most widely applied metallic nanomaterials in biomedical and biological applications. Among them, Cu, Fe, Ag, and Au are the most broadly explored ones. Research in synthetic biology and metallic nanomaterials is linked to each other. More importantly, metallic nanomaterials, as well as the others, can be synthesized and even modified with suitable functional agents which let them bind to ligands, drugs, and antibodies, which are of high interest and importance in biomedical science. Figure 3.6 shows the main application areas of metallic nanobiomaterials (Mody et al. 2010).

4.1.5 Ceramic Nanobiomaterials

Over the recent decades, remarkable advancements in the ceramics field have resulted in the improvement of nanobiomaterials for scaffolds of tissue engineering, hip replacements, and dental implants. Ceramic nanobiomaterials, such as hydroxyapatite-tricalcium phosphate (HA/TCP), silicon nitride, alumina, and zirconia, have a lot of desirable properties, namely, biocompatibility, chemical stability, low density, and good wear resistance (Chen et al. 2009).

4.1.6 Organic Carbon-Based Nanobiomaterials

They are nanoscale structures that are created by organic materials and have attracted significant attention in life and materials science. Fullerenes and carbon nanotubes (CNTs) are two of the prominent carbon-based nanomaterials that are extensively employed in biomedical applications. CNTs are graphene-based cylindrical structures with exceptional chemical and physical characteristics such as excellent electrical and thermal conductivity and supreme mechanical strength, while fullerene, also known as buckyball, is a hollow geodesic structure made completely up of carbon. It is reported to exhibit antiviral and antioxidant activity. These carbon-based nanomaterials are hydrophobic; therefore, diverse surface modification techniques have been applied to make these nanostructures water soluble for biomedical purposes. Hence, by virtue of their unique photochemical and photophysical characteristics, they have been employed in different biomedical applications, including cell tracking, pressure sensors, tissue engineering, protein and gene microarrays, photoacoustic, microwave, etc. (Sinha and Yeow 2005).

4.1.7 Polymeric Nanocomposites and Nanobiomaterials

In the production of polymeric nanobiomaterials, both synthetic and biological polymers can be used. Biological polymers comprise proteins (silk, fibrin gel, and collagen) and polysaccharides (alginate, derivatives of hyaluronic acid, chitin/chitosan, and starch). The synthetic ones contain polylactic acid (PLA), polyhydroxybutyrate (PHB), poly-Ɛ-caprolactone (PCL), and polyglycolic acid (PGA). Biocompatibility that facilitates tissue regeneration and cell adhesion is the major advantage of applying biological polymers in developing nanobiomaterials. Nevertheless, the disadvantage of these polymers is their poor mechanical features. In fact, in terms of mechanical strength, synthetic polymers are better than biological types. In addition, they can be manipulated synthetically to let biological degradation. However, they display lower biocompatibility versus biological polymers. Polymeric nanocomposites are composites in which nanomaterials are utilized as fillers to improve their surface or bulk characteristics. By virtue of their role in improving the polymer matrix's physicochemical attributes, these nanomaterials have received a lot of attention. Carbon-based nanoparticles, metal nanoparticles, and hydroxyapatite (HA) are the common nanomaterials applied as fillers in the matrix polymer (Sitharaman et al. 2008).

4.1.8 Organic-Inorganic Hybrid Nanobiomaterials

The most important improvement in this field was accelerated by several applications in physics, chemistry, medicine, life science, and technology. They include two or more various elements, usually inorganic elements (metal particles or clusters, oxides, salts, sulfides, metal ions, nonmetallic components and their derivatives, and so on) and organic elements (organic molecules or groups, biomolecules, ligands, polymers, pharmaceutical matters, etc.), which are connected to each other using special interactions that lead to the synergistic increase of their functional characteristics. A wide range of interactions, including the construction of molecules (π-complexation, covalent bonds, etc.), nanoscale binding, microstructuring (cooperative interactions in several modes), and self-assembly (different intermolecular interactions containing H-bonding, electrostatic interactions, dispersion interactions, and so on). The mixture of various elements and structural designs using diverse kinds of interactions leads to an almost unlimited diversity of unique materials for specific applications. These kinds of nanobiomaterials can be classified into three major groups based on the materials applied for the formation of either the hybrid core or its shell: (a) Nanoparticles with an inorganic core which is surrounded by organic layers that are linked to each other covalently and form the outer layer that is also known as the shell. This shell characterizes the hybrid's chemical features and the interaction with its surrounding environment, while the physical features of the aforementioned hybrid are based on the shape, size, and type of its organic core. (b) Hybrids of organic core/inorganic shell, in which the shells are made up of silicone, silica, or metals (gold or silver) while the organic cores are composed of polylactide, polyethylene, or polymers. These kinds of hybrids are broadly applied in joint replacements owing to their supreme strength and excellent resistance to abrasion and corrosion. (c) Organic/inorganic hybrids based on dendrimers that have a core based on either metallic (copper, silver, or gold) or semiconductor quantum dots (cadmium selenium (CdSe) or cadmium sulfur (CdS)). They let controlled surface chemistry to gain favorable nonimmunogenic characteristics and biocompatibility. They have the potential to be used as probes for MRI, X-ray computed tomography (CT), and fluorescence imaging (Lazić and Nedeljković 2019).

5 Nanobiomaterials Applications

As mentioned in previous sections, nanomaterials apply nanoscale engineering knowledge and system combinations of the available materials to create superior materials and crops. Nanomaterials' extensive applications have led to their strong presence in diverse areas such as health care, prostheses, implants, defense, surveillance, security, energy generation and its conservation using special materials and extremely efficient batteries, smart textiles, etc. Nanobiomaterials research is a novel interdisciplinary frontier in materials and life sciences fields. Significant developments in nanomotors, nano-biochips, nanosized biomimetic materials, nanoscale systems of drug delivery, nanocomposites, nanobiosensors, interface biomaterials, etc., have a great prospect in clinical medicine, defense, and industrial applications.

5.1 Tissue Engineering

It is a novel field with the intention of growing living organs and tissues using natural or synthetic scaffolds to regenerate or substitute worn-out or damaged organs and tissues. Fundamentally, scaffolds are synthetic substrates that support the differentiation and proliferation of cells as well as maintaining their stability. The perfect scaffold should have sufficiently large pore networks that are open enough for penetration of blood vessels and cells. Moreover, they should be able to attach to the bones. The appropriate scaffold for orthopedic usage should do the initial mineralization, help with the formation of new bone, and concurrently allow for the substitution of new bone. Polymers of polyglycolic acid and polylactic acid and the biodegradable elastomer of polyglycerol sebacate have been utilized for tissue engineering purposes. Additionally, artificial hydrogels are noteworthy for the improvement of scaffolds by virtue of their hydrophilicity, tissue-like structure, and excellent biocompatibility. Furthermore, in order to replace the heart valve and develop cell growth on it, hydrogels of polylactic acid-γ-polyvinyl alcohol have been created (Choudhary et al. 2007).

5.2 Drug Delivery

Nanobiomaterials are extensively used in drug delivery systems for treating different kinds of diseases. Particularly, they are employed as carriers in drug delivery systems and span a broad range of geometries, chemistries, and forms. Up until now, approximately all the materials (such as metals, polymers, semiconductors, ceramics, sol-gels, etc.) in zero to three dimensions have been employed to deliver different kinds of biomolecules and small-molecule drugs with bio-distribution and particular kinetics of release. In fact, for drug delivery systems, nanobiomaterials are reservoirs with controlled release. These systems can be constructed with controlled size, shape, morphology, and composition. Their surface characteristics can also be managed to improve immunocompatibility, cellular uptake, and solubility. The restrictions of prevalent delivery systems include possible cytotoxicity, finite targeting capabilities, and suboptimum bioavailability. Versatile and favorable nanoscale kinds of drug delivery systems comprise nanoparticles, nanotubes, nanocapsules, dendrimers, and nanogels. They can be employed to deliver diverse groups of bio-macromolecules (proteins, peptides, artificial oligodeoxynucleotides, plasmid DNA, etc.) as well as small-molecule drugs (Fattal and Barratt 2009).

5.3 Biomimetics

These kinds of materials completely include synthetic metals, ceramics, or polymers with bulk or surface modifications leading to the material's biocompatibility and their suitability for tissue engineering or tissue implants. Innumerable composites were developed, composed of nanocomposites with both organic-inorganic and biological bases. They are made to imitate the tissues and produce 3D scaffolds, which can help with special cell functions including cell growth, differentiation, adhesion, and expression of tissue-specific types of genes while preventing reactions that are toxic and immune responses. In the case of hard tissues, nanobiomaterials based on metal and ceramic have been applied for teeth and bone implants. They mimic the durability, biocompatibility, stable adhesiveness, and support of in vivo natural structures (Webster et al. 2000).

5.4 Bioimaging

This kind of imaging strongly depends on the advancement of complicated probes with the aim of detecting and studying biological procedures at the molecular and cellular levels. Nanosized probes have displayed exceptional benefits compared to the agents, which are molecule-based. The aforementioned advantages are composed of the ability to integrate several features (such as multiple kinds of contrast-creating materials), generate better contrast, and the feasibility to contain high payloads of drugs. Therefore, diverse promising agents and novel systems for imaging have been created based on nanomaterials. In this regard, the application of nanoparticles has increased the advancement of diagnostic agents in bioimaging. Recently, nanoparticles, known as multimodal agents, have attracted much attention for imaging, therapy, and diagnosis. For instance, quantum dots (QDs), by virtue of their size-tunable narrow emission spectra, long photostability, and supreme brightness, have been broadly employed as probes in systems of optical imaging. QDs targeting using different antibodies could lead to various pathology diagnoses. In addition, nanoparticles of dendritic manganese developed as contrast agents in MRI resulted in enhancements of relaxivity and hydrophobicity. Also, superparamagnetic iron oxide (SPIO) nanoparticles were explored for different applications (Sitharaman et al. 2008).

5.5 Biofunctionalized Nanoelectromechanical Systems (BioNEMs)

Nanoelectromechanical systems (NEMs), the nanoscopic apparatus with a length of less than 100 nanometers, have the capability to merge mechanical and electrical components. The NEMs made using novel nanobiomaterials are applied as BioNEMs for clinical and biological usages. They recognize variations induced by analytes, which quantifiably change the properties of the dynamical devices. Hence, they are known as intelligent nanosystems that have the ability to sense, process, and/or actuate. The variations in features of dynamical systems include variations of the properties of the nanomechanical device (particularly the force constant), alterations to the system damping, and the direct imposing of extra forces on the apparatus. The BioNEMs are applied as tweezers with the aim of handling the manipulation of single molecules (nanomolecules) like proteins and DNA to provide extremely useful and valuable data about the composition of molecules, the organization of chromatin, or the dynamics of biomolecular interactions. In general, the tweezer tips are made in such a way that they allow the detection of variations in the applied electric field in molecular solutions to realize their dynamics (Strick et al. 2000).

5.6 Point-of-Care (POC) Diagnostics

Over the past few years, the advancements in medical science have been remarkable. However, lack of on-time detection or proper monitoring of diseases is still the leading cause of death. Diabetes, respiratory infections, bacterial infections, namely, diarrheal diseases or tuberculosis, and ischemic heart disease are examples of the worldwide main causes of death. But they can be prevented by proper early detection. Today, there are potential tools and technologies to detect all kinds of diseases. In this respect, in order to provide superior health care, it is of vital importance to present health management with superior quality. Also, higher standards in the management of health care can be gained by making the best decisions on time on the basis of timely diagnostics, informatics, and smart data analyses. This needs smart diagnostic devices, therapeutics, and analytical tools to improve health. Disease progression efficacious management and monitoring that is too important to realize and manage epidemic diseases, rely on therapeutic optimizations. Therefore, developing smart diagnostic tools, namely, point-of-care systems, with the aim of personalizing health care is crucial. These kinds of devices can carry out precise diagnostics and rapid tests at or near the place where the patient first encounters the system of health care (Chandra 2016). They are also known as bedside tests. The ideal kinds of POC devices should be straightforward and simple enough to be easily used even by users who have no laboratory or medical knowledge. Additionally, cost-effectiveness is a significant and desirable property of POC devices to ensure that everyone can provide them everywhere (Syedmoradi et al. 2017). Accordingly, by virtue of its low cost, abundance, biosustainability, and recyclability, paper is one of the most favored materials which is used as a substrate in POC systems. POC devices have a fast turnaround period (almost 15 min) and provide practical data that can guide a considerable variation in disease management. Quick results decrease the necessity for several patient visits, authorize on-time treatments, and ease the control of infectious disease prevalence. Additionally, they decrease the trust in possible therapy. Fast diagnostic experiments function via the detection of analytes, which are extracted from or found in clinical samples. Moreover, the other attributes that POC devices should have are sensitivity (the ability to distinguish between the same values), selectivity (the quality to respond to a special parameter or analyte and not to be influenced by interferences), and robustness (the capacity to endure the variations of environmental conditions). There are various approaches in POC systems for signal production, and in most of them, the selected method is based on the applied transducer. In this respect, electrochemical and optical devices are likely the most desired ones. Glucometers and pregnancy tests are examples of these kinds of POC devices. POC systems can be classified into two groups: small handheld devices and larger bench-top instruments. Handheld systems are made based on microfabrication methods that automatically perform sample preparation, steps of assay, analytes, and signal detection. They propose quantitative or qualitative evaluations of a broad spectrum of analytes. The latter ones are basically miniaturized forms of laboratory instruments that have been reduced in both complexity and size. Actually, recent advancements in these devices are the consequence of continuous developments in microfluidic, lab-on-a-chip technologies, biosensors, assay formats, bioanalytical platforms, and supplementary technologies. The following are examples of POC testing systems (Vashist 2017; Noah and Ndangili 2019). Figure 3.7 shows the comparison of common testing processes and point-of-care testing.

5.7 Strip-Based Tests: Capillary Flow Assays

5.7.1 Dipsticks

Analytical devices that have emerged based on paper, appearing as dipstick tests and paper-based indicators, have been employed for rapid determination of a broad spectrum of analytes owing to their uncomplicated design, facile production, and ease of use. These paper-based dipsticks were first created in the 1950s, aiming to detect the glucose level in urine samples. Today, urine test strips are used to measure metabolic products such as glucose, salt, and protein in patients with diabetes or nephritic diseases (Liana et al. 2012).

5.7.2 Lateral Flow Assays (LFA)

The capillary flow assay platform, which is also recognized as a test strip or LFA, is a promising apparatus to detect various analytes at home and in POC applications. They offer a relatively rapid and low-cost test with the ability to be performed by untrained people in regions where no complicated laboratory instrumentations are available. In these kinds of sensing platforms, the liquid specimens move across a membrane, which is paper-based too, via capillary force. More importantly, in LFA, no pressure is applied. They need small amounts of liquid specimens and 5–15 min for the detection of analytes in samples (Yamada et al. 2015). In the presence of antibodies and their fragments as bioreceptors, the platform is known as “lateral flow immunoassay (LFIA).” Commercially, they are one of the most prosperous microfluidic POC systems. Nucleic acid lateral flow immunoassay (NALFIA) is a novel and promising use of LFA for the determination of genetic materials. This test is designed in order to study the presence of a double-stranded sequence of nucleic acid

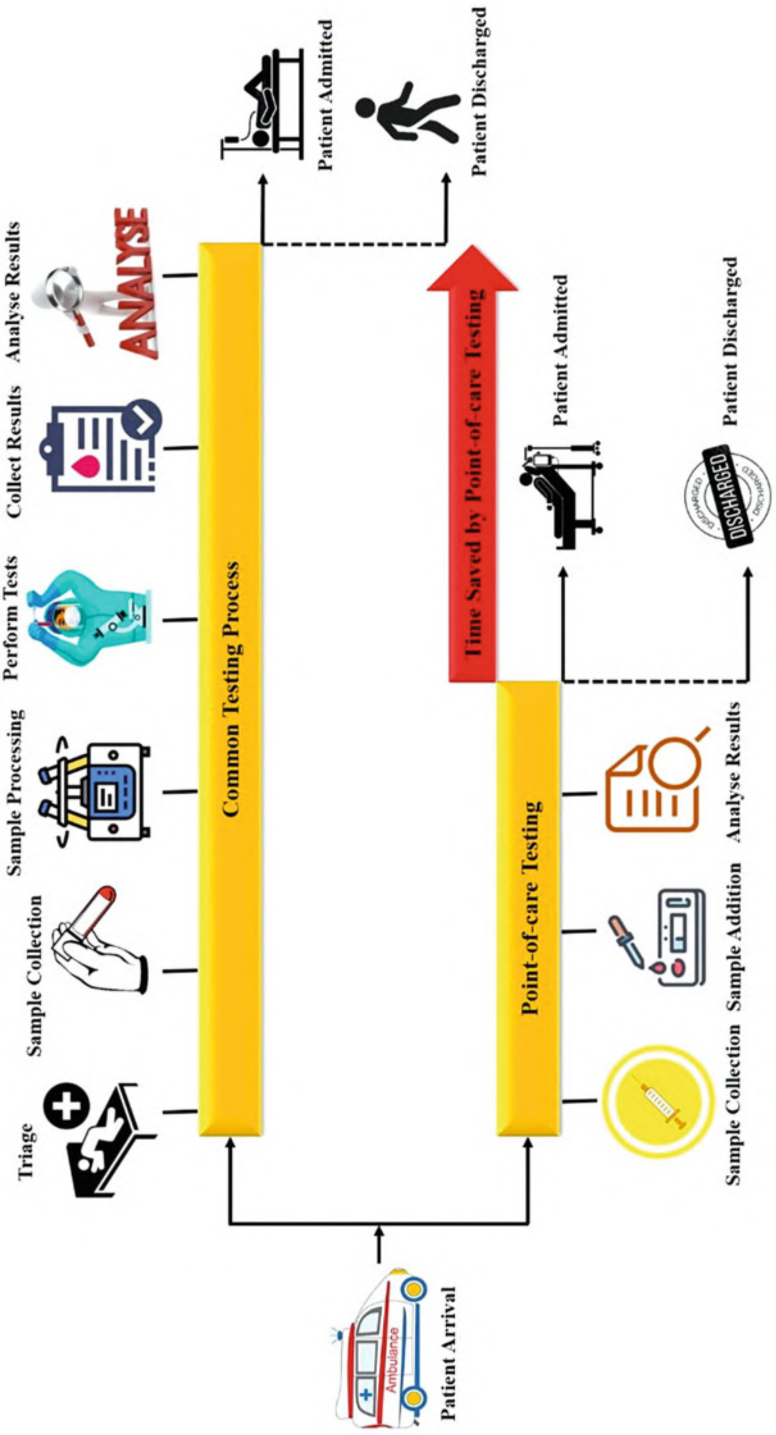
Patient Arrival
Ambulance
Triage
Sample Collection
Sample Processing
Perform Tests
Collect Results
Analyse Results
ANALYSE
Common Testing Process
Patient Admitted
Patient Discharged
Time Saved by Point-of-care Testing
Point-of-care Testing
Sample Collection
Sample Addition
Analyse Results
Patient Admitted
Patient Discharged
DISCHARGED

Fig. 3.7 Comparison of common testing processes and point-of-care testing

after amplification that is unique to the organism studied via primers with two various tags. Another kind of this test is the “nucleic acid lateral flow assay (NALF),” which is specific hybridization between amplicons and the immobilized probes (Goudarzi et al. 2015).

5.7.3 Advancements of Capillary Flow Assays

Lab-on-paper or paper-based microfluidics are a group of microfluidic approaches that present a modern platform for fluid analyses and handling for different medical utilizations such as disease screening and health care in developing countries (Gomez 2014). These devices merge the user-friendliness, disposability, portability, and cost-effectiveness of paper-based strip tests with the complications of the conventional POC systems. In essence, these analytical apparatuses demonstrate a novel category of POC tools that combine the flexibility of test strips with a number of microfluidic system capabilities. Paper is a very cheap and ubiquitous cellulosic material, so it is an attractive substrate for microfluidic systems. It is suitable for a variety of medical applications. Also, it transports liquids through capillary forces without any external force. In addition, its chemical composition and high ratio of surface area to volume allow the easy physical immobilization of chemicals onto its surface. Cellulose is a main constituent of the walls in plant cells. It has a few agents of carboxylic acid (-COOH) and many hydroxyl groups (-OH) on the surface of fibers (Alila et al. 2005). They can be employed as scaffolds for the chemical and physical immobilization of biomolecules. Usually, covalent bonds are applied for the bioactive compounds strong attachments. Molecules nonspecific adsorption at the surface is a problem in utilizing paper as the substrate. This disadvantage can result in the reduction of the number of analyte molecules that reach the test area and need to be offset via calibration. By developing microchannels that are patterned on the substrate (paper), liquid flows are restricted inside the channels. Therefore, liquid samples can be conducted in a controlled procedure. Up until now, a spectrum of two- and even three-dimensional microfluidic channels has been established in papers. They are capable of transforming liquids in predefined pathways, separately, to carry out single or even multistep assays and measure the concentrations of various analytes in our body fluid. Practically, several methods can be utilized for creating microfluidic paper-based analytical devices (μPADs), including etching, photolithography, writing, printing, dipping, spraying, and stamping (Dossi et al. 2013). The main basis of these techniques is to design hydrophobic-hydrophilic contrast on the paper in order to create capillary channels at the microscale on the fibers of the paper. Aiming to choose the appropriate technique, a wide range of parameters, including material costs, simplicity of the production process, instrument availability, and the considered applications of microfluidic paper-based devices, should be investigated. One of the most common methods with minimum hydrophobic material consumption is printing. Wax printing and inkjet printing using alkyl ketene dimer (AKD) are two promising techniques as a result of their rapid and easy fabrication procedures and patterning low-cost agents. Both of these techniques can fabricate several devices and multiple zones on a small piece of paper. Electrochemical, colorimetric, chemiluminescence, electrochemiluminescence, and fluorescence are detecting methods that have been applied in µPADs for detecting analytes (Cate et al. 2015; Cho et al. 2015).

6 POC Assay Based on Printed Electrodes

The technology of screen printing is one of the most broadly used techniques of microfabrication for the fabrication of very low cost and yet significantly reproducible kinds of electrochemical biosensors in large scale (Mahato et al. 2018). This technology proposes inexpensive and simple approaches to fabricate disposable systems at large scale for on-site, rapid, real-time, and low-cost analyses or monitoring various clinical biomarkers (Omidfar et al. 2011; Omidfar et al. 2012). Recent advancements in nano-characterization and microfabrication have resulted in the preparation of these disposable and inexpensive devices via printing different self-made or commercial inks on various kinds of substrates. Plastics (polycarbonate and polyvinyl chloride), alumina, and ceramics are usual matrices in the fabrication of screen-printed electrodes (SPEs), although, fiberglass, silver, iron, and gold are also not uncommon. The surface of these electrodes can be simply modified using different materials to meet several aims related to various analytes and to attain diverse betterments in their stability, sensitivity, and selectivity (Ahmed et al. 2016; Daneshpour et al. 2016). They usually include three electrodes: the working electrode, which is the major one and the electrochemical reactions take place on their surface, and the reference and counter electrodes, both of which are applied with the aim of completing the electronic circuit. Carbon and silver inks are the most common pastes used in the course of SPEs printing procedures. The working electrodes are usually printed applying inks based on carbon, while silver inks are used to print conductive tracks. Other materials like platinum and gold inks also can be used for SPEs preparation. It has been proven that changes in the composition of inks such as type and particle loading or size can remarkably affect the electron transfer and vary the fabricated biosensors analytical performance totally. Their compositions specify the sensitivity and selectivity needed for each test. During the analysis and detection processes, unknown ingredients in inks can lead to unpredictable outcomes. These pastes are often made on the basis of polymeric binders with graphite or metallic dispersions. Additionally, they can contain mediators, cofactors, and stabilizers as functional materials (Ahmed et al. 2016). Particularly for sensing usages, carbon-based inks are more attractive because of their low background currents, chemical inertness, low cost, and wide potential windows. While gold paste, due to its higher cost, is less applied in SPEs versus carbon. Despite that, preparation of self-assembled monolayers (SAMs) via strong bonds of Au-S increases the interest in applying gold in the production of SPEs. The low rate of electron transfers or the printing ink's adhesion to the surface of the substrate can be improved by employing diverse materials. Resins, cyclohexane, ethylene glycol, and cellulose acetate are examples of adhesive materials that can be utilized to attach the inks to the electrode substrate. Aiming to improve the selectivity, sensitivity, or ratio of signal to noise (S/N), additives can be combined with the printing inks. High versatility is one of the SPEs major advantages. This property is mainly due to the broad range of methods for modification of the surfaces of electrodes via changing the composition of inks or deposition of different materials such as enzymes, polymers, metal films, etc., on the surfaces of electrodes (Rao et al. 2006; Taleat et al. 2014). Moreover, significant developments were made in the production of SPEs through the application of nanostructured materials. Recently, CNTs, metallic nanoparticles, graphene, various nanowires, and their nanocomposites have also been employed in the aforementioned pastes or as the next step on the working electrodes (Daneshpour et al. 2016; Khorsand et al. 2013).

7 POC Assays Based on Nanomaterials

The relationship between nanotechnology and medical diagnostics, treatments, monitoring, and therapeutics has provided “Nanomedicine” as a novel concept in the world of science. It is an interdisciplinary field in science in which numerous scientists with diverse expertise, namely, chemists, biochemists, mathematicians, physicians, computer scientists, and engineers must work together (Vinogradov and Wei 2012; Quesada-González and Merkoçi 2018). A broad spectrum of nanomaterials and nanocomposites of them have been extensively applied in medicine. They have presented a number of the most promising outcomes in imaging, therapeutics, and diagnostics (Baker 2010; Chi et al. 2012; Kumar et al. 2019). Over the recent decade, nanomedicine has been widely studied and a considerable amount of literature has been published. Especially, CNTs, metal nanoparticles, and graphene and their nanocomposites have been broadly used for the development of POC biosensors. Nanomaterials can be used for loading signal markers as carriers or as signal reporters for specific and sensitive determination of analytes. Also, as the functional substances on the electrode surface, they can accelerate the rate of electron transfer. Their chemical and physical features such as shape, size, construction, composition, etc., can be improved to produce appropriate materials with different specific properties (Yang et al. 2013). Nanomaterials are capable of improving the specificity and sensitivity of detection devices as well as increasing the reliability and reproducibility of tests owing to their exceptional characteristics such as chemical stability, good electrical features, and excellent surface-to-volume ratios (Holzinger et al. 2014). In addition, the integration of these materials in micro-biosensors provides easy-to-use, inexpensive, and portable sensors by virtue of the simplicity of the miniaturization of the system transduction and these materials (Sadabadi et al. 2013). Applying nanomaterials to biosensing systems allows the simultaneous detection of multiple biomarkers and the timely diagnosis of various diseases. They also offer the possibility of detecting ultra-trace amounts of analytes and the design of rapid, inexpensive, and ultrasensitive assays with minimum amounts of specimens (Janegitz et al. 2014). Nevertheless, the major promising usage of nanotechnology will be in POC devices, which will let the physicians of primary care and patients to attain clinical diagnostic measurements at their own respective settings. The aforementioned developments in this field will be widely useful in varying the late-stage and expensive diagnosis and socially onerous treatments to cheaper and less invasive on-time diagnosis (Song et al. 2014). In the following, a number of the most common nanomaterials used in the production of POC systems will be reviewed.

7.1 Nanoparticles

Over the last decade, metallic nanoparticles owing to their variety and broad applications have attracted the attention of many scientists and researchers. By virtue of their excellent surface area and small size, they offer exceptional physical, chemical, and electronic characteristics, which are interestingly useful for developing reliable POC tests performed in screen-printed and microfluidic devices (Medina-Sánchez et al. 2012).

7.1.1 Gold Nanoparticles (AuNPs)

Up until now, among the various nanoparticles, AuNPs (containing gold nanorods, hollow nanospheres, and nanorings) are the most preferred ones, which are applied as the label in producing the suitable signals and consequently, providing the increase and advantage versus the molecular reagents. In addition to good biocompatibility, excellent stability, and simple functionalization, AuNPs have outstanding optoelectronic features that are affected by their shape, size, and surroundings. Generally, they are synthesized via liquid or colloidal chemical synthesis by reduction of the tetrachloroauric (III) acid solution in water. Through controlling different synthesis conditions, including reaction steps, thermal conditions, and the applied reducer, nanoparticles of various shapes and sizes can be synthesized. This can improve their effectiveness and usage in various applications (Omidfar et al. 2013).

7.1.2 Magnetic Nanoparticles

They have found broad usage in catalysis, magnetic fluids, bioseparation, drug delivery, medical imaging, treatment of hyperthermia, and targeted detection. Moreover, owing to their excellent properties (low cost, easy manipulation via magnetic field, and simple size control), they have been employed as an important element in biosensing devices in modern biomedical applications. More importantly, using suitable strategies of surface functionalization, the use of these nanoparticles can be increased while enhancing their stability (Mahdavi et al. 2013).

7.1.3 Carbon-Based Nanomaterials

CNTs

Since the early 1990s, CNTs have attracted remarkable attention by virtue of their supreme electrical, chemical, and physical properties. They are mainly categorized into two groups: single-walled and multi-walled CNTs. They are applied in various modern devices and technologies due to their excellent specificity, low cost, user-friendliness, and sensitivity. CNTs are under consideration for employing in POC devices in order to study biological analytes such as DNA, proteins, viruses, and glucose (Gao et al. 2014).

Graphene

Graphene has attracted the great attention of scientists due to its interesting thermal, electronic, and mechanical features. Recently, this honeycomb lattice and its derivatives have become a favorable platform used for sensitive clinical monitoring and POC diagnostics, including lab-on-a-chip technologies and screen-printed electrodes based on graphene (Pumera 2011).

Silver Nanoparticles (AgNPs)

Silver is an important metal in the history of medical treatment. Nanoparticles of silver are one of the most applied nanomaterials all over the world. Based on their applications, they are synthesized in multiple shapes, while spherical AgNPs are the most commonly applied form of them. AgNPs have excellent electrical, thermal, and optical characteristics. These days they are used in various products from photovoltaics to chemical and biological sensors. The features of AgNPs appropriate for use in human treatments are still under assessment for investigating their potential toxicity, efficacy, and costs (Chaloupka et al. 2010). However, based on their novel optical characteristics, AgNPs are broadly used in photonic devices and molecular diagnostics (Al-Saedy et al. 2020). Moreover, AgNPs have a series of properties such as simple synthesis process, high surface to volume ratio, tunable morphology, intracellular delivery system, etc., which make them appropriate for different biomedical applications. In this respect, for tissue regeneration, AgNPs are considered as gene delivery systems. Also, they have been used in various therapeutic applications. Up until now, cancer therapy (Jeyaraj et al. 2013), antimicrobial activities (Durán et al. 2016), catalysis (Bindhu and Umadevi 2015), antibacterial activities (Gnanadesigan et al. 2012), antiviral activities (Xiang et al. 2013), antifungal treatments (Tran and Le 2013), wound healing and dressing (Leaper 2006; Wilkinson et al. 2011), tissue engineering, implanted material, medical devices (prostheses, catheters, and vascular grafts) and diagnostic applications in dental preparations, biosensing devices, and antipermeability agents are examples of AgNps most common biomedical applications (Chaloupka et al. 2010; Graham et al. 2006; Zhao and Tripp 2007).

8 Conclusions

Over the recent decade, several modern POC devices have been developed in academic studies and commercial productions. Through offering fast and accurate tests at patients' locations, these assays optimize the procedure of diagnosis, improve therapy management, and permit attaining cost-effective and efficient clinical results. Actually, it can be deduced that POC devices have the potential to transform the health care system in both developing and developed countries. In this regard, the synergy of nanostructured materials with diverse biosensing devices and communication technologies may result in the creation of innovative POC devices, which are sensitive, selective, affordable, easy to use, portable, rapid, and robust for diagnostic applications.

References

Ahmed MU, Hossain MM, Safavieh M, Wong YL, Rahman IA, Zourob M, Tamiya E (2016) Toward the development of smart and low cost point-of-care biosensors based on screen printed electrodes. Crit Rev Biotechnol 36:495–505

Alila S, Boufi S, Belgacem MN, Beneventi D (2005) Adsorption of a cationic surfactant onto cellulosic fibers I. Surface charge effects. Langmuir 21:8106–8113

Al-Saedy M, Ali A, Sabah R, Hamed WM, Kafi M (2020) Preparation method of silver Nano particles. J Adv Sci Technol 3:1–8

Amna T, Hassan MS, Sheikh FA (2020) Nanocamptothecins as new generation pharmaceuticals for the treatment of diverse cancers: overview on a natural product to nanomedicine. In: Application of Nanotechnology in Biomedical Sciences, pp 39–49

Atala A (2005) Technology insight: applications of tissue engineering and biological substitutes in urology. Nat Clin Pract Urol 2:143–149

Bajpai VK, Kamle M, Shukla S, Mahato DK, Chandra P, Hwang SK, Kumar P, Huh YS, Han Y-K (2018) Prospects of using nanotechnology for food preservation, safety, and security. J Food Drug Anal 26:1201–1214

Baker M (2010) Nanotechnology imaging probes: smaller and more stable. Nat Methods 7:957–962

Baranwal A, Srivastava A, Kumar P, Bajpai VK, Maurya PK, Chandra P (2018) Prospects of nanostructure materials and their composites as antimicrobial agents. Front Microbiol 9:422

Bindhu M, Umadevi M (2015) Antibacterial and catalytic activities of green synthesized silver nanoparticles. Spectrochim Acta A Mol Biomol Spectrosc 135:373–378

Cate DM, Adkins JA, Mettakoonpitak J, Henry CS (2015) Recent developments in paper-based microfluidic devices. Anal Chem 87:19–41

Chaloupka K, Malam Y, Seifalian AM (2010) Nanosilver as a new generation of Nanoproduct in biomedical applications. Trends Biotechnol 28:580–588

Chandra P (2016) Nanobiosensors for personalized and onsite biomedical diagnosis. The Institution of Engineering and Technology

Chen C-B, Chen J-Y, Lee W-C (2009) Fast transfection of mammalian cells using super-paramagnetic nanoparticles under strong magnetic field. J Nanosci Nanotechnol 9:2651–2659

Chi X, Huang D, Zhao Z, Zhou Z, Yin Z, Gao J (2012) Nanoprobes for in vitro diagnostics of cancer and infectious diseases. Biomaterials 33:189–206

Cho S, San Park T, Nahapetian TG, Yoon J-Y (2015) Smartphone-based, sensitive μpad detection of urinary tract infection and gonorrhea. Biosens Bioelectron 74:601–611

Choudhary S, Haberstroh KM, Webster TJ (2007) Enhanced functions of vascular cells on nanostructured Ti for improved stent applications. Tissue Eng 13:1421–1430

Daneshpour M, Izadi P, Omidfar K (2016) Femtomolar level detection of RASSF1A tumor suppressor gene methylation by electrochemical nano-genosensor based on Fe_3O_4/TMC/au nanocomposite and PT-modified electrode. Biosens Bioelectron 77:1095–1103

Dossi N, Toniolo R, Pizzariello A, Impellizzieri F, Piccin E, Bontempelli G (2013) Pencil-drawn paper supported electrodes as simple electrochemical detectors for paper-based fluidic devices. Electrophoresis 34:2085–2091

Duncan TV (2011) Applications of nanotechnology in food packaging and food safety: barrier materials, antimicrobials and sensors. J Colloid Interface Sci 363:1–24

Durán N, Durán M, De Jesus MB, Seabra AB, Fávaro WJ, Nakazato G (2016) Silver nanoparticles: a new view on mechanistic aspects on antimicrobial activity. Nanomedicine 12:789–799

Fakruddin M, Hossain Z, Afroz H (2012) Prospects and applications of nanobiotechnology: a medical perspective. J Nanobiotechnol 10:1–8

Fattal E, Barratt G (2009) Nanotechnologies and controlled release systems for the delivery of antisense oligonucleotides and small interfering RNA. Br J Pharmacol 157:179–194

Fiipponi L, Sutherland D (2012) Nanotechnologies: principles, applications, implications and hands-on activities: a compendium for educators. European Union, Directorate General for Research and Innovation

Gao X, Xu L-P, Zhou S-F, Liu G, Zhang X (2014) Recent advances in nanoparticles-based lateral flow biosensors. Am J Biomed Sci 6

Gartland KM, Gartland JS (2018) Opportunities in biotechnology. J Biotechnol 282:38–45

Gnanadesigan M, Anand M, Ravikumar S, Maruthupandy M, Ali MS, Vijayakumar V, Kumaraguru A (2012) Antibacterial potential of biosynthesised silver nanoparticles using Avicennia Marina mangrove plant. Appl Nanosci 2:143–147

Gomez FA (2014) Paper microfluidics in bioanalysis. Bioanalysis 6:2911–2914

Goudarzi S, Ahmadi A, Farhadi M, Kamrava SK, Mobarrez F, Omidfar K (2015) A new gold nanoparticle based rapid Immunochromatographic assay for screening EBV-VCA specific IgA in nasopharyngeal carcinomas. J Appl Biomed 13:123–129

Graham D, Faulds K, Smith WE (2006) Biosensing using silver nanoparticles and surface enhanced resonance Raman scattering. Chem Commun:4363–4371

Holzinger M, Le Goff A, Cosnier S (2014) Nanomaterials for biosensing applications: a review. Front Chem 2:63

Ige OO, Umoru LE, Aribo S (2012) Natural products:a minefield of biomaterials. Int Sch Res Notices 2012:983062

Jampílek J, Kráľová K (2015) Application of nanotechnology in agriculture and food industry, its prospects and risks. Ecol Chem Eng S 22:321–361

Janegitz BC, Cancino J, Zucolotto V (2014) Disposable biosensors for clinical diagnosis. J Nanosci Nanotechnol 14:378–389

Jeyaraj M, Sathishkumar G, Sivanandhan G, Mubarakali D, Rajesh M, Arun R, Kapildev G, Manickavasagam M, Thajuddin N, Premkumar K (2013) Biogenic silver nanoparticles for cancer treatment: an experimental report. Colloids Surf B: Biointerfaces 106:86–92

Khorsand F, Azizi MD, Naeemy A, Larijani B, Omidfar K (2013) An electrochemical biosensor for 3-hydroxybutyrate detection based on screen-printed electrode modified by coenzyme functionalized carbon nanotubes. Mol Biol Rep 40:2327–2334

Kumar A, Roy S, Srivastava A, Naikwade MM, Purohit B, Mahato K, Naidu V, Chandra P (2019) Nanotherapeutics: a novel and powerful approach in modern healthcare system. In: Nanotechnology in modern animal biotechnology. Elsevier

Lazić V, Nedeljković JM (2019) Organic–inorganic hybrid nanomaterials: synthesis, characterization, and application. Nanomat Synt 2019:419–449

Leaper DJ (2006) Silver dressings: their role in wound management. Int Wound J 3:282–294

Liana DD, Raguse B, Gooding JJ, Chow E (2012) Recent advances in paper-based sensors. Sensors 12:11505–11526

Mahato K, Maurya PK, Chandra P (2018) Feundamentals and commercial aspects of nanobiosensors in point-of-care clinical diagnostics. 3 Biotech 8:1–14

Mahdavi M, Ahmad MB, Haron MJ, Namvar F, Nadi B, Rahman MZA, Amin J (2013) Synthesis, surface modification and characterisation of biocompatible magnetic iron oxide nanoparticles for biomedical applications. Molecules 18:7533–7548

Maheshwari N, Tekade M, Chourasiya Y, Sharma MC, Deb PK, Tekade RK (2019a) Nanotechnology in tissue engineering. In: Biomaterials and bionanotechnology. Elsevier

Maheshwari R, Joshi G, Mishra DK, Tekade RK (2019b) Bionanotechnology in pharmaceutical research. In: Basic fundamentals of drug delivery. Elsevier

Medina-Sánchez M, Miserere S, Merkoçi A (2012) Nanomaterials and lab-on-a-chip technologies. Lab Chip 12:1932–1943

Mody VV, Siwale R, Singh A, Mody HR (2010) Introduction to metallic nanoparticles. J Pharm Bioallied Sci 2:282

Noah NM, Ndangili PM (2019) Current trends of nanobiosensors for point-of-care diagnostics. J Anal Methods Chem 2019:2179718

Nouailhat A (2010) First published in Great Britain and the United States in 2008 by ISTE Ltd and John Wiley & Sons, Inc.

Omidfar K, Dehdast A, Zarei H, Sourkohi BK, Larijani B (2011) Development of urinary albumin Immunosensor based on colloidal AuNP and PVA. Biosens Bioelectron 26:4177–4183

Omidfar K, Zarei H, Gholizadeh F, Larijani B (2012) A high-sensitivity electrochemical Immunosensor based on Mobile crystalline material-41-polyvinyl alcohol nanocomposite and colloidal gold nanoparticles. Anal Biochem 421:649–656

Omidfar K, Khorsand F, Azizi MD (2013) New analytical applications of gold nanoparticles as label in antibody based sensors. Biosens Bioelectron 43:336–347

Park JB, Bronzino JD (2002) Biomaterials: principles and applications. CRC Press, Taylor & Francis, London

Patra JK, Das G, Fraceto LF, Campos EVR, Del Pilar Rodriguez-Torres M, Acosta-Torres LS, Diaz-Torres LA, Grillo R, Swamy MK, Sharma S (2018) Nano based drug delivery systems: recent developments and future prospects. J Nanobiotechnol 16:1–33

Pumera M (2011) Graphene-based nanomaterials for energy storage. Energy Environ Sci 4: 668–674

Purohit B, Vernekar PR, Shetti NP, Chandra P (2020) Biosensor nanoengineering: design, operation, and implementation for biomolecular analysis. Sens Int 1:100040

Quesada-González D, Merkoçi A (2018) Nanomaterial-based devices for point-of-care diagnostic applications. Chem Soc Rev 47:4697–4709

Rao V, Sharma M, Pandey P, Sekhar K (2006) Comparison of different carbon ink based screen-printed electrodes towards amperometric immunosensing. World J Microbiol Biotechnol 22: 1135–1143

Sadabadi H, Badilescu S, Packirisamy M, Wüthrich R (2013) Integration of gold nanoparticles in PDMS microfluidics for lab-on-a-chip plasmonic biosensing of growth hormones. Biosens Bioelectron 44:77–84

Sekhon BS (2014) Nanotechnology in agri-food production: an overview. Nanotechnol Sci Appl 7:31

Shi J, Votruba AR, Farokhzad OC, Langer R (2010) Nanotechnology in drug delivery and tissue engineering: from discovery to applications. Nano Lett 10:3223–3230

Singh TG, Dhiman S, Jindal M, Sandhu IS, Chitkara M (2016) Nanobiomaterials: applications in biomedicine and biotechnology. In: Fabrication and self-assembly of nanobiomaterials, Elsevier, pp 401–429

Sinha N, Yeow J-W (2005) Carbon nanotubes for biomedical applications. IEEE Trans Nanobioscience 4:180–195

Sitharaman B, Zakharian TY, Saraf A, Misra P, Ashcroft J, Pan S, Pham QP, Mikos AG, Wilson LJ, Engler DA (2008) Water-soluble fullerene (C60) derivatives as nonviral gene-delivery vectors. Mol Pharm 5:567–578

Song Y, Huang Y-Y, Liu X, Zhang X, Ferrari M, Qin L (2014) Point-of-care technologies for molecular diagnostics using a drop of blood. Trends Biotechnol 32:132–139

Strick TR, Croquette V, Bensimon D (2000) Single-molecule analysis of DNA uncoiling by a type II topoisomerase. Nature 404:901–904

Suh WH, Suslick KS, Stucky GD, Suh Y-H (2009) Nanotechnology, nanotoxicology, and neuroscience. Prog Neurobiol 87:133–170

Syedmoradi L, Daneshpour M, Alvandipour M, Gomez FA, Hajghassem H, Omidfar K (2017) Point of care testing: the impact of nanotechnology. Biosens Bioelectron 87:373–387

Taleat Z, Khoshroo A, Mazloum-Ardakani M (2014) Screen-printed electrodes for biosensing: a review (2008–2013). Microchim Acta 181:865–891

Thirumavalavan M, Settu K, Lee J-F (2016) A short review on applications of nanomaterials in biotechnology and pharmacology. Curr Bionanotechnol (Discontinued) 2:116–121

Tran QH, Le A-T (2013) Silver nanoparticles: synthesis, properties, toxicology, applications and perspectives. Adv Nat Sci Nanosci Nanotechnol 4:033001

Vashist SK (2017) Point-of-care diagnostics: recent advances and trends. Biosensors 7:62

Vinogradov S, Wei X (2012) Cancer stem cells and drug resistance: the potential of nanomedicine. Nanomedicine 7:597–615

Webster TJ, Ergun C, Doremus RH, Siegel RW, Bizios R (2000) Enhanced functions of osteoblasts on nanophase ceramics. Biomaterials 21:1803–1810

Wheeldon I, Farhadi A, Bick AG, Jabbari E, Khademhosseini A (2011) Nanoscale tissue engineering: spatial control over cell-materials interactions. Nanotechnology 22:212001

Wieling R (2008) Carbon fibre reinforced peek medical implants. Eur Cell Mater 16:8

Wilkinson L, White R, Chipman J (2011) Silver and nanoparticles of silver in wound dressings: a review of efficacy and safety. J Wound Care 20:543–549

Wu Y, Yang P (2001) Direct observation of vapor – liquid – solid nanowire growth. J Am Chem Soc 123:3165–3166

Wu Y, Yan H, Huang M, Messer B, Song JH, Yang P (2002) Inorganic semiconductor nanowires: rational growth, assembly, and novel properties. Chemistry 8:1260–1268

Xiang D, Zheng Y, Duan W, Li X, Yin J, Shigdar S, O'conner ML, Marappan M, Zhao X, Miao Y (2013) Inhibition of a/human/Hubei/3/2005 (H3n2) influenza virus infection by silver nanoparticles in vitro and in vivo [corrigendum]. Int J Nanomedicine 8:4703–4704

Yamada K, Henares TG, Suzuki K, Citterio D (2015) Paper-based inkjet-printed microfluidic analytical devices. Angew Chem Int Ed 54:5294–5310

Yang D, Ma J, Zhang Q, Li N, Yang J, Raju PA, Peng M, Luo Y, Hui W, Chen C (2013) Polyelectrolyte-coated gold magnetic nanoparticles for immunoassay development: toward point of care diagnostics for syphilis screening. Anal Chem 85:6688–6695

Zhao Y, Tripp RA (2007) Spherical and anisotropic silver nanomaterials in medical diagnosis. In: Nanotechnologies for the life sciences. Online https://onlinelibrary.wiley.com/doi/abs/10.1002/9783527610419.ntls0127

Всё для победы! НАРОДНЫЙ ФРОНТ
https://pobeda.onf.ru/
LET'S HELP THE RUSSIA

Nanobioelectrochemical Sensors in Clinical Diagnosis

4

B. Jurado-Sánchez

Contents

1 Introduction 70
2 Enzyme- and Non-Enzyme-Based Nanoelectrochemical Biosensors 71
  2.1 Enzyme-Based Nanoelectrochemical Biosensors 72
  2.2 Nonenzymatic Nanoelectrochemical Biosensors 74
3 Nanoelectrochemical Immunosensors 78
4 Nanoelectrochemical Genosensors 81
5 Nanoelectrochemical Cytosensors 83
6 Conclusions 84
References 85

Abstract

The development of ready-to-use point of care sensing devices is of paramount significance in healthcare and for the well-being of society. The aim of this chapter is to provide an overview of recent progress in the development of nanoelectrochemical biosensors for clinical diagnosis. The use of nanomaterials in connection with electrochemical sensors can greatly increase its performance, allowing for the detection of very low levels of clinical biomarkers and aiming in the quest for identification of new ones. In this chapter, selected examples on the design and applications of relevant enzymatic and nonenzymatic biosensors, immunosensors, genosensors, and cytosensors are given. Important diseases such as cancer and bacterial infections are specifically covered, to conclude with future perspectives of such a novel area of research.

B. Jurado-Sánchez (✉)
Department of Analytical Chemistry, Physical Chemistry, and Chemical Engineering, Universidad de Alcala, Alcala de Henares, Spain
e-mail: beatriz.jurado@uah.es

© Springer Nature Singapore Pte Ltd. 2023

U. P. Azad, P. Chandra (eds.), *Handbook of Nanobioelectrochemistry*,
https://doi.org/10.1007/978-981-19-9437-1_4

Keywords

Nanomaterial · Biosensor · Enzymatic · Immunosensing · Genosensing · Cytosensing · Diagnosis

1 Introduction

The development of fast, sensible, and ready-to-use point of care and sensing devices is of paramount significance for clinical diagnosis. Indeed, the fast diagnosis of biomarkers, such as proteins, circulating RNA, bacteria, and endotoxins, allows for immediate treatment, decreasing overall sanitary costs and improving the health and well-being of populations (Chandra 2016; Chamorro-Garcia and Merkoçi 2016). Biosensors are analytical devices that rely on biological elements-receptors for recognition of the analyte. The receptor is integrated within a physical or chemical transducer. Such devices generate a digital electronic signal in response to the target analyte, which is subsequently converted into a measurable response, allowing for fast and specific detection of a myriad of analytes with negligible sample treatment (Turner 2000; Mahato et al. 2018b; Purohit et al. 2020). In electrochemical biosensors, electrical signal changes in response to the analyte are measured by amperometry, potentiometry, impedance spectroscopy, or conductometry. Since the first glucose sensor in 1967 (Updike and Hicks 1967), a myriad of biosensors for healthcare monitoring and diagnosis have been developed.

Advances in nanofabrication and nanotechnology revolutionize many aspects in chemistry and overall science. In the biosensors field, nanomaterials (NMs) can be combined with the transducer leading to the so-called nanobiosensors or nanoelectrochemical biosensors (Mckeating et al. 2016; Mahato et al. 2018a). To this end, different nanoparticles, nanomaterials, and nanostructured surfaces have been explored. Nanomaterials possess sizes ranging from 1 to 100 nm in a 0 dimensional (D), 1D, 2D, or 3D structure arrangement, with a high volume-to-surface ratio. Such remarkable properties can greatly benefit electrochemical sensing thorough signal amplification, also facilitating electrode surface modification with different receptors. As such, such functional nanomaterials have been used in electrochemical sensing to increase the surface area of the electrode –increasing the sensitivity – facilitating thus the immobilization of different receptors, to enhance electronic transfer and even as efficient tags (Wongkaew et al. 2019; Zhang et al. 2021). Figure 4.1 illustrates a summary of different nanomaterials explored for connection with electrochemical biosensors. These include metallic and semiconductor nanoparticles (NPs), carbon NMs, and other 2D like NMs, mesoporous and nanoporous structures, and nanopillar structures. For modification, antibodies, DNA, or whole cells can be incorporated and used as the specific bioreceptors.

The aim of this chapter is to give an updated summary in the development of nanoelectrochemical biosensors for clinical diagnosis. The chapter is organized according to the type of bioreceptor used for connection with different NMs. In each subsection, comprehensive tables comparing the strategies will be included,

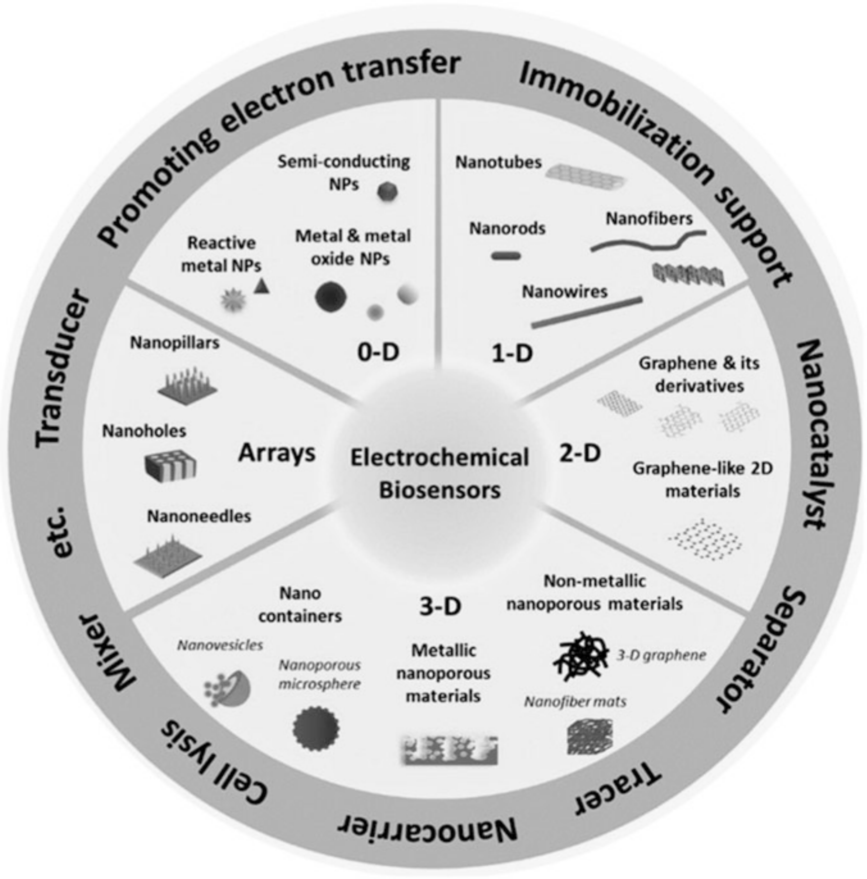
Promoting electron transfer
Immobilization support
Nanocatalyst
Separator
Tracer
Nanocarrier
Cell lysis
Mixer
etc.
Transducer
Semi-conducting NPs
Reactive metal NPs
Metal & metal oxide NPs
0-D
Nanotubes
Nanorods
Nanofibers
Nanowires
1-D
Graphene & its derivatives
Graphene-like 2D materials
2-D
Non-metallic nanoporous materials
3-D graphene
Nanofiber mats
Metallic nanoporous materials
3-D
Nano containers
Nanovesicles
Nanoporous microsphere
Nanopillars
Nanoholes
Nanoneedles
Arrays
Electrochemical Biosensors

Fig. 4.1 Classification of nanomaterials used for electrochemical biosensing. (Reprinted with permission from (Wongkaew et al. 2019). Copyright 2019, American Chemical Society)

along with an overview of different sensors for the determination of relevant biomarkers of important diseases such as bacterial infections, cancer, etc., to finish with brief conclusions and some future perspectives.

2 Enzyme- and Non-Enzyme-Based Nanoelectrochemical Biosensors

Enzyme-based electrochemical biosensors have an immobilized enzyme on the working electrode. In this case, the enzyme is the selective probe that catalyzes the generation of electroactive products in response to a specific analyte. The most known enzymatic sensor is the glucose biosensor, which use glucose oxidase (GOx) to convert glucose into measurable hydrogen peroxide (Yoo and Lee 2010).

The main enzymatic electrochemical sensors suffer from the low stability of enzymes, which are prone to inactivation, and the efficient immobilization in the electrode with adequate conformation to avoid loss of catalytic activity. Nanomaterials can offer a convenient solution to avoid the abovementioned challenges, incrementing the overall surface area for enzyme immobilization, protecting the enzyme, or providing adequate functional groups to avoid conformational changes. Recent advances also illustrate the enzyme-mimic activity of some nanomaterials, allowing the replacement of enzyme, increasing the overall stability since a synthetic material is used, without hampering the analytical performance (Dong et al. 2021). Table 4.1 lists a summary of recent (last 3 years) enzymatic and nonenzymatic biosensors based on nanomaterials. As can be seen, most applications have been devoted to glucose and hydrogen peroxide detection. In addition, current trends are aimed at the replacement of enzymes with NPs based in oxides and carbon nanomaterials as an alternative to enzymes due to the abovementioned drawbacks.

2.1 Enzyme-Based Nanoelectrochemical Biosensors

Recent trends in nanomaterial-based electrochemical biosensors rely on the use of nanostructured materials to enhanced enzyme immobilization and increase the electronic transport properties. Three-dimensional (3D) carbon nanostructures contain macropores and micropores and a cage structure for the immobilization of enzymes, which can be very beneficial in electrochemical sensing. For example, an enzymatic electrode for glucose detection has been assembled by immobilization of GOx in a 3D graphene framework prepared by coating mesoporous silica with graphene (see Fig. 4.2). The large surface area of the 3D template and enhanced electron and mass transfer rate improve glucose sensing when compared with common electrodes and flat materials (Shen et al. 2019). Thus, as illustrated in Fig. 4.2c, the cyclic voltammetry (CV) signals greatly increased along with the scan rate. 3D graphene in connection with MXenes ($Ti_3C_2T_x$) have been also explored for glucose sensing in human serum samples. The incorporation of the MXene material increase the hydrophilicity of the networks and the surrounding environment, increasing the enzyme affinity due to this facilitates GOx access to the internal pores. Such biosensor displays excellent performance in raw human serum (Gu et al. 2019).

Cholesterol detection is of great importance to prevent serious cardiovascular diseases. Electrochemical cholesterol detection can be achieved using cholesterol esterase or cholesterol oxidase that ultimately generate hydrogen peroxide, which can be measured in Pt electrodes. Yet, these electrodes have low sensitivity, and as an alternative, novel nanomaterials have been explored. Eom et al. (2020) explored the use of Pt nanoclusters for cholesterol determination in saliva samples. The resulting electrodes possess enhanced electron transfer properties, allowing for the detection of cholesterol in saliva samples with low limit of detection (2 μM) and good specificity.

Table 4.1 Enzymatic and nonenzymatic biosensors based on nanomaterials

Nanomaterial	Analyte	Sample	Analytical characteristics	References
Enzymatic sensors				
3D graphene	Glucose	–	–	Shen et al. (2019)
$Ti_3C_2T_x$ MXene–graphene	Glucose	Serum	LOD: 0.1 mM	Gu et al. (2019)
MWCNTs	Abiraterone	Serum	LOD: 230 nM	Aliakbarinodehi et al. (2018)
Pt nanoclusters	Cholesterol	Saliva	LR: 2–486 μM LOD: 2 μM	Eom et al. (2020)
Nonenzymatic sensors				
GO/MoS_2 aerogel	Glucose	–	LR: 2–20 mM LOD: 0.3 mM	Jeong et al. (2017)
MWCNTs/ZnO QDs	Glucose	Urine	LR: 0.1–2.5 μM LOD: 0.2 μM	Vinoth et al. (2021)
MWCNTs-Z-AuNiNPs	Glucose	Serum	LR: 1–1900 μM LOD: 0.063 μM	Amiripour et al. (2021)
Carbon cloths/MOF-74 (Cu)	Glucose	Serum	LR: 1–100 μM LOD: 0.41 μM	Hu et al. (2020)
AuSn alloys	Glucose	–	LR: 2–8110 μM LOD: 0.36 μM	Pei et al. (2018)
ZnO on carbon cloth	Glucose	Serum	LR: 1–1450 μM LOD: 0.43 μM	Wang et al. (2020b)
CuO nanocuboids	Glucose	–	LOD: 0.6 mM	Lynch et al. (2020)
CuO nanobelts	Glucose	Serum	LR: 0.1–2000 μM LOD: 60 nM	Li et al. (2020)
CeO_2@CuO NPs	Glucose	Serum	LOD: 0.02 μM	Dayakar et al. (2018)
$C_3N_4/Co(OH)_2$	Glucose	Serum	LR: 0.03–420 mM 6.6–9800 μM	Tashkhourian et al. (2018)
Cu nanoflowers/ AuNPs	Glucose	Biofluids	LR: 0.001–0.1 mM LOD: 0.02 μM	Baek et al. (2020)
Co_3O_4 nanobooks	Glucose	Serum	LOD: 7.9 μM	Wang et al. (2020a)
Co/Cu nanocolumn arrays	Glucose	Serum	LR: 0.005–1 mM LOD: 0.4 μM	Pak et al. (2020)
Ni nanopillar arrays	Glucose	Blood	LR: 0.01–12 mM LOD: 0.44 μM	Ding et al. (2020)
RhO nanocorals	Glucose	Serum	LOD: 3.1 μM	Dong et al. (2018)
Co_3O_4 needles on Au honeycomb	Glucose	Saliva	LR: 20–100 μM	Coyle et al. (2019)
CB/PdCu	Hydrogen peroxide	Cellular media	LR: 0.4–5000 μM LOD: 0.054 μM	Liu et al. (2019)
2D Cu-tetrakis (4-carboxyphenyl) porphyrin MOF	Hydrogen peroxide	Cellular media	LOD: 0.13 μM	Qiao et al. (2021)
Fe-hemin-MOFs	Hydrogen peroxide	Cellular media	LOD: 0.6 μM	Zhao et al. (2020)
$CuCo_2O_4$ nanosheets	Hydrogen peroxide	Cellular media	LR: 1–730 μM LOD: 0.16 μM	Xie et al. (2020)

(continued)

Table 4.1 (continued)

Nanomaterial	Analyte	Sample	Analytical characteristics	References
CuO-ZnO	Hydrogen peroxide	–	LR: 3–530 μM LOD: 2.4 μM	Daemi et al. (2019)
Ag nanosheets	Hydrogen peroxide	Cellular media	LR: 6–6000 μM LOD: 0.17 μM	Ma et al. (2018)
Ag_2WO_4 nanorods	Hydrogen peroxide	–	LR: 0.06–2.4 mM LOD: 6.25 μM	Koyappayil et al. (2020)
Hollow sphere NiS	Lactic acid	Urine	LR: 0.5–89 μM LOD: 0.023 μM	Arivazhagan et al. (2020)
MWCNTs/Mo	Dopamine	Serum	LR: 0.01–1609 μM LOD: 1.3 nM	Keerthi et al. (2019)
Ni_6MnO_8@C nanosheets	Epinephrine	Serum	LR: 0.01–800 μM LOD: 3.33 nM	Lei et al. (2021)

LOD limit of detection, *LR* linear range *MWCNT* multi-walled carbon nanotubes, *QDs* quantum dots, *MOF* metal-organic framework, *CB* carbon black

2.2 Nonenzymatic Nanoelectrochemical Biosensors

Enzyme-free electrochemical biosensors are replacing the traditionally used enzyme-based sensors as reflected by the increasing number of publications during the last 3 years (see Table 4.2). In addition, the performance of the new sensors is equal and even better to the traditional ones. Most works are related with glucose and hydrogen peroxide detection, with few applications for the determination of neurotransmitters and other analytes such as dopamine.

Carbon-based nanomaterials have been greatly explored in electrobiosensing for glucose and other bioanalytes detection due to a remarkable electron transfer along with the large surface-to-volume ratio. Combined with other nanomaterials, highly selective and sensitive enzyme-free detection can be achieved (Cai and Chen 2004). As in the case of enzymatic sensor, a 3D graphene aerogel has been combined with MoS_2 for glucose detection via flow injection amperometric detection (Jeong et al. 2017). The resulting 3D biosensor exhibits better analytical performance than 2D MoS_2/rGO-based biosensor, which was attributed mainly to an improved diffusion of the ions due to the particular 3D structural conformation. Detection was achieved with a LOD of 0.3 mM. MWCNTs were combined with immobilized ZnO QDs, resulting in a nanocomposite material with synergetic properties for glucose detection at a LOD as low as 200 nM in urine samples with high selectivity (Vinoth et al. 2021). Similarly, MWCNTs have been combined in a nanozeolite as a substrate for AuNiNPs immobilization for direct detection of glucose in human serum samples with a LOD of 63 nM (Amiripour et al. 2021). A carbon cloth has been used as template for the immobilization of a MOF-74(Cu) by bottom-up self-assembly. The resulting nanohybrid oxidizes glucose into gluconate, improving the redox properties as compared with the MOFs or carbon cloth alone. As such, a LR from 1.0 to 1000 μM was obtained, with a LOD of 410 nM for glucose detection in human serum (Hu et al. 2020). Similarly, ZnO have been explored in connection with a

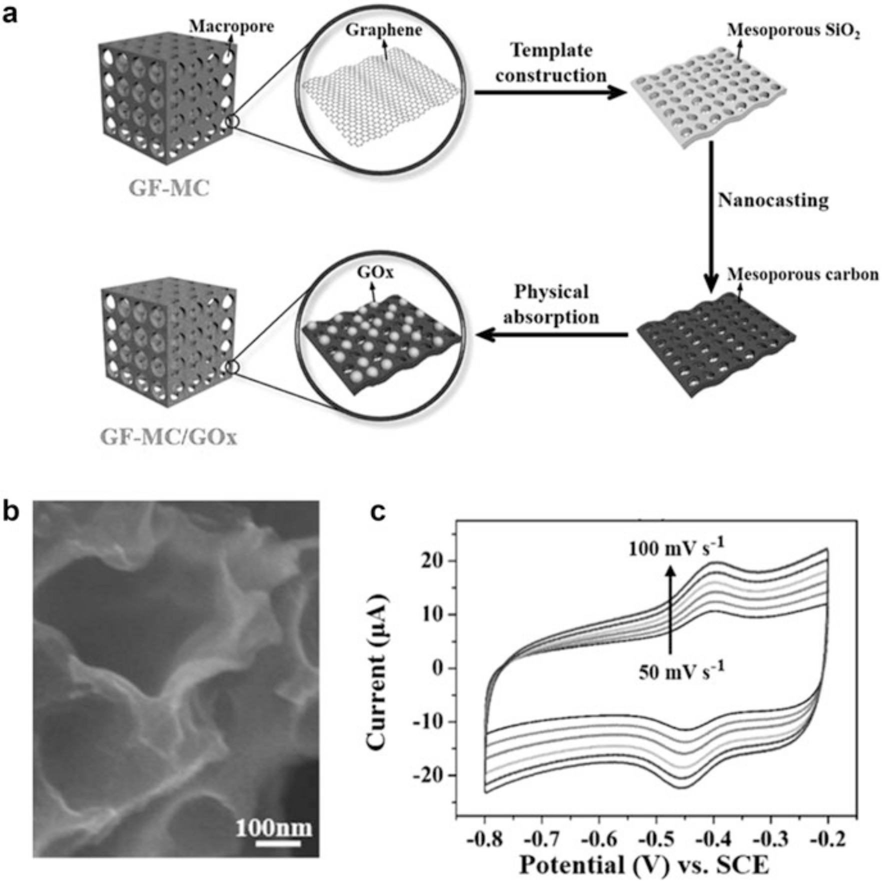
a
Macropore
Graphene
Template construction
Mesoporous SiO$_2$
GF-MC
Nanocasting
Mesoporous carbon
GOx
Physical absorption
GF-MC/GOx
b
100nm
c
100 mV s^{-1}
50 mV s^{-1}
Current (μA)
20
10
0
-10
-20
-0.8
-0.7
-0.6
-0.5
-0.4
-0.3
-0.2
Potential (V) vs. SCE

Fig. 4.2 3D Graphene electrodes for enzymatic glucose detection. (**a**) Schematic of the preparation. (**b**) Scanning-electron microscopy images showing the morphology of the 3D composites. (**c**) Cyclic voltammograms at different scan rates under the presence of glucose. (Reprinted with permission from Shen et al. (2019). Copyright 2019, Elsevier)

carbon cloth for the same application. The resulting nanobiosensor has excellent analytical performance with a LOD of 430 nM (Wang et al. 2020b). Nanoporous gold/Sn alloy has been employed as substrate to fabricate a nanoporous film for amperometric glucose detection in alkaline media. Excellent analytical performance with a low LOD of 360 nM was obtained (Pei et al. 2018).

Layered double hydroxides and copper have been used for direct detection of glucose, avoiding the use of enzymes, due to mainly the hydrophilicity and adequate dispersion in aqueous media (Lynch et al. 2020). The preparation of the oxides into ordered nanostructures can improve the analytical performance. For example, CuO nanobelts have been used for glucose determination in serum samples, with a wide linear range and excellent LOD of 60 nM (Li et al. 2020). CuO materials have also

Table 4.2 Immunosensors based on nanomaterials

Nanomaterial	Analyte	Sample	Analytical characteristics	References
Magnetic beads	SARS-CoV-2	Saliva	LOD: 8 ng mL^{-1}	Fabiani et al. (2021)
CNTs/CuAu on carbon nanospheres	Carcinoembryonic antigen	Serum	LR: 0.025–25 ng mL^{-1} LOD: 0.5 pg mL^{-1}	Tran et al. (2018)
CoS_2@C hollow nanotubes as secondary antibody tags	Carcinoembryonic antigen	Serum	LR: 0.001–80 ng mL^{-1} LOD: 0.3 pg mL^{-1}	Ma et al. (2019a)
Au@PtPd nanorods as secondary antibody tags	Carcinoembryonic antigen	Serum	LR: 0.005–100 ng mL^{-1} LOD: 17 fg mL^{-1}	Jia et al. (2020)
MoS_2 nanoflowers decorated with Au@AgPt nanocubes as secondary antibody tags	Carcinoembryonic antigen	Serum	LR: 0.01–100 ng mL^{-1} LOD: 3 fg mL^{-1}	Ma et al. (2019b)
Worm-like Pt as tags for the secondary antibody	Alpha fetoprotein	Serum	LR: 0.0001–100 ng mL^{-1} LOD: 0.028 pg mL^{-1}	Li et al. (2021)
Mesoporous silica coated Au nanorods	Procalcitonin	Serum	LR: 0.001–100 ng mL^{-1} LOD: 0.39 pg mL^{-1}	Feng et al. (2021)
IRMOFs and Pd@PtRh hybrids as secondary antibody tags	Procalcitonin	Serum	LR: 0.002–100 ng mL^{-1} LOD: 7.8 fg mL^{-1}	Dong et al. (2020)
$Cu_3(PO_4)_2$ nanoflowers	C-reactive protein	–	LR: 0.005–1 ng mL^{-1} LOD: 1.3 pg mL^{-1}	Tang et al. (2019)
Porous graphene decorated with Pd@Au nanocubes supported on β-cyclodextrins	Cardiac troponin I	Serum	LOD: 33 fg mL^{-1}	Zhang et al. (2019)
MOF/rGO/AuPt	Lymphocyte activation gene-3	Serum	LR: 0.01–1000 ng mL^{-1} LOD: 1.1 pg mL^{-1}	Xu et al. (2018)
AuNPs-PtNPs-MOFs	Nuclear matrix protein 22	Urine	LR: 0.005–20 ng mL^{-1} LOD: 1.7 pg mL^{-1}	Zhao et al. (2019)
rGO-TEPA-Thi-Au RuPdPt NPs as secondary antibody tag	Monocyte chemoattractant protein-1	Serum	LR: 0.02–1000 pg mL^{-1} LOD: 9 pg mL^{-1}	Mao et al. (2019)
AuNPs on PPY nanosheet RhPt nanodendrites as secondary antibody tags	Hepatitis B surface antigen	Serum	LR: 0.0005–10 ng mL^{-1} LOD: 166 fg mL^{-1}	Pei et al. (2019)

PPY polypyrrole

been combined with other oxides, such as CeO_2, resulting in a composite material with synergetic properties, i.e., enhanced electron transfers due to the combination of the electronic levels. Indeed, enhanced analytical properties with a LOD of 20 nM in serum were achieved (Dayakar et al. 2018). $Co(OH)_2$ has been electrodeposited on graphitic carbon nitride (C_3N_4) and used for glucose detection in raw human serum. The synergetic effect among both nanomaterials allows to increase the electronic transfer for enhanced detection at nM ranges (Tashkhourian et al. 2018).

Another convenient strategy to increase sensitivity and selectivity in nonenzymatic glucose sensing relies on the preparation of well-defined nanostructures with the aim to increase the overall native electrocatalytic activity of different nanoparticles. As such, Cu nanoflowers decorated with AuNPs (Baek et al. 2020), Co_3O_4 nanobooks (Wang et al. 2020a), Co/Cu nanocolumn arrays (Pak et al. 2020), Ni nanopillar arrays (Ding et al. 2020), RhO nanocorals (Dong et al. 2018), or Co_3O_4 needles on Au honeycomb (Coyle et al. 2019) have been applied to electrochemical glucose detection in human serum and saliva with LOD within the nM range and excellent operation linear ranges (see Table 4.1 for more details).

Hydrogen peroxide is another relevant bioanalyte of great importance to detect cell stress in the diagnosis of serious illnesses such as heart attacks and even cancer. In addition, most enzymatic sensors are based on the direct measurement of hydrogen peroxide, thus such biosensors can be also applied in the detection of a myriad of analytes only limited by our imagination (Zhang and Chen 2017; Miller et al. 2005). Traditionally, Pd was the most used noble metal for hydrogen peroxide detection using nonenzymatic methods, due to its excellent catalytic properties for peroxide decomposition and subsequent electronic transfer generation. Yet, such metal is highly expensive, thus recent trends are aimed at exploring alternative nanomaterials with high electrocatalytic activity. Bimetallic PdCu NPs have been combined with CB to detect hydrogen peroxide generated from RAW 264.7 cells in physiological media. The CB possesses a large density of highly active sites and results in a low LOD (54 nM) for in situ detection of hydrogen peroxide (Liu et al. 2019). Figure 4.3 illustrates the schematic of the procedure for real-time detection along with corresponding chronoamperometric response. A 2D Cu-tetrakis(4-carboxyphenyl) porphyrin (TCPP) MOF hybrid have been used for hydrogen peroxide determination in cellular media by square-wave voltammetry, providing a LOD of 130 nM (Qiao et al. 2021). Similarly, a hemin-based MOF was used for hydrogen peroxide monitoring in living cells with a LOD of 600 nM (Zhao et al. 2020). Cu and Cu oxide nanohybrids can also be used for peroxide detection following a similar principle to that explained for nonenzymatic glucose biosensors (better dispersibility and electronic transfer) at the nM range (Xie et al. 2020; Daemi et al. 2019). Ag is an alternative metal to Pd with similar catalytic properties for peroxide decomposition. The performance is limited, yet, by dissolution of the silver. For example, concave Ag nanosheets allow for the detection of peroxide released from SH-SY5Y cells with a LOD of 170 nM and LR of 5–6000 μM (Ma et al. 2018). Ag NPs have been assembled into Ag_2WO_4 nanorods, leading to a nanohybrid very promising for peroxide detection at μM levels (Koyappayil et al. 2020).

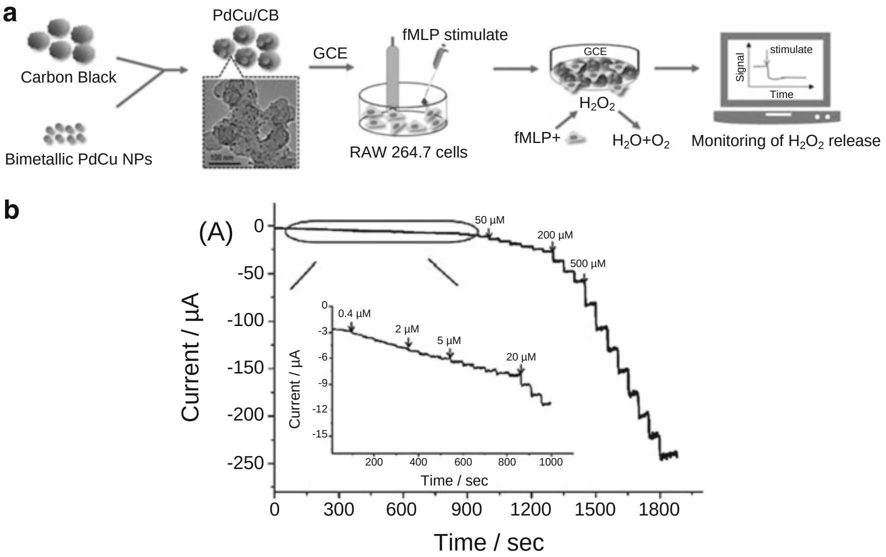

Fig. 4.3 PdCu nanoparticles/carbon black nonenzymatic electrochemical sensor for hydrogen peroxide detection. (**a**) Schematic of the sensing protocol. (**b**) Chronoamperometric response under the presence of different concentrations of hydrogen peroxide. (Reprinted with permission from Liu et al. (2019). Copyright 2019, Elsevier)

Lactic acid is a nonspecific biomarker that can be nevertheless monitored to follow lactic acidosis, related to serious illnesses such as sepsis or to follow the metabolism during intense exercise (Gladden 2004). Hollow sphere structured NiS have been used for enzyme-free electrochemical sensing of lactic acid in urine. The material acts as enzyme mimic for the electrocatalytic oxidation of lactic acid into pyruvic acid. Excellent analytical performance with a LOD of 23 nM (Arivazhagan et al. 2020) is achieved. Dopamine is another important clinical biomarker monitored in neurological diseases. Molybdenum nanoparticles have been assembled into MWCNTs and used for the electrochemical detection of such important analyte with a low LOD of 1.3 nM directly in human serum (Keerthi et al. 2019). Epinephrine, another important neurotransmitter, can be determined in human serum using a nonenzymatic sensor constructed using Ni_6MnO_8@C nanosheets with a LOD of 3 nM (Lei et al. 2021).

3 Nanoelectrochemical Immunosensors

Immunoassays rely on antigen–antibody recognition, both in competitive or noncompetitive modes (Darwish 2006; Wan et al. 2013). Table 4.2 lists a summary of recent nanoelectrochemical immunosensors for clinical diagnosis of virus, proteins, and biomarkers of cancer and infectious diseases (Pallela et al. 2016; Chandra et al. 2015). In most of them, the nanomaterial increases the overall surface area and conductivity of the electrode to improve the analytical signal or is used as tag of the secondary antibody. More details are given below.

Magnetic beads composed of Fe_2O_3 or other magnetic materials and coated with silica have been widely used to perform immunoassays for clinical diagnosis due to a better control of the immobilization of the antibody. In addition, the washing and modification steps can be easily controlled by magnetic actuation, facilitating the overall process. A wide variety of magnetic beads are commercially available. As a representative example, a very recent sandwich immunoassay for SARS-CoV-2 coronavirus detection relies on the modification of magnetic beads with a specific antibody targeting the spike and nucleocapsid protein of the virus. The secondary antibody is tagged with alkaline phosphatase as immunological label. After the immunoassay, the magnetic beads were dropped onto a carbon black screen-printed electrode and mixed with 1-naphthyl phosphate to generate 1-naphtol as electroactive material. The use of carbon black greatly enhanced the analytical signal, achieving a LOD of 8 ng mL^{-1}. The method was applied to the direct analysis of the virus in saliva samples (Fabiani et al. 2021).

Several competitive and sandwich-type electrochemical immunoassays have been devoted for the detection of carcinoembryonic antigen protein, which is present in serum at abnormal levels in cancer patients and can also act as a biomarker. Carbon nanospheres modified with carbon nanotubes-Cu-Au arrays provides a high density of active sites and rough area for the immobilization of carcinoembryonic antibody for the detection of such analyte. Excellent analytical performance for detection in serum samples is achieved, with a wide LR (0.025–25 ng mL^{-1}) and a LOD of 0.5 pg mL^{-1} (Tran et al. 2018). Nanomaterials containing high surface area and electrocatalytic activity have been also used as tags of the secondary antibody in the detection of the carcinoembryonic antigen. Thus, CoS_2@C hollow nanotubes have been used as tags with electrocatalytic ability towards hydrogen peroxide reduction in the detection of such analyte in a sandwich format. The signal produced was monitored by current response, with a low LOD of 0.3 pg mL^{-1} due to the amplification of the signal by the rough nanomaterial (Ma et al. 2019a). In a similar configuration, Au@PtPd nanorods have been also used as tags for the secondary antibody. In this case, a doubled amplification strategy in the sandwich assay was adopted by modifying the electrode with MoS_2/CuS-Au hybrids to increase the loading of primary antibody. After carcinoembryonic antigen and interaction with the Au@PtPd tagged secondary antibody, an excellent LOD of 17 fg mL^{-1} was achieved in serum samples (Jia et al. 2020). Such LODs have been further decreased to 3 fg mL^{-1} in a similar sandwich assay using trimetallic yolk-shell Au@AgPt nanocubes loaded on MoS_2 nanoflowers as secondary antibody tag (Ma et al. 2019b). Alpha fetoprotein is another important complementary cancer biomarker for liver cancer diagnosis and monitoring of treatment. Worm-like platinum nanoparticles have been used as tags for the secondary antibody in the determination of such compound in serum samples. The signal amplification and catalytic abilities of such tags result in a low LOD of 0.03 pg $mL^{-1}$with good accuracy as compared with the standard method (Li et al. 2021).

Procalcitonin is a relevant protein used in the diagnosis and prognosis of septicemia. PCT content in the serum of healthy people is extremely low (0.1 ng mL^{-1}), thus an increase of such levels is a good indicator of infections and septicemia. An immunoassay method for the analysis of PCT was assembled by immobilizing porous silica-coated gold nanorods containing electroactive thionine on the electrode surface. The rods act both as containers for the electroactive materials and increase the surface area for the immobilization of the specific antibody. The immunosensor exhibited a good LR (0.001–100 ng mL^{-1}) with a LOD of 0.4 pg mL^{-1} (Feng et al. 2021). A sandwich immunoassay was assembled by using an organometallic frame (Au/IRMOF-3) for electrode modification and primary antibody immobilization and Pd@PtRh nanorods as secondary antibody labels for hydrogen peroxide reduction. The amplification strategy allows for procalcitonin detection at 7.8 fg mL^{-1} levels in serum samples (Dong et al. 2020). C-reactive protein is another typical biomarker used for the monitoring of infections, which in some cases is monitored along with procalcitonin. $Cu_2(PO_4)_2$ nanoflowers have been explored as tags in the secondary antibody for the detection of such analyte via peroxide reduction with a LOD of 1.3 pg mL^{-1} (Tang et al. 2019).

Cardiac troponin is a relevant biomarker used for the monitoring of myocardial infracts. A sandwich-type immunoassay was designed by using porous graphene decorated with Pd@Au nanocubes functionalized with β-cyclodextrins. To further amplify the electrochemical signal, the electrode surface was modified with AuNPs/carbon spheres nanocomposites for immobilization of a high loading of primary antibody. The immunosensor exhibited high selectivity, with a low LOD of 33 fg mL^{-1} in serum samples (Zhang et al. 2019). Lymphocyte activation gene-3 protein is a type I transmembrane protein that holds considerable promise in the detection of diseases such as HIV, cardiovascular diseases, etc. A sandwich immunosensor for the detection of such biomarker was assembled by using MOFs@AuPt hybrids on rGO as nanomaterial for electrode modification and immobilization of the primary antibody and silica nanoparticles tagged with the secondary antibody. The silica-antibody 2 is used as signal-decreasing label due to the steric hindrance property. For the electrode configuration and signal profile, see Fig. 4.4. The immunosensor exhibited a wide LR with a low LOD 1.1 pg mL^{-1} with excellent performance in serum samples (Xu et al. 2018).

Nuclear matrix protein 22 has been recognized as a urinary biomarker for the detection of bladder cancer. The determination of such compounds was assembled by using rGO for supporting AuNPs-PtNPs-MOFs. This increased the loading of the specific antibody, allowing for the direct detection of such analyte in urine samples with a LOD of 1.7 pg mL^{-1} (Zhao et al. 2019). Monocyte chemoattractant protein-1, a cardiovascular biomarker, have been determined directly in serum samples with a sandwich immunoassay using RuPdPt NPs as secondary antibody tags and rGO for electrode modification, with a LOD of 9 pg mL^{-1} (Mao et al. 2019). Similarly, RhPt nanodendrites have been used as tags for the secondary antibody in the detection of hepatitis B surface antigen with high selectivity and a LOD as low as 166 fg mL^{-1} (Pei et al. 2019).

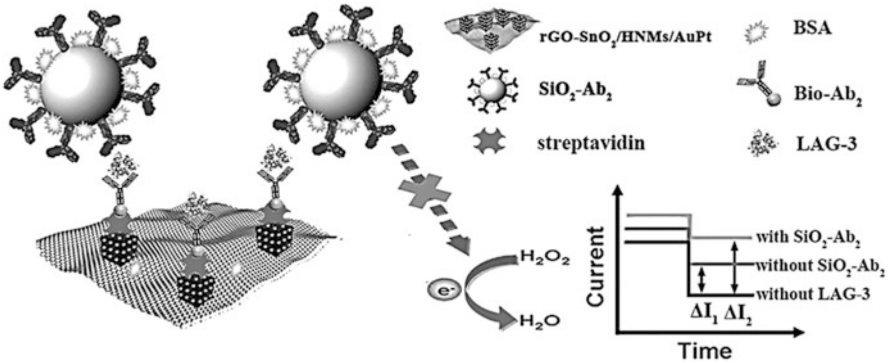

Fig. 4.4 Sandwich immunoassay for lymphocyte activation gene-3 protein detection in serum using MOFs@AuPt hybrids on rGO as nanomaterial for electrode modification and silica nanoparticles tagged with the secondary antibody. (Reprinted with permission from Xu et al. (2018). Copyright 2018, Elsevier)

4 Nanoelectrochemical Genosensors

Electrochemical genosensors rely on the use of single-stranded DNA as recognition probes immobilized onto the electrode surface. In the presence of the target analyte, hybridization occurs, generating an electrochemical signal by different mechanisms, as will be further explained. In this type of sensors, nanomaterials can be used for modification of the electrode to increase the surface area for probe immobilization or as tags to generate the electrochemical signal (Sadighbayan et al. 2019; Manzanares-Palenzuela et al. 2015). Table 4.3 lists a summary of recent nanoelectrochemical genosensors applied for clinical diagnosis.

CdS nanosheets have been electrodeposited in a carbon electrode and used as transducer in a genosensor for *Leishmania infantum* detection in skin cells. Such disease is caused by the intracellular pathogen Leishmania, infecting macrophages and dendritic cells and causing severe adverse health effects. The proposed genosensor is constructed by immobilization of specifically designed oligonucleotides, which hybridized selectively in the presence of the target analyte. Impedimetric detection was performed without the need of any additional tag with an excellent LOD of 1.2 ng μL^{-1} (Nazari-Vanani et al. 2020). In another sensor for Leishmaniosis detection, gold nanoleaves were explored for electrode surface modification and immobilization of the specific DNA. After hybridization, methylene blue was used as redox marker for detection via differential pulse voltammetry measurements. The peak current of the biosensors was higher after interaction with the specific analyte and hybridization, due to methylene blue can interact with both DNA strands, incrementing thus the analytical signal. A LOD of 0.07 ng μL^{-1} was achieved (Moradi et al. 2016). The detection of the infectious bacteria *Enterococcus faecalis* detection have been achieved using electrodeposited gold nanostructures in connection with toluidine blue as redox probe. Such bacteria

Table 4.3 Genosensors based on nanomaterials

Nanomaterial	Analyte	Sample	Analytical characteristics	References
CdS nanosheets	*Leishmania infantum*	Skin	LR: 5–50 ng μL^{-1} LOD: 1.2 ng μL^{-1}	Nazari-Vanani et al. (2020)
Au nanoleaves	Leishmania parasites	Skin	LR: 0.5–20 ng μL^{-1} LOD: 0.07 ng μL^{-1}	Moradi et al. (2016)
AuNPs	*Enterococcus faecalis*	–	LOD: 30 ng μL^{-1}	Nazari-Vanani et al. (2018)
rGO-Au	Hemoglobin A1c	Blood	LR: 0.001–14 μM LOD: 1 nM	Shajaripour Jaberi et al. (2019)
SWCNT-grafted dendritic Au nanostructure	miRNA-21	Serum	LOD: 0.01 fM	Sabahi et al. (2020)
MWCNTs-rGO	HPV16	–	LR: 0.009–11 μM LOD: 1.3 nM	Farzin et al. (2020)
GO	Hepatitis C virus	Serum	LOD: 1.4 nM	Oliveira et al. (2019)
$WS_{2/}Au$	Maternally expressed gene3	Serum	LR: 1 fM-100 pM LOD: 0.3 fM	Li et al. (2018)
Co oxide nanoflakes	Influenza A	Huma swabs	LR: 0.5–10 ng μL^{-1} LOD: 0.3 ng μL^{-1}	Mohammadi et al. (2017)

SWCNTs single-walled carbon nanotubes

can cause infections and adverse health effect in elderly immunocompromised patients. Differential pulse voltammetry was used to monitor DNA hybridization, achieving a low LOD of 30 ng μL^{-1} in the detection of such bacteria in relevant clinical samples (Nazari-Vanani et al. 2018).

Genosensors can be also useful for the detection of specific biomarkers beyond the identification of microorganism as previously described. Hemoglobin A1c can be used for long-term monitoring of diabetes. A genosensor for the identification of such compounds directly in blood samples was assembled by using rGO/gold for modification of the electrode and modification with the thiolated DNA aptamer as specific probe. As redox label, the $Fe(CN)_6$ system was used. Figure 4.5 illustrate a schematic of the detection protocol and representative signals. The detection relies on the decrease of the peak current in the presence of the target analyte, reaching LODs of 1 nM (Shajaripour Jaberi et al. 2019).

Micro-RNA-21, a novel cancer biomarker, have been detected using a genosensor assembled using SWCNTs/dendritic gold nanostructures in the electrode for self-assembly or the specific receptor. The target miRNA-21 was labeled with cadmium ions as redox mediators. The oxidation of the Cd ions was measured by differential pulse voltammetry, achieving a LOD of 0.01 fM in serum samples (Sabahi et al. 2020). MWCTs/rGO hybrids were used for the assembly of a genosensor for HPV detection using anthraquinone as redox mediators due to its binding capacities with

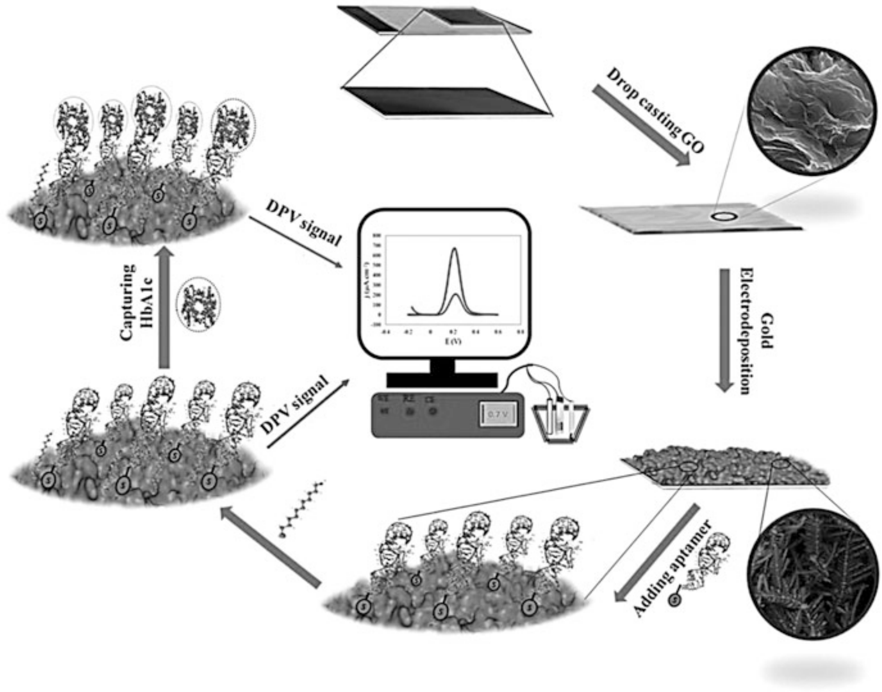

Fig. 4.5 Genosensor for Hemoglobin A1c detection in blood. (Reprinted with permission from Shajaripour Jaberi et al. (2019). Copyright 2019, Elsevier)

the DNA (Farzin et al. 2020). Hepatitis C virus determination have been also achieved by electrode modification with GO using the $Fe(CN)_6$ system as redox mediator (Oliveira et al. 2019). 2D nanomaterials analogous to graphene, such as WS_2, have been used for electrode modification, following assembly of gold for immobilization of specific DNA probes for the determination of maternally expressed gene3 RNA, a biomarker for the detection of lung cancer. Using ferrocene and methylene blue as redox probes, an LOD of 0.3 fM was achieved (Li et al. 2018). Cobalt oxide nanoflakes have been used for electrode modification and immobilization of single-stranded DNA specific to influenza A. Using methylene blue as redox indicators, direct detection from human swab samples was achieved with a LOD of 0.3 ng μL^{-1} (Mohammadi et al. 2017).

5 Nanoelectrochemical Cytosensors

Cytosensors rely on the capture of cells, normally cancer cells, using electrodes modified with specific receptors (aptamers, antibodies, etc.) that can interact with the cells via specific binding with overexpressed components on the surfaces of cancer cells such as glycans, etc. The nanomaterials here can play a vital role for increasing

Table 4.4 Cytosensors based on nanomaterials

Nanomaterial	Analyte	Sample	Analytical characteristics	References
AuNPs and Pt@Ag nanoflowers as tags	Circulating tumor cells	Blood	LOD: 3 cells mL^{-1}	Tang et al. (2018)
Iron oxide NPs	MCF-7 cells	Blood	LOD: 6 cells mL^{-1}	Zhang et al. (2020)
Peptide nanoparticles	DLD-1 cells		LOD: 100 cells mL^{-1}	Yaman et al. (2018)
Folic acid functionalized silica NPs	HT 29 cells	Serum	LOD: 50 cells mL^{-1}	Soleymani et al. (2019)

the surface area of the electrode for the incorporation of a higher amount of receptors (Xu et al. 2020). Table 4.4 lists some representative cytosensors based on nanomaterials for the detection of cancer cells.

A sensor for the detection of circulating tumor cells has been assembled using AuNPs acetylene black for electrode modification and assembly of specific antibodies. Pt@Ag nanoflowers were used as tags of the secondary antibody after MCF-7 cell capture, for reduction of peroxide and highly selective detection in blood samples with a LOD of 3 cells mL^{-1} (Tang et al. 2018). The detection of such MCF-7 has also been performed using graphene/iron oxide nanoparticles for electrode modification and immobilization of a specific aptamer for specific detection with a LOD of 6 cells mL^{-1} in blood samples (Zhang et al. 2020).

Peptide nanoparticles were used for modification of a pencil graphite electrodes in the detection of DLD-1 cancer cells by electrochemical impedance spectroscopy, with a LOD of 100 cells mL^{-1} (Yaman et al. 2018). Folic acid functionalized nanosilica was used as electrode modification materials for the detection of HT 29 colorectal cancer cells with a LOD of 50 cells mL^{-1} (Soleymani et al. 2019).

6 Conclusions

Electrochemical biosensors are highly useful tools in clinical diagnosis, allowing for fast detection directly in the samples using very low volumes. The use of nanomaterials and nanostructures in connection with electrochemical sensors can greatly increase the performance, allowing for the detection of very low levels or clinical biomarkers and aiming in the quest for identification of new ones, which were not possible to detect due to the low performance of traditional sensors. Enzymatic electrochemical biosensors were the most employed in the last 20 decades. The field is evolving now to adapt the working principle of enzymatic biosensors using NMs as enzyme mimics, solving the problems of enzyme instability and loss of activity due to changes in conformation after immobilization. NMs can also be used to modify the working electrode to increase the surface area for the incorporation of a large number or receptors or to increase the electronic transfer properties. For example, immunosensors and genosensors based on NMs explore the large surface area for the incorporation and protection a larger number of antibodies or DNA to decrease the LOD to fM levels for practical applicability. Compared with the progress in the previous configurations, cytosensors are still under development due to the complexity for specific detection and the low abundance of circulating tumor cells in blood.

Future efforts should be aimed at the portability and end-user applicability of the previously mentioned nanomaterials-based biosensors. Great progress in this direction have been made with the development of wearable biosensors, which can greatly benefit from the great properties of NMs for further development in the not-so-distant future.

Acknowledgments B. J-S acknowledges the Spanish Ministry of Innovation (PID2020-118154GB-I00) and Comunidad de Madrid (CM/JIN/2021-012) for funding.

References

Aliakbarinodehi N, De Micheli G, Carrara S (2018) Highly sensitive enzymatic MWCNTs-based biosensors for detection of abiraterone in human serum. BioNanoScience 8:675

Amiripour F, Ghasemi S, Azizi SN (2021) A novel non-enzymatic glucose sensor based on gold-nickel bimetallic nanoparticles doped aluminosilicate framework prepared from agro-waste material. Appl Surf Sci 537:147827

Arivazhagan M, Shankar A, Maduraiveeran G (2020) Hollow sphere nickel sulfide nanostructures–based enzyme mimic electrochemical sensor platform for lactic acid in human urine. Microchim Acta 187:468

Baek SH, Roh J, Park CY, Kim MW, Shi R, Kailasa SK, Park TJ (2020) Cu-nanoflower decorated gold nanoparticles-graphene oxide nanofiber as electrochemical biosensor for glucose detection. Mater Sci Eng C 107:110273

Cai C, Chen J (2004) Direct electron transfer of glucose oxidase promoted by carbon nanotubes. Anal Biochem 332:75–83

Chamorro-Garcia A, Merkoçi A (2016) Nanobiosensors in diagnostics. Nano 3:1849543516663574

Chandra, P. Nanobiosensors for personalized and onsite biomedical diagnosis. 2016

Chandra P, Noh H-B, Pallela R, Shim Y-B (2015) Ultrasensitive detection of drug resistant cancer cells in biological matrixes using an amperometric nanobiosensor. Biosens Bioelectron 70: 418–425

Coyle VE, Kandjani AE, Field MR, Hartley P, Chen M, Sabri YM, Bhargava SK (2019) Co_3O_4 needles on Au honeycomb as a non-invasive electrochemical biosensor for glucose in saliva. Biosens Bioelectron 141:111479

Daemi S, Ghasemi S, Akbar Ashkarran A (2019) Electrospun CuO-ZnO nanohybrid: tuning the nanostructure for improved amperometric detection of hydrogen peroxide as a non-enzymatic sensor. J Colloid Interface Sci 550:180–189

Darwish IA (2006) Immunoassay methods and their applications in pharmaceutical analysis: basic methodology and recent advances. Int J Biomed Sci 2:217–235

Dayakar D, Rao KV, Bikshalu K, Malapati V, Sadasivuni KK (2018) Non-enzymatic sensing of glucose using screen-printed electrode modified with novel synthesized CeO_2@CuO core shell nanostructure. Biosens Bioelectron 111:166–173

Ding J, Li X, Zhou L, Yang R, Yan F, Su B (2020) Electrodeposition of nickel nanostructures using silica nanochannels as confinement for low-fouling enzyme-free glucose detection. J Mater Chem B 8:3616–3622

Dong Q, Huang Y, Song D, Wu H, Cao F, Lei Y (2018) Dual functional rhodium oxide nanocorals enabled sensor for both non-enzymatic glucose and solid-state pH sensing. Biosens Bioelectron 112:136–142

Dong H, Cao L, Zhao H, Liu S, Liu Q, Wang P, Xu Z, Wang S, Li Y, Zhao P, Li Y (2020) “Gold-plated” IRMOF-3 and sea cucumber-like Pd@PtRh SNRs based sandwich-type immunosensor for dual-mode detection of PCT. Biosens Bioelectron 170:112667

Dong Q, Ryu H, Lei Y (2021) Metal oxide based non-enzymatic electrochemical sensors for glucose detection. Electrochim Acta 370:137744

Eom KS, Lee YJ, Seo HW, Kang JY, Shim JS, Lee SH (2020) Sensitive and non-invasive cholesterol determination in saliva via optimization of enzyme loading and platinum nano-cluster composition. Analyst 145:908–916

Fabiani L, Saroglia M, Galatà G, De Santis R, Fillo S, Luca V, Faggioni G, D’amore N, Regalbuto E, Salvatori P, Terova G, Moscone D, Lista F, Arduini F (2021) Magnetic beads combined with carbon black-based screen-printed electrodes for COVID-19: a reliable and miniaturized electrochemical immunosensor for SARS-CoV-2 detection in saliva. Biosens Bioelectron 171:112686

Farzin L, Sadjadi S, Shamsipur M, Sheibani S (2020) Electrochemical genosensor based on carbon nanotube/amine-ionic liquid functionalized reduced graphene oxide nanoplatform for detection of human papillomavirus (HPV16)-related head and neck cancer. J Pharm Biomed Anal 179:112989

Feng Y-G, Wang X-Y, Wang Z-W, Wang A-J, Mei L-P, Luo X, FENG J-J (2021) A label-free electrochemical immunosensor based on encapsulated signal molecules in mesoporous silica-coated gold nanorods for ultrasensitive assay of procalcitonin. Bioelectrochemistry 140:107753

Gladden LB (2004) Lactate metabolism: a new paradigm for the third millennium. J Physiol 558: 5–30

Gu H, Xing Y, Xiong P, Tang H, Li C, Chen S, Zeng R, Han K, Shi G (2019) Three-dimensional porous Ti3C2Tx MXene–graphene hybrid films for glucose biosensing. ACS Appl Nano Mater 2:6537–6545

Hu S, Lin Y, Teng J, Wong W-L, Qiu B (2020) In situ deposition of MOF-74(Cu) nanosheet arrays onto carbon cloth to fabricate a sensitive and selective electrocatalytic biosensor and its application for the determination of glucose in human serum. Microchim Acta 187:670

Jeong J-M, Yang M, Kim DS, Lee TJ, Choi BG, Kim DH (2017) High performance electrochemical glucose sensor based on three-dimensional MoS2/graphene aerogel. J Colloid Interface Sci 506: 379–385

Jia Y, Li Y, Zhang S, Wang P, Liu Q, Dong Y (2020) Mulberry-like Au@PtPd porous nanorods composites as signal amplifiers for sensitive detection of CEA. Biosens Bioelectron 149:111842

Keerthi M, Boopathy G, Chen S-M, Chen T-W, Lou B-S (2019) A core-shell molybdenum nanoparticles entrapped f-MWCNTs hybrid nanostructured material based non-enzymatic bio-sensor for electrochemical detection of dopamine neurotransmitter in biological samples. Sci Rep 9:13075

Koyappayil A, Berchmans S, Lee M-H (2020) Dual enzyme-like properties of silver nanoparticles decorated Ag2WO4 nanorods and its application for H2O2 and glucose sensing. Colloids Surf B: Biointerfaces 189:110840

Lei P, Zhou Y, Zhu R, Dong C, Wu S, Shuang S (2021) Facilely synthesized ultrathin Ni_6MnO_8@C nanosheets: excellent electrochemical performance and enhanced electrocatalytic epinephrine sensing. Sensors Actuators B Chem 326:128863

Li X, Peng G, Cui F, Qiu Q, Chen X, Huang H (2018) Double determination of long noncoding RNAs from lung cancer via multi-amplified electrochemical genosensor at sub-femtomole level. Biosens Bioelectron 113:116–123

Li Y-Y, Kang P, Huang H-Q, Liu Z-G, Li G, Guo Z, Huang X-J (2020) Porous CuO nanobelts assembly film for nonenzymatic electrochemical determination of glucose with high fabrication repeatability and sensing stability. Sensors Actuators B Chem 307:127639

Li S-S, Tan Y-Y, Zhang Y, Liu M, Liu A (2021) A simple electrochemical immunosensor based on worm-like platinum for highly sensitive determination of alpha-fetoprotein. Bioelectrochemistry 140:107804

Liu Y, Li H, Gong S, Chen Y, Xie R, Wu Q, Tao J, Meng F, Zhao P (2019) A novel non-enzymatic electrochemical biosensor based on the nanohybrid of bimetallic PdCu nanoparticles/carbon black for highly sensitive detection of H_2O_2 released from living cells. Sensors Actuators B Chem 290:249–257

Lynch PJ, Amorim Graf A, Ogilvie SP, Large MJ, Salvage JP, Dalton AB (2020) Surfactant-free liquid-exfoliated copper hydroxide nanocuboids for non-enzymatic electrochemical glucose detection. J Mater Chem B 8:7733–7739

Ma B, Kong C, Hu X, Liu K, Huang Q, Lv J, Lu W, Zhang X, Yang Z, Yang S (2018) A sensitive electrochemical nonenzymatic biosensor for the detection of H2O2 released from living cells based on ultrathin concave Ag nanosheets. Biosens Bioelectron 106:29–36

Ma C, Zhao C, Li W, Song Y, Hong C, Qiao X (2019a) Sandwich-type electrochemical immunosensor constructed using three-dimensional lamellar stacked CoS_2@C hollow nanotubes prepared by template-free method to detect carcinoembryonic antigen. Anal Chim Acta 1088:54–62

Ma E, Wang P, Yang Q, Yu H, Pei F, Li Y, Liu Q, Dong Y (2019b) Electrochemical immunosensor based on MoS2 NFs/Au@AgPt YNCs as signal amplification label for sensitive detection of CEA. Biosens Bioelectron 142:111580

Mahato K, Kumar A, Maurya PK, Chandra P (2018a) Shifting paradigm of cancer diagnoses in clinically relevant samples based on miniaturized electrochemical nanobiosensors and microfluidic devices. Biosens Bioelectron 100:411–428

Mahato K, Maurya PK, Chandra P (2018b) Fundamentals and commercial aspects of nanobiosensors in point-of-care clinical diagnostics. 3 Biotech 8:149

Manzanares-Palenzuela CL, Martín-Fernández B, Sánchez-Paniagua López M, López-Ruiz B (2015) Electrochemical genosensors as innovative tools for detection of genetically modified organisms. TrAC Trends Anal Chem 66:19–31

Mao W, He J, Tang Z, Zhang C, Chen J, Li J, Yu C (2019) A sensitive sandwich-type immunosensor for the detection of MCP-1 based on a rGO-TEPA-Thi-Au nanocomposite and novel RuPdPt trimetallic nanoalloy particles. Biosens Bioelectron 131:67–73

Mckeating KS, Aubé A, Masson J-F (2016) Biosensors and nanobiosensors for therapeutic drug and response monitoring. Analyst 141:429–449

Miller EW, Albers AE, Pralle A, Isacoff EY, Chang CJ (2005) Boronate-based fluorescent probes for imaging cellular hydrogen peroxide. J Am Chem Soc 127:16652–16659

Mohammadi J, Moattari A, Sattarahmady N, Pirbonyeh N, Yadegari H, Heli H (2017) Electrochemical biosensing of influenza A subtype genome based on meso/macroporous cobalt (II) oxide nanoflakes-applied to human samples. Anal Chim Acta 979:51–57

Moradi M, Sattarahmady N, Rahi A, Hatam GR, Sorkhabadi SMR, Heli H (2016) A label-free, PCR-free and signal-on electrochemical DNA biosensor for Leishmania major based on gold nanoleaves. Talanta 161:48–53

Nazari-Vanani R, Sattarahmady N, Yadegari H, Heli H (2018) A novel and ultrasensitive electrochemical DNA biosensor based on an ice crystals-like gold nanostructure for the detection of Enterococcus faecalis gene sequence. Colloids Surf B Biointerfaces 166:245–253

Nazari-Vanani R, Heli H, Sattarahmady N (2020) An impedimetric genosensor for Leishmania infantum based on electrodeposited cadmium sulfide nanosheets. Talanta 217:121080

Oliveira DA, Silva JV, Flauzino JMR, Sousa HS, Castro ACH, Moço ACR, Soares MMCN, Madurro JM, Brito-Madurro AG (2019) Carbon nanomaterial as platform for electrochemical genosensor: a system for the diagnosis of the hepatitis C in real sample. J Electroanal Chem 844: 6–13

Pak M, Moshaii A, Siampour H, Abbasian S, Nikkhah M (2020) Cobalt-copper bimetallic nanostructures prepared by glancing angle deposition for non-enzymatic voltammetric determination of glucose. Microchim Acta 187:276

Pallela R, Chandra P, Noh H-B, Shim Y-B (2016) An amperometric nanobiosensor using a biocompatible conjugate for early detection of metastatic cancer cells in biological fluid. Biosens Bioelectron 85:883–890

Pei Y, Hu M, Tu F, Tang X, Huang W, Chen S, Li Z, Xia Y (2018) Ultra-rapid fabrication of highly surface-roughened nanoporous gold film from AuSn alloy with improved performance for nonenzymatic glucose sensing. Biosens Bioelectron 117:758–765

Pei F, Wang P, Ma E, Yang Q, Yu H, Gao C, Li Y, Liu Q, Dong Y (2019) A sandwich-type electrochemical immunosensor based on RhPt NDs/NH_2-GS and Au NPs/PPy NS for quantitative detection hepatitis B surface antigen. Bioelectrochemistry 126:92–98

Purohit B, Vernekar PR, Shetti NP, Chandra P (2020) Biosensor nanoengineering: design, operation, and implementation for biomolecular analysis. Sens Int 1:100040

Qiao X, Arsalan M, Ma X, Wang Y, Yang S, Wang Y, Sheng Q, Yue T (2021) A hybrid of ultrathin metal-organic framework sheet and ultrasmall copper nanoparticles for detection of hydrogen peroxide with enhanced activity. Anal Bioanal Chem 413:839–851

Sabahi A, Salahandish R, Ghaffarinejad A, Omidinia E (2020) Electrochemical nano-genosensor for highly sensitive detection of miR-21 biomarker based on SWCNT-grafted dendritic Au nanostructure for early detection of prostate cancer. Talanta 209:120595

Sadighbayan D, Sadighbayan K, Khosroushahi AY, Hasanzadeh M (2019) Recent advances on the DNA-based electrochemical biosensing of cancer biomarkers: analytical approach. TrAC Trends Anal Chem 119:115609

Shajaripour Jaberi SY, Ghaffarinejad A, Omidinia E (2019) An electrochemical paper based nanogenosensor modified with reduced graphene oxide-gold nanostructure for determination of glycated hemoglobin in blood. Anal Chim Acta 1078:42–52

Shen L, Ying J, Ren L, Yao Y, Lu Y, Dong Y, Tian G, Yang X-Y, Su B-L (2019) 3D graphene-based macro-mesoporous frameworks as enzymatic electrodes. J Phys Chem Solids 130:1–5

Soleymani J, Hasanzadeh M, Somi MH, Shadjou N, Jouyban A (2019) Highly sensitive and specific cytosensing of HT 29 colorectal cancer cells using folic acid functionalized-KCC-1 nanoparticles. Biosens Bioelectron 132:122–131

Tang S, Shen H, Hao Y, Huang Z, Tao Y, Peng Y, Guo Y, Xie G, Feng W (2018) A novel cytosensor based on Pt@Ag nanoflowers and AuNPs/Acetylene black for ultrasensitive and highly specific detection of circulating tumor cells. Biosens Bioelectron 104:72–78

Tang Q, Zhang L, Tan X, Jiao L, Wei Q, Li H (2019) Bioinspired synthesis of organic–inorganic hybrid nanoflowers for robust enzyme-free electrochemical immunoassay. Biosens Bioelectron 133:94–99

Tashkhourian J, Nami-Ana SF, Shamsipur M (2018) A new bifunctional nanostructure based on two-dimensional nanolayered of $Co(OH)_2$ exfoliated graphitic carbon nitride as a high performance enzyme-less glucose sensor: impedimetric and amperometric detection. Anal Chim Acta 1034:63–73

Tran DT, Hoa VH, Tuan LH, Kim NH, Lee JH (2018) Cu-Au nanocrystals functionalized carbon nanotube arrays vertically grown on carbon spheres for highly sensitive detecting cancer biomarker. Biosens Bioelectron 119:134–140

Turner APF (2000) Biosensors – sense and sensitivity. Science 290:1315–1317

Updike SJ, Hicks GP (1967) The enzyme electrode. Nature 214:986–988

Vinoth V, Subramaniyam G, Anandan S, Valdés H, Manidurai P (2021) Non-enzymatic glucose sensor and photocurrent performance of zinc oxide quantum dots supported multi-walled carbon nanotubes. Mater Sci Eng B 265:115036

Wan Y, Su Y, Zhu X, Liu G, Fan C (2013) Development of electrochemical immunosensors towards point of care diagnostics. Biosens Bioelectron 47:1–11

Wang M, Shi M, Meng E, Gong F, Li F (2020a) Non-enzymatic glucose sensor based on three-dimensional hierarchical Co3O4 nanobooks. Micro Nano Lett 15:191–195

Wang Z, Zhang J, Jian R, Liao J, Xiong X, Huang K (2020b) Room temperature ultrafast synthesis of zinc oxide nanomaterials via hydride generation for non-enzymatic glucose detection. Microchem J 159:105396

Wongkaew N, Simsek M, Griesche C, Baeumner AJ (2019) Functional nanomaterials and nanostructures enhancing electrochemical biosensors and lab-on-a-chip performances: recent Progress, applications, and future perspective. Chem Rev 119:120–194

Xie J, Cheng D, Zhou Z, Pang X, Liu M, Yin P, Zhang Y, Li H, Liu X, Yao S (2020) Hydrogen peroxide sensing in body fluids and tumor cells via in situ produced redox couples on two-dimensional holey CuCo2O4 nanosheets. Microchim Acta 187:469

Xu W, Qin Z, Hao Y, He Q, Chen S, Zhang Z, Peng D, Wen H, CHEN J, QIU J, LI, C. (2018) A signal-decreased electrochemical immunosensor for the sensitive detection of LAG-3 protein based on a hollow nanobox-MOFs/AuPt alloy. Biosens Bioelectron 113:148–156

Xu J, Hu Y, Wang S, Ma X, Guo J (2020) Nanomaterials in electrochemical cytosensors. Analyst 145:2058–2069

Yaman YT, Akbal O, Bolat G, Bozdogan B, Denkbas EB, Abaci S (2018) Peptide nanoparticles (PNPs) modified disposable platform for sensitive electrochemical cytosensing of DLD-1 cancer cells. Biosens Bioelectron 104:50–57

Yoo E-H, Lee S-Y (2010) Glucose biosensors: an overview of use in clinical practice. Sensors (Basel, Switzerland) 10:4558–4576

Zhang R, Chen W (2017) Recent advances in graphene-based nanomaterials for fabricating electrochemical hydrogen peroxide sensors. Biosens Bioelectron 89:249–268

Zhang X, Lv H, Li Y, Zhang C, Wang P, Liu Q, Ai B, Xu Z, Zhao Z (2019) Ultrasensitive sandwich-type immunosensor for cardiac troponin I based on enhanced electrocatalytic reduction of H_2O_2 using β-cyclodextrins functionalized 3D porous graphene-supported Pd@Au nanocubes. J Mater Chem B 7:1460–1468

Zhang H, Liang F, Wu X, Liu Y, Chen A (2020) Recognition and sensitive detection of CTCs using a controllable label-free electrochemical cytosensor. Mikrochim Acta 187:487

Zhang L, Gu C, Wen J, Liu G, Liu H, Li L (2021) Recent advances in nanomaterial-based biosensors for the detection of exosomes. Anal Bioanal Chem 413:83–102

Zhao S, Zhang Y, Ding S, Fan J, Luo Z, Liu K, Shi Q, Liu W, Zang G (2019) A highly sensitive label-free electrochemical immunosensor based on AuNPs-PtNPs-MOFs for nuclear matrix protein 22 analysis in urine sample. J Electroanal Chem 834:33–42

Zhao P, Chen S, Zhou J, Zhang S, Huo D, Hou C (2020) A novel Fe-hemin-metal organic frameworks supported on chitosan-reduced graphene oxide for real-time monitoring of H_2O_2 released from living cells. Anal Chim Acta 1128:90–98

Nanomaterials for Biosensors

5

Luís M. C. Ferreira, Rodrigo V. Blasques, Fernando C. Vicentini, and Bruno C. Janegitz

Contents

1 Introduction: Use of Nanobiomaterials in Biosensors 92
2 Use of Gold Nanoparticles in Electrochemical Biosensors 93
3 Use of Magnetic Nanoparticles in Electrochemical Biosensors 94
4 Use of Carbon-Based Nanomaterials in Electrochemical Biosensors 95
5 Use of Hybrid Nanoparticles in Electrochemical Biosensors 98
6 Quartz Crystal Microbalance-Based Biosensors 99
7 Nanobiomaterials for Optical Analysis 100
8 Conclusion 105
References 105

Abstract

The current challenges in Analytical Chemistry have demanded the use of nanostructured materials associated with biomolecules, which have emerged as an essential strategy for the development of biosensors comprising many different analytical techniques. The nanobiomaterials have enabled the development of multifunctional analytical platforms by the combination of interesting features to improve analytical parameters, including high surface area, biocompatibility, specificity, and stability. Also, the possibility of increasing charge transfer rates and tuning of surface plasmons has been established as an exceptional tool for signal enhancement in electrochemical and optical analysis, respectively. This

---

L. M. C. Ferreira · F. C. Vicentini (✉)
Center of Nature Sciences, Federal University of São Carlos, São Carlos, Brazil
e-mail: fcvicentini@ufscar.br

R. V. Blasques · B. C. Janegitz (✉)
Department of Nature Sciences, Mathematics and Education, Federal University of São Carlos, São Carlos, Brazil
e-mail: brunocj@ufscar.br

© Springer Nature Singapore Pte Ltd. 2023

U. P. Azad, P. Chandra (eds.), *Handbook of Nanobioelectrochemistry*,
https://doi.org/10.1007/978-981-19-9437-1_5

chapter presents the recent achievements in the development of biosensors, emphasizing the inherent versatility and application for environmental monitoring, clinical diagnoses, and point-of-care analysis.

Keywords

Nanomaterials · Biosensors · Sample analysis · Electrochemistry

1 Introduction: Use of Nanobiomaterials in Biosensors

The use of nanobiomaterials in the development of biosensors has gained strength in recent years, particularly due to their outstanding features, including stability, biocompatibility, the possibility of miniaturization, and signal enhancement, presenting a great range of applications in several areas. In this sense, the use of nanosized materials, such as metallic nanoparticles, graphene, carbon nanotubes, quantum dots, and magnetic nanoparticles, has emerged as an expanding field of study. These materials function as sensor components owing to attractive physicochemical properties, such as high surface area (Paul and Sharma 2020), which is very desirable for immobilization of biomolecules, acting as a biorecognition element integrated within a transducing system. The wide group of proteins includes a collection of multifunctional elements that often appear as a preferable choice for attachment on the transducer's surfaces in biosensor manufacturing (Fig. 5.1). Enzymes, antibodies, and even structural proteins can carry the recognition of target molecules out through catalysis, affinity, or any signaling process that allows specific identification (Kurbanoglu et al. 2020; Zhu et al. 2020; Oliveira et al. 2020).

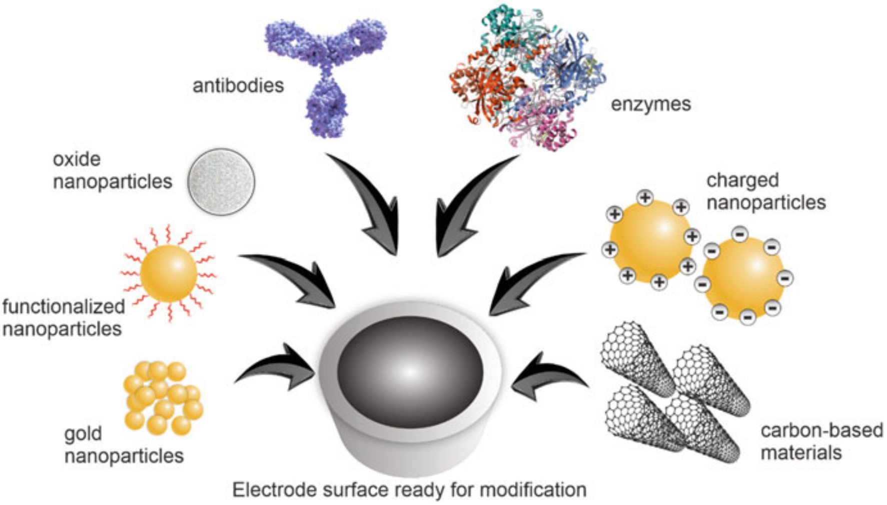
antibodies
enzymes
oxide nanoparticles
charged nanoparticles
functionalized nanoparticles
gold nanoparticles
carbon-based materials
Electrode surface ready for modification

Fig. 5.1 Construction of biosensors with nanobiomaterials

Thus, new electrochemical or optical devices containing nanomaterials associated with biological materials bring new perspectives that have triggered the interest of researchers. Nanobiomaterials have achieved promising results in terms of improved sensitivity, stability, low limits of detection, response speed, and noise reduction. For this reason, significant advances have been accomplished in environmental monitoring, food quality control, and especially in clinical analysis to diagnose infectious, congenital, and hereditary diseases.

2 Use of Gold Nanoparticles in Electrochemical Biosensors

Among the numerous nanoparticles explored for the development of nanobiomaterials, the gold nanoparticles (AuNPs) present great interest in the area of biosensors due to the low toxicity, surface reactivity, and localized surface plasmon resonance (LSPR) phenomena. The AuNPs can be purchased from commercial sources or synthesized in laboratories by simple or laborious procedures, according to the size and shape of interest, which significantly affect the sensor performance and the immobilization of biomolecules on the transducer surface. On this matter, the fabrication of biosensors has improved thanks to the functionalization of nanoparticles surfaces with different functional groups for further attachment of biomolecules. A enzyme biosensor based on an AuNP is combined with a multi-nanomaterial electrode film modified with acetylcholinesterase for the detection of the insecticide paraoxon (Jia et al. 2020). The device operated via differential pulse voltammetry (DPV) presented a current response of 0.49 V (vs. Hg/Hg_2Cl_{2sat}) during the hydrolysis process of acetylcholine chloride, in addition to a sensitivity of 4.44 uA μg^{-1} mL^{-1} and a limit of detection (LOD) of 0.0014 $\mu g\ mL^{-1}$. The use of nanobiomaterials led to improved catalytic processes, decreased toxicity, and greater efficiency in enzymatic immobilization methods. A label-free immunosensor proposed by Choosang et al. (2020) for the determination of human serum albumin (HSA) was built over a carbon screen-printed electrode (SPE) modified with ferrocene nanocomposite as an immobilized redox probe and AuNPs to anchor anti-HSA antibodies. The proposed sensor presented a LOD of 5.4×10^{-10} $\mu g\ mL^{-1}$ and showed stability of approximately 30 days. Label-free immunosensors do not require markings to detect target molecules, having an advantage over another electrode framework by simplifying the assembly process. Since the labeling steps are eliminated, the time and reagent consumption are reduced. Other examples of immunosensors for HSA detection are described in Table 5.1.

Also developing label-free immunosensors, Zhao et al. (2019) determined the nuclear matrix protein 22 in urine samples, using AuNPs in conjunction with platinum nanoparticles (PtNPs). The target protein is a urinary biomarker used in bladder cancer detection and its monitoring is essential for diagnosis and prevention. The authors' work demonstrated a LOD of 1.7 pg mL^{-1} and was considered a reliable approach for the detection of protein biomarkers in urine. Proteins can also be determined using electrochemical biosensors, as they combine the advantages of simplicity, low background signal, and high sensitivity. This way, the work of Liu

Table 5.1 Comparison of different electrochemical immunosensors for HSA

Electrode materials	Detection	Linear range	LOD	References
Ab/AuNPs/HDT/AuNPs/MWCNT-CILE	EIS	0.1 to 100 μg mL^{-1}	15.4 ng mL^{-1}	Arkan et al. (2014)
Ab/PS-Ag/SPCE	EIS	30 to 300 μg mL^{-1}	1.0 μg mL^{-1}	Shaikh et al. (2019)
Ab/COOH-SPCE	Amperometry	10 to 300 μg mL^{-1}	9.77 μg mL^{-1}	Tsai et al. (2016)
Ab/AuNPs/PVA/SPCE	DPV	2.5 to 200 μg mL^{-1}	25 μg mL^{-1}	Omidfar et al. (2011)
Ab/AuNPs/TU/AuNPs/Pty/Au	Capacitive	6.8×10^{-12} to 6.8×10^{-3} mg L^{-1}	6.8×10^{-15} mg L^{-1}	Samanman et al. (2012)

Ab antibodies, *AuNPs* gold nanoparticles, *HDT* 1,6-hexanedithiol, *MWCNT* multi-walled carbon nanotube, *CILE* carbon ionic liquid electrodes, *EIS* electrochemical impedance spectroscopy, *PS* polystyrene, *Ag* silver, *SPCE* screen-printed carbon electrode, *COOH* carboxylic acid, *PVA* polyvinyl acetate, *TU* thiourea, *Pty* poly-tyramine, *Au* gold electrode, *DPV* differential pulse voltammetry

et al. (2018) demonstrates the detection of C-peptide through the functionalization of AuNPs with a LOD of 14.2 ng L^{-1}. Recent advances in nanobiotechnology for the development of biosensors with virus detection capability, such as MERS-CoV and SARS-CoV-2, are addressed (Qiu et al. 2020; Layqah and Eissa 2019).

3 Use of Magnetic Nanoparticles in Electrochemical Biosensors

The use of magnetic nanoparticles (MNPs) has increased in the electrochemistry field due to the versatility of applications, their varied size from nm to μm, and intrinsic properties, such as super magnetic behavior and high saturation magnetization (Nkurikiyimfura et al. 2020), which allowed the advance of new analytical methodologies for biomedical analysis. MNPs applied in electrochemistry accelerate analytical signal transduction, reflecting as a sensitivity gain of biosensors in the detection of various analytes. For its synthesis, several processes are described in the literature, such as the synthesis in microemulsions (Chin and Yaacob 2007), synthesis through electrospray (Basak et al. 2007), electrodeposition (Janegitz et al. 2012) flow injection (Salazar-Alvarez et al. 2006), and microfluidic flow (Abou-Hassan et al. 2010). All the synthetic routes are performed according to the system's need to the function of MNPs, aiming for better dispersion and biocompatibility by the attachment of proper functional groups. In consequence, the use of MNPs shows great potential in the development of biosensors, by increasing their sensitivity and stability for the detection of pathogenic targets, in addition to facilitating the process of immobilization of enzymes. In this context, He et al. (2020) immobilized the enzyme tyrosinase (Tyr) in GCE with biochar nanoparticles (BCNPs) functionalized with Fe_3O_4 nanoparticles (MNPs) and carboxylic functional groups (-COOH). Due to the biocatalytic activity to Tyr and conductivity provided by BCNPs, the bisphenol A detection signal was significantly improved, presenting a limit of detection (LOD) of 2.78 nM with linear ranges from 0.01 to 1.01 μM. Other examples of Tyr immobilization in Fe_3O_4-chitosan magnetic nanoparticle compounds are described recently (Zhou et al. 2018; Polatoğlu 2019). The MNPs can also be used for the detection of protein biomarkers in the detection of varieties of cancer due to synergic exploration in electrochemical biosensors. As previously mentioned, the size and three-dimensional shapes of MNPs can provide excellent versatility for bioassays with biomolecules of different sizes. Once the biosensor surface has been modified, the use of an external magnet favors the maneuvering of the magnetic nanoparticles together with the genetic material at the base of the transducer, thus reducing additional modification steps. In this perspective, Luo et al. (2020) presented the use of magnetic nanospheres remodeled with anti-EpCAM for the detection of circulating tumor cells (CTSs) of breast cancer MCF-7. The CTCs were isolated on the transducer surface of a photoelectrochemical biosensor. The photoelectrochemical method in this perspective gains prominence in the development of biosensors since it opens possibilities in the improvement of sensitivity and by presenting a low noise signal. Its operation occurs through an excitation source, where it is possible to project such devices to detect signal transduction on the surface of organic and inorganic materials, using potentiometric or amperometric detection.

4 Use of Carbon-Based Nanomaterials in Electrochemical Biosensors

High-performance electrochemical biosensors require electrode materials owing to high conductivity and fast electron transfer rate, as well as a substrate that allows the easy anchoring of biomolecules. These characteristics are essentially found in carbon-based materials containing sp^2 hybridization with the elevated number of conjugated atoms and endowed with appreciable surface area, such as carbon nanotubes (Janegitz et al. 2011), graphene (Janegitz et al. 2017), and, the least known, carbon black (Vicentini et al. 2016) (Fig. 5.2).

Graphene, for example, is a semi-infinite-sized one-atom-thick 2D-foil, which makes its surface area incredibly high. Such a property associated with the equally notable conductivity enables the development of third-generation electrochemical biosensors (López Marzo et al. 2020; Díaz Nieto et al. 2018). Graphene also presents two different derived forms: graphene oxide (GO) and reduced graphene oxide (rGO). GO has an increased interlayer space and is rich in oxygenated functional groups that give greater hydrophilicity and good capacity for protein binding, both covalently and electrostatically. Meanwhile, having a reduced oxygen content, rGO is endowed with better electrical conductivity, around eight orders of magnitude larger than GO. The choice of graphene form will depend, of course, on the sensor purpose (Taniselass et al. 2019; Felix et al. 2015).

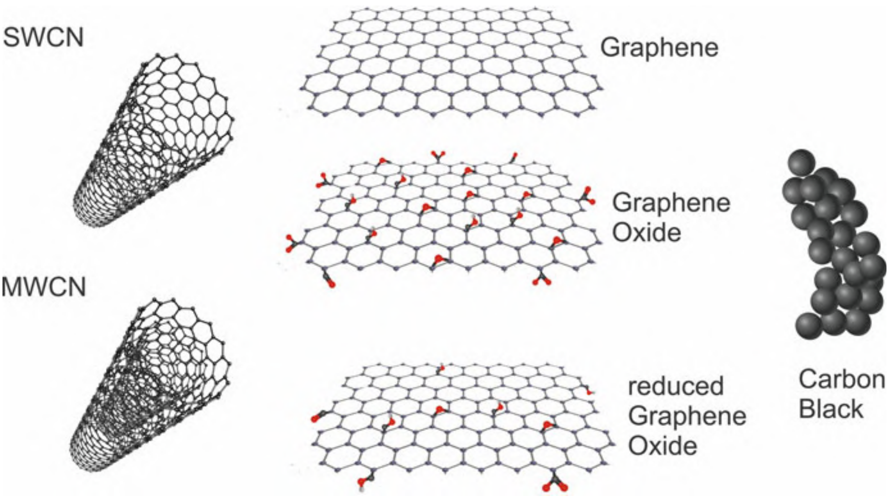

Fig. 5.2 Carbon-based nanomaterials for manufacturing of protein-based biosensors

Reduced graphene oxide (rGO) was applied together to Fe_3O_4 magnetic nanoparticles for the determination of glucose by a third-generation biosensor proposed by Pakapongpan and Poo-arporn, including a novel enzyme immobilization procedure based on electrostatic pairing between positively charged F_3O_4 and negatively charged glucose oxidase (GOx) at pH 7.0 (Pakapongpan and Poo-Arporn 2017). Third-generation biosensors are known for the ability to promote direct electron transfer between enzyme cofactor and the electrode surface. In this case, intensive electrochemical characterization suggested that rGO directly exchanges charge with GOx from flavin adenine dinucleotide (FAD). However, Bartlett and Al-Lolage recently claimed that it lacks strong evidence to support the hypothesis of direct charge transfer between GOx and carbon materials such as graphene and nanotubes (Bartlett and Al-Lolage 2018). Regarding enzyme-based biosensors, GOx is usually presented as a general model for new analytical methodologies, especially due to its robustness towards abrupt oscillations in the chemical environment. Also, they have been provided easy probing for either electrochemical or spectroscopic techniques and has a well-known reaction mechanism. Once this model is revealed to be promising, it turns into a "proof of concept" that can be applied to other enzymatic reactions or protein interactions.

Exploiting the presence of high-numbered oxygenated terminal groups in GO, Kazemi et al. (2016) reported an impedimetric immunosensor for the detection of cardiac troponin I, a biomarker protein for heart attack. In this work, GO was converted into a porous nanosheet framework, preserving the oxygenated groups. The resulting porous graphene oxide (PrGO) is endowed by a larger surface area compared to non-treated GO, increasing the efficiency of immobilization of anti-cardiac troponin I immunoglobulin on GCE by the covalent attachment of amino-terminated antibody and carboxyl-terminated PrGO. The performance of the immunosensor was evaluated by cyclic voltammetry and electrochemical impedance spectroscopy, showing a significant intensification of charge transfer resistance in the presence of the target protein, indicating the biorecognition response. Further study of analytical performance resulted in a wide linear concentration range from 0.1 to 10 ng mL^{-1} and a LOD of 0.07 ng mL^{-1}. Additionally, the evaluation of potential interfering of serum albumin and myoglobin showed that the sensor was suitable for analysis of blood samples.

As a noteworthy nanomaterial, carbon nanotubes (CNT) have physicochemical properties similar to graphene, which differ in conformational structure. CNT are based on a tubular framework built through rolled concentric graphene foils, generating the called multiple-walled carbon nanotubes (MWCNT) (Vicentini et al. 2013). Or, they can be found as a single sheet or simply a single-walled carbon nanotube (SWCNT), being both attractive as biosensor material and being able to undergo a functionalization process to immobilize biomolecules (Arduini et al. 2014; Liu et al. 2005; Ortolani et al. 2019). To demonstrate the possibilities of this material, Gulati et al. (2019) and Silva et al. (2014) used vertically aligned MWCNT dispersed on a flexible PET substrate to produce an impedimetric immunosensor for leukemia-related K-562 cells. The modification process started with the treatment of nanotubes with oxygen plasma, to provide oxygenated groups and improve antibody covalent attachment. The extensive morphological characterization analysis of the resulting electrode showed that the aligned framework of MWCNT allowed an increased surface area and electron transfer, resulting in a larger charge transfer resistance variation response. The sensor presented a very extensive linear range of 1.5×10^2 to 1.5×10^7 cells mL^{-1} and a striking LOD of 10 cells mL^{-1}, demonstrating its suitability to perform diagnostic analysis.

The underexplored carbon material is carbon black (CB), which emerges as a non-expanse alternative for electrode fabrication. CB is a petroleum-derivative nanoparticle-like material with particle size varying between 3 and 100 nm, and it is generally found in industrial process applications, presenting comparable features to graphene and CNT, including high electrical conductivity and elevated surface area. The interest in CB rises to supply the increasing demand for fast, low cost, disposable/reusable, and reliable analytical devices for diagnosis and substances of environmental interest. For this reason, CB has been subjected to study for its application in the production of electrochemical analytical devices. Additionally, CB has high adsorption potential and its structure contains oxygenated functional groups localized on its edges that allow the functionalization by the anchoring of other molecules, which confers great suitability for the development of biosensors (Silva et al. 2017; Laurinavicius et al. 2013; Ma et al. 2007).

The use of CB on enzyme-based biosensors has already been reported. Arduini et al. (2014), for example, proposed detection of paraoxon through its inhibition activity over the butyrylcholinesterase. The enzyme was immobilized on CB nanoparticles using glutaraldehyde as a cross-linking agent to produce a modified SPE. In this system, the analytical signal was based on the variations of the oxidation current by using the electrochemical probe thiocholine, the main product of enzymatic hydrolysis of butyrylcholine. The sensor also presented an excellent response for thiocholine oxidation, which occurred at lower potential (300 mV vs. Ag ink) when compared to bare SPE and other electrode modified with carbon nanomaterials, including carbon nanotubes CNT and rGO (Liu et al. 2005; Li et al. 2013). Also, the biosensor was successfully applied to the analysis of the organophosphate in waste and drink water samples with no pretreatment, showing a LOD of 5 μg L^{-1}, as well as presenting high operation and shelf stability.

Xiao-He et al. (2007) studied the efficiency of GOx immobilization on aniconic polymer-grafted CB supported on hydrophilic fumed SiO_2 nanoparticles as hybrid material for modification of carbon paste SPE. They managed how to manipulate the material architecture to improve the conformational exposure of hydrophilic and hydrophobic regions of GOx. The resulting material was evaluated to enhance the enzymatic kinetic process and to achieve a better electrode response in chronoamperometric assay.

Quantum dots are also excellent platforms for electrochemical detection of tumor biomarkers. For example, Hasanzadeh et al. (2018) proposed a voltammetric immunosensor for ultrasensitive detection of cancer antigen 15-3 (CA15-3) in unprocessed human plasma and lysates of breast cancer cells MCF-7 using electrochemical gold nanospheres (AuNSs) mounted on violated GQDs. The immunosensor has shown a LOD of 0.11 U mL^{-1}, demonstrating considerable analytical performance. Liu et al. (2013), in the same perspective, proposed an amperometric enzymatic immunosensor amplified sensitivity for the determination of the tumor marker alpha-fetoprotein (AFP) with a set layer by layer of poly (3,4-ethylenedioxythiophene) (PEDOT)/nano-Au/Azure I/ZnSe QDs on the surface of the Pt electrode. The immunosensor exhibited high sensitivity, fast analytical time, a low LOD of 1.1×10^{-6} ng mL^{-1}, and an impressive linear range response to AFP from 5×10^{-5} to 250 ng mL^{-1}. Another example of immunoassay was performed by Liu et al. (2016) for the detection of Golgi-73 protein, a biomarker for the liver tumor, using quantum points of CdTe/CdS modified with manganese. First, CdTe/CdS QDs modified with Mn functionalized with carboxylic were synthesized. Then, the A/G protein agarose granules were specifically combined with the Ab conjugated with QDs to form the QD-Ab-granules conjugate. The biosensor presented the clinical testing potential for the Golgi-73 biomarker with a LOD of 10 ng mL^{-1}. It has been observed in the cited examples of immunosensors that these may vary according to the type of transducer used as well as the type of antigen and antibody immobilized on the surface of the transducer.

5 Use of Hybrid Nanoparticles in Electrochemical Biosensors

Other examples of nanomaterials used in biosensors are oxide/hydroxide-based hybrid nanoparticles, which have demonstrated innovative ideas in the field of materials science. This interest is related to the fact that metallic oxide or hydroxide nanostructures present interesting applications for the manufacture of optical, electronic, and electrochemical devices on a miniaturized scale. Before the synthesis of these nanostructures, the bandgap and pore size distribution must be taken into consideration, because in this way, it is possible to orient the material in different matrices and quantitative analytical applications in electrochemical analysis. These nanoparticles can be synthesized from the reduction of a metallic precursor or by processing routes such as hydrothermal, coprecipitation, chemical decomposition, electrodeposition, and sol-gel. The sol-gel method stands out, considering several factors, such as the ease of preparation (high purity and homogeneity), the acid characters of Brønsted and Lewis, those of high surface area and high thermal and chemical stability (Blasques et al. 2020; Martins et al. 2014). Based on the characteristics addressed, the work of Peng et al. (2014) develops a new platform for the manufacture of a glucose biosensor, where it was built by imprisoning GOx in an organically modified (ormosil)/chitosan (CS)/graphene oxide nanocomposite. The graphene acted as support in the GO immobilization process, as well as in the promotion of electron transfer on the electrode/solution surface. The biosensor designed for glucose displayed a wide and useful linear range of 0.02–5.39 mM with a low LOD of 6.5 μM. Another work was presented by Kochana et al. (2015), where a tyrosinase (Tyr) based biosensor for bisphenol A (BPA) detection in a loop-flow system was developed. The Tyr was trapped in the sol-gel matrix of modified TiO_2 with MWCNTs and Nafion. The MWCNTs facilitated the electrical conductivity of the material and helped in the enzyme immobilization. Other researchers have reported the use of metal oxides synthesized in sol-gel matrices, such as Glezer and Lev (1993), which took advantage of the high conduction of vanadium pentoxide to project a glucose biosensor. Liu et al. (2003) proposed a new enzyme biosensor based on a mesoporous matrix of ZrO_2. Zirconia was chosen by the authors due to its excellent chemical inertness and biocompatibility, as well as its acidic and basic properties. It should be noted that in all the synthesis routes presented, some desirable characteristics should be taken into consideration, such as pore volume, high surface area, type of porosity (microporous, mesoporous, and macroporous), leading to a better cost-benefit for immobilization of enzymes.

6 Quartz Crystal Microbalance-Based Biosensors

Quartz crystal microbalance (QCM) is also an example of the usual system in the development of interfacial-based analysis and that with the combination of nano-biomaterials has presented performance improvements regarding sensitivity and selectivity for the detection of several analytes. QCM is an analytical technique that is based on piezoelectric principle, where typically occurs a gravimetric loading on a quartz crystal surface, leading to a decrease in the resonant oscillation frequency of the crystal, which is interpreted as mass variation proportional to the load (Dayal et al. 2019). However, other mechanical properties, including density and viscoelasticity can also be tracked by this technique, as well as the dynamics of interfacial chemical events. This working principle allows that specific affinity interactions between the piezoelectric surface and a target molecule to be monitored with no trouble, making QCM platforms a very convenient transducer for protein-based biosensing, especially for label-free immunosensors.

To mediate and improve the interactions of the crystal surface, nanomaterials arise as an important component for piezoelectric biosensor manufacturing, since they can provide an extensive matrix that facilitates biomolecules attachment. Additionally, the typical increase of surface area assigned to nanoparticles directly affects the number of binding sites, yielding significant signal amplification. Considering such characteristics and principles, Pohanka established a piezoelectric biosensor based on magnetic nanospheres for the detection of tumor necrosis factor-alpha (TNFα) (Pohanka 2018). In this study, the immobilization of the antibody TNFα on the surface of the QCM sensor was reported, where it demonstrated a LOD of 1.62 pg mL^{-1}. Following the same principle of the previous work, Pirich et al. (2017) used a piezoelectric immunochip coated with cellulose crystal nanofilm for the detection of the NS1 antigen of dengue fever.

Besides the great applicability for immunosensor development, the association of metallic nanoparticles with QCM also has been shown to be suitable for building enzymatic biosensors. Since enzyme-substrate reaction can induce secondary events that change the oscillating crystal frequency, a readable signal can be produced for specific biochemical recognition of target molecules. A compelling methodology centered on this principle was presented in a study conducted by Park and Lee (2018), where the signal response of enzymatic biosensor for the detection of glycated hemoglobin (HbA1c) was based on mass changes caused by the increase in the size of the AuNPs attached on the sensor surface via conjugated thiol terminated self-assembled monolayers. The nanoparticle enlargement was triggered by a reaction catalyzed by the enzyme fructosyl amino acid oxidase, which uses HbA1c as the substrate for proteolytic digestion, H_2O_2 in a media containing Au^{3+} ions that are readily reduced to metallic form and deposited on nanoparticles surfaces that act as nucleation sites for Au staining. The QCM HbA1c enzymatic assay was applied in whole blood analysis, achieving a LOD of 0.147% related to the total hemoglobin. Although the studied HbA1c concentration range (4.61–13.5%) presented a nonlinear behavior, the presented methodology has shown enough sensitivity and reproducibility, being considered a useful platform for clinical analysis.

7 Nanobiomaterials for Optical Analysis

While in electrochemistry metallic nanoparticles offer interesting applications with the aim of increase of electroactive area, promote the arising of electrocatalyst sites, and speed up charge transfer rate to improve analytical features, in spectroscopic techniques, they can have valuable use to generate and/or significantly intensify analytical signal through localized surface plasmon tuning. Optical techniques based on surface-enhanced Raman scattering (SERS) and localized surface plasmon resonance (LSPR) can use space-confined electrical oscillations on nanoparticles surfaces caused by incident radiation to investigate variations in the localized chemical environment. Furthermore, resonating plasmon absorption in the visible spectrum associated with metallic nanostructures, especially gold and silver nanoparticles, may occasionally be useful for colorimetric analysis. Conventional surface plasmon resonance (SPR) spectroscopy can also gain improvements by using nanomaterials, like signal enhancement by inducing LSPR phenomena, or promoting feasibility for biomolecules attachment (Mohammadzadeh-Asl et al. 2018).

Metal nanoparticles comprise a range of important substrates for SERS. The eventual attachment of a molecule on nanoparticles can create a Raman hot spot, that is, micro- or nanosized restricted regions localized on the metallic surface with high roughness, such as nanoparticles, where there is intense local field enhancement. The localized surface plasmon interaction with incident radiation is considered to be the main cause of this produced enhancement (McNay et al. 2011). Moreover, the light absorption of the same localized plasmons can give information of molecular targets by changes in absorption patterns as they interact with the surface of the nanoparticles. This information is interpreted as small changes in the absorbance wavelength. That is the basis of LSPR spectroscopy. On the other hand, conventional SPR signal is acquired from changes in minimum reflection angle on incident light source due to local refractive index indicating variations on surface plasmon profile caused by adsorptive interactions of interesting species with the surface of a continuous metal layer.

Returning to glucose enzymatic analysis, it is known that most methodologies for GOx-based glucose detection are based on H_2O_2-derived signals due to its high reactivity and a countless number of reactions that can be managed to generate the analytical response. In this way, H_2O_2 reactions combined with metallic nanostructures were extensively explored to produce SERS hot spots (Zhong et al. 2019; Fu et al. 2017). Gu et al. (2016) established a novel H_2O_2 approach to analyze glucose in urine using boronic acid-derived thiol to modify gold nanospheres (Au-NS) by covalent attachment. The functionalizing molecule reacts with H_2O_2 generating a phenol-terminated Au-NS. Moreover, due to the high specificity of this reaction, the method may be suitable for other oxidases since catalytic oxidation of their substrates also results in H_2O_2 generation.

An interesting concept of controlling chemical environment was developed by Sun and co-authors for indirect detection of glucose in blood serum (Sun et al. 2017), attaching GOx electrostatically to silver nanospheres (Ag-NS) negatively charged by functionalization with the cationic poly(dimethyl diallyl ammonium). As the SERS signal response was based on chromophore group FAD present in the enzyme, the mechanism of "*turning off*" Raman signal was triggered by the generation of localized acidic environment post-enzymatic reaction: glucose is converted to gluconic acid, leading to pH dropping below GOx isoelectric point, causing electrostatic impairment. The signal quenching produced by enzyme detachment from Ag-NS showed to be proportional to glucose concentration in a linear range from 2.0 to 14.0 mM, reaching a LOD of 1.0 μM.

The wide applicability of metallic nanoparticles in optical-based analytical techniques is due to their unique tunable plasmonic properties. Localized plasmon oscillations can be easily tweaked by controlling either size, shape, or aggregation state, which are related to variations in electronic conduction band arrangement and plasmon-plasmon interactions. Moreover, plasmonic tuning can also be achieved by functionalization of nanoparticle surfaces, which changes the local refractive index and, therefore, their plasmonic pattern. Those endeavors will significantly change the absorption wavelength of nanoparticles, and this change can be easily monitored.

In this way, one of the first experimental changes is often observed in plasmon light absorption, which mostly occurs at visible or near-infrared regions when we talk about silver and gold nanomaterials. This property can be managed in other to develop very simple but highly sensitive analytical assays, like the one presented by Zhang et al. (2020) for glucose determination in urine samples that exploited the generation H_2O_2 by GOx/glucose reaction to oxidizing I^- to I_3^-, creating a controlled corrosive environment that changes the shape of gold nanobipyramids (AuNBPs), that particularly own a strong local electric field enhancement (Chow et al. 2019; Lin et al. 2019; Bhardwaj et al. 2021). The oxidative process leads to different nanostructures derived from AuNBPs according to glucose concentration causing significant alteration on the visible light LSPR spectrum that can be detected by eyes: longitudinal surface plasmons of AuNBP show a pronounced band at 800 nm that suffers a blue shift as the axial tips start etching in the presence of small concentrations of glucose, reaching a maximum shift at 520 nm. Throughout this process, a polychromic change of the dispersion is visually detected from pale brown to yellow, blue, purple, and finally to red, indicating glucose saturation. Additionally, a visual sensitivity scale was presented and a linear range for glucose concentration was evaluated by instrumental analysis of wavelength shift. Moreover, the proposed procedure presented no need for enzyme attachment on the surface of the nanoparticles.

A considerable number of studies involving colorimetric LSPR are available (Zhang et al. 2016; Russell and de la Rica 2018; Tang and Li 2017). However, a protein-mediated control of the morphological states of nanoparticles can create a highly specific colorimetric probe for biosensing, as summarized in Fig. 5.3. Exploring protein functionality, such as specific binding or catalysis, has demonstrated a great potential for point-of-care colorimetric analysis, especially for diagnosis and environmental measurements. To illustrate this potential, a variety of works involving LSPR-based colorimetric analysis is summarized in Table 5.2.

Protein interactions can also be employed to initiate aggregation of nanostructures to promote analyte concentration-dependent modulation of LSPR since the electromagnetic field of the assembly differs significantly from a single particle, as well as the number and the relative position of particles aggregated (Fan et al. 2010). Metal nanoparticles can produce clusters by electrostatic interactions or specific molecular bonding which can be achieved by antibody/antigen pairing, which turns out to be very convenient to the development of immunosensor. In this way, a simples methodology for SARS-CoV-2 detection was released by Della Ventura et al. (2020) based on absorbance quenching at 560 nm of antibody-functionalized AuNPs that aggregate throughout the virus surface, creating an active AuNP layer with distinct characteristics that causes a wavelength redshift. The alterations on the absorbance profile are observed as a color change of the dispersion from red to purple. The immunoglobulins for biorecognition of spike, envelope, and

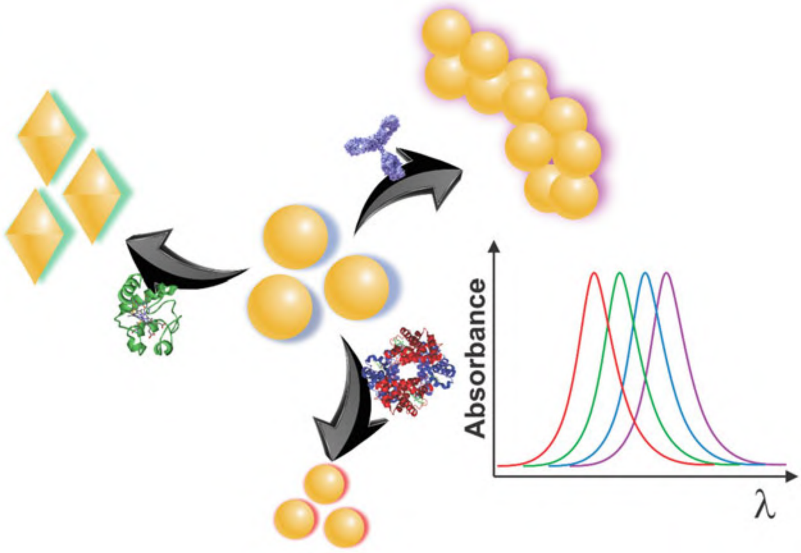

Fig. 5.3 Control management of protein systems can induce changes in metallic nanoparticles morphology, including size, shape, and aggregation state, leading to readable changes in LSPR absorption pattern

Table 5.2 Comparison of different LSPR-based colorimetric methodologies

Nanostructured material	Biomaterial	Analyte	LSPR-inducing mechanism	LOD	References
AuNBPs	Gox	Glucose	Particle etching	0.34 μmol L^{-1}	Zhang et al. (2020)
Ag nanoprisms	Gox	Glucose	Particle etching	0.20 μmol L^{-1}	Xia et al. (2013)
AgNPs	Ascorbic acid-2-phosphate	Alkaline phosphatase	Particle growth	0.50 pmol L^{-1}	Guo et al. (2016)
AuNPs	Antibody set	SARS-CoV-2	Aggregation	$C_t = 36.5^a$	Della Ventura et al. (2020)
AuNPs	Anti-EV71 immunocomplex	Enterovirus 71	Particle growth	0.65 ng mL^{-1}	Xiong et al. (2017)

AuNBPs gold nano bipyramids, *GOx* glucose oxidase, *AgNPs* silver nanoparticles, *AuNPs* gold nanoparticles, *SARS-CoV-2* severe acute respiratory syndrome coronavirus 2, *EV71* enterovirus 71

[a] Ct: cycle threshold, in PCR analysis, is the number of cycles needed for the fluorescent signal to exceeds the background. Ct level is inversely proportional to the amount of target molecule

membrane proteins were attached to AuNPs by photochemical immobilization technique that allows direct binding with no need of crosslinkers (Della Ventura et al. 2019), generating three different functionalized nanospheres. The colorimetric immunoassay was compared to conventional real-time polymerase chain reaction analysis (PCR). The proposed assay could detect significantly low virus loads, allowing to distinguish different stages of contamination.Immuno-sensorial platforms based on antibody-functionalized nanoparticles have also demonstrated good feasibility for implantation in SERS probing (Wang et al. 2017). An antibody capturing of analytes can create either a high specificity or signal amplification for ultrasensitive detection by creating new bonds over nanoparticle-induced hot spots. Furthermore, molecular attachments on functionalized nanoparticle surfaces caused by biorecognition lead to readable changes on the local refractive index that can be easily verified via LSPR. Those features offer great applicability in targeting specific biomarkers that are found in a trace level range that eventually are demanded in disease screening (Rissin et al. 2010).

An interesting concept demonstrating human IgG and streptavidin detection at the picomolar range was presented by Campu et al. (2018) using dual detection via SERS and LSPR. This approach is also an excellent example of how functionalization can significantly affect the plasmonic behavior of nanostructures. The group demonstrated how they manage to functionalize selectively AuNBP tips with para-aminothiophenol for further attachment of anti-IgG and biotin for analyte recognition. The choice of AuNBPs is related to the sharp tips that endow them with a singular plasmonic enhancement, as we discussed in the previous colorimetric methodology for glucose detection. The enhanced field is localized at the tips of AuNBP, which provides a distinct longitudinal plasmon absorbance spectrum with high sensitivity, providing the required setting to detect very small changes on the local refractive index arising from antigen capture.

Although metallic nanoparticles have been predominantly favored for their direct plasmonic response as substrates in optical analytical techniques, oxide nanoparticles have proven to be quite interesting for SPR analysis. Zinc oxide, for example, is a transparent material with a high refractive index, which is very convenient in approaches to increase sensitivity in fiber optic-based probing in SPR (Li et al. 2010; Zhang et al. 2018, 2019). Fiber-optic sensors have been described to perform exceptionally due, among many features, to the possibility of miniaturization and development of small probes, especially for continuous monitoring of chemical species in clinical applications. Indeed, when the wavelength of incident radiation reaches the metallic surface, the light absorption by the resonating metal plasmons leads to a dropping in the reflected light intensity, which is detected as an absorbance response by a spectrometer (Liu et al. 2021; Usha et al. 2016).

When it comes to oxide materials for SPR, ZnO is one that allows relatively easy control of particle dimensions at nanosized levels, and, due to its high isoelectric point, a simple approach for electrostatic protein attachment can be carried out for GOx at physiological pH, just as the methodology purposed by Usha et al. (2016), where GOx was immobilized on a ZnO nanorod-coated silver layer covering the fiber optic pathway. The SPR signal arises from changes in local refractive index in the fiber surroundings promoted by reactive interaction between glucose and GOx and interpreted as absorbance changes at the detector. This multilayer probe was applied to detect abnormal glucose blood levels below 2.2 mM, owing to a LOD of 0.012 mM, acting as a supporting tool for insulinoma diagnosis, a rare pancreatic carcinogenic condition.

8 Conclusion

To adress the new demands in analytical chemistry by exploring the boundaries of this field, the use of nanostructured materials associated with biomolecules has emerged as an essential strategy for the development of biosensors based on different analytical techniques. The advantage of the so-called nanobiomaterials lies in the combination of electrical and optical properties associated with intrinsic surface phenomena of nanosized materials and the specificity of biomolecules, which allows the precise recognition of target species, enabling the development of multifunctional sensing platforms endowed with improved analytical parameters, including high sensitivity, detectability, selectivity, and stability. Moreover, the possibility of increasing charge transfer rates and tuning surface plasmons has clearly been set up as an exceptional tool for signal enhancement in electrochemical and optical analysis, respectively.

The overview presented here illustrates the recent achievements in biosensors application, emphasizing the inherent versatility and application for environmental monitoring, clinical diagnoses, and point-of-care analysis. Some of these applications are, at this moment, well consolidated, and many others are still at an early stage of development, indicating a continuous growth of this research field in the coming years, with the development of new proof-of-concept systems and therefore new solutions for analytical issues and new strategies for real-life applications.

References

Abou-Hassan A, Sandre O, Cabuil V (2010) Microfluidics in inorganic chemistry. Angew Chem Int Ed 49(36):6268–6286. https://doi.org/10.1002/anie.200904285

Arduini F, Forchielli M, Amine A, Neagu D, Cacciotti I, Nanni F, Moscone D, Palleschi G (2014) Screen-printed biosensor modified with carbon black nanoparticles for the determination of paraoxon based on the inhibition of butyrylcholinesterase. Microchim Acta 182(3–4):643–651. https://doi.org/10.1007/s00604-014-1370-y

Arkan E, Saber R, Karimi Z, Mostafaie A, Shamsipur M (2014) Multiwall carbon nanotube-ionic liquid electrode modified with gold nanoparticles as a base for preparation of a novel impedimetric immunosensor for low level detection of human serum albumin in biological fluids. J Pharm Biomed Anal 92:74–81. https://doi.org/10.1016/j.jpba.2014.01.005

Bartlett PN, Al-Lolage FA (2018) There is no evidence to support literature claims of direct electron transfer (DET) for native glucose oxidase (GOx) at carbon nanotubes or graphene. J Electroanal Chem 819:26–37. https://doi.org/10.1016/j.jelechem.2017.06.021

Basak S, Chen D-R, Biswas P (2007) Electrospray of ionic precursor solutions to synthesize iron oxide nanoparticles: modified scaling law. Chem Eng Sci 62(4):1263–1268. https://doi.org/10.1016/j.ces.2006.11.029

Bhardwaj H, Sumana G, Marquette CA (2021) Gold nanobipyramids integrated ultrasensitive optical and electrochemical biosensor for Aflatoxin B1 detection. Talanta 222:121578. https://doi.org/10.1016/j.talanta.2020.121578

Blasques RV, Pereira MAA, Mendes AMRV, Filho NEM, Gomes WC, Arenas LT, Marty J-L, Gurgo MIP, Nunes GS, Villis PCM (2020) Synthesis and characterization of a new ceramic nanomaterial SiO_2/NPsSm$_2$O$_3$/C-graphite for the development of electrochemical sensors. Mater Chem Phys 243:122255. https://doi.org/10.1016/j.matchemphys.2019.122255

Campu A, Lerouge F, Chateau D, Chaput F, Baldeck P, Parola S, Maniu D, Craciun AM, Vulpoi A, Astilean S, Focsan M (2018) Gold NanoBipyramids performing as highly sensitive dual-modal optical immunosensors. Anal Chem 90(14):8567–8575. https://doi.org/10.1021/acs.analchem.8b01689

Chin AB, Yaacob II (2007) Synthesis and characterization of magnetic iron oxide nanoparticles via w/o microemulsion and Massart's procedure. J Mater Process Technol 191(1):235–237. https://doi.org/10.1016/j.jmatprotec.2007.03.011

Choosang J, Thavarungkul P, Kanatharana P, Numnuam A (2020) AuNPs/PpPD/PEDOT:PSS-Fc modified screen-printed carbon electrode label-free immunosensor for sensitive and selective determination of human serum albumin. Microchem J 155:104709. https://doi.org/10.1016/j.microc.2020.104709

Chow TH, Li N, Bai X, Zhuo X, Shao L, Wang J (2019) Gold nanobipyramids: an emerging and versatile type of plasmonic nanoparticles. Acc Chem Res 52(8):2136–2146. https://doi.org/10.1021/acs.accounts.9b00230

Dayal H, Ng WY, Lin XH, Li SFY (2019) Development of a hydrophilic molecularly imprinted polymer for the detection of hydrophilic targets using quartz crystal microbalance. Sensors Actuators B Chem 300:127044. https://doi.org/10.1016/j.snb.2019.127044

Della Ventura B, Banchelli M, Funari R, Illiano A, De Angelis M, Taroni P, Amoresano A, Matteini P, Velotta R (2019) Biosensor surface functionalization by a simple photochemical immobilization of antibodies: experimental characterization by mass spectrometry and surface enhanced Raman spectroscopy. Analyst 144(23):6871–6880. https://doi.org/10.1039/c9an00443b

Della Ventura B, Cennamo M, Minopoli A, Campanile R, Censi SB, Terracciano D, Portella G, Velotta R (2020) Colorimetric test for fast detection of SARS-CoV-2 in nasal and throat swabs. ACS Sens 5(10):3043–3048. https://doi.org/10.1021/acssensors.0c01742

Díaz Nieto CH, Granero AM, Lopez JC, Pierini GD, Levin GJ, Fernández H, Zon MA (2018) Development of a third generation biosensor to determine hydrogen peroxide based on a composite of soybean peroxidase/chemically reduced graphene oxide deposited on glassy carbon electrodes. Sensors Actuators B Chem 263:377–386. https://doi.org/10.1016/j.snb.2018.02.094

Fan JA, Wu C, Bao K, Bao J, Bardhan R, Halas NJ, Manoharan VN, Nordlander P, Shvets G, Capasso F (2010) Self-assembled plasmonic nanoparticle clusters. Science 328:1135–1138. https://doi.org/10.1126/science.1187949

Felix FS, Ferreira LMC, Vieira F, Trindade GM, Ferreira VSSA, Angnes L (2015) Amperometric determination of promethazine in tablets using an electrochemically reduced graphene oxide modified electrode. New J Chem 39(1):696–702. https://doi.org/10.1039/c4nj00887a

Fu C, Jin S, Oh J, Xu S, Jung YM (2017) Facile detection of glucose in human serum employing silver-ion-guided surface-enhanced Raman spectroscopy signal amplification. Analyst 142(16): 2887–2891. https://doi.org/10.1039/c7an00604g

Glezer V, Lev O (1993) Sol-gel vanadium pentaoxide glucose biosensor. J Am Chem Soc 115(6): 2533–2534. https://doi.org/10.1021/ja00059a072

Gu X, Wang H, Schultz ZD, Camden JP (2016) Sensing glucose in urine and serum and hydrogen peroxide in living cells by use of a novel boronate nanoprobe based on surface-enhanced Raman spectroscopy. Anal Chem 88(14):7191–7197. https://doi.org/10.1021/acs.analchem.6b01378

Gulati P, Kaur P, Rajam MV, Srivastava T, Mishra P, Islam SS (2019) Vertically aligned multi-walled carbon nanotubes based flexible immunosensor for extreme low level detection of multidrug resistant leukemia cells. Sensors Actuators B Chem 301:127047. https://doi.org/10.1016/j.snb.2019.127047

Guo Y, Wu J, Li J, Ju H (2016) A plasmonic colorimetric strategy for biosensing through enzyme guided growth of silver nanoparticles on gold nanostars. Biosens Bioelectron 78:267–273. https://doi.org/10.1016/j.bios.2015.11.056

Hasanzadeh M, Tagi S, Solhi E, Mokhtarzadeh A, Shadjou N, Eftekhari A, Mahboob S (2018) An innovative immunosensor for ultrasensitive detection of breast cancer specific carbohydrate

(CA 15-3) in unprocessed human plasma and MCF-7 breast cancer cell lysates using gold nanospear electrochemically assembled onto thiolated graphene quantum dots. Int J Biol Macromol 114:1008–1017. https://doi.org/10.1016/j.ijbiomac.2018.03.183

He L, Yang Y, Kim J, Yao L, Dong X, Li T, Piao Y (2020) Multi-layered enzyme coating on highly conductive magnetic biochar nanoparticles for bisphenol a sensing in water. Chem Eng J 384: 123276. https://doi.org/10.1016/j.cej.2019.123276

Janegitz BC, Pauliukaite R, Ghica ME, Brett CMA, Fatibello-Filho O (2011) Direct electron transfer of glucose oxidase at glassy carbon electrode modified with functionalized carbon nanotubes within a dihexadecylphosphate film. Sensors Actuators B Chem 158(1):411–417. https://doi.org/10.1016/j.snb.2011.06.048

Janegitz BC, Medeiros RA, Rocha-Filho RC, Fatibello-Filho O (2012) Direct electrochemistry of tyrosinase and biosensing for phenol based on gold nanoparticles electrodeposited on a boron-doped diamond electrode. Diam Relat Mater 25:128–133. https://doi.org/10.1016/j.diamond.2012.02.023

Janegitz BC, Silva TA, Wong A, Ribovski L, Vicentini FC, Taboada Sotomayor MDP, Fatibello-Filho O (2017) The application of graphene for in vitro and in vivo electrochemical biosensing. Biosens Bioelectron 89:224–233. https://doi.org/10.1016/j.bios.2016.03.026

Jia L, Zhou Y, Wu K, Feng Q, Wang C, He P (2020) Acetylcholinesterase modified AuNPs-MoS2-rGO/PI flexible film biosensor: towards efficient fabrication and application in paraoxon detection. Bioelectrochemistry 131:107392. https://doi.org/10.1016/j.bioelechem.2019.107392

Kazemi SH, Ghodsi E, Abdollahi S, Nadri S (2016) Porous graphene oxide nanostructure as an excellent scaffold for label-free electrochemical biosensor: detection of cardiac troponin I. Mater Sci Eng C Mater Biol Appl 69:447–452. https://doi.org/10.1016/j.msec.2016.07.005

Kochana J, Wapiennik K, Kozak J, Knihnicki P, Pollap A, Woźniakiewicz M, Nowak J, Kościelniak P (2015) Tyrosinase-based biosensor for determination of bisphenol a in a flow-batch system. Talanta 144:163–170. https://doi.org/10.1016/j.talanta.2015.05.078

Kurbanoglu S, Erkmen C, Uslu B (2020) Frontiers in electrochemical enzyme based biosensors for food and drug analysis. TrAC Trends Anal Chem 124:115809. https://doi.org/10.1016/j.trac.2020.115809

Laurinavicius V, Razumiene J, Gureviciene V (2013) Bioelectrochemical conversion of urea on carbon black electrode and application. IEEE Sensors J 13(6):2208–2213. https://doi.org/10.1109/jsen.2013.2250711

Layqah LA, Eissa S (2019) An electrochemical immunosensor for the corona virus associated with the Middle East respiratory syndrome using an array of gold nanoparticle-modified carbon electrodes. Microchim Acta 186(4):224. https://doi.org/10.1007/s00604-019-3345-5

Li L, Mu Q, Zhang B, Yan B (2010) Analytical strategies for detecting nanoparticle–protein interactions. Analyst 135(7):1519. https://doi.org/10.1039/c0an00075b

Li Y, Bai Y, Han G, Li M (2013) Porous-reduced graphene oxide for fabricating an amperometric acetylcholinesterase biosensor. Sensors Actuators B Chem 185:706–712. https://doi.org/10.1016/j.snb.2013.05.061

Lin Y, Kannan P, Zeng Y, Qiu B, Guo L, Lin Z (2019) Enzyme-free multicolor biosensor based on Cu^{2+}–modified carbon nitride nanosheets and gold nanobipyramids for sensitive detection of neuron specific enolase. Sensors Actuators B Chem 283:138–145. https://doi.org/10.1016/j.snb.2018.12.007

Liu B, Cao Y, Chen D, Kong J, Deng J (2003) Amperometric biosensor based on a nanoporous ZrO_2 matrix. Anal Chim Acta 478(1):59–66. https://doi.org/10.1016/S0003-2670(02)01480-0

Liu G, Riechers SL, Mellen MC, Lin Y (2005) Sensitive electrochemical detection of enzymatically generated thiocholine at carbon nanotube modified glassy carbon electrode. Electrochem Commun 7(11):1163–1169. https://doi.org/10.1016/j.elecom.2005.08.025

Liu K, Zhang J, Liu Q, Huang H (2013) Electrochemical immunosensor for alpha-fetoprotein determination based on ZnSe quantum dots/azure I/gold nanoparticles/poly (3,4-ethylenedioxythiophene) modified Pt electrode. Electrochim Acta 114:448–454. https://doi.org/10.1016/j.electacta.2013.10.018

Liu W, Zhang A, Xu G, Wei F, Yang J, Hu Q (2016) Manganese modified CdTe/CdS quantum dots as an immunoassay biosensor for the detection of Golgi protein-73. J Pharm Biomed Anal 117: 18–25. https://doi.org/10.1016/j.jpba.2015.08.020

Liu X, Fang C, Yan J, Li H, Tu Y (2018) A sensitive electrochemiluminescent biosensor based on AuNP-functionalized ITO for a label-free immunoassay of C-peptide. Bioelectrochemistry 123: 211–218. https://doi.org/10.1016/j.bioelechem.2018.05.010

Liu Y, Li X, Zhang Y-N, Zhao Y (2021) Fiber-optic sensors based on Vernier effect. Measurement:167. https://doi.org/10.1016/j.measurement.2020.108451

López Marzo AM, Mayorga-Martinez CC, Pumera M (2020) 3D-printed graphene direct electron transfer enzyme biosensors. Biosens Bioelectron 151:111980. https://doi.org/10.1016/j.bios.2019.111980

Luo J, Liang D, Zhao D, Yang M (2020) Photoelectrochemical detection of circulating tumor cells based on aptamer conjugated Cu_2O as signal probe. Biosens Bioelectron 151:111976. https://doi.org/10.1016/j.bios.2019.111976

Ma G-X, Lu T-H, Xia Y-Y (2007) Direct electrochemistry and bioelectrocatalysis of hemoglobin immobilized on carbon black. Bioelectrochemistry 71(2):180–185. https://doi.org/10.1016/j.bioelechem.2007.04.002

Martins PR, Ferreira LMC, Araki K, Angnes L (2014) Influence of cobalt content on nanostructured alpha-phase-nickel hydroxide modified electrodes for electrocatalytic oxidation of isoniazid. Sensors Actuators B Chem 192:601–606. https://doi.org/10.1016/j.snb.2013.11.029

McNay G, Eustace D, Smith WE, Faulds K, Graham D (2011) Surface-enhanced Raman scattering (SERS) and surface-enhanced resonance Raman scattering (SERRS): a review of applications. Appl Spectrosc 65(8):825–837. https://doi.org/10.1366/11-06365

Mohammadzadeh-Asl S, Keshtkar A, Ezzati Nazhad Dolatabadi J, de la Guardia M (2018) Nanomaterials and phase sensitive based signal enhancment in surface plasmon resonance. Biosens Bioelectron 110:118–131. https://doi.org/10.1016/j.bios.2018.03.051

Nkurikiyimfura I, Wang Y, Safari B, Nshingabigwi E (2020) Temperature-dependent magnetic properties of magnetite nanoparticles synthesized via coprecipitation method. J Alloys Compd 846:156344. https://doi.org/10.1016/j.jallcom.2020.156344

Oliveira GCMD, Carvalho JHDS, Brazaca LC, Vieira NCS, Janegitz BC (2020) Flexible platinum electrodes as electrochemical sensor and immunosensor for Parkinson's disease biomarkers. Biosens Bioelectron 152:112016. https://doi.org/10.1016/j.bios.2020.112016

Omidfar K, Dehdast A, Zarei H, Sourkohi BK, Larijani B (2011) Development of urinary albumin immunosensor based on colloidal AuNP and PVA. Biosens Bioelectron 26(10):4177–4183. https://doi.org/10.1016/j.bios.2011.04.022

Ortolani TS, Pereira TS, Assumpção MHMT, Vicentini FC, Gabriel De Oliveira G, Janegitz BC (2019) Electrochemical sensing of purines guanine and adenine using single-walled carbon nanohorns and nanocellulose. Electrochim Acta 298:893–900. https://doi.org/10.1016/j.electacta.2018.12.114

Pakapongpan S, Poo-Arporn RP (2017) Self-assembly of glucose oxidase on reduced graphene oxide-magnetic nanoparticles nanocomposite-based direct electrochemistry for reagentless glucose biosensor. Mater Sci Eng C Mater Biol Appl 76:398–405. https://doi.org/10.1016/j.msec.2017.03.031

Park HJ, Lee SS (2018) A quartz crystal microbalance-based biosensor for enzymatic detection of hemoglobin A1c in whole blood. Sensors Actuators B Chem 258:836–840. https://doi.org/10.1016/j.snb.2017.11.170

Paul W, Sharma CP (2020) Inorganic nanoparticles for targeted drug delivery. In: Sharma CP (ed) Biointegration of medical implant materials, 2nd edn. Woodhead Publishing, pp 333–373

Peng H, Huang Z, Zheng Y, Chen W, Liu A, Lin X (2014) A novel nanocomposite matrix based on graphene oxide and ferrocene-branched organically modified sol–gel/chitosan for biosensor application. J Solid State Electrochem 18(7):1941–1949. https://doi.org/10.1007/s10008-014-2415-1

Pirich CL, de Freitas RA, Torresi RM, Picheth GF, Sierakowski MR (2017) Piezoelectric immunochip coated with thin films of bacterial cellulose nanocrystals for dengue detection. Biosens Bioelectron 92:47–53. https://doi.org/10.1016/j.bios.2017.01.068

Pohanka M (2018) Piezoelectric biosensor for the determination of tumor necrosis factor alpha. Talanta 178:970–973. https://doi.org/10.1016/j.talanta.2017.10.031

Polatoğlu İ (2019) Electrochemical sensing platform based on Tyrosinase immobilized magnetite chitosan Nanobiocomposite film and its application as catechol biosensor. J Electrochem Soc 166(15):B1620–B1629. https://doi.org/10.1149/2.1041915jes

Qiu G, Gai Z, Tao Y, Schmitt J, Kullak-Ublick GA, Wang J (2020) Dual-functional Plasmonic Photothermal biosensors for highly accurate severe acute respiratory syndrome coronavirus 2 detection. ACS Nano 14(5):5268–5277. https://doi.org/10.1021/acsnano.0c02439

Rissin DM, Kan CW, Campbell TG, Howes SC, Fournier DR, Song L, Piech T, Patel PP, Chang L, Rivnak AJ, Ferrell EP, Randall JD, Provuncher GK, Walt DR, Duffy DC (2010) Single-molecule enzyme-linked immunosorbent assay detects serum proteins at subfemtomolar concentrations. Nat Biotechnol 28(6):595–599. https://doi.org/10.1038/nbt.1641

Russell SM, de la Rica R (2018) Paper transducers to detect plasmon variations in colorimetric nanoparticle biosensors. Sensors Actuators B Chem 270:327–332. https://doi.org/10.1016/j.snb.2018.05.052

Salazar-Alvarez G, Muhammed M, Zagorodni AA (2006) Novel flow injection synthesis of iron oxide nanoparticles with narrow size distribution. Chem Eng Sci 61(14):4625–4633. https://doi.org/10.1016/j.ces.2006.02.032

Samanman S, Kanatharana P, Asawatreratanakul P, Thavarungkul P (2012) Characterization and application of self-assembled layer by layer gold nanoparticles for highly sensitive label-free capacitive immunosensing. Electrochim Acta 80:202–212. https://doi.org/10.1016/j.electacta.2012.07.016

Shaikh MO, Zhu P-Y, Wang C-C, Du Y-C, Chuang C-H (2019) Electrochemical immunosensor utilizing electrodeposited au nanocrystals and dielectrophoretically trapped PS/ag/ab-HSA nanoprobes for detection of microalbuminuria at point of care. Biosens Bioelectron 126:572–580. https://doi.org/10.1016/j.bios.2018.11.035

Silva TA, Zanin H, Saito E, Medeiros RA, Vicentini FC, Corat EJ, Fatibello-Filho O (2014) Electrochemical behaviour of vertically aligned carbon nanotubes and graphene oxide nanocomposite as electrode material. Electrochim Acta 119:114–119. https://doi.org/10.1016/j.electacta.2013.12.024

Silva TA, Moraes FC, Janegitz BC, Fatibello-Filho O (2017) Electrochemical biosensors based on nanostructured carbon black: a review. J Nanomater 2017:1–14. https://doi.org/10.1155/2017/4571614

Sun D, Qi G, Cao F, Xu W, Chen Q, Xu S (2017) A recyclable silver ions-specific surface-enhanced Raman scattering (SERS) sensor. Talanta 171:159–165. https://doi.org/10.1016/j.talanta.2017.04.052

Tang L, Li J (2017) Plasmon-based colorimetric nanosensors for ultrasensitive molecular diagnostics. ACS Sens 2(7):857–875. https://doi.org/10.1021/acssensors.7b00282

Taniselass S, Arshad MKM, Gopinath SCB (2019) Graphene-based electrochemical biosensors for monitoring noncommunicable disease biomarkers. Biosens Bioelectron 130:276–292. https://doi.org/10.1016/j.bios.2019.01.047

Tsai J-Z, Chen C-J, Settu K, Lin Y-F, Chen C-L, Liu J-T (2016) Screen-printed carbon electrode-based electrochemical immunosensor for rapid detection of microalbuminuria. Biosens Bioelectron 77:1175–1182. https://doi.org/10.1016/j.bios.2015.11.002

Usha SP, Shrivastav AM, Gupta BD (2016) FO-SPR based dextrose sensor using ag/ZnO nanorods/GOx for insulinoma detection. Biosens Bioelectron 85:986–995. https://doi.org/10.1016/j.bios.2016.05.082

Vicentini FC, Janegitz BC, Brett CMA, Fatibello-Filho O (2013) Tyrosinase biosensor based on a glassy carbon electrode modified with multi-walled carbon nanotubes and 1-butyl-3-

methylimidazolium chloride within a dihexadecylphosphate film. Sensors Actuators B Chem 188:1101–1108. https://doi.org/10.1016/j.snb.2013.07.109

Vicentini FC, Raymundo-Pereira PA, Janegitz BC, Machado SAS, Fatibello-Filho O (2016) Nanostructured carbon black for simultaneous sensing in biological fluids. Sensors Actuators B Chem 227:610–618. https://doi.org/10.1016/j.snb.2015.12.094

Wang Z, Zong S, Wu L, Zhu D, Cui Y (2017) SERS-activated platforms for immunoassay: probes, encoding methods, and applications. Chem Rev 117(12):7910–7963. https://doi.org/10.1021/acs.chemrev.7b00027

Xia Y, Ye J, Tan K, Wang J, Yang G (2013) Colorimetric visualization of glucose at the submicromole level in serum by a homogenous silver nanoprism-glucose oxidase system. Anal Chem 85(13):6241–6247. https://doi.org/10.1021/ac303591n

Xiao-He Y, Qiang Y, Hao Y, Li W, Yu-Quan C (2007) Performance and mechanism of screen-printed carbon paste electrode glucose biosensors based on functional carbon black. Chin J Anal Chem 35(12):1751–1755. https://doi.org/10.1016/s1872-2040(08)60007-9

Xiong LH, He X, Xia J, Ma H, Yang F, Zhang Q, Huang D, Chen L, Wu C, Zhang X, Zhao Z, Wan C, Zhang R, Cheng J (2017) Highly sensitive naked-eye assay for enterovirus 71 detection based on catalytic nanoparticle aggregation and Immunomagnetic amplification. ACS Appl Mater Interfaces 9(17):14691–14699. https://doi.org/10.1021/acsami.7b02237

Zhang Y, McKelvie ID, Cattrall RW, Kolev SD (2016) Colorimetric detection based on localised surface plasmon resonance of gold nanoparticles: merits, inherent shortcomings and future prospects. Talanta 152:410–422. https://doi.org/10.1016/j.talanta.2016.02.015

Zhang H, Chen Y, Wang H, Hu S, Xia K, Xiong X, Huang W, Lu H, Yu J, Guan H, He M, Liu W, Zhang J, Luo Y, Xie Z, Chen Z (2018) Titanium dioxide nanoparticle modified plasmonic interface for enhanced refractometric and biomolecular sensing. Opt Express 26(25): 33226–33237. https://doi.org/10.1364/OE.26.033226

Zhang L, Luo Z, Su L, Tang D (2019) A surface plasmon resonance enhanced photoelectrochemical immunoassay based on perovskite metal oxide@gold nanoparticle heterostructures. Analyst 144(19):5717–5723. https://doi.org/10.1039/c9an01395d

Zhang X, Sucre-Rosales E, Byram A, Hernandez FE, Chen G (2020) Ultrasensitive visual detection of glucose in urine based on the iodide-promoted etching of gold bipyramids. ACS Appl Mater Interfaces 12(44):49502–49509. https://doi.org/10.1021/acsami.0c16369

Zhao S, Zhang Y, Ding S, Fan J, Luo Z, Liu K, Shi Q, Liu W, Zang G (2019) A highly sensitive label-free electrochemical immunosensor based on AuNPs-PtNPs-MOFs for nuclear matrix protein 22 analysis in urine sample. J Electroanal Chem 834:33–42. https://doi.org/10.1016/j.jelechem.2018.12.044

Zhong Y, Yu X, Fu W, Chen Y, Shan G, Liu Y (2019) Colorimetric and Raman spectroscopic array for detection of hydrogen peroxide and glucose based on etching the silver shell of au@ag core-shell nanoparticles. Mikrochim Acta 186(12):802. https://doi.org/10.1007/s00604-019-3991-7

Zhou G, Sun J, Yaseen M, Zhang H, He H, Wang Y, Yang H, Liang J, Zhang M, Zhou L, Liao D (2018) Synthesis of highly selective magnetite (Fe_3O_4) and tyrosinase immobilized on chitosan microspheres as low potential electrochemical biosensor. J Electrochem Soc 165:G11–G17. https://doi.org/10.1149/2.1031802jes

Zhu Y, Xu Z, Gao J, Ji W, Zhang J (2020) An antibody-aptamer sandwich cathodic photoelectrochemical biosensor for the detection of progesterone. Biosens Bioelectron 160:112210. https://doi.org/10.1016/j.bios.2020.112210

Nanoelectrodes and Nanopores Ensembles for Electrobioanalytical Applications

6

Fernando Battaglini

Contents

1 Introduction 112
2 Nanoelectrodes and Nanopores: Types and Construction 112
  2.1 Nanoelectrodes 112
  2.2 Nanopores 114
3 Electrochemical Response and Modeling 115
  3.1 Nanoelectrodes 115
  3.2 Nanopores 117
4 Functionalization 119
  4.1 Nanoelectrodes 119
  4.2 Nanopores 121
5 Applications 121
  5.1 Nanoelectrodes 121
  5.2 Nanopores 123
6 Concluding Remarks 124
References 125

Abstract

Electrochemistry at the nanoscale can achieve bioanalytical information from single entities (molecules, cells, and nanoparticles). This chapter focuses on the construction, modeling, functionalization, and applications of nanoelectrochemical probes (nanoelectrodes and nanopores combined with electrochemical detection) regarding bioanalytical sciences, highlighting the advances achieved in the last ten years and discussing the future challenges.

F. Battaglini (✉)
INQUIMAE (CONICET), Departamento de Química Inorgánica, Analítica y Química Física,
Facultad de Ciencias Exactas y Naturales, Universidad de Buenos Aires, Buenos Aires, Argentina
e-mail: battagli@qi.fcen.uba.ar

© Springer Nature Singapore Pte Ltd. 2023

U. P. Azad, P. Chandra (eds.), *Handbook of Nanobioelectrochemistry*,
https://doi.org/10.1007/978-981-19-9437-1_6

Keywords

Nanoelectrodes · Single · Array · Ensembles · Modeling · Selective modification · Extracellular biosensing · Intracellular sensing

1 Introduction

Electrochemistry at the nanoscale has been a goal since the early 1980s when microelectrodes began to be designed to make measurements of chemical concentrations inside the mammalian brain (Wightman 1981), since then the downsize of the electrode and pore dimensions to achieve single-molecule information in biosciences push the imagination and resources of the academic community to accomplish very ingenious systems able to perform such tasks.

Nanoscale in electrochemistry refers to a critical dimension involving electrodes or pores with less than 50 nm. The advantages of size decreasing in electrochemistry impact in several ways, allowing to work in tiny spaces, reducing sample volume, enhancing mass transport, producing low background charging current achieving faster time scales, and identifying single molecules.

This chapter focuses on the construction, modeling, functionalization, and applications of nanoelectrochemical probes regarding bioanalytical sciences. The research in nanoelectrochemistry has been dramatically increasing in the last 30 years, and several reviews have been lately published devoted to different areas (Oja et al. 2013; Clausmeyer and Schuhmann 2016; Oja et al. 2016; Karimian and Ugo 2019; Wongkaew et al. 2019; Fu and Bohn 2018; Kumar et al. 2018; Purohit et al. 2020; Sharma et al. 2018).

2 Nanoelectrodes and Nanopores: Types and Construction

2.1 Nanoelectrodes

Nanoelectrodes can be used as single electrodes or as a set of electrodes, named nanoelectrode arrays when the units are ordered or nanoelectrode ensembles when they are randomly distributed. Different means of production have been developed. Here, we focus on those with a significant impact on bioanalytical chemistry.

Disk nanoelectrodes are mainly built from a metal wire sealed in a glass cylinder working as insulator material. Recently, the modification of this well-established procedure allowed the production of Pt nanoelectrodes, achieving 1 nm radius. The basis of the procedure is fully described elsewhere (Li et al. 2009). Difficulties arise when a metal different from Pt wants to be used due to the high melting point of quartz glass. Alternatively, the electrochemical deposition of gold onto platinum allows the fabrication of gold nanoelectrodes (Kumar Jena et al. 2010).

Nanopore electrodes result from the combination of a solid-state nanopore with a nanoelectrode that follows the flux of a redox species able to cross the nanopore. The pore material can be glass acquiring conical (Zhang et al. 2004) or cylindrical shapes (Sun 2010). The fabrication of a nanopore electrode resembles the previous one; a microwire is sealed in a capillary tube, then pulled and cut at the thinnest diameter. Then, the Pt or Au disk is etched in a sodium chloride solution applying a voltage (Zhang et al. 2007). The nanopore electrode can be used to carry out single-molecule experiments regarding its redox properties.

Measuring extremely small electrical currents represents a significant drawback of individual nanoelectrodes. This limitation can be partially overcome using a nanoelectrode set encompassing many nanoelectrodes that carry out the same process. A recent review on this topic is available (Karimian and Ugo 2019). The nanoelectrode sets are divided into two types: nanoelectrode arrays, where the nanoelectrode units are perfectly ordered, and the nanoelectrode ensembles, where the nanoelectrode units are randomly distributed.

In the last 20 years, several strategies were carried out to construct these systems; those based on methods applied in the semiconductor industry are frequently used. They can be considered a top-down approach since their features are created on the sample surface by instruments like an electronic microscope able to create a nanometric pattern (Bruchhaus et al. 2017). These sets can be built by electron beam lithography (EBL). In this way, a nanopattern can be achieved similarly that devices at the micrometer scale that can be made by photolithography. This technique allows a resolution of 3 nm (Manheller et al. 2012). In the academy, usually, an electron microscope is adapted into an electron beam lithography system implementing some accessories. These adapted microscopes can produce linewidths of 10 nm or smaller. A recent example of the application of this technique in nanoelectrodes arrays is given by Dincer et al. (Dincer et al. 2015). They build boron-doped diamond nanoelectrode arrays by patterning boron-doped diamond on silicon, obtaining an array of nanoelectrodes (320 nm diameter, 10 μm interelectrode distance).

Focus ion beam lithography is another alternative. Here ions are used for the exposure of the resist. The ion beam has a higher resolution due to a low scattering in the target. Also, the direct nature of processing can greatly simplify sample preparation allowing milling, deposition, and etching. These features allow to produce three-dimensional structures (Joshi-Imre and Bauerdick 2014). The pioneering work of Arrigan's group fabricated nanopore electrode arrays using direct-write local ion milling, achieving pores between 150 and 400 nm diameter (Lanyon et al. 2007). Even though these techniques have been applied in some extension, and can be scaled up with relative facility, their cost may be prohibitive for routinary clinical applications.

Distinct periodic cup-like nanostructures can be generated on indium tin oxide (ITO). Figure 6.1 illustrates the steps used to obtain these nanostructures. A homogenous photoresist (PR) pattern is produced on ITO using laser interference lithography. Then, the PR nanoholes work as a template to deposit gold. This represents an attempt to manage the experimental conditions and different cup-like and dot-like nanostructures that can be fabricated (Kim et al. 2015).

A bottom-up approach is possible through chemical processes. Several strategies can be found in the literature. In the last years, great attention was placed on the

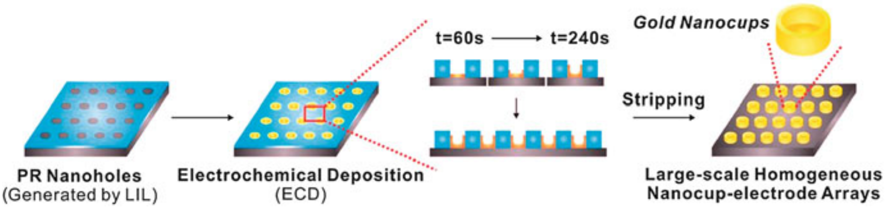

Fig. 6.1 Sequential steps involved in the fabrication of the nanocup-electrode array on ITO (Kim et al. 2015). (Reproduced with permission from John Wiley and Sons)

construction of vertically configured nanostructure arrays (nanoneedles, nanopillars, and nanowires). Anodic aluminum oxide (AAO) can work as a template to construct these arrays using metals such as Ag, Ni, Au, Pt, and even more complex composites (Lee and Park 2014; Ganapathi et al. 2019). Electrolyte concentration, current density, and deposition time are commonly used variables to obtain well-shaped arrays. Alternatively, polycarbonate (PC) and polyethylene terephthalate (PET) membranes can work as porous templates (Scho et al. 1997). Peinetti et al. have used hexagonally ordered porous AAO of 10 nm pore diameter to produce gold nanoelectrodes of ~2 nm diameter using pulsed electrodeposition (Peinetti et al. 2013) constituting a hybrid nanopore-nanoelectrode system. Chen et al. fabricated Fe_3O_4 nanotube electrodes by growing ZnO nanowires on a glass substrate conveniently coated with fluorine-doped tin oxide and then chemically transforming them in Fe_3O_4 by immersion into $FeCl_3$ solution obtaining nanotubes of 130 ± 40 nm diameter and 4 μm height (Chen et al. 2017).

2.2 Nanopores

With a pore size like the size of biomolecules, nanopores can be part of a label-free electrochemical biosensing platform. These sensors exploit the Coulter counter principle. In the 1950s, Coulter (Coulter 1953) developed a method able to determine the concentration and size of micrometric size particles using a pore at the same scale fixed on a membrane. The membrane separates two compartments filled with saline solutions. Electrodes of opposite charges are placed in each compartment as a particle pass, an increase in the resistance produces a change in the signal that can be correlated to the particle concentration. This type of signal generation is called resistive pulse sensing (RPS). The miniaturization of this pore to the nanometer scale allows nowadays the determination of physical and chemical properties of single molecules (Bayley and Martin 2000; Yameen et al. 2009; Kaya and Keçeci 2020; Xue et al. 2020).

Details regarding nanopore fabrication technologies can be found elsewhere (Xue et al. 2020) (Chen and Liu 2019). Here we introduce the cases frequently discussed in the literature.

Routinary access to heavy-ion accelerators has popularized the use of ion beams. They produce tracks with a straight trajectory in the membrane. The most widely used materials are polyethylene-terephthalate, polycarbonate, polyimide, and polyvinylidene fluoride. Ion density irradiation can be controlled, achieving even down to 1 ion/membrane; therefore, single-track membranes can be produced. Then, the shape and diameter of the pore(s) are shaped using NaOH, KOH, or NaClO depending on the polymeric material (Kaya and Keçeci 2020).

A simpler alternative is the use of commercially available alumina or polycarbonate track-etched membranes. Alumina membranes can be chemically modified in different ways (e.g., covalent link and self-assembly); also, pore sizes in the range of biomolecules can be obtained (González et al. 2010; Md Jani et al. 2013). On the other hand, polycarbonate membranes have been widely used. Martin developed an innovative approach where Au nanotubes are produced from electroless deposition on track-etched polycarbonate membranes obtaining pores with effective inside diameters less than 1 nm (Wirtz et al. 2002).

3 Electrochemical Response and Modeling

3.1 Nanoelectrodes

Nanoelectrodes are generally used as amperometric sensors. Therefore, the modeling of chronoamperometry and cyclic voltammetry experiments is of great interest. Cyclic voltammetry as an experimental technique is very simple, affordable, and can render information on the mass transfer mechanisms, electron transfer processes, and coupled homogeneous chemical reactions. However, the analysis of voltammetric data sometimes becomes complex. Numerical simulation is an adequate tool to model these systems (Compton et al. 2008; Henstridge and Compton 2012).

The size reduction enhances the mass transport rate, which in turn allows the investigation of fast electrode kinetics. However, other mass transport mechanisms should be considered at the nanoscale, for example, migration, since the diffusion layer becomes close to the Debye length, an essential effect in single nanopore electrodes and nanoelectrode arrays. White’s group investigated the mass transport of species with different charges. They conclude that the faradaic currents generated depend on both factors (migration and diffusion) crossing the pore in the case of nanopore electrodes and can be described assuming Nernst-Planck transport and electroneutrality (Zhang et al. 2006).

A different theoretical framework is needed to model the electrochemical behavior in nanoelectrode arrays (Davies et al. 2005; Amatore et al. 2009; Guo and Lindner 2009; Peinetti et al. 2016). The current response for an electrode array in a cyclic voltammetry experiment mainly depends on three factors: scan rate, electrode radius, and interelectrode distance, producing four different diffusional patterns (Fig. 6.2a). Cases 1 and 4 can be described by planar diffusion and corresponds to a one-dimensional problem. Case 2 is easily modeled as individual electrodes. In

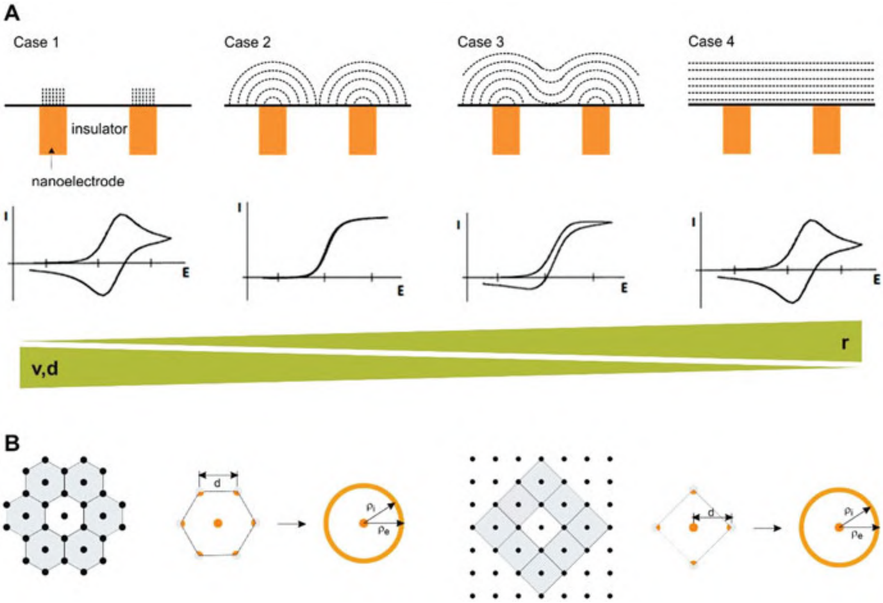

Fig. 6.2 (**a**) Diffusion profiles in a nanoelectrode array (above), corresponding cyclic voltammograms (below). (**b**) ANSA model unit cell definition for hexagonal array (left) and square array (right)

Case 3, the overlapping of the adjacent diffusional layers does not allow its treatment as independent electrodes; however, the diffusional fields are not enough overlapped to assume a linear diffusion case (Case 4), making Case 3 the most complex to model. This situation is noticeable in nanoelectrode arrays since the participation of the radial diffusion increases as the electrode diameter decreases. This process scales with the inverse of the electrode diameter, being of paramount influence at the nanometer scale.

We have introduced a computational model consisting in dividing a regular electrode array into cells (Fig. 6.2b). A central electrode surrounded by neighbor electrodes is represented in this model as a disk surrounded by a ring (Fig. 6.2b), maintaining the same active electrode area. This approach was called axial neighbor symmetry approximation (ANSA) and allows to model the diffusional behavior with a cylindrical symmetry model, which also considers the diffusion and current produced in the neighbors (Peinetti et al. 2016).

Electrochemical impedance spectroscopy (EIS) is frequently used for label-free detection combined with nanoelectrode arrays. Lantiat et al. performed a simulation of the impedance experiments for a single nanoelectrode and nanoelectrode arrays (Lantiat et al. 2010). They observe three frequency regions (Fig. 6.3): (1) a high-frequency loop (500 Hz–100 kHz), due to the charge transfer at each nanoelectrode; (2) a low-frequency loop (0.01–10 Hz) equivalent to the electrochemical response of

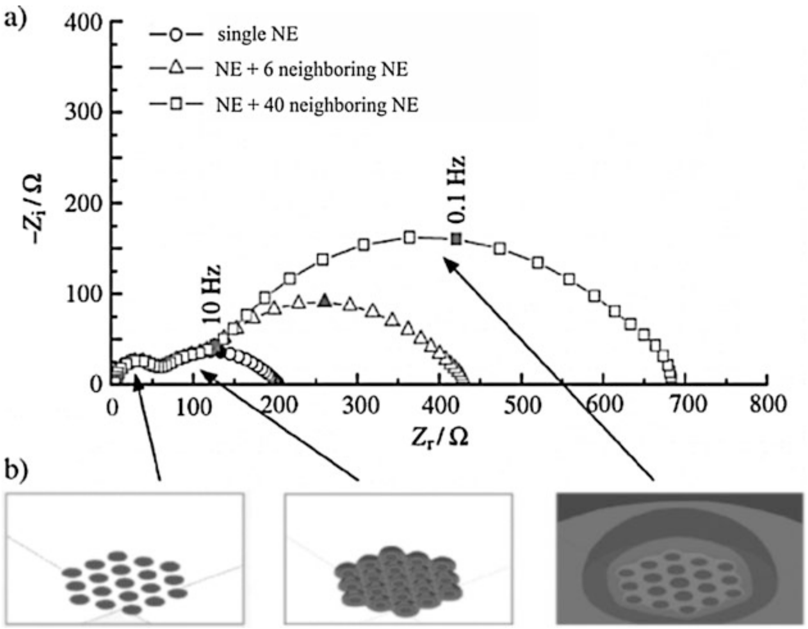

Fig. 6.3 (**a**) Impedance response as a function of the number of nanoelectrodes (NE). (**b**) 3D representation of the diffusion layers as a function of the frequency (Lantiat et al. 2010). (Reproduced with permission from John Wiley and Sons)

a macroscopic electrode, and (3) a medium-frequency loop (10–500 Hz) where the diffusion layer partially overlaps.

3.2 Nanopores

Resistive pulse sensing allows getting information on the chemical interactions occurring in the nanopores through a straightforward technique. Two reservoirs filled with an electrolyte (e.g., KCl solution) are separated by a thin, nonpermeable membrane and linked via one or several nanopores. Electrodes are immersed in the two compartments (Fig. 6.4a), and a constant voltage across the nanopores is applied, generating a steady-state ionic current flux through the pore. The resistance increases as the analyte crosses the pores, owing to hindered access of ions to the pore. The generated current signal presents three main features: amplitude, duration, and noise (Fig. 6.4b), containing relevant information on the analyte. Finally (Fig. 6.4c), the frequency of these modulations carries information on the analyte concentration (Xue et al. 2020).

Ionic charges on the pore surface combined with a conical pore shape induce an asymmetric electrostatic potential along the pore axis, affecting the anion and cation concentrations within the pore when a voltage is applied, producing the rectification of the ionic current. Azzaroni's group has intensively worked in modeling single

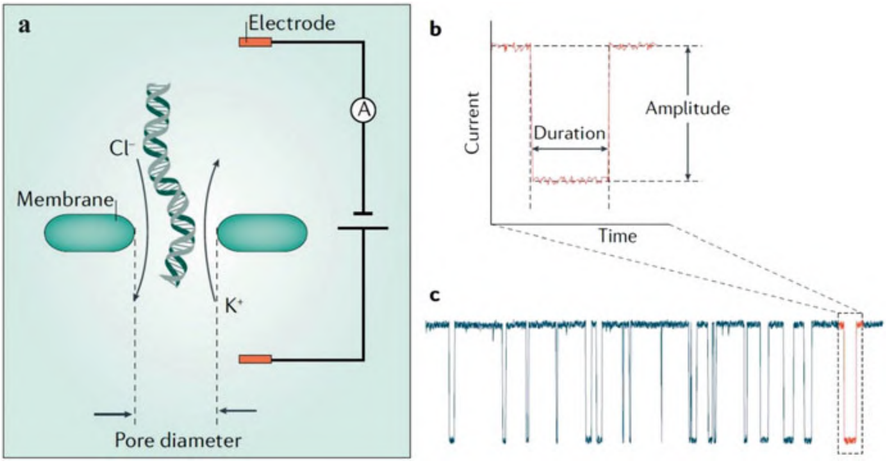
a
Electrode
A
Cl⁻
Membrane
K⁺
Pore diameter
b
Current
Duration
Amplitude
Time
c

Fig. 6.4 Resistive pulse signal generation. (**a**) Scheme of the experimental setup. (**b**) Details of the generated signal. (**c**) Train of pulses during an experiment (Xue et al. 2020). (Reproduced with permission from Springer Nature)

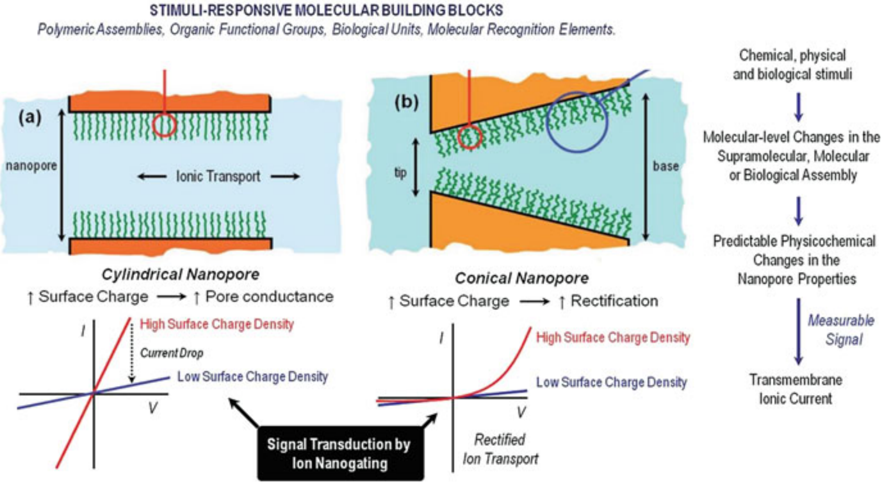
STIMULI-RESPONSIVE MOLECULAR BUILDING BLOCKS
Polymeric Assemblies, Organic Functional Groups, Biological Units, Molecular Recognition Elements.
(a)
nanopore
Ionic Transport
Cylindrical Nanopore
↑ Surface Charge ⟶ ↑ Pore conductance
I
High Surface Charge Density
Current Drop
Low Surface Charge Density
V
(b)
tip
base
Conical Nanopore
↑ Surface Charge ⟶ ↑ Rectification
I
High Surface Charge Density
Low Surface Charge Density
V
Rectified
Ion Transport
Signal Transduction by
Ion Nanogating
Chemical, physical
and biological stimuli
Molecular-level Changes in the
Supramolecular, Molecular
or Biological Assembly
Predictable Physicochemical
Changes in the
Nanopore Properties
Measurable
Signal
Transmembrane
Ionic Current

Fig. 6.5 Schemes of cylindrical (**a**) and conical (**b**) functionalized nanopores. The figure shows the type of response of the ionic current depending on the pore shape leading to high and low surface charge density states in the responsive layer (Perez-Mitta et al. 2017). (Reproduced with permission from Creative Commons Attribution 3.0 Unported Licence)

nanopore systems (Perez-Mitta et al. 2017). They establish the current-voltage response for nanochannels with different symmetries, observing a rectified ion transport in conical nanopores, considered an ionic diode. Figure 6.5 schematized the current-potential behavior for cylindrical and conical nanopores.

Kant et al. proposed the use of electrochemical impedance spectroscopy to characterize nanoporous alumina with different diameters. They found that the concentration and ion species of electrolytes affect the nanopores' resistance, while the capacitance is independent of them (Kant et al. 2014).

Our group has applied dynamic electrochemical techniques (square wave voltammetry and cyclic voltammetry) to model mesoporous membranes. Digital simulations of both types of experiments permit comparing the responses for different situations considering how the membrane is blocked by the sample, evaluating different variables such as the pore diameter, analyte, and probe sizes (González et al. 2010; Peinetti et al. 2010).

4 Functionalization

4.1 Nanoelectrodes

Bioanalytical electrochemical applications are characterized for surface modification with selective recognition elements. When conventional electrodes are used, this modification can be easily performed by depositing solutions with the needed components. Controlling the functionalization of the individual elements in nanoelectrode arrays is however complex. Techniques used to modify one sensor in the presence of many others include microcontact printing (Libioulle et al. 1999; Salomon et al. 2012), dip-pen nanolithography (Zhang et al. 2003), and the modification of inkjet printers (Bietsch et al. 2004; Falconnet et al. 2006). Haag et al. introduced different functionalities in a gold electrode array using selective potential-assisted electrochemical deposition and inhibition of thiol adsorption (Haag et al. 2016). They exploit the adsorption/desorption kinetics of alkanethiols on gold at different applied potentials. A positive potential (higher than 200 mV vs. Ag/AgCl) can increase the adsorption rate. On the other hand, cathodic potentials (less than −200 mV vs. Ag/AgCl) slow the rate of chemisorption of alkanethiols, while at potentials less than -600 mV, chemisorbed alkanethiols are reductively desorbed. They use three different potentials to produce a selective immobilization: E_{adsorb} (adsorption), E_{desorb} (desorption), and E_{hold} (holding). The first one promotes chemisorption, and the second one maintains the electrode in the reductive desorption state. In contrast, the third one is an intermediate potential that is neither reductive enough to desorb an already formed monolayer nor sufficiently anodic to promote the adsorption of new alkanethiols. In Fig. 6.6, a scheme of the procedure is presented using two ferrocene alkanethiols (Fc–CO–C11-SH and Fc–C11–SH); in (A), both electrodes are immersed in a Fc–CO–C11–SH solution. Different potentials are applied to the two electrodes so that the alkanethiol is only deposited onto electrode 1. Then, in step (B), the solution is changed to the second adsorbate, Fc–C11–SH, while the applied potential targets the Fc–C11–SH to the second electrode exclusively. In this way, each electrode was modified with a different ferrocene derivative and present an electrochemical signal at different potentials.

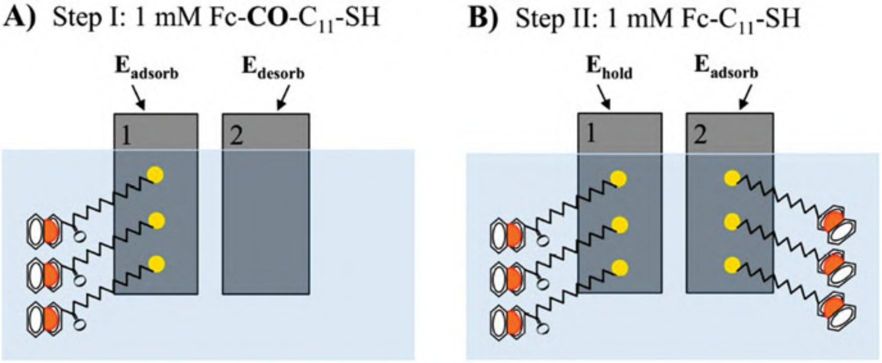
A) Step I: 1 mM Fc-**CO**-C_{11}-SH
E_{adsorb}
E_{desorb}
1
2
B) Step II: 1 mM Fc-C_{11}-SH
E_{hold}
E_{adsorb}
1
2

Fig. 6.6 Steps involved in the individual modification of a set of nanoelectrodes with thiol moieties (Haag et al. 2016). (Reproduced with permission from IOP Publishing, Ltd.)

Contemporarily, Jambrec et al. (2015) proposed a method for the potential-assisted adsorption on gold electrodes of ssDNA that takes into account the role of ions close to the electrodes, the DNA strands, and the shift of the potential of zero charge (pzc) of the electrode produced by the surface modification with ssDNA. This change requires a careful selection of the applied pulse potentials to control the ssDNA adsorption process. This method was later applied to the preparation of microarrays (Jambrec et al. 2019).

Alternative methods for selective electrochemical modification can be achieved through the electropolymerization of organic species containing functional groups that produce a selective imprinted polymer (Azevedo Beluomini et al. 2019) or by introducing functional groups where the recognition element can be further coupled (Yanez-Heras et al. 2010). Electrochemical reduction of diazonium salts is extensively exploited and can be applied on different surfaces such as gold, carbon, and fluorine tin oxide (Bahr et al. 2001; Siepenkoetter et al. 2017). Details regarding this technique applied to the construction of bioanalytical devices can be found elsewhere (Hetemi et al. 2020).

We only have to consider the chemical properties of the surface when single nanoelectrodes or the whole array is modified with the same adsorbate. For example, as previously described, gold readily reacts with thiol groups, introducing a myriad of functional groups for further functionalization (Peinetti et al. 2015, 2018). The same procedure can be followed using some amino derivatives (Ashwell et al. 2011). Glass and ITO (indium-doped tin oxide) allow silane modification, whereas silane derivatives also can introduce multiple functional groups (Aydin and Kemal Sezgintürk 2017). Layer-by-layer assembly can also be used as a method to control a surface modification; in this case, the surface should have the ability to interact with the substrate through opposite charges, hydrogen bridges, and molecular recognition, among others (Richardson et al. 2016). Also, the difference in chemical composition between the electrode and the surrounding insulator can be exploited to build a more complex structure; for example, gold nanoelectrodes can be modified with thiol-containing molecules while the surrounding insulator, polycarbonate, can be modified with a protein (Silvestrini et al. 2011).

4.2 Nanopores

Electrostatic interactions have been applied to modify polyethyleneterphtalate and polycarbonate-based nanopores due to the negative charges present in the pores (Pérez-Mitta et al. 2018; Laucirica et al. 2019), and also by self-polymerization of dopamine (Pérez-Mitta et al. 2015b). Sputter coating of the nanochannels also allows the deposition of a gold layer, allowing the further electropolymerization of polyaniline (Pérez-Mitta et al. 2015a). Nanopores can also be covered by gold by electroless techniques and further modified with thiol-containing biomolecules (Siwy et al. 2005).

Alumina nanopores can easily be modified with silane derivatives to immobilize biomolecules further (Ko et al. 2009; Chaturvedi et al. 2016; Santos et al. 2020). Alternatively, versatility in the modification of porous membranes can be achieved using a polyallyamine–dodecylsulfate complex. The complex can be directly applied to different types of surfaces (Peinetti et al. 2012).

5 Applications

The applications of these devices are mainly oriented to single-molecule, low concentration detection, and monitoring species in a limited volume in real time, generally living cells. Electrochemical sensors can directly detect many biomolecular species or by assisted means in a short time. The nanoscale adds more advantages, e.g., improved signal/noise ratio, faster scan rates, and reduced RC time decay, enabling determinations in high resistive media. As its size is equivalent to the target analyte, it enhances the signal produced, decreasing the limit of detection.

5.1 Nanoelectrodes

The application in biomedicine of single nanoelectrodes is a major drive in their development. In the last five years, impressive results have been obtained using these devices. Ewing's group found that carbon electrodes spontaneously adsorb and stochastically rupture cellular vesicles. The authors refer to the method as intracellular vesicle impact electrochemical cytometry. It is carried out using a carbon fiber electrode of nanometric dimensions to pierce the plasma membrane of a single secretory cell; in this way, the carbon fiber reaches the vesicles in the cytoplasm, allowing to follow the fate of molecules in an exocytosis process at living neurons. These results lead to the conclusion that only a small fraction of the vesicular content is released, suggesting new theoretical modalities for understanding the initial plastic changes in learning (Li et al. 2015; Li et al. 2016; Larsson et al. 2020).

Different nanoelectrode arrays based on metal nanoparticles or metal oxides have been used to directly determine small biomolecules such as hydrogen peroxide, glucose, and neurotransmitters (Wang et al. 2021). Improved sensitivities and higher currents are obtained due to the bigger electroactive area of these ensembles. Recently, this trend was extended to metal nitride and phosphide compounds; for example, Ni phosphide nanoensembles supported on conductive carbon cloth can oxidize glucose in alkaline media. It was tested as a nonenzymatic glucose sensor showing a short response time, selectivity, and reproducibility (Chen et al. 2016). Cobalt nitride nanowire array on Ti mesh was used as a glucose sensor in serum, being sensitive also to H_2O_2 at physiological pH (Xie et al. 2018). In the same trend, different strategies developed to detect glutamate were presented (Schultz et al. 2020).

Peinetti et al. constructed isolated 2 nm gold nanoelectrodes inside nanoporous alumina and then modified them with an aptamer selective to adenosine monophosphate. The aptamer exhibits two possible configurations: as a random coil in the absence of the analyte, or as a stem−loop structure when the aptamer binds to the AMPs, creating a loop of 2 nm diameter. Here, each nanoelectrode has a similar size to the size changes in the aptamer chemical structure, producing a strong effect in the electron transfer process of an electrochemical probe present in the solution, which is assessed by electrochemical impedance spectroscopy (EIS). In this way, a label-free sensor-based EIS assay for small molecules can be produced, overcoming the low sensitivity of this technique when detecting small molecules (Peinetti et al. 2015).

In the last decade, vertically configured nanostructures (VN, nanopillars, nanowires, nanoneedles, and nanocups) expand their application beyond biosensing (Li et al. 2020; Shokouhi et al. 2020). They provide an optimal platform to handle and assess intracellular information by penetrating the cell membrane, which other means cannot achieve. The use of patterned VN arrays could detect intracellular signals and collect high-throughput and long-term intracellular signals (Abbott et al. 2017, 2020). Fig. 6.7 shows the biomedical information obtained in different

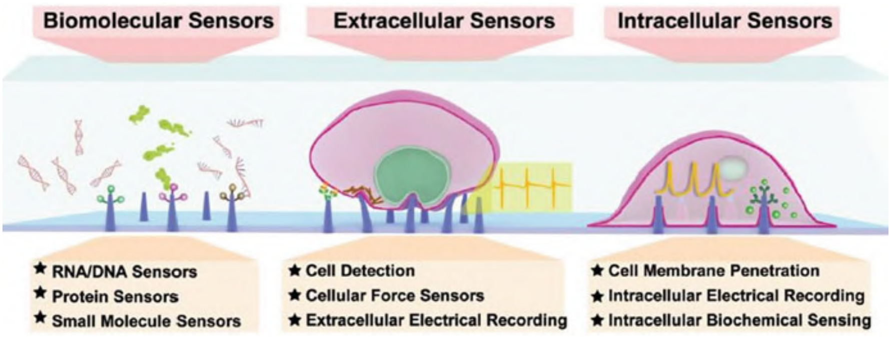
Biomolecular Sensors
Extracellular Sensors
Intracellular Sensors
★ RNA/DNA Sensors
★ Protein Sensors
★ Small Molecule Sensors
★ Cell Detection
★ Cellular Force Sensors
★ Extracellular Electrical Recording
★ Cell Membrane Penetration
★ Intracellular Electrical Recording
★ Intracellular Biochemical Sensing

Fig. 6.7 VN array–based biosensors. The schemes show different applications depending on the interaction between VN and cells (Li et al. 2020). (Reprinted with permission from Royal Society of Chemistry)

environments, solution/fluids (biomolecules), extracellular, and intracellular (Li et al. 2020).

Several biomolecular applications of VN arrays can be found in the literature; RNA, DNA, and other small molecules (H_2O_2, glucose, etc.) have been detected (Huang et al. 2014; Lee et al. 2016; Ahmad et al. 2017). For example, HIV-1 Rev response element (RRE) RNA was determined using modified gold-coated silicon VN arrays with an artificial peptide that recognizes the target RNAs. A detection limit of 1.5 fM was achieved (Lee et al. 2016). Jamal et al. produced a nanowire array composed of Pd nanoparticles/Au nanowires (Au@Pd) to detect H_2O_2 (Jamal et al. 2012). The nanowire array can determine hydrogen peroxide at -0.2 V with a sensitivity higher than other nonenzymatic sensors and avoid the interference of species such as ascorbate, uric acid, acetaminophen, and dopamine.

VN arrays have typical diameters and heights proper to work in an intracellular environment since the high aspect ratio and minimal invasiveness allow the application of a lower voltage to produce pores through the cell membrane, minimizing damage to the cells (Chiappini 2017; Shokouhi et al. 2020). For example, a sensing platform based on nanocup electrode arrays can achieve real-time and highly sensitive assessment of neurotransmitters allowing differentiation of dopaminergic neurons from other cells in a completely noninvasive and label-free mode (Kim et al. 2015).

5.2 Nanopores

Several research groups worldwide have modified single and nanopore ensembles in different ways to detect biomolecules using resistive pulse or current rectification as signal generation means (Choi et al. 2006; Ongaro and Ugo 2013; Perez-Mitta et al. 2017). Electrogenerated chemiluminescence (ECL) can also be used as a signal generator, using a gold-modified nanopore membrane ensemble as a detection platform. The working principle encompasses an antibody immobilized on a polycarbonate track-etched membrane. The target analyte binds to the antibody, then a biotinylated secondary antibody is bound, which in turn captures a streptavidin-modified ruthenium-based ECL label. A potential is applied on the gold surface that oxidizes a tri-n-propylamine solution, generating an ECL signal (Habtamu et al. 2015).

Pan et al. introduced a nanopipette as a scanning ion conductance microscopy tip. Vesicles and nanoparticles can be determined inside cells following localized resistive pulses. This method allows the detection of cellular vesicles inside a macrophage and 10 nm Au nanoparticles in cytoplasm selectively. Also, they developed an alternative version of the resistive pulse technique using conductive carbon nanopipettes, the reduction and oxidation processes produced on the carbon nanopipette allow the analysis of the electroactive species contained in the cell. Figure 6.8 schematized the different approaches (Pan et al. 2019, 2020).

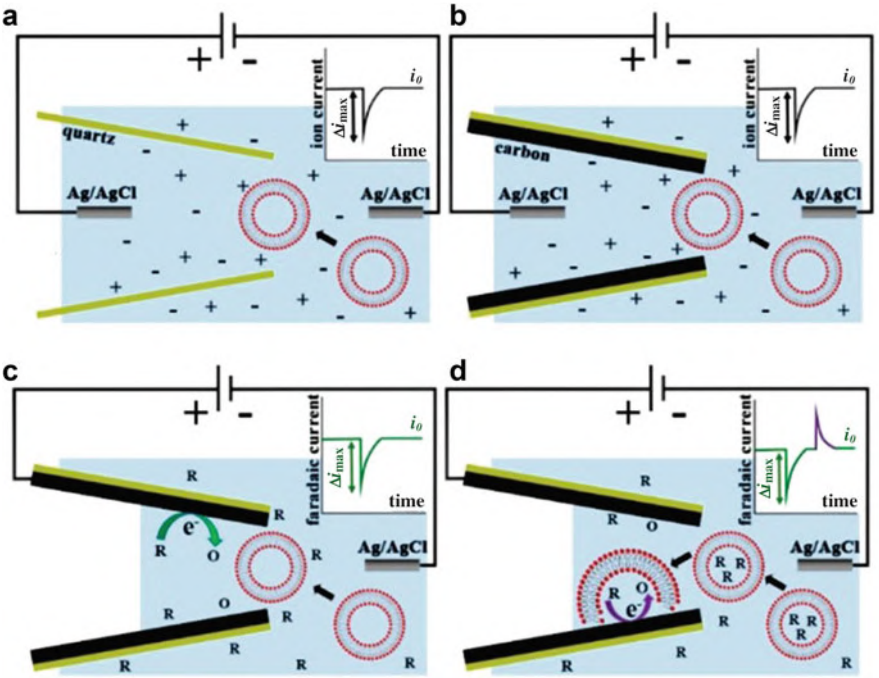
a
+
-
quartz
ion current
Δi_{max}
i_0
time
Ag/AgCl
Ag/AgCl
b
carbon
ion current
Δi_{max}
i_0
time
Ag/AgCl
Ag/AgCl
c
faradaic current
Δi_{max}
i_0
time
e⁻
R
O
Ag/AgCl
d
faradaic current
Δi_{max}
i_0
time
e⁻
R
O
Ag/AgCl

Fig. 6.8 Four types of resistive pulse experiments involving translocation of liposomes through quartz (**a**) and carbon (**b–d**) nanopipettes. The insets depict the ion current changes due to the blockage in resistive pulse configurations (**a, b**). In **c** and **d**, faradaic current spikes are produced by either a blockage of the pore (downward peaks) or a redox process inside a liposome (upward peak in **d**) (Pan et al. 2019). (Reprinted with permission from American Chemical Society)

6 Concluding Remarks

Nanopores and nanoelectrodes in their different configurations are becoming a powerful tool in basic research studies in biomedicine (Li et al. 2015, 2020; Li et al. 2016; Pan et al. 2019; Larsson et al. 2020). As soon as some bottlenecks can be solved to scale their fabrication, these devices will have an immediate application in cell studies replacing or complementing current techniques such as patch-clamp or fluorescent reporters. On the other hand, its application in routine clinical chemistry to get a myriad of information from a simple drop of blood looks more distant. Here, mass-scale production must be solved, and the proper working conditions must be achieved; for example, most of the devices presented for nonenzymatic glucose detection work at alkaline pH, a drawback for a clinical sensor. This fact highlights a limitation in the techniques for adequately modifying these nanostructures, and, to a greater extent, selectively modifying a single or a restricted number of the electrodes conforming the array. In this sense, the works devoted to controlling mercapto-surface derivatization (Jambrec et al. 2015; Haag et al. 2016), target electropolymerization (Yanez-Heras et al. 2010; Azevedo Beluomini et al. 2019), and selective reduction of diazonium salts (Hetemi et al. 2020) deserve further research. Also, developments for electrical addressing individual elements in nanoelectrode ensembles should be carried out.

Acknowledgments The author gratefully acknowledges financial support from ANPCYT (Argentina) and Universidad de Buenos Aires. The author is a research staff of CONICET (Argentina).

References

Abbott J et al (2017) CMOS nanoelectrode array for all-electrical intracellular electrophysiological imaging. Nat Nanotechnol 12:460–466. https://doi.org/10.1038/NNANO.2017.3

Abbott J et al (2020) A nanoelectrode array for obtaining intracellular recordings from thousands of connected neurons. Nat Biomed Eng 4(2):232–241. https://doi.org/10.1038/s41551-019-0455-7

Ahmad R et al (2017) Highly efficient non-enzymatic glucose sensor based on CuO modified vertically-grown ZnO Nanorods on electrode OPEN. Sci Rep 7:5715–5724. https://doi.org/10.1038/s41598-017-06064-8

Amatore C, Oleinick AI, Svir I (2009) Numerical simulation of diffusion processes at recessed disk microelectrode arrays using the quasi-conformal mapping approach. Anal ChemAmerican Chemical Society 81(11):4397–4405. https://doi.org/10.1021/ac9003419

Ashwell J, G. et al (2011) Self-assembly of amino−thiols via gold−nitrogen links and consequence for in situ elongation of molecular wires on surface-modified electrodes. J Phys Chem C 115(10):4200–4208. https://doi.org/10.1021/jp200006j

Aydin EB, Kemal Sezgintürk M (2017) Indium tin oxide (ITO): a promising material in biosensing technology. Trends Anal Chem 97:309–315. https://doi.org/10.1016/j.trac.2017.09.021

Azevedo Beluomini M et al (2019) Tailor-made 3D-nanoelectrode ensembles modified with molecularly imprinted poly(o-phenylenediamine) for the sensitive detection of L-arabitol. Sensors Actuators B Chem 284:250–257. https://doi.org/10.1016/j.snb.2018.12.091

Bahr JL et al (2001) Functionalization of carbon nanotubes by electrochemical reduction of aryl diazonium salts: a bucky paper electrode. J Am Chem Soc 123(27):6536–6542. Available at: http://www.ncbi.nlm.nih.gov/pubmed/11439040

Bayley H, Martin CR (2000) Resistive-pulse SensingFrom microbes to molecules. Chem Rev ACS 100(7):2575–2594. https://doi.org/10.1021/cr980099g

Bietsch A et al (2004) Rapid functionalization of cantilever array sensors by inkjet printing. Nanotechnology 15(8):873–880. https://doi.org/10.1088/0957-4484/15/8/002

Bruchhaus L et al (2017) Comparison of technologies for nano device prototyping with a special focus on ion beams: a review. Appl Phys Rev. American Institute of Physics Inc.:11302. https://doi.org/10.1063/1.4972262

Chaturvedi P et al (2016) Simple and versatile detection of viruses using anodized alumina membranes. ACS Sens 1:488–492. https://doi.org/10.1021/acssensors.6b00003

Chen Q, Liu Z (2019) Fabrication and applications of solid-state nanopores. Sensors 19:1886. https://doi.org/10.3390/s19081886

Chen T et al (2016) Three-dimensional Ni2P Nanoarray: an efficient catalyst electrode for sensitive and selective non-enzymatic glucose sensing with high specificity. Anal Chem. American Chemical Society 88(16):7885–7889. https://doi.org/10.1021/acs.analchem.6b02216

Chen YC et al (2017) Fabrication of Fe_3O_4 nanotube arrays for high-performance non-enzymatic detection of glucose. J Electroanal Chem. Elsevier BV 788:144–149. https://doi.org/10.1016/j.jelechem.2017.02.007

Chiappini C (2017) Nanoneedle-based sensing in biological systems. ACS Sensors., American Chemical Society 2(8):1086–1102. https://doi.org/10.1021/acssensors.7b00350

Choi Y et al (2006) Biosensing with conically shaped nanopores and nanotubes. Phys Chem Chem Phys. The Royal Society of Chemistry 8(43):4976–4988. https://doi.org/10.1039/B607360C

Clausmeyer J, Schuhmann W (2016) Nanoelectrodes: applications in electrocatalysis, single-cell analysis and high-resolution electrochemical imaging. 79:46–59. https://doi.org/10.1016/j.trac.2016.01.018

Compton RG et al (2008) Design, fabrication, characterisation and application of nanoelectrode arrays. Chem Phys Lett 459(1–6):1–17. https://doi.org/10.1016/j.cplett.2008.03.095

Coulter WH (1953) Means for counting particles suspended in a fluid. United States patent 2,656,508, p 9. Available at: www.google.com/patents/US2656508

Davies TJ et al (2005) The cyclic and linear sweep voltammetry of regular arrays of microdisc electrodes: fitting of experimental data. J Electroanal Chem 585(1):51–62. https://doi.org/10.1016/j.jelechem.2005.07.021

Dincer C et al (2015) Nanocrystalline boron-doped diamond nanoelectrode arrays for ultrasensitive dopamine detection. Electrochim Acta. Elsevier Ltd 185:101–106. https://doi.org/10.1016/j.electacta.2015.10.113

Falconnet D et al (2006) Surface engineering approaches to micropattern surfaces for cell-based assays. Biomaterials 27(16):3044–3063. https://doi.org/10.1016/j.biomaterials.2005.12.024

Fu K, Bohn PW (2018) Nanopore electrochemistry: a nexus for molecular control of electron transfer reactions. 4:20. https://doi.org/10.1021/acscentsci.7b00576

Ganapathi A, Swaminathan P, Neelakantan L (2019) Anodic aluminum oxide template assisted synthesis of copper nanowires using a galvanic displacement process for electrochemical denitrification. ACS Appl NanoMat. UTC 2:5981–5988. https://doi.org/10.1021/acsanm.9b01409

González G et al (2010) Mass transport effect of mesoscopic domains in the amperometric response of an electroactive species: modeling for its applications in biomolecule detection. Sensors Actuators B Chem 144(2):349–353. https://doi.org/10.1016/j.snb.2008.11.006

Guo J, Lindner E (2009) Cyclic Voltammograms at coplanar and shallow recessed microdisk electrode arrays: guidelines for design and experiment. Anal Chem. American Chemical Society 81(1):130–138. https://doi.org/10.1021/ac801592j

Haag A-L et al (2016) Selective in situ potential-assisted SAM formation on multi electrode arrays. Nanotechnology 27(45):455501. https://doi.org/10.1088/0957-4484/27/45/455501

Habtamu B, H. et al (2015) A sensitive electrochemiluminescence immunosensor for celiac disease diagnosis based on nanoelectrode ensembles. Anal Chem 87(24):12080–12087. https://doi.org/10.1021/acs.analchem.5b02801

Henstridge MC, Compton RG (2012) Mass transport to micro- and nanoelectrodes and their arrays: a review. Chem Rec. Wiley 12(1):63–71. https://doi.org/10.1002/tcr.201100032

Hetemi D, Noël V, Pinson J (2020) Grafting of Diazonium salts on surfaces: application to biosensors. Biosensors 10:4. https://doi.org/10.3390/bios10010004

Huang J et al (2014) Dispersed CuO nanoparticles on a silicon nanowire for improved performance of non-enzymatic H_2O_2 detection. ACS Appl Mater Interfaces. American Chemical Society 6(10):7055–7062. https://doi.org/10.1021/am501799w

Jamal M et al (2012) Non-enzymatic and highly sensitive H_2O_2 sensor based on Pd nanoparticle modified gold nanowire Array electrode. J Electrochem Soc 159(11):B825–B829. https://doi.org/10.1149/2.010212jes

Jambrec D et al (2015) Potential-assisted DNA immobilization as a prerequisite for fast and controlled formation of DNA monolayers. Angew Chem Int Ed Engl. Wiley-VCH Verlag 54(50):15064–15068. https://doi.org/10.1002/anie.201506672

Jambrec D, Kayran YU, Schuhmann W (2019) Controlling DNA/surface interactions for potential pulse-assisted preparation of multi-probe DNA microarrays. Electroanalysis. Wiley-VCH Verlag 31(10):1943–1951. https://doi.org/10.1002/elan.201900233

Joshi-Imre A, Bauerdick S (2014) Direct-write ion beam lithography. J Nanotechnol. Hindawi Publishing Corporation. https://doi.org/10.1155/2014/170415

Kant K et al (2014) The influence of nanopore dimensions on the electrochemical properties of nanopore arrays studied by impedance spectroscopy. Sensors 14:21316–21328. https://doi.org/10.3390/s141121316

Karimian N, Ugo P (2019) Recent advances in sensing and biosensing with arrays of nanoelectrodes * this review comes from a themed issue on sensors and biosensors. Curr Opin Electrochem 16:106–116. https://doi.org/10.1016/j.coelec.2019.04.026

Kaya D, Keçeci K (2020) Review – track-etched nanoporous polymer membranes as sensors: a review. J Electrochem Soc 167(3):037543. https://doi.org/10.1149/1945-7111/ab67a7

Kim T-H et al (2015) Large-scale nanoelectrode arrays to monitor the dopaminergic differentiation of human neural stem cells. Adv Mater. Wiley-VCH Verlag 27(41):6356–6362. https://doi.org/10.1002/adma.201502489

Ko H, Chang S, Tsukruk VV (2009) Porous substrates for label-free molecular level detection of nonresonant organic molecules. ACS Nano 3(1):181–188. https://doi.org/10.1021/nn800569f

Kumar Jena B, Percival J, S. and Zhang, B. (2010) Au disk nanoelectrode by electrochemical deposition in a nanopore. Anal Chem 82(15):6737–6743. https://doi.org/10.1021/ac101261m

Kumar A et al (2018) Nanoengineered material based biosensing electrodes for enzymatic biofuel cells applications. Mater Sci Ener Technol. Elsevier 1(1):38–48. https://doi.org/10.1016/J.MSET.2018.04.001

Lantiat D et al (2010) Gold nanoelectrode arrays and their evaluation by impedance spectroscopy and cyclic voltammetry. Chem Phys Chem. Wiley-VCH Verlag 11(9):1971–1977. https://doi.org/10.1002/cphc.200900929

Lanyon YH et al (2007) Fabrication of nanopore array electrodes by focused ion beam milling. Anal Chem. American Chemical Society 79(8):3048–3055. https://doi.org/10.1021/ac061878x

Larsson A et al (2020) Intracellular electrochemical Nanomeasurements reveal that exocytosis of molecules at living neurons is subquantal and complex. Angew Chem Int Ed. Wiley-VCH Verlag 59(17):6711–6714. https://doi.org/10.1002/anie.201914564

Laucirica G et al (2019) Amine-phosphate specific interactions within nanochannels: binding behavior and nanoconfinement effects. J Phys Chem C. American Chemical Society 123(47): 28997–29007. https://doi.org/10.1021/acs.jpcc.9b07977

Lee W, Park S-J (2014) Porous anodic aluminum oxide: anodization and templated synthesis of functional nanostructures. Chem Rev. American Chemical Society 114(15):7487–7556. https://doi.org/10.1021/cr500002z

Lee J et al (2016) Sensitive and selective detection of HIV-1 RRE RNA using vertical silicon nanowire electrode array. Nanoscale Res Lett 11:341. https://doi.org/10.1186/s11671-016-1504-8

Li Y, Bergman D, Zhang B (2009) Preparation and electrochemical response of 1−3 nm Pt disk electrodes. Anal Chem 81(13):5496–5502. https://doi.org/10.1021/ac900777n

Li X et al (2015) Electrochemical cytometry quantitative Measurementof transmitters in individual vesicles in the cytoplasm of single cells with nanotip electrodes. Angew Chem Int Ed Engl 54: 11978–11982. https://doi.org/10.1002/ange.201504839

Li X, Dunevall J, Ewing G, A. (2016) Quantitative chemical measurements of vesicular transmitters with electrochemical cytometry. Acc Chem Res 49(10):2347–2354. https://doi.org/10.1021/acs.accounts.6b00331

Li X et al (2020) Vertical nanowire array-based biosensors: device design strategies and biomedical applications. J Mater Chem B. The Royal Society of Chemistry 8(34):7609–7632. https://doi.org/10.1039/D0TB00990C

Libioulle L et al (1999) Contact-inking stamps for microcontact printing of alkanethiols on gold. Langmuir., American Chemical Society 15(2):300–304. https://doi.org/10.1021/la980978y

Manheller M et al (2012) Reliable fabrication of 3 nm gaps between nanoelectrodes by electron-beam lithography. Nanotechnology 23(12):125302. https://doi.org/10.1088/0957-4484/23/12/125302

Md Jani AM, Losic D, Voelcker NH (2013) Nanoporous anodic aluminium oxide: advances in surface engineering and emerging applications. Prog Mater Sci 58(5):636–704. https://doi.org/10.1016/j.pmatsci.2013.01.002

Oja SM, Wood M, Zhang B (2013) Nanoscale electrochemistry. Anal Chem 85(2):473–486. https://doi.org/10.1021/ac3031702

Oja M, S. et al (2016) Nanoscale electrochemistry revisited. Anal Chem. American Chemical Society 88(1):414–430. https://doi.org/10.1021/acs.analchem.5b04542

Ongaro M, Ugo P (2013) Bioelectroanalysis with nanoelectrode ensembles and arrays. Anal Bioanal Chem 405(11):3715–3729. https://doi.org/10.1007/s00216-012-6552-z

Pan R et al (2019) Electrochemical resistive-pulse sensing. J Am Chem Soc. UTC 141:49. https://doi.org/10.1021/jacs.9b10329

Pan R et al (2020) Resistive-pulse sensing inside single living cells. J Am Chem Soc 142(12): 5778–5784. https://doi.org/10.1021/jacs.9b13796

Peinetti AS, González GA, Battaglini F (2010) Modeling the electrochemical response of mesoporous materials toward its application to biomolecular detection. Electroanalysis 22(12): 1329–1336. https://doi.org/10.1002/elan.200900572

Peinetti AS et al (2012) A polyelectrolyte-surfactant complex as support layer for membrane functionalization. J Colloid Interface Sci 386(1):44–50. https://doi.org/10.1016/j.jcis.2012.07.015

Peinetti AS et al (2013) Synthesis of atomic metal clusters on nanoporous alumina. Chem Commun. The Royal Society of Chemistry 49(96):11317–11319. https://doi.org/10.1039/C3CC47170E

Peinetti AS et al (2015) Confined gold nanoparticles enhance the detection of small molecules in label-free impedance aptasensors. Nanoscale 7(17):7763–7769. https://doi.org/10.1039/c5nr01429h

Peinetti AS et al (2016) Numerical simulation of the diffusion processes in nanoelectrode arrays using an axial neighbor symmetry approximation. Anal Chem 88(11):5752–5759. https://doi.org/10.1021/acs.analchem.6b00039

Peinetti AS et al (2018) Characterization and electrochemical response of DNA functionalized 2 nm gold nanoparticles confined in a nanochannel array. Bioelectrochemistry 121:169–175. https://doi.org/10.1016/j.bioelechem.2018.02.002

Pérez-Mitta G, Marmisollé WA et al (2015a) Nanofluidic diodes with dynamic rectification properties stemming from reversible electrochemical conversions in conducting polymers. J Am Chem Soc. American Chemical Society 137(49):15382–15385. https://doi.org/10.1021/jacs.5b10692

Pérez-Mitta G, Tuninetti JS et al (2015b) Polydopamine meets solid-state nanopores: a bioinspired integrative surface chemistry approach to tailor the functional properties of nanofluidic diodes. J Am Chem Soc 137(18):6011. https://doi.org/10.1021/jacs.5b01638

Perez-Mitta G et al (2017) Bioinspired integrated nanosystems based on solid-state nanopores: ‘iontronic’ transduction of biological, chemical and physical stimuli. Chem Sci 8:890–913. https://doi.org/10.1039/c6sc04255d

Pérez-Mitta G et al (2018) Highly sensitive biosensing with solid-state nanopores displaying enzymatically reconfigurable rectification properties. Nano Lett. American Chemical Society 18(5):3303–3310. https://doi.org/10.1021/acs.nanolett.8b01281

Purohit B et al (2020) Biosensor nanoengineering: design, operation, and implementation for biomolecular analysis. Sens Int. Elsevier 1:100040. https://doi.org/10.1016/J.SINTL.2020.100040

Richardson JJ et al (2016) Innovation in layer-by-layer assembly. Chem Rev 116(23): 14828–14867. https://doi.org/10.1021/acs.chemrev.6b00627

Salomon S et al (2012) Arrays of nanoelectromechanical biosensors functionalized by microcontact printing. Nanotechnology 23(49):495501. https://doi.org/10.1088/0957-4484/23/49/495501

Santos A et al (2020) Porous alumina membrane-based electrochemical biosensor for protein biomarker detection in chronic wounds. Front Chem | wwwfrontiersinorg 8:155. https://doi.org/10.3389/fchem.2020.00155

Scho C et al (1997) Template synthesis of nanowires in porous polycarbonate membranes: electrochemistry and morphology. J Phys Chem B 101:5497–5505. Available at: https://pubs.acs.org/sharingguidelines

Schultz J et al (2020) Glutamate sensing in biofluids: recent advances and research challenges of electrochemical sensors. Analyst. Royal Society of Chemistry 145:321–347. https://doi.org/10.1039/c9an01609k

Sharma S et al (2018) Engineered nanoporous materials mediated heterogeneous catalysts and their implications in biodiesel production. Mater. Sci Ener Technol. Elsevier 1(1):11–21. https://doi.org/10.1016/J.MSET.2018.05.002

Shokouhi A-R et al (2020) Vertically configured nanostructure-mediated electroporation: a promising route for intracellular regulations and interrogations. Materi Horiz. The Royal Society of Chemistry 7(11):2810–2831. https://doi.org/10.1039/D0MH01016B

Siepenkoetter T et al (2017) Immobilization of redox enzymes on nanoporous gold electrodes: applications in biofuel cells. ChemPlusChem. Wiley-VCH Verlag GmbH & Co KGaA 82(4): 553–560. https://doi.org/10.1002/cplu.201600455

Silvestrini M et al (2011) Modification of nanoelectrode ensembles by thiols and disulfides to prevent non specific adsorption of proteins. Electrochim Acta 56:7718–7724. https://doi.org/10.1016/j.electacta.2011.06.034

Siwy Z et al (2005) Protein biosensors based on biofunctionalized conical gold nanotubes. J Am Chem Soc 127(14):5000–5001. https://doi.org/10.1021/ja043910f

Sun P (2010) Cylindrical nanopore electrode and its application to the study of electrochemical reaction in several hundred attoliter volume. Anal Chem 82(1):276–281. https://doi.org/10.1021/ac9019335

Wang J, Li Z, Gu Z (2021) A comprehensive review of template-synthesized multi-component nanowires: from interfacial design to sensing and actuation applications. Sens Actuators Rep. Elsevier BV 3:100029. https://doi.org/10.1016/j.snr.2021.100029

Wightman RM (1981) Microvoltammetric Electrodes. Anal Chem. UTC 53:1125A–1134A. https://doi.org/10.1021/ac00232a004

Wirtz M, Yu S, Martin CR (2002) Template synthesized gold nanotube membranes for chemical separations and sensing. Analyst. Royal Society of Chemistry:871–879. https://doi.org/10.1039/b201939f

Wongkaew N et al (2019) Functional Nanomaterials and nanostructures enhancing electrochemical biosensors and lab-on-a-chip performances: recent Progress, applications, and future perspective. Chem Rev. American Chemical Society 119(1):120–194. https://doi.org/10.1021/acs.chemrev.8b00172

Xie F et al (2018) Cobalt nitride nanowire array as an efficient electrochemical sensor for glucose and H2O2 detection. Sensors Actuators B 255:1254–1261. https://doi.org/10.1016/j.snb.2017.08.098

Xue L et al (2020) Solid-state nanopore sensors. Nat Rev Mater 5(12):931–951. https://doi.org/10.1038/s41578-020-0229-6

Yameen B et al (2009) Single conical nanopores displaying pH-tunable rectifying characteristics. Manipulating ionic transport with Zwitterionic polyer brushes. J Am Chem Soc. American Chemical Society 131(6):2070–2071. https://doi.org/10.1021/ja8086104

Yanez-Heras J, Pallarola D, Battaglini F (2010) Electronic tongue for simultaneous detection of endotoxins and other contaminants of microbiological origin. Biosens Bioelectron 25(11): 2470–2476. https://doi.org/10.1016/j.bios.2010.04.004

Zhang H et al (2003) Biofunctionalized nanoarrays of inorganic structures prepared by dip-pen nanolithography. Nanotechnology 14(10):1113–1117. https://doi.org/10.1088/0957-4484/14/10/308

Zhang B, Zhang Y, White HS (2004) The nanopore electrode. Anal Chem. American Chemical Society 76(21):6229–6238. https://doi.org/10.1021/ac049288r

Zhang Y, Zhang B, White S, H. (2006) Electrochemistry of nanopore electrodes in low ionic strength solutions. J Phys Chem B. American Chemical Society 110(4):1768–1774. https://doi.org/10.1021/jp054704c

Zhang B et al (2007) Bench-top method for fabricating glass-sealed nanodisk electrodes, glass nanopore electrodes, and glass nanopore membranes of controlled size. Anal Chem 79(13): 4778–4787. https://doi.org/10.1021/ac070609j

Nanoscale Electrochemical Sensors for Intracellular Measurements at the Single Cell

7

Amir Hatami, Xinwei Zhang, Pieter E. Oomen, and Andrew G. Ewing

Contents

1 Introduction 132
2 Electrochemistry at Micro-/Nanoelectrodes and Instrumental Aspects 133
3 Fabrication Methods of Nano-/Microscale Electrochemical Sensors 134
4 Modification of Nanoscale Electrochemical Sensors and Their Combination with Other Analytical Techniques 141
5 Intracellular Analytes 145
  5.1 Intracellular Analysis of Electroactive Targets 146
  5.2 Intracellular Analysis of Nonelectroactive Targets 147
6 Conclusion and Outlook 148
References 148

A. Hatami (✉)
Department of Chemistry and Molecular Biology, University of Gothenburg, Gothenburg, Sweden

Department of Chemistry, Institute for Advanced Studies in Basic Sciences, Zanjan, Iran
e-mail: amir.hatami@gu.se

X. Zhang
College of Chemistry and Molecular Sciences, Wuhan University, Wuhan, China
e-mail: xinweizhang@whu.edu.cn

P. E. Oomen
Department of Chemistry and Molecular Biology, University of Gothenburg, Gothenburg, Sweden

ParaMedir B.V, Groningen, The Netherlands

A. G. Ewing (✉)
Department of Chemistry and Molecular Biology, University of Gothenburg, Gothenburg, Sweden
e-mail: andrewe@chem.gu.se

© Springer Nature Singapore Pte Ltd. 2023

U. P. Azad, P. Chandra (eds.), *Handbook of Nanobioelectrochemistry*,
https://doi.org/10.1007/978-981-19-9437-1_7

Abstract

The single cell is an important target for bioelectrochemical analysis. It is noteworthy that most biological processes occur at the cellular level, such as production, storage, and secretion of most neurotransmitters and hormones, and other vital biomolecules. Due to the small size of the cells (micrometer range), low concentrations of intracellular biological targets (nM to μM range), the high rate of most intracellular processes and reactions (subsecond), and vulnerability of cells, tiny probes with adequate sensitivity and high spatiotemporal resolution are required for their assessment. In this chapter, we have discussed the development and recent examples of real-time intracellular electrochemical sensing. Thanks to their superior temporal and spatial resolution, sensors based on micro- and nanoelectrodes have allowed researchers to quantitatively analyze a wide range of (bio)molecules and ions in real time, both inside cells and organelles (e.g., vesicles). Although electrochemistry has been employed for intracellular analysis for decades, many challenges regarding microfabrication, attaining sufficient sensitivity and selectivity, and measuring multiple parameters in a parallel fashion still remain.

Keywords

Nanoscale sensors · Intracellular measurement · Single cell analysis · Vesicles

1 Introduction

The single cell is a key target for electroanalysis. It is noteworthy that most biological processes happen at the cellular level, such as production, storage, and secretion of most neurotransmitters and hormones and other vital biomolecules. Due to the small size of the cells (micrometer range), low concentrations of intracellular biological targets (nM to μM range), the high rate of most intracellular processes and reactions (subsecond), and vulnerability of cells, tiny probes with adequate sensitivity and high spatiotemporal resolution are required for their assessment. Among analytical techniques, ultramicro- and nano-electrochemical methods are powerful tools for intracellular analysis, because they can be performed in the cytoplasm and quantify electroactive and some nonelectroactive targets inside the cell. The miniaturization of (bio)sensors unlocks the study of intracellular phenomena that have been unreachable by existing other analytical methods. Intracellular sensing has revealed fundamental details of cellular processes that are essential for medical research and disease treatment. To date, many micro-/nanoscale electrodes with different shapes and geometries have been fabricated and applied. In this chapter, we review the unique advantages, fabrication methods, and recent progress of micro-/nanoscale electrodes applied to electrochemical analysis inside single cells, alone or combined with other methods.

2 Electrochemistry at Micro-/Nanoelectrodes and Instrumental Aspects

The introduction of microscale electrodes to in vivo analysis by professors Wightman and Fleischmann in the 1980s (Pons and Fleischmann 1987; Wightman 1981; Zoski 2002) has triggered extraordinary advances in electroanalytical chemistry. Initially, this type of electrode was known as “ultramicroelectrode,” but over time the term “microelectrode” became widely accepted. Compared to macroelectrodes, microelectrodes have small dimensions ranging from tens of micrometers or less, down to the submicrometer range. To date, a myriad of this type of electrodes (Chen et al. 2020a; Sun et al. 2008; Van Leeuwen et al. 2002; Zoski 2002) has been developed and applied, exhibiting various geometries (e.g., cylinder, disk, ring, etc.,), dimensions (nm to μm), and different materials such as carbon, platinum, gold, mercury, and silver (Clausmeyer and Schuhmann 2016; Ying et al. 2017; Zhang et al. 2020). Many excellent discussions of the relation between electrochemical performance and electrode material, size, and geometry have been presented previously (Arrigan 2004; Forster and Keyes 2007; Heinze 1993). Here, we will focus on the advantages of electrode size reduction.

When electrode dimensions are small enough to be comparable to the electrical double layer thickness, new properties are introduced that make the performance of micro-/nanoelectrodes different from that of larger macroelectrodes. In summary, the unique advantages of micro-/nanoelectrodes are comprised of the following:

(a) The analysis can be performed in small volumes or at microscopically small objects, such as tissue sections, single cells, and intracellular organelles.
(b) Reducing the electrode size down to the diffusion layer thickness can affect mass transport by giving rise to a three-dimensional, radial, rather than planar (which is dominant in micro-/nanoelectrodes) diffusion profile. Because of the high transport rates of analyte from the bulk of solution toward the electrode surface seen in radial diffusion, the steady state for a faradaic process under constant potential can be established very rapidly (~milliseconds to seconds).
(c) The ratio between faradaic and charging currents is improved, as the charging current decreases with the reducing electrode area, while the faradaic current reduces less. This low charging current benefits measurements employing potentiodynamic electrochemical techniques, like cyclic voltammetry and potential step techniques. A unique application of this is found in fast-scan cyclic voltammetry (FSCV). FSCV is a variant of the well-established cyclic voltammetry technique, employing much higher scan rates (less than or equal to ~10^6 V.s^{-1}), leading to a high temporal resolution (~msec) of measurements (Bard and Faulkner 2001; Amatore 1995; Zoski 1996; Wightman and Wipf 1989; Schulte and Schuhmann 2007). This has proven mainly useful for monitoring biomolecules in neuroscience areas.
(d) Short electrochemical response time can be achieved. Benefitting from the fast discharging, microelectrodes allow the monitoring of small and rapid variations in the amount of electroactive species with high temporal resolution (≤ms). This

also makes it possible to monitor rapid electrode processes (e.g., chemical reactions associated with electrode charge transfer).

(e) The small currents measured at microelectrodes induce significantly less influence of ohmic drop (IR drop) on the signal. This permits measurements in highly resistive solutions that have little or no electrolytes, such as organic solvents. Moreover, this advantage allows use of a two-electrode system (Reference and working electrodes), instead of the three-electrode system (Reference, working, and counter electrodes) necessary for the reduction of IR drop influence when working with macroelectrodes.

(f) The signal-to-noise ratio is improved. This improvement results from the radial diffusion profile around the micro-/nanoelectrode, which provides a higher flux of electroactive species and induces a higher sensitivity of electrodes.

These properties make micro-/nanoelectrodes advantageous in many areas of electrochemistry, such as studying electrochemical reaction mechanisms, in vivo measurements in biomedical research, and scanning electrochemical microscopy imaging. Additionally, access to highly sensitive, low-noise amplifiers allows the monitoring of extremely small current variations (~100 fA). This opens up possible applications of electrochemical probes in trace analysis and motoring of fast biological processes. In fact, the above-listed advantages depend on the reliability and sensitivity of the instrumentation employed for cellular analysis and fabrication techniques of micro-/nanoelectrodes (Bard and Faulkner 2001; Amatore 1995; Zoski 1996; Wightman and Wipf 1989; Pons and Fleischmann 1987; Wightman 1981).

In order to realize intracellular electrochemical analysis, the first important practical challenge is maintaining cell viability during experiments. To reduce cell damage, it is crucial to reduce the dimensions of the electrode tip to the submicrometer range – although some micrometer-size electrodes have been applied for intracellular analysis of giant cells, like frog oocytes (Fulati et al. 2010). Moreover, insertion of small electrodes into cells is a challenge in itself and needs complementary instruments, such as optical microscopes and micromanipulators. Generally, each electrode is controlled with a micromanipulator, while the whole process of the electrode penetration into a target cell should be observed using an optical microscope. Typically, the tip of the electrode is placed on top of a single cell. The electrode is then pressed through the cell membrane by use of a micromanipulator to enter the cytoplasm of the cell. Depending on the electrochemical techniques used, the potential or current can be recorded (Table 7.1). In some cases, the electrochemical analysis is combined with other analytical methods, allowing improved quality of the measurement or collection of new, complementary data.

3 Fabrication Methods of Nano-/Microscale Electrochemical Sensors

Because of the unique advantages of micro-/nanoelectrodes, a lot of effort has been made to improve their fabrication, leading to various efficient and controllable fabrication strategies. Typically, these can be categorized into “top-down” and

Table 7.1 Detected intracellular targets by micro-/nanoscale electrodes

Intracellular target(s)	Cell type(s)	Electrochemical sensors/dimension	Electrochemical method	References
Oxygen	Gracilis muscle cells of guinea pig	Wood's metal and gold in micropipette/D[1]: 1–2 μm	Amperometry	Whalen and Nair (1967)
Oxygen	Protoplast of *Bryopsis plumosa*	Silver-ring microelectrodes/D: ≤ 1 μm	Amperometry	Uchida et al. (1990)
Glucose	Human adipocytes and frog oocytes	Coated glass microcapillary with nanoflake ZnO/N.R[2]	Potentiometry	Fulati et al. (2010)
Glucose	Human umbilical vein endothelial cells	Enzymatic platinized SiC@C@Au nanowire/L[3]: 10 μm and D: 500–600 nm	Amperometry	Liao et al. (2019)
Glucose	HeLa cells	Platinum ("nano-kit") on nanopipette/Pt layer: thickness 70 nm and D: 200 nm	Amperometry	Pan et al. (2016)
Glucose	Breast cancer cell lines: MDA-MB-231 and MCF-7	Enzyme-modified nanopipettes/D: ~90 nm	Potentiometry	Nascimento et al. (2016)
Catecholamines	PC12 [4] and chromaffin cells	Conical carbon-fiber electrode/D: 500 nm and tip diameter: ~50 nm	Amperometry	Li et al. (2015, 2016a); Majdi et al. (2017); Ren et al. (2017); Ye et al. (2018)
Catecholamines	Chromaffin cells	Nanopore carbon electrode/D range: 50–500 nm	Amperometry	Hu et al. (2020)
Catecholamines	PC12 cells	Conical carbon-fiber electrode/L: 5 μm and tip diameter: ~300 nm	Amperometry and fast-scan cyclic voltammetry	Roberts et al. (2020)
Serotonin	Beta cells	Conical CFE[5]/D: 500 nm and tip diameter: ~50 nm	Amperometry	Hatamie et al. (2020)

(continued)

Table 7.1 (continued)

Intracellular target(s)	Cell type(s)	Electrochemical sensors/dimension	Electrochemical method	References
ROS and RNS[6]	Noncancerous and metastatic human breast cells	Platinized carbon Nanoelectrodes/D: 80 nm	Voltammetry and amperometry	Hu et al. (2019)
ROS and RNS	RAW 264.7 macrophages	Platinized carbon nanoelectrodes/ D:≤100 nm)	Voltammetry and Amperometry	Li et al. (2017)
ROS and RNS	RAW 264.7 macrophages	Platinized SiC@C nanowire/L:10 μm D: 300–600 nm	Amperometry	Zhang et al. (2017, 2019)
Mitochondrial ROS	NIH 3 T3 cell	Platinized SiC@C nanowire/L:10 μm D: 300–600 nm	Amperometry	Jiang et al. (2019)
ROS	HEK293 and LNCaP cancer cells	Platinized commercial carbon electrodes/D: 60–100 nm	Amperometry	Erofeev et al. (2018)
H_2O_2	Murine macrophage J774A.1 Human embryonic kidney TSA201 cells	Carbon nanoelectrodes modified with Prussian blue/D: 50–200 nm	Amperometry	Marquitan et al. (2016)
H2O2	HeLa cells	Platinum (“nano-kit”)/Pt film thickness: 70 nm and D:200 nm	Amperometry	Pan et al. (2018)
H2O2	HeLa cells	Composite electrode/D: 1–2 μm	Electrochemiluminescence	He et al. (2016)
$OH^{\bullet}$	RAW 264.7 macrophages	Open gold nanopipette electrode	Voltammetry	Chen et al. (2020b)

K^+	Human oocytes	Modified glass microcapillary with ZnO nanowire and K^+ membrane	Potentiometry	Usman Ali et al. (2011)
H^+ (pH)	Human fibroblasts, HeLa, MDA-MB-231, and MCF-7	Modified nanopipettes/D: ~100 nm	Potentiometry	Özel et al. (2015)
H^+ (pH)	Human adipocytes	Modified glass microcapillary with ZnO nanorod	Potentiometry	Al-Hilli et al. (2007)
Ca^{2+}	HeLa cells	Nanopipette-based field effect transistor/thickness metal layers: 10–30 nm	Fluorescence and Conductometry	Son et al. (2011)
Ca^{2+}	Human adipocytes	Modified glass microcapillary with ZnO nanorod and Ca^{2+}-selective membrane/N.R.	Potentiometry	Asif et al. (2009)
Mg^{2+}	Human adipocyte and frogoocyte	Modified glass microcapillary with ZnO nanorod and Mg^{2+} – selective membrane/N.R.	Potentiometry	Asif et al. (2010)
PO_4^{3-}	HeLa cells	Platinum (“nano-kit”)/Pt thickness: 70 nm and D:200 nm	Amperometry	Xu et al. (2019)

Abbreviations: *D* diameter, *N.R.* not reported, *L* length, *PC12 cell* pheochromocytoma cells, *CFE* carbon fiber electrode, and *ROS* and *RNS* reactive oxygen/nitrogen species "bottom-up" approaches. We will first provide a number of examples of "bottom-up" strategies for manufacturing electrodes for intracellular applications.

In 1967, a small probe was reported for the detection of intracellular oxygen (O_2). To construct this oxygen electrode, a prepulled glass micropipette was filled with an alloy consisting of Wood's metal and gold. The microelectrode had a 4-μm diameter and could detect O_2 in gracilis muscle cells (Whalen and Nair 1967). Later, Ewing's group (Kim et al. 1986) made carbon microring electrodes (tip diameters in the range of 1–4 μm) through pyrolysis of methane gas as a carbon precursor. In this method, methane gas was passed through the quartz capillary continually, while a Bunsen burner outside the capillary was used to pyrolyze the gas to pyrolytic carbon. The carbon layer was deposited on the internal wall of the glass pipette, forming a conductive surface there. After filling the pipette with epoxy and beveling the tip to expose a carbon ring, the electrode was used to detect intracellular dopamine in the presence of ascorbic acid with high selectivity.

In 1990, Tomokazu et al. (Uchida et al. 1990) deposited Ag inside a glass capillary, through the classic silver mirror reaction, and then filled the inside space with epoxy resin. Furthermore, to increase sensitivity of the Ag-ring electrode, Pt was electrochemically deposited on the electrode surface. The modified Pt-ring microelectrodes (tip diameter $\leq$ 1 μm) allowed detection of intracellular O_2 levels in living protoplasts (*Bryopsis plumosa*, Fig. 7.1a). When using this silver mirror method, it is important to control the chemical reaction rate and restrict the silver plating to the inside of the glass capillary, as this greatly affects the size and geometry of the ring electrode.

Noble metal sputtering is another common technique that has been used to fabricate micro-/nanoelectrodes. Using this approach, Long et al. deposited an ultrathin Au layer (Ying et al. 2018) on the inner wall of a glass pipette (tip diameter ~ 100 nm). Chen et al. (Pan et al. 2016) coated both the outer and inner walls of a nanopipette tip with a Pt layer in order to fabricate metallic nanoscale electrodes (tip diameter ~ 200–300 nm). Despite the convenience of this method, precise control of the thickness of the metal layer is cumbersome. In addition, other issues such as insulation and electrical connection often prove challenging.

Recently, Mirkin's group (Hu et al. 2019; Li et al. 2017) presented a nanocavity electrode with a nanoscale dimension (40 nm). To fabricate the nanoelectrode, the orifice at the tip of the glass nanopipette was filled with pyrolytic carbon via a chemical vapor deposition (CVD) technique (Singhal et al. 2010). Generally, these glass micropipettes can have tips at nanoscale ranges, can be fabricated easily, and have been applied extensively for cell injection. Next, the cavity at the tip was packed with Pt nanoparticles using an electrochemical deposition technique. The sharp electrode was used to measure trace concentrations and fluxes of different reactive oxygen/nitrogen species (ROS/RNS) species in different cancer cells (Hu et al. 2019; Li et al. 2017).

Considering the crucial role of vesicles (nanoscale packages consisting of liquid or cytoplasm enclosed by a lipid bilayer) and their cargo in cell-to-cell communications, analysis of stored neurotransmitters or hormones inside these intracellular vesicles is an important issue (Phan et al. 2017). In the 2010s, the Ewing research

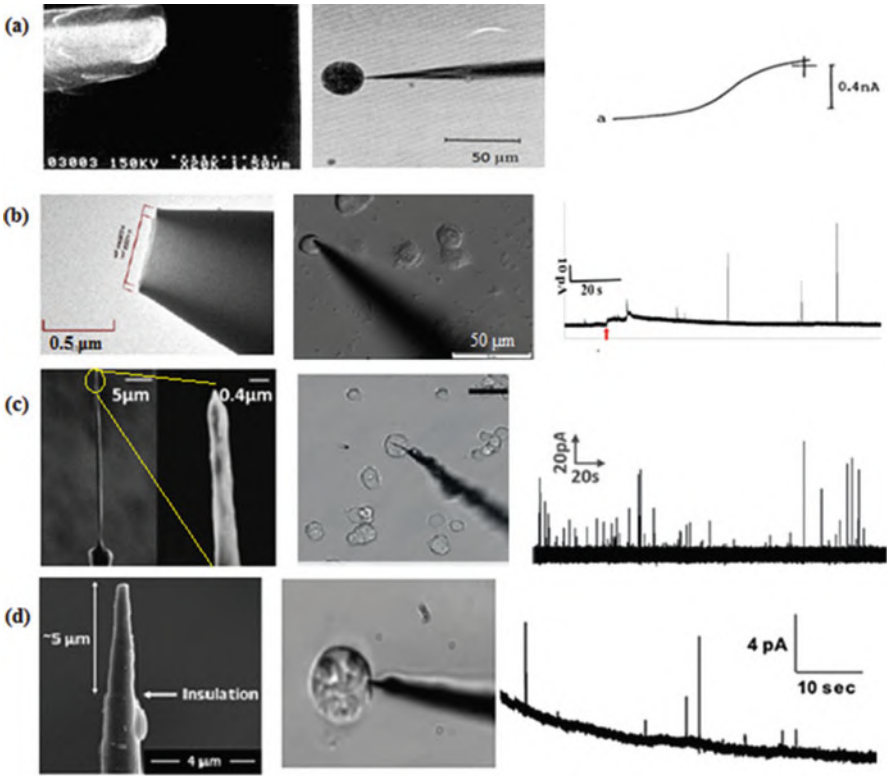

Fig. 7.1 Microscopic images of nanoscale electrodes for intracellular analysis and associated electrochemical signals: (**a**) Images of a silver ring electrode (left), during analysis of oxygen molecules inside a single protoplast (middle) and voltammogram (right) (Uchida et al. 1990) (Reproduced with permission from the Chemical Society of Japan (CSJ), Copyright © 1990): (**b**) images of an open CNP (left), during IVIEC analysis inside a single chromaffin cell (middle) and representative amperometric trace (right) (Hu et al. 2020) (Reproduced with permission from the American Chemical Society (ACS), Copyright © 2020); (**c**) images of nanotip CFE (left), placed in the cytoplasm of a single PC12 cell (middle) and a recorded amperometric trace of an IVIEC measurement (right) (Li et al. 2015) (Reproduced with permission from the WILEY-VCH, Copyright © 2015); and (**d**) image of a conical carbon-fiber electrode (left), inserted into a PC12 cell (middle) and an amperometric trace recorded during IVIEC analysis (right) (Roberts et al. 2020) (Reproduced with permission from the American Chemical Society (ACS), Copyright © 2020)

group introduced two techniques for the quantification of catecholamines. The first, vesicle impact electrochemical cytometry (VIEC), is performed in isolated vesicles (Dunevall et al. 2015). The second, intracellular vesicle impact electrochemical cytometry (IVIEC), is performed inside living, single cells (Li et al. 2015; Phan et al. 2017). Typically, VIEC is done using a carbon disk microelectrode, whereas in IVIEC a flame-etched nanotip carbon-fiber electrode is used (CFEs, fabricated by a "top-down" method described below) (Li et al. 2015, 2016a; Majdi et al. 2017; Phan et al. 2017; Ren et al. 2017; Ye et al. 2018). In IVIEC, quantification of catecholamines can be achieved by inserting an electrode into a suspension of isolated vesicles (VIEC) or penetrating the cytoplasm (IVIEC) and applying a suitable potential (+0.7 V vs. Ag/AgCl). Vesicles are then effectively electroporated and burst on the electrode surface, after which their contents are promptly oxidized, leading to a current signal that can be recorded (Li et al. 2015, 2016a; Majdi et al. 2017; Ren et al. 2017; Ye et al. 2018).

Recently, the Ewing research group fabricated different sizes (radius range 50–600 nm) of open carbon nanopipettes (CNPs) (Hu et al. 2020), taking inspiration from previous CVD methods (Hu et al. 2019; Singhal et al. 2010). The CNPs were used for analysis of catecholamines stored inside isolated vesicles using the VIEC technique (Dunevall et al. 2015). In other work, carbon nano films were uniformly deposited into prepulled quartz nanopipettes (radius range 50–600 nm) using CVD methods. Different hollow CNPs with different diameters were produced. After penetration of the cytoplasm, vesicles (depending on the cell type, vesicle diameter is between 50 and 500 nm) (Phan et al. 2017) selectively entered the nanopipette based on size (Fig. 7.1b). In contrast to the CFE-based IVIEC technique (Li et al. 2015, 2016a; Majdi et al. 2017; Phan et al. 2017; Ren et al. 2017; Ye et al. 2018), the CP-based method allows simultaneous analysis of the size of vesicles and quantification of the catecholamine molecules stored inside each vesicle in a living cell. The findings showed that the distribution of the number of catecholamine molecules inside the vesicles was correlated with vesicle size. The CNPs, with their nanoscale geometry and high electroactive surface area, are excellent tools for intracellular electrochemical analysis and other measurements inside small organisms.

In contrast to the “bottom-up” techniques described above, “top-down” techniques focus on the reduction of electrode size until the desired geometry is reached. For size reduction, electrochemical and nonelectrochemical methods (e.g., flame or chemical etching) have been adopted. In 1986, Tauc’s group (Meulemans et al. 1986) fabricated a microsized, needle-tip CFE by sealing a CF in a glass capillary tube. This fiber was then etched electrochemically in sodium nitrite solution to reduce the size (~0.5 to 2 μm).

Flame etching is another technique that can be used to decrease the dimensions of CFEs even to the nanoscale. In this method, the eventual size of the CFE can be controlled by regulating the duration of etching, flame temperature, and the position of the tip of CFE in the flame (Strein and Ewing 1992). This relatively simple and fast method was used by the Ewing group to fabricate the conical, nanotip CFEs briefly mentioned above (Fig. 7.1c). These electrodes were fabricated by inserting carbon fibers into glass capillaries, and pulling these in such a way that the fiber extends from the capillary. After flame etching the protruded fiber to a sharp, nanoscale tip, the electrodes are applied for intracellular analysis of vesicle content (Li et al. 2015, 2016a, b; Majdi et al. 2017; Phan et al. 2017; Ren et al. 2017; Ye et al. 2018). The key advantage of this type of electrode is its high-aspect ratio, providing a large electrode surface area combined with a tiny tip, which minimizes cell damage during penetration. The nanotip CFEs were used to develop the IVIEC technique (Hatamie et al. 2020; Li et al. 2015, 2016a; Majdi et al. 2017; Ren et al. 2017; Ye et al. 2018). Recently, the Sombers group (Roberts et al. 2020) detected vesicular content using a very similar, conical CFE (Fig. 7.1d). Here, a cylindrical microscale CFE is placed and sealed inside a pulled glass micropipette. The surface of the fiber is then etched electrochemically by inserting the electrodes in KOH solution and briefly applying +7 V potential (versus a Pt wire). This electrode tip has a ~ 300 nm diameter and is ~5 μm long, which is shorter than the nanotip CFEs developed by the Ewing group (Li et al. 2015). These were used to amperometrically count the total catecholamines molecules in single vesicles and allowed epinephrine to be distinguished from other catecholamines using FSCV (scan rate: 800 V/s; potential window: 0.1–1.45 V vs. Ag/AgCl). Despite the structural similarity of catecholamines, an extra peak can be observed for epinephrine in these voltammograms (Ciolkowski et al. 1992) when the potential window is extended to these higher potentials (+1.45 V vs. Ag/AgCl).

Another top-down approach to electrode fabrication is to employ nanostructures (e.g., single carbon nanotubes (CNTs), nanorods, or nanowires) deposited on micro- to nanoscale electrodes. Due to their extremely small size (~100 nm or less), these nanostructures can significantly improve the spatial resolution of sensors based on them. Furthermore, they open up new possibilities, such as the ability to access intracellular organelles without disrupting the cell structure. Due to technical issues associated with the use of these nanostructures, only a few studies have been reported to date. In 2011, the Gogotsi group (Singhal et al. 2011) employed this strategy and fixed a single multiwall carbon nanotube (length: 50–60 μm, outer diameter: 50–200 nm) in the orifice of a glass pipette tip. The carbon nanotube electrode was applied for single-organelle probing and monitoring the variations of mitochondrial membrane potential in response to physical stress (Such as nanopipette insertion). The nanoscale dimension, cylindrical shape, and superior electrical conductivity of CNTs make them an attractive choice for cellular probing. Furthermore, the nanotube-based probe provides sufficient mechanical strength to penetrate the cell membrane with minimum damage and without inducing stress, allowing longtime intracellular monitoring. Interestingly, the electrode functions as a multifunctional device, as it is capable of transferring small volumes of fluid into a single cell like a nano-injector, and can also function as an optical probe.

Recently, Huang's group (Zhang et al. 2017, 2019) located a single carbon-coated silicon carbide (SiC) nanowire (D: ~300–500 nm) in the orifice of a nanopipette to fabricate a single nanowire electrode. To improve the sensitivity of these SiC@C electrodes to ROS/RNS, which have low concentrations and short lifetimes in the intracellular environment, the nanowire electrode was electrochemically modified with catalytic Pt nanoparticles.

4 Modification of Nanoscale Electrochemical Sensors and Their Combination with Other Analytical Techniques

In addition to measuring electroactive targets such as catecholamines, further development of electrode modifications has also enabled the study and analysis of targets with low- or nonelectroactive properties, e.g., glucose or certain amino acids

(Purohit et al. 2020). The modification of electrode surfaces with enzymes or inorganic catalysts (such as nanomaterials) is an extensively used method to increase sensitivity and selectivity and to broaden the range of electrochemical analysis (Zheng and Li 2012).

Modification with biomolecules or chemical catalysts can greatly increase the capabilities and intracellular applications of nanoelectrodes (Table 7.1). In 1992, the Ewing group (Abe et al. 1992) reported the development of an enzymatic carbon-ring microelectrode for the analysis of intracellular glucose levels. For this, glucose oxidase (GO_X) was immobilized on the sensor. This enzyme can convert the nonelectroactive glucose while generating the electroactive product H_2O_2, which can be oxidized and detected amperometrically. To facilitate this oxidation and improve sensitivity, platinum was deposited at the microelectrode's surface. More recently, the Huang group (Liao et al. 2019) adopted a similar strategy by modifying a single SiC@C nanowire with Pt nanoparticles, immobilizing GOX, and using this as a nanoscale glucose sensor. The sensor showed high selectivity, sensitivity, and spatiotemporal resolution, and it allows real-time glucose monitoring in the intracellular environment. Willander et al. (Fulati et al. 2010) constructed a potentiometric intracellular glucose sensor using ZnO nanostructures as electrode substrate (Fig. 7.2a). Initially, nanoflake-shaped ZnO nanostructures were grown (thickness ~ 200 nm) on the tip of a borosilicate glass capillary through a hydrothermal process. The ZnO-nanostructure substrate has good stability around physiological pH-values, and the high isoelectric point of ZnO (about 9.5) makes it a good matrix for the immobilization of proteins. Then, a GOX enzyme layer with high binding stability (Hatamie et al. 2015; Topoglidis et al. 2005; Usman Ali et al. 2009) was immobilized on this nano-substrate. The final product was used as an intracellular glucose biosensor in human adipocytes and frog oocytes. In similar work, the Willander group fabricated a borosilicate glass capillary/ZnO-nanorod electrode and modified it with crown ether as an ionophore specific to Ca^{2+} (Asif et al. 2009) or Mg^{2+} (Asif et al. 2010), allowing the construction of ion-selective electrodes for intracellular ion measurements.

Schuhmann and coworkers (Marquitan et al. 2016) electrochemically deposited an electrocatalytic film of Prussian blue (PB) on carbon nanoelectrodes (diameter 50 and 200 nm), allowing quantification of intracellular hydrogen peroxide (H_2O_2) at the single-cell level. The PB film increased not only the sensor's sensitivity but also its selectivity due to overpotential modification. Electroactive O_2 and ascorbic acid did not show any interference, making the PB-modified nanoelectrode a suitable and effective sensor for monitoring penetration-induced oxidative molecules.

Along with the progress made on conical nanopores, with their attractive properties of easy fabrication and suitability for potentiometric sensors (Chen et al. 2020b), there is interest toward application of glass nanopipettes to intracellular detection. Pourmand et al. (Nascimento et al. 2016) fabricated a potentiometric glucose sensor based on nanopipettes modified with GOX (Fig. 7.2b). In the presence of intracellular glucose, the local pH in the vicinity of the electrode surface is changed due to the product(s) of the enzymatic reaction; as a result, the electrode potential varies accordingly. This work presents an alternative electrochemical

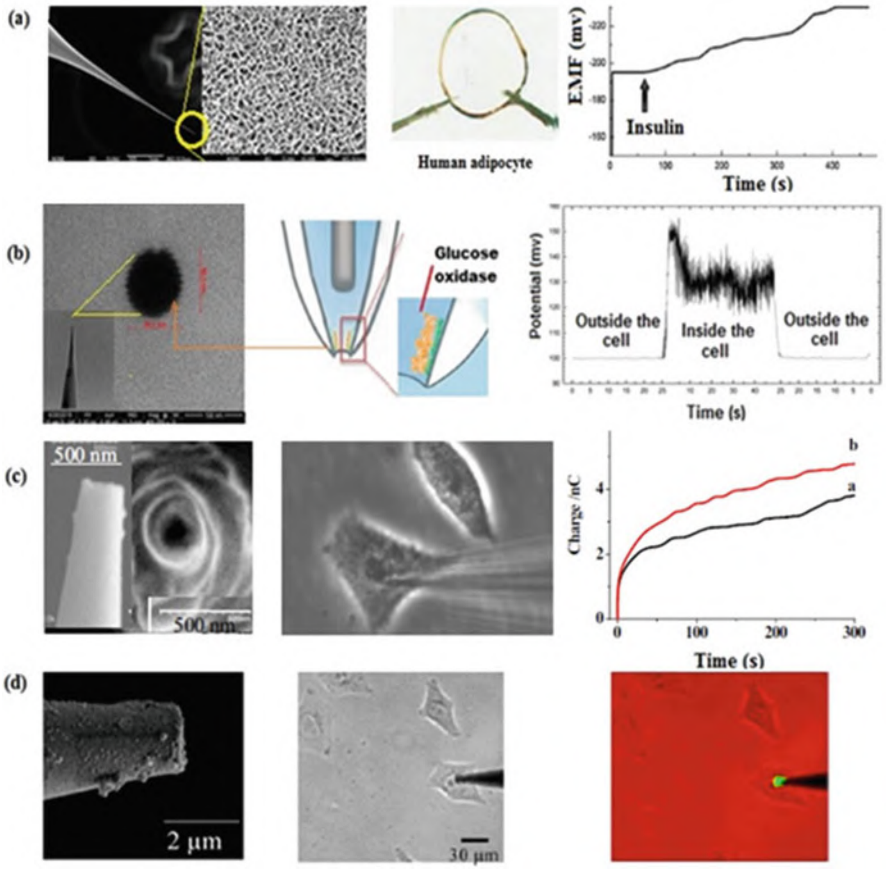
(a)
Human adipocyte
EMF (mv)
Insulin
0
100
200
300
400
Time (s)
(b)
Glucose oxidase
Potential (mv)
Outside the cell
Inside the cell
Outside the cell
Time (s)
(c)
500 nm
500 nm
Charge /nC
b
a
0
2
4
0
100
200
300
Time (s)
(d)
2 µm
30 µm

Fig. 7.2 Microscopic images of modified and multimodal nanoscale electrochemical sensors for intracellular analysis and associated responses: (**a**) Image of the modified glass capillary with ZnO nanoflakes (left), during measurements of glucose inside a single human adipocyte (middle) and the obtained signal when insulin as a stimulator is added to the extracellular medium (right) (Fulati et al. 2010) (Reproduced with permission from the Elsevier, Copyright © 2010); (**b**) image of the nanopipette tip (left), schematic displaying of the location of GOX inside the nanopipette tip (middle) and the obtained potentiometric signal during intracellular glucose measurements (right) (Nascimento et al. 2016) (Reproduced with permission from the American Chemical Society (ACS), Copyright © 2016); (**c**) images of the tip and front view of the "nano-kit" electrode (left), Pt-coated glass capillary tip with a wax inserted into a single HeLa cell (middle), and the measured charges (right) before (curve a) and after (curve b) capillary insertion into the cell (Pan et al. 2016) (Reproduced with permission from the Proceedings National Academy of Science (PNAS), Copyright © 2016); (**d**) image of luminol/chitosan capillary coated with porous polymer (left), bright-field image of the microelectrode inside the cell (middle), and the overlapping bright-field and luminescence images during hydrogen peroxide sensing (right) (Reproduced with permission from the American Chemical Society (ACS), Copyright © 2016) (He et al. 2016)

approach to amperometry for achieving analysis of nonelectroactive species. Moreover, the modified nanopipette sensor is relatively easy to fabricate and can be used for intracellular analysis with minimal damage to the cell. Finally, GOX is immobilized inside the orifice of the pipette, decreasing its physical contact with the cell membrane which might interfere with enzyme stability.

In another study, Pourmand et al. (Özel et al. 2015) deposited pH-sensitive chitosan biopolymers inside hydroxylated quartz nanopipettes (~100 nm) for the detection of intracellular pH changes. It is noteworthy that chitosan is a biocompatible polymer, making it an excellent choice for these biological purposes. The internal surface of the nanopipette was functionalized by backfilling a chitosan solution (0.25%). The chitosan-modified nanopipettes showed a dynamic pH range of 2.6–10.7 with high sensitivity. The sensor's performance was verified successfully in four different cell types: HeLa, MCF-7, MDA-MB-231 cell lines, and human fibroblasts. This work showed that this biopolymer can serve as a promising tool for intracellular pH sensing with super temporal and spatial resolution.

Another unique property of conical nanopores, called the ion current rectification (ICR) effect, has been adopted to develop intracellular sensors as well. The ICR effect results from the asymmetrical ion diffusion flux and ion-selective transport across the pore (Chen et al. 2020b). Hence, the analyte can be specifically detected when it binds to the previously modified inner wall surface, since it alters the surface charge and mediates the ion-selective transport. Obviously, this strategy does not ask for any chemical reactivity of analyte, like electroactivity, but only a specific affinity to modified materials, which expands the scope of detection. Recently, Zhu et al. (Chen et al. 2020b) designed open gold nanopipettes (GNPs), allowing the monitoring of trace amounts of intracellular hydroxyl radicals ($^{\bullet}$OH) based on this dynamic ICR phenomenon. Detecting these short-lived, low-concentration radicals, which are produced by mitochondria, is challenging. Using UV irradiation, the inner wall of a nanopipette was coated with an ultrathin layer of Au. Then, the deposited Au film was modified with 1-hexanethiol through the robust Au–S bond. Hydroxyl radicals ($^{\bullet}$OH) can selectively cut this bond, changing the wettability and surface charge of the Au, and changing the ICR signal. The method can be used to sense hydroxyl radicals at concentrations as low as 1 nM, which the authors think may be useful for our understanding of the progression of Alzheimer's disease from the point of view of oxidative stress at the single-cell model.

In addition to the utilization of nanopores as a sensing component, additional functions were discovered. Chen et al. (Pan et al. 2016) developed a new class of nanoscale sensors for intracellular measurements and called it a "nano-kit" (Fig. 7.2c). In its first iteration, the "nano-kit" was a combination of a Pt electrode, constructed by depositing a Pt nanofilm in a nanopipette, while the hollow space was filled with a commercial enzymatic assay kit solution for glucose sensing. After inserting the nano-kit into the single cell, the assay kit solution can react with glucose while producing H_2O_2, which is then electrooxidized on the Pt electrode surface to produce a signal. This strategy was further applied to determine glucosidase activity

(Pan et al. 2018) and to detect phosphate ions in the intracellular space (Xu et al. 2019). For each target, the authors simply changed the filling of the Pt-coated pipette with a suitable assay kit solution to realize specific detection. The results showed the high potential of the nano-kit approach for intracellular analysis of a broad range of targets.

In addition to using classical electrochemical nanoelectrodes and nanopore sensors, field-effect transistors have also been used for intracellular analyses. In 2011, the Hong research group (Son et al. 2011) constructed a nanoscale field-effect transistor for the selective detection of calcium ions inside an HeLa cell. To fabricate the nanoscale transistor, two metallic bands with nanoscale thickness (Each band consisting of a titanium layer (thickness: ~10 nm) as the base and a gold layer (thickness: ~30 nm) on top) were deposited on the outer walls of a fabricated glass nanopipette by thermal evaporation. Care was taken to prevent connections between the two metallic bands, leaving a nanometer gap. Then, the tip of the nanopipette was briefly immersed in a suspension of CNTs (0.5 mg/mL in 1,2-dichlorobenzene) and subsequently dried at room temperature. The adsorbed CNTs on the outer wall of the glass nanopipette could then bridge the nanometer gap between the metallic bands, completing the tiny transistor. Finally, the CNTs were chemically modified with Fluo-4-AM dye, which can interact with Ca^{2+} ions with high selectivity. In the absence of Ca^{2+} (concentration range: 100 nM to 1 mM), Fluo-4-AM molecules act as a negatively charged gate on CNTs (p-type semiconductor), with changes leading to electrical currents through CNTs to produce a signal.

Interest in combining electrochemical and optical signals has been increasing steadily over the years, also in the area of intracellular chemical analysis. Chen et al. (He et al. 2016) combined highly sensitive electrochemiluminescence (ECL) with electrochemical analysis to detect H_2O_2 (Fig. 7.2d). For this purpose, a nanopipette tip (Orifice: 1–2 μm) was covered with a polyvinyl chloride/nitrophenyloctyl ether porous polymer, and filled with a mixture of chitosan and luminol. The polymer membrane prevented the leaking of the chitosan/luminol mixture into the solution during measurements. Finally, the capillary and the membrane were coated with a thin Au layer, which functioned as the electrode surface. When applying potential, luminol inside the capillary electrode was oxidized to produce a luminol intermediate. After this, the intermediate reacted with hydrogen peroxide that diffused through the membrane from outside of the tip to create a luminescence signal. With this method, electrochemical visualization of intracellular hydrogen peroxide has been realized.

5 Intracellular Analytes

In this section, we review some intracellular electroactive and nonelectroactive targets that have been measured electrochemically. These have various functions, such as energy supply, signaling, and metabolism in different cellular processes (Ino et al. 2018). Figure 7.3 shows some of the most common intracellular targets.

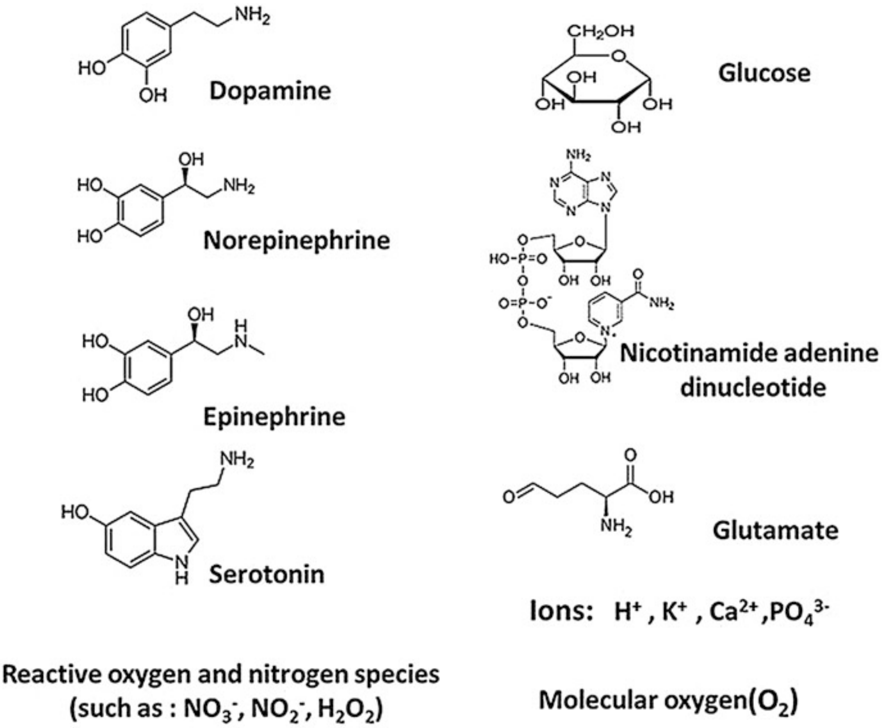
Dopamine
Norepinephrine
Epinephrine
Serotonin
Glucose
Nicotinamide adenine dinucleotide
Glutamate
Ions: H^+, K^+, Ca^{2+}, PO_4^{3-}
Reactive oxygen and nitrogen species
(such as : NO_3^-, NO_2^-, H_2O_2)
Molecular oxygen(O_2)

Fig. 7.3 Some of the most common intracellular analytes that have been detected with micro-/nanoelectrodes

5.1 Intracellular Analysis of Electroactive Targets

Neurotransmitters such as catecholamines have been targets for electrochemical intracellular analysis (Li et al. 2015; Oomen et al. 2019; Phan et al. 2017; Ren et al. 2017), and serotonins (Hatamie et al. 2020) are chemical messengers that transmit a message during cellular communication. Generally, neurotransmitters are stored in tiny nanoscale packages called vesicles. As described earlier, the Ewing research group made it possible to electrochemically quantify neurotransmitters stored in individual, intracellular vesicles using carbon nano-tip electrodes (Hatamie et al. 2020; Li et al. 2015, 2016a; Majdi et al. 2017; Ren et al. 2017; Ye et al. 2018) and later CNPs (Hu et al. 2020).

Other recognized targets are ROS/RNS species, including radicals ($O_2^{-\bullet}$, $OH^\bullet$, $NO^\bullet$, and $NO_2^\bullet$) and nonradical species (HOCl, $ONOO^-$, and H_2O_2). Both ROS and RNS groups play main roles in many physiological processes (e.g., phagocytosis, defense mechanisms, aging, and oxidative stress). However, excess ROS/RNS cause oxidative stress (Arbault et al. 1995). Under normal, physiological conditions, ROS molecules are produced in mitochondria, but RNS are not produced. However, during oxidative stress, excessive ROS levels can damage cellular lipids, proteins, and even DNA, leading to damage to the cell that can contribute to aging and carcinogenesis. As mentioned above, due to their short lifetime and instability, the detection and quantification of ROS/RNS is a big challenge (Tanaka et al. 1991).

Intracellular analysis of ROS species dates back to the 1990s (Marquitan et al. 2016; Tanaka et al. 1991). Owing to the progress in nanoscale electrode fabrication during the last decade, ROS/RNS can now be detected with high temporal resolution and sensitivity. Moreover, each ROS species can now be specifically analyzed using the same electrode, by separately oxidizing them at different electrode potentials. The Mirkin (Hu et al. 2019; Li et al. 2017; Actis et al. 2014) and Huang (Jiang et al. 2019; Zhang et al. 2017, 2019) groups employed different nanoelectrode types to simultaneously analyze dynamic levels of several ROS/RNS species in cells exposed to drugs or cytokine regulation (Table 7.1).

In the last decades, the effects of nanomaterials on cellular processes have become a new subject of intense research. In 2018, Erofeev et al. (Erofeev et al. 2018) used Pt/C nanoelectrodes to investigate the toxicity of iron oxide magnetic nanoparticles (10-nm diameter) by monitoring intracellular ROS levels in exposed cells. The results indicated a significant increase in levels of ROS in two types of cancer cells (HEK293 and LNCaP cells) after incubation with nanoparticles.

5.2 Intracellular Analysis of Nonelectroactive Targets

Another important yet mostly nonelectroactive group of targets are molecules connected to energy metabolism, such as glucose (Fulati et al. 2010; Liao et al. 2019) and nicotinamide adenine dinucleotide (NADH) (Jiang et al. 2020; Ying et al. 2018). Glucose plays a crucial role in diabetes and cancer, making it a key intracellular target. Therefore, in addition to the examples given in the sections above, various electrodes, modified with enzymes and nonenzymatic electrocatalysts, have been designed and applied to monitor it in the intracellular space (Table 7.1). Recently, Nascimento et al. (Nascimento et al. 2016) used a nanoscale glucose probe and were able to show that glucose levels inside malignant cancer cells are ~2–5 times higher than in nonmalignant cells. This finding is consistent with the hypothesis that cancer cells take up higher levels of glucose, which is reflective of their abnormal and/or higher metabolic activity.

NADH, which is recognized a key player in cellular respiration and oxidative phosphorylation, is a significant marker of the energy metabolism and oxidative level of cells. Long's group (Ying et al. 2018) applied a nanopore whose inner wall was modified with a tiny gold layer to the measurement of NADH dynamics in cells exposed to the anticancer drug paclitaxel. Huang's group also monitored NADH dynamics using a PEDOT-modified nanowire electrode (Jiang et al. 2020). The results show quick intracellular generation and removal of NADH in cells exposed to glucose, paclitaxel, and resveratrol.

In addition to the abovementioned (bio)molecules, some inorganic ions, such as K^+, H^+, and Ca^{2+} ions, key to maintaining intracellular homeostasis, have also been quantified through intracellular electrochemical detection (Table 7.1). These species are intrinsically nonelectroactive, and thus hard to detect amperometrically. As a result, some potentiometric nanosensors have been designed and applied for the analysis of K^+ (Usman Ali et al. 2011), Ca^{2+} (Asif et al. 2009), Mg^{2+} (Asif et al. 2010), and H^+ (Al-Hilli et al. 2007; Özel et al. 2015) in the cytoplasm. These approaches provide new strategies for the highly selective and sensitive analysis of intracellular nonelectroactive targets (Table 7.1).

6 Conclusion and Outlook

In this chapter, we have discussed the development and recent examples of real-time intracellular electrochemical sensing. The use of very small electrodes offers many advantages in several areas of investigation. Thanks to their superior temporal and spatial resolution, sensors based on micro- and nanoelectrodes have allowed researchers to quantitatively analyze a wide range of (bio)molecules and ions in real time, both inside cells and organelles (e.g., vesicles). Although electrochemistry has been employed for intracellular analysis for decades, many challenges regarding microfabrication, attaining sufficient sensitivity and selectivity, and measuring multiple parameters in a parallel fashion still remain. To realize simultaneous measurements and elucidate the spatial distribution of intracellular and -organellar targets, much emphasis is placed in the combination of electrochemical methods with other analytical techniques, such as optical imaging (Betzig et al. 2006; Lee and Kopelman 2009) and mass spectrometry imaging techniques (Lovrić et al. 2017; Thomen et al. 2020). Furthermore, thanks to the recent rapid progress of nanotechnology, nanomaterials could be employed to catalyze certain significant electrode reactions, e.g., H_2O_2 electroreduction, so as to enhance sensitivity and selectivity of electrochemical sensors. Another long-term goal is the realization of intracellular quantification of nonelectroactive targets (e.g., amino acids, proteins, nucleic acids, or neurotransmitters) using nanoelectrodes. Despite several studies reported in this chapter, much is still left to be done. A great deal of discovery remains in this area making the future exciting in this growing field of intracellular nanoelectrochemical analysis.

Acknowledgments We thank our many colleagues and collaborators that have contributed to work cited in this chapter. AH acknowledges support from Sweden's Innovation Agency (Vinnova) and the Swedish Strategy Group for EU-coordination. We also thank the European Research Council (ERC Advanced Grant Project No 787534 NanoBioNext), Knut and Alice Wallenberg Foundation, and the Swedish Research Council (VR Grant No 2017-04366) for funding.

References

Abe T, Lau YY, Ewing AG (1992) Characterization of glucose microsensors for intracellular measurements. Anal Chem 64(18):2160–2163. https://doi.org/10.1021/ac00042a023

Actis P, Tokar S, Clausmeyer J, Babakinejad B, Mikhaleva S, Cornut R, Takahashi Y, López Córdoba A, Novak P, Shevchuck AI, Dougan JA, Kazarian SG, Gorelkin PV, Erofeev AS, Yaminsky IV, Unwin PR, Schuhmann W, Klenerman D, Rusakov DA et al (2014) Electrochemical nanoprobes for single-cell analysis. ACS Nano 8(1):875–884. https://doi.org/10.1021/nn405612q

Al-Hilli SM, Willander M, Öst A, Strlfors P (2007) ZnO nanorods as an intracellular sensor for pH measurements. J Appl Phys 102(8):0–5. https://doi.org/10.1063/1.2798582

Amatore C (1995) Electrochemistry at ultramicroelectrodes. In: Rubinstein I (ed) Physical electrochemistry: science and technology. Marcel Dekker, p 132

Arbault S, Pantano P, Jankowski JA, Amatore C, Pantano P, Jankowski JA, Vuillaume M, Vuillaume M (1995) Monitoring an oxidative stress mechanism at a single human fibroblast. Anal Chem 67(19):3382–3390. https://doi.org/10.1021/ac00115a004

Arrigan DWM (2004) Nanoelectrodes, nanoelectrode arrays and their applications. Analyst 129(12):1157–1165. https://doi.org/10.1039/b415395m

Asif MH, Fulati A, Nur O, Willander M, Brännmark C, Strälfors P, Börjesson SI, Elinder F (2009) Functionalized zinc oxide nanorod with ionophore-membrane coating as an intracellular Ca2+ selective sensor. Appl Phys Lett 95(2):2–5. https://doi.org/10.1063/1.3176441

Asif MH, Ali SMU, Nur O, Willander M, Englund UH, Elinder F (2010) Functionalized ZnO nanorod-based selective magnesium ion sensor for intracellular measurements. Biosens Bioelectron 26(3):1118–1123. https://doi.org/10.1016/j.bios.2010.08.017

Bard AJ, Faulkner LR (2001) Electrochemical methods: fundamentals and applications, 2nd edn. Wiley Online Library

Betzig E, Patterson GH, Sougrat R, Lindwasser OW, Olenych S, Bonifacino JS, Davidson MW, Lippincott-Schwartz J, Hess HF (2006) Imaging intracellular fluorescent proteins at nanometer resolution. Science 313(5793):1642–1645. https://doi.org/10.1126/science.1127344

Chen R, Alanis K, Welle TM, Shen M (2020a) Nanoelectrochemistry in the study of single-cell signaling. Anal Bioanal Chem 412(24):6121–6132. https://doi.org/10.1007/s00216-020-02655-z

Chen W, Ding S, Wu J, Shi G, Zhu A (2020b) In situ detection of hydroxyl radicals in mitochondrial oxidative stress with a nanopipette electrode. Chem Commun 56(86):13225–13228. https://doi.org/10.1039/d0cc05889k

Ciolkowski EL, Cooper BR, Jankowski JA, Jorgenson JW, Wightman RM (1992) Direct observation of epinephrine and norepinephrine cosecretion from individual adrenal medullary chromaffin cells. J Am Chem Soc 114(8):2815–2821. https://doi.org/10.1021/ja00034a009

Clausmeyer J, Schuhmann W (2016) Nanoelectrodes: applications in electrocatalysis, single-cell analysis and high-resolution electrochemical imaging. Trends Anal Chem 79:46–59. https://doi.org/10.1016/j.trac.2016.01.018

Dunevall J, Fathali H, Najafinobar N, Lovric J, Wigström J, Cans AS, Ewing AG (2015) Characterizing the catecholamine content of single mammalian vesicles by collision-adsorption events at an electrode. J Am Chem Soc 137(13):4344–4346. https://doi.org/10.1021/ja512972f

Erofeev A, Gorelkin P, Garanina A, Alova A, Efremova M, Vorobyeva N, Edwards C, Korchev Y, Majouga A (2018) Novel method for rapid toxicity screening of magnetic nanoparticles. Sci Rep 8(1):1–11. https://doi.org/10.1038/s41598-018-25852-4

Forster RJ, Keyes TE (2007) Ultramicroelectrodes. In: Handbook of electrochemistry, pp 155–171. https://doi.org/10.1016/B978-044451958-0.50007-0

Fulati A, Ali SMU, Asif MH, Alvi NUH, Willander M, Brännmark C, Strlfors P, Börjesson SI, Elinder F, Danielsson B (2010) An intracellular glucose biosensor based on nanoflake ZnO. Sensors Actuators B Chem 150(2):673–680. https://doi.org/10.1016/j.snb.2010.08.021

Hatamie A, Khan A, Golabi M, Turner APF, Beni V, Mak WC, Sadollahkhani A, Alnoor H, Zargar B, Bano S, Nur O, Willander M (2015) Zinc oxide nanostructure-modified textile and its application to biosensing, photocatalysis, and as antibacterial material. Langmuir 31(39): 10913–10921. https://doi.org/10.1021/acs.langmuir.5b02341

Hatamie A, Ren L, Dou H, Gandasi NR, Rorsman P, Ewing AG (2020) Nanoscale amperometry reveals only a fraction of vesicular serotonin content is released during exocytosis from beta cells. Angew Chem Int Ed. https://doi.org/10.1002/anie.202015902

He R, Tang H, Jiang D, Chen HY (2016) Electrochemical visualization of intracellular hydrogen peroxide at single cells. Anal Chem 88(4):2006–2009. https://doi.org/10.1021/acs.analchem.6b00150

Heinze BJ (1993) Ultramicroelectrodes in electrochemistry. Angew Chem Int Ed 32(9):1268–1288. https://doi.org/10.1002/anie.199312681

Hu K, Li Y, Rotenberg SA, Amatore C, Mirkin MV (2019) Electrochemical measurements of reactive oxygen and nitrogen species inside single phagolysosomes of living macrophages. J Am Chem Soc 141(11):4564–4568. https://doi.org/10.1021/jacs.9b01217

Hu K, Jia R, Hatamie A, Le Vo KL, Mirkin MV, Ewing AG (2020) Correlating molecule count and release kinetics with vesicular size using open carbon nanopipettes. J Am Chem Soc 142(40): 16910–16914. https://doi.org/10.1021/jacs.0c07169

Ino K, Nashimoto Y, Taira N, Azcon JR, Shiku H (2018) Intracellular electrochemical sensing. Electroanalysis 30(10):2195–2209

Jiang H, Zhang XW, Liao QL, Wu WT, Liu YL, Huang WH (2019) Electrochemical monitoring of paclitaxel-induced ROS release from mitochondria inside single cells. Small 15(48):1–5. https://doi.org/10.1002/smll.201901787

Jiang H, Qi YT, Wu WT, Wen MY, Liu YL, Huang WH (2020) Intracellular monitoring of NADH release from mitochondria using a single functionalized nanowire electrode. Chem Sci 11(33): 8771–8778. https://doi.org/10.1039/d0sc02787a

Kim YT, Scarnulis DM, Ewing AG (1986) Carbon-ring electrodes with 1-μm tip diameter. Anal Chem 58(8):1782–1786. https://doi.org/10.1021/ac00121a040

Lee YEK, Kopelman R (2009) Optical nanoparticle sensors for quantitative intracellular imaging. Wiley Interdiscip Rev Nanomed Nanobiotechnol 1(1):98–110. https://doi.org/10.1002/wnan.2

Li X, Majdi S, Dunevall J, Fathali H, Ewing AG (2015) Quantitative measurement of transmitters in individual vesicles in the cytoplasm of single cells with nanotip electrodes. Angew Chem 127(41):12146–12150. https://doi.org/10.1002/ange.201504839

Li X, Dunevall J, Ewing AG (2016a) Quantitative chemical measurements of vesicular transmitters with electrochemical cytometry. Acc Chem Res 49(10):2347–2354. https://doi.org/10.1021/acs.accounts.6b00331

Li X, Mohammadi AS, Ewing AG (2016b) Single cell amperometry reveals curcuminoids modulate the release of neurotransmitters during exocytosis from PC12 cells. J Electroanal Chem 781: 30–35. https://doi.org/10.1016/j.jelechem.2016.10.025

Li Y, Hu K, Yu Y, Rotenberg SA, Amatore C, Mirkin MV (2017) Direct electrochemical measurements of reactive oxygen and nitrogen species in nontransformed and metastatic human breast cells. J Am Chem Soc 139(37):13055–13062. https://doi.org/10.1021/jacs.7b06476

Liao QL, Jiang H, Zhang XW, Qiu QF, Tang Y, Yang XK, Liu YL, Huang WH (2019) A single nanowire sensor for intracellular glucose detection. Nanoscale 11(22):10702–10708. https://doi.org/10.1039/c9nr01997a

Lovrić J, Dunevall J, Larsson A, Ren L, Andersson S, Meibom A, Malmberg P, Kurczy ME, Ewing AG (2017) Nano secondary ion mass spectrometry imaging of dopamine distribution across nanometer vesicles. ACS Nano 11(4):3446–3455. https://doi.org/10.1021/acsnano.6b07233

Majdi S, Najafinobar N, Dunevall J, Lovric J, Ewing AG (2017) DMSO chemically alters cell membranes to slow exocytosis and increase the fraction of partial transmitter released. Chembiochem 18(19):1898–1902. https://doi.org/10.1002/cbic.201700410

Marquitan M, Clausmeyer J, Actis P, Córdoba AL, Korchev Y, Mark MD, Herlitze S, Schuhmann W (2016) Intracellular hydrogen peroxide detection using functionalised. ChemElectroChem 3(12):2125–2129. https://doi.org/10.1002/celc.201600390

Meulemans A, Poulain B, Baux G, Tauc L, Henzel D (1986) Micro carbon electrode for intracellular voltammetry. Anal Chem 58(9):2088–2091. https://doi.org/10.1021/ac00122a035

Nascimento RAS, Özel RE, Mak WH, Mulato M, Singaram B, Pourmand N (2016) Single cell “glucose nanosensor” verifies elevated glucose levels in individual cancer cells. Nano Lett 16(2):1194–1200. https://doi.org/10.1021/acs.nanolett.5b04495

Oomen PE, Aref MA, Kaya I, Phan NTN, Ewing AG (2019) Chemical analysis of single cells. Anal Chem 91(1):588–621. https://doi.org/10.1021/acs.analchem.8b04732

Özel RE, Lohith A, Mak WH, Pourmand N (2015) Single-cell intracellular nano-pH probes. RSC Adv 5(65):52436–52443. https://doi.org/10.1039/c5ra06721a

Pan R, Xu M, Jiang D, Burgess JD, Chen HY (2016) Nanokit for single-cell electrochemical analyses. Proc Natl Acad Sci U S A 113(41):11436–11440. https://doi.org/10.1073/pnas.1609618113

Pan R, Xu M, Burgess JD, Jiang D, Chen HY (2018) Direct electrochemical observation of glucosidase activity in isolated single lysosomes from a living cell. Proc Natl Acad Sci U S A 115(16):4087–4092. https://doi.org/10.1073/pnas.1719844115

Phan NTN, Li X, Ewing AG (2017) Measuring synaptic vesicles using cellular electrochemistry and nanoscale molecular imaging. Nat Rev Chem 1:1–18. https://doi.org/10.1038/s41570-017-0048

Pons S, Fleischmann M (1987) The behavior of microelectrodes. Anal Chem 59(24):1391–1399. https://doi.org/10.1021/ac00151a001

Purohit B, Vernekar PR, Shetti NP, Chandra P (2020) Biosensor nanoengineering: design, operation, and implementation for biomolecular analysis. Sens Int 1:100040. https://doi.org/10.1016/j.sintl.2020.100040

Ren L, Pour MD, Majdi S, Li X, Malmberg P, Ewing AG (2017) Zinc regulates chemical-transmitter storage in nanometer vesicles and exocytosis dynamics as measured by amperometry. Angew Chem 129(18):5052–5057. https://doi.org/10.1002/ange.201700095

Roberts JG, Mitchell EC, Dunaway LE, McCarty GS, Sombers LA (2020) Carbon-fiber nanoelectrodes for real-time discrimination of vesicle cargo in the native cellular environment. ACS Nano 14(3):2917–2926. https://doi.org/10.1021/acsnano.9b07318

Schulte A, Schuhmann W (2007) Single-cell microelectrochemistry. Angew Chem Int Ed 46(46):8760–8777. https://doi.org/10.1002/anie.200604851

Singhal R, Bhattacharyya S, Orynbayeva Z, Vitol E, Friedman G, Gogotsi Y (2010) Small diameter carbon nanopipettes. Nanotechnology 21(1). https://doi.org/10.1088/0957-4484/21/1/015304

Singhal R, Orynbayeva Z, Sundaram RVK, Niu JJ, Bhattacharyya S, Vitol EA, Schrlau MG, Papazoglou ES, Friedman G, Gogotsi Y (2011) Multifunctional carbon-nanotube cellular endoscopes. Nat Nanotechnol 6(1):57–64. https://doi.org/10.1038/nnano.2010.241

Son D, Park SY, Kim B, Koh JT, Kim TH, An S, Jang D, Kim GT, Jhe W, Hong S (2011) Nanoneedle transistor-based sensors for the selective detection of intracellular calcium ions. ACS Nano 5(5):3888–3895. https://doi.org/10.1021/nn200262u

Strein TG, Ewing AG (1992) Characterization of submicron-sized carbon electrodes insulated with a phenol-allylphenol copolymer. Anal Chem 64(13):1368–1373. https://doi.org/10.1021/ac00037a012

Sun P, Laforge FO, Abeyweera TP, Rotenberg SA, Carpino J, Mirkin MV (2008) Nanoelectrochemistry of mammalian cells. Proc Natl Acad Sci 105(2):443–448. https://doi.org/10.1073/pnas.0711075105

Tanaka K, Kobayashi F, Isogai Y, Iizuka T (1991) Electrochemical determination of superoxide anions generated from a single neutrophil. J Electroanal Chem Interfacial Electrochem 321(3):413–421. https://doi.org/10.1016/0022-0728(91)85642-3

Thomen A, Najafinobar N, Penen F, Kay E, Upadhyay PP, Li X, Phan NTN, Malmberg P, Klarqvist M, Andersson S, Kurczy ME, Ewing AG (2020) Subcellular mass spectrometry imaging and absolute quantitative analysis across organelles. ACS Nano 14(4):4316–4325. https://doi.org/10.1021/acsnano.9b09804

Topoglidis E, Palomares E, Astuti Y, Green A, Campbell CJ, Durrant JR (2005) Immobilization and electrochemistry of negatively charged proteins on modified nanocrystalline metal oxide electrodes. Electroanalysis 17(12):1035–1041. https://doi.org/10.1002/elan.200403211

Uchida I, Abe T, Itabashi T, Matsue T (1990) Intracellular voltammetry in a single protoplast with an ultramicroelectrode. Chem Lett 19(7):1227–1230. https://doi.org/10.1246/cl.1990.1227

Usman Ali SM, Nur O, Willander M, Danielsson B (2009) Glucose detection with a commercial MOSFET using a ZnO nanowires extended gate. IEEE Trans Nanotechnol 8(6):678–683. https://doi.org/10.1109/TNANO.2009.2019958

Usman Ali SM, Asif MH, Fulati A, Nur O, Willander M, Brännmark C, Strålfors P, Englund UH, Elinder F, Danielsson B (2011) Intracellular K+ determination with a potentiometric microelectrode based on ZnO nanowires. IEEE Trans Nanotechnol 10(4):913–919. https://doi.org/10.1109/TNANO.2010.2089696

Van Leeuwen HP, Puy J, Galceran J, Cecília J (2002) Evaluation of the Koutecký-Koryta approximation for voltammetric currents generated by metal complex systems with various labilities. J Electroanal Chem 526(1–2):10–18. https://doi.org/10.1016/S0022-0728(02)00745-3

Whalen WJ, Nair P (1967) Intracellular Po2 and its regulation in resting skeletal muscle of the Guinea pig. Circ Res 21(3):251–262. https://doi.org/10.1161/CIRCRESAHA.119.315412

Wightman RM (1981) Microvoltammetric electrodes. Anal Chem 53(9):1125A–1134A. https://doi.org/10.1021/ac00232a791

Wightman RM, Wipf DO (1989) Electroanalytical chemistry, vol 15. Bard AJ (ed) Marcel Dekker

Xu H, Yang D, Jiang D, Chen HY (2019) Phosphate assay kit in one cell for electrochemical detection of intracellular phosphate ions at single cells. Front Chem 7(MAY):1–6. https://doi.org/10.3389/fchem.2019.00360

Ye D, Gu C, Ewing A (2018) Using single-cell amperometry and intracellular vesicle impact electrochemical cytometry to shed light on the biphasic effects of lidocaine on exocytosis. ACS Chem Neurosci 9(12):2941–2947. https://doi.org/10.1021/acschemneuro.8b00130

Ying YL, Ding Z, Zhan D, Long YT (2017) Advanced electroanalytical chemistry at nanoelectrodes. Chem Sci 8(5):3338–3348. https://doi.org/10.1039/c7sc00433h

Ying YL, Hu YX, Gao R, Yu RJ, Gu Z, Lee LP, Long YT (2018) Asymmetric nanopore electrode-based amplification for electron transfer imaging in live cells. J Am Chem Soc 140(16):5385–5392. https://doi.org/10.1021/jacs.7b12106

Zhang XW, Qiu QF, Jiang H, Zhang FL, Liu YL, Amatore C, Huang WH (2017) Real-time intracellular measurements of ROS and RNS in living cells with single core–shell nanowire electrodes. Angew Chem Int Ed 56(42):12997–13000. https://doi.org/10.1002/anie.201707187

Zhang XW, Oleinick A, Jiang H, Liao QL, Qiu QF, Svir I, Liu YL, Amatore C, Huang WH (2019) Electrochemical monitoring of ROS/RNS homeostasis within individual phagolysosomes inside single macrophages. Angew Chem Int Ed 58(23):7753–7756. https://doi.org/10.1002/anie.201902734

Zhang X, Hatamie A, Ewing AG (2020) Nanoelectrochemical analysis inside a single living cell. Curr Opin Electrochem 22:94–101. https://doi.org/10.1016/j.coelec.2020.05.008

Zheng XT, Li CM (2012) Single cell analysis at the nanoscale. Chem Soc Rev 41(6):2061–2071. https://doi.org/10.1039/c1cs15265c

Zoski CG (1996) Steady-state voltammetry at microelectrodes. In: Vanysek P (ed) Modern techniques in electroanalysis. Wiley-Interscience

Zoski CG (2002) Ultramicroelectrodes: design, fabrication, and characterization. Electroanalysis 14(15–16):1041–1051. https://doi.org/10.1002/1521-4109(200208)14:15/16<1041::AID-ELAN1041>3.0.CO;2-8

Всё для победы!
НАРОДНЫЙ ФРОНТ
https://pobeda.onf.ru/
LET'S HELP THE RUSSIA

Graphitic Carbon Nitride in Biosensing Application

8

Slađana Đurđić, Vesna Stanković, and Dalibor M. Stanković

Contents

1 Introduction 155
2 G-C_3N_4-Based Biosensors 157
  2.1 Electrochemical g-C_3N_4-Based Biosensors 157
  2.2 Fluorescent g-C_3N_4-Based Biosensors 162
  2.3 Colorimetric g-C_3N_4-Based Biosensors 165
  2.4 Photoelectrochemical g-C_3N_4-Based Biosensors 166
  2.5 Electrochemiluminescence g-C_3N_4-Based Biosensors 168
3 Conclusion 171
References 172

Abstract

Development of nanotechnology has led to the preparation of the different nanomaterials with excellent physicochemical properties, application-oriented morphologies, electrochemical and catalytic properties, and so on. Similar properties and potential-wide application in different fields from electronics, imaging, sensing and biosensing, energy conversation, etc. were reported for carbon nitride materials (CNM). CNM is a class of 2D polymeric materials dominantly composed from carbon and nitrogen. Generally, CNMs are known from the nineteenth

---

S. Đurđić (✉)
University of Belgrade, Faculty of Chemistry, Belgrade, Serbia
e-mail: sladjanadj@chem.bg.ac.rs

V. Stanković
Scientific Institution, Institute of Chemistry, Technology and Metallurgy, National Institute
University of Belgrade, Belgrade, Serbia
e-mail: vvukojevic@chem.bg.ac.rs

D. M. Stanković
University of Belgrade, Faculty of Chemistry, Belgrade, Serbia

The "Vinča" Institute of Nuclear Sciences, University of Belgrade, Belgrade, Serbia
e-mail: dalibors@chem.bg.ac.rs; daliborstankovic@vin.bg.ac.rs

© Springer Nature Singapore Pte Ltd. 2023

U. P. Azad, P. Chandra (eds.), *Handbook of Nanobioelectrochemistry*,
https://doi.org/10.1007/978-981-19-9437-1_8

century. However, interest for this structure was aroused at the end of the twentieth century, when theoretical prediction of dense sp^3-bonded C_3N_4 phase showed that this material can have high hardness values and significantly high bulk modulus. It is worth mentioning that single-phase CN is difficult to synthesize due to their insufficient thermodynamic stability and that application of CNM are connected with their graphitic phase (graphitic carbon nitride, g-C_3N_4), as a most stabile allotrope at ambient conditions. g-C_3N_4 is characterized by graphite-like structure, where distance between layers is around 3.3 nm. g-C_3N_4 structure can be presented as two-dimensional frameworks of tri-s-triazine or s-triazine linked via tertiary amines. Second structure due to the thermodynamic stability is much more favorable.

Keywords

Biosensors · Carbon nitride materials · Electrochemistry · Graphitic carbon nitride · Sensing

Abbreviations

ALP	alkaline phosphatase
AuNPs	gold nanoparticles
BPA	bisphenol A
C-g-C_3N_4	carboxylated graphitic carbon nitride
ChOx	cholesterol oxidase
CNM	carbon nitride materials
CySH	L-cysteine
DGX	Digoxin
DNA	deoxyribonucleic acid
dsDNA	double-stranded DNA
Dox	doxorubicin
ECL	electrochemiluminescence
ECL-ET	electrochemiluminescence energy transfer
EDC	1-ethyl-3-(3-dimethylaminopropyl)-carbodiimide
FRET	fluorescence resonance energy transfer
g-C_3N_4	graphitic carbon nitride
g-C_3N_4NSs	g-C_3N_4 nanosheets
g-C_3N_4NSQDs	g-C_3N_4 quantum dots
GCE	glassy carbon electrode
GO_x	glucose oxidase
ITO	indium-tin-oxide glass
MB	methylene blue
mpg-g-C_3N_4	mesoporous-g-C_3N_4
NHS	*N*-hydroxysuccinimide
PEC	photoelectrochemical
PET	photoinduced electron transfer
PPi	pyrophosphate

RNA	ribonucleic acid
ROX	carboxy-X-rhodamine
SBA	soybean agglutinin
ssDNA	single-stranded nucleic acid
TEM	transmission electron microscopic
TMB	3,3′,5,5′-tetramethylbenzidine

1 Introduction

In the last two decades, carbon- and graphene-based nanomaterials had experienced expansion in biosensor application, due to their unique electronic, magnetic, optical, mechanical, and thermal properties. Many developed carbon- and graphene-based biosensors were characterized by electroanalytical parameters such as wide linear range, low limit of detection, and excellent repeatability and reproducibility, as well as high stability and selectivity (Nirbhaya et al. 2021; Xiong et al. 2017). However, there is a constant need to develop new matrices for the immobilization of biological compounds, with the aim of developing highly sensitive and highly selective biosensors.

Graphitic carbon nitride (g-C_3N_4) belongs to the promising carbon-based matrices for production of immobilization matrixes of biosensors (Nirbhaya et al. 2021). g-C_3N_4 represents two-dimensional (2D) polymeric nanomaterial, where the structure primarily contains carbon and nitrogen atoms (Ju et al. 2018; Mandal et al. 2020; Wang et al. 2019a), with a minimum content of hydrogen atoms (Fig. ▶ 5.1). The existence of a stable π-conjugated system within condensed tri-s-triazine rings (Fig. 8.1) provides typical semiconductor properties of g-C_3N_4 with a band gap of 2.7 eV (Nirbhaya et al. 2021; Ju et al. 2018). The nitrogen-rich structure of g-C_3N_4 highly contributes to the catalytic activity of the material due to the effect of nitrogen as a strong electron donor (Vinoth et al. 2021). Semiconductor capability of g-C_3N_4 has been significantly used for energy production and storage (Fidan et al. 2021; Vinoth et al. 2021), photocatalysis (Bellamkonda et al. 2019), and electrocatalysis (Barrio et al. 2020). C-N network in g-C_3N_4 structure provided high surface area, fast electron transmission, and high chemical and thermal stability (Barrio et al. 2020; Vinoth et al. 2021; Xiong et al. 2017). Also, since it is defined as a semiconductor free from metal, the g-C_3N_4-based materials were found significant application in the environment as a green material (Barrio et al. 2020; Eswaran et al. 2021; Fidan et al. 2021). On the other hand, g-C_3N_4 structure allows potential chelation between nitrogen and metal ions, causing an improvement in the sensitivity of g-C_3N_4-based assays. This capability of g-C_3N_4 materials has expanded its application in heavy metals detection (Eswaran et al. 2021; Radhakrishnan et al. 2020).

Methods such as synthesis based on solvothermal (Montigaud et al. 2000), solid-state reactions (Zhang et al. 2001), and electrodeposition (Li et al. 2004) can be used to synthesize g-C_3N_4 material. Contrarily, thermal decomposition method has found the widest application for production of bulk g-C_3N_4 materials (Lotsch and Schnick 2006; Xiong et al. 2017). Thermal decomposition method is based on the gradual

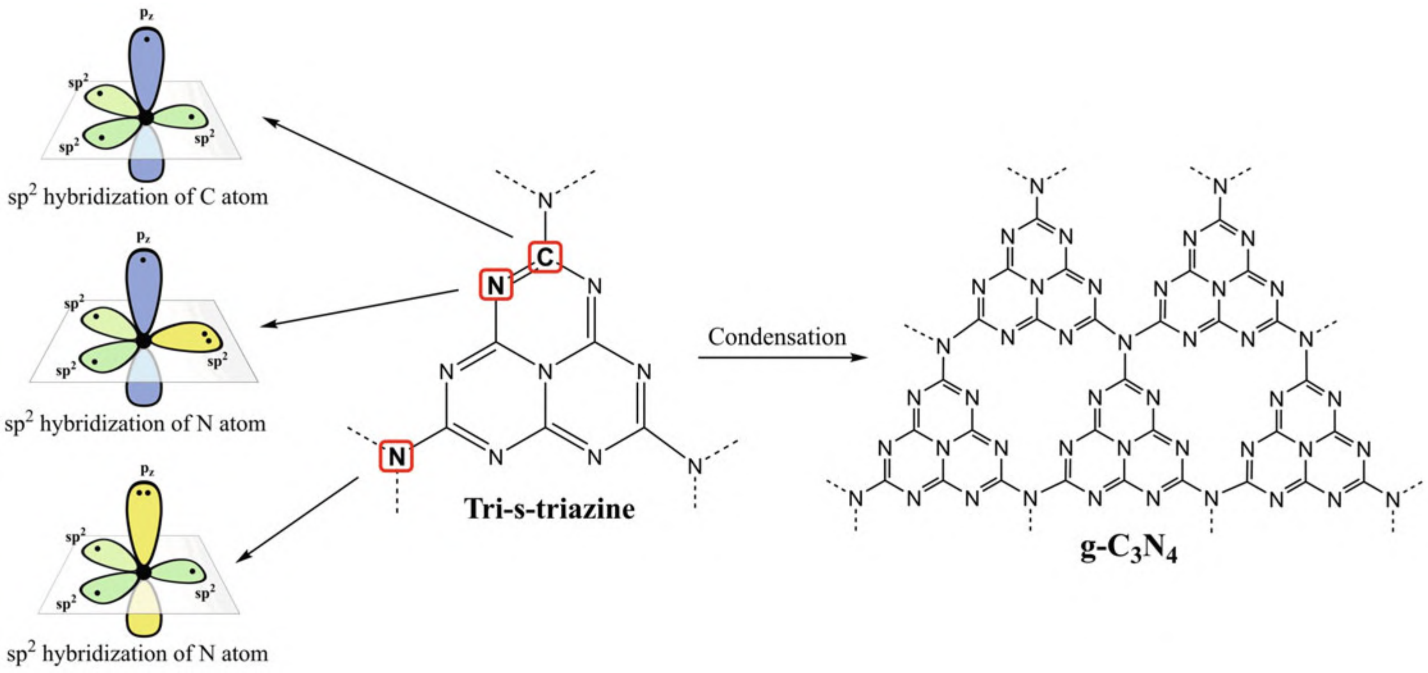
p_z
sp²
sp² hybridization of C atom
sp² hybridization of N atom
sp² hybridization of N atom
C
N
N
Tri-s-triazine
Condensation
g-C₃N₄

Fig. 8.1 π-conjugated system of the tri-s-triazine ring. Chemical structure of g-C_3N_4

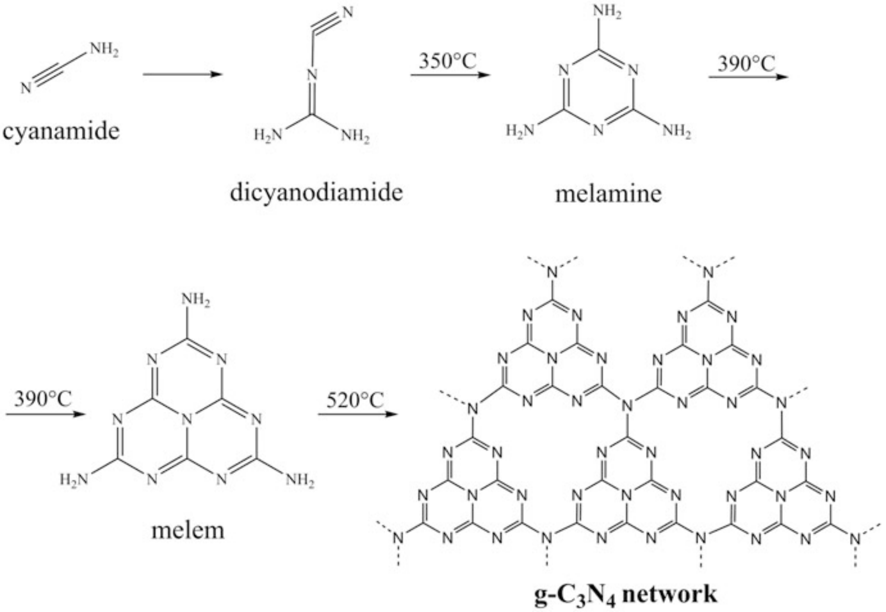

Fig. 8.2 Synthesis of g-C_3N_4 material from cyanamide by thermal decomposition method

heating of the cyanamide precursor. Then, in a heating period of 60–600 °C, the corresponding oligomers, then polymers, are formed, which is finalized by obtaining the g-C_3N_4 network (Fig. 8.2).

g-C_3N_4 materials, due to their exceptional chemical/catalytic properties, have pulled up considerable interest in the scientific world, and the industrial and environmental association. Various researchers utilize g-C_3N_4 materials to construct multiple sensors and biosensors, due to the enviable physicochemical stability and biocompatibility of this material with certain analytes and biologically active compounds (Nirbhaya et al. 2021; Vinoth et al. 2021). Therefore, this chapter provides a detailed overview of the g-C_3N_4 to construct sensors and biosensors, based on various detection principles (Fig. 8.3).

2 G-C_3N_4-Based Biosensors

2.1 Electrochemical g-C_3N_4-Based Biosensors

Sensor platform for successful immobilization of the primary antibodies (Ab1) was developed on the mesoporous g-C_3N_4 by Zhou et al. (2016) for quantification of subgroup J of avian leucosis viruses (ALVs-J). For the first time, the composite of thionine and mesoporous-g-C_3N_4 (mpg-g-C_3N_4) was synthesized and served not only as the carrier of secondary antibodies, but also as the electroactive probe. They

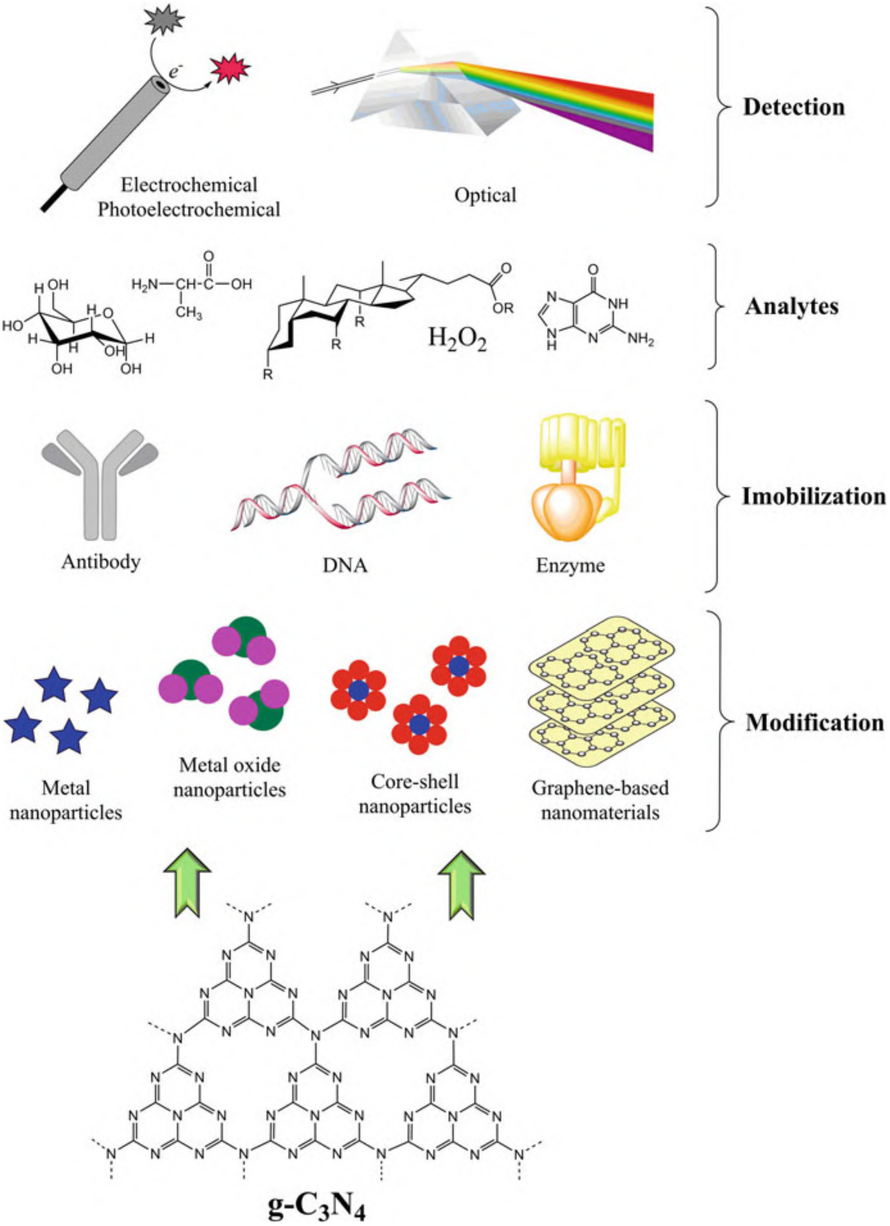
e⁻
Electrochemical
Photoelectrochemical
Optical
Detection
H₂O₂
Analytes
Antibody
DNA
Enzyme
Imobilization
Metal nanoparticles
Metal oxide nanoparticles
Core-shell nanoparticles
Graphene-based nanomaterials
Modification
g-C₃N₄

Fig. 8.3 Schematic illustration of the preparation of g-C_3N_4-based biosensors with several modification and immobilization concepts and the various detection principles

took advantages of the mpg-g-C_3N_4 such as small electrochemical resistance, large effective working area, and abundant active sites to build immunosensor. Using differential pulse voltammetry, after parameters optimization, the immunosensor provided remarkable analytical characteristics for the quantification of ALVs-J with remarkable accuracy of the developed approach which was obtained in the analysis of ALV-J in normal avian serum.

Abdul Rasheed et al. (2017) reported electrochemical geno-based sensor for the highly sensitive quantification of deoxyribonucleic acid (DNA), where breast cancer gene was used as model gene. This sensor was based on the well-known sandwich-based strategy. This strategy involved immobilization of capture probe DNA on glassy carbon electrode (GCE) previously modified with g-C_3N_4. In this work, target DNA was detected down to 10 aM with application of an Au nanoparticle cluster as electrochemical label in DNA reporter probe and immobilization of DNA capture probe to g-C_3N_4 platform. Using chronoamperometry as detection technique, the proposed approach showed linearity from 10 aM to 1 nM. In this work, authors reported that the effective surface area of the g-C_3N_4 is slightly lower compared to reduced graphene oxide. This is attributed to the few-layer structure of reduced graphene oxide. However, thanking to the properties of the g-C_3N_4, final biosensor characteristics were better with this material. Authors reported that modified electron transmission resistance of g-C_3N_4 after immobilization of DNA-c was responsible for improvement of biosensor performances. Similar to the previous study, Li and He (2021) develop a sandwich-type electrochemical biosensor for the sulfamethazine detection, based on the expressed affinity of aptamer and antibody to target molecule. They functionalized g-C_3N_4 nanosheets (g-C_3N_4NSs) with poly (ethylenimine) which, in combination with octahedral gold nanoparticles (AuNPs), served for modification of gold electrode. Through Au-N bound sulfamethazine, monoclonal antibody was stationed at the working surface. Nanocomposites based on Au@Pt core-shell, aptamers, and methylene blue (MB) were used for signal monitoring. Once sulfamethazine existed, the certain quadruplex complex is formed and the MB redox probe was linked to the electrode via Au@Pt core-shell nanoparticles. Picomolar limit of detection was obtained. Practical applicability of this method was tested in the spiked milk samples with excellent recovery and accuracy. The prepared composite in this study, based on the g-C_3N_4 as carrier, showed excellent chemical and physical properties. Authors reported that g-C_3N_4-based carrier accelerated electron transfer and provided larger binding sites for antibody. Current signal amplification and improvement of biosensor performance were achieved by the use of Au@Pt core-shell nanocomposites as carriers of aptamer and MB. In addition, highly sensitive and selective determination of sulfamethazine was realized based on the specificity of aptamer and antibody. More importantly, this study extends the analytical application of g-C_3N_4-based composites in the fields of electroanalytical sensing and bioanalysis.

Kumar Shrestha et al. (2017) exfoliated bulk g-C_3N_4 into ultrathin two-dimensional nanosheets (~3.4 nm), functionalized with proton. Using chemical polymerization method, these g-C_3N_4NSs were additionally modified with the introduction of cylindrical spongy shaped polypyrrole. This platform serves as basis for the utilization of the cholesterol biosensors. Cholesterol oxidase (ChOx) was immobilized at the composite at physiological pH, with help of strong electrostatic attraction of positively charged composite and negatively charged ChOx. Very fast response time (~3 s) and excellent sensitivity of 645.7 μA/mMcm^2 are reported for g-C_3N_4 material. Developed g-C_3N_4-based material was applied in the human samples. The engineered composite material, produced in this work exhibited effective and large active area due to exfoliation of g-$C_3N_4^+$ into ultrathin nanosheets. In addition, during immobilization of ChOx enzyme, positively enriched structure obtained with composite preparation strongly binds to the negatively charged enzymes. These interactions additionally expressed the synergetic effects for electroconductive network and electrocatalytic ability.

Puente-Santiago et al. (2019) indicate that electron-transfer processes via biomaterials with the improved electrocatalytic properties can be controlled by adjusting the surface properties of materials. They improved electron-transfer process in g-C_3N_4 material with involvement of sulfonic groups in the structure with the aim of preparation of the recombinant laccase biosensor for the detection of syringol and catechol. Remarkable charge-transfer rate constant of 12 ± 0.5 1/s was obtained for such material as the highest recorded to date for a direct electron-transfer reaction of copper-based oxidases bound to carbon-based materials. These facts were used for the preparation of amperometric biosensor which provided outstanding bioelectrocatalytic activities in the oxidation of syringol and catechol, which are relevant environmental pollutants. The sensitivities of the developed electrode were 0.41 and 0.95 A/Mcm^{-2} for syringol and catechol, respectively, dominating most of the laccase-based biosensors reported in the literature. Remarkable stability of the proposed system was reported from the authors. Such approach retained 93.2% and 94.3% of its primary electrochemical response to syringol and catechol after 57 days. Using the platform of an electrostatic self-assembly approach, a unique hybrid electrically active biocomposite based on a sulfonated g-C_3N_4 material and recombinant laccase has been provided. The developed biocomposites exhibited remarkable electron-transport efficiencies with an apparent electron-transfer rate constant (over 1200 times higher than rate constant of the free enzyme). This study represents a significant progress in the field of bioelectronics and provides the experimental and theoretical tools to discovering pathways for modification of the CNM surface properties. This strategy is significant for optimization of the structural properties of genetically engineered metalloenzymes with the aim of significantly increasing their electron-transfer efficiency for the production of ultrasensitive amperometric biosensors.

Pd wormlike nanochains/g-C_3N_4 nanocomposites serve as basis for the preparation of new electroanalytical biosensor for detection of organophosphorus pesticides and huperzine-A, where biosensor was based on the acetylcholinesterase as sensing platform. This approach was proposed by Wang et al. (2016). Synthesized structure successfully binds enzymes and promotes the signal amplification, based on the composite morphology – large number of wormlike Pd structures randomly deposited on the stacked flake-like form of g-C_3N_4 with high surface area-to-volume ratio. In this structure, Pd material acts as electron traps and facilitates the segmentation of electron-hole pairs. Further, loading of Pd affects the interfacial electron transfer efficiency, resulting in improvement of electrochemical signal. Prepared Pd wormlike nanochains/g-C_3N_4 composites successfully catalyzed the redox reaction of the analyte, but most importantly enhanced the loading of acetylcholinesterase and thus improved the sensitivity of the sensor.

Highest number of g-C_3N_4 electrochemical biosensors were developed for glucose and H_2O_2 detection, using two principles enzymatic and nonenzymatic. For the synthesis of g-C_3N_4/iron, oxide@copper nanocomposite was used as one-step pyrolysis of melamine and $Cu_3[Fe(CN)_6]_2$ (Liu et al. 2018). The iron oxide and copper nanomaterials were decorated g-C_3N_4NSs, which can productively defend the g-C_3N_4NSs from restacking. The derived Cu and Fe_2O_3 nanomaterials directly improve the electro-catalytic properties of as-prepared composites. These three components cooperatively enhance the electrochemical characteristics of nonenzymatic glucose quantification, due to excellent electrocatalytic properties of Cu nanomaterial, while good mimicking of peroxidase activity was attributed to thin-layered g-C_3N_4 and Fe_2O_3. Thin layers of g-C_3N_4, with a relatively high effective surface area, can supply a large number of active groups in order to stabilize Fe_2O_3 and Cu nanostructures. This also improves the stability of as-fabricated modified electrode. In addition, N-rich thin layered g-C_3N_4 could interact with glucose in the solution, resulting in the accumulation of glucose in the surface of as-fabricated electrode. The synergistic effect of these three components in the as-prepared composites provides improvement of electrocatalytic activity toward glucose oxidation. For the first time, Tian et al. (2013) demonstrated ultrathin g-C_3N_4NSs as a highly efficient, green, and low-cost electrocatalyst for reduction of H_2O_2. Nano-layered $Co(OH)_2$ deposited on polymeric g-C_3N_4 linked by chemical bath deposition was used as support for the construction of novel nonenzymatic glucose biosensor (Tashkhourian et al. 2018). Authors used this two-dimensional nanocomposite for modification of carbon paste electrode and improvement of its electrochemical characteristics. This material revealed a noticeably synergistic effect as a result of appropriate exfoliation of g-C_3N_4 in the presence of $Co(OH)_2$, as well as remarkable electrocatalytic properties. Also, authors reported separate effect of the material components, where the catalytic current generally originated from the active site of $Co(OH)_2$ toward the catalytic glucose oxidation, while g-C_3N_4 affected the electrochemical characteristics of the modified electrode. Actually, the presence of g-C_3N_4 provided a large surface area, leading to an increase in the quality of Co $(OH)_2$ active sites and causing the development of $Co(OH)_2$ in the form of a two-dimensional nanolayer. In addition, authors noted that the appearance of Co $(OH)_2$ helps flaking of the g-C_3N_4 layers, resulting in the $Co(OH)_2$ deposition in the form of nanolayers on it. This is confirmed and with morphological characterization of the material. The high surface area-to-volume ratio of g-C_3N_4 nanostructure improves oxidation of glucose over its large total surface area.

Imran et al. (2021a) apply knowledge about synergetic effect of metal-metal oxides and g-C_3N_4 on electrocatalytic properties of the electrode surfaces for the preparation of electrochemical nonenzymatic glucose sensor based on the modification of g-C_3N_4 with zinc oxide and platinum. The interactions between g-C_3N_4, ZnO, and Pt were studied using various physicochemical methods. Combination of these materials resulted in the electrochemical response of glucose at low potential of +0.20 V (vs. Ag/AgCl), fast response time of 5 s, and high sensitivity of 3.34 μA/

mMcm^2. Similar results were achieved with the Na,O-co-doped-g-C_3N_4 (Na,O-g-C_3N_4) which was prepared by subsequent heat treatment in the presence of alkaline, reported by Mohammad et al. (2020). The Na,O-g-C_3N_4, obtained from urea, showed relative surface area and adjusted optical characteristics with sheet-like properties. This nanomaterial was used for the modification of GCE. Remarkable results for the nonenzymatic H_2O_2 detection by electrochemical method were reported. Urea as a base for the synthesis of ultrathin layered g-C_3N_4 was used by Imran et al. (2021b). In this work, g-C_3N_4 was additionally decorated using niobium (Nb) metal nanoparticle. The composite was prepared by pyrolysis method and used for direct glucose determination in human blood samples. Two different oxidation peaks during cyclic voltammetry scanning were observed (similar to metal electrodes), showing the metallic behavior of the Nb-g-C_3N_4 composite. The oxidation peak at +0.39 V corresponds to oxidation of glucose to gluconolactone. Appearance of very intense reverse peak in reverse scan originates from oxidation of gluconolactone to CO_2 and H_2O. This good electrocatalytic behavior of Nb-g-C_3N_4 may be described by successful doping of niobium into g-C_3N_4 with aim to increase the numbers of electro-active sites and improve the electron transportation. This result indicates the metallic behavior of the Nb-g-C_3N_4 composite. The mechanism of glucose oxidation at metal/metal oxide surfaces is highly reported in literature. The gold electrode modified with Nb-g-C_3N_4 composite catalyzes the formation of adsorbed hydroxyl ions and acts as a mediator for reactions such as oxidation of glucose and reduction oxygen at electrode surface.

2.2 Fluorescent g-C_3N_4-Based Biosensors

g-C_3N_4 is characterized by unique fluorescent properties. The excitation wavelength of g-C_3N_4 is 320 nm. Contrarily, g-C_3N_4 emits strong fluorescence at ~440 nm (blue light region) with increased fluorescence quantum yield of ~20% (Xiong et al. 2017). This optical characteristic of g-C_3N_4 has found wide application in the production of label-free biosensors and the quantification of a wide range of biological/chemical compounds. Determinations are mostly based on monitoring the quenching of g-C_3N_4 fluorescence intensity. In most experiments, metal ions such as Cu^{2+}, Ag^+, and Fe^{3+} are used to quench g-C_3N_4 fluorescence (Xiong et al. 2017). For this purpose, the capability of g-C_3N_4 to chelate with metal ions via photoinduced electron transfer (PET) was used (Xiang et al. 2016; Xiong et al. 2017). In addition, quenching of g-C_3N_4 fluorescence can be performed by the biomolecule heparin, as well as certain nitrobenzene derivatives (Xiong et al. 2017).

Fluorescent properties of g-C_3N_4 were used to determine enzyme activity. A design principle of enzyme determination with label-free g-C_3N_4-based biosensors is explained using enzyme alkaline phosphatase (ALP) and pyrophosphate (PPi) as its substrate (Xiang et al. 2016). The experimental procedure for determining enzyme activity is based on the chelation of Cu^{2+} (added in order to quench the fluorescence of g-C_3N_4) by PPi (Fig. 8.4). In parallel, g-C_3N_4 exhibits its fluorescence capabilities, and the corresponding signals are detected using an appropriate

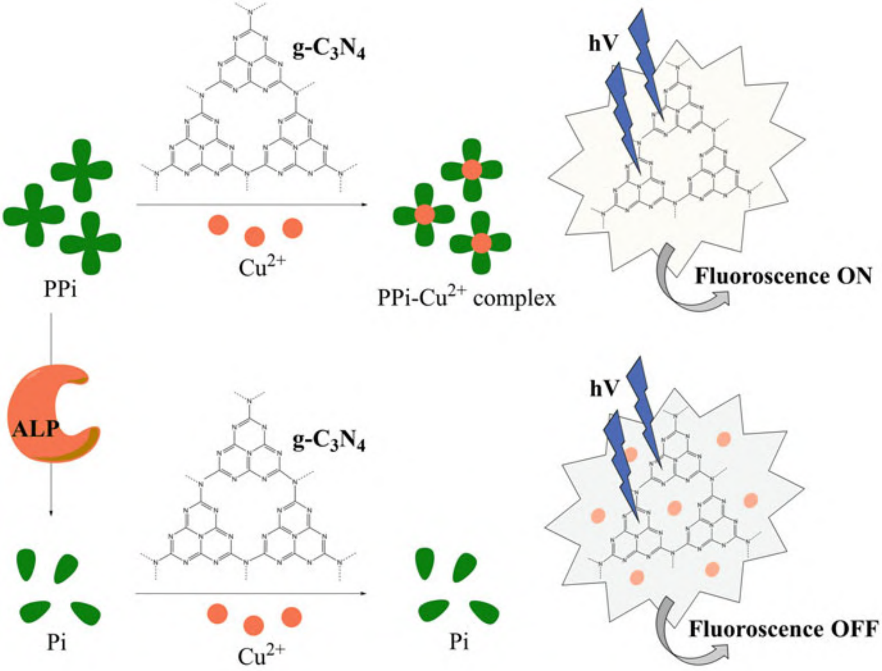

Fig. 8.4 Schematic illustration of label-free biosensing strategy for ALP using of g-C_3N_4 quenching platform

spectrofluorometer. The addition of ALP catalyzes the hydrolysis of PPi to phosphate (Pi), resulting in the loose of Cu^{2+} from the PPi-Cu complex. Then, the released Cu^{2+} was chelated by g-C_3N_4. The g-C_3N_4-Cu complex does not have the capability to fluoresce, which is noted as a decrease in the signal on the instrument. Precisely, the quenching of g-C_3N_4 fluorescence is labeled as an indicator of enzyme activity. Using this principle and procedure, Xiang et al. (2016) reported a g-C_3N_4NSs-based biosensor for determination of ALP activity. Bulk g-C_3N_4 was synthesized by treatment of cyanamide at 600 °C. g-C_3N_4NSs were obtained by chemical oxidation of bulk g-C_3N_4 with HNO_3, accompanied with exfoliation of oxidized bulk g-C_3N_4 in order to obtain nanosheets. Further, the transmission electron microscopic (TEM) imaging confirmed the g-C_3N_4NSs thickness of 1.25 nm. After optimization of experimental parameters (the content of PPi, the content of Cu^{2+}, the reaction time, and the reaction temperature between ALP and PPi), the developed g-C_3N_4-based biosensor provided a wide concentration range toward ALP (0.1–1000 U/L), with a limit of detection of 0.08 U/L. In addition, the biosensor was giving high selectivity during the determination of ALP activity in the presence of other enzymes. Accordingly, the developed g-C_3N_4-based biosensor provided a selective and sensitive platform for quantification of ALP in biomedical samples and clinical diagnostics.

Intense of g-C_3N_4 fluorescence was used to produce aptasensor. Shirani et al. (2020) developed an aptasensor based on g-C_3N_4, AuNPs and single-stranded nucleic acid (ssDNA) for quantification of the cardiac drug Digoxin (DGX). Bulk g-C_3N_4 was prepared by the polymerization of melamine. Exfoliation of bulk g-C_3N_4 in water regia resulted in formation of g-C_3N_4NSs. The TEM method confirmed the planner shape of g-C_3N_4NSs form, with a size of ~100 nm and a thickness of ~2 nm. Colloidal AuNPs were synthesized from $HAuCl_4$. DGX aptamer (ssDNA) with the appropriate nucleotide sequence was adsorbed on the obtained AuNPs, by electrostatic interactions. The fluorescence of g-C_3N_4NSs, in presence of NaCl, was monitored at 445 nm (*fluorescence ON*). Following the addition of AuNPs-aptamer conjugate to the g-C_3N_4NSs/NaCl suspension, g-C_3N_4NSs interacts with AuNPs via fluorescence resonance energy transfer (FRET) mechanism, resulting in g-C_3N_4NSs fluorescence quenching and signal reduction (*fluorescence OFF*). The addition of DGX as a substrate leads to the interaction of aptamer and DGX, while AuNPs were aggregated in the presence of NaCl. In parallel, g-C_3N_4NSs fluorescence was recovered (*fluorescence ON*). The determination was based on measuring the fluorescence intensity of g-C_3N_4NSs before and after the addition of DGX. After optimizing experimental parameters (amount of g-C_3N_4NSs, aptamer/AuNPs molar ratio, NaCl concentration, incubation period of aptamer/AuNPs, and incubation period of aptamer/DGX interactions), the developed g-C_3N_4-aptasensor provided a linear concentration scale from 10 to 500 ng/L for DGX, with ultrasensitive LOD of 3.2 ng/L. In addition, the proposed g-C_3N_4-aptasensor provided high selectivity if it is accompanied with various coexisting drugs and heavy metal ions. Finally, the *ON-OFF-ON* fluorescence aptasensor was effectively used for determination of DGX in human plasma, without prior sample preparation.

Liu et al. (2019a) showed a ratiometric fluorescent g-C_3N_4-based aptasensor for the detection of the biomarker adenosine. g-C_3N_4 network was doped with phenyl groups in order to achieve strong green fluorescence of the material (λ_{max} = 505 nm). Urea and trimesic acid were involved in the preparation of phenyl-doped g-C_3N_4 nanosheets (PDCN-NS). TEM imaging confirmed the thickness of composite of 6 nm and the size of 130 nm. Preparation of the aptasensor included labeling the antiadenosine aptamer with fluorescent dye. Carboxy-X-rhodamine (ROX), which emits fluorescence at 620 nm, was used as the dye. The resulting ROX-aptamer was adsorbed to the PDCN-NS surface through π-π stacking and hydrophobic interactions. In this way, the fluorescence of the ROX-aptamer at 620 nm was quenched, while the green fluorescence of the PDCN-NS did not change significantly. Precisely, the constant fluorescence of PDCN-NS was used to develop a ratiometric nanoprobe for adenosine analysis. After the addition of adenosine, the fluorescence of the ROX-aptamer was recovered due to the formation of the aptamer-adenosine complex. Analytical procedure was based on normalization of the fluorescence strength of ROX-aptamer by the fluorescence intensity of PDCN-NS. After optimization of experimental parameters (PDCN-NS concentration, buffer pH, and incubation time between ROX-aptamer and adenosine), PDCN-NS@ROX-aptamer biosensor was shown linear calibration curve from 10 to 1000 μM, with detection limit of 6.86 μM. Also, the PDCN-NS-based aptasensor showed high selectivity in the appearance of various biological important compounds and essential metal ions and has been effectively applied for the quantification of the adenosine in human serum samples.

Also, g-C_3N_4 was used to produce "turn off" fluorescence biosensors to detect metal ions. Li et al. (2017) reported g-C_3N_4-based aptasensor for detection of Hg^{2+}. Strong adsorption of ssDNA by g-C_3N_4 via Van der Waals interactions was used for quantification of Hg^{2+}. g-C_3N_4 was obtained by melamine polymerization at 500 °C. The resulting yellow precipitate of g-C_3N_4 was subjected to HNO_3 in order to obtain g-C_3N_4NSs. *N*-hydroxysuccinimide (NHS) and 1-ethyl-3-(3-dimethylaminopropyl)-carbodiimide (EDC) were used for preparation of g-C_3N_4@ssDNA conjugate. The analytical procedure was based on monitoring the fluorescence intensity at 440 nm of the g-C_3N_4@ssDNA aptasensor before and after the addition of analyte. Hg^{2+}, after addition to the assay solution, chelates with tymine from ssDNA and forms the thymine-Hg^{2+}-thymine complex, resulting in the formation of hairpin-shaped double-stranded DNA (dsDNA). Thus, Hg^{2+} was closer to the surface of g-C_3N_4NSs, whereby fluorescence was quenched and fluorescence signal was reduced. The influence of g-C_3N_4NSs concentration on the fluorescence signal was examined to increase the optical performances of the developed g-C_3N_4@ssDNA aptasensor. In addition, the reaction time between g-C_3N_4@ssDNA aptasensor and analyte was optimized. Developed g-C_3N_4@ssDNA showed ultrasensitive LOD of 0.17 nM, as well as high selectivity during detection og Hg^{2+} accompanied with the different metal ions. Finally, proposed g-C_3N_4-based aptasensor was used for detection of Hg^{2+} in water samples.

2.3 Colorimetric g-C_3N_4-Based Biosensors

g-C_3N_4 has found significant application in nanozyme production. Nanozymes are new nano/functional materials with the properties of natural enzymes. Nanozymes are characterized by the ability to catalyze typical enzymatic reactions by mimicking oxidases, catalases, and peroxidases. Their advantage over enzymes is reflected in large surface area, high catalytic activity, high stability in various media, and simple synthesis, as well as low costs (Ju et al. 2018). In order to increase catalytic activity, g-C_3N_4 is most commonly modified with metal/metal oxides nanoparticles. Colorimetric detection is based on an appropriate reaction catalyzed by a g-C_3N_4-supported nanozyme without the addition of a natural enzyme, resulting in the formation of a colored compound. Then, the absorbance of the colored compound is monitored on an appropriate spectrophotometer (Wu et al. 2019a; Zhu et al. 2018).

Wu et al. (2019b) reported g-C_3N_4-supported colorimetric approach for detection of H_2O_2 and glucose. The nanozyme probe was based on the modification of g-C_3N_4NSs with plasmonic AuNPs. g-C_3N_4NSs was synthesized by melamine polymerization at 550 °C, while $HAuCl_4$ was used to obtain AuNPs. The thickness of g-C_3N_4NSs of around 1 nm was confirmed by the atomic force microscopic method, while the size of AuNPs of around 10 nm was reveal by TEM imaging.

Preparation of g-C_3N_4NSs@AuNPs hybrid catalyst was based on “in situ” grown of AuNPs on g-C_3N_4NSs surface. The aim of the research was to develop and examine the performances of the g-C_3N_4NSs@AuNPs nanozymes probe which in the experiment mimics the enzyme peroxidase. The first experimental step was to examine the peroxidase-like activity of g-C_3N_4NSs@AuNPs hybrid. As substrate was used 3,3′,5,5′-tetramethylbenzidine (TMB). The determination was based on the addition of g-C_3N_4NSs@AuNPs to the TMB/H_2O_2/phosphate buffer mixture. Then, g-C_3N_4NSs@AuNPs catalyzes the TMB oxidation, the existence of H_2O_2, resulting in blue color formation. Absorbance of blue color was monitored at 652 nm using an appropriate spectrophotometer. Consequently, the intensity of absorption depends on the H_2O_2 concentration, enabling its detection. After optimization of pH of phosphate buffer solution, reaction temperature, and TMB concentration, the g-C_3N_4NSs@AuNPs hybrid showed an LOD of 1.0 μM toward H_2O_2. In addition, H_2SO_4 was added to the TMB/H_2O_2 mixture to increase parameters for the determination. Addition of an acid solution leads to the protonation of TMB and formation of yellow-colored TBM^{2+}, characterized with an absorption at 451 nm. In the H_2SO_4 medium, the g-C_3N_4NSs@AuNPs hybrid showed an LOD of 0.31 μM for H_2O_2. The second experimental step involved the detection of glucose via H_2O_2. Glucose oxidase (GO_x) was added to phosphate buffer solution containing different concentrations of glucose. GO_x enzyme induces glucose oxidation to the corresponding lactone and H_2O_2. The obtained H_2O_2 was detected with g-C_3N_4NSs@AuNPs hybrid according to the explained procedure in H_2SO_4 medium. The obtained concentration of H_2O_2 is directly proportional to the glucose concentration. g-C_3N_4NSs@AuNPs hybrid provided the LOD of 0.75 μM for glucose. Finally, g-C_3N_4NSs@AuNPs hybrid catalyst as a peroxidase nanozyme was used to quantify glucose in urine and human serum samples.

2.4 Photoelectrochemical g-C_3N_4-Based Biosensors

Photoelectrochemical (PEC) determination is based on irradiation of photoexcited material by appropriate lamps. The resulting photocurrent is converted to electrical by the electrode as a transducer, causing signal recording. PEC platform uses two different signal forms for excitation and detection, making this platform potentially more sensitive compared to classical electrochemical measurements (Zhao et al. 2014). In a biosensing application, biological recognition systems (enzymes, DNA, ribonucleic acid (RNA), and antibodies) respond to biochemical changes (interactions, analyte concentration) and transmit a specific change to the photoactive electrode environment. The resulting PEC signal is linearly dependent on the applied analyte concentration (Xu et al. 2020). The main step in PEC determinations is the construction of a photoactive electrode. g-C_3N_4 has proven to be a potential candidate for developing the PEC platform. As mentioned, this promising material is characterized by appropriate photoactivity, as well as tunable bandgap. In addition, by intercalating certain sensitizers within the g-C_3N_4 structure, the photoactivity of the material can be significantly increased. Also, g-C_3N_4 modification can be performed with metal/metal oxide NP in order to increase the catalytic activity of the target material, which directly affects the improvements in the electrochemical performances of biosensors. In recent years, standard electrochemical sensors have been modified with g-C_3N_4-based nanomaterial to develop PEC assays (Wang et al. 2019b; Xu et al. 2020).

Xu et al. (2020) proposed a g-C_3N_4-based aptasensor for the detection of bisphenol A (BPA). Proposed aptasensor was based on the modification of g-C_3N_4 with Cu(I). g-C_3N_4 was synthesized from urea, while g-C_3N_4@Cu composite was obtained from bis (1-hexadecyl-3-methylimidazolium) tetrachlorocuprate(II) after the solvothermal treatment. Indium-tin-oxide glass (ITO) was modified with the g-C_3N_4@Cu composite to construct a working electrode (ITO/g-C_3N_4@Cu). The surface of ITO/g-C_3N_4@Cu was modified with BPA aptamer of the appropriate nucleotide sequence to produce aptasensors. Photocurrent was monitored for each electrode modification step after a 20-second interval of irradiation of the PEC cell with a xenon lamp. A decrease in photocurrent was observed after the application of aptamer due to the coating of the electrode surface with the organic layer, which caused a decrease in electron transfer. This proved the successful immobilization of the aptamer on the electrode. After the addition of BPA as an analyte, an additional decrease in photocurrent was observed due to successful interactions between aptamer and BPA. The developed g-C_3N_4-based aptasensor showed a linear dependence between the logarithm of the concentration and photocurrent, with an ultrasensitive LOD of 70 fM toward BPA. After selectivity testing in the presence of hexafluorobisphenol A and bromophenol blue, the developed ITO/g-C_3N_4@Cu aptasensor was successfully applied to quantify BPA in wastewater.

Wang et al. (2019b) reported g-C_3N_4@AuNPs biosensor for microRNA-141 detection supported with a target-activated enzyme-free DNA walker. g-C_3N_4@AuNPs composite was prepared by electrodeposition of AuNPs on the surface of g-C_3N_4. GCE surface was adopted with g-C_3N_4@AuNPs composite with the aim of preparing a working electrode. The DNA hairpin (H1) was immobilized on the GCE/g-C_3N_4@AuNPs surface, while the other DNA hairpins (H2-H5), in the existence of target miRNA-141, reacted with H1 and added to each other. After completion of the cycle, a dsDNA copolymer was formed on GCE/g-C_3N_4@AuNPs. The immobilized dsDNA copolymer is characterized by cavities. Doxorubicin (Dox), used as a sensitizer, increased the photoactivity of g-C_3N_4 after its intercalation within dsDNA cavities. After irradiation of the PEC cell, the PEC responses of the biosensor were monitored after each immobilization step. The photocurrent response of the developed g-C_3N_4-based biosensor was tested at different concentrations of microRNA-141, under optimized experimental conditions. LOD of 83 aM toward microRNA-141 was recorded. Finally, the g-C_3N_4@AuNPs biosensor provided satisfactory selectivity in the presence of coexisting compounds (microRNA-122, microRNA-126, and microRNA-21).

2.5 Electrochemiluminescence g-C_3N_4-Based Biosensors

Electrochemiluminescence (ECL) is an electrogenerated chemiluminescence process where species are formed at the electrode surface, subject to reaction of high-energy electron transfer, with formation of excited states that emit light during relaxation process. In another word, after bringing additional energy in the form of external voltage, a stable precursor will produce an intermediate near the electrode. Then in the medium, an intermediate interacts with coreactants to redintegrate an excited state (Xavier et al. 2019). The main advantages of this method, compared to luminescence induced by chemical reaction (chemiluminescence), are the ability to initiate and control luminescence mainly by the electrode voltage (Richter 2004) as well as the low background emission, which allows lower detection limits to be achieved (Kulmala and Kankare 2013).

Since the first studies in the 1960s, several thousands of papers, patents, and book chapters have been published on ECL. A significant number of commercial platforms that use ECL are commercially available for the detection of the clinically significant analytes (steroid hormones, antibodies, proteins. . .), with high accuracy and selectivity. Furthermore, use of ECL active species to label biological molecules enabled the application of this technique in immunoassay and DNA analysis (Kulmala and Kankare 2013).

There are three different mechanisms used in ECL sensing: the ion annihilation process, hot electron-induced cathodic process, and coreactant process. Ion annihilation process requires a rapid change in the potential of the working electrode among the two values, generating an oxidative and a reduced species (radical cations and radical anions) that react close to the electrode surface to form an excited state of the species, which emits light after relaxing to the ground state (Kulmala and Kankare 2013). This activity is mainly carried out in nonaquas solvents, in order to achieve the required stability of cation and anion radicals, due to which it is not suitable for biosensing applications (Qi and Zhang 2020). The hot electron-induced cathodic process is based on the injection of hot electrons in a semiconductor/insulating film into an aqueous regia which is a supporting electrolyte. This leads to the formation of hydrated electrons as reducing mediators, followed by oxidation/reduction processes between these electrons and luminophores/oxidized luminophores, directing to its emission (Qi and Zhang 2020). In the coreactant process, ECL is generated in one potential step by species, e.g., coreactant which, after oxidation or reduction, produces an intermediate. Then, the intermediate reacts with ECL luminophore to produce excited states (Richter 2004). For the purposes of ECL biosensing, coreactants mostly use peroxydisulfate ($S_2O_8{}^{2-}$) for the cathodic coreactant process. Contrary, anodic coreactant process involves hydrogen peroxide (H_2O_2), while luminophores include inorganic complex (for example, tris(2,20-bipyridyl) ruthenium(II), $Ru(bpy)_3{}^{2+}$), organic compound (luminol), and nanomaterials (g-C_3N_4) (Fig. 8.5) (Qi and Zhang 2020).

Since the first report on the cathodic electrochemiluminescence behavior of g-C_3N_4 in 2012 was published (Cheng et al. 2012), this material has been intensively researched to obtain new biosensors with improved analytical performance. Compared to other

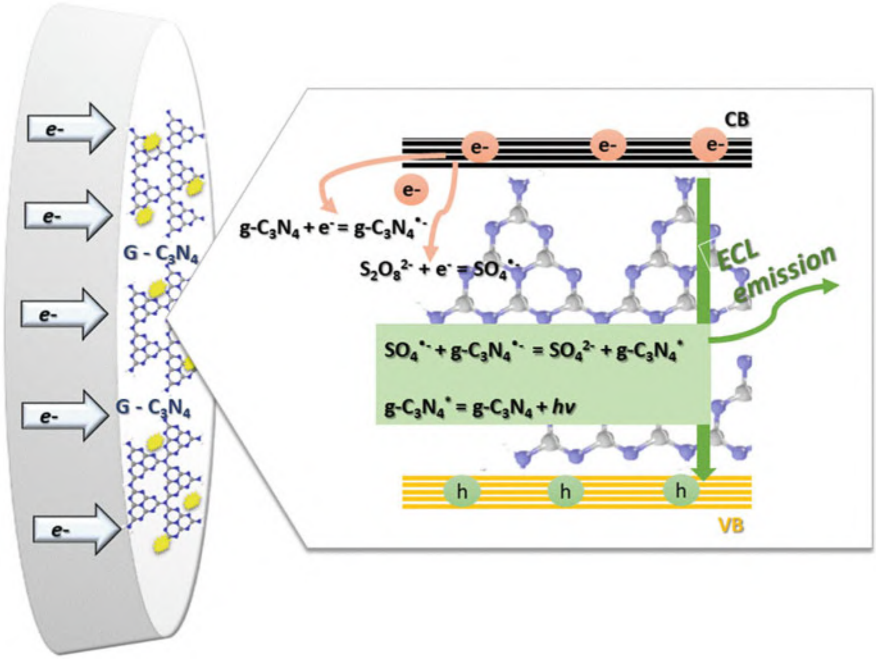
e-
e-
e-
e-
e-
G - C_3N_4
G - C_3N_4
CB
e-
e-
e-
e-
$g\text{-}C_3N_4 + e^- = g\text{-}C_3N_4^{\bullet -}$
$S_2O_8^{2-} + e^- = SO_4^{\bullet -}$
ECL emission
$SO_4^{\bullet -} + g\text{-}C_3N_4^{\bullet -} = SO_4^{2-} + g\text{-}C_3N_4^{*}$
$g\text{-}C_3N_4^{*} = g\text{-}C_3N_4 + hv$
h
h
h
VB

Fig. 8.5 Schematic representation of ECL emission mechanism

conventional ECL emitters, g-C_3N_4 possesses a number of distinct properties such as higher thermal and chemical stability, cheaper raw materials as well as facile preparation mode, nontoxicity, and generally good biocompatibility (Zou et al. 2020). It is important to emphasize that all ECL occurrence in g-C_3N_4 have been established on the coreactant pathway, where a coreactant ($S_2O_8{}^{2-}$; Et_3N...) produced intermediate species. Then, an intermediate reacts with the radical ions of g-C_3N_4 to produce excited state when convenient potential is applied. Problems that can occur during the practical application of this material in ECL sensing are due to the small effective area, poor conductivity, low dispersion, and chemical inertness of material itself, which together with the appearance of the electrode passivation ultimately lead to reduced stability, reproducibility, and sensitivity of the entire system (Chen et al. 2014; Feng et al. 2018). Significant improvement of sensing performance of g-C_3N_4 can be achieved by its modification with different nanomaterials including metal-oxide nanoparticles, metal nanoparticles, carbon-based nanoparticles, etc.

Wang et al. (2018) proposed an ECL biosensor for detecting dopamine using nanocomposite of silver-carbon nitride (Ag-g-C_3N_4) as signal probe. The bulk GCE was modified with Ag-g-C_3N_4 nanocomposite and chitosan which were applied to immobilize the substrate material on electrode surface. This system produces a weak ECL signal in a solution containing $K_2S_2O_8$ as coreactant. After addition of dopamine to the main solution, a strong ECL signal was recorded based on the amino group of dopamine that fostered the coreactant transformation of anion $S_2O_8{}^{2-}$ into radical anion $SO_4^{\cdot-}$, which is followed by an increase of ECL intensity of Ag-g-C_3N_4. Obtained ECL biosensor have wide linear calibration curve (from 0.015 to 150 mM), high sensitivity and good stability, and low limit of detection (0.005 mM) and, according to authors, can be used for the quantification of dopamine in human serum samples (Wang et al. 2018).

Cao et al. (2018) developed aptasensor for ECL determination of BPA by using g-C_3N_4. The only modification of the g-C_3N_4 was its carboxylation. Carboxylated g-C_3N_4 (C-g-C_3N_4) has better conductivity and solubility in aqueous regia compared with g-C_3N_4. The authors pointed out that obtained composite possesses improved shortened electronic transmission distance and luminous stability thanks to the carboxyl groups on the material surface which can be covalently linked to various other functional groups (hydroxy, amido, etc.). In this study, the amide bond was formed between NH_2 groups of aptamers and the COOH groups of C-g-C_3N_4. In the presence of BPA, the aptamer would discriminately interact with BPA, resulting in the decrease of the ECL response, originated from the buffer solution containing C-g-C_3N_4 and coreactant ($K_2S_2O_8$). Using this approach, authors produce a new platform for BPA determination with excellent sensitivity (the detection limit is 30 fM), outstanding stability, and high selectivity (Cao et al. 2018).

Construction of a "turn off-on" electrochemiluminescence (ECL) sensing platform for L-cysteine detection was described by Wu et al. (2019c). Authors used composite made of C-g-C_3N_4 and MnO_2 nanosheets as the probe. $K_2S_2O_8$ was used as the coreactant. Large specific surface area and numerous functional groups of C-g-C_3N_4 nanosheet offer support for in situ expansion of MnO_2 nanosheet. Under the coreactant synergy, C-g-C_3N_4 is able to generate strong ECL emission. After formation of the MnO_2 and C-g-C_3N_4 nanocomposite, the ECL is markedly quenched due to the transfer of the energy based on ECL from g-C_3N_4 to MnO_2. Further, the addition of CySH could lead to the ECL-ET elimination, because it reduced MnO_2 to Mn^{2+} and recovery of ECL signal. Using the abovementioned method, authors developed a new ECL biosensor that has fast response, high sensitivity, excellent selectivity, good stability, and with low detection limit (0.18 nM) (Wu et al. 2019c).

Zhang et al. (2019) also performed only g-C_3N_4 carboxylation, instead of other types of material functionalization with metal nanoparticles or other nanomaterials. This group of authors developed a sandwich-structured electrochemiluminescence platform for the determination of soybean agglutinin (SBA). Biosensor was prepared using D-galactosamine (galM) as a recognition platform and C-g-C_3N_4 as luminophore. The authors showed the following steps to achieve the sensitive determination of SBA. GCE was modified with AuNPs for capturing the galM via Au-N link, which is followed by further capturing the SBA by specific recognition between galM and SBA. After addition of SBA, the C-g-C_3N_4-galM composite was immobilized at the electrode surface. The ECL signal from C-g-C_3N_4 increased with the increasing of SBA concentration, resulting in a signal on detection of SBA. Here, authors used C-g-C_3N_4 not only as a luminophore, but also as an immobilization matrix for recognition element, and achieved the detection limit for SBA of 0.33 ng/mL (Zhang et al. 2019).

Liu et al. (2019b) recently proposed an electrochemiluminescence sensing platform for ultrasensitive detection of DNA. Platform was based on resonance energy transfer between Au nanoparticles and graphitic carbon nitride quantum dots (g-C_3N_4QDs). In this research, authors used a solid-state approach under low temperature to produce g-C_3N_4QDs. g-C_3N_4QDs composite showed an energetic ECL answer based on the use of coreactant ($K_2S_2O_8$). Furthermore, AuNPs were used because of their extraordinary properties such as catalytical effect and superior biocompatibility as well as possibility to use these nanoparticles as a quencher in order to establish an energy transfer-based sensing support. For the preparation of biosensors, the authors followed the next procedure: g-C_3N_4QDs was cast on the prepared GCE, and then certain amount of the AuNPs-modified hairpin DNA (Hai-DNA) probe solution was spread on the g-C_3N_4QDs/GCE. The g-C_3N_4QDs on the unmodified GCE provided a robust ECL response, in the presence of $K_2S_2O_8$. After immobilization of AuNPs-modified Hai-DNA at the electrode surface, the ECL signal decreased due to the donor/acceptor pair energy transfer in the system AuNPs/C_3N_4QDs. When the hybridization between DNA and Hai-DNA occurs, ECL signal is recovered. Developed sensor, used for DNA quantification, after optimization of experimental conditions, showed excellent performance with detection limit of 0.01 fM (Liu et al. 2019a).

Recently, Jian et al. (2020) published a new, interesting immunosensing approach where they developed a highly sensitive ECL sensor focused on the supersandwich sensing platform (the ratio of target-to-signal probe is 1: N^n). In their work, porous Au-based electrode was used to provide an increased number of bonding sites for immobilization of the primary antibody (Ab1 – goat antirabbit IgG). As signal probes, the biocompatible, ultrathin two-dimensional g-C_3N_4NSs, decorated with AuNP and ssDNA, were used. Formation of a double helix, from two ssDNA (DNA_1 and DNA_2) with complementary base sequences, result in electrode surface rich in a g-C_3N_4NSs. A hybridization process provided a drastically expanded ECL signal, which also implies increased sensitivity, with unusually low detection limits, necessary in clinical analyses of biomarkers. The ECL immunosensor proposed in this work possesses a wide linear working range – from 0,01 pg/L to 1 mg/L with limit of detection of 0.001 pg/L as well as excellent selectivity. Authors suggested that proposed sensing platform could be developed into a real-time analysis for the disease-related molecular targets (Jian et al. 2020).

3 Conclusion

This chapter has highlighted developments in g-C_3N_4-based biosensors, immunosensors, and aptasensors that have been reported in the literature, in recent years. The review clearly shows that the g-C_3N_4 materials are very suitable for various modifications. Also, the g-C_3N_4 materials have proven to be very suitable for immobilization of various enzymes, antibodies, or genetic material, due to its biocompatibility with biological compounds. In addition, it is noticed that the developed g-C_3N_4-based biosensors show excellent essential electroanalytical parameters such as extremely low LOD, wide linear range, high stability, and high sensitivity.

The chapter also shows how the unique properties of the g-C_3N_4 material were used to develop different detection methods. Although g-C_3N_4 provided semiconductor capability, electrochemical and photoelectrochemical detection of various analytes was carried out thanks not only to the fast electron transfer (due to the action of nitrogen as an electron donor), but also to the large specific surface area of the material. Strong fluorescence of g-C_3N_4 has been used to develop fluorescent-based methods. Quenching of the g-C_3N_4 fluorescence after interaction/reaction/chelation of the different compounds (metal ion, nanoparticles, and analyte) with the material is most commonly monitored. On the other hand, colorimetric detection of analyte is enabled due to the creation of color formed after a certain ox-red reaction catalyzed by the g-C_3N_4-based hybrid. This detection method is widely used in the development of g-C_3N_4-based nanozyme assays. In addition, the development of electrochemiluminescence-based methods is possible due to the high chemical and thermal stability of the g-C_3N_4 material, during the interaction/reaction of the material with the coreagents in the medium, in order to achieve the excited state.

Finally, carbon-based materials have once again proven their wide application in various fields and activities. Carbon nitride materials are one of the promising materials whose era is just beginning. g-C_3N_4-based materials, thanks to the abovementioned unique properties from which numerous detection methods for quantifying a wide range of analytes have emerged, have shown that they can be major components of bio-/immuno-/aptasensors and sensors generally. Therefore, wide applications of these materials in industrial/technological activities, food quality assessment, clinical diagnosis, and environmental assessment are inevitable.

References

Abdul Rasheed P, Radhakrishnan T, Nambiar SR et al (2017) Graphitic carbon nitride as immobilization platform for ssDNA in a genosensor. Sens Actuators B Chem 250:162–168

Barrio J, Volokh M, Shalom M (2020) Polymeric carbon nitrides and related metal-free materials for energy and environmental applications. J Mater Chem A 8:11075

Bellamkonda S, Shanmugamand R, Ranga Rao G (2019) Extending the π-electron conjugation in 2D planar graphitic carbon nitride: efficient charge separation for overall water splitting. J Mater Chem A 7:3757–3771

Cao HX, Wang L, Pan CG et al (2018) Aptamer based electrochemiluminescent determination of bisphenol A by using carboxylated graphitic carbon nitride. Microchim Acta 185:463–470

Chen L, Zeng X, Si P et al (2014) Gold nanoparticle-graphite-like C3N4 nanosheet nanohybrids used for electrochemiluminescent immunosensor. Anal Chem 86:4188–4195

Cheng C, Huang Y, Tian X et al (2012) Electrogenerated chemiluminescence behavior of graphite-like carbon nitride and its application in selective sensing Cu2+. Anal Chem 84:4754–4759

Eswaran M, Tsai PC, Wu MT et al (2021) Novel nano-engineered environmental sensor based on polymelamine/graphitic-carbon nitride nanohybrid material for sensitive and simultaneous monitoring of toxic heavy metals. J Hazard Mater 418:126267

Feng Y, Shi L, Wu H et al (2018) Detection of cyanide by etching-induced electrochemiluminescence recovery. Electrochim Acta 261:29–34

Fidan T, Torabfam M, Saleem Q et al (2021) Functionalized graphitic carbon nitrides for environmental and sensing applications. Adv Energy Sustain Res 2:2000073

Imran H, Vaishali K, Francy SA et al (2021a) Platinum and zinc oxide modified carbon nitride electrode as non-enzymatic highly selective and reusable electrochemical diabetic sensor in human blood. Bioelectrochemistry 137:107645

Imran H, Nagarajan Manikandan P, Dharuman V (2021b) Highly selective and rapid non-enzymatic glucose sensing at ultrathin layered Nb doped C_3N_4 for extended linearity range. Microchem J 160:105774

Jian X, Li Y, Zhao C et al (2020) Introducing graphitic carbon nitride nanosheets as supersandwich-type assembly on porous electrode for ultrasensitive electrochemiluminescence immunosensing. Anal Chim Acta 1097:62–70

Ju P, He Y, Wang M et al (2018) Enhanced peroxidase-like activity of MoS_2 quantum dots functionalized g-C_3N_4 nanosheets towards colorimetric detection of H_2O_2. Nano 8:976–992

Kulmala S, Kankare J (2013) CHEMILUMINESCENCE | Electrogenerated. In: Reference module in chemistry, molecular sciences and chemical engineering, vol 52. Elsevier, Netherlands, p 391

Kumar Shrestha B, Ahmad R, Shrestha S et al (2017) In situ synthesis of cylindrical spongy polypyrrole doped protonated graphitic carbon nitride for cholesterol sensing application. Biosens Bioelectron 94:686–693

Li C, Cao CB, Zhu H (2004) Graphitic carbon nitride thin films deposited by electrodeposition. Mater Lett 58:1903–1906

Li J, Wang H, Guo Z et al (2017) A “turn-off” fluorescent biosensor for the detection of mercury (II) based on graphite carbon nitride. Talanta 162:46–51

Li M, He B (2021) Ultrasensitive sandwich-type electrochemical biosensor based on octahedral gold nanoparticles modified poly (ethylenimine) functionalized graphitic carbon nitride nanosheets for the determination of sulfamethazine. Sens Actuators B: Chem 329:129158

Liu L, Wang M, Wang C (2018) In-situ synthesis of graphitic carbon nitride/iron oxide-copper composites and their application in the electrochemical detection of glucose. Electrochim Acta 265:275–283

Liu X, Zhang H, Song Z et al (2019a) A ratiometric nanoprobe for biosensing based on green fluorescent graphitic carbon nitride nanosheets as an internal reference and quenching platform. Biosens Bioelectron 129:118–123

Liu Z, Zhang X, Ge X et al (2019b) Electrochemiluminescence sensing platform for ultrasensitive DNA analysis based on resonance energy transfer between graphitic carbon nitride quantum dots and gold nanoparticles. Sens Actuators B: Chem 297:126790

Lotsch BV, Schnick W (2006) From Triazines to Heptazines: novel nonmetal tricyanomelaminates as precursors for graphitic carbon nitride materials. Chem Mater 18:1891–1900

Mandal D, Biswas S, Chowdhury A et al (2020) Utilizing 2D graphite carbon nitride for industrial applications – from supercapacitors to biosensors. Meet Abstr MA2020-01:821. https://doi.org/10.1149/MA2020-0110821mtgabs

Mohammad A, Ehtisham Khan M, Yoon T et al (2020) Na,O-co-doped-graphitic-carbon nitride (Na,O-g-C_3N_4) for nonenzymatic electrochemical sensing of hydrogen peroxide. Appl Surf Sci 525:146353

Montigaud H, Tanguy B, Demazeau G et al (2000) C_3N_4: dream or reality? Solvothermal synthesis as macroscopic samples of the C_3N_4 graphitic form. J Mater Sci 35:2547–2552

Nirbhaya V, Chauhan D, Jain R et al (2021) Nanostructured graphitic carbon nitride based ultrasensing electrochemical biosensor for food toxin detection. Bioelectrochemistry 139:107738

Puente-Santiago A, Rodríguez-Padrón D, Quan X et al (2019) Unprecedented wiring efficiency of sulfonated graphitic carbon nitride materials: toward high-performance amperometric recombinant CotA laccase biosensors. ACS Sustain Chem Eng 7:1474–1484

Qi H, Zhang C (2020) Electrogenerated chemiluminescence biosensing. Anal Chem 92:524–534

Radhakrishnan K, Sivanesan S, Panneerselvam P (2020) Turn-on fluorescence sensor based detection of heavy metal ion using carbon dots@graphitic-carbon nitride nanocomposite probe. J Photochem Photobiol A 389:112204

Richter MM (2004) Electrochemiluminescence (ECL). Chem Rev 104:3003–3036

Shirani M, Kalantari H, Khodayar MJ et al (2020) A novel strategy for detection of small molecules based on aptamer/gold nanoparticles/graphitic carbon nitride nanosheets as fluorescent biosensor. Talanta 219:121235

Tashkhourian J, Fatemeh Nami-Ana S, Shamsipur M (2018) A new bifunctional nanostructure based on two-dimensional nanolayered of Co(OH)2 exfoliated graphitic carbon nitride as a high performance enzyme-less glucose sensor: impedimetric and amperometric detection. Anal Chim Acta 1034:63–73

Tian J, Liu Q, Ge C et al (2013) Ultrathin graphitic carbon nitride nanosheets: a low-cost, green, and highly efficient electrocatalyst toward the reduction of hydrogen peroxide and its glucose biosensing application. Nanoscale 5:8921–8924

Vinoth S, Shalini Devi KS, Pandikumar A (2021) A comprehensive review on graphitic carbon nitride based electrochemical and biosensors for environmental and healthcare applications. Trends Anal Chem 140:116274

Wang B, Ye C, Zhong X et al (2016) Electrochemical biosensor for organophosphate pesticides and Huperzine-A detection based on Pd wormlike Nanochains/graphitic carbon nitride nanocomposites and acetylcholinesterase. Electroanalysis 28:304–311

Wang Y, Guo W, Jia N (2018) High-sensitivity electrochemiluminescence biosensor based on silver-carbon nitride for the detection of dopamine utilizing enhancement effects. Chem Electro Chem 5:3786–3792

Wang X, Qin L, Lin M et al (2019a) Fluorescent graphitic carbon nitride-based nanozymes with peroxidase-like activities for ratiometric biosensing. Anal Chem 91:10648–10656

Wang Y, Xia L, Wei C et al (2019b) Ultrasensitive photoelectrochemical microRNA biosensor based on doxorubicin sensitized graphitic carbon nitride assisted by a target-activated enzyme-free DNA walker. Chem Commun 55:13082

Wu Y, Chen Q, Liu S et al (2019a) Surface molecular imprinting on g-C_3N_4 photooxidative nanozyme for improved colorimetric biosensing. Chin Chem Lett 30:2186–2190

Wu N, Wang YT, Wang XY et al (2019b) Enhanced peroxidase-like activity of AuNPs loaded graphitic carbon nitride nanosheets for colorimetric biosensing. Anal Chim Acta 1091:69–75

Wu Q, Wang P, Yang X et al (2019c) Turn off-on electrochemiluminescence sensor based on MnO2/carboxylated graphitic carbon nitride nanocomposite for ultrasensitive L-cysteine detection. J Electrochem Soc 166:B994–B999

Xavier MM, Radhakrishnan Nair P, Suresh M (2019) Emerging trends in sensors based on carbon nitride materials. Analyst 144:1475–1491

Xiang MH, Liu JW, Li N et al (2016) A fluorescent graphitic carbon nitride nanosheet biosensor for highly sensitive, label-free detection of alkaline phosphatase. Nanoscale 8:4727–4732

Xiong M, Rong Q, Meng HM et al (2017) Two-dimensional graphitic carbon nitride nanosheets for biosensing applications. Biosens Bioelectron 89:212–223

Xu L, Duan W, Chen F et al (2020) A photoelectrochemical aptasensor for the determination of bisphenol A based on the Cu (I) modified graphitic carbon nitride. J Hazard Mater 400:123162

Zhang Z, Leinenweber K, Bauer M et al (2001) High-pressure bulk synthesis of crystalline $C_6N_9H_3{\cdot}HCl$: a novel C_3N_4 graphitic derivative. J Am Chem Soc 123:7788–7796

Zhang C, Hu F, Zhang H et al (2019) An electrochemiluminescence biosensor for the detection of soybean agglutinin based on carboxylated graphitic carbon nitride as luminophore. Anal Bioanal Chem 411:6049–6056

Zhao WW, Xu JJ, Chen HY (2014) Photoelectrochemical bioanalysis: the state of the art. Chem Soc Rev 44:729–741

Zhou D, Wang M, Dong J et al (2016) A novel electrochemical Immunosensor based on mesoporous graphitic carbon nitride for detection of subgroup J of avian Leukosis viruses. Electrochim Acta 205:95–101

Zhu J, Nie W, Wang Q et al (2018) In situ growth of copper oxide-graphite carbon nitride nanocomposites with peroxidase-mimicking activity for electrocatalytic and colorimetric detection of hydrogen peroxide. Carbon 129:29–37

Zou R, Teng X, Lin Y et al (2020) Graphitic carbon nitride-based nanocomposites electrochemiluminescence systems and their applications in biosensors. Trends Anal Chem 132:116054

Flexible Nanobiosensors in Biomolecular Detection and Point of Care Testing

9

Nimet Yildirim-Tirgil

Contents

1 Introduction 176
2 Nanobiosensors for Point of Care Testing 177
  2.1 Nanobiosensors Based on Electrochemistry 178
  2.2 Nanobiosensors with an Optical Component 179
  2.3 Nanobiosensors with High Mass Sensitivity 179
  2.4 Nanobiosensor with a Calorimetric Sensor 179
3 The Structure of Flexible Nanobiosensors 179
  3.1 Materials and Configurations 180
  3.2 Substrate Materials on Flexible Nanobiosensors 181
4 Fabrication Techniques for Flexible Biosensing Platforms 184
  4.1 Sputtering 184
  4.2 Lithography 186
  4.3 Printing 187
  4.4 Other Techniques 188
5 Current Applications of Flexible Nanobiosensors 188
  5.1 Nanobiosensors with a Wide Range of Flexibility for In Vitro Monitoring 188
  5.2 Flexible Nanobiosensors with Body-Attached Devices 191
6 Conclusion and Future Perspectives 192
References 193

Abstract

Nano-scaled analytical frameworks or nanobiosensors use nano-conjugated biological materials as a transducing mechanism to detect extremely small amounts of biological, chemical, or physical analytes. Wearable technology, particularly smart gadgets, is becoming increasingly popular, and they have much promise for use in wearable healthcare equipment like ECG monitoring watches and POCT systems. This feature might open the way for personalized diagnosis and analysis,

---

N. Yildirim-Tirgil (✉)
Biomedical Engineering, Faculty of Engineering and Natural Sciences, Ankara Yildirim Beyazit University, Ankara, Turkey
e-mail: nyildirimtirgil@ybu.edu.tr

© Springer Nature Singapore Pte Ltd. 2023

U. P. Azad, P. Chandra (eds.), *Handbook of Nanobioelectrochemistry*,
https://doi.org/10.1007/978-981-19-9437-1_9

allowing biosensors to achieve their main goal of identifying target molecules early, accurately, and individually. Many key qualities, such as remarkable flexibility and the capacity to transmit conductivity onto the flexible material, must be addressed to produce more flexible nanobiosensors. As a result, much research has gone into creating flexible conductive substrates with cutting-edge nanomaterials and manufacturing processes. Low conductivity, brittleness, and the challenge of achieving high flexibility and conductivity in materials should be addressed by inventing and researching novel substrates that combine conductivity and flexibility. This chapter covers a variety of flexible biosensor construction methodologies and flexible material structures. The reported flexible nanobiosensors are also divided and discussed in this chapter depending on the types of target molecules and the biosensors' operating environment. Flexible nanobiosensors for body-attached biosensors for direct and in vitro molecule monitoring are the two study domains, with the hope that these approaches will help overcome and address current constraints and barriers on POCT systems.

Keywords

Nanobiosensors · Flexible sensors · Point of Care Testing · Medical Diagnosis · Polymers

1 Introduction

Point of Care Testing (POCT) and diagnosis are utilized to increase the quality of life and minimize illness, hospitalization, and death linked to a sedentary lifestyle (Price 2001). Although POCT will never totally replace standard laboratory testing, it provides several benefits in patients' health monitoring. Benefits include reduced testing time, continuous monitoring of biomolecular indicators, early detection of emergencies, no requirement for specialists (Noah and Ndangili 2019), user-friendly application, and noninvasiveness measurement. Wearable sensor signals can evaluate personal health issues (Zarei 2017; Pandya et al. 2015). In ordinary life, wearable sensors might be utilized more than simply health monitoring (Daneshpour et al. 2016; Sheeparamatti et al. 2007). They are also used for fitness and sport (Zhang et al. 2009; Lyberopoulou et al. 2016), communications (e.g., human-machine interface) (Altintas 2017; Dahlin 2012), security, business, and lifestyle needs.

Portable and flexible nanobiosensors are becoming increasingly important and popular on POCT (Noah and Ndangili 2019; Zarei 2017). Nano-scaled analytical frameworks or nanobiosensors detect extremely minute quantities of biological, chemical, or physical analytes using nano-conjugated biological materials as a transducing mechanism. The structures apply electrochemical, optical, piezoelectric, thermometric, micromechanical, or magnetic techniques to communicate the needed evidence in signals (Fig. 9.1). The generated signals are based on the idea of the linked antibody or bioligands selectively biorecognizing intracellular or surface biomarkers associated with cancer cells.

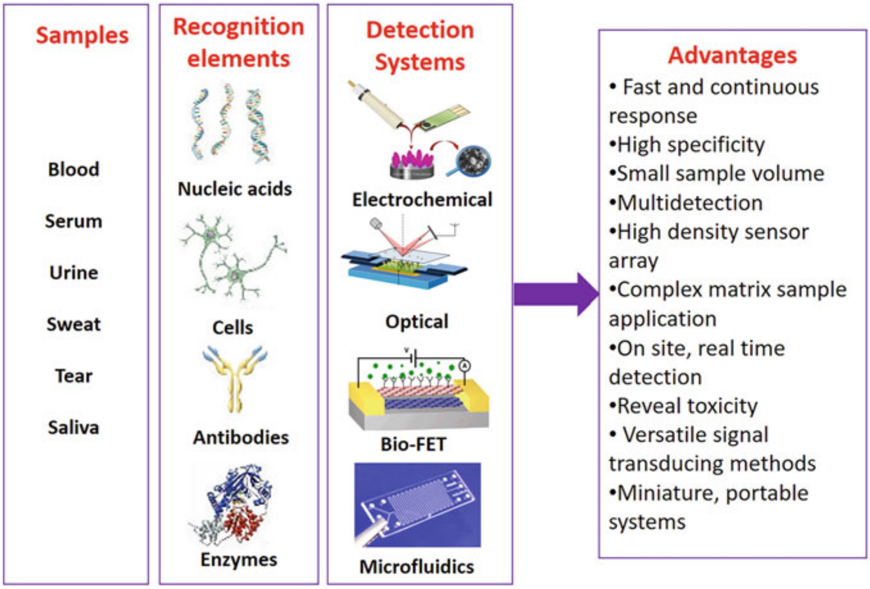
Samples
Blood
Serum
Urine
Sweat
Tear
Saliva
Recognition elements
Nucleic acids
Cells
Antibodies
Enzymes
Detection Systems
Electrochemical
Optical
Bio-FET
Microfluidics
Advantages
• Fast and continuous response
•High specificity
•Small sample volume
•Multidetection
•High density sensor array
•Complex matrix sample application
•On site, real time detection
•Reveal toxicity
• Versatile signal transducing methods
•Miniature, portable systems

Fig. 9.1 Nanobiosensor components include target samples, biorecognition elements, and such examples of transduction systems with their advantages in analyzing tools

Nanobiosensors that are portable and flexible offer several major advantages: (1) They are more user-friendly; (2) test results may be acquired immediately without having to wait a long time; (3) manufacturing costs are low, which advantages resource-constrained areas; and (4) more appropriate for the application, they may be applied to the skin to achieve more real-time sampling (Pandya et al. 2015; Daneshpour et al. 2016; Price 2001).

2 Nanobiosensors for Point of Care Testing

Nanotechnology is a branch of science that discovers the operation of substances at the molecular and atomic levels. It entails developing and using biological, chemical, and physical systems on a 1–100 nm scale. These materials, also known as nanomaterials or nanoparticles, are revolutionizing science due to their superior chemical, physical, and biological properties, compared to their bulk complements (Sheeparamatti et al. 2007; Zhang et al. 2009), and have a wider variety of applications, particularly in optical, biomedical, catalysis, medical imaging, and electronics (Lyberopoulou et al. 2016; Zhang et al. 2009). Because of their increased catalytic characteristics, electron transport, and ability to be employed in biomolecule labeling and adsorption, they are ideally suited for biosensing (Altintas 2017). Nanoparticles' unique physicochemical features have managed to invent biosensors, such as nanosensors for illness diagnostics at the point of care.

Biosensors established on nanotechnology have several advantages. The ever-intensifying discoveries in the field of nano-biotechnology-based sensors have produced tremendous technological momentum (Dahlin 2012; Patel et al. 2016), owing to the following benefits:

1. Biomarker identification and data creation that is quick, sensitive, and accurate.
2. Consolidation of traditional detection methods into a single platform.
3. Analysis that is user-friendly, simple, and cost-effective.
4. Test sample reduction for analysis.
5. Multiplexed data can be generated from a single test.
6. The constructions have high stability, repeatability, and portability.

Despite the advantages of nanobiosensors, there are several obstacles to their clinical use (Dahlin 2012; Quesada-González and Merkoçi 2018; Dincer et al. 2017). Here are a few examples:

1. Difficulty integrating result support services that can be observed and controlled by separate devices in POC systems.
2. Additional expenditures associated with the development of biosensors for diagnostics.
3. Developing a generally applicable diagnostic test is difficult because various cancer subtypes have diverse biomarkers.
4. Multiplexing complicates design and manufacture, test formulation, and clarification.
5. Stringent characterization parameters are required to offer meaningful information on nanomaterial storage, functionalization, modification, and usage.
6. Worldwide nanomaterial safety recommendations do not address the toxicological effects of nanomaterials.
7. Valid correlation with existing technology must be demonstrated.

Nano-scaled analytical structures or nanobiosensors detect extremely minute quantities of biological, chemical, or physical analytes using nano-conjugated biological materials as a transducing mechanism. To transfer the necessary data in the formula of signals, the structures utilize electrochemical, optical, thermometric, piezoelectric, magnetic, or micromechanical methods. Nanobiosensors may be classified based on their signal transduction method and biorecognition components. Targets interact with recognition components through these nano-contexts, recognizing a quantifiable or observable signal (Fig. 9.1). The kind of detected signals is used to characterize these biosensors further.

2.1 Nanobiosensors Based on Electrochemistry

The sensor molecules in electrochemical nanosensors are physically attached to the probe surface. A detectable electrochemical signal is generated when the probe interacts strongly and specifically with the target analyte. These sensors are the most well-known sensing systems because of their great stability, sensitivity, quick reaction, and small intrusions (Pandya et al. 2015; Hu et al. 2018; Chandra et al. 2012).

2.2 Nanobiosensors with an Optical Component

Luminescence, fluorescence, FRET (fluorescence resonance energy transfer), phosphorescence, absorption, refraction, and dispersion based detection systems are all used in optical nanobiosensors to provide single or multiplexed analyte detection. Spectroscopic methods identify differentiating features such as energy, amplitude, polarization, phase, or decay time (Han et al. 2017). According to recent articles, optical nanobiosensors may successfully detect cancer biomarkers such as cysteine and miRNAs (Wang et al. 2016; Yang et al. 2017).

2.3 Nanobiosensors with High Mass Sensitivity

These biosensors use micro- or nano-dimensional cantilevers to differentiate living species automatically. The shift in the resonance frequency of the unbound and biomolecule attached cantilevers due to mechanical stimulation shows the observed mass change. Acoustic piezoelectric crystal-based sensors are widely used in mass-sensitive nanobiosensors (Wang et al. 2020; Manjakkal et al. 2019).

2.4 Nanobiosensor with a Calorimetric Sensor

Calorimetric nanobiosensors are based on the energy generated in heat during diverse biological processes. The temperature change between before and after the solution enters and departs is measured with thermistors. Heat may be used as a marker for various biological processes, allowing for nondestructive metabolic evaluations of live cells (Nantaphol et al. 2017; Khan et al. 2014).

3 The Structure of Flexible Nanobiosensors

“Flexible” biosensors, like their “stiff” counterparts, are made up of three elements: (A) a substrate that acts as the system’s basic mechanical support; (B) bioreceptor (s) that has a specific interest in the analyte(s); and (C) active materials that, depending on the detection method, transduce the signal from the bioreceptor(s). The human operator, generally using software, then translates the signals corresponding to the parameter of interest into a readable interface. Figure 9.2 depicts the main substrate components of nanobiosensors, particularly in a flexible design. Figure 9.2 also depicts some of the regions where it is planned to be used. They indicate places that have previously been targeted to detect certain biochemical

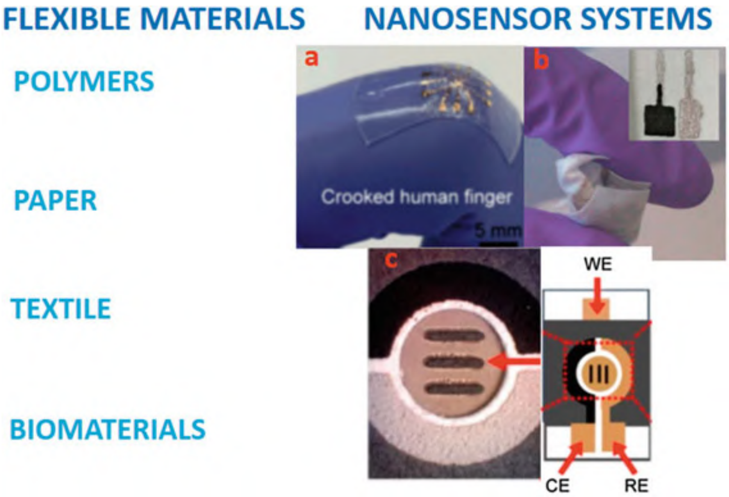

Fig. 9.2 The main substrate components of nanobiosensors, particularly in a flexible design, and some of the regions where they were previously used: (**a**) The stretchable biosensor can change the shape with the movement of the human body. (Adapted with permission from (Wang et al. 2020)); (**b**) the real picture of flexible and wrinkled pH sensor on cloth. (Reformed with permission from (Manjakkal et al. 2019)); (**c**) picture of the paper-based electrochemical device. (Adapted with permission from (Nantaphol et al. 2017). Copyright 2017 American Chemical Society)

targets or are being targeted. Mechanical flexibility, bendability, stretchability, thermal/chemical stability, transparency, biocompatibility, and biodegradability are just a few of the qualities that the substrate (A) must exhibit (Han et al. 2017; Yang et al. 2017; Wang et al. 2016).

It is worth noting that a single system can have one or more of these features, and all of them in many cases. The substrate (A) is the device's most important component, as it provides strong support, interacts with the surface, keeps the biosensor parts together, and guarantees that the device functions properly. The recognition (B) and transduction (C) elements must be combined on the substrate and stable and adaptive to the same mechanical conformations without delaminating or removing due to deformation. The following part covers the materials and fabrication/design principles used in flexible nanosensors.

3.1 Materials and Configurations

One of the most important processes in device manufacture is selecting the substrate, which serves as the basis for the biosensor. The qualities and functions result from the substrate's ability to sustain them (Khan et al. 2014; Windmiller and Wang 2013). By explanation, mechanical elasticity is a significant characteristic because it allows analytes and sensing/transducing components to interact more efficiently by adapting to the physical dynamics of essentially nonrigid and frequently nonlinear settings. For example, a substrate that adheres better to the surface's contours is more probable to offer a broad interaction area for collecting samples such as physiological liquids. While such devices are principally intended to extend the range of biomolecular recognition, they can be utilized for other applications (e.g., medication administration) (Wang et al. 2016).

Material selection may be influenced by the intended use location (e.g., external or internal location on the biological system). Some of the instances of location-based demands put on flexible devices are shown in Fig. 9.2. Surface conformability is affected by mechanical deformations. Bendability, conformability, stretchability, and wear resistance. Fracture resistance is frequently imparted using two methods: (1) use rigid conductive or semiconductive materials with specific geometrical or structural designs to impart flexibility, or (2) use stiff conductive or semiconductive materials with specific structural or geometrical designs to impart flexibility (e.g., twisting or wave patterns). While some materials and procedures discussed below were created for larger flexible devices, they represent basic design perceptions that may be adapted to flexible biosensors or have already been done. First, we will go over some of the features of mostly used flexible substrate materials.

3.2 Substrate Materials on Flexible Nanobiosensors

3.2.1 Synthetic Polymers

Because of their versatility and processability, synthetic polymers have become one of the greatest widely used substrates, enabling the creation of flexible designs and low prices with high efficiency. Some of the well-studied polymers used to produce flexible substrates utilized in bioanalysis systems include polyimide (PI,) polyethylene terephthalate (PET), polyethylene naphthalate (PEN), and polydimethylsiloxane (PDMS) (Lau et al. 2013; Liao et al. 2015; Segev-Bar et al. 2013). PET is an artificial polyester fiber extensively used in plastic bottles, clothes, and as an electrical insulator (Reddish 1950). Because of its thermal stability, mechanical properties, inertness, and low price, it is a feasible alternative to silicon-based materials. The polymer is routinely pressed into ultratiny films to provide high-interaction surfaces, optically transparent, that offer flexibility and adaptability to various shapes and configurations (MacDonald 2004). PEN (also known as Teonex®) is an artificial polyester with increased intrinsic properties (hydrolytic and chemical resistance, thermooxidative and thermal resistance, and UV resistance), which makes it appropriate for use as a plastic substrate (Murakami et al. 1995). PEN has superior optical transparency and an oxygen barrier in optical devices, providing it an advantage. Although PEN is stiffer than PET, its inherent bendability allows it to be flexible (Barlow et al. 2002; Lechat et al. 2006).

Screen printing technology has prepared it simpler to create ultrathin microelectrodes and additional micro contact devices, increasing their application (Mościcki et al. 2017). Polyimides (PI) are flexible polymer fibers that can easily bend, mold, and fold and are widely utilized in industrial applications (Kapton® is one commercially accessible version). They exhibit excellent dielectric, structural, thermal stability, and dynamic tensile strength. These materials are versatile and easy, and they may be used for various purposes. Metal deposited PIs can increase conductivity, and photo-sensitive PIs have been created (Liaw et al. 2012). In bioelectronics, thin-film and double-layer films have been employed as substrates for fuel cells, brain implants, and other devices (Xiao et al. 2008; Lee et al. 2004).

PDMS (polydimethylsiloxane) is a silicone-based elastomer widely used in soft lithography and microfluidics (Qin et al. 2010). PDMS is used in various biomedical devices, including catheters, cartilage implants, and membrane oxygenators. PDMS devices' low cost, thermal stability, chemical inertness, and oxygen permeability have aided their rapid acceptance (Mata et al. 2005). PDMS is preferred as a flexible substrate above most other polymer-based flexible substrates because of its high elasticity, low modulus, and optical transparency. Because it is oxygen permeable, nontoxic, and biocompatible, it is suitable for in vitro and in vivo applications (Patrito et al. 2007). Other nanomaterials and nanoparticles can be combined with PDMS to make multifaceted structures such as implantable electrodes (SadAbadi et al. 2013) and lab-on-a-chip (Klemic et al. 2002).

3.2.2 Paper

Paper is an esthetically appealing and cost-effective semisynthetic/seminatural substrate for generating rapid POC diagnostics, principally in weak-facilities environments. Paper is adaptable, widespread, and simple to use (Chinnasamy et al. 2014; Martinez et al. 2010). It is commonly employed as a device substrate, either alone or with paper-based structures. Paper substrates may accept various sensing modalities when detecting biotargets, including optical, electrochemical, and electrical (Parolo and Merkoçi 2013; Qiu et al. 2017). Reduce the thickness of cellulose fibers from cm to nm, for example, to obtain optical transparency in the paper (Yao et al. 2017). Paper may be easily molded into composites because of its low weight and porous composition. Paper-based electrodes with multilayer topologies may now be manufactured more easily using screen-printing, nanopatterning, inkjet printing, and other processing methods (Siegel et al. 2010). Because paper absorbs by capillary action, it may be utilized to make lateral flow assays like pregnancy test strips for detecting human chorionic gonadotrophin (Choi et al. 2016). For example, there has been interest in creating quick nucleic acid testing paper tests (Ngom et al. 2010).

While individual cellulose strands may be easily manipulated to change the mechanical characteristics of paper, they can also be delicate and prone to ripping, with limited stability in moist settings. The bioactive paper has been proposed as a composite of paper and other biomaterials. Strengthening polymers such as polyamide-epichlorohydrin and/or glyoxalated polyacrylamides (GPAM) can be used to make cellulose fibers and nanofibers (CNFs) have a stronger and longer-lasting wet-strength impact (PAE) (Pelton 2009). Because cellulose does not break down naturally, efforts to create more biodegradable cellulose fibers have been developed (Jung et al. 2015). Because it is a synthetic material with poor conductivity, biomolecule labeling and doping with metal oxides or conducting polymers are typically required to provide electrochemical capabilities (Pelton 2009).

3.2.3 Textiles and Fibers

To provide strong support for the active sensing region, textiles can be manufactured as filaments (1D), woven, knitted, or shaped into various 2D structures (Stoppa and Chiolerio 2014; Windmiller and Wang 2013). Because of their natural flexibility, durability, and stability, wool, cotton, and synthetics (polyester, nylon, etc.) are excellent possibilities. Various manufacturing procedures can be used to mix textile substrates with conductive materials. To make conductive filaments, fabrics have been immersed in or drop-coated onto conductive polymers (Ding et al. 2010). Textiles can also produce conductive strands (Akşit et al. 2009). Lightweight, convenient, integrated functions, low cost, simple operation, and real-time display are just some of the benefits of migrated electrochemical/electrical structures on textile substrates, bridging the gap among influential electroanalytical devices and meeting the demands of daily, even dense usage.

Stability throughout long wash cycles is also a concern when using wearable clothing. The creation of textile-based carbon electrodes (TCEs) on the flexible waistband of clothes was prepared by screen-printing carbon-based ink deposited by thermal curing (Yang et al. 2010). These electrodes can withstand much mechanical stress without breaking or peeling. The TCEs' electrochemical performance was outstanding despite repeated stretching or bending, and they could sense 0–25 mM H2O2 and 0–100 M NADH for glucose detecting on sweat samples. Conductive fabrics have been used to manufacture transistors and traditional electrochemical biosensors. PEDOT: PSS was screen-printed on a textile substrate to create flexible TCEs (Gualandi et al. 2016).

3.2.4 Metals

Flexible substrates have also been made using thin metallic foils. While they can benefit biosensors, their application in conventional electronics has been more prevalent (Huang et al. 2011). Metal foils (made of titanium, stainless steel, copper, and molybdenum) can provide great thermal strength for roll-to-roll processing with a depth of 0.05 mm or less (Liao et al. 2012). The foils may readily bend at this point while still delivering the improved conductivity associated with metal substrates (Qu et al. 2001). Furthermore, flexible foil substrates are beneficial because they may be manufactured to any size while allowing for functionality tuning by stacking or depositing additional metals (Mathew et al. 2003). Metallic foils have shown potential as thin-film and solar cell transistor substrates, notwithstanding their scarcity in producing flexible biosensors (Howell et al. 2000; Park et al. 2003). External bending and compression are more robust to metallic foil substrates than stretched substrates (Gleskova et al. 2002). Metallic foils as flexible biosensor substrates have obvious limitations. Metallic foils are more expensive to manufacture than plastic foil materials such as PI or PEN.

The deposition of practical electronic designs on metallic foil materials is a high-temperature procedure. These approaches are generally incompatible with sensitive bioreceptor molecules and are energy and time-intensive (Howell et al. 2000). External bending and compression are more robust to metallic foil substrates than stretched substrates (Gleskova et al. 2002). Metallic foils as flexible biosensor substrates have obvious limitations. To begin with, metallic foils are more expensive to manufacture than plastic foil substrates such as PI or PEN.

3.2.5 Biomaterials

Biomaterials (sometimes called biobased materials) are made from reusable sources. Biomaterials are created through bioprocessing, biosynthesis, and biological refinement from basic materials such as legumes (Voisin et al. 2014), grains (Diouf-Lewis et al. 2017), bamboo powder (Hsieh et al. 2006), straw (Paranthaman et al. 2009), and other rare materials (Nair and Laurencin 2007; Kumar et al. 2018; Stagner 2016; Rivas et al. 2016). Polymer materials are used in almost every aspect of people's life.

However, excluding natural plastics/rubber and a few other materials, most polymer resources rely extensively on fossil fuels (coal and mostly oil), resulting in major pollution, human health issues, and environmental damage (Brunner and Rechberger 2016). Polymers that are both environmentally friendly and sustainable have become more important in preserving fossil energy and decreasing greenhouse gas emissions. Many attempts to make biodegradable materials with biobased components have been made (Sheldon 2014; Ummartyotin and Pechyen 2016).

Chemically manufactured biomaterials include the following: Agricultural feedstock such as potatoes, maize, and other carbohydrate feedstock was used to make the first generation of biobased polymers. Another form of biomaterial is natural biopolymers, such as nucleic acids, proteins, and polysaccharides (chitin, cellulose). Chemical synthesis may also be used to make biodegradable polymers like polyhydroxyalkanoates (PHAs), polyurethanes (PUs), polylactic acid (PLA), and polydopamine (PDA).

4 Fabrication Techniques for Flexible Biosensing Platforms

Nanobiosensors technologies have piqued attention in recent decades to track one's health in real time. However, many of these gadgets still lack significant flexibility, size, and comfortability because of a lack of logical design and production procedures. It is necessary to build next-generation integrated nanobiosensing systems with needed flexibility and downsizing for improved devices. The main fabrication techniques for the flexible nanoobiosensors are detailed below.

4.1 Sputtering

While nanobiosensors must meet various requirements, imparting conductivity is the greatest critical improvement on behalf of the deployment of electrochemical flexible biosensors. Sputtering conductive metals over nonconductive flexible substrates is one of the many techniques to impart conductivity. It can be a quick, straightforward, and operative approach to producing an electrochemical biosensor system. The development of conductive layers is dependent on physical processes in the sputtering process. In particular, conductive metal layers over nonconductive substrates can be uniformly generated by removing metal elements from metal targets' surfaces and blasting them onto the substrate surface using plasma or gas energetic particles (Libansky et al. 2017; Baptista et al. 2018). This technology has been used to create a tinny metallic conductive layer in numerous disciplines, including electrode creation and biosensor development (Hallot et al. 2018; Rahmanian et al. 2018). Sputtering has also been utilized to build high-conductivity electrochemical biosensors by deposition of new metals on the electrode and these applications (Roditi et al. 2019).

Sputtering has been utilized in various studies to build flexible nanobiosensors because it is easier to employ than other methods for producing conductive layers. Sputtering indium oxide (In_2O_3) on a PET substrate was allegedly used to create a very sensitive and flexible electrochemical biosensor for monitoring glucose levels in body liquids (Fig. 9.3a). The additional study employed the sputtering procedure

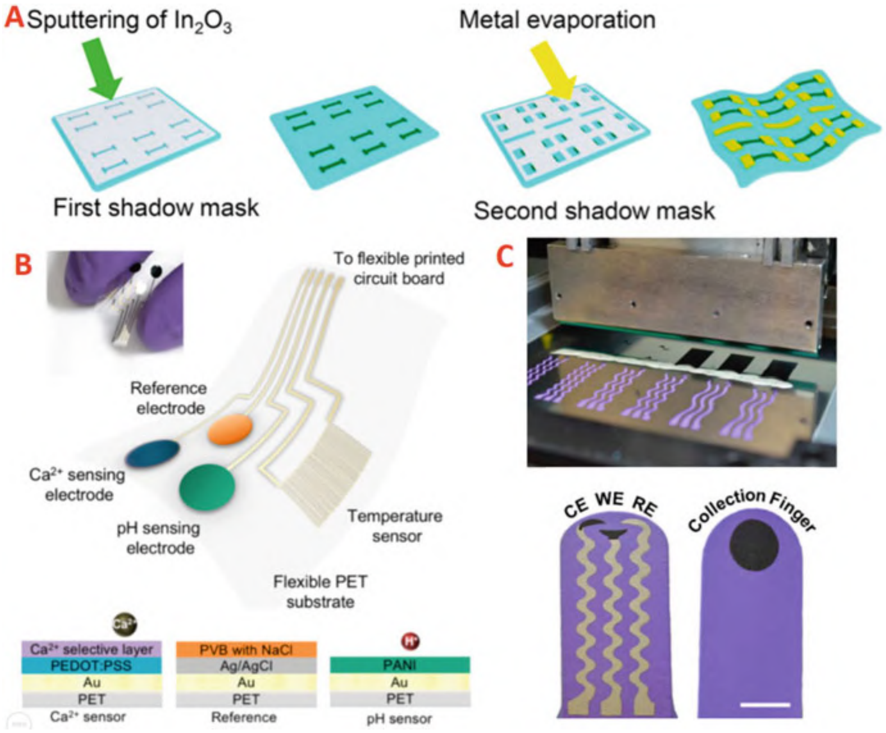
A
Sputtering of In_2O_3
Metal evaporation
First shadow mask
Second shadow mask
B
To flexible printed circuit board
Reference electrode
Ca^{2+} sensing electrode
pH sensing electrode
Temperature sensor
Flexible PET substrate
Ca^{2+}
Ca^{2+} selective layer
PEDOT:PSS
Au
PET
Ca^{2+} sensor
PVB with NaCl
Ag/AgCl
Au
PET
Reference
H^+
PANI
Au
PET
pH sensor
C
CE WE RE
Collection Finger

Fig. 9.3 Flexible nanoobiosensor fabrication techniques: (**a**) a schematic depiction of In2O3 sputtering on PET. (Adapted with permission from (Liu et al. 2018). Copyright 2018 American Chemical Society); (**b**) a diagram representation of a flexible biosensor produced by photolithography for observing various targets covering pH, ions, and temperature. (Adapted with permission from (Nyein et al. 2016). Copyright 2018 American Chemical Society); and (**c**) using printing technique to make a flexible glove biosensor with a three-electrode setup. (Adapted with permission from (Mishra et al. 2017). Copyright 2017 American Chemical Society, further permissions related to the material excerpted should be directed to the ACS)

to cover a flexible PET substrate with nickel oxide (NiO) to develop a flexible lactate biosensor evaluated using a potentiometric device (Chou et al. 2018). Choi et al. employed metal sputtering on nonconductive polymer material while introducing original nanostructures (i.e., MoS_2 nanoparticles). To enhance the electron transfer process and generate a highly sensitive biosensor system to detect HIV-1 surface protein and glucose, the researchers constructed a sandwich assembly consisting of sputtered gold coatings and a spin-coated MoS_2 layer positioned among the sputtered gold films (Yoon et al. 2019). However, the sputtering technique has drawbacks when introducing three- or two-electrode structures made up of reference or counter electrodes on conductive and flexible electrodes.

More innovative approaches for the direct usage of electrode structures on flexible materials are needed to develop flexible electrochemical biosensors that can be used in wearable devices, even if they are not as practical and simple as the sputtering approach.

4.2 Lithography

Finer techniques capable of exquisitely granting conductivity on flexible substrates beyond the nonspecific deposition that results from sputtering are required to establish an electrochemical system directly on flexible substrates or to develop multiple-target monitoring systems on a miniaturized chip. One example of such implementations is advanced conductive nano-electrodes (Smith 1986). The lithography technique, widely utilized for silicon-based electronic devices, fits the characteristics listed above (Barcelo and Li 2016). Photolithography is a contemporary lithography technique that employs a photo-sensitive photoresistor that may be imprinted on a substrate using a predesigned photomask and laser exposure. This approach might be used, for example, to make tiny conductive electrodes on flexible substrates.

Furthermore, employing an electrochemical structure constructed on a flexible material using the photolithography approach, a flexible multiple-target detecting system was described to observe pH changes and temperature simultaneously (Fig. 9.3b) (Nyein et al. 2016). Other lithography methods, like soft lithography, electrochemical lithography, or electron-beam lithography are frequently used in addition to photolithography to construct flexible nanobiosensors (Chen 2015). Flexible silver nanowire films created by soft lithography, for example, have been proposed for hydrogen peroxide (H_2O_2) detection (Lee et al. 2016; Zhang et al. 2017). Lithography technologies have been employed to construct intricate electrochemical flexible biosensors with completely joined electrochemical systems or biosensors accomplished by concurrently distinguishing several targets, similar to the experiments detailed above.

Although sensitive lithography methods are among the most efficient tools for building electrochemical flexible biosensors that can sense many targets or produce a completely integrated circuit system, they have downsides such as expensive equipment, difficult processes, and high expenses. As a result, processes for producing adaptable electrochemical biosensors that are reasonably inexpensive, simpler, and more accessible are required. As a result, several studies are being conducted, containing the use of current lithography procedures such as etching inkjet maskless lithography (E-IML) and salt impregnated inkjet maskless lithography (SIIML), to reimburse for lithographic techniques' boundaries and increase their performance, allowing the development of extremely well-organized flexible nanobiosensors (Hondred et al. 2019, 2020).

4.3 Printing

Due to its capacity to effectively construct gentle structures on any substrate by covering any chemical in the solution, printing has also benefited from widespread adoption because of its accessibility (Parameswaran and Gupta 2019). Many printing methods have commenced being applied in medicine and biology, notably in biosensors, as spraying sophistication and printing velocity improve. Printing technology has been utilized to construct various biosensors due to its ability to appropriately print biomolecules and new nanomaterials on substrates to build functional and biocompatible coatings to improve compact biosensors. Printed microfluidic-based bioanalysis devices, for example, have been created by printing (e.g., inkjet printing) polymer layers on surfaces (Loo et al. 2019; Ali et al. 2018).

The benefits of printing technologies, in particular, allow for fine control of the conductive substrate structure, which is essential for the construction of electrochemical flexible biosensors. Many biomaterials and unique conductive nanomaterials may be printed on flexible surfaces to provide conductivity or construct electrochemical systems (e.g., paper-based substrates). In one work, SNP ink was used to print silver inter-digital electrodes on a PET material via an inkjet printer for pathogen detection (Ali et al. 2018). A flexible enzymatic biosensor was developed in another investigation for simultaneous glucose observing (Pu et al. 2018).

Furthermore, printing is a low-cost way of generating reusable paper-based biosensors for POCT, lately involving much interest in the biosensor business (Arduini et al. 2019; Cao et al. 2020). In addition to paper-based biosensors, wearable lab-on-a-glove structures have been built using three-electrode systems: the counter, working, and reference electrodes on flexible gloves (Fig. 9.3c) (Barfidokht et al. 2019). Furthermore, 3D printing has recently attracted much interest as a breakthrough new-generation production technique. In biology, 3D printing has much potential for various applications, containing tissue engineering (Patra and Young 2016), because of its exceptional capability to build precise biological assemblies such as three-dimensional synthetic organs or tissues. These benefits of 3D printing might be leveraged to create flexible electrochemical biosensors (Sharafeldin et al. 2018).

4.4 Other Techniques

There are other efficient and inventive ways to build flexible electrochemical biosensors in addition to the three fundamental manufacturing procedures listed above; however, they are not as extensively utilized as the approaches listed above. Using metal ion solutions and basic electrochemical procedures, electrodeposition is a common approach for producing highly conductive films on superficial semiconductive or conductive surfaces. To make an ultrasensitive glucose biosensor, electrodeposition of platinum nanoparticles was used on a flexible graphene-modified PI substrate.

Electrospinning has also been utilized on several substrates to create patterned polymer membranes. Flexible polysulfone fiber mats were made by combining this technology with spray-based layer-by-layer deposition processes. A CNT-based conductive film was generated on these flexible rugs to develop a biosensor system (Saetia et al. 2014). An additional recent study (Cho et al. 2015) described producing biosensor devices employing a high-rate nanoscale offset printing procedure with guided nanomaterial assembly and transfer. By adjusting assembly settings, SWCNTs were formed at the required places with good homogeneity and controlled high density, resulting in a more stable and reusable biosensor device. They overcame some challenges connected with nanosensors, including unstable, non-reproducible detecting ability because of the unpredictable and chaotic SWCNTs assembly arrangement and the high price and difficult CVD construction technique. To make this platform, electrospinning was employed for polyacrylonitrile (PAN) nanofibers, subsequently carbonized. Chemical vapor deposition (CVD) and electrochemical/mechanical exfoliation are two additional novel ways to build flexible biosensors that have been effective (Luo et al. 2020; Zhang et al. 2019).

5 Current Applications of Flexible Nanobiosensors

Many electrochemical flexible biosensors have been built and published using the unique materials and manufacturing processes represented in this chapter. This chapter divides and discusses the reported flexible nanobiosensors based on the sorts of target molecules and the biosensors' working environment. The two research fields are flexible nanobiosensors for body-attached biosensors for direct and in vitro molecule monitoring.

5.1 Nanobiosensors with a Wide Range of Flexibility for In Vitro Monitoring

Flexible nanobiosensor research's ultimate objective is to be used in the creation of wearable biosensors. When using wearable biosensors to directly observe target molecules on the body, it is important to select target molecules and compensate for the biosensor's high sensitivity by removing noise signals from the environment and other undesirable molecules. As a result, current flexible nanobiosensor research focuses on improving selectivity and sensitivity while maintaining flexibility and stability under various physical situations. Small biological molecules that may affect health (e.g., lactate and glucose) and are linked to certain illnesses are the major target molecules of flexible nanobiosensors. Although many in vivo measurable glucose biosensors have progressed to the point that they are no longer required, flexible glucose biosensors for real-time observing glucose levels in the body to avoid diabetes mellitus are still required. As a result, a series of flexible glucose biosensors (Anusha et al. 2018; Pu et al. 2018) have recently been revealed. Choi et al. employed MoS_2 nanoparticles to procedure a sandwich assembly of MoS_2/gold/gold nanofilms on a PI material to greatly increase the sensitivity of flexible biosensors (Yoon et al. 2019). Sputtering was employed to construct the sandwich structural film quickly and effectively, resulting in gold films and a spin-coating MoS_2 coating (Fig. 9.4a). The developed flexible biosensor has outstanding glucose detection capabilities (detection limit: 10 nM), great selectivity, and the capacity to maintain its structure and function even after being bent repeatedly.

Furthermore, electrochemical flexible glucose biosensors based on graphene and carbon nanomaterials such as CNT have recently been produced (Bandodkar et al. 2016; Yoon et al. 2020) by utilizing the extremely conductive features of these carbon nanomaterials. Flexible nanobiosensors based on hybrid nanomaterials, including 3D porous graphene and platinum nanoparticles were also created to simultaneously monitor many targets (such as pH, electrocardiographic signals, and glucose), which might be used to create wearable smart devices (Xuan et al. 2018). To create this integrated system, the graphene nanowall-modified copper foil was created on the PET material using the CVD process, and the three-electrode system was printed straight on the flexible material. The recently constructed lactate biosensor displayed exceptional resiliency even after twisting and bending.

Additionally, it is claimed that a flexible alcohol nanobiosensor has been deployed in various contexts (Cinti et al. 2017). This biosensor can even differentiate among different beers' alcohol levels with its high sensitivity. Most research has focused on glucose and lactate as target molecules for electrochemical flexible biosensors because these substances are easily accessible and can be observed on the body via a wearable biosensor, which is the long-term objective of electrochemical flexible biosensors. However, there have recently been attempts to progress electrochemical flexible biosensors for in vitro observing of other chemicals, which might widen the target molecules' wearable biosensors in the future.

Electrochemical flexible biosensors may also be used to observe the states of live cells in vitro, and these investigations detect other target chemicals. Living cells are influenced by their surroundings, including the microenvironment and niches, which affect cell-substrate interactions and the chemicals produced by affected cells. Some researchers have used electrochemical flexible systems to analyze cell-secreted chemicals, including the cytokine tumor necrosis factor-a (TNF-a) and dopamine (Kim et al. 2019; Park et al. 2019). A flexible conductive PANI/PVAN bilayer-modified bacterial cellulose film was recently used to detect the release of neurotransmitters by neural stem cells cultured on a flexible material during differentiation

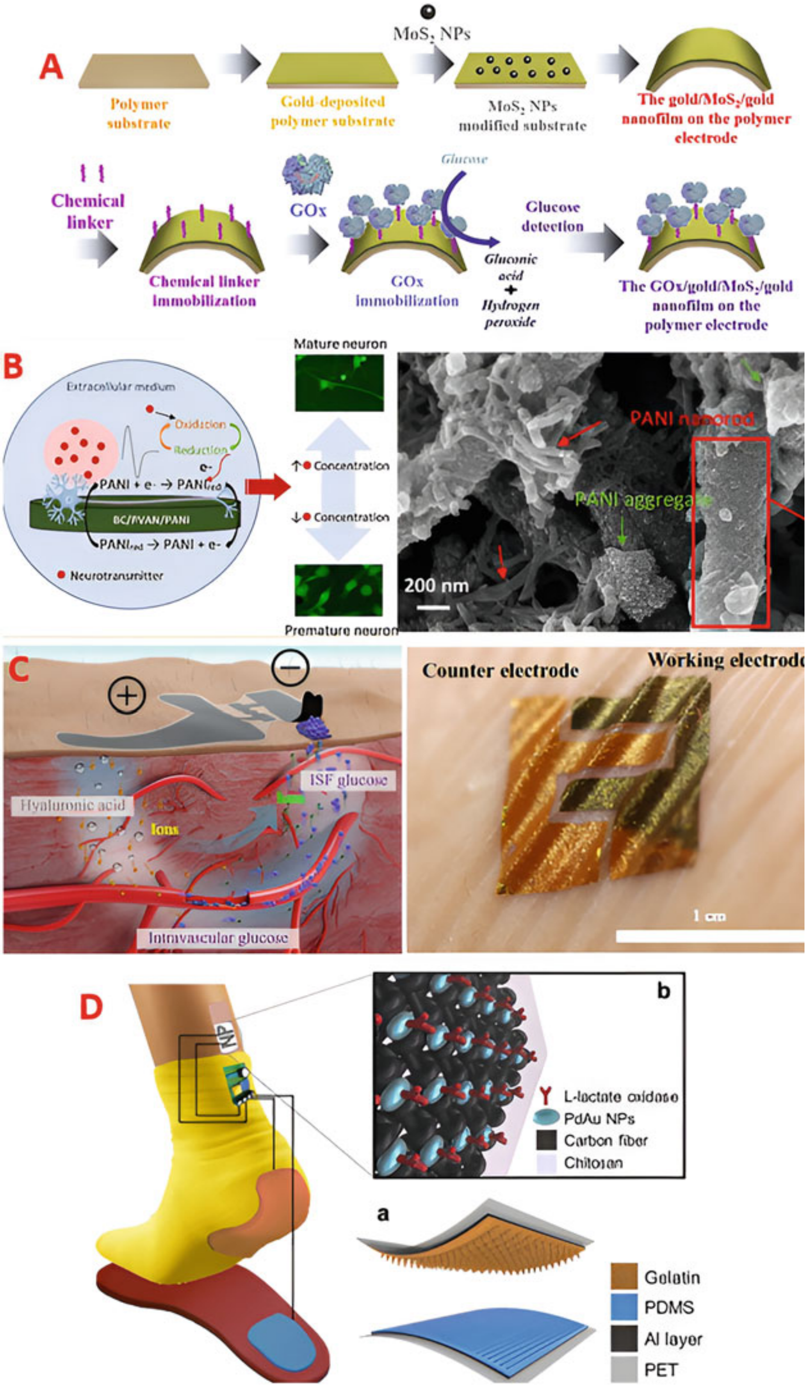
A
Polymer substrate
Gold-deposited polymer substrate
MoS_2 NPs
MoS_2 NPs modified substrate
The gold/MoS_2/gold nanofilm on the polymer electrode
Chemical linker
Chemical linker immobilization
GOx
GOx immobilization
Glucose
Gluconic acid + Hydrogen peroxide
Glucose detection
The GOx/gold/MoS_2/gold nanofilm on the polymer electrode
B
Extracellular medium
Oxidation
Reduction
e-
PANI + e- → $PANI_{red}$
BC/PVAN/PANI
$PANI_{red}$ → PANI + e-
Neurotransmitter
Mature neuron
↑● Concentration
↓● Concentration
Premature neuron
PANI nanorod
PANI aggregate
200 nm
C
+
−
Hyaluronic acid
Ions
ISF glucose
Intravascular glucose
Counter electrode
Working electrode
1 cm
D
NP
b
L-lactate oxidase
PdAu NPs
Carbon fiber
Chitosan
a
Gelatin
PDMS
Al layer
PET

Fig. 9.4 (**a**) The glucose-detecting capabilities of the suggested flexible nanobiosensor from ref., as well as the fabrication technique of a glucose biosensor based on a sandwich assembly of gold/

(Rebelo et al. 2019). The differentiation of brain stem cells was electrochemically measured straight on the flexible biosensor due to its dual monitoring and cell development (Fig. 9.4b). Many studies on flexible nanobiosensors are underway, intending to lay the framework for developing extremely sensitive wearable biosensing devices.

Another recent study developed a sensitive electrochemical nanobiosensor for diagnosing Invasive Aspergillosis (IA) by detecting the pathogenic glip target gene (glip-T) in a miniaturized experimental setup. 1,6-Hexanedithiol and chitosan stabilized gold nanoparticle-mediated self-assembly of glip probes (glip-P) on gold electrodes were used to make the sensor probe. UV-visible spectroscopy, cyclic voltammetry, and electrochemical impedance spectroscopy were used to characterize it (Bhatnagar et al. 2018).

5.2 Flexible Nanobiosensors with Body-Attached Devices

A few cases have only described flexible nanobiosensors that sense objective molecules straight on the body. Flexible biosensors that are biocompatible and noninvasive and may be attached directly to the body are required. Furthermore, monitoring target molecules in physiological fluids, including blood, tears, and sweat, necessitates a high level of sensitivity. As a result, biosensors have been integrated into particular wearable structures such as mouthguards, wristbands, gloves, and adhesive plasters that may be readily connected to the body while maintaining biocompatibility and high sensitivity (Kim et al. 2015).

A disposable and wearable glove-shaped electrochemical biosensor for detecting synthetic opioids and fentanyl was developed by one research group. Using 3D-printed molds, the researchers developed a three-electrode system on the glove-shaped material. They then created a three-electrode system with a working electrode (carbon ink layer), a counter electrode (carbon ink layer), and a reference electrode (Ag/AgCl ink layer) using screen-printing technology (Mishra et al. 2017).

A composite nanomaterial comprised of ionic solution (IL, 4-(3-butyl-1-imidazolio)-1-butanesulfonate), polyethyleneimine (PEI), and carbon nanotubes (CNT) was produced over the working electrode to improve the biosensor's sensitivity. The developed biosensor successfully detected fentanyl in a timely and

◀

Fig. 9.4 (continued) MoS_2/gold nanofilms on a PI material utilizing spin-coating and sputtering methods. (Reprinted from (Yoon et al. 2019), Copyright (2019), with permission from Elsevier.); (**b**) conductive PANI/PVAN bilayer-modified flexible bacterial cellulose sheet for observing neurotransmitters generated by neural stem cells throughout stem cell separation, and fluorescent photographs of segregated cells created on flexible materials. (Reprinted (adapted) with permission from (Rebelo et al. 2019). Copyright 2019 American Chemical Society.); (**c**) a diagram of the ETC system for blood glucose observing, as well as a photograph of the created wearable biosensor on the body (Y. Chen et al. 2017b); and (**d**) schematic pictures of a self-powered electrochemical lactate nanobiosensor from ref., which is made up of two separate flexible systems (one for lactate detection and other for energy harvesting). (Reprinted from (C.-H. Chen et al. 2017a). Copyright (2017), with permission from Elsevier) efficient manner (detection limit: 10 mM). A lactate nanobiosensor made up of the two devices stated above displayed good lactate detection capacity using the energy supplied by physiological action. This self-powered nanosensor system is a novel technique to create compact, wearable sensing devices that can run for long periods, are biocompatible, and do not require external power (C.-H. Chen et al. 2017a). To establish this new system, the authors created two flexible electrochemical systems: one made of PDMS, an aluminum, and gelatin film on a PET material to produce biochemical energy from human running or walking when worn straight on foot, and another made of LOx, carbon fibers, Pd/Au bimetallic nanoparticles, and chitosan for lactate sensing coupled to an energy-harvesting system (Fig. 9.4c).

Furthermore, tattoo-style wearable biosensors can be used to observe important bioindicators in real time (Mishra et al. 2018; Jia et al. 2013). Patch-shaped or bandage electrochemical wearable biosensors that can be straight and noninvasively implanted at any place on the body are the most actively explored among the many types of structures used in wearable devices in the current study (Imani et al. 2016; Bariya et al. 2018). Wearable nanobiosensors based on electrochemical twin channels (ETC) were employed to detect blood glucose noninvasively (Y. Chen et al. 2017b). Prussian blue, GOx, gold, poly(methyl methacrylate) (PMMA), and PI were used to make this biosensor. Intravascular blood glucose might be pushed out of the vessel and dejected to the skin's surface, where the biosensor was worn, piercing hyaluronic acid and enduring glucose refiltration and external conveyance, using the proposed ETC system (Fig. 9.4d). This biosensor offered an attractive solution for nonstop glucose observing for noninvasive medical claims based on the properties of this ETC system, which included glucose transit and noninvasive sensitivity detection. Modified microneedle sensors on the bandage-shaped biosensor were constructed to sense tyrosinase, a cancer-based target molecule linked to melanoma (Ciui et al. 2018).

In recent work, the researchers produced a new nanocomposite containing Au-nanorattles-reduced graphene oxide for the label-free detection of serotonin using a glassy carbon probe electrode device. In addition, the probe was utilized to determine serotonin in standard settings, including dose-dependent research and analytical results produced using differential pulse voltammetry (DPV). The probe's practical implications were investigated using the spike and recovery approach in serum, urine, and in vitro cell samples (Mahato et al. 2019).

6 Conclusion and Future Perspectives

Flexible nanobiosensing technologies have shown to be a significant step forward in developing next-generation analytical tools. Given the growing popularity of wearable technology, particularly smart devices, they offer much potential for usage in wearable healthcare devices like electrocardiogram monitoring watches and POCT systems. This capability might pave the way for individualized diagnosis and analysis, allowing biosensors to meet their primary aim of detecting target molecules early, precisely, and individually.

Because they encounter all of the conditions for flexible biosensor improvement, electrochemical methods are among the numerous existing biosensor measurement techniques suited for biosensing applications. The best strategy for the work may be identified and applied using various electrochemical techniques available, including DPV, CV, and EIS. Electrochemical technologies also have a variety of advantages, including quick response, high sensitivity and selectivity, natural shrinkage, ease of operation, and mobility, which make them ideal for building flexible biosensors. As a result, a wide range of flexible nanobiosensors as wearable biosensor technologies have been thoroughly researched recently. To develop further flexible nanobiosensors, many critical properties must be addressed, including exceptional flexibility and the ability to transfer conductivity onto the flexible material. As a result, much study has been accompanied on developing flexible conductive substrates using cutting-edge nanomaterials and manufacturing techniques.

Low conductivity, brittleness, or the difficulty of obtaining high flexibility and conductivity in materials should be addressed by developing and studying new substrates that combine conductivity and flexibility. The production of unique and new materials and the synthesis of materials under research are thought to improve the benefits of individual materials and counteract the disadvantages. Furthermore, rather than manufacturing a substrate using a single manufacturing method, it is envisaged that a novel fabrication procedure may be designed to reimburse for the constraints of each method by concurrently integrating two or more fabrication processes. These techniques will help overwhelm and resolve existing limits and barriers.

Furthermore, even if the best substrate materials and manufacturing methods are established, obstacles remain, such as developing acceptable energy resource solutions and biosensors' capability to function on the frame without extra apparatus. Several obstacles must be explained to build functional wearable biosensors in the future. Converging biosensor research with other critical disciplines like electronics and energy might tackle these issues shortly. Additionally, for commercialization, the mass construction system of flexible conductive materials should be accomplished by lowering the complicated production procedure for new materials and reducing the tough manufacturing procedures for biosensors. If these contests are overcome, flexible nanobiosensors will likely be employed in customized POCT systems.

References

Akşit AC et al (2009) Electromagnetic and electrical properties of coated cotton fabric with barium ferrite doped polyaniline film. J Appl Polym Sci. Wiley Online Library 113(1):358–366

Ali S et al (2018) Disposable all-printed electronic biosensor for instantaneous detection and classification of pathogens. Sci Rep. Nature Publishing Group 8(1):1–11

Altintas Z (2017) Biosensors and nanotechnology: applications in health care diagnostics. Wiley, Hoboken

Anusha JR et al (2018) Performance of α-and β-chitosan in enzymatic glucose biosensor on gold nanoparticles coated flexible electrodes. Adv Sci Eng Med. American Scientific Publishers 10(9):887–893

Arduini F et al (2019) Origami multiple paper-based electrochemical biosensors for pesticide detection. Biosens Bioelectron. Elsevier 126:346–354

Bandodkar AJ et al (2016) Highly stretchable fully-printed CNT-based electrochemical sensors and biofuel cells: combining intrinsic and design-induced stretchability. Nano Lett. ACS Publications 16(1):721–727

Baptista A et al (2018) Sputtering physical vapour deposition (PVD) coatings: a critical review on process improvement and market trend demands. Coatings. Multidisciplinary Digital Publishing Institute 8(11):402

Barcelo S, Li Z (2016) Nanoimprint lithography for nanodevice fabrication. Nano Convergence. SpringerOpen 3(1):1–9

Barfidokht A et al (2019) Wearable electrochemical glove-based sensor for rapid and on-site detection of fentanyl. Sensors Actuators B Chem. Elsevier 296:126422

Bariya M et al (2018) Roll-to-roll gravure printed electrochemical sensors for wearable and medical devices. ACS Nano. ACS Publications 12(7):6978–6987

Barlow F, Lostetter A, Elshabini A (2002) Low cost flex substrates for miniaturized electronic assemblies. Microelectron Reliab. Elsevier 42(7):1091–1099

Bhatnagar I et al (2018) Chitosan stabilized gold nanoparticle mediated self-assembled gliP nanobiosensor for diagnosis of invasive Aspergillosis. Int J Biol Macromol. Elsevier 110: 449–456

Brunner PH, Rechberger H (2016) Handbook of material flow analysis: for environmental, resource, and waste engineers. CRC Press, Boca Raton

Cao L et al (2020) A novel 3D paper-based microfluidic electrochemical glucose biosensor based on rGO-TEPA/PB sensitive film. Anal Chim Acta. Elsevier 1096:34–43

Chandra P et al (2012) In vitro monitoring of i-NOS concentrations with an immunosensor: the inhibitory effect of endocrine disruptors on i-NOS release. Biosens Bioelectron. Elsevier 32(1): 278–282

Chen Y (2015) Nanofabrication by electron beam lithography and its applications: a review. Microelectron Eng. Elsevier 135:57–72

Chen C-H et al (2017a) Utilization of self-powered electrochemical systems: metallic nanoparticle synthesis and lactate detection. Nano Energy. Elsevier 42:241–248

Chen Y et al (2017b) Skin-like biosensor system via electrochemical channels for noninvasive blood glucose monitoring. Sci Adv. American Association for the Advancement of Science 3(12):e1701629

Chinnasamy T et al (2014) Point-of-care vertical flow allergen microarray assay: proof of concept. Clin Chem. Oxford University Press 60(9):1209–1216

Cho H et al (2015) High-rate nanoscale offset printing process using directed assembly and transfer of nanomaterials. Adv Mater. Wiley Online Library 27(10):1759–1766

Choi JR et al (2016) An integrated paper-based sample-to-answer biosensor for nucleic acid testing at the point of care. Lab Chip. Royal Society of Chemistry 16(3):611–621

Chou J-C et al (2018) Reaction of NiO film on flexible substrates with buffer solutions and application to flexible arrayed lactate biosensor. Microelectron Reliab. Elsevier 83:249–253

Cinti S et al (2017) A paper-based nanomodified electrochemical biosensor for ethanol detection in beers. Anal Chim Acta. Elsevier 960:123–130

Ciui B et al (2018) Finger-based printed sensors integrated on a glove for on-site screening of *Pseudomonas aeruginosa* virulence factors. Anal Chem. ACS Publications 90(12):7761–7768

Dahlin AB (2012) Size matters: problems and advantages associated with highly miniaturized sensors. Sensors. Molecular Diversity Preservation International 12(3):3018–3036

Daneshpour M, Omidfar K, Ghanbarian H (2016) A novel electrochemical nanobiosensor for the ultrasensitive and specific detection of femtomolar-level gastric cancer biomarker miRNA-106a. Beilstein J Nanotechnol. Beilstein-Institut 7(1):2023–2036

Dincer C et al (2017) Multiplexed point-of-care testing–xPOCT. Trends Biotechnol. Elsevier 35(8): 728–742

Ding Y, Invernale MA, Sotzing GA (2010) Conductivity trends of PEDOT-PSS impregnated fabric and the effect of conductivity on electrochromic textile. ACS Appl Mater Interfaces. ACS Publications 2(6):1588–1593

Diouf-Lewis A, Commereuc S, Verney V (2017) Toward greener polyolefins: antioxidant effect of phytic acid from cereal waste. Eur Polym J. Elsevier 96:190–199

Gleskova H et al (2002) Electrical response of amorphous silicon thin-film transistors under mechanical strain. J Appl Phys. American Institute of Physics 92(10):6224–6229

Gualandi I et al (2016) Textile organic electrochemical transistors as a platform for wearable biosensors. Sci Rep. Nature Publishing Group 6(1):1–10

Hallot M et al (2018) Sputtered LiMn1. 5Ni0. 5O4 thin films for Li-ion micro-batteries with high energy and rate capabilities. Energy Storage Mater. Elsevier 15:396–406

Han S et al (2017) An overview of the development of flexible sensors. Adv Mater. Wiley Online Library 29(33):1700375

Hondred JA, Medintz IL, Claussen JC (2019) Enhanced electrochemical biosensor and supercapacitor with 3D porous architectured graphene via salt impregnated inkjet maskless lithography. Nanoscale Horizons. Royal Society of Chemistry 4(3):735–746

Hondred JA, Johnson ZT, Claussen JC (2020) Nanoporous gold peel-and-stick biosensors created with etching inkjet maskless lithography for electrochemical pesticide monitoring with microfluidics. J Mater Chem C. Royal Society of Chemistry 8(33):11376–11388

Howell RS et al (2000) Poly-Si thin-film transistors on steel substrates. IEEE Electron Device Lett. IEEE 21(2):70–72

Hsieh C-W et al (2006) Molecular cloning and functional identification of invertase isozymes from green bamboo Bambusa oldhamii. J Agric Food Chem. ACS Publications 54(8):3101–3107

Hu Q et al (2018) Electrochemically mediated in situ growth of electroactive polymers for highly sensitive detection of double-stranded DNA without sequence-preference. Biosens Bioelectron. Elsevier 101:1–6

Huang Y et al (2011) Graphene-based biosensors for detection of bacteria and their metabolic activities. J Mater Chem. Royal Society of Chemistry 21(33):12358–12362

Imani S et al (2016) A wearable chemical–electrophysiological hybrid biosensing system for real-time health and fitness monitoring. Nat Commun. Nature Publishing Group 7(1):1–7

Jia W et al (2013) Electrochemical tattoo biosensors for real-time noninvasive lactate monitoring in human perspiration. Anal Chem. ACS Publications 85(14):6553–6560

Jung YH et al (2015) High-performance green flexible electronics based on biodegradable cellulose nanofibril paper. Nat Commun. Nature Publishing Group 6(1):1–11

Khan S, Lorenzelli L, Dahiya RS (2014) Technologies for printing sensors and electronics over large flexible substrates: a review. IEEE Sensors J. IEEE 15(6):3164–3185

Kim J et al (2015) Wearable salivary uric acid mouthguard biosensor with integrated wireless electronics. Biosens Bioelectron. Elsevier 74:1061–1068

Kim B-Y, Lee H-B, Lee N-E (2019) A durable, stretchable, and disposable electrochemical biosensor on three-dimensional micro-patterned stretchable substrate. Sensors Actuators B Chem. Elsevier 283:312–320

Klemic KG et al (2002) Micromolded PDMS planar electrode allows patch clamp electrical recordings from cells. Biosens Bioelectron. Elsevier 17(6–7):597–604

Kumar M et al (2018) Carbon dioxide capture, storage and production of biofuel and biomaterials by bacteria: a review. Bioresour Technol. Elsevier 247:1059–1068

Lau PH et al (2013) Fully printed, high performance carbon nanotube thin-film transistors on flexible substrates. Nano Lett. ACS Publications 13(8):3864–3869

Lechat C et al (2006) Mechanical behaviour of polyethylene terephthalate & polyethylene naphthalate fibres under cyclic loading. J Mater Sci. Springer 41(6):1745–1756

Lee K et al (2004) Polyimide based neural implants with stiffness improvement. Sensors Actuators B Chem. Elsevier 102(1):67–72

Lee JH et al (2016) Fabrication of flexible, transparent silver nanowire electrodes for amperometric detection of hydrogen peroxide. Sensors Actuators B Chem. Elsevier 224:789–797

Liao J-Y et al (2012) Oriented hierarchical single crystalline anatase TiO_2 nanowire arrays on Ti-foil substrate for efficient flexible dye-sensitized solar cells. Energy Environ Sci. Royal Society of Chemistry 5(2):5750–5757

Liao C et al (2015) Flexible organic electronics in biology: materials and devices. Adv Mater. Wiley Online Library 27(46):7493–7527

Liaw D-J et al (2012) Advanced polyimide materials: syntheses, physical properties and applications. Prog Polym Sci. Elsevier 37(7):907–974

Libansky M et al (2017) Basic electrochemical properties of sputtered gold film electrodes. Electrochim Acta. Elsevier 251:452–460

Liu Q et al (2018) Highly sensitive and wearable In_2O_3 nanoribbon transistor biosensors with integrated on-chip gate for glucose monitoring in body fluids. ACS Nano. ACS Publications 12(2):1170–1178

Loo JFC et al (2019) Integrated printed microfluidic biosensors. Trends Biotechnol. Elsevier 37(10):1104–1120

Luo Y et al (2020) A flexible CVD graphene platform electrode modified with L-aspartic acid for the simultaneous determination of acetaminophen, epinephrine and tyrosine. J Electroanal Chem. Elsevier 856:113737

Lyberopoulou A, Efstathopoulos EP, Gazouli M (2016) Nanotechnology-based rapid diagnostic tests. In: Proof and concepts in rapid diagnostic tests and technologies. https://doi.org/10.5772/63908

MacDonald WA (2004) Engineered films for display technologies. J Mater Chem. Royal Society of Chemistry 14(1):4–10

Mahato K et al (2019) Novel electrochemical biosensor for serotonin detection based on gold nanorattles decorated reduced graphene oxide in biological fluids and in vitro model. Biosens Bioelectron. Elsevier 142:111502

Manjakkal L et al (2019) Textile-based potentiometric electrochemical pH sensor for wearable applications. Biosensors. Multidisciplinary Digital Publishing Institute 9(1):14

Martinez AW et al (2010) Diagnostics for the developing world: microfluidic paper-based analytical devices. Anal Chem. ACS Publications 82:3

Mata A, Fleischman AJ, Roy S (2005) Characterization of polydimethylsiloxane (PDMS) properties for biomedical micro/nanosystems. Biomed Microdevices. Springer 7(4):281–293

Mathew X et al (2003) Development of CdTe thin films on flexible substrates – a review. Sol Energy Mater Sol Cells. Elsevier 76(3):293–303

Mishra RK et al (2017) Wearable flexible and stretchable glove biosensor for on-site detection of organophosphorus chemical threats. ACS Sensors. ACS Publications 2(4):553–561

Mishra RK et al (2018) Wearable potentiometric tattoo biosensor for on-body detection of G-type nerve agents simulants. Sensors Actuators B Chem. Elsevier 273:966–972

Mościcki A et al (2017) Ink for ink-jet printing of electrically conductive structures on flexible substrates with low thermal resistance. J Electron Mater. Springer 46(7):4100–4108

Murakami S et al (1995) A study on the structural changes during uniaxial drawing and/or heating of poly (ethylene naphthalene-2, 6-dicarboxylate) films. Polymer 36(2):291–297

Nair LS, Laurencin CT (2007) Biodegradable polymers as biomaterials. Prog Polym Sci. Elsevier 32(8–9):762–798

Nantaphol S et al (2017) Boron doped diamond paste electrodes for microfluidic paper-based analytical devices. Anal Chem. ACS Publications 89(7):4100–4107

Ngom B et al (2010) Development and application of lateral flow test strip technology for detection of infectious agents and chemical contaminants: a review. Anal Bioanal Chem. Springer 397(3):1113–1135

Noah NM, Ndangili PM (2019) Current trends of nanobiosensors for point-of-care diagnostics. J Anal Methods Chem. Hindawi 2019:2179718

Nyein HYY et al (2016) A wearable electrochemical platform for noninvasive simultaneous monitoring of Ca2+ and pH. ACS Nano. ACS Publications 10(7):7216–7224

Pandya HJ, Park K, Desai JP (2015) Design and fabrication of a flexible MEMS-based electro-mechanical sensor array for breast cancer diagnosis. J Micromech Microeng. IOP Publishing 25(7):75025

Parameswaran C, Gupta D (2019) Large area flexible pressure/strain sensors and arrays using nanomaterials and printing techniques. Nano Convergence. SpringerOpen 6(1):1–23

Paranthaman R et al (2009) Production of tannin acyl hydrolase and HPLC determination of flavonoids from fermented rice bran. Int J Appl Chem. Research India Publications 5(2):93–101

Park JH et al (2003) High temperature crystallized poly-Si on Mo substrates for TFT application. Thin Solid Films. Elsevier 427(1–2):303–308

Park S et al (2019) Hydrogel nanospike patch as a flexible anti-pathogenic scaffold for regulating stem cell behavior. ACS Nano. ACS Publications 13(10):11181–11193

Parolo C, Merkoçi A (2013) Based nanobiosensors for diagnostics. Chem Soc Rev. Royal Society of Chemistry 42(2):450–457

Patel S et al (2016) Biosensors in health care: the milestones achieved in their development towards lab-on-chip-analysis. Biochem Res Int. Hindawie 2016:3130469

Patra S, Young V (2016) A review of 3D printing techniques and the future in biofabrication of bioprinted tissue. Cell Biochem Biophys. Springer 74(2):93–98

Patrito N et al (2007) Spatially controlled cell adhesion via micropatterned surface modification of poly (dimethylsiloxane). Langmuir. ACS Publications 23(2):715–719

Pelton R (2009) Bioactive paper provides a low-cost platform for diagnostics. TrAC Trends Anal Chem. Elsevier 28(8):925–942

Price CP (2001) Point-of-care testing: impact on medical outcomes. Clin Lab Med. Elsevier 21(2): 285–304

Pu Z et al (2018) A flexible enzyme-electrode sensor with cylindrical working electrode modified with a 3D nanostructure for implantable continuous glucose monitoring. Lab Chip. Royal Society of Chemistry 18(23):3570–3577

Qin D, Xia Y, Whitesides GM (2010) Soft lithography for micro-and nanoscale patterning. Nat Protoc. Nature Publishing Group 5(3):491

Qiu Z, Shu J, Tang D (2017) Bioresponsive release system for visual fluorescence detection of carcinoembryonic antigen from mesoporous silica nanocontainers mediated optical color on quantum dot-enzyme-impregnated paper. Anal Chem. ACS Publications 89(9):5152–5160

Qu W, Ploetner M, Fischer W-J (2001) Microfabrication of thermoelectric generators on flexible foil substrates as a power source for autonomous microsystems. J Micromech Microeng. IOP Publishing 11(2):146

Quesada-González D, Merkoçi A (2018) Nanomaterial-based devices for point-of-care diagnostic applications. Chem Soc Rev. Royal Society of Chemistry 47(13):4697–4709

Rahmanian R et al (2018) Development of sensitive impedimetric urea biosensor using DC sputtered Nano-ZnO on TiO2 thin film as a novel hierarchical nanostructure transducer. Sensors Actuators B Chem. Elsevier 256:760–774

Rebelo AR et al (2019) Poly (4-vinylaniline)/polyaniline bilayer-functionalized bacterial cellulose for flexible electrochemical biosensors. Langmuir. ACS Publications 35(32):10354–10366

Reddish W (1950) The dielectric properties of polyethylene terephthalate (terylene). Trans Faraday Soc. Royal Society of Chemistry 46:459–475

Rivas D et al (2016) MALDI-TOF MS imaging evidences spatial differences in the degradation of solid polycaprolactone diol in water under aerobic and denitrifying conditions. Sci Total Environ. Elsevier 566:27–33

Roditi E et al (2019) Integrated on-chip sensor with sputtered Ag-Au-Au electrodes for the voltammetric determination of trace Hg (II). Sensors Actuators B Chem. Elsevier 286:125–130

SadAbadi H et al (2013) Integration of gold nanoparticles in PDMS microfluidics for lab-on-a-chip plasmonic biosensing of growth hormones. Biosens Bioelectron. Elsevier 44:77–84

Saetia K et al (2014) Spray-layer-by-layer carbon nanotube/electrospun fiber electrodes for flexible chemiresistive sensor applications. Adv Funct Mater. Wiley Online Library 24(4):492–502

Segev-Bar M et al (2013) Tunable touch sensor and combined sensing platform: toward nanoparticle-based electronic skin. ACS Appl Mater Interfaces. ACS Publications 5(12): 5531–5541

Sharafeldin M, Jones A, Rusling JF (2018) 3D-printed biosensor arrays for medical diagnostics. Micromachines. Multidisciplinary Digital Publishing Institute 9(8):394

Sheeparamatti BG, Sheeparamatti RB, Kadadevaramath JS (2007) Nanotechnology: inspiration from nature. IETE Tech Rev. Taylor & Francis 24(1):5–8

Sheldon RA (2014) Green and sustainable manufacture of chemicals from biomass: state of the art. Green Chem. Royal Society of Chemistry 16(3):950–963

Siegel AC et al (2010) Foldable printed circuit boards on paper substrates. Adv Funct Mater. Wiley Online Library 20(1):28–35

Smith HI (1986) A review of submicron lithography. Superlattice Microst. Elsevier 2(2):129–142

Stagner J (2016) Methane generation from anaerobic digestion of biodegradable plastics – a review. Int J Environ Stud. Taylor & Francis 73(3):462–468

Stoppa M, Chiolerio A (2014) Wearable electronics and smart textiles: a critical review. Sensors. Multidisciplinary Digital Publishing Institute 14(7):11957–11992

Ummartyotin S, Pechyen C (2016) Strategies for development and implementation of bio-based materials as effective renewable resources of energy: a comprehensive review on adsorbent technology. Renew Sust Energ Rev. Elsevier 62:654–664

Voisin A-S et al (2014) Legumes for feed, food, biomaterials and bioenergy in Europe: a review. Agron Sustain Dev. Springer 34(2):361–380

Wang S et al (2016) Flexible substrate-based devices for point-of-care diagnostics. Trends Biotechnol. Elsevier 34(11):909–921

Wang Z et al (2020) A wearable and deformable graphene-based affinity nanosensor for monitoring of cytokines in biofluids. Nano. Multidisciplinary Digital Publishing Institute 10(8):1503

Windmiller JR, Wang J (2013) Wearable electrochemical sensors and biosensors: a review. Electroanalysis. Wiley Online Library 25(1):29–46

Xiao SY et al (2008) A novel fabrication process of MEMS devices on polyimide flexible substrates. Microelectron Eng. Elsevier 85(2):452–457

Xuan X et al (2018) A highly stretchable and conductive 3D porous graphene metal nanocomposite based electrochemical-physiological hybrid biosensor. Biosens Bioelectron. Elsevier 120: 160–167

Yang Y-L et al (2010) Thick-film textile-based amperometric sensors and biosensors. Analyst. Royal Society of Chemistry 135(6):1230–1234

Yang Y et al (2017) Recent progress in flexible and wearable bio-electronics based on nanomaterials. Nano Res. Springer 10(5):1560–1583

Yao B et al (2017) Paper-based electrodes for flexible energy storage devices. Adv Sci. Wiley Online Library 4(7):1700107

Yoon J et al (2019) Flexible electrochemical glucose biosensor based on GOx/gold/MoS_2/gold nanofilm on the polymer electrode. Biosens Bioelectron. Elsevier 140:111343

Yoon H et al (2020) A chemically modified laser-induced porous graphene based flexible and ultrasensitive electrochemical biosensor for sweat glucose detection. Sensors Actuators B Chem. Elsevier 311:127866

Zarei M (2017) Portable biosensing devices for point-of-care diagnostics: recent developments and applications. TrAC Trends Anal Chem. Elsevier 91:26–41

Zhang X, Guo Q, Cui D (2009) Recent advances in nanotechnology applied to biosensors. Sensors. https://doi.org/10.3390/s90201033

Zhang X et al (2017) Beyond conventional patterns: new electrochemical lithography with high precision for patterned film materials and wearable sensors. Anal Chem. ACS Publications 89(4):2569–2574

Zhang P et al (2019) Electrochemically exfoliated high-quality 2H-MoS_2 for multiflake thin film flexible biosensors. Small. Wiley Online Library 15(23):1901265

Electrochemical Determination of Promethazine Hydrochloride Using Carbon Paste Electrode Modified with Activated Carbon and Silver Nanoparticles

10

Arnaldo César Pereira, Anna Paula Santos,
Ana Elisa Ferreira de Oliveira, and Lucas Franco Ferreira

Contents

1 Introduction 200
2 Experimental Setup 202
  2.1 Instrumentation and Chemicals 202
  2.2 Synthesis of Silver Nanoparticles 203
  2.3 Preparation of Electrodes and Electrochemical Behavior 203
  2.4 Optimization of PMZ Analysis Conditions 204
  2.5 Analytical Characteristics 204
  2.6 Tablet Form Samples 204
3 Results and Discussion 205
  3.1 AgNPs Characterization 205
  3.2 Electrochemical Behavior of CPE/AC/AgNPs 205
  3.3 Kinetic Parameters Evaluation 206
  3.4 Optimization of Experimental Conditions 208
  3.5 Performance of Electrochemical Sensor 211
  3.6 Application in Pharmaceutical Samples 213
4 Conclusions 214
References 214

Abstract

In this work, an electrochemical sensor was developed for the determination of promethazine hydrochloride (PMZ), an antihistamine used to relieve the symptoms of allergies. The sensor was prepared using a carbon paste electrode (CPE) modified with activated carbon (AC) and silver nanoparticles (AgNPs) described as CPE/AC/AgNPs. The analytical response obtained with CPE/AC/AgNPs was 88% higher compared to unmodified CPE. The optimization of experimental

---

A. C. Pereira (✉) · A. P. Santos · A. E. F. de Oliveira
Department of Natural Sciences, Federal University of São João del-Rei, São João del-Rei, Brazil

L. F. Ferreira
Institute of Science and Technology, Federal University of the Jequitinhonha and Mucuri Valleys, Diamantina, Brazil

© Springer Nature Singapore Pte Ltd. 2023

U. P. Azad, P. Chandra (eds.), *Handbook of Nanobioelectrochemistry*,
https://doi.org/10.1007/978-981-19-9437-1_10

conditions contributed to increasing the sensitivity of the proposed electrochemical sensor. The followed experimental conditions were optimized: the proportion of graphite, AC, and AgNPs was 55/25/20 (% m/m), respectively, with 0.05 mol L^{-1} phosphate buffer solution (PBS) at pH 7.00 as support electrolyte. Under optimized conditions, a linear range from 5–40 μmol L^{-1} was obtained for PMZ with a limit of detection (LOD) of 1.30 μmol L^{-1} and a limit of quantification (LOQ) of the 4.20 μmol L^{-1}. The determination of PMZ in Phenergan® tablets showed recovery values between 98.4 and 102.2%, which indicates that the CPE/AC/AgNPs can be used as a viable alternative to the determination of the promethazine in pharmaceutical samples.

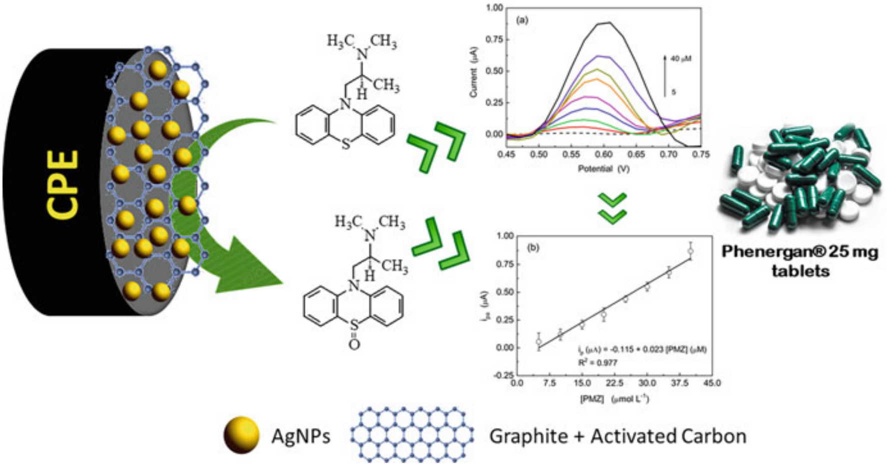
CPE
H_3C CH_3 N CH_3 H N S
H_3C CH_3 N CH_3 H N S O
(a)
Current (μA)
1.00
0.75
0.50
0.25
0.00
40 μM
5
0.45 0.50 0.55 0.60 0.65 0.70 0.75
Potential (V)
(b)
I_{pa} (μA)
1.00
0.75
0.50
0.25
0.00
-0.25
I_p (μA) = -0.115 + 0.023 [PMZ] (μM)
R^2 = 0.977
0.0 7.5 15.0 22.5 30.0 37.5 45.0
[PMZ] (μmol L^{-1})
Phenergan® 25 mg tablets
AgNPs
Graphite + Activated Carbon

Representation of the CPE/AC/AgNPs sensor for determination of Phenergan®.

Keywords

Promethazine hydrochloride · Electrochemical sensor · Carbon paste electrode · Activated carbon · Silver nanoparticles

1 Introduction

Promethazine hydrochloride (PMZ) shown in Fig. 10.1 is a compound phenothiazines derivative with antihistamine and anticholinergic properties (Alizadeh and Akhoundian 2010). This compound is extensively marketed in the form of a pharmaceutical drug known as Fenergan®. The drug is indicated for the treatment of symptoms of anaphylactic and allergic reactions, also having antiemetic activity and sedative action, but it has also side effects like respiratory depression, photosensitization of the skin tissue, paresthesia, etc. (Idris et al. 2006; Ribeiro et al. 2008; Maurya et al. 2018). As antiallergic, its main function is to resist the effects of the production of histamine, a substance that is produced naturally by the body during an

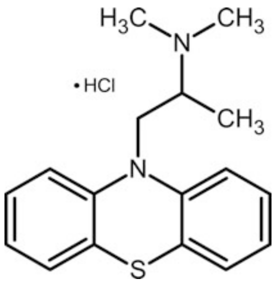

Fig. 10.1 Structure of promethazine hydrochloride

allergic reaction process mainly in the skin, the vessels, and the mucous membranes. The clinical effects of Fenergan® are reached 20 min after the drug is administered, and usually last for 4–6 h, but they can persist for up to 12 h, according to some manufacturers. However, overuse of these medications can lead to some adverse effects, such as cardiac and reproductive changes, drowsiness and excessive sedation, mental confusion, and blood pressure modification (Silveira and Tarley 2008; Wei et al. 2008; AlAqad et al. 2018).

Idris et al. (2006) describe the importance of the determination of PMZ, justified by the therapeutic interest and the worldwide consumption of the drug. According to the authors, the drug is analyzed spectrophotometrically in tablet form according to the British Pharmacopoeia and the United States Pharmacopoeia. However, other nonofficial methods including titrimetric, spectrophotometric, fluorimetric, chemiluminescence, high-performance liquid chromatographic, electrophoresis, voltammetric, potentiometric, conductimetric, coulometric, nephelometric, and flow injection analysis are reported in the literature (Idris et al. 2006). In Brazilian Pharmacopoeia, the method described for the assay of PMZ in tablet form is also ultraviolet absorption spectrophotometry in an acid medium (HCl) at a wavelength of 249 nm (ANVISA 2010). Ribeiro et al. (2008) report that the quantification of PMZ using these methods has excellent sensitivity, but for several procedures an extraction step is necessary. Idris et al. (2006) also present some disadvantages of the UV-Vis spectrophotometric method presented by pharmacopeias, mainly concerning the analysis time, consumption of reagents, and extraction steps.

Hence, new methodologies based on electrochemical sensors have been proposed for various analytes to develop devices with high sensitivity, specificity, rapid response, low application cost, and that do not require extraction steps or pre-concentration. Electrochemical sensors are being increasingly used for analytical purposes, as they present themselves as a promising alternative when compared to existing official methods, presenting unique advantages that allow a real-time response, low reagent consumption, including the possibility of miniaturization of the system, and in many cases can be used in complex samples without pretreatment (Brett 2001; Hanrahan et al. 2004; Wang et al. 2008; Privett et al. 2010; Jadon et al. 2016; Hamzah et al. 2018; Purohit et al. 2020; Karimi-Maleh et al. 2020).

Electroanalytical methods have aroused great interest in recent years, as they allow the use of chemically modified electrodes since the immobilization of a certain substance on the surface of an electrode can provide devices with greater sensitivity and specificity for the development of electroanalytical procedures and more efficient methods, allowing to obtain the desired characteristics of the system under study when compared to unmodified electrodes. The use of chemically modified electrodes is an area in increasing expansion, mainly in the aspect of the development of new materials for modifying the surface of the electrodes, which aims to expand and enhance the applications of these devices (Wang 1991; Pereira et al. 2002; Piletsky and Turner 2002; Zhao et al. 2002; Stradiotto et al. 2003; Ramanavičius et al. 2006; Wu et al. 2013; Thiyagarajan et al. 2014; Zhu et al. 2015; Beluomini et al. 2019; Vernekar et al. 2021).

Consequently, these electrochemical methods can be used to monitor analytes of clinical interest because of all the advantages presented, which is also interesting for the quantification of PMZ in pharmaceutical preparations or biospecimen. As a result, some studies are described in the literature for the electrochemical determination of PMZ (Bosáková et al. 2002; Xi et al. 2011; Saleh et al. 2012; Gu et al. 2012; McClure et al. 2013; Marco et al. 2013; Honarmand et al. 2014, 2016; Akram et al. 2019; Sakthivel et al. 2019; Akhoundian and Alizadeh 2020; Promsuwan et al. 2020; Alagumalai et al. 2020; Arumugam et al. 2020; de Oliveira et al. 2020).

In this sense, in this work we present a proposal for an electrochemical sensor for quantification of the PMZ in pharmaceutical samples using a carbon paste electrode (CPE) modified with activated carbon (AC) and silver nanoparticles (AgNPs) described as CPE/AC/AgNPs. This sensor had some advantages over other sensors developed, and to our knowledge, no studies were found using AC and AgNPs for this purpose. AC is a porous material with a high surface area, ensuring a great physical adsorption capacity of liquids and gases (Arroyo-Gómez et al. 2018; Vicentini et al. 2019; Wei et al. 2019; Partlan et al. 2020). Because of this, the AC increases conductivity when used as an electrochemical sensor modifier. Additionally, the material pores can allow the adsorption of many substances, including nanoparticles. The metallic nanoparticles (NPs), such as the silver nanoparticles, have been frequently used in electrochemical sensors, because of their good conductivity, stability, and reactivity (Vanitha Kumari et al. 2016; Donini et al. 2018). A carbon paste sensor modified with activated carbon and silver nanoparticles will increase the conductivity by increasing the surface area, which will promote a better charge transport between the electrode and solution.

2 Experimental Setup

2.1 Instrumentation and Chemicals

All electrochemical measurements were performed in a potentiostat/galvanostat from Autolab model PGSTAT101 coupled to a computer with the Nova 1.11 software. A conventional three-electrode electrochemical cell was used to obtain the electrochemical measurements where: Ag/AgCl (KCl 3.0 M) was used as a reference electrode, a platinum wire as an auxiliary electrode, and a carbon paste electrode (CPE) as the working electrode (12.6 mm^2).

Sodium borohydride ($NaBH_4$), sodium citrate ($Na_3C_6H_5O_7$), dibasic sodium phosphate heptahydrate ($Na_2HPO_4.7H_2O$), monobasic sodium phosphate monohydrate ($NaH_2PO_4.H_2O$), nitric acid (HNO_3), ethyl alcohol (EtOH), pure graphite powder, and silver nitrate were obtained from Synth®. Powdered activated carbon, mineral oil, sodium tetrachloroaurate ($NaAuCl_4.2H_2O$), and promethazine hydrochloride ($C_{17}H_{20}N_2S$) were purchased from Sigma-Aldrich®. All chemical reagents used were of analytical purity and all solutions were prepared with deionized water by the Millipore Milli-Q system (resistivity 18.2 MΩ.cm).

2.2 Synthesis of Silver Nanoparticles

Silver nanoparticles were synthesized according to the procedure proposed by Jana et al. (2001) with minor modifications. Briefly, 50 mL of 0.50 mmol L^{-1} $AgNO_3$ and 50 mL of 0.50 mmol L^{-1} sodium citrate were prepared and cooled to approximately 4 °C. Subsequently, 10 mL of sodium borohydride ($NaBH_4$) 2.9 mmol L^{-1} was added to a burette and dripped dropwise per second, which was kept in an ice bath with vigorous stirring and protected against light. In this step, it was possible to observe a change in the color of the solution, from transparent to yellow, evidencing the formation of silver nanoparticles in suspension. Thus, the solution was slowly stirred for 2 h in an ice bath protected from light, to remove excess salts and ions present, and the nanoparticles were stored in an amber flask in a refrigerated environment. After synthesis, the absorbance of the AgNPs was evaluated by an ultraviolet spectrophotometer using a Shimadzu UV-2550 spectrometer.

2.3 Preparation of Electrodes and Electrochemical Behavior

The CPE/AC/AgNPs was prepared by direct mixing initially of 21 mg of graphite powder, 9.0 mg of activated carbon, 9.0 μL of mineral oil, and 7.5 μL solution containing silver nanoparticles followed by grounding in an agate mortar until a homogeneous paste obtained. The obtained paste was introduced into the cavity of a glass tube (4.0 mm internal diameter), which, before each modification, was cleaned with ethyl alcohol and nitric acid 5% (v/v) and subsequently washed with deionized water. Before use, the CPE/AC/AgNPs were polished with weighing paper until a uniform surface was obtained.

The electrochemical behavior of the developed sensor was evaluated in the absence and the presence of 35 μmol L^{-1} of PMZ, using the cyclic voltammetry in the potential range of +0.3 to +0.8 V at 20 mV/s, using 0.10 mol L^{-1} PBS buffer at pH 7.00 as supporting electrolyte. For this study, different sensor configurations were proposed to analyze which configuration (CPE; CPE/AC; CPE/AC/AgNPs) was more suitable for the electrooxidation of PMZ, to further improve the performance of the sensor.

To carry out the electrochemical characterization, the kinetic properties of the system were evaluated, such as the determination of the number of electrons (n_e), electron transfer coefficient (α), and electron transfer rate constant (κ), studying the influence of the scan rate on the oxidation process of PMZ, obtaining the cyclic voltammograms from 5–500 mV/s. For this, an electrochemical cell with 10 mL of support electrolyte (0.10 mol L^{-1} PBS buffer at pH 7.00) containing 35 μmol L^{-1} of PMZ was used.

2.4 Optimization of PMZ Analysis Conditions

The amount of activated carbon was optimized concerning the amount of graphite powder. To carry out this study, the amount of AgNPs was kept fixed at 15% and the mass/mass ratio (%) of graphite powder and activated carbon was assessed at 75:10, 70:15, 60:25, and 50:35, respectively. Then, with the amount of activated carbon optimized, the amount of the AgNPs solution was evaluated using 10, 15, 20, and 25% of the colloidal suspension next to the carbon paste, keeping the amount of mineral oil fixed at 8.0 uL. The influence of the pH of PBS buffer from 4.00 to 8.00 was studied in search of the system that presented the highest sensitivity. Lastly, the effect of the ionic strength was investigated by changing the concentration of the PBS buffer solution from 0.025 to 0.20 mol L^{-1}.

2.5 Analytical Characteristics

Differential pulse voltammetry (DPV) was selected for the electrochemical determination of PMZ. The analyzes were performed from +0.45 to +0.75 V at 40 mV/s with a modulation amplitude of 60 mV. PMZ solutions prepared in 0.05 mol L^{-1} PBS buffer at concentrations from 5–40 μmol L^{-1} were used to obtain the analytical parameters of the sensor under optimized conditions, such as linear range, and limit of detection (LOD), the limit of quantification (LOQ) and sensitivity. The LOD was calculated as $3 \times Sb/b$, and the LOQ as $10 \times Sb/b$, where Sb is the blank standard deviation ($n = 10$) and b the sensitivity of the analytical curve.

2.6 Tablet Form Samples

For the application of the method Fenergan® tablets were used, which contain 25 mg of promethazine hydrochloride. Then, one tablet was macerated until obtaining a fine and homogeneous powder to prepare a 1.0 mmol L^{-1} PMZ solution. This stock solution was then diluted in PBS buffer at pH 7.00 to obtain the concentrations of 15 and 30 μmol L^{-1} of PMZ. All analyzes were performed using DPV.

3 Results and Discussion

3.1 AgNPs Characterization

Figure 10.2 shows UV-Vis spectra for silver nanoparticles. The absorption spectrum is responsible for indicating absorption bands corresponding to electronic transitions, that is, the passage of the electron from a molecular orbital to an unoccupied orbital (Viol et al. 2011). The spectra show the absorption spectrum for the band corresponding to the silver nanoparticles at 410 nm. According to Melo Jr. et al. (2012), the characteristic yellow color observed in colloidal silver is the result of the absorption of electromagnetic radiation in resonance with surface plasmons. With the increase of silver particles, the yellow color characteristic of the standard solution changes to orange and, later, violet until reaching the characteristic coloration of silver on a macroscopic scale.

Also, one of the most striking characteristics of the nanoparticles is related in addition to the optical properties, since the noble metal nanoparticles have characteristic stains (yellow for AgNPs) with the electrochemical properties, since they have high conductivity, reactivity, and stability, improving the sensitivity of sensors when modified with these materials.

3.2 Electrochemical Behavior of CPE/AC/AgNPs

Promethazine, belonging to the phenothiazine drug class, has in its chemical structure electroactive functional groups which oxidize in the potential range of

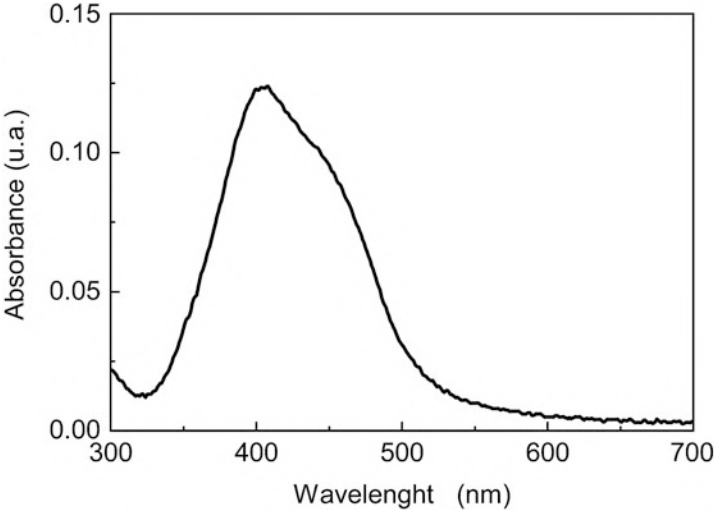

Fig. 10.2 UV-Vis spectra of the silver nanoparticles obtained in an aqueous solution

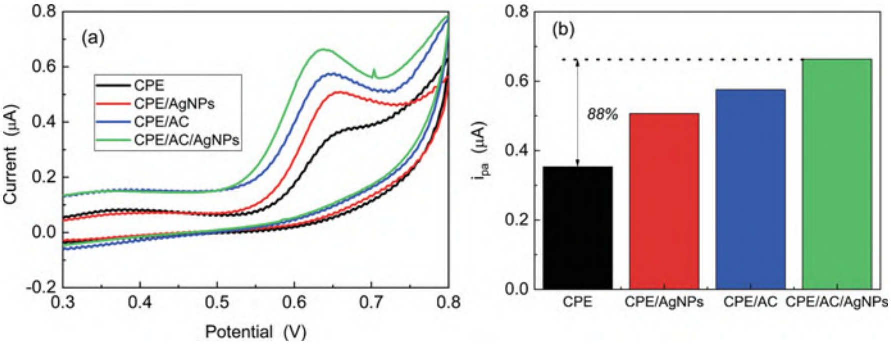

Fig. 10.3 (**a**) Cyclic voltammograms obtained for: CPE, CPE/AgNPs, CPE/AC, and CPE/AC/AgNPs composite in the presence of 35 μmol L^{-1} PMZ in 0.10 mol L^{-1} PBS at pH 7.00. (**b**) Comparison of sensors performance

approximately +0.65 V, which corresponds to the oxidation of sulfur present in the structure, forming promethazine sulfoxide. Analyzing the voltammetric behavior, in Fig. 10.3, it was observed that the PMZ presented a low-intensity oxidation peak when only the CPE was used. Observing the CPE/AC/AgNPs response, there was found a significant increase in the faradaic current at approximately 88% when compared to the CPE under the same analysis conditions.

This could be justified by the fact that the AC, besides having a high surface area and large porosity, also presents good conductivity (Arroyo-Gómez et al. 2018). The use of AgNPs has also contributed to improved sensitivity, justified by the fact that the smaller the particle size, the larger the surface area, thus allowing it to adhere to the AC surface, improving efficiency when applied to sensors (de Lima et al. 2016).

3.3 Kinetic Parameters Evaluation

To obtain information on the kinetic parameters of CPE/AC/AgNPs the influence of the scan rate on the electrochemical oxidation of PMZ was investigated. The results obtained were analyzed by evaluating the anodic peak current (i_{pa}) as a function of the scan rate applied. Figure 10.4a shows that as the scan rate increases, a shift in PMZ oxidation peak potentials to more positive values is observed, as well as an increase in peak current values.

A graph relating the i_{pa} values as a function of the scan rate was constructed in Fig. 10.4b. The result was linear with $R^2 = 0.995$, suggesting that this electrode process is controlled by the adsorption of the electroactive species on the surface electrode. Figure 10.4c shows the relationship between log i_{pa} versus log ν, where the linearity can be verified, obtaining a slope value equal to 0.844. This value indicates that the electron transfer process between the electrode and the solution is controlled by PMZ adsorption (Ghoneim and Tawfik 2004). It can also be verified that in the obtained voltammograms peak is absent during the inverse scan,

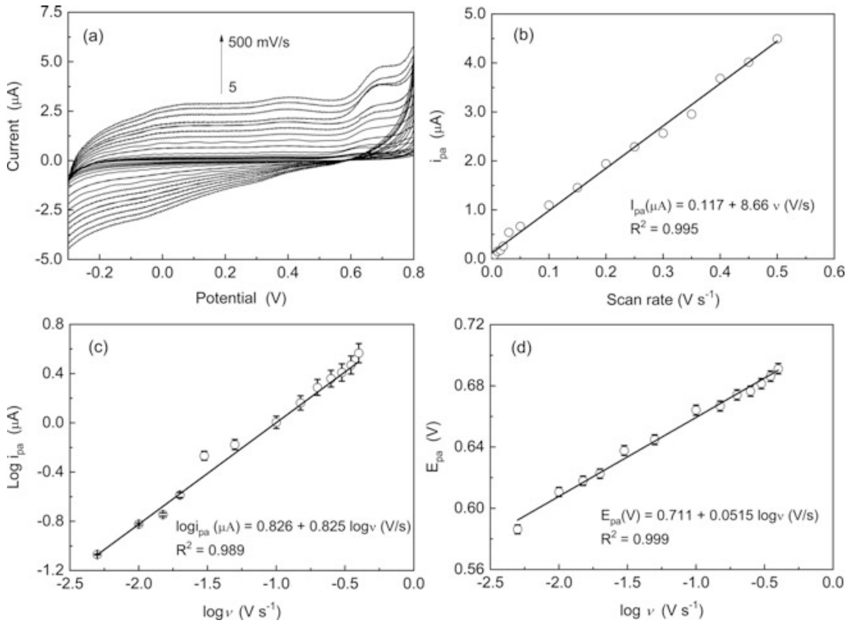

Fig. 10.4 (**a**) Cyclic voltammogram obtained at different scan rates for PMZ; (**b**) peak current dependence as a function of scan rate, (**c**) Log(i_{pa}) versus log(ν), and (**d**) potential dependence as a function of the scan rate logarithm. [PMZ]: 35 μmol L^{-1} in 0.10 mol L^{-1} PBS at pH 7.00

indicating that this process is considered irreversible. This fact can be proven by analyzing Fig. 10.4d, which indicates that the peak potential is linear for log(ν) (Laviron 1979). So, the number of electrons involved in the reaction is 2.

Following this study, we proceeded to calculate the number of electrons involved in the redox process, and, in this sense, the theory demonstrates that the width of the peak's half-height ($\delta_{0.5}$) measured in millivolts (mV) must be equal to 90.6/n for the ideal case (Laviron 1982). This methodology proposed by Laviron is simpler and its application is restricted to adsorbed species, as occurs in this case. In this way, the CPE/AC/AgNPs sensor shows at a low scanning rate (10 mV/s) a $\delta_{0.5}$ around 47 mV. Applying this value in the previously mentioned relation, for the developed sensor a value of n_e was found to be 1.92 electrons ($n_e = 2$).

With the number of electrons calculated, it was possible to estimate the value of the electron transfer coefficient by analyzing the E_{pa} as a function of the log(ν) (Fig. 10.4d) as described in Eq. 10.1. The theory proposed by Laviron (1979) indicates that:

$$S_a = \frac{2.3RT}{\alpha n_e F} \tag{10.1}$$

where: S_a is the angular coefficient, F is Faraday's constant (96485.34 C mol^{-1}), R is the ideal gas constant (8.314 J K^{-1} mol^{-1}), n is the number of electrons, and T is the temperature (298.15 K).

Knowing that the angular coefficient is 0.0515 according to Fig. 10.4d, α was estimated at 0.573. This fact indicates that the studied system is not reversible, as expected, and this corroborates the previous analyzes, where only one oxidation peak and no reduction peak could be observed for PMZ. So, this result implies that this process probably is irreversible.

With the values of α and n calculated, it was also possible to calculate the electron transfer speed of the process according to Eq. 10.2.

$$k = \frac{\alpha n F v}{RT} \tag{10.2}$$

Thus, replacing the values previously found, the estimated value for K at 1 V/s was 44.7 s^{-1}. This result, together with the other factors mentioned, indicates that the proposed sensor has kinetic viability and is considered irreversible in a process controlled by adsorption. Therefore, it is considered that the constructed sensor is viable for the determination of PMZ in tablet forms.

3.4 Optimization of Experimental Conditions

3.4.1 Chemical Modifiers Concentration

To further improve the performance of the proposed sensor, the ratio of the amount of activated carbon (AC) and graphite powder (GFT) that constituted the composite material used to modify the electrode was optimized. For this, the amount of silver nanoparticles was kept fixed at 15% (w/w) and the proportions were varied between 75:10, 70:15, 60:25, and 50:35 (% m/m). Figure 10.5a shows that there was an

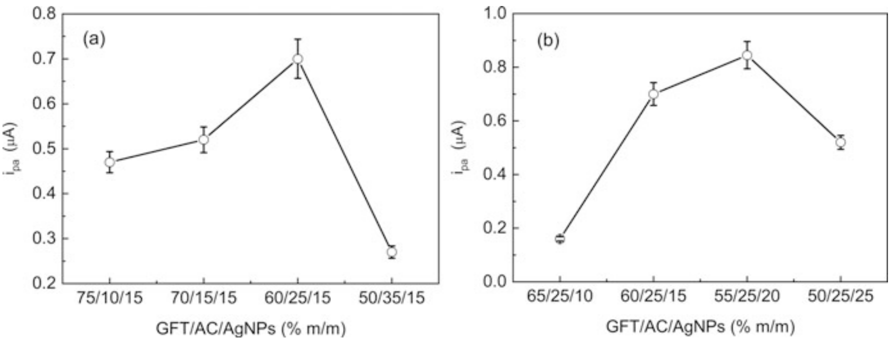

Fig. 10.5 Peak current variation values obtained for different proportions of AC in relation to GFT and AgNPs, where: (**a**) GFT:AC amounts with AgNPs fixed at 15% and (**b**) GFT:AgNPs amounts with AC fixed at 25%. [PMZ] = 35 μmol L^{-1} in 0.10 mol L^{-1} PBS at pH 7.00

increase in current variation up to a ratio of 60:25% (w/w) followed by a decrease at higher concentrations.

Also, it was possible to verify that the sensor sensitivity presented higher values with the increase in the percentage of AC used, as expected, since the AC has a high surface area, and large porosity, allowing a larger contact area between the sensor and the analyte, and good conductivity. However, for AC amounts greater than 25%, relative to the amount of GFT, there was a loss of sensitivity of the proposed sensor, and material leaching may have occurred. It is also known that there is a minimum amount of graphite required in the carbon paste composition since graphite acts as a support for other modifiers so that the conductivity of the sensor is not affected.

Subsequently, the amount of AgNPs was evaluated along with the carbonaceous material that would facilitate the electron transfer process between the electrode-solution interface (de Lima et al. 2016). For this, the amount of carbonaceous material (in this case, AC) was kept fixed at 25% and the amount of AgNPs was evaluated from 10–25% (% w/w). Figure 10.5b shows that the best amount of AgNPs in the carbon paste was 20%. Such behavior is expected because as the amount of AgNPs increases, this material is likely to promote better electron transfer as nanometric materials increase the contact surface between the electrode and the solution. For values lower than this, the lower i_{pa} values may be related to the amount of AgNPs, which is inadequate to promote electron transfer in the PMZ oxidation process.

On the other hand, for amounts greater than 20%, there is a decrease in current variation, which implies lower sensor sensitivity, and this may be related to the possible blockage of AC pores by AgNPs, reducing the surface area and consequently the faradaic current, which may be hindering the transport of electrons. An observed fact is also that a very high concentration of nanoparticle colloidal suspension leads to a loss of material by leaching.

3.4.2 pH Studies

The electrolyte pH is a parameter of extreme importance in the chemical analysis since it is necessary to know if the molecule is protonated or deprotonated in the medium. Thus, the influence of pH from 4.0–8.0 on the oxidation PMZ was studied.

Figure 10.6a shows that i_{pa} values increased linearly until pH 7.00. Above this pH there was a decrease in sensitivity, indicating that the concentration of OH^- ions in the solution negatively affects the oxidation of PMZ (Alizadeh and Akhoundian 2010). Hence, the optimized value was pH 7.00, a condition used for all subsequent studies.

Figure 10.6b shows the influence of pH on the anodic peak oxidation potential of PMZ where a linear relationship is observed. This behavior is explained by assuming that protons also participate in the PMZ oxidation process. The slope obtained was -0.035, which is about half for a Nernstian system(-0.059). So, the number of protons involved in the electrochemical oxidation of PMZ is half the number of electrons (Chen et al. 2013). This fact can be corroborated with the PMZ reaction mechanism proposed by Honarmand et al. (2016) in Fig. 10.6c, where promethazine hydrochloride is oxidized in more than one step, involving two electrons and only

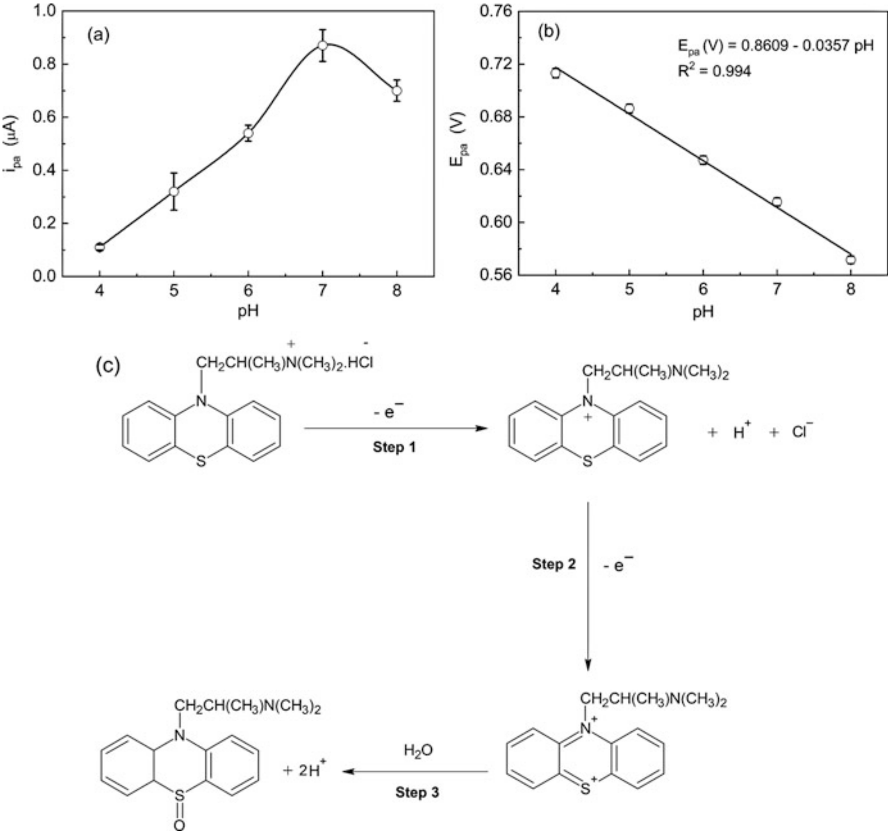

Fig. 10.6 (**a**) Peak current values obtained by the influence of pH in the PHZ oxidation and (**b**) relationship between pH and cathodic peak potential for the reduction of PHZ, where (PHZ): 35 μmol L^{-1} in 0.10 mol L^{-1} phosphate buffer. (**c**) PMZ oxidation mechanism proposed by Honarmand et al. (2016) which was reproduced with permission conveyed through Copyright Clearance Center, Inc., License Number 5293821484331 (Ebrahim et al. 2016)

one proton. In the first stage, a nitrogen atom is removed to form a stable radical cation (step 2), which is then oxidized to promethazine sulfoxide through the hydrolysis reaction of the molecule (step 3).

3.4.3 Ionic Strength Effect

To investigate the influence of ionic strength on the electrochemical response of PMZ, PBS buffer solutions were prepared varying the concentration from 0.025–0.200 mol. L^{-1} keeping the pH at 7.00. The results obtained are presented in Table 10.1.

Analyzing the results, it was concluded that the 0.05 mol L^{-1} concentration generated the highest sensitivity for the proposed sensor. Since the supporting electrolyte has as goal to transport the electroactive species charges to keep the

Table 10.1 Influence of the PBS buffer (at pH 7.00) concentration on the i_{pa} values obtained for the electrochemical oxidation of 35 μmol L^{-1} PMZ

Electrolyte (mol L^{-1})	Δi_{pa} (μA)
0.025	0.62
0.050	0.81
0.100	0.73
0.150	0.48
0.200	0.22

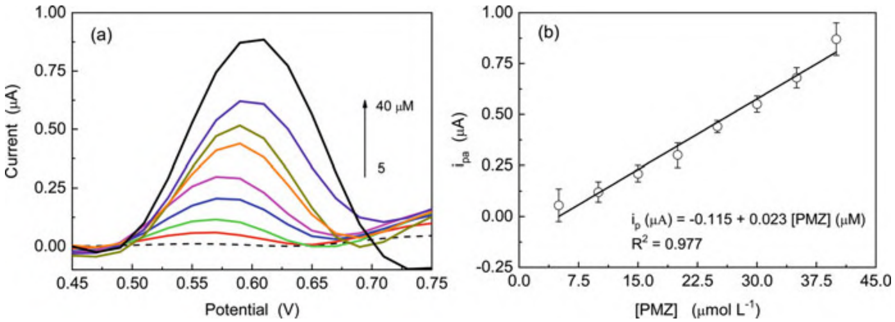

Fig. 10.7 (**a**) VPD obtained for different concentrations of PMZ with additions of 5–40 μmol L^{-1} of PMZ in 0.05 mol L^{-1} PBS buffer at pH 7.00, and (**b**) calibration curve

charge number constant in the solution, the fact that the 0.05 mol L^{-1} concentration presented the highest value can be explained because more dilute solutions may compromise the system due to insufficient load carriers. Alternatively, for much more concentrated solutions (above 0.05 mol L^{-1}), excess ions also affect sensitivity, as they can compete with the analyte, decreasing the electrochemical signal.

3.5 Performance of Electrochemical Sensor

DPV can be considered one of the most important for the determination of electroactive species since it consists of the application of pulses. Therefore, the current is measured before and after the application of the differential pulse and the value obtained is the subtraction of the second by the first. It is a more sensitive technique when compared to the cyclic voltammetry technique (Pacheco et al. 2013).

Figure 10.7a shows the voltammograms after successive additions of 5–40 μmol L^{-1} of PMZ, where the calibration curve obtained can be seen in Fig. 10.7b.

Validation of analytical processes is of fundamental importance for the analysis of any substance, as it is necessary to ensure that the proposed methodology is accurate and sensitive, presents a good linear response range, and is stable for the proposed analyses. Based on these aspects, the method validation was performed according to the Brazilian National Health Surveillance Agency (Agência Nacional de Vigiância Sanitária - ANVISA) standards for drug analysis (ANVISA 2017). So, from the analytical curve constructed, important parameters were obtained, such as linear response range, sensitivity, the limit of detection, and the limit of quantification.

As a brief explanation, the linear response range can be determined using the analyte concentration range in which the method can be accurately applied. Sensitivity can be described as the smallest value distinguished between two close concentrations. The LOD indicates the lowest detectable concentration but is not precisely quantifiable. The LOQ reports the lowest concentration of the quantifiable analyte (Brito et al. 2003; Armbruster and Pry 2008).

Analyzing the analytical curve obtained by VPD (Fig. 10.7b), a linear range from 5–40 μmol L^{-1} with the sensitivity of 0.023 μA L μmol L^{-1} was found. LOD and LOQ values were calculated as 1.30 and 4.20 μmol L^{-1}, respectively. The values obtained are acceptable when compared to other works involving the electrochemical analysis of PMZ, as can be seen in Table 10.2. The CPE/AC/AgNPs show relevant characteristics such as ease of preparation, sensibility for the PMZ detection, stability, and regeneration capacity, which allows the same electrode to be used in several measures, thus reducing the time analysis.

Table 10.2 Comparison of the analytical performance of the proposed method with other electrochemical sensors used for promethazine detection

Sensor	Technique	Linear range (μM)	LOD (μM)	Sample	References
BDD[a]	SWAV[b]	0.596–4.76	0.0266 and 0.0461	Commercial formulations	Ribeiro et al. (2008)
MIP[c]	PSA[d]	0.5–100,000	0.1	Pharmaceutical and serum	Alizadeh and Akhoundian (2010)
MWCNT/GCE[e]	LSV[f]	0.05–400	0.01	Drug, human serum, and urine	Xi et al. (2011)
PNR/CPE[g]	SWV[h]	1.0–1000.	0.20	Tablets	Gu et al. (2012)
MWCN/SN/DNA[i]	SWV[h]	20–100	5.90	Pharmaceutical	Marco et al. (2013)
Au-NPs/CPE[j]	DPV[k]	2.0–225.0	0.0648	Pharmaceutical and urine	Honarmand et al. (2014)
rGO-GCE[l]	Amp[m]	1.99–1030	0.199	Pharmaceutical	Felix et al. (2015)
MPSI-au SAM[n]	DPV[k]	1.0–240	0.00246	Urine and blood serum	Honarmand et al. (2016)
GCE-Ni-Bi_2S_3[o]	Amp[m]	0.001–163.17	0.0004	Human serum and urine	Sakthivel et al. (2019)
Graphite/MIP[p]	SWV[h]	0.004–0.4 and 0.4–7.0	0.0014	Plasma	Akhoundian and Alizadeh (2020)
CW/CGE[q]	DPV[k]	0.01–436	0.0159	Lake water and commercial tablet	Alagumalai et al. (2020)

(continued)

Table 10.2 (continued)

Sensor	Technique	Linear range (μM)	LOD (μM)	Sample	References
FeMo NPs/GCE[r]	DPV[k]	0.01–68.65	0.01	Lake water and commercial tablet	Arumugam et al. (2020)
*f*MWCNT-PEI/GCE[s]	SWV[h]	0.497–5.03	0.231	Pharmaceutical	de Oliveira et al. (2020)
AuNP-GrNP/GCE[t]	AdSV[u]	0.001–1.0 and 1.0–10	0.0004	Biological fluids and forensic	Promsuwan et al. (2020)
CPE/AC/AgNPs[v]	DPV[k]	5.0–40.0	1.30	Pharmaceutical samples	This work.

[a]**BDD:** boron-doped diamond electrode; [b]**SWAV:** square wave adsorptive voltammetry; [c]**MIP:** molecularly imprinted polymer; [d]**PSA:** potentiometry; [e]**MWCNT/GCE:** multiwall carbon nanotube modified glassy carbon electrode; [f]**LSV:** linear sweep voltammetry; [g]**PNR/CPE:** poly(neutral red) modified carbon paste electrode; [h]**SWV:** square wave voltammetry; [i]**MWCN/SiAlNb/DNA:** multiwall carbon nanotubes paste, and an inorganic material based on silica – $SiO_2/Al_2O_3/Nb_2O_5$ with DNA; [j]**Au-NPs/CPE**: carbon paste electrode modified with gold nanoparticles; [k]**DPV:** differential pulse voltammetry; [l]**rGO-GCE:** glassy carbon electrode modified with reduced graphene oxide; [m]**Amp:** amperometry; [n]**MPSI-Au SAM:** gold electrode modified with self-assembled monolayer of bis-N-(2-mercaptophenyl) salicylaldimine; [o]**GCE-Ni-Bi_2S_3:** glassy carbon electrode modified with nickel-doped bismuth sulphide; [p]**graphite/MIP:** carbon paste electrode modified with nano-sized molecularly imprinted polymer; [q]**CW/CGE:** glassy carbon electrode modified with structured cobalt tungstate; [r]**FeMo NPs/GCE:** FeMo NPs modified glassy carbon electrode; [s]**fMWCNT-PEI/GCE:** polyethylenimine-functionalized multiwalled carbon nanotubes/glassy carbon electrode; [t]**AuNP-GrNP/GCE:** gold nanoparticle-graphene nanoplatelet–modified glassy carbon electrode; [u]**AdSV:** adsorptive stripping voltammetry; [v]**CPE/AC/AgNPs:** carbon paste electrode modified with activated carbon and silver nanoparticles

3.6 Application in Pharmaceutical Samples

After plotting the analytical curve and evaluating all the necessary parameters to prove that the proposed sensor is applicable in Phenergan® tablets, where a 1.0 mmol L^{-1} solution containing one of these tablets was prepared, it was macerated until a fine homogeneous powder was obtained. This stock solution was diluted to concentrations of 15, 30, and 45 μmol L^{-1} to determine the concentration of PMZ in the tablet.

Table 10.3 shows the results obtained for the determination of PMZ in Fernegan tablets for each of the concentrations analyzed. Addition and recovery studies showed values between 98.4 and 101.4% for CPE/AC/AgNPs.

Evaluating the results obtained in the determination of PMZ using the CPE/AC/AgNPs presented a relative standard deviation and relative error values below 5%, which can ensure that the results were acceptable, and can be considered a promising alternative. For application in pharmaceutical samples such as Phenergan®, the sensor had low detection and quantification limits, simplicity in preparation and application, low cost of analysis for using financially accessible equipment and materials, and fast response.

Table 10.3 Determination of PMZ in Fenergan tables using CPE/AC/AgNPs

[PMZ] added (μmol L^{-1})	[PMZ] found (μmol L^{-1})	Recovery (%)	ER (%)
15	15.21 ± 0.25	101.4	1.41
30	30.65 ± 0.21	102.2	2.03
45	44.27 ± 0.43	98.4	1.62

4 Conclusions

The proposed electrochemical sensor can be considered as an alternative method for the determination of promethazine in pharmaceutical formulations, such as Phenergan® tablets, using the differential pulse voltammetry technique. The CPE/AC/AgNPs has advantages when compared to unmodified electrodes, where a considerable increase in i_{pa} values was observed, which can be attributed to the conductive properties of activated carbon. We can also emphasize that, after the optimization of the main experimental parameters of analysis, it was possible to notice an increase in the sensitivity of the sensor, obtaining a linear range, limits of detection, and quantification satisfactory when compared to some studies described in the literature. Based on these aspects, the validation of the method was carried out following the rules of ANVISA (Brazil).

Considering all the factors mentioned, it was possible to apply the electrochemical sensor developed for the determination of PMZ in pharmaceutical samples, which resulted in good sample recovery values, making the sensor viable for this purpose. In addition, we can consider that the analysis methodology is fast and easy to perform, presenting sufficient sensitivity for the proposed analyses. The working electrode can be easily prepared and regenerated, being a good alternative for the electrochemical determination of promethazine.

Acknowledgments The authors gratefully acknowledge financial support from Fundação de Amparo à Pesquisa do Estado de Minas Gerais (FAPEMIG) and Conselho Nacional de Desenvolvimento Científico e Tecnológico (CNPq), INCT-DATREM (465571/2014-0). This study was financed in part by Coordenação de Aperfeiçoamento de Pessoal de Nível Superior – Brasil (CAPES) – Finance Code 001.

References

Akhoundian M, Alizadeh T (2020) In situ voltammetric determination of promethazine on carbon paste electrode modified with Nano-sized molecularly imprinted polymer. Anal Bioanal Electrochem 12:1014–1024

Akram M, Anwar S, Kabir-ud-Din (2019) Biophysical investigation of promethazine hydrochloride binding with micelles of biocompatible gemini surfactants: combination of spectroscopic and electrochemical analysis. Spectrochim Acta Part A Mol Biomol Spectrosc 215:249–259. https://doi.org/10.1016/j.saa.2019.02.082

Alagumalai K, Balamurugan M, Chen S-M, Selvaganapathy M (2020) One-pot engineering of novel cashew like cobalt tungstate; dynamic electrocatalyst for the selective detection of promethazine hydrochloride. Microchem J 159:105381. https://doi.org/10.1016/j.microc.2020.105381

AlAqad KM, Suleiman R, Al Hamouz OCS, Saleh TA (2018) Novel graphene modified carbon-paste electrode for promazine detection by square wave voltammetry. J Mol Liq 252:75–82. https://doi.org/10.1016/j.molliq.2017.12.108

Alizadeh T, Akhoundian M (2010) A novel potentiometric sensor for promethazine based on a molecularly imprinted polymer (MIP): the role of MIP structure on the sensor performance. Electrochim Acta 55:3477–3485. https://doi.org/10.1016/j.electacta.2010.02.010

ANVISA (2010) Farmacopeia Brasileira, 5ª edição. Brazil, São Paulo

ANVISA (2017) Resolução RDC Nº 166, de 24 de julho de 2017 – Imprensa Nacional. In: Diário Of. da União. https://www.in.gov.br/materia/-/asset_publisher/Kujrw0TZC2Mb/content/id/19194581/do1-2017-07-25-resolucao-rdc-n-166-de-24-de-julho-de-2017-19194412. Accessed 1 Dec 2020

Armbruster DA, Pry T (2008) Limit of blank, limit of detection and limit of quantitation. Clin Biochem Rev 29(Suppl 1):S49–S52

Arroyo-Gómez JJ, Villarroel-Rocha D, de Freitas-Araújo KC et al (2018) Applicability of activated carbon obtained from peach stone as an electrochemical sensor for detecting caffeine. J Electroanal Chem 822:171–176. https://doi.org/10.1016/j.jelechem.2018.05.028

Arumugam B, Muthukutty B, Chen S-M et al (2020) Ultrasonication-aided synthesis of nanoplates-like iron molybdate: fabricated over glassy carbon electrode as an modified electrode for the selective determination of first generation antihistamine drug promethazine hydrochloride. Ultrason Sonochem 66:104977. https://doi.org/10.1016/j.ultsonch.2020.104977

Beluomini MA, da Silva JL, de Sá AC et al (2019) Electrochemical sensors based on molecularly imprinted polymer on nanostructured carbon materials: a review. J Electroanal Chem 840:343–366. https://doi.org/10.1016/j.jelechem.2019.04.005

Bosáková Z, Kloučková I, Tesařová E (2002) Study of the stability of promethazine enantiomers by liquid chromatography using a vancomycin-bonded chiral stationary phase. J Chromatogr B 770:63–69. https://doi.org/10.1016/S0378-4347(01)00559-X

Brett CMA (2001) Electrochemical sensors for environmental monitoring. Strategy and examples. Pure Appl Chem 73:1969–1977. https://doi.org/10.1351/pac200173121969

Brito NM, De Amarante Junior OP, Polese L, Ribeiro ML (2003) Validação de métodos analíticos: estratégia e discussão. Pestic Rev Ecotoxicologia e Meio Ambient 13. https://doi.org/10.5380/pes.v13i0.3173

Chen M, Meng Y, Zhang W et al (2013) β-Cyclodextrin polymer functionalized reduced-graphene oxide: application for electrochemical determination imidacloprid. Electrochim Acta 108:1–9. https://doi.org/10.1016/j.electacta.2013.06.050

de Lima CA, Santana ER, Piovesan JV, Spinelli A (2016) Silver nanoparticle-modified electrode for the determination of nitro compound-containing pesticides. Anal Bioanal Chem 408:2595–2606. https://doi.org/10.1007/s00216-016-9367-5

de Oliveira RC, Sousa CP, Morais S et al (2020) Polyethylenimine-multi-walled carbon nanotubes/glassy carbon electrode as an efficient sensing platform for promethazine. J Electrochem Soc 167:107506. https://doi.org/10.1149/1945-7111/ab995f

Donini CA, da Silva MKL, Simões RP, Cesarino I (2018) Reduced graphene oxide modified with silver nanoparticles for the electrochemical detection of estriol. J Electroanal Chem 809:67–73. https://doi.org/10.1016/j.jelechem.2017.12.054

Ebrahim H, Mohammad HM, Mojtaba H, Hossein M (2016) Electro-oxidation study of promethazine hydrochloride at the surface of modified gold electrode using molecular self-assembly of a novel bis-thio Schiff base from ethanol media. J Mol Liq 216:429–439

Felix FS, Ferreira LMC, Vieira F et al (2015) Amperometric determination of promethazine in tablets using an electrochemically reduced graphene oxide modified electrode. New J Chem 39:696–702. https://doi.org/10.1039/C4NJ00887A

Ghoneim MM, Tawfik A (2004) Assay of anti-coagulant drug warfarin sodium in pharmaceutical formulation and human biological fluids by square-wave adsorptive cathodic stripping voltammetry. Anal Chim Acta 511:63–69. https://doi.org/10.1016/j.aca.2004.01.037

Gu L, Zhang M, He Y (2012) Electrochemical behaviors and determination of promethazine hydrochloride on poly (neutral red) modified carbon paste electrode. Chinese J Pharm Anal 32:1443–1447

Hamzah HH, Shafiee SA, Abdalla A, Patel BA (2018) 3D printable conductive materials for the fabrication of electrochemical sensors: a mini review. Electrochem Commun 96:27–31. https://doi.org/10.1016/j.elecom.2018.09.006

Hanrahan G, Patil DG, Wang J (2004) Electrochemical sensors for environmental monitoring: design, development and applications. J Environ Monit 6:657–664. https://doi.org/10.1039/B403975K

Honarmand E, Motaghedifard MH, Ghamari M (2014) Electroanalytical approach for determination of promethazine hydrochloride on gold nanoparticles-incorporated carbon paste electrode as a nanosensor. RSC Adv 4:35511–35521. https://doi.org/10.1039/C4RA02712D

Honarmand E, Motaghedifard MH, Hadi M, Mostaanzadeh H (2016) Electro-oxidation study of promethazine hydrochloride at the surface of modified gold electrode using molecular self assembly of a novel bis-thio Schiff base from ethanol media. J Mol Liq 216:429–439. https://doi.org/10.1016/j.molliq.2015.12.094

Idris AM, Assubaie FN, Sultan SM (2006) Chemometric optimization of a SIA promethazine hydrochloride assay method. Microchem J 83:7–13. https://doi.org/10.1016/j.microc.2005.12.004

Jadon N, Jain R, Sharma S, Singh K (2016) Recent trends in electrochemical sensors for multianalyte detection – a review. Talanta 161:894–916. https://doi.org/10.1016/j.talanta.2016.08.084

Jana NR, Gearheart L, Murphy CJ (2001) Wet chemical synthesis of silver nanorods and nanowires of controllable aspect ratio. Chem Commun:617–618. https://doi.org/10.1039/B100521I

Karimi-Maleh H, Karimi F, Alizadeh M, Sanati AL (2020) Electrochemical sensors, a bright future in the fabrication of portable kits in analytical systems. Chem Rec 20:682–692. https://doi.org/10.1002/tcr.201900092

Laviron E (1979) General expression of the linear potential sweep voltammogram in the case of diffusionless electrochemical systems. J Electroanal Chem Interfacial Electrochem 101:19–28. https://doi.org/10.1016/S0022-0728(79)80075-3

Laviron E (1982) Voltammetric methods for the study of adsorbed species. In: Bard AJ (ed) Electroanalytical chemistry, vol 12. Marcel Dekker, New York, pp 53–157

Marco JP, Borges KB, Tarley CRT et al (2013) Development of a simple, rapid and validated square wave voltametric method for determination of promethazine in raw material and pharmaceutical formulation using DNA modified multiwall carbon nanotube paste electrode. Sensors Actuators B Chem 177:251–259. https://doi.org/10.1016/j.snb.2012.11.005

Maurya N, ud din Parray M, Maurya JK et al (2018) Interaction of promethazine and adiphenine to human hemoglobin: a comparative spectroscopic and computational analysis. Spectrochim Acta Part A Mol Biomol Spectrosc 199:32–42. https://doi.org/10.1016/j.saa.2018.03.023

McClure RA, Chumbley CW, Reyzer ML et al (2013) Identification of promethazine as an amyloid-binding molecule using a fluorescence high-throughput assay and MALDI imaging mass spectrometry. NeuroImage Clin 2:620–629. https://doi.org/10.1016/j.nicl.2013.04.015

Melo MA Jr, Santos LSS, Gonçalves M, do C, Nogueira AF (2012) Preparação de nanopartículas de prata e ouro: um método simples para a introdução da nanociência em laboratório de ensino. Química Nov 35:1872–1878

Pacheco WF, Semaan FS, De Almeida VGK et al (2013) Voltammetry: a brief review about concepts. Rev Virtual Quim 5:516–537. https://doi.org/10.5935/1984-6835.20130040

Partlan E, Ren Y, Apul OG et al (2020) Adsorption kinetics of synthetic organic contaminants onto superfine powdered activated carbon. Chemosphere 253:126628. https://doi.org/10.1016/j.chemosphere.2020.126628

Pereira AC, Santos A de S, Kubota LT (2002) Tendências em modificação de eletrodos amperométricos para aplicações eletroanalíticas. Química 25:1012–1021

Piletsky SA, Turner APF (2002) Electrochemical sensors based on molecularly imprinted polymers. Electroanalysis 14:317–323. https://doi.org/10.1002/1521-4109(200203)

Privett BJ, Shin JH, Schoenfisch MH (2010) Electrochemical sensors. Anal Chem 82:4723–4741. https://doi.org/10.1021/ac101075n

Promsuwan K, Kanatharana P, Thavarungkul P, Limbut W (2020) Subnanomolar detection of promethazine abuse using a gold nanoparticle-graphene nanoplatelet-modified electrode. Microchim Acta 187:646. https://doi.org/10.1007/s00604-020-04616-w

Purohit B, Vernekar PR, Shetti NP, Chandra P (2020) Biosensor nanoengineering: design, operation, and implementation for biomolecular analysis. Sensors Int 1:100040. https://doi.org/10.1016/j.sintl.2020.100040

Ramanavičius A, Ramanavičienė A, Malinauskas A (2006) Electrochemical sensors based on conducting polymer – polypyrrole. Electrochim Acta 51:6025–6037. https://doi.org/10.1016/j.electacta.2005.11.052

Ribeiro FWP, Cardoso AS, Portela RR et al (2008) Electroanalytical determination of promethazine hydrochloride in pharmaceutical formulations on highly boron-doped diamond electrodes using square-wave adsorptive voltammetry. Electroanalysis 20:2031–2039. https://doi.org/10.1002/elan.200804286

Sakthivel R, Kubendhiran S, Chen S-M (2019) Facile one-pot sonochemical synthesis of Ni doped bismuth sulphide for the electrochemical determination of promethazine hydrochloride. Ultrason Sonochem 54:68–78. https://doi.org/10.1016/j.ultsonch.2019.02.013

Saleh TA, Abulkibash AM, Ibrahim AE (2012) Portable system of programmable syringe pump with potentiometer for determination of promethazine in pharmaceutical applications. Saudi Pharm J 20:155–160. https://doi.org/10.1016/j.jsps.2011.08.005

Silveira G, Tarley CRT (2008) Determinação turbidimétrica do antidepressivo amitriptilina em sistema fia explorando a formação do par iônico com lauril sulfato de sódio. Quim Nova 31: 1653–1659

Stradiotto NR, Yamanaka H, Zanoni MVB (2003) Electrochemical sensors: a powerful tool in analytical chemistry. J Braz Chem Soc 14:159–173

Thiyagarajan N, Chang J-L, Senthilkumar K, Zen J-M (2014) Disposable electrochemical sensors: a mini review. Electrochem Commun 38:86–90. https://doi.org/10.1016/j.elecom.2013.11.016

Vanitha Kumari G, Ananth N, Asha et al (2016) Synthesis and characterization of folic acid conjugated silver/gold nanoparticles for biomedical applications. Mater Today Proc 3: 4215–4219. https://doi.org/10.1016/j.matpr.2016.11.099

Vernekar PR, Purohit B, Shetti NP, Chandra P (2021) Glucose modified carbon paste sensor in the presence of cationic surfactant for mefenamic acid detection in urine and pharmaceutical samples. Microchem J 160:105599. https://doi.org/10.1016/j.microc.2020.105599

Vicentini R, Nunes WG, Costa LH et al (2019) Highly stable nickel-aluminum alloy current collectors and highly defective multi-walled carbon nanotubes active material for neutral aqueous-based electrochemical capacitors. J Energy Storage 23:116–127. https://doi.org/10.1016/j.est.2019.01.013

Viol LC de S, Silva FO, Ferreira DL et al (2011) Precipitação seletiva de tamanhos em nanopartículas semicondutoras coloidais de CdTe e CdSe: um estudo por espectroscopia UV-VIS. Química 34:595–600

Wang J (1991) Modified electrodes for electrochemical sensors. Electroanalysis 3:255–259. https://doi.org/10.1002/elan.1140030404

Wang Y, Xu H, Zhang J, Li G (2008) Electrochemical sensors for clinic analysis. Sensors 8: 2043–2081. https://doi.org/10.3390/s8042043

Wei X, Hao Q, Zhou Q et al (2008) Interaction between promethazine hydrochloride and DNA and its application in electrochemical detection of DNA hybridization. Electrochim Acta 53: 7338–7343. https://doi.org/10.1016/j.electacta.2008.04.007

Wei Q, Chen Z, Cheng Y et al (2019) Preparation and electrochemical performance of orange peel based-activated carbons activated by different activators. Colloids Surfaces A Physicochem Eng Asp 574:221–227. https://doi.org/10.1016/j.colsurfa.2019.04.065

Wu S, He Q, Tan C et al (2013) Graphene-based electrochemical sensors. Small 9:1160–1172. https://doi.org/10.1002/smll.201202896

Xi X, Ming L, Liu J (2011) Voltammetric determination of promethazine hydrochloride at a multi-wall carbon nanotube modified glassy carbon electrode. Drug Test Anal 3:182–186. https://doi.org/10.1002/dta.205

Zhao Q, Gan Z, Zhuang Q (2002) Electrochemical sensors based on carbon nanotubes. Electroanalysis 14:1609–1613. https://doi.org/10.1002/elan.200290000

Zhu C, Yang G, Li H et al (2015) Electrochemical sensors and biosensors based on nanomaterials and nanostructures. Anal Chem 87:230–249. https://doi.org/10.1021/ac5039863

Porous Nanostructured Materials for Electroanalytical Applications

11

Nutthaya Butwong

Contents

1 Nanoporous Materials 220
2 Nanoporous Synthesis Method for Electroanalytical Application 221
3 Application of Nanomaterials for Electroanalytical Sensor 221
  3.1 Nanoporous Metals for Electroanalytical Application 223
  3.2 Nanoporous Oxide Compounds for Electroanalytical Application 226
  3.3 Nanoporous Carbon for Electroanalytical Application 229
  3.4 Nanoporous Polymer-based Composites for Electroanalytical Application 232
4 Conclusion and Future Perspectives 235
References 236

Abstract

Nanoporous materials having a porosity of 1–100 nm and excellent functional moieties are unique with high surface area and selective adsorption. Nanomaterials are a subset of porous materials with a high surface-to-volume ratio. The most challenging work is synthesizing a uniform porous structure because the particular electrochemical sensor depends on the uniform size of the pores. This chapter explains the electrochemical application of nanoporous materials, including metal, alloy, metal oxide, carbon, and polymer. In this chapter, the detection mechanisms of the different forms of nanoporous materials and their unique roles are discussed together with their advantages/disadvantages. Different strategies for their functionalization are also emphasized from a sensor development perspective. Finally, the perspective and current challenges of nanoporous metal-based sensing are outlined.

N. Butwong (✉)
Applied Chemistry Department, Faculty of Sciences and Liberal Arts, Rajamangala University of Technology Isan, Nakhon Ratchasima, Thailand

© Springer Nature Singapore Pte Ltd. 2023
U. P. Azad, P. Chandra (eds.), *Handbook of Nanobioelectrochemistry*,
https://doi.org/10.1007/978-981-19-9437-1_11

Keywords

Nanoporous materials · Electrochemical sensor · Nanoporous metals · Nanoporous carbon · Nanoporous polymer

1 Nanoporous Materials

The porous material with a 3D pore size in the range of 1–1000 nm is the nanoporous material (Jiao et al. 2016). The nanoporous materials can be classified into three types in terms of pore size, including micropore (0.2 nm), mesopore (2–5 nm), and macropore (>50 nm). A highly functional surface area per volume is a superior property of nanoporous nanomaterials compared to other nanomaterials. There is the two-pore type which generates nanoporous materials, closed pore and open pore. In comparison, the open pore surface area has a greater surface area, making the open pore a more suitable choice for sorbent, catalyst, and electrochemical applications. Since the pore shape and size mainly affect the conductivity of the nanoporous materials, the homogeneity of the pore is the challenging step for the synthesis of these materials. Although nanoporous nanomaterials have the advantage of having active surface area in the heterogeneous reactions, there are significant obstacles to using these materials in practical applications, such as their pore structure's stability, the analyte's adsorption after use, and the re-treatment.

Nanoporous materials commonly used in electroanalytical applications are shown in Table 11.1. It is primarily the porous properties that make it possible to escalate the specific surface area of the electrochemical sensor for redox species and have a high electron transfer rate. The primary mechanism for determining the analyte is the diffusion control mechanism to generate the faradic current. Therefore, the nanomaterial has to be conductive or semiconductor materials. These are divided into four groups with different advantages and disadvantages, as shown in Table 11.1.

Using electrodes in electrical analytical chemistry and biosensor applications depends on the specific pore size, contact surface area, and analyte reactivity. The selectivity of nanoporous electrodes can be increased by modifying with other nanoporous materials, designing the specific porous size and functionalized groups specific to the target substance.

Table 11.1 Comparison table of the nanoporous materials properties

Material type	Surface area	Catalyst	Chemical stability	Conductivity	Life	Cost
Metal	Low	√	High	High	Long	Medium
Metal oxide	High	√	Excessive	Semiconductor	Long	Medium
Carbon	Medium	–	High	Medium-high	Long	Medium
Polymer	Low	–	Low-medium	Low-medium	Short	High

2 Nanoporous Synthesis Method for Electroanalytical Application

An ideal nanoporous material has homogenous pore size and structure; therefore, the synthesis method is crucial to design their properties to fit the proposal, as shown in Fig. 11.1. The nanoporous material is mainly synthesized using template methods (hard templating and soft templating), template-free, and electrochemical processes (Jérôme and Valange 2017). Hard-templating method uses rigid porous substrates such as silica, zeolite, carbon, or polymer as templates. After the precursor self-assembly on the layer, the templates are removed by thermal treatment or solvent elution. This method can prepare highly uniform structures and even single-crystal materials because the rigid template and the pore structure depend on the form of the template (Polarz and Smarsly 2002). However, this synthetic approach is quite tedious since much effort and various steps are required, such as calcite temperature conditions. Soft-templating method refers to the self-assembled arrangements of structure-directing molecules like surfactants, organic ligands, or block copolymers, leading to mesopores up to 30 nm. This approach's disadvantage is that the resulting nanoporous material is often amorphous because heat treatments resulted in structural collapse. However, eliminating templates in the soft-templating method is more comfortable than a hard-templating process because of their thermodynamic properties. Besides, the use of surfactant, ligand, and block copolymers can facilitate a highly uniform pore (Jérôme and Valange 2017). The template-free method is generated via the salt precursors' thermal decomposition from micrometer-sized polyhedron particles in the gas. Thermal decomposition of inorganic salts such as nitrates, sulfates, carbonates, and oxalates were generally used to synthesize metal oxide powders (Hulicova-Jurcakova et al. 2008). The nanomaterials' pore size is typically in micropore (sub-nanometer) or mesopore (several nanometers) and disorganized shape.

The electrochemical method provides the rough surface of nanoporous materials by varying the oxidation/reduction cycle duration, wave frequency (or sweep rate), and the potential transferring limits. This method can synthesize intrinsic nanoporous materials without using a template. However, it is not very easy to operate, and the types of the selected materials depend on their oxidation potentials. These requirements make the existing nanoporous materials limited on a small scale and cannot be applied more widely. The nanomaterial structures are typically found in the sphere, rod, layers, and bicontinuous shapes.

3 Application of Nanomaterials for Electroanalytical Sensor

Since the structural properties, electrical conductivity, and electron transmission of nanoporous material are related to pore size and shape, they have been used as catalysts rather than sensors in an electrochemical perspective (Menzel et al. 2012). There have been some efforts to introduce nanoporous materials to increase the sensitivity of the measurement in the electrochemical sensors. However, to improve the probe's specificity, functionalizing with other nanomaterials or biomolecules is

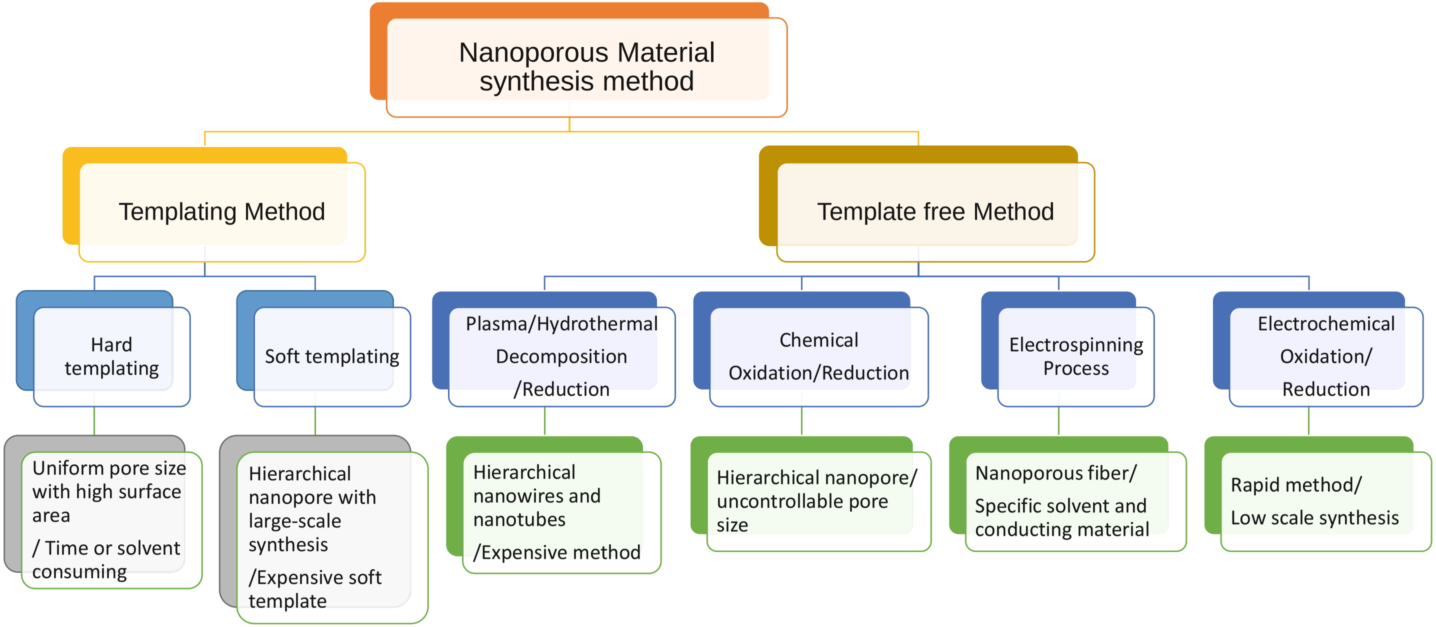
Nanoporous Material synthesis method
Templating Method
Template free Method
Hard templating
Soft templating
Plasma/Hydrothermal Decomposition /Reduction
Chemical Oxidation/Reduction
Electrospinning Process
Electrochemical Oxidation/ Reduction
Uniform pore size with high surface area / Time or solvent consuming
Hierarchical nanopore with large-scale synthesis /Expensive soft template
Hierarchical nanowires and nanotubes /Expensive method
Hierarchical nanopore/ uncontrollable pore size
Nanoporous fiber/ Specific solvent and conducting material
Rapid method/ Low scale synthesis

Fig. 11.1 Summary of synthesis methods for nanoporous metal

still necessary. Here are the summarized applications of nanoporous materials classified based on the materials used as sensor and biosensor electrodes.

3.1 Nanoporous Metals for Electroanalytical Application

The pores in metals are classified into two types: closed and open pore with a porosity between 0.2 and 0.9 (Stanev et al. 2016). The open pore is preferable for the electrochemical application because of its high active surface area to penetrate, electrocatalytic property, low adsorption, and low thermal conductivity (Stanev et al. 2016). The nanoporous metals can be fabricated by alloying/dealloying techniques, either electrochemical or chemical methods. The porosity is evaluated by the dissolution of the minor noble metal in the alloy. Most of Au's binary or tertiary alloy with other noble metals, including Pt, Ag, Pd, Cu, and Al, have been used as the starting alloy (Zhang and Li 2012). The cracking during the dealloying process to generate the pore is the problem, but annealing can reduce these effects. Dealloying plays an essential role in the pore structure, while alloy composition strongly affects the porosity. The chemical dealloying immerges the alloy in the concentrated mineral acids such as nitric acid and sulfuric acid (Summerlot et al. 2011). The corrosion of the most minor noble consistent is the mechanism to generate the pore. Time, temperature, and acid concentration are the most critical factors to control the pore size. Electrochemical dealloying can be processed by immerging the alloy as suitable electrolytes and applying the specific potential in a period. The pore size and surface area are strongly dependent on the condition used. The critical parameters for electrodeposition are as follows: the substrate has to be a conductive material. The thickness and configuration of nanoporous on the electrode surface depend on the applied potential and time used. The film, wire, and ribbon of nanoporous can be prepared in this method. The morphology of nanoporous alloy is shown in Fig. 11.2.

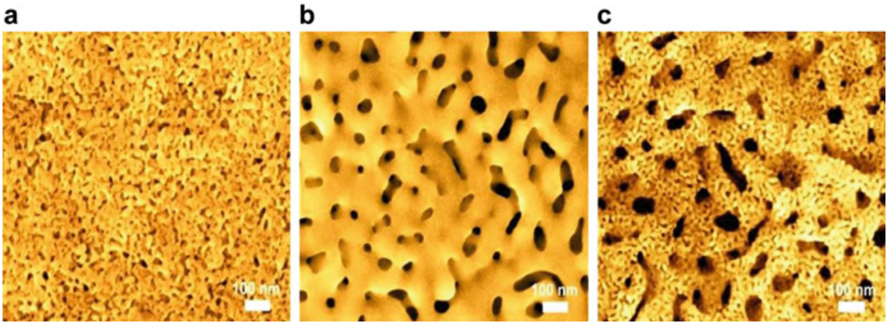

Fig. 11.2 SEM images of the nanoporous AuAg alloy with an average nanopore (**a**), roughened nanoporous AuAg alloy with a roughened pore size of ~80–100 nm (**b**), and SEM image of the ordered nanoporous Au with ~5–20 nm small pores on the ~80–100 nm ligaments (**c**) (Taken from Guo et al. (2016))

Nanoporous metals have an electron-rich surface area which provided the electrocatalytic ability to oxidize small organic molecules such as organic acids, alcohols, and biomolecules. Platinum is intensively used in catalysts among conductive metals, because it is the most stable noble metal (Xu and Zhang 2014). At the same time, gold is widely used in enzymatic sensors because of its biocompatibility via forming covalent bonds with an amino group on protein moieties. In general, nanoporous metals have been used as electrodes or modified on carbon electrodes (van der Zalm et al. 2020). Most nanoporous metal applications in electroanalytical applications are nonenzymatic electrochemical sensors, because they have catalytic properties toward analytes (Collinson 2013). The roughness of nanoporous Pt can reduce the adsorption of interferences occurring on the smooth Pt electrode (Kim et al. 2013). Therefore, most nanoporous Pt applications are the nonenzymatic sensor of H_2O_2 and glucose (Liu et al. 2017) (McCormick and McCrudden 2020). However, the oxidation peak of the glucose still has interference from ascorbic acid (AA).

The direct electrochemical method using a nanoporous Pt electrode had adsorption and a slow electron transfer rate as obstacles; nanoporous Pt thin films modified by other conducting materials can solve this problem. For an instant, nanoporous Pt-modified carbon electrodes provided a better result (Park et al. 2010). The faradic current of glucose oxidation is related to the kinetically controlled reaction. Therefore, the chronoamperometric method can be used for glucose determination with sub-millimolar sensitivity. Kim et al. (2013) revealed the dealloying of PtSi to fabricate nanoporous Pt electrodes by sputtering Pt_xSi_{x-1} on the Pt, then dealloying Si. The pore structure of nanoporous Pt was opened and cylindrical. The sensitivity of glucose determination increased with increasing Pt roughness. The signal was still stable after cleaning in the H_2SO_4 solution. However, the glucose assay limit was as low as the micromolar (50 μM), AA, and uric acid (UA) continued to interfere with the measurement.

Au is an ideal material for biosensor electrodes because of its biocompatibility and chemical stability. Nanoporous Au has been used as the electrode of the nonenzymatic sensors of AA, UA, dopamine (DA), glucose, and H_2O_2 as the application of Pt (Su et al. 2013). However, a few works demonstrated the nanoporous Au electrodes to analyze macromolecules via functionalized them with amino moieties. The small nanopores in the 3D open framework of Au can limit the transport of large biomolecules. Therefore, it can minimize the accessibility of the inner sides by permitting only a tiny redox analyte to access the pore. The electrochemical synthesis method via anodizing Au in anionic surfactant provided the ordered nanoporous Au. For example, the anionic surfactant assisted the reducing of intermediate product adsorption on the electrode surface. The nanoporous Au provided a highly active surface area. Therefore, the sensitivity of quercetin (QU) detection was two times higher than that of the bare electrode (Nasrollahi et al. 2020). Another work is the modified nanoporous Au on the indium tin oxide (ITO) by dealloying AuCu in 0.5 M H_2SO_4 and used for As (III) determination (Chen et al. 2020). The determination response increased three times with no significant Cu(II) interference after being modified by nanoporous Au. These may occur due to the difference in nanoporous Au's metallic formation rate. A three-dimensional (3D) bicontinuous nanoporous Au has also been used as an electrochemical biosensor to detect DA by differential pulse voltammetry (DPV). The fabrication was processed by electrodepositing palladium nanoparticles (Pd) onto the nanoporous Au wire. The decorated Pd on Au wire provides great superiority in detection. Besides, the proposed DA biosensor had good stability, reproducibility, reusability, and selectivity (Yi et al. 2017).

Due to the price limit, the other metal nanomaterials with lower electrical conductivity, such as Ag (Zhao et al. 2020b) and Cu (Regiart et al. 2020), were introduced. Zhao et al. (2020b) revealed nanoporous Ag electrode fabrication by pulse laser deposition and used as the electrode for H_2O_2 determination. Because of its high surface area, the nanoporous Ag provided a higher sensitivity for H_2O_2 determination than another form of Ag nanoparticles electrode. Apart from Ag, the microelectrode of nanoporous Cu was fabricated by electrodeposition and used as a glyphosate (Glyp) sensor. The Cu film structure is influenced by potential and time. The reduction of CuO peak at -0.2 V was directly linear with the concentration of Glyp, resulting from the formation of Cu(II)-Glyp complex.

Since the stability of nanoporous metal is their primary obstacle, dealloying conditions are the crucial rule of using them. In recent years, nanoporous alloys have been used to develop stability in conditions of use (Qiu et al. 2019). Although their high electrocatalytic activity affects the conductivity, the pore size is not stable in alkaline and acidic solutions (Regiart et al. 2020). The major drawback of using nanoporous metals is their chemical stability. Alloying of metals can solve this problem and also increase the electrocatalytic activity of the probe. Pt and Au alloys with cheaper transition metals can reduce the number of noble metals, improve their stability and also catalytic activity. For instance, the bimetallic alloy of the sponge-like structure of PtNi is fabricated by dealloying trimetallic PtNiAl alloy. Nanoporous PtNi is stable for 2 weeks and showed sensitivity towards ethanol and H_2O_2 with no significant interference from glucose, AA, UA, and DA (Xu et al. 2013). Nanoporous PtAu was also used as the H_2O_2 and glucose sensor. The uniform ligament of nanoporous PtAu was obtained by dealloying Pt4Au16Cu80 foil. Although nanoporous PtAu showed better sensitivity than PtNi, it was found that AA still severely interferes in detecting glucose (Wang et al. 2014). Because of Cu alloy's reasonable cost and electrocatalytic property, it has been considered an alternative nanoporous material to replace the noble metal alloy. Nanoporous PdCu with a 3D bicontinuous nanosponge structure was synthesized by dealloying PdCuAl alloy. Although nanoporous PdCu shows stability and selectivity towards H_2O_2 and glucose detections, the sensitivity was lower than Au- and Pt-based alloys (Yang et al. 2017). Liu et al. (2019) synthesized the nanoporous CuAg film from the CuAgZn dealloying. A small amount of Ag in the alloy induced the agglomeration of the alloy and enhanced the glucose's electrooxidation. The nanoporous CuAg provided long-term stability (4 weeks). Nanoporous CuCr was fabricated by co-sputtering on polyamide film and dealloying of Cu by dipping the film in 22.5%(v/v) HNO_3. The CuCr alloy film exhibited an average pore size between 20 and 40 nm. The CuCr alloy electrode was used as the moisture sensor in the oil sample using the electrostatic capacity transient method. The amount of Cu dealloying strongly affected the moisture detection response (Yoshii et al. 2019).

3.2 Nanoporous Oxide Compounds for Electroanalytical Application

The well-known oxide compounds with nanoporous such as silica, alumina, zeolite, and metal oxide have been used in verities applications because of their high relevance in catalysis, stability, and cheaper than metals. Zeolite and silica are widely used as catalyst substrates and sorbents (Liang et al. 2017). In comparison, nanoporous metal oxides are widely used as electrocatalysts for the production of H_2 (Sapountzi et al. 2017), energy storage (Salunkhe et al. 2017), biodiesel production (Sharma et al. 2018), and also gas sensors (Mirzaei et al. 2019). Transition metal oxides have been interested in electrochemical applications because of their variable redox species and catalytic and magnetic properties. Nanoporous oxide compound materials possess large surface areas, high sensitivity to the analyte, heterogeneous catalytic properties, and chemical stability in the environment. These materials' structure strongly affects their catalytic performance. To control the growth of transition metal oxide, the metal and oxide precursor are the critical rule. The sol-gel process with surfactants to generate the structure and calcine over 600 °C is the simple method to synthesize oxide compounds. Most frameworks begin to crystalline in the sol-gel process and restructure the pore and size structure after calcination (Li et al. 2015b), which is time-consuming. The different shapes of metal oxide are shown in Fig. 11.2. This obstacle can be overcome by using ligands instead of surfactants to generate the inorganic framework, especially transition metal oxides. The nanoporous MgO (Dong et al. 2015) was synthesized via the hydrothermal method at low temperatures. It was found that the bandgap energy of MgO can be reduced by decreasing the synthesis temperature. The shape and size of the pore are uniform (450 nm). The plasma processing with ligands such as porphyrin and phthalocyanine recently provided a large area scale of CuO, Fe_2O_3, TiO_2, and ZnO (Obrero et al. 2020).

The electrodeposition in hydroxide electrolyte and applied voltage was also used for metal oxides (Biswal et al. 2019). Even though their morphology is highly controlled, the synthetic yield is relatively small, making them difficult to apply on a large scale. Metal oxides such as alumina, silica, zeolite, and titanium dioxide are often used as a support in a catalyst rather than a direct electrode in electrochemical applications due to its low electrical conductivity as with metals, making most of the work used in the form of composite materials.

Some applications use these materials as direct electrodes (Nasir et al. 2018) and (Chen et al. 2017). Nanoporous MgO (Dong et al. 2015) was modified on GCE via dispersed in Nafion before dropping on the GCE surface and evaluated as the nonenzymatic H_2O_2 sensor. The oxidation peak of H_2O_2 was detected at +0.9 V, occasioning little significant interference from AA, UA, and DA. The anatase nanoporous TiO_2 can also be synthesized without using surfactant as a template

(Chen et al. 2017). The sensor provided an increased surface area (147.17 $m^2.g^{-1}$) to facilitate the high sensitivity and fast response to acetone detection. Though the electrochemical properties of silica and alumina are not as good as transition metal oxide, silicon is an element that is readily available and has a low production cost in terms of marketing for real-world use. Nanoporous silica has an ordered mesopore, an excellent choice for hosting and adsorption of biomolecules in electrochemical sensors. The mesoporous silica film was modified on a glassy carbon electrode (GCE) by electrodeposition in tetraethyl orthosilicate (TEOS) and cetyltrimethylammonium bromide (CTAB) under galvanostatic conditions. The obtained sensitivity of paraquat detection was higher than bare GCE for one magnitude order. The selectivity of the determination depended on the electrostatic force between the ionic wall of the pore and the positive charge of paraquat (Nasir et al. 2018). The nanoporous TiO_2 has been used as an electronic resistant sensor to determine acetone vapor.

Most nanoporous CuO and NiO have been extensively interested in CO_2 reduction applications (Giziński et al. 2020). Among the different CuO sensor nanostructures, only a few works have been used as the electrochemical sensor (Xiao et al. 2014; Huang et al. 2015). A freestanding porous CuO nanowire array and nanowires pile was used as nonenzymatic glucose sensing. The CuO nanowire array electrode exhibited extensively promoted electrochemistry characterized by higher sensitivity over fivefold of the CuO nanowires pile complement, beneficial to the binder-free nanoarray structure (Huang et al. 2015). The micro hollow-sphere nano CuO has also been synthesized using a hydrothermal method with pluronic F-127 surfactant as a template (Haghparas et al. 2020). The electrocatalytic activities of microstructure and hydroxide ions influenced the glucose oxidation mechanism. Nanoporous NiO has a catalyst activity towards glucose based on Ni(III)/Ni(II) redox couple. The glucose converts to gluconolactone related to NiOOH catalytic property. Nanoporous has been fabricated via hydrothermal and modified on the fluorine-doped tin oxide (FTO) (Mishra et al. 2018) and Au electrode (Ahmad et al. 2020). The nanoporous NiO shows a good anti-interference for AA and UA. Recently, the laser-induced method has synthesized nanoporous NiO, which provided a better pore size uniform (2–50 nm). The obtained NiO was very selective to glucose without interfering with AA, UA, and DA. The porous aluminum anodic oxide (AAO) was recently used as the membrane in electrochemical biosensors due to its unique properties. Mainly they can synthesize by self-ordering electrochemical anodization with orderly nanochannels, as shown in Fig. 11.3a. The suitable pore size and shape of nanoporous Al_2O_3 can be the membrane to block the Flightless (Flii) protein in the biosensor, which results in decreasing the current of the redox species on the electrode surface (Rajeev et al. 2020).

Apart from using one metal oxide material, the composite nanoporous oxide nanomaterials are also attractive and have been used as electrodes in electroanalytical applications because of their synergetic electrocatalytic properties. The thickness of porous ZnO-CuO hierarchical nanocomposites (HNCs) is varied by controlling the electrospinning. The superior electrocatalytic property of the ZnO-CuO HNCs was mainly from the small CuO nanoparticles (NPs), which

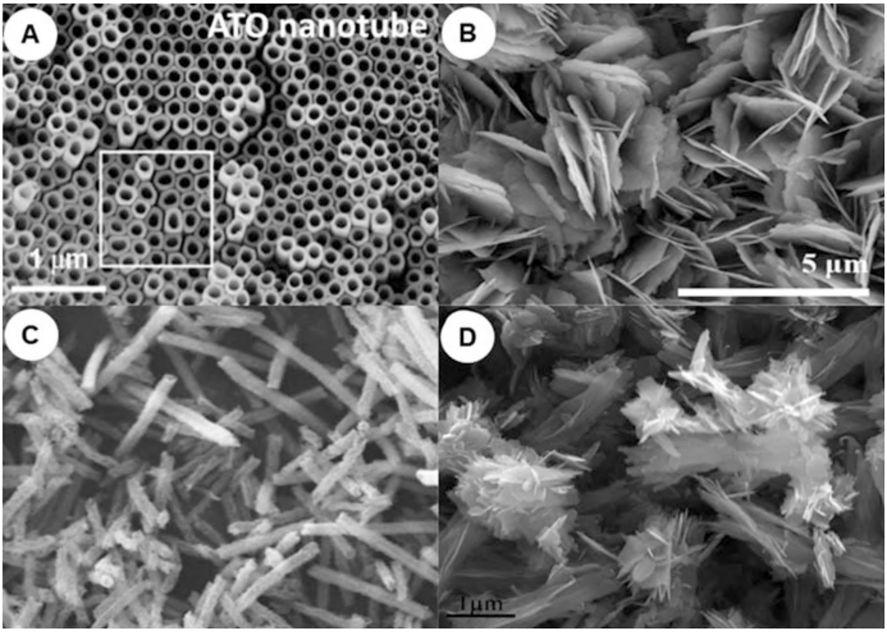

Fig. 11.3 The SEM image of anodic titanium oxide (ATO) nanotube arrays (**a**) (Su and Zhou 2008), the pristine porous ZnO nanosheets (**b**) (Liang et al. 2020), NiO nanofibers sintered at 600 °C (**c**) (Kong et al. 2016), and CuO-ZnO nanocomposite (**d**) (Das and Srivastava 2018)

decorated the ZnO-CuO HNCs' outer surface. The sensitivity and selectivity of the sensing electrode were significantly improved and depended strongly on the thickness of the HNCs. Under the optimum condition, the electrode was highly sensitive (3066.4 $\mu AmM^{-1}\ cm^{-2}$). Not only the excellent selectivity, but it also showed long-term stability and good reproducibility. Besides, the porous zinc oxide-nickel oxide (ZnO-NiO) composite nanosheets were produced via sputtering the NiO to generate a thin film on the porous ZnO nanosheet. The rough surface of the nanosheet structure displayed more excellent sensing responses to ethanol vapor than the pristine ZnO at the same concentrations. The ethanol detection sensitivity is related to the ZnO/NiO heterojunction amounts and specific porous nanosheet structure with a high surface area. The coating of NiO on the porous ZnO nanosheet with a suitable particle size can increase the sensor's selectivity (Liang et al. 2020). The hollow structure porous nanofiber of SnO_2-CuO can be fabricated by electrospinning combined with a hydrothermal process, which provides high sensitivity for H_2S gas detection. The unique structures are caused by the different diffusion rates of SnO_2-CuO and Sn/Cu. The operating temperatures for H_2S sensing were low, promising that SnO_2-CuO is a good candidate for a gas sensor (Park et al. 2020). The hierarchical heterojunction and the orderly 3D structure were the primary reason for enhancing the sensor's sensitivity (Zhou et al. 2014). For example, the Fe_3O_4 magnetic nanoparticles and material-41 (Fe_3O_4 MNP-MCM-41) were synthesized for sensing cardiovascular drugs. The Fe_3O_4 MNP-MCM-41 structure is designed to capably capture and enhance cardiovascular drugs' electrochemical signals. The Fe_3O_4 MNP-MCM-41 exhibited a greater oxidative current of the analyte than the bare carbon paste electrode (CPE). Magnetic and specific properties of the Fe_3O_4 MNPMCM-41 act as the fit size cage to capture and pre-concentrate the drugs molecules, which are essential for increasing the selectivity of large molecule detection (Hasanzadeh et al. 2016).

3.3 Nanoporous Carbon for Electroanalytical Application

The crystalline carbon is primarily found in graphite and diamond forms, whereas the activated carbon is amorphous. The uniform carbon nanomaterials have been explored as electrode materials because of their high surface area, surface wettability by electrolyte, cost, and high electron transfer rate. Carbon materials with a pore size smaller than 100 nm are namely nanoporous carbon (Ray et al. 2020). Nanoporous carbon materials could be excellent for energy storage applications (Shao et al. 2020) and electrochemical sensing applications (Poh and Pumera 2012). The nanoporous carbon capacity was significantly increased when the pore size was close to electrolyte ions' size (Raymundo-Piñero et al. 2006). Nanoporous carbon provides a lower overpotential of biomarkers and forensics-related compounds. Moreover, the faradic currents significantly improved compared to bare GCE, graphite microparticles, and carbon nanotubes.

If the porosity is used to classify carbon nanomaterials, then carbon nanotubes and graphene multilayers fall into this category. These materials' porosity is structural porosity and inter-particle porosity, which have different electrical properties. CNTs and graphene are intensively used as sensors because of their high electron transfer rate, which is generated from their 1D and 2D structure, respectively (Poh and Pumera 2012). Activated nanocarbon has been markedly used in energy storage. The conductive carbon mainly contains sp2 carbon atoms with a high surface area and consistent pore size. In general, nanoporous carbon is synthesized by pyrolysis of highly carbon source materials at high temperatures (200–400 °C) with chemical or physical activations. This method's limitation is that the obtained nanoporous carbon has defects that result in low conductivity and electron transfer rate (Jänes et al. 2007). Chemical vapor deposition (CVD) is the greatest method to synthesize nanoporous carbon. The obtained nanoporous carbon provided superior sensing performance over the bare GCE, graphite microparticles, and carbon nanotube as exhibited a fast heterogeneous electron transfer. The nanoporous carbon can also be used as a biosensor because of its physisorption, H-bonding, and electrostatic interaction with protein.

Moreover, the nanoporous carbon can also reduce the overpotential oxidation/reduction of biomarkers, including DNA, AA, UA, DA, NADH, and nitroaromatic compounds (Poh and Pumera 2012). However, the stability of the biosensor probes depends on the pH ionic strength and temperature; therefore, the composite of nanoporous carbon with other metal nanoparticles has been presented to solve this problem. The nanoporous carbon has also been used as the sorbent host for other nanomaterials to detect the analyte in the electrochemical sensor in the differential pulse voltammetry (DPV). For instance, the composite of Fe_3O_4-doped nanoporous carbon (Fe_3O_4-NC) was fabricated by the carbonization of the Fe-porous metal-organic framework (MOF). The Fe_3O_4-NC modified GCE was employed as a sensor electrode for the diethylstilbestrol (DES) and 17β-estradiol (E2) simultaneous analysis, as shown in Fig. 11.4a. The adsorptive and catalytic property of Fe_3O_4-NC plays a crucial role in the sensor's high sensitivity (Chen et al. 2018).

The 3D graphene network (3DGN) delivers multiplexed conductive and rapid charge transfer pathways. These factors contribute to enhance the performance of the electrochemical electrode. 3D porous graphene has recently attracted interest as an electrochemical electrode because of its superior features, including multiple electron paths from the 3D network and an excellent inner and outer surface to attach the analyte. The 3D graphene network can be synthesized by carbon templating substrates, chemical, electrochemical, and hydrothermal reduction (Ma and Chen 2015). Among several synthesis methods, direct electrochemical methods are simplifying by immersing the electrode in graphene oxide (GO) suspension and applying constant negative or swiped the potential to generate the 3D reduced graphene oxide (rGO). However, the orderly 3DGN structure properties, including the growth of layers, pore size, and porosity, are the barrier to overcome. Most 3DGNs' pore sizes were in several hundreds of micrometers, and single-layered 3DGNs are a hard-to-synthesize structure, outstanding for their delicate mechanical properties. The uniform meso/micropores and controlled layers 3DGNs is the most structure that provides the suitable catalytic property. In comparison, the assembly method needs more control over the growth of layers and size of the GO/graphene sheets. To improve the mechanical and electrical properties of the 3DGNs, cross-linking between the graphene/GO sheets is needed to increase the surface functional moieties or add cross-linkers. The application of electrochemical sensors of the different pore structures of 3D graphene is intensive on the dopamine determination without the interference from UA (Dong et al. 2012; Li et al. 2015a; Baig and Saleh 2018). The 3D graphene with biopolymers/surfactants were highly selective for hemoglobin (Sun et al. 2015), biomarker serotonin (Khoshnevisan et al. 2019), and levodopa (Gao et al. 2018) without using the electron mediator. The 3D graphene was also evaluated as the methyl phosphonate (DMMP) gas sensor. The graphene oxide was accumulated on the Au electrode over the electrostatic interaction followed by hydrazine reduction. The multilayer framework of GO/rGO increased the active surface area for DMMP adsorption (Wang et al. 2019a). The enzymatic sensor of 3D graphene was interested because it can be the selective biocompatible pore for enzymes. The 3D graphene-based nanomaterials with hierarchical macro-mesoporous structures (GF-MC) have been synthesized using silica as the template shown in Fig. 11.4. The synthesized GF-MC was applied to detect glucose by decorating the enzyme. The GF-MC/GOx electrode exhibited good glucose-sensing performance due to enzymes' well-organized immobilization and improved electron and mass transfer rates. It is supposed that these 3D graphene-based macro-

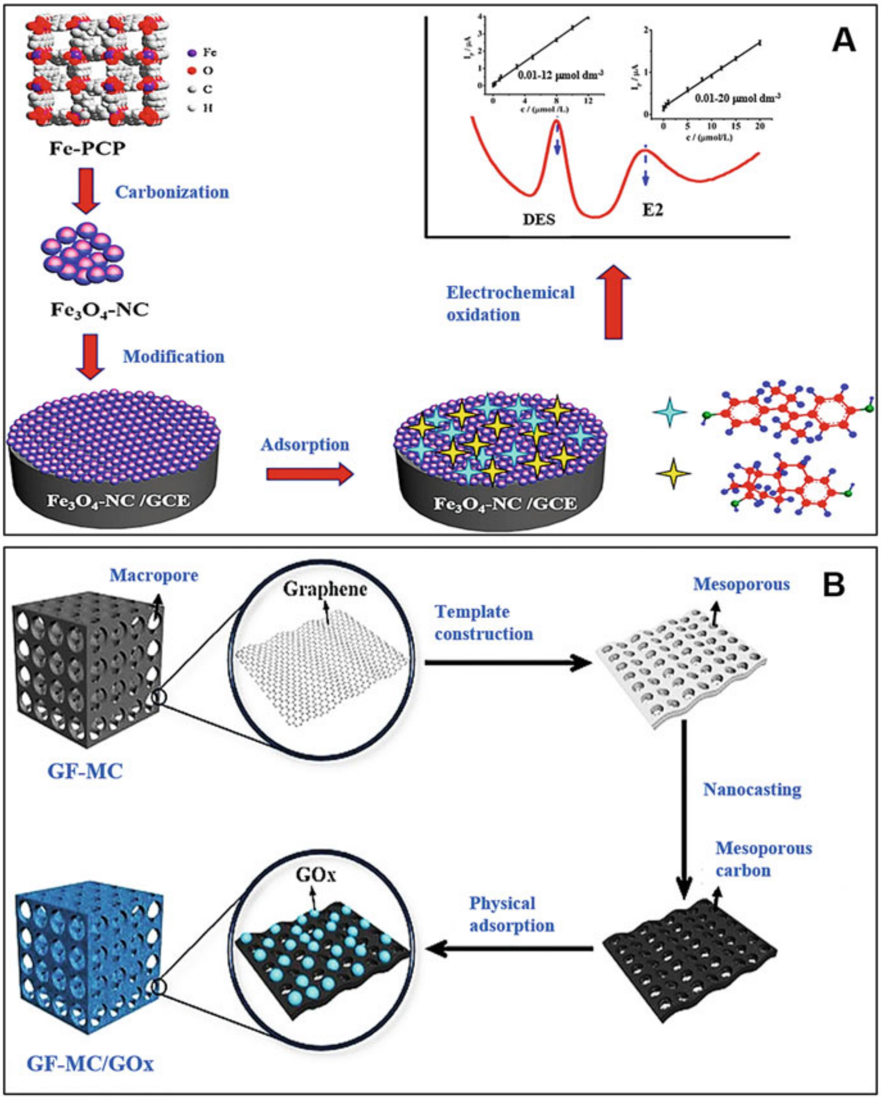
A
Fe
O
C
H
Fe-PCP
Carbonization
Fe$_3$O$_4$-NC
Modification
Fe$_3$O$_4$-NC /GCE
Adsorption
Fe$_3$O$_4$-NC /GCE
Electrochemical oxidation
DES
E2
I$_p$ / μA
0.01-12 μmol dm^{-3}
c / (μmol /L)
0 4 8 12
0 1 2 3 4
I$_p$ / μA
0.01-20 μmol dm^{-3}
c / (μmol/L)
0 5 10 15 20
0 1 2
B
Macropore
Graphene
GF-MC
Template construction
Mesoporous
Nanocasting
Mesoporous carbon
Physical adsorption
GOx
GF-MC/GOx

Fig. 11.4 The electrodeposition of nanoporous carbon-doped Fe$_3$O$_4$ on GCE (**a**) (Chen et al. 2018) and 3D graphene-based frameworks with hierarchical macro and mesoporous structures (GF-MC) are created and used as platforms to immobilize glucose oxidase (GOx) (**b**) (Shen et al. 2019)

mesoporous nanomaterials are promising scaffolds for enzymes in the future (Shen et al. 2019).

Besides 3D graphene, carbon nanofibers (CNFs) have also been interested in using them as electrodes due to their similar properties with CNTs. They have exclusively basal graphite planes and edge planes with a high potential for surface modification or functionalization (Wang et al. 2019b). CNFs with mesoporous pores provided a large specific surface area with few defects and high electrical conductivity, making them suitable for electrochemical sensing. The most effective method for CNFs synthesis is the electrospinning method. The polymer forms a Taylor cone, and then the fiber is pre-oxidized in air and carbonized under N_2 conditions to get the uniform CNFs. For example, Seven et al. (2020) demonstrated CNFs microelectrode to detect H_2O_2 and DA. The increase in the C:O ratio favors the escalation of conductivity and electron transfer rate. A single fiber of CNFs was tripped at the end of Cu wire by Ag paste. It was found that AA at six times higher than DA did not significantly influence the DA's square wave voltammetry signal.

Exceptionally 3D graphene and CNFs, graphitic nanoporous carbon were fabricated as the thin film electrode for ammonia and water vapor sensor (Slobodian et al. 2020). The graphite film obtained from acetylene gave a higher porosity and low resistivity than CH_4 (Hulicova-Jurcakova et al. 2008). The graphitic nanoporous carbon was created by plasma-enhanced decomposition of CH_4 and acetylene on the silicon substrate. Graphitic carbon nitride (g-C_3N_4)/graphite nanocomposite was also produced by the thermal polymerization of melamine and applied for sub-micromolar detection of oxalic acid. The sensor showed a very high sensitivity of 1945 $\mu A\ mM^{-1}\ cm^{-2}$ for oxalic acid (Alizadeh et al. 2019). Zhao et al. (2020a) presented macroporous carbon for tyrosine's enantioselective sensor. The macroporous carbon was implanted with sulfato-β-cyclodextrin (MPC-SCD) and dispersed in Nafion before dropping on the GCE surface. The pore was favorable for the adsorption of cyclodextrin, which is the host for L-tyrosine. The macroporous carbon has excellent electrical conductivity to promote sensitivity, while sulfato-β-cyclodextrin acted as the enantiomer selective cage, as shown in Fig. 11.5.

3.4 Nanoporous Polymer-based Composites for Electroanalytical Application

Over the last several years, conductive polymers are used in electrochemical applications because they are biocompatible and comfortable functionalizing with biomolecules, increasing the method's specificity. Recently, there has been intense research and development on these novel materials, because most of the researchers assumed that reducing the pore size to the nanometer range could strongly influence some of the properties of porous polymers. The nanoporous polymers provide unexpected and enhanced properties compared to other available porous and microporous polymers and nonporous solids (Notario et al. 2016). The polymer network with the pore in the nanoscale range has been synthesized using phase separation, colloidal imprinting, microemulsion, foaming, and molecular imprinting. The conductivity of the nanoporous polymer increased by reducing the pore size of the polymer. Among several synthesis methods, molecular imprinting is an exciting method for electrochemical application. The imprinted molecule's length can control the pore size and structure as the template. The thin film of the polymer, such as polyaniline (PANI), polypyrrole (PPy), diaminonaphthalene (DAN), poly

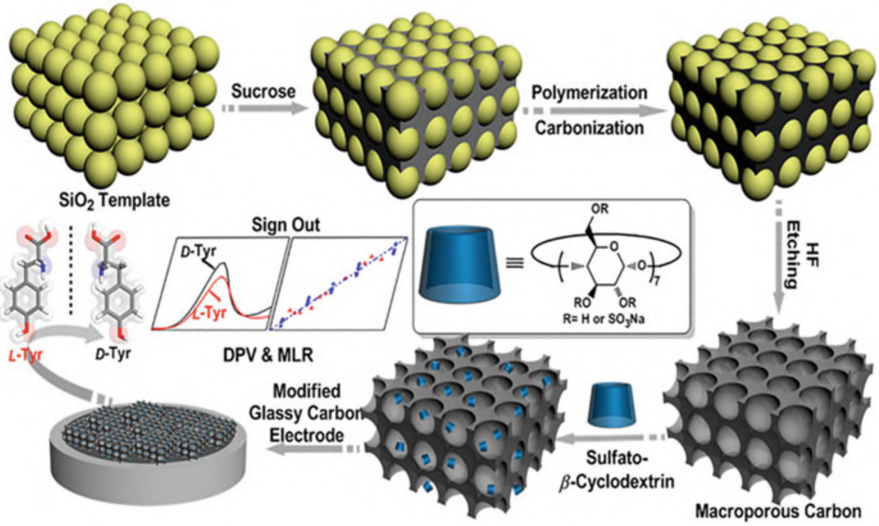

Fig. 11.5 The synthesis route of MPC-SCD hybrid and the chemically modified electrode production diagram (Zhao et al. 2020a)

3,4-ethylene dioxythiophene (PEDOT), has been widely used with other nanomaterials for the fabrication of the electrode (Tonelli et al. 2019). However, the limitation of polymer-modified electrodes is the film's fouling, adsorption, and resistance from the polymer's electrode modification. Therefore, some synthesis of the conductive polymer's nanoporous thin film has been used the carbon nanomaterial as the template (Feng et al. 2019). The nanoporous conductive polymer of polyphonic acid doped nanoporous conductive polyaniline (PANI) was modified on the carbon fiber electrode and used as the vivo sensor for monitoring dopamine in the rat brain. The using polymer film improved the aliphatic organic functional groups on the surface area, which related to the electrode's specific active surface area. The cyclotrimerization reaction of amine or nitro functionalized 4,4'diacetylbiphenyl were synthesized porous polymer and introduced as the chemiresistive gas sensors for alcohol and ketone. Because of their unique pore types and pore functionalization, amine-functionalized polymers display the utmost selectivity towards alcohols, whereas the nitro-functionalized ones show the highest towards ketones. The different selectivity associated with the porous polymer's swelling behavior through vapor adsorption (Liu et al. 2018). The molecularly imprinted polymers (MIPs) become a good candidate because of their greater chemical and physical stability, low-cost manufacture, and high selectivity and sensitivity. MIPs combined with diminished electrochemical transducers such as metal nanoparticles can detect target analytes in situ and increase the sensor's selectivity. For example, the conducting poly(4-amino thiophenol) nanostructures layered on Au nanodots decorated indium tin oxide (ITO) electrode was synthesized using the self-assembly method followed by electrochemical polymerization of 4-amino thiophenol molecules. The polymer-modified Au nanodots/ITO electrode showed an outstanding electrocatalytic activity toward adenine and guanine oxidation reaction (El-Said and Choi 2014). In addition, the imidazolium-based porous polymer-loaded Pt nanoparticles were electrodeposited on GCE via silane chemistry and alkylation (Fang et al. 2018). The modified electrode showed the efficient catalyst for hydrogen evolution reaction (HER). The imidazolium-based porous organic polymer acted as the supporter to stabilize Pt nanoparticles. Most of the porous polymer in the electrochemical application is the biomolecular sensors (Tonelli et al. 2019). The alpha-fetoprotein (AFP) sensor was established based on 3D macroporous PANI doped with poly (sodium 4-styrene sulfonate) (PSS). The macroporous PANI delivered an outstanding substrate for immobilization of alpha-fetoprotein (AFP) antibodies. The PANI's porous essential the redox signal change. The AFP immunosensor showed a satisfactory sensing performance to AFP. This sensor's response sensitivity was about two times higher than that of using only PANI-modified electrode, revealing an excellent improvement result associated with the 3D macroporous structure, as shown in Fig. 11.6.

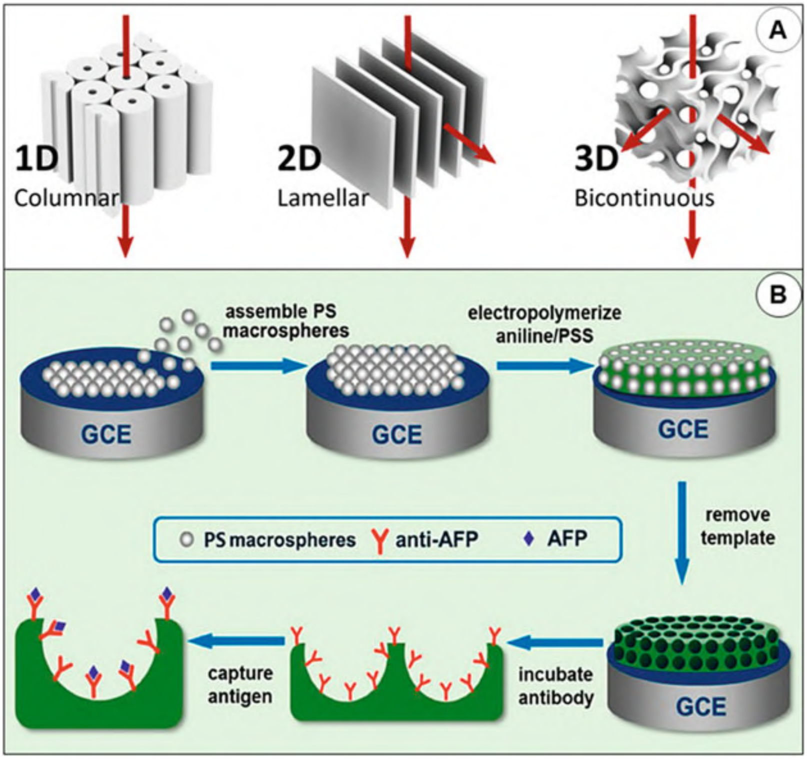
A
1D
Columnar
2D
Lamellar
3D
Bicontinuous
B
assemble PS macrospheres
electropolymerize aniline/PSS
GCE
GCE
GCE
remove template
PS macrospheres
anti-AFP
AFP
capture antigen
incubate antibody
GCE

Fig. 11.6 (**a**) Different nanoporous polymer structures (Lugger et al. 2018) and (**b**) biosensor fabrication uses a porous polymer as the adsorbent electrodeposition on the electrode (Liu et al. 2018)

Recently, the Au nanoparticles decorated PEDOT-modified GCE has been used as the glutathione sensor. The electrodeposition of PEDOT film followed by Au nanoparticles provided the pore in nano dimension. The Au nanoparticles assisted the electrocatalytic activity towards glutathione via Au-S interaction. The mechanism is diffusion-controlled rather than surface control (Rajaram et al. 2020). The electrochemical sensor of As^{3+} has been established based on ion-imprinted polymer (IIP) and nanoporous gold (NPG) modified Au electrode (Ma et al. 2020). The IIP and NPG modified Au electrode (IIP/NPG/GE) by electropolymerization, in which using o-phenylenediamine as a functional monomer. The resulting polymer membrane provided several precise binding moieties that complement the template ion As^{3+} in the spatial site and chemical bonding, therefore increasing the selectivity. The composite of chitosan membrane and CNTs can improve large molecules' signal via the analyte molecule's absorption (Butwong et al. 2020; (Park et al. 2020). A nanocomposite comprising Ag@AgCl/Ag_2S nanoparticles dispersed in chitosan was decorated on multi-walled carbon nanotubes and modified on GCE. Chitosan also played a significant role in interacting strongly with arbutin (AR) glucose moiety and ascorbyl glucoside (AA2G). The electrode showed good electrocatalysis towards the analytes by reducing the anodic peak potential with ≈ a fivefold higher current (Butwong et al. 2020). An electrochemical sensor based on double-template molecularly imprinted polymer (MIP) with nanoporous Au leaf (NPGL) was established to determine DA and UA simultaneously. The MIP layer was synthesized in situ in the existence of 15.0 mM o-phenylenediamine, DA, and UA, to provide specific recognition. The dual templates were confirmed to play a major role in the sensing performance, as the sensing signals of the analyte are significantly different from interfering species. The sensor was stable for 30 days, and the result of the determination of DA and UA in bovine serum was in good agreement with those from high-performance liquid chromatography (Li et al. 2020).

4 Conclusion and Future Perspectives

Electrochemical sensors must be highly conductive materials to improve measurement agility and increase specificity by using target-specific materials where these properties are difficult to find in a macro-materials. For this reason, the application of nanomaterials in analytical chemistry as electrochemical sensors is generally the conductive porous thin film of composites because of their specific properties from the synthetic porosity to fit the target molecule with good electrical conductivity. However, to synthesize any material, its purpose is to consider the material design and currently still needs to be developed continuously due to the uniform pore size and stable materials used today is always an ideal material. Conducted polymers make the electrode surface more hydrophilic and act as the membrane, while metal oxides are the regular and robust catalyst. The metal nanomaterial provides better conductivity and electron transfer. The developed 3D nanoporous materials from 2D nanomaterials can improve the 2D material properties. 3D nanoporous with nanopore structure can be a semipermeable membrane for increasing the electrochemical sensor's active surface area and sensor selectivity. From the perspective of the analytical chemist, the molecular imprinting of the conductive polymer and nanoporous graphene with the metal nanoparticles is willing used as the flexible electrochemical sensor.

References

Ahmad R, Khan M, Tripathy N, Khan MIR, Khosla A (2020) Hydrothermally synthesized nickel oxide nanosheets for nonenzymatic electrochemical glucose detection. J Electrochem Soc 167(10):107504. https://doi.org/10.1149/1945-7111/ab9757

Alizadeh T, Nayeri S, Hamidi N (2019) Graphitic carbon nitride (g-C_3N_4)/graphite nanocomposite as an extraordinarily sensitive sensor for sub-micromolar detection of oxalic acid in biological samples. RSC Adv 9(23):13096–13103. https://doi.org/10.1039/C9RA00982E

Baig N, Saleh TA (2018) Electrodes modified with 3D graphene composites: a review on methods for preparation, properties and sensing applications. Microchim Acta 185(6):283. https://doi.org/10.1007/s00604-018-2809-3

Biswal A, Panda P, Jiang Z-T, Tripathy B, Minakshi M (2019) Facile synthesis of a nanoporous sea sponge architecture in a binary metal oxide. Nanoscale Adv 1(5):1880–1892. https://doi.org/10.1039/C8NA00402A

Butwong N, Kunawong T, Luong JHT (2020) Simultaneous analysis of hydroquinone, arbutin, and ascorbyl glucoside using a nanocomposite of Ag@AgCl nanoparticles, Ag_2S nanoparticles, multiwall carbon nanotubes, and chitosan. Nano 10(8). https://doi.org/10.3390/nano10081583

Chen N, Li Y, Deng D, Liu X, Xing X, Xiao X, Wang Y (2017) Acetone sensing performances based on nanoporous TiO_2 synthesized by a facile hydrothermal method. Sensors Actuators B Chem 238:491–500. https://doi.org/10.1016/j.snb.2016.07.094

Chen X, Shi Z, Hu Y, Xiao X, Li G (2018) A novel electrochemical sensor based on Fe_3O_4-doped nanoporous carbon for simultaneous determination of diethylstilbestrol and 17β-estradiol in toner. Talanta 188:81–90. https://doi.org/10.1016/j.talanta.2018.05.063

Chen C, Yu S, Jiang S, Liu J, Wang Z, Ye B-C (2020) A novel and sensitive electrochemical sensor based on nanoporous gold for determination of As(III). Microchim Acta 187(7):395. https://doi.org/10.1007/s00604-020-04365-w

Collinson MM (2013) Nanoporous gold electrodes and their applications in analytical chemistry. ISRN Anal Chem 2013:1–21. https://doi.org/10.1155/2013/692484

Das S, Srivastava VC (2018) An overview of the synthesis of CuO-ZnO nanocomposite for environmental and other applications. Nanotechnol Rev 7(3):267–282. https://doi.org/10.1515/ntrev-2017-0144

Dong X, Wang X, Wang L, Song H, Zhang H, Huang W, Chen P (2012) 3D graphene foam as a monolithic and macroporous carbon electrode for electrochemical sensing. ACS Appl Mater Interfaces 4(6):3129–3133. https://doi.org/10.1021/am300459m

Dong X, Li M, Feng N, Sun Y, Yang C, Xu Z (2015) A nanoporous MgO based nonenzymatic electrochemical sensor for rapid screening of hydrogen peroxide in milk. RSC Adv 5(105): 86485–86489. https://doi.org/10.1039/C5RA18560B

El-Said WA, Choi J-W (2014) Electrochemical biosensor consisted of conducting polymer layer on gold nanodots patterned indium tin oxide electrode for rapid and simultaneous determination of purine bases. Electrochim Acta 123:51–57. https://doi.org/10.1016/j.electacta.2013.12.144

Fang H, Chen J, Balogun M-S, Tong Y-X, Zhang J (2018) Covalently modified electrode with Pt nanoparticles encapsulated in porous organic polymer for efficient electrocatalysis. ACS Appl Nano Mater 1(11):6477–6482. https://doi.org/10.1021/acsanm.8b01697

Feng T, Ji W, Tang Q, Wei H, Zhang S, Mao J, Zhang Y, Mao L, Zhang M (2019) Low-fouling nanoporous conductive polymer-coated microelectrode for in vivo monitoring of dopamine in the rat brain. Anal Chem 91(16):10786–10791. https://doi.org/10.1021/acs.analchem.9b02386

Gao X, Yue H, Song S, Huang S, Li B, Lin X, Guo E, Wang B, Guan E, Zhang H, Wu P (2018) 3-dimensional hollow graphene balls for voltammetric sensing of levodopa in the presence of uric acid. Microchim Acta 185(2):91. https://doi.org/10.1007/s00604-017-2644-y

Giziński D, Brudzisz A, Santos JS, Trivinho-Strixino F, Stępniowski WJ, Czujko T (2020) Nanostructured anodic copper oxides as catalysts in electrochemical and photoelectrochemical reactions. Catalysts 10(11). https://doi.org/10.3390/catal10111338

Guo X, Han J, Liu P, Chen L, Ito Y, Jian Z, Jin T, Hirata A, Li F, Fujita T, Asao N, Zhou H, Chen M (2016) Hierarchical nanoporosity enhanced reversible capacity of bicontinuous nanoporous metal based Li-O_2 battery. Sci Rep 6(1):33466. https://doi.org/10.1038/srep33466

Haghparas Z, Kordrostami Z, Sorouri M, Rajabzadeh M, Khalifeh R (2020) Fabrication of nonenzymatic electrochemical glucose sensor based on nano-copper oxide micro hollow-spheres. Biotechnol Bioproc E 25(4):528–535. https://doi.org/10.1007/s12257-020-0058-x

Hasanzadeh M, Shadjou N, Pournaghi-Azar MH, Jouyban A (2016) Magnetic mesoporous silica: a novel nano-material towards electrochemical sensing. J Electroceram 37(1–4):85–91. https://doi.org/10.1007/s10832-016-0033-2

Huang J, Zhu Y, Yang X, Chen W, Zhou Y, Li C (2015) Flexible 3D porous CuO nanowire arrays for enzymeless glucose sensing: in situ engineered versus ex situ piled. Nanoscale 7(2): 559–569. https://doi.org/10.1039/C4NR05620E

Hulicova-Jurcakova D, Li X, Zhu Z, de Marco R, Lu GQ (2008) Graphitic carbon nanofibers synthesized by the chemical vapor deposition (CVD) method and their electrochemical performances in supercapacitors. Energy Fuel 22(6):4139–4145. https://doi.org/10.1021/ef8004306

Jänes A, Kurig H, Lust E (2007) Characterisation of activated nanoporous carbon for supercapacitor electrode materials. Carbon 45(6):1226–1233. https://doi.org/10.1016/j.carbon.2007.01.024

Jérôme F, Valange S (2017) Rational design of nanostructured carbon materials: contribution to cellulose processing. In: Van de Voorde M, Sels B (eds) Nanotechnology in catalysis. Wiley-VCH Verlag GmbH & Co. KGaA, Weinheim, pp 627–654

Jiao K, Flynn KT, Kohli P (2016) Synthesis, characterization, and applications of nanoporous materials for sensing and separation. In: Aliofkhazraei M (ed) Handbook of nanoparticles. Springer International Publishing, Cham, pp 429–454

Khoshnevisan K, Maleki H, Honarvarfard E, Baharifar H, Gholami M, Faridbod F, Larijani B, Faridi Majidi R, Khorramizadeh MR (2019) Nanomaterial based electrochemical sensing of the biomarker serotonin: a comprehensive review. Microchim Acta 186(1):49. https://doi.org/10.1007/s00604-018-3069-y

Kim SH, Choi JB, Nguyen QN, Lee JM, Park S, Chung TD, Byun JY (2013) Nanoporous platinum thin films synthesized by electrochemical dealloying for nonenzymatic glucose detection. Phys Chem Chem Phys 15(16):5782–5787. https://doi.org/10.1039/C2CP43097E

Kong XW, Zhang RL, Zhong SK, Wu L (2016) Electrospinning synthesis of 3D porous NiO nanorods as anode material for lithium-ion batteries. Mater Sci-Pol 34(2):227–232. https://doi.org/10.1515/msp-2016-0040

Li M, Liu C, Zhao H, An H, Cao H, Zhang Y, Fan Z (2015a) Tuning sulfur doping in graphene for highly sensitive dopamine biosensors. Carbon 86:197–206. https://doi.org/10.1016/j.carbon.2015.01.029

Li Z, Zhu Y, Wang L, Wang J, Guo Q, Li J (2015b) A facile method for the structure control of TiO_2 particles at low temperature. Appl Surf Sci 355:1051–1056. https://doi.org/10.1016/j.apsusc.2015.07.162

Li N, Nan C, Mei X, Sun Y, Feng H, Li Y (2020) Electrochemical sensor based on dual-template molecularly imprinted polymer and nanoporous gold leaf modified electrode for simultaneous determination of dopamine and uric acid. Microchim Acta 187(9):496. https://doi.org/10.1007/s00604-020-04413-5

Liang J, Liang Z, Zou R, Zhao Y (2017) Heterogeneous catalysis in zeolites, mesoporous silica, and metal-organic frameworks. Adv Mater 29(30):1701139. https://doi.org/10.1002/adma.201701139

Liang Y-C, Chang Y-C, Zhao W-C (2020) Design and synthesis of novel 2D porous zinc oxide-nickel oxide composite nanosheets for detecting ethanol vapor. Nano 10(10). https://doi.org/10.3390/nano10101989

Liu H, Weng L, Yang C (2017) A review on nanomaterial-based electrochemical sensors for H_2O_2, H_2S and NO inside cells or released by cells. Microchim Acta 184(5):1267–1283. https://doi.org/10.1007/s00604-017-2179-2

Liu S, Ma Y, Cui M, Luo X (2018) Enhanced electrochemical biosensing of alpha-fetoprotein based on three-dimensional macroporous conducting polymer polyaniline. Sensors Actuators B Chem 255:2568–2574. https://doi.org/10.1016/j.snb.2017.09.062

Liu S, Liu B, Gong C, Li Z (2019) A nanoporous Cu-Ag thin film at the Cu-Ag-Zn alloy surface by spontaneous dissolution of Zn and Cu in different degrees as a highly sensitive nonenzymatic glucose sensor. Electrochim Acta 320:134599. https://doi.org/10.1016/j.electacta.2019.134599

Lugger J, Mulder DJ, Sijbesma R, Schenning A (2018) Nanoporous polymers based on liquid crystals. Materials 11(1):104. https://doi.org/10.3390/ma11010104

Ma Y, Chen Y (2015) Three-dimensional graphene networks: synthesis, properties and applications. Natl Sci Rev 2(1):40–53. https://doi.org/10.1093/nsr/nwu072

Ma W, Chang Q, Zhao J, Ye B-C (2020) Novel electrochemical sensing platform based on ion imprinted polymer with nanoporous gold for ultrasensitive and selective determination of As^{3+}. Microchim Acta 187(10):571. https://doi.org/10.1007/s00604-020-04552-9

McCormick W, McCrudden D (2020) Development of a highly nanoporous platinum screen-printed electrode and its application in glucose sensing. J Electroanal Chem 860:113912. https://doi.org/10.1016/j.jelechem.2020.113912

Menzel N, Ortel E, Kraehnert R, Strasser P (2012) Electrocatalysis using porous nanostructured materials. ChemPhysChem 13(6):1385–1394. https://doi.org/10.1002/cphc.201100984

Mirzaei A, Lee J-H, Majhi SM, Weber M, Bechelany M, Kim HW, Kim SS (2019) Resistive gas sensors based on metal-oxide nanowires. J Appl Phys 126(24):241102. https://doi.org/10.1063/1.5118805

Mishra S, Yogi P, Sagdeo PR, Kumar R (2018) Mesoporous nickel oxide (NiO) nanopetals for ultrasensitive glucose sensing. Nanoscale Res Lett 13(1):16. https://doi.org/10.1186/s11671-018-2435-3

Nasir T, Herzog G, Hébrant M, Despas C, Liu L, Walcarius A (2018) Mesoporous silica thin films for improved electrochemical detection of paraquat. ACS Sens 3(2):484–493. https://doi.org/10.1021/acssensors.7b00920

Nasrollahi S, Ghoreishi SM, Khoobi A (2020) Nanoporous gold film: surfactant-assisted synthesis, anodic oxidation and sensing application in electrochemical determination of quercetin. J Electroanal Chem 864:114097. https://doi.org/10.1016/j.jelechem.2020.114097

Notario B, Pinto J, Rodriguez-Perez MA (2016) Nanoporous polymeric materials: a new class of materials with enhanced properties. Prog Mater Sci 78–79:93–139. https://doi.org/10.1016/j.pmatsci.2016.02.002

Obrero JM, Filippin AN, Alcaire M, Sanchez-Valencia JR, Jacob M, Matei C, Aparicio FJ, Macias-Montero M, Rojas TC, Espinos JP, Saghi Z, Barranco A, Borras A (2020) Supported porous nanostructures developed by plasma processing of metal phthalocyanines and porphyrins. Front Chem 8:520. https://doi.org/10.3389/fchem.2020.00520

Park S, Song YJ, Han J-H, Boo H, Chung TD (2010) Structural and electrochemical features of 3D nanoporous platinum electrodes. Electrochim Acta 55(6):2029–2035. https://doi.org/10.1016/j.electacta.2009.11.026

Park K-R, Cho H-B, Lee J, Song Y, Kim W-B, Choa Y-H (2020) Design of highly porous SnO_2-CuO nanotubes for enhancing H_2S gas sensor performance. Sensors Actuators B Chem 302:127179. https://doi.org/10.1016/j.snb.2019.127179

Poh HL, Pumera M (2012) Nanoporous carbon materials for electrochemical sensing. Chem Asian J 7(2):412–416. https://doi.org/10.1002/asia.201100681

Polarz S, Smarsly B (2002) Nanoporous materials. J Nanosci Nanotechnol 2(6):581–612. https://doi.org/10.1166/jnn.2002.151

Qiu H-J, Fang G, Wen Y, Liu, P, Xie G, Liu X, Sun, S (2019) Nanoporous high-entropy alloys for highly stable and efficient catalysts. J Mater Chem A 7(11):6499–6506. https://doi.org/10.1039/C9TA00505F

Rajaram R, Kanagavalli P, Senthilkumar S, Mathiyarasu J (2020) Au nanoparticle-decorated nanoporous PEDOT modified glassy carbon electrode: a new electrochemical sensing platform for the detection of glutathione. Biotechnol Bioprocess Eng 25(5):715–723. https://doi.org/10.1007/s12257-020-0065-y

Rajeev G, Melville E, Cowin AJ, Prieto-Simon B, Voelcker NH (2020) Porous alumina membrane-based electrochemical biosensor for protein biomarker detection in chronic wounds. Front Chem 8:155. https://doi.org/10.3389/fchem.2020.00155

Ray SS, Gusain R, Kumar N (2020) Chapter seven – carbon nanomaterials: synthesis, functionalization, and properties. In: Ray SS, Gusain R, Kumar N (eds) Carbon nanomaterial-based adsorbents for water purification. Elsevier, pp 137–179

Raymundo-Piñero E, Kierzek K, Machnikowski J, Béguin F (2006) Relationship between the nanoporous texture of activated carbons and their capacitance properties in different electrolytes. Carbon 44(12):2498–2507. https://doi.org/10.1016/j.carbon.2006.05.022

Regiart M, Kumar A, Gonçalves JM, Silva Junior GJ, Masini JC, Angnes L, Bertotti M (2020) An electrochemically synthesized nanoporous copper microsensor for highly sensitive and selective determination of glyphosate. ChemElectroChem 7(7):1558–1566. https://doi.org/10.1002/celc.202000064

Salunkhe RR, Kaneti YV, Yamauchi Y (2017) Metal–organic framework-derived nanoporous metal oxides toward supercapacitor applications: progress and prospects. ACS Nano 11(6):5293–5308. https://doi.org/10.1021/acsnano.7b02796

Sapountzi FM, Gracia JM, (Kees-J) Weststrate CJ, HOA F, (Hans) Niemantsverdriet JW (2017) Electrocatalysts for the generation of hydrogen, oxygen and synthesis gas. Prog Energy Combust Sci 58:1–35. https://doi.org/10.1016/j.pecs.2016.09.001

Seven F, Gölcez T, Şen M (2020) Nanoporous carbon-fiber microelectrodes for sensitive detection of H_2O_2 and dopamine. J Electroanal Chem 864:114104. https://doi.org/10.1016/j.jelechem.2020.114104

Shao H, Wu Y-C, Lin Z, Taberna P-L, Simon P (2020) Nanoporous carbon for electrochemical capacitive energy storage. Chem Soc Rev 49(10):3005–3039. https://doi.org/10.1039/D0CS00059K

Sharma S, Saxena V, Baranwal A, Chandra P, Pandey LM (2018) Engineered nanoporous materials mediated heterogeneous catalysts and their implications in biodiesel production. Mater Sci Energy Technol 1(1):11–21. https://doi.org/10.1016/j.mset.2018.05.002

Shen L, Ying J, Ren L, Yao Y, Lu Y, Dong Y, Tian G, Yang X-Y, Su B-L (2019) 3D graphene-based macro-mesoporous frameworks as enzymatic electrodes. J Phys Chem Solids 130:1–5. https://doi.org/10.1016/j.jpcs.2019.02.007

Slobodian OM, Gomeniuk YV, Vasin AV, Rusavsky AV, Okholin PN, Gudymenko OY, Khyzhun OY, Nikolenko A, Lytvyn P, Korchovyy A, Yatskiv R, Nazarova TM, Stepanov V, Kisyl D, Nazarov AN (2020) Graphitic nanoporous carbon thin films: fabrication method, structural, electrical and gas sensor properties. ECS Trans 97(5):151–156. https://doi.org/10.1149/09705.0151ecst

Stanev L, Kolev M, Drenchev B, Drenchev L (2016) Open-cell metallic porous materials obtained through space holders—part I: production methods. A review. J Manuf Sci Eng 139(050801). https://doi.org/10.1115/1.4034439

Su Z, Zhou W (2008) Formation mechanism of porous anodic aluminium and titanium oxides. Adv Mater 20(19):3663–3667. https://doi.org/10.1002/adma.200800845

Su S-H, Cheng H, Chen P-Y (2013) Electrochemical oxidation and determination of glucose using cyclic voltammetry and a one-step prepared nanoporous gold wire electrode. J Chin Chem Soc 60(11):1380–1386. https://doi.org/10.1002/jccs.201300301

Summerlot D, Kumar A, Das S, Goldstein L, Seal S, Diaz D, Cho HJ (2011) Nanoporous gold electrode for electrochemical sensors in biological environment. Procedia Engineering 25: 1457–1460. https://doi.org/10.1016/j.proeng.2011.12.360

Sun W, Hou F, Gong S, Han L, Wang W, Shi F, Xi J, Wang X, Li G (2015) Direct electrochemistry and electrocatalysis of hemoglobin on three-dimensional graphene modified carbon ionic liquid electrode. Sensors Actuators B Chem 219:331–337. https://doi.org/10.1016/j.snb.2015.05.015

Tonelli D, Scavetta E, Gualandi I (2019) Electrochemical deposition of nanomaterials for electrochemical sensing. Sensors 19(5). https://doi.org/10.3390/s19051186

van der Zalm J, Chen S, Huang W, Chen A (2020) Review—recent advances in the development of nanoporous Au for sensing applications. J Electrochem Soc 167(3):037532. https://doi.org/10.1149/1945-7111/ab64c0

Wang J, Gao H, Sun F, Xu C (2014) Nanoporous PtAu alloy as an electrochemical sensor for glucose and hydrogen peroxide. Sensors Actuators B Chem 191:612–618. https://doi.org/10.1016/j.snb.2013.10.034

Wang Y, Yang M, Liu W, Dong L, Chen D, Peng C (2019a) Gas sensors based on assembled porous graphene multilayer frameworks for DMMP detection. J Mater Chem C 7(30):9248–9256. https://doi.org/10.1039/C9TC02299F

Wang Z, Wu S, Wang J, Yu A, Wei G (2019b) Carbon nanofiber-based functional nanomaterials for sensor applications. Nano 9(7). https://doi.org/10.3390/nano9071045

Xiao X, Wang M, Li H, Pan Y, Si P (2014) Nonenzymatic glucose sensors based on controllable nanoporous gold/copper oxide nanohybrids. Talanta 125:366–371. https://doi.org/10.1016/j.talanta.2014.03.030

Xu Y, Zhang B (2014) Recent advances in porous Pt-based nanostructures: synthesis and electrochemical applications. Chem Soc Rev 43(8):2439. https://doi.org/10.1039/c3cs60351b

Xu C, Wang J, Zhou J (2013) Nanoporous PtNi alloy as an electrochemical sensor for ethanol and H_2O_2. Sensors Actuators B Chem 182:408–415. https://doi.org/10.1016/j.snb.2013.03.035

Yang H, Wang Z, Li C, Xu C (2017) Nanoporous PdCu alloy as an excellent electrochemical sensor for H_2O_2 and glucose detection. J Colloid Interface Sci 491:321–328. https://doi.org/10.1016/j.jcis.2016.12.041

Yi X, Wu Y, Tan G, Yu P, Zhou L, Zhou Z, Chen J, Wang Z, Pang J, Ning C (2017) Palladium nanoparticles entrapped in a self-supporting nanoporous gold wire as sensitive dopamine biosensor. Sci Rep 7(1):7941. https://doi.org/10.1038/s41598-017-07909-y

Yoshii Y, Sakurai J, Mizoshiri M, Hata S (2019) Fabrication of a novel nanoporous film via chemical dealloying of a Cu–Cr alloy for sensing moisture in oil. J Microelectromech Syst 28(2):279–289. https://doi.org/10.1109/JMEMS.2019.2895164

Zhang J, Li CM (2012) Nanoporous metals: fabrication strategies and advanced electrochemical applications in catalysis, sensing and energy systems. Chem Soc Rev 41(21):7016–7031. https://doi.org/10.1039/C2CS35210A

Zhao J, Cong L, Ding Z, Zhu X, Zhang Y, Li S, Liu J, Chen X, Hou H, Fan Z, Guo M (2020a) Enantioselective electrochemical sensor of tyrosine isomers based on macroporous carbon embedded with sulfato-β-Cyclodextrin. Microchem J 159:105469. https://doi.org/10.1016/j.microc.2020.105469

Zhao X, Deng Z, Zhao W, Feng B, Wang M, Huang M, Liu L, Zou G, Shao Y, Zhu H (2020b) Nanoporous silver using pulsed laser deposition for high-performance oxygen reduction reaction and hydrogen peroxide sensing. Nanoscale 12(37):19413–19419. https://doi.org/10.1039/D0NR05395C

Zhou C, Xu L, Song J, Xing R, Xu S, Liu D, Song H (2014) Ultrasensitive nonenzymatic glucose sensor based on three-dimensional network of ZnO-CuO hierarchical nanocomposites by electrospinning. Sci Rep 4(1):7382. https://doi.org/10.1038/srep07382

Nanobiomaterial-Based Biosensors for the Diagnosis of Infectious Diseases

12

Fereshteh Vajhadin and Mohammad Mazloum-Ardakani

Contents

1 Introduction 242
2 Electrochemical Nanobiomaterial-Based Biosensors for the Detection of Pathogens 243
3 Metal-Based Nanomaterials for the Detection of Infectious Diseases 243
  3.1 Gold and Silver Nanomaterials 243
  3.2 Magnetic Nanomaterials 247
4 Carbon-Based Nanomaterials 249
  4.1 Graphene-Based Nanomaterials 249
  4.2 Carbon Nanotubes 252
5 Conclusion and Future Perspectives 253
References 253

Abstract

Infectious diseases are among the primary causes of millions of deaths every year. Early detection of these diseases is a crucial step in controlling outbreaks. Therefore, the development of reliable, rapid, inexpensive, convenient, and point-of-care devices for diagnosing infectious diseases is at the forefront of research. In recent decades, the utilization of nanostructures in biosensing platforms has led to significant advancements in disease diagnosis. This is due to the diverse range of available nanostructures and the ability to customize their physicochemical properties. This chapter provides an overview of the application of nanobiomaterials in constructing biosensors for monitoring infectious diseases. Additionally, it explains strategies to create high-performance biosensors by harnessing the benefits of gold, silver, magnetic, and carbon-based nanobiomaterials.

Keywords

Biosensor · Infectious disease · Nanobiomaterial · Diagnosis · Point-of-care device

---

F. Vajhadin · M. Mazloum-Ardakani (✉)
Department of Chemistry, Faculty of Science, Yazd University, Yazd, Iran

© Springer Nature Singapore Pte Ltd. 2023

U. P. Azad, P. Chandra (eds.), *Handbook of Nanobioelectrochemistry*,
https://doi.org/10.1007/978-981-19-9437-1_12

1 Introduction

Infectious diseases have emerged as one of the main global healthcare concerns due to the high mortality rates. Pathogenic infections are induced by bacteria, viruses, parasites, and fungi (Qasim et al. 2014; Pashchenko et al. 2018; Zhou et al. 2020). Until November 2020, SARS-CoV-2 virus has affected the lives of >45 million people (Deng et al. 2020). Acute respiratory infections including influenza, tuberculosis, and pneumonia lead to five million deaths every year (Pashchenko et al. 2018). Pathogenic bacterial infections are responsible for one-third of mortalities (Deng et al. 2020). For each hour of delay in the treatment of blood infection, the survival rate of patients is reduced by 8% (Campuzano et al. 2017). The common approaches for the diagnosis of infectious diseases include culturing, staining, polymerize chain reactions (PCR) amplification, and the use of immunological assays such as ELISA based on antibodies-antigen recognition events (Amiri et al. 2018; Gill et al. 2019). These mentioned approaches are often costly and need multistep sample preparation procedures and also expert persons. Thus, it is important to develop sensing platforms with features such as high detection speed, low cost, and ease of use to combat infectious pathogens and reduce the treatment costs and delays, which ultimately helps to prevent disease transmission.

Biosensors are analytical devices that generate semi-quantitative/quantitative analytical data by converting biological incidents, such as the binding of aptamers/antibodies and targets, into detectable output signals, including thermal, optical, and electrochemical signals (Hassanpour et al. 2018). The monitoring of infectious diseases using biosensors is performed either directly based on the detection of pathogens or indirectly by the assessment of biomarkers associated with a specific pathogen such as genes, proteins, antigens, and antibodies (Campuzano et al. 2017; Kashish et al. 2017). Developing point-of-care devices (POC) that are easy to use at home is of great significance to prevent the spread of diseases (Mahapatra and Chandra 2020). Moreover, the design of smartphone-based biosensors, as the next-generation sensors, has gained considerable attention for enabling remote data collection and processing by the general population.

Among various biosensors, electrochemical platforms are outstanding due to their attractive features such as portability, rapid response, easy operation, miniaturized size, as well as low cost (Maduraiveeran et al. 2018; Bhatnagar et al. 2018). In recent decades, the incorporation of nanobiomaterials into electrochemical biosensing platforms has played a critical role in boosting the functionality of these platforms. Nanobiomaterials, which refer to nanosized materials applied in biomedical applications, can be classified as inorganic, organic, or a combination of both. Developing new nanomaterials has introduced new horizons to combat infectious diseases by providing novel diagnostic platforms and novel therapeutic agents (Gill et al. 2019; Rabbani et al. 2021; Haghniaz et al. 2021; Baranwal et al. 2018).

The early detection of a disease is a key step to control it. There is a very low level of biomarkers in body fluids at an early stage of a disease, highlighting the need to develop ultra-sensitive biosensors for diagnostic applications. Many efforts have been made to leverage nanobiomaterials to enhance the performance of sensing platforms for the monitoring of infectious pathogens (Deng et al. 2020). These materials in electrochemical platforms can serve as a transducer and signal amplifiers owing to their excellent electronic and catalytic activities (Zhu et al. 2015). The careful engineering of the size, shape, and morphology of nanobiomaterials increases their functionality in terms of binding efficiency and the number of immobilized biorecognition elements, thereby improving the biosensing detection limits. Besides, the fabrication of nanohybrids and nanocomposites is a well-established strategy to boost the favorable properties of nanobiomaterials through synergetic effects. In addition to the mentioned benefits of nanobiomaterials, their incorporation into electrochemical platforms enhances the generation of optical signals, such as colorimetric and fluorescence signals, simultaneously with electrochemical signals. This capability is due to its unique optical characteristics. Generally speaking, such platforms are capable of supporting dual-signals for the detection of targets of interest.

Here, we describe the progress in nanomaterial-based biosensors for the monitoring of infectious pathogens. We only cover the biosensors that are based on electrochemical transducers (i.e., impedimetric, amperometric, and voltammetric ones). The roles of nanobiomaterials in the fabrication of various biosensors are also highlighted.

2 Electrochemical Nanobiomaterial-Based Biosensors for the Detection of Pathogens

In general, to fabricate functional nanobiomaterial-based biosensors, several criteria should be considered. They include (a) selective and sensitive detection of pathogens, (b) ease of fabrication, (c) cost-effectiveness, (d) measurement of analytes at clinically relevant levels, (e) rapid analysis, (f) low reagent volumes, and (g) disposability. The following sections discuss several important biosensing platforms whose sensing performance is improved by the use of nanobiomaterials including gold and silver as well as magnetic and carbon-based nanomaterials.

3 Metal-Based Nanomaterials for the Detection of Infectious Diseases

3.1 Gold and Silver Nanomaterials

Among the metals implemented in electrochemical biosensing platforms, nanomaterials of gold and silver received much attention. They are favored due to their high biocompatibility. In particular, their high electrical conductivity makes them have special importance in electrochemical sensing platforms. They are synthesized by chemical, physical, electrochemical, and plant-based approaches reported in several reviews, such as Lee et al. (2020), Sengani et al. (2017), Beyene et al. (2017). By virtue of their great biocompatibility and large surface area, metal nanoparticles (NPs) can serve as a stable substrate to immobilize a high amount of targeting ligands such as aptamers, antibodies, and peptides by forming a link between the metal and the SH and NH groups of targeting ligands (Kumar et al. 2015; Steinmetz et al. 2019). The high conductivity of metal NPs provides improved electrochemical properties for a transducer, such as rapid electron transfer, suitable signal-to-noise ratio, and high detection sensitivity (Liu and Lin 2007). Furthermore, metal NPs have found a broad application as labels and signal amplifiers in nanosensor arrays (Guo and Wang 2007; Li et al. 2015a; de la Escosura-Muniz et al. 2010).

Replication of Hepatitis B Virus (HBV) in the liver might cause complications such as inflammation, damage, and even liver cancer in chronic cases (Böttcher et al. 1997). Biosensors intended to employ in HIV diagnosis can evaluate biomarkers including a soluble antigen Hepatitis B e antigen (HBeAg), Hepatitis B surface antigen (HBsAg), and HBV genomic DNA (de la Escosura-Muniz et al. 2010; Ahangar and Mehrgardi 2017). In a trial, a biosensor was exploited using nanoporous Au and horseradish peroxidase (HRP) as a co-catalyst. It dramatically amplified the output signals associated with the recognition of HBeAg and achieved a linear range from 0.1 pg mL^{-1} to 500 pg mL^{-1} with the limit of detection (LOD) of 0.064 pg mL^{-1} in a solution containing H_2O_2 and catechol (Zhang et al. 2019). The fabrication of biosensing platforms using the high enzyme-like activities of nanomaterials as the analogs of natural enzymes such as HRP and glucose oxide is very common. This is because they lower the cost and increase the stability of platforms (Meng et al. 2019; Golchin et al. 2018). The good catalytic activity of the sensors is due to the functional groups present as a capping agent and the interstice properties of nanomaterials (Lin et al. 2014).

In 2021, a smartphone-based biosensor was constructed by Near Field Communication (NFC) for the real-time detection of Hepatitis B (HB) (Teengam et al. 2021). To prepare Au NPs, the electrodeposition method on a graphite screen-printed electrode (GSPE) was employed. An electropolymerized β-cyclodextrin (CD)-Au NPs-modified GSPE was then coupled to antibodies for the selective monitoring of HBsAg concentrations. The cost of each platform is reported to be less than $10, while conducting a diagnosis in 60 min with a LOD of less than 0.17 μg/mL. There might be either a lack or a very low level of antigens at the early stage of infectious disease, limiting the reliability-functionality of antigen-based biosensors in the disease diagnosis. In comparison to antigen-based biosensors, DNA-based ones might indicate better performance (Ahangar and Mehrgardi 2017).

Early disease diagnosis based on the detection of pathogens' genomes by biosensors has gained great importance to provide simple sensing platforms that assist in controlling a disease spread by the rapid identification of infected persons (Campuzano et al. 2017; Sharifi et al. 2021; Hassanpour et al. 2018). These biosensors utilize synthetic oligonucleotides as biorecognition elements that are complementary to the target DNA or RNA (Mahshid et al. 2020). The detection of DNA/RNA hybridization requires high sensitivity and often depends on signal amplification strategies such as isothermal amplification methods, PCR, and ligase chain reaction (LCR) techniques (Wang 2005b; Fan et al. 2019). While such methods are very robust and sensitive, their byproducts might introduce measurement bias (Cesewski and Johnson 2020). In a notable study, Li et al. (2015a) proposed Ag NPs and magnetic microbeads for signal amplification by paper-based devices (PADs) termed "oSlip-DNA" to monitor the DNA of HBV. This assay was based on ex-situ sandwich formation between the label DNA-Ag NPs and the captured DNA-magnetic microbeads along with the DNA of HBV. The use of Ag NPs and magnetic microbeads resulted in 250,000-fold and 25-fold signal amplification, respectively, highlighting the potential of nanomaterials as a signal amplifier. The cost of each biosensor is estimated to be $ 0.37, while it does very fast detection (the testing time is reported to be nearly 5 min) with the LOD of 85 pM. Obviously, the role of metal nanoparticles in signal amplification is incredible, yet amplification strategies such as PCR are required to meet the demands in practical applications.

The application of Au NPs as a tag in biosensors to detect DNA hybridization dates back to 1996, and there is still a growing interest in applying them for disease diagnosis (Qasim et al. 2014; Cui et al. 2015). For instance, as Fig. 12.1 shows, the amplification of target DNA with colloidal Au NPs was conducted to electrochemically detect mycobacterium tuberculosis (Mtb) DNA down to 1 CFU (Ng et al. 2015). The cost of the assay was calculated to be under $10 per run with an analysis time of about 90 min. Feng et.al (2020) also employed Au NPs in hybridization chain reaction (HCR) amplification. Indeed, they used an isothermal enzyme-free amplification method that generated long double-stranded nucleic acids from a primarily hairpin construct to detect the 16S rRNA fragments of *Staphylococcus aureus* (*Staph. aureus*) bacteria as a product of HCR. They also deposited a silver wire on Au NPs coupled to DNA-RNA (HCR products) and made some changes in the electrical parameters of an interdigital electrode. They could, thus, measure the targeted bacteria in milk and human serum samples with the LOD of 50 CFU/ml within100 min**.** In another study, Au NPs functionalized with silsesquioxane polymer modified an oxidized glassy carbon electrode, preparing a substrate for the attachment of thiolate Zika DNA via covalent binding (Au-S) (Steinmetz et al. 2019). The hybridization of Zika DNA with its target (Zika ssDNA) t caused a change in the current. This was performed with the LOD of 0.82 pmol L^{-1} in real human serum samples.

Paper-based lateral-flow test strip biosensors offer the great advantage of being commercially available, which makes them greatly potential to meet the demands for reliable-simple disease diagnosis in healthcare systems. In recent years, the incorporation of Au NPs into lateral-flow immunosensors has gained importance to raise the detection sensitivity by the use of Au NPs as a label and a carrier (Sinawang et al. 2016; Rivas et al. 2014). An electrochemical lateral-flow immunosensor is often composed of a lateral-flow paper strip and a screen-printed electrode. In a study by Sinawang et al. (2016), gold screen-printed electrodes were coupled with capture antibodies. Next, they bonded to dengue NS1 protein as a target analyte. In this assay, Au NPs served as a matrix to anchor ferrocene-detection dengue NS1 antibody through physical adsorption. The detection of the dengue NS1 protein concentration took place with a LOD of lower than 0.5 ng/mL.

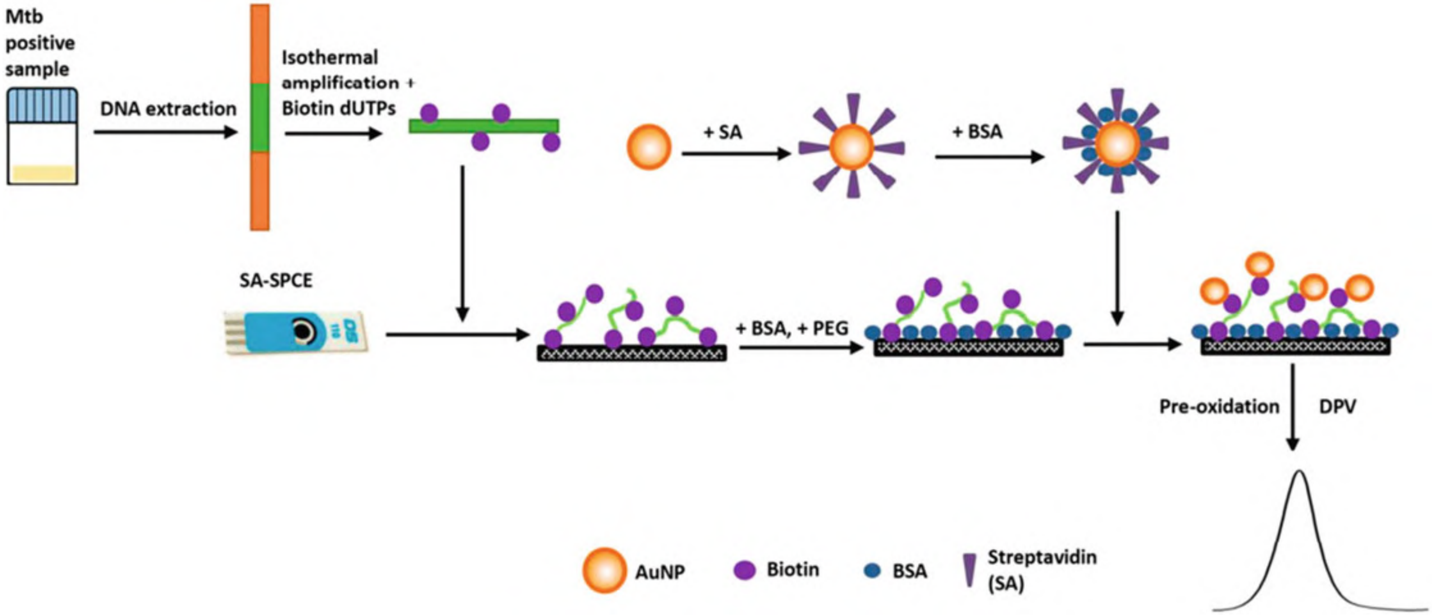
Mtb
positive
sample
DNA extraction
Isothermal
amplification +
Biotin dUTPs
+ SA
+ BSA
SA-SPCE
+ BSA, + PEG
Pre-oxidation
DPV
AuNP
Biotin
BSA
Streptavidin
(SA)

Fig. 12.1 Schematic display of an electrochemical sensing platform for monitoring the target DNA using isothermal amplification of target DNA: An electrochemical signal correlates to the presence of Au NPs. Adapted with permission from (Ng et al. 2015). Copyright (2015) American Chemical Society

3.2 Magnetic Nanomaterials

Magnetic nanomaterials, which have magnetic properties, are composed of pure metals (e.g., Co and Ni), alloys (e.g., FeCo,) or oxides (e.g., Fe_3O_4 and $CoFe_2O_4$) (Wang et al. 2020). They can be obtained by various approaches such as hydrothermal, co-precipitation or microemulsion, sol-gel, sonochemical decomposition, and electrochemical deposition (Dadfar et al. 2019). The integration of the advantages of nanoscale materials with magnetic properties allows magnetic nanomaterials to be widely utilized in clinical diagnosis for a few reasons (de la Escosura-Muniz et al. 2010; Nourani et al. 2013). First, the analyte can be preconcentrated on the surface of magnetic nanomaterials through binding to biorecognition elements that are immobilized by physical adsorption or covalent coupling. Second, analyte-magnetic nanomaterial complexes can be isolated from the complex matrix of samples to minimize the matrix effect on the electrochemical responses and increase the selectivity of the bioassay. Third, their small size makes it possible to miniaturize bioassay platforms.

Among magnetic nanomaterials, Fe_3O_4 has received the most attention for application in biosensors. This is due to its high biocompatibility, good magnetism, and interesting catalytic performance (Wei et al. 2020; Li et al. 2013). Fe_3O_4 nanoparticles might be unstable when exposed to oxygen due to certain interactions between the surface of Fe (II) cations and the adsorbed oxygen, which leads to the formation of γ-Fe_2O_3 as a shell (Urbanova et al. 2014). To address this problem and provide highly stable and functional Fe_3O_4 nanoparticles, it is a common practice to use core-shell structures and do surface coating with inorganic/ organic layers such as silica, surfactants, polymers, and noble metals (Freitas et al. 2016; Dzudzevic Cancar et al. 2016). Besides, coating layers might contribute to the advantage of antifouling to reduce non-specific protein adsorption and improve the functionality of nanomaterials in complex matrixes. Among materials with antifouling properties, poly(ethylene glycol) (PEG), zwitterionic polymers, and dextran can be mentioned (Chen et al. 2018). The synergistic effects of chondroitin sulfate (CSA) and poly (ethylene glycol) (PEG) as a coating layer on magnetic nanoparticles (Fe_3O_4@Au@PEG@CSA NPs), created an outstanding antifouling property (Chen et al. 2018).

Detection of biomarkers in complex samples such as blood often involves separation with magnetic nanomaterials, use of microfluidic devices, centrifugation, filtering, and employing multi-biorecognition elements in biosensing platforms to ensure the selectivity of bioassays. The most widely reported application of magnetic nanomaterials in biosensors is magnetic separation from complex samples (Sayhi et al. 2018; Markwalter et al. 2019; Nourani et al. 2013). Electrochemical platforms for the diagnosis of HIV/AIDS infection are based on biomarkers such as $CD4^+$ T lymphocyte, HIV antibodies, viral DNA (RNA), viral P24, p17, and also HIV-related enzymes (Farzin et al. 2020). In a study by Carinelli et al. (2015), antiCD3 antibody-magnetic materials were employed to monitor $CD4^+$ T lymphocytes as an HIV

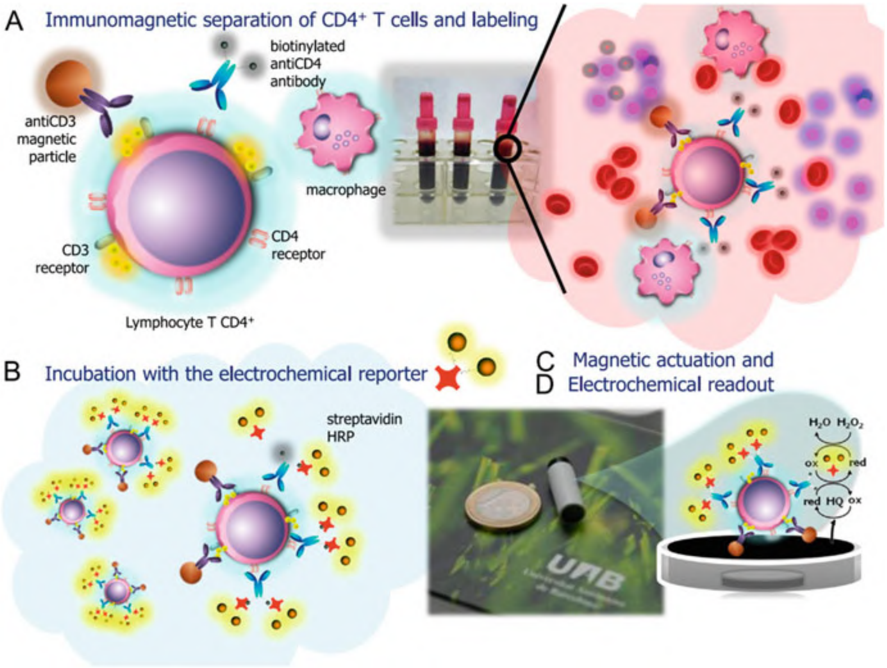
A Immunomagnetic separation of CD4⁺ T cells and labeling
biotinylated antiCD4 antibody
antiCD3 magnetic particle
macrophage
CD3 receptor
CD4 receptor
Lymphocyte T CD4⁺
B Incubation with the electrochemical reporter
streptavidin HRP
C Magnetic actuation and
D Electrochemical readout
H₂O H₂O₂
ox red
red HQ ox
UAB

Fig. 12.2 Schematic display of a magnetic-based sensing platform (Carinelli et al. 2015): (**a**) Magnetic separation of CD4$^+$ T lymphocytes from the blood sample and labeling them with antibodies, (**b**) Coupling magnetic CD4$^+$ T lymphocytes with the electrochemical reporter, (**c**) Magnetic actuation, and (**d**) Electrochemical measurement

biomarker in whole blood. During the magnetic cell separation with these materials, the studied cells were tagged with an antiCD4 antibody (Fig. 12.2). In such cases, the use of two different antibodies often improves the selectivity of the sensor to exclude monocytes and macrophages that express CD4 molecules. This ultimately improves the functionality of the biosensor in whole blood samples.

Beyond magnetic separation, the development of novel and functional magnetic nanomaterials to construct electrochemical interfaces is an interesting application of magnetic nanomaterials in bioelectronic devices (Urbanova et al. 2014). Li et al. (2021) constructed an electrochemical platform for the monitoring of HBsAg in serum. In this examination, a sensing layer was fabricated using a magnetic 3D Fe_3O_4 nanoflower coupled with hepatitis B antibodies that were magnetically attached to an indium tin oxide (ITO) electrode. Therefore, 3D Fe_3O_4 nanoflower served to transfer the current signals. Through a heterogeneous chain reaction (HCR), the sandwich-type biosensor achieved an excellent LOD of 0.16 pgmL^{-1}.

4 Carbon-Based Nanomaterials

4.1 Graphene-Based Nanomaterials

Graphene nanosheets belong to the class of two-dimensional materials c. Due to the presence of a high number of oxygen-containing groups in graphene oxide compared with graphene, it provides more active sites for conjugation to biorecognition elements and more available sites for chemical activities (Vajhadin et al. 2020). Graphene-based nanomaterials have gained wide applications in biosensors owing to their advantages such as a high surface-area-to-volume ratio, good biocompatibility, outstanding electrical conductivity, cost-effectiveness, and convenient synthesis (Kumar et al. 2015). In particular, graphene as an electrochemical interface is favorable because not only does it have a specific physicochemical surface and electronic structure that improves the electron transfer but also it provides a direct electron transfer between its surface and the active sites of bioreceptors with no need for a mediator.

Over the recent decades, significant studies have focused on developing new graphene nanocomposites to improve graphene limitations such as agglomeration. Furthermore, many studies have aimed to modulate the properties of graphene-based nanomaterials, so as to improve their functionality and achieve very low LODs.

Fabrication of graphene-Nafion nanocomposites is a simple example of how to improve graphene dispersity and stability for evaluating HIV-1 genes with the LOD of 2.3×10^{-14} M (Fig. 12.3). The integration of conductive polymers (i.e., polyaniline, polypyrrole, polythiophene) into graphene nanosheets is a considerable approach that might provide favorable dispersibility, and fast electron transfer as well as active sites for the immobilization of biorecognition elements (Dakshayini et al. 2019). Gong et al. (2019) prepared polyaniline-graphene nanocomposites as an electrode modifier to monitor HIV-1 genes with the LOD of 1.0×10^{16} M. Polyaniline not only enhanced the conductivity of the platform but also improved the stability of graphene for the immobilization of single-strand DNA so as to identify the hybridization of target HIV-1 genes. Similarly, a genosenor was developed using graphene and a polytyramine-conducting polymer to recognize Zika virus genomic RNA in samples taken from infected patients (Moço et al. 2019). The analysis time of the resulting biosensor was about 20 min.

Graphene oxide nanosheets are extensively exploited as a platform to support nanoparticles and signal producers (Gu et al. 2015; Sanati et al. 2019). The decoration of graphene nanosheets with nanoparticles not only hampers nanoparticle agglomeration but also increases their stability. Besides, graphene might synergistically enhance the functionality of nanomaterials such as their enzyme-like catalytic activity. Li et al. (2015b) sought to use graphene oxide (GOx) as an anchoring matrix warped with thionine (Thi) (as a redox probe) and Au NPs-coated SiO_2 nanocomposites (GOx–Thi–Au@SiO_2) through electrostatic adsorption. Hemin/G-quadruples, serving as DNAzyme, was added to GOx–Thi–Au@SiO_2 to provide a signal tag for the monitoring of Escherichia coli O157:H7 with the LOD of 0.01 nM in the presence of H_2O_2. It is to be noted that silica coating not only

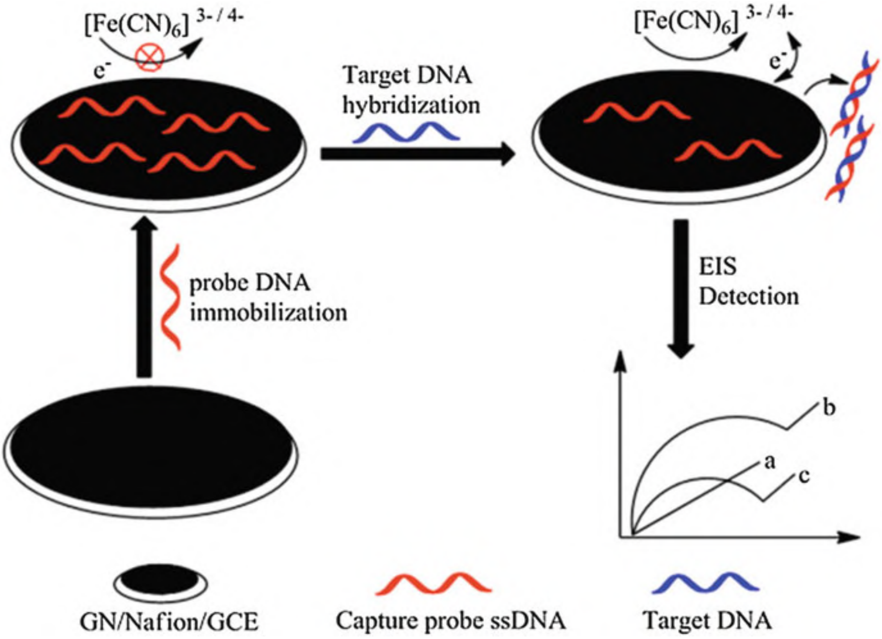

Fig. 12.3 Schematic illustration of an impedimetric DNA biosensor to detect target DNA using graphene-Nafion nanocomposites (Gong et al. 2017)

promotes the biocompatibility of nanomaterials but also prevents the core materials from degradation (Markwalter et al. 2019). In another study, Wei et al. (2020) applied a nanocomposite of graphene oxide decorated with Fe_3O_4 nanoparticles and Prussian blue (PB) (as a redox probe) to modify screen-printed electrodes. This enhanced the electron transfer capability of those electrodes. In this platform, Au NPs served as a matrix for anchoring antibodies and as a signal amplifier. In that study, a LOD of less than 0.166 pg mL^{-1} was achieved for HBsAg. In this line of research, Jin et al. (2016) used an electrochemical interface composed of graphene oxide functionalized with 3-Aminopropyltriethoxysilane (APTES) and warped with SiO_2 nanoparticles to detect dengue RNA with the LOD of less than 1 fM.

Electrochemical sandwich-type immunosensors are a popular type of biosensors often fabricated by the sandwiching of a target of interest between two antibodies, a primary antibody (Ab1) and a secondary antibody (Ab2). In such biosensors, Ab1 is often immobilized on nanomaterials as an electrochemical interface, and Ab2 is often coupled to labels including natural enzymes and artificial enzymes such as nanomaterials and nanocomposites (Li et al. 2015b; Maduraiveeran et al. 2018; Nourani et al. 2013; Huang et al. 2016). For instance, Pei et al. (2019) developed an electrochemical interface by the immobilization of Ab1 on Au NPs that decorated pyrrole nanosheets (Au NPs/PPy NSs). In this system, Au NPs served as a matrix to immobilize antibodies with amine groups through Au-NH binding and accelerate the electron transfer among PPy NSs. Graphene was also applied as a substrate

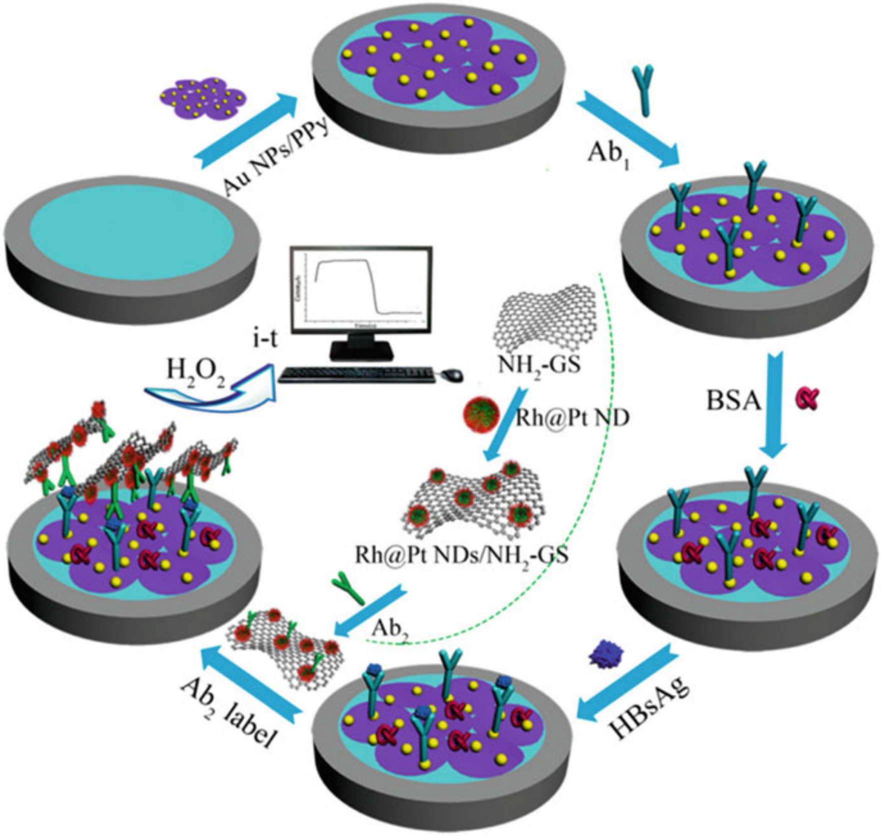

Fig. 12.4 Schematic display of an immunosensor with a sandwich-type structure (Pei et al. 2019)

decorated with Pt shell nanodenderites and Rh core (RhPt NDs) and then coupled to Ab2 to support signal tags (Fig. 12.4). The detection limit of HBsAg was found to be 166 fg/mL.

Bio field-effect transistor (bio-FET) platforms measure the conductance change in the "source-drain". The change is induced by the changes in the surface potential due to the target binding to biorecognition elements immobilized onto the gate surface (Kergoat et al. 2012; Furst and Francis 2019). A biosensor of this type has a great potential for clinical diagnosis owing to its easy mass-production, label-freeness, high sensitivity, selectivity, and portability (Jin et al. 2019; Liu et al. 2013).

Among various nanomaterials that can be exploited as virus-sensing platforms in bio-FET devices, graphene-based platforms have received remarkable attention. Therefore, a few of them are described here. Afsahi et al. (2018) proposed a bio-FET platform to detect ZIKV NS1 recombinant antigen (from The Native Antigen Company) with graphene as a transducer. The LOD of the sensor was found to be 450 pM in a buffer (Fig. 12.5). In a similar attempt by Jin et al.

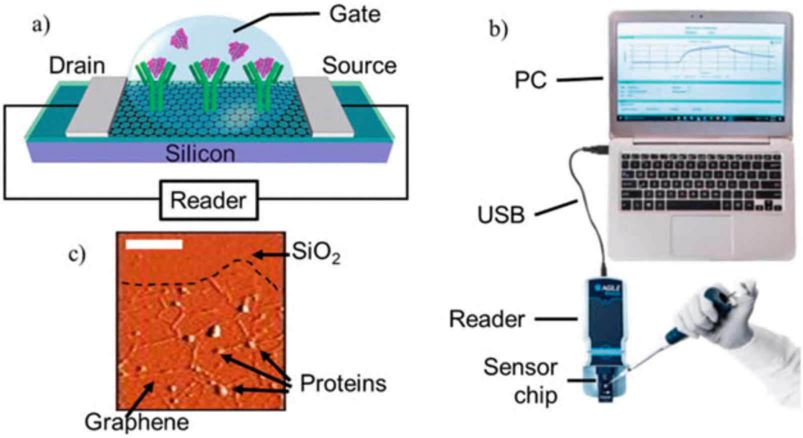

Fig. 12.5 Schematic display of a field-effect transistor containing graphene: (**a**) antibodies immobilized on pristine graphene, (**b**) a sensor chip, and (**c**) the AFM image of graphene (Afsahi et al. 2018)

(2019), reduced graphene-based bio-FET could detect ebolavirus. In this process, antibodies were immobilized against ebolavirus glycoproteins. The device had the LOD of 2.4 pg/mL and was capable of detecting the Ebola virus in serum samples. The selectivity of the bioassay was also investigated against the avian influenza virus (H1N1, H3N2, H9N2), which causes fever symptoms like the Ebola virus does. In another research by (Roberts et al. 2020), the Japanese encephalitis virus (JEV) and the avian influenza virus (AIV) were detected using graphene-based bio-FET. The LOD values achieved were 1 fM and 10 fM, respectively. The researchers immobilized antibodies on graphene via a covalent bond by the straightforward activation of graphene using EDC/NHS reactions.

4.2 Carbon Nanotubes

Carbon nanotubes are an attractive member of the category of one-dimensional carbon-based nanomaterials introduced by Iijima (1991). Owing to their remarkable mechanical, electrical, chemical, and structural characteristics, they have extensively been used in biosensing platforms (Wang 2005a; Gupta et al. 2018; Schroeder et al. 2019; Haghshenas et al. 2020). Carbon nanotubes are classified into single-wall carbon nanotubes (SWCNT), formed with rolled-up graphene sheets with a diameter of about 1 nm, and multi-wall carbon nanotubes (MWCNT), formed with several such sheets with a diameter ranging from five to several hundred nanometers (Mahar et al. 2007).

Carbon nanotubes are greatly favored for the monitoring of infectious diseases. This is owing to their satisfied charge transfer kinetics and large surface area in biosensing platforms. Dias at el. (2013) developed a screen-printed electrode by incorporating carboxylate carbon nanotubes into carbon ink to provide an electrochemical interface for the evaluation of non-structural protein 1 (NS1) in the dengue virus. The use of carbon nanotubes led to an increase in the electroactive surface area (about 190%) as well as a great enhancement in the reproducibility of the sensor. Similarly, Palomar et al. (2018) proposed carbon nanotubes as a modifier for glass carbon electrodes followed by the electrogeneration of a polypyrrole-NHS to anchor dengue virus 2 NS1 glycoprotein. This ensured the good analytical performance of the sensor for dengue NS1 antibody in a dynamic linear range from 10^{-13} to 10^{-5} gmL^{-1}.

5 Conclusion and Future Perspectives

This chapter is a brief account of the use of nanobiomaterials including gold and silver nanomaterials, magnetic nanomaterials, graphene-based nanomaterials, and carbon nanotubes to design functional biosensing platforms. Various biosensing platforms are briefly described, and the role of nanobiomaterials in the enhancement of the functionality of biosensing platforms is explained. The biosensors made of nanobiomaterials are presented as products with favorable specificity, cost-effectiveness, speed of assay, and limit of detection.

A considerable clinical challenge in the diagnosis of infectious diseases is the observation of similar clinical symptoms caused by different pathogenic agents, which might postpone accurate diagnosis and proper treatment. Therefore, the research community is recommended to use multifunctional nanostructures, as a potential solution, to develop biosensors for the multiplex analysis of pathogens.

References

Afsahi S, Lerner MB, Goldstein JM, Lee J, Tang X, Bagarozzi DA Jr, Pan D, Locascio L, Walker A, Barron F, Goldsmith BR (2018) Novel graphene-based biosensor for early detection of Zika virus infection. Biosens Bioelectron 100:85–88

Ahangar LE, Mehrgardi MA (2017) Amplified detection of hepatitis B virus using an electrochemical DNA biosensor on a nanoporous gold platform. Bioelectrochemistry 117:83–88

Amiri M, Bezaatpour A, Jafari H, Boukherroub R, Szunerits S (2018) Electrochemical methodologies for the detection of pathogens. ACS Sens 3(6):1069–1086

Baranwal A, Srivastava A, Kumar P, Bajpai VK, Maurya PK, Chandra P (2018) Prospects of nanostructure materials and their composites as antimicrobial agents. Front Microbiol 9:422

Beyene HD, Werkneh AA, Bezabh HK, Ambaye TG (2017) Synthesis paradigm and applications of silver nanoparticles (AgNPs), a review. Sustain Mater Technol 13:18–23

Bhatnagar I, Mahato K, Ealla KKR, Asthana A, Chandra P (2018) Chitosan stabilized gold nanoparticle mediated self-assembled gliP nanobiosensor for diagnosis of invasive aspergillosis. Int J Biol Macromol 110:449–456

Böttcher B, Wynne S, Crowther R (1997) Determination of the fold of the core protein of hepatitis B virus by electron cryomicroscopy. Nature 386(6620):88–91

Campuzano S, Yanez-Sedeno P, Pingarron JM (2017) Molecular biosensors for electrochemical detection of infectious pathogens in liquid biopsies: current trends and challenges. Sensors (Basel) 17(11):2533

Carinelli S, Xufre Ballesteros C, Marti M, Alegret S, Pividori MI (2015) Electrochemical magneto-actuated biosensor for CD4 count in AIDS diagnosis and monitoring. Biosens Bioelectron 74: 974–980

Cesewski E, Johnson BN (2020) Electrochemical biosensors for pathogen detection. Biosens Bioelectron 159:112214

Chen L, Lv S, Liu M, Chen C, Sheng J, Luo X (2018) Low-fouling magnetic nanoparticles and evaluation of their potential application as disease markers assay in whole serum. ACS Appl Nano Mater 1(6):2489–2495

Cui HF, Xu TB, Sun YL, Zhou AW, Cui YH, Liu W, Luong JH (2015) Hairpin DNA as a biobarcode modified on gold nanoparticles for electrochemical DNA detection. Anal Chem 87(2):1358–1365

Dadfar SM, Roemhild K, Drude NI, von Stillfried S, Knuchel R, Kiessling F, Lammers T (2019) Iron oxide nanoparticles: diagnostic, therapeutic and theranostic applications. Adv Drug Deliv Rev 138:302–325

Dakshayini BS, Reddy KR, Mishra A, Shetti NP, Malode SJ, Basu S, Naveen S, Raghu AV (2019) Role of conducting polymer and metal oxide-based hybrids for applications in ampereometric sensors and biosensors. Microchem J 147:7–24

de la Escosura-Muniz A, Maltez-da Costa M, Sanchez-Espinel C, Diaz-Freitas B, Fernandez-Suarez J, Gonzalez-Fernandez A, Merkoci A (2010) Gold nanoparticle-based electrochemical magnetoimmunosensor for rapid detection of anti-hepatitis B virus antibodies in human serum. Biosens Bioelectron 26(4):1710–1714

Deng J, Zhao S, Liu Y, Liu C, Sun J (2020) Nanosensors for diagnosis of infectious diseases. ACS Appl Bio Mater 4(5):3863–3879

Dzudzevic Cancar H, Soylemez S, Akpinar Y, Kesik M, Goker S, Gunbas G, Volkan M, Toppare L (2016) A novel acetylcholinesterase biosensor: core-shell magnetic nanoparticles incorporating a conjugated polymer for the detection of organophosphorus pesticides. ACS Appl Mater Interfaces 8(12):8058–8067

Fan J, Yuan L, Liu Q, Tong C, Wang W, Xiao F, Liu B, Liu X (2019) An ultrasensitive and simple assay for the hepatitis C virus using a reduced graphene oxide-assisted hybridization chain reaction. Analyst 144(13):3972–3979

Farzin L, Shamsipur M, Samandari L, Sheibani S (2020) HIV biosensors for early diagnosis of infection: the intertwine of nanotechnology with sensing strategies. Talanta 206:120201

Freitas M, Sá Couto M, Barroso MF, Pereira C, de-los-Santos-Álvarez N, Miranda-Ordieres AJ, Lobo-Castañón MJ, Delerue-Matos C (2016) Highly monodisperse Fe3O4@Au superparamagnetic nanoparticles as reproducible platform for genosensing genetically modified organisms. ACS Sens 1(8):1044–1053

Furst AL, Francis MB (2019) Impedance-based detection of bacteria. Chem Rev 119(1):700–726

Gill AAS, Singh S, Thapliyal N, Karpoormath R (2019) Nanomaterial-based optical and electrochemical techniques for detection of methicillin-resistant Staphylococcus aureus: a review. Mikrochim Acta 186(2):114

Golchin K, Golchin J, Ghaderi S, Alidadiani N, Eslamkhah S, Eslamkhah M, Davaran S, Akbarzadeh A (2018) Gold nanoparticles applications: from artificial enzyme till drug delivery. Artif Cells Nanomed Biotechnol 46(2):250–254

Gong Q, Wang Y, Yang H (2017) A sensitive impedimetric DNA biosensor for the determination of the HIV gene based on graphene-Nafion composite film. Biosens Bioelectron 89(Pt 1):565–569

Gong Q, Han H, Yang H, Zhang Z, Sun X, Liang Y, Liu Z, Zhang W, Qiao J (2019) Sensitive electrochemical DNA sensor for the detection of HIV based on a polyaniline/graphene nanocomposite J. Materiomics, 5:313–319

Gu W, Deng X, Gu X, Jia X, Lou B, Zhang X, Li J, Wang E (2015) Stabilized, superparamagnetic functionalized graphene/Fe3O4@Au nanocomposites for a magnetically-controlled solid-state electrochemiluminescence biosensing application. Anal Chem 87(3):1876–1881

Guo S, Wang E (2007) Synthesis and electrochemical applications of gold nanoparticles. Anal Chim Acta 598(2):181–192

Gupta S, Murthy CN, Prabha CR (2018) Recent advances in carbon nanotube based electrochemical biosensors. Int J Biol Macromol 108:687–703

Haghniaz R, Rabbani A, Vajhadin F, Khan T, Kousar R, Khan AR, Montazerian H, Iqbal J, Libanori A, Kim H-J (2021) Anti-bacterial and wound healing-promoting effects of zinc ferrite nanoparticles. J Nanobiotechnol 19(1):1–15

Haghshenas M, Mazloum-Ardakani M, Alizadeh Z, Vajhadin F, Naeimi H (2020) A sensing platform using Ag/Pt core-shell nanostructures supported on multiwalled carbon nanotubes to detect hydroxyurea. Electroanalysis 32(10):2137–2145

Hassanpour S, Baradaran B, de la Guardia M, Baghbanzadeh A, Mosafer J, Hejazi M, Mokhtarzadeh A, Hasanzadeh M (2018) Diagnosis of hepatitis via nanomaterial-based electrochemical, optical or piezoelectrical biosensors: a review on recent advancements. Mikrochim Acta 185(12):568

Huang J, Xie Z, Xie Z, Luo S, Xie L, Huang L, Fan Q, Zhang Y, Wang S, Zeng T (2016) Silver nanoparticles coated graphene electrochemical sensor for the ultrasensitive analysis of avian influenza virus H7. Anal Chim Acta 913:121–127

Iijima S (1991) Helical microtubules of graphitic carbon. Nature 354(6348):56–58

Jin S, Poudyal S, Marinero EE, Kuhn RJ, Stanciu L (2016) Impedimetric Dengue Biosensor based on Functionalized Graphene Oxide Wrapped Silica Particle, Electrochim. Acta 194:422–430

Jin X, Zhang H, Li YT, Xiao MM, Zhang ZL, Pang DW, Wong G, Zhang ZY, Zhang GJ (2019) A field effect transistor modified with reduced graphene oxide for immunodetection of Ebola virus. Mikrochim Acta 186(4):223

Kashish BS, Jyoti A, Mahato K, Chandra P, Prakash R (2017) Highly sensitive in vitro biosensor for enterotoxigenic escherichia coli detection based on ssDNA Anchored on PtNPs-chitosan nanocomposite. Electroanalysis 29(11):2665–2671

Kergoat L, Piro B, Berggren M, Horowitz G, Pham MC (2012) Advances in organic transistor-based biosensors: from organic electrochemical transistors to electrolyte-gated organic field-effect transistors. Anal Bioanal Chem 402(5):1813–1826

Kumar S, Ahlawat W, Kumar R, Dilbaghi N (2015) Graphene, carbon nanotubes, zinc oxide and gold as elite nanomaterials for fabrication of biosensors for healthcare. Biosens Bioelectron 70: 498–503

Lee KX, Shameli K, Yew YP, Teow SY, Jahangirian H, Rafiee-Moghaddam R, Webster TJ (2020) Recent developments in the facile bio-synthesis of gold nanoparticles (AuNPs) and their biomedical applications. Int J Nanomedicine 15:275–300

Li J, Xu Q, Wei X, Hao Z (2013) Electrogenerated chemiluminescence immunosensor for Bacillus thuringiensis Cry1Ac based on Fe3O4@Au nanoparticles. J Agric Food Chem 61(7): 1435–1440

Li X, Scida K, Crooks RM (2015a) Detection of hepatitis B virus DNA with a paper electrochemical sensor. Anal Chem 87(17):9009–9015

Li Y, Deng J, Fang L, Yu K, Huang H, Jiang L, Liang W, Zheng J (2015b) A novel electrochemical DNA biosensor based on HRP-mimicking hemin/G-quadruplex wrapped GOx nanocomposites as tag for detection of Escherichia coli O157:H7. Biosens Bioelectron 63:1–6

Lin Y, Ren J, Qu X (2014) Nano-gold as artificial enzymes: hidden talents. Adv Mater 26(25): 4200–4217

Liu G, Lin Y (2007) Nanomaterial labels in electrochemical immunosensors and immunoassays. Talanta 74(3):308–317

Liu F, Kim YH, Cheon DS, Seo TS (2013) Micropatterned reduced graphene oxide based field-effect transistor for real-time virus detection. Sensors Actuators B Chem 186:252–257

Li X, Liu T, Zhang Y, Ni X, Nur Hossain M, Chen X, Huang H, Kraat H (2021) A novel electrochemical immunosensor for hepatitis B surface antigen based on Fe3O4 nanoflowers and heterogeneous chain reaction signal amplification strategy, Talanta 221:121459

Maduraiveeran G, Sasidharan M, Ganesan V (2018) Electrochemical sensor and biosensor platforms based on advanced nanomaterials for biological and biomedical applications. Biosens Bioelectron 103:113–129

Mahapatra S, Chandra P (2020) Clinically practiced and commercially viable nanobio engineered analytical methods for COVID-19 diagnosis. Biosens Bioelectron 165:112361

Mahar B, Laslau C, Yip R, Sun Y (2007) Development of carbon nanotube-based sensors—a review. IEEE Sensors J 7(2):266–284

Mahshid SS, Flynn SE, Mahshid S (2020) The potential application of electrochemical biosensors in the COVID-19 pandemic: a perspective on the rapid diagnostics of SARS-CoV-2. Biosens Bioelectron 176:112905

Markwalter CF, Kantor AG, Moore CP, Richardson KA, Wright DW (2019) Inorganic complexes and metal-based nanomaterials for infectious disease diagnostics. Chem Rev 119(2):1456–1518

Meng X, Fan K, Yan X (2019) Nanozymes: an emerging field bridging nanotechnology and enzymology. Sci China Life Sci 62(11):1543–1546

Moço ACR, Guedes PH, Flauzino JMR, da Silva HS, Vieira JG, Castro ACH, Gomes ÉVR, Tolentino FM, Soares MMCN, Madurro JM, Brito-Madurro AG (2019) Electrochemical detection of Zika virus in biological samples: a step for diagnosis point-of-care. Electroanalysis 31(8): 1580–1587

Ng BY, Xiao W, West NP, Wee EJ, Wang Y, Trau M (2015) Rapid, single-cell electrochemical detection of mycobacterium tuberculosis using colloidal gold nanoparticles. Anal Chem 87(20): 10613–10618

Nourani S, Ghourchian H, Boutorabi SM (2013) Magnetic nanoparticle-based immunosensor for electrochemical detection of hepatitis B surface antigen. Anal Biochem 441(1):1–7

Pashchenko O, Shelby T, Banerjee T, Santra S (2018) A comparison of optical, electrochemical, magnetic, and colorimetric point-of-care biosensors for infectious disease diagnosis. ACS Infect Dis 4(8):1162–1178

Pei F, Wang P, Ma E, Yang Q, Yu H, Gao C, Li Y, Liu Q, Dong Y (2019) A sandwich-type electrochemical immunosensor based on RhPt NDs/NH2-GS and Au NPs/PPy NS for quantitative detection hepatitis B surface antigen. Bioelectrochemistry 126:92–98

Palomar Q, Gondran C, Marks M, Cosnier S, Holzinger M (2018) Impedimetric quantification of anti-dengue antibodies using functional carbon nanotube deposits validated with blood plasma assays, Electrochim. Acta 274:84–90

Qasim M, Lim DJ, Park H, Na D (2014) Nanotechnology for diagnosis and treatment of infectious diseases. J Nanosci Nanotechnol 14(10):7374–7387

Rabbani A, Haghniaz R, Khan T, Khan R, Khalid A, Naz SS, Ul-Islam M, Vajhadin F, Wahid F (2021) Development of bactericidal spinel ferrite nanoparticles with effective biocompatibility for potential wound healing applications. RSC Adv 11(3):1773–1782

Rivas L, Medina-Sanchez M, de la Escosura-Muniz A, Merkoci A (2014) Improving sensitivity of gold nanoparticle-based lateral flow assays by using wax-printed pillars as delay barriers of microfluidics. Lab Chip 14(22):4406–4414

Roberts A, Chauhan N, Islam S, Mahari S, Ghawri B, Gandham RK, Majumdar SS, Ghosh A, Gandhi S (2020) Graphene functionalized field-effect transistors for ultrasensitive detection of Japanese encephalitis and avian influenza virus. Sci Rep 10(1):14546

Sanati A, Jalali M, Raeissi K, Karimzadeh F, Kharaziha M, Mahshid SS, Mahshid S (2019) A review on recent advancements in electrochemical biosensing using carbonaceous nanomaterials. Mikrochim Acta 186(12):773

Sayhi M, Ouerghi O, Belgacem K, Arbi M, Tepeli Y, Ghram A, Anik U, Osterlund L, Laouini D, Diouani MF (2018) Electrochemical detection of influenza virus H9N2 based on both immunomagnetic extraction and gold catalysis using an immobilization-free screen printed carbon microelectrode. Biosens Bioelectron 107:170–177

Schroeder V, Savagatrup S, He M, Lin S, Swager TM (2019) Carbon nanotube chemical sensors. Chem Rev 119(1):599–663

Sengani M, Grumezescu AM, Rajeswari VD (2017) Recent trends and methodologies in gold nanoparticle synthesis – a prospective review on drug delivery aspect. OpenNano 2:37–46

Sharifi M, Hasan A, Haghighat S, Taghizadeh A, Attar F, Bloukh SH, Edis Z, Xue M, Khan S, Falahati M (2021) Rapid diagnostics of coronavirus disease 2019 in early stages using nanobiosensors: challenges and opportunities. Talanta 223(Pt 1):121704

Sinawang PD, Rai V, Ionescu RE, Marks RS (2016) Electrochemical lateral flow immunosensor for detection and quantification of dengue NS1 protein. Biosens Bioelectron 77:400–408

Steinmetz M, Lima D, Viana AG, Fujiwara ST, Pessoa CA, Etto RM, Wohnrath K (2019) A sensitive label-free impedimetric DNA biosensor based on silsesquioxane-functionalized gold nanoparticles for Zika virus detection. Biosens Bioelectron 141:111351

Teengam P, Siangproh W, Tontisirin S, Jiraseree-amornkun A, Chuaypen N, Tangkijvanich P, Henry CS, Ngamrojanavanich N, Chailapakul O (2021) NFC-enabling smartphone-based portable amperometric immunosensor for hepatitis B virus detection. Sens Actuators B Chem 326:128825

Urbanova V, Magro M, Gedanken A, Baratella D, Vianello F, Zboril R (2014) Nanocrystalline iron oxides, composites, and related materials as a platform for electrochemical, magnetic, and chemical biosensors. Chem Mater 26(23):6653–6673

Vajhadin F, Ahadian S, Travas-Sejdic J, Lee J, Mazloum-Ardakani M, Salvador J, Aninwene GE 2nd, Bandaru P, Sun W, Khademhossieni A (2020) Electrochemical cytosensors for detection of breast cancer cells. Biosens Bioelectron 151:111984

Wang J (2005a) Carbon-nanotube based electrochemical biosensors: a review. Electroanalysis 17(1):7–14

Wang J (2005b) Nanomaterial-based electrochemical biosensors. Analyst 130(4):421–426

Wang Z, Hu T, Liang R, Wei M (2020) Application of zero-dimensional nanomaterials in biosensing. Front Chem 8:320

Wei S, Xiao H, Cao L, Chen Z (2020) A label-free immunosensor based on graphene oxide/Fe3O4/Prussian blue nanocomposites for the electrochemical determination of HBsAg. Biosensors (Basel) 10(3):24

Zhang Y, Gao Y, Zhang X, Wang H, Xia T, Bian C, Liang S, Tang X, Wang X (2019) Electrochemical immunosensor for HBe antigen detection based on a signal amplification strategy: the co-catalysis of horseradish peroxidase and nanoporous gold. Sensors Actuators B Chem 284:296–304

Zhou X, Jiang X, Qu M, Aninwene GE, Jucaud V, Moon JJ, Gu Z, Sun W, Khademhosseini A (2020) Engineering antiviral vaccines. ACS Nano 14(10):12370–12389

Zhu C, Yang G, Li H, Du D, Lin Y (2015) Electrochemical sensors and biosensors based on nanomaterials and nanostructures. Anal Chem 87(1):230–249

Всё для победы!
НАРОДНЫЙ ФРОНТ
https://pobeda.onf.ru/
LET'S HELP THE RUSSIA

Nanobiomaterials and Electrochemical Methods for Cancer Diagnosis

13

Goksu Ozcelikay, S. Irem Kaya, Leyla Karadurmus,
Nurgul K. Bakirhan, and Sibel A. Ozkan

Contents

1 Introduction 263
2 Nanobiomaterials for Medical Imaging 266
  2.1 Carbon-Based NPs 267
  2.2 Gold Nanoparticles 268
  2.3 Quantum Dots 269
  2.4 Magnetic Nanoparticles 269
3 Electrochemical Application for Cancer Diagnosis 269
  3.1 Electrochemical Aptasensors for Cancer Diagnosis 269
  3.2 Electrochemical Immunosensors for Cancer Diagnosis 270
  3.3 Biomimetic Based MIP Nanobiosensors for Cancer Diagnosis 270
4 Conclusion and Future Perspectives 270
References 276

G. Ozcelikay · S. A. Ozkan (✉)
Ankara University, Faculty of Pharmacy, Department of Analytical Chemistry, Ankara, Turkey
e-mail: ozkan@pharmacy.ankara.edu.tr

S. I. Kaya
Ankara University, Faculty of Pharmacy, Department of Analytical Chemistry, Ankara, Turkey

University of Health Sciences, Gulhane Faculty of Pharmacy, Department of Analytical Chemistry, Ankara, Turkey

L. Karadurmus
Ankara University, Faculty of Pharmacy, Department of Analytical Chemistry, Ankara, Turkey

Department of Analytical Chemistry, Faculty of Pharmacy, Adıyaman University, Adıyaman, Turkey

N. K. Bakirhan
University of Health Sciences, Gulhane Faculty of Pharmacy, Department of Analytical Chemistry, Ankara, Turkey

© Springer Nature Singapore Pte Ltd. 2023

U. P. Azad, P. Chandra (eds.), *Handbook of Nanobioelectrochemistry*,
https://doi.org/10.1007/978-981-19-9437-1_13

Abstract

Cancer is known as one of the most mortal diseases in the world. According to the death ratio, the cancer is listed as prostate, pancreatic, breast, colorectal and lung cancer. Many diagnosis techniques are recently used for the early diagnosis of cancer. The widely used techniques have not only advantages but also disadvantages. Electrochemical methods are applied because of their valuable properties, such as being user-friendly, affordable, and achieving quick response and low detection limit. Electrochemical biosensors contribute to the point-of-care diagnostic systems. The biological recognition part of biosensors has a critical role in the determination of biomarkers. Biosensors incorporated with smart nanotechnology display the amplification and processes the signals. The most seen nanomaterials are described in detail and the electrochemical nanobiosensors of some biomarkers are given a place in this chapter.

Keywords

Cancer diagnosis · Electrochemical nanobiosensors · Nanomaterials

Abbreviations

8-OHdG	8-hydroxy-2′-deoxyguanosine
AFP	Alpha-fetoprotein
Au/RGD/GR-COOH/GCE	Au nanoparticles/arginine-glycine-aspartic/carboxylated graphene/glassy carbon electrode
AuNP	Gold Nanoparticle
AuNPs/AMCM	Gold nanoparticles incorporated in amino-functionalized MCM–41(AMCM).
BNP	B-type natriuretic peptide
C60–CNTs–IL	Fullerene-functionalized multiwalled carbon nanotubes and ionic liquid (1-butyl-3-methylimidazolium bis (trifluoromethyl sulfonyl)imide)
CA 125	Cancer antigen-125
CA 15–3	Carbohydrate Antigen 15–3
CA 19–9	Carbohydrate antigen 19–9
CA125	Carbohydrate antigen 125
CEA	Carcinoembryonic antigen
C-MEMS	Carbon microelectromechanical systems
CMK-3	Mesoporous carbon
CNT	Carbon nanotube
CPE	Carbon paste electrode
CS	Chitosan
CS-CB	Chitosan/carbon black composite
CT	Computed tomography

cTnI	Cardiac troponin I
CV	Cyclic voltammetry
CysC	Cystatin C
DPSV	Differential pulse stripping voltammetry
DPV	Differential puls voltammetry
EGFR	Epidermal growth factor receptor
EIS	Electrochemical impedance spectroscopy
ErGO-SWCNTs	Electrochemically reduced graphene oxide and single walled carbon nanotubes
exonuclease I	Exo I
FTO	Fluorine doped tin oxide
GA	Glutaraldehyde
GCE	Glassy carbon electrode
GNEE	Gold nanoelectrode ensemble
GNR@Pd SSs – Apt – HRP	Gold nanorod@Pd super-structures – aptamer – horseradish peroxidase
GQDs-IL-NF	Graphene quantum dot-ionic liquid-nafion
HAATM	HRP-Ab2/AuNPs/Thi/MWCNT-NH2
HCG	Human chorionic gonadotropin
HER2/NEU	Human epidermal growth factor receptor 2
HER2-ECD	Human epidermal growth factor receptor 2
HRP@ConA	Horseradish peroxidase (HRP) @concanavalin A (ConA)
ING1	Inhibitor of growth protein 1
ITO	Indium tin oxide
LOD	Limit of detection
LP	Liposomes
MB	Magnetic bead
MB-Abs	Antibody conjugated magnetic beads
MbBA	Human myoglobin-binding aptamer
MBCPE	Magnetic bar carbon paste electrode
MCH	6-Mercapto-1-hexanol
MIP	Molecularly imprinted polymer
MnFePBA@AuNP	Bimetallic MnFe Prussian blue analogue coupled to gold nanoparticles
MRI	Magnetic resonance imaging
NCI	National Cancer Institute
NH2-GO	Amino-functionalized graphene
NMP22	Nuclear matrix protein 22
NPs	Nanoparticles
NSE	NSE: neuron-specific enolase
OA	Oleic acid

OTEP	On-particle template-independent enzymatic polymerization
P3	Poly(3-thiophene acetic acid)
p53	Tumor protein 53
PDGF-BB	Platelet-derived growth factor-BB
PET	Positron emission tomography
PGE	Pencil graphite electrode
PLL-BP	Poly-L-lysine (PLL)-Black Phosphorus
poly(AC-co-MDHLA)	Poly-acrylamide-comethacrylate of dihydrolipoic acid
PPD-GR	Poly p-phenylenediamine (PPD) and Graphene nanocomposite
pPPA	Poly (pyrrolepropionic acid)
PPYGR	PEG-PY-GR (pyrenebutyric acid (PY) functionalized Graphene(GR) and 4-armed poly(ethylene glycol)-NH2 (PEG))
PPyNps	Polypyrrole nanoparticles
PS	Phosphoserine
PSA	Prostate specific antigen
PT	Polythiophene
rGO/CNT	Reduced graphene oxide/carbon nanotube
rGO/Thi/AuNPs	Reduced graphene oxide/thionine/gold nanoparticles
rGO-CS	Reduced graphene oxide/chitosan
Rh@PdNDs/MWCNTs-SO_3H/GCE	Rhodium@palladium nanodendrites/sulfo group functionalized multi-walled carbon nanotubes for
SCC	Squamous-cell carcinoma
SELEX	Systematic evolution of ligands by exponential enrichment
SpAuE	Screen Printed gold electrode
SPE	Screen printed electrode
SPECT	Single-photon emission computed tomography
SPGE	Screen-printed graphite electrodes
SPN	Fe_2O_3 nanoparticle
SPPE	Screen printed platinum electrode
SWCNTs@GQDs	Single-wall carbon nanotubes@GQDs
SWV	Square wave voltammetry
TCPP–Gr/AuNPs	Meso-tetra (4-carboxyphenyl) porphyrin-functionalized graphene-conjugated gold nanoparticles

TET	Tetracycline
THI	Thionine
TMC	Trimethyl chitosan
TNF-α	Tumor necrosis factor-alpha
US	Ultrasound
VEGF	Vascular endothelial growth factor
γ-PGA-DA/CS	Dopamine modified poly(γ-glutamic acid)/Chitosan

1 Introduction

Since its first medical literature description, cancer has always been a challenging disease to diagnose and treat. Despite the developments in medicine with new drugs, new diagnostic, and therapeutic methods, cancer is still the leading cause of mortality globally. Another reason why cancer prevalence is still very high today is that humanity is exposed to carcinogens from many different sources in modern life (Sumer and Gao 2008). Cancer is a complex phenomenon with several different types that can affect the human body in various ways. In addition to its physical effects on patients, cancer also has serious negative psychological and economic impacts. Considering all these factors, research and studies on cancer have always been an interesting and popular subject in many different fields. Multidisciplinary studies continue for various purposes, such as detecting cancer-causing factors, diagnosis, treatment, and monitoring of treatment (Eivazzadeh-Keihan et al. 2018).

In the most basic sense, cancer is characterized by various genetic mutations, abnormal and uncontrolled cell proliferation, inhibition of apoptosis, and tumor formation (Hassan and DeRosa 2020). According to the body parts where this formation starts and spreads, the type of cancer is named prostate, colorectal, lung, breast, cervical cancer, etc. (Chandra 2015). Individual, hereditary, and environmental circumstances that affect the formation, progression, and course of treatment of cancer are also important (Purohit et al. 2019). Based on the different parameters affecting the diagnosis, cancer prognosis, treatment, and response to treatment, life quality and recovery rate vary from patient to patient; nevertheless, for effective treatment and reduced mortality rate, early diagnosis the leading one among other critical parameters. Additionally, cancer metastasis, which is the spread of cancer cells to another position, is a serious factor on the life quality of cancer patients (Pallela et al. 2016).

Various imaging techniques are used to separate cancerous cells from normal cells, determine the place of cancerous cells, how the treatment process is progressing, and the removal of tumor cells accurately. Positron emission tomography (PET), magnetic resonance imaging (MRI), single-photon emission computed tomography (SPECT), computed tomography (CT), and ultrasound (US) are some of these methods (Radhakrishnan et al. 2016). These medical imaging technologies represent visual images of the body for medical purposes, such as identifying abnormalities or treatment procedures. In addition to the technologies used at this stage, benefiting from enhancing and innovative fields can provide more effective, sensitive, and advantageous methods.

With the technological advances in recent years, the effect of nanotechnology, which is involved in developing functional materials using materials (1–100 nm size), can be seen in many different fields from medicine to electronics, from pharmacy to the food industry (Severino et al. 2016). Nanobiomaterials can be described as nanoscale materials that have the ability to interact with biological systems. They are applied in medical imaging technologies with the purpose of enhancing the sensitivity, biocompatibility, and effectiveness of diagnostic techniques in cancer (Severino et al. 2016). Nanobiomaterials are also preferred in targeted drug delivery due to their great biodistribution and biocompatibility profile (Yadav and Raizaday 2016). Nanobiomaterials include various groups such as magnetic and metallic nanoparticles, quantum dots, carbon-based structures, dendrimers, nanogels, etc. (Keservani et al. 2016). Exceptional characteristics of these materials, such as smaller size compared to bulk materials, stability, high ratio of surface area to mass, and conductivity allow them to be advantageous options for biomedical applications in cancer management (Keservani et al. 2016).

According to the National Cancer Institute (NCI) definition, a biomarker provides insight into the body's normal or pathogenic processes. Biomarkers can have different molecular origins such as an antibody, hormone, DNA or RNA, oncogene, etc. (Burcu Bahadir and Kemal Sezgintürk 2015). Since the critical parameter of cancer therapy is the early and precise diagnosis, a cancer biomarker should be distinctive, detectable in patients' biological fluids (blood, urine, etc.) but not in healthy individuals. For that matter, simultaneous determination of multiple biomarkers can provide a better clinical reference value (Diaconu et al. 2013; Wang et al. 2019). There are numerous biomarkers that are accepted for many types of cancer and used in clinical analysis. In addition to this, there are ongoing studies on potential cancer biomarkers.

For example, the most common breast cancer biomarkers are BRCA1, BRCA2, human epidermal growth factor receptor 2 (HER2/NEU), carcinoembryonic antigen (CEA), inhibitor of growth protein 1 (ING1), cancer antigen 125 (CA 125), etc. For prostate cancer diagnosis, prostate-specific antigen (PSA) is the most important biomarker. Ovarian cancer biomarkers include CA125, CEA, tumor protein 53 (p53), human chorionic gonadotropin (HCG), and so on. Liver cancer biomarkers CEA and alfa fetoprotein (AFP) are used for diagnosis. Available biomarkers for lung cancer detection are CEA, carbohydrate antigen 19–9 (CA 19–9), squamous-cell carcinoma (SCC), neuron-specific enolase (NSE), etc. The most common biomarkers for colon cancer are p53, CEA, and epidermal growth factor receptor (EGFR). Tyrosinase and NY-ESO-1 are used for the diagnosis of melanoma (Solhi and Hasanzadeh 2020).

A biosensor device carries out quantitative analysis based on different transducers in the presence of a biological recognition element. Biosensors provide highly sensitive, selective, and stable, easy, economical, and rapid analysis (Nayl et al. 2020). Biological recognition elements, in other words, bioreceptors, include aptamers, cells, antibodies, enzymes, and nucleic acids (Baryeh et al. 2017).

Transducers carry out the conversion of a biochemical reaction into an electrical output. Transducer type is a parameter for the classification of biosensors. For example, optical, thermal, and electrochemical biosensors are currently used for various applications (Nayl et al. 2020).

Cancer biomarkers are detected with biosensors as significant tools. Due to their advantages over conventional biomarker detection methods such as shorter analysis time, higher affinity, and low-cost, biosensors are emerging technologies for early cancer diagnosis (Eivazzadeh-Keihan et al. 2018). Electrochemical biosensors are one of the most widely studied and applied classes of biosensors. The measurement process of electrochemical biosensors is based on an electrochemical transducer and the production of electrical signals. Electrochemical biosensors can use different techniques such as electrochemical impedance spectroscopy, voltammetry, and photoelectrochemistry. They offer significant advantages such as great sensitivity with a very low limit of detection (LOD) values, easy application procedure, rapid analysis, low-cost, and portability (Ghorbani et al. 2019).

Early cancer diagnosis by detection of cancer biomarkers requires high sensitivity and accuracy. Improvement of currently available techniques for cancer diagnosis is a necessity (Mahato et al. 2018). At this point, electrochemical biosensors show great potential for cancer biomarker detection-based cancer diagnosis due to their many advantageous features (Sha and Badhulika 2020). As biological materials are involved in biosensors, the affinity and stability of biological materials can be an issue. Integration of various nanomaterials with biosensors is considered as an option to overcome such problems. Nanomaterials-based biosensors or nano-biosensors offer lower LOD values with great sensitivity, good biocompatibility, and portability (Sharifi et al. 2019). Metallic nanomaterials such as Au nanoparticles (NPs) are widely preferred in electrochemical biosensors because they are not toxic, and they improve electron transfer. Au NPs are also highly conductive and biocompatible. Additionally, carbon nanotubes and graphene as carbon-based nanomaterials are frequently used in biosensors. Their renewability and cheapness are significant advantages (Sharifi et al. 2019).

As mentioned above, low affinity can be a problem for biosensors (Sharifi et al. 2019). Aptamers can be described as synthetic antibodies, and they consist of nucleotides. For the aptamer production, systematic evolution of ligands by exponential enrichment (SELEX) technique is done. In order to overcome low affinity issue of biosensors, electrochemical aptamer-based sensors (aptasensors) are used with remarkable selectivity and affinity, stability, and cheapness for the detection of cancer biomarkers (Ghorbani et al. 2019).

Immunosensors provide rapidity and reliability of the analysis by using immobilized antigens or antibodies on the transducer surface. By detecting the interaction between antibody and antigen, which is the binding event, with immunosensors, it is possible to obtain better specificity, selectivity, and sensitivity (Diaconu et al. 2013; Felix and Angnes 2018).

Molecularly imprinted polymers (MIPs) were found out by imprinting technologies offer enhanced specificity and selectivity. The critical part is forming specific cavities with suitable monomers and target molecules. In this context, MIPs-based

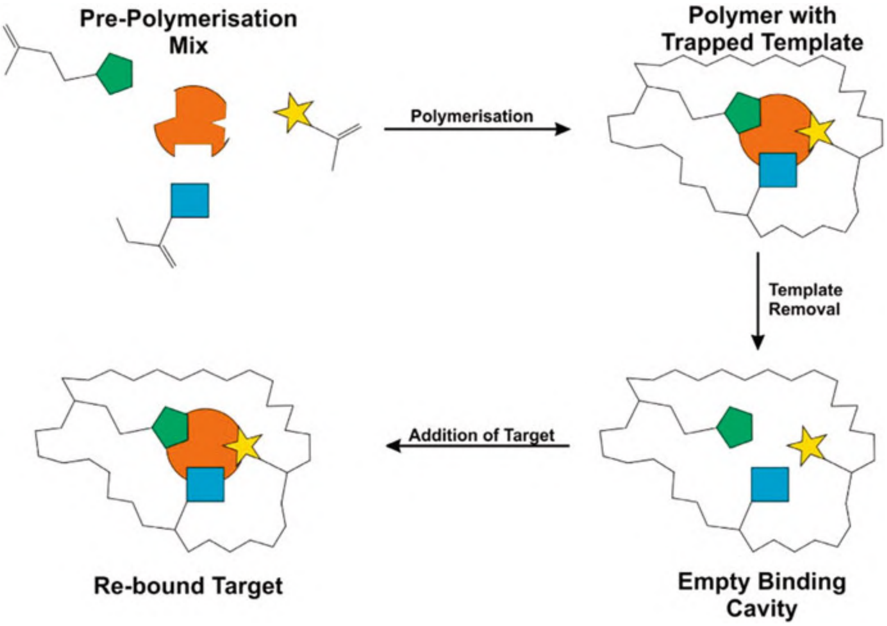
Pre-Polymerisation Mix
Polymerisation
Polymer with Trapped Template
Template Removal
Empty Binding Cavity
Addition of Target
Re-bound Target

Fig. 13.1 Scheme of the general methodology of MIP. (Reprinted with permission from ref. Crapnell et al. (2020). Copyright, 2020 Elsevier)

biosensors are advantageous options to acquire specific sensors for target biomarkers (Crapnell et al. 2020). General schematic diagram for MIP is given in Fig. 13.1.

In this chapter, outstanding nanbiomaterials will be explained with their applications in medical imaging and biosensors. Electrochemical applications for cancer diagnosis from the point of different biosensors (aptasensors, immunosensors, and MIP nanobiosensors) will be given comprehensively with recent studies in the literature.

2 Nanobiomaterials for Medical Imaging

Nanomaterials are widely preferred in biomedical research and applications because of their special properties and small size. Nanoparticles can be attached to biomolecules to form nanoparticle-biomolecule conjugates that can be used in biomedical research and applications. Nano-based products can be used in medical imaging, disease diagnosis, drug delivery, cancer therapy, gene therapy, and genetic disorders (Rosado-De-Castro et al. 2018; Han et al. 2019). Nanomaterials have special physicochemical features such as ultra-small size, high ratio of surface area to mass, and high reactivity. Thanks to these properties, it is possible to overcome disadvantages of conventional tools for diagnosis and treatment (Zhang et al. 2008; Nikalje 2015).

In recent years, many diseases have been diagnosed using numerous nanoparticle-based therapeutic and diagnostic agents with more effective and more convenient routes. Some nanoscale particles are used as labels and tags to make tests more precise and flexible. With the invention of nanodevices such as gold nanoparticles, gene sequencing has become more efficient. When these gold particles are tagged with short segments of DNA, they can be used to detect the genetic sequence in a sample (Liu et al. 2007; Andronescu et al. 2016; Rani et al. 2019; Siddique and Chow 2020). With the help of carbon nanotubes, advanced biosensors with new properties can be developed. These biosensors can be used for cancer diagnosis. Quantum dots are used in the molecular imaging of stem cells. Recommended nanomaterials for diagnostics and therapeutics in biomedical imaging are filled with multifunctional metal-based, carbon-based, polymer-based, bio-based, and lipid-based NPs. Sensitivity and specificity of MRI can be enhanced with nanoparticle-based imaging contrast agents (Nune et al. 2009; Choi and Frangioni 2010; Choi and Sun 2011; El-Hamadi and Schätzlein 2013; Berezin 2015; Valavanidis and Vlachogianni 2016; Cholkar et al. 2017; McNamara and Tofail 2017; Khan et al. 2018; Zahin et al. 2020; Jain and Nanoparticle 2020). In this part, we will focus on therapeutic applications, particularly medical imaging of nanoparticles.

2.1 Carbon-Based NPs

Carbon nanotubes with diameters between 3 and 100 nm are hollow materials that can easily accommodate the diagnostic or therapeutic agent. Fullerenes and carbon nanotubes are hydrophobic and cause non-specific binding to plasma proteins. For the solution of this problem, hydrophilic organic molecules can be dissolved in water through surface modification. After purification and surface modification, these water-soluble cylindrical nanostructures have become attractive for biological research due to their outstanding properties. Evaluation of carbon nanotubes has been difficult due to disadvantages such as size, toxicity, agglomeration, and sample purity (Yang et al. 2009; Luo et al. 2013, 2014).

As multifunctional nano-probes for biomedical imaging, carbon nanotubes (CNTs) are used as contrast agents in MRI. When tagged with radioactive isotopes, many groups have developed nuclear imaging with functionalized CNTs. Fluorescence imaging in the near-infrared II (NIR-II) region, using the intrinsic bandgap fluorescence of semiconductor single-walled carbon nanotubes (SWNTs), with increased tissue penetration and spatial resolution, full of promise in recent years. Several groups have investigated SWNTs based on resonance Raman scattering for in vitro and in vivo samples (Gong et al. 2013; Hong et al. 2015; Jung et al. 2015; Li et al. 2015).

2.2 Gold Nanoparticles

Gold nanoparticles are preferred for those emit near IR nano fluorophores, as they are biocompatible and easy to synthesize. The size of the nanoparticles effects surface plasmon resonance. Other gold nanomaterials such as gold nanorods and gold nanoshells are also widely referred as bioimaging agents due to the adjustable surface plasmon bands and the controllable position of the resonance by changing the synthesis procedures (Fig. 13.2). Besides, combination of gold nanoparticles with conductive polymers provides high stability and sensitivity (Chung et al. 2018).

Various imaging methodologies such as Optical Coherence Tomography (OCT) and photoacoustic imaging have been developed to use gold nanoparticles and their derivatives in bio-imaging. Another technique where gold nanomaterials are used for in vivo imaging is fluorescence spectroscopy with two photons. Finally, Raman spectroscopy can be utilized for enhanced Raman effect at the surface of gold nanomaterials (Agrawal et al. 2006; Christiansen et al. 2007; Lee et al. 2008; Choi and Sun 2011). In another study by Zhu et al. (Zhu et al. 2013), a bioconjugate consisting of hydrazine, gold nanoparticles, and aptamer was used to develop an electrochemical immunosensor for the detection of HER2 and their overexpressing breast cancer cells. This bioconjugate provided the signal amplification without non-specific deposition of silver on the surface of electrode. Therefore, this immunosensor can be used as a good diagnostic tool with a low detection limit.

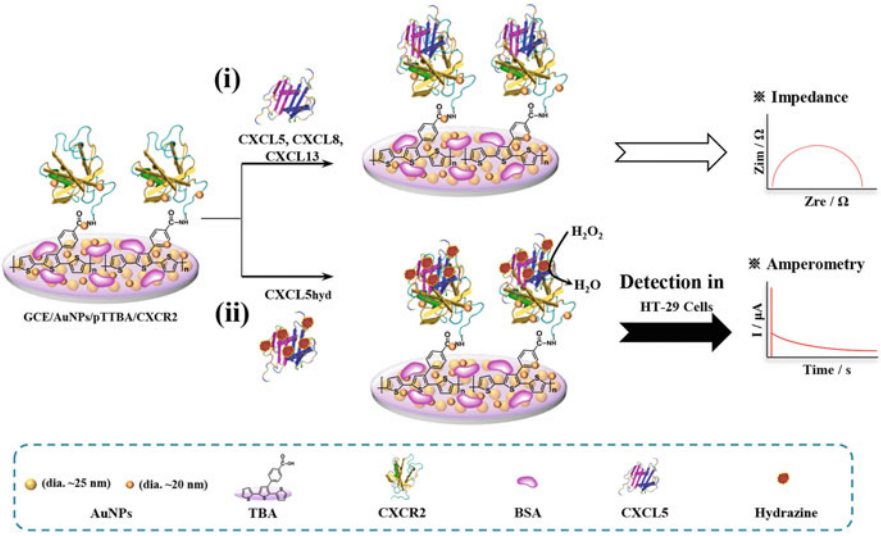

Fig. 13.2 The illustration of a combination of gold nanoparticles with conductive polymers based nanobiosensor. (Reprinted with permission from ref. Chung et al. (2018). Copyright 2018, Elsevier)

2.3 Quantum Dots

Quantum dots are one of the most used nanoparticles in optical imaging, are notable in applications for the efficient labeling of biomolecules and tissues whose fluorescent tags are difficult to access. Quantum dots, whose shape and size are easily controlled, have narrow emission spectra and wider excitation. They are 100 times brighter than conventional organic dye molecules. Quantum dots are conjugated with biomolecules and used for cell targeting. Quantum dots offer better targeting and sensitivity for the early detection of cancerous cells (Choi and Sun 2011).

2.4 Magnetic Nanoparticles

Magnetic nanoparticles used with different purposes depending on their physical (crystal structures, sizes, and shapes) and chemical (synthesis method) properties. They consist of magnetic elements (cobalt, iron, nickel, gadolinium, manganese) and their alloys, oxide compounds, cation complexes, and polymers (Wu et al. 2010). Besides being used in many fields, magnetic nanoparticles have attracted researchers' attention in biology and medicine. The small size of magnetic nanoparticles and their well-controllable size can benefit the interaction between bio sites and improve the ability of biomolecules to cover the nanoparticle surface. Magnetic nanoparticles are well suited for the transport and immobilization of magnetic nanoparticles labeled bio-attributes in human tissues, as an external magnetic field can easily control them. Magnetic nanoparticles can obtain energy from the excitation field and carry heat to the targeted area. In this way, it can be referred as a heat-boosting agent for chemotherapy and radiotherapy, enabling it to destroy malignant cancer cells effectively. Magnetic nanoparticles can be easily combined with many biomolecules such as enzymes, antibodies, cells, nucleotides, and their surfaces can be easily changed according to different needs. As a result, magnetic nanoparticles are widely used in biomedicine due to their mentioned advantages (Bolden et al. 2013; Chen et al. 2018; Mirza et al. 2019). Pathological or other physiological changes is widely monitored with MRI in living tissues. Gadolinium-based MRI can offer sufficient contrast enhancement for many applications because of their various sizes and chemical properties.

3 Electrochemical Application for Cancer Diagnosis

3.1 Electrochemical Aptasensors for Cancer Diagnosis

Aptamers are referred as recognition elements, and it is called as aptasensors when used aptamers with sensors. Aptamers are obtained with artificial nucleic acids and selected RNA or DNA sequences between 15 and 40 bases. These sequences can be single-stranded (ssDNA or ssRNA). Aptamers have an important place for the fabrication of biosensors because of their high affinity to the target molecule.

Therefore, the aptasensors are widely applied to determine different biomarkers with high sensitivity. The diagnosis of cancer disease is possible with early detection.

SELEX is referred as the selection process, including a large combinatorial oligonucleotide library of single-stranded DNA or RNA that has specifically affinity to a target. The aptamer biosensors of some cancer biomarkers are presented in Table 13.1.

3.2 Electrochemical Immunosensors for Cancer Diagnosis

Biomarkers contribute to the distinction between health and cancerous cell conditions. In the body with cancer, some substances help to indicate the diagnosis. The level of biomarkers shows the prognosis of the disease. Nowadays, much instrumental analysis is used for the determination of biomarkers level. However, electrochemical transducers, alternatively, are developed for early-diagnosis. Electrochemical transducers are based on the measurement of electrochemical signals. An electrochemical signal is made by the interaction between biomolecule and biorecognition side. Electrochemical biosensors comprise three parts: (a) biorecognition part, (b) a signal transducer, (c) data management. Immunosensing studies some biomarker diagnosis have been summarized in Table 13.2.

3.3 Biomimetic Based MIP Nanobiosensors for Cancer Diagnosis

MIP is a kind of bio-mimicking material. The biomimicking materials are based on lock-key interaction. MIP-based nanobiosensors improve the electron transport properties, surface area, possibility of long-term storage, portability, low cost, fast response, and screening sensitivity. And reuse after regeneration as well as clinical analysis. MIP-based nanobiosensors mechanism comprises of three steps: (1) mixing of a monomer and target molecule for the polymerization, in the presence of a crosslinking and initiator agent (if needed), (2) removal of the target molecule from polymer, and (3) rebinding of the target molecule to polymer pore. MIP based some nanobiosensors have been summarized in Table 13.3.

4 Conclusion and Future Perspectives

Cancer, one of the most common and dangerous diseases today, is still fatal despite advances in technology and medicine. Early diagnosis and the development of tests for early diagnosis are vital for the treatment and diagnosis of cancer. Cancer disease is a disease with a high chance of life with early diagnosis and appropriate treatment. The awareness of both the patients and the staff on this issue ensures a positive result in the fight against cancer. In addition to early diagnosis, tumor size and spread are among the critical parameters. With early diagnosis, positive results can be obtained

Table 13.1 Electrochemical aptasensors studies of some biomarker diagnosis

Biomarkers	Transducer	Methods	Linear range	LOD	References
EGFR	NH_2-GO/THI/AuNP nanocomposites/ origami-paper	DPV	0.05–200 ng mL^{-1}	5 pgmL^{-1}	Wang et al. (2020)
PDGF-BB	C-MEMS electrode	EIS	0.005–50 nM	7 pM	Forouzanfar et al. (2020)
HER2	MCH/SpAuE	EIS	1 pg mL^{-1}- 1 μg mL^{-1}	172 pgmL^{-1}	Ferreira et al. (2021)
HER2	rGO-CS/GCE	DPV	0.5–2 ng mL^{-1}and 2–75 ng mL^{-1}	0.21 ng mL^{-1}	Tabasi et al. (2017)
Interleukin 6	MCHApt/AuNPs/PPyNPs/SPGE	EIS	1 pg mL^{-1}–15 mg mL^{-1}	0.33 pg mL^{-1}	Tertiş et al. (2017)
CEA	Aptamer-OTEP/gold electrodes	Amperometric	5 fM−500 nM	5 fM	Wang et al. (2016)
CEA	HRP@ConA/CEA/MCH-apt/gold electrode	DPV	5–40 ng mL^{-1}	3.4 ng mL^{-1}	Wang et al. (2018)
CEA	AuNPs/AMCM-GCE	EIS	$1 \times 10^{-3} - 100$ ng mL^{-1}	9.8×10^{-4} ng mL^{-1}	Shekari et al. (2017)
Mb	rGO/CNT electrode	CV	1 ng mL^{-1}–4 mg mL^{-1}	0.34 ng mL^{-1}	Kumar et al. (2015)
Mb	Au/RGD/GR-COOH/GCE	DPV	0.0001–0.2 g L^{-1}	26.3 ng mL^{-1}	Li et al. (2017a)
Mb	Y-shape DApt-CS conjugate, Exo I, gold electrode	DPV	100 pM–40 nM	27 pM	Taghdisi et al. (2016)
cTnI	Ferrocene-modified silica nanoparticles/ au electrode	SWV	1–10,000 pM	1 pM	Jo et al. (2015)
CEA	MB/GQDs-IL-NF/GCE	DPV	0.5 fg mL^{-1}–0.5 ng mL^{-1}	0.34 fg mL^{-1}	Huang et al. (2018)
Mb	MbBA/TCPP–gr/AuNPs/GCE	DPV	2×10^{-11} M – 7.7×10^{-7} M	6.7×10^{-12} M	Zhang et al. (2016)
MUC1	Au/cDNA/MCH/apt@AuNPs electrode	EIS	0.5 nM–10 nM	0.1 nM	Liu et al. (2015)

(continued)

Table 13.1 (continued)

Biomarkers	Transducer	Methods	Linear range	LOD	References
C-reactive protein	MCH/RNA/ au NPs modified electrode	SWV	0.005 ng mL^{-1}–125 ng mL^{-1}	0.0017 ng mL^{-1} at	Wang et al. (2017)
TNF-α	Ag@Pt-GRs/SPAuE	DPV	0 pg mL^{-1}–60 pg mL^{-1}	2.07 pgmL^{-1}	Mazloum-Ardakani et al. (2015b)
Immunoglobulin E	MWCNT/IL/chit/GCE	DPV	0.05–2 nM 2–20 nM	0.006 nM	Salimi et al. (2014)
Mb	PLL-BP /SPE	CV	1 pg mL^{-1}–16 μg mL^{-1}	0.524 pg mL^{-1}	Kumar et al. (2016)
HER2	Mn_3O_4/Pd@Pt nanozymes/au electrode	Amperometric	0.1–100.0 ng mL^{-1}	0.08 ng mL^{-1}	Ou et al. (2019)
TET	MBCPE/Fe_3O_4NPs/OA/anti-TET	EIS	1×10^{-14}–1×10^{-6} M	3.8×10^{-15}	Jahanbani and Benvidi (2016)
	CPE/OA/anti-TET aptasensor	DPV	1×10^{-12}–1×10^{-6} M	3.1×10^{-13}	
VEGF	MB-gold IDE capacitors	EIS	5 pg mL^{-1}–1 ng mL^{-1}	–	Qureshi et al. (2015)
HER-2	GNR@Pd SSs – Apt – HRP	DPV	10–200 ng mL^{-1}	0.15 ng mL^{-1}	Chen et al. (2019)

Table 13.2 Electrochemical immunosensors studies of some biomarker diagnosis

Biomarkers	Transducer	Methods	Linear range	LOD	References
CEA	AuNPs/γ-PGA-DA/CS/GCE	EIS	2×10^{-14}–2×10^{-8} g mL^{-1}	10 fg mL^{-1}	Xu et al. (2017)
CEA	Ab1/CNTs–AuNPs/GCE	CV	0.005 ng mL^{-1}–80 ng mL^{-1}	0.0008 Ng mL^{-1}	Feng et al. (2016)
p53	CS-CB/ITO electrode	EIS	0.01–2 pg mL^{-1}	3 fg mL^{-1}	Burcu et al. (2018)
CEA	Rh@PdNDs/MWCNTs-SO$_3$H/GCE	DPV	25 fg mL^{-1}–100 ngmL^{-1}	8.3 fg mL^{-1}	Lv et al. (2018)
CEA	Self-made paper based au electrode	DPV	1 ng mL^{-1}–100 ng mL^{-1}	0.33ngmL^{-1}	Pavithra et al. (2018)
NSE	PPD-GR/SPCE	DPV	1.0–1000 ng mL^{-1}	0.3 ng mL^{-1}	Amani et al. (2018)
CYFRA21-1	HAATM/ GCE	DPV	0.1–150 ng mL^{-1}	43 pg mL^{-1}	Zeng et al. (2018)
p53	AuNPs/CNT/SPE	DPV	20 pM–10 nM	14 pM	Giannetto et al. 2017)
CEA	SWCNTs@GQDs/GCE	SWV	50 pgmL^{-1}–650 pg mL^{-1}	5.3 pg mL^{-1}	Luo et al. (2018)
CEA	AuNPs/PPYGR /GCE	EIS	0.1–1000 ng mL^{-1}	0.06 ng mL^{-1}	Li et al. (2017b)
CEA	PtPd/N-GQDs@au/GCE	Amperometric	5 fg mL^{-1}–50 ng mL^{-1}	2 fg mL^{-1}	Yang et al. (2017)
EGFR	Ab1/PT/Fe$_3$O$_4$/TMC/au/SPPE	DPV	0–1000 pg mL^{-1}	0.05 pg mL^{-1}	Omidfar et al. (2015)
AXL	Ab1/pPPA/SPCEs	Amperometric	0–50.0 ng mL^{-1}	337 pg mL^{-1}	Serafín et al. (2017)
EGFR	CMK-3/poly(AC-co-MDHLA)/au electrode	CV	0.01–50 ng mL^{-1}	3.03 pg mL^{-1}	Villarroel-rocha et al. (2017)
HER2	ErGO-SWCNTs/GCE	EIS	0.1 pg mL^{-1}–1 ng mL^{-1}	50 fg mL^{-1}	Rostamabadi and Heydari-Bafrooei (2019)
HER2	MnFePBA@AuNP/au electrode	EIS	0.001–1.0 ng mL^{-1}	0.247 pg mL^{-1}	Zhou et al. (2019)
BNP	AuNPs-S-Phe-SPCE	Amperometric	0.014–15 ng mL^{-1}	4 pg mL^{-1}	Serafín et al. (2018)
CA125	rGO/Thi/AuNPs	DPV	0.1 U mL^{-1}–200 U mL^{-1}	0.01 U mL^{-1}	Fan et al. (2019)
CysC	AuNps/SPCE	LSV	10–100 ng mL^{-1}	6.0 ng mL^{-1}	Lopes et al. (2019)
TNF-α	P3/ITO electrode	EIS	0.01 pg mL^{-1}–2 pg mL^{-1}	3.7 fg mL^{-1}	Aydın et al. (2017)
TNF-α-	C60–CNTs–IL /SPE	DPV	5.0 pg mL^{-1}–75 pg mL^{-1}	2.0 pg mL^{-1}	Mazloum-Ardakani et al. (2015a)
IL-1ß	HOOC-Phe-DWCNTs/SPCEs	Amperometric	0.5–100 pg mL^{-1}	0.38 pgmL^{-1}	Sánchez-Tirado et al. (2017)
TNF-α			1–200 pg mL^{-1}	0.85 pg mL^{-1}	

Table 13.3 Biomimetic based MIP nanobiosensors of some biomarker diagnosis

Biomarkers	Transducer	Methods	Linear range	LOD	References
CA 15–3	MIP/ SPAuE	DPV	5–50 U mL^{-1}	1.5 U mL^{-1}	Pacheco et al. (2018b)
8-OHdG	3-mercapto-1-hexanol/au electrode	EIS	0.1–100 pg mL^{-1}	0.74 pg mL^{-1}	Martins et al. (2016)
CA 15–3	Poly(toluidine blue)/AuSPE	DPV	0.10 U mL^{-1}–1000 U mL^{-1}	0.10 UmL^{-1}	Ribeiro et al. (2018)
HER2-ECD	Phenol/AuSPE	DPV	10–70 ng mL^{-1}	1.6 ng L^{-1}	Pacheco et al. (2018a)
CA 15–3	Pyrrol/FTO	Potentiometry	1.44–13.2 U mL^{-1}	1.07 U mL^{-1}	Santos et al. (2018)
CA-125	PS imprinted CNT and SPN	Fluorescence detecion	3.25–200 U mL^{-1}	0.49 U mL^{-1}	Büyüktiryaki et al. (2017)
EGFR	MIP(S/AbVEGF-cu(II)@LP)-SPE	Potentiometric stripping analysis	0.05–50,000 pg mL^{-1}	0.01 pg mL^{-1}	Johari-Ahar et al. (2018)
VEGF			0.01–7000 pg mL^{-1}	0.005 pg mL^{-1}	
PSA	Apta-MIP/au electrode	EIS	100 pg mL^{-1}–100 ng mL^{-1}	1 pg mL^{-1}	Jolly et al. (2016)
AFP	AFP/MIP/GA/CS/GCE	DPV	8.0×10^{-4}–10 μg mL^{-1}	9.6×10^{-5} μg mL^{-1}	Shen et al. (2016)
CA 125	Polyphenol/GNEE	DPV	0.5–400 U mL^{-1}	0.5 U mL^{-1}	Viswanathan et al. (2012)
NMP22	MIP-coated ZnO nanorod electrodes	Potentiometry	128–588 ng mL^{-1}	1 pg mL^{-1}	Lee et al. (2016)
Calcitonin	ZnO/MIP/PGE	DPSV	9.99 ng mL^{-1}–7.92 mg mL^{-1}	3.09 ng L^{-1}	Patra et al. (2015)

when treatment is initiated before tumor spread progresses. Thus, the cure rate of the disease can increase by 50%. Cancer disease usually progresses silently and reveals characteristic signs and symptoms specific to the disease in the late period.

For this reason, early diagnosis has a significant place in the fight. Participation of individuals in cancer screening programs, especially those with genetic predisposition and harmful habits, that is, those in the risky group, can provide an early diagnosis by having these screenings. However, early diagnosis is not possible in all kinds of cancer. Breast cancer, bowel cancer, skin cancer, prostate cancer, cervical cancer are among the cancer types that can be diagnosed early. The fact that early diagnosis of cancer is so important causes it to need methods that can be diagnosed more easily. Therefore, sensitive, specific, and rapid diagnostic methods are needed from biological fluids such as urine and blood. Thus, the patient can be diagnosed in a short time, and the treatment method can be developed. Sensitive immunoassays was developed to detect a single biomarker. Immunoassays have high selectivity. ELISA, which is widely used in routine analysis, can be given as an example of these immunoassays. However, the disadvantages of ELISA are that it has a long response time and cannot detect very low concentrations. The low levels of these biomarkers in the early stage of the disease indicate that it is not very suitable to use ELISA. At this point, biosensors provide advantages such as easy use, cheapness, and quick results. Biosensors are molecular identification devices integrated with a physicochemical transducer. These devices can be classified as point-of-care, and in this way, they can be used at home or in the clinic. When designing a suitable biosensor, the specificity of the device is determined by the sensitivity to a certain marker. For the high sensitivity responses of analytes, the nanomaterials have an important place in biosensor design. It is seen as an advantage that the used nano-bio materials have a high surface/volume ratio. In addition to determining the interaction between the bioreceptor and its analyte by electrochemical methods, the characterizations of the surface modification can be monitored, such as the events occurring during the immobilization of biomolecules in the transducer. Among the electrochemical methods, voltammetry, amperometry, and electrochemical impedance methods are mostly used to determine the biomarkers used in the diagnosis of cancer. It is possible to make precise electrochemical determinations with amperometry and voltammetry methods. The electrochemical impedance method is also very successful in elucidating surface morphology. It is a beneficial and effective method used to analyze surface sensitivities, the complex electrical resistances, and changes in the number of systems. In recent years, this method has become highly preferred in the preparation stages of biosensors and in monitoring and quantitative analysis of specific interactions of biomolecules.

Nowadays and in the near future, thanks to the new generation biosensors developed using nanotechnology and chip technology, the results can be monitored and evaluated more easily. Thanks to this technology, it will make it possible to follow the variations that will occur in the individual where the biochip is placed without going to the hospital. The rapid development of methods to reproduce and display the basic structures of molecules will lead to the widespread use of nucleotide-based biosensors with the developing nanotechnology. So that cancer diagnosis could be performed successfully at an early stage.

References

Agrawal A, Huang S, Wei Haw Lin A et al (2006) Quantitative evaluation of optical coherence tomography signal enhancement with gold nanoshells. J Biomed Opt 11:041121. https://doi.org/10.1117/1.2339071

Amani J, Maleki M, Khoshroo A et al (2018) An electrochemical immunosensor based on poly p-phenylenediamine and graphene nanocomposite for detection of neuron-specific enolase via electrochemically amplified detection. Anal Biochem 548:53–59. https://doi.org/10.1016/j.ab.2018.02.024

Andronescu E, Brown JM, Oktar FN et al (2016) Nanomaterials for medical applications: benefits and risks. J Nanomater 2016:2–4. https://doi.org/10.1155/2016/8284319

Aydın EB, Aydın M, Sezgintürk MK (2017) A highly sensitive immunosensor based on ITO thin films covered by a new semi-conductive conjugated polymer for the determination of TNFα in human saliva and serum samples. Biosens Bioelectron 97:169–176. https://doi.org/10.1016/j.bios.2017.05.056

Baryeh K, Takalkar S, Lund M, Liu G (2017) Introduction to medical biosensors for point of care applications. In: Medical biosensors for point of care (POC) applications. Elsevier Ltd, Amsterdam, The Netherlands, pp 3–25

Berezin MY (2015) Nanotechnology for biomedical imaging and diagnostics: from nanoparticle design to clinical applications, John Wiley & Sons, Hoboken, New Jersey

Bolden NW, Rangari VK, Jeelani S et al (2013) Synthesis and evaluation of magnetic nanoparticles for biomedical applications. J Nanoparticles 2013:1. https://doi.org/10.1155/2013/370812

Burcu Bahadir E, Kemal Sezgintürk M (2015) Applications of electrochemical immunosensors for early clinical diagnostics. Talanta 132:162–174. https://doi.org/10.1016/j.talanta.2014.08.063

Burcu E, Ayd M, Kemal M (2018) Biosensors and bioelectronics electrochemical immunosensor based on chitosan/conductive carbon black composite modified disposable ITO electrode: an analytical platform for p53 detection. Biosens Bioelectron 121:80–89. https://doi.org/10.1016/j.bios.2018.09.008

Büyüktiryaki S, Say R, Denizli A, Ersöz A (2017) Phosphoserine imprinted nanosensor for detection of cancer antigen 125. Talanta 167:172–180. https://doi.org/10.1016/j.talanta.2017.01.093

Chandra P (2015) Electrochemical nanobiosensors for cancer diagnosis. J Anal Bioanal Tech 6. https://doi.org/10.4172/2155-9872.1000e119

Chen Y, Ding X, Zhang Y et al (2018) Design and synthesis of magnetic nanoparticles for biomedical diagnostics. Quant Imaging Med Surg 8:957–970. https://doi.org/10.21037/qims.2018.10.07

Chen D, Wang D, Hu X et al (2019) A DNA nanostructured biosensor for electrochemical analysis of HER2 using bioconjugate of GNR@Pd SSs – Apt – HRP. Sens. Actuators B Chem 296. https://doi.org/10.1016/j.snb.2019.126650

Choi HS, Frangioni JV (2010) Nanoparticles for biomedical imaging: fundamentals of clinical translation. Mol Imaging 9:291–310. https://doi.org/10.2310/7290.2010.00031

Choi J, Sun N (2011) Nanoparticles in biomedical applications and their safety concerns. Biomed Eng. https://doi.org/10.5772/18452

Cholkar K, Hirani ND, Natarajan C (2017) Nanotechnology-based medical and biomedical imaging for diagnostics. In Emerging nanotechnologies for diagnostics, drug delivery and medical devices. Elsevier, Amsterdam, The Netherlands, pp 355–374

Christiansen SH, Becker M, Fahlbusch S et al (2007) Signal enhancement in nano-Raman spectroscopy by gold caps on silicon nanowires obtained by vapour-liquid-solid growth. Nanotechnology:18. https://doi.org/10.1088/0957-4484/18/3/035503

Chung S, Chandra P, Koo JP, Shim YB (2018) Development of a bifunctional nanobiosensor for screening and detection of chemokine ligand in colorectal cancer cell line. Biosens Bioelectron 100:396–403. https://doi.org/10.1016/j.bios.2017.09.031

Crapnell RD, Dempsey-Hibbert NC, Peeters M et al (2020) Molecularly imprinted polymer based electrochemical biosensors: overcoming the challenges of detecting vital biomarkers and speeding up diagnosis. Talanta Open 2:100018. https://doi.org/10.1016/j.talo.2020.100018

Diaconu I, Cristea C, Hârceagă V et al (2013) Electrochemical immunosensors in breast and ovarian cancer. Clin Chim Acta 425:128–138. https://doi.org/10.1016/j.cca.2013.07.017

Eivazzadeh-Keihan R, Pashazadeh-Panahi P, Baradaran B et al (2018) Recent advances on nanomaterial based electrochemical and optical aptasensors for detection of cancer biomarkers. TrAC – Trends Anal Chem 100:103–115. https://doi.org/10.1016/j.trac.2017.12.019

El-Hamadi M, Schätzlein AG (2013) Nanoparticles in medical imaging. Fundam Pharm Nanosci 6: 543–566. https://doi.org/10.1007/978-1-4614-9164-4_20

Fan Y, Shi S, Ma J, Guo Y (2019) A paper-based electrochemical immunosensor with reduced graphene oxide/thionine/gold nanoparticles nanocomposites modification for the detection of cancer antigen 125. Biosens Bioelectron 135:1–7. https://doi.org/10.1016/j.bios.2019.03.063

Felix FS, Angnes L (2018) Electrochemical immunosensors – a powerful tool for analytical applications. Biosens Bioelectron 102:470–478. https://doi.org/10.1016/j.bios.2017.11.029

Feng T, Qiao X, Wang H et al (2016) A porous CuO nanowire-based signal amplification immunosensor for the detection of carcinoembryonic antigens. RSC Adv 6:16982–16987. https://doi.org/10.1039/c5ra26828a

Ferreira DC, Batistuti MR, Bachour B, Mulato M (2021) Aptasensor based on screen-printed electrode for breast cancer detection in undiluted human serum. Bioelectrochemistry:137. https://doi.org/10.1016/j.bioelechem.2020.107586

Forouzanfar S, Alam F, Pala N, Wang C (2020) Highly sensitive label-free electrochemical aptasensors based on photoresist derived carbon for cancer biomarker detection. Biosens Bioelectron 170:112598. https://doi.org/10.1016/j.bios.2020.112598

Ghorbani F, Abbaszadeh H, Dolatabadi JEN et al (2019) Application of various optical and electrochemical aptasensors for detection of human prostate specific antigen: a review. Biosens Bioelectron 142:111484. https://doi.org/10.1016/j.bios.2019.111484

Giannetto M, Bianchi MV, Mattarozzi M, Careri M (2017) Competitive amperometric immunosensor for determination of p53 protein in urine with carbon nanotubes/gold nanoparticles screen-printed electrodes: a potential rapid and noninvasive screening tool for early diagnosis of urinary. Anal Chim Acta 991:133–141. https://doi.org/10.1016/j.aca.2017.09.005

Gong H, Peng R, Liu Z (2013) Carbon nanotubes for biomedical imaging: the recent advances. Adv Drug Deliv Rev 65:1951–1963. https://doi.org/10.1016/j.addr.2013.10.002

Han X, Xu K, Taratula O, Farsad K (2019) Applications of nanoparticles in biomedical imaging. Nanoscale 11:799–819. https://doi.org/10.1039/c8nr07769j

Hassan EM, DeRosa MC (2020) Recent advances in cancer early detection and diagnosis: role of nucleic acid based aptasensors. TrAC – Trends Anal Chem 124:115806. https://doi.org/10.1016/j.trac.2020.115806

Hong G, Diao S, Antaris AL, Dai H (2015) Carbon nanomaterials for biological imaging and nanomedicinal therapy. Chem Rev 115:10816–10906. https://doi.org/10.1021/acs.chemrev.5b00008

Huang JY, Zhao L, Lei W et al (2018) A high-sensitivity electrochemical aptasensor of carcinoembryonic antigen based on graphene quantum dots-ionic liquid-nafion nanomatrix and DNAzyme-assisted signal amplification strategy. Biosens Bioelectron 99:28–33. https://doi.org/10.1016/j.bios.2017.07.036

Jahanbani S, Benvidi A (2016) Comparison of two fabricated aptasensors based on modified carbon paste/oleic acid and magnetic bar carbon paste/Fe_3O_4@oleic acid nanoparticle electrodes for tetracycline detection. Biosens Bioelectron 85:553–562. https://doi.org/10.1016/j.bios.2016.05.052

Jain S, Nanoparticle AV (2020) The role of nanoparticles for biomedical application. Asian Biomed 13:121–122. https://doi.org/10.1515/abm-2019-0050

Jo H, Gu H, Jeon W et al (2015) Electrochemical aptasensor of cardiac troponin i for the early diagnosis of acute myocardial infarction. Anal Chem 87:9869–9875. https://doi.org/10.1021/acs.analchem.5b02312

Johari-Ahar M, Karami P, Ghanei M et al (2018) Development of a molecularly imprinted polymer tailored on disposable screen-printed electrodes for dual detection of EGFR and VEGF using nano-liposomal amplification strategy. Biosens Bioelectron 107:26–33. https://doi.org/10.1016/j.bios.2018.02.005

Jolly P, Tamboli V, Harniman RL et al (2016) Aptamer-MIP hybrid receptor for highly sensitive electrochemical detection of prostate specific antigen. Biosens Bioelectron 75:188–195. https://doi.org/10.1016/j.bios.2015.08.043

Jung YK, Choi Y, Kim BS (2015) Functionalized carbon nanodots for biomedical applications. In carbon nanomaterials for biomedical applications cham: Springer International Publishing, Switzerland, pp 299–317

Keservani RK, Kesharwani RK, Sharma AK (2016) Nanobiomaterials involved in medical imaging technologies. Elsevier Inc.

Khan HA, Sakharkar MK, Nayak A et al (2018) Nanoparticles for biomedical applications: an overview. In Nanobiomaterials in Medical Imaging. William Andrew Publishing, Elsevier, Amsterdam, The Netherlands, pp 303–337

Kumar V, Shorie M, Ganguli AK, Sabherwal P (2015) Graphene-CNT nanohybrid aptasensor for label free detection of cardiac biomarker myoglobin. Biosens Bioelectron 72:56–60. https://doi.org/10.1016/j.bios.2015.04.089

Kumar V, Brent JR, Shorie M et al (2016) Nanostructured aptamer-functionalized black phosphorus sensing platform for label-free detection of myoglobin, a cardiovascular disease biomarker. ACS Appl Mater Interfaces 8:22860–22868. https://doi.org/10.1021/acsami.6b06488

Lee S, Cha EJ, Park K et al (2008) A near-infrared-fluorescence-quenched gold-nanoparticle imaging probe for in vivo drug screening and protease activity determination. Angew Chemie – Int Ed 47:2804–2807. https://doi.org/10.1002/anie.200705240

Lee MH, Thomas JL, Chang YC et al (2016) Electrochemical sensing of nuclear matrix protein 22 in urine with molecularly imprinted poly(ethylene-co-vinyl alcohol) coated zinc oxide nanorod arrays for clinical studies of bladder cancer diagnosis. Biosens Bioelectron 79:789–795. https://doi.org/10.1016/j.bios.2016.01.005

Li J, Madiyar FR, Swisher L (2015) Carbon nanotubes with special architectures for biomedical applications. In Carbon nanomaterials for biomedical applications. Cham: Springer International Publishing. Switzerland, pp 113–143

Li C, Li J, Yang X et al (2017a) A label-free electrochemical aptasensor for sensitive myoglobin detection in meat. Sensors Actuators B Chem 242:1239–1245. https://doi.org/10.1016/j.snb.2016.09.087

Li Y, Chen Y, Deng D et al (2017b) Water-dispersible graphene/amphiphilic pyrene derivative nanocomposite: high AuNPs loading capacity for CEA electrochemical immunosensing. Sens Actuators B Chem 248:966–972. https://doi.org/10.1016/j.snb.2017.02.138

Liu Y, Miyoshi H, Nakamura M (2007) Nanomedicine for drug delivery and imaging: a promising avenue for cancer therapy and diagnosis using targeted functional nanoparticles. Int J Cancer 120:2527–2537. https://doi.org/10.1002/ijc.22709

Liu X, Qin Y, Deng C et al (2015) Talanta a simple and sensitive impedimetric aptasensor for the detection of tumor markers based on gold nanoparticles signal amplification. Talanta 132:150–154. https://doi.org/10.1016/j.talanta.2014.08.072

Lopes P, Costa-Rama E, Beirão I et al (2019) Disposable electrochemical immunosensor for analysis of cystatin C, a CKD biomarker. Talanta 201:211–216. https://doi.org/10.1016/J.TALANTA.2019.04.006

Luo PG, Sahu S, Yang ST et al (2013) Carbon "quantum" dots for optical bioimaging. J Mater Chem B 1:2116–2127. https://doi.org/10.1039/c3tb00018d

Luo PG, Yang F, Yang ST et al (2014) Carbon-based quantum dots for fluorescence imaging of cells and tissues. RSC Adv 4:10791–10807. https://doi.org/10.1039/c3ra47683a

Luo Y, Wang Y, Yan H et al (2018) SWCNTs@GQDs composites as nanocarriers for enzyme-free dual-signal amplification electrochemical immunoassay of cancer biomarker. Anal Chim Acta 1042:44–51. https://doi.org/10.1016/j.aca.2018.08.023

Lv H, Li Y, Zhang X et al (2018) The label-free immunosensor based on rhodium@palladium nanodendrites/sulfo group functionalized multi-walled carbon nanotubes for the sensitive analysis of carcino embryonic antigen. Anal Chim Acta 1007:61. https://doi.org/10.1016/j.aca.2017.12.030

Mahato K, Kumar A, Maurya PK, Chandra P (2018) Shifting paradigm of cancer diagnoses in clinically relevant samples based on miniaturized electrochemical nanobiosensors and microfluidic devices. Biosens Bioelectron 100:411–428. https://doi.org/10.1016/j.bios.2017.09.003

Martins GV, Marques AC, Fortunato E, Sales MGF (2016) 8-hydroxy-2′-deoxyguanosine (8-OHdG) biomarker detection down to picoMolar level on a plastic antibody film. Biosens Bioelectron 86:225–234. https://doi.org/10.1016/j.bios.2016.06.052

Mazloum-Ardakani M, Hosseinzadeh L, Khoshroo A (2015a) Label-free electrochemical immunosensor for detection of tumor necrosis factor α based on fullerene-functionalized carbon nanotubes/ionic liquid. J Electroanal Chem 757:58–64. https://doi.org/10.1016/j.jelechem.2015.09.006

Mazloum-Ardakani M, Hosseinzadeh L, Taleat Z (2015b) Synthesis and electrocatalytic effect of ag@Pt core-shell nanoparticles supported on reduced graphene oxide for sensitive and simple label-free electrochemical aptasensor. Biosens Bioelectron 74:30–36. https://doi.org/10.1016/j.bios.2015.05.072

McNamara K, Tofail SAM (2017) Nanoparticles in biomedical applications. Adv Phys X 2:54–88. https://doi.org/10.1080/23746149.2016.1254570

Mirza S, Ahmad MS, Shah MIA, Ateeq M (2019) Magnetic nanoparticles: drug delivery and bioimaging applications. In: Metal nanoparticles for drug delivery and diagnostic applications. Elsevier Inc, pp 189–213

Nayl AA, Abd-Elhamid AI, El-Moghazy AY et al (2020) The nanomaterials and recent progress in biosensing systems: a review. Trends Environ Anal Chem 26:e00087. https://doi.org/10.1016/j.teac.2020.e00087

Nikalje AP (2015) Nanotechnology and its applications in medicine. Med Chem 5:81–089. https://doi.org/10.4172/2161-0444.1000247

Nune SK, Gunda P, Thallapally PK et al (2009) Nanoparticles for biomedical imaging. Expert Opin Drug Deliv 6:1175–1194. https://doi.org/10.1517/17425240903229031

Omidfar K, Darzianiazizi M, Ahmadi A et al (2015) A high sensitive electrochemical nanoimmunosensor based on Fe_3O_4/TMC/au nanocomposite and PT-modified electrode for the detection of cancer biomarker epidermal growth factor receptor. Sens Actuators B Chem 220:1311–1319. https://doi.org/10.1016/j.snb.2015.07.021

Ou D, Sun D, Lin X et al (2019) A dual-aptamer-based biosensor for specific detection of breast cancer biomarker HER2 via flower-like nanozymes and DNA nanostructures. J Mater Chem B 7:3661–3669. https://doi.org/10.1039/c9tb00472f

Pacheco JG, Rebelo P, Freitas M et al (2018a) Breast cancer biomarker (HER2-ECD) detection using a molecularly imprinted electrochemical sensor. Sens Actuators B Chem 273:1008–1014. https://doi.org/10.1016/j.snb.2018.06.113

Pacheco JG, Silva MSV, Freitas M et al (2018b) Molecularly imprinted electrochemical sensor for the point-of-care detection of a breast cancer biomarker (CA 15-3). Sensors Actuators B Chem 256:905–912. https://doi.org/10.1016/j.snb.2017.10.027

Pallela R, Chandra P, Noh HB, Shim YB (2016) An amperometric nanobiosensor using a biocompatible conjugate for early detection of metastatic cancer cells in biological fluid. Biosens Bioelectron 85:883–890. https://doi.org/10.1016/j.bios.2016.05.092

Patra S, Roy E, Madhuri R, Sharma PK (2015) Imprinted ZnO nanostructure-based electrochemical sensing of calcitonin: a clinical marker for medullary thyroid carcinoma. Anal Chim Acta 853: 271–284. https://doi.org/10.1016/j.aca.2014.10.030

Pavithra M, Muruganand S, Parthiban C (2018) Sensors and actuators B: chemical development of novel paper based electrochemical immunosensor with self-made gold nanoparticle ink and quinone derivate for highly sensitive carcinoembryonic antigen. Sensors Actuators B Chem 257:496–503. https://doi.org/10.1016/j.snb.2017.10.177

Purohit B, Kumar A, Mahato K et al (2019) Cancer cytosensing approaches in miniaturized settings based on advanced nanomaterials and biosensors. Elsevier Inc.

Qureshi A, Gurbuz Y, Niazi JH (2015) Capacitive aptamer-antibody based sandwich assay for the detection of VEGF cancer biomarker in serum. Sensors Actuators B Chem 209:645–651. https://doi.org/10.1016/j.snb.2014.12.040

Radhakrishnan N, Kanagesan S, Pandurangan A, Padmanabhan P (2016) Basics to different imaging techniques, different nanobiomaterials for image enhancement. Elsevier Inc.

Rani R, Sethi K, Singh G (2019) Nanomaterials and their applications in. Bioimaging:429–450. https://doi.org/10.1007/978-3-030-16379-2_15

Ribeiro JA, Pereira CM, Silva AF, Sales MGF (2018) Disposable electrochemical detection of breast cancer tumour marker CA 15-3 using poly(toluidine blue) as imprinted polymer receptor. Biosens Bioelectron 109:246–254. https://doi.org/10.1016/j.bios.2018.03.011

Rosado-De-Castro PH, Morales MDP, Pimentel-Coelho PM et al (2018) Development and application of nanoparticles in biomedical imaging. Contrast Media Mol Imaging 2018:1. https://doi.org/10.1155/2018/1403826

Rostamabadi PF, Heydari-Bafrooei E (2019) Impedimetric aptasensing of the breast cancer biomarker HER2 using a glassy carbon electrode modified with gold nanoparticles in a composite consisting of electrochemically reduced graphene oxide and single-walled carbon nanotubes. Microchim Acta 186:1. https://doi.org/10.1007/s00604-019-3619-y

Salimi A, Khezrian S, Hallaj R, Vaziry A (2014) Highly sensitive electrochemical aptasensor for immunoglobulin e detection based on sandwich assay using enzyme-linked aptamer. Anal Biochem 466:89–97. https://doi.org/10.1016/j.ab.2014.08.019

Sánchez-Tirado E, Salvo C, González-Cortés A et al (2017) Electrochemical immunosensor for simultaneous determination of interleukin-1 beta and tumor necrosis factor alpha in serum and saliva using dual screen printed electrodes modified with functionalized double – walled carbon nanotubes. Anal Chim Acta 959:66–73. https://doi.org/10.1016/j.aca.2016.12.034

Santos ART, Moreira FTC, Helguero LA, Sales MGF (2018) Antibody biomimetic material made of pyrrole for CA 15-3 and its application as sensing material in ion-selective electrodes for potentiometric detection. Biosensors 8. https://doi.org/10.3390/bios8010008

Serafín V, Torrente-Rodríguez RM, Batlle M et al (2017) Electrochemical immunosensor for receptor tyrosine kinase AXL using poly(pyrrolepropionic acid)-modified disposable electrodes. Sens Actuators B Chem 240:1251–1256. https://doi.org/10.1016/j.snb.2016.09.109

Serafín V, Torrente-Rodríguez RM, González-Cortés A et al (2018) An electrochemical immunosensor for brain natriuretic peptide prepared with screen-printed carbon electrodes nanostructured with gold nanoparticles grafted through aryl diazonium salt chemistry. Talanta 179:131–138. https://doi.org/10.1016/j.talanta.2017.10.063

Severino P, De Hollanda LM, Santini A, et al (2016) Advances in nanobiomaterials for oncology nanomedicine. Nanobiomaterials Cancer Ther Appl Nanobiomaterials 91–115. https://doi.org/10.1016/B978-0-323-42863-7.00004-9

Sha R, Badhulika S (2020) Recent advancements in fabrication of nanomaterial based biosensors for diagnosis of ovarian cancer: a comprehensive review. Microchim Acta 187:187. https://doi.org/10.1007/s00604-020-4152-8

Sharifi M, Avadi MR, Attar F et al (2019) Cancer diagnosis using nanomaterials based electrochemical nanobiosensors. Biosens Bioelectron 126:773–784. https://doi.org/10.1016/j.bios.2018.11.026

Shekari Z, Zare HR, Falahati A (2017) Developing an impedimetric aptasensor for selective label–free detection of CEA as a cancer biomarker based on gold nanoparticles loaded in functionalized mesoporous silica films. J Electrochem Soc 164:B739–B745. https://doi.org/10.1149/2.1991713jes

Shen X, Ma Y, Zeng Q et al (2016) Molecularly imprinted electrochemical sensor for advanced diagnosis of alpha-fetoprotein. Anal Methods 8:7361–7368. https://doi.org/10.1039/c6ay01922f

Siddique S, Chow JCL (2020) Application of nanomaterials in biomedical imaging and cancer therapy. Nano 10:1–41. https://doi.org/10.3390/nano10091700

Solhi E, Hasanzadeh M (2020) Critical role of biosensing on the efficient monitoring of cancer proteins/biomarkers using label-free aptamer based bioassay. Biomed Pharmacother 132:110849. https://doi.org/10.1016/j.biopha.2020.110849

Sumer B, Gao J (2008) Theranostic nanomedicine for cancer. Nanomedicine 3:137–140. https://doi.org/10.2217/17435889.3.2.137

Tabasi A, Noorbakhsh A, Sharifi E (2017) Reduced graphene oxide-chitosan-aptamer interface as new platform for ultrasensitive detection of human epidermal growth factor receptor 2. Biosens Bioelectron 95:117–123. https://doi.org/10.1016/j.bios.2017.04.020

Taghdisi SM, Danesh NM, Ramezani M et al (2016) A novel electrochemical aptasensor based on Y-shape structure of dual-aptamer-complementary strand conjugate for ultrasensitive detection of myoglobin. Biosens Bioelectron 80:532–537. https://doi.org/10.1016/j.bios.2016.02.029

Tertiş M, Ciui B, Suciu M et al (2017) Label-free electrochemical aptasensor based on gold and polypyrrole nanoparticles for interleukin 6 detection. Electrochim Acta 258:1208–1218. https://doi.org/10.1016/j.electacta.2017.11.176

Valavanidis A, Vlachogianni T (2016) Engineered nanomaterials for pharmaceutical and biomedical products new trends, benefits and opportunities. Pharm Bioprocess 4:13–24. https://doi.org/10.4172/jpr.1000105

Villarroel-rocha J, Regiart M, Fern MA, Raba J (2017) Micro fluidic immunosensor based on mesoporous silica platform and CMK-3/poly-acrylamide-co-methacrylate of dihydrolipoic acid modified gold electrode for cancer biomarker detection. 963:83–92. https://doi.org/10.1016/j.aca.2017.01.029

Viswanathan S, Rani C, Ribeiro S, Delerue-Matos C (2012) Molecular imprinted nanoelectrodes for ultra sensitive detection of ovarian cancer marker. Biosens Bioelectron 33:179–183. https://doi.org/10.1016/j.bios.2011.12.049

Wang P, Wan Y, Deng S et al (2016) Aptamer-initiated on-particle template-independent enzymatic polymerization (aptamer-OTEP) for electrochemical analysis of tumor biomarkers. Biosens Bioelectron 86:536–541. https://doi.org/10.1016/j.bios.2016.07.025

Wang J, Guo J, Zhang J et al (2017) RNA aptamer-based electrochemical aptasensor for C-reactive protein detection using functionalized silica microspheres as immunoprobes. Biosens Bioelectron 95:100–105. https://doi.org/10.1016/j.bios.2017.04.014

Wang QL, Cui HF, Song X et al (2018) A label-free and lectin-based sandwich aptasensor for detection of carcinoembryonic antigen. Sensors Actuators B Chem 260:48–54. https://doi.org/10.1016/j.snb.2017.12.105

Wang Y, Luo J, Liu J et al (2019) Label-free microfluidic paper-based electrochemical aptasensor for ultrasensitive and simultaneous multiplexed detection of cancer biomarkers. Biosens Bioelectron 136:84–90. https://doi.org/10.1016/j.bios.2019.04.032

Wang Y, Sun S, Luo J et al (2020) Low sample volume origami-paper-based graphene-modified aptasensors for label-free electrochemical detection of cancer biomarker-EGFR. Microsyst Nanoeng 6:1. https://doi.org/10.1038/s41378-020-0146-2

Wu A, Ou P, Zeng L (2010) Biomedical applications of magnetic nanoparticles. Nano 5:245–270. https://doi.org/10.1142/S1793292010002165

Xu S, Zhang R, Zhao W et al (2017) Self-assembled polymeric nanoparticles film stabilizing gold nanoparticles as a versatile platform for ultrasensitive detection of carcino-embryonic antigen. Biosens Bioelectron 92:570–576. https://doi.org/10.1016/j.bios.2016.10.058

Yadav HKS, Raizaday A (2016) Inorganic nanobiomaterials for medical imaging. Elsevier Inc.

Yang ST, Cao L, Luo PG et al (2009) Carbon dots for optical imaging in vivo. J Am Chem Soc 131: 11308–11309. https://doi.org/10.1021/ja904843x

Yang Y, Liu Q, Liu Y et al (2017) Biosensors and bioelectronics a novel label-free electrochemical immunosensor based on functionalized nitrogen-doped graphene quantum dots for carcinoembryonic antigen detection. Biosens Bioelectron 90:31–38. https://doi.org/10.1016/j.bios.2016.11.029

Zahin N, Anwar R, Tewari D et al (2020) Nanoparticles and its biomedical applications in health and diseases: special focus on drug delivery. Environ Sci Pollut Res 27:19151–19168. https://doi.org/10.1007/s11356-019-05211-0

Zeng Y, Bao J, Zhao Y et al (2018) A sandwich-type electrochemical immunoassay for ultrasensitive detection of non-small cell lung cancer biomarker CYFRA21-1. Bioelectrochemistry 120:183–189. https://doi.org/10.1016/j.bioelechem.2017.11.003

Zhang L, Gu FX, Chan JM et al (2008) Nanoparticles in medicine: therapeutic applications and developments. Clin Pharmacol Ther 83:761–769. https://doi.org/10.1038/sj.clpt.6100400

Zhang G, Liu Z, Wang L, Guo Y (2016) Electrochemical aptasensor for myoglobin-specific recognition based on porphyrin functionalized graphene-conjugated gold nanocomposites. Sensors (Switzerland) 16. https://doi.org/10.3390/s16111803

Zhou N, Su F, Li Z et al (2019) Gold nanoparticles conjugated to bimetallic manganese(II) and iron (II) Prussian blue analogues for aptamer-based impedimetric determination of the human epidermal growth factor receptor-2 and living MCF-7 cells. Microchim Acta 186:3–12. https://doi.org/10.1007/s00604-018-3184-9

Zhu Y, Chandra P, Shim YB (2013) Ultrasensitive and selective electrochemical diagnosis of breast cancer based on a hydrazine-au nanoparticle-aptamer bioconjugate. Anal Chem 85:1058–1064. https://doi.org/10.1021/ac302923k

Carbon Quantum Dots: Green Nanobiomaterials in the Future of Biosensing

14

Barbara Vercelli

Contents

1 Introduction 284
2 Synthesis and Optical Properties 286
  2.1 Synthesis 286
  2.2 Optical Properties 289
3 Biosensing Applications 293
  3.1 Optical Biosensors 293
  3.2 Electrochemical Biosensors 295
  3.3 Enzymatic Biosensors 297
4 Conclusions 300
References 300

Abstract

Since their casual discovery in 2004, carbon quantum dots (CDs), fluorescent carbon-based nanomaterials, were highly studied by the research community, by virtue of their particular properties, which enable a wide range of biological applications, going from chemo- and biosensing to fluorescence imaging and drug delivery. They are characterized by excellent fluorescence emission, which can be modulated from the visible to near-infrared (NIR), and their surface is rich in functional groups, which enable their functionalization with a wide range of receptors and bio-functionalities (i.e., enzymes, etc.). They also exhibit extremely low toxicity and excellent biocompatibility, which are useful for real-world biological applications. On the other hand, CDs are also expected to reduce the cost of biosensors by replacing both the noble metal substrates and the well-known quantum dots based on metal chalcogenides. Their synthesis is based on simple and sustainable approaches that could employ cheap and "greener"

B. Vercelli (✉)
Istituto di Chimica della Materia Condensata e di Tecnologie per l'Energia, ICMATE-CNR, Milan, Italy
e-mail: barbara.vercelli@cnr.it

© Springer Nature Singapore Pte Ltd. 2023

U. P. Azad, P. Chandra (eds.), *Handbook of Nanobioelectrochemistry*,
https://doi.org/10.1007/978-981-19-9437-1_14

starting materials coming from biomass or agro-industrial waste. In this context, the present chapter will focus on CDs as new sustainable nanomaterials for biosensor applications, with particular care to optical and electrochemical biosensors. A short overview of the green synthesis strategies of CDs and their optical properties is also presented.

Keywords

Carbon quantum dot · Green synthesis · Biosensors

1 Introduction

Carbon quantum dots (CQDs) (Lim et al. 2015), also called carbon dots (CDs) (Sun et al. 2006; Baker and Baker 2010), constitute a new class of carbon-based nanomaterials, characterized by diameters less than 10 nm and featured by peculiar fluorescence properties. Xu et al. casually discovered CDs during the electrophoretic purification of single-walled carbon nanotubes (SWCNTs) (Xu et al. 2004), and since then, they have seen a rapid development and were considered a case study in materials science (Zhou et al. 2020b; Zheng et al. 2020; Peng et al. 2017). By comparison with the traditional luminescent nanoparticles, CDs present numerous superior characteristics like high photostability, nontoxicity, and low cost (Dou et al. 2016; Zhao et al. 2011; Zheng et al. 2017; Zhou et al. 2017; Dong et al. 2017; Chen et al. 2018; Feng et al. 2016; Li et al. 2014; Zhang et al. 2018; Gao et al. 2016).

In 2016, Valcárcel's group (Cayuela et al. 2016) classified CDs into three different species depending on their nature, crystalline structure, and quantum confinement. They defined carbon nanodots (CNDs) as the amorphous nanodots that are quasi-spherical and do not present quantum confinement; carbon quantum dots (CQDs) as the nanodots that are spherical and show a crystalline structure with quantum confinement; and graphene quantum dots (GQDs) as the single sheets that are π-conjugated. Literature reports that the formation of the above reported different species of CDs depends on both the synthesis strategies developed for their fabrication and the precursors employed as starting materials. The production of CDs comprises a variety of approaches, which are classified into two main groups: "top-down" and "bottom-up." The "top-down" approaches are based on harsh processes that breakdown large pieces of raw carbon materials into CDs. They include approaches like laser ablation (Li et al. 2011), arc discharge (Xu et al. 2004), electrochemical exfoliation (Tan et al. 2015; Lu et al. 2009), and oxidation acid treatment (Lu et al. 2020; Ray et al. 2009), and employ as precursors materials like carbon soot (Tian et al. 2009), carbon fiber (Peng et al. 2012), activated carbon (Qiao et al. 2009), carbon black (Dong et al. 2012), graphene (Pan et al. 2010), and carbon nanotubes (Xu et al. 2004). On the other side, the "bottom-up" approaches employ small molecules as carbon sources, which are converted into CDs through "decomposition–polymerization–carbonization" processes. The usually employed carbon-source molecules include small organic molecules like citric acid (Peng et al. 2020b; Li et al. 2020; Schneider et al. 2017), polyols (Liu et al. 2014), and amino acids (Sahiner et al. 2019); synthetic polymers like polyethylene glycol (PEG) (Ji et al. 2020; Li et al. 2015) and polythiophene (Ge et al. 2015); and natural products like carbohydrates (Peng and Travas-Sejdic 2009) and polysaccharides (Zhou et al. 2013). The most commonly employed bottom-up synthetic methods are pyrolysis-solvothermal (Chen et al. 2020; Wang et al. 2010), hydrothermal carbonization (Liu et al. 2012), and microwave/ultrasonication (Zhu et al. 2009). Recently, many research efforts were devoted to the development of more sustainable approaches that are based on the following two strategies: the substitution of the organic compound precursors with materials coming from biomass (like orange juice, honey, betel nut shells, silk, etc.) (Jiang et al. 2020a; Huang et al. 2020; Meng et al. 2019; Mandani et al. 2017; Wu et al. 2013); and the development of new processes that should be both efficient and do not require high expenditures of external energy. Thus, owing to the possibility of green preparation methods together with the abovementioned peculiar properties, CDs are expected to replace the conventional inorganic quantum dots or noble metal nanoclusters in biosensing applications and become promising sustainable luminescent nanoprobes. A typical nanoprobe for biosensing applications has to present the following features: (1) wavelength in the near-infrared (NIR) region because the high energy of ultraviolet rays may damage living organisms and biological tissues easily absorb visible light; (2) it has to exhibit chemical inertness and photoluminescence (PL) emission stability; (3) it should be harmless to organisms. Regarding point 1, it was shown that through suitably designed synthetic approaches (Loi et al. 2017; Kozák et al. 2013), adequate selection of carbon sources (Ge et al. 2015), and doping with heteroatoms (Jiang et al. 2020; Sun et al. 2019; Zhang et al. 2012), it is possible to modulate the PL emission of CDs from the visible to the NIR; for point 2, CDs, compared to organic dyes, present the advantage of not being easily metabolized by cells and remain stable in the body; and for point 3, CDs, unlike traditional nanomaterials, are nontoxic materials because of their carbon-based nature (Ji et al. 2020). Furthermore, the surface of CDs is rich in functional groups of different nature that can function as binding sites for a variety of bioreceptors, which is peculiar for CDs employment as nanoprobes in biosensors, and finally, their simple and sustainable synthesis approaches are expected to achieve production on a large scale, which is crucial for CDs industrial development and commercial application in biosensing. Thus, from the above reported characteristics, CDs demonstrate great potential as components for biosensors (Campuzano et al. 2019; Haitang et al. 2014; Koutsogiannis et al. 2020; Fan et al. 2015; Qu et al. 2020).

It is well known that a biosensor is composed of three parts: a detector, for the recognition of the signal of the target analyte; a converter, for the conversion of the signal into an appropriate output; and a signal processor, for the analysis and the processing of the output signal (Perumal and Hashim 2014). Usually in the sensing systems reported in literature, CDs are employed as converters, i.e., they convert the signals of the target analyte into useful signals that could be recognized and processed by the signal processor. The abovementioned presence of various functional groups on CDs surface that can function as binding sites for specific bioreceptors makes it possible to design biosensors, where CDs are directly sensitive to specific biomolecules (Zhou et al. 2020a; Wang et al. 2017) and function as both detectors and converters simultaneously without the further addition of bioreceptors.

In this context, the present chapter deals with CDs as new sustainable nanomaterials for biosensor applications and is organized into two main sections. The first one is devoted to describing the synthesis methods of CDs, mainly focusing on the green approaches and both the biocompatibility and toxicity of the obtained materials. The optical properties of CDs will also be treated by summarizing the most accepted explanations for their luminescence origin. The second section is devoted to the biosensing applications of CDs, focusing on the optical and electrochemical approaches.

2 Synthesis and Optical Properties

2.1 Synthesis

The sustainable strategies for the preparation of CDs are mainly devoted to the selection of "greener" precursors, i.e., materials obtained from biomass, and the development of new processes that should be both efficient and do not require high expenditures of external energy. In comparison with conventional synthesis methods for CDs, the approach based on biomass employs precursors that are natural and renewable in place of traditional carbon sources. On the one hand, the method presents disadvantages related to the variable properties and structures exhibited by the obtained CDs, which depend on the diversity of the employed renewable starting materials; on the other hand, the renewability of starting materials enables the inexpensive mass production of CDs, which is crucial for their industrial applications. In other words, the reaction temperature required in the biomass synthesis of CDs (usually 100–200 °C) is lower than that required for the preparation of CDs starting from traditional precursors (usually higher than 200 °C). Furthermore, the selection of solvents necessary for the CDs synthesis is related to the solubility of their precursor materials. Usually, materials obtained from biomass are soluble in aqueous media, while some traditional precursors usually require organic media because of their limited water solubility. The biomass synthesis of CDs is usually based on "bottom-up" strategies, currently including hydrothermal/solvothermal treatment and microwave irradiation. For example, Liu et al. (2017b) developed a green, facile, and low-cost approach based on the one-pot hydrothermal treatment of rose-heart radish for the preparation of fluorescent CDs with well-distributed size. The obtained CDs are highly fluorescent with a PL emission quantum yield of 13.6%, extremely biocompatible, chemically stable, and nontoxic. In another study, garlic was employed for the hydrothermal synthesis of nitrogen and sulfur co-doped CDs (Zhao et al. 2015). The obtained CDs are soluble in water, fluorescent in the blue region with a PL emission quantum yield of 17.5%, photo- and pH-stable, and noncytotoxic. Furthermore, they proved to be resistant to the interference of metal ions, biomolecules, and high ionic strength environments.

Wang and Zhou (2014) reported a green, simple, and sustainable strategy for the preparation of fluorescent nitrogen-doped CDs using milk as a precursor (Fig. 14.1a). In practice, by hydrothermal heating of milk, they produced monodispersed CDs of ca. 3 nm of diameter, which showed to be extremely fluorescent and did not present noticeable toxicity to the cells even at high concentrations of CDs (Wang and Zhou 2014). Another sustainable and green approach employed honey for the production of CDs with a quantum yield of about 19.8%, for imaging and sensing applications (Yang et al. 2014).

The prepared CDs are also nontoxic and proved to be both photo- and chemically stable. In another work by Edison et al. (2016), fluorescent nitrogen-doped CDs (N-CDs) were prepared through a fast and simple microwave approach. L-ascorbic acid and β-alanine were employed as carbon and nitrogen sources, respectively; the N-CDs exhibited excitation-dependent emission properties with a quantum yield of ca. 14% and low cytotoxicity. Eutrophic algal blooms were employed by Vadivel et al. (2016) as the carbon source for the development of a facile and rapid strategy for mass production of CDs. The produced CDs exhibit a QY of 13%, high water solubility, a nanosecond fluorescence lifetime characterized by high photostability and luminescence stability in different environments, low cytotoxicity, and excellent cell permeability. CDs were also prepared from the direct employment of fruit juice, like orange juice (Sahu et al. 2012), grape juice (Huang et al. 2014), banana juice (De and Karak 2013), *Chionanthus retusus* (*C. retusus*) fruit juice (Atchudan et al. 2017), etc. For example, Atchudan et al. (2017) developed a simple hydrothermal strategy for the preparation of N-CDs starting from *C. retusus* fruit juice (Fig. 14.1b). In another work, Atchudan et al. (2018) proposed a low-cost hydrothermal route for preparing N-CDs through the employment of *Phyllanthus acidus* (*P. acidus*) as a precursor. Furthermore, due to the growing attention towards environmental sustainability, some waste materials are employed for the synthesis of CDs. In fact, the concept of upcycling waste for the industrial production of significant amounts of CDs has recently gained a growing attraction. In particular, in order to reduce human impact on the environment through zero waste generation, agro-industrial waste, intended as products and byproducts, has become an object of interest. To this end, the work of Sangam et al. (2018) reports the development of a simple, economic, and large-scale synthetic strategy for the preparation of sulfur-doped GQDs (S-GQDs) employing as starting material biowastes of the second generation (Fig. 14.1c). The proposed approach, which could be considered a promising strategy for the sustainable preparation of CDs, employs sugarcane molasses as a green precursor. The obtained S-GQDs are highly crystalline, soluble in water, stable, highly fluorescent with a PL emission QY of 47%, and biocompatible. In another work, Zhang et al. (2015) propose a one-step hydrothermal method that employs egg white for the preparation of fluorescent CDs with a QY of 61%, which were used for the detection of Fe^{3+} ions and for living cell imaging.

Toxicity – Recent studies on CD toxicity report that, unlike heavy metal-based quantum dots, which are usually located in cells' cytoplasm, CDs enter into the nucleus. Furthermore, it was observed that the location of CDs in normal rat kidney (NRK) cells depends on their dose of exposure. In particular, upon exposure to

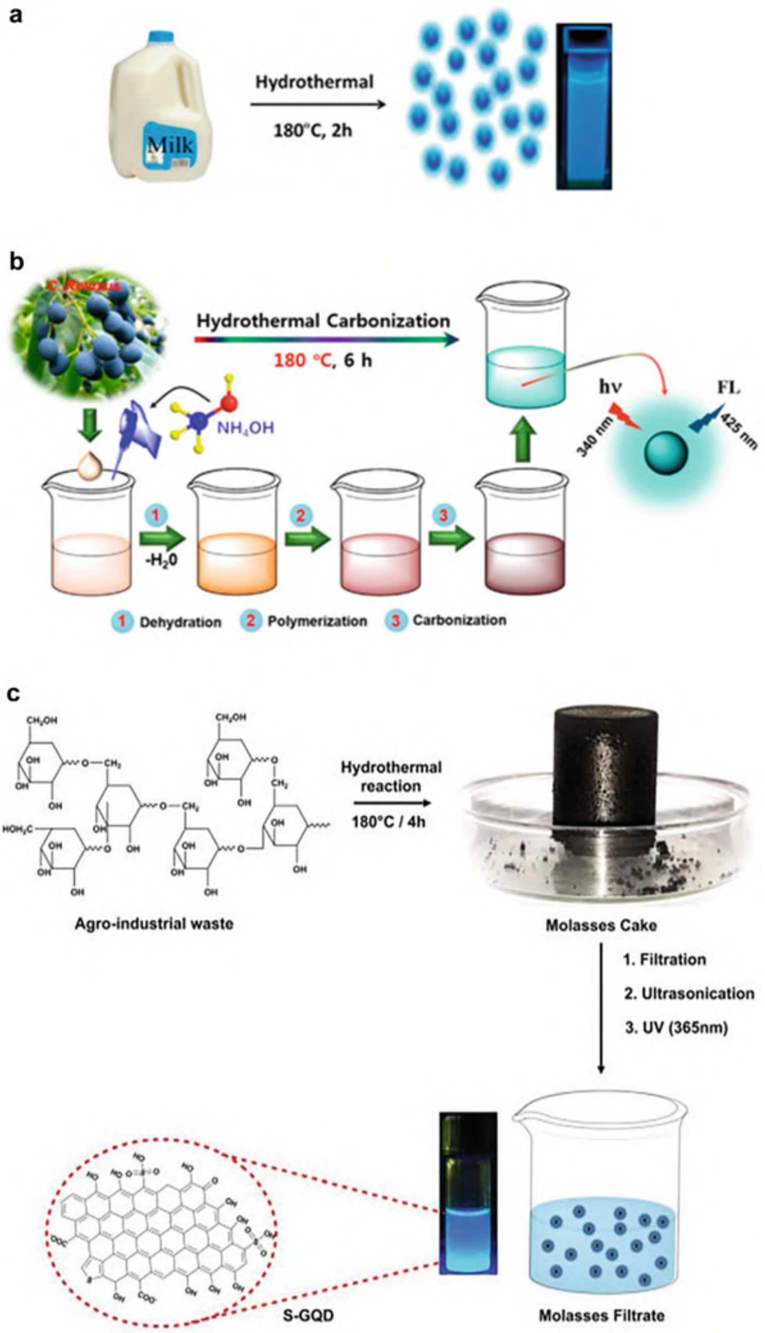
a
Milk
Hydrothermal
180°C, 2h
b
C. Retusus
Hydrothermal Carbonization
180 °C, 6 h
NH$_4$OH
hv
FL
340 nm
425 nm
1
-H$_2$0
2
3
1 Dehydration
2 Polymerization
3 Carbonization
c
Agro-industrial waste
Hydrothermal reaction
180°C / 4h
Molasses Cake
1. Filtration
2. Ultrasonication
3. UV (365nm)
S-GQD
Molasses Filtrate

Fig. 14.1 (**a**) Illustration of the formation process of carbon dots from milk by hydrothermal treatment. (Reproduced with permission from Wang and Zhou (2014), © 2014 American Chemical

3 mg mL^{-1} CDs for 6 h, the CDs were located in the cytoplasm, while after exposure to 6 mg mL^{-1} CDs for the same time, they could enter the nucleus (Song et al. 2019). Furthermore, it is interesting to note that after exposures for 6 h to CDs 3 and 6 mg mL^{-1}, they did not induce the normal rat kidney cell apoptosis and necrosis, but they did cause autophagy and change the mitochondrial energy metabolism from aerobic to glycolytic metabolism (Song et al. 2019). It was also found that CDs cytotoxicity is mild; in fact, it was reported that the cell viability of HepG2 cells was greater than 90% after 4 h of incubation at a CDs concentration of 2 mg mL^{-1}. Even more, it was observed that CDs helped HepG2 cells to clear hydroxyl radicals induced by H_2O_2 (Wang et al. 2019).

2.2 Optical Properties

One of the most appealing features of CDs is their PL emission, which makes them good candidates as nanoprobes in optical biosensors. In general, optical biosensors convert the intangible information of the target analytes into recognizable optical signals, i.e., fluorescence intensity/wavelength and color change. As above reported, an optical biosensor requires that the wavelength of the nanoprobe should be in the near-infrared (NIR) region (Zhang et al. 2016) because the high energy of ultraviolet rays may damage living organisms (Sinha and Häder 2002; Moan and Peak 1989) and biological tissues easily absorb visible light. To this end, most studies report that through suitably designed synthetic approaches (Loi et al. 2017; Kozák et al. 2013), adequate selection of carbon sources (Ge et al. 2015), and doping with heteroatoms (Jiang et al. 2020a; Sun et al. 2019; Zhang et al. 2012), it is possible to modulate the PL emission of CDs from the visible to the NIR. For example, a series of CDs with different emissions was obtained by Bao et al. (2015) through the manipulation of the reaction conditions. Ding et al. (2016) developed a hydrothermal strategy followed by further separation via silica gel column chromatography to prepare CDs with tunable fluorescence, which goes from blue to red under single-wavelength UV light. Although the literature is rich in studies on the argument, the origin of the fluorescence of CDs is still not clear and continues to be the object of scientific discussion. In fact, CDs revealed themselves to be more complex systems than expected because they exhibit dissimilar optical properties that are related to the synthetic strategies, the employed precursors, and the post-synthesis treatments. According to recent reported studies, it is possible to consider three main points of view on the fluorescence origin of CDs: (i) surface-state emission, which

◀

Fig. 14.1 (continued) Society). (**b**) Schematic illustration for the preparation and formation mechanism of N–CDs from *Chionanthus retusus* (*C. retusus*) fruit juice. (Reproduced with permission from Atchudan et al. (2017), © 2016 Elsevier B.V.). (**c**) Schematic illustration of the mass synthesis of S-GQDs from agro-industrial waste. (Reproduced with permission from Sangam et al. (2018), © 2018 The Royal Society of Chemistry) regards the carbon backbone and the surface functionalities (Song et al. 2015); (ii) core-state emission (quantum confinement), which depends on the crystallinity of CDs and their surface groups; (iii) molecular fluorescence, which is generated by fluorescent impurities/byproducts produced during CDs synthesis (Essner et al. 2018).

(i) *Surface state emission* – It is the most widely accepted luminescence mechanism of CDs, and it is ascribed to their surface oxidation degree or their surface functional groups. Regarding CDs surface oxidation degree, Bao et al. (2011) showed that the oxygen content on CDs surface is responsible of the redshift of their PL emission. They suggested that a higher degree of surface oxidation may generate a greater number of surface defects that can act as exciton traps. Thus, the redshift of the PL emission is considered to be the result of the recombination of these trapped excitons. An example is the series of CDs prepared by Ding et al. (2016) through purification with column chromatography, which exhibit an excitation-independent fluorescence from blue to red (Fig. 14.2a). The authors showed that the surface oxidation degree of CDs gradually increases, going from blue to red emission. On the one hand, surface oxidation is considered responsible for the production of defects, which act as capture centers for excitons and cause a fluorescence emission that is related to the surface states (Bao et al. 2015). On the other hand, the incorporated oxygen species strongly affect the bandgap of CDs (Hu et al. 2015), i.e., by increasing the degree of surface oxidation of CDs, their bandgap reduces, causing the redshifted fluorescence emission (Fig. 14.2a). Green and yellow emissive CDs were prepared by Liu et al. (2017a) through a simple and sustainable room temperature method. These two CDs samples exhibit the same size distribution and chemical surface composition, but they are characterized by different surface oxidation degrees. In particular, the author observed that by increasing the surface oxidation degree, the emission wavelength shifted to lower energies, passing from 518 nm to 543 nm and ascribed the phenomenon to the decrease of their bandgaps. On the other hand, regarding the CDs surface functional groups, other research studies correlate the surface state emission of CDs with their surface functional groups, also known as molecular states, like C=O and C=N. It is suggested that different fluorophores or energy levels can be introduced in CDs by the functional groups present on their surface. The multicolor nitrogen-doped CDs (N-CDs) reported by Zhang et al. (2017) could be an example. The authors show that the PL emission can be modulated from dark blue to red or even white (Fig. 14.2b). As these full-color N-CDs exhibit similar oxygen content, the authors ascribed their PL emission to their surface functional groups rather than to their surface oxidation degree. In fact, they propose (Fig. 14.2b) that except for the HOMO–2(π) energy level, the functional groups (C=O and C=N) present on the surface of their N-CDs insert the two new energy levels HOMO-1 and HOMO, and determine the new level transitions from HOMO-1 and HOMO to LUMO (π*). A possible redshift of the emission is supposed to take place when the electrons in the N-related defect states return to the HOMO level.

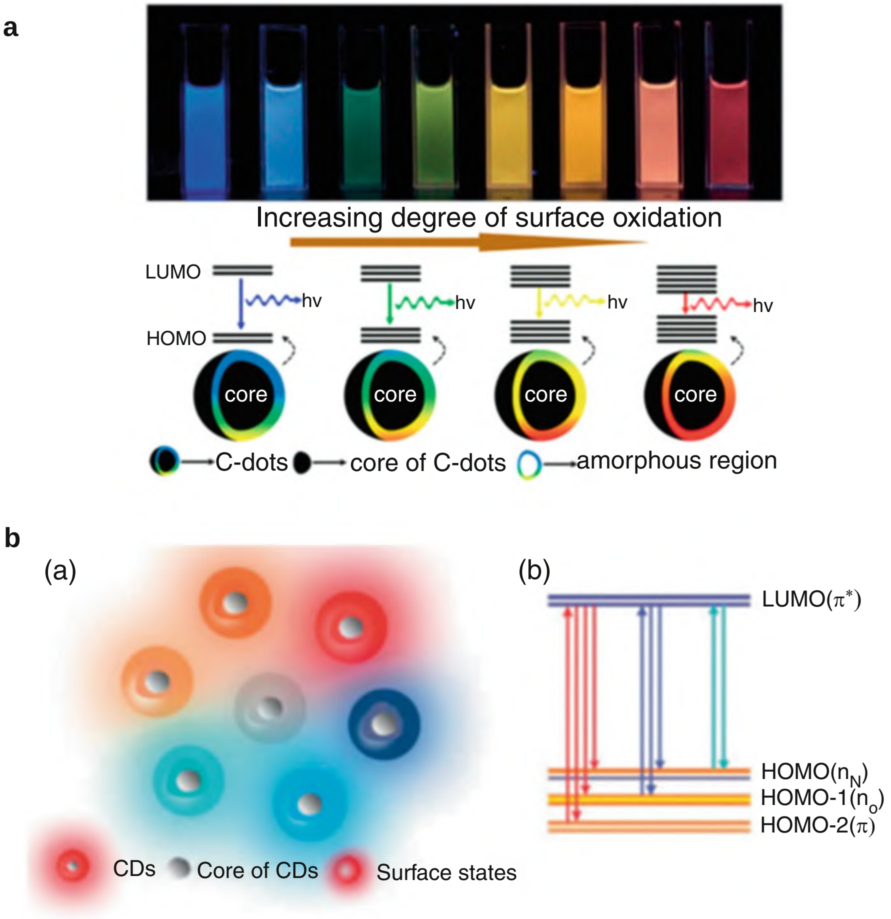
a
Increasing degree of surface oxidation
LUMO
HOMO
hv
hv
hv
hv
core
core
core
core
C-dots
core of C-dots
amorphous region
b
(a)
CDs
Core of CDs
Surface states
(b)
LUMO(π*)
HOMO(n_N)
HOMO-1(n_O)
HOMO-2(π)

Fig. 14.2 (**a**) Model for the tunable PL of CDs with different degrees of oxidation. (Reproduced with permission from Ding et al. (2016), © 2015 American Chemical Society). (**b**) (a) Structure of the multicolor CDs. (b) Schematic illustration of the proposed energy level and electron transition diagrams of the multicolor CDs. (Reproduced with permission from Zhang et al. (2017), © 2017 The Royal Society of Chemistry)

(ii) *Core state emission (quantum confinement)* – The quantum confinement effect can be observed when the dimensions of a particle are comparable to the wavelength of the electron. Compared to the bulk material, in nanoparticles with diameters in the range of ca. 2–10 nm, the bandgap is increased because of the quantum size effect, and it causes different color emission depending on the small differences in the size of the particles. For example, three types of CDs, showing bright red, green, and blue PL emissions, respectively, under single ultraviolet-light excitation were reported by Jiang (2015a). These CDs exhibited similar chemical composition but different particle size distributions.

Thus, the authors ascribed the observed different PL emissions of these CDs to the quantum confinement effect. In another work, Li et al. (2010) observed that, when the oxygen on the surface of CDs is removed through hydrogen plasma, their PL emission remained unchanged. So, they suggested that the PL emission of their CDs may be ascribed to effects of quantum confinement and properties depending on particles dimensions. Sun et al. (2006) reported that the quantum confinement effect of the emissive energy traps present on CDs surface may be responsible for their PL emission upon surface passivation. In some reported cases, the PL emission of CDs is due to a combination of surface state and quantum confinement effect (Zhu et al. 2017). A series of CDs with different degree of surface oxidation and dimensions were synthetized by Bao et al. (2015). They proposed that the PL emission of their CDs is related to their surface oxidation degree and the π-electron system. In particular, a higher surface oxidation degree or an extended π-electron system corresponds to a smaller energy gap. Thus, they concluded that the redshift of the PL emission of their CDs is due to the increase in their particle size or their surface oxidation degree.

(iii) *Molecular fluorescence* – Essner et al. (2018) observed that during the bottom-up synthesis strategies of preparation of CDs, some fluorescent impurities may form and contribute to increasing their PL emission (i.e., molecular fluorescence). In the CDs obtained employing citric acid and ethylenediamine, Song et al. (2015); Zhu et al. (2016) revealed the presence of the fluorescent molecule (imidazo[1,2-a]pyridine-7-carboxylic acid, 1,2,3,5-tetrahydro-5-oxo-, IPCA). They suggested that the observed high PL emission QY is ascribed to the contribution of IPCA and showed that their CDs consist of IPCA, polymers, and carbon cores. In further work, Schneider et al. (2017), through the preparation of three types of CDs employing citric acid and three different N-containing precursors, showed that the contribution to the PL emission of the obtained CDs samples may be ascribed to different molecular fluorophores. Furthermore, the authors showed that the molecular fluorophores are not reaction by-product free in the solution but are directly bonded to CDs and contribute to their emission behavior (Fig. 14.3).

Righetto et al. (2017) employed fluorescence correlation spectroscopy and time-resolved electron paramagnetic resonance spectroscopy to show that the PL emission of their CDs may be due to the small fluorophores present in solution or to their carbon-cores, depending on the excitation wavelength. In particular, in the excitation range from 320 to 450 nm the PL emission is mainly ascribed to the small fluorophores, while at excitation above 480 nm is dominated by poorly emitting carbon cores. Thus, they concluded that, although carbon cores are present, the PL emission of their CDs is mainly ascribed to the contribution of the small fluorophores present in the solution.

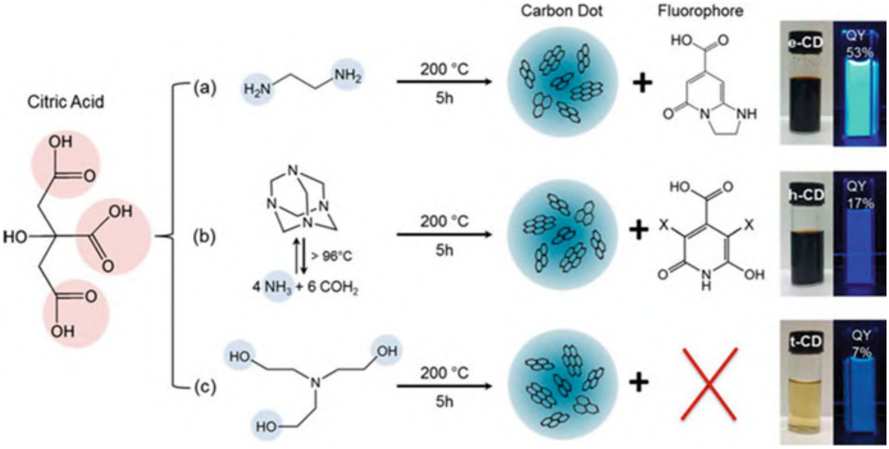

Fig. 14.3 Synthesis conditions of citric acid-based CDs using three different nitrogen-containing precursors. (**a**) Reaction of citric acid and ethylenediamine, resulting in e-CDs and the fluorophore IPCA, as previously reported by Song et al. (2015); (**b**) Reaction of citric acid with hexamethylenetetramine, producing h-CDs and citrazinic acid and/or 3,5 derivatives (marked by −X), due to the decomposition of hexamethylenetetramine to ammonia and formaldehyde at temperatures exceeding 96 °C; (**c**) Reaction of citric acid and triethanolamine, resulting in t-CDs and no derivatives of citrazinic acid since the tertiary amine prohibits their formation. (**a**–**c**) Images of the purified reaction products under ambient light and corresponding diluted solutions under UV light excitation, which reveal blue emission with PL QYs as labeled on the graph. (Reproduced with permission from Schneider et al. (2017), © 2016 American Chemical Society)

3 Biosensing Applications

3.1 Optical Biosensors

In general, an optical biosensor designed with CDs is based on the variation of the CDs optical properties (i.e., PL emission intensity or PL emission wavelength shift) caused by the interaction between the CDs and the target analytes whose related information can be provided depending on the impact (Ji et al. 2020). For the realization of an effective optical biosensor, the mechanism of sensing has to be taken into account for the application of the suited strategy. For CDs-based optical biosensors, there are two main strategies: (i) "on-off" strategy and (ii) "on-off-on" strategy.

(i) *"on-off" strategy* – In an "on-off" strategy, the interaction between CDs and the target molecules causes a decrease of the intensity of their PL emission (PL quenching); this means that due to the quenching effect, the PL emission of CDs decreases with the increase of the concentration of the target analytes. Thus, the amount of the target analytes can be determined through a simple linear relationship, through calibration curves. The PL quenching mechanisms exploited in the design optical biosensors based on CDs are: Förster resonance energy transfer (FRET), photoinduced electron transfer (PET), and inner filter effect (IFE), see Fig. 14.3. In a FRET quenching, the energy of the excited donor (i.e., CDs) is transferred without emission of radiation to the ground state of the proximal acceptor (i.e., quencher/target molecules). However, to have a FRET quenching, the following condition have to be satisfied: (a) the energy of the excitation-state of the donor should be comparable with the one of the ground-state of the acceptor, i.e., the emission spectrum of the donor should overlap with the absorption spectrum of the acceptor; (b) the distance between the donor and the acceptor should be in the range from 1 nm to 10 nm; (c) the transition dipoles of the donor and acceptor molecules must be close to parallel; (d) the PL emission lifetime of the donor should be enough long to enable the energy transfer to occur.

In a PET quenching, an electron transfer from an electron donor (i.e., CDs) to an electron acceptor (i.e., the target analyte) occurs. Under the suitable conditions, the electrons photoexcited from CDs are transferred to the target analytes; thus, the PL emission of CDs is quenched because the number of the excited electron that return to the ground state is diminished. In an IFE process, the PL emission of CDs is blocked by the target analyte before reaching the detector of a fluorometer. In this case, the emission and absorption spectra of the donor (i.e., CDs) and acceptor (i.e., target analytes), respectively, need to overlap very well; thus, the target analytes can absorb the light emitted by the CDs, before reaching the detector, and cause a decrease in their PL intensity. The target analyte is determined through the analysis of the degree of PL quenching (Yang et al. 2019).

(ii) *"on-off-on" strategy* – In an "on-off-on" strategy, the CDs firstly interact with non-analytes that quench (turn-off) their PL emission which will be then restored (turn-on) by the addition of the analytes (Fig. 14.4). The analysis of the PL restoration degree of CDs gives the amount of the target analytes. The above reported PL quenching mechanisms (FRET, PET, or IFE) can be exploited for PL quenching of CDs by non-analyte quenchers. The interaction between the target analyte and the quencher has to be stronger than that between the quencher and CDs to cause the release of CDs from quenchers and thus restore the PL emission of CDs.

For example, Shen and Xia (2016) reported the realization of an optical biosensor for glucose, based on CDs obtained from phenylboronic acid. The interaction between glucose and the boronic functionalities present on CDs surface cause the quenching of their PL emission. The amounts of glucose levels in the body were determined through the degree of PL quenching, reaching a sensitivity that is 10–250 times higher than the one of the previous fluorescent nanosensing detection system based on boric acid.

In most cases, optical biosensors were developed for the detection of metal ions, because their interaction with CDs could effectively quench their PL via PET. A singular example is the sensitive detection of Fe^{3+} developed by Liu et al. (2016).

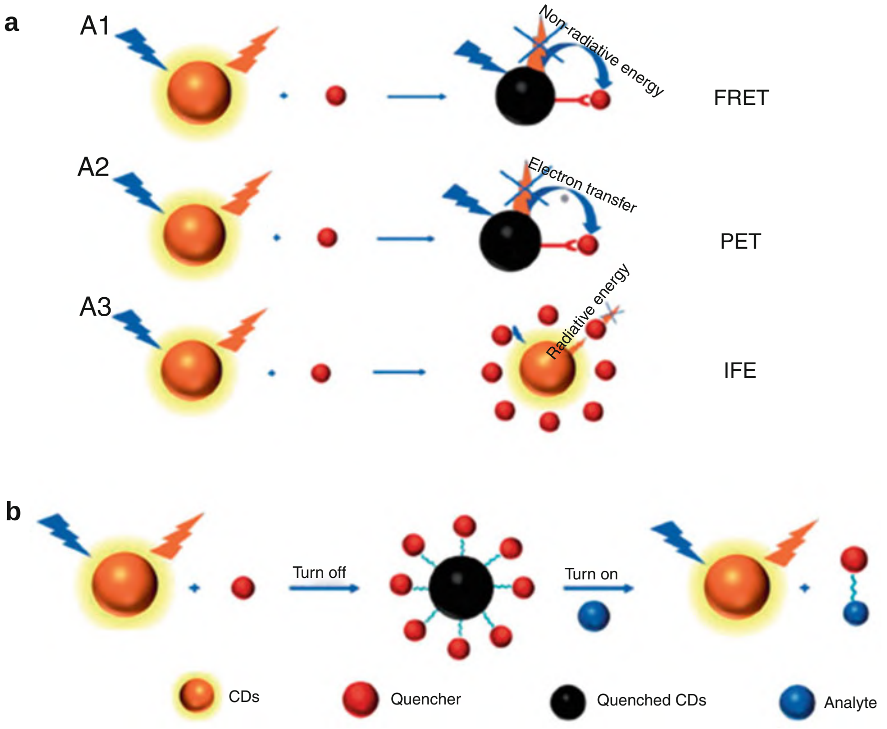

Fig. 14.4 Typical optical biosensing strategies: (**a**) Three fluorescence-quenching mechanisms of "on-off" strategy, (A1) FRET, (A2) PET, and (A3) IFE. (**b**) Scheme for "on-off-on" strategy. (Reproduced with permission from Ji et al. (2020), © 2020 American Chemical Society)

They found that the PL quenching of CDs is not ascribed to a PET between Fe^{3+} and CDs but to the aggregation of CDs caused by the ferric ions. Other detection strategies developed by scientists are based on the detection of the products of the target analytes obtained by reactions with known mechanisms. It is possible to analyze the target analytes retrospectively from the information obtained from their products. For example, an efficient strategy for the detection of p-nitrophenylphosphate was developed by Li et al. (2016). The analysis was based on the IFE-quenching of the PL emission of CDs determined by p-nitrophenol, the catalytic product of p-nitrophenylphosphate (Fig. 14.5).

3.2 Electrochemical Biosensors

According to the International Union of Pure and Applied Chemistry (IUPAC) (Thevenot et al. 1999), an electrochemical biosensor is an integrated device that provides information on the target analytes by employing bioreceptors, which are put in direct contact with the electrochemical conduction element. In an

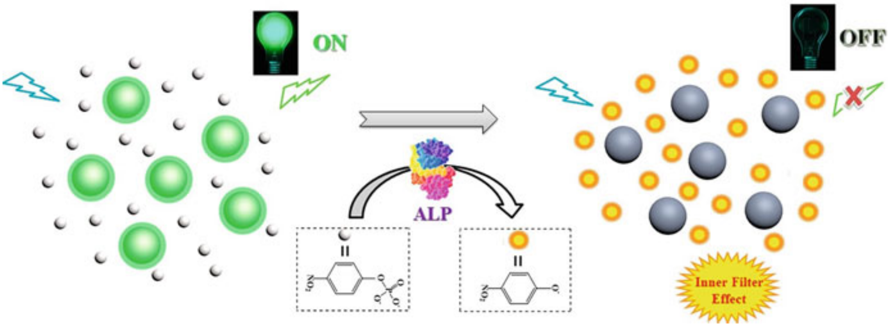

Fig. 14.5 Working principle for alkaline phosphate (ALP) sensing based on inner filter effect (IFE). (Reproduced with permission from Li (2016), © 2016 American Chemical Society)

electrochemical biosensor, the biological information of the target analytes is directly converted into detectable electrical signals (i.e., current, potential, resistivity, capacitance, impedance, etc.). Another important aspect of electrochemical biosensors is that they can be easily miniaturized to satisfy the trend for modern medical applications, based on rapid diagnosis of diseases at low cost. Tool for electrochemical analyses with the dimensions of mobile phones able to realize simple testing without special training can be easily designed and fabricated, thanks to the advancements in the processes at microscale and nanoscale level. Furthermore, electrochemical biosensors are characterized by strong anti-interference capability and high sensitivity. As above reported, the surface of CDs is rich in functional groups of different nature that can function as binding sites for specific bioreceptors and that make CDs good candidates for the realization of electrochemical biosensors. Furthermore, CDs are good electronic conductors and are able to realize simple and rapid transfer of electrons between the sensing interface and the electrodes. In general, in an electrochemical biosensor, the electrode surface is directly modified with CDs, and the detection/analysis of the target analytes is performed through the collection of the signals (i.e., current) altered by the interaction between CDs and the target analytes. For example, N-CDs were prepared by Jiang et al. (2015b) through a sustainable strategy that did not employ organic solvent or catalyst. The CDs, whose surface was rich in carboxyl groups, were employed for the realization of an electrochemical biosensor for the direct detection of dopamine (Fig. 14.6). Thus, when an electrode modified with CDs is put in contact with dopamine, the interaction between CDs carboxylic groups and dopamine causes a change of the current of the electrode which shows a linear relationship with the concentration of dopamine.

The sensor was employed by the authors for the detection of dopamine in human fluids. The obtained linear range goes from 5×10^{-8} to 8×10^{-6} mol L^{-1} and a detection limit is of 1.2×10^{-9} mol L^{-1}. In a different study, a similar biosensor was developed by Jiang et al. (2015c) for the monitoring of dopamine in real time.

CDs can also be employed for the realization of photo-electrochemical biosensors where a simple photo-irradiation causes an electron transfer at the electrode (Wang

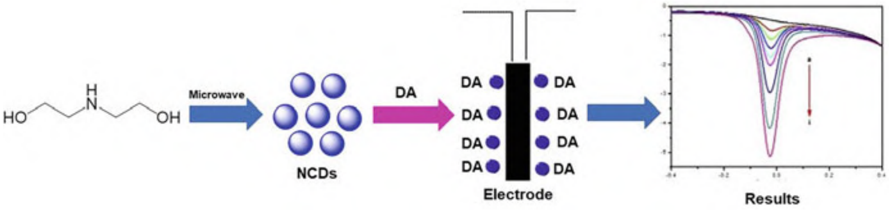

Fig. 14.6 Scheme of an electrode loaded with CDs for the sensing of dopamine (DA). (Reproduced with permission from Jiang (2015a), © 2015 Elsevier Inc.)

et al. 2018b). For example, the first self-powdered photo-electrochemical biosensor based on N-CDs/TiO_2 for detection of chlorpyrifos was developed by Cheng et al. (2019). They found that the photocurrent response under visible light of the CDs-based electrode is about 42 times higher than the one without the CDs.

3.3 Enzymatic Biosensors

Biosensors based on the combination of CDs and enzymes were also designed and developed, by exploiting the simplicity and specificity of the enzymatic catalytic reactions. As above reported, indirect detection of the target analytes could be realized by the analysis of the variations of the signal caused by the interaction between the products (or side products) of the enzymatic reaction and CDs. Furthermore, enzymatic biosensors based on CDs have high sensing specificity, as the reaction catalyzed by enzymes is very specific. Thus, they could be very useful for the detection of particular biomolecules and enzymes.

Enzymatic optical biosensors are based on the PL quenching (FRET, PET, or IFE mechanisms) caused by the interaction between CDs and the product of the enzymatic reaction of the target analytes (Fig. 14.7).

For example, H_2O_2 is the product of the enzymatic oxidation reactions of acetylcholine, uric acid, and glucose; thus, the amounts of these target analytes in human fluids could be determined through the analysis of the PL quenching due to the interaction between CDs and H_2O_2 (Cho and Park 2019; Wang et al. 2016; Ren et al. 2015; Wang et al. 2018b). An interesting CD-based enzymatic biosensor was designed and developed by Lu et al. (2016) for the determination of the β-glucuronidase. They exploited the IFE quenching effect caused by the interaction between CDs and p-nitrophenol, which is the product of the enzymatic reaction of 4-nitrophenyl-β-D-glucuronide. On the other side, the enzymatic biosensors could be employed for the detection and evaluation of the catalytic performance of specific enzymes. In this case, the "on-off-on" strategy was exploited for the design/realization of the biosensors (Fig. 14.7). The strategy simply consists of the formation of a complex between the substrate and the CDs, which causes the PL quenching of CDs; then the substrate is decomposed upon the interaction with the specific enzyme and the PL emission of CDs is restored. Thus, the presence and the amount of the specific

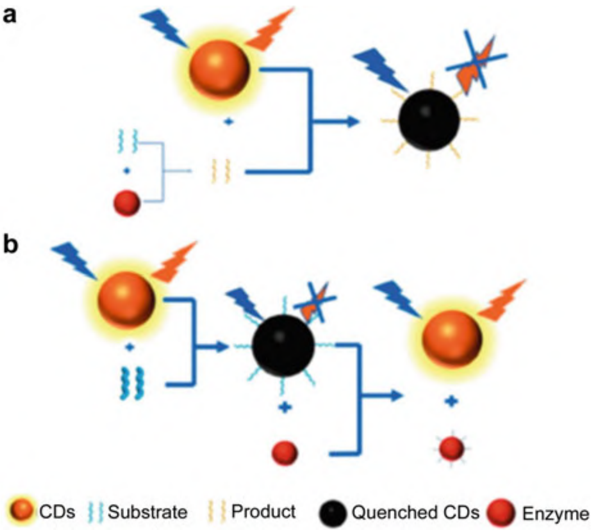

Fig. 14.7 Two sensing strategies of CD biosensors based on enzymatic reactions. (Reproduced with permission from Ji et al. (2020), © 2020 American Chemical Society)

enzyme could be determined by the analysis of the restored PL emission of CDs. An example is a biosensor for the detection of hyaluronidase reported by Liu et al. (2015). It is based on CDs, whose surface consists of positively charged functional groups and gold nanoparticles (AuNPs, known to be negatively charged) functionalized with hyaluronic acid. The PL emission of the CDs is firstly quenched by the interaction with AuNPs and then restored by the introduction of hyaluronidase that determined the decomposition of hyaluronic acid (Fig. 14.8a).

Enzymatic electrochemical biosensors are based on the determination of the target analysts through the analysis of the variations of the electrochemical signal caused by the enzymatic reactions. On the one hand, the employment of CDs in these systems provides rich binding sites for enzymes that favor their stable absorption on the electrode, and on the other hand, it improves the transmission of the electrical signals from the interfaces to the electrode because CDs are also good electron transfer materials. For example, the redox reaction between oxidoreductase and its substrates could be exploited for the design of biosensors based on the electrochemical detection of its substrates, like glucose, galactose, and H_2O_2. When an electrode modified with an oxidase is put into contact with a solution containing the substrate, a redox reaction takes place at the electrode interface that causes the transfer of an electron. Thus, through the analysis of the electrode current variations determined by this electron transfer, it is possible to detect the target analytes (i.e., oxidoreductase substrates). Following this strategy, various CDs-based electrochemical biosensors were designed and realized for the detection of oxidoreductase substrates (i.e., glucose (Buk and Pemble 2019) (Fig. 14.8b), H_2O_2 (Wang et al. 2015), and galactose (Sharma et al. 2019)).

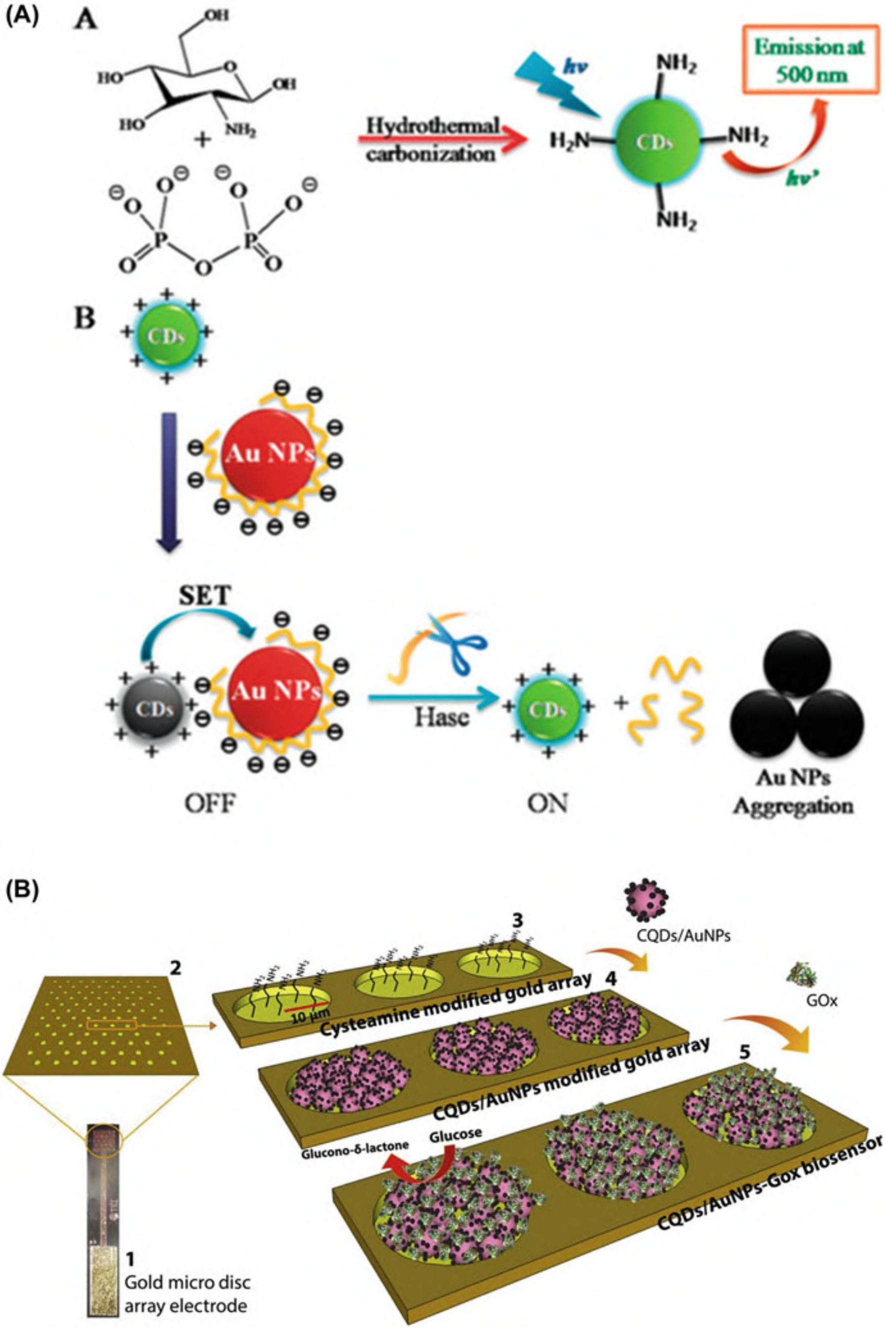
(A)
A
OH
HO
O
OH
HO
NH2
+
Hydrothermal carbonization
hv
NH2
H2N
CDs
NH2
NH2
Emission at 500 nm
hv'
B
CDs
Au NPs
SET
CDs
Au NPs
Hase
CDs
OFF
ON
Au NPs Aggregation
(B)
2
3
CQDs/AuNPs
10 µm
Cysteamine modified gold array
4
GOx
CQDs/AuNPs modified gold array
5
Glucono-δ-lactone
Glucose
CQDs/AuNPs-Gox biosensor
1
Gold micro disc array electrode

Fig. 14.8 (**a**) The schematic illustration of the synthetic process of amino-functionalized CDs (A) and the use of prepared CDs and Au NPs as a SET biosensor system for hyaluronidase

4 Conclusions

In summary, with this chapter, it was possible to show how the peculiar properties of CDs make them extremely versatile nanomaterials for application in biosensing. In fact, they exhibit an excellent intrinsic fluorescence, which could be modulated from the visible to NIR, and their surface is rich in functional groups, which enable their functionalization with different bioreceptors and functionalities (i.e., enzymes, etc.); they are also characterized by extremely low toxicity and excellent biocompatibility useful for their real-world biological applications. On the other hand, CDs are also expected to reduce the cost of biosensors by replacing both the noble metal substrates and the well-known quantum dots based on metal chalcogenides. In fact, their synthesis is based on simple and sustainable approaches that could employ cheap and "greener" starting materials coming from biomass or agro-industrial waste. They proved to be applied with excellent results both in optical and electrochemical biosensors. As a final remark, the gap between the development of CD-based optical biosensors and other types of CD-based biosensors, like electrochemical ones, could be highlighted. Compared with optical biosensors, the development of electrochemical ones should be improved, also in light of their excellent detection limits, strong anti-interference capability, and miniaturization possibilities.

References

Atchudan R, Edison TNJI, Chakradhar D, Perumal S, Shim JJ, Lee YR (2017) Facile green synthesis of nitrogen-doped carbon dots using *Chionanthus retusus* fruit extract and investigation of their suitability for metal ion sensing and biological applications. Sensors Actuators B Chem 246:497–509

Atchudan R, Edison TNJI, Aseer KR, Perumal S, Karthik N, Lee YR (2018) Highly fluorescent nitrogen-doped carbon dots derived from Phyllanthus acidus utilized as a fluorescent probe for label-free selective detection of Fe^{3+}ions, live cell imaging and fluorescent ink. Biosens Bioelectron 99:303–311

Baker SN, Baker GA (2010) Luminescent carbon nanodots: emergent nanolights. Angew Chem Int Ed 49:6726–6744

Bao L, Zhang ZL, Tian ZQ, Zhang L, Liu C, Lin Y, Qi BP, Pang DW (2011) Electrochemical tuning of luminescent carbon nanodots: from preparation to luminescence mechanism. Adv Mater 23: 5801–5806

Bao L, Liu C, Zhang ZL, Pang DW (2015) Photoluminescence-tunable carbon nanodots: surface-state energy-gap tuning. Adv Mater 27:1663–1667

◄

Fig. 14.8 (continued) (B) (Reproduced with permission from Liu (2015), © 2015 The Royal Society of Chemistry); (**b**) Schematic diagram of the biosensor preparation process: (1) the bare individual disk array electrode, (2) magnified surface of the array, (3) amine-functionalized gold surface after cysteamine modification, (4) CQDs/AuNPs attached surface, and (5) GOx enzyme immobilized overall CQDs/AuNPs-GOx biosensor. Note that the size of the electrodes, nanomaterials, and biomolecules showed are not drawn to scale. (Reproduced with permission from Buk (2019), © 2018 Elsevier Ltd.)

Buk V, Pemble ME (2019) A highly sensitive glucose biosensor based on a micro disk array electrode design modified with carbon quantum dots and gold nanoparticles. Electrochim Acta 298:97–105

Campuzano S, Yáñez-Sedeño P, José M, Pingarrón JM (2019) Carbon dots and graphene quantum dots in electrochemical biosensing. Nanomaterials 9(4):634

Cayuela A, Soriano ML, Carrillo-Carrion C, Valcárcel M (2016) Semiconductor and carbon-based fluorescent nanodots: the need for consistency. Chem Commun 52:1311–1326

Chen S, Yu YL, Wang JH (2018) Inner filter effect-based fluorescent sensing systems: a review. Anal Chim Acta 999:13–26

Chen YQ, Sun XB, Wang XY, Pan W, Yu GF, Wang JP (2020) Carbon dots with red emission for bioimaging of fungal cells and detecting Hg2+ and ziram in aqueous solution. Spectrochim Acta Part A 233:118230

Cheng W, Zheng Z, Yang J, Chen M, Yao Q, Chen Y, Gao W (2019) The visible light-driven and self-powered photoelectrochemical biosensor for organophosphate pesticides detection based on nitrogen doped carbon quantum dots for the signal amplification. Electrochim Acta 296: 627–636

Cho M-J, Park S-Y (2019) Carbon-dot-based ratiometric fluorescence glucose biosensor. Sensors Actuators B Chem 282:719–729

De B, Karak N (2013) A green and facile approach for the synthesis of water soluble fluorescent carbon dots from banana juice. RSC Adv 3:8286–8290

Ding H, Yu SB, Wei JS, Xiong HM (2016) Full-color light-emitting carbon dots with a surface-state-controlled luminescence mechanism. ACS Nano 10:484–491

Dong Y, Chen C, Zheng X, Gao L, Cui Z, Yang H, Guo C, Chi Y, Li CM (2012) One-step and high yield simultaneous preparation of single-and multi-layer graphene quantum dots from CX-72 carbon black. J Mater Chem 22:8764–8766

Dong SQ, Yuan ZQ, Zhang LJ, Lin YJ, Lu C (2017) Rapid screening of oxygen states in carbon quantum dots by chemiluminescence probe. Anal Chem 89:12520–12526

Dou XN, Zheng YZ, Uchiyama K, Lin JM (2016) Fluorescent carbon nanoparticles: mimicking hydrogen peroxide properties in a chemiluminescence system. Chem Commun 52: 14137–14140

Edison TNJI, Atchudan R, Sethuraman MG, Shim J-J, Lee YR (2016) Microwave assisted green synthesis of fluorescent N-doped carbon dots: cytotoxicity and bio-imaging applications. J Photochem Photobiol B 161:154–161

Essner JB, Kist JA, Polo-Parada L, Baker GA (2018) Artifacts and errors associated with the ubiquitous presence of fluorescent impurities in carbon nanodots. Chem Mater 30:1878–1887

Fan Z, Li S, Yuan F, Fan L (2015) Fluorescent graphene quantum dots for biosensing and bioimaging. RSC Adv 5:19773–19789

Feng J, Wang WJ, Hai X, Yu YL, Wang JH (2016) Green preparation of nitrogen-doped carbon dots derived from silkworm chrysalis for cell imaging. J Mater Chem B 4:387–393

Gao MX, Yang L, Zheng Y, Yang XX, Zou HY, Han J, Liu ZX, Li YF, Huang CZ (2016) “Click” on Alkynylated carbon quantum dots: an efficient surface functionalization for specific biosensing and bioimaging. Chem Eur J 23:2171–2178

Ge J, Jia Q, Liu W, Guo L, Liu Q, Lan M, Zhang H, Meng X, Wang P (2015) Red-emissive carbon dots for fluorescent, photoacoustic, and thermal theranostics in living mice. Adv Mater 27: 4169–4177

Haitang S, Jianfei W, Li Q, Xue C, Xianwei M (2014) Fluorescent carbon dots for bioimaging and biosensing applications. J Biomed Nanotechnol 10(10):2677–2699

Hu SL, Trinchi A, Atkin P, Cole I (2015) Tunable photoluminescence across the entire visible spectrum from carbon dots excited by white light. Angew Chem Int Ed 54:2970–2974

Huang H, Xu Y, Tang CJ, Chen JR, Wang AJ, Feng JJ (2014) Facile and green synthesis of photoluminescent carbon nanoparticles for cellular imaging. New J Chem 38:784–789

Huang Q, Bao C, Wang Q, Dong C, Guan H (2020) Tuning the microwave absorption capacity of TiP2O7 by composited with biomass carbon. Appl Surf Sci 515:145974

Ji C, Zhou Y, Leblanc RM, Peng Z (2020) Recent developments of carbon dots in biosensing: a review. ACS Sensors 5:2724–2741

Jiang K, Sun S, Zhang L, Lu Y, Wu AG, Cai CZ, Lin HW (2015a) Red, green, and blue luminescence by carbon dots: full-color emission tuning and multicolor cellular imaging. Angew Chem Int Ed 127:5450–5453

Jiang Y, Wang B, Meng F, Cheng Y, Zhu C (2015b) Microwaveassisted preparation of N-doped carbon dots as a biosensor for electrochemical dopamine detection. J Colloid Interface Sci 452: 199–202

Jiang G, Jiang T, Zhou H, Yao J, Kong X (2015c) Preparation of N-doped carbon quantum dots for highly sensitive detection of dopamine by an electrochemical method. RSC Adv 5:9064–9068

Jiang H, Geng X, Li S, Tu H, Wang J, Bao L, Yang P, Wan Y (2020a) Multi-3D hierarchical biomass-based carbon particles absorber for solar desalination and thermoelectric power generator. J Mater Sci Technol 59:180–188

Jiang L, Ding HZ, Lu SY, Geng T, Xiao GJ, Zou B, Bi H (2020b) Photoactivated fluorescence enhancement in F,N-doped carbon dots with piezochromic behavior. Angew Chem Int Ed 59: 9986–9991

Koutsogiannis P, Thomou E, Stamatis H, Gournis D, Rudolf P (2020) Advances in fluorescent carbon dots for biomedical applications. Adv Phys X 5(1):1758592

Kozák O, Datta KKR, Greplová M, Ranc VC, Kašlík J, Zbořil R (2013) Surfactant-derived amphiphilic carbon dots with tunable photoluminescence. J Phys Chem C 117:24991–24996

Li HT, He XD, Kang ZH, Huang H, Liu Y, Liu JL, Lian SY, Tsang CA, Yang XB, Lee ST (2010) Water-soluble fluorescent carbon quantum dots and photocatalyst design. Angew Chem Int Ed 49:4430–4434

Li XY, Wang HQ, Shimizu Y, Pyatenko A, Kawaguchi K, Koshizaki N (2011) Preparation of carbon quantum dots with tunable photoluminescence by rapid laser passivation in ordinary organic solvents. Chem Commun 47:932–934

Li YS, Zhong XX, Rider AE, Furman SA, Ostrikov K (2014) Fast, energy-efficient synthesis of luminescent carbon quantum dots. Green Chem 16:2566–2570

Li H, Liu J, Guo SJ, Zhang YL, Huang H, Liu Y, Kang ZH (2015) Carbon dots from PEG for highly sensitive detection of levodopa. J Mater Chem B 3:2378–2387

Li G, Fu H, Chen X, Gong P, Chen G, Xia L, Wang H, You J, Wu Y (2016) Facile and sensitive fluorescence sensing of alkaline phosphatase activity with photoluminescent carbon dots based on inner filter effect. Anal Chem 88:2720–2726

Li H, Zheng Z, Liu M, Jiang H, Hu D, Zhang X, Xia L, Geng X, Lu J, Cheng X, Wan Y, Yang P (2020) Visible light phototreatment of simulated wastewater activated by high-efficient photocatalyst: a novel heterojunction of Bi2MoO6 balls and Pd nanoskeletons. Appl Surf Sci 510:145468

Lim SY, Shen W, Gao Z (2015) Carbon quantum dots and their applications. Chem Soc Rev 44: 362–381

Liu S, Tian JQ, Wang L, Zhang YW, Qin XY, Luo YL, Asiri AM, Al-Youbi AO, Sun XP (2012) Hydrothermal treatment of grass: a low-cost, green route to nitrogen-doped, carbon-rich, photoluminescent polymer nanodots as an effective fluorescent sensing platform for label-free detection of Cu(II) ions. Adv Mater 24:2037–2041

Liu Y, Xiao N, Gong N, Wang H, Shi X, Gu W, Ye L (2014) One-step microwave-assisted polyol synthesis of green luminescent carbon dots as optical nanoprobes. Carbon 68:258–264

Liu S, Zhao N, Cheng Z, Liu H (2015) Amino-functionalized green fluorescent carbon dots as surface energy transfer biosensors for hyaluronidase. Nanoscale 7:6836–6842

Liu M, Xu Y, Niu F, Gooding JJ, Liu J (2016) Carbon quantum dots directly generated from electrochemical oxidation of graphite electrodes in alkaline alcohols and the applications for specific ferric ion detection and cell imaging. Analyst 141:2657–2664

Liu ML, Yang L, Li RS, Chen BB, Liu H, Huang CZ (2017a) Large-scale simultaneous synthesis of highly photoluminescent green amorphous carbon nanodots and yellow crystalline graphene quantum dots at room temperature. Green Chem 19:3611–3617

Liu W, Diao H, Chang H, Wang H, Li T, Wei W (2017b) Green synthesis of carbon dots from rose-heart radish and application for Fe^{3+} detection and cell imaging. Sensors Actuators B Chem 241: 190–198

Loi E, Ng RWC, Chang MMF, Fong JFY, Ng YH, Ng S (2017) One-pot synthesis of carbon dots using two different acids and their respective unique photoluminescence property. Luminescence 32:114–118

Lu J, Yang JX, Wang JZ, Lim AL, Wang S, Loh KP (2009) One-pot synthesis of fluorescent carbon nanoribbons, nanoparticles, and graphene by the exfoliation of graphite in ionic liquids. ACS Nano 3:2367–2375

Lu S, Li G, Lv Z, Qiu N, Kong W, Gong P, Chen G, Xia L, Guo X, You J, Wu Y (2016) Facile and ultrasensitive fluorescence sensor platform for tumor invasive biomaker beta-glucuronidase detection and inhibitor evaluation with carbon quantum dots based on inner-filter effect. Biosens Bioelectron 85:358–362

Lu Q, Zhou S, Zhang Y, Chen M, Li B, Wei H, Zhang D, Zhang J, Liu Q (2020) Nanoporous carbon derived from green material by an ordered activation method and its high capacitance for energy storage. Nanomaterials 10:1058

Mandani S, Dey D, Sharma B, Sarma TK (2017) Natural occurrence of fluorescent carbon dots in honey. Carbon 119:569–572

Meng W, Bai X, Wang B, Liu Z, Lu S, Yang B (2019) Biomassderived carbon dots and their applications. Energy Environ Mater 2:172–192

Moan J, Peak MJ (1989) Effects of UV radiation on cells. J Photochem Photobiol B 4:21–34

Pan DY, Zhang JC, Li Z, Wu MH (2010) Hydrothermal route for cutting graphene sheets into blue-luminescent graphene quantum dots. Adv Mater 22:734–738

Peng H, Travas-Sejdic J (2009) Simple aqueous solution route to luminescent carbogenic dots from carbohydrates. Chem Mater 21:5563–5565

Peng J, Gao W, Gupta BK, Liu Z, Romero-Aburto R, Ge L, Song L, Alemany LB, Zhan X, Gao G, Vithayathil SA, Kaipparettu BA, Marti AA, Hayashi T, Zhu J-J, Ajayan PM (2012) Graphene quantum dots derived from carbon fibers. Nano Lett 12:844–849

Peng Z, Han X, Li S, Al-Youbi AO, Bashammakh AS, El-Shahawi MS, Leblanc RM (2017) Carbon dots: biomacromolecule interaction, bioimaging and nanomedicine. Coord Chem Rev 343: 256–277

Peng Z, Ji C, Zhou Y, Zhao T, Leblanc RM (2020a) Polyethylene glycol (PEG) derived carbon dots: preparation and applications. Appl Mater Today 20:100677

Peng Z, Zhao T, Zhou Y, Li S, Li J, Leblanc RM (2020b) Bone tissue engineering via carbon-based nanomaterials. Adv Healthc Mater 9:1901495

Peng Z, Zhou Y, Ji C, Pardo J, Mintz KJ, Pandey RR, Chusuei CC, Graham RM, Yan G, Leblanc RM (2020c) Facile synthesis of "boron-doped" carbon dots and their application in visible-light-driven photocatalytic degradation of organic dyes. Nanomaterials 10:1560

Perumal V, Hashim U (2014) Advances in biosensors: principle, architecture and applications. J Appl Biomed 12:1–15

Qiao Z-A, Wang Y, Gao Y, Li H, Dai T, Liu Y, Huo Q (2009) Commercially activated carbon as the source for producing multicolor photoluminescent carbon dots by chemical oxidation. Chem Commun 46:8812–8814

Qu D, Wang X, Bao Y, Sun Z (2020) Recent advance of carbon dots in bio-related applications. J Phys Mater 3:022003

Ray SC, Saha A, Jana NR, Sarkar R (2009) Fluorescent carbon nanoparticles: synthesis, characterization, and bioimaging application. J Phys Chem C 113:18546–18551

Ren X, Wei J, Ren J, Qiang L, Tang F, Meng X (2015) A sensitive biosensor for the fluorescence detection of the acetylcholinesterase reaction system based on carbon dots. Colloids Surf B Biointerfaces 125:90–95

Righetto M, Privitera A, Fortunati I, Mosconi D, Zerbetto M, Curri ML, Corricelli M, Moretto A, Agnoli S, Franco L, Bozio R, Ferrante C (2017) Spectroscopic insights into carbon dot systems. J Phys Chem Lett 8:2236–2242

Sahiner N, Suner SS, Sahiner M, Silan C (2019) Nitrogen and sulfur doped carbon dots from amino acids for potential biomedical applications. J Fluoresc 29:1191–1200

Sahu S, Behera B, Maiti TK, Mohapatra S (2012) Simple one-step synthesis of highly luminescent carbon dots from orange juice: application as excellent bio-imaging agents. Chem Commun 48: 8835–8837

Sangam S, Gupta A, Shakeel A, Bhattacharya R, Sharma AK, Suhag D, Chakrabarti S, Garg SK, Chattopadhyay S, Basu B, Kumar V, Rajput SK, Dutta MK, Mukherjee M (2018) Sustainable synthesis of single crystalline sulphur-doped graphene quantum dots for bioimaging and beyond. Green Chem 20:4245–4259

Schneider J, Reckmeier CJ, Xiong Y, von Seckendorff M, Susha AS, Kasák P, Rogach AL (2017) Molecular fluorescence in citric acid-based carbon dots. J Phys Chem C 121:2014–2022

Sharma SK, Micic M, Li S, Hoar B, Paudyal S, Zahran EM, Leblanc RM (2019) Conjugation of carbon dots with betagalactosidase enzyme: surface chemistry and use in biosensing. Molecules 24:3275

Shen P, Xia Y (2016) Synthesis-modification integration: one-step fabrication of boronic acid functionalized carbon dots for fluorescent blood sugar sensing. Anal Chem 86:5323–5329

Sinha RP, Häder D-P (2002) UV-induced DNA damage and repair: a review. Photochem Photobiol Sci 1:225–236

Song YB, Zhu SJ, Zhang ST, Fu Y, Wang L, Zhao XH, Yang B (2015) Investigation from chemical structure to photoluminescent mechanism: a type of carbon dots from the pyrolysis of citric acid and an amine. J Mater Chem C 3:5976–5984

Song Y, Wu Y, Wang H, Liu S, Song L, Li S, Tan M (2019) Carbon quantum dots from roasted Atlantic salmon (Salmo salar L.): formation, biodistribution and cytotoxicity. Food Chem 293: 387–395

Sun YP, Zhou B, Lin Y, Wang W, Fernando KAS, Pathak P, Meziani MJ, Harruff BA, Wang X, Wang HF, Luo PG, Yang H, Kose ME, Chen BL, Veca LM, Xie SY (2006) Quantum-sized carbon dots for bright and colorful photoluminescence. J Am Chem Soc 128:7756–7757

Sun S, Guan Q, Liu Y, Wei B, Yang Y, Yu Z (2019) Highly luminescence manganese doped carbon dots. Chin Chem Lett 30:1051–1054

Tan XY, Li YC, Li XH, Zhou SX, Fan LZ, Yang SH (2015) Electrochemical synthesis of small-sized red fluorescent grapheme quantum dots as a bioimaging platform. Chem Commun 51: 2544–2546

Thevenot DR, Toth K, Durst RA, Wilson GS (1999) Electrochemical biosensors: recommended definitions and classification. Pure Appl Chem 71:2333–2348

Tian L, Ghosh D, Chen W, Pradhan S, Chang X, Chen S (2009) Nanosized carbon particles from natural gas soot. Chem Mater 21:2803–2809

Vadivel R, Thiyagarajan SK, Raji K, Suresh R, Sekar R, Ramamurthy P (2016) Outright green synthesis of fluorescent carbon dots from eutrophic algal blooms for in vitro imaging. ACS Sustain Chem Eng 4:4724–4731

Wang L, Zhou HS (2014) Green synthesis of luminescent nitrogen-doped carbon dots from milk and its imaging application. Anal Chem 86:8902–8905

Wang F, Pang SP, Wang L, Li Q, Kreiter M, Liu CY (2010) One-step synthesis of highly luminescent carbon dots in noncoordinating solvents. Chem Mater 22:4528–4530

Wang Y, Wang Z, Rui Y, Li M (2015) Horseradish peroxidase immobilization on carbon nanodots/CoFe layered double hydroxides: direct electrochemistry and hydrogen peroxide sensing. Biosens Bioelectron 64:57–62

Wang H, Lu Q, Hou Y, Liu Y, Zhang Y (2016) High fluorescence S, N co-doped carbon dots as an ultra-sensitive fluorescent probe for the determination of uric acid. Talanta 155:62–69

Wang R, Wang X, Sun Y (2017) One-step synthesis of self-doped carbon dots with highly photoluminescence as multifunctional biosensors for detection of iron ions and pH. Sensors Actuators B Chem 241:73–79

Wang B, Shen J, Huang Y, Liu Z, Zhuang H (2018a) Graphene quantum dots and enzyme-coupled biosensor for highly sensitive determination of hydrogen peroxide and glucose. Int J Mol Sci 19:1696

Wang Y, Zhou Y, Xu L, Han Z, Yin H, Ai S (2018b) Photoelectrochemical apta-biosensor for zeatin detection based on graphene quantum dots improved photoactivity of graphite-like carbon nitride and streptavidin induced signal inhibition. Sensors Actuators 257:237–244

Wang H, Xie Y, Na X, Bi J, Liu S, Zhang L, Tan M (2019) Fluorescent carbon dots in baked lamb: formation, cytotoxicity and scavenging capability to free radicals. Food Chem 286:405–412

Wu ZL, Zhang P, Gao MX, Liu CF, Wang W, Leng F, Huang CZ (2013) One-pot hydrothermal synthesis of highly luminescent nitrogen-doped amphoteric carbon dots for bioimaging from Bombyx mori silk–natural proteins. J Mater Chem B 1:2868–2873

Xu XY, Ray R, Gu YL, Ploehn HJ, Gearheart L, Raker K, Scrivens WA (2004) Electrophoretic analysis and purification of fluorescent single-walled carbon nanotube fragments. J Am Chem Soc 126:12736–12737

Yang X, Zhuo Y, Zhu S, Luo Y, Feng Y, Dou Y (2014) Novel and green synthesis of high-fluorescent carbon dots originated from honey for sensing and imaging. Biosens Bioelectron 60:292–298

Yang Y, Zou T, Wang Z, Xing X, Peng S, Zhao R, Zhang X, Wang Y (2019) The fluorescent quenching mechanism of N and S co-doped graphene quantum dots with Fe^{3+} and Hg^{2+} ions and their application as a novel fluorescent sensor. Nanomaterials 9:738

Zhang Y-Q, Ma D-K, Zhuang Y, Zhang X, Chen W, Hong L-L, Yan Q-X, Yu K, Huang S-M (2012) One-pot synthesis of N doped carbon dots with tunable luminescence properties. J Mater Chem 22:16714–16718

Zhang ZH, Sun WH, Wu PY (2015) Highly photoluminescent carbon dots derived from egg white: facile and green synthesis, photoluminescence properties, and multiple applications. ACS Sustain Chem Eng 3:1412–1418

Zhang H, Salo DC, Kim DM, Komarov S, Tai Y-C, Berezin MY (2016) Penetration depth of photons in biological tissues from hyperspectral imaging in shortwave infrared in transmission and reflection geometries. J Biomed Opt 21:126006

Zhang YJ, Yuan RR, He ML, Hu GC, Jiang JT, Xu T, Zhou L, Chen W, Xiang WD, Liang XJ (2017) Multicolour nitrogen-doped carbon dots: tunable photoluminescence and sandwich fluorescent glass-based light-emitting diodes. Nanoscale 9:17849–17858

Zhang QQ, Yang T, Li RS, Zou HY, Li YF, Guo J, Liu XD, Huang CZ (2018) A functional preservation strategy for the production of highly photoluminescent emerald carbon dots for lysosome targeting and lysosomal pH imaging. Nanoscale 10:14705–14711

Zhao HX, Liu LQ, Liu ZD, Wang Y, Zhao XJ, Huang CZ (2011) Highly selective detection of phosphate in very complicated matrixes with an off–on fluorescent probe of europium-adjusted carbon dots. Chem Commun 47:2604–2606

Zhao S, Lan M, Zhu X, Xue H, Ng T-W, Meng X, Lee C-S, Wang P, Zhang W (2015) Green synthesis of bifunctional fluorescent carbon dots from garlic for cellular imaging and free radical scavenging. ACS Appl Mater Interfaces 7:17054–17060

Zheng YZ, Zhang DK, Shah SNA, Li HF, Lin JM (2017) Ultra-weak chemiluminescence enhanced by facilely synthesized nitrogen-rich quantum dots through chemiluminescence resonance energy transfer and electron hole injection. Chem Commun 53:5657–5660

Zheng Z, Li H, Zhang X, Jiang H, Geng X, Li S, Tu H, Cheng X, Yang P, Wan Y (2020) High-absorption solar steam device comprising Au@ Bi2MoO6-CDs: extraordinary desalination and electricity generation. Nano Energy 68:104298

Zhou L, He BZ, Huang JC (2013) Amphibious fluorescent carbon dots: one-step green synthesis and application for light emitting polymer nanocomposites. Chem Commun 49:8078–8080

Zhou WJ, Dong SQ, Lin YJ, Lu C (2017) Insights into the role of nanostructure in the sensing properties of carbon nanodots for improved sensitivity to reactive oxygen species in living cells. Chem Commun 53:2122–2125

Zhou X, Qu Q, Wang L, Li L, Li S, Xia K (2020a) Nitrogen dozen carbon quantum dots as one dual function sensing platform for electrochemical and fluorescent detecting ascorbic acid. J Nanopart Res 22:1–13

Zhou Y, Mintz KJ, Cheng L, Chen J, Ferreira B, Hettiarachchi SD, Liyanage PY, Seven ES, Miloserdov N, Pandey RR, Quiroga B, Blackwelder PL, Chusuei CC, Li S, Peng Z, Leblanc RM (2020b) Direct conjugation of distinct carbon dots as Lego-like building blocks for the assembly of versatile drug nanocarriers. J Colloid Interface Sci 576:412–425

Zhu H, Wang XL, Li YL, Wang ZJ, Yang F, Yang XR (2009) Microwave synthesis of fluorescent carbon nanoparticles with electrochemiluminescence properties. Chem Commun 2009: 5118–5120

Zhu SJ, Zhao XH, Song YB, Lu SY, Yang B (2016) Beyond bottom-up carbon nanodots: citric-acid derived organic molecules. Nano Today 11:128–132

Zhu SJ, Song YB, Wang J, Wan H, Zhang Y, Ning Y, Yang B (2017) Photoluminescence in graphene quantum dots. Nano Today 13:10–14

Metal Nanoclusters and Their Composites for Clinical Diagnosis

15

Nurgul K. Bakirhan

Contents

1 Introduction 308
  1.1 Metal Nanoclusters 309
  1.2 Properties of Metal Nanoclusters 309
2 Synthesis of Metallic Nanoparticles 309
3 Electrochemical Applications of Metal-Based Biosensors for Clinical Diagnosis 310
4 Other Application Fields of Metal-Based Nanomaterials 312
5 Conclusion 326
References 327

Abstract

Fast diagnosis of disease is especially crucial in certain illnesses. Biological compound detection methods, equipment, and processes have been of great interest in the determination of the early level of diseases. Electroanalytical methods are frequently studied by researchers to investigate biomarkers or other important biological compounds due to their excellent properties such as easy usage, no need for pretreatment steps, fast response, and inexpensive equipment. In line with the increasing interest in nanotechnology, sensors development has also gained much interest. In this chapter, metal nanoclusters have been explained to develop biosensors in detail. They are preferred due to their excellent features such as optical, mechanical, physical, and chemical. Metal nanomaterials-based sensors have been presented by electrochemical methods to determine important compounds.

Keywords

Metal nanoclusters · Electrochemistry · Metal nanoparticles · Biomolecules

---

N. K. Bakirhan (✉)
Department of Analytical Chemistry, Gulhane Faculty of Pharmacy, University of Health Sciences, Ankara, Turkey

© Springer Nature Singapore Pte Ltd. 2023

U. P. Azad, P. Chandra (eds.), *Handbook of Nanobioelectrochemistry*,
https://doi.org/10.1007/978-981-19-9437-1_15

1 Introduction

Nanotechnology is a crucial and rapidly developing technology. It is used in the production of materials at the molecular level and at the atomic level, which includes the processes of separating, combining, and decomposing materials by an atom or a molecule as a science that covers the design, production, characterization, and application of nanometer-sized structures. In terms of nanomaterials, structures with a size smaller than 100 nm should be considered. On the other hand, nanoclusters are structures formed by nanomaterials with a dimension of 1–10 nm (Fronzi et al. 2016; Jin et al. 2016). The small dimensions of these structures and their high surface-to-volume ratio provide advantages over bulk materials. The variation of these size-dependent physicochemical properties compared to bulk materials causes a rapid increase in nanoproduct and nanomaterial production (Jeevanandam et al. 2018).

Nanomaterials are divided into three main groups (Jeevanandam et al. 2018):

(a) Carbon-based nanomaterials: fullerenes, nanofibers, and nanotubes are materials in the form of spheres, ellipsoids, or tubes in this group.
(b) Metal and/or metal oxide-based nanomaterials: these include gold, silver, iron oxide, zinc oxide, and quantum dots that are several nanometers in size.
(c) Composite nanomaterials: these include nanostructures containing various combinations such as carbon-metal, carbon-polymer, metal-polymer, polymer-polymer, metal-metal, and carbon-carbon. The purpose of the production of composite materials is to obtain a material with new and improved properties from materials that are insoluble in each other. These properties are mechanical properties such as durability, flexibility and dimensional stability, thermomechanical properties, and water permeability. Nanocomposites are separated into three main parts according to their composition: firstly, ceramic-based nanocomposites like Al_2O_3/CNT, Al_2O_3/SiO_2, and Al_2O_3/SiC; secondly, metal-based nanocomposites like Fe-MgO, Fe-Cr/Al_2O_3, and Co/Cr; and lastly, polymer-based nanocomposites like polyester/TiO_2 and polymer/CNT. Among these three groups of nanomaterials, metal-based nanomaterials have received the most attention due to their unique size-dependent features such as photoluminescence (Xu and Suslick 2010), catalysis (Chen and Chen 2009), electrochemical characteristics (Ingram et al. 1997), intrinsic magnetism (Santiago González et al. 2010), and chirality (Cathcart and Kitaev 2010), which deviate significantly from those of their corresponding bulk metals and large nanoparticles.

Gold and silver nanomaterials have been used extensively in various application fields. Specifically, they are preferred for use with alkanethiols and other ligands as protecting agents via thiol, phosphines, or amides to noble metal surfaces, and are known for their excellent stability in different media (Murray 2008; Jin 2010; Díez and Ras 2011).

1.1 Metal Nanoclusters

Metal nanomaterials attract a great deal of attention for their extraordinary electronic, optical, magnetic, and catalytic properties. The fact that nano-sized materials have physical, chemical, and biological differences compared to bulk materials has also caused differentiation in their electronic, magnetic, and optical properties due to quantum mechanics. The surface areas of the nanoclusters are higher than the bulk materials. The smaller number of atoms on the surface, or the more they settle on the surface, increases the interaction with other molecules or atoms around it. The increased surface area shows higher catalytic properties and chemical activity. Electrons of metal materials in bulk are constantly in motion in irregular orbits. The distances of the moving electrons in the orbits to the atomic nucleus, that is, the electron levels, are very small, that is, the energy difference is small enough to be ignored. In nanometal clusters, electrons move away from each other and the energy difference is high. This causes a difference in nanometal material. For example, while the conductive bulk material is in the nanostructure, it may not be conductive. Or it can be the other way around. It is clear that gold nanoparticles with different sizes have different colors and properties. Due to these superior properties of metal materials, they are preferred in the production or modification of electrode materials and in the catalysis of various redox reactions.

1.2 Properties of Metal Nanoclusters

Due to the distance between a large number of atoms in the structure of nanomaterials, they can exhibit different magnetic properties according to their stack states. The magnetic moment in the nanocluster is expected to be greater. The large surface-to-volume ratios of the nanoclusters and the low coordination of the atoms on the surface give these structures unique reactivity and catalytic properties. The optical properties of metal nanoclusters depend on their electronic structure. The energy gap between the highest occupied molecular orbital and the lowest unoccupied molecular orbital determines the optical behavior of a nanocluster. These gaps can differ in the new structures formed by different ligands or materials around the metal materials. Thus, it is possible to design new materials by adjusting the energy gaps in metal nanoclusters.

2 Synthesis of Metallic Nanoparticles

It is possible to synthesize metal nanoparticles using various reduction methods of metal ions. Chemical reduction, electrochemical reduction, thermal reduction, reduction by ionizing radiation, and photochemical reduction can be listed among these methods (Khan et al. 2019). Nanostructures can be obtained quickly with nucleation and growth steps in reduction reactions. The creation of nanoparticles in these two steps is carried out by two approaches: physical methods, also known as the top-down approach, and chemical methods, also known as the bottom-up approach (Khan et al. 2019). The reduction of bulk materials to nano-size by physical and mechanical processes (shredding, cutting, grinding methods) involves the top-down approach. In this method, it is advantageous that no chemical material is needed and the processes applied are simple. The negative aspect of this method is that the nanoparticles formed are of irregular, inhomogeneous sizes and there is a great deal of material loss. With the bottom-up approach, it is possible to reach the nanoparticle structure in a controlled manner starting from the atomic and molecular levels. The dimensions of nanoparticles obtained in this approach can be formed at the desired level and kept under control. Therefore, this approach is more preferred in the synthesis of nanoparticles. The instability of metal nanoparticles has shed light on the preparation of metal composites. Ensuring the control of composites and observing stable structures increase the importance of using metal composites.

3 Electrochemical Applications of Metal-Based Biosensors for Clinical Diagnosis

Biosensor systems include many disciplines and come to the forefront in making this diagnosis (Monošik et al. 2012; Tao et al. 2015). Biosensors are defined as transmitter systems that are based on the interaction between a receptor and an analyte and transform the information generated as a result of this interaction into a measurable signal (Florea et al. 2015). The most important component affecting sensor performance consists of two parts: the bioreceptor and the transducer. Structures such as enzymes, cells, antibodies, and nucleic acids with properties such as high sensitivity and selectivity to the target substance are used as receptors. Transducer systems transform the biological response that occurs as a result of the interaction between receptors and the target analyte into a measurable signal such as electrochemical, optical, piezoelectric, calorimetric, or impedimetric. In addition, an ideal biosensor definition made by the World Health Organization (CSL STYLE ERROR: reference with no printed form) is: affordable, precise and specific, user-friendly, fast and robust, without equipment, and can be delivered to those in need. Based on this definition, point of care (POC) tests (da Silva et al. 2017), known as a biosensor system, is a term used to describe the tests that can be applied at or near the patient's location (Omidfar et al. 2012). The most important feature of these tests is that they do not require laboratory personnel or laboratory experience. In addition, in these tests, while proteins, metabolites, nucleic acids, human cells, drugs, dissolved ions, gases, and micro-organisms form target analytes, blood, saliva, urine, and other body fluids are samples for analysis. POC products are needed in a broad range of fields such as monitoring disease in hospitals, clinics, or private practices or at home, monitoring water or food safety, and monitoring legal regulations. Because these products respond in a very short time with very small samples and without pre-preparation, they practically detect multiple analytes or markers with simple instructions for use. These diagnostic platforms provide fast access to analytical information with important advantages such as being sensitive, environmentally friendly, portable, applicable on-site, and low cost.

Antibodies are ideal bio-recognized materials thanks to their high specificity and strong affinity for their antigens. They contain a large number of functional groups or can be functionalized. Using electrochemical methods and antibody–antigen relationships, it is possible to apply various analyses and determinations of disease-specific markers used in clinical practice.

Metal nanoparticles have excellent properties which mean they are preferred in biosensor design with the proper size, shape, and modification procedure. Metal salts have been used to synthesize metal nanomaterials in aqueous and organic solutions. Stabilizers like ions, nanomaterials, polymers, or biological molecules are needed for preventing the degradation of reduced metal particles.

Biosensors attract a great deal of interest from researchers due to their many potential application fields in clinical diagnosis, environmental monitoring, food analysis, etc. (Wang 2008). Glucose biosensors have wide application in many laboratories due to the high number of people suffering from diabetes. The glucose biosensor is one of the most used devices all over the world (Wang 2001). Fast response, accuracy, and low cost have been important factors in developing a sensor (Magner 1998). AuNP-based sensors for glucose quantification present a high-stability surface and remove enzyme leakage problems (Luo et al. 2004; Wu et al. 2007; Bai et al. 2007). A composite of AuNPs with conductive polymers (Xian et al. 2006), as well as graphene and nanotubes, was fabricated as glucose sensors (Liu et al. 2007). AuNPs size was found to be an important criterion in modification with the polypyrrole polymerization process (German et al. 2012). According to the result of this study, smaller size AuNPs had a greater effect on amperometric responses. PtNPs showed good performance on the activity of hydrogen peroxide to quantification precise glucose (Wang et al. 2007; Pang et al. 2009). PtNP can present sensitive properties for the detection of glucose when they used with other nanoparticles such as iron oxide, nanotube and chitosan (Li et al. 2010c). Titania nanotube arrays have also been used for glucose sensing (Pang et al. 2009). Cholesterol blood level is so important on the control of health. Electrochemical methods and metal-based sensors provide an opportunity for sensitive and selective detection of cholesterol. In one study, amperometry was applied for the measurement of cholesterol up to 0.5 nM by Pt/Graphene and Pt/CNT modified electrodes (Dey and Raj 2010; Yang et al. 2012). AuNPs were also applied for the development of an enzymatic sensor with limit of detection (LOD) 1.28 μM (Sharma et al. 2017). Composite metal structures such as zinc, silver, titanium molybdenum, and palladium have been used for cholesterol biosensor design (Giri et al. 2014; Dey and Raj 2014; Xu et al. 2015; Wang et al. 2015c; Vc and Berchmans 2016; Komathi et al. 2016). The simple and accurate detection of biological compounds such as ascorbic acid (AA), uric acid (UA), and dopamine (DA) is important for the investigation of diseases. The simultaneous detection with well-separated peaks of these compounds was achieved by palladium graphene composite (Wang et al. 2013b). Silver nanowire/reduced graphene oxide (AgNW/rGO) as silver composite was also used for sensitive simultaneous determination of AA, DA, and UA. AgNW plays a role in

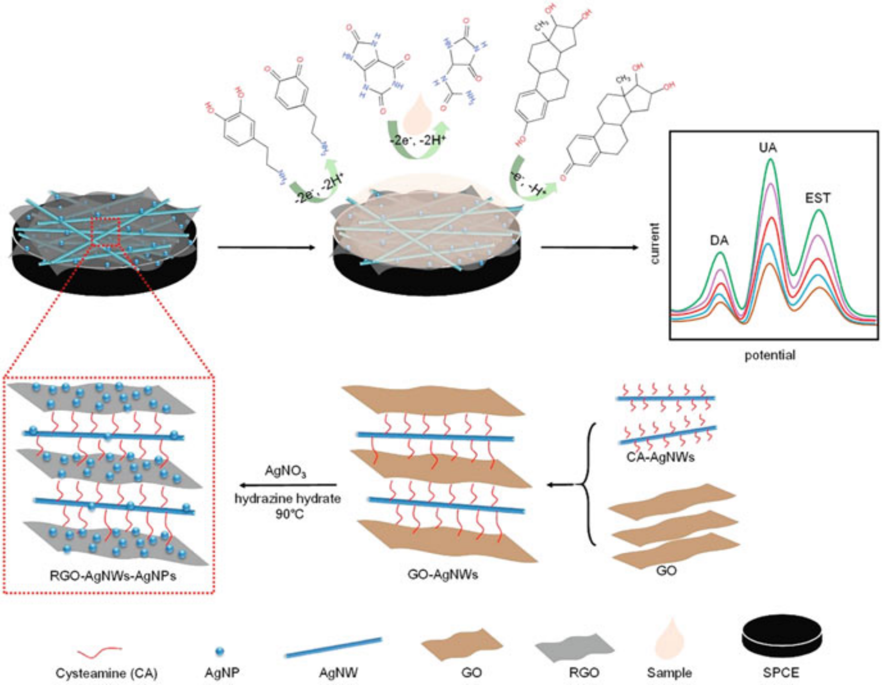

Fig. 15.1 The design of nanoparticle-based sensors and their electrochemical performances for the analysis of DA, UA, and EST. (Reprinted with permission from Elsevier (Zhao et al. 2020a))

preventing the agglomeration of rGO suspension and acceleration of electron transfer between conductive pathways (Kaur et al. 2013; Li et al. 2015). The electrochemical impedance spectroscopy method was applied via AuNPs for simultaneous sensing of biomolecules (Wang et al. 2013a). AuNPs with graphene hydrogel composite could succeed in the selective determination of AA, DA, and UA with nanomolar-level LOD values (Zhu et al. 2017; Zhao et al. 2020a) (Fig. 15.1).

The aim of this chapter is to briefly explain metal nanomaterials which are used for surface modification of electrodes, which can increase electron transfer rate in the redox process. Biomolecular recognition and signal enhancement are also possible with metal nanoclusters (Chandra et al. 2013; Tao et al. 2015; Zhang et al. 2017; Wong et al. 2021). This chapter mainly discusses the selected research articles which are related to clinically important compounds or biomarkers (Table 15.1).

4 Other Application Fields of Metal-Based Nanomaterials

Metal nanoparticles smaller than 100 nanometers show excellent potential as highly active and selective catalysts. Metal nanoparticles have a large proportion of catalytically active atoms due to their higher volumetric surface (Astruc 2020). In addition to their high activity and selectivity, they are generally isolated,

Table 15.1 Metal-based nanoclusters; composites for detection of biological compounds

Type of Metal	Analyte	Technique	LOD	Medium	Ref.
Pt/Cu NPs	PSA	Amperometry	0.55 fM	0.1 M PBS (pH 7.7)	(Feng et al. 2017)
Fe_3O_4@GO	PSA	Amperometry	15 fg mL^{-1}	Patient serum samples	(Sharafeldin et al. 2017)
AuNPs	Cancer antigen 125	SWV	6 μUmL^{-1}	Human serum	(Samadi Pakchin et al. 2020)
rGO/Fe_3O_4/Cu_2O NSs Ag@RF-Ag NPs	PSA	DPV	6.2 $pgmL^{-1}$	0.1 M PBS (pH 7.0)	(Zhao et al. 2020b)
PtNPs/MWCNT	Ascorbic acid Dopamine Uric acid	DPV	20 μM 0.0483 μM 0.35 μM	Not reported	(Dursun and Gelmez 2010)
PtNPs	Alpha-fetoprotein	DPV	0.001 pM	0.2 M PBS (pH 7.0) containing 0.2 M KCl	(Chang et al. 2016)
Fe_3O_4@PDA/CuxO	Cysteine	SWV	83 pM	Real sample	(Zhou et al. 2018)
Fe_3O_4/Ag/Au	IgG	Amperometry	0.33 fM	0.1 M PBS (pH = 7.4)	(Zhang et al. 2016)
AgNPs/CuOHCs/Fe_3O_4	Glucose	Amperometry	15 nM	Human serum Human urine	(Baghayeri et al. 2020)
GO- Fe_3O_4/GOD	Glucose	Amperometry	0.1 μM	0.1 M PBS (pH = 7)	(Pakapongpan and Poo-arporn 2017)
Fe_3O_4 nanoparticles-polyvinyl alcohol	Glucose	CV		0.1 M PBS (pH = 7)	(Sanaeifar et al. 2017)
AuNPs/AZA/MWCNTs	Ascorbic acid Dopamine Uric acid	DPV	16 μM 0.014 μM 0.028 μM	Human urine	(Filik et al. 2016)

(continued)

Table 15.1 (continued)

Type of Metal	Analyte	Technique	LOD	Medium	Ref.
AuNPs/BSA/ Fe_3O_4	Glucose	Amperometry	3.54 μM	0.05 M PBS (pH = 7.4)	(He et al. 2016)
$CuFe_2O_4$-MNPs	Lysozyme	DPV	1.58 × 10–3 μg mL^{-1}	Biological samples	(Liang et al. 2019a)
AuNPs	CEA	DPV	0.01 pM	10 mM $K_3[Fe(CN)_6]$ (pH 5.0)	(Cai et al. 2016)
$ZnxFe_3$-xO_4	Glucose	Amperometry	0.03 mM	Real samples	(Ognjanović et al. 2019)
La-MWCNT	Ascorbic acid Dopamine Uric acid	Chronoamperometry	0.14 μM 0.013 μM 0.015 μM	Human urine Human serum	(Zhang et al. 2012)
SOx/Pt– Fe_3O_4@C	Sarcosine	Amperometry	0.43 μM	Serum sample	(Yang et al. 2019)
AgNPs	PSA	ECL	0.1 pM	1/15 M PBS (pH 8.0)	(Ma et al. 2016)
Fe_3O_4–Au@Ag	CaMV35S (tDNA)	Amperometry	1.26×10^{-17} M	Tomato samples	(Ye et al. 2020)
AgNPs	H5N1	CV	1×10^{-15} M	0.1 M KCl	(Zhang et al. 2009a)
PDA-AuNPs	Ascorbic acid Dopamine Uric acid	SWV	5.0 μM 0.08 μM 0.06 μM	Human blood, serum, and urine	(Zhang et al. 2013)
Au NPs/BPene/Fe_3O_4–COF	PSA	DPV	30 fg mL^{-1}	Real sample	(Liang et al. 2019b)
AgNCs	H_2O_2	Chronoamperometry	2 μM	0.05 M PBS (pH 6.5, 25 °C)	(Yang et al. 2018)
3DGH-AuNPs	Ascorbic acid Dopamine Uric acid	DPV	0.028 μM 0.0026 μM 0.005 μM	Human serum	(Zhu et al. 2017)

MgO/Gr	Ascorbic acid Dopamine Uric acid	DPV	0.03 μM 0.15 μM 0.12 μM	Human serum	(Zhao et al. 2015b)
AgNPs	Hepatitis B virus (HBV)	DPV	1×10^{-18} M	Not reported	(Li et al. 2010b)
Ti_3C_2	Carcinoembryonic antigen (CEA)	CV	0.018 pg/mL	50 mM PBS (pH 7.4, 0.9% NaCl) containing 5 mM $[Ru(NH_3)_6]^{3+}$	(Kumar et al. 2018)
MNPs-anti-M2/influenza virus/fetuin-AuNPs	Influenza virus H9N2	Amperometry	16 HAU	PBS	(Sayhi et al. 2018)
AuNPs	Hepatitis C virus RNA	DPV	3.1×10^{-22} M	Not reported	(Liu et al. 2011a)
MoS_2	VP40	Electrolysis	2 fM	Not reported	(Zhang et al. 2019)
AuNPs	Escherichia coli	Chronocoulometry	9×10^{-13} M	10 mM Tris–HCl buffer (pH 7.4) +50 μM $[Ru(NH_3)_6]^{3+}$	(Wang et al. 2011b)
CNT-NiNC carbon nanotube with prophyrinoid nickel (II) norcorrole complex	Ascorbic acid Dopamine Uric acid	DPV	2.0 μM 0.1 μM 0.4 μM	Human urine and serum	(Deng et al. 2016)
Silica-coated Fe_2O_3 NPs/Nafion	Hydrazine	DPV	76.0 pM	0.1 M pH 7.0 PBS	(Akhter et al. 2017)
AuNPs	microRNA-21	DPV		0.01 M PBS	(Tian et al. 2018)
AgNPs/PPy	Ascorbic acid Dopamine Uric acid	DPV	1.8 μM 0.1 μM 0.5 μM	Hydrochloride Injection and human urine	(Ghanbari and Hajheidari 2015)
CuNPs/p-TAOX	Ascorbic acid Dopamine Uric acid	DPV	5.0 μM 0.03 μM 0.16 μM	Human blood, serum, and urine	(Wang et al. 2015a)

(continued)

Table 15.1 (continued)

Type of Metal	Analyte	Technique	LOD	Medium	Ref.
AuNPs	Single and double-base mismatch	DPV	DNA bases	Not reported	(Du et al. 2010)
Fe_3O_4@rGO/PANI	Insulin	DPV	3 pM	Real serum samples	(Zhu et al. 2016)
Au/MoS_2/Au nanofilm	Glucose	Amperometry	10 nM	PBS	(Yoon et al. 2019)
$[Ni(phen)_2]^{2+}$/SWCNTs	Ascorbic acid Dopamine Uric acid	DPV	12.0 μM 1.0 μM 0.7 μM	Human urine Dopamine Vitamin C tablets	(Yan et al. 2016)
Au@Fe_3O_4	Eosinophil cationic protein (ECP)	SWV, EIS, Chronocoulometry	0.3 nM	10 mM PBS (pH 7.4)	(Lee et al. 2018)
rMWCNTs-PdNTs reduced MWCNTs and palladium nanotubes	Ascorbic acid Dopamine Uric acid	DPV	1.7×10^{-5} μM 0.18 μM 3.6×10^{-4} μM	Not reported	(Shruthi et al. 2018)
AuNPs	H_2O_2	Direct electrochemistry	0.1 μM	0.1 M pH 7.0 PBS	(Huang et al. 2011)
AuNPs@ MoS_2	Ascorbic acid Dopamine Uric acid	DPV	100 μM 0.05 μM 10 μM	Human serum	(Sun et al. 2014)
AuNPs	H_2O_2	Direct electrochemistry	0.67 μM	0.2 M pH 7.0 PBS	(Liu et al. 2011b)
AuNPs	Galactose	Direct electrochemistry		20 mM MES buffer pH 7.5	(Abad et al. 2009)
AuNCs/AGR/MWCNT	Ascorbic acid Dopamine Uric acid	SWV	0.27 μM 0.08 μM 0.1 μM	Human urine	(Abdelwahab and Shim 2015)
MWCNT/PSVM/Au	Dopamine	DPV	56 nM	Real sample analysis	(Liu et al. 2017)

AuNPs	H_2O_2	Direct electrochemistry	0.08 μM	0.1 M PBS (pH 5.0)	(Wang et al. 2009a)
AgNW/rGO	Ascorbic acid Dopamine Uric acid	LSV	0.81 μM 0.26 μM 0.30 μM	Not reported	(Li et al. 2015)
PtNPs	H_2O_2	Direct electrochemistry	0.028 μM	0.1 M PBS (pH 7.0)	(Jia et al. 2009)
Graphene/SnO_2	Ascorbic acid Dopamine Uric acid	DPV	100 μM 1 μM 3 μM	Not reported	(Xie et al. 2015)
AgNPs	H_2O_2	Direct electrochemistry	0.3 μM	0.1 M PBS (pH 7.0)	(Lu et al. 2010)
AuNPs modified TiO_2 nanotube array	Glucose	Direct electrochemistry	3.1×10^{-4} M	0.067 M PBS (pH 6.8)	(Zhang et al. 2011b)
Fe_3O_4-SnO_2-Gr	Ascorbic acid Dopamine Uric acid	DPV	0.062 μM 0.0071 μM 0.005 μM	Urine Serum Tablet	(Bagheri et al. 2017)
HRP-Strept-Biotin-Ab-Cor/AuNPs/MrGO/Nafion	Cortisol	DPV	0.05 $ngmL^{-1}$	Human Plasma	(Sun et al. 2017)
AuNPs	H_2O_2	Direct electrochemistry	1.7 μM	0.1 M PBS (pH 6.5)	(Zhou et al. 2010b)
MWCNTs/FeNAZ/CH iron ion-doped natrolite zeolite, chitosan and MWCNTs	Ascorbic acid Dopamine Uric acid	LSV	1.11 μM 1.05 μM 0.033 μM	Human urine Human serum	(Noroozifar et al. 2011)
AuNPs	H_2O_2	Direct electrochemistry	9 μM	0.1 M PBS (pH 7.0)	(Xiang et al. 2009)
AuNPs	Glucose	Direct electrochemistry	1.8×10^{-4} M	Human blood sample	(Shan et al. 2010)

(continued)

Table 15.1 (continued)

Type of Metal	Analyte	Technique	LOD	Medium	Ref.
MoS_2/rGO	Ascorbic acid Dopamine Uric acid	DPV	0.72 μM 0.05 μM 0.46 μM	Human serum	(Xing and Ma 2016)
CTAB/rGO/ZnS	Ascorbic acid Dopamine Uric acid	DPV	30 μM 0.5 μM 0.4 μM	Urine sample	(Yang 2015)
AuNPs/AgNPs	Alpha-fetoprotein	DPV, CV, and EIS	5×10^{-13} g mL^{-1}	0.1 M acetic acid-buffered saline (pH 5.5)	(Su et al. 2011a)
Fe_3O_4–MWCNT–poly(BCG)	Serotonin	DPV	80 nM	Spiked human serum	(Ran et al. 2017)
AuNPs	H_2O_2	Direct electrochemistry	0.1 μM	0.1 M N_2-saturated PBS (pH 7.0)	(Li et al. 2010a)
AuNPs	SNP	DPV	1×10^{-14} M,	100 mM PBS (pH = 6.5)	(Du et al. 2011)
Fe(III)P/MWCNTs	Ascorbic acid Dopamine Uric acid	CV	3.0 μM 0.09 μM 0.3 μM	Human urine and serum	(Wang et al. 2012)
AuNPs	CEA	EIS and CV	1×10^{-10} g·mL^{-1}	0.02 M PBS (pH = 7.0)	(Yuan et al. 2009)
AgNPs	CEA and AFP	LSV	LOD of CEA 9.3 × 10^{-14} g mL^{-1}; LOD of AFP 6.1× 10^{-14} g mL^{-1}	1.0 M KCl	(Lai et al. 2011)
MWCNTs/FeNAZ/CH iron ion-doped natrolite zeolite, chitosan, and multiwalled carbon nanotubes	Ascorbic acid Dopamine Uric acid	LSV	1.11 μM 1.05 μM 0.033 μM	Human urine Human serum	(Noroozifar et al. 2011)

Fe_3O_4@GQD/ f–MWCNTs	Progesterone	LSV	2.18 nM	Human serum samples Pharmaceutics	(Arvand and Hemmati 2017)
AgNPs	PSA	LSV	9×10^{-13} g mL^{-1}	10 mM PBS (0.1 M NaCl, pH 7.4) and 20 mM Tris-HCl buffer (pH 8.0)	(Huang et al. 2009)
Hnp Pt/Cu alloy	Ascorbic acid Dopamine Uric acid	DPV	17.5 μM 2.8 μM 5.7 μM	Not reported	(Zhao et al. 2015a)
AuNPs	α-Synuclein (α-SYN)	EIS	3.4×10^{-11} g·mL^{-1}	0.05 M PBS (pH 7.0)	(An et al. 2010)
PtNPs	Glucose	Direct electrochemistry	4 μM	0.1 M deoxygenated PBS (pH 6.0) Beverage drinks	(Han et al. 2010)
AuNPs	Progastrin releasing-peptide (ProGRP)	CV	3×10^{-12} g·mL^{-1}	0.1 M PBS (pH 7.4)	(Zhuo et al. 2011)
AuNPs	H_2O_2	Direct electrochemistry	1.5 μM	0.1 M PBS (pH 7.0)	(Villalonga et al. 2011)
AuNPs	Hepatitis B	ASV	8.7×10^{-11} g mL^{-1}	0.05 M PBS (pH 7.0)	(Shen and Zhang 2010)
Pt-Gr/CNT	Ascorbic acid Dopamine Uric acid	DPV	50 μM 0.01 μM 0.1 μM	Vitamin C Urine Serum	(Ramakrishnan et al. 2015)
AuNPs	Escherichia coli (E. Coli)	ASV	30 CFU·mL^{-1}	0.1 M PBS (pH 7.4)	(Zhang et al. 2009b)
MgO nanobelts	Ascorbic acid Dopamine Uric acid	CV	0.2 μM 0.05 μM 0.04 μM	Not reported	(Li et al. 2014)
AgNPs	Bacillus globigii (BG)	CV	602 spores/mL	Not reported	(Mwilu et al. 2009)
PtNPs	H_2O_2	Direct electrochemistry	1.1 μM	0.1 M PBS (pH 7.0)	(Zhang et al. 2010d)

(continued)

Table 15.1 (continued)

Type of Metal	Analyte	Technique	LOD	Medium	Ref.
PtNPs	Single-base mismatch	CV and DPV	CA, GA, GT, and TT mismatches	0.1 M KCl	(Ahangar and Mehrgardi 2011)
Pd NPs/GR/CS	Ascorbic acid Dopamine Uric acid	DPV	20 μM 0.1 μM 0.17 μM	Not reported	(Wang et al. 2013b)
AuNPs	Carcinoembryonic antigen (CEA)	CV	1×10^{-11} g·mL^{-1}	0.1 M PBS (pH 7.0)	(Zhong et al. 2010)
AuNPs	H_2O_2	Direct electrochemistry	99 μM	67 mM PBS (pH 7.0)	(Wang et al. 2009b)
AgNPs/rGO	Ascorbic acid Dopamine Uric acid	LSV	9.6 μM 5.4 μM 8.2 μM	Not reported	(Kaur et al. 2013)
AgNPs	Platelet-derived growth factor-BB (PDGF-BB)	CV and SWV	5×10^{-12} g·mL^{-1}	5 mM $Fe_3(CN)_6^{3-}$ + 0.1 M KCl	(Qu et al. 2011)
Ru/Pty	Ascorbic acid Dopamine Uric acid	LSSV	0.31 μM 0.08 μM 0.58 μM	Human blood and serum	(Khudaish et al. 2014)
Poly(DPA)/SiO_2@Fe_3O_4	Ascorbic acid Dopamine Uric acid	DPV	0.4 μM	Human blood, serum, and urine	(Veera Manohara Reddy et al. 2018)
AuNPs	Prostate-specific antigen (PSA)	CV and rotating disk amperometry	5×10^{-13} g·mL^{-1}	Undiluted serum	(Mani et al. 2009)
Nano-Au/p-TA	Ascorbic acid Dopamine Uric acid	DPV	1.1 μM 0.05 μM 0.08 μM	Human blood, serum, and urine	(Wang et al. 2011a)

AuNPs	IL-6	Amperometry	1×10^{-11} g·mL^{-1}	0.01 M PBS (pH 7.2)	(Munge et al. 2009)
PtNPs	PSA	CV	1×10^{-15} g·mL^{-1}	10 mM of HCl + 1 M of KCl	(Zhang et al. 2010a)
RGO/PAMAM/MWCNT/AuNP	Ascorbic acid Dopamine Uric acid	DPV	6.7 μM 3.3 μM 0.33 μM	Not reported	(Wang et al. 2015b)
AuNPs	Alpha-fetoprotein	DPV	8×10^{-16} g·mL^{-1}	0.1 M acetic acid-buffered saline (pH 8)	(Tang et al. 2011b)
AuNPs	Cardiac troponin I (cTnI) and C-reactive protein (CRP)	SWV	LOD of cTnI 4×10^{-12} g·mL^{-1}, LOD of CRP 2.2×10^{-10} g·mL^{-1}	Not reported	(Zhou et al. 2010a)
Pd_3Pt_1/PDDA-RGO	Ascorbic acid Dopamine Uric acid	DPV	0.61 μM 0.04 μM 0.10 μM	Human urine Serum samples	(Yan et al. 2013)
AuNPs	Alpha-fetoprotein	EIS, CV and amperometry	6×10^{-10} g·mL^{-1}	0.1 M BRB (pH 9.0)	(Lin et al. 2009)
AuNPs	Jurkat cells during early apoptosis	EIS	–	HEPES buffer (pH 7.4)	(Tong et al. 2009)
PdAg NFs/rGO	Ascorbic acid Dopamine Uric acid	DPV	0.185 μM 0.017 μM 0.654 μM	Not reported	(Chen et al. 2015)
AuNPs	Single nucleotide polymorphism (SNP)	LSV	1×10^{-15} M	Not reported	(Das and Yang 2009)
AuNPs	Drug-sensitive leukemia K562/B.W. cells and drug-resistant K562/ ADM cells	EIS and DPV	8.0×10^{2} cells/mL	0.02 M PBS (pH 7.2)	(Wu et al. 2011)
Fe_3O_4-NH_2@GS	Ascorbic acid Dopamine Uric acid	DPV	0.074 μM 0.126 μM 0.056 μM	Urine samples	(Wu et al. 2014)

(continued)

Table 15.1 (continued)

Type of Metal	Analyte	Technique	LOD	Medium	Ref.
AuNPs	Glucose	Direct electrochemistry	1.2 μM	0.1 M pH 7.0 PBS	(Li et al. 2011)
Fe-Meso-PANI	Ascorbic acid Dopamine Uric acid	LSV	6.5 μM 9.8 μM 5.3 μM	Human blood, serum, and urine	(Anu Prathap and Srivastava 2013)
AuNPs	Neomycin (Neo)	CV and Amperometry	$6.76 \pm 0.17 \times 10^{-9}$ g·mL^{-1}	Not reported	(Zhu et al. 2010)
AuNPs	Insulin-like growth factor-1 (IGF-1)	CV and EIS	1.5×10^{-13} g·mL^{-1}	0.1 M PBS + 0.1 M KCl (pH = 4.4)	(Rezaei et al. 2011)
AgNPs	DNA hybridization	DPV	3.2 pM	0.1 M PBS (pH 7.0)	(Zhang et al. 2009c)
Pd-NP/ (MWCNTs/IL/G)	Ascorbic Acid Dopamine Uric Acid	DPV	0.2 μM 0.03 μM 0.15 μM	Human serum Urine	(Abbas Rafati et al. 2014)
AuNPs	DNA hybridization	ECL	1.9×10^{-16} M	Not reported	(Chai et al. 2010)
PtNPs	Human immunoglobulin G (IgG)	QCM and LSV	1.8×10^{-11} g·mL^{-1}	0.1 M PBS (pH 7.4)	(Fu et al. 2010)
AuNPs/ AgNPs	H_2O_2	Direct electrochemistry	6.3 μM	0.1 M PBS (pH 7.0)	(Zhu et al. 2009)
MoS2/PEDOT	Ascorbic acid Dopamine Uric acid	DPV	5.83 μM 0.52 μM 0.95 μM	Human urine	(Li et al. 2016)
AuNPs	Glucose	Direct electrochemistry	2.4×10^{-2} M	Human blood sample	(Li et al. 2009)
AuNPs	H_2O_2	Direct electrochemistry	0.6 μM	0.1 M PBS (pH 6.0)	(Cao et al. 2008)

AuNPs	Brevetoxin B (BTX-2)	CV and DPV	1×10^{-11} g·mL^{-1}	0.1 M PBS (pH 6.8)	(Tang et al. 2011a)
AuNPs	H_2O_2	Direct electrochemistry	2.35×10^{-4} M	0.1 M PBS (pH 7.0)	(Xie et al. 2010)
PEDOT-modified Ni/Si	Ascorbic acid Dopamine Uric acid	DPV	10 μM 1.5 μM 2.7 μM	Human urine	(Yu et al. 2013)
AuNPs	Gene fragments isolated from Bacillus anthracis	QCM	3.5×10^2 CFU·mL^{-1}	0.3 M NaCl +10 mM 0.1 M PBS (pH 7.4)	(Hao et al. 2011b)
AuNPs/PtNPs	Alpha-fetoprotein	DPV	1.7×10^{-12} g·mL^{-1}	0.1 M PBS (pH 7.4)	(Su et al. 2011b)
AgNPs	Single-base mismatch AgNPs	EIS and DPV	CA GA GT TT	0.15 M PBS (pH 5.5)	(Mehrgardi and Ahangar 2011)
Au/RGO	Ascorbic acid Dopamine Uric acid	DPV	51 μM 1.4 μM 1.8 μM	Serum samples	(Wang et al. 2014)
AgNPs	IgG	DPV	4×10^{-10} g·mL^{-1}	0.1 M PBS (pH 7.4)	(Hao et al. 2011a)
AuNPs	Burkitt's lymphoma cells	ASV and ECL	67 cells/mL	Not reported	(Ding et al. 2010)
AuNPs	IL-6	CV and EIS	3.3×10^{-14} g·mL^{-1}	Not reported	(Zhang et al. 2011a)
Au@Pd-RGO	Ascorbic acid Dopamine Uric acid	DPV	0.28 μM 0.024 μM 0.02 μM	Urine samples	(Jiang and Du 2014)
AuNPs	Cancer-associated glycosylation	DPV	7.0×10^3 cells/mL	Not reported	(Zhang et al. 2010c)
AuNPs	Hepatitis B	CV and DPV	4×10^{-11} g·mL^{-1}	0.1 M acetate buffer solution (pH 5.5)	(Qiu et al. 2011)

(continued)

Table 15.1 (continued)

Type of Metal	Analyte	Technique	LOD	Medium	Ref.
AuNPs	HeLa cervix cancer cells	CV	5×10^2 cells/mL	0.1 M PBS (pH 7.4)	(Zhang et al. 2010b)
AuNPs	CA-125	CV and DPV	1×10^{-10} g·mL^{-1}	Not reported	(Das and Kelley 2011)
PtNPs	Alpha-fetoprotein	ECL	3.3×10^{-12} g·mL^{-1}	Not reported	(Cao et al. 2011)
AuNPs/ AgNPs	DNA hybridization	ASV	1×10^{-16} M	Not reported	(Bai et al. 2010)
AuNPs/ PdNPs	Evaluation of DNA damage and antioxidant activity of sericin	CV	0.05 ~ 0.90 g·L^{-1}	Acetate buffer (pH 4.7) + 1.0×10^{-2} M NaCl	(Qian et al. 2010)
AuNPs/PtNPs	H_2O_2	Direct electrochemistry	2.8 µM	0.1 M PBS (pH 6.0)	(Chen et al. 2011)
AuNPs	Glucose	Direct electrochemistry	1.3×10^{-3} M	0.1 M PBS (pH 7.0)	(Barbadillo et al. 2009)
Au-NP/(MWCNTs/IL/G)	Ascorbic acid Dopamine Uric acid	DPV	0.12 µM 0.03 µM 0.03 µM	Human serum and urine	(Afraz et al. 2014)
AuNPs	Glucose	Direct electrochemistry	20 µM	0.1 M PBS (pH 6.5)	(Gu et al. 2010)

NiCo-NPs-in-N	Ascorbic acid Dopamine Uric acid	DPV	0.091 μM 0.080 μM 0.014 μM	Human urine	(Zhang et al. 2015)
AuNPs	H_2O_2	Direct electrochemistry	0.1 μM	0.1 M PBS (pH 7.4)	(Wang et al. 2011c)
AuNCs/PDA	Ascorbic acid Dopamine Uric acid	CV DPV	Not reported	Not reported	(Palanisamy 2014)
Ni/sG	Ascorbic acid Dopamine Uric acid	DPV	30 μM 0.12 μM 0.46 μM	Human serum Urine	(Nancy and Kumary 2014)

Abbreviations: *AgNP* silver nanoparticle, *AuNPs* gold nanoparticles, *PtNPs* platinum nanoparticles, *PdNPs* palladium nanoparticles, *DPV* differential pulse voltammetry, *AdSDPV* adsorptive stripping differential pulse voltammetry, *LSV* linear sweep voltammetry, *CV* cyclic voltammetry, *CA* chronoamperommetry, *EIS* electrochemical impedance spectroscopy, *CV* cyclic voltammetry, *ECL* electrochemiluminescence, *QCM* quartz crystal microbalance, *LOD* limit of detection, *SNP* single nucleotide polymorphism, *IL-6* interleukin-6, MoS_2 molybdenum disulfide, *CS* chitosan, *PDA* polydopamine, *IL* ionic liquid, *G* graphene, *DPA* dipicolinic acid, *PPy* polypyrrole, *CuNPs* copper nanoparticles, *SWCNT* single-walled carbon nanotubes, *MWCNT* multi-walled carbon nanotubes, *AuNW* gold nanowire, *ZnS* zinc sulfide, *PdAgNFs* palladium silver nanofibers, *BCG* bromocresol green, *CTAB* cetrimonium bromide, *PBS* phosphate buffer solution

redispersible, and reusable as catalysts (Poliakoff et al. 2002; Dhakshinamoorthy and Garcia 2012). Due to the excellent results of this property, the use of metal nanoparticles as catalysts has increased in recent years.

In areas where nanotechnology is used, it is known that functionalization, efficiency, quality increase, and harmful products decrease. For example, in the textile industry, the production of self-cleaning, non-flammable fabrics and the synthesis of antibacterial, water-repellent products can be achieved with nanotechnology. In addition, photovoltaic batteries, anti-stain smart fabrics, nano-particle paint, biocompatible implants, magnetic memory, and nanotube fuel cells are new-generation products produced with nanotechnology.

In the field of health, nanotechnology has benefits such as carrying medicines, eliminating physical damage with the nanorobots produced, repairing heart damage, and diagnosing diseases easily and quickly. Nanotechnology is also used in drug development (Sowa et al. 2005; Li et al. 2010d).

In the field of electronics, organic transistors are useful in the production of fabrics that can generate electricity. In terms of the environment, nanotechnology is used in the production of protective paints in cars and in removing organic and inorganic pollution.

One of the most popular areas where nanotechnology is used is energy. In order to meet current energy needs, it is necessary to find new renewable energy sources. Solar energy has an important place among renewable energy sources. It is of great importance that solar energy can be used and stored. Nanotechnology is used in solar cells, fuel cells, and energy storage.

5 Conclusion

Nanoclusters are similar to nanoparticles, whose features are similar to the properties of molecules and are therefore said to fill the gap between nanoparticles and atoms. They have advantageous features that are completely different from their bulk forms. In this chapter, metal nanoclusters have been presented for the clinical diagnosis of important compounds or biomarkers. Electrochemical methods have been used to develop sensors because of their unique features such as easy usage, fast response, small volume of solutions, sensitive responses, easy modification processes, no need for pretreatment steps, and inexpensive equipment. Metal nanoclusters, especially gold nanomaterials, have been preferred because of their unique physical, mechanical, optical, and chemical properties. According to developing technology and equipment, clinical studies need lab on a chip system to easy processes for patients and specialists in the hospital, so that diagnosis of diseases such as cancer and cardiovascular disease can be determined at early stages.

References

Abad JM, Gass M, Bleloch A, Schiffrin DJ (2009) Direct electron transfer to a metalloenzyme redox center coordinated to a monolayer-protected cluster. J Am Chem Soc 131:10229–10236. https://doi.org/10.1021/ja9026693

Abbas Rafati A, Afraz A, Hajian A, Assari P (2014) Simultaneous determination of ascorbic acid, dopamine, and uric acid using a carbon paste electrode modified with multiwalled carbon nanotubes, ionic liquid, and palladium nanoparticles. Microchim Acta. https://doi.org/10.1007/s00604-014-1293-7

Abdelwahab AA, Shim YB (2015) Simultaneous determination of ascorbic acid, dopamine, uric acid and folic acid based on activated graphene/MWCNT nanocomposite loaded Au nanoclusters. Sensors Actuators B Chem 221:659–665. https://doi.org/10.1016/j.snb.2015.07.016

Afraz A, Rafati AA, Najafi M (2014) Optimization of modified carbon paste electrode with multiwalled carbon nanotube/ionic liquid/cauliflower-like gold nanostructures for simultaneous determination of ascorbic acid, dopamine and uric acid. Mater Sci Eng C 44:58–68. https://doi.org/10.1016/j.msec.2014.07.065

Ahangar LE, Mehrgardi MA (2011) Nanoparticle-functionalized nucleic acids: a strategy for amplified electrochemical detection of some single-base mismatches. Electrochim Acta 56: 2725–2729. https://doi.org/10.1016/j.electacta.2010.12.051

Akhter H, Murshed J, Rashed MA et al (2017) Fabrication of hydrazine sensor based on silica-coated Fe2O3magnetic nanoparticles prepared by a rapid microwave irradiation method. J Alloys Compd 698:921–929. https://doi.org/10.1016/j.jallcom.2016.12.266

An Y, Tang L, Jiang X et al (2010) A photoelectrochemical immunosensor based on Au-doped TiO_2 nanotube arrays for the detection of α-Synuclein. Chem – A Eur J 16:14439–14446. https://doi.org/10.1002/chem.201001654

Anu Prathap MU, Srivastava R (2013) Tailoring properties of polyaniline for simultaneous determination of a quaternary mixture of ascorbic acid, dopamine, uric acid, and tryptophan. Sensors Actuators B Chem 177:239–250. https://doi.org/10.1016/j.snb.2012.10.138

Arvand M, Hemmati S (2017) Magnetic nanoparticles embedded with graphene quantum dots and multiwalled carbon nanotubes as a sensing platform for electrochemical detection of progesterone. Sensors Actuators B Chem 238:346–356. https://doi.org/10.1016/j.snb.2016.07.066

Astruc D (2020) Introduction: nanoparticles in catalysis. Chem Rev 120:461–463

Baghayeri M, Nodehi M, Amiri A et al (2020) Electrode designed with a nanocomposite film of CuO Honeycombs/Ag nanoparticles electrogenerated on a magnetic platform as an amperometric glucose sensor. Anal Chim Acta 1111:49–59. https://doi.org/10.1016/j.aca.2020.03.039

Bagheri H, Pajooheshpour N, Jamali B et al (2017) A novel electrochemical platform for sensitive and simultaneous determination of dopamine, uric acid and ascorbic acid based on Fe_3O_4[sbnd]SnO_2[sbnd]Gr ternary nanocomposite. Microchem J 131:120–129. https://doi.org/10.1016/j.microc.2016.12.006

Bai Y, Yang H, Yang W et al (2007) Gold nanoparticles-mesoporous silica composite used as an enzyme immobilization matrix for amperometric glucose biosensor construction. Sensors Actuators B Chem 124:179–186. https://doi.org/10.1016/j.snb.2006.12.020

Bai YH, Li JY, Xu JJ, Chen HY (2010) Ultrasensitive electrochemical detection of DNA hybridization using Au/Fe_3O_4 magnetic composites combined with silver enhancement. Analyst 135: 1672–1679. https://doi.org/10.1039/b923847f

Barbadillo M, Casero E, Petit-Domínguez MD et al (2009) Gold nanoparticles-induced enhancement of the analytical response of an electrochemical biosensor based on an organic-inorganic hybrid composite material. Talanta 80:797–802. https://doi.org/10.1016/j.talanta.2009.07.064

Cai X, Weng S, Guo R et al (2016) Ratiometric electrochemical immunoassay based on internal reference value for reproducible and sensitive detection of tumor marker. Biosens Bioelectron 81:173–180. https://doi.org/10.1016/j.bios.2016.02.066

Cao W, Wei C, Hu J, Li Q (2008) Direct electrochemistry and electrocatalysis of myoglobin immobilized on gold nanoparticles/carbon nanotubes nanohybrid film. Electroanalysis 20: 1925–1931. https://doi.org/10.1002/elan.200804272

Cao Y, Yuan R, Chai Y et al (2011) A solid-state electrochemiluminescence immunosensor based on MWCNTs-Nafion and Ru(bpy)32+/Nano-Pt nanocomposites for detection of α-fetoprotein. Electroanalysis 23:1418–1426. https://doi.org/10.1002/elan.201000611

Cathcart N, Kitaev V (2010) Silver nanoclusters: single-stage scaleable synthesis of monodisperse species and their chirooptical properties. J Phys Chem C . American Chemical Society 114: 16010–16017

Chai Y, Tian D, Wang W, Cui H (2010) A novel electrochemiluminescence strategy for ultrasensitive DNA assay using luminol functionalized gold nanoparticles multi-labeling and amplification of gold nanoparticles and biotin-streptavidin system. Chem Commun 46:7560–7562. https://doi.org/10.1039/c0cc02356f

Chandra P, Singh J, Singh A et al (2013) Gold nanoparticles and nanocomposites in clinical diagnostics using electrochemical methods. J Nanopart 2013:1–12. https://doi.org/10.1155/2013/535901

Chang H, Zhang H, Lv J et al (2016) Pt NPs and DNAzyme functionalized polymer nanospheres as triple signal amplification strategy for highly sensitive electrochemical immunosensor of tumour marker. Biosens Bioelectron 86:156–163. https://doi.org/10.1016/j.bios.2016.06.048

Chen W, Chen S (2009) Oxygen electroreduction catalyzed by gold nanoclusters: strong core size effects. Angew Chemie 121:4450–4453. https://doi.org/10.1002/ange.200901185

Chen S, Fu P, Yin B et al (2011) Immobilizing Pt nanoparticles and chitosan hybrid film on polyaniline nanofibers membrane for an amperometric hydrogen peroxide biosensor. Bioprocess Biosyst Eng 34:711–719. https://doi.org/10.1007/s00449-011-0520-4

Chen LX, Zheng JN, Wang AJ et al (2015) Facile synthesis of porous bimetallic alloyed PdAg nanoflowers supported on reduced graphene oxide for simultaneous detection of ascorbic acid, dopamine, and uric acid. Analyst 140:3183–3192. https://doi.org/10.1039/c4an02200a

da Silva ETSG, Souto DEP, Barragan JTC et al (2017) Electrochemical biosensors in point-of-care devices: recent advances and future trends. ChemElectroChem 4:778–794

Das J, Kelley SO (2011) Protein detection using arrayed microsensor chips: tuning sensor footprint to achieve ultrasensitive readout of CA-125 in serum and whole blood. Anal Chem 83: 1167–1172. https://doi.org/10.1021/ac102917f

Das J, Yang H (2009) Enhancement of electrocatalytic activity of DNA-conjugated gold nanoparticles and its application to DNA detection. J Phys Chem C 113:6093–6099. https://doi.org/10.1021/jp809850f

Deng K, Li X, Huang H (2016) A glassy carbon electrode modified with a nickel(II) norcorrole complex and carbon nanotubes for simultaneous or individual determination of ascorbic acid, dopamine, and uric acid. Microchim Acta 183:2139–2145. https://doi.org/10.1007/s00604-016-1843-2

Dey RS, Raj CR (2010) Development of an amperometric cholesterol biosensor based on graphene-Pt nanoparticle hybrid material. J Phys Chem C 114:21427–21433. https://doi.org/10.1021/jp105895a

Dey RS, Raj CR (2014) Enzyme-integrated cholesterol biosensing scaffold based on in situ synthesized reduced graphene oxide and dendritic Pd nanostructure. Biosens Bioelectron 62: 357–364. https://doi.org/10.1016/j.bios.2014.06.063

Dhakshinamoorthy A, Garcia H (2012) Catalysis by metal nanoparticles embedded on metal–organic frameworks. Chem Soc Rev 41:5262–5284. https://doi.org/10.1039/c2cs35047e

Díez I, Ras RHA (2011) Fluorescent silver nanoclusters. Nanoscale 3:1963–1970

Ding C, Ge Y, Zhang S (2010) Electrochemical and electrochemiluminescence determination of cancer cells based on aptamers and magnetic beads. Chem – A Eur J 16:10707–10714. https://doi.org/10.1002/chem.201001173

Du M, Yang T, Jiao K (2010) Immobilization-free direct electrochemical detection for DNA specific sequences based on electrochemically converted gold nanoparticles/graphene composite film. J Mater Chem 20:9253–9260. https://doi.org/10.1039/c0jm01549k

Du Y, Guo S, Dong S, Wang E (2011) An integrated sensing system for detection of DNA using new parallel-motif DNA triplex system and graphene-mesoporous silica-gold nanoparticle hybrids. Biomaterials 32:8584–8592. https://doi.org/10.1016/j.biomaterials.2011.07.091

Dursun Z, Gelmez B (2010) Simultaneous determination of ascorbic acid, dopamine and uric acid at Pt nanoparticles decorated multiwall carbon nanotubes modified GCE. Electroanalysis 22: 1106–1114. https://doi.org/10.1002/elan.200900525

Feng J, Li Y, Li M et al (2017) A novel sandwich-type electrochemical immunosensor for PSA detection based on PtCu bimetallic hybrid (2D/2D) rGO/g-C_3N_4. Biosens Bioelectron 91: 441–448. https://doi.org/10.1016/j.bios.2016.12.070

Filik H, Avan AA, Aydar S (2016) Simultaneous detection of ascorbic acid, dopamine, uric acid and tryptophan with Azure A-interlinked multi-walled carbon nanotube/gold nanoparticles composite modified electrode. Arab J Chem 9:471–480. https://doi.org/10.1016/j.arabjc.2015.01.014

Florea A, Guo Z, Cristea C et al (2015) Anticancer drug detection using a highly sensitive molecularly imprinted electrochemical sensor based on an electropolymerized microporous metal organic framework. Talanta 138:71–76. https://doi.org/10.1016/J.TALANTA.2015.01.013

Fronzi M, Iwaszuk A, Lucid A, Nolan M (2016) Metal oxide nanocluster-modified TiO_2 as solar activated photocatalyst materials. J Phys Condens Matter 28:074006

Fu Y, Li P, Wang T et al (2010) Novel polymeric bionanocomposites with catalytic Pt nanoparticles label immobilized for high performance amperometric immunoassay. Biosens Bioelectron 25: 1699–1704. https://doi.org/10.1016/j.bios.2009.12.010

German N, Ramanavicius A, Voronovic J, Ramanaviciene A (2012) Glucose biosensor based on glucose oxidase and gold nanoparticles of different sizes covered by polypyrrole layer. Colloids Surf A Physicochem Eng Asp 413:224–230. https://doi.org/10.1016/j.colsurfa.2012.02.012

Ghanbari K, Hajheidari N (2015) Simultaneous electrochemical determination of dopamine, uric acid and ascorbic acid using silver nanoparticles deposited on polypyrrole nanofibers. J Polym Res 22:1–9. https://doi.org/10.1007/s10965-015-0797-0

Giri AK, Charan C, Saha A et al (2014) An amperometric cholesterol biosensor with excellent sensitivity and limit of detection based on an enzyme-immobilized microtubular ZnO@ZnS heterostructure. J Mater Chem A 2:16997–17004. https://doi.org/10.1039/c4ta03627a

Gu M, Wang J, Tu Y, Di J (2010) Fabrication of reagentless glucose biosensors: a comparison of mono-enzyme GOD and bienzyme GOD-HRP systems. Sensors Actuators B Chem 148: 486–491. https://doi.org/10.1016/j.snb.2010.05.057

Han X, Zhu Y, Yang X, Li C (2010) Amperometric glucose biosensor based on platinum nanoparticle encapsulated with a clay. Microchim Acta 171:233–239. https://doi.org/10.1007/s00604-010-0424-z

Hao N, Li H, Long Y et al (2011a) An electrochemical immunosensing method based on silver nanoparticles. J Electroanal Chem 656:50–54. https://doi.org/10.1016/j.jelechem.2011.01.029

Hao R-Z, Song H-B, Zuo G-M et al (2011b) DNA probe functionalized QCM biosensor based on gold nanoparticle amplification for Bacillus anthracis detection. Biosens Bioelectron 26: 3398–3404. https://doi.org/10.1016/j.bios.2011.01.010

He C, Xie M, Hong F et al (2016) A highly sensitive glucose biosensor based on gold nanoparticles/ bovine serum albumin/Fe3O4 biocomposite nanoparticles. Electrochim Acta 222:1709–1715. https://doi.org/10.1016/j.electacta.2016.11.162

Huang Y, Wang T-H, Jiang J-H et al (2009) Prostate specific antigen detection using microgapped electrode array immunosensor with enzymatic silver deposition. Clin Chem 55:964–971. https://doi.org/10.1373/clinchem.2008.116582

Huang KJ, Sun JY, Jin CX et al (2011) Direct electrochemistry and electrocatalytic behavior of hemoglobin entrapped in chitosan/gold colloid/3-aminopropyl triethylene silane/Prussian blue composite film. Thin Solid Films 519:3925–3930. https://doi.org/10.1016/j.tsf.2011.01.342

Ingram RS, Hostetler MJ, Murray RW et al (1997) 28 kDa alkanethiolate-protected Au clusters give analogous solution electrochemistry and STM coulomb staircases. J Am Chem Soc 119: 9279–9280. https://doi.org/10.1021/ja972319y

Jeevanandam J, Barhoum A, Chan YS et al (2018) Review on nanoparticles and nanostructured materials: history, sources, toxicity and regulations. Beilstein J Nanotechnol 9:1050–1074

Jia S, Fei J, Tian T, Zhou F (2009) Reagentless biosensor for hydrogen peroxide based on the immobilization of hemoglobin in platinum nanoparticles enhanced poly(chloromethyl thiirane) cross-linked chitosan hybrid film. Electroanalysis 21:1424–1431. https://doi.org/10.1002/elan.200804531

Jiang J, Du X (2014) Sensitive electrochemical sensors for simultaneous determination of ascorbic acid, dopamine, and uric acid based on Au@Pd-reduced graphene oxide nanocomposites. Nanoscale 6:11303–11309. https://doi.org/10.1039/c4nr01774a

Jin R (2010) Quantum sized, thiolate-protected gold nanoclusters. Nanoscale 2:343–362

Jin R, Zeng C, Zhou M, Chen Y (2016) Atomically precise colloidal metal nanoclusters and nanoparticles: fundamentals and opportunities. Chem Rev 116:10346–10413

Kaur B, Pandiyan T, Satpati B, Srivastava R (2013) Simultaneous and sensitive determination of ascorbic acid, dopamine, uric acid, and tryptophan with silver nanoparticles-decorated reduced graphene oxide modified electrode. Colloids Surf B Biointerfaces 111:97–106. https://doi.org/10.1016/j.colsurfb.2013.05.023

Khan II, Saeed K, Khan II (2019) Nanoparticles: properties, applications and toxicities. Arab J Chem 12:908–931

Khudaish EA, Al-Ajmi KY, Al-Harthi SH (2014) A solid-state sensor based on ruthenium (II) complex immobilized on polytyramine film for the simultaneous determination of dopamine, ascorbic acid and uric acid. Thin Solid Films 564:390–396. https://doi.org/10.1016/j.tsf.2014.05.056

Komathi S, Muthuchamy N, Lee KP, Gopalan AI (2016) Fabrication of a novel dual mode cholesterol biosensor using titanium dioxide nanowire bridged 3D graphene nanostacks. Biosens Bioelectron 84:64–71. https://doi.org/10.1016/j.bios.2015.11.042

Kumar S, Lei Y, Alshareef NH et al (2018) Biofunctionalized two-dimensional Ti_3C_2 MXenes for ultrasensitive detection of cancer biomarker. Biosens Bioelectron 121:243–249. https://doi.org/10.1016/j.bios.2018.08.076

Lai G, Wu J, Ju H, Yan F (2011) Streptavidin-functionalized silver-nanoparticle-enriched carbon nanotube tag for ultrasensitive multiplexed detection of tumor markers. Adv Funct Mater 21: 2938–2943. https://doi.org/10.1002/adfm.201100396

Lee CY, Wu LP, Chou TT, Hsieh YZ (2018) Functional magnetic nanoparticles–assisted electrochemical biosensor for eosinophil cationic protein in cell culture. Sensors Actuators B Chem 257:672–677. https://doi.org/10.1016/j.snb.2017.11.033

Li F, Song J, Li F et al (2009) Direct electrochemistry of glucose oxidase and biosensing for glucose based on carbon nanotubes@SnO_2-Au composite. Biosens Bioelectron 25:883–888. https://doi.org/10.1016/j.bios.2009.08.044

Li F, Feng Y, Wang Z et al (2010a) Direct electrochemistry of horseradish peroxidase immobilized on the layered calcium carbonate-gold nanoparticles inorganic hybrid composite. Biosens Bioelectron 25:2244–2248. https://doi.org/10.1016/j.bios.2010.03.006

Li H, Sun Z, Zhong W et al (2010b) Ultrasensitive electrochemical detection for DNA arrays based on silver nanoparticle aggregates. Anal Chem 82:5477–5483. https://doi.org/10.1021/ac101193e

Li J, Yuan R, Chai Y, Che X (2010c) Fabrication of a novel glucose biosensor based on Pt nanoparticles- decorated iron oxide-multiwall carbon nanotubes magnetic composite. J Mol Catal B Enzym 66:8–14

Li Z, Huang P, Lin J et al (2010d) Arginine-glycine-aspartic acid-conjugated dendrimer-modified quantum dots for targeting and imaging melanoma. J Nanosci Nanotechnol 10:4859–4867

Li J, Yuan R, Chai Y (2011) Simple construction of an enzymatic glucose biosensor based on a nanocomposite film prepared in one step from iron oxide, gold nanoparticles, and chitosan. Microchim Acta 173:369–374. https://doi.org/10.1007/s00604-011-0544-0

Li M, Guo W, Li H et al (2014) Electrochemical biosensor based on one-dimensional MgO nanostructures for the simultaneous determination of ascorbic acid, dopamine, and uric acid. Sensors Actuators B Chem 204:629–636. https://doi.org/10.1016/j.snb.2014.08.022

Li SM, Wang YS, Hsiao ST et al (2015) Fabrication of a silver nanowire-reduced graphene oxide-based electrochemical biosensor and its enhanced sensitivity in the simultaneous determination of ascorbic acid, dopamine, and uric acid. J Mater Chem C 3:9444–9453. https://doi.org/10.1039/c5tc01564b

Li Y, Lin H, Peng H et al (2016) A glassy carbon electrode modified with MoS_2 nanosheets and poly (3,4-ethylenedioxythiophene) for simultaneous electrochemical detection of ascorbic acid, dopamine and uric acid. Microchim Acta 183:2517–2523. https://doi.org/10.1007/s00604-016-1897-1

Liang A, Tang B, Hou HP et al (2019a) A novel $CuFe_2O_4$ nanospheres molecularly imprinted polymers modified electrochemical sensor for lysozyme determination. J Electroanal Chem 853: 113465. https://doi.org/10.1016/j.jelechem.2019.113465

Liang H, Xu H, Zhao Y et al (2019b) Ultrasensitive electrochemical sensor for prostate specific antigen detection with a phosphorene platform and magnetic covalent organic framework signal amplifier. Biosens Bioelectron 144. https://doi.org/10.1016/j.bios.2019.111691

Lin J, He C, Zhang L, Zhang S (2009) Sensitive amperometric immunosensor for α-fetoprotein based on carbon nanotube/gold nanoparticle doped chitosan film. Anal Biochem 384:130–135. https://doi.org/10.1016/j.ab.2008.09.033

Liu Y, Wu S, Ju H, Xu L (2007) Amperometric glucose biosensing of gold nanoparticles and carbon nanotube multilayer membranes. Electroanalysis 19:986–992. https://doi.org/10.1002/elan.200603814

Liu S, Wu P, Li W et al (2011a) Ultrasensitive and selective electrochemical identification of hepatitis C virus genotype 1b based on specific endonuclease combined with gold nanoparticles signal amplification. Anal Chem 83:4752–4758. https://doi.org/10.1021/ac200624f

Liu Y, Han T, Chen C et al (2011b) A novel platform of hemoglobin on core-shell structurally Fe_3O_4@Au nanoparticles and its direct electrochemistry. Electrochim Acta 56:3238–3247. https://doi.org/10.1016/j.electacta.2011.01.037

Liu J, Xie Y, Wang K et al (2017) A nanocomposite consisting of carbon nanotubes and gold nanoparticles in an amphiphilic copolymer for voltammetric determination of dopamine, paracetamol and uric acid. Microchim Acta 184:1739–1745. https://doi.org/10.1007/s00604-017-2185-4

Lu C, Shen Q, Zhao X et al (2010) Ag nanoparticles self-supported on Ag_2V_4O 11 nanobelts: novel nanocomposite for direct electron transfer of hemoglobin and detection of H_2O_2. Sensors Actuators B Chem 150:200–205. https://doi.org/10.1016/j.snb.2010.07.016

Luo XL, Xu JJ, Du Y, Chen HY (2004) A glucose biosensor based on chitosan-glucose oxidase-gold nanoparticles biocomposite formed by one-step electrodeposition. Anal Biochem 334: 284–289. https://doi.org/10.1016/j.ab.2004.07.005

Ma H, Li X, Yan T et al (2016) Electrochemiluminescent immunosensing of prostate-specific antigen based on silver nanoparticles-doped Pb (II) metal-organic framework. Biosens Bioelectron 79:379–385. https://doi.org/10.1016/j.bios.2015.12.080

Magner E (1998) Trends in electrochemical biosensors. Analyst. Royal Society of Chemistry 123: 1967–1970

Mani V, Chikkaveeraiah BV, Patel V et al (2009) Ultrasensitive immunosensor for cancer biomarker proteins using gold nanoparticle film electrodes and multienzyme-particle amplification. ACS Nano 3:585–594. https://doi.org/10.1021/nn800863w

Mehrgardi MA, Ahangar LE (2011) Silver nanoparticles as redox reporters for the amplified electrochemical detection of the single base mismatches. Biosens Bioelectron 26:4308–4313. https://doi.org/10.1016/j.bios.2011.04.020

Monošik R, Stred'anský M, Šturdík E (2012) Application of electrochemical biosensors in clinical diagnosis. J Clin Lab Anal 26:22–34. https://doi.org/10.1002/jcla.20500

Munge BS, Krause CE, Malhotra R et al (2009) Electrochemical immunosensors for interleukin-6. Comparison of carbon nanotube forest and gold nanoparticle platforms. Electrochem Commun 11:1009–1012. https://doi.org/10.1016/j.elecom.2009.02.044

Murray RW (2008) Nanoelectrochemistry: metal nanoparticles, nanoelectrodes, and nanopores. Chem Rev 108:2688–2720

Mwilu SK, Aluoch AO, Miller S et al (2009) Identification and quantitation of Bacillus globigii using metal enhanced electrochemical detection and capillary biosensor. Anal Chem 81: 7561–7570. https://doi.org/10.1021/ac900834e

Nancy TEM, Kumary VA (2014) Synergistic electrocatalytic effect of graphene/nickel hydroxide composite for the simultaneous electrochemical determination of ascorbic acid, dopamine and uric acid. Electrochim Acta 133:233–240. https://doi.org/10.1016/j.electacta.2014.04.027

Noroozifar M, Khorasani-Motlagh M, Akbari R, Bemanadi Parizi M (2011) Simultaneous and sensitive determination of a quaternary mixture of AA, DA, UA and Trp using a modified GCE by iron ion-doped natrolite zeolite-multiwall carbon nanotube. Biosens Bioelectron 28:56–63. https://doi.org/10.1016/j.bios.2011.06.042

Ognjanović M, Stanković DM, Ming Y et al (2019) Bifunctional (Zn, Fe)3O4 nanoparticles: tuning their efficiency for potential application in reagentless glucose biosensors and magnetic hyperthermia. J Alloys Compd 777:454–462. https://doi.org/10.1016/j.jallcom.2018.10.369

Omidfar K, Zarei H, Gholizadeh F, Larijani B (2012) A high-sensitivity electrochemical immunosensor based on mobile crystalline material-41-polyvinyl alcohol nanocomposite and colloidal gold nanoparticles. Anal Biochem 421:649–656. https://doi.org/10.1016/j.ab.2011.12.022

Pakapongpan S, Poo-arporn RP (2017) Self-assembly of glucose oxidase on reduced graphene oxide-magnetic nanoparticles nanocomposite-based direct electrochemistry for reagentless glucose biosensor. Mater Sci Eng C 76:398–405. https://doi.org/10.1016/J.MSEC.2017.03.031

Palanisamy S (2014) Polydopamine supported gold nanoclusters for sensitive and simultaneous detection of dopamine in the presence of excess ascorbic acid and uric acid. Electrochim Acta 138:302–310. https://doi.org/10.1016/j.electacta.2014.06.131

Pang X, He D, Luo S, Cai Q (2009) An amperometric glucose biosensor fabricated with Pt nanoparticle-decorated carbon nanotubes/TiO_2 nanotube arrays composite. Sensors Actuators B Chem 137:134–138. https://doi.org/10.1016/j.snb.2008.09.051

Poliakoff M, Fitzpatrick JM, Farren TR, Anastas PT (2002) Green chemistry: science and politics of change. Science (80-) 297:807–810

Qian P, Ai S, Yin H, Li J (2010) Evaluation of DNA damage and antioxidant capacity of sericin by a DNA electrochemical biosensor based on dendrimer-encapsulated Au-Pd/chitosan composite. Microchim Acta 168:347–354. https://doi.org/10.1007/s00604-009-0280-x

Qiu JD, Huang H, Liang RP (2011) Biocompatible and label-free amperometric immunosensor for hepatitis B surface antigen using a sensing film composed of poly(allylamine)-branched ferrocene and gold nanoparticles. Microchim Acta 174:97–105. https://doi.org/10.1007/s00604-011-0585-4

Qu F, Lu H, Yang M, Deng C (2011) Electrochemical immunosensor based on electron transfer mediated by graphene oxide initiated silver enhancement. Biosens Bioelectron 26:4810–4814. https://doi.org/10.1016/j.bios.2011.06.018

Ramakrishnan S, Pradeep KR, Raghul A et al (2015) One-step synthesis of Pt-decorated graphene-carbon nanotubes for the electrochemical sensing of dopamine, uric acid and ascorbic acid. Anal Methods 7:779–786. https://doi.org/10.1039/c4ay02487g

Ran G, Chen X, Xia Y (2017) Electrochemical detection of serotonin based on a poly(bromocresol green) film and Fe_3O_4 nanoparticles in a chitosan matrix. RSC Adv 7:1847–1851. https://doi.org/10.1039/c6ra25639b

Rezaei B, Majidi N, Rahmani H, Khayamian T (2011) Electrochemical impedimetric immunosensor for insulin like growth factor-1 using specific monoclonal antibody-nanogold modified electrode. Biosens Bioelectron 26:2130–2134. https://doi.org/10.1016/j.bios.2010.09.020

Samadi Pakchin P, Fathi M, Ghanbari H et al (2020) A novel electrochemical immunosensor for ultrasensitive detection of CA125 in ovarian cancer. Biosens Bioelectron 153:112029. https://doi.org/10.1016/j.bios.2020.112029

Sanaeifar N, Rabiee M, Abdolrahim M et al (2017) A novel electrochemical biosensor based on Fe_3O_4 nanoparticles-polyvinyl alcohol composite for sensitive detection of glucose. Anal Biochem 519:19–26. https://doi.org/10.1016/j.ab.2016.12.006

Santiago González B, Rodríguez MJ, Blanco C et al (2010) One step synthesis of the smallest photoluminescent and paramagnetic PVP-protected gold atomic clusters. Nano Lett 10:4217–4221. https://doi.org/10.1021/nl1026716

Sayhi M, Ouerghi O, Belgacem K et al (2018) Electrochemical detection of influenza virus H_9N_2 based on both immunomagnetic extraction and gold catalysis using an immobilization-free screen printed carbon microelectrode. Biosens Bioelectron 107:170–177. https://doi.org/10.1016/j.bios.2018.02.018

Shan C, Yang H, Han D et al (2010) Graphene/AuNPs/chitosan nanocomposites film for glucose biosensing. Biosens Bioelectron 25:1070–1074. https://doi.org/10.1016/j.bios.2009.09.024

Sharafeldin M, Bishop GW, Bhakta S et al (2017) Fe_3O_4 nanoparticles on graphene oxide sheets for isolation and ultrasensitive amperometric detection of cancer biomarker proteins. Biosens Bioelectron 91:359–366. https://doi.org/10.1016/j.bios.2016.12.052

Sharma D, Lee J, Seo J, Shin H (2017) Development of a sensitive electrochemical enzymatic reaction-based cholesterol biosensor using Nano-sized carbon interdigitated electrodes decorated with gold nanoparticles. Sensors (Switzerland) 17:2128. https://doi.org/10.3390/s17092128

Shen G, Zhang Y (2010) Highly sensitive electrochemical stripping detection of hepatitis B surface antigen based on copper-enhanced gold nanoparticle tags and magnetic nanoparticles. Anal Chim Acta 674:27–31. https://doi.org/10.1016/j.aca.2010.06.007

Shruthi CD, Venkataramanappa Y, Suresh GS (2018) Reduced MWCNTs/palladium nanotubes hybrid fabricated on graphite electrode for simultaneous detection of ascorbic acid, dopamine and uric acid. J Electrochem Soc 165:B458–B465. https://doi.org/10.1149/2.1161810jes

Sowa B, Rauw G, Davood A et al (2005) Design and biological evaluation of phenyl-substituted analogs of β-phenylethylidenehydrazine. Bioorganic Med Chem 13:4389–4395. https://doi.org/10.1016/j.bmc.2005.04.072

Su B, Tang D, Li Q et al (2011a) Gold–silver–graphene hybrid nanosheets-based sensors for sensitive amperometric immunoassay of alpha-fetoprotein using nanogold-enclosed titania nanoparticles as labels. Anal Chim Acta 692:116–124. https://doi.org/10.1016/j.aca.2011.02.061

Su H, Yuan R, Chai Y et al (2011b) Ferrocenemonocarboxylic-HRP@Pt nanoparticles labeled RCA for multiple amplification of electro-immunosensing. Biosens Bioelectron 26:4601–4604. https://doi.org/10.1016/j.bios.2011.04.043

Sun H, Chao J, Zuo X et al (2014) Gold nanoparticle-decorated MoS2 nanosheets for simultaneous detection of ascorbic acid, dopamine and uric acid. RSC Adv 4:27625–27629. https://doi.org/10.1039/c4ra04046e

Sun B, Gou Y, Ma Y et al (2017) Investigate electrochemical immunosensor of cortisol based on gold nanoparticles/magnetic functionalized reduced graphene oxide. Biosens Bioelectron 88:55–62. https://doi.org/10.1016/j.bios.2016.07.047

Tang D, Tang J, Su B, Chen G (2011a) Gold nanoparticles-decorated amine-terminated poly (amidoamine) dendrimer for sensitive electrochemical immunoassay of brevetoxins in food samples. Biosens Bioelectron 26:2090–2096. https://doi.org/10.1016/j.bios.2010.09.012

Tang J, Tang D, Su B et al (2011b) Enzyme-free electrochemical immunoassay with catalytic reduction of p-nitrophenol and recycling of p-aminophenol using gold nanoparticles-coated carbon nanotubes as nanocatalysts. Biosens Bioelectron 26:3219–3226. https://doi.org/10.1016/j.bios.2010.12.029

Tao Y, Li M, Ren J, Qu X (2015) Metal nanoclusters: novel probes for diagnostic and therapeutic applications. Chem Soc Rev 44:8636–8663. https://doi.org/10.1039/C5CS00607D

Tian L, Qian K, Qi J et al (2018) Gold nanoparticles superlattices assembly for electrochemical biosensor detection of micro RNA-21. Biosens Bioelectron 99:564–570. https://doi.org/10.1016/j.bios.2017.08.035

Tong C, Shi B, Xiao X et al (2009) An Annexin V-based biosensor for quantitatively detecting early apoptotic cells. Biosens Bioelectron 24:1777–1782. https://doi.org/10.1016/j.bios.2008.07.040

Vc S, Berchmans S (2016) Flower like Bi structures on Pt surface facilitating effective cholesterol biosensing. Mater Sci Eng C 64:183–189. https://doi.org/10.1016/j.msec.2016.03.075

Veera Manohara Reddy Y, Sravani B, Agarwal S et al (2018) Electrochemical sensor for detection of uric acid in the presence of ascorbic acid and dopamine using the poly(DPA)/$SiO_2@Fe_3O_4$ modified carbon paste electrode. J Electroanal Chem 820:168–175. https://doi.org/10.1016/j.jelechem.2018.04.059

Villalonga R, Díez P, Yáñez-Sedeño P, Pingarrón JM (2011) Wiring horseradish peroxidase on gold nanoparticles-based nanostructured polymeric network for the construction of mediatorless hydrogen peroxide biosensor. Electrochim Acta 56:4672–4677. https://doi.org/10.1016/j.electacta.2011.02.108

Wang J (2001) Glucose biosensors: 40 years of advances and challenges – Wang – 2001 – Electroanalysis – Wiley Online Library. In: Electroanalysis. https://analyticalsciencejournals.onlinelibrary.wiley.com/doi/abs/10.1002/1521-4109(200108)13:12%3C983::AID-ELAN983%3E3.0.CO;2-%23?casa_token=bhm8MJx6KzUAAAAA%3A1VACsKf-Hx8e_yIZCDlZdl6uwdpO8hY9K2YrNAJTmzP6JIQnewC4_b3bx_WDSv2H0z7xLI6qpEKnXgdV. Accessed 12 May 2021

Wang J (2008) Electrochemical glucose biosensors. Chem Rev 108:814–825

Wang A, Ye X, He P, Fang Y (2007) A new technique for chemical deposition of Pt nanoparticles and its applications on biosensor design. Electroanalysis 19:1603–1608. https://doi.org/10.1002/elan.200703890

Wang Y, Chen X, Zhu JJ (2009a) Fabrication of a novel hydrogen peroxide biosensor based on the AuNPs-C@SiO2 composite. Electrochem Commun 11:323–326. https://doi.org/10.1016/j.elecom.2008.11.056

Wang Y, Ma X, Wen Y et al (2009b) Electrochemistry and electrocatalytic properties of mixed assemblies of horseradish peroxidase, poly(diallyl dimethylammonium chloride) and gold nanoparticles on a glassy carbon electrode. Microchim Acta 166:283–288. https://doi.org/10.1007/s00604-009-0202-y

Wang C, Yuan R, Chai Y et al (2011a) Au-nanoclusters incorporated 3-amino-5-mercapto-1,2,4-triazole film modified electrode for the simultaneous determination of ascorbic acid, dopamine, uric acid and nitrite. Biosens Bioelectron 30:315–319. https://doi.org/10.1016/j.bios.2011.08.035

Wang Q, Yang L, Yang X et al (2011b) Electrochemical biosensors for detection of point mutation based on surface ligation reaction and oligonucleotides modified gold nanoparticles. Anal Chim Acta 688:163–167. https://doi.org/10.1016/j.aca.2011.01.004

Wang W, Zhang T-J, Zhang D-W et al (2011c) Amperometric hydrogen peroxide biosensor based on the immobilization of heme proteins on gold nanoparticles–bacteria cellulose nanofibers nanocomposite. Talanta 84:71–77. https://doi.org/10.1016/j.talanta.2010.12.015

Wang C, Yuan R, Chai Y et al (2012) Non-covalent iron(III)-porphyrin functionalized multi-walled carbon nanotubes for the simultaneous determination of ascorbic acid, dopamine, uric acid and nitrite. Electrochim Acta 62:109–115. https://doi.org/10.1016/j.electacta.2011.11.115

Wang C, Ye F, Wu H, Qian Y (2013a) Depositing Au nanoparticles onto graphene sheets for simultaneous electrochemical detection ascorbic acid, dopamine and uric acid. Int J Electrochem Sci 8:2440–2448

Wang X, Wu M, Tang W et al (2013b) Simultaneous electrochemical determination of ascorbic acid, dopamine and uric acid using a palladium nanoparticle/graphene/chitosan modified electrode. J Electroanal Chem 695:10–16. https://doi.org/10.1016/j.jelechem.2013.02.021

Wang C, Du J, Wang H et al (2014) A facile electrochemical sensor based on reduced graphene oxide and Au nanoplates modified glassy carbon electrode for simultaneous detection of ascorbic acid, dopamine and uric acid. Sensors Actuators B Chem 204:302–309. https://doi.org/10.1016/j.snb.2014.07.077

Wang C, Zou X, Zhao X et al (2015a) Cu-nanoparticles incorporated overoxidized-poly(3-amino-5-mercapto-1,2,4-triazole) film modified electrode for the simultaneous determination of ascorbic acid, dopamine, uric acid and tryptophan. J Electroanal Chem 741:36–41. https://doi.org/10.1016/j.jelechem.2015.01.014

Wang S, Zhang W, Zhong X et al (2015b) Simultaneous determination of dopamine, ascorbic acid and uric acid using a multi-walled carbon nanotube and reduced graphene oxide hybrid functionalized by PAMAM and Au nanoparticles. Anal Methods 7:1471–1477. https://doi.org/10.1039/c4ay02086c

Wang T, Du K, Liu W et al (2015c) Electrochemical sensors based on molybdenum disulfide nanomaterials. Electroanalysis 27:2091–2097

WHO | World Health Organization. https://www.who.int/. Accessed 11 May 2021

Wong XY, Quesada-González D, Manickam S et al (2021) Integrating gold nanoclusters, folic acid and reduced graphene oxide for nanosensing of glutathione based on “turn-off” fluorescence. Sci Rep 111(11):1–12. https://doi.org/10.1038/s41598-021-81677-8

Wu BY, Hou SH, Yin F et al (2007) Amperometric glucose biosensor based on layer-by-layer assembly of multilayer films composed of chitosan, gold nanoparticles and glucose oxidase modified Pt electrode. Biosens Bioelectron 22:838–844. https://doi.org/10.1016/j.bios.2006.03.009

Wu X, Jiang H, Zheng J et al (2011) Highly sensitive recognition of cancer cells by electrochemical biosensor based on the interface of gold nanoparticles/polylactide nanocomposites. J Electroanal Chem 656:174–178. https://doi.org/10.1016/j.jelechem.2010.11.035

Wu D, Li Y, Zhang Y et al (2014) Sensitive electrochemical sensor for simultaneous determination of dopamine, ascorbic acid, and uric acid enhanced by amino-group functionalized mesoporous Fe_3O_4@Graphene sheets. Electrochim Acta 116:244–249. https://doi.org/10.1016/j.electacta.2013.11.033

Xian Y, Hu Y, Liu F et al (2006) Glucose biosensor based on Au nanoparticles-conductive polyaniline nanocomposite. Biosens Bioelectron. Elsevier 21:1996–2000

Xiang C, Zou Y, Sun LX, Xu F (2009) Direct electrochemistry and enhanced electrocatalysis of horseradish peroxidase based on flowerlike ZnO-gold nanoparticle-Nafion nanocomposite. Sensors Actuators B Chem 136:158–162. https://doi.org/10.1016/j.snb.2008.10.058

Xie W, Kong L, Kan M et al (2010) Introduction of gold nanoparticles into myoglobin-nafion film for direct electrochemistry application. J Nanosci Nanotechnol 10:6720–6724. https://doi.org/10.1166/jnn.2010.2544

Xie YL, Yuan J, Ye HL et al (2015) Facile ultrasonic synthesis of graphene/SnO_2 nanocomposite and its application to the simultaneous electrochemical determination of dopamine, ascorbic acid, and uric acid. J Electroanal Chem 749:26–30. https://doi.org/10.1016/j.jelechem.2015.04.035

Xing L, Ma Z (2016) A glassy carbon electrode modified with a nanocomposite consisting of MoS_2 and reduced graphene oxide for electrochemical simultaneous determination of ascorbic acid, dopamine, and uric acid. Microchim Acta 183:257–263. https://doi.org/10.1007/s00604-015-1648-8

Xu H, Suslick KS (2010) Sonochemical synthesis of highly fluorescent Ag nanoclusters. ACS Nano 4:3209–3214. https://doi.org/10.1021/nn100987k

Xu L, Hou Y, Zhang M et al (2015) Electrochemical sensor based on a silver nanowires modified electrode for the determination of cholesterol. Anal Methods 7:5649–5653. https://doi.org/10.1039/c5ay01164g

Yan J, Liu S, Zhang Z et al (2013) Simultaneous electrochemical detection of ascorbic acid, dopamine and uric acid based on graphene anchored with Pd-Pt nanoparticles. Colloids Surf B Biointerfaces 111:392–397. https://doi.org/10.1016/j.colsurfb.2013.06.030

Yan S, Li X, Xiong Y et al (2016) Simultaneous determination of ascorbic acid, dopamine and uric acid using a glassy carbon electrode modified with the nickel(II)-bis(1,10-phenanthroline) complex and single-walled carbon nanotubes. Microchim Acta 183:1401–1408. https://doi.org/10.1007/s00604-016-1776-9

Yang YJ (2015) One-pot synthesis of reduced graphene oxide/zinc sulfide nanocomposite at room temperature for simultaneous determination of ascorbic acid, dopamine and uric acid. Sensors Actuators B Chem 221:750–759. https://doi.org/10.1016/j.snb.2015.06.150

Yang J, Lee H, Cho M et al (2012) Nonenzymatic cholesterol sensor based on spontaneous deposition of platinum nanoparticles on layer-by-layer assembled CNT thin film. Sensors Actuators B Chem 171–172:374–379. https://doi.org/10.1016/j.snb.2012.04.070

Yang P, Pang J, Hu F et al (2018) An ultrasensitive biosensing flexible chip using a novel silver@Prussian blue core-shell nanocube composite. Sensors Actuators B Chem 276:31–41. https://doi.org/10.1016/j.snb.2018.08.070

Yang Q, Li N, Li Q et al (2019) Amperometric sarcosine biosensor based on hollow magnetic Pt–Fe3O4@C nanospheres. Anal Chim Acta 1078:161–167. https://doi.org/10.1016/j.aca.2019.06.031

Ye Y, Mao S, He S et al (2020) Ultrasensitive electrochemical genosensor for detection of CaMV35S gene with Fe_3O_4-Au@Ag nanoprobe. Talanta 206:120205. https://doi.org/10.1016/j.talanta.2019.120205

Yoon J, Lee SN, Shin MK et al (2019) Flexible electrochemical glucose biosensor based on GOx/gold/MoS_2/gold nanofilm on the polymer electrode. Biosens Bioelectron 140:111343. https://doi.org/10.1016/j.bios.2019.111343

Yu S, Luo C, Wang L et al (2013) Poly(3,4-ethylenedioxythiophene)-modified Ni/silicon micro-channel plate electrode for the simultaneous determination of ascorbic acid, dopamine and uric acid. Analyst 138:1149–1155. https://doi.org/10.1039/c2an36335f

Yuan YR, Yuan R, Chai YQ et al (2009) Electrochemical amperometric immunoassay for carcinoembryonic antigen based on bi-layer nano-Au and nickel hexacyanoferrates nanoparticles modified glassy carbon electrode. J Electroanal Chem 626:6–13. https://doi.org/10.1016/j.jelechem.2008.10.031

Zhang J, Ting BP, Jana NR et al (2009a) Ultrasensitive electrochemical dna biosensors based on the detection of a highly characteristic solid-state process. Small 5:1414–1417. https://doi.org/10.1002/smll.200900073

Zhang X, Geng P, Liu H et al (2009b) Development of an electrochemical immunoassay for rapid detection of E. coli using anodic stripping voltammetry based on Cu@Au nanoparticles as antibody labels. Biosens Bioelectron 24:2155–2159. https://doi.org/10.1016/j.bios.2008.11.019

Zhang Y, Zhang K, Ma H (2009c) Electrochemical DNA biosensor based on silver nanoparticles/poly(3-(3-pyridyl) acrylic acid)/carbon nanotubes modified electrode. Anal Biochem 387:13–19. https://doi.org/10.1016/j.ab.2008.10.043

Zhang J, Ting BP, Khan M et al (2010a) Pt nanoparticle label-mediated deposition of Pt catalyst for ultrasensitive electrochemical immunosensors. Biosens Bioelectron 26:418–423. https://doi.org/10.1016/j.bios.2010.07.112

Zhang JJ, Cheng FF, Zheng TT, Zhu JJ (2010b) Design and implementation of electrochemical cytosensor for evaluation of cell surface carbohydrate and glycoprotein. Anal Chem 82:3547–3555. https://doi.org/10.1021/ac9026127

Zhang X, Teng Y, Fu Y et al (2010c) Lectin-based biosensor strategy for electrochemical assay of glycan expression on living cancer cells. Anal Chem 82:9455–9460. https://doi.org/10.1021/ac102132p

Zhang Y, Yuan R, Chai Y et al (2010d) An amperometric hydrogen peroxide biosensor based on the immobilization of HRP on multi-walled carbon nanotubes/electro-copolymerized nano-Pt-poly(neutral red) composite membrane. Biochem Eng J 51:102–109. https://doi.org/10.1016/j.bej.2010.06.001

Zhang JJ, Liu Y, Hu LH et al (2011a) "Proof-of-principle" concept for ultrasensitive detection of cytokines based on the electrically heated carbon paste electrode. Chem Commun 47: 6551–6553. https://doi.org/10.1039/c1cc11565k

Zhang Z, Xie Y, Liu Z et al (2011b) Covalently immobilized biosensor based on gold nanoparticles modified TiO2 nanotube arrays. J Electroanal Chem 650:241–247. https://doi.org/10.1016/j.jelechem.2010.10.016

Zhang W, Yuan R, Chai YQ et al (2012) A simple strategy based on lanthanum-multiwalled carbon nanotube nanocomposites for simultaneous determination of ascorbic acid, dopamine, uric acid and nitrite. Sensors Actuators B Chem 166–167:601–607. https://doi.org/10.1016/j.snb.2012.03.018

Zhang Y, Ren W, Zhang S (2013) Simultaneous determination of epinephrine, dopamine, ascorbic acid and uric acid by polydopamine-nanogold composites modified electrode. Int J Electrochem Sci 8:6839–6850

Zhang X, Yan W, Zhang J et al (2015) NiCo-embedded in hierarchically structured N-doped carbon nanoplates for the efficient electrochemical determination of ascorbic acid, dopamine, and uric acid. RSC Adv 5:65532–65539. https://doi.org/10.1039/c5ra10937j

Zhang H, Ma L, Li P, Zheng J (2016) A novel electrochemical immunosensor based on non-enzymatic Ag@Au-Fe_3O_4 nanoelectrocatalyst for protein biomarker detection. Biosens Bioelectron 85:343–350. https://doi.org/10.1016/j.bios.2016.04.100

Zhang Q, Yang M, Zhu Y, Mao C (2017) Metallic nanoclusters for cancer imaging and therapy. Curr Med Chem 25:1379–1396. https://doi.org/10.2174/0929867324666170331122757

Zhang P, Yang S, Pineda-Gómez R et al (2019) Electrochemically exfoliated high-quality 2H-MoS_2 for multiflake thin film flexible biosensors. Small 15:1901265. https://doi.org/10.1002/smll.201901265

Zhao D, Fan D, Wang J, Xu C (2015a) Hierarchical nanoporous platinum-copper alloy for simultaneous electrochemical determination of ascorbic acid, dopamine, and uric acid. Microchim Acta. https://doi.org/10.1007/s00604-015-1450-7

Zhao L, Li H, Gao S et al (2015b) MgO nanobelt-modified graphene-tantalum wire electrode for the simultaneous determination of ascorbic acid, dopamine and uric acid. Electrochim Acta 168: 191–198. https://doi.org/10.1016/j.electacta.2015.03.215

Zhao Q, Faraj Y, Liu LY et al (2020a) Simultaneous determination of dopamine, uric acid and estriol in maternal urine samples based on the synergetic effect of reduced graphene oxide, silver nanowires and silver nanoparticles in their ternary 3D nanocomposite. Microchem J 158: 105185. https://doi.org/10.1016/J.MICROC.2020.105185

Zhao Y, Liu H, Shi L et al (2020b) Electroactive Cu_2O nanoparticles and Ag nanoparticles driven ratiometric electrochemical aptasensor for prostate specific antigen detection. Sensors Actuators B Chem 315:128155. https://doi.org/10.1016/j.snb.2020.128155

Zhong Z, Wu W, Wang D et al (2010) Nanogold-enwrapped graphene nanocomposites as trace labels for sensitivity enhancement of electrochemical immunosensors in clinical immunoassays: carcinoembryonic antigen as a model. Biosens Bioelectron 25:2379–2383. https://doi.org/10.1016/j.bios.2010.03.009

Zhou F, Lu M, Wang W et al (2010a) Electrochemical immunosensor for simultaneous detection of dual cardiac markers based on a poly(dimethylsiloxane)-gold nanoparticles composite microfluidic chip: a proof of principle. Clin Chem 56:1701–1707. https://doi.org/10.1373/clinchem.2010.147256

Zhou K, Zhu Y, Yang X et al (2010b) A novel hydrogen peroxide biosensor based on Au-graphene-HRP-chitosan biocomposites. Electrochim Acta 55:3055–3060. https://doi.org/10.1016/j.electacta.2010.01.035

Zhou H, Ran G, Masson JF et al (2018) Rational design of magnetic micronanoelectrodes for recognition and ultrasensitive quantification of cysteine enantiomers. Anal Chem 90: 3374–3381. https://doi.org/10.1021/acs.analchem.7b05006

Zhu A, Tian Y, Liu H, Luo Y (2009) Nanoporous gold film encapsulating cytochrome c for the fabrication of a H_2O_2 biosensor. Biomaterials 30:3183–3188. https://doi.org/10.1016/j.biomaterials.2009.02.019

Zhu Y, Son JI, Shim Y-B (2010) Amplification strategy based on gold nanoparticle-decorated carbon nanotubes for neomycin immunosensors. Biosens Bioelectron 26:1002–1008. https://doi.org/10.1016/J.BIOS.2010.08.023

Zhu W, Xu L, Zhu C et al (2016) Magnetically controlled electrochemical sensing membrane based on multifunctional molecularly imprinted polymers for detection of insulin. Electrochim Acta 218:91–100. https://doi.org/10.1016/j.electacta.2016.09.108

Zhu Q, Bao J, Huo D et al (2017) 3D graphene hydrogel – gold nanoparticles nanocomposite modified glassy carbon electrode for the simultaneous determination of ascorbic acid, dopamine and uric acid. Sensors Actuators B Chem 238:1316–1323. https://doi.org/10.1016/j.snb.2016.09.116

Zhuo Y, Chai YQ, Yuan R et al (2011) Glucose oxidase and ferrocene labels immobilized at Au/TiO2 nanocomposites with high load amount and activity for sensitive immunoelectrochemical measurement of ProGRP biomarker. Biosens Bioelectron 26:3838–3844. https://doi.org/10.1016/j.bios.2011.02.043

Electrochemical Sensing and Biosensing-Based on Carbon Nanodots

16

Alyah Buzid and John H. T. Luong

Contents

1 Introduction 340
2 Hydrogen Peroxide (H_2O_2) and Glucose (GLC) Sensing 342
3 Detection of Organic Compounds 343
4 Metal Ion Sensing 350
5 Aptasensing and Immunosensing 352
6 Trends and Conclusions 356
References 358

Abstract

Carbon quantum dots (CQDs) or simply carbon nanodots (CNDs) represent emerging materials in the form of nanocarbon, which have been advocated for diversified applications. Different top-down and bottom-up procedures are applicable to synthesize inexpensive 2-D nanomaterials. Based on their superconductivity and rapid electron transfer, CNDs with diameters below 10 nm form nanocomposites with metal nanoparticles, carbon graphene/nanotubes, and conducting polymers with enhanced catalytic activity and electrical conductivity. The surface of CNDs with abundant reactive groups facilitates bioconjugation with recognition biomolecules or the preparation of complex catalysts with enhanced charge transfer. CNDs can be doped with N, S, or P, which acts as reactive catalytic sites for electrocatalysis. Such distinct features are attributed to the fabrication of reliable biosensing platforms to target important analytes encompassing simple biomolecules, metal ions, proteins, and macromolecules.

A. Buzid
Department of Chemistry, College of Science, King Faisal University, Al-Ahsa, Saudi Arabia

J. H. T. Luong (✉)
Innovative Chromatography Group, Irish Separation Science Cluster (ISSC), School of Chemistry and Analytical & Biological Chemistry Research Facility (ABCRF), University College Cork, Cork, Ireland
e-mail: j.luong@ucc.ie

© Springer Nature Singapore Pte Ltd. 2023

U. P. Azad, P. Chandra (eds.), *Handbook of Nanobioelectrochemistry*,
https://doi.org/10.1007/978-981-19-9437-1_16

This chapter also unravels technical issues and potential uses of CNDs in electroanalysis toward developing ideal devices with low cost, high detection sensitivity, and selectivity.

Keywords

Carbon nanodots · Graphene quantum dots · Electrochemical sensing · Biosensing · Synthesis · Applications

1 Introduction

Carbon nanodots (CNDs) comprising carbon dots (CNDs) or (ii) graphene quantum dots (GQDs) with strong fluorescence characteristics have attracted interest in a plethora of applications. Besides their low toxicity, biocompatibility, and high aqueous solubility, they exhibit superior π-π conjugation structure, chemical inertness, and high electrical conductivity (Lim et al. 2015b). Such quasi-spherical nanoparticles can be nanocrystalline or amorphous with sp^2/sp^3 carbon clusters and sizes below 10 nm (Song-Ling et al. 2017), whereas GQDs resemble nanosheets of graphene with less than 100 nm and a mix of sp^2 and sp^3 carbon (Ponomarenko et al. 2008). Carbon dots can be graphitic carbon quantum dots, polymer dots, or amorphous carbon dots. In comparison to organic dyes or conventional semiconductor quantum dots, photoluminescent CNDs exhibit high resistance to photobleaching and facile modification. To date, diversified procedures have been developed for the synthesis of CNDs (Table 16.1) (Anwar et al. 2019; Deng et al. 2014; Doñate-Buendia et al. 2018; Shen et al. 2018; Thoda et al. 2018; Xu et al. 2004; Zhang et al. 2017). Detailed information on the synthesis of CNDs and doped CNDs has been well documented (Lu and Yang 2017; Mosconi et al. 2015; Naik et al. 2019; Wu et al. 2017; Ngo et al. 2020), whereas electrochemiluminescence (ECL) applications of CNDs were also reviewed (Namdari et al. 2017; Hassanvand et al. 2021; Ngo et al. 2020; Ji et al. 2020; Molaei 2020).

To date, multifunctional CNDs have been advocated for applications in nanomedicine, antimicrobials, bioimaging, solar cells, chemical/biosensing sensing, etc. Besides their well-characterized optical properties such as absorbance (Li et al. 2018a), photoluminescence (Yuan et al. 2018), and electroluminescence (Hasan et al. 2018), CNDs exhibit sufficient active reaction sites and good electric conductivity. Thus, hybrid materials based on CND have been applied to the electrocatalytic hydrogen evolution reaction (HER) (Tian et al. 2019). CNDs with nitrogen or oxygen functional groups are stable in organic solvents and water. For instance, a nanocomposite of CNDs with graphene nanoribbons serves as catalysts for the oxygen reduction reaction (ORR) (Jin et al. 2015). The abundant -OH, -COOH, and $-NH_2$ on the surface of CNDs serve as the coordination sites with transition metal ions. Thus, the adsorption of heavy metals is improved by CNDs via electrostatic interaction. CNDs also form stable complexes with unmodified oligonucleotides via non-covalent interactions owing to the richness of the hydrophobic plane

Table 16.1 Synthesis of CNDs by top-down and bottom-up methods

Methods of synthesis	General procedures and key points	Ref.
Top-down		
Laser ablation	A laser pulse with high energy is applied to blast the surface of the target to a thermodynamic state. Nanoparticles (NPs) with a narrow size distribution are formed. Albeit this is a high-cost operation, fluorescent NPs are highly water-soluble	(Doñate-Buendia et al. 2018)
Arc discharge	A sealed reactor with an anodic electrode driven by gas plasma (up to 4000 K), carbon atoms are decomposed from the bulk carbon substrates. The carbon vapor assembles on the cathode to form CNDs with Nanoparticles have good water solubility but possess a large particle size distribution.	(Xu et al. 2004)
Acid hydrolysis	Acids (HNO_3, H_2SO_4, $NaClO_3$, etc.) can exfoliate and decompose bulk carbon into nanoparticles with hydroxyl or carboxyl groups. A hydrothermal reduction step follows the acid treatment. The method is inexpensive and amenable to scale-up production.	(Zhang et al. 2017)
Bottom-up		
Microwave pyrolysis	Microwave pyrolysis of a mixture of organic molecules and simple sugars. This approach is simple and fast for synthesizing CNDs with high oxygen-containing groups.	(Shen et al. 2018)
Hydrothermal/ Solvothermal	Under a relatively high temperature, an aqueous or solvent solution of small organic molecules and/or polymers tends to form carbon-seeding cores and becomes CNDs. The method is suitable for the synthesis of doped CNDs.	(Anwar et al. 2019)
Combustion/ Thermal	Combustion of an organic acid, followed by functionalization with acetic acid under high temperature. CNDs are uniform with high carboxyl groups.	(Thoda et al. 2018)
Electrochemical	Electrochemical carbonization of an aqueous solution of sodium citrate and urea. NPs have an average diameter of 2.4 nm.	(Deng et al. 2014)

and hydrophilic edges. Consequently, CNDs are considered low cost electrode materials compared to noble metals. Considering more active catalytic reaction sites delivered by CNDs, nanocomposites stemming from CNDs exhibit enhanced electronic conductivity and charge transfer during the electrocatalytic process.

The electrical conductivity of CNDs has been confirmed using ferro/ferricyanide as the redox couple (Lim et al. 2015a). Therefore, CNDs have been used for the modification of electrode materials or together with other metallic nanoparticles, carbon nanotubes, graphene, etc. for a plethora of electroanalysis. Beyond the hydrogen/oxygen evolution reduction as well as oxygen/CO_2 reduction reaction, this chapter extends the prospective applications of CNDs and GQDs in the electroanalysis of important analytes in analytical and clinical chemistry. The potential uses of CNDs in immunosensing and aptasensing platforms are also reported.

2 Hydrogen Peroxide (H_2O_2) and Glucose (GLC) Sensing

H_2O_2 is an important compound that is often used as an oxidant in the industrial process, and high H_2O_2 levels may be dangerous for humans. Therefore, accurate determination of H_2O_2 is of most importance (Su et al. 2018). H_2O_2 can be measured by different approaches, including electrochemical sensors based on enzymes, e.g., horseradish peroxidase (HRP), or proteins (hemoglobin and myoglobin). Despite being sensitive and specific for H_2O_2 detection, they are expensive and have a limited lifetime (Saleh Ahammad 2013). Electrochemical sensors based on carbon nanomaterials, metal, and metal oxides have been used for H_2O_2 detection. In this context, CNDs have been described as enzyme-free or enzymeless sensing of H_2O_2 as they mimic enzyme activity (Mollarasouli et al. 2017). A nanostructure-sensing film modified glassy carbon electrode (GCE) is fabricated from GQDs functionalized chitosan (CS) (GQDs-CS) for the covalent attachment of methylene blue (MB) to an amino hydroxyl group of GCE. The synergistic effect between GQDs-CS and MB enables a significant activity for H_2O_2 reduction. The fabricated sensor hinders the potential interference of endogenous species such as dopamine, uric and ascorbic acids, caffeine, glucose, and inorganic salts (Mollarasouli et al. 2017). Selective electroanalysis of dopamine could be feasible when a cyclodextrin derivative is deposited on the electrode (Shang et al. 2009).

Of interest is a novel biosensor constructed from rGO QDs (reduced graphene oxide quantum dots) and zinc oxide (ZnO) by a nanofiber (NFs) template. The sensor is applicable for detecting intercellular H_2O_2 released from normal cells (BPH-1) and cancerous prostate cells (PC-3) after treatment with anticancer drugs. The amount detected of H_2O_2 is ~320 ± 12 and 210 ± 6 amoles per cell for PC-3 cancer cells and BPH-1 non-cancer cells, respectively, evincing the effective role of the rGO QDs/ZnO for detecting H_2O_2 (Yang et al. 2015).

Silver nanoparticles (AgNPs) can be implanted on the CND surface by ultraviolet (UV) irradiation. The AgNPs-CND_S are simply dropping cast on the GCE to prepare the H_2O_2 sensor. With a 80 nM ($S/N = 3$) as a limit of detection, the sensor can detect H_2O_2 in purified bovine serum samples (Jahanbakhshi and Habibi 2016). A GCE modified with CND-MWCNT (multiwalled carbon nanotubes) nanocomposite exhibits significant electrocatalytic activity for the reduction of H_2O_2 compared to CNDs or MWCNTs (Bai et al. 2016). Of note is the design of an electrochemical biosensor for H_2O_2 by immobilizing HRP using CNDs and CoFe layered double hydroxy composites (CNDs/LDHs) on a GCE (Wang et al. 2015b). The HRP/CND/LDHs/GCE shows good electrocatalytic reduction activity toward H_2O_2.

Blood glucose (GLC) plays a major role in human health. Various techniques with electrochemical approaches have been developed as GLC sensors. Glucose oxidase (GOx) is commonly applied for catalyzing GLC and subsequently producing a response current, which can be linked to the GLC concentration (Hrapovic et al. 2004). A high-performance GLC sensor is fabricated by introducing GQDs as a novel substrate to immobilize GOx on a carbon-ceramic electrode (CCE) (Razmi and Mohammad-Rezaei 2013). The enzyme adheres firmly to the large surface area of highly porous GQDs with abundant hydrophobic planes and hydrophilic edges, (Razmi and Mohammad-Rezaei 2013). A gold microdisk array electrode is modified by gold nanoparticles (AuNPs) and carbon quantum dots (CQDs), followed by the immobilization of GOx on the active surface area. Based on chronoamperometry, the GOx/CQDs-AuNPs/Au microdisk array electrode exhibits 13 times increase in sensitivity over the planar electrode (Buk and Pemble 2019).

A novel nanostructured electrocatalyst of CQDs and octahedral-cuprous oxide (Cu_2O) is exploited for the determination of GLC and H_2O_2 (Li et al. 2015). The enzymeless approach, CQDs/Cu_2O/GCE, shows preferable electrolysis to the GLC oxidation and H_2O_2 reduction compared to the Cu_2O/GCE. Nitrogen-doped CNDs (N-CNDs) can be synthesized from polyacrylamide, mixed with CS, and drop-cast on a GCE, followed by the immobilization of GOx on the electrode surface by the amino-carboxyl reaction (Ji et al. 2016). The performances of CNDs and GQDs based sensors for H_2O_2 and GLC detection are brief in Table 16.2.

3 Detection of Organic Compounds

The importance of detecting organic compounds encompassing nicotinamide adenine dinucleotide (NADH), uric acid (UA), dopamine (DA), and ascorbic acid (AA) is due to their vital significance. The electrochemical approaches can be utilized for the determination of vitamins, amino acids, drugs, explosives, and chemical pollutants because of their simplicity, low cost, and high sensitivity. The electrode modification by CNDs could effectively enhance the interaction between the electrochemically active surface area and electroactive substances, i.e., the rate of electrochemical reaction as reflected by the signal response can be augmented by CNDs.

Abnormalities of DA levels are linked to several neurological illnesses; therefore, the determination of DA is critical in clinical chemistry (Hu et al. 2014). A DA sensor is fabricated from rGO and a CND composite film. Electrostatic interaction between the amine functional group of DA and carboxylic groups of CNDs enhances the specific detection of DA. Electron communication and the interaction between DA and rGO are governed by the π-π stacking force (Hu et al. 2014). The rGO-CNDs/GCE shows a high response contrasted to a bare GCE, GO/GCE, or CNDs/GCE. An N-CQD modified GCE can be used for detection. The sensor exhibits excellent performance with broad linearity and a low LOD for DA detection (Jiang et al. 2015). In this context, another sensor for DA is based on a Cu_2O-CNDs/Nafion film (Cu_2O-CNDs/NF) (Huang et al. 2015). The electrode conductivity is enhanced by Cu_2O nanoparticles, while the carboxylic groups of CNDs and sulfo groups of NF attract DA via electrostatic interaction but exclude AA and UA, The Cu_2O-CNDs/NF/GCE detects successfully DA in human serum with high selectivity.

A GCE can be modified with layers of ferrocene@β-cyclodextrin (Fc@β-CD) and N-CNDs for selective detection of UA (Zhang et al. 2014). A novel approach for chiral separation of D-AA and L-AA is achieved using electropolymerized molecularly imprinted (MI) polyaniline ferrocene sulfonic acid (PANI-FSA) on a CND

Table 16.2 Analytical performances of CNDs-based sensors for H_2O_2 and GLC detection

Fabricated electrode	Analyte	Linear range	(LOD) Limit of detection	Method	Reference
GQDs-CS/MB/GCE	H_2O_2	1–11.78 × 10^{-3} μM	0.7 μM	Amperometry	(Mollarasouli et al. 2017)
rGO QDs/ZnO NFs/ITO	H_2O_2	1–22.48 μM	0.025 μM	Amperometry	(Yang et al. 2015)
AgNPs/CNDs/GCE	H_2O_2	0.2–27 μM	80 nM	Amperometry	(Jahanbakhshi and Habibi 2016)
CNDs/MWCNTs	H_2O_2	3.5–30 × 10^{-3} μM	0.25 μM	Amperometry	(Bai et al. 2016)
HRP/CNDs/LDHs/GCE	H_2O_2	0.1–23.1 μM	40 nM	Amperometry	(Wang et al. 2015b)
GOx-GQDs/GCE	GLC	5–1270 μM	1.73 μM	Amperometry	(Razmi and Mohammad-Rezaei 2013)
GOx/CQDs-AuNPs/Au microdisk array electrode	GLC	0.16–4.32 mM	13.6 μM	Chronoamperometry	(Buk and Pemble 2019)
CQDs/Cu_2O/GCE	GLC	0.02–4.3 mM	8.4 μM	Amperometry	(Li et al. 2015)
GOx/N-CNDs/GCE	GLC	1–12 mM	0.25 mM	CV (cyclic voltammetry)	(Ji et al. 2016)

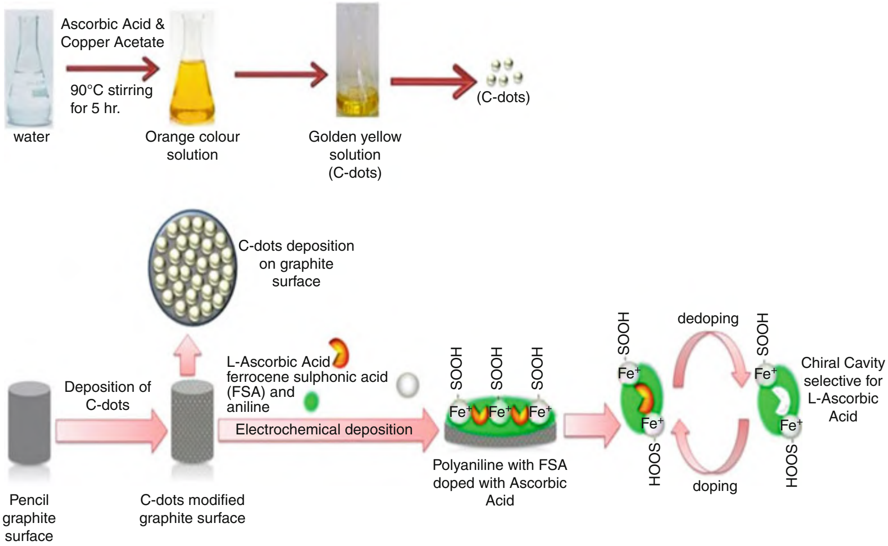
Ascorbic Acid &
Copper Acetate
90°C stirring
for 5 hr.
water
Orange colour
solution
Golden yellow
solution
(C-dots)
(C-dots)
C-dots deposition
on graphite
surface
Deposition of
C-dots
L-Ascorbic Acid
ferrocene sulphonic acid
(FSA) and
aniline
Electrochemical deposition
SOOH
Fe+
Polyaniline with FSA
doped with Ascorbic
Acid
dedoping
doping
Chiral Cavity
selective for
L-Ascorbic
Acid
HOOS
Pencil
graphite
surface
C-dots modified
graphite surface

Fig. 16.1 The fabrication of MI-PANI-FSA/CND/PGE electrode (Pandey and Jha 2015). (Reproduced with permission from Ref. (Pandey and Jha 2015) Copyright (2015) Elsevier)

modified pencil graphite electrode. The developed sensor can be successfully applied to human plasma samples and pharmaceuticals for determining L-AA (Fig. 16.1) (Pandey and Jha 2015). CNDs are synthesized by ultrasonic methods using glucose as a carbon source. The CND modified GCE electrode (CNDs/GCE) simultaneously detects DA, L-tryptophan (TRP), UA, and theophylline (TP). The CNDs/GCE shows a strong anti-interference effect and good stability (Wang et al. 2021).

Creatinine is produced in the body by creatinine metabolism and then filtered by the kidney. Abnormal levels of creatinine are linked to chronic kidney disease and hypothyroidism, thus the accurate measurement of creatinine is of clinical importance. A sensor for creatinine is based on CNDs doped on tungstic anhydride (WO_3), which are embedded on a GO-modified GCE. This sensing approach detects creatinine in blood and urine samples without any interference (Ponnaiah and Prakash 2020). Of interest is the electrochemical detecting of NADH by a screen-printed electrode (SPE) modified with hybrid magnetic nanoparticles-CQDs (Fig. 16.2) (Canevari et al. 2017).

As a nonessential amino acid, hydrophilic L-cysteine (L-Cys) has been considered an antitoxin antioxidant and cancer biomarker in biological systems. Electrochemical methods are one of the most desired approaches used for the analysis of amino acids, including L-Cys (Hou et al. 2015). Polypyrrole (PPy), a conducting polymer, and GQDs@Prussian blue (PB) are grafted on graphite felt for electroanalysis of L-Cys (Wang et al. 2016). GQDs are simply immobilized on GF ultrasonically, followed by the adsorption of PB. The PPy film is then electropolymerized to enhance the electrochemical stability of the fabricated electrode.

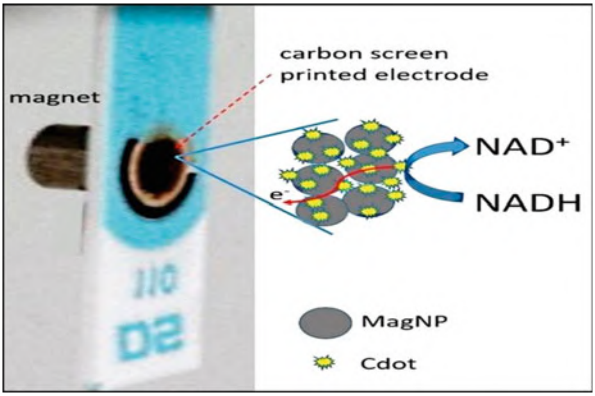

Fig. 16.2 Illustration of SPE with MgNPs-CQDs (Canevari et al. 2017). (Reproduced with permission from Ref. (Canevari et al. 2017) Copyright (2017) Wiley-VCH GmbH)

An enantio-recognition interface for the tryptophan (TRP) isomers has been achieved by GQDs incorporating into β-CD via hydrogen bonds between the oxygen-containing and hydroxyl groups on GQDs and β-CD, respectively. The resulting GQDs/β-CD could be electrodeposited on the GCE because of highly negative charges due to the carboxylic groups' ionization. The hydrophobic cavity of β-CD also plays an important role as a chiral interface for the TRP enantiomer measurement and separation (Fig. 16.3) (Ou et al. 2015).

Vitamin D_2 can be detected by an electrochemical biosensor platform using CNDs embedded in CS. A thin film of CNDs-CS is deposited on indium tin oxide (ITO) coated glass. Vitamin D_2 antibody (Ab-VD_2) and BSA are co-immobilized on CNDs-CS/ITO (Sarkar et al. 2018). A diversified range of electrochemical sensors for detecting organic compounds such as UA, AA, DA, creatinine, NADH, amino acids, and vitamins based on CNDs is presented in Table 16.3.

As mentioned above, the performance of drug characterization can be improved using CNDs due to their electrical property and sizable specific surface area. For instance, an electrochemical sensor for doxorubicin hydrochloride (DOX) is based on AgNPs, CNDs, and rGO electrodeposited on a GCE, without any reducing agents or toxic solvents (Fig. 16.4) (Guo et al. 2017). Electrocatalytic activities for DOX reduction are significantly affected by $Ag(NH_3)_2OH$ concentrations and become optimal when the volume ratio of CNDs-GO to $Ag(NH_3)_2OH$ is set at 1:1.

p-acetamidophenol can be detected by AuNPs/amino-acids functionalized GQDs. In brief, 20 amino acids-GQDs are prepared by a simple pyrolysis step of one amino acid and citric acid, which subsequently reacts with $HAuCl_4$ to form AuNPs/amino acid-GQDs. Among different amino acids-GQDs, the proline (Pro)-GQD scheme offers a fast reaction rate for the preparation of AuNPs/Pro-GQDs, resulting in high detection sensitivity for this analyte (Xiaoyan et al. 2016).

Mesalazine (MSA) is commonly utilized for treating bowel disease inflammation, e.g., ulcerative colitis and Crohn's illness (Bergman and Parkes 2006). Electrochemical sensing of MSA is realized by a CS-CNDs-hexadecyltrimethylammonium bromide (CTAB) modified GCE (CS/CNDs-CTAB/GCE). CTAB serves as an adsorbent due to its positive charge that effectively assembles with negative

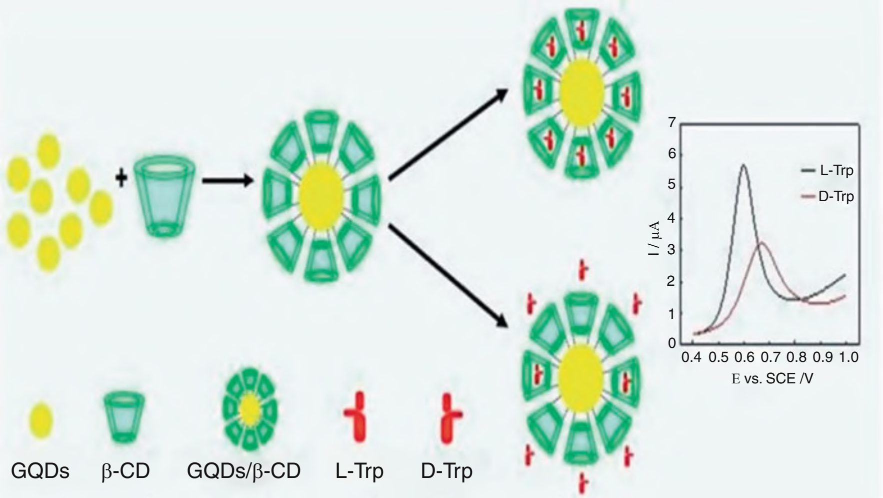

Fig. 16.3 The preparation of electrochemical chiral interface GQDs/β-CNDs and the application in the recognition of TRP isomers (Ou et al. 2015). (Reproduced with permission from Ref. (Ou et al. 2015) Copyright (2015) Elsevier)

Table 16.3 Various electrochemical sensors for detecting UA, AA, DA, creatinine, NADH, amino acids based on CNDs

Fabricated electrode	Analyte	Linear range	LOD	Technique	Ref.
rGO-CNDs/GCE	DA	10–450 × 10^{-3} nM	1.5 nM	DPV	(Hu et al. 2014)
NCQDs/GCE	DA	0–1 mM	1.1 nM	DPV	(Jiang et al. 2015)
Cu_2O-CNDs/NF/GCE	DA	0.05–45 μM	1.1 nM	DPV	(Huang et al. 2015)
Fc@β-CD/N-CNDs/GCE	UA	5–120 μM	0.08 μM	DPV	(Zhang et al. 2014)
MI-PANI-FSA/CNDs/PGE	L-AA	6–165 nM	0.001 nM	DPV	(Pandey and Jha 2015)
CNDs/WO_3@GO/GCE	Creatinine	0.2–112 nM	220 pM	DPV	(Wang et al. 2021)
MgNPs-CQDs/SPE	NADH	0.2–5 μM	20 nM	DPV	(Canevari et al. 2017)
PPy/GQDs@PB/GF	L-Cys	50–1000 μM	0.15 μM	Amperometry	(Wang et al. 2016)
BSA/Ab-VD_2/CNDs-CS/ITO	Vitamin D_2	10–50 ng/mL	1.35 ng/mL	DPV	(Sarkar et al. 2018)

CNDs. The CNDs-CTAB mixture is simply drop-cast on the GCE, followed by the addition of CS. This sensing approach can detect MSA in human blood serum (Jalali et al. 2020). The detection of lactose is feasible by β-galactosidase, crosslinked with

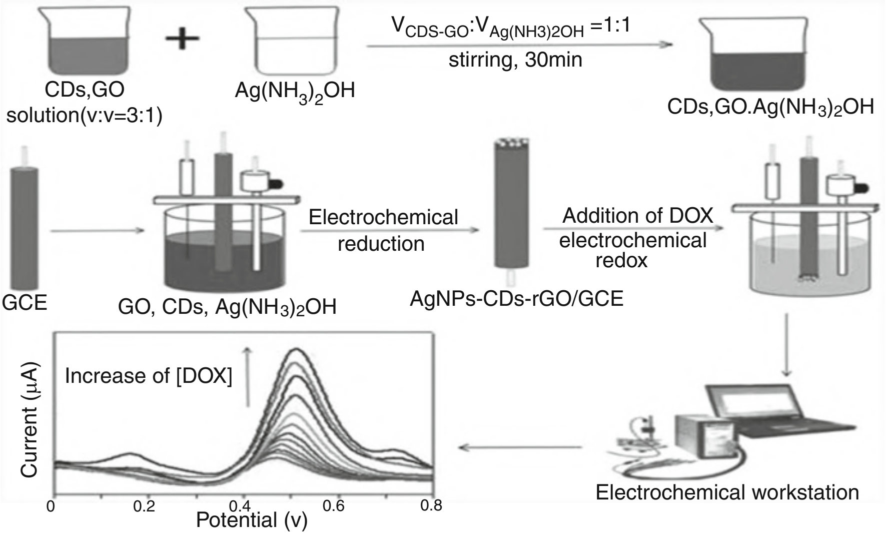
CDs,GO
solution(v:v=3:1)
+
Ag(NH3)2OH
VCDS-GO:VAg(NH3)2OH =1:1
stirring, 30min
CDs,GO.Ag(NH3)2OH
GCE
GO, CDs, Ag(NH3)2OH
Electrochemical reduction
AgNPs-CDs-rGO/GCE
Addition of DOX electrochemical redox
Electrochemical workstation
Current (µA)
Increase of [DOX]
Potential (v)
0
0.2
0.4
0.6
0.8

Fig. 16.4 The preparation of the developing electrochemical sensing AgNOs-CNDs-rGO/GCE and its application toward DOX detection (Guo et al. 2017). (Reproduced with permission from Ref.(Guo et al. 2017) Copyright (2017) Elsevier)

CNDs by 1-ethyl-1-3-(3-dimethylaminopropyl) carbodiimide (Sharma et al. 2019). The determination of pharmaceuticals and organic molecules by electrochemical sensing using CNDs is shown in Table 16.4.

Using a layer-by-layer (LBL) technique, NF/MWCNTs/CNDs/MWCNTs are fabricated for simultaneous analysis of catechol (CC), hydroquinone (HQ), and resorcinol (RS) (Wei et al. 2014). Electrostatic interaction between MWCNTs with an amido group and CNDs can be exploited to fabricate the electrode (Fig. 16.5). For catechol detection, a novel sensing approach is based on fluorine laccase and nitrogen co-doped CNDs (Lac/F, N-CNDs/GCE). F, N-CNDs are prepared by the hydrothermal carbonization procedure from *p*-phenylenediamine (p-PD) and 5-fluorouracil (5-Fu). The detecting enzyme, laccase, forms a complex with the as-synthesized F, N-CNDs and is deposited on the GCE. The sensor detects catechol in lake water, tap water, composite bioremediate, and seafood (Liu et al. 2019). A stable and sensitive sensor for capsaicin is attained using CNDs grafted onto ITO. CNDs are synthesized from iota-carrageenan via the hydrothermal method (Supchocksoonthorn et al. 2021). Carrageenan is a sulfated polysaccharide obtained from red seaweed (Eccles et al. 2015).

As one of the most dangerous and explosive chemicals, 2,4,6-trinitrotoluene (TNT) causes several diseases including hepatotoxicity and hemolysis as it affects the level of the hepatic enzyme (Rodgers and Bunce 2001). An electrochemical sensor for TNT detection is fabricated from N-CNDs. TNT with an electron-deficient nitro-aromatic ring interacts strongly with electron-rich amino groups of N-CNDs occurs (Zhang et al. 2015). *N*-nitrosamines are extremely toxic compounds observed in meat and foods as potent mutagens and carcinogens are formed in processing meat

Table 16.4 Electrochemical sensors based on CNDs for detecting drugs and pharmaceuticals

Fabricated electrode	Analyte	Linear range	LOD	Method	Ref.
AgNPs-CNDs-rGO/GCE	DOX	0.01–2.5 μM	2 nM	DPV	(Guo et al. 2017)
AuNPs/Pro-GQDs/GCE	p-acetamidophenol	0.08–100 μM	0.02 μM	DPV	(Xiaoyan et al. 2016)
CS/CNDs-CTAB/GCE	MSA	0.1–10 μM	0.05 μM	Amperometry	(Jalali et al. 2020)
β-galactosidase-CNDs/GCE	Lactose	0.29–2 mM	0.29 mM	CV	(Sharma et al. 2019)

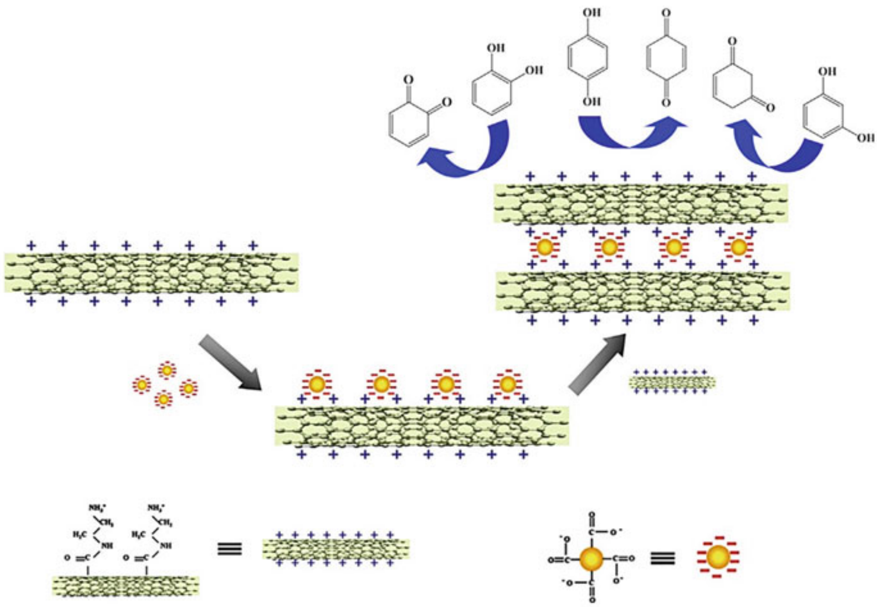

Fig. 16.5 LBL assembly between MWCNTs and CNDs (Wei et al. 2014). (Reproduced with permission from Ref. (Wei et al. 2014) Copyright (2014) Elsevier)

during curing, smoking, or salting (Minami et al. 2012; Tung et al. 2017). A DNA biosensor for the determination of mutagenic nitrosamines; NDMA and NDEA (*N*-nitrosodimethylamine *N*-nitrosodiethanolamine, respectively) is based on a CS-CND modified GCE electrode, in which DNA is electrostatically immobilized on the CS-CND/GCE surface (Majumdar et al. 2020). CNDs can also be used as a reducing agent for the in situ growth of CND/AuNPs on the GCE, followed by the drop cast of NF solution on GCE to retain CNDs/AuNPs on the electrode. The synergistic effect between CNDs and AuNPs is attributed to the oxidation of nitrite (NO_2^-) (Zhuang et al. 2016).

CNDs and GQDs are used in the detection of important bases of RNA and DNA. For example, simultaneous electrochemical detection of adenine (A) and guanine (G) is achieved using AgNPs and GQDs base (Wang et al. 2015a). A and G as RNA/DNA bases are important in the biosynthesis of protein and storage of genetic information (Wang et al. 2008). Electrochemical sensors based on CNDs for detecting pollutants, organophosphates, explosives, insecticides, and inorganic compounds are presented in Table 16.5.

4 Metal Ion Sensing

The development of a sensing system of heavy ions is important to obtain a fast and low-cost detection tool. Electrochemical sensors based on CNDs and GQDs for detecting heavy metals have been extensively developed. Such efforts are

Table 16.5 CNDs based sensors for pollutants, organophosphates, explosives, insecticides, and inorganic compounds

Modified electrode	Target	Linear range	Detection limit	Method	Ref.
NF/MWCNTs/CNDs/MWCNTs/GCE	CC HQ RS	4–200 μM 1–200 μM 3–400 μM	0.06 μM 0.07 μM 0.15 μM	DPV	(Wei et al. 2014)
Lac/F, N-CNDs/GCE	CC	12–450 μM	0.014 μM	Amperometry	(Liu et al. 2019)
CNDs/ITO	Capsaicin	0.05–500 μM	5.4 nM	CV	(Supchocksoonthorn et al. 2021)
N-CNDs/GCE	TNT	10 nM–1.5 μM	1 nM	DPV	(Zhang et al. 2015)
DNA/CS-CNDs/GCE	NDMA NDEA	9.9 nM –74 μM 9.6 nM – 40.2 μM	9.9 nM 9.6 nM	DPV	(Majumdar et al. 2020)
NF/CND-Au/GCE	NO_2^-	0.1 μM–2 mM	60 nM	Amperometry	(Zhuang et al. 2016)

anticipated because oxygen-containing groups on the surface of CNDs and GQDs significantly affect re-oxidizing metals to ions for stripping analysis.

A PANI/GQDs modified SPCE (screen-printed carbon electrode) is useful for detecting Cr(VI) (Punrat et al. 2016). GQDs are synthesized from citric acid and an optimal ratio of (1:4, v/v) aniline and GQDs is needed for the electropolymerization of aniline to PANI. The PANI/GQDs/SPCE detects Cr(VI) in mineral-drinking water using linear sweep voltammetry (LSV). For Cu^{2+} detection, a GCE is modified by CNDs and (*N*-(2-aminoethyl)-*N*,*N′*,*N′*,tris(pyridine-2-methyl)ethane-1,2,diamine) (AE-TPEA). CNDs are attached to methoxy functional groups on (3-aminopropyl) trimethoxysilane (APTMS) through salinization interaction. The AE-TPEA receptor is conjugated with -OH and/or -COOH groups of CNDs. Of importance is the specific recognition of TPEA toward Cu^{2+}, along with the amplified properties of CNDs. The (TPEA/CNDs/APTMS/GCE) using differential pulse anodic stripping voltammetry (DPASV) detects Cu^{2+} in rat brain microdialysate (Fig. 16.6) (Shao et al. 2013). A GQD-modified PG electrode can also detect Cu^{2+} ions (Ahour and Taheri 2018). Another scheme for sensitive detection of Cu^{2+} in water is based on a CD-CS modified GCE (Echabaane et al. 2021).

Cadmium (Cd^{2+}) and lead (Pb^{2+}) ions are distributed in soil and groundwaters because of their widespread industrial uses (Verma and Dwivedi 2013). Simultaneous electrochemical detection of Cd^{2+} and Pb^{2+} is feasible by a GCE modified by N-CQDs and GO (NCQDs-GO/GCE) by anodic stripping voltammetry (ASV). The hybrid composed of NCQDs-GO with abundant oxygen-containing groups and a sizeable specific surface area enhances the efficient adsorption of Cd^{2+} and Pb^{2+} via electrostatic interaction, resulting in significantly improved detection sensitivity (Li et al. 2018b).

The accumulation of mercury (Hg^{2+}) ions can be linked to several risky issues including renal and neural problems (Rice et al. 2014). The determination of Hg^{2+} and Cu^{2+} is based on a GCE modified by AuNPs and GQDs. Cysteamine-capped AuNPs are synthesized from the electrochemical reduction of gold chloride and conjugated with GQDs. The GQD-AuNP/GCE shows great affinity with Hg^{2+} compared to the AuNP/GCE (Ting et al. 2015). An SPCE is modified by CNDs for the determination of ferric ion (Fe^{3+}). Spent battery carbon dots are used for the synthesis of CNDs and the result obtained from the sensor is validated by atomic absorption spectroscopy (AAS) (Tan et al. 2017). Sensing heavy metal ions by CNDs and GQDs is summarized in Table 16.6.

5 Aptasensing and Immunosensing

Effective and sensitive analysis of proteins, biomarkers, and DNA is significantly vital in clinical analysis. CNDs and GQDs represent unique features of increasing electrocatalytic activity of aptasensors and immunosensors (Campuzano et al. 2019). Avian leukosis viruses (ALVs), the commonest naturally occurring avian retroviruses are corresponding to neoplastic diseases (Zhou et al. 2011). The Avian leukosis virus subgroup J (ALVs-J) is considered a recombination between an endogenous

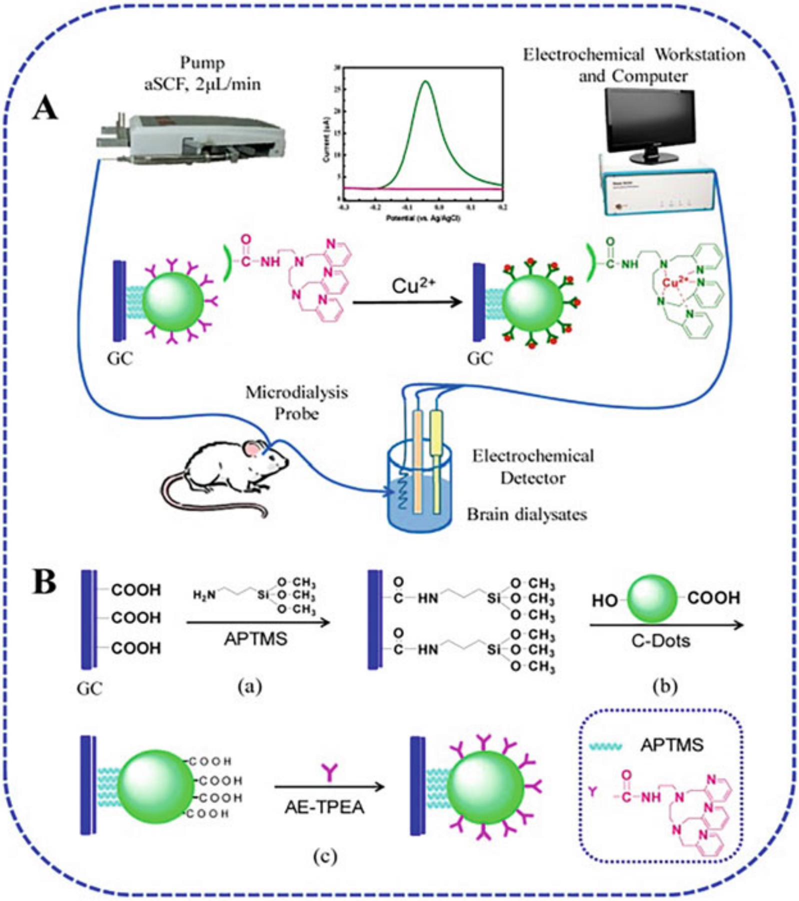
A
Pump
aSCF, 2μL/min
Electrochemical Workstation
and Computer
Current (μA)
Potential (vs. Ag/AgCl)
GC
Cu2+
GC
Microdialysis
Probe
Electrochemical
Detector
Brain dialysates
B
COOH
COOH
COOH
GC
APTMS
(a)
C-Dots
(b)
AE-TPEA
(c)
APTMS

Fig. 16.6 Diagram illustration (**a**) the determination of cerebral Cu^{2+} by TPEA/CNDs/APTMS/GC, and (**b**) modified electrode preparation (Shao et al. 2013). (Reproduced with permission from Ref. (Shao et al. 2013) Copyright (2013) American Chemical Society)

retrovirus and a known exogenous avian leukosis virus (Pan et al. 2011). An ultrasensitive electrochemical sandwich immunoassay for detecting ALVs-J is based on hybrid Fe_3O_4@GQDs and apoferritin-encapsulated Cu (Cu-apoferritin) (Fig. 16.7) (Wang et al. 2013). The Fe_3O_4@GQDs are used to link apoferritin with secondary antibodies (Ab_2). After the assembly of a sandwich-type between the antigen (ALVs-J) and Ab_2, Cu released from the cavity of apoferritin is detected by DPV.

Of note is the sensitive detection of tumor suppressor protein p53 antigen. The p53 antibody is immobilized onto a conductive matrix and dual amplification elements of poly-L-cysteine (P-Cys) and GQDs/AuNPs, respectively. P-Cys-GQDs/AuNPs are immobilized on the Au electrode by electrochemical

Table 16.6 CNDs-based electrochemical sensors for heavy metal ions

Fabricated electrode	Analyte	Linear range	LOD	Method	Ref.
PANI/GQDs/SPCE	Cr(VI)	0.1–10 mg/L	0.097 mg/L	LSV	(Punrat et al. 2016)
TPEA/CND/APTMS/GC	Cu^{2+}	1–60 μM	100 nM	DPASV	(Shao et al. 2013)
GQDs/PGE	Cu^{2+}	$50–4 \times 10^{-3}$ pM	12 pM	SWV	(Ahour and Taheri 2018)
CNDs-CS/GCE	Cu^{2+}	1 nM–10 mM	50 nM	EIS	(Echabaane et al. 2021)
NCQDs-GO/GCE	Cd^{2+} Pd^{2+}	11.24–11,241 μg/L 20.72–10,360 μg/L	7.45 μg/L 1.17 μg/L	ASV	(Li et al. 2018b)
GQDs-AuNPs/GCE	Hg^{2+} Cu^{2+}	0.02–1.5 nM $0.05–0.5 \times 10^{-3}$ nM	0.02 nM 0.05 nM	LSV	(Ting et al. 2015)
CNDs/SPCE	Fe^{3+}	0.5–25 ppm	0.44 ppm	CV	(Tan et al. 2017)

deposition. The resulting immunosensor exhibits long-term stability and excellent sensitivity (Hasanzadeh et al. 2018). A biosensing approach for gene mutation detection is proposed, based on CNDs/AuSPEs modified by a 25-mer sequence of *Helicobacter pylori* (HP1) (García-Mendiola et al. 2018). Oligonucleotides like HP1 are firmly adsorbed on CNDs through π-π stacking interaction and hydrogen bonding (Manohar et al. 2008). The biosensor based on HP1/CNDs/AuNPs offers sensitive and accurate hybridization monitoring using safranine as a redox probe that binds to double-stranded DNA (dsDNA) selectively (Garcia-Mendiola et al. 2016). An aptamer-based sensor is fabricated for ultrasensitive analysis of the hepatitis C virus (HCV) core antigen. In this approach, the aptamer (Apt) is immobilized onto GQDs via non-covalent interactions of electrostatics, π-π stacking, and hydrogen bonding types. The fabricated device detects HCV core antigen in human serum with good accuracy and precision by electrochemical impedance spectroscopy (EIS) (Ghanbari et al. 2017). CNDs can be used as a stabilizer and reducing agent to synthesize Pd-Au@CNDs nanocomposites. Single-stranded probe DNA (S1) is anchored on a Pd-Au@CNDs/GCE by coupling with CNDs through carboxylic groups (Fig. 16.8). The sensor detects colitoxin in human serum with excellent stability and reproducibility (Huang et al. 2017). CNDs stabilized AgNPs lipid nanohybrid offer selective, sensitive, and label-free electrochemical DNA sensing. CNDs-AgNPs are used to binary lipid vesicles to form a biocomposite, designated as lipid-CNDs-AgNPs. The biocomposite is then tethered on a 3-mercaptopropionic acid (MPA) monolayer via electrostatic interaction on the Au electrode. The detection scheme based on MPA/lipid/CNDs-AgNPs detects 1 μM target DNA with great selectivity (Divya et al. 2019). The application of CNDs and GQDs for detecting protein and DNA/RNA is itemized in Table 16.7.

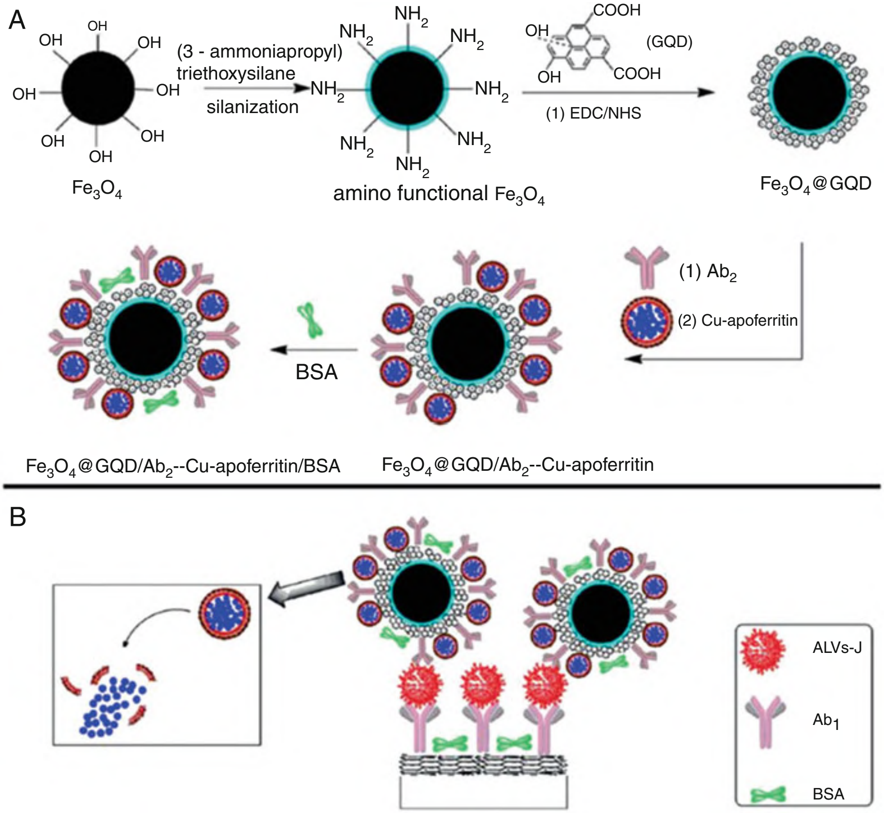
A
OH
OH
OH
OH
OH
OH
OH
OH
Fe_3O_4
(3 - ammoniapropyl) triethoxysilane
silanization
NH_2
amino functional Fe_3O_4
OH
COOH
OH
COOH
(GQD)
(1) EDC/NHS
Fe_3O_4@GQD
(1) Ab_2
(2) Cu-apoferritin
BSA
Fe_3O_4@GQD/Ab_2--Cu-apoferritin/BSA
Fe_3O_4@GQD/Ab_2--Cu-apoferritin
B
ALVs-J
Ab_1
BSA

Fig. 16.7 Schematic illustration (**a**) fabrication of Fe_3O_4@GQDs/Ab_2-Cu-apoferritin/BSA and (**b**) immunosensor (Wang et al. 2013). (Reproduced with permission from Ref. (Wang et al. 2013) Copyright (2013) Elsevier)

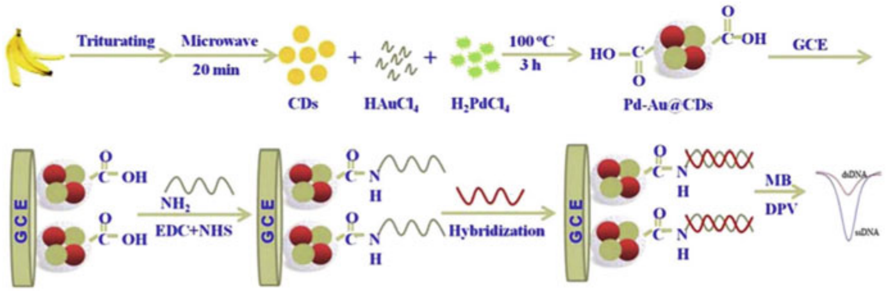
Triturating
Microwave
20 min
CDs
$HAuCl_4$
H_2PdCl_4
100 °C
3 h
HO–C
O
C–OH
Pd-Au@CDs
GCE
C–OH
NH_2
EDC+NHS
GCE
C–N
H
Hybridization
GCE
MB
DPV
dsDNA
ssDNA

Fig. 16.8 The green synthesis of CNDs from banana peels and its application as s a stabilizer and reducing agent for Pd-Au@CNDs for colitoxin (a toxin of *Escherichia coli*) sensing (Huang et al. 2017). (Reproduced with permission from Ref. (Huang et al. 2017) Copyright (2017) Elsevier)

Table 16.7 The electrochemical sensors-based CNDs for detecting proteins and DNA/RNA

Fabricated electrode	Analyte	Linear range	LOD	Method	Reference
Fe_3O_4@GQDs/ Ab_2-Cu-appferritin/ BSA/Ab_1/GCE	ALVs-J	$10^{2.08}$–$10^{4.50}$ $TCID_{50}$/mL[a]	115 $TCID_{50}$/mL	DPV	(Wang et al. 2013)
AuNPs/GQDs/ P-Cys/Au electrode	p53	0.000197–0.016 pM	0.065 fM	SWV	(Hasanzadeh et al. 2018)
HP1/CNDs/AuNPs	HP1	0.001–20 μM	0.16 nM	DPV	(García-Mendiola et al. 2018)
BSA/Apt/GQDs/ GCE	HCV	10–400 pg/mL	3.3 pg/mL	EIS	(Ghanbari et al. 2017)
S1/Pd-Au@CNDs/ GCE	Colitoxin	0.5 fM-5 nM	0.0182 fM	DPV	(Huang et al. 2017)
MPA/lipid/CNDs-AgNPs	Target DNA	10^{-16}–10^{-11} M	10^{-16} M	EIS	(Divya et al. 2019)

[a]TCID: Median Tissue Culture Infection Dose

6 Trends and Conclusions

CNDs have been advocated for important applications in electrocatalysis and electroanalysis (Nekoueian et al. 2019). As their electronic and chemical structures are related to their shape, size, surface functional groups, and heteroatom doping, different approaches can be used for the synthesis of CNDs and doped CNDs from different precursors. Another technique for improving the electrocatalytic and electronic characteristics of CNDs is to form nanocomposites of CNDs with other nanoscale materials. In particular, doped heteroatoms (N, S, P, etc.) serve as reactive catalytic sites during the electrocatalytic process. To date, the hydrothermal method is a promising route to control the structure and composition of doped CNDs via precursor optimization. Also, electrochemical synthesis of CQDs produces CNDs with low nanoscale particles. The absorbance and photoluminescence properties of CNDs have been advocated in the development of optical sensing platforms. Undoubtedly, this feature can be combined with electrocatalytic properties for developing sensing platforms with a dual-mode of detection: optical and electrochemical toward the improvement of detection selectivity. This combined feature is intriguing and could become an active and hot research topic in analytical chemistry. Conducting polymers can form polymer composites with CNDs with enhanced DC electrical conductivity. One typical example is the electrical conductivity of the CND- polyvinylidene fluoride (PVDF) films, which increases sixfolds over the PVDF film (Badawi et al. 2019). The direct energy bandgap of the composite film decreases from 5.28 to 2.96 eV as the wt % ratio of CNDs/PVDF increases from 0% to 10.0%. Such films will find various optoelectronic applications and in the field of biosensing, they can be used to entrap or bioconjugate with a biorecognition molecule toward the development of simple devices for field testing or point of care.

CNDs play a dual role (electron donors and acceptors) and have diversified applications in optronics, catalysis, and sensing (Hutton et al. 2017). Another feature is the tunable surface chemistry of CNDs that accommodates their functionalization or integration with different materials, biomolecules, nanoparticles, etc. Compared with CNDs, other carbon-based materials have some shortcomings, e.g., graphene contains fewer functional groups and defects, whereas high-cost carbon nanotubes are difficult to synthesize with poor aqueous solubility. Black phosphorus is also a new 2-D material with highly unique electrical and optical properties (Huang and Ling 2017). However, it is unstable and exhibits low biological compatibility. Lastly, g-C_3N_4 with poor electrical conductivity is uncompetitive in the field of electroanalysis. Nevertheless, the combination of CNDs with carbon-based materials opens an opportunity to examine the effect of chemical compositions and structural parameters on the electrocatalytic performance of such electrocatalysts. This is a relatively new field, and their new chemical and physical properties will be unraveled for novel applications, including electrochemical sensing and biosensing. For mass production of biosensing platforms, CNDs must be produced by a simple procedure with low-cost precursors, and in this context, graphite can be a good carbon source. However, CNDs can be synthesized with other functional groups from carbon sources to improve detection sensitivity and linearity.

From an academic viewpoint, very little is known about the electrical properties of CNDs (Liu and Wu 2013). The efficient and complex interaction between carbon core, various functional groups, and doped heteroatoms is attributed to their key electrochemical (electrical) features, similar to quantum dots (Ambrosi et al. 2014). Other contributing factors include their ample edge sites and sizeable specific surface area, which enable efficient electron transfer of CNDs, a subject of future endeavors. Recently, CNDs form nanocomposites with conducting polymers (Maruthapandi et al. 2021b), which are emerging materials for the construction of electrochemical biosensors. CNDs also exhibit antibacterial properties (Maruthapandi et al. 2021a), which could be exploited to develop biosensors with anti-fouling activities.

GQD exhibits electrochemiluminescence (Xu et al. 2004) but this important property has not been established for CNDs. However, GQDs outperform CNDs in electrochemical sensing as the former exhibits intrinsic electrochemical activity, and enhanced electrical conductivity with facilitated electron transfer (Campuzano et al. 2019). Nevertheless, doping CNDs or GQDs with various heteroatoms, e.g., nitrogen, boron, etc., is a distinct possibility to tune their electrochemical properties, a subject of future endeavors. Hybrid nanomaterials of CNDs with metal/metal oxide nanoparticles, organic compounds, conducting polymers, etc. could also lead to an increase in electrical conductivity owing to the increase of active surface areas and active sites. To date, CND-based biosensors require enzymes, aptamers, antibodies, nucleic acids, etc. It is of uttermost importance to develop CNDs with some intrinsic properties to mimic the biological properties of such biomolecules. Of note is the development of the nanostructure electrocatalyst of CNDs/octahedral-cuprous oxide (Cu_2O) as an enzymeless sensor for the determination of GLC and H_2O_2 (Li et al. 2015).

From a commercial viewpoint, the production of CNDs must be scalable with low cost, i.e., only limited methods and precursors are suitable to fulfill this stringent requirement. Therefore, future endeavors must focus on pertinent carbon-nitrogen sources and synthesis strategies toward the development of inexpensive CNDs “en masse” with extreme active sites and functional groups.

References

Ahour F, Taheri M (2018) Anodic stripping voltammetric determination of copper (II) ions at a graphene quantum dot-modified pencil graphite electrode. J Iran Chem Soc 15:343–350

Ambrosi A, Chua CK, Bonanni A, Pumera M (2014) Electrochemistry of graphene and related materials. Chem Rev 114:7150–7188

Anwar S, Ding H, Xu M, Hu X, Li Z, Wang J, Liu L, Jiang L, Wang D, Dong C (2019) Recent advances in synthesis, optical properties, and biomedical applications of carbon dots. ACS Appl Bio Mater 2:2317–2338

Badawi A, Alharthi SS, Mostafa NY, Althobaiti MG, Altalhi T (2019) Effect of carbon quantum dots on the optical and electrical properties of polyvinylidene fluoride polymer for optoelectronic applications. Appl Phys A Mater Sci Process 125:858

Bai J, Sun C, Jiang X (2016) Carbon dots-decorated multiwalled carbon nanotubes nanocomposites as a high-performance electrochemical sensor for detection of H_2O_2 in living cells. Anal Bioanal Chem 408:4705–4714

Bergman R, Parkes M (2006) Systematic review: the use of mesalazine in inflammatory bowel disease. Aliment Pharmacol Ther 23:841–855

Buk V, Pemble ME (2019) A highly sensitive glucose biosensor based on a micro disk array electrode design modified with carbon quantum dots and gold nanoparticles. Electrochim Acta 298:97–105

Campuzano S, Yanez-Sedeno P, Pingarron JM (2019) Carbon dots and graphene quantum dots in electrochemical biosensing. Nanomaterials 9:634

Canevari TC, Cincotto FH, Gomes D, Landers R, Toma HE (2017) Magnetite nanoparticles bonded carbon quantum dots magnetically confined onto screen printed carbon electrodes and their performance as electrochemical sensor for NADH. Electroanalysis 29:1968–1975

Deng J, Lu Q, Mi N, Li H, Liu M, Xu M, Tan L, Xie Q, Zhang Y, Yao S (2014) Electrochemical synthesis of carbon nanodots directly from alcohols. Chem Eur J 20:4993–4999

Divya KP, Karthikeyan R, Sinduja B, Grace AA, John SA, Hahn JH, Dharuman V (2019) Carbon dots stabilized silver–lipid nano hybrids for sensitive label free DNA detection. Biosens Bioelectron 133:48–54

Doñate-Buendia C, Torres-Mendieta R, Pyatenko A, Falomir E, Fernández-Alonso M, Mínguez-Vega G (2018) Fabrication by laser irradiation in a continuous flow jet of carbon quantum dots for fluorescence imaging. ACS Omega 3:2735–2742

Eccles R, Winther B, Johnston S, Robinson P, Trampisch M, Koelsch S (2015) Efficacy and safety of iota-carrageenan nasal spray versus placebo in early treatment of the common cold in adults: the ICICC trial. Respir Res 16:1–11

Echabaane M, Hfaiedh S, Smiri B, Saidi F, Dridi C (2021) Development of an impedimetric sensor based on carbon dots and chitosan nanocomposite modified electrode for Cu(II) detection in water. J Solid State Chem 25:1797–1806

Garcia-Mendiola T, Cerro MR, López-Moreno JM, Pariente F, Lorenzo E (2016) Dyes as bifunctional markers of DNA hybridization on surfaces and mutation detection. Bioelectrochemistry 111:115–122

García-Mendiola T, Bravo I, López-Moreno JM, Pariente F, Wannemacher R, Weber K, Popp J, Lorenzo E (2018) Carbon nanodots based biosensors for gene mutation detection. Sens Actuator B-Chem 256:226–233

Ghanbari K, Roushani M, Azadbakht A (2017) Ultra-sensitive aptasensor based on a GQD nanocomposite for detection of hepatitis C virus core antigen. Anal Biochem 534:64–69

Guo H, Jin H, Gui R, Wang Z, Xia J, Zhang F (2017) Electrodeposition one-step preparation of silver nanoparticles/carbon dots/reduced graphene oxide ternary dendritic nanocomposites for sensitive detection of doxorubicin. Sens Actuator B-Chem 253:50–57

Hasan MT, Gonzalez-Rodriguez R, Ryan C, Faerber N, Coffer JL, Naumov AV (2018) Photo-and electroluminescence from nitrogen-doped and nitrogen–sulfur codoped graphene quantum dots. Adv Funct Mater 28:1804337

Hasanzadeh M, Baghban HN, Shadjou N, Mokhtarzadeh A (2018) Ultrasensitive electrochemical immunosensing of tumor suppressor protein p53 in unprocessed human plasma and cell lysates using a novel nanocomposite based on poly-cysteine/graphene quantum dots/gold nanoparticle. Int J Biol Macromol 107:1348–1363

Hassanvand Z, Jalali F, Nazari M, Parnianchi F, Santoro C (2021) Carbon nanodots in electrochemical sensors and biosensors: a review. ChemElectroChem 8:15–35

Hou C, Fan S, Lang Q, Liu A (2015) Biofuel cell based self-powered sensing platform for L-cysteine detection. Anal Chem 87:3382–3387

Hrapovic S, Liu Y, Male KB, Luong JH (2004) Electrochemical biosensing platforms using platinum nanoparticles and carbon nanotubes. Anal Chem 76:1083–1088

Hu S, Huang Q, Lin Y, Wei C, Zhang H, Zhang W, Guo Z, Bao X, Shi J, Hao A (2014) Reduced graphene oxide-carbon dots composite as an enhanced material for electrochemical determination of dopamine. Electrochim Acta 130:805–809

Huang S, Ling X (2017) Black phosphorus: optical characterization, properties and applications. Small 13:1700823

Huang Q, Lin X, Lin C, Zhang Y, Hu S, Wei C (2015) A high performance electrochemical biosensor based on Cu_2O–carbon dots for selective and sensitive determination of dopamine in human serum. RSC Adv 5:54102–54108

Huang Q, Lin X, Zhu J-J, Tong Q-X (2017) Pd-Au@ carbon dots nanocomposite: facile synthesis and application as an ultrasensitive electrochemical biosensor for determination of colitoxin DNA in human serum. Biosens Bioelectron 94:507–512

Hutton GA, Martindale BC, Reisner E (2017) Carbon dots as photosensitisers for solar-driven catalysis. Chem Soc Rev 46:6111–6123

Jahanbakhshi M, Habibi B (2016) A novel and facile synthesis of carbon quantum dots via salep hydrothermal treatment as the silver nanoparticles support: application to electroanalytical determination of H_2O_2 in fetal bovine serum. Biosens Bioelectron 81:143–150

Jalali F, Hassanvand Z, Barati A (2020) Electrochemical sensor based on a nanocomposite of carbon dots, hexadecyltrimethylammonium bromide and chitosan for mesalazine determination. J Anal Chem 75:544–552

Ji H, Zhou F, Gu J, Shu C, Xi K, Jia X (2016) Nitrogen-doped carbon dots as a new substrate for sensitive glucose determination. Sensors 16:630

Ji C, Zhou Y, Leblanc RM, Peng Z (2020) Recent developments of carbon dots in biosensing: a review. ACS Sens 5:2724–2741

Jiang G, Jiang T, Zhou H, Yao J, Kong X (2015) Preparation of N-doped carbon quantum dots for highly sensitive detection of dopamine by an electrochemical method. RSC Adv 5:9064–9068

Jin H, Huang H, He Y, Feng X, Wang S, Dai L, Wang J (2015) Graphene quantum dots supported by graphene nanoribbons with ultrahigh electrocatalytic performance for oxygen reduction. J Am Chem Soc 137:7588–7591

Li Y, Zhong Y, Zhang Y, Weng W, Li S (2015) Carbon quantum dots/octahedral Cu_2O nanocomposites for non-enzymatic glucose and hydrogen peroxide amperometric sensor. Sens Actuator B-Chem 206:735–743

Li F, Li Y, Yang X, Han X, Jiao Y, Wei T, Yang D, Xu H, Nie G (2018a) Highly fluorescent chiral N-S-doped carbon dots from cysteine: affecting cellular energy metabolism. Angew Chem Int Ed 57:2377–2382

Li L, Liu D, Shi A, You T (2018b) Simultaneous stripping determination of cadmium and lead ions based on the N-doped carbon quantum dots-graphene oxide hybrid. Sens Actuator B-Chem 255: 1762–1770

Lim CS, Hola K, Ambrosi A, Zboril R, Pumera M (2015a) Graphene and carbon quantum dots electrochemistry. Electrochem Commun 52:75–79

Lim SY, Shen W, Gao Z (2015b) Carbon quantum dots and their applications. Chem Soc Rev 44: 362–381

Liu Y, Wu P (2013) Graphene quantum dot hybrids as efficient metal-free electrocatalyst for the oxygen reduction reaction. ACS Appl Mater Interfaces 5:3362–3369

Liu L, Anwar S, Ding H, Xu M, Yin Q, Xiao Y, Yang X, Yan M, Bi H (2019) Electrochemical sensor based on F, N-doped carbon dots decorated laccase for detection of catechol. J Electroanal Chem 840:84–92

Lu S, Yang B (2017) One step synthesis of efficient orange-red emissive polymer carbon nanodots displaying unexpect two photon fluorescence. Acta Polym Sin 7:1200–1206

Majumdar S, Thakur D, Chowdhury D (2020) DNA carbon-nanodots based electrochemical biosensor for detection of mutagenic nitrosamines. ACS Appl Bio Mater 3:1796–1803

Manohar S, Mantz AR, Bancroft KE, Hui C-Y, Jagota A, Vezenov DV (2008) Peeling single-stranded DNA from graphite surface to determine oligonucleotide binding energy by force spectroscopy. Nano Lett 8:4365–4372

Maruthapandi M, Das P, Saravanan A, Natan M, Banin E, Kannan S, Michaeli S, Luong JH, Gedanken A (2021a) Biocompatible N-doped carbon dots for the eradication of methicillin-resistant *S. aureus* (MRSA) and sensitive analysis for europium (III). Nano-Struct Nano-Objects 26:100724

Maruthapandi M, Saravanan A, Manohar P, Luong JH, Gedanken A (2021b) Photocatalytic degradation of organic dyes and antimicrobial activities by polyaniline–nitrogen-doped carbon dot nanocomposite. Nano 11:1128

Minami T, Esipenko NA, Zhang B, Kozelkova ME, Isaacs L, Nishiyabu R, Kubo Y, Anzenbacher P Jr (2012) Supramolecular sensor for cancer-associated nitrosamines. J Am Chem Soc 134: 20021–20024

Molaei MJ (2020) Principles, mechanisms, and application of carbon quantum dots in sensors: a review. Anal Methods 12:1266–1287

Mollarasouli F, Asadpour-Zeynali K, Campuzano S, Yanez-Sedeno P, Pingarron JM (2017) Non-enzymatic hydrogen peroxide sensor based on graphene quantum dots-chitosan/methylene blue hybrid nanostructures. Electrochim Acta 246:303–314

Mosconi D, Mazzier D, Silvestrini S, Privitera A, Marega C, Franco L, Moretto A (2015) Synthesis and photochemical applications of processable polymers enclosing photoluminescent carbon quantum dots. ACS Nano 9:4156–4164

Naik V, Zantye P, Gunjal D, Gore A, Anbhule P, Kowshik M, Bhosale SV, Kolekar G (2019) Nitrogen-doped carbon dots via hydrothermal synthesis: naked eye fluorescent sensor for dopamine and used for multicolor cell imaging. ACS Appl Bio Mater 2:2069–2077

Namdari P, Negahdari B, Eatemadi A (2017) Synthesis, properties and biomedical applications of carbon-based quantum dots: An updated review. Biomed Pharmacother 87:209–222

Nekoueian K, Amiri M, Sillanpää M, Marken F, Boukherroub R, Szunerits S (2019) Carbon-based quantum particles: an electroanalytical and biomedical perspective. Chem Soc Rev 48:4281–4316

Ngo Y-LT, Jana J, Chung JS, Hur SH (2020) Electrochemical biosensors based on nanocomposites of carbon-based dots. Korean Chem Eng Res 58:499–513

Ou J, Zhu Y, Kong Y, Ma J (2015) Graphene quantum dots/β-cyclodextrin nanocomposites: a novel electrochemical chiral interface for tryptophan isomer recognition. Electrochem Commun 60: 60–63

Pan W, Gao Y, Sun F, Qin L, Liu Z, Yun B, Wang Y, Qi X, Gao H, Wang X (2011) Novel sequences of subgroup J avian leukosis viruses associated with hemangioma in Chinese layer hens. Virol J 8:1–9

Pandey I, Jha SS (2015) Molecularly imprinted polyaniline-ferrocene-sulfonic acid-Carbon dots modified pencil graphite electrodes for chiral selective sensing of D-Ascorbic acid and L-Ascorbic acid: a clinical biomarker for preeclampsia. Electrochim Acta 182:917–928

Ponnaiah SK, Prakash P (2020) Carbon dots doped tungstic anhydride on graphene oxide nanopanels: a new picomolar-range creatinine selective enzymeless electrochemical sensor. Mater Sci Eng C 113:111010

Ponomarenko LA, Schedin F, Katsnelson MI, Yang R, Hill EW, Novoselov KS, Geim AK (2008) Chaotic Dirac billiard in graphene quantum dots. Science 320:356–358

Punrat E, Maksuk C, Chuanuwatanakul S, Wonsawat W, Chailapakul O (2016) Polyaniline/graphene quantum dot-modified screen-printed carbon electrode for the rapid determination of Cr(VI) using stopped-flow analysis coupled with voltammetric technique. Talanta 150:198–205

Razmi H, Mohammad-Rezaei R (2013) Graphene quantum dots as a new substrate for immobilization and direct electrochemistry of glucose oxidase: application to sensitive glucose determination. Biosens Bioelectron 41:498–504

Rice KM, Walker EM Jr, Wu M, Gillette C, Blough ER (2014) Environmental mercury and its toxic effects. J Prev Med Public Health 47:74

Rodgers JD, Bunce NJ (2001) Electrochemical treatment of 2,4,6-trinitrotoluene and related compounds. Environ Sci Technol 35:406–410

Saleh Ahammad A (2013) Hydrogen peroxide biosensors based on horseradish peroxidase and hemoglobin. J Biosens Bioelectron 9:2

Sarkar T, Bohidar H, Solanki PR (2018) Carbon dots-modified chitosan based electrochemical biosensing platform for detection of vitamin D. Int J Biol Macromol 109:687–697

Shang F, Zhou L, Mahmoud KA, Hrapovic S, Liu Y, Moynihan HA, Glennon JD, Luong JHT (2009) Selective nanomolar detection of dopamine using a boron-doped diamond electrode modified with an electropolymerized sulfobutylether-β-cyclodextrin-doped poly(*n*-acetyltyramine) and polypyrrole composite film. Anal Chem 81(10):4089–4098

Shao X, Gu H, Wang Z, Chai X, Tian Y, Shi G (2013) Highly selective electrochemical strategy for monitoring of cerebral Cu^{2+} based on a carbon dot-TPEA hybridized surface. Anal Chem 85: 418–425

Sharma SK, Micic M, Li S, Hoar B, Paudyal S, Zahran EM, Leblanc RM (2019) Conjugation of carbon dots with β-galactosidase enzyme: surface chemistry and use in biosensing. Molecules 24:3275

Shen Z, Zhang C, Yu X, Li J, Wang Z, Zhang Z, Liu B (2018) Microwave-assisted synthesis of cyclen functional carbon dots to construct a ratiometric fluorescent probe for tetracycline detection. J Mater Chem C 6:9636–9641

Song-Ling Y, Huang J-J, Lin L, Hui-Jun F, Yuan-Ming S, Yu-Dong S, Hong-Tao L, Zhen-Lin X (2017) Preparation of carbon dots and their application in food analysis as signal probe. Chin J Anal Chem 45:1571–1581

Su Y, Zhou X, Long YM, Li WF (2018) Immobilization of horseradish peroxidase on amino-functionalized carbon dots for the sensitive detection of hydrogen peroxide. Microchim Acta 185:114

Supchocksoonthorn P, Thongsai N, Wei W, Gopalan P, Paoprasert P (2021) Highly sensitive and stable sensor for the detection of capsaicin using electrocatalytic carbon dots grafted onto indium tin oxide. Sens Actuator B-Chem 329:129160

Tan SC, Chin SF, Pang SC (2017) Disposable carbon dots modified screen printed carbon electrode electrochemical sensor strip for selective detection of ferric ions. Sesnors 2017:1–7

Thoda O, Xanthopoulou G, Vekinis G, Chroneos A (2018) Review of recent studies on solution combustion synthesis of nanostructured catalysts. Adv Eng Mater 20:1800047

Tian L, Qiu G, Shen Y, Wang X, Wang J, Wang P, Song M, Li J, Li T, Zhuang W (2019) Carbon quantum dots modulated NiMoP hollow nanopetals as efficient electrocatalysts for hydrogen evolution. Ind Eng Chem Res 58:14098–14105

Ting SL, Ee SJ, Ananthanarayanan A, Leong KC, Chen P (2015) Graphe ne quantum dots functionalized gold nanoparticles for sensitive electrochemical detection of heavy metal ions. Electrochim Acta 172:7–11

Tung NT, Tue PT, Lien TTN, Ohno Y, Maehashi K, Matsumoto K, Nishigaki K, Biyani M, Takamura Y (2017) Peptide aptamer-modified single-walled carbon nanotube-based transistors for high-performance biosensors. Sci Rep 7:1–9

Verma R, Dwivedi P (2013) Heavy metal water pollution-a case study. Recent Res Sci Technol 5: 98–99

Wang W, Zhou L, Wang S, Luo Z, Hu Z (2008) Rapid and simple determination of adenine and guanine in DNA extract by micellar electrokinetic chromatography with indirect laser-induced fluorescence detection. Talanta 74:1050–1055

Wang X, Chen L, Su X, Ai S (2013) Electrochemical immunosensor with graphene quantum dots and apoferritin-encapsulated Cu nanoparticles double-assisted signal amplification for detection of avian leukosis virus subgroup. J Biosens Bioelectron 47:171–177

Wang G, Shi G, Chen X, Yao R, Chen F (2015a) A glassy carbon electrode modified with graphene quantum dots and silver nanoparticles for simultaneous determination of guanine and adenine. Microchim Acta 182:315–322

Wang Y, Wang Z, Rui Y, Li M (2015b) Horseradish peroxidase immobilization on carbon nanodots/CoFe layered double hydroxides: direct electrochemistry and hydrogen peroxide sensing. Biosens Bioelectron 64:57–62

Wang L, Tricard S, Yue P, Zhao J, Fang J, Shen W (2016) Polypyrrole and graphene quantum dots@Prussian Blue hybrid film on graphite felt electrodes: application for amperometric determination of L-cysteine. Biosens Bioelectron 77:1112–1118

Wang Z, An R, Dai Y, Luo H (2021) A simple strategy for the simultaneous determination of dopamine, uric acid, l-tryptophan and theophylline based on a carbon dots modified electrode. Int J Electrochem Sci 16:1–15

Wei C, Huang Q, Hu S, Zhang H, Zhang W, Wang Z, Zhu M, Dai P, Huang L (2014) Simultaneous electrochemical determination of hydroquinone, catechol and resorcinol at Nafion/multiwalled carbon nanotubes/carbon dots/multiwalled carbon nanotubes modified glassy carbon electrode. Electrochim Acta 149:237–244

Wu M, Zhan J, Geng B, He P, Wu K, Wang L, Xu G, Li Z, Yin L, Pan D (2017) Scalable synthesis of organic-soluble carbon quantum dots: superior optical properties in solvents, solids, and LEDs. Nanoscale 9:13195–13202

Xiaoyan Z, Ruiyi L, Zaijun L, Zhiguo G, Guangli W (2016) Ultrafast synthesis of gold/proline-functionalized graphene quantum dots and its use for ultrasensitive electrochemical detection of p-acetamidophenol. RSC Adv 6:42751–42755

Xu X, Ray R, Gu Y, Ploehn HJ, Gearheart L, Raker K, Scrivens WA (2004) Electrophoretic analysis and purification of fluorescent single-walled carbon nanotube fragments. J Am Chem Soc 126: 12736–12737

Yang C, Hu LW, Zhu HY, Ling Y, Tao JH, Xu CX (2015) rGO quantum dots/ZnO hybrid nanofibers fabricated using electrospun polymer templates and applications in drug screening involving an intracellular H_2O_2 sensor. J Mater Chem B 3:2651–2659

Yuan JM, Zhao R, Wu ZJ, Li W, Yang XG (2018) Graphene oxide quantum dots exfoliated from carbon fibers by microwave irradiation: two photoluminescence centers and self-assembly behavior. Small 14:1703714

Zhang H, Dai P, Huang L, Huang Y, Huang Q, Zhang W, Wei C, Hu S (2014) A nitrogen-doped carbon dot/ferrocene@ β-cyclodextrin composite as an enhanced material for sensitive and selective determination of uric acid. Anal Methods 6:2687–2691

Zhang L, Han Y, Zhu J, Zhai Y, Dong S (2015) Simple and sensitive fluorescent and electrochemical trinitrotoluene sensors based on aqueous carbon dots. Anal Chem 87:2033–2036

Zhang Q, Sun X, Ruan H, Yin K, Li H (2017) Production of yellow-emitting carbon quantum dots from fullerene carbon soot. Sci China Mater 60:141–150

Zhou G, Cai W, Liu X, Niu C, Gao C, Si C, Zhang W, Qu L, Han L (2011) A duplex real-time reverse transcription polymerase chain reaction for the detection and quantitation of avian leukosis virus subgroups A and B. J Virol Methods 173:275–279

Zhuang Z, Lin H, Zhang X, Qiu F, Yang H (2016) A glassy carbon electrode modified with carbon dots and gold nanoparticles for enhanced electrocatalytic oxidation and detection of nitrite. Microchim Acta 183:2807–2814

Organic-Inorganic Hybrid Nanomaterials in Biosensing Applications

17

Guilherme Figueira Alves, Thalles Pedrosa Lisboa, and
Renato Camargo Matos

Contents

1 Introduction 364
2 Organic and Inorganic Hybrid Nanomaterials 365
  2.1 Organic Nanomaterials 365
  2.2 Inorganic Nanomaterials 366
3 Hybrid Nanomaterials Synthesis 368
  3.1 Chemical Reduction 368
  3.2 Electrochemical Methods 369
  3.3 Hydrothermal and Solvothermal 369
4 Applications 372
  4.1 Carbon Nanotubes–Based Hybrid Nanomaterials 372
  4.2 Graphene-Based Hybrid Nanomaterials 373
  4.3 Carbon Black–Based Hybrid Nanomaterials 374
  4.4 Carbon Dots–Based Hybrid Nanomaterials 375
5 Conclusions and Future Outlooks 375
References 376

Abstract

Extensive research on the development of biosensors has been conducted. In particular, electrochemical biosensors have flourished with the advancement of nanomaterials, since the modification of electric biosensing devices can offer enhanced sensitive and selective personalized diagnostics. The performance of these sensors can be pushed further away with the use of organic-inorganic nanostructures, where a synergic effect may arise due to this combination. In

---

G. F. Alves (✉) · R. C. Matos
Chemistry Department, Institute of Exact Science, Federal University of Juiz de Fora, Juiz de Fora, Brazil
e-mail: alves@ice.ufjf.br

T. P. Lisboa
College of Exact Sciences and Technology, Federal University of Grande Dourados, Dourados, Brazil

© Springer Nature Singapore Pte Ltd. 2023

U. P. Azad, P. Chandra (eds.), *Handbook of Nanobioelectrochemistry*,
https://doi.org/10.1007/978-981-19-9437-1_17

the previous chapter, different classes of nanomaterials such as nanoclay, nanoclusters, and nanodendrite were discussed. Herein, the different organic and inorganic nanomaterials used in the fabrication of electrochemical biosensors are summarized, the advantages and disadvantages of each one of them are discussed, and current trends and research opportunities are highlighted. Besides that, the structure, properties, and some synthetic routes for obtaining its hybrid counterparts are presented. Finally, an overview of the applications of these materials in biosensing is reviewed.

Keywords

Graphene · Carbon nanotubes · Carbon black · Chalcogenides · Layered double hydroxides · MXenes

1 Introduction

The advance in nanomaterials engineering and nanotechnology casts new possibilities for the synthesis of materials with tailored properties and application in many research fields, such as electronics (Gong and Cheng 2017; Wu 2017), drug delivery (Hassan et al. 2017; Saxena et al. 2018; Mei et al. 2020), energy conversion and storage (Dai et al. 2012; Zhang et al. 2013), building/construction (Jones et al. 2019; Lum et al. 2019), cosmetics (Katz et al. 2015; Fytianos et al. 2020), aerospace and automotive industries (Srinivasan et al. 2015), and biosensors, in chemistry (Wang 2005; Choudhary et al. 2016; Lv et al. 2018). In this sense, biosensors can be defined as self-contained integrated analytical devices that convert a biological response into quantifiable and processable signals (Jadhav et al. 2021).

The development of biosensors has increased in past years due to the demand for personalized health care and cheaper diagnostics. Thus, the fabrication of high-performance biosensors with high sensitivity, selectivity, and compatibility with biological systems is required (Ray and Jana 2017; Bhatnagar et al. 2018; Bolotsky et al. 2019). For this purpose, electrochemical biosensors (EB) have been investigated because they offer advantages such as simplicity of construction, low detection limits, ease of miniaturization, and portability (Alves et al. 2020, 2022a, b, 2023; de Faria LV et al. 2020; Lisboa et al. 2021; Vinícius de Faria et al. 2021). EB can be an amperometric/voltammetric biosensor (the working electrode is responsible for measuring the current produced by a redox reaction), a potentiometric biosensor (where changes in potential are recorded in respect of a reference electrode), or an impedimetric biosensor (where changes in charge, conductance, and capacitance at the sensor surface are tracked) (Jadhav et al. 2021).

Currently, a variety of nanomaterials (NMs) have been applied as labeling tags aiming to enhance the performance of EB by increasing electrochemical surface area, which will result in higher sensitivity, improving electron transfer across the electrode-electrolyte interface, leading to a faster current response for a target molecule, and providing electrocatalytic sites. NMs are materials that possess at least one of their dimensions on a nanometric scale and can be classified as 0D, 1D, and 2D NMs. If all dimensions are nano-sized, this is a 0D NM (e.g., nanoparticles, quantum dots, fullerenes, and carbon dots). If two dimensions possess nanometric size, this material is called 1D NM, like nanowires, nanoribbons, and carbon nanotubes. If only one dimension is nanometric, this is a 2D NM (e.g., nanolayers, nanosheets, graphene, layered double hydroxides, and chalcogenides) (Naresh and Lee 2021). Meanwhile, the combination of nanomaterials in hybrid nanostructures integrates characteristics of both organic and inorganic materials, which can produce new features due to the formation of a composite and thus improve the EB analytical performance.

Therefore, in this chapter, the properties, the synthetic route, and applications of organic (graphene, carbon nanotubes, carbon black, and carbon dots) and inorganic (metal nanostructures, layered double hydroxides, chalcogenides, and quantum dots) hybrid nanomaterials will be discussed.

2 Organic and Inorganic Hybrid Nanomaterials

2.1 Organic Nanomaterials

Carbon atoms can be arranged in different configurations which result in different materials with unique structural configurations and properties. Figure 17.1 shows the carbon allotropes nanomaterials used organic nanomaterial for electrochemical biosensors assembly. The scientific literature reports are mainly focused on the use of

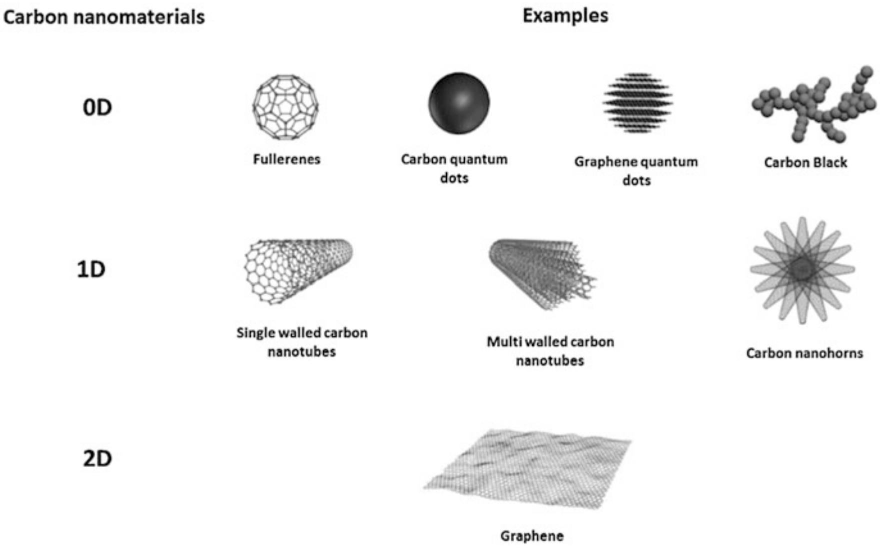
Carbon nanomaterials
Examples
0D
Fullerenes
Carbon quantum dots
Graphene quantum dots
Carbon Black
1D
Single walled carbon nanotubes
Multi walled carbon nanotubes
Carbon nanohorns
2D
Graphene

Fig. 17.1 The different categories of carbon nanomaterials used in the assembly of EB

EB based on graphene, reduced graphene oxide (rGO), graphene oxide (GO), and carbon nanotubes (CNT) (Sanati et al. 2019). In this sense, the use of other carbon nanomaterials such as fullerenes, carbon dots (CDs), carbon black (CB), and carbon nanohorns (CNHs) for biosensing applications represent new research opportunities.

Graphene is a single layer of sp^2-hybridized carbon atoms, linked covalently in a hexagonal honeycomb structure; this structure is responsible for its properties such as high surface area, and electric and thermal conductivity. Graphene is the building block of graphitic materials such as fullerenes, CNTs, and graphite, and these materials share, to some extent, the same properties as graphene (Malard et al. 2009).

Carbon nanotubes are cylindrical nanostructures that can be formed by rolling a sole graphene sheet into a tube (SWCNTs), or several layers in a concentric cylindrical structure (MWCNTS). The main properties of CNTs are high conductivity, fast electrode kinetics, and large surface area, these properties can be modulated by inserting functional groups on their surface by chemical modification, also called functionalization (Kour et al. 2020). CNHs are cone-shaped 1D nanostructures like CNTs and possess similar properties, the main advantages of CNH over CNTs are large-scale industrial synthesis with high yield and no need for purification (Karfa et al. 2019).

Fullerenes can be seen as wrapped graphene sheets, where carbon atoms (C_n; $n > 20$) are located in the vertices of a regular truncated icosahedron structure (Kroto et al. 1985). Like fullerenes, CD and graphene quantum dots (GQDs) are zero-dimensional carbon nanomaterials, consisting of carbon atoms with a size below 10 nm, sharing the same optical and electronic properties as that of quantum dots. CD and GQDs possess low toxicity, biocompatibility, and chemical inertness making these ideal materials for the fabrication of EB (Tajik et al. 2020). Another organic 0D nanomaterial is CB, an amorphous form of carbon with spherical morphology and particles size in the range from 3–100 nm, that is produced as soot from partial combustion of hydrocarbons, and the properties of CB are comparable to those above mentioned (Arduini et al. 2020).

2.2 Inorganic Nanomaterials

Inorganic nanomaterials comprise a variety of materials with different morphologies, such as quantum dots and nanoparticles. By tuning, size and morphology is possible to tailor its properties for specific applications (Pingarrón et al. 2008). Nanoparticles possesses physical, chemical, and electronic properties different than its bulk counterpart, due to the number and kind of atoms. Metal nanoparticles (MeNP), such as Ag, Au, and Pt, possess high conductivity and catalytic properties, thus MeNP act by increasing the electron transfer between redox centers and the electrode surface. Oxide nanoparticles are often used to immobilize biomolecules, while semiconductor nanoparticles are used as labels or tracers for electrochemical analysis (Luo et al. 2006). Another type of zero-dimension nanomaterial used for the fabrication of biosensors is quantum dots (QD). QD are semiconductor nanomaterials composed of groups II-VI, III-V, or IV elements and possess similar characteristics as

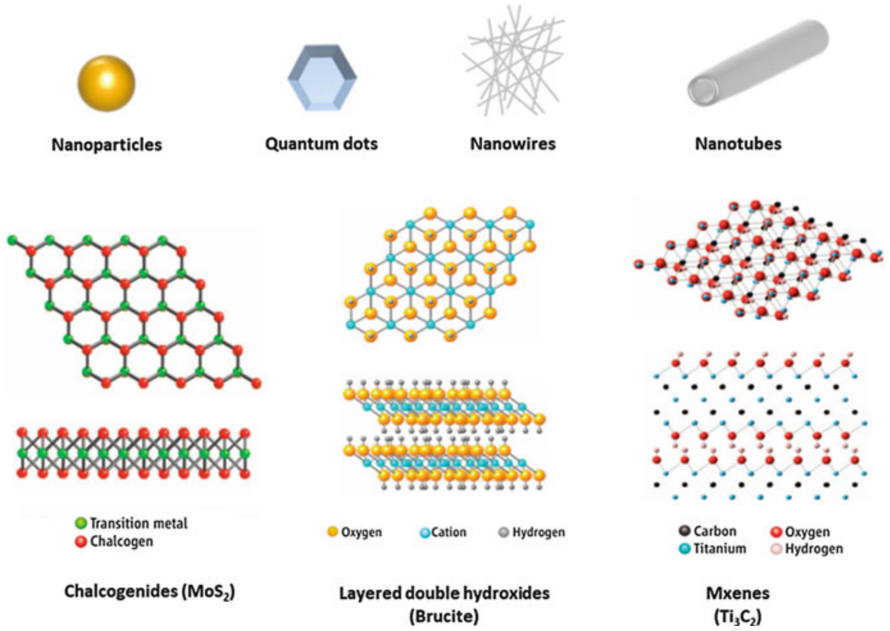
Nanoparticles
Quantum dots
Nanowires
Nanotubes
Transition metal
Chalcogen
Chalcogenides (MoS2)
Oxygen
Cation
Hydrogen
Layered double hydroxides (Brucite)
Carbon
Oxygen
Titanium
Hydrogen
Mxenes (Ti3C2)

Fig. 17.2 The different inorganic nanomaterials used for the assembly of EB

nanoparticles (Farzin and Abdoos 2021). Nanoparticles can be used as a precursor to producing nanowires (NW) and nanotubes (NT), where NT is hollow and NW are solid, with a cylindrical form (García et al. 2014; Cho et al. 2020). Figure 17.2 shows different examples of inorganic nanomaterials used in biosensing.

Since the discovery of graphene in 2004, a growing interest in inorganic 2D nanostructures has emerged, among these are chalcogenides and transition metal dichalcogenides (TMDs), MXenes, and layered double hydroxides (LDHs). Chalcogenides are layered compounds formed by the elements of group 16 that possess a variety of stoichiometry, the atoms in the layers are held by covalent bonds, while the planes are linked by a weak van der Waals bond, which allows the isolation of single individual layers from the bulk material (Wang et al. 2017). The largest subset of this group are TMDs, these compounds possess the formula MX_2, where M is a transition metal of groups 4–10 (e.g., Mo, W, Nb, Ti, and Ta) and X represents a chalcogen (S, Se, and Te) (Chhowalla et al. 2013; Tan and Zhang 2015). The electronic properties of TMDs are directly related to their composition, for example, semiconducting (as MoS_2 and WSe_2), semi-metallic (as $PtSe_2$ and TiS_2), metallic (as $NbSe_2$), and superconducting (as NbS) (Qi et al. 2018).

Another type of 2D nanomaterial discovered recently, MXenes are an emerging class constituted of transition metal carbides, nitrides, or carbonitrides with a general formula of $M_{n+1}X_nT_x$ ($n = 1–3$). This nanomaterial has $n + 1$ layers structure of M (early transition metal [e.g., Ti, Nb, Ta, Mo, V, and Cr]), n layer of X (carbon or nitrogen), and T represents surface functional groups (OH, O, and F) (Lin et al. 2021;

Sajid 2021). When compared to other nanomaterials MXenes possess some advantages such as biocompatibility, hydrophilicity, and prone availability of functional groups for analytes adsorption and/or modification (Sinha et al. 2018; Kalambate et al. 2019; Soomro et al. 2020; Lin et al. 2021).

Concerning multilayer nanomaterial, LDHs are a category of anionic clays, with lamellar structure and general formula that can be represented as $\left[M^{2+}_{(1-x)}M^{3+}_{x}(OH)_2\right]^{x+}[A^{n-}]_{x/n}\cdot zH_2O$, where M^{2+} is a divalent cation such as Mg^{2+}, Zn^{2+}, and Co^{2+}, M^{3+} represents a trivalent metal cation such as Al^{3+}, Co^{3+}, and Fe^{3+}, and A^{n-} is the interlayer anion such as $CO_3{}^{2-}$, $SO_4{}^{2-}$, and $NO_3{}^{-}$. The x is the molar ratio of $M^{3+}/(M^{2+} + M^{3+})$ and has a value ranging from 0.2–0.33 (Bukhtiyarova 2019; Jing et al. 2020). The poor electrical conductivity of LDHs hinders their electrochemical performance, though they have high chemical reactivity, thus the formation of hybrid composites with other nanomaterials, such as graphene and nanotubes, for modified electrodes has great appeal (Cao et al. 2016).

The main properties of the abovementioned materials are large surface areas and energy, preferential orientation of crystallographic planes, lattice defects, porous structure, and edges. All these features contribute to the improvement of the electrochemical response of electrodes, which is highly desirable since biomolecules are present in low concentrations in biofluids (Nikolaev et al. 2018; Shi et al. 2018).

3 Hybrid Nanomaterials Synthesis

A variety of methods can be used to produce composites nanomaterials such as chemical reduction, electrochemical methods, hydrothermal and solvothermal, chemical vapor deposition, laser ablation, and layer-by-layer assembling. In this session, only an overview of the first three mentioned methods will be explored since they are the most commonly used. A deeper discussion and particularities of each one of these methods are beyond the scope of this chapter, and readers may refer to further readings for this purpose (Huang et al. 2012; Tajik et al. 2020; Wang et al. 2020).

3.1 Chemical Reduction

This is the most used process for the decoration of carbon nanomaterials such as CNTs and rGO with MeNP, NW, and NR. TMDs/rGO composites can be produced by this method as well (Thanh et al. 2018), whereby mixing of metal salts (e.g., Au, Ag, Pt, Pd, Mo, and Ti) with a suspension of carbon material such as GO and derivatives (Tan et al. 2013; Ruffino and Giannazzo 2017; Darabdhara et al. 2019), CNTs (Satishkumar et al. 1996; Gao et al. 2012; Kharisov et al. 2016), and CQDs (Shen et al. 2013; Song et al. 2020) followed by the simultaneous reduction using a reducing agent such as hydrazine, sodium borohydrade, hydroxylamine, or ascorbic acid.

The growth of MeNP, NW, and NR takes place in the negatively charged functional groups on the surface of carbon materials. The same method can be applied to the synthesis of LDH/rGO and LDH/CNTs composites. For this purpose, the pH of the medium must be controlled to promote the precipitation of both M^{2+}/M^{3+} cations simultaneously and prevent residues of $M(OH)_2$ impurities (Daud et al. 2016). The resulting material is composed of a sandwich-like structure of LDHs and rGO, or CNTs (Cao et al. 2016; Asif et al. 2019).

3.2 Electrochemical Methods

This method has been used to produce rGO/MeNM (Darabdhara et al. 2019), CNT/MeNM (Vairavapandian et al. 2008), and TMDs/rGO (Thanh et al. 2018) with high purity in a simple and rapid way, without the need of toxic reagents. Electrochemical synthesis can be used to deposit MeNP and TMDs over CNTs and rGO surfaces. The first step consists in modifying the working electrode with a carbon nanomaterial, usually by drop-casting technique. After that the electrode is immersed in a solution containing the metal precursor. By applying a potential, the metals are reduced on the electrode surface. The functionalization of carbon nanomaterial and some parameters (applied potential, reaction time, and metal concentration) can be used to control the size, morphology, and amount of nanoparticles deposited on the electrode surface (Chu et al. 2010; Palanisamy et al. 2015).

Electrochemical techniques, such as chronoamperometry and cyclic voltammetry, can be used to generate LDHs/rGO composites. The working electrode is coated with GO and then immersed in a solution containing the divalent and trivalent salts of the metal, generally nitrates or sulfate salts. Hydroxide ions are formed due to the reduction of nitrate, or sulfate ions, to nitrite and sulfite respectively, which leads to a local pH decrease in the working electrode vicinities, and consequently the deposition of the LDH film (Yarger et al. 2008; Shao et al. 2015). Even though there is a variety of LDHs can be produced and associated with rGO by this method, only NiAl, ZnAl-LDHs/rGO, composites have been reported (Mousty and Walcarius 2015). Figure 17.3 shows the use of electrochemical and other techniques for the fabrication of hybrid nanomaterials.

3.3 Hydrothermal and Solvothermal

Hydrothermal and solvothermal methods are the most common synthetic route used to produce inorganic and organic nanomaterials. Elevated temperatures are applied to a sealed or open reactor that contains water (hydrothermal), organic solvents (solvothermal) and the precursor's materials (Feng and Li 2017). These conditions increase the solvent's ability to dissolve solids and speed up reactions between solid species. Temperature controls the product formation kinetics, pressure is essential for solubilization and directs the crystallization process, and both control the product

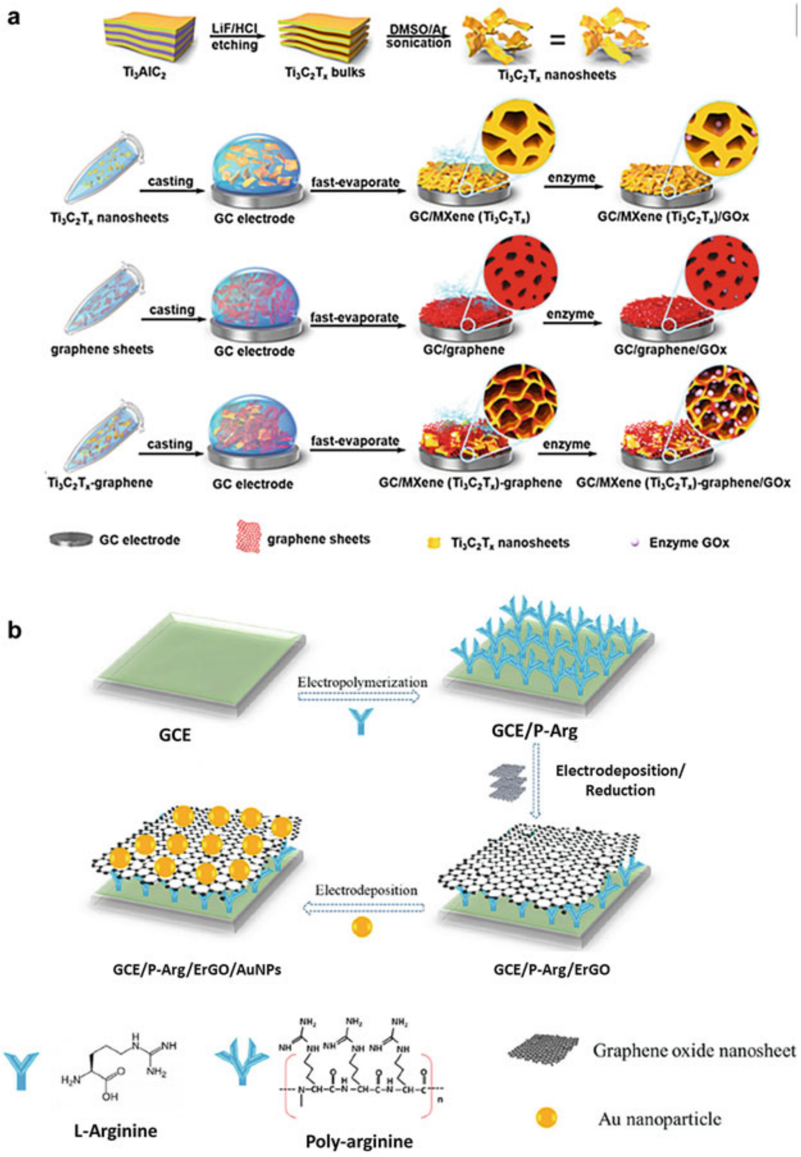
a
Ti_3AlC_2
LiF/HCl etching
$Ti_3C_2T_x$ bulks
DMSO/Ar sonication
$Ti_3C_2T_x$ nanosheets
casting
fast-evaporate
enzyme
$Ti_3C_2T_x$ nanosheets
GC electrode
GC/MXene ($Ti_3C_2T_x$)
GC/MXene ($Ti_3C_2T_x$)/GOx
graphene sheets
GC electrode
GC/graphene
GC/graphene/GOx
$Ti_3C_2T_x$-graphene
GC electrode
GC/MXene ($Ti_3C_2T_x$)-graphene
GC/MXene ($Ti_3C_2T_x$)-graphene/GOx
GC electrode
graphene sheets
$Ti_3C_2T_x$ nanosheets
Enzyme GOx
b
GCE
Electropolymerization
GCE/P-Arg
Electrodeposition/ Reduction
Electrodeposition
GCE/P-Arg/ErGO/AuNPs
GCE/P-Arg/ErGO
L-Arginine
Poly-arginine
Graphene oxide nanosheet
Au nanoparticle

Fig. 17.3 (**A**) Fabrication of rGO/Ti_3C_2 biosensor, (**B**) electrodeposition of AuNP on rGO modified electrode, (**C**) hydrothermal synthesis of rGO/LDHs nanomaterial, (**D**) chemical reduction of rGO/Sb_2O_5 biosensor, and (**E**) chemical reduction of rGO/NiAl-LDH. Panel **A**, **B**, **C**, **D**, and **E** were adapted and reproduced with permission from (Cincotto et al. 2015; Huang et al. 2018; Aziz et al. 2019; Gu et al. 2019; Khan et al. 2019), Copyright 2019 with permission from American Chemical Society, Copyright 2018 with permission from Springer, Copyright 2018 with permission from Elsevier B.V, Copyright 2015, with permission from Elsevier B.V, Copyright with 2019, with permission from Elsevier B.V, respectively

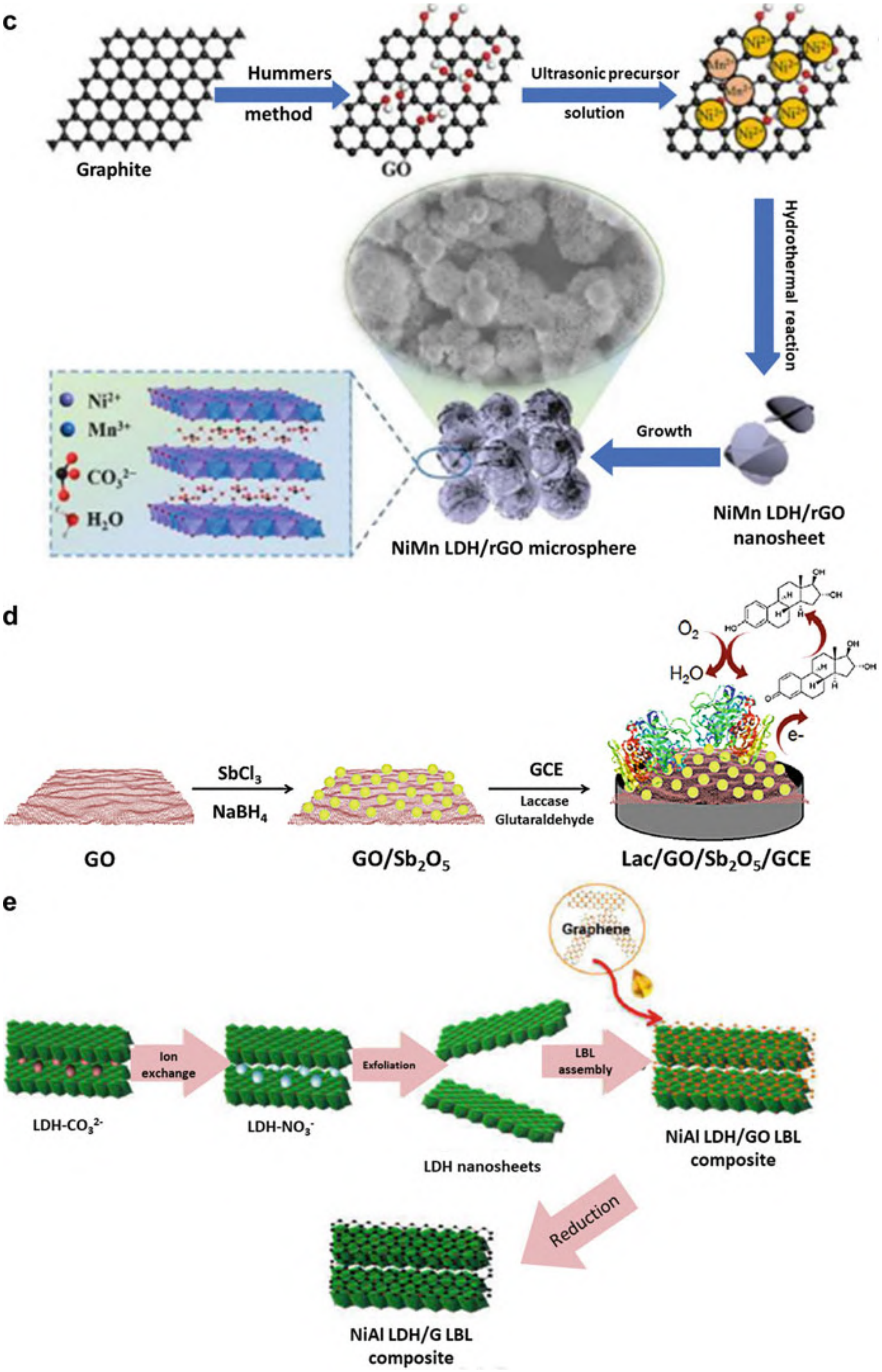
c
Graphite
Hummers method
GO
Ultrasonic precursor solution
Ni^{2+}
Mn^{3+}
Hydrothermal reaction
NiMn LDH/rGO nanosheet
Growth
NiMn LDH/rGO microsphere
Ni^{2+}
Mn^{3+}
CO_3^{2-}
H_2O
d
O_2
H_2O
e-
GO
$SbCl_3$
$NaBH_4$
GO/Sb_2O_5
GCE
Laccase
Glutaraldehyde
$Lac/GO/Sb_2O_5/GCE$
e
Graphene
$LDH-CO_3^{2-}$
Ion exchange
$LDH-NO_3^-$
Exfoliation
LDH nanosheets
LBL assembly
NiAl LDH/GO LBL composite
Reduction
NiAl LDH/G LBL composite

Fig. 17.3 (continued)

thermodynamic stability (Schäf et al. 2004). In this sense, these parameters can be used to tailor the size and morphology of the nanomaterials synthesized.

This method has been used to produce MeNP/rGO (Teymourian et al. 2014; Ding et al. 2015; Nazarpour et al. 2020), MeNW/rGO(Zhang et al. 2019), NR/rGO (Zhang et al. 2016), TMD/rGO (Li et al. 2015, 2016; Chiu and Chen 2018), LDHs/rGO (Cai et al. 2015; Huang et al. 2018; Kumaresan et al. 2019), and MXene/rGO (Yang et al. 2021). For this purpose, graphene oxide is first obtained and then added to the reactor with other precursors of the desired inorganic nanomaterials. The functional groups on the graphene surface help to attach the precursors to its surface, then the thermal and pressure treatments promote the reduction of graphene and, nucleation of inorganic nanomaterials and, the formation of composites.

To produce CQDs and GQDs by hydrothermal or solvothermal methods, a carbon source is required such as ethylene glycol, organic acids, and GO. Aiming the use of less hazardous chemical reagents other sources of carbon have been used such as apple juice, carrot, beer, garlic, honey, and, mango leaves (Chen et al. 2018; Iravani and Varma 2020). Four steps are involved in the formation of CQDs and GQDs: (i) dehydration, (ii) polymerization, (iii) carbonization, and (iv) passivation (Ghosh et al. 2021). Thus, the carbon source precursor will produce CQDs and GQDs with different morphologies, sizes, and properties. This method can be used to produce QD/GQDs (Min et al. 2017), TMDs/GQDs (Sangabathula and Sharma 2020), MeNP/CQDs (Lu et al. 2018), and NR/CQDs (Yang et al. 2015). CNTs, CB, and fullerenes can also be produced by this method even though there are only a few reports concerning the use of hydrothermal or solvothermal methods to produce hybrid inorganic composites with these materials (Ding et al. 2013; Wayu et al. 2013; Lorestani et al. 2015; Cao et al. 2017).

4 Applications

4.1 Carbon Nanotubes–Based Hybrid Nanomaterials

Several applications of hybrid-MWCNTs-based biosensors have been reported in the scientific literature. For example, the neurotransmitter dopamine was detected using an enzymaticless sensor based on self-supporting molybdenum nanoparticles functionalized in MWCNTs modified screen-printed carbon electrode (SPCE). The SPCE was used to analyze samples of biological interest (Keerthi et al. 2019). The electrochemical performance of the sensor was comparable to other reported sensors with a linear working range in the order of 0.01–1609 μmol L^{-1} and a detection limit (LD) of 1.26 nmol L^{-1}. The sensor was used to evaluate real samples of rat brain, human blood serum, and dopamine injection showing recovery percentages ranging from 99.6–107%.

On the other hand, MWCNT associated with polypyrrole nanowires, gold nanoparticles, and DNA aptamer were used for the electrochemical detection of the avian influenza virus (Liu et al. 2011). This biosensor is based on the hybridization and preferred orientation of an immobilized DNA aptamer on the surface of a working electrode modified with its target (a sequence specific to the H5N1). The analytical performance of the biosensor was comparable to other biosensors reported for DNA detection and showed a higher sensitivity with an LD in the order of 4.6×10^{-13} mol L^{-1}.

Hybrid composites of CNTs and NiAl-LDH modified glassy carbon electrode (GCE) were used for the real-time quantification of L-cysteine released by PC-12, MCF-7, MDA-MB-231 cells, serum, and urine (Aziz et al. 2022). First, the CNT was functionalized, for the formation of active sites for the growth of the NiAl-LDH by a coprecipitation method, followed by hydrothermal treatment, resulting in a wrapped hybrid structure. Furthermore, the Ni mediated the oxidation of L-cysteine to L-cystine, with LD of 3 nm L^{-1}, and three linear ranges, from 0.005–11, 16–96, and 116–780 μmol L^{-1}.

By combining titanium carbide MXene, MWCNT, and molecularly imprinted polymer a biosensor for amyloid-β protein, a Alzheimer biomarker, was fabricated for the analysis of plasma samples (Özcan et al. 2020). This composite was drop-casted on the surface of a GCE, the modified sensor had an electroactive area fivefold greater, and charge transfer resistance fivefold smaller than the bare electrode. Even when compared to its sole counterparts, there is a superior electrochemical performance of the sensor. Moreover, it can be highlighted the wide linear range of 1.0–100 ng L^{-1} and high sensitivity of 0.3 nmol L^{-1}.

4.2 Graphene-Based Hybrid Nanomaterials

Like MWCNT, graphene has been widely used to build hybrid sensors. In this sense, a bimetallic (platinum and silver) graphene hybrid biosensor was developed for the quantification of dopamine in injections (Anuar et al. 2020). The sensor showed a wide linear range, and a significantly lower LD (0.012 μmol L^{-1}) when compared to other sensors reported in the literature. The sensor presented adequate recovery percentages ranging from 91.4–99.0%.

The use of graphene associated with metal nanoparticles has been extensively explored. For example, silver vanadate nanorods decorated with silver nanoparticles were synthesized by using a simple hydrothermal technique and anchored onto nitrogen-doped rGO. This biosensor was applied in the determination of levofloxacin using a screen-printed carbon paste electrode (Sharma and Hwa 2021). The sensor performed significantly better than others reported in the literature, with a linear working range ranging from 0.09–671 μmol L^{-1} and an LD of 8.0 nmol L^{-1}. The sensor was also applied to samples of human blood serum, human urine, river water, and pharmaceutical tablets.

A hybrid sensor based on rGO-AuNP and poly(L-arginine) was used for the simultaneous determination of dopamine, serotonin, and L-tryptophan in real urine samples (Khan et al. 2018). Poly-aminoacid-modified electrodes have been the focus of current interest due to their electrocatalytic properties. Thus, due to the ease of its electropolymerization on the electrode surface, poly(L-arginine) has been highlighted. Its interaction with the negatively charged groups of graphene-based materials has also been reported. The hybrid material was used to modify a GCE to produce a sensor with excellent analytical performance. Two linear ranges were obtained, the smallest ranging from 1.0–50 nmol L^{-1}, 10–500 nmol L^{-1}, and 10–70 nmol L^{-1} for dopamine, serotonin, and L-tryptophan, respectively. Moreover, the observed LD were 1.0, 30.0, and 100.0 nmol L^{-1}, for the same analytes respectively. This method was applied to urine samples with recovery percentages ranging from 98.0–102.6%, which shows adequate performance.

Serotonin was analyzed in blood serum, and urine using a novel nanocomposite comprising gold nanorattles and reduced graphene oxide nanocomposite coated onto the gold nanoparticles deposited in a glassy carbon electrode surface, the sensor presented a wide linear range from 0.003–1.00 mmol L1 and high sensitivity, as well as LD 0.39 μmol L1, and the biosensor was selective among several interferents and presented long-term stability of 8 weeks (Mahato et al. 2019).

Association of graphene and LDHs also has been reported, a composite made of graphene, ZnAl-LDHs, and cobalt ferrite nanoparticles ($CoFe_2O_4$) was used for the quantification of etoposide, an anticancer agent used to treat lungs, lymphoma, and leukemia. Both ZnAL-LDHs and $CoFe_2O_4$ were synthesized using a hydrothermal method, the composite was obtained by the adsorption of the nanoparticles and graphene on the ZnAl-LDHs. The sensor presented an LD of 1 nm L^{-1}, and it was applied in the analysis of serum, blood plasma, and urine with recovery values ranging from 97–104%; it can be highlighted that the long-term stability of the sensor retains 95% of its initial activity after 7 weeks (Vajedi and Dehghani 2020).

4.3 Carbon Black–Based Hybrid Nanomaterials

The sensitive determination of the antihistamine, promethazine, was achieved by using an SPCE modified with a hybrid nanocomposite of barium tungstate ($BaWO_4$) modified and functionalized carbon black (*f*-CB) through an ecological synthesis technique (Muthukutty et al. 2021). The $BaWO_4$ particles were synthesized using aqueous media by coprecipitation technique. The sensor presented two linear working ranges and an LD in the order of 0.029 μmol L^{-1}, being applied for the determination of promethazine hydrochloride in lake water samples. Carbon black was also used to develop a hybrid sensor modified with polypyrrole and doped with iron oxide for the quantification of catechol in tap water (Ahmed et al. 2021). The sensor had a wide linear working range, ranging from 0.5–1188 μmol L^{-1}, and a low LD (52.8 nmol L^{-1}). In addition, the recovery percentages ranged from 96.4–98.1%.

In contrast, a nonenzymatic bimetallic alloy (palladium and copper) and carbon black hybrid nanostructure were developed for monitoring hydrogen peroxide released by living cells (Liu et al. 2019). Hydrogen peroxide is the main metabolite of oxygen in living organisms. In addition, its monitoring is of great importance, since hydrogen peroxide is a biomarker related to several diseases. The results suggest that carbon black increases the dispersibility and stability of metallic nanoparticles, in addition to preserving the nanostructure of the bimetallic alloy. The sensor had a wide linear working range (0.4 μmol L^{-1} to 5.0 mmol L^{-1}) and a low

LD (54 nmol L^{-1}). Furthermore, it was applied for real-time monitoring of hydrogen peroxide released from RAW 264.7 cells, showing that the sensor was promising for monitoring physiological processes.

4.4 Carbon Dots–Based Hybrid Nanomaterials

CD was synthesized through hydrothermal treatment of salep, a type of flour made of flower, as a new source of biopolymer by a simple, low-cost, and eco-friendly process, in the presence of only pure water (Jahanbakhshi and Habibi 2016). Silver nanoparticles were incorporated into the surface of the carbon quantum dots by ultraviolet irradiation. The sensor was applied to the determination of hydrogen peroxide in samples in the disinfected fetal bovine serum samples using amperometry. Furthermore, under optimal conditions, the linear working range achieved was 0.2–27.0 μmol L^{-1} and the LD was 80 nmol L^{-1}.

Similarly, green and fast methods to synthesize CD by microwave treatment of banana peels were reported, without the use of any surface passivation agents (Huang et al. 2017). The CD was also used as a reducing and stabilizing agent for the synthesis of a nanocomposite of Pd-Au@CD and applied to the modification surface of a GCE. A single-stranded DNA probe was immobilized on the surface of the modified electrode. The biosensor was applied for monitoring colitoxin in human serum samples. Using optimized conditions, the sensor could detect target DNA in very little concentrations in the range from 5.0×10^{-16} to 1.0×10^{-10} mol L^{-1}, the LD was in the order of attomole (1.82×10^{-17} mol L^{-1}).

CD was used to decorate NiAL-LDH for the nonenzymatic amperometric detection of acetylcholine (Wang et al. 2016), the hybrid nanomaterial was fabricated using a hydrothermal method, using a wood-based carbon as the precursor, and the LDH was prepared by a coprecipitation method. In the oxidation process, Ni is oxidized to NiO_2H, which oxidizes acetylcholine. The biosensor presented a wide linear range of 5–6885 μmol L^{-1}, high sensibility, the limit of detection of 1.7 μmol L^{-1}, and long-term stability, of 8 weeks.

5 Conclusions and Future Outlooks

The use of electrochemical platforms for (bio)sensors has great appeal since they offer fast, cheap, and easy-to-use techniques. However, since (bio)molecules are in low concentration, nanomolar to picomolar, in a complex matrix, such as biofluids, the need to obtain sensors that exhibit broad sensitivity and selectivity is increasing.

To face these challenges, composite nanomaterials have been used due to their unique morphologies and electrocatalytic properties. Furthermore, hybrid composite nanomaterials also provide long-term stability and high reproducibility, which are highly desirable characteristics of (bio)sensors. Since the discovery of CNTs, and rGO, these materials have been widely used for the fabrication of hybrid composite nanomaterials, while only a few reports applied carbon black, carbon dots, and fullerenes-based nanomaterials for (bio)sensing.

In this sense, there is still plenty of opportunities for the use of hybrid nanomaterials, since new materials, organic and inorganic, are discovered each year. For example, MXenes are in the early stages of their development, where titanium carbides are the most studied, and the new materials of this class may offer new features for the quantification of biomarkers and biomolecules. Furthermore, different combinations can be used for the fabrication of hybrid nanomaterials, and more than one nanomaterial, organic or inorganic, can be synthesized generating a complex structure where a synergic effect arises due to the combination of these materials.

However, there are still issues that must be addressed, even though a variety of synthetic routes are available, including hydrothermal/solvothermal, chemical reduction, electrochemical, chemical vapor deposition, and layer-by-layer assembling, are fundamental studies and scalable production and the control of the quality of the synthesized materials are yet to be demostrated. The correlation between structure and physiochemical properties, crystallinity, composition, phase structure, layer numbers, and interface of the heterojunction are not complete resolved. Thus the characterization of these materials, must be evaluated to understand how these factors affect the properties of the electrochemical (bio)sensor.

Besides, it can be believed that the development and integration of these functional hybrid nanomaterials in wearable sensors can significantly improve health care diagnostics. However, the biocompatibility of these materials should be evaluated, and they differ from those of the single material. Regardless of that, hybrid nanomaterials have been developed and applied to the monitoring of several drugs, bioactive molecules, and DNA residues, helping in the detection of viruses and diseases, which demonstrates their importance both for electrochemistry and for medical and diagnostic areas.

References

Ahmed J, Faisal M, Jalalah M, Alsaiari M, Alsareii SA, Harraz FA (2021) An efficient amperometric catechol sensor based on novel polypyrrole-carbon black doped α-Fe_2O_3 nanocomposite. Colloids Surf A Physicochem Eng Asp 619:126469

Alves GF, Lisboa TP, de Faria LV, de Farias DM, Matos MAC, Matos RC (2020) Disposable pencil graphite electrode for ciprofloxacin determination in pharmaceutical formulations by square wave voltammetry. Electroanalysis 33(2):543–549

Alves GF, de Faria LV, Lisboa TP, Costa Matos MA, Abarza Muñoz RA, Matos RC (2022a) Simple and fast batch injection analysis method for monitoring diuron herbicide residues in juice and tap water samples using reduced graphene oxide sensor, Journal of Food Composition and Analysis, 106:104284. ISSN 0889-1575. https://doi.org/10.1016/j.jfca.2021.104284

Alves GF, de Faria LV, Lisboa TP, de Souza CC, Mendes Fernandes BL, Costa Matos MA, Matos RC (2022b) A portable and affordable paper electrochemical platform for the simultaneous detection of sunset yellow and tartrazine in food beverages and desserts, Microchemical Journal 181:107799, ISSN 0026-265X. https://doi.org/10.1016/j.microc.2022.107799

Alves GF, de Faria LV, Lisboa TP, et al. (2023) Electrochemical exfoliation of graphite from pencil lead to graphene sheets: a feasible and cost-effective strategy to improve ciprofloxacin sensing. J Appl Electrochem 53, 39–48. https://doi.org/10.1007/s10800-022-01755-1

Anuar NS, Basirun WJ, Shalauddin M, Akhter S (2020) A dopamine electrochemical sensor based on a platinum–silver graphene nanocomposite modified electrode. RSC Adv 10(29): 17336–17344

Arduini F, Cinti S, Mazzaracchio V, Scognamiglio V, Amine A, Moscone D (2020) Carbon black as an outstanding and affordable nanomaterial for electrochemical (bio)sensor design. Biosens Bioelectron 156:112033

Asif M, Aziz A, Wang Z, Ashraf G, Wang J, Luo H, Chen X, Xiao F, Liu H (2019) Hierarchical CNTs@CuMn layered double hydroxide nanohybrid with enhanced electrochemical performance in H_2S detection from live cells. Anal Chem 91(6):3912

Aziz A, Asif M, Azeem M, Ashraf G, Wang Z, Xiao F, Liu H (2019) Self-stacking of exfoliated charged nanosheets of LDHs and graphene as biosensor with real-time tracking of dopamine from live cells. Anal Chim Acta 1047

Aziz A, Asif M, Ashraf G, Iftikhar T, Ajmal M, Liu H, Wang S (2022) Showcasing advanced electrocatalytic behavior of layered double hydroxide wrapped on carbon nanotubes: real-time monitoring of L-cysteine in biological matrices. Chem Eng J 440:135985

Bhatnagar I, Mahato K, Ealla KKR, Asthana A, Chandra P (2018) Chitosan stabilized gold nanoparticle mediated self-assembled gliP nanobiosensor for diagnosis of invasive aspergillosis. Int J Biol Macromol 110:449–456

Bolotsky A, Butler D, Dong C, Gerace K, Glavin NR, Muratore C, Robinson JA, Ebrahimi A (2019) Two-dimensional materials in biosensing and healthcare: from in vitro diagnostics to optogenetics and beyond. ACS Nano 13(9):9781

Bukhtiyarova MV (2019) A review on effect of synthesis conditions on the formation of layered double hydroxides. J Solid State Chem 269

Cai X, Shen X, Ma L, Ji Z, Xu C, Yuan A (2015) Solvothermal synthesis of NiCo-layered double hydroxide nanosheets decorated on RGO sheets for high performance supercapacitor. Chem Eng J 268

Cao Y, Li G, Li X (2016) Graphene/layered double hydroxide nanocomposite: properties, synthesis, and applications. Chem Eng J 292

Cao P, Peng J, Li J, Zhai M (2017) Highly conductive carbon black supported amorphous molybdenum disulfide for efficient hydrogen evolution reaction. J Power Sources 347

Chen W, Lv G, Hu W, Li D, Chen S, Dai Z (2018) Synthesis and applications of graphene quantum dots: a review. Nanotechnol Rev 7:157

Chhowalla M, Shin HS, Eda G, Li LJ, Loh KP, Zhang H (2013) The chemistry of two-dimensional layered transition metal dichalcogenide nanosheets. Nat Chem 5:263

Chiu CT, Chen DH (2018) One-step hydrothermal synthesis of three-dimensional porous Ni-Co sulfide/reduced graphene oxide composite with optimal incorporation of carbon nanotubes for high performance supercapacitors. Nanotechnology 29(17):175602

Cho IH, Kim DH, Park S (2020) Electrochemical biosensors: perspective on functional nanomaterials for on-site analysis. Biomater Res 24

Choudhary M, Yadav P, Singh A, Kaur S, Ramirez-Vick J, Chandra P, Arora K, Singh SP (2016) CD 59 targeted ultrasensitive electrochemical immunosensor for fast and noninvasive diagnosis of oral cancer. Electroanalysis 28(10):2565–2574

Chu H, Wei L, Cui R, Wang J, Li Y (2010) Carbon nanotubes combined with inorganic nanomaterials: preparations and applications. Coord Chem Rev 254:1117

Cincotto FH, Canevari TC, Machado SAS, Sánchez A, Barrio MAR, Villalonga R, Pingarrón JM (2015) Reduced graphene oxide-Sb_2O_5 hybrid nanomaterial for the design of a laccase-based amperometric biosensor for estriol. Electrochim Acta 174

Dai L, Chang DW, Baek JB, Lu W (2012) Carbon nanomaterials for advanced energy conversion and storage. Small 8

Darabdhara G, Das MR, Singh SP, Rengan AK, Szunerits S, Boukherroub R (2019) Ag and Au nanoparticles/reduced graphene oxide composite materials: synthesis and application in diagnostics and therapeutics. Adv Colloid Interface Sci 271

Daud M, Kamal MS, Shehzad F, Al-Harthi MA (2016) Graphene/layered double hydroxides nanocomposites: a review of recent progress in synthesis and applications. Carbon N Y 104

de Faria LV et al. (2020) Electrochemical study of different sensors for simple and fast quantification of ciprofloxacin in pharmaceutical formulations and bovine milk. Electroanalysis, 32(10):2266

Ding K, Wang Y, Liu L, Liu L, Zhang X, Guo Z (2013) Hydrothermal process synthesized electrocatalytic multi-walled carbon nanotubes-inserted gold composite microparticles toward ethanol oxidation reaction. J Appl Electrochem 43(6):567

Ding J, Zhu S, Zhu T, Sun W, Li Q, Wei G, Su Z (2015) Hydrothermal synthesis of zinc oxide-reduced graphene oxide nanocomposites for an electrochemical hydrazine sensor. RSC Adv 5(29):22935

Farzin MA, Abdoos H (2021) A critical review on quantum dots: from synthesis toward applications in electrochemical biosensors for determination of disease-related biomolecules. Talanta 224

Feng S-H, Li G-H (2017) Chapter 4 – hydrothermal and solvothermal syntheses. In: Xu R, Xu YBT-MISC (eds) Modern inorganic synthetic chemistry, 2nd edn. Elsevier, Amsterdam, pp 73–104

Fytianos G, Rahdar A, Kyzas GZ (2020) Nanomaterials in cosmetics: recent updates. Nanomaterials 10

Gao C, Guo Z, Liu JH, Huang XJ (2012) The new age of carbon nanotubes: an updated review of functionalized carbon nanotubes in electrochemical sensors. Nanoscale 4(6):1948

García M, Batalla P, Escarpa A (2014) Metallic and polymeric nanowires for electrochemical sensing and biosensing. TrAC – Trends Anal Chem 57:6

Ghosh D, Sarkar K, Devi P, Kim KH, Kumar P (2021) Current and future perspectives of carbon and graphene quantum dots: from synthesis to strategy for building optoelectronic and energy devices. Renew Sust Energ Rev 135:110391

Gong S, Cheng W (2017) One-dimensional nanomaterials for soft electronics. Adv Electron Mater 3:1600314

Gu H, Xing Y, Xiong P, Tang H, Li C, Chen S, Zeng R, Han K, Shi G (2019) Three-dimensional porous Ti_3C_2Tx MXene-graphene hybrid films for glucose biosensing. ACS Appl Nano Mater 2(10):6537

Hassan S, Prakash G, Bal Ozturk A, Saghazadeh S, Farhan Sohail M, Seo J, Remzi Dokmeci M, Zhang YS, Khademhosseini A (2017) Evolution and clinical translation of drug delivery nanomaterials. Nano Today 15:91

Huang X, Qi X, Boey F, Zhang H (2012) Graphene-based composites. Chem Soc Rev 41(2): 666–686

Huang Q, Lin X, Zhu JJ, Tong QX (2017) Pd-Au@carbon dots nanocomposite: facile synthesis and application as an ultrasensitive electrochemical biosensor for determination of colitoxin DNA in human serum. Biosens Bioelectron 94:507

Huang L, Liu B, Hou H, Wu L, Zhu X, Hu J, Yang J (2018) Facile preparation of flower-like NiMn layered double hydroxide/reduced graphene oxide microsphere composite for high-performance asymmetric supercapacitors. J Alloys Compd 730

Iravani S, Varma RS (2020) Green synthesis, biomedical and biotechnological applications of carbon and graphene quantum dots. A review. Environ Chem Lett 18:703

Jadhav DA, Chendake AD, Ghosal D, Mathuriya AS, Kumar SS, Pandit S (2021) Advanced microbial fuel cell for biosensor applications to detect quality parameters of pollutants. In: L Singh, DM Mahapatra, S Thakur, Bioremediation, Nutrients, and Other Valuable Product Recovery. Elsevier, 125–139. ISBN 9780128217290. https://doi.org/10.1016/B978-0-12-821729-0.00003-8

Jahanbakhshi M, Habibi B (2016) A novel and facile synthesis of carbon quantum dots via salep hydrothermal treatment as the silver nanoparticles support: application to electroanalytical determination of H_2O_2 in fetal bovine serum. Biosens Bioelectron 81:143–150

Jing C, Dong B, Zhang Y (2020) Chemical modifications of layered double hydroxides in the supercapacitor. Energy Environ Mater 3

Jones W, Gibb A, Goodier C, Bust P, Song M, Jin J (2019) Nanomaterials in construction-what is being used, and where? Proc Inst Civ Eng Constr Mater 172(2):49

Kalambate PK, Gadhari NS, Li X, Rao Z, Navale ST, Shen Y, Patil VR, Huang Y (2019) Recent advances in MXene–based electrochemical sensors and biosensors. TrAC – Trends Anal Chem 120

Karfa P, De S, Majhi KC, Madhuri R, Sharma PK (2019) Functionalization of carbon nanostructures. In: David L. Andrews, Robert H. Lipson, Thomas Nann, Comprehensive Nanoscience and Nanotechnology (Second Edition). Academic Press, 123–144. ISBN 9780128122969. https://doi.org/10.1016/B978-0-12-803581-8.11225-1

Katz LM, Dewan K, Bronaugh RL (2015) Nanotechnology in cosmetics. Food Chem Toxicol 85:127

Keerthi M, Boopathy G, Chen SM, Chen TW, Lou BS (2019) A core-shell molybdenum nanoparticles entrapped f-MWCNTs hybrid nanostructured material based non-enzymatic biosensor for electrochemical detection of dopamine neurotransmitter in biological samples. Sci Rep 9(1)

Khan MZH, Liu X, Tang Y, Zhu J, Hu W, Liu X (2018) A glassy carbon electrode modified with a composite consisting of gold nanoparticle, reduced graphene oxide and poly(L-arginine) for simultaneous voltammetric determination of dopamine, serotonin and L-tryptophan. Microchim Acta 185(9)

Khan F, Akhtar N, Jalal N, Hussain I, Szmigielski R, Hayat MQ, Ahmad HB, El-Said WA, Yang M, Janjua HA (2019) Carbon-dot wrapped ZnO nanoparticle-based photoelectrochemical sensor for selective monitoring of H_2O_2 released from cancer cells. Microchim Acta 186(2)

Kharisov BI, Kharissova OV, Ortiz Méndez U, De La Fuente IG (2016) Decoration of carbon nanotubes with metal nanoparticles: recent trends. Synth React Inorg Met Nano-Metal Chem 46(1):55

Kour R, Arya S, Young S-J, Gupta V, Bandhoria P, Khosla A (2020) Review – recent advances in carbon nanomaterials as electrochemical biosensors. J Electrochem Soc 167(3):037555

Kroto HW, Heath JR, O'Brien SC, Curl RF, Smalley RE (1985) C60: buckminsterfullerene. Nature 318(6042):162

Kumaresan A, Yang S, Zhao K, Ahmad N, Zhou J, Zheng Z, Zhang Y, Gao Y, Zhou H, Tang Z (2019) Facile development of CoAl-LDHs/RGO nanocomposites as photocatalysts for efficient hydrogen generation from water splitting under visible-light irradiation. Inorg Chem Front 6(7):1753

Li X, Shen J, Li N, Ye M (2015) Fabrication of γ-MnS/rGO composite by facile one-pot solvothermal approach for supercapacitor applications. J Power Sources 282:194

Lin X, Li Z, Qiu J, Wang Q, Wang J, Zhang H, Chen T (2021) Fascinating MXene nanomaterials: emerging opportunities in the biomedical field. Biomater Sci 9:5437

Lisboa TP, de Faria LV, Alves GF, Matos MAC, Matos RC (2021) Development of paper devices with conductive inks for sulfanilamide electrochemical determination in milk, synthetic urine, and environmental and pharmaceutical samples. J Solid State Electrochem 25(8–9):2301–2308

Liu X, Cheng Z, Fan H, Ai S, Han R (2011) Electrochemical detection of avian influenza virus H5N1 gene sequence using a DNA aptamer immobilized onto a hybrid nanomaterial-modified electrode. Electrochim Acta 56(18):6266

Liu G, Wang B, Wang L, Yuan Y, Wang D (2016) A facile hydrothermal synthesis of a reduced graphene oxide modified cobalt disulfide composite electrode for high-performance supercapacitors. RSC Adv 6(9):7129

Liu Y, Li H, Gong S, Chen Y, Xie R, Wu Q, Tao J, Meng F, Zhao P (2019) A novel non-enzymatic electrochemical biosensor based on the nanohybrid of bimetallic PdCu nanoparticles/carbon black for highly sensitive detection of H_2O_2 released from living cells. Sensors Actuators B Chem 290

Lorestani F, Shahnavaz Z, Mn P, Alias Y, Manan NSA (2015) One-step hydrothermal green synthesis of silver nanoparticle-carbon nanotube reduced-graphene oxide composite and its application as hydrogen peroxide sensor. Sensors Actuators B Chem 208:389

Lu Y, Feng Y, Wang F, Zou X, Chen ZF, Chen P, Liu H, Su Y, Zhang Q, Liu G (2018) Facile hydrothermal synthesis of carbon dots (CDs) doped $ZnFe_2O_4/TiO_2$ hybrid materials with high photocatalytic activity. J Photochem Photobiol A Chem 353

Lum WC, Lee SH, Ahmad Z, Halip JA, Chin KL (2019) Lignocellulosic nanomaterials for construction and building applications. In: Sabu Thomas, Yves Grohens, Yasir Beeran Pottathara, In Micro and Nano Technologies, Industrial Applications of Nanomaterials. Elsevier, 423–439. ISBN 9780128157497. https://doi.org/10.1016/B978-0-12-815749-7.00015-3

Luo X, Morrin A, Killard AJ, Smyth MR (2006) Application of nanoparticles in electrochemical sensors and biosensors. Electroanalysis 18:319

Lv M, Liu Y, Geng J, Kou X, Xin Z, Yang D (2018) Engineering nanomaterials-based biosensors for food safety detection. Biosens Bioelectron 106:122

Mahato K, Purohit B, Bhardwaj K, Jaiswal A, Chandra P (2019) Novel electrochemical biosensor for serotonin detection based on gold nanorattles decorated reduced graphene oxide in biological fluids and in vitro model. Biosens Bioelectron 142:111502

Malard LM, Pimenta MA, Dresselhaus G, Dresselhaus MS (2009) Raman spectroscopy in graphene. Phys Rep 473(5–6):51–87

Mei X, Hu T, Wang Y, Weng X, Liang R, Wei M (2020) Recent advancements in two-dimensional nanomaterials for drug delivery. Wiley Interdiscip Rev Nanomed Nanobiotechnol 12

Min S, Hou J, Lei Y, Ma X, Lu G (2017) Facile one-step hydrothermal synthesis toward strongly coupled TiO2/graphene quantum dots photocatalysts for efficient hydrogen evolution. Appl Surf Sci 396:1375–1382

Mousty C, Walcarius A (2015) Electrochemically assisted deposition by local pH tuning: a versatile tool to generate ordered mesoporous silica thin films and layered double hydroxide materials. J Solid State Electrochem 19

Muthukutty B, Vivekanandan AK, Chen S-M, Sivakumar M, Chen S-H (2021) Designing hybrid barium tungstate on functionalized carbon black as electrode modifier for low potential detection of antihistamine drug promethazine hydrochloride. Compos Part B Eng 215:108789

Naresh V, Lee N (2021) A review on biosensors and recent development of nanostructured materials-enabled biosensors. Sensors (Switzerland) 21

Nazarpour S, Hajian R, Sabzvari MH (2020) A novel nanocomposite electrochemical sensor based on green synthesis of reduced graphene oxide/gold nanoparticles modified screen printed electrode for determination of tryptophan using response surface methodology approach. Microchem J 154

Nikolaev KG, Ermolenko YE, Offenhäusser A, Ermakov SS, Mourzina YG (2018) Multisensor systems by electrochemical nanowire assembly for the analysis of aqueous solutions. Front Chem 6(Jun)

Özcan N, Medetalibeyoglu H, Akyıldırım O, Atar N, Yola ML (2020) Electrochemical detection of amyloid-β protein by delaminated titanium carbide MXene/multi-walled carbon nanotubes composite with molecularly imprinted polymer. Mater Today Commun 23:101097

Palanisamy S, Thirumalraj B, Chen SM, Ali MA, Al-Hemaid FMA (2015) Palladium nanoparticles decorated on activated fullerene modified screen printed carbon electrode for enhanced electrochemical sensing of dopamine. J Colloid Interface Sci 448

Pingarrón JM, Yáñez-Sedeño P, González-Cortés A (2008) Gold nanoparticle-based electrochemical biosensors. Electrochim Acta 53(19):5848

Qi H, Wang L, Sun J, Long Y, Hu P, Liu F, He X (2018) Production methods of Van der Waals heterostructures based on transition metal dichalcogenides. Crystals 8(1):35

Ray SC, Jana NR (2017) Application of carbon-based nanomaterials as biosensor In: Micro and Nano Technologies, Carbon Nanomaterials for Biological and Medical Applications. Elsevier, 87–127. ISBN 9780323479066. https://doi.org/10.1016/B978-0-323-47906-6.00003-5

Ruffino F, Giannazzo F (2017) A review on metal nanoparticles nucleation and growth on/in graphene. Crystals 7

Sajid M (2021) MXenes: are they emerging materials for analytical chemistry applications? A review. Anal Chim Acta 1143:267

Sanati A, Jalali M, Raeissi K, Karimzadeh F, Kharaziha M, Mahshid SS, Mahshid S (2019) A review on recent advancements in electrochemical biosensing using carbonaceous nanomaterials. Microchim Acta 186

Sangabathula O, Sharma CS (2020) One-pot hydrothermal synthesis of molybdenum nickel sulfide with graphene quantum dots as a novel conductive additive for enhanced supercapacitive performance. Mater Adv 1(8):2763

Satishkumar BC, Vogl EM, Govindaraj A, Rao CNR (1996) The decoration of carbon nanotubes by metal nanoparticles. J Phys D Appl Phys 29(12):3173

Saxena V, Chandra P, Pandey LM (2018) Design and characterization of novel Al-doped ZnO nanoassembly as an effective nanoantibiotic. Appl Nanosci 8(8):1925–1941

Schäf O, Ghobarkar H, Knauth P (2004) Hydrothermal synthesis of nanomaterials. In: Nanostructured materials. Kluwer Academic Publishers, Boston, pp 23–41

Shao M, Zhang R, Li Z, Wei M, Evans DG, Duan X (2015) Layered double hydroxides toward electrochemical energy storage and conversion: design, synthesis and applications. Chem Commun 51:15880

Sharma TSK, Hwa K-Y (2021) Facile synthesis of Ag/AgVO$_3$/N-rGO hybrid nanocomposites for electrochemical detection of levofloxacin for complex biological samples using screen-printed carbon paste electrodes. Inorg Chem 60(9):6585–6599

Shen L, Chen M, Hu L, Chen X, Wang J (2013) Growth and stabilization of silver nanoparticles on carbon dots and sensing application. Langmuir 29(52):16135

Shi PC, Guo JP, Liang X, Cheng S, Zheng H, Wang Y, Chen CH, Xiang HF (2018) Large-scale production of high-quality graphene sheets by a non-electrified electrochemical exfoliation method. Carbon N Y 126

Sinha A, Dhanjai ZH, Huang Y, Lu X, Chen J, Jain R (2018) MXene: an emerging material for sensing and biosensing. TrAC – Trends Anal Chem 105:424

Song C, Wei Q, Li H, Gao H, An J, Qi B (2020) Highly sensitive electrochemical sensor based on carbon dots reduced gold nanoparticles for ractopamine detection in pork meat. Int J Electrochem Sci 15

Soomro RA, Jawaid S, Zhu Q, Abbas Z, Xu B (2020) A mini-review on MXenes as versatile substrate for advanced sensors. Chinese Chem Lett 31(4):922

Srinivasan S, Kannan AM, Kothurkar N, Khalil Y, Kuravi S (2015) Nanomaterials for energy and environmental applications. J Nanomater 2015:1

Tajik S, Dourandish Z, Zhang K, Beitollahi H, Van Le Q, Jang HW, Shokouhimehr M (2020) Carbon and graphene quantum dots: a review on syntheses, characterization, biological and sensing applications for neurotransmitter determination. RSC Adv 10:15406

Tan C, Zhang H (2015) Two-dimensional transition metal dichalcogenide nanosheet-based composites. Chem Soc Rev 44:2713

Tan C, Huang X, Zhang H (2013) Synthesis and applications of graphene-based noble metal nanostructures. Mater Today 16

Teymourian H, Salimi A, Firoozi S, Korani A, Soltanian S (2014) One-pot hydrothermal synthesis of zirconium dioxide nanoparticles decorated reduced graphene oxide composite as high performance electrochemical sensing and biosensing platform. Electrochim Acta 143:143

Thanh TD, Chuong ND, Van Hien H, Kshetri T, Tuan LH, Kim NH, Lee JH (2018) Recent advances in two-dimensional transition metal dichalcogenides-graphene heterostructured materials for electrochemical applications. Prog Mater Sci 96:51

Vairavapandian D, Vichchulada P, Lay MD (2008) Preparation and modification of carbon nanotubes: review of recent advances and applications in catalysis and sensing. Anal Chim Acta 626: 119–129

Vajedi F, Dehghani H (2020) A high-sensitive electrochemical DNA biosensor based on a novel ZnAl/layered double hydroxide modified cobalt ferrite-graphene oxide nanocomposite electrophoretically deposited onto FTO substrate for electroanalytical studies of etoposide. Talanta 208:120444

Vinícius de Faria L, Lisboa TP, Alves GF, Costa Matos MA, Abarza Muñoz RA, Matos RC (2021) Adsorptive stripping voltammetric determination of chloramphenicol residues in milk samples using reduced graphene oxide sensor. Anal Methods 13(47):5711–5718

Wang J (2005) Carbon-nanotube based electrochemical biosensors: a review. Electroanalysis 17

Wang L, Chen X, Liu C, Yang W (2016) Non-enzymatic acetylcholine electrochemical biosensor based on flower-like NiAl layered double hydroxides decorated with carbon dots. Sensors Actuators B Chem 233:199–205

Wang YH, Huang KJ, Wu X (2017) Recent advances in transition-metal dichalcogenides based electrochemical biosensors: a review. Biosens Bioelectron 97:305

Wang B, Ruan T, Chen Y, Jin F, Peng L, Zhou Y, Wang D, Dou S (2020) Graphene-based composites for electrochemical energy storage. Energy Storage Mater 24

Wayu MB, Spidle RT, Devkota T, Deb AK, Delong RK, Ghosh KC, Wanekaya AK, Chusuei CC (2013) Morphology of hydrothermally synthesized ZnO nanoparticles tethered to carbon nanotubes affects electrocatalytic activity for H_2O_2 detection. Electrochim Acta 97

Wu W (2017) Inorganic nanomaterials for printed electronics: a review. Nanoscale 9

Yang Y, Ji X, Jing M, Hou H, Zhu Y, Fang L, Yang X, Chen Q, Banks CE (2015) Carbon dots supported upon N-doped TiO_2 nanorods applied into sodium and lithium ion batteries. J Mater Chem A 3(10):5648

Yang C, He H, Jiang Q, Liu X, Shah SP, Huang H, Li W (2021) Pd nanocrystals grown on MXene and reduced graphene oxide co-constructed three-dimensional nanoarchitectures for efficient formic acid oxidation reaction. Int J Hydrog Energy 46(1):589

Yarger MS, Steinmiller EMP, Choi KS (2008) Electrochemical synthesis of Zn-Al layered double hydroxide (LDH) films. Inorg Chem 47(13):5859

Zhang Q, Uchaker E, Candelaria SL, Cao G (2013) Nanomaterials for energy conversion and storage. Chem Soc Rev 42(7):3127

Zhang X, Li K, Li H, Lu J, Fu Q, Zhang L (2016) Hydrothermal synthesis of cobalt oxide porous nanoribbons anchored with reduced graphene oxide for hydrogen peroxide detection. J Nanopart Res 18(8)

Zhang S, Gao H, Zhou J, Jiang F, Zhang Z (2019) Hydrothermal synthesis of reduced graphene oxide-modified $NiCo_2O_4$ nanowire arrays with enhanced reactivity for supercapacitors. J Alloys Compd 792

Всё для победы!
НАРОДНЫЙ ФРОНТ
https://pobeda.onf.ru/
LET'S HELP THE RUSSIA

Nanopapers-Based Biosensors for Point-of-Care Diagnostics

18

Yachana Gupta, Aditya Sharma, and Chandra Mouli Pandey

Contents

1 Introduction . . . 384
  1.1 Origin of Paper . . . 385
2 Paper Substrates Used for POC Diagnostics . . . 385
  2.1 Whatman Paper . . . 386
  2.2 Cellulose Paper . . . 386
  2.3 Fiber-Based Paper . . . 390
  2.4 Glossy Paper . . . 393
3 Nanomaterial-Modified Paper Substrate . . . 393
  3.1 Conducting Polymer-Modified Paper . . . 393
  3.2 Carbonaceous Nanomaterial-Based Nanopapers . . . 395
  3.3 CNTs-Modified Nanopapers . . . 395
  3.4 Graphene Nanopapers . . . 395
  3.5 Miscellaneous Carbon-Based Nanopapers . . . 396
  3.6 Metal- and Metal Oxide-Modified Nanopaper . . . 397
4 Nanopaper for POC Diagnostics . . . 398
  4.1 Nanopaper-Based Nucleic Acid Detection . . . 398
  4.2 Nanopapers for Immunosensor Application . . . 398
  4.3 Nanopapers for Aptamer Detection . . . 399
  4.4 Nanopapers for Enzymatic Biosensors . . . 400
5 Conclusion . . . 400
References . . . 403

Y. Gupta · A. Sharma (✉)
Applied Science Department, The NorthCap University, Gurugram, Haryana, India
e-mail: adityasharma@ncuindia.edu

C. M. Pandey (✉)
Department of Chemistry, Faculty of Science, SGT University, Gurugram, Haryana, India
e-mail: cmp.npl@gmail.com; chandramouli_fosc@sgtuniversity.org

© Springer Nature Singapore Pte Ltd. 2023

U. P. Azad, P. Chandra (eds.), *Handbook of Nanobioelectrochemistry*,
https://doi.org/10.1007/978-981-19-9437-1_18

Abstract

The emerging demand for low-cost biosensors has resulted in the introduction of non-rigid precursors that are flexible, disposable, biocompatible, and environment friendly. In this context, the nanopaper-based substrate has drawn significant interest among the research community as it has paved a new way to substitute the conventional substrate. In this chapter, we will describe different types of paper that are being used to produce affordable, low-cost biosensing platforms. The modification of the paper substrate with nanomaterials and its various biosensing applications have been discussed. The emerging application of nano paper in point-of-care diagnostics has been highlighted. Furthermore, the challenges and the prospects of these nano paper-based biosensors are summarized.

Keywords

Nanopapers · Nanomaterials · Conducting polymers · Point-of-care devices · Biosensors

1 Introduction

The application of nano papers in biosensor devices has been assessed day after day since it has been proven that the on-site diagnosis can radically retard the development of a disease. In clinical trial guidelines, the World Health Organization (WHO) concluded that nano paper-based sensors are sensitive, specific, and available for diagnosis at the point-of-care (POC) (Solanki and Pandey 2016). Paper substrates offer resourceful technology as they are readily available in various forms and have unique properties such as portability, ease of access, and low cost (Byrnes et al. 2013, Lee and Lee 2021). Furthermore, incorporating nanomaterials with paper is anticipated to spur potential approaches for discovery, including advances in their stability/strength, lifespan, and other analytical performance enhancements such as in various detection techniques (Jaiswal et al. 2018, Khan et al. 2019, Yaqoob et al. 2020). Due to their permeable and hydrophilic properties cellulose-based papers are widely used for POC diagnostics, allowing on-site diagnosis of disease and inflammation without needing sophisticated equipment (Nayak et al. 2017, Nishat et al. 2021). In recent years, paper-based microfluidics (MF) have been explored by sequencing paper with lyophobic obstacles to describe lipophilic channels and regions to constrain fluid flow at a predicted position or maintain fluid flow in preferred imprints. Several techniques have been developed for manufacturing hydrophobic barriers, such as laser processing, wax printing, flexography, photolithography, screen printing, plasma processing, and flexography. Several methods such as chemiluminescence, colorimetric detection, fluorescence, mass spectrum, electrochemical detection, and Raman spectroscopy with surface enhancement (SERS) have been used to develop paper-based sensors and devices. Regarding the main objective to be accomplished, numerous modification techniques and analytical methods have been used to meet the end-user's requirements in paper-based biosensors (Pandey et al. 2016). In this context, nanopaper-based biosensors provide requisite sensitivity, selection, and discriminatory treatment of multiple analytes and can better serve today's objectives with cost-efficient and portable equipment (Kumar et al. 2016a).

1.1 Origin of Paper

Paper has been introduced to the analytical world for centuries, starting from the 1800s, when Gay-Lussac discovered a litmus test to determine acid (Nye 1979). In 1906, a chromatographic-based spot test was performed to analyze bilirubin in urine samples (Morgan and Wilson 2004). Paper-based device has been developed using paraffin stamping for chromatographic discrimination in diagnosing pigments and dyes (Müller and Clegg 1949). The history of paper-based biosensors began with Synge and Martin's invention of chromatography paper, for which they received the Nobel Prize in chemistry in 1952. After that various techniques such as electrophoresis and colorimetric were introduced to develop hydrophobic barriers on a paper substrate. The electrophoresis technique was used on paper to separate multiple proteins, and the colorimetric technique was presented on filter paper (Noviana et al. 2020a). The dextro-stix glucose dipstick using commercial paper was first introduced in 1964 (Doumas 2006). Singer and Plotz achieved yet another milestone in 1956 when they developed the first lateral flow assay POC biosensor to diagnose rheumatoid arthritis (Singer and Plotz 1956). The first lateral flow assay (LFA) for identifying human chorionic gonadotropin hormone in urine was introduced (Vaitukaitis et al. 1972). Following the urine test, the LFA device has been consistently used for POC detection of multiple infectious diseases (Koczula and Gallotta 2016, Gupta and Ghrera 2021). The Whiteside group introduced a reliable and robust POC platform for various research applications based on the MF paper (Martinez et al. 2010). In 2011, a team at McMaster University developed another form of bioactive paper (Pelton 2009) to detect food, aquatic bacteria and pesticides (Gupta and Ghrera 2021). Nowadays, various paper-based biosensors are being used for diagnostic purposes, and in the following section, we will discuss some of the widely used paper substrates for POC applications.

2 Paper Substrates Used for POC Diagnostics

In developing POC devices, the choice of paper substrate for the desired applications is critical because each type of paper has its own properties, such as retention capacity, pore size, flow rate, hydrophilic and hydrophobic properties. Whatman paper, glass fiber paper, cellulose paper, and glossy paper seem to be the most frequently used. The different type of papers used in nanopaper fabrication and their potential application has been summarized in Fig. 18.1.

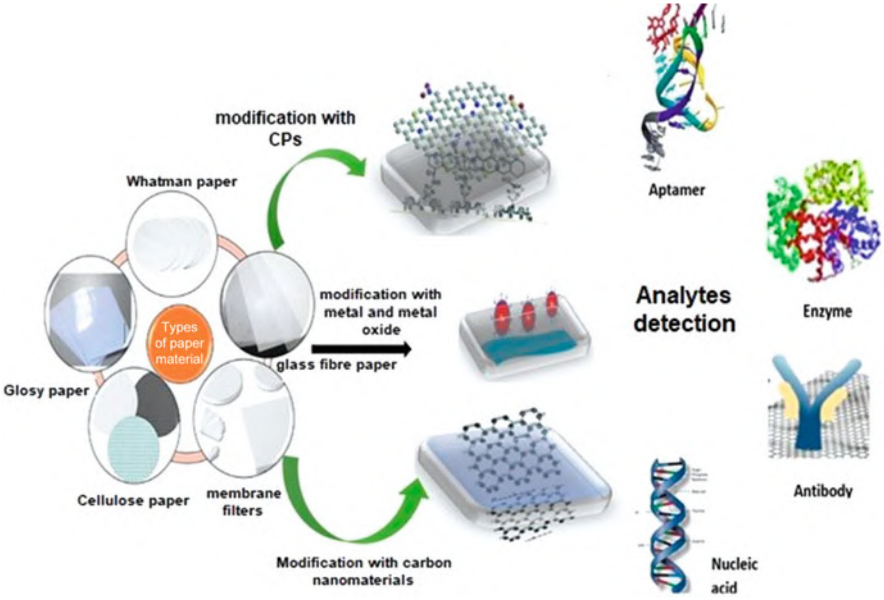
modification with CPs
Whatman paper
Aptamer
Enzyme
Analytes detection
modification with metal and metal oxide
glass fibre paper
Types of paper material
Glosy paper
Antibody
Cellulose paper
membrane filters
Modification with carbon nanomaterials
Nucleic acid

Fig. 18.1 Schematic showing different types of nanopaper used for biosensor fabrication

2.1 Whatman Paper

Whatman paper (WP) is one of the most common papers used in chromatography because of its excellent wicking ability. WP shows good chemical compatibility with the solution, and thus, it is suitable for POC diagnostics. WP are available in different grades, and each grade differs in its pore size and the fluidic rate, which further affects the absorbance of the sample from the surface, diffusion of reagents, chemical interference, manufacturing method, and time required to coat the surface. Various techniques such as wax printing, wax dipping, photolithography, polydimethylsiloxane (PDMS) ink, SU-8 photoresist, and screen printing are used to develop a hydrophobic pattern in WP. Some of the reported literature on the biosensing application of WP has been summarized in Table 18.1.

2.2 Cellulose Paper

Cellulose is formulated with the most renewable biopolymer as it exhibits good saturation and absorption ability. It is naturally derived from plants and non-pathogenic bacteria, particularly from the *Gluconacetobacter* genus. *Gluconacetobacter* is associated with producing a unique type of cellulose with good mechanical and structural properties that can be used in various sensor applications (Kumar Gupta et al. 2019, Ratajczak and Stobiecka 2020). Nanoporous

Table 18.1 Various categories of WP grades are used for the detection of different analytes

WP grade type	Pore size	Detection method	Target analyte	References
Whatman#1	11 um	Electrochemical, Electrochemiluminescence	1. Glucose, lactate, and uric acid,	Dungchai et al. (2009)
			2. Heavy-metal ions and glucose	Nie et al. (2010)
			3. Troponin	Jagadeesan et al. (2012)
			4. Glucose oxidase	Tan et al. (2012)
			5. Neomycin	Wu et al. (2012)
			6. Glucose	Määttänen et al. (2013),
			7. Carbohydrate antigen	Määttänen et al. (2013), Yang et al. (2014)
			8. Zika virus	Jiang et al. (2017)
Whatman# 903	0.1–0.45 μm	ELISA, Serological method, Microscopic agglutination test Blood spot screening	Dengu virus, Chikungunya virus Human leptospirosis, Syphilis	Tran et al. (2006), Grivard et al. (2007), Desvars et al. (2011), Stevens et al. (1992)
Whatman CHR # 1	0.18 mm	ELISA	Haptoglobin	Busin et al. (2016)
Whatman 42	2.5 um	ELISA	T7 bacteriophage	Khan et al. (2015)
Whatman # 3	6 μm	Colorimetric Loop-mediated isothermal amplification	Drug-resistant in antibiotics, Multiple schistosome parasites	Punjabi et al. (2020), Lodh et al. (2017)
Whatman# BA85	0.45 μm	Electrochemical	Glucose	Li et al. (2015)
Whatmann# 41	20 μm	ELISA	Fluidic device for multiple analytes	Gerbers et al. (2014)
Whatman # 113	150 mm	Microscopic agglutination test	Device formation of unknown blood samples and ABO type blood samples	Songjaroen et al. (2018)
Whatman# 5	2.5 μm	Matrix composite method	Human serum albumin	Shen et al. (2019)

cellulose paper-based SERS platform has been reported for precise and accurate diagnosis of multiple synthetic insecticides. Different ratios of gold nanoparticles (AuNP) were deposited on a nano-cellulose paper substrate (Kwon et al. 2019). Based on the results, it was concluded that the properties of cellulose fiber-based papers and the new properties of nano-cellulose make cellulose polymer among the most enticing and innovative materials in several research applications. Cellulose has been activated in various forms such as aerosols, sponges, plastics, fibers, and films, used for several biosensing applications (Lin and Dufresne 2014, Ciolacu et al. 2016, Nicu et al. 2021). The different forms of cellulose-based paper that have been used for POC applications have been summarized in Table 18.2.

2.2.1 Cellulose Acetate

Cellulose is hydrophilic, whereas cellulose acetate (CA) is hydrophobic, and both of them are thermoplastic polymers. Due to the highly packed structure, cellulose is insoluble in organic solvents, whereas soluble in organic solvents and can flow with heat. CA is the ester form of cellulose that can be used for film formation (Kamel and Khattab 2020), membrane fibers (Khan et al. 2016), and sensor applications. The amperometric signal detection technique used CA paper to identify glucose from whole blood (Ahmadi et al. 2021). In another report a conductive CA paper using the electro-spinning technique has been prepared for the 25-hydroxyvitamin-D3 detection (Chauhan and Solanki 2019). The DNA-AuNP conjugated-CA nanofiber was used to establish portable colorimetric strips for kanamycin detection (Abedalwafa et al. 2020). In this work, pyromellitic dianhydride was cross-linked with CA film to enhance the signals. Using coated CA on the electrode, a mouth-guard biosensor for the interpretation of salivary glucose was evaluated. The different characteristics of coated CA biosensor were predicted by artificial saliva and the sensor was successfully used for the diabetic patients (Arakawa et al. 2020). CA can often be used before enzyme immobilization and it may improve the process of incorporating biological elements into cellulose or for increasing the efficiency of the biosensor.

2.2.2 Nitrocellulose Membrane

The hydrophobic nitrocellulose membrane (NCM) is formed by the interaction of hydrochloric acid and cellulose (Jamal et al. 2020). The NCM has a negatively charged surface owing to the influence of a nitro group. It can accumulate positively charged functional groups of biomolecules. NCM has been used as a predominant matrix in protein staining due to its compatibility, pore size, and high binding affinity to the protein. NCM is available in pore sizes of about 0.1, 0.2, or 0.45 μm, which are well suited for fabricating POC devices. The pore size of the NCM has a significant impact on adsorption capacity because varying NCM pore sizes display different adsorbing affinities for biomolecules (Fridley et al. 2013). The primary benefit of NCM-based biosensors is their ability to incorporate biorecognition principles into analytical devices, making them hypersensitive and innovative over sophisticated instrumental techniques.

Table 18.2 Existing modification and detection approaches used for the development of cellulose-based biosensor strip

Type of cellulose	Detection technique	Modifications	Types of sensors	Target analyte/ Molecules	Limit of detection/ sensitivity	References
NCM	Colorimetric assay	PDMS as the polymeric matrix;	Color sensor	Acinetobacterbaumannii	450 CFU per reaction	Wu et al. (2018)
NCM	Spectroscopy	Quartz crystal microbalance	Humidity sensor	Humidity	25.6 Hz/% RH	Tang et al. (2021a,b)
NCM	Photoluminescence	molecularly imprinted nanoparticles	Photoluminescent-based nanosensor	Tributyltin	0.23 ppt	Sari et al. (2019)
NCM	ELISA	Magnetic beads	Magnetic sensors	Influenza A virus	–	Hong et al. (2011)
NCM	LFIA	Electrospin-coating polycaprolactone		Nucleic acid	–	Yew et al. (2018)
NCM	Fluorometric assay	Molecularly imprinted nanoparticles	Fluorescent nanosensors	BisphenolA	43.9 ± 0.8 μg·L – 1	Üzek et al. (2019)
CA	Electro-spinning	Tungsten oxide (WO3) nanoparticles	Gas sensor	H2S	1 ppm.	Abdel Rahman et al. (2021)
CA	Fluorescence	Pluronic and polyethylene glycol	Optical sensor	Ethanol	0.29%	Mulijani et al. (2018)
CA	Spectrophotometry	Pyrogallol red	Optical sensor	Co(II)	3.6×10^{-7} M	Ensafi and Aboutalebi (2005)
CA	Electrochemical	Chitosan	Electrochemical sensor	Glucose	–	Yezer and Demirkol (2020)

2.3 Fiber-Based Paper

Fiber-based paper is usually cotton rag fibers or high-grade wood pulp, upon which an ink-receptive coating is directly applied. Fiber-based paper is coated with a photographic emulsion and used for improved wet strength and grease resistance. According to WHO recommendations, fiber sensing platforms are currently of great importance for POC diagnosis and much attention is being paid to their efficient implementation in biosensors to identify various analytes. Fiber-based paper sensors are typically inexpensive and provide a large area for biomolecular contact owing to

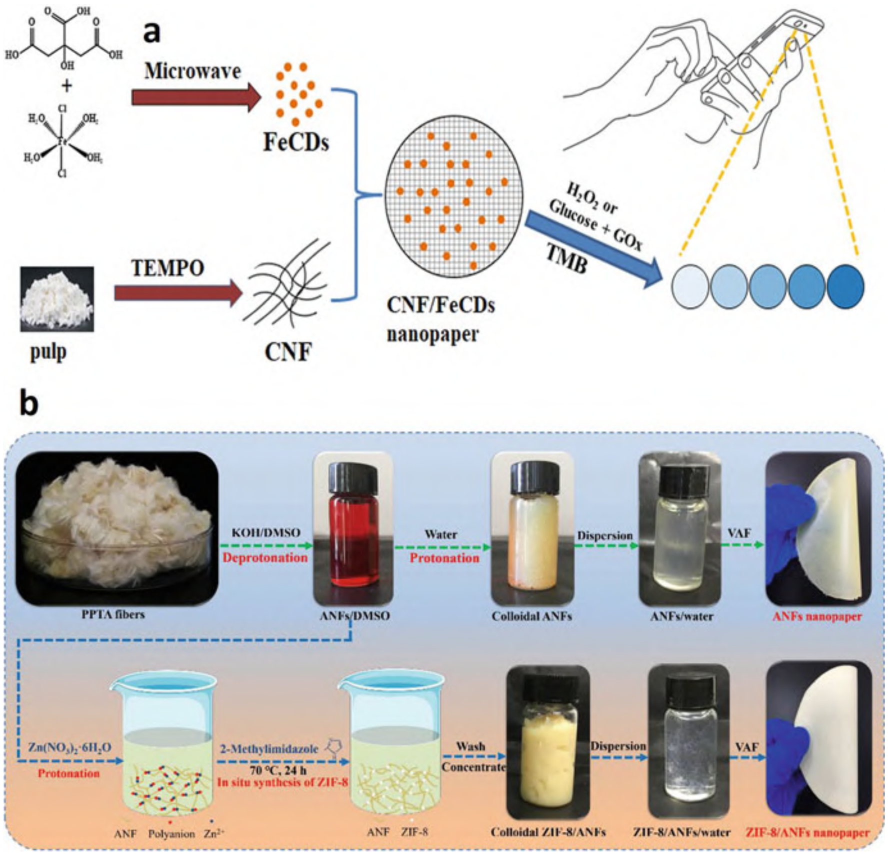
a
Microwave
FeCDs
TEMPO
pulp
CNF
CNF/FeCDs nanopaper
H2O2 or Glucose + GOx
TMB
b
KOH/DMSO
Deprotonation
Water
Protonation
Dispersion
VAF
PPTA fibers
ANFs/DMSO
Colloidal ANFs
ANFs/water
ANFs nanopaper
Zn(NO3)2·6H2O
Protonation
2-Methylimidazole
70 °C, 24 h
In situ synthesis of ZIF-8
Wash
Concentrate
Dispersion
VAF
ANF Polyanion Zn2+
ANF ZIF-8
Colloidal ZIF-8/ANFs
ZIF-8/ANFs/water
ZIF-8/ANFs nanopaper

Fig. 18.2 Modification of paper substrate with different nanomaterials (**a**) Scheme shows the development of cellulose nanofibrils/carbon dots composite nanopapers for hydrogen peroxide and glucose (Bandi et al. 2021). (**b**) Fabrication of zeolitic imidazolate framework-8/aramid nanofibers composite nanopaper (Yang et al. 2020). (**c**) Schematic representation of the process of obtaining cellulose nanofibrils composite nanopapers (Ma et al. 2019). (**d**) Nanostructured iron oxide-modified conducting paper sensor for cancer biomarker detection (Kumar et al. 2019b)

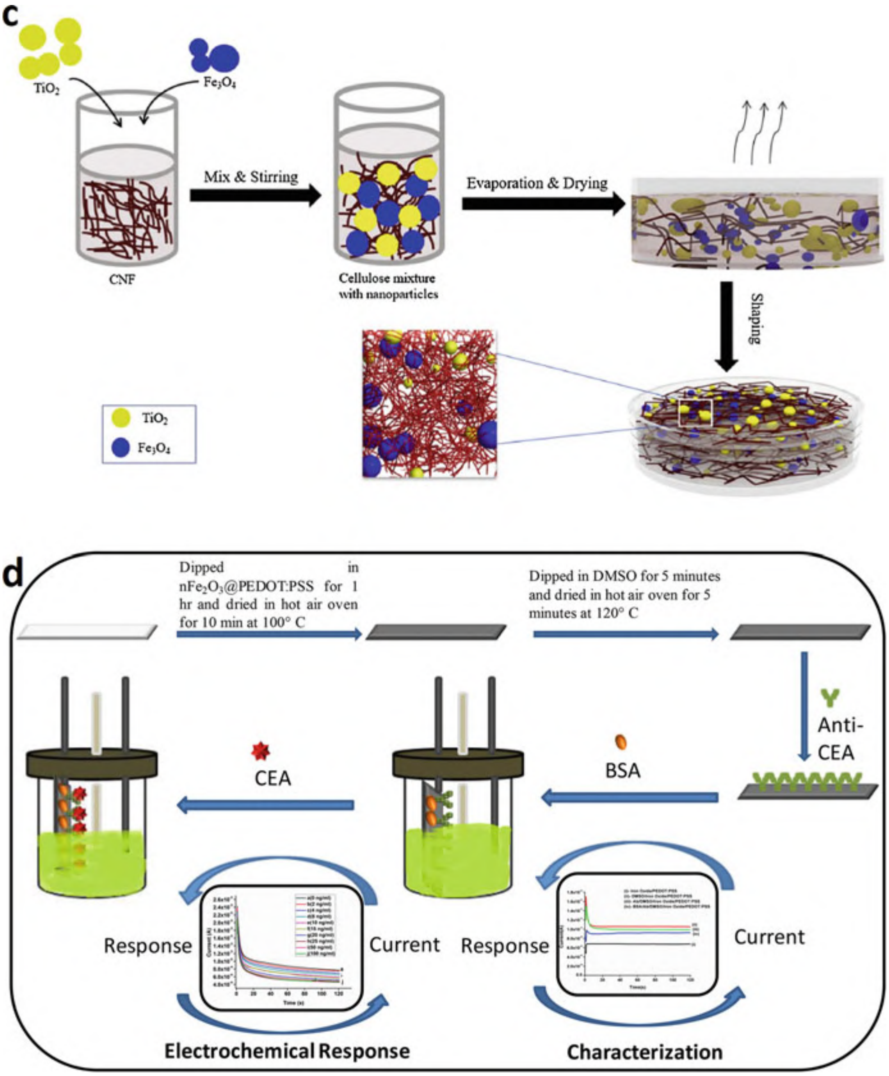
c
TiO$_2$
Fe$_3$O$_4$
CNF
Mix & Stirring
Cellulose mixture with nanoparticles
Evaporation & Drying
Shaping
TiO$_2$
Fe$_3$O$_4$
d
Dipped in nFe$_2$O$_3$@PEDOT:PSS for 1 hr and dried in hot air oven for 10 min at 100° C
Dipped in DMSO for 5 minutes and dried in hot air oven for 5 minutes at 120° C
Anti-CEA
BSA
CEA
Response
Current
Response
Current
Electrochemical Response
Characterization

Fig. 18.2 (continued)

their high permeability. They are commonly used for high-quality printing, display, and archiving for sensing applications. Fibers are usually tiny in size ranging from 0.0007 μm to 8 μm. The weight of fiber-based paper is about 255 g per square meter or higher. Currently, glass fiber and nylon-based paper have gained much attention in POC diagnostic applications (Fig. 18.2).

2.3.1 Glass Fiber

Glass fiber comprises a silica matrix and has a pore size of 0.7 μm. It has thermal insulation properties, heat resistance, and outstanding stability and thus, presents little extension and retrenchment under various experimental conditions. Because of its good absorption ability and very high loading capacity, glass fiber can readily absorb nanoparticles and biomolecules (proteins and nucleic acids), making it a promising matrix for POC application. A variety of glass fiber-based sensing platforms has been reported in the literature. Cadmium telluride quantum dots-modified glass fiber paper (GFP)-based fluorescent sensor was evaluated for the rapid and multiplex detection of Hg^{2+} and Cu^{2+} ions (Qi et al. 2017). The reduction method was assessed for the deposition of silver nanoparticles (AgNP) on a glass fiber paper surface for signal enhancement to diagnose malachite green in fish (Deng et al. 2019). Another study used the SERS detection technique on AgNP-modified glass fiber paper substrate to detect dibenzothiophene (Ye et al. 2020). For the early screening of methyl parathion pesticides, a GFP-based optical biosensor was evaluated. As a biocomponent, whole cells of *Flavobacterium* were immobilized on the GFP surface, presenting homogeneity and high methyl parathion reproducibility (Kumar et al. 2006). A molecular imprinted polymer-based 3D rotary MF paper device was developed, where an aqueous solution of ZnSe quantum dots imprinted polymers was transferred to the solid GFP for the testing of Cd^{2+} and Pb^{2+} ions (Zhou et al. 2020b). The above-mentioned GFP sensor studies have shown that the SERS detection technique can be used for POC detection of multiple analytes.

2.3.2 Nylon Fiber-Based Paper

Nylon is a polyamide formed through the condensation reaction of the amine group and carboxylic acid groups. Since it contains terminal functional groups such as carboxylic acid and amine, it enables covalent immobilization of the biomolecule over the paper membrane, making it suitable as a sensory platform. Nylon is mainly used for chemical and thermal stability because it has water-resistant and strong mechanical properties (Wang et al. 2021). The most commonly known forms of nylon are nylon-6,6 and nylon-6. However, the nylon-6 paper membrane has been widely used for biosensing applications. The covalently modified Nylon-6 nanofibrous membrane (N6NFM) was used for spectrophotometric verification of carcinogenic alkylating fumigants (Tang et al. 2019). In another study, the authors used the same sensing platform for the colorimetric detection of chloropicrin vapor in the air. This study was based on the detoxification response of biological thiols such as cysteamine, thioglycolic acid, homocysteine, glutathione, and N-acetyl-L-cysteine. N6NFM was used as a compact surface for chloropicrin vapor adsorption (Tang et al. 2018). Another quantitative N6NFM sensor was evaluated for formaldehyde detection by using electro-spinning. After interacting with formaldehyde, the sensor provided a significant spectral response band at 550 nm, causing the graphic appearance to change from yellow to red color (Wang et al. 2012). A nylon-based solid-phase colorimetric plasmon sensor was developed for detecting volatile sulfide compounds such as $(CH_3)_2S$, H_2S, and CH_3SH in breath samples. AgNP was used as auxiliary material, and the nature of AgNP was investigated using spectroscopy

(Jornet-Martínez et al. 2019). The chemical and physical stability of the evaluated sensors based on nylon fiber eliminates the possibility of quantitative performance errors and ensures precise detection results. Thus, nylon fiber-based paper can be used as an excellent sensor platform for various biomedical applications due to its film thickness for biomolecular stabilization and its good strength, desirable SERS functionality, low cost, and durability.

2.4 Glossy Paper

Glossy paper-based devices have recently been explored as a sensing platform for POC diagnostics. For biosensor fabrication, glossy papers are coated with various polymeric nanocomposites. However, it is a good substitute for the fibrous matrix-like filter paper, especially when the surface is modified with nanomaterials. The glossy paper was modified with indium tin oxide nanopowder and poly-diallyl dimethyl ammonium chloride composite for ethanol sensing using electron micro-spectroscopy technique (Arena et al. 2010). The Cole-Cole impedance model has been used to develop an inkjet-printed graphene sensor on glossy photo paper to monitor breathing rate (Lu et al. 2019). In another application, an electrochemical system on a patterned glossy paper was designed for the expansion of a glucose sensor for diabetic patients. The electrochemical setup was designed on copper tape and fixed on the patterned glossy paper (Khoshroo et al. 2020).

3 Nanomaterial-Modified Paper Substrate

A wide variety of nanomaterials have recently been used in the advancement of paper-based POC devices (Gupta et al. 2022). The modification of paper with nanomaterials enhances the chemical and physical properties such as surface charge, wet strength, and so on. Further, the lyophilic and lyophobic of the paper can be altered, and various functional groups can be introduced to the paper substrate by modifying it with suitable nanomaterials. Modification of paper substrate with the nanomaterials is a way that allows them to interact with the biomolecules on the surface. Because of the outstanding intermolecular interactions between the nanomaterial and the paper surface. Paper modified with nanomaterials has received much interest when compared to the un-modified paper surface. Several nanomaterials such as conducting polymers, carbonaceous materials (such as CNTs, graphene), and metallic nanoparticles have been employed for the modifications of the paper substrate.

3.1 Conducting Polymer-Modified Paper

Conducting polymers (CPs) are organic polymers with alternating double and single bonds along the polymer backbone and have intrinsically high electrical conductivities (Soni et al. 2015). The prime advantage of CP lies in its processability, mainly through dispersion. The commonly used CP for biosensor application includes polycarbazoles, polyaniline (PANI), polyindoles. Poly(3,4-ethylene dioxythiophene) (PEDOT), polyvinylpyrrolidone (PVP), polypyrrole (PPy), poly (p-phenylene sulfide), polyvinylpyrrolidone (PVP), and so on. CPs have been used in various biosensing applications, particularly for electrical and electrochemical biosensor fabrication (Nezakati et al. 2018). A composite polymer graphene/PVP/PANI-based disposable sensor was reported for the electrochemical detection of cholesterol (Ruecha et al. 2014). For the detection of ascorbic acid, a screen-printed disposable paper-based electrochemical sensor was fabricated using PANI (Kit-Anan et al. 2012). Whatman paper-1was sputtered with Au, which was further modified with PANI. The modified paper electrode was further used to detect anti-carcinoembryonic antigen (CEA) protein (Kumar et al. 2016a). The same group has also fabricated an impedimetric biosensor using PEDOT:PSS, which was self-assembled on the WP, resulting in an enhanced electrochemical signal (Kumar et al. 2016b). The electrochemical performance of the PEDOT:PSS-modified WP has been further improved by incorporating iron oxide nanoparticles with the conducting paper (Kumar et al. 2019b). Graphene was incorporated with PEDOT:PSS-modified WP to obtain an improved electrochemical signal. The modified paper was used for CEA detection using electrochemical impedance spectroscopy (Yen et al. 2020). A novel label-free potentiometric paper-based immunosensor has been reported, where the sensor was modified with PEDOT:PSS that showed remarkable performance for detecting *Salmonella typhimurium*. As sensitive layers, PEDOT:PSS and multi-wall carbon nanotubes (MWCNT) composite material were used to develop a gas sensor to detect volatile organic compounds in the air (George et al. 2019). PEDOT:PSS polymer showed a remarkable performance in enhancing the signal and real-time detection of the food-borne pathogen (Silva et al. 2019). PPy has also been widely used to modify paper for improving electroactivity and electrical conductivity. An electrochemical sensor has been developed by electrodepositing ruthenium-phosphate on PPy-modified carbon fiber paper. The sensor was successfully used to detect ultra-low cholesterol in human serum samples without the use of enzymes (Akshaya et al. 2019). A potentiometric sensor was developed on a typical PPy-based ion-selective membrane with the modification of PPy nanoparticles (Jaworska et al. 2017). The gas sensing applications were studied, followed by vapor phase polymerization on PPy-coated filter paper (Majumdar et al. 2020). For the development of an advanced combination of fabrics with nanoparticles, the paper substrate was modified with PES for the detection of Fe^{3+}. This combination of sensors exhibited excellent solvent resistance and thermal stability (Yu et al. 2021). In another approach, the CA membrane was modified with graphene-based materials and their composite with polyindole. The GO/polyindole composites-modified paper was used to determine methanol vapor (Phasuksom et al. 2020). The use of conductive polymer and its nanocomposites leads to the formation of a more allosteric site on a substrate surface, which improves the sensing capability of the paper substrate. The paper modification with CPs and its nanocomposite may lead to the development of cost-effective, affordable POC devices having high sensitivity and selectivity.

3.2 Carbonaceous Nanomaterial-Based Nanopapers

Carbonaceous nanomaterials (CNMs) have received considerable attention in biosensor applications because of their unique physicochemical properties. Carbon in its various allotropic forms (graphite, amorphous carbon, and diamond) has been widely used in the growth of advanced biosensors. The most commonly used CNMs for the paper substrate modification include graphene oxide (GO), carbon nanotubes (CNTs), and graphene quantum dots. These CNMs exhibit unique properties are discussed in detail in the following section (Maiti et al. 2019, Yue et al. 2020, Wei et al. 2021).

3.3 CNTs-Modified Nanopapers

Carbon nanotubes (CNTs) have received considerable attention in the field of biosensors since they have structural diversity, excellent thermal conductivity, and mechanical and electrical properties. Because of their high tensile strength and hollow structure, CNTs have unique properties that allow them to absorb a substantial percentage of biomolecules on their surface via electronic interactions. The electrical properties of CNTs demonstrate excellent carrier mobility, near-ideal quantum efficiency, and an ultra-thin package, which allows them to be used on a scale of less than 8 nm (Bandaru 2007). Modifying a paper substrate with CNT may elucidate the signal intensity, conductivity, and catalytic activity and facilitate electron transfer due to the high surface area (Power et al. 2018; Tang et al. 2021b). For detecting bacteria in food samples, antibodies-modified SWCNT were used to minimize the functionalization step and enhance the stability of the paper electrochemical sensor (Bhardwaj et al. 2017). In another study, a glucose sensor was fabricated using SWCNT on a nitrocellulose membrane. With the modification of the paper substrate with SWCNT, the biosensor shows high conductivity and robust adhesion (Tran et al. 2018). An art paper-based electrochemical sensor was reported for bisphenol detection by loading AuNP onto MWCNT (Li et al. 2016). In another study, MWCNT, the fabricated paper was used for the detection of 17β-estradiol (Wang et al. 2018). CNTs have several unique properties that can be used to develop biosensors. Paper modifications with CNTs have demonstrated a remarkable combination of mechanical, electrical, thermal, optical, and electrochemical properties. Because of these characteristics, paper substrates serve as a unique platform for biosensor fabrication.

3.4 Graphene Nanopapers

Graphene is a monoatomic layer of sp^2 hybridized carbon atoms, and the exclusion of few and single-layer graphene can open a new avenue for the development of highly sensitive biosensors (Jalil et al. 2021). These graphene sheets have been considered to be a building block for the construction of various novel nanomaterials. Graphene oxide (GO), one of graphene's derivatives, has been identified as a versatile 2D building block for various applications owing to its unique structure and outstanding physicochemical characteristics. Recently, free-standing GO nanopapers have drawn much attention due to their flexibility and high physical properties. Reduced graphene oxide (rGO) nanopapers are indeed a promising candidate for sensing purposes because of their remarkable mechanical properties, stability, ionic conductivity, and biocompatibility. The GO-based nanopapers can be made by arranging the GO sheets onto the nanopapers so that the basal planes of the nanoplatelets are associated with one another and the interlayer spacing between parallel layers is reduced to achieve maximum interlayer interactions. Bottom-up and top-down synthetic strategies are often used to explore a range of graphene-based nanopapers. GO-based nanopapers with superior mechanical strength, flexibility, and tensile strength were produced in this perspective. TiO_2 nanobelts and graphene-based nanopapers were used to fabricate the paper substrate. The developed paper shows excellent electron transport properties and is used to develop photo-electrochemical biosensors. An amperometric biosensor has been fabricated to detect the htrA gene of Orientia (Kala et al. 2021). For the detection of POC tumor biomarkers, a low-cost, portable paper-based sensor modified with GO, thionine, and AuNP was reported. Graphene and its raw material modification results in excellent biocompatibility with the surface molecules (Fan et al. 2019),

Numerous studies have reported the outstanding properties of GO-modified nanopapers like low detection limit, sensitivity, ease of use, fast response and recovery times, and good selectivity. However, it is still necessary to determine parameters such as the number of optimal graphene layers or the best way to measure the response and the commercialization of the GO-modified nanopapers (Mahato et al. 2019, Patil et al. 2019, Yusof et al. 2019, Islam et al. 2021).

3.5 Miscellaneous Carbon-Based Nanopapers

Besides CNTs, GO, quantum dots, and so on, the nanopapers are also modified with other CNMs. Carbon black nanoparticles were used as a modifier to enhance the electrochemical signal of paper-based biosensors, which were further used to detect ascorbic acid (Cinti et al. 2018). A fluorescent paper-based sensor was developed by modifying the paper with PDMS and carbon dots hybrid to detect folic acid in orange juice samples (Li et al. 2020). An AuNP-modified graphite paper was used for the electrochemical detection of hydroquinone (Fan et al. 2016). Similarly, a graphite paper-based electrochemical sensor was evaluated for the tertiary butyl hydroquinone detection. In another report, an electrochemical biosensor was designed to determine bisphenol A (Li et al. 2016). For the fabrication of the sensor, AuNP was used and developed with AuNP (Chandra et al. 2012; Yue et al. 2016; Fan et al. 2017; Bhatnagar et al. 2018; Noviana et al. 2020b; Tang et al. 2021a). A non-enzymatic glucose sensor was developed by modifying the disposable paper screen-printed carbon electrode along with graphene and cobalt phthalocyanine (Chaiyo et al. 2018). A glucose biosensor was fabricated on the paper substrate by modifying the paper with carbon ink (Amor-Gutiérrez et al. 2017). For monitoring Parkinson's disease and hypertension, an electrochemical biosensing platform based on carbon dots graphite paper has been reported (Pandey et al. 2019). An affordable, paper-based sensor was developed to identify bacteria in water where the paper substrate was modified with screen-printed carbon electrodes, which led to enhanced electron transfer properties (Rengaraj et al. 2018). Homemade carbon ink was used on a CA membrane to produce a glucose sensor, which shows many advantageous properties such as fast analysis, requirements of low sample volume, and low cost (Rungsawang et al. 2016). To study the morphology of the paper-based sensor or to enhance the electrochemical signal, carbon black has been used on the paper surface (Cinti et al. 2017).

3.6 Metal- and Metal Oxide-Modified Nanopaper

In the development of nanopaper-based biosensors, metal and metal oxide are being used to increase the conductivity, surface charge resistance, sensitivity, and hydrophilic and hydrophobic interactions, as these metal and their oxides are surrounded by many small voids or holes that help in the movement of electrons from one place to another place. Various metals and their oxides such as Fe_2O_3, Cr_2O_3, TiO_2, NiO, Mn_2O_3, CuO, ZnO, Co_3O_4, MoO_3, SrO, WO_3, GeO_2, (Pandey et al. 2014, Deka et al. 2018, Saxena et al. 2018), and so on were used for surface modification because they provide exclusive characteristics such as biocompatibility, less cytotoxicity, and so on compared to equivalent larger-sized metals (Neouze and Schubert 2008, Cartwright et al. 2020). Due to their excellent chemical and physical properties, metal nanoparticles has been widely used in POC devices and can be applied directly as signaling agents (Shafey 2020). Pt nanoparticles-modified flexible electrochemical biosensor was developed on graphene paper using MnO_2 nanowire network. This modified sensor has been used for various applications in bioelectronics, biosensors, and lab-on-a-chip devices (Xiao et al. 2012). An AuNP-modified paper substrate-based impedimetric immunosensor was fabricated for the detection of *Escherichia coli*. The developed paper-based immunosensor shows promising results in terms of sensitivity, reproducibility, and stability (Wang et al. 2013). A flexible silanized-titanium dioxide-modified paper-based sensor has been used for quantitative analysis of Cr(VI) with the leaching of AuNP (Guo et al. 2016). A disposable art paper electrode was modified with AuNP and MWCNTs to determine bisphenol A (Li et al. 2016). An AuNP-deposited graphene-modified carbon electrode was used to develop a single device for the multiple steps of electrode modification for anti-C-reactive protein detection in human serum samples (Boonkaew et al. 2019).

4 Nanopaper for POC Diagnostics

Biosensing on paper is designed to detect various analytes such as nucleic acid, biomarker, aptamer, and so on, and evaluate MF devices. Analytes can be easily identified on the paper substrate because sensing on the paper substrate has several advantages: low thermal expansion, availability of raw material in excess, less expensive, biodegradable, high mechanical properties and reusability, and so on. The recent application of paper substrates for different analyte detection has been discussed in the following sections.

4.1 Nanopaper-Based Nucleic Acid Detection

For nucleic acid (NA) detection, the paper-based sensor serves as a POC (Hu et al. 2019) diagnostic platform with high sensitivity and specificity compared to other immunoassays. Some critical challenges, such as sample preparation, amplicon detection, and NA amplification, can be easily accomplished on a paper substrate (Choi et al. 2017). An electrochemical DNA biosensor has been reported to detect a synthetic 14-base oligonucleotide target with a sequence consistent with human papillomavirus (HPV) type 16 DNA. For this purpose, the paper electrode was modified with an anthraquinone-labeled pyrrolidinyl peptide NA probe and graphene-PANI nanocomposite (Teengam et al. 2017a). Further, a fluorescent and the colorimetric paper-based sensor was developed to detect DNA and RNA of *Mycobacterium tuberculosis*, Middle East Respiratory Syndrome coronavirus, and human papillomavirus (Teengam et al. 2017b). Further studies developed a fluorescent paper-based DNA sensor for hepatitis C virus detection in clinical samples (Teengam et al. 2021). In another work, a POC DNA amplification test was proposed to detect multiple genes of different analytes. This developed biosensor has been used for DNA amplification, sample transportation, and storage (Liu et al. 2020). An integrated DNA amplification, extraction, and detection system were evaluated for *Listeria monocytogenes*. A variety of gene sensing applications was studied on the paper substrate by the same authors (Fu et al. 2018). For the detection of miRNA-492, a paper-based electrochemical peptide nucleic acid biosensor was designed. This activity was performed on screen-printed office paper (Moccia et al. 2020). A sensitive and simple paper-based sensor has been reported to detect Zika virus RNA. The paper sensor was coupled with CRISPR/Cas9 molecule (Meagher et al. 2016). The nano paper-based sensing approach is an easy, cost-effective, and simple path for developing POC for NA detection.

4.2 Nanopapers for Immunosensor Application

Nanopapers have been used for various immunosensor applications such as chemiluminescence, plasmon surface resonance, optical, fluorescence, and so on. Wax and screen-printed paper-based electrochemical immunosensor were developed to modify paper substrate with MWCNTs/AuNP/thionine nanocomposite. The paper electrode was used for the early detection of 17β-estradiol (Wang et al. 2018). A paper strip integrated with a filter paper pad-based potentiometric immunosensor was developed to detect *Salmonella typhimurium*. The proposed design showed an expedient platform for sampling and antibody immobilization (Silva et al. 2019). Paper was modified with PANI/graphene to detect human interferon-gamma using a label-free paper-based electrochemical immunosensor (Ruecha et al. 2019). To detect the H1N1 influenza virus, a homemade, low-cost paper-based immunosensor was developed (Devarakonda et al. 2017). A cost-effective, MF paper-based immunosensor was designed for the early recognition of Aflatoxin B1in maize flour samples (Migliorini et al. 2020). The chief benefit of nanopaper-based immunosensors is the incessant and discriminating diagnosis of the analyte, resulting in real-time response. Nanopaper-based immunosensor also support quality control measures for on-site detection and help in the kinetic study of antigen-antibody reactions.

4.3 Nanopapers for Aptamer Detection

The single-stranded RNA/DNA or peptide molecules that can bind antigen-antibody for a specific target are aptamers or synthetic antibodies (Gopinath et al. 2012). Aptamers are generally used in envisaging, segregating, and tracing the cells. Aptamers offer a high affinity against a target compared to antibodies and are widely used in many areas of interest, and they play an essential role in clinical practice for the prevention and treatment of disease. A colorimetric polydiacetylene paper strip sensor detected target-specific aptamer *Bacillus thuringiensis*, HD-73 spores. The fabricated biosensor can detect the target without pre-treatment paper strips (Zhou et al. 2020a). A paper-based oligonucleotide aptamer recognition device was developed to detect multiple small molecule analytes in complex samples (Liu et al. 2021). Another paper-based potentiometric sensor was propoed to detect the Zika virus, in which the paper was dipped in a buffer solution containing oligonucleotides designed to bind to the Zika virus capsid proteins (Dolai and Tabib-Azar 2020). Paper-based colorimetric aptasensor was evaluated for the determination of lead ions. This study was performed on Whatman paper and nylon filter paper (Fakhri et al. 2018). An inkjet-printed RNA aptasensor was proposed for the detection of fluoroquinolone ciprofloxacin. Authors characterized the secondary structure of aptamer to determine antibiotic adulteration (Jaeger et al. 2019). A conjugated aptamer-AuNP fluorescent sensor was evaluated for the sensitive detection of recombinant human erythropoietin-α. In their study, 12 nm-sized AuNP is used as a function of nano quench and nano-scaffold (Sun et al. 2011). So, for the on-site detection of aptamer, paper-based POC sensors have been revealed to have appealing characteristics such as small sample requirement, high sensitivity, and real-time measurement capability (Huang et al. 2021).

4.4 Nanopapers for Enzymatic Biosensors

In developing enzymatic biosensors, the application of nanopapers has received enormous attention (Li et al. 2012, Janyasupab and Liu 2014, Hooda et al. 2018, Kumar et al. 2019a, Cho et al. 2020, Wang et al. 2020), because these biosensors are the largest group of biosensors with the most significant innovations. Electrochemical biosensors based on enzymatic nanopaper have been used to detect clinical biomarkers, small biomolecules, food contaminants, and environmental pollutants (Saylan et al. 2019). An enzymatic glucose biosensor based on the Nafion membrane modified with rGO-activated carbon composite has been reported. This developed biosensor exhibits negligible interference response and superior electrocatalytic activity for target glucose detection (Hossain and Park 2016). In developing a colorimetric paper sensor, a cellulose-binding recombinant enzyme was used for lactate dehydrogenase detection. The obtained results suggest that the biosensor can bind the enzyme to the paper substrate (Dai et al. 2017). Enzymatic activity was studied on the paper substrate, where the enzyme horseradish peroxidase and glucose oxidase were covalently immobilized on the paper surface (Böhm et al. 2018). Conducting paper modified with PEDOT:PSS-grafted rGO-titanium dioxide nanohybrid has been used to immobilize glucose oxidase for the quantitative estimation of glucose. The impacts of various solvents (methanol, glycerine, and ethylene glycol [EG]) on the conductivity of the paper were also studied, and it was found that with EG the conductivity of the paper significantly increases from 6.9 10^{-5} S/cm to 1.1 10^{-4} S/cm (Paul et al. 2021). In the advancement of the sensor strip, enzymatic biosensors have shown excellent performance due to the expansion of specific identification characteristics that can be used for in situ detection (Fig. 18.3).

5 Conclusion

Nanopapers have recently gained much attention in device fabrication due to their cost-effectiveness, easy availability, and non-toxic and biodegradable properties. The modification of paper with nanomaterial further improves its physicochemical characteristics, making it a more promising substrate for fabricating opto/electronic devices such as optical, electrical, and electrochemical biosensors. We have discussed various types of paper substrates used for biosensing applications and have compared their properties. This will help the reader better understand and select suitable paper substrates for biosensor fabrication. Furthermore, detailed literature has been presented on different nanomaterials class that is being used to tailor the paper substrate to achieve improved biosensing performance. With the recent developments in nanopaper-based biosensors, it can be predicted that it will emerge as the most appropriate sensing platform for POC diagnostics. Further, efforts should be made to develop paper-based biosensors with improved performance that can be combined with smartphones and Internet of Medical Things applications, leading to more versatile, user-friendly, and robust POC devices.

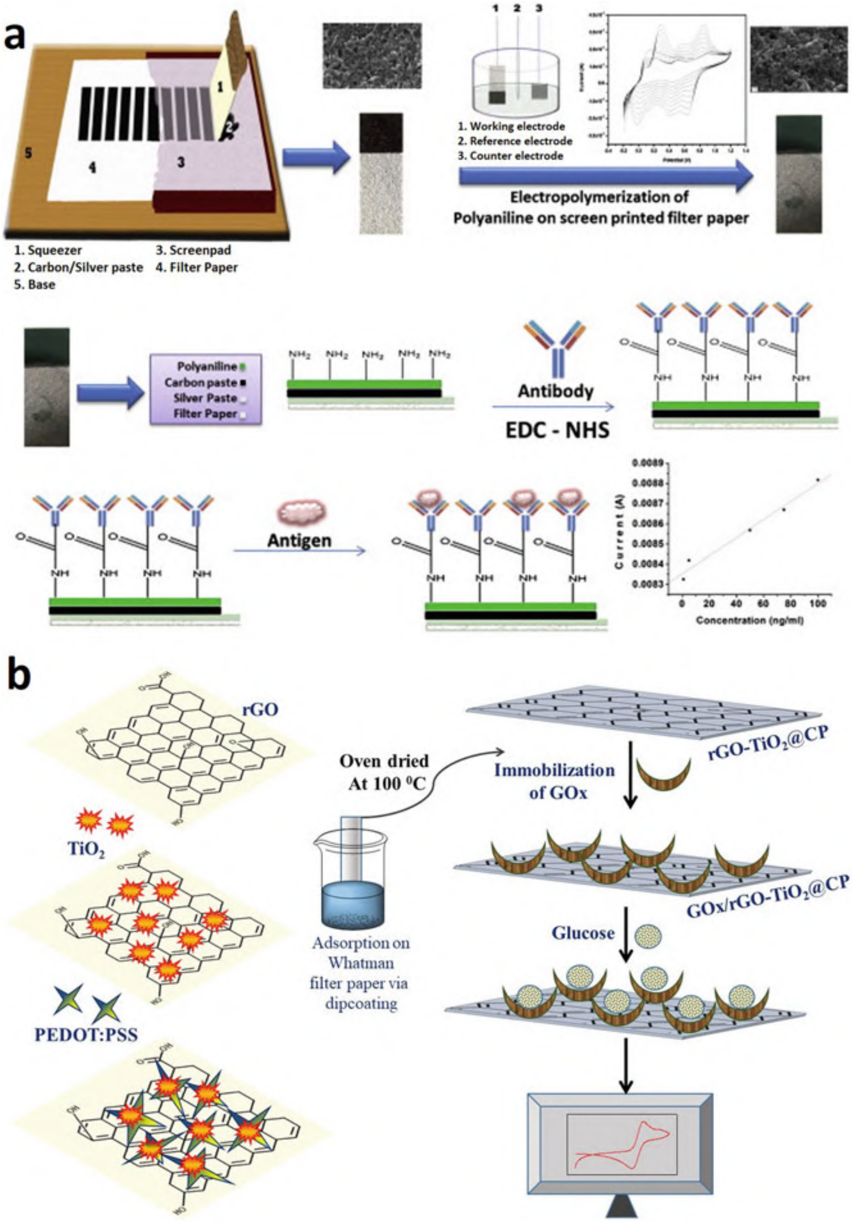
a
1
2
3
4
5
1. Squeezer
2. Carbon/Silver paste
3. Screenpad
4. Filter Paper
5. Base
1 2 3
1. Working electrode
2. Reference electrode
3. Counter electrode
Electropolymerization of Polyaniline on screen printed filter paper
Polyaniline
Carbon paste
Silver Paste
Filter Paper
NH₂ NH₂ NH₂ NH₂ NH₂
Antibody
EDC - NHS
NH
Antigen
Current (A)
0.0089
0.0088
0.0087
0.0086
0.0085
0.0084
0.0083
0 20 40 60 80 100
Concentration (ng/ml)
b
rGO
TiO₂
PEDOT:PSS
Oven dried At 100 °C
Adsorption on Whatman filter paper via dipcoating
Immobilization of GOx
rGO-TiO₂@CP
GOx/rGO-TiO₂@CP
Glucose

Fig. 18.3 Biosensing applications of nanopapers: (**a**) Screen-printed paper electrodes to detect cardiovascular markers (Jagadeesan et al. 2012). (**b**) Scheme showing the fabrication of rGO-TiO_2@CP-based enzymatic biosensor (Paul et al. 2021). (**c**) Schematic illustration of (i) electrode modification and (ii) immobilization and hybridization steps of a paper-based electrochemical DNA biosensor (Teengam et al. 2017a). (**d**) Schematic diagram of aptamer-based LFA (i), sandwich (ii), competitive (iii), and adsorption-desorption (iv) formats of aptamer-based LFAs (Huang et al. 2021)

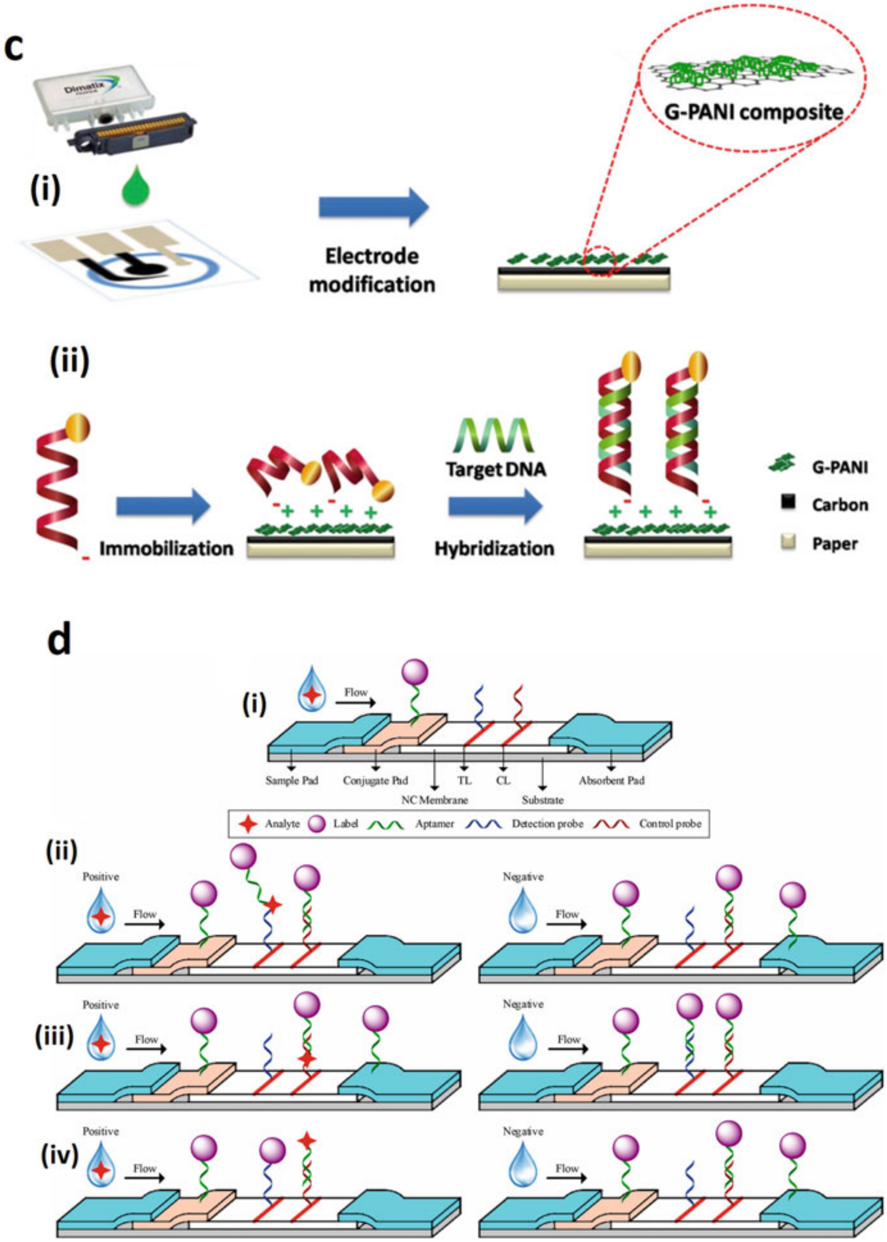
c
Dimatix
(i)
Electrode modification
G-PANI composite
(ii)
Immobilization
Target DNA
Hybridization
G-PANI
Carbon
Paper
d
(i)
Flow
Sample Pad
Conjugate Pad
NC Membrane
TL
CL
Substrate
Absorbent Pad
Analyte
Label
Aptamer
Detection probe
Control probe
(ii)
Positive
Flow
Negative
Flow
(iii)
Positive
Flow
Negative
Flow
(iv)
Positive
Flow
Negative
Flow

Fig. 18.3 (continued)

These nano paper-based devices can be used for mass testing and can help improve the healthcare system. Moreover, nano paper-based POC must not be limited to detecting disease, but efforts should also be made to use these nanopapers for agricultural and environmental applications.

References

Abdel Rahman NS, Greish YE, Mahmoud ST, Qamhieh NN, El-Maghraby HF, Zeze D (2021) Fabrication and characterization of cellulose acetate-based nanofibers and nanofilms for H_2S gas sensing application. Carbohydr Polym 258:117643

Abedalwafa MA, Tang Z, Qiao Y, Mei Q, Yang G, Li Y, Wang L (2020) An aptasensor strip-based colorimetric determination method for kanamycin using cellulose acetate nanofibers decorated DNA–gold nanoparticle bioconjugates. Microchim Acta 187(6):360

Ahmadi A, Khoshfetrat SM, Kabiri S, Fotouhi L, Dorraji PS, Omidfar K (2021) Impedimetric paper-based enzymatic biosensor using electrospun cellulose acetate nanofiber and reduced graphene oxide for detection of glucose from whole blood. IEEE Sensors J 21(7):9210–9217

Akshaya KB, Varghese A, Nidhin M, George L (2019) Amorphous Ru-Pi nanoclusters coated on polypyrrole modified carbon fiber paper for non-enzymatic electrochemical determination of cholesterol. J Electrochem Soc 166(12):B1016–B1027

Amor-Gutiérrez O, Costa Rama E, Costa-García A, Fernández-Abedul MT (2017) Paper-based maskless enzymatic sensor for glucose determination combining ink and wire electrodes. Biosens Bioelectron 93:40–45

Arakawa T, Tomoto K, Nitta H, Toma K, Takeuchi S, Sekita T, Minakuchi S, Mitsubayashi K (2020) A wearable cellulose acetate-coated mouthguard biosensor for in vivo salivary glucose measurement. Anal Chem 92:12201–12207

Arena A, Donato N, Saitta G, Bonavita A, Rizzo G, Neri G (2010) Flexible ethanol sensors on glossy paper substrates operating at room temperature. Sensors Actuators B Chem 145(1): 488–494

Bandaru PR (2007) Electrical properties and applications of carbon nanotube structures. J Nanosci Nanotechnol 7(4–5):1239–1267

Bandi R, Alle M, Park C-W, Han S-Y, Kwon G-J, Kim N-H, Kim J-C, Lee S-H (2021) Cellulose nanofibrils/carbon dots composite nanopapers for the smartphone-based colorimetric detection of hydrogen peroxide and glucose. Sensors Actuators B Chem 330:129330

Bhardwaj J, Devarakonda S, Kumar S, Jang J (2017) Development of a paper-based electrochemical immunosensor using an antibody-single walled carbon nanotubes bio-conjugate modified electrode for label-free detection of foodborne pathogens. Sensors Actuators B Chem 253: 115–123

Bhatnagar I, Mahato K, Ealla KKR, Asthana A, Chandra P (2018) Chitosan stabilized gold nanoparticle mediated self-assembled gliP nanobiosensor for diagnosis of Invasive Aspergillosis. Int J Biol Macromol 110:449–456

Böhm A, Trosien S, Avrutina O, Kolmar H, Biesalski M (2018) Covalent attachment of enzymes to paper fibers for paper-based analytical devices. Front Chem 6:214

Boonkaew S, Chaiyo S, Jampasa S, Rengpipat S, Siangproh W, Chailapakul O (2019) An origami paper-based electrochemical immunoassay for the C-reactive protein using a screen-printed carbon electrode modified with graphene and gold nanoparticles. Microchim Acta 186(3):153

Busin V, Burgess S, Shu W (2016) A novel multi-pad paper plate (MP3) based assays for rapid animal disease diagnostics. Procedia Eng 168:1418–1421

Byrnes S, Thiessen G, Fu E (2013) Progress in the development of paper-based diagnostics for low-resource point-of-care settings. Bioanalysis 5(22):2821–2836

Cartwright A, Jackson K, Morgan C, Anderson A, Britt DW (2020) A review of metal and metal-oxide nanoparticle coating technologies to inhibit agglomeration and increase bioactivity for agricultural applications. Agronomy 10(7):1018

Chaiyo S, Mehmeti E, Siangproh W, Hoang TL, Nguyen HP, Chailapakul O, Kalcher K (2018) Non-enzymatic electrochemical detection of glucose with a disposable paper-based sensor using a cobalt phthalocyanine–ionic liquid–graphene composite. Biosens Bioelectron 102:113–120

Chandra P, Koh WCA, Noh H-B, Shim Y-B (2012) In vitro monitoring of i-NOS concentrations with an immunosensor: The inhibitory effect of endocrine disruptors on i-NOS release. Biosens Bioelectron 32(1):278–282

Chauhan D, Solanki PR (2019) Hydrophilic and insoluble electrospun cellulose acetate fiber-based biosensing platform for 25-hydroxy vitamin-D3 detection. ACS Applied Polymer Materials 1(7):1613–1623

Cho I-H, Kim DH, Park S (2020) Electrochemical biosensors: perspective on functional nanomaterials for on-site analysis. Biomater Res 24(1):6

Choi JR, Yong KW, Tang R, Gong Y, Wen T, Li F, Pingguan-Murphy B, Bai D, Xu F (2017) Advances and challenges of fully integrated paper-based point-of-care nucleic acid testing. TrAC Trends Anal Chem 93:37–50

Cinti S, Mazzaracchio V, Cacciotti I, Moscone D, Arduini F (2017) Carbon black-modified electrodes screen-printed onto paper towel, waxed paper and parafilm M®. Sensors 17(10):2267

Cinti S, Colozza N, Cacciotti I, Moscone D, Polomoshnov M, Sowade E, Baumann RR, Arduini F (2018) Electroanalysis moves towards paper-based printed electronics: carbon black nano-modified inkjet-printed sensor for ascorbic acid detection as a case study. Sensors Actuators B Chem 265:155–160

Ciolacu D, Rudaz C, Vasilescu M, Budtova T (2016) Physically and chemically cross-linked cellulose cryogels: Structure, properties and application for controlled release. Carbohydr Polym 151:392–400

Dai G, Hu J, Zhao X, Wang P (2017) A colorimetric paper sensor for lactate assay using a cellulose-Binding recombinant enzyme. Sensors Actuators B Chem 238:138–144

Deka S, Saxena V, Hasan A, Chandra P, Pandey LM (2018) Synthesis, characterization and in vitro analysis of α-Fe_2O_3-$GdFeO_3$ biphasic materials as therapeutic agent for magnetic hyperthermia applications. Mater Sci Eng C 92:932–941

Deng D, Lin Q, Li H, Huang Z, Kuang Y, Chen H, Kong J (2019) Rapid detection of malachite green residues in fish using a surface-enhanced Raman scattering-active glass fiber paper prepared by in situ reduction method. Talanta 200:272–278

Desvars A, Gigan J, Hoarau G, Gérardin P, Favier F, Michault A (2011) Short report: Seroprevalence of human leptospirosis in Reunion Island (Indian Ocean) assessed by microscopic agglutination test on paper disc-absorbed whole blood. Am J Trop Med Hyg 85(6):1097–1099

Devarakonda S, Singh R, Bhardwaj J, Jang J (2017) Cost-effective and handmade paper-based immunosensing device for electrochemical detection of influenza virus. Sensors 17(11):2597

Dolai S, Tabib-Azar M (2020) Whole virus detection using aptamers and paper-based sensor potentiometry. Med Dev Sens 3(6):e10112

Doumas BT (2006) Landmark papers in clinical chemistry. Clin Chem 52:1977

Dungchai W, Chailapakul O, Henry CS (2009) Electrochemical detection for paper-based microfluidics. Anal Chem 81(14):5821–5826

Ensafi AA, Aboutalebi A (2005) A versatile stable cobalt optical sensor based on pyrogallol red immobilization on cellulose acetate film. Sensors Actuators B Chem 105(2):479–483

Fakhri N, Hosseini M, Tavakoli O (2018) Aptamer-based colorimetric determination of Pb2+ using a paper-based microfluidic platform. Anal Methods 10(36):4438–4444

Fan L, Li X, Kan X (2016) Disposable graphite paper based sensor for sensitive simultaneous determination of hydroquinone and catechol. Electrochim Acta 213:504–511

Fan L, Hao Q, Kan X (2017) Three-dimensional graphite paper based imprinted electrochemical sensor for tertiary butylhydroquinone selective recognition and sensitive detection. Sensors Actuators B Chem 256:520–527

Fan Y, Shi S, Ma J, Guo Y (2019) A paper-based electrochemical immunosensor with reduced graphene oxide/thionine/gold nanoparticles nanocomposites modification for the detection of cancer antigen 125. Biosens Bioelectron 135:1–7

Fridley GE, Holstein CA, Oza SB, Yager P (2013) The evolution of nitrocellulose as a material for bioassays. MRS Bull 38(4):326–330

Fu Y, Zhou X, Xing D (2018) Integrated paper-based detection chip with nucleic acid extraction and amplification for automatic and sensitive pathogen detection. Sensors Actuators B Chem 261: 288–296

George J, Abdelghani A, Bahoumina P, Tantot O, Baillargeat D, Frigui K, Bila S, Hallil H, Dejous C (2019) CNT-based inkjet-printed RF gas sensor: modification of substrate properties during the fabrication process. Sensors 19(8):1768

Gerbers R, Foellscher W, Chen H, Anagnostopoulos C, Faghri M (2014) A new paper-based platform technology for point-of-care diagnostics. Lab Chip 14(20):4042–4049

Gopinath SCB, Awazu K, Fujimaki M (2012) Waveguide-mode sensors as aptasensors. Sensors 12(2):2136

Grivard P, Le Roux K, Laurent P, Fianu A, Perrau J, Gigan J, Hoarau G, Grondin N, Staikowsky F, Favier F, Michault A (2007) Molecular and serological diagnosis of Chikungunya virus infection. Pathol Biol 55(10):490–494

Guo J-f, Huo D-q, Yang M, Hou C-j, Li J-j, Fa H-b, Luo H-b, Yang P (2016) Colorimetric detection of Cr (VI) based on the leaching of gold nanoparticles using a paper-based sensor. Talanta 161: 819–825

Gupta Y, Ghrera AS (2021) Recent advances in gold nanoparticle-based lateral flow immunoassay for the detection of bacterial infection. Arch Microbiol 203(7):3767–3784

Gupta Y, Kalpana K, Ghrera AS (2022) Electrochemical studies of lateral flow assay test results for procalcitonin detection. J Electrochem Sci Eng 12(2):265–274

Hong H-B, Krause H-J, Song K-B, Choi C-J, Chung M-A, Son S-w, Offenhäusser A (2011) Detection of two different influenza A viruses using a nitrocellulose membrane and a magnetic biosensor. J Immunol Methods 365(1):95–100

Hooda V, Kumar V, Gahlaut A, Hooda V (2018) Alcohol quantification: recent insights into amperometric enzyme biosensors. Artif Cells Nanomed Biotechnol 46(2):398–410

Hossain MF, Park JY (2016) Plain to point network reduced graphene oxide – activated carbon composites decorated with platinum nanoparticles for urine glucose detection. Sci Rep 6(1):21009

Hu J, Xiao K, Jin B, Zheng X, Ji F, Bai D (2019) Paper-based point-of-care test with xeno nucleic acid probes. Biotechnol Bioeng 116(10):2764–2777

Huang L, Tian S, Zhao W, Liu K, Ma X, Guo J (2021) Aptamer-based lateral flow assay on-site biosensors. Biosens Bioelectron 186:113279

Islam S, Shaheen Shah S, Naher S, Ali Ehsan M, Aziz MA, Ahammad AJS (2021) Graphene and carbon nanotube-based electrochemical sensing platforms for dopamine. Chem Asian J 16(22): 3516–3543

Jaeger J, Groher F, Stamm J, Spiehl D, Braun J, Dörsam E, Suess B (2019) Characterization and inkjet printing of an RNA aptamer for paper-based biosensing of ciprofloxacin. Biosensors (Basel) 9(1):7

Jagadeesan KK, Kumar S, Sumana G (2012) Application of conducting paper for selective detection of troponin. Electrochem Commun 20:71–74

Jaiswal N, Pandey CM, Soni A, Tiwari I, Rosillo-Lopez M, Salzmann CG, Malhotra BD, Sumana G (2018) Electrochemical genosensor based on carboxylated graphene for detection of water-borne pathogen. Sensors Actuators B Chem 275:312–321

Jalil O, Pandey CM, Kumar D (2021) Highly sensitive electrochemical detection of cancer biomarker based on anti-EpCAM conjugated molybdenum disulfide grafted reduced graphene oxide nanohybrid. Bioelectrochemistry 138:107733

Jamal SH, Roslan NJ, Shah NAA, Noor SAM, Ong KK, Yunus WMZW (2020) Preparation and characterization of nitrocellulose from bacterial cellulose for propellant uses. Mater Today: Proc 29:185–189

Janyasupab M, Liu C-C (2014) Enzymatic electrochemical biosensors. In: Kreysa G, Ota K-I, Savinell RF (eds) Encyclopedia of applied electrochemistry. Springer New York, New York, pp 872–882

Jaworska E, Gniadek M, Maksymiuk K, Michalska A (2017) Polypyrrole nanoparticles based disposable potentiometric sensors. Electroanalysis 29(12):2766–2772

Jiang Q, Chandar YJ, Cao S, Kharasch ED, Singamaneni S, Morrissey JJ (2017) Rapid, point-of-care, paper-based plasmonic biosensor for Zika virus diagnosis. Adv Biosyst 1(9):1700096

Jornet-Martínez N, Hakobyan L, Argente-García AI, Molins-Legua C, Campíns-Falcó P (2019) Nylon-Supported Plasmonic Assay Based on the Aggregation of Silver Nanoparticles: In Situ Determination of Hydrogen Sulfide-like Compounds in Breath Samples as a Proof of Concept. ACS Sens 4(8):2164–2172

Kala D, Sharma TK, Gupta S, Verma V, Thakur A, Kaushal A, Trukhanov AV, Trukhanov SV (2021) Graphene oxide nanoparticles modified paper electrode as a biosensing platform for detection of the htrA gene of O. tsutsugamushi. Sensors 21(13):4366

Kamel S, Khattab TA (2020) Recent advances in cellulose-based biosensors for medical diagnosis. Biosensors (Basel) 10(6):67

Khan MS, Pande T, van de Ven TG (2015) Qualitative and quantitative detection of T7 bacteriophages using paper based sandwich ELISA. Colloids Surf B Biointerfaces 132:264–270

Khan A, Abas Z, Kim HS, Kim J (2016) Recent progress on cellulose-based electro-active paper, its hybrid nanocomposites and applications. Sensors 16(8):1172

Khan I, Saeed K, Khan I (2019) Nanoparticles: properties, applications and toxicities. Arab J Chem 12(7):908–931

Khoshroo A, Sadrjavadi K, Taran M, Fattahi A (2020) Electrochemical system designed on a copper tape platform as a nonenzymatic glucose sensor. Sensors Actuators B Chem 325:128778

Kit-Anan W, Olarnwanich A, Sriprachuabwong C, Karuwan C, Tuantranont A, Wisitsoraat A, Srituravanich W, Pimpin A (2012) Disposable paper-based electrochemical sensor utilizing inkjet-printed Polyaniline modified screen-printed carbon electrode for Ascorbic acid detection. J Electroanal Chem 685:72–78

Koczula KM, Gallotta A (2016) Lateral flow assays. Essays Biochem 60(1):111–120

Kumar Gupta P, Sai Raghunath S, Venkatesh Prasanna D, Venkat P, Shree V, Chithananthan C, Choudhary S, Surender K, Geetha K (2019) An update on overview of cellulose, its structure and applications. IntechOpen

Kumar J, Jha SK, D'Souza SF (2006) Optical microbial biosensor for detection of methyl parathion pesticide using Flavobacterium sp. whole cells adsorbed on glass fiber filters as disposable biocomponent. Biosens Bioelectron 21(11):2100–2105

Kumar S, Kumar S, Pandey CM, Malhotra BD (2016a) Conducting paper based sensor for cancer biomarker detection. J Phys Conf Ser 704:012010

Kumar S, Sen A, Kumar S, Augustine S, Yadav B, Mishra S, Malhotra B (2016b) Polyaniline modified flexible conducting paper for cancer detection. Appl Phys Lett 108:203702

Kumar A, Purohit B, Maurya PK, Pandey LM, Chandra P (2019a) Engineered nanomaterial assisted signal-amplification strategies for enhancing analytical performance of electrochemical biosensors. Electroanalysis 31(9):1615–1629

Kumar S, Umar M, Saifi A, Kumar S, Augustine S, Srivastava S, Malhotra BD (2019b) Electrochemical paper based cancer biosensor using iron oxide nanoparticles decorated PEDOT:PSS. Anal Chim Acta 1056:135–145

Kwon G, Kim J, Kim D, Ko Y, Yamauchi Y, You J (2019) Nanoporous cellulose paper-based SERS platform for multiplex detection of hazardous pesticides. Cellulose 26(8):4935–4944

Lee D, Lee JH (2021) Paper-based biosensors with lateral/vertical flow assay. In: Lee JH (ed) Paper-based medical diagnostic devices: as a part of bioanalysis-advanced materials, methods, and devices. Springer Singapore, Singapore, pp 115–136

Li J, Li S, Yang CF (2012) Electrochemical biosensors for cancer biomarker detection. Electroanalysis 24(12):2213–2229

Li Z, Li F, Hu J, Wee WH, Han YL, Pingguan-Murphy B, Lu TJ, Xu F (2015) Direct writing electrodes using a ball pen for paper-based point-of-care testing. Analyst 140(16):5526–5535

Li H, Wang W, Lv Q, Xi G, Bai H, Zhang Q (2016) Disposable paper-based electrochemical sensor based on stacked gold nanoparticles supported carbon nanotubes for the determination of bisphenol A. Electrochem Commun 68:104–107

Li W, Zhang X, Miao C, Li R, Ji Y (2020) Fluorescent paper–based sensor based on carbon dots for detection of folic acid. Anal Bioanal Chem 412(12):2805–2813

Lin N, Dufresne A (2014) Nanocellulose in biomedicine: Current status and future prospect. Eur Polym J 59:302–325

Liu M, Zhao Y, Monshat H, Tang Z, Wu Z, Zhang Q, Lu M (2020) An IoT-enabled paper sensor platform for real-time analysis of isothermal nucleic acid amplification tests. Biosens Bioelectron 169:112651

Liu Y, Alkhamis O, Liu X, Yu H, Canoura J, Xiao Y (2021) Aptamer-integrated multianalyte-detecting paper electrochemical device. ACS Appl Mater Interfaces 13(15):17330–17339

Lodh N, Mikita K, Bosompem KM, Anyan WK, Quartey JK, Otchere J, Shiff CJ (2017) Point of care diagnosis of multiple schistosome parasites: species-specific DNA detection in urine by loop-mediated isothermal amplification (LAMP). Acta Trop 173:125–129

Lu R, Haider MR, Gardner S, Alexander JID, Massoud Y (2019) A paper-based inkjet-printed graphene sensor for breathing-flow monitoring. IEEE Sens Lett 3(2):1–4

Ma L, Xu Z, Zhang X, Lin J, Tai R (2019) Facile and quick formation of cellulose nanopaper with nanoparticles and its characterization. Carbohydr Polym 221:195–201

Määttänen A, Vanamo U, Ihalainen P, Pulkkinen P, Tenhu H, Bobacka J, Peltonen J (2013) A low-cost paper-based inkjet-printed platform for electrochemical analyses. Sensors Actuators B Chem 177:153–162

Mahato K, Purohit B, Bhardwaj K, Jaiswal A, Chandra P (2019) Novel electrochemical biosensor for serotonin detection based on gold nanorattles decorated reduced graphene oxide in biological fluids and in vitro model. Biosens Bioelectron 142:111502

Maiti D, Tong X, Mou X, Yang K (2019) Carbon-based nanomaterials for biomedical applications: a recent study. Front Pharmacol 9:1401

Majumdar S, Sarmah K, Mahanta D (2020) A simple route to prepare polypyrrole-coated filter papers via vapor phase polymerization and their gas sensing application. ACS Appl Poly Mater 2(5):1933–1942

Martinez AW, Phillips ST, Whitesides GM, Carrilho E (2010) Diagnostics for the developing world: microfluidic paper-based analytical devices. Anal Chem 82(1):3–10

Meagher RJ, Negrete OA, Van Rompay KK (2016) Engineering paper-based sensors for Zika virus. Trends Mol Med 22(7):529–530

Migliorini FL, dos Santos DM, Soares AC, Mattoso LHC, Oliveira ON, Correa DS (2020) Design of a low-cost and disposable paper-based immunosensor for the rapid and sensitive detection of aflatoxin B1. Chemosensors 8(3):87

Moccia M, Caratelli V, Cinti S, Pede B, Avitabile C, Saviano M, Imbriani AL, Moscone D, Arduini F (2020) Paper-based electrochemical peptide nucleic acid (PNA) biosensor for detection of miRNA-492: a pancreatic ductal adenocarcinoma biomarker. Biosens Bioelectron 165:112371

Morgan ED, Wilson ID (2004) An early description of paper chromatography? Chromatographia 60(1):135–136

Mulijani S, Iswantini D, Wicaksono R, Notriawan D (2018) Optical sensor based chemical modification as a porous cellulose acetate film and its application for ethanol sensor. IOP Conf Ser: Mater Sci Eng 333:012014

Müller RH, Clegg DL (1949) Automatic paper chromatography. Anal Chem 21(9):1123–1125

Nayak S, Blumenfeld NR, Laksanasopin T, Sia SK (2017) Point-of-care diagnostics: recent developments in a connected age. Anal Chem 89(1):102–123

Neouze M-A, Schubert U (2008) Surface modification and functionalization of metal and metal oxide nanoparticles by organic ligands. Monatshefte für Chemie – Chemical Monthly 139: 183–195

Nezakati T, Seifalian A, Tan A, Seifalian AM (2018) Conductive polymers: opportunities and challenges in biomedical applications. Chem Rev 118(14):6766–6843

Nicu R, Ciolacu F, Ciolacu DE (2021) Advanced functional materials based on nanocellulose for pharmaceutical/medical applications. Pharmaceutics 13(8):1125

Nie Z, Nijhuis CA, Gong J, Chen X, Kumachev A, Martinez AW, Narovlyansky M, Whitesides GM (2010) Electrochemical sensing in paper-based microfluidic devices. Lab Chip 10(4):477–483

Nishat S, Jafry AT, Martinez AW, Awan FR (2021) Paper-based microfluidics: Simplified fabrication and assay methods. Sensors Actuators B Chem 336:129681

Noviana E, Carrão DB, Pratiwi R, Henry CS (2020a) Emerging applications of paper-based analytical devices for drug analysis: A review. Anal Chim Acta 1116:70–90

Noviana E, McCord CP, Clark KM, Jang I, Henry CS (2020b) Electrochemical paper-based devices: sensing approaches and progress toward practical applications. Lab Chip 20(1):9–34

Nye MJ (1979) Maurice crosland. Gay-Lussac: scientist and bourgeois. New York: Cambridge University Press. 1978. pp xvi, 333. $36.00. Am Hist Rev 84(5):1397–1398

Pandey CM, Sumana G, Tiwari I (2014) Copper oxide assisted cysteine hierarchical structures for immunosensor application. Appl Phys Lett 105(10):103706

Pandey CM, Dewan S, Chawla S, Yadav BK, Sumana G, Malhotra BD (2016) Controlled deposition of functionalized silica coated zinc oxide nano-assemblies at the air/water interface for blood cancer detection. Anal Chim Acta 937:29–38

Pandey I, Tiwari JD, Furukawa H, Khosla A, Sekhar PK (2019) Flexible Prussian blue/Carbon dots nanocomposite modified exfoliated graphite paper based sensor for simultaneous monitoring of hypertension and Parkinson disease. Microsyst Technol 28:109

Patil PO, Pandey GR, Patil AG, Borse VB, Deshmukh PK, Patil DR, Tade RS, Nangare SN, Khan ZG, Patil AM, More MP, Veerapandian M, Bari SB (2019) Graphene-based nanocomposites for sensitivity enhancement of surface plasmon resonance sensor for biological and chemical sensing: A review. Biosens Bioelectron 139:111324

Paul G, Verma S, Jalil O, Thakur D, Pandey CM, Kumar D (2021) PEDOT: PSS-grafted graphene oxide-titanium dioxide nanohybrid-based conducting paper for glucose detection. Polym Adv Technol 32(4):1774–1782

Pelton R (2009) Bioactive paper provides a low-cost platform for diagnostics. TrAC Trends Anal Chem 28(8):925–942

Phasuksom K, Prissanaroon-Ouajai W, Sirivat A (2020) A highly responsive methanol sensor based on graphene oxide/polyindole composites. RSC Adv 10(26):15206–15220

Power AC, Gorey B, Chandra S, Chapman J (2018) Carbon nanomaterials and their application to electrochemical sensors: a review. Nanotechnol Rev 7(1):19–41

Punjabi K, Adhikary RR, Patnaik A, Bendale P, Singh S, Saxena S, Banerjee R (2020) Core–shell nanoparticles as platform technologies for paper based point-of-care devices to detect antimicrobial resistance. J Mater Chem B 8(29):6296–6306

Qi J, Li B, Wang X, Zhang Z, Wang Z, Han J, Chen L (2017) Three-dimensional paper-based microfluidic chip device for multiplexed fluorescence detection of Cu_2+ and Hg_2+ ions based on ion imprinting technology. Sensors Actuators B Chem 251:224–233

Ratajczak K, Stobiecka M (2020) High-performance modified cellulose paper-based biosensors for medical diagnostics and early cancer screening: a concise review. Carbohydr Polym 229:115463

Rengaraj S, Cruz-Izquierdo Á, Scott JL, Di Lorenzo M (2018) Impedimetric paper-based biosensor for the detection of bacterial contamination in water. Sensors Actuators B Chem 265:50–58

Ruecha N, Rangkupan R, Rodthongkum N, Chailapakul O (2014) Novel paper-based cholesterol biosensor using graphene/polyvinylpyrrolidone/polyaniline nanocomposite. Biosens Bioelectron 52:13–19

Ruecha N, Shin K, Chailapakul O, Rodthongkum N (2019) Label-free paper-based electrochemical impedance immunosensor for human interferon gamma detection. Sensors Actuators B Chem 279:298–304

Rungsawang T, Punrat E, Adkins J, Henry C, Chailapakul O (2016) Development of electrochemical paper-based glucose sensor using cellulose-4-aminophenylboronic acid-modified screen-printed carbon electrode. Electroanalysis 28(3):462–468

Sari E, Üzek R, Merkoçi A (2019) Paper based photoluminescent sensing platform with recognition sites for tributyltin. ACS Sens 4(3):645–653

Saxena V, Chandra P, Pandey LM (2018) Design and characterization of novel Al-doped ZnO nanoassembly as an effective nanoantibiotic. Appl Nanosci 8(8):1925–1941

Saylan Y, Erdem Ö, Ünal S, Denizli A (2019) An alternative medical diagnosis method: biosensors for virus detection. Biosensors (Basel) 9(2):65

Shafey AME (2020) Green synthesis of metal and metal oxide nanoparticles from plant leaf extracts and their applications: a review. Green Process Synth 9(1):304–339

Shen Y, Tran T-T, Modha S, Tsutsui H, Mulchandani A (2019) A paper-based chemiresistive biosensor employing single-walled carbon nanotubes for low-cost, point-of-care detection. Biosens Bioelectron 130:367–373

Silva NFD, Almeida CMR, Magalhães JMCS, Gonçalves MP, Freire C, Delerue-Matos C (2019) Development of a disposable paper-based potentiometric immunosensor for real-time detection of a foodborne pathogen. Biosens Bioelectron 141:111317

Singer JM, Plotz CM (1956) The latex fixation test: I. Application to the serologic diagnosis of rheumatoid arthritis. Am J Med 21(6):888–892

Solanki S, Pandey CM (2016) Biological applications of microfluidics system. In: Dixit CK, Kaushik A (eds) Microfluidics for biologists: fundamentals and applications. Springer International Publishing, Cham, pp 191–221

Songjaroen T, Primpray V, Manosarn T, Khumchanta W, Sakuldamrongpanich T, Kulkeratiyut S, Laiwattanapaisal W (2018) A simple and low-cost portable paper-based ABO blood typing device for point-of-care testing. J Immunoass Immunochem 39(3):292–307

Soni A, Pandey CM, Solanki S, Sumana G (2015) One-pot synthesis of a polyaniline–gold nanocomposite and its enhanced electrochemical properties for biosensing applications. RSC Adv 5(57):45767–45774

Stevens R, Pass K, Fuller S, Wiznia A, Noble L, Duva S, Neal M (1992) Blood spot screening and confirmatory tests for syphilis antibody. J Clin Microbiol 30(9):2353–2358

Sun J, Guo A, Zhang Z, Guo L, Xie J (2011) A conjugated aptamer-gold nanoparticle fluorescent probe for highly sensitive detection of rHuEPO-α. Sensors 11(11):10490

Tan SN, Ge L, Tan HY, Loke WK, Gao J, Wang W (2012) Paper-based enzyme immobilization for flow injection electrochemical biosensor integrated with reagent-loaded cartridge toward portable modular device. Anal Chem 84(22):10071–10076

Tang P, Leung HT, Gomez MT, Sun G (2018) Sensitivity-tunable colorimetric detection of chloropicrin vapor on nylon-6 nanofibrous membrane based on a detoxification reaction with biological thiols. ACS Sens 3(4):858–866

Tang P, Nguyen NT-H, Lo JG, Sun G (2019) Colorimetric detection of carcinogenic alkylating fumigants on a nylon 6 nanofibrous membrane. Part II: self-catalysis of 2-diethylaminoethyl-modified sensor matrix for improvement of sensitivity. ACS Appl Mater Interfaces 11(14): 13632–13641

Tang J, Zheng S-B, Jiang S-X, Li J, Guo T, Guo J-H (2021a) Metal organic framework (ZIF-67)-derived co nanoparticles/N-doped carbon nanotubes composites for electrochemical detecting of tert-butyl hydroquinone. Rare Metals 40(2):478–488

Tang L, Chen W, Chen B, Lv R, Zheng X, Rong C, Lu B, Huang B (2021b) Sensitive and renewable quartz crystal microbalance humidity sensor based on nitrocellulose nanocrystals. Sensors Actuators B Chem 327:128944

Teengam P, Siangproh W, Tuantranont A, Henry CS, Vilaivan T, Chailapakul O (2017a) Electrochemical paper-based peptide nucleic acid biosensor for detecting human papillomavirus. Anal Chim Acta 952:32–40

Teengam P, Siangproh W, Tuantranont A, Vilaivan T, Chailapakul O, Henry CS (2017b) Multiplex paper-based colorimetric dna sensor using pyrrolidinyl peptide nucleic acid-induced AgNPs aggregation for detecting MERS-CoV, MTB, and HPV oligonucleotides. Anal Chem 89(10): 5428–5435

Teengam P, Nisab N, Chuaypen N, Tangkijvanich P, Vilaivan T, Chailapakul O (2021) Fluorescent paper-based DNA sensor using pyrrolidinyl peptide nucleic acids for hepatitis C virus detection. Biosens Bioelectron 189:113381

Tran TN, de Vries PJ, Hoang LP, Phan GT, Le HQ, Tran BQ, Vo CM, Nguyen NV, Kager PA, Nagelkerke N, Groen J (2006) Enzyme-linked immunoassay for dengue virus IgM and IgG antibodies in serum and filter paper blood. BMC Infect Dis 6:13

Tran V-K, Ko E, Geng Y, Kim MK, Jin GH, Son SE, Hur W, Seong GH (2018) Micro-patterning of single-walled carbon nanotubes and its surface modification with gold nanoparticles for electrochemical paper-based non-enzymatic glucose sensor. J Electroanal Chem 826:29–37

Üzek R, Sari E, Şenel S, Denizli A, Merkoçi A (2019) A nitrocellulose paper strip for fluorometric determination of bisphenol A using molecularly imprinted nanoparticles. Microchim Acta 186(4):218

Vaitukaitis JL, Braunstein GD, Ross GT (1972) A radioimmunoassay which specifically measures human chorionic gonadotropin in the presence of human luteinizing hormone. Am J Obstet Gynecol 113(6):751–758

Wang X, Si Y, Wang J, Ding B, Yu J, Al-Deyab SS (2012) A facile and highly sensitive colorimetric sensor for the detection of formaldehyde based on electro-spinning/netting nano-fiber/nets. Sensors Actuators B Chem 163(1):186–193

Wang Y, Ping J, Ye Z, Wu J, Ying Y (2013) Impedimetric immunosensor based on gold nanoparticles modified graphene paper for label-free detection of Escherichia coli O157:H7. Biosens Bioelectron 49:492–498

Wang Y, Luo J, Liu J, Li X, Kong Z, Jin H, Cai X (2018) Electrochemical integrated paper-based immunosensor modified with multi-walled carbon nanotubes nanocomposites for point-of-care testing of 17β-estradiol. Biosens Bioelectron 107:47–53

Wang C-F, Sun X-Y, Su M, Wang Y-P, Lv Y-K (2020) Electrochemical biosensors based on antibody, nucleic acid and enzyme functionalized graphene for the detection of disease-related biomolecules. Analyst 145(5):1550–1562

Wang W-Y, Ma X, Shao Y-W, Qi X-D, Yang J-H, Wang Y (2021) Flexible, multifunctional, and thermally conductive nylon/graphene nanoplatelet composite papers with excellent EMI shielding performance, improved hydrophobicity and flame resistance. J Mater Chem A 9(8): 5033–5044

Wei Q, Zhang P, Liu T, Pu H, Sun D-W (2021) A fluorescence biosensor based on single-stranded DNA and carbon quantum dots for acrylamide detection. Food Chem 356:129668

Wu X, Kuang H, Hao C, Xing C, Wang L, Xu C (2012) Paper supported immunosensor for detection of antibiotics. Biosens Bioelectron 33(1):309–312

Wu J-H, Wang C-H, Ma Y-D, Lee G-B (2018) A nitrocellulose membrane-based integrated microfluidic system for bacterial detection utilizing magnetic-composite membrane microdevices and bacteria-specific aptamers. Lab Chip 18(11):1633–1640

Xiao F, Li Y, Zan X, Liao K, Xu R, Duan H (2012) Growth of metal–metal oxide nanostructures on freestanding graphene paper for flexible biosensors. Adv Funct Mater 22(12):2487–2494

Yang H, Kong Q, Wang S, Xu J, Bian Z, Zheng X, Ma C, Ge S, Yu J (2014) Hand-drawn&written pen-on-paper electrochemiluminescence immunodevice powered by rechargeable battery for low-cost point-of-care testing. Biosens Bioelectron 61:21–27

Yang B, Ding X, Zhang M, Wang L, Huang X (2020) A flexible, strong, heat- and water-resistant zeolitic imidazolate framework-8 (ZIF-8)/aramid nanofibers (ANFs) composite nanopaper. Composites Communications 17:192–196

Yaqoob AA, Ahmad H, Parveen T, Ahmad A, Oves M, Ismail IMI, Qari HA, Umar K, Mohamad Ibrahim MN (2020) Recent advances in metal decorated nanomaterials and their various biological applications: a review. Front Chem 8:341

Ye T, Huang Z, Zhu Z, Deng D, Zhang R, Chen H, Kong J (2020) Surface-enhanced Raman scattering detection of dibenzothiophene and its derivatives without π acceptor compound using multilayer Ag NPs modified glass fiber paper. Talanta 220:121357

Yen Y-K, Chao C-H, Yeh Y-S (2020) A graphene-PEDOT:PSS modified paper-based aptasensor for electrochemical impedance spectroscopy detection of tumor marker. Sensors 20(5):1372

Yew C-HT, Azari P, Choi JR, Li F, Pingguan-Murphy B (2018) Electrospin-coating of nitrocellulose membrane enhances sensitivity in nucleic acid-based lateral flow assay. Anal Chim Acta 1009: 81–88

Yezer I, Demirkol DO (2020) Cellulose acetate–chitosan based electrospun nanofibers for bio-functionalized surface design in biosensing. Cellulose 27(17):10183–10197

Yu Y, Pan D, Qiu S, Ren L, Huang S, Liu R, Wang L, Wang H (2021) Polyphenylene sulfide paper-based sensor modified by Eu-MOF for efficient detection of Fe3+. React Funct Polym 165:104954

Yue X, Zhu W, Ma S, Yu S, Zhang Y, Wang J, Wang Y, Zhang D, Wang J (2016) Highly sensitive and selective determination of tertiary butylhydroquinone in edible oils by competitive reaction induced “On–Off–On” fluorescent switch. J Agric Food Chem 64(3):706–713

Yue X-Y, Zhou Z-J, Wu Y-M, Li Y, Li J-C, Bai Y-H, Wang J-L (2020) Application progress of fluorescent carbon quantum dots in food analysis. Chin J Anal Chem 48(10):1288–1296

Yusof NA, Rahman SFA, Muhammad A (2019) Chapter 9 – Carbon nanotubes and graphene for sensor technology. In: Rashid SA, Othman RNIR, Hussein MZ (eds) Synthesis, technology and applications of carbon nanomaterials. Elsevier, pp 205–222

Zhou C, You T, Jang H, Ryu H, Lee E-S, Oh M-H, Huh YS, Kim SM, Jeon T-J (2020a) Aptamer-conjugated polydiacetylene colorimetric paper chip for the detection of bacillus thuringiensis spores. Sensors (Basel) 20(11):3124

Zhou J, Li B, Qi A, Shi Y, Qi J, Xu H, Chen L (2020b) ZnSe quantum dot based ion imprinting technology for fluorescence detecting cadmium and lead ions on a three-dimensional rotary paper-based microfluidic chip. Sensors Actuators B Chem 305:127462

Micro-Nano Structured Materials for DNA/RNA Amplification-Based Electrochemical Tests

19

Federico Figueredo, Mónica Mosquera-Ortega, and
Eduardo Cortón

Contents

1 Introduction 414
2 Nucleic Acid Amplification Methods 416
3 Integration of Micro-nano Structured Materials with Nucleic Acid Amplification-Based Tests 418
  3.1 Nanolabels 418
  3.2 Electrode Nanomaterials 422
4 Characteristics and Applications of Magnetic Micro-Nano Structured Materials 426
  4.1 Introduction 426
  4.2 Applications in Amplification-Based Tests 429
5 Future Perspectives 432
References 432

Abstract

Nucleic acid amplification is now a standardized analytical technique, allowing precise and rapid determination of the presence of a determined DNA/RNA sequence. Moreover, some sophisticated equipment allows the exquisite quantification of the number of copies originally presented in a sample; many different protocols, enzymes, labels, and equipment have been developed over time, allowing high throughput and automatization. In the same way, modern nanotechnology has been developed over several decades, and now almost any laboratory can synthesize and characterize nanoparticles of different materials

---

F. Figueredo · E. Cortón (✉)
Laboratory of Biosensors and Bioanalysis (LABB), Biological Chemistry Department and IQUIBICEN-CONICET, Science School, University of Buenos Aires, Buenos Aires, Argentina
e-mail: eduardo@qb.fcen.uba.ar

M. Mosquera-Ortega
Laboratory of Biosensors and Bioanalysis (LABB), Biological Chemistry Department and IQUIBICEN-CONICET, Science School, University of Buenos Aires, Buenos Aires, Argentina

Basic Science Department, National Technology University - FRGP, General Pacheco, Buenos Aires, Argentina

© Springer Nature Singapore Pte Ltd. 2023

U. P. Azad, P. Chandra (eds.), *Handbook of Nanobioelectrochemistry*,
https://doi.org/10.1007/978-981-19-9437-1_19

and tune size and shape. We believe there is then an opportunity to merge both already mature technological areas and find new and exciting applications to improve the analytical performance, lower the per-analysis cost, and make the whole process (from reagents elaboration to disposal) more environmentally friendly. Here we explore some of the possibilities for nanoscience and nucleic acid amplification to come together to obtain better analytical systems.

Keywords

Electrochemical assays · Electrode nanomaterial · LAMP · Magnetic nanomaterial · Nanostructures · Nanolabel · PCR

1 Introduction

The detection of DNA and RNA sequences employing nucleic acid amplification tests has made great progress since the polymerase chain reaction (PCR) appeared in the 1980s. While PCR and quantitative PCR are the gold standard methods used in the laboratory field, they present complex operational procedures and portability limitations. Today, there is an urgent need for the development of simple, portable, and practical analytical devices for nucleic acid detection. For the last 20 years, electrochemical biosensors have shown great advances toward DNA and RNA detection, comprising high sensitivity, low cost, and potential application as portable analytical devices.

Although the field of electrochemical nucleic acid biosensors has increased and different strategies and detection methods have appeared, complex or unprocessed samples, including cell lysates, and genomic DNA and RNA extracts, among others, remain a challenge for practical applications. The nature of the sample could, in some cases, decrease the signal-to-noise ratio when electroactive molecules react with the electrode or impair the electrochemical cell performance (the electrodes can become fouled or poisoned). Moreover, the concentration of a given sequence (target) is usually extremely low. To overcome these limitations, there are two principal strategies: the use of nanomaterials and the use of nucleic acid amplification methods (Fig. 19.1).

Nanomaterials are characterized by their superior physicochemical properties, principally concerning their small size, high surface area, nontoxicity (mostly), biocompatibility, high surface reactivity, and super-paramagnetic behavior (some materials). They can be used to modify the surface of the electrodes (increasing the electroactive surface area or including more recognition elements/reaction sites) and as nanolabels or magnetic nanocarriers.

Nucleic acid amplification methods can be used to increase the number of target DNA/RNA copies present in the original sample, to overcome problems associated

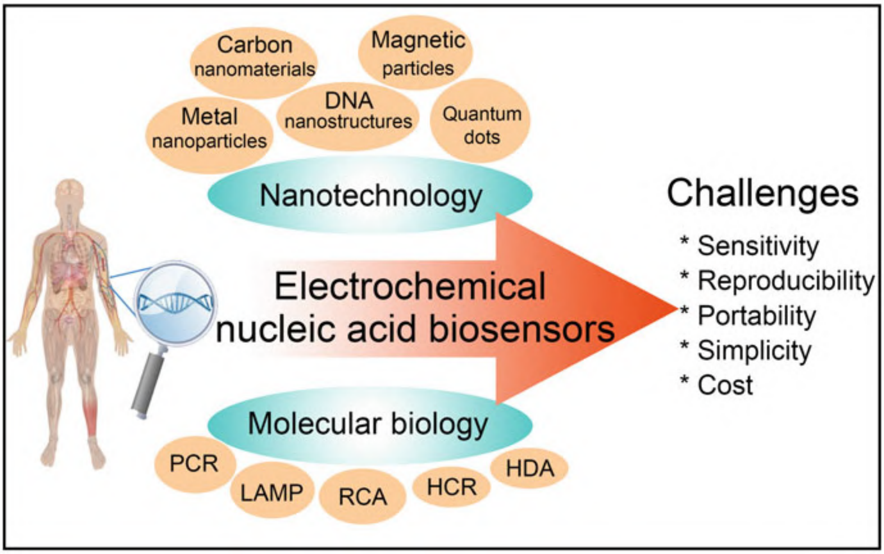
Carbon nanomaterials
Magnetic particles
Metal nanoparticles
DNA nanostructures
Quantum dots
Nanotechnology
Challenges
* Sensitivity
* Reproducibility
* Portability
* Simplicity
* Cost
Electrochemical nucleic acid biosensors
Molecular biology
PCR
LAMP
RCA
HCR
HDA

Fig. 19.1 Schematic diagram showing the combination of nanotechnology and molecular biology toward the development of electrochemical nucleic acid biosensors

with the interference and low concentration of the analyte (Tosar et al. 2010). In recent years, new nucleic acid amplification tests have emerged as viable and simpler alternatives to PCR-based amplification tests. Some of them include isothermal amplification methods, such as loop-mediated isothermal amplification (LAMP), recombinase polymerase amplification (RPA), helicase dependent amplification (HDA), and rolling circle amplification (RCA). One of the most important advantages of the isothermal methods is that they can be performed over solid substrates such as electrodes or micro-nano structured materials.

Several reviews focus on different aspects, including applications and design of nanomaterial-assisted nucleic acid amplification methods; for example, Wei et al. (2010) concentrate on the detection of small sequence change useful for genetic disease diagnostics, intending to design point-of-care biosensors. Other reviews have focused on the possibilities of integrating the technology from an engineering perspective and considering the possibilities of miniaturized integration (lab on a chip paradigm), multiplexing sensors, and the use of smartphones as convenient interphase for diagnostic chips (Zhu et al. 2015a; Purohit et al. 2020; Liu et al. 2020).

In this chapter, we will review the recent advances in electrochemical nucleic acid biosensors that combine micro- and nanostructures with DNA/RNA amplification methods. Herein, we summarize the progress in the development of biosensors that combine elements of nanotechnology and molecular biology, in particular those strategies that employ nucleic acid amplification approaches. In this sense, electrochemical biosensors have shown the potential to serve as suitable devices for point-of-care diagnostics, in particular for the detection of DNA and microRNAs (miRNA) (Labib and Berezovski 2015).

2 Nucleic Acid Amplification Methods

Polymerase chain reaction (PCR) is a DNA amplification method that has continued to improve since it was first developed in 1985 (Saiki et al. 1985, 1988), and is one of the most important techniques in applied medical research and diagnostics. The use of a pair of primers, a DNA thermostable polymerase and dNTPs, ensures the amplification of a target sequence, making the technique highly specific. The reaction is performed with a thermal cycler that raises and lowers the temperature of the sample n times, allowing the denaturation and reannealing of DNA molecules in a controlled manner (Fig. 19.2a). The amplicons (the amplified DNA products) are double-stranded oligonucleotides that can be identified through traditional post-PCR detection methods, such as DNA blotting gel electrophoresis, after performing several PCR cycles (typically 20–40). Although PCR is the most well-established approach to amplify nucleic acids, it presents some disadvantages, such as easy contamination, sensitivity to inhibiting substances that can be present in real samples, and high cost, as well as being time-consuming. However, point-of-care diagnostic platforms that alleviate some limitations of PCR have been proposed (Zhu et al. 2020). On the other hand, the isothermal amplification of target DNA sequences offers great advantages since it can be performed by employing simple and affordable equipment, which is more attractive for applications in resource-limited settings (Nguyen et al. 2020).

Rolling circle amplification (RCA) is an isothermal nucleic acid amplification technique discovered in the mid-1990s. It can be conducted at room temperature (up to 37 °C) in solution, on a solid support, or in a complex biological environment (e.g., on the cell surface or inside the cell) (Feng et al. 2016). In a typical RCA, a linear DNA probe, complementary to the target sequence, is used as a ligation template to circulate a padlock probe with a DNA ligase, obtaining a DNA ring that serves as a template. Once prepared, the circular template is used to hybridize with the target sequence. Then, a DNA polymerase (e.g., Phi29 DNA polymerase) continuously adds dNTPs to the circular template to produce ssDNA with several tandem repeats (Fig. 19.2b). The elongated ssDNA can be customized to contain functional sequences, including DNA aptamers and DNA nanostructures, among others (Ali et al. 2014). Since RCA is a versatile tool, many approaches have been developed in research areas such as genomics, proteomics, diagnosis, biosensing, drug discovery, and nanotechnology (Zhao et al. 2008).

Loop-mediated isothermal amplification (LAMP), first reported in 2000 (Notomi et al. 2000), is a molecular technique that amplifies the target DNA sequence at a constant temperature of around 64–65 °C, producing around 100 times more amplicons than PCR (Nagamine et al. 2002). LAMP employs four (up to six) primers that recognize six or more specific regions of the target DNA sequence, and a DNA polymerase with strand-displacement activity (Fig. 19.2c). These

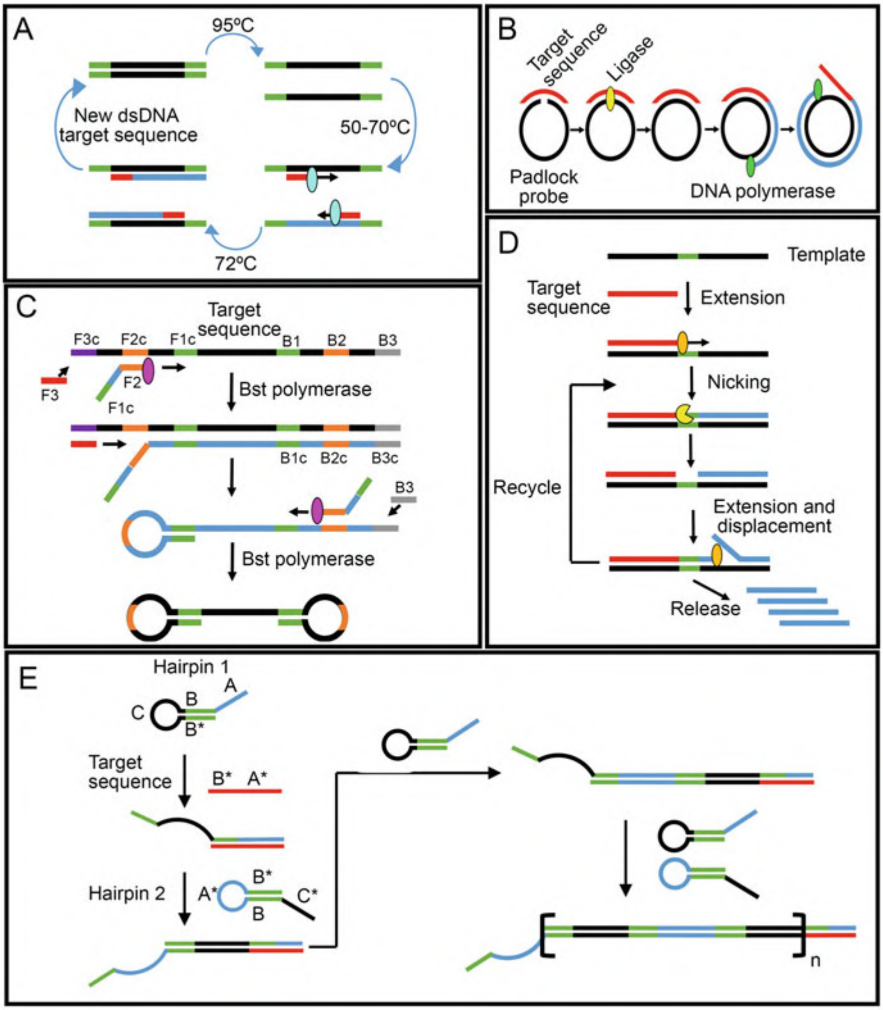
A
95°C
New dsDNA target sequence
50-70°C
72°C
B
Target sequence
Ligase
Padlock probe
DNA polymerase
C
Target sequence
F3c F2c F1c B1 B2 B3
F3 F2 F1c
Bst polymerase
B1c B2c B3c
B3
Bst polymerase
D
Template
Target sequence
Extension
Nicking
Recycle
Extension and displacement
Release
E
Hairpin 1
C B A B*
Target sequence
B* A*
Hairpin 2
A* B* C* B
n

Fig. 19.2 Schematic representation of nucleic acid amplification methods. (**a**) PCR, (**b**) RCA, (**c**) LAMP, (**d**) SDR, and (**e**) HCR

characteristics make LAMP an extremely sensitive and selective technique, used for the amplification of very low DNA concentrations in less than 1 h. One of the most important features of LAMP is that the amplification reaction can be detected and monitored by a diverse range of sensing techniques, including optical, magnetic, piezoelectric, electrochemical, and magneto-resistive transducers (Becherer et al. 2020).

Strand displacement reactions (SDRs) and toehold mediated strand displacement reactions are molecular techniques widely used for many applications in biotechnology. They use DNA sequences containing overhangs that are designed to have more complementary bases and hybridize completely with the target DNA sequence, displacing another (shorter) complementary strand (Fig. 19.2d; Gillespie et al. 2019). The hybridization chain reaction (HCR) is a particular SDR, first reported in 2004 (Dirks and Pierce 2004). The HCR is a non-enzymatic amplification method with high sensitivity and good selectivity toward the target detection, widely used in biosensing applications. The HCR needs two auxiliary DNA hairpins that are composed of a stem, toehold, and loop domain. The HCR process starts when the target DNA hybridizes to the complementary single-stranded overhang region (toehold) of a DNA hairpin. The target DNA opens the first hairpin, which opens the second, and the cycle continues following a cascade reaction, with enzyme-free amplification of the DNA (Fig 19.2e; Bi et al. 2017).

3 Integration of Micro-nano Structured Materials with Nucleic Acid Amplification-Based Tests

3.1 Nanolabels

In recent years, many electrochemical tests have been developed for the detection of RCA or HCR amplification products triggered by target DNA/RNA sequences. In contrast to PCR, isothermal nucleic acid amplification methods coupled with DNA and RNA biosensors were widely studied. The electrochemical detection strategies include the use of metal nanoparticles (NPs) modified with DNA probes to tag complementary sequences, metal NPs that bind electrostatically to DNA amplified molecules, and the DNA-templated synthesis of metal NPs or nanoclusters (NCs), used as electrochemical labels.

3.1.1 Gold and Other Nanoparticles

Gold nanoparticles (AuNPs) were one of the first types of metal NPs used to label DNA probes, and still have a particularly important role in several tests, for many reasons. They are highly stable and can be stored in a proper solution for years, maintaining their high quality and dispersion characteristics. They have good biocompatibility, low toxicity, and well-known bioconjugation chemistry (Liu and Liu 2017). A DNA sequence target can be electrochemically detected by performing a metal NP-based DNA hybridization assay. After the hybridization reaction with the NP-labeled probe is performed, there are three main detection strategies: (1) based on the intrinsic signal of the NPs, (2) dissolving the NPs for the detection of the metal ions, and (3) instead of dissolving the NPs, performing electrodeposition of silver over the metal NP-labeled probe.

In 2001, Authier et al. (2001) developed one of the first electrochemical DNA detection methods for the sensitive determination of PCR amplicons. They labeled a DNA probe with 20 nm AuNPs that were hybridized with the complementary PCR amplicons previously immobilized on the surface of a carbon electrode. They obtained oxidative fragments of the AuNPs by treating the complex with acidic bromine-bromide. The gold ion, with its high solubility, is reduced electrochemically and is detected by anodic stripping voltammetry. However, other strategies based on the oxidation signal of AuNP-labeled probes without the dissolution step were proposed by Ozsoz et al. (2003). In their study, the authors preconcentrated the DNA amplicons on the surface of the electrode by a simple polarization procedure, decreasing the assay time. Park et al. (2002) showed that the AuNPs can be used to label the DNA probe immobilized at the electrode surface, and, after hybridization with the target sequence, the silver deposition over the AuNPs produced a change in the conductivity signal. Later, other electrochemical detection techniques were employed, based on the anodic shift of silver reduction potential in typical cyclic voltammetry (Cai et al. 2004) or the detection of the dissolved silver ions after chronoamperometric stripping (Li et al. 2004). Recently, the dual labeled primers approach was developed for the electrochemical detection of PCR or RPA (isothermal alternative to PCR) amplicons: one of the primers was labeled with metal NPs (de la Escosura-Muñiz et al. 2016) or carbon nanostructures (Ang et al. 2020), and the second primer was labeled with magnetic particles (MPs). The magnetic nanolabel is important to separate/concentrate the amplicon over the surface of the electrode (Fig. 19.3a). The AuNPs, used as labels, were electrochemically detected in HCl 1 M by performing chronoamperometry to detect the reduction of H^+ to H_2, catalyzed by the Au (de la Escosura-Muñiz et al. 2016). An interesting alternative is to label the primers with graphene oxide materials to make use of their intrinsic electroactivity (Ang et al. 2020).

A particularly interesting study showed that a sandwich assay can be performed by using AuNPs modified with two different DNA probes. The particularity of the assay is that they used AuNPs with a dual purpose, to immobilize the DNA complementary target probe and DNA primers that recognized the circular template used for the RCA. Therefore, when a target DNA is present, it can hybridize between the AuNP-DNA probe and a DNA probe immobilized at the surface of the electrode. The RCA then amplifies the AuNP-DNA probe, complementary to the circular template. The amplification product of the RCA, a long single-stranded DNA with many tandem repeats of a particular DNAzyme (DNA with peroxidase-like activity), was used for the formation of polyaniline, catalyzed by the peroxidase-mimicking DNAzyme (Fig. 19.3b). Finally, the presence of polyaniline was electrochemically detected by the cascade of signal amplification triggered by the target DNA previously hybridized at the electrode surface (Hou et al. 2014).

3.1.2 Quantum Dots

Along with gold, other metal NPs were employed to label and immobilize DNA probes. An interesting approach was employed using CdTe quantum dots (CdTe-QDs) as nanolabels. The quantum dots (QDs) were conjugated with a DNA probe to tag RCA (Ji et al. 2012) or HCR (Liu et al. 2016) amplification products. For example, Ji and colleagues detected DNA molecules down to attomolar concentrations by employing a particular strategy (Ji et al. 2012). First, they attached a molecular beacon over the electrode surface, which was used to hybridize with assistants and target DNAs to form a ternary "Y-junction." The Y-junction was designed to be attacked by a nicking endonuclease that can open the molecular

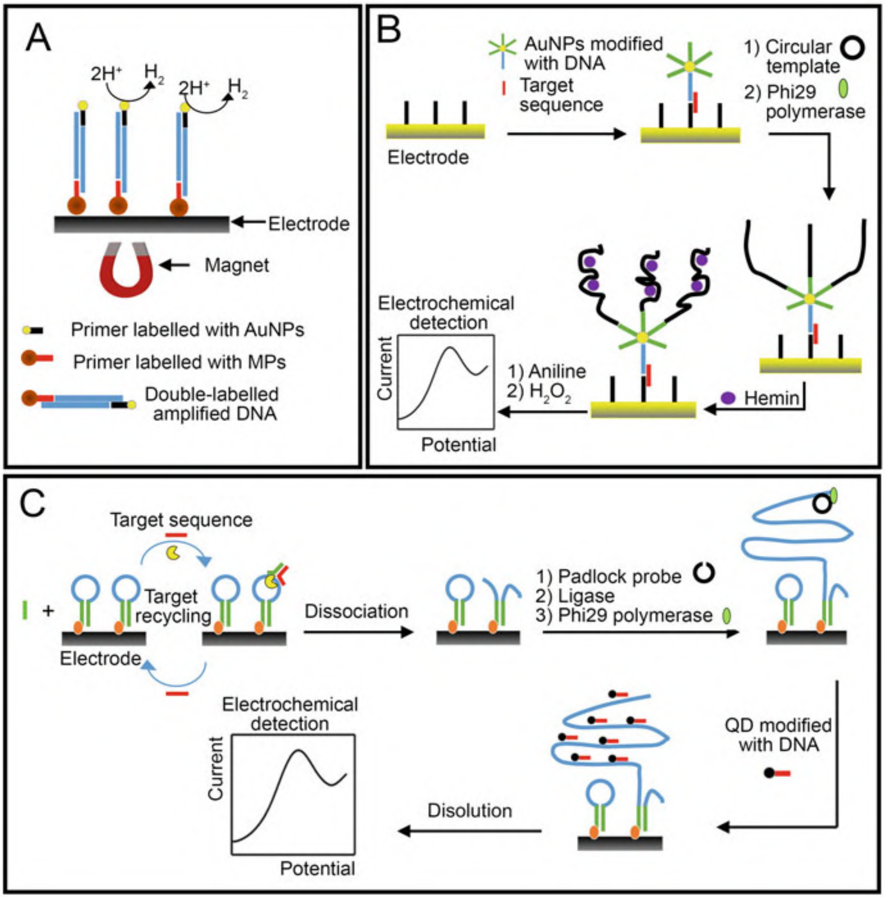
A
2H⁺
H₂
2H⁺
H₂
Electrode
Magnet
Primer labelled with AuNPs
Primer labelled with MPs
Double-labelled amplified DNA
B
AuNPs modified with DNA
Target sequence
Electrode
1) Circular template
2) Phi29 polymerase
Electrochemical detection
Current
Potential
1) Aniline
2) H₂O₂
Hemin
C
Target sequence
+
Target recycling
Electrode
Dissociation
1) Padlock probe
2) Ligase
3) Phi29 polymerase
Electrochemical detection
Current
Potential
Disolution
QD modified with DNA

Fig. 19.3 Metal nanoparticles are used to label DNA amplification products. (**a**) Double labeled DNA strategy, (**b**) Aniline synthesis over DNA amplification product, and (**c**) Detection of quantum dots (QDs) previously used to label the RCA amplification product. (**a** was inspired by de la Escosura-Muñiz et al. 2016, **b** was inspired by Hou et al. 2014, and **c** was inspired by Ji et al. 2012)

beacon to expose the sequence used for the second hybridization process. The exposed sequence acted as the primer of the RCA reaction that produced several oligonucleotide repetitions. The RCA amplification products were tagged with a CdTe-QD containing a complementary DNA probe. After dissolving the CdTe-QDs with acid, the Cd ions were detected by square wave voltammetry (Fig. 19.3c).

3.1.3 Silver Nanostructures

Taking advantage of the specificity for the detection of the target DNA sequence that is given by the SDRs, electrochemical tests were designed, employing metal NPs to tag the amplification product. For example, Zhuang and colleagues employed cetyltrimethylammonium bromide-capped silver NPs (CTAB-AgNPs) to tag the HCR product to detect HIV DNA (Zhuang et al. 2013). They started by immobilizing the capture probe over a gold electrode, which can hybridize with the target DNA. After the hybridization reaction, a pair of hairpins were added to start the HCR. The long-range self-assembled DNA linear structure produced at the electrode surface was tagged with CTAB-AgNPs. The CTAB provided a net positive charge over the surface of the AgNPs, which allowed them to electrostatically interact with the DNA molecules, particularly with the sugar-phosphate backbone that carries the nucleotide bases. Here, the specificity is given by the hybridization reaction that triggers the HCR, and the CTAB-AgNPs are only used to detect the HCR self-assembled structures. Once the nanotags were added, and the unbound ones removed by washing, linear sweep voltammetry was used for the electrochemical detection of the CTAB-AgNPs, which correlates with the amplification products triggered by the target DNA. Similar strategies were reported for miRNA detection (Liu et al. 2017). Hairpin DNA probes were assembled onto AuNPs displayed at the surface of the electrode. After the target mRNA sequence hybridized with the hairpin, 4-mercaptophenylboronic acid (MPBA) was added to interact with the cis-diol at the 3′-terminal of the miRNA to produce a covalent bond. Then, citrate-capped AgNPs were added to interact with the MPBA anchored at the miRNA's 3′ terminal through an Ag-S bond and to interact with each other through covalent interactions between the α-hydroxycarboxylate of the citrate and the boronate of the MPBA. These amplification strategies, based on the aggregation of the AgNPs, successfully increased the sensitivity, resulting in a limit of detection (LOD) of 20 aM of miRNA. Again, the specificity was given by the HCR; meanwhile, the detection does not require the specific modification of NPs or DNA probes.

3.1.4 DNA-Templated Synthesis of Nanolabels

DNA metallization is a particular kind of biomolecule-templated bottom-up nanofabrication, where metal nanostructures can be deposited on DNA scaffolds by the reduction of metal salts. The concept was first introduced in 1998, with a focus on the fabrication of nanoscale electronics, as a way of producing conductive nanowires (Richter 2003). Further metal nanostructures with different compositions, such as Au, Pt, Pd, Cu, Co, Ni, Te, Rh, and their alloys, have been produced over DNA templates for a variety of applications (Aryal et al. 2020). The general procedure, based on in situ, DNA-templated NP synthesis, can be performed by employing wet chemistry approaches, such as photo-induced metal deposition or electrochemical deposition (Chen et al. 2018). Chemical reduction methods involve three main steps: activation, chemical reduction, and growth. The activation step is based either on exchanging ions into the DNA backbone or on the insertion of metal complexes between the DNA bases. The second step is reduction, where reducing agents trigger the nucleation of metal NPs. Finally, the previously deposited metal nanostructures can grow in a particular media. While the chemical method is the most popular, it is difficult to control the growth kinetics and thus obtain small NPs. Furthermore, the reducing agents can, in some cases, contaminate, denature, or even destroy the DNA strands. To minimize the disadvantages associated with DNA metallization, some authors began to control the size of the NPs growing at the DNA template. For example, regular PdO nanowires with a thickness of 20 nm were efficiently grown over DNA templates (Nguyen et al. 2008). The procedure involved two steps: the insertion of metal complexes (Pd salt) between the DNA bases and then, instead of adding reducing agents, the PdO nanowires were allowed to precipitate, at a relatively low rate, in a hydrogen atmosphere for 20 h.

The possibility of precipitating metal nanostructures for use as DNA labels was recently investigated for the electrochemical detection of miRNA (Zhang et al. 2019). The reaction was performed entirely at the surface of the gold electrodes, where a pair of hairpins were used to recognize the target miRNA. RCA was then employed to elongate a hairpin sequence, producing a guanine-rich long ssDNA. PdNPs were successfully synthesized over DNA templates in just 60 min, taking advantage of the affinity between Pd and guanine DNA bases. The electrochemical signal provided by the PdNPs was detected by employing differential pulse voltammetry after acid dissolution, obtaining an miRNA-21 LOD of 8.6 aM (Fig. 19.4a). Like PdNPs, other metal nanostructures were shown to be more stable in particular DNA bases; for example, cytosine (C)-rich ssDNA stabilized Ag nanoclusters (AgNCs) (Chen et al. 2018; Yang et al. 2015), and (C)-rich dsDNA stabilized Cu nanoclusters (CuNCs) (Wang et al. 2017). Metal NCs are ultrasmall particles (<2 nm) containing few atoms. Recently, many studies have demonstrated the tremendous advantages of using Ag, Au, and Cu metal NCs in combination with DNA amplification strategies for electrochemical biosensor applications (Xu et al. 2020). Metal NCs, especially Ag and Cu, are widely used for fluorescent and colorimetric assays. However, some metal NCs such as CuNCs were employed to be electrochemically detected after acid dilution, showing a wide linear range of detection (10 aM–100 fM) (Wang et al. 2017). The biosensor uses the exonuclease T7, which is part of a reaction that involves two DNA templates and a cycle of amplification reactions that continuously recycles the target molecule and one of the DNA templates (Fig. 19.4b). The other DNA template hybridizes with a DNA probe immobilized at the surface of a gold electrode. A second DNA probe is then added to form a Y-shaped dsDNA over the electrode, and then an HCR takes place when a pair of hairpins trigger the dsDNA assembly that serves as a template for the formation of the CuNCs.

3.2 Electrode Nanomaterials

The unique and attractive properties of nanostructured materials make them one of the most important components when an electrochemical biosensor is designed. Nanostructured materials are used to modify the electrode surface owing to their remarkable chemical stability, biocompatibility, high surface area, and good conductivity. The bare electrode can be modified with the nanostructured material by employing a wide range of methods, such as drop-casting, deep coating, or electrodeposition, among others. An important step in designing an electrochemical DNA biosensor is the immobilization of the DNA probe (linear ssDNA, hairpins, or aptamers) on the surface of the electrode. The immobilization method varies with the type and composition of the nanomaterial exposed at the electrode surface. The most common DNA immobilization methods include physical adsorption, adsorption at a controlled potential, covalent attachment, and employing the avidin-biotin

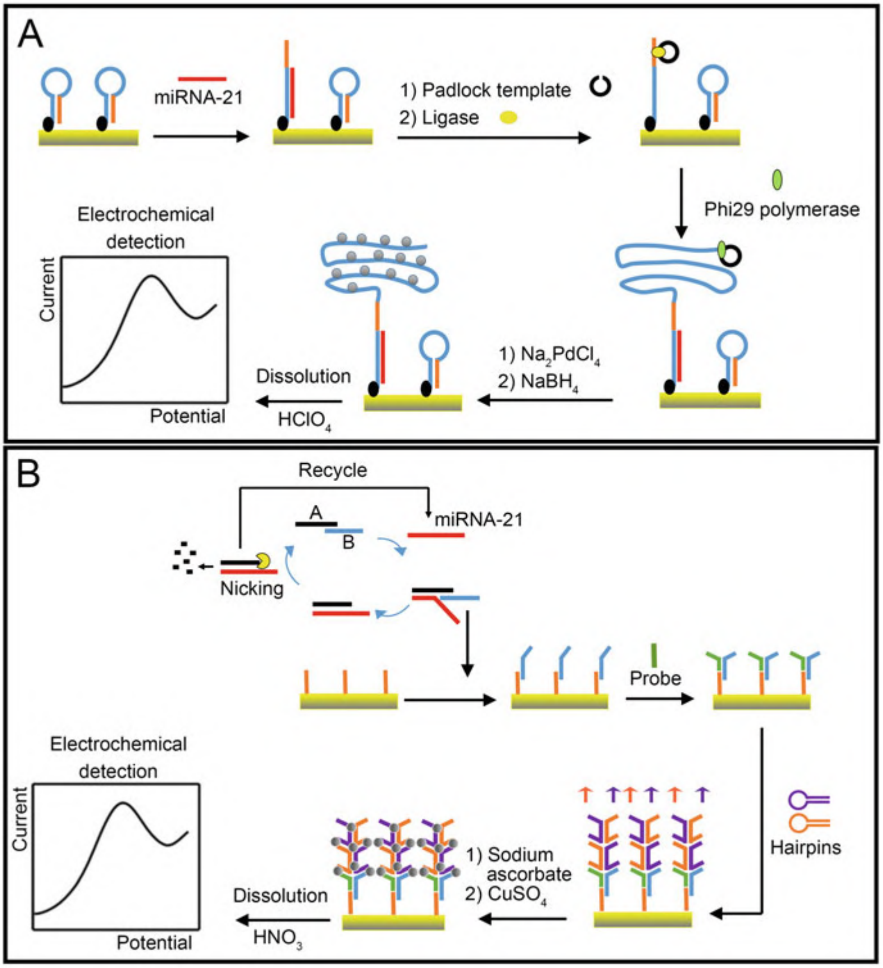
A
miRNA-21
1) Padlock template
2) Ligase
Phi29 polymerase
Electrochemical detection
Current
Potential
Dissolution
$HClO_4$
1) Na_2PdCl_4
2) $NaBH_4$
B
Recycle
A
B
miRNA-21
Nicking
Probe
Hairpins
Electrochemical detection
Current
Potential
Dissolution
HNO_3
1) Sodium ascorbate
2) $CuSO_4$

Fig. 19.4 Synthesis of metal nanoparticles over DNA amplified products. (**a**) PdNP synthesis over RCA amplification product and (**b**) CuNCs synthesis over HCR amplification product. (**a** was inspired by Zhang et al. 2019 and **b** was inspired by Wang et al. 2017)

complex chemistry. In general, the chemistry behind DNA immobilization follows the traditional procedures used for bulk materials (Au and carbon graphite, among others), but with minor modifications.

Metal NPs, carbon-based nanomaterials, and DNA nanostructures have been used to modify the electrode surface, to develop nucleic acid amplification-based tests. Hybridization biosensors have been widely studied and many designs developed. Since the sensitivity of hybridization biosensors is generally low, several alternatives have been developed to increase the analytical performance. One of the main problems is the poor accessibility of target molecules to the probes immobilized at the electrode surface, and great effort has been taken to control the surface chemistry, conformation, and packing density of the probes.

3.2.1 Carbon-Based Nanostructures

PCR amplicons can be detected with high accuracy with a hybridization biosensor constructed with DNA probes covalently attached at the surface of carbon-based nanostructures, such as multi-walled carbon nanotubes (MWCNT) (Koehne et al. 2003), carbon nanofibers (Koehne et al. 2009), or nanocomposites containing polyaniline nanofibers and MWCNTs (Yang et al. 2009). However, better analytical performance was obtained for electrochemical biosensors coupled to solid-state nucleic acid amplification methods. For example, carbon nanotubes (CNTs) were used as the solid substrate to immobilize a hairpin structured probe that recognizes the target miRNA sequence (Tian et al. 2015). The miRNA hybridizes with the hairpin and opens the loop to be recognized by the circular probe and start the RCA. The amplification product, ssDNAs elongated at the surface of the electrode, can be electrochemically detected by measuring the oxidation current of a soluble redox compound. The ssDNA at the electrode surface acts as a barrier affecting the free diffusion of a redox marker, resulting in a current signal decrease. The CNTs help to increase the electroactive surface and enhance the nucleic acid amplification reaction, resulting in an LOD of 1.2 fM.

3.2.2 Metal Nanostructures

Metal NPs can be used to modify the surface of the electrode and attach DNA probes. Electrodes containing AuNPs (Brasil de Oliveira Marques et al. 2009), $AuTiO_2$ microspheres (Zhang et al. 2008), and reduced graphene oxide (RGO)/AuNP nanostructured interfaces (Lei et al. 2015) were used to detect PCR amplicons. Meanwhile, metal NPs can be used to improve and control the dispersion and density of DNA probes over the electrode: the LOD achieved was close to 10 fM (Brasil de Oliveira Marques et al. 2009). Detection of enterotoxigenic *E. coli* was developed by immobilizing specific probes over Pt nanoparticles, and then deposited over SP electrodes with the help of chitosan (Bansal et al. 2017).

3.2.3 DNA Nanostructures

Since the introduction of nanometer-sized DNA structures, an extraordinary breakthrough in structural DNA nanotechnology has appeared. The bottom-up nanofabrication is mainly based on the predictable Watson–Crick base-pairing rules of DNA self-assembly. This nanofabrication method is based on the folding of a long ssDNA strand into a specific shape, guided by a great number of short ssDNAs. The resulting folded DNA structure can turn into 2D or even 3D shapes, such as triangular prisms, tetrahedrons, cubes, octahedrons, icosahedrons, buckyballs, and more complicated DNA origami structures (Su et al. 2019). Three-dimensional DNA nanostructures present many advantages for electrochemical biosensor applications, for several reasons:

1. The precise predictability and reproducibility, both based on the strict base-pairing principle.
2. The strong nuclease resistance in comparison with ssDNA, dsDNA, and duplex DNA probes.

3. The great biocompatibility and biodegradability.
4. They can adopt an ordered and upright orientation at the sensor surface.
5. The DNA nanostructured interfaces have fast molecular diffusion and convection.
6. They can be functionalized with aptamers, peptides, antibodies, and QDs, among others.

The DNA tetrahedron, one of the most popular nanostructures, has been widely used for electrochemical biosensor applications (Goodman et al. 2005; Lin et al. 2016). Typically, these nanostructures are assembled employing four strands, heated for a few minutes at high temperatures (around 95 °C), and cooled at 4 °C for a few seconds to obtain the nanostructures (Fig. 19.5a). The resulting nanostructures are immobilized face down onto a gold electrode through three thiol groups, leaving the remaining vertex, carrying the probe of interest, facing upward. Ge et al. (2014) modified a gold electrode with a thiol-modified DNA tetrahedron and performed HCR amplification to detect DNA and miRNA target molecules at concentrations as low as 100 and 10 aM, respectively. Later, the LOD of miRNA was improved (2 aM) when a dual amplification strategy was employed (Miao et al. 2015a). The target miRNA opens the DNA tetrahedron's hairpin domain, releasing the sequence that can hybridize with the complementary DNA sequence exposed at the surface of the AuNPs. Then, the hairpins are added to initiate an HCR over the surface of the AuNPs. Finally, AgNPs are used to tag the amplification product, which can be further electrochemically detected by performing linear sweep voltammetry (Fig. 19.5b). A similar approach employs a DNA tetrahedron and RCA amplification. For example, AgNPs were used to tag the amplification product, obtaining an LOD of 50 aM for miRNA (Miao et al. 2015b). Another possibility that has been studied recently is the addition of enzyme-like functionality to the RCA amplification product. For example, a DNAzyme that reduces methylene blue in the presence of H_2O_2 was studied, obtaining an LOD of 100 aM for methylated DNA sequences (Liu et al. 2018).

Recent studies have shown the development of electrochemical biosensors following the idea of in situ assemblies of DNA nanostructures to tag nucleic acid amplification products (Meng et al. 2020, Zhang et al. 2020). Zhang et al. (2020) developed an electrochemical biosensor for the detection of circulating miRNA, obtaining an LOD of 3.6 fM. The closed hairpin at the electrode surface changes the conformation in the presence of miRNA and a second hairpin then recognizes the exposed sequence, producing a dsDNA and recycling the miRNA for a new cycle of amplification. After *n* cycles, the second amplification results in the addition of three DNA strands that hybridize with the hairpin's tails and form a 3D nanostructure, similar to a net, which is electrochemically detected using a DNA electroactive intercalant (Fig. 19.6a). On the other hand, better LODs for miRNA can be accomplished when 3D nanostructured nets are formed starting from Pd-modified DNA strands, as shown by Meng et al. (2020). The LOD obtained by the authors was 63.1 aM, showing the advantage of the 3D nanostructure to increase the Pd loading capacity. The authors added paracetamol, an electroactive substance, for the indirect detection of miRNA through the reaction with PdNPs (Fig. 19.6b).

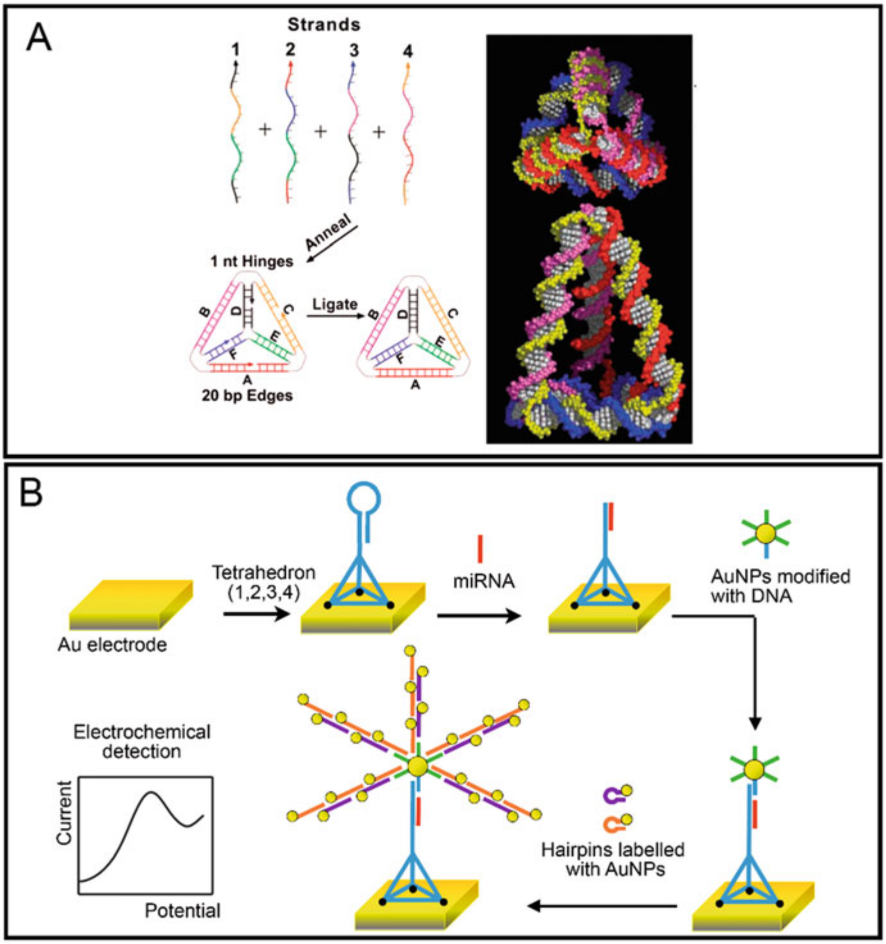
A
Strands
1
2
3
4
+
+
+
Anneal
1 nt Hinges
B
D
C
E
F
A
20 bp Edges
Ligate
B
D
C
E
F
A
B
Tetrahedron
(1,2,3,4)
miRNA
AuNPs modified
with DNA
Au electrode
Electrochemical
detection
Current
Potential
Hairpins labelled
with AuNPs

Fig. 19.5 DNA tetrahedron-based nucleic acid electrochemical biosensors. (**a**) Scheme illustrating the DNA tetrahedron structure and a 3D space-filling representation and (**b**) Example of a DNA tetrahedron biosensor. (**a** was reproduced from Goodman et al. 2005 and **b** was inspired by Miao et al. 2015a)

4 Characteristics and Applications of Magnetic Micro-Nano Structured Materials

4.1 Introduction

MPs have been used as useful tools for nucleic acid purification, amplification, and detection processes (Chen et al. 2020). One of the main features of MPs is their large surface area to volume ratio. The surface of the MPs can be modified to serve as

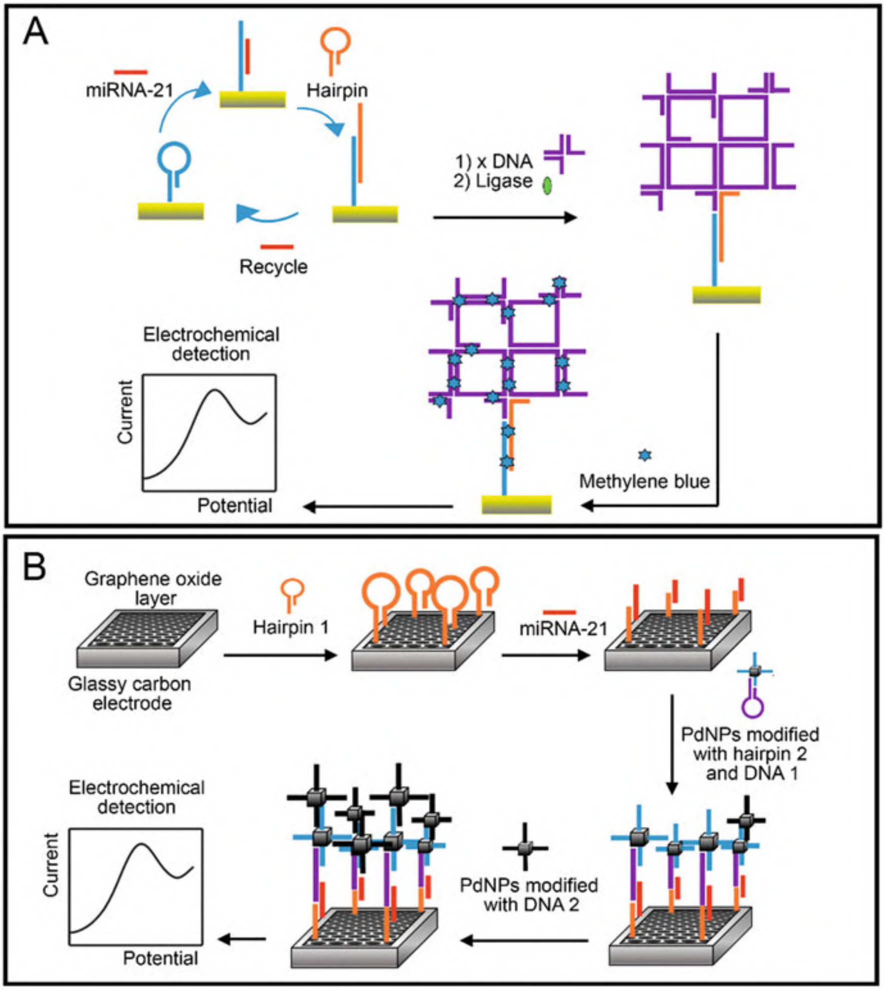
A
miRNA-21
Hairpin
Recycle
1) x DNA
2) Ligase
Electrochemical detection
Current
Potential
Methylene blue
B
Graphene oxide layer
Glassy carbon electrode
Hairpin 1
miRNA-21
PdNPs modified with hairpin 2 and DNA 1
Electrochemical detection
Current
Potential
PdNPs modified with DNA 2

Fig. 19.6 DNA nanostructure-based electrochemical biosensors. (**a**) 3D nanostructure produced over the hairpins disposed at the electrode surface and (**b**) 3D nanostructure produced with PdNPs modified with ssDNAs and hairpins. (**a** was inspired by Zhang et al. 2020 and **b** was inspired by Meng et al. 2020)

detection markers (nanolabels). In this way, MPs act as dispersible biocapture surfaces and, in some cases, as dispersible electrodes (Goon et al. 2010).

Due to their paramagnetic properties and their small size (typically ~20 nm for iron oxide), MPs do not agglomerate in solution. Nonetheless, once an external magnetic field is applied, MPs selectively capture the molecular target, separating them from the rest of the components present in the matrix and avoiding non-specific absorption of interference. MPs can also concentrate nucleic acids, resulting in LOD at aM concentration levels when electrochemical methods are used (Pastucha et al. 2019).

The applicability of MPs will depend on their final size and composition, as well as the binding characteristics of the material used to modify the surface of the MPs (Masud et al. 2019; Wu et al. 2016).

4.1.1 Composition

The most widely used materials to obtain MPs are pure metals (Fe, Co, and Ni), some ferrites ($BaFe_{12}O_{19}$ and $CoFe_2O_4$), and metallic oxides, such as magnetite Fe_3O_4 and maghemite γ-Fe_2O (Gloag et al. 2019, Shan et al. 2016). They are used for several medical and industrial applications due to their low toxicity, chemical stability at room temperature, and biocompatibility, both in vivo and in vitro (Cardoso et al. 2018). Other materials commonly used in the manufacture of MPs are conductive polymers, such as poly-(2,2′:5′,5″-terthiophene-3′-*p*-benzoic acid), and spherical polymeric particles, known as magnetic beads (MBs) marketed under the name Dynabeads™ (Pastucha et al. 2019). There are hybrid MPs formed by a compound with paramagnetic properties and others that facilitate the redox reaction, such as Fe_3O_4-graphene (Wang et al. 2015).

4.1.2 Size

The superparamagnetic properties of MPs depend on their size, which is mainly controlled during the synthesis. When the dimensions of MPs are below the "critical size," they present paramagnetic mono-domain behavior; thus, they become rapidly magnetized only when a magnetic field is applied. For example, the critical size of Fe_3O_4 was estimated to be below ~20 nm, but it has not been determined exactly, since it changes with the crystalline structure (70 nm and 128 nm for cubic and spherical structures, respectively) (Li et al. 2017).

4.1.3 Coating

Coatings have been widely used to improve the stability and performance of MPs, preventing unwanted reactions from taking place, as well as oxidation reactions, which easily occur with Fe_3O_4 NPs. The use of a suitable coating can increase the bioavailability of the MPs and also provide some signal amplification characteristics, making them not only a tool to capture and separate the analyte but also a fundamental part of the transduction mechanism of the sensors (Gloag et al. 2019). Thus, the coating material composition will depend on the application of the MPs in the nucleic acid extraction process. There are several coating materials, such as Au, polymeric membranes (e.g., polyethylenamine, polystyrene), porous materials (especially SiO_2) (Berensmeier 2006), and proteins, such as avidin and streptavidin. Coating materials provide an ideal ionic surface that can trap nucleic acids, since they incorporate functional groups such as amino, thiol, carboxylic, hydroxyl, tosyl, and activated N-hydroxysuccinate groups. Hence, the surface properties (porosity, size, and shape) play an important role in the absorption and isolation of nucleic acids (Fig. 19.7; Zhu et al. 2015b, Tosar et al. 2010, Yeung and Hsing 2006).

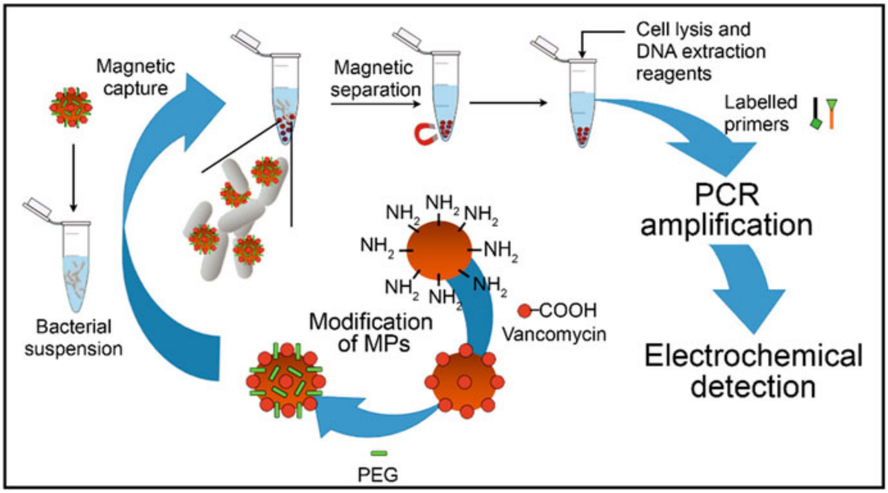
Magnetic capture
Magnetic separation
Cell lysis and DNA extraction reagents
Labelled primers
Bacterial suspension
PCR amplification
NH_2
Modification of MPs
COOH
Vancomycin
Electrochemical detection
PEG

Fig. 19.7 Application of magnetic particles in the separation and lysis of bacterial cells, DNA extraction, and amplification of their nucleic acids for electrochemical detection. (Inspired by Zhu et al. 2015b)

4.1.4 Functionalization

MPs by themselves do not capture or detect the analyte; therefore, they must be efficiently functionalized to capture molecular targets and subsequently separate them through the use of an external magnetic field in a quick and convenient step. In this way, MPs improve the analysis in terms of specificity and sensitivity, since the purity of the sample can be increased by the elimination of interferences (Pastucha et al. 2019). The functionalization of MPs is related to the characteristics of the molecule to be studied; this is expected since there will be an interaction with the functional groups of the target biomolecules (Gloag et al. 2019).

The coating and functionalization of MPs provides an ideal surface for the immobilization of nucleic acids and can occur by (1) electrostatic adsorption between the positive charge of the functional groups of the coating and the phosphate group of the DNA amplicon; (2) covalent bonding between negatively charged groups with nucleic acids labeled with the thiol or amino group; (3) an affinity interaction to the protein, for example, an avidin/streptavidin-biotin-binding interaction; and (4) direct conjugation with the MPs using a linker, for example, Au-thiol (Masud et al. 2020, Rashid and Yusof 2017).

4.2 Applications in Amplification-Based Tests

The most common application of MPs in the electrochemical detection of nucleic acids involves techniques such as electrochemiluminescence and amperometry, as well as linear sweep and cyclic voltammetry.

Nowadays, nucleic acid separation with the help of MPs produces excellent results with very low LODs (Pastucha et al. 2019). This has led to the design of several biosensors, for example, the point-of-care electrochemical biosensor for *Mycoplasma pneumoniae* DNA detection presented by Zhao et al. (2020). In this work, the authors used Fe_3O_4 MPs coated with Au, polyethylene glycol (PEG), and chondroitin sulfate (CS) to obtain the Fe_3O_4@Au@PEG@CS MPs. The MPs were deposited on the surface of the carbon electrode and measured by cyclic voltammetry, achieving an LOD of 3.3 aM.

More sensitive biosensor development with better LODs can be obtained by employing nucleic acid amplification techniques. Thus, using the functionality of MPs to separate and concentrate the molecular target, Yeung et al. (2006) reported the design of a microchip to electrochemically detect DNA amplicons of *E. coli* and *Bacillus subtilis*. They employed avidin-coated MPs functionalized with biotinylated DNA probes to capture specific genomic DNA sequences and subsequently carried out PCR amplification. Amplicons were labeled with AuNPs, and the amplification signal on indium tin oxide-based electrodes was detected by performing linear voltammetry.

In another study, PCR amplification of nucleic acids using MPs was reported employing a sandwich detection method strategy (Lermo et al. 2007). The authors reported an in situ DNA PCR amplification method for the *Salmonella* genome, employing labeled primers to obtain double-labeled PCR products. One of the primers was labeled with biotin, to immobilize DNA in streptavidin MBs. The second primer was labeled with digoxigenin (Fig. 19.8). The authors designed a real-time PCR reactor in which the double-labeling on the streptavidin-coated MPs can be electrochemically detected, as shown in Fig. 19.8. An anti-digoxigenin antibody labeled with peroxidase was used to label the digoxigenin. After the addition of peroxide and hydroquinone (a redox mediator), the authors determined the PCR amplification product using a carbon electrode and performing chronoamperometric detection.

The good results obtained using MPs in PCR-based amplification assays have generated interest from other researchers to apply other amplification techniques such as LAMP and RCA (Sharif et al. 2019), to reduce the assay time and achieve the selective separation of genetic material.

Recently, LAMP was used to detect the DNA of various foodborne pathogens (*E. coli*, *Vibro parahaemolyticus*, *Staphylococcus aureus*, and *Listeria monocytogenes*) (Sharif et al. 2019). The detection was performed through an impedimetric microfluidic sensor employing gold electrodes. After the LAMP reaction, the amplicons were separated using MBs and washed with deionized water, and the MB-DNA suspension was injected into the microfluidic compartment for further detection, obtaining an LOD of 10 copies.

In addition, Fig. 19.8b shows the study carried out by Barreda-García et al. (2014). They reported the detection of DNA from *Mycobacterium tuberculosis***,** performing electrochemical detection. The authors combined asymmetric HDA amplification and hybridization techniques, using MBs of streptavidin functionalized with a biotin-amplicon and obtaining an LOD of 0.5 aM. Other

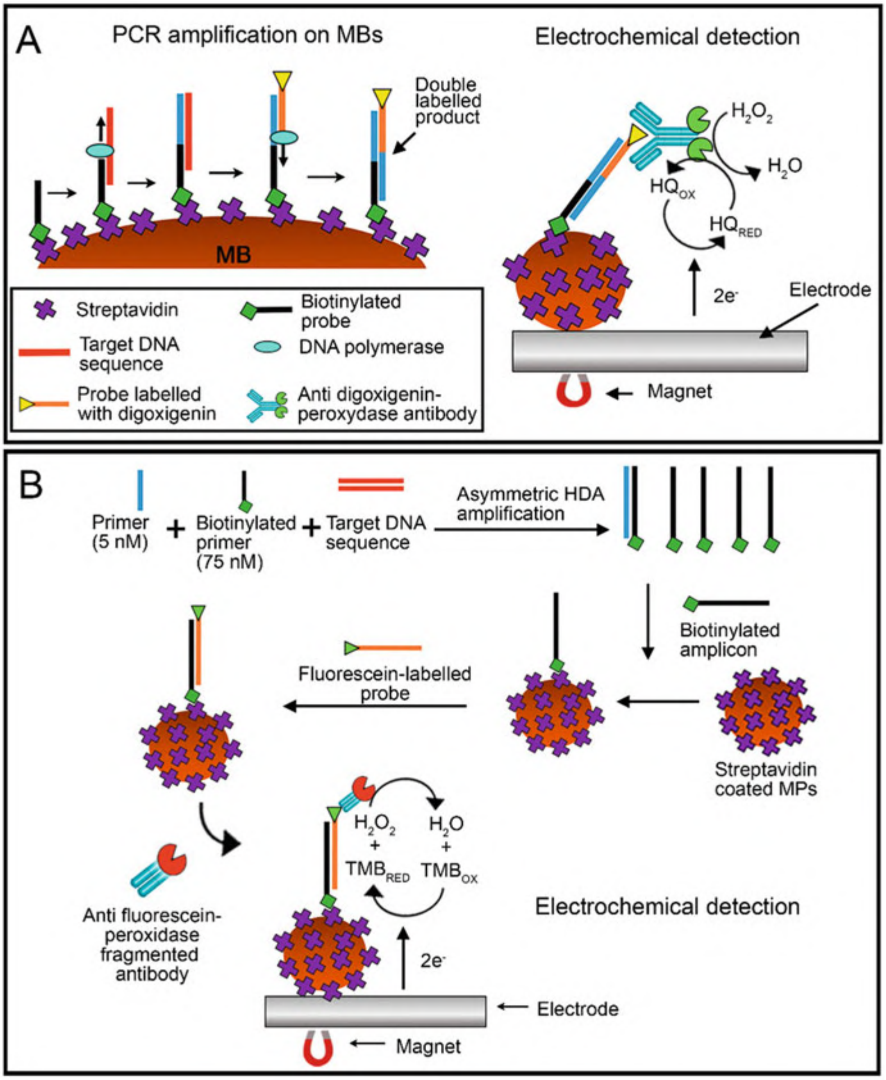
A
PCR amplification on MBs
Electrochemical detection
Double labelled product
MB
Streptavidin
Target DNA sequence
Probe labelled with digoxigenin
Biotinylated probe
DNA polymerase
Anti digoxigenin-peroxydase antibody
H₂O₂
H₂O
HQ_OX
HQ_RED
2e⁻
Electrode
Magnet
B
Primer (5 nM)
+
Biotinylated primer (75 nM)
+
Target DNA sequence
Asymmetric HDA amplification
Biotinylated amplicon
Fluorescein-labelled probe
Streptavidin coated MPs
H₂O₂ + TMB_RED
H₂O + TMB_OX
Anti fluorescein-peroxidase fragmented antibody
Electrochemical detection
2e⁻
Electrode
Magnet

Fig. 19.8 Magnetic particles are used in the separation and amplification of nucleic acids using electrochemical determinations. (**a**) PCR and (**b**) HDA amplification methods applying magnetic particles and magnetic beads in nucleic acid determinations for electrochemical techniques. (**a** was inspired by Lermo et al. 2007 and **b** was inspired by Barreda-García et al. 2014)

nucleic acid amplification methods, such as the padlock exponential rolling circle, have been reported by Yu et al. (2017), who determined miRNA-21 using $CoFe_2O_4$ MPs functionalized with poly (diallyldimethylammonium chloride) and AuNPs (Au@$CoFe_2O_4$/Tb-Gra) to capture miRNA. A redox molecule was used (toluidine blue), co-immobilized onto the graphene in the absence of substrate (H_2O_2).

Toluidinde blue was used to amplify the electrochemical signal at the electrode surface. The electrochemical detection was performed by cyclic voltammetry and electrochemical impedance spectroscopy, obtaining an LOD of 0.3 fM.

5 Future Perspectives

Great progress has been made by coupling micro-nano structured materials and nucleic acid amplification methods. However, there are specific problems that need to be solved for the development of practical and sensitive biosensors. The high reactivity of micro-nano structured materials toward the biomolecules that increase the background signals, the multistep fabrication of nanomaterials, and the particularly long time needed to assemble DNA nanostructures are not good enough for most standardized clinical (and some other) analyses. If these problems can be overcome in the future, the possibility of coupling micro-nano structured materials with nucleic acid amplification methods is a fact. The amplification methods can increase the signal-to-noise ratio, which is highly efficient for miRNA detection or target sequences belonging to a complex matrix. Future perspectives may focus on the development of complete, fully disposable miniaturized devices, allowing sample clean-up, amplification and electrochemical detection, and minimal sample manipulation (avoiding cross-contamination and safety issues), and minimizing the time-to-result window, which is a particular challenge for the tests that employ DNA nanostructures.

References

Ali MM, Li F, Zhang Z, Zhang K, Kang D-K, Ankrum JA, Le XC, Zhao W (2014) Rolling circle amplification: a versatile tool for chemical biology, materials science and medicine. Chem Soc Rev 43:3324–3341

Ang WL, Seah XY, Koh PC, Caroline C, Bonanni A (2020) Electrochemical polymerase chain reaction using electroactive graphene oxide nanoparticles as detection labels. ACS Appl Nano Mater 3:5489–5498

Aryal BR, Ranasinghe DR, Westover TR, Calvopiña DG, Davis RC, Harb JN, Woolley AT (2020) DNA origami mediated electrically connected metal-semiconductor junctions. Nano Res 13: 1419–1426

Authier L, Grossiord C, Brossier P, Limoges B (2001) Gold nanoparticle-based quantitative electrochemical detection of amplified human cytomegalovirus DNA using disposable microband electrodes. Anal Chem 73:4450–4456

Bansal KS, Jyoti A, Mahato K, Chandra P, Prakash R (2017) Highly sensitive in vitro biosensor for enterotoxigenic *Escherichia coli* detection based on ssDNA anchored on PtNPs-chitosan nanocomposite. Electroanalysis 29:2665–2671

Barreda-García S, González-Álvarez MJ, de-los-Santos-Álvarez N, Palacios-Gutiérrez JJ, Miranda-Ordieres AJ, Lobo-Castañón MJ (2014) Attomolar quantitation of *Mycobacterium tuberculosis* by asymmetric helicase-dependent isothermal DNA-amplification and electrochemical detection. Biosens Bioelectron 68:122–128

Becherer L, Borst N, Bakheit M, Frischmann S, Zengerle R, von Stetten F (2020) Loop-mediated isothermal amplification (LAMP) – Review and classification of methods for sequence-specific detection. Anal Methods 12:717–746

Berensmeier S (2006) Magnetic particles for the separation and purification of nucleic acids. Appl Microbiol Biotechnol 73:495–504

Bi S, Yue S, Zhang S (2017) Hybridization chain reaction: a versatile molecular tool for biosensing, bioimaging, and biomedicine. Chem Soc Rev 46:4281–4298

Brasil de Oliveira Marques PR, Lermo A, Campoy S, Yamanaka H, Barbé J, Alegret S, Pividori MI (2009) Double-tagging polymerase chain reaction with a thiolated primer and electrochemical genosensing based on gold nanocomposite sensor for food safety. Anal Chem 81:1332–1339

Cai H, Shang C, Hsing I-M (2004) Sequence-specific electrochemical recognition of multiple species using nanoparticle labels. Anal Chim Acta 523:61–68

Cardoso VF, Francesko A, Ribeiro C, Bañobre-López M, Martins P, Lanceros-Mendez S (2018) Advances in magnetic nanoparticles for biomedical applications. Adv Healthc Mater 7:1700845

Chen Z, Liu Y, Xin C, Zhao J, Liu S (2018) A cascade autocatalytic strand displacement amplification and hybridization chain reaction event for label-free and ultrasensitive electrochemical nucleic acid biosensing. Biosens Bioelectron 113:1–8

Chen Y, Li Y, Shi Y, Ping J, Wu J, Chen H (2020) Magnetic particles for integrated nucleic acid purification, amplification and detection without pipetting. Trends Anal Chem 127:115912

de la Escosura-Muñiz A, Baptista-Pires L, Serrano L, Altet L, Francino O, Sánchez A, Merkoçi A (2016) Magnetic bead/gold nanoparticle double-labeled primers for electrochemical detection of isothermal amplified *Leishmania* DNA. Small 12:205–213

Dirks RM, Pierce NA (2004) From the cover: triggered amplification by hybridization chain reaction. Proc Natl Acad Sci 101:15275–15278

Feng C, Mao X, Yang Y, Zhu X, Yin Y, Li G (2016) Rolling circle amplification in electrochemical biosensor with biomedical applications. J Electroanal Chem 781:223–232

Ge Z, Lin M, Wang P, Pei H, Yan J, Shi J, Huang Q, He D, Fan C, Zuo X (2014) Hybridization chain reaction amplification of microRNA detection with a tetrahedral DNA nanostructure-based electrochemical biosensor. Anal Chem 86:2124–2213

Gillespie P, Ladame S, O'Hare D (2019) Molecular methods in electrochemical microRNA detection. Analyst 144:114–129

Gloag L, Mehdipour M, Chen D, Tilley RD, Gooding JJ (2019) Advances in the application of magnetic nanoparticles for sensing. Adv Mater 31:1904385

Goodman RP, Schaap IAT, Tardin CF, Erben CM, Berry RM, Schmidt CF, Turberfield AJ (2005) Chemistry: rapid chiral assembly of rigid DNA building blocks for molecular nanofabrication. Science 310:1661–1665

Goon IY, Lai LMH, Lim M, Amal R, Gooding JJ (2010) "Dispersible electrodes": a solution to slow response times of sensitive sensors. Chem Commun 46:8821–8823

Hou T, Liu X, Wang X, Jiang A, Liu S, Li F (2014) DNAzyme-guided polymerization of aniline for ultrasensitive electrochemical detection of nucleic acid with bio-bar codes-initiated rolling circle amplification. Sensors Actuators B Chem 190:384–388

Ji H, Yan F, Lei J, Ju H (2012) Ultrasensitive electrochemical detection of nucleic acids by template enhanced hybridization followed with rolling circle amplification. Anal Chem 84:7166–7171

Koehne J, Chen H, Li J, Cassell AM, Ye Q, Ng HT, Han J, Meyyappan M (2003) Ultrasensitive label-free DNA analysis using an electronic chip based on carbon nanotube nanoelectrode arrays. Nanotechnology 14:1239–1245

Koehne JE, Chen H, Cassell A, Liu G, Li J, Meyyappan M (2009) Arrays of carbon nanofibers as a platform for biosensing at the molecular level and for tissue engineering and implantation. Biomed Mater Eng 19:35–43

Labib M, Berezovski MV (2015) Electrochemical sensing of microRNAs: avenues and paradigms. Biosens Bioelectron 68:83–94

Lei Y, Yang F, Tang L, Chen K, Zhang G-J (2015) Identification of Chinese herbs using a sequencing-free nanostructured electrochemical DNA biosensor. Sensors 15:29882–29892

Lermo A, Campoy S, Barbé J, Hernández S, Alegret S, Pividori MI (2007) In situ DNA amplification with magnetic primers for the electrochemical detection of food pathogens. Biosens Bioelectron 22:2010–2017

Li LL, Cai H, Lee TMH, Barford J, Hsing IM (2004) Electrochemical detection of PCR amplicons using electroconductive polymer modified electrode and multiple nanoparticle labels. Electroanalysis 16:81–87

Li Q, Kartikowati CW, Horie S, Ogi T, Iwaki T, Okuyama K (2017) Correlation between particle size/domain structure and magnetic properties of highly crystalline Fe_3O_4 nanoparticles. Sci Rep 7:1–7

Lin M, Song P, Zhou G, Zuo X, Aldalbahi A, Lou X, Shi J, Fan C (2016) Electrochemical detection of nucleic acids, proteins, small molecules and cells using a DNA-nanostructure-based universal biosensing platform. Nat Protoc 11:1244–1263

Liu B, Liu J (2017) Methods for preparing DNA-functionalized gold nanoparticles, a key reagent of bioanalytical chemistry. Anal Methods 9:2633–2643

Liu H, Bei X, Xia Q, Fu Y, Zhang S, Liu M, Fan K, Zhang M, Yang Y (2016) Enzyme-free electrochemical detection of microRNA-21 using immobilized hairpin probes and a target-triggered hybridization chain reaction amplification strategy. Microchim Acta 183:297–304

Liu L, Chang Y, Xia N, Peng P, Zhang L, Jiang M, Zhang J, Lin L (2017) Simple, sensitive and label–free electrochemical detection of microRNAs based on the in situ formation of silver nanoparticles aggregates for signal amplification. Biosens Bioelectron 94:235–242

Liu H, Luo J, Fang L, Huang H, Deng J, Huang J, Zhang S, Li Y, Zheng J (2018) An electrochemical strategy with tetrahedron rolling circle amplification for ultrasensitive detection of DNA methylation. Biosens Bioelectron 121:47–53

Liu Y, Li X, Chen J, Yuan C (2020) Micro/nano electrode array sensors: advances in fabrication and emerging applications in bioanalysis. Front Chem 8:1102

Masud MK, Na J, Younus M, Hossain MSA, Bando Y, Shiddiky MJA, Yamauchi Y (2019) Superparamagnetic nanoarchitectures for disease-specific biomarker detection. Chem Soc Rev 48:5717–5751

Masud MK, Na J, Lin TE, Malgras V, Preet A, Ibn Sina AA, Wood K, Billah M, Kim J, You J, Kani K, Whitten AE, Salomon C, Nguyen NT, Shiddiky MJA, Trau M, Hossain MSA & Yamauchi Y (2020) Nanostructured mesoporous gold biosensor for microRNA detection at attomolar level. Biosens Bioelectron 168:112429

Meng T, Jia H, An S, Wang H, Yang X, Zhang Y (2020) Pd nanoparticles-DNA layered nanoreticulation biosensor based on target-catalytic hairpin assembly for ultrasensitive and selective biosensing of microRNA-21. Sensors Actuators B Chem 323:128621

Miao P, Tang Y, Yin J (2015a) MicroRNA detection based on analyte triggered nanoparticle localization on a tetrahedral DNA modified electrode followed by hybridization chain reaction dual amplification. Chem Commun 51:15629–15632

Miao P, Wang B, Meng F, Yin J, Tang Y (2015b) Ultrasensitive detection of microRNA through rolling circle amplification on a DNA tetrahedron decorated electrode. Bioconjug Chem 26: 602–607

Nagamine K, Hase T, Notomi T (2002) Accelerated reaction by loop-mediated isothermal amplification using loop primers. Mol Cell Probes 16:223–229

Nguyen K, Monteverde M, Filoramo A, Goux-Capes L, Lyonnais S, Jegou P, Viel P, Goffman M, Bourgoin JP (2008) Synthesis of thin and highly conductive DNA-based palladium nanowires. Adv Mater 20:1099–1104

Nguyen T, Chidambara VA, Andreasen SZ, Golabi M, Huynh VN, Linh QT, Bang DD, Wolff A (2020) Point-of-care devices for pathogen detections: the three most important factors to realise towards commercialization. TrAC Trends Anal Chem 131:116004

Notomi T, Okayama H, Masubuchi H, Yonekawa T, Watanabe K, Amino N, Hase T (2000) Loop-mediated isothermal amplification of DNA. Nucleic Acids Res 28:63e

Ozsoz M, Erdem A, Kerman K, Ozkan D, Tugrul B, Topcuoglu N, Ekren H, Taylan M (2003) Electrochemical genosensor based on colloidal gold nanoparticles for the detection of factor V Leiden mutation using disposable pencil graphite electrodes. Anal Chem 75:2181–2187

Park SJ, Taton TA, Mirkin CA (2002) Array-based electrical detection of DNA with nanoparticle probes. Science 295:1503–1506

Pastucha M, Farka Z, Lacina K, Mikušová Z, Skládal P (2019) Magnetic nanoparticles for smart electrochemical immunoassays: a review on recent developments. Microchim Acta 186:312

Purohit B, Vernekar PR, Shetti NP, Chandra P (2020) Biosensor nanoengineering: design, operation, and implementation for biomolecular analysis. Sensors International 1:100040

Rashid JIA, Yusof NA (2017) The strategies of DNA immobilization and hybridization detection mechanism in the construction of electrochemical DNA sensor: a review. Sens Bio-Sensing Res 16:19–31

Richter J (2003) Metallization of DNA. Phys E Low-dimensional Syst Nanostructures 16:157–173

Saiki R, Scharf S, Faloona F, Mullis K, Horn G, Erlich H, Arnheim N (1985) Enzymatic amplification of beta-globin genomic sequences and restriction site analysis for diagnosis of sickle cell anemia. Science 230:1350–1354

Saiki R, Gelfand D, Stoffel S, Scharf S, Higuchi R, Horn G, Mullis K, Erlich H (1988) Primer-directed enzymatic amplification of DNA with a thermostable DNA polymerase. Science 239: 487–491

Shan J, Wang L, Yu H, Ji J, Amer WA, Chen Y, Jing G, Khalid H, Akram M, Abbasi NM (2016) Recent progress in Fe_3O_4 based magnetic nanoparticles: from synthesis to application. Mater Sci Technol 32:602–614

Sharif S, Wang Y, Ye Z, Wang Z, Qiu Q, Ying S, Ying Y (2019) A novel impedimetric sensor for detecting LAMP amplicons of pathogenic DNA based on magnetic separation. Sensors Actuators B Chem 301:127051

Su Y, Li D, Liu B, Xiao M, Wang F, Li L, Zhang X, Pei H (2019) Rational design of framework nucleic acids for bioanalytical applications. ChemPlusChem 84:512–523

Tian Q, Wang Y, Deng R, Lin L, Liu Y, Li J (2015) Carbon nanotube enhanced label-free detection of microRNAs based on hairpin probe triggered solid-phase rolling-circle amplification. Nanoscale 7:987–993

Tosar JP, Brañas G, Laíz J (2010) Electrochemical DNA hybridization sensors applied to real and complex biological samples. Biosens Bioelectron 26:1205–1217

Wang Y, Ma H, Wang X, Pang X, Wu D, Du B, Wei Q (2015) Novel signal amplification strategy for ultrasensitive sandwich-type electrochemical immunosensor employing Pd-Fe_3O_4-GS as the matrix and SiO_2 as the label. Biosens Bioelectron 74:59–65

Wang Y, Zhang X, Zhao L, Bao T, Wen W, Zhang X, Wang S (2017) Integrated amplified aptasensor with in-situ precise preparation of copper nanoclusters for ultrasensitive electrochemical detection of microRNA 21. Biosens Bioelectron 98:386–391

Wei F, Lillehoj P, Ho CM (2010) DNA diagnostics: nanotechnology-enhanced electrochemical detection of nucleic acids. Pediatr Res 67:458–468

Wu J, Pei L, Xuan S, Yan Q, Gong X (2016) Particle size dependent rheological property in magnetic fluid. J Magn Magn Mater 408:18–25

Xu J, Zhu X, Zhou X, Khusbu FY, Ma C (2020) Recent advances in the bioanalytical and biomedical applications of DNA-templated silver nanoclusters. TrAC Trends Anal Chem 124:115786

Yang T, Zhou N, Zhang Y, Zhang W, Jiao K, Li G (2009) Synergistically improved sensitivity for the detection of specific DNA sequences using polyaniline nanofibers and multi-walled carbon nanotubes composites. Biosens Bioelectron 24:2165–2170

Yang C, Shi K, Dou B, Xiang Y, Chai Y, Yuan R (2015) In situ DNA-templated synthesis of silver nanoclusters for ultrasensitive and label-free electrochemical detection of microRNA. ACS Appl Mater Interfaces 7:1188–1193

Yeung SW, Hsing IM (2006) Manipulation and extraction of genomic DNA from cell lysate by functionalized magnetic particles for lab on a chip applications. Biosens Bioelectron 21: 989–997

Yeung S, Lee TM-H, Cai H, Hsing IH (2006) A DNA biochip for on-the-spot multiplexed pathogen identification. Nucleic Acids Res 34:e118

Yu N, Wang Z, Wang C, Han J, Bu H (2017) Combining padlock exponential rolling circle amplification with $CoFe_2O_4$ magnetic nanoparticles for microRNA detection by nano-electrocatalysis without a substrate. Anal Chim Acta 962:24–31

Zhang Y, Yang T, Zhou N, Zhang W, Jiao K (2008) Nano Au/TiO_2 hollow microsphere membranes for the improved sensitivity of detecting specific DNA sequences related to transgenes in transgenic plants. Sci China Ser B Chem 51:1066–1073

Zhang C, Li D, Li D, Wen K, Yang X, Zhu Y (2019) Rolling circle amplification-mediated in situ synthesis of palladium nanoparticles for the ultrasensitive electrochemical detection of micro-RNA. Analyst 144:3817–3825

Zhang W, Xu H, Zhao X, Tang X, Yang S, Yu L, Zhao S, Chang K, Chen M (2020) 3D DNA nanonet structure coupled with target-catalyzed hairpin assembly for dual-signal synergistically amplified electrochemical sensing of circulating microRNA. Anal Chim Acta 1122:39–47

Zhao W, Ali MM, Brook MA, Li Y (2008) Rolling circle amplification: applications in nanotechnology and biodetection with functional nucleic acids. Angew Chemie Int Ed 47:6330–6337

Zhao S, Zhou Y, Wei L, Chen L (2020) Low fouling strategy of electrochemical biosensor based on chondroitin sulfate functionalized gold magnetic particle for voltammetric determination of mycoplasma ovipneumonia in whole serum. Anal Chim Acta 1126:91–99

Zhu C, Yang G, Li H, Du D, Lin Y (2015a) Electrochemical sensors and biosensors based on nanomaterials and nanostructures. Anal Chem 87:230–249

Zhu M, Liu W, Liu H, Liao Y, Wei J, Zhou X, Xing D (2015b) Construction of Fe_3O_4/vancomycin/PEG magnetic nanocarrier for highly efficient pathogen enrichment and gene sensing. ACS Appl Mater Interfaces 7:12873–12881

Zhu H, Zhang H, Ni S, Korabečná M, Yobas L, Neuzil P (2020) The vision of point-of-care PCR tests for the COVID-19 pandemic and beyond. TrAC Trends Anal Chem 130:115984

Zhuang J, Fu L, Xu M, Yang H, Chen G, Tang D (2013) Sensitive electrochemical monitoring of nucleic acids coupling DNA nanostructures with hybridization chain reaction. Anal Chim Acta 783:17–23

Current Overview of Drug Delivery, Bioimaging, and Electrochemical Biosensors on Mesoporous Silica Nanomaterials

20

Julia Oliveira Fernandes, Cassiano Augusto Rolim Bernardino,
Bernardo Ferreira Braz, Claudio Fernando Mahler,
Ricardo Erthal Santelli, and Fernando Henrique Cincotto

Contents

1 Introduction ... 438
2 Types of Mesoporous Silica ... 438
3 Synthetic Techniques of Mesoporous Silica Nanoparticles (MSNs) ... 440
4 Applications of Mesoporous Sílicas ... 442
5 Drug and Genes Deliveries ... 442
6 Bioimaging ... 444
7 Biosensor ... 444
8 Final Considerations ... 449
References ... 450

Abstract

Mesoporous silicas are materials that have aroused the interest of the industries and scientific community in the medical field. These nanomaterials present several relevant characteristics, and their application has been in drug delivery, bioimaging, and electrochemical biosensors to solve and prevent problems related to human health. The main silicas used for this purpose are the MCM-n and SBA-n families due to their high surface area, good biocompatibility, excellent hydrothermal stability, and absence of toxicity. Furthermore, these

---

J. O. Fernandes · B. F. Braz
Department of Analytical Chemistry, Institute of Chemistry, Federal University of Rio de Janeiro, Rio de Janeiro, Brazil

C. A. R. Bernardino · C. F. Mahler
Department of Civil Engineering, COPPE, Federal University of Rio de Janeiro, Rio de Janeiro, Brazil

R. E. Santelli · F. H. Cincotto (✉)
Department of Analytical Chemistry, Institute of Chemistry, Federal University of Rio de Janeiro, Rio de Janeiro, Brazil

National Institute of Science & Technology of Bioanalytics (INCTBio), São Paulo, Brazil
e-mail: fernandocincotto@iq.ufrj.br

© Springer Nature Singapore Pte Ltd. 2023

U. P. Azad, P. Chandra (eds.), *Handbook of Nanobioelectrochemistry*,
https://doi.org/10.1007/978-981-19-9437-1_20

synthesized nanomaterials are extremely inexpensive and have a low analysis time than conventional techniques. Therefore, the chapter shows the recent developments in drug delivery, bioimaging, and electrochemical biosensors based on various nanomaterials created with mesoporous silicas. This proposal focuses on providing an overview of the types of nanomaterials with mesoporous silicas that are being developed in several scientific studies. In addition, this work will show a history of the main silica families used in the development of various biosensors, bioimaging techniques, and the application of drug delivery for different analytes. Finally, the chapter proposes a reflection on the perspectives and challenges of new research on drug delivery, bioimaging, and electrochemical biosensors composed of mesoporous silicas.

Keywords

Mesoporous silica · Biosensor · Bioimaging · Drug delivery

1 Introduction

Porous materials are nanomaterials that have been of great interest to the evolution of medical treatments and the detection of diseases in humans. The International Union of Pure and Applied Chemistry (IUPAC) categorize the porous solids according to pore size (diameter, Ø). This classification is known as microporous (Ø < 2 nm), mesoporous (2 nm < Ø < 50 nm), and macroporous (Ø > 50 nm) (Sing et al. 1985). Mesoporous silicas are nanomaterials that have great relevance in nanomedicine because of important characteristics such as excellent surface reactivity and thermal, mechanical, and chemical stability. Moreover, the presence of active sites is well distributed on the external and internal surfaces, the high surface area (above 600 m^2 g^{-1}) and the mesoporous structure allow easy diffusion to the reaction on active sites (Costa et al. 2021). Given these characteristics, mesoporous silicas have been developed over the years. The scientific community and the industry have advanced in developing several families of silicas that have been applied for drug delivery, bioimaging, and the manufacture of biosensors.

2 Types of Mesoporous Silica

Synthetic silicas have shown excellent efficiency in biosensing. Then, several families of silica have been studied, such as Mobil Crystalline Materials (MCM-n), Santa Barbara Amorphous (SBA-n), Michigan State University (MSU-n), Korean Institute of Technology (KIT-n), Folded Sheet Materials (FSM-n), Fudan University (FDU-n), and Anionic Mesoporous Silica (AMS-n) (Vallet-Regí et al. 2013).

The first family of porous silicas, called M41S, was created by the *Mobil Corporation Laboratories* in 1992. This family has three mesoporous materials

(MCM-41, MCM-48, and MCM-50) containing silicate and aluminosilicate in diverse pore arrangements. The MCM-41 has two dimensions (2D), a hexagonal structure with P6mm space-group symmetry; the MCM-48 presents a three-dimensional (3D) cubic system with Ia3d space-group symmetry; and the MCM-50 shows a lame form without space-group symmetry (Beck et al. 1992; Kresge et al. 1992; Vartuli et al. 1994).

Another important family is the SBA-n (n ranges from 1 to 16), developed in 1998 at the University of Santa Barbara. This family of amorphous mesoporous silica nanomaterial was produced using a copolymer with a targeting agent and tetraorthosilicate (TEOS) as a silicon source (Zhao et al. 1998). From this technique, several materials were created with several pore geometric forms such as SBA-1 (cubic), SBA-3 (hexagonal), SBA-11 (cubic), SBA-12 (hexagonal 3D), SBA-14 (lame), SBA-15 (hexagonal 2D), and SBA-16 (cubic). In SBA-n family, the SBA-15 has been extensively studied because it has high hydrothermal stability due to the size of the silica walls (3.1–6.4 nm), larger pores (4.6–30 nm), and high surface area (Huo et al. 1995; Zhao et al. 1998).

In the case of the MSU-n family (n ranges from 1 to 4), the materials have a porous structure of “wormhole” in 3D with ill-defined crystallographic symmetry. The literature reports that this family is more active in reactions of limited diffusion; and non-ionic surfactants and block copolymers form this material (Boissière et al. 2000; Gong et al. 2001; Prouzet and Boissière 2005).

The KIT-n family (where n = 1, 5 or 6) was developed at the Korea Advanced Institute of Science and Technology (KAIST). Among the mesoporous silicas (KIT-1, KIT-5 and KIT-6), the most studied by the scientific community are KIT-5 and KIT-6 (Dongyuan Zhao et al. 2013). KIT-1 has a disordered 3D structure (Sanaeishoar et al. 2016). On the other hand, KIT-5 and KIT-6 materials have well-ordered 3D mesopores (cage) in a compact cubic structure centered on the face with Fm3m space-group symmetry, interconnected spherical amorphous walls. The KIT-5 and KIT-6 also present good hydrothermal stability, high surface area, large pore diameter and volume (He et al. 2020; Mahdizadeh Ghohe et al. 2019).

The FSM-n family (e.g., FSM-16) are folded sheets of mesoporous materials and can be synthesized using surfactant of quaternary ammonium and kanemite of polysilicate (Narayan et al. 2018; Tozuka et al. 2005). Regarding AMS-n, this mesoporous family with anionic surfactants has been studied due to the new interaction between inorganic and surfactant species, good cost-benefit, and lower toxicity of anionic surfactants compared to cationic surfactants. This synthetic route can produce several mesoporous forms such as cubic, lamelar, hexagonal, and disordered structures (Che et al. 2003).

The FDU-n family was developed at the University of Fudan and can be displayed in some classifications, such as FDU-1, FDU-2, FDU-5, FDU-12, FDU-14, and FDU-15. FDU-n can present different characteristics such as pore arrangements and well-ordered structures, large and uniform pore diameter distribution, amorphous pore wall structure, high surface area, mechanical and thermal stability (da Silva et al. 2011; Shen et al. 2002; Wu et al. 2018; Dongyuan Zhao et al. 2013). The Fig. 20.1 shows a scheme of some structures of mesoporous silicas.

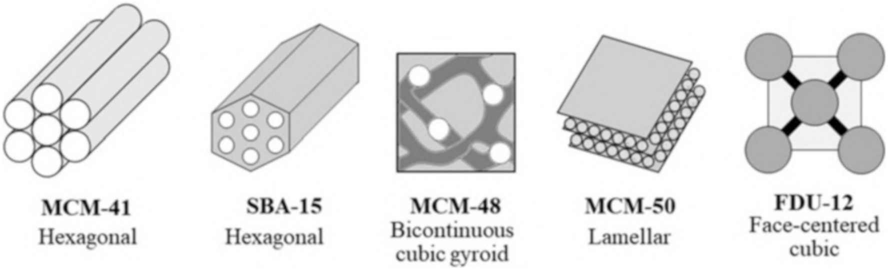

Fig. 20.1 Scheme of some structures of mesoporous silicas

3 Synthetic Techniques of Mesoporous Silica Nanoparticles (MSNs)

The synthetic techniques of mesoporous silica nanoparticles (MSNs) use three main components: (1) template; (2) silica source; and (3) acid/base. The template is usually a surfactant, which has the function of creating pores. The silica source has the function of forming the walls around the pores and the third component (acid/base) works as a facilitator of formation. The synthetic techniques of MSNs are three: (1) sol-gel; (2) hydrothermal; and (3) green method (Isa et al. 2021). Table 20.1 presents some examples of template and source of silica associated with the synthesis technique reference.

Stober et al. (1968) were the first to produce monodispersed silica particles in the spherical form of micrometric size by means of a set of chemical reactions, a method that became known as Stober synthesis, a process of sol-gel nature. This synthesis consists of hydrolysis of tetraalkyl silicates in a mixture of ethanol and water, and ammonia as a catalyst. In this process, the alkoxide monomers, in the presence of a base or acid as catalyst, are hydrolyzed and condensed into a colloidal solution (sol) from which an ordered network of particles (gel) is formed. Different models of structural-directing agents such as surfactants, copolymers, and organic compounds can be used (Kumar et al. 2017; Narayan et al. 2018; Stober et al. 1968; Wu and Lin 2013).

Over the years, this synthesis was submitted the several changes according to conditions and parameters. Grün et al. (1997) performed the first study of modifications to the Stober synthesis, by adding a cationic surfactant to the reaction, which resulted in spherical microparticles of MCM-41 (Grün et al. 1997; Isa et al. 2021; Narayan et al. 2018; Wu and Lin 2013). Since then, several studies have been conducted to obtain silica particles with different sizes and volumes of the pore, dimensions, and particle morphology. The use of traditional cationic surfactants results in simple mesoporous materials, with ordered pores and thin walls; however, they present limited pore size adjustment and low hydrothermal stability. Currently, instead of the traditional quaternary ammonium cationic surfactant have been studied new ionic liquid surfactants as a template (Wang et al. 2021).

Table 20.1 Some examples of template and silica sources associated with the synthetic technique reference

Synthesis technique	*Template*	Silica source	References
Sol-gel	PEG	Sodium silicate	Hwang et al. (2021)
Sol-gel	CTAC	TEOS	Khalil et al. (2020)
Sol-gel	CTAB	TEOS	Oliveira and Andrada (2019)
Sol-gel	CTAB	TEOS	Muthusami et al. (2020)
Sol-gel	CTAB	TEOS	Vazquez et al. (2017)
Hydrothermal	Pluronic F-127	TEOS	Ferreira Soares et al. (2020)
Hydrothermal	Ionic liquid surfactants	TEOS	Wang et al. (2021)
Hydrothermal	CTAB	TEOS	Song et al. (2019)
Green	Pluronic F-127	Rice husk	Vanichvattanadecha et al. (2020)
Green	CTAB	Banana peels ash (sodium silicate)	Mohamad et al. (2019)
Green	Pluronic P-123	TEOS	Feng et al. (2018)

PEG polyethylene glycol, *CTAC* cetyltrimethylammonium chloride, *CTAB* cetyltrimethylammonium bromide, *TEOS* tetraethylorthosilicate

The modified Stober method consists of four steps: (1) Mixing water, template and base; (2) Addition of the silica source and agitation, stage where occurs hydrolysis, condensation, and formation of the sol; (3) Sol aging and gel formation; (4) Obtaining MSN powder and calcination or extraction, by solvent to template removal (Isa et al. 2021; Singh et al. 2014).

The synthetic hydrothermal methodology is a chemical reaction under high temperature and pressure that results in a mesoporous material with better hydrothermal stability, larger pore size, and mesoscopic regularity. The steps of this synthesis method are five: (1) Mixture among water, template, and catalyst; (2) Addition of silica source; (3) Aging or short stirring of the mixture and transfer to a Teflon autoclave; (4) Heating of the autoclave for a certain period of time; (5) Getting MSN powder and removing the template. Despite the improvements observed when using this synthesis method, it requires expensive and specific equipment, which leads most researchers to opt for the sol-gel method (Feng et al. 2018; Isa et al. 2021; Yu et al. 2012).

Studies show that pH directly affects the morphology and size of mesoporous silica particles because it influences the hydrolysis rate, condensation rate, and interaction between the template and silica. Another important factor to be controlled is the rate of agitation. If it is slow, long fibers are produced and if it is quick, fine powder is produced. The adjustment of the pore width can be made by hydrothermal treatment (during or after synthesis). The use of additives during the synthesis assists the pore width. Mesythylene (1,3,5-trimethylbenzene), for example, is an additive used to expand the pores without changing the particle size. The hydrothermal treatment consists of pressurizing the newly synthesized particle and subjecting it to temperatures ranging from 373 to 423 K, with or without additives. In medical application, it is important to highlight that the amount of drug adsorbed on the mesoporous silica matrix is directly proportional to its surface area, pore volume, and affinity in both (Mehmood et al. 2017).

It is common for mesoporous materials to be synthesized under strongly acidic or basic conditions. However, this makes large-scale production unfeasible, since the widespread use of such reagents is *eco-unfriendly*. Neutral synthesis is also possible, but these conditions often result in poorly organized materials, because hydrolysis is incomplete and organic residues are present (Dai et al. 2012; Feng et al. 2018).

More recently, green synthetic routes, *environmentally friendly* and/or employing waste as a source of silica, have been studied (Isa et al. 2021). Feng et al. (2018) proposed a green synthesis strategy for SBA-15 and Fe-SBA-15 silicas without the use of strong acid. A method that uses hydroxyl free radicals (·OH) was presented as a green alternative, resulting in highly ordered materials with a high surface area than the synthetic method in an acid medium. This study also demonstrated that, for hydrolysis of tetraethylorthosilicate (TEOS), free radicals OH have higher catalytic activity than H^+ ions.

4 Applications of Mesoporous Sílicas

Mesoporous silica nanoparticles are for various purposes such as drug delivery, biosensor, bioimaging, catalysis, optical devices, antimicrobial activity, protein delivery, polymer filling, adsorption, separation, and purification. These applications of mesoporous silicas are due to several attractive properties such as biocompatibility, high thermal stability, efficient absorption by mammalian cells, small pore diameter, high surface area and pore volume, adjustable pore structure, and mechanical stability (Kumar et al. 2017). This chapter will focus on the first three applications mentioned: drug delivery, bioimaging, and biosensor.

5 Drug and Genes Deliveries

Nanomedicine is the term commonly used to refer to nanomaterials for the distribution of drugs in the body. The first transporters, reported in 1960, were liposomes. Then, several drug deliveries were developed to increase the effectiveness of treatment. The nanoparticles used in this transport may be organic or inorganic, but it has already been observed that inorganic ones are more stable. Vallet-Regi et al. (2001) were the pioneers in applying MCM-41 to the transport of drugs (Ibuprofen) (Gisbert-Garzarán et al. 2020; Vallet-Regi et al. 2001).

Nanoparticles used for drug delivery need to have properties, such as: biocompatibility, that is, rapid internalization by human being, without cytotoxicity, maximizing the amount of drug loading within the pore channels, reaching the target and minimizing premature release (Gisbert-Garzarán et al. 2020).

Inorganic mesoporous silica nanomaterials are promising carriers for drug administration. The interaction between mesoporous silica nanoparticles (MSN) and the drug occurs through hydrogen and/or electrostatic bonds. MSNs are biocompatible and have an extremely porous and open structure, so that drug release to the target is minimized. It is necessary to adapt the nanoparticles to make the drug available only when stimulus is applied; this adaptation is the *gatekeeper* (Gisbert-Garzarán et al. 2017; Pal et al. 2020).

Several types of *gatekeepers* of the various natures can be used, each with its specific stimulus for removing MSNs. Some examples are polymers, quantum dots, gold nanoparticles, silver nanoparticles, fullerenes, cyclodextrins, pilararenes, nucleic acids, proteins, peptides, etc. The stimuli are also varied with pH, redox potential, temperature, enzyme, complementary sequence, irradiation, and others (Gisbert-Garzarán et al. 2017; Wen et al. 2017).

MSNs present promising prospects for diagnosing and treating serious diseases such as cancer. Despite recent advances in research related to this disease, developing more specific and effective treatments is still necessary. Chemotherapy and radiation therapy have serious side effects on the patient. Metastasis is a challenge, and in many cases, surgical removal is impossible. In this scenario, multifunctional drug delivery agents utilizing different nanomaterials can be an important alternative (Isa et al. 2021).

In general, MSNs can be used to carry various types of drugs. Each type of MSN associated with a type of drug has an ability to transport that needs to be studied. Examples of carried drugs are Ibuprofen, 5-Fluorouracil, Captopril, Doxorubicin, and Lendronate (Balas et al. 2006; Chen et al. 2014; Narayan et al. 2018; Qu et al. 2006; She et al. 2015; Vallet-Regi et al. 2001; Zhu et al. 2005). Table 20.2 shows some MSNs used in drug delivery, *gatekeeper*, and stimulus.

Mesoporous silica with hybrid materials are also found in the literature, enabling the combination of several components in entities of nanometric dimension. Among some of these hybrid materials, it can mention magnetic nanocomposites of mesoporous silica, nanocomposites of mesoporous silica responsive to the light, and

Table 20.2 Some mesoporous silica nanoparticles (MSNs) used in drug delivery

Silica	Gatekeeper	Stimulus	Drug	References
MSN-SS-Au	Au	Redox	Doxorubicin	Zhang et al. (2020a)
MSN-NA-CS	CS	Redox	Rhodamine 6G	Chen et al. (2020)
MSN-SS-GQD	Graphene	Redox	Rhodamine B	Gao et al. (2019)
HA-FMSN	HA	Enzyme	5-Fluorouracil	Jiang et al. (2018)
MSN	Iron oxide	Enzyme	Doxorubicin	Qiao et al. (2019)
MSN-PAA-FA	PAA	pH	Umbelliferone	Kundu et al. (2020)
MSNR	Albumin	pH	Lamivudine	Zhang et al. (2020b)

FA folic acid, *PAA* polyacrylic acid, *HA* hyaluronic acid, *CS* chitosan, *Au* gold, *NA* 1,8-Naphthalimide fluorophore, *SS* disulfide bonds, *GQD* graphene quantum dot, *MSNR* mesoporous silica nanorod multicomponent nanocomposites containing mesoporous silica (Castillo and Vallet-Regí 2019).

In addition, the use of MSNs have also been an alternative in the application of gene delivery. MSNs have been developed to encapsulate abundant genes and protect genes from nucleases. Through cationic modification, MSNs have been able to complex with genes and be successfully transfected into multiple cells (Zhou et al. 2018). Finally, drugs and genetic materials in-vitro can be selected and co-delivered by mesoporous silica nanoparticles to be applied in different therapeutic objectives (Paris and Vallet-Regí 2020).

6 Bioimaging

The adjustment properties of the morphology and size of MSNs have allowed the broad development of its use as a flexible, biocompatible imaging platform with a functionalizable surface. MSNs can be used to obtain quantitative images. The excellent benefit is that MSNs are cleared from the patient's body when the imaging process is finished. Images are usually obtained by optical or magnetic resonance (Mehmood et al. 2017; Yuan et al. 2020).

The filling of mesopores is performed with drugs, quantum dots, and/or fluorescent dyes, since bioimaging aims to monitor infected cells, drug molecules, and even biological processes in vivo, resulting in an important diagnostic resource (Pal et al. 2020; Pratiwi et al. 2018). Table 20.3 describes some functionalized MSNs used in bioimaging.

There are several strategies developed in recent years to fill the pores or surface of MSNs with fluorescent dyes, giving rise to FMSNs (fluorescent mesoporous silica nanoparticles) (Pratiwi et al. 2018).

7 Biosensor

Nanomedicine has focused on producing new biosensors to advance the development of therapeutic and clinical diagnostics for the detection, prevention, and treatment of diseases, which result in expressive improvements in human health (Niculescu 2020; Slowing et al. 2007). Thus, the scientific community has studied

Table 20.3 Some functionalized mesoporous silica nanoparticles used in bioimaging

Silica synthesis	Modifier	Analyte	References
CTAB/TEOS	Rhodamine B	Cu^{2+}	Liu et al. (2011)
CTAC/TEOS	Folic acid	Cancer cells	Palantavida et al. (2013)
CTAB/TEOS	FITC/PEG	Cancer cells	Song et al. (2012)
CTAB/TEOS	Iridium (III) complexes	Hypochlorite	Zhang et al. (2015)

FITC fluorescein isothiocyanate, *PEG* Polyethylene glycol, *CTAC* cetyltrimethylammonium chloride, *CTAB* cetyltrimethylammonium bromide, *TEOS* tetraethylorthosilicate

MSNs in biosensors to detect several analytes that are highly important in nanomedicine. Table 20.4 presents several biosensors based on several MSNs that have been recently explored to detect different types of analytes.

Zheng et al. (2009) determined Dopamine, Ascorbic acid, and Uric acid in ordered mesoporous carbon (OMC)/Nafion composite film in human urine. The synthesis of OMC was performed through an nanocastification process using mesoporous silica (KIT-6) as the rigid model and a commercially available PF resin (Mw = 4500), as the precursor without catalysts (Zhou et al. 2006). The authors showed that the electrode presented a total pore volume of 1.09 $cm^3\ g^{-1}$, a pore size of 3.9 nm, and a surface area of 886 $m^2\ g^{-1}$. The analysis results indicated a recovery between 100.6 and 103% of the analytes (Dopamine, Ascorbic acid, and Uric acid).

Zhang et al. (2014) developed the ordered two-dimensional mesoporous carbon nitride biosensor (OMCN-800). This material was treated by pyrolysis at 800 °C and prepared with mesoporous silica (SBA-15 and Melamine to determine Hydrogen peroxide (H_2O_2), Nitrobenzene and Adenine nicotinamide dinucleotide (NADH). The advantage of using OMCN-800 is the improvement of the mechanical, conductive, field emission and energy storage properties. This biosensor presented a surface area of 659.2 $m^2\ g^{-1}$, pore volume of 0.52 $cm^3\ g^{-1}$, and pore diameter of 5.24 nm. The OMCN-800/GCE indicated high sensitivity, wide linear range, good stability, and low detection limit.

Bagheri Hashkavayi et al. (2016) presented a system based on a Chloramphenicol-binding aptamer that is a molecular recognition element and mesoporous silica supported by 1,4-Diazabicyclo [2.2.2] octane (DABCO) and SBA-15 on the surface of a graphite electrode printed on canvas for the formation of dendritic gold nanostructures to improve the conductivity of the biosensor. The detection of the biosensor for the determination of Chloramphenicol was applied to blood serum samples. The results showed that the biosensor had good selectivity and high sensitivity for determining chloramphenicol and a wide linear range.

Khalilzadeh et al. (2016) reported an electrode composed of electrodeposited on a modified vitreous carbon electrode HRP-MB-BP-AuNP-S-MCM-41 to measure Caspase-3 activity in stem cell. The results showed a low detection limit (less than 5 fM). The detection method for Caspase-3 activity in stem cell proved to be reliable, fast, sensitive and inexpensive for application in medicine. Figure 20.2 shows a schematic of the electrochemical biosensor developed.

Chen et al. (2016) developed a chemiluminescence biosensor composed of MSNs modified with the amino group (NH_2) and aimed to determine Cocaine in human serum. The synthesis of the MSNs was based on a controlled release delivery system composed of the MCM-41 that is responsive to stimuli and chemically inert to the compounds trapped in the matrix. The system consists of a mesoporous silica nanosphere material functionalized with 2-(Propyldisulfanyl) ethylamine with an average pore diameter of 2.3 nm and an average particle size of 200 nm (Lai et al. 2003). Chemiluminescence (CL), which is the light emission (luminescence) based on the chemical reaction, was coupled to this system due to some relevant advantages such as simplicity and low cost of the equipment, high sensitivity, tiny sample required, and the results are unchanged by side reactions. The material synthesized

Table 20.4 Biosensors developed with MSNs and used in nanomedicine

Analyte	Matrix	Sensor with silica	Method	LOD	Linear range	References
Cocaine	Human serum	MSN-NH_2	CL	1.43 μM	5.0–60 μM	Chen et al. (2016)
Ascorbic acid	Human urine	CMK-1 (KIT-6/PF resin)	DPV	20 μM	40–800 μM	Zheng et al. (2009)
Dopamine				0.5 μM	1–90 μM	
Uric acid				40 μM	5–80 μM	
Hydrogen peroxide	Neutral solution	OMCN-800/GCE (SBA-15)	DPV	1.52 μM	4–40 μM	Zhang et al. (2014)
Nitrobenzene				0.18 μM	0.5–1000 μM	
Adenine nicotinamide dinucleotide				0.82 μM	2–2200 μM	
Dopamine	–	PPy/C#SiO_2/GCE	DPV	0.7 μM	1–200 μM	Liu et al. (2020)
Cholesterol	Human serum	AF-MSN-QD@ZIF-8-ChOx	Ratiometric fluorescence	2.39 μM	5.17–258.6 μM	Wang et al. (2018)
Glucose	Human blood	Se-MCM-41/GOD	CV	100 μM	10–200 μM	Yusan et al. (2018)
Caspase-3 activity	Stem cell	HRP-MB-BP-AuNP-S-MCM-41	SWV	5 fM	10 fM-10 nM	Khalilzadeh et al. (2016)
Chloramphenicol	Blood serum	HEM/Apt/AuNPs/SBA-15@DABCO/SPE	CV, EIS, and DPV	4.0 nM	0.03–0.15 μM 0.15–7.0 μM	Bagheri Hashkavayi et al. (2016)
Carcinoembryonic antigen	Buffered solutions	Apt/AuNP-MSN/SPE	DPV	280 fg mL^{-1}	1–160 ng mL^{-1}	Jimenez-Falcao et al. (2019)
	Human serum			510 fg mL^{-1}		
S1 nuclease	Milk and drinking water	hemin–MSN@DNA	CL	0.1 mU	0.1–10 U	Gu et al. (2019)
Escherichia coli				3 cfu mL^{-1}	10^1–10^9 cfu mL^{-1}	
Staphylococcus aureus				2.5 cfu mL^{-1}		
H_2O_2	Live cells	Ag-mSiO_2 NPs/GCE	AMP	3 μM	4 μM–10 mM	Yang et al. (2019)

CL chemiluminescence, *CV* cyclic voltammetry; *DPV* differential pulse voltammetry, *EIS* electrochemical impedance spectroscopy, *SWV* square wave voltammetry, *AMP* amperometric analysis, *LOD* limit of detection

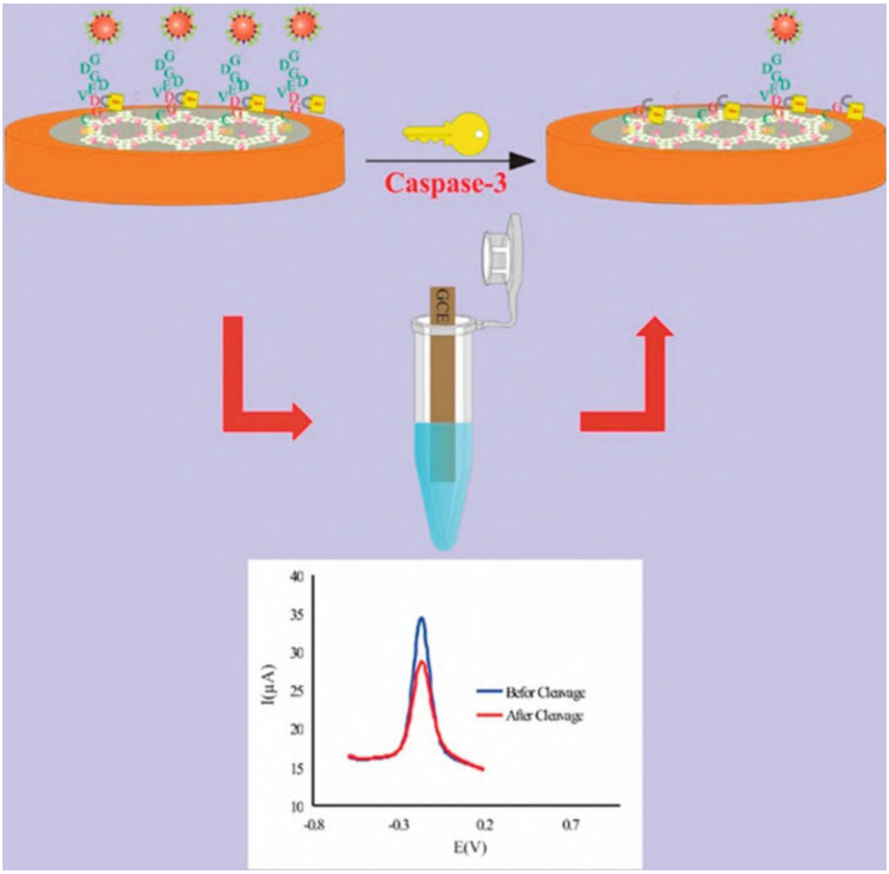

Fig. 20.2 Schematic presentation of the electrochemical biosensor engineered by gold nanoparticle functionalized MCM-41. (Reprinted with permission from Khalilzadeh et al. (2016). Copyright 2021 Elsevier)

with modified MSNs had a surface area of 956 $m^2 g^{-1}$, a pore diameter of 2.2 nm, and a pore volume of 0.42 $cm^3 g^{-1}$. The biosensor for the determination of Cocaine in human serum was efficient, with recovery between 94.1% and101%.

Yusan et al. (2018) created a bioenzyme glucose biosensor for glucose detection that was developed by immobilizing Glucose oxidase (GOD) in a selenium mesoporous silica nanoparticle (MCM-41) composite matrix and prepared as a carbon paste electrode (CPE). The biosensor had the potential to determine the Glucose concentration in human blood due to low detection limit (1×10^{-4} M), high sensitivity (0.34 μA mM^{-1}), good reproducibility (RSD of 2.8%), high affinity for glucose (Km = 0.02 mM), and stability of about 10 days when stored dry at +4 ° C.

Wang et al. (2018) demonstrated that a biosensor with a raciometric fluorescence detection system composed of MSNs coupled with quantum dots could be used to determine Cholesterol in human serum. 5-Aminofluorescein (AF) was used to charge the pores of the MSNs, which were involved in quantum red emission CdTe dots (QDs) on the surface to seal in the dye molecules, forming the signal display unit (AF-MSN-QDs) encapsulated with a zeolytic imidazolate structure (ZIF-8). Therefore, the Cholesterol oxidase (ChOx) self-organized on the surface of AF-MSN-QDs encapsulated in ZIF-8 via chemo-physical adsorption, forming new composites core-shell (AF-MSN-QD @ ZIF-8-ChOx) as a detection platform for Cholesterol detection. The results showed a linear variation of 5.17–258.6 μM and a quantification limit of 2.39 μM for human serum, suggesting the effectiveness of the biosensor.

Liu et al. (2020) used a biosensor with electrode based on conductive polypyrrole/carbon-coated mesoporous silica to determine Dopamine. The MSNs (SiO2) were synthesized with the cationic surfactant Cetyltrimethylammonium bromide. The silica nanoparticles were coated with a carbon layer (C # SiO_2) and were also used as a core for the in situ chemical-oxidative polymerization of conductive polypyrrole (PPy). The authors concluded that the biosensor detected Dopamine and was successful in the presence of Uric acid and *L*-ascorbic acid. In addition, the excellent performance and great sensitivity of the biosensor were related to the low limit of detection (0.7 μM) and the good linear range (1–200 μM).

Jimenez-Falcao et al. (2019) employed a signal amplification approach for affinity electrochemical biosensors based on MSN loaded with a redox probe and capped with an avidin/imminobiotin pH-responsive ensemble. This signal amplification was validated by an electrochemical aptasensor for the detection of carcinoembryonic antigen. The aptasensor was constructed carbon screen-printed electrodes modified with gold nanoparticles (AuNP/SPE). The limit of detection was 280 and 510 fg mL^{-1} in buffered solutions and diluted human serum samples, respectively. Figure 20.3 shows a schematic of the electrochemical biosensor developed.

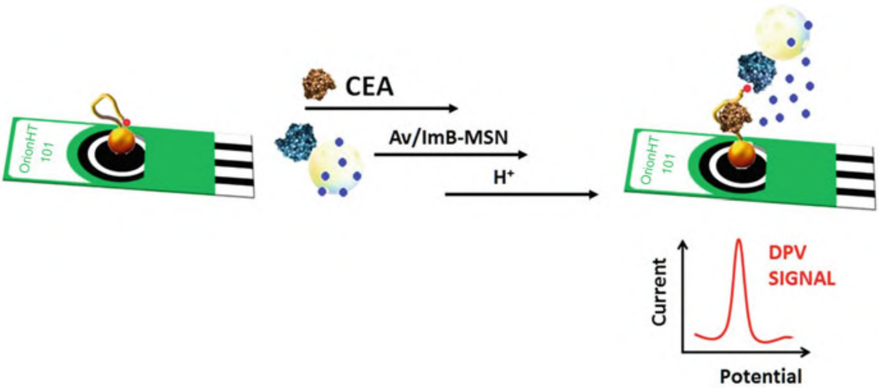

Fig. 20.3 Schematic presentation a electrochemical biosensor using Avidin-gated mesoporous silica nanoparticles. (Reprinted with permission from Jimenez-Falcao et al. (2019). Copyright 2021 Elsevier)

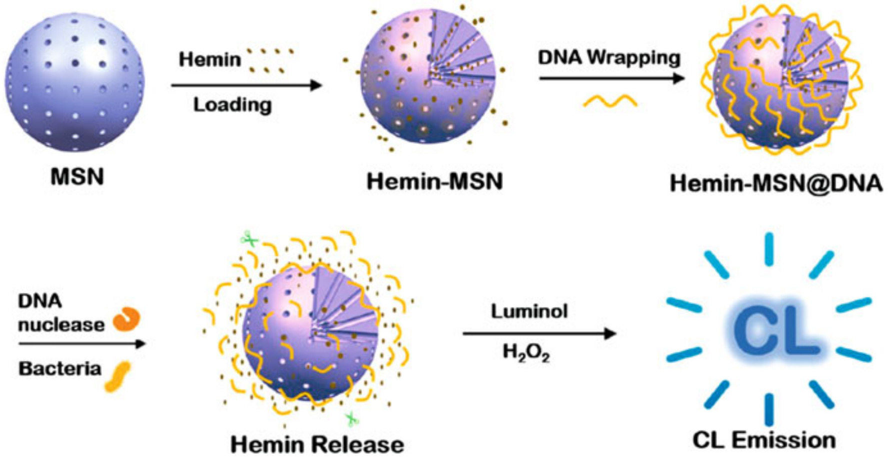

Fig. 20.4 Schematic presentation a chemiluminescence biosensor for DNA nuclease and bacteria detection. (Reprinted with permission from Gu et al. (2019). Copyright 2021 American Chemical Society)

Gu et al. (2019) developed a chemiluminescence biosensor aimed at simple and convenient detection of S1 nuclease and bacteria in fields such as bacterial contamination of food, pharmaceuticals, and clinical analysis. The limits of detection were 0.1 mU, 3.0 and 2.5 cfu mL^{-1} for the S1 nuclease, *Escherichia coli,* and *Staphylococcus aureus*. Figure 20.4 shows a schematic of the chemiluminescence biosensor developed.

Yang et al. (2019) studied silver-doped mesoporous silica nanoparticles-based enzyme-less electrochemical sensor for the determination of hydrogen peroxide (H_2O_2) released from live cells. The authors found a wide linear range (4 μM to 10 mM), a low detection limit of 3 μM, and an optimized potential of −0.5 V with high selectivity over biological interferents such as uric acid, ascorbic acid, and glucose.

8 Final Considerations

The nanomaterials composed of mesoporous silicas aimed at drug delivery, bioimaging, and electrochemical biosensors are highly relevant to the detection, control, and resolution of problems related to human health. MSNs, due to their properties such as high surface area, without toxicity, excellent biocompatibility, and excellent thermal, mechanics and chemistry stability have contributed to the development of different drug delivery, bioimaging and electrochemical biosensors. Several studies with different strategies for creating biosensors based on MSNs, mainly related to the families of SBA-n, MCM-n, and modified silicas, aim to increase the effectiveness of these nanomaterials in human health. Another interesting and relevant factor is the search for biosensors with great efficiency, wide linear range and increasingly lower detection limits to diagnose, control, and prevent adverse effects on human health cheaply and accurately. It is essential to highlight that detecting analytes by biosensors in blood samples has been challenging because of the highly complex and dynamic biological matrix. Therefore, the biomonitoring through biosensors and drug delivery composed of mesoporous silicas has contributed to the diagnosis and treatment of diseases and improved human health. For this reason, the drug delivery, bioimaging, and electrochemical biosensors based on nanomaterials of mesoporous silicas have had great relevance by the scientific community and industries due to their efficiency, recovery rates, and trace detection limits of several analytes in the nanomedicine. Finally, when financial resources are scarce, these sensors have a high-speed analysis time and are more inexpensive than conventional techniques.

References

Bagheri Hashkavayi A, Raoof JB, Azimi R, Ojani R (2016) Label-free and sensitive aptasensor based on dendritic gold nanostructures on functionalized SBA-15 for determination of chloramphenicol. Anal Bioanal Chem 408(10):2557–2565. https://doi.org/10.1007/s00216-016-9358-6

Balas F, Manzano M, Horcajada P, Vallet-Regi M (2006) Confinement and controlled release of bisphosphonates on ordered mesoporous silica-based materials. J Am Chem Soc 128(25): 8116–8117. https://doi.org/10.1021/ja062286z

Beck JS, Vartuli JC, Roth WJ, Leonowicz ME, Kresge CT, Schmitt KD et al (1992) A new family of mesoporous molecular sieves prepared with liquid crystal templates. J Am Chem Soc 114(27): 10834–10843. https://doi.org/10.1021/ja00053a020

Boissière C, Larbot A, van der Lee A, Kooyman PJ, Prouzet E (2000) A new synthesis of mesoporous MSU-X silica controlled by a two-step pathway. Chem Mater 12(10):2902–2913. https://doi.org/10.1021/cm991188s

Castillo RR, Vallet-Regí M (2019) Functional mesoporous silica nanocomposites: biomedical applications and biosafety. Int J Mol Sci 20(4). https://doi.org/10.3390/ijms20040929

Che S, Garcia-Bennett AE, Yokoi T, Sakamoto K, Kunieda H, Terasaki O, Tatsumi T (2003) A novel anionic surfactant templating route for synthesizing mesoporous silica with unique structure. Nat Mater 2(12):801–805. https://doi.org/10.1038/nmat1022

Chen F, Hong H, Shi S, Goel S, Valdovinos HF, Hernandez R et al (2014) Engineering of hollow mesoporous silica nanoparticles for remarkably enhanced tumor active targeting efficacy. Sci Rep:4. https://doi.org/10.1038/srep05080

Chen Z, Tan Y, Xu K, Zhang L, Qiu B, Guo L et al (2016) Stimulus-response mesoporous silica nanoparticle-based chemiluminescence biosensor for cocaine determination. Biosens Bioelectron 75:8–14. https://doi.org/10.1016/j.bios.2015.08.006

Chen Y, Chen Y, Chen Y, Lu W, Lu W, Guo Y et al (2020) Chitosan-gated fluorescent mesoporous silica nanocarriers for the real-time monitoring of drug release. Langmuir 36(24):6749–6756. https://doi.org/10.1021/acs.langmuir.0c00832

Costa JAS, de Jesus RA, Santos DO, Neris JB, Figueiredo RT, Paranhos CM (2021) Synthesis, functionalization, and environmental application of silica-based mesoporous materials of the M41S and SBA-n families: a review. J Environ Chem Eng 9(3):105259. https://doi.org/10.1016/j.jece.2021.105259

da Silva LCC, Infante CMC, Lima AWO, Cosentino IC, Fantini MCA, Rocha FRP et al (2011) Immobilization of glucose oxidase enzyme (GOD) in large pore ordered mesoporous cage-like

FDU-1 silica. J Mol Catal B Enzym 70(3–4):149–153. https://doi.org/10.1016/j.molcatb.2011.02.014

Dai H, Yang J, Ma J, Chen F, Fei Z, Zhong M (2012) A green process for the synthesis of controllable mesoporous silica materials. Microporous Mesoporous Mater 147(1):281–285. https://doi.org/10.1016/j.micromeso.2011.06.029

Feng G, Wang J, Boronat M, Li Y, Su JH, Huang J et al (2018) Radical-facilitated green synthesis of highly ordered mesoporous silica materials. J Am Chem Soc 140(14):4770–4773. https://doi.org/10.1021/jacs.8b00093

Ferreira Soares DC, Soares LM, Miranda de Goes A, Melo EM, Branco de Barros AL, Alves Santos Bicalho TC et al (2020) Mesoporous SBA-16 silica nanoparticles as a potential vaccine adjuvant against *Paracoccidioides brasiliensis*. Microporous Mesoporous Mater 291(June 2019):109676. https://doi.org/10.1016/j.micromeso.2019.109676

Gao Y, Zhong S, Xu L, He S, Dou Y, Zhao S et al (2019) Mesoporous silica nanoparticles capped with graphene quantum dots as multifunctional drug carriers for photo-thermal and redox-responsive release. Microporous Mesoporous Mater 278(July 2018):130–137. https://doi.org/10.1016/j.micromeso.2018.11.030

Gisbert-Garzarán M, Manzano M, Vallet-Regí M (2017) pH-responsive mesoporous silica and carbon nanoparticles for drug delivery. Bioengineering 4(1). https://doi.org/10.3390/bioengineering4010003

Gisbert-Garzarán M, Manzano M, Vallet-Regí M (2020) Mesoporous silica nanoparticles for the treatment of complex bone diseases: bone cancer, bone infection and osteoporosis. Pharmaceutics 12(1). https://doi.org/10.3390/pharmaceutics12010083

Gong YJ, Hong Li Z, Wu D, Sun YH, Deng F, Luo Q, Yue Y (2001) Synthesis and characterization of ureidopropyl-MSU-X silica. Microporous Mesoporous Mater 49(1–3):95–102. https://doi.org/10.1016/S1387-1811(01)00406-1

Grün M, Lauer I, Unger KK (1997) The synthesis of micrometer- and submicrometer-size spheres of ordered mesoporous oxide MCM-41. Adv Mater 9(3):254–257. https://doi.org/10.1002/adma.19970090317

Gu Z, Fu A, Ye L, Kuerban K, Wang Y, Cao Z (2019) Ultrasensitive chemiluminescence biosensor for nuclease and bacterial determination based on hemin-encapsulated mesoporous silica nanoparticles. ACS Sensors 4(11):2922–2929. https://doi.org/10.1021/acssensors.9b01303

He J, Li H, Xu Y, Yang S (2020) Dual acidic mesoporous KIT silicates enable one-pot production of γ-valerolactone from biomass derivatives via cascade reactions. Renew Energy 146:359–370. https://doi.org/10.1016/j.renene.2019.06.105

Huo Q, Leon R, Petroff PM, Stucky GD (1995) Mesostructure design with gemini surfactants: supercage formation in a three-dimensional hexagonal array. Science 268:1324–1327. https://doi.org/10.1126/science.268.5215.1324

Hwang J, Lee JH, Chun J (2021) Facile approach for the synthesis of spherical mesoporous silica nanoparticles from sodium silicate. Mater Lett 283:128765. https://doi.org/10.1016/j.matlet.2020.128765

Isa EDM, Ahmad H, Rahman MBA, Gill MR (2021) Progress in mesoporous silica nanoparticles as drug delivery agents for cancer treatment. Pharmaceutics 13(2):1–33. https://doi.org/10.3390/pharmaceutics13020152

Jiang H, Shi X, Yu X, He X, An Y, Lu H (2018) Hyaluronidase enzyme-responsive targeted nanoparticles for effective delivery of 5-fluorouracil in colon cancer. Pharm Res 35(4). https://doi.org/10.1007/s11095-017-2302-4

Jimenez-Falcao S, Parra-Nieto J, Pérez-Cuadrado H, Martínez-Máñez R, Martínez-Ruiz P, Villalonga R (2019) Avidin-gated mesoporous silica nanoparticles for signal amplification in electrochemical biosensor. Electrochem Commun 108:106556. https://doi.org/10.1016/j.elecom.2019.106556

Khalil M, Amanda A, Yunarti RT, Jan BM, Irawan S (2020) Synthesis and application of mesoporous silica nanoparticles as gas migration control additive in oil and gas cement. J Pet Sci Eng 195(July):107660. https://doi.org/10.1016/j.petrol.2020.107660

Khalilzadeh B, Charoudeh HN, Shadjou N, Mohammad-Rezaei R, Omidi Y, Velaei K et al (2016) Ultrasensitive caspase-3 activity detection using an electrochemical biosensor engineered by gold nanoparticle functionalized MCM-41: its application during stem cell differentiation. Sensors Actuators B Chem 231:561–575. https://doi.org/10.1016/j.snb.2016.03.043

Kresge CT, Leonowicz ME, Roth WJ, Vartuli JC, Beck JS (1992) Ordered mesoporous molecular sieves synthesized by a liquid-crystal template mechanism. Nature 359(6397):710–712. https://doi.org/10.1038/359710a0

Kumar S, Malik MM, Purohit R (2017) Synthesis methods of mesoporous silica materials. Mater Today Proc 4(2):350–357. https://doi.org/10.1016/j.matpr.2017.01.032

Kundu M, Chatterjee S, Ghosh N, Manna P, Das J, Sil PC (2020) Tumor targeted delivery of umbelliferone via a smart mesoporous silica nanoparticles controlled-release drug delivery system for increased anticancer efficiency. Mater Sci Eng C 116(June):111239. https://doi.org/10.1016/j.msec.2020.111239

Lai CY, Trewyn BG, Jeftinija DM, Jeftinija K, Xu S, Jeftinija S, Lin VSY (2003) A mesoporous silica nanosphere-based carrier system with chemically removable CdS nanoparticle caps for stimuli-responsive controlled release of neurotransmitters and drug molecules. J Am Chem Soc 125(15):4451–4459. https://doi.org/10.1021/ja028650l

Liu J, Li C, Li F (2011) Fluorescence turn-on chemodosimeter-functionalized mesoporous silica nanoparticles and their application in cell imaging. J Mater Chem 21(20):7175–7181. https://doi.org/10.1039/c1jm10803d

Liu YC, Hsu WF, Wu TM (2020) Electrochemical determination of dopamine using a conductive polypyrrole/carbon-coated mesoporous silica composite electrode. J Appl Electrochem 50(3): 311–319. https://doi.org/10.1007/s10800-019-01391-2

Mahdizadeh Ghohe N, Tayebee R, Amini MM (2019) Synthesis and characterization of mesoporous Nb Zr/KIT-6 as a productive catalyst for the synthesis of benzylpyrazolyl coumarins. Mater Chem Phys 223:268–276. https://doi.org/10.1016/j.matchemphys.2018.10.067

Mehmood A, Ghafar H, Yaqoob S, Gohar UF, Ahmad B (2017) Mesoporous silica nanoparticles: a review. J Develop Drugs 6(2). https://doi.org/10.4172/2329-6631.1000174

Mohamad DF, Osman NS, Nazri MKHM, Mazlan AA, Hanafi MF, Esa YAM et al (2019) Synthesis of mesoporous silica nanoparticle from banana peel ash for removal of phenol and methyl orange in aqueous solution. Mater Today Proc 19:1119–1125. https://doi.org/10.1016/j.matpr.2019.11.004

Muthusami R, Kesavan A, Ramachandran V, Vasudevan V, Irena K, Rangappan R (2020) Synthesis of mesoporous silica nanoparticles with a lychee-like morphology and dual pore arrangement and its application towards biomimetic activity via functionalization with copper(II) complex. Microporous Mesoporous Mater 294(November 2019):109910. https://doi.org/10.1016/j.micromeso.2019.109910

Narayan R, Nayak U, Raichur A, Garg S (2018) Mesoporous silica nanoparticles: a comprehensive review on synthesis and recent advances. Pharmaceutics 10(3):118. https://doi.org/10.3390/pharmaceutics10030118

Niculescu V-C (2020) Mesoporous silica nanoparticles for bio-applications. Front Mater 7. https://doi.org/10.3389/fmats.2020.00036

Oliveira DM, Andrada AS (2019) Synthesis of ordered mesoporous silica MCM-41 with controlled morphology for potential application in controlled drug delivery systems. Cerâmica 65(374): 170–179. https://doi.org/10.1590/0366-69132019653742509

Pal N, Lee JH, Cho EB (2020) Recent trends in morphology-controlled synthesis and application of mesoporous silica nanoparticles. Nanomaterials 10(11):1–38. https://doi.org/10.3390/nano10112122

Palantavida S, Guz NV, Woodworth CD, Sokolov I (2013) Ultrabright fluorescent mesoporous silica nanoparticles for prescreening of cervical cancer. Nanomedicine 9(8):1255–1262. https://doi.org/10.1016/j.nano.2013.04.011

Paris JL, Vallet-Regí M (2020) Mesoporous silica nanoparticles for co-delivery of drugs and nucleic acids in oncology: a review. Pharmaceutics 12(6). https://doi.org/10.3390/pharmaceutics12060526

Pratiwi FW, Kuo CW, Wu SH, Chen YP, Mou CY, Chen P (2018) The bioimaging applications of mesoporous silica nanoparticles. In: Enzymes, vol 43, 1st edn. Elsevier Inc. https://doi.org/10.1016/bs.enz.2018.07.006

Prouzet É, Boissière C (2005) A review on the synthesis, structure and applications in separation processes of mesoporous MSU-X silica obtained with the two-step process. C R Chim 8(3–4):579–596. https://doi.org/10.1016/j.crci.2004.09.011

Qiao H, Jia J, Shen H, Zhao S, Chen E, Chen W et al (2019) Capping silica nanoparticles with tryptophan-mediated cucurbit[8]uril complex for targeted intracellular drug delivery triggered by tumor-overexpressed IDO1 enzyme. Adv Healthc Mater 8(13):1–10. https://doi.org/10.1002/adhm.201900174

Qu F, Zhu G, Huang S, Li S, Sun J, Zhang D, Qiu S (2006) Controlled release of captopril by regulating the pore size and morphology of ordered mesoporous silica. Microporous Mesoporous Mater 92(1–3):1–9. https://doi.org/10.1016/j.micromeso.2005.12.004

Sanaeishoar H, Sabbaghan M, Mohave F, Nazarpour R (2016) Disordered mesoporous KIT-1 synthesized by DABCO-based ionic liquid and its characterization. Microporous Mesoporous Mater 228:305–309. https://doi.org/10.1016/j.micromeso.2016.04.003

She X, Chen L, Li C, He C, He L, Kong L (2015) Functionalization of hollow mesoporous silica nanoparticles for improved 5-fu loading. J Nanomater 2015. https://doi.org/10.1155/2015/872035

Shen S, Li Y, Zhang Z, Fan J, Tu B, Zhou W, Zhao D (2002) A novel ordered cubic mesoporous silica templated with tri-head group quaternary ammonium surfactantElectronic supplementary information (ESI) available: projections of a typical diamond structure with Fd3m space group; 1H NMR data; elemental analysis; SE. Chem Commun 19:2212–2213. https://doi.org/10.1039/b206993h

Sing KSW, Everett DH, Haul RAW, Moscou L, Pierotti RA, Rouquérol J, Siemieniewska T (1985) Reporting physisorption data for gas/solid systems with special reference to the determination of surface area and porosity (recommendations 1984). Pure Appl Chem 57(4):603–619. https://doi.org/10.1351/pac198557040603

Singh LP, Bhattacharyya SK, Kumar R, Mishra G, Sharma U, Singh G, Ahalawat S (2014) Sol-gel processing of silica nanoparticles and their applications. Adv Colloid Interf Sci 214:17–37. https://doi.org/10.1016/j.cis.2014.10.007

Slowing II, Trewyn BG, Giri S, Lin VSY (2007) Mesoporous silica nanoparticles for drug delivery and biosensing applications. Adv Funct Mater 17(8):1225–1236. https://doi.org/10.1002/adfm.200601191

Song G, Li C, Hu J, Zou R, Xu K, Han L et al (2012) A simple transformation from silica core-shell-shell to yolk-shell nanostructures: a useful platform for effective cell imaging and drug delivery. J Mater Chem 22(33):17011–17018. https://doi.org/10.1039/c2jm32382f

Song T, Zhao H, Hu Y, Sun N, Zhang H (2019) Facile assembly of mesoporous silica nanoparticles with hierarchical pore structure for CO2 capture. Chin Chem Lett 30(12):2347–2350. https://doi.org/10.1016/j.cclet.2019.07.024

Stober W, Fink A, Bohn E (1968) Controlled growth of monodisperse silica spheres in the micron size range. J Colloid Interface Sci 26:62–69. https://doi.org/10.1589/jpts.29.112

Tozuka Y, Wongmekiat A, Kimura K, Moribe K, Yamamura S, Yamamoto K (2005) Effect of pore size of FSM-16 on the entrapment of flurbiprofen in mesoporous structures. Chem Pharm Bull 53(8):974–977. https://doi.org/10.1248/cpb.53.974

Vallet-Regi M, Rámila A, Del Real RP, Pérez-Pariente J (2001) A new property of MCM-41: drug delivery system. Chem Mater 13(2):308–311. https://doi.org/10.1021/cm0011559

Vallet-Regí M, García MM, Colilla M (2013) Biomedical applications of mesoporous ceramics. CRC Press. https://doi.org/10.1201/b12959

Vanichvattanadecha C, Singhapong W, Jaroenworaluck A (2020) Different sources of silicon precursors influencing on surface characteristics and pore morphologies of mesoporous silica nanoparticles. Appl Surf Sci 513(September 2019):145568. https://doi.org/10.1016/j.apsusc.2020.145568

Vartuli JC, Schmitt KD, Kresge CT, Roth WJ, Leonowicz ME, McCullen SB et al (1994) Effect of surfactant/silica molar ratios on the formation of mesoporous molecular sieves: inorganic mimicry of surfactant liquid-crystal phases and mechanistic implications. Chem Mater 6(12): 2317–2326. https://doi.org/10.1021/cm00048a018

Vazquez NI, Gonzalez Z, Ferrari B, Castro Y (2017) Synthesis of mesoporous silica nanoparticles by sol-gel as nanocontainer for future drug delivery applications. Bol SECV 56(3):139–145. https://doi.org/10.1016/j.bsecv.2017.03.002

Wang K, Ren H, Li N, Tan X, Dang F (2018) Ratiometric fluorescence sensor based on cholesterol oxidase-functionalized mesoporous silica nanoparticle@ZIF-8 core-shell nanocomposites for detection of cholesterol. Talanta 188(January):708–713. https://doi.org/10.1016/j.talanta.2018.06.019

Wang J, Zhang C, Bai Y, Li Q, Yang X (2021) Synthesis of mesoporous silica with ionic liquid surfactant as template. Mater Lett 291:129556. https://doi.org/10.1016/j.matlet.2021.129556

Wen J, Yang K, Liu F, Li H, Xu Y, Sun S (2017) Diverse gatekeepers for mesoporous silica nanoparticle based drug delivery systems. Chem Soc Rev 46(19):6024–6045. https://doi.org/10.1039/c7cs00219j

Wu SH, Lin HP (2013) Synthesis of mesoporous silica nanoparticles. Chem Soc Rev 42(9): 3862–3875. https://doi.org/10.1039/c3cs35405a

Wu Q, Li Y, Hou Z, Xin J, Meng Q, Han L et al (2018) Synthesis and characterization of Beta-FDU-12 and the hydrodesulfurization performance of FCC gasoline and diesel. Fuel Process Technol 172:55–64. https://doi.org/10.1016/j.fuproc.2017.12.003

Yang D, Ni N, Cao L, Song X, Alhamoud Y, Yu G et al (2019) Silver doped mesoporous silica nanoparticles based electrochemical enzyme-less sensor for determination of H2O2 released from live cells. Micromachines 10(4):268. https://doi.org/10.3390/mi10040268

Yu Q, Hui J, Wang P, Xu B, Zhuang J, Wang X (2012) Hydrothermal synthesis of mesoporous silica spheres: effect of the cooling process. Nanoscale 4(22):7114–7120. https://doi.org/10.1039/c2nr31834b

Yuan D, Ellis CM, Davis JJ (2020) Mesoporous silica nanoparticles in bioimaging. Materials 13(17):16–18. https://doi.org/10.3390/ma13173795

Yusan S, Rahman MM, Mohamad N, Arrif TM, Latif AZA, Mohd Aznan MA, Wan Nik WSB (2018) Development of an amperometric glucose biosensor based on the immobilization of glucose oxidase on the Se-MCM-41 mesoporous composite. J Analyt Methods Chem 2018. https://doi.org/10.1155/2018/2687341

Zhang Y, Bo X, Nsabimana A, Luhana C, Wang G, Wang H et al (2014) Fabrication of 2D ordered mesoporous carbon nitride and its use as electrochemical sensing platform for H_2O_2, nitrobenzene, and NADH detection. Biosens Bioelectron 53:250–256. https://doi.org/10.1016/j.bios.2013.10.001

Zhang KY, Zhang J, Liu Y, Liu S, Zhang P, Zhao Q et al (2015) Core–shell structured phosphorescent nanoparticles for detection of exogenous and endogenous hypochlorite in live cells via ratiometric imaging and photoluminescence lifetime imaging microscopy. Chem Sci 6(1): 301–307. https://doi.org/10.1039/C4SC02600D

Zhang L, Wei F, Al-Ammari A, Sun D (2020a) An optimized mesoporous silica nanosphere-based carrier system with chemically removable Au nanoparticle caps for redox-stimulated and targeted drug delivery. Nanotechnology 31(47):475102. https://doi.org/10.1088/1361-6528/ab9391

Zhang H, Xia Q, Zhou D (2020b) Albumin-gated zwitterion-stabilized mesoporous silica nanorod as a pH-responsive drug delivery system. Colloids Surf B: Biointerfaces 193(April):111107. https://doi.org/10.1016/j.colsurfb.2020.111107

Zhao D, Feng J, Huo Q, Melosh N, Fredrickson GH, Chmelka BF, Stucky GD (1998) Triblock copolymer syntheses of mesoporous silica with periodic 50 to 300 angstrom pores. Science 279(5350):548–552. https://doi.org/10.1126/science.279.5350.548

Zhao D, Wan Y, Zhou W (2013) Ordered mesoporous materials. Wiley-VCH Verlag GmbH & Co. KGaA, Weinheim. https://doi.org/10.1002/9783527647866

Zheng D, Ye J, Zhou L, Zhang Y, Yu C (2009) Simultaneous determination of dopamine, ascorbic acid and uric acid on ordered mesoporous carbon/Nafion composite film. J Electroanal Chem 625(1):82–87. https://doi.org/10.1016/j.jelechem.2008.10.012

Zhou L, Li H, Yu C, Zhou X, Tang J, Meng Y et al (2006) Easy synthesis and supercapacities of highly ordered mesoporous polyacenes/carbons. Carbon 44(8):1601–1604. https://doi.org/10.1016/j.carbon.2006.02.025

Zhou Y, Quan G, Wu Q, Zhang X, Niu B, Wu B et al (2018) Mesoporous silica nanoparticles for drug and gene delivery. Acta Pharm Sin B 8(2):165–177. https://doi.org/10.1016/j.apsb.2018.01.007

Zhu Y, Shi J, Chen H, Shen W, Dong X (2005) A facile method to synthesize novel hollow mesoporous silica spheres and advanced storage property. Microporous Mesoporous Mater 84(1–3):218–222. https://doi.org/10.1016/j.micromeso.2005.05.001

Functionalized Nanobiomaterials in Electroanalysis and Diagnosis of Biomolecules

21

Gözde Aydoğdu Tığ, Derya Koyuncu Zeybek, and Bülent Zeybek

Contents

1 Introduction 458
2 Nanomaterials 459
  2.1 Biofunctionalization of Nanomaterials 460
  2.2 Applications of Nanomaterials for Diagnosis of Biomolecules 462
3 Conclusion 476
References 476

Abstract

Functional nanomaterials have been broadly studied due to their role in ultrasensitive bioassays and miniaturized platforms. They can generate a synergic impact for catalytic activity, electrical conductivity, and feasibility to enhance the analyte response and supply high-affinity recognitions by conjugating several signal tags, causing highly sensitive and selective biosensing. This chapter will focus on recent prominent progressions in biofunctionalization strategies assembling multidisciplinary areas including chemistry, pharmacy, biology, and materials science. Some critical implementations of biofunctional nanomaterials have been highlighted as superior electronic signal labels for sensitive bioanalysis. The biofunctional nanomaterial-modified biosensing applications provide a series of different concepts and propose promising tools for detecting trace amounts of various analytes in clinical, environmental, and industrial implementations.

G. A. Tığ (✉)
Department of Chemistry, Faculty of Science, Ankara University, Ankara, Turkey
e-mail: gaydogdu@science.ankara.edu.tr

D. K. Zeybek
Department of Biochemistry, Faculty of Arts and Science, Kütahya Dumlupınar University, Kütahya, Turkey

B. Zeybek
Department of Chemistry, Faculty of Arts and Science, Kütahya Dumlupınar University, Kütahya, Turkey

© Springer Nature Singapore Pte Ltd. 2023

U. P. Azad, P. Chandra (eds.), *Handbook of Nanobioelectrochemistry*,
https://doi.org/10.1007/978-981-19-9437-1_21

Keywords

Nanobiomaterials · Electrocatalysis · Biomolecules · Biosensing · Functionalization

1 Introduction

The most significant side of nanomaterials is their remarkable features connected with nanoscale sizes. Nano-sized materials, which are attracting a lot of attention today, present some extreme properties that were never thought of before with bulk materials (Silva et al. 2021). The most elementary property of nanomaterials is their large surface-area-to-volume ratio. This circumstance provides many extraordinary physical and chemical characteristics such as increased chemical and biological efficiencies, high catalytic impacts, improved molecular adsorption, and excessive mechanical resistance (Chae et al. 2004; Barbieri et al. 2005; Tuantranont 2013). Another distinctive characteristic of nanomaterials is the quantum size impact, which causes separate electronic band structures as those of molecules. In contrast to the increasing surface-to-volume proportion that appears when moving from the macro to the micro sizes, the quantum impact is solely particular to nanoscale sizes less than a few tens of nanometers (Tsai et al. 2008; Acharya et al. 2009; Tuantranont 2013). Nowadays, studies on the preparation of new and functional nanomaterials by researchers continue at full speed.

The nanomaterials are therefore very functional for a broad variety of nanotechnology areas involving nanoelectronics (Tsai et al. 2008), nanophotonics (Chung et al. 2005; Jiang et al. 2007), nanobiotechnology (Soto and Ratna 2010), biochemistry (Geng et al. 2009; Soto and Ratna 2010), biomedicine (Pierstorff and Ho 2007), electrochemistry (Chen et al. 2007), and so on. These cause a wide diversity of implementations such as solar cells (Bernardi et al. 2010; Yu et al. 2012), catalysts (Jakhmola et al. 2010), photocatalysts (Banerjee 2011), the molecular electronic instrument (Pashchanka et al. 2010), fuel cells (Antolini 2009; Guo and Wang 2011), drug delivery systems (Ochekpe et al. 2009; Board et al. 2011), nanosensors (Wang 2005; Di Francia et al. 2009; Sugiyama et al. 2010; Bhatnagar et al. 2018), energy-storage systems (Aricò et al. 2005; Simon and Gogotsi 2008; Lee and Cho 2011), surface-enhanced Raman spectroscopy (SERS) (Guo and Dong 2011), and nano-actuators (Ma et al. 2018). Within these application areas, sensors are one of the fields of study that attract a lot of attention in both daily life and the scientific world. Sensors may be divided into various classes such as optical, thermal, mechanical, gas, magnetic, chemical, and biological. The sensors usually contain sensing material that replies to alterations in analytes and a transducer that transforms alters into electrical signals (Tuantranont 2013). Biosensing platforms based on electrochemical measurements are widely used (Drummond et al. 2003; Wang 2005, 2007; Wang et al. 2009a, b). Biosensing implementations also include a comprehensive series of biologically suitable materials involving analytes existing in alive organisms such as uric acid, cholesterol, glucose, proteins, organelles, DNAs, RNAs, cells, and so on

(Drummond et al. 2003; Chopra et al. 2007; Wang 2007; Dong and Dae 2008; Lu et al. 2009; Bhatnagar et al. 2018).

Our overview here has focused on functional nanomaterials used in the diagnosis and electroanalysis of biomolecules in recent years.

2 Nanomaterials

Nanomaterial science, one of the leading fields of nanotechnology, includes the synthesis, characterization, and applications of nano-sized materials. The nanoscale is generally described as a dimension less than 100 nm. But this definition is enlarged to a size smaller than 1 μm. The European Commission describes nanomaterial as a native, fortuitous, or produced material involving unbound, aggregated, or agglomerated particles with a dimension between 1 and 100 nm. Nanomaterials can be classified as 0D, 1D, 2D, and 3D nanostructures according to their properties' dimensionality (D) (Tuantranont 2013; Malhotra and Ali 2018). Due to the small size of nanomaterials, new energy levels are created, and a quantum effect occurs. Besides, nanomaterials are characterized by an enlarged surface area due to the surface/volume proportion increment. Nanomaterials' unique optical, electrical, magnetic, mechanical, or chemical features make them indispensable for analytical applications (López-Sanz et al. 2019; Rathee and Ojha 2022). Nanomaterials are available in almost all areas of our lives: medicine, textiles, food, environment, and others (López-Sanz et al. 2019). It is seen that the utilization of nanomaterials is quite high in biosensor systems developed for the analysis of various biomolecules. Figure 21.1 shows a schematic of the different pieces of a biosensor and some nanomaterials that can be used for the modification of the sensing platform.

Electrochemical biosensors are defined as analytical tools that can convert a biochemical event, which is formed by the interaction between molecules such as enzyme-substrate and antigen-antibody, into an electrical signal. The biocomponent (enzyme, antibody, nucleic acid, etc.) is immobilized to a solid matrix (transducer or electrode) in the biosensor structure. The immobilization procedure may result in loss of activity and specificity of the biocomponent. Nanomaterials are used to immobilize enzymes and other molecules because of their extraordinary surface modification properties obtained by their functionalization during or after production (T.sriwong et al. 2022). In addition, the use of suitable functional nanomaterials is an effective alternative for developing the performance of biosensors. Thanks to the numerous nanomaterials with a great surface area, the analytical performance of electrochemical biosensors can be improved in terms of increased loading capacity and facilitated mass transport (Cho et al. 2020). Nanomaterials that we can list as metal NPs such as gold, silver, metal oxide NPs such as Fe_3O_4, CuO, NiO, and ZnO; carbon-based NPs such as MWCNT, SWCNT, graphene, and its derivatives; quantum dots (QDs), and polymeric nanomaterials are the most used in electrochemical biosensors (Harish et al. 2022). The types and size-based classification of nanomaterials used for the biosensing platform are shown in Fig. 21.2.

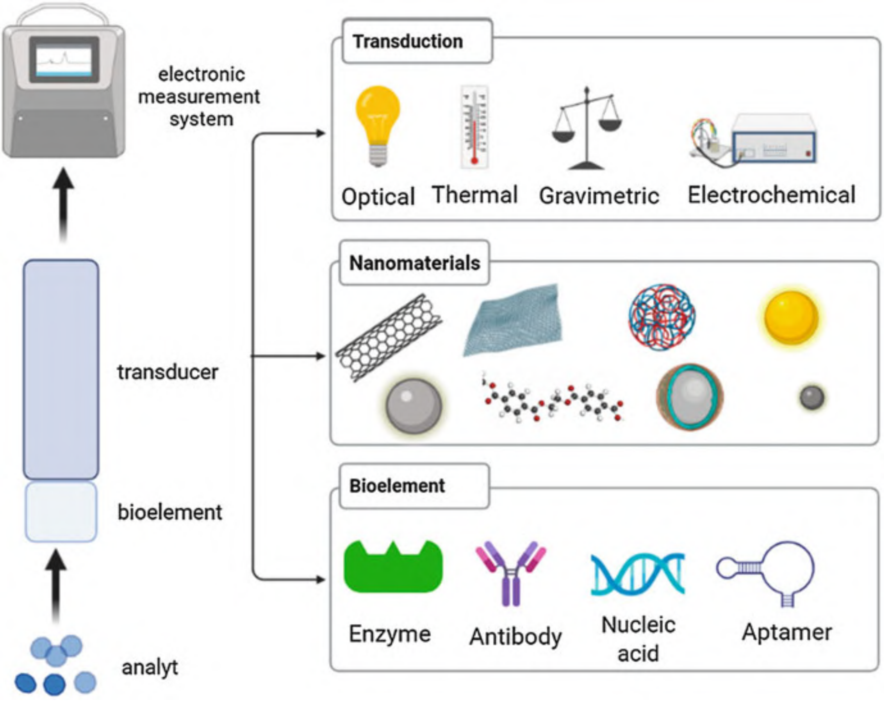
electronic measurement system
transducer
bioelement
analyt
Transduction
Optical
Thermal
Gravimetric
Electrochemical
Nanomaterials
Bioelement
Enzyme
Antibody
Nucleic acid
Aptamer

Fig. 21.1 Schematic of different parts of a biosensor. (Created in BioRender)

2.1 Biofunctionalization of Nanomaterials

Nanomaterials used in biosensing interfaces are functionalized to lower the activation energy, accelerate electron transfer, and determine the target analyte. By functionalizing nanostructures with biomolecules such as DNA, antibodies/antigens, proteins, aptamers, lectins, and peptides, they can be used as specific recognition or signal triggering elements. With the development of sensitive biosensing methods, it is frequently used for signal generation of biological events. This process provides excellent selectivity and specificity and improves biosensing response. In recent studies, functional nanomaterials have been synthesized and conjugated with several biomolecules for precise and sensitive detection of diverse biomolecules in vivo and in vitro (Deka et al. 2018).

Biofunctionalization of nanomaterials acts an essential role in their catching properties because the surface modification can lead to alterations in the electrochemical answers acquired from the transducer involving the sensor surface. Accordingly, nanomaterials can be appropriately synthesized for biomolecule immobilization, which is covalent or non-covalent, and the surface of these nanomaterials bearing amine or carboxyl groups is activated before biomodification. Modifying the biomolecules with amine ($-NH_2$), carboxyl (-COOH), thiol (-SH), avidin/streptavidin, or biotin is also possible (Choudhary et al. 2016; Erkmen et al. 2022).

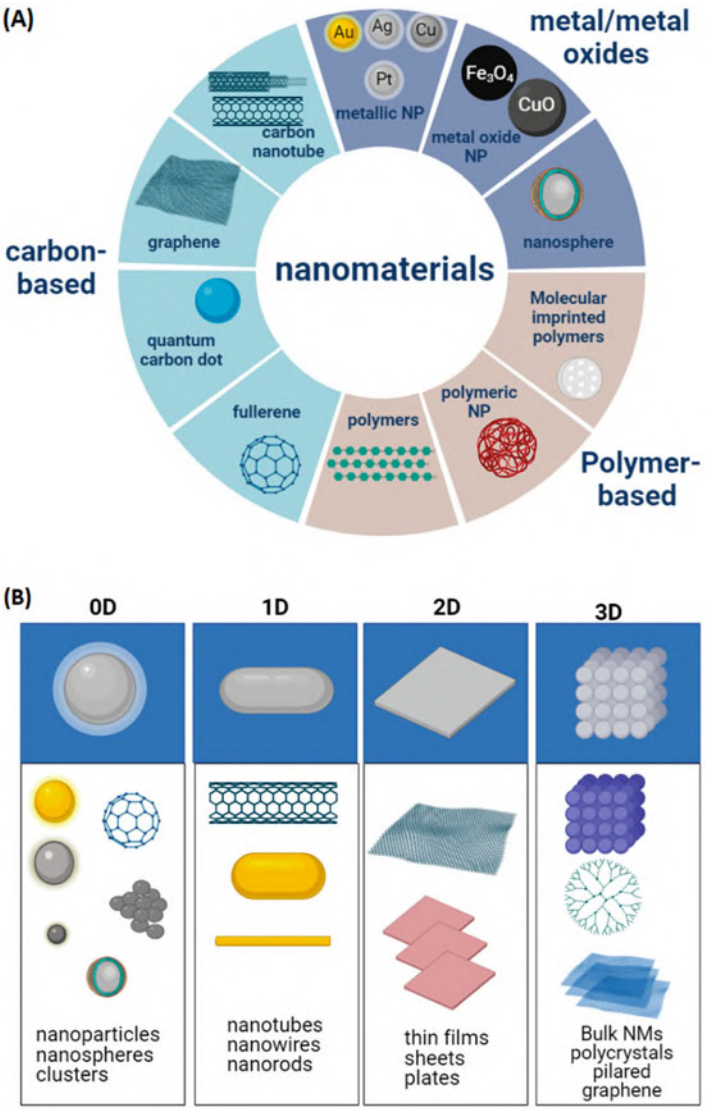
(A)
metal/metal oxides
Au
Ag
Cu
Pt
metallic NP
Fe_3O_4
CuO
metal oxide NP
nanosphere
carbon nanotube
graphene
carbon-based
nanomaterials
quantum carbon dot
fullerene
polymers
polymeric NP
Molecular imprinted polymers
Polymer-based
(B)
0D
1D
2D
3D
nanoparticles
nanospheres
clusters
nanotubes
nanowires
nanorods
thin films
sheets
plates
Bulk NMs
polycrystals
pilared
graphene

Fig. 21.2 (**a**) Types of nanomaterials used for bio-sensing platform. (**b**) Classification of nanomaterials based on dimensionality. (Created in BioRender)

These functionalized nano biomaterials allowed the rapid detection of many analytes in trace amounts. For example, an electrochemical immunosensor was prepared via a GCE modified with molybdenum disulfide nanosheet-loaded gold nanoparticles (MoS_2/AuNPs). The primary antibody was immobilized onto the electrode via Au-S chemistry. Then, the target analyte, insulin, was incubated with MoS_2/AuNPs modified GCE. After that, the secondary antibody (Ab2) was conjugated with copper(I) oxide decorated with titanium(IV) oxide octahedral loaded dendritic platinum–copper nanoparticles ($Cu_2O@TiO_2$-PtCuNPs) conjugated via Pt-N chemistry. This sandwich platform enables an enhanced signal amplification due to its reproducible, selective, and stable properties (Li et al. 2019).

A promising electrochemical platform for the dsDNA adsorption was recently prepared through in-situ synthesized keratin-SH (KerSH) particles from the waste product of wool fabric and Pd^{2+} by Kalkan Erdoğan et al. (2021). The drop-casted KerSH-Pd^{2+} particles were electrochemically reduced onto the GCE via chronoamperometry at the optimized conditions(-0.4 V, for 500 s). It was reported that after the electrochemical PdNPs deposition, the KerSH particles were obtained onto electrode surface self-assembly with their functional NH_2 groups to adsorb negatively structured biomolecule dsDNA. The electrochemical oxidation signals of guanine and adenine bases revealed the presence of dsDNA. The authors emphasized the potential application area of the prepared platform in the environmental, pharmaceutical, and medicinal fields (Kalkan Erdoğan et al. 2021).

2.2 Applications of Nanomaterials for Diagnosis of Biomolecules

2.2.1 Carbon-Based Nanomaterials

Carbon-based nanomaterials have shown significant progress in many scientific and technological areas with different applications such as biosensors, environmental control, biomedicine, pharmaceutical chemistry, clinical diagnosis, tissue engineering, bioimaging, targeted drug delivery, and energy devices. The history of carbon nanomaterials begins with the exploration of fullerenes in 1985, pursued by carbon nanotubes in 1991, graphene in 2004, and their derivatives. Recent developments in carbon-based nanomaterials include synthesizing carbon and QDs in 2004 and 2008, respectively (Namdari et al. 2017). These promising nanostructures can be produced by top-down or bottom-up techniques (Baptista et al. 2015; Campuzano et al. 2019). Carbon-based nanomaterials can be investigated in terms of their structure; zero (0D), one (1D), and two (2D) dimensional, owing to their superior properties and different applications. Among them, while 0D carbon QDs have high fluorescence, high quantum yield, low toxicity, small size, and considerable biocompatibility (Liu et al. 2020), 1D carbon nanotubes have been extensively employed in biosensing, bioimaging, nanomedicine, and catalysis due to their matchless chemical and physical features consisting of thermal stability, high conductivity, high surface to volume proportion, easy functionalization, adsorption capacity (Xu et al. 2019). In addition, 2D graphene nanosheets exhibit promising electrical, mechanical, and optical properties with lots of functional groups for sensing several biomolecules (Soozanipour and Taheri-Kafrani 2018; Sastry et al. 2021). The integration of carbon-based nanomaterials with biomolecules is the ultimate tool for generating complex nanostructures and functions.

Researchers and several studies have preferred carbon-based nanomaterials, i.e., carbon nanotubes with carboxyl or amine group, graphene, graphene oxide (GO), graphene QDs, and carbon dots.

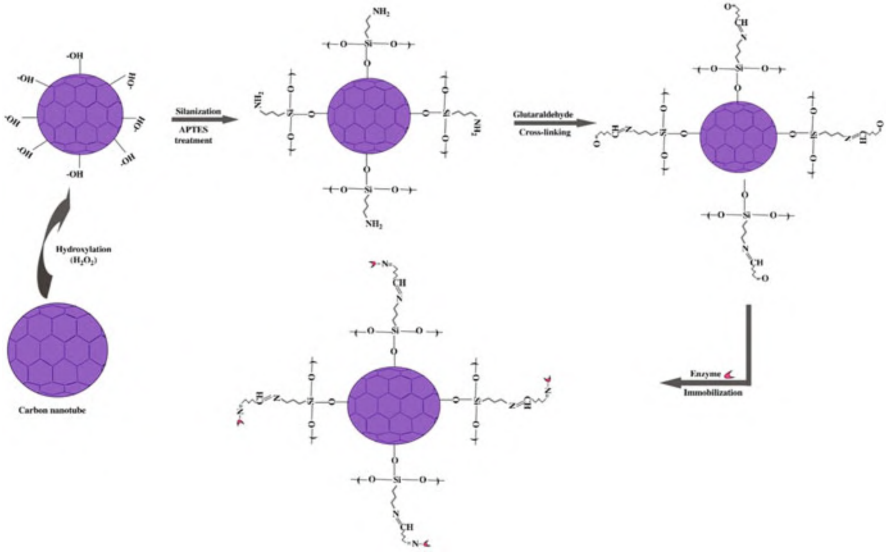

Fig. 21.3 Functionalization of carbon nanotubes with 3-aminopropyl-triethoxysilane (APTES) and glutaraldehyde (GA) for enzyme immobilization. (Reproduced with permission from Methods in Enzymology. Reproduced with permission Singh and Chauhan (2020))

Multiwalled carbon nanotubes (MWCNTs) for functionalizing biomolecules occupy numerous commercial and scientific applications such as gas storage, electronic devices, environmental remediation, and immobilization of several biomolecules. They can also be used as nanocarriers for enzyme immobilization, especially with specific chemicals to add active groups (Meng et al. 2009). Immobilization of various enzymes such as catalase (Canbay et al. 2021), lipase, and peroxidase (Fu et al. 2020), etc. have been prepared with MWCNTs to fabricate an immobilized biocatalyst for several applications. Li et al. manufactured an electrochemical glucose biosensor based on MWCNTs coated with cobalt(II) sulfide (CoS) nanoparticles. Firstly, CoS-MWCNTs suspension was prepared by the in-situ hydrothermal method, followed by the addition of GOx into the prepared composite. Different spectroscopic and microscopic techniques characterized the GOx biosensor. The determination of glucose was achieved at −0.43 V (vs. SCE). A wide working range between 8 μM and 1.5 mM, a high sensitivity value of 15 mA M^{-1} cm^{-2}, and a limit of detection (LOD) of 5 μM were obtained. The finding demonstrates that the prepared CoS-MWCNTs nanostructure with a broad specific surface area supplies the direct electron transfer between the enzyme and the surface. In addition, human serum samples from a local hospital were selected and tested to measure glucose levels by the developed enzyme electrode (Li et al. 2020). In another study, carboxylic acid modifies MWCNTs were conjugated with (3-aminopropyl) triethoxysilane (APTES) and glutaraldehyde (GA) for enzyme immobilization (Fig. 21.3) (Singh and Chauhan 2020).

In another study, Rezaei and coworkers suggested an aptamer-based method for the electrochemical assay of lysozyme, which is an essential enzyme in living organisms. A new composite consisting of MWCNTs, poly(diallyldimethylammonium chloride) (PDDA), and CQD (MWCNT/PDDA/CQD) was used to modify the aptasensor and obtain a high analytical response. PDDA was recognized as a dispersing agent for carbon-based nanomaterials. It was noticed that the modified aptasensor exhibits unique superiorities for the immobilization of amino-linkage anti-lysozyme aptamer utilizing the amine coupling procedure. A signal of $Fe(CN)_6^{3-/4-}$ redox probe at about +0.15 V (vs. Ag/AgCl) was selected as an electrochemical indicator to perform the relationship between the peak signal and lysozyme concentration. The authors calculated a low LOD value of 12.9 fmol L^{-1} and a wide linear range from 50 fmol L^{-1} to 10 nmol L^{-1}. A synergistic effect between MWCNT, PDDA, and CQD provides better aptamer immobilization and enhanced aptasensor characteristics. The method is used as a sensing platform for white, serum, and urine actual specimens (Rezaei et al. 2018).

An ultra-sensitive aptasensor for Thrombin detection was constructed based on fullerene (C_{60}), MWCNTs, polyethyleneimine (PEI), and polymer quantum dots (PQdot) modified screen-printed carbon electrode (SPCE) (Fig. 21.4). In this study, first, C60/MWCNTs-PEI was prepared by sonication procedure. Then, the freshly prepared PQdots were mixed with C60/MWCNTs-PEI. It is emphasized that a high amount of aptamer molecules could be attached to the electrode surface by using both carbon-based nanomaterials having a negative charge which helps create a strong interaction between MWCNTs and PEI. DPV signal for redox probe solution was employed as an indicator for the connection of the aptamer to thrombin protein. The fabricated aptasensor exhibited a low LOD (6 fmol L^{-1}) and a wide linear range (50 fmol L^{-1} and 20 nmol L^{-1}). The application of the suggested strategy was evaluated in human serum specimens, and high recovery values were found (Jamei et al. 2021).

Recently, Liu et al. improved an HRP electrochemical biosensor based on a zeolite imidazolate framework-67(Co)/multiwalled carbon nanotube composite (ZIF-67(Co)/MWCNT) modified GCE [60]. MWCNTs solution (1 mg mL^{-1}) was firstly mixed with ZIF-67(Co) suspension (1 mg mL^{-1}), then the HRP solution was mixed with the prepared composite mixture. This mixture was drop-casted onto the GCE surface. ZIF-67(Co)/MWCNT modified GCE exhibited higher affinity toward detection of H_2O_2 (Michaelis constant K_m decreased by ~75%) compared to ZIF-67 (Co) or MWCNTs based HRP electrochemical biosensors. It is indicated that the prepared ZIF-67(Co)/MWCNT composite has a stabilized hydrophilic/hydrophobic characteristic that provides an appropriate microenvironment for the interplay between the active region of the HRP enzyme and its substrate H_2O_2. Finally, the developed biosensor is considered to be applicable for other MOF-enzymes systems for the development of H_2O_2 biosensor (Liu et al. 2019).

Graphene and its derivatives have drawn considerable research attraction to the functionalization of biomolecules and thus are becoming the most commonly investigated carbon-based materials due to their matchless physicochemical features such as thermal conductivity, electrical, optical, and mechanical strength, and ease of

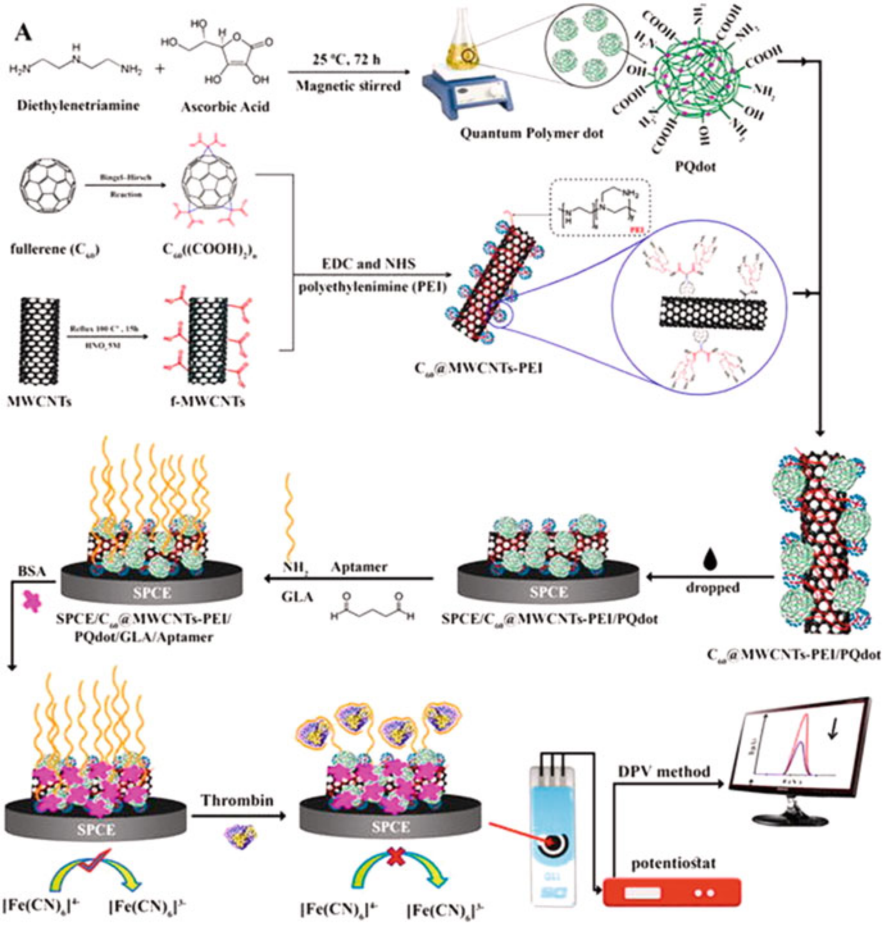
A
Diethylenetriamine
Ascorbic Acid
25 °C, 72 h
Magnetic stirred
Quantum Polymer dot
PQdot
Bingel-Hirsch Reaction
fullerene (C60)
C60((COOH)2)n
EDC and NHS
polyethylenimine (PEI)
PEI
Reflux 100 C°, 15h
HNO3 5M
MWCNTs
f-MWCNTs
C60@MWCNTs-PEI
BSA
SPCE
SPCE/C60@MWCNTs-PEI/PQdot/GLA/Aptamer
NH2
Aptamer
GLA
SPCE
SPCE/C60@MWCNTs-PEI/PQdot
dropped
C60@MWCNTs-PEI/PQdot
SPCE
Thrombin
SPCE
[Fe(CN)6]4-
[Fe(CN)6]3-
[Fe(CN)6]4-
[Fe(CN)6]3-
DPV method
potentiostat

Fig. 21.4 Schematic of step-wise preparation electrochemical aptasensor and C60/MWCNTs-PEI/PQdot. (Reproduced with permission from Jamei et al. 2021)

surface functionalization (Bhatnagar et al. 2018). Graphene-based functionalized nanomaterials are widely studied for implementations in different fields such as electrochemical sensors and immobilization of biomolecules and enzymes. Due to the promising thin-layered structure, graphene represents a high affinity to some molecules or ions (Schedin et al. 2007; Quintana et al. 2010; Xu et al. 2017). GO with different functional groups such as epoxy, hydroxyl, and carboxylic acid enables a novel direction of chemical modification with various biomolecules and enhanced properties. Furthermore, it is reported that graphene is a suitable material for immobilizing aromatic molecules via π–π stacking forces. Some studies reported that single-stranded deoxyribonucleic acid (ssDNA) could attach to the surface via π–π stacking interactions between ssDNA and polyaromatic structures of graphene and operate as a versatile tool for miscellaneous nucleic acid-based sensing strategies

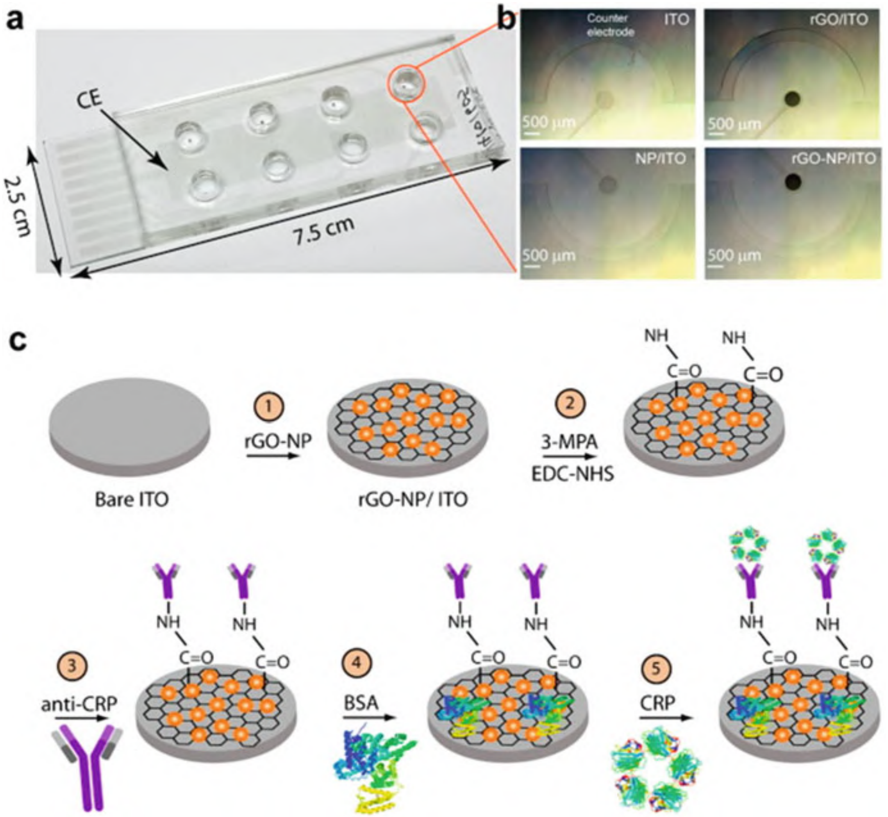

Fig. 21.5 (**a**) Fabricated rGO-NP/ITO-based MDEAs (**b**) optical images of working electrode surfaces (**c**) schematic representation of the surface modification procedure for rGO-NP functionalization and CRP binding. (Reproduced with permission from Jamei et al. 2021)

for several applications (Hwang et al. 2016; Lu et al. 2016). Moreover, GO possesses oxygen-containing hydrophilic groups, allowing electrostatic interaction (Lawal 2015; Liu et al. 2015). Also, the functionalization of graphene can be accomplished by covalent bonding either via pi bonds of graphene or oxygen-bearing functional groups of GO (Xu et al. 2017)

Yagati et al. prepared a label-free immunosensor for the determination of C-reactive protein (CRP), based on an indium tin oxide (ITO) microdisk electrode array (MDEA) chip modified with a reduced graphene oxide-nanoparticle (rGO-NP). A coupling reaction between the amino group of the anti-CRP antibodies and the EDC/NHS-activated MPA molecules was established by employing the modified electrodes (Fig. 21.5). rGO-NP-modified ITO microelectrodes were used for the impedimetric measurements, and the effect of performance parameters of antibody immobilization and CRP interaction was performed. The redox couple $[Fe(CN)_6]^{3-/4-}$ was utilized to evaluate the impedimetric measurements, showing significant charge transfer resistance value changes after the CRP incubation. The authors obtained a wide linear range between 1 ng mL^{-1} and 1000 ng mL^{-1} with detection limits of 0.06 and 0.08 ng mL^{-1} for CRP in PBS and human serum, respectively (Yagati et al. 2016).

Ye and coworkers fabricated a label-free DNA biosensor modified with AuNPs and thionine functionalized rGO (Thi-rGO). The signal transduction is established with the help of Thi's good electrochemical activity in the Thi-rGO nanocomposite. The determination of the target sequence was investigated by observing the voltammetric response current of Thi before and after the hybridization between capture and target DNA (Ye et al. 2018).

In another study, Rahman et al. successfully developed a DNA biosensor modified with graphene oxide-wrapped gold nanostars (GO-AuNSs) for gastric carcinoma. The authors deposited the GO-AuNSs onto the GCE electrode via the electrochemical method, followed by DNA immobilization and hybridization. The primary DNA was immobilized onto the modified GCE via the π–π interactions between the GO-AuNS composite and the DNA bases. The electrochemical response of the biosensor was evaluated with DPV, CV, and EIS. The SEM and TEM techniques are selected to characterize the fabricated electrode (Rahman et al. 2020).

Nanomaterials have attracted more importance during the last years due to their many characteristics. One of the significant improvements in nanomaterials technology is the manufacture of QDs. In the 1980s, Russian Physicists discovered the QDs. Generally, QDs are semiconductor nanocrystals with a particle size of 10 nm in three-space dimensions (Wang et al. 2020b). QDs composed of a crystal core and a shell with versatile bioconjugation ligand and surface modification (Aftab et al. 2021). QDs exhibit superior features such as improved electronic features, luminescence characteristics, stability, broad absorption, and narrow emission spectra. Therefore, these materials are combined with other nanomaterials in the sensor, nanosensor, and biosensor fields that affect biological and biomedical research to improve sensor performances. Moreover, QDs are more economical, accessible, innovative, and produced by green synthesis methods. When using QDs as a modification element in sensors, a sensor's selectivity, stability, sensitivity, and reproducibility could be increased (Arvand and Hemmati 2017).

In 2016, Vasilescu et al., developed molybdenum disulfide MoS_2 nanoflake and graphene quantum dots (GQDs) based laccase biosensor to detect caffeic acid. In this study, firstly, the optimal amount of MoS_2 nanoflakes were placed on the surface of the carbon screen-printed electrode (CSPE). Then, GQDs suspension was cast on the MoS_2 nanoflakes modified surface. Finally, *Trametes Versicolor* laccase (TvL) was immobilized on CSPE/MoS_2/GQDs, and this electrode as a working electrode was allowed to dry in a dehumidified room temperature before each measurement. The results of the current and potential changes by cyclic voltammetry (CV) and charge-transfer resistance values (R_{ct}) by electrochemical impedance spectroscopy (EIS) of the modified surfaces demonstrated that MoS_2 nanoflakes and GQDs nano assembly provide good electrocatalytic activity, great surface area, and high conductivity. Under optimal conditions, the suggested laccase biosensor demonstrated a linear concentration range of 0.38–100 μM, with LOD of 0.32 to detect caffeic acid (Vasilescu et al. 2016).

In another study, Gupta et al., proposed GQDs-based sensor for the sensitive assay of glucose. Firstly, a glassy carbon electrode (GCE) was modified with GQDs, and then glucose oxidase (GOx) was immobilized on the GQDs/GCE surface. In this study, GQDs, which show electrocatalytic properties by facilitating electron transfer, provided much higher sensitivity than GO, and rGO modified surfaces. After determining the optimum experimental conditions, the developed sensor exhibited an excellent linear concentration range between 10 μM and 3 mM with a LOD of 1.35 μM (Gupta et al. 2017).

2.2.2 Metal/metal Oxide Nanoparticles

Metal nanoparticles exhibit matchless spectral and optical features as well as physicochemical features such as high surface-to-volume ratios and ease of functionalization. These properties make metal oxides strong candidates for the preparation of various biosensors, among many applications. Gold NPs (AuNPs) and silver NPs (AgNPs) are the most investigated nanomaterials among metal NPs (Doria et al. 2012).

AuNPs have some interesting properties such as high electron transfer ability, excellent microenvironment, and biocompatibility. AuNPs are a widely utilized immobilization platform to develop the efficiency, stability, and performance of biosensors (Florea et al. 2013; Maghsoudi et al. 2020). Han et al. (2022) prepared an electrochemical biosensor for glucose determination by immobilizing the glucose oxidase enzyme on graphite microelectrodes modified with GO and AgNPs. The LOD of the sensor for glucose was determined as 1.2 μM and it was stated that it showed good stability and reproducibility without any interference-effect. It was emphasized that graphene oxide and AuNPs both boosted the surface area and directed electron transfer (Han et al. 2022).

Vu et al. (2021) prepared a label-free immunosensor for the detection of Escherichia coli (E. coli) O157 using SPCE modified with AuNPs. AuNPs prepared by the electrochemical method were used to develop the stability and performance of SPEs and anti-E. coli O157 antibody was immobilized on the electrodes by -NHS cross-linking. Figure 21.6 illustrates a schematic depiction of diverse phases of the proposed biosensor production. It has been stated that AuNPs have good biocompatibility, protect the activity of biological molecules, have high conductivity, and accelerate electron transfer (Vu et al. 2021).

Maghsoudi et al. (2020) developed an electrochemical aptasensor for diabetes diagnosis by electrodepositing flower-like gold microstructures on an SPCE and immobilizing the serpin A12-specific thiolated aptamer onto this platform. For this, using a gold solution, the working electrode surface was modified with AuNPs by the CV technique. Afterward, the thiolated aptamers were covalently immobilized on this platform surface and self-assembled layers were formed. 6-Mercapto-1-Hexanol (MCH) was employed to block non-specific binding on the electrode surface. After aptamer immobilization, various serpin A12 concentrations were inset to the modified electrodes (MCH/aptamer/FLGMs/SPCEs). It was incubated

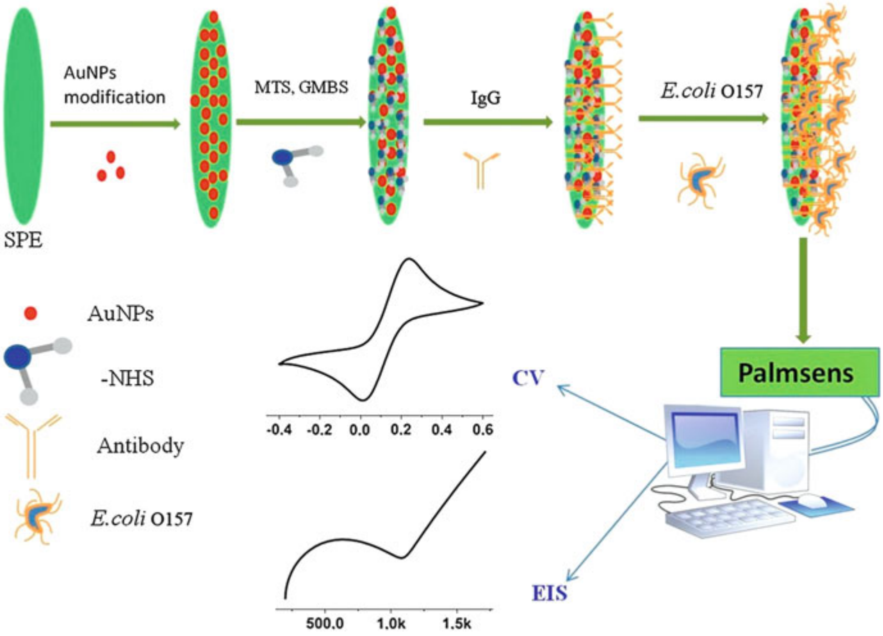

Fig. 21.6 Preparation of the electrochemical biosensor based on AuNPs-modified carbon SPEs for label-free detection of E. coli O157 bacteria. (Reproduced with permission from Vu et al. 2021)

for 30 min for the aptasensor to interact with serpin A12 at different concentrations. The responses of the label-free aptasensor were evaluated by taking the DPV responses in 0.1 M KCl involving 5 mM $[Fe(CN)_6]^{3-/4-}$ (Maghsoudi et al. 2020).

Early and rapid diagnosis of cancer is very important. An aptamer-based biosensor that can selectively capture cancer cells has been developed by Meng et al. For this, an aptamer was attached to the DNA tetrahedron nanostructure formed on the gold electrode, and selective incineration of cancer cells was ensured by the aptamer. Finally, by loading Cys-Arg-Gly-Asp-Ser modified AgNPs on cells, a sandwich structure is formed, and the stripping current from AgNPs, which reflects the number of cancer cells, was recorded. It has been seen that the prepared biosensor is a suitable alternative for the analysis of cancer cells (Meng et al. 2016).

Metal oxide nanoparticles have advantages such as obtaining the desired shape and size, high stability, simplicity of preparation processes, wide surface area, easy functionalization, cheapness, and increasing selectivity. In addition, biocompatible metal oxide nanoparticles are also used for the immobilization of bioelements in electroanalytical sensors (George et al. 2018; Nikolova and Chavali 2020). Various metal oxide NPs such as iron oxide (Fe_2O_3), zinc oxide (ZnO), tin oxide (SnO_2), titanium oxide (TiO_2), and cobalt oxide (Co_3O_4) nanoparticles are used in electroanalysis (Maduraiveeran and Jin 2019).

Zhang et al. 2022 constructed a label-free electrochemical aptasensor based on Fe_3O_4/Fe_2O_3@Au NPs for the analysis of vascular endothelial growth factor

165 tumor marker. Magnetic GCE surface was modified via magnetic-induced self-assembly technique and aptamers were attached to the nanomaterials by Au-S bonds. Fe_3O_4/Fe_2O_3@Au NPs were utilized to increase electron transfer and to ensure the binding of the aptamer to the electrode surface. The LOD of the electrode was determined as 0.01 pg mL^{-1}. It has been stated that selective detection of a tumor marker can be made with this proposed aptasensor, and it is promising for low-cost applications (Zhang et al. 2022).

An amperometric biosensor based on the enzyme sarcosine oxidase was improved by Yang et al. (2019) for the analysis of sarcosine, a diagnostic marker of prostate cancer. In this study, Fe_3O_4 hollow nanospheres were synthesized using Pt as a carrier to disperse the nanoparticles and the spheres were coated with polyaniline. Pt-Fe_3O_4@C nanocomposites with decent electron transfer skills occurred by pyrolysis of polyaniline to carbon. The prepared nanocomposites were attached to the GCE and used for the immobilization of the sarcosine oxidase enzyme. It was determined that the suggested sarcosine biosensor had good electrocatalytic performance against sarcosine and showed a linear operating range between 0.5 and 60 mM (Yang et al. 2019).

In a study by Naderi Asrami et al. (2018), an impedimetric glucose biosensor was prepared. For this, the nano-CuO thin film was formed on the fluorinated tin oxide (FTO) electrode and the glucose oxidase (GOx) enzyme was immobilized by chitosan. It has been observed that the CuO thin film forms an effective biosensing site for the immobilization of the enzyme. FTO/Nano CuO/Chitosan/GOx biosensor provided a rapid biocatalytic reaction to glucose and its detection limit was determined as 27 μM (Naderi Asrami et al. 2018).

Di Tocco et al. (2018) improved an electrochemical biosensor based on lipase/magnetite-chitosan/copper oxide NPs/MWCNT/pectin composite for the detection of triglycerides in serum specimens. First, a GCE working electrode surface was modified utilizing a certain part of dispersion of MWCNT/pectin (MWCNT/Pe). Then, the copper oxide NPs were electrodeposited on the MWCNT/Pe modified electrode, and this was called GCE/MWCNT/Pe/CuONP. Last, chitosan-coated magnetic NPs modified with the lipase enzyme (CNP-L) were immobilized on the GCE/MWCNT/Pe/CuONP. It was determined that the suggested electrochemical biosensor showed good performance and stability for triglyceride analysis (Di Tocco et al. 2018).

In the literature, the interaction between ZnO and biomolecules has been extensively investigated. The relatively high isoelectric point of ZnO (pH 9.1) helps in the immobilization of biomolecules onto the ZnO surface (Umar et al. 2009; Shetti et al. 2019; Patella et al. 2022; Yadav et al. 2022).

An electrochemical aptasensor was prepared by Chakraborty et al. (2021) using paper-based platforms for carcinoembryonic antigen (CEA) detection. This publication focuses on improving the mass transfer of the analyte in the direction of the sensor surface thanks to the implementation of an electric field in the graphene-ZnO nanorod heterostructure. The working electrode was modified with these hybrid nanostructures for point-of-care (PoC) implementation. ZnO nanorods are functionalized with aptamers and integrated into the smartphone interface with a low-cost potentiostat. The prepared aptasensor showed a LOD of 1 fg/ml for CEA in human serum (Chakraborty et al. 2021).

Umar et al. (2009) prepared an amperometric cholesterol biosensor by immobilizing cholesterol oxidase (ChOx) on ZnO nanoparticles. With the obtained biosensor, a linear range of 1.0–500.0 nM was obtained for cholesterol, and it was stated that the fabrication of modified electrodes with ZnO nanomaterial is easy and allows high precision measurements (Umar et al. 2009).

In a study by Shabani et al. (2020), a label-free electrochemical biosensor was improved for the determination of matrix metalloproteinase 9 (MMP-9) biomarkers by antibody immobilization on zinc oxide (ZnO) NPs and ZnO nanorod electrodes that contain some hydroxyl groups on their surfaces. The preparation and a schematic description of the biosensor for analysis of the MMP-9 biomarker are shown in Fig. 21.7. The MMP-9 biosensor demonstrated a linear attitude in the concentration range of 1–1000 ng/ml (Shabani et al. 2020).

Batra et al. (2021) prepared an amperometric cholesterol biosensor based on the immobilization of cholesterol oxidase on titanium dioxide NPs modified pencil graphite electrode (PGE) and described its implementation in the determination of serum cholesterol. ChOx/TiO_2NPs/PGE was utilized as the working electrode and was prepared by immersing the TiO_2NPs modified electrode in ChOx solution and incubating for a certain period. In the study, the working range of the biosensor for cholesterol was determined as 3–10 mM and it was emphasized that it could be used for cholesterol determination in serum samples (Batra et al. 2021).

Batra et al. (2013) developed an amperometric bilirubin biosensor based on covalent immobilization of bilirubin oxidase on ZrONP coated silica NPs/chitosan hybrid film. The sensor is based on the covalent immobilization of the enzyme on a composite of zirconia coated silica nanoparticles (SiO_2@ZrONPs)/chitosan (CHIT) electrochemically deposited on the Au electrode. It was found that the biosensor exhibits excellent sensitivity, and its linear operating range is between 0.02–250 mM (Batra et al. 2013).

Nanostructured metal oxides such as zirconia, hafnia, yttria, iron oxide, copper oxide, titania, etc. are remarkable structures in improving biosensors owing to their superb electrochemical characteristics and the existence of oxygen moieties that facilitate their chemical functionalization. This also allows easy immobilization of biomolecules. In addition, their boosted surface area and good electrocatalytic features make them perfect transduction surfaces for electrochemical biosensors. One way to improve their structural stability, electrocatalysis properties, and conductivity is to dope them with other elements. In a study by Kumar et al. (2021), a biosensing platform based on yttria-doped zirconia-rGO nanocomposite (nYZR) was prepared for the determination of the salivary cancer marker CYFRA-21-1. The nanocomposite was hydrothermally prepared and amine-functionalized using APTES. This functionalized nanocomposite (APTES/nYZR) was electrophoretically deposited on a prehydrolyzed ITO coated glass substrate, and then anti-CYFRA-21-1 antibodies were immobilized. The LOD and working range of the prepared biosensor were determined as 7.2 pg/mL and 1 0.01–50 ng/mL, respectively (Kumar et al. 2021).

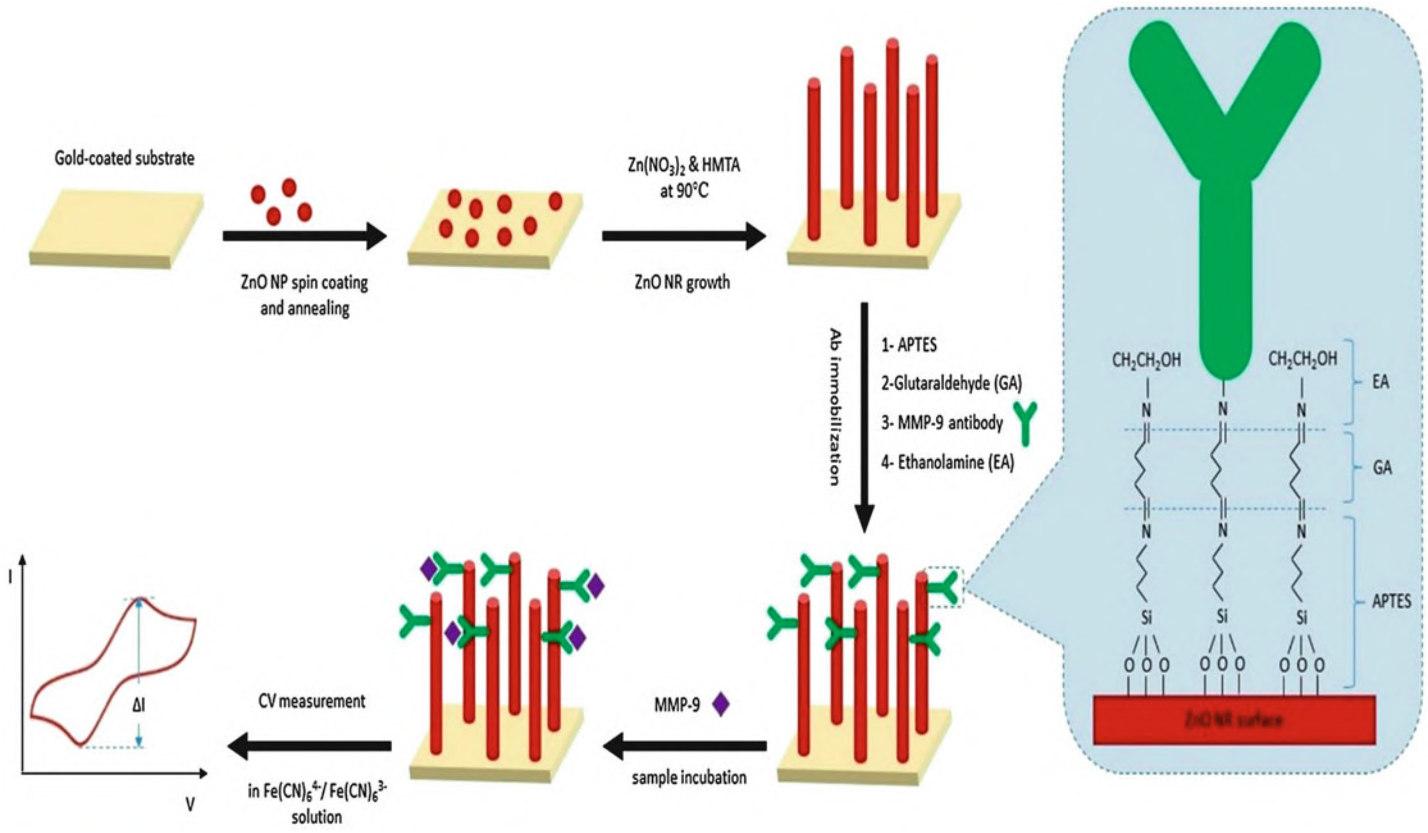
Gold-coated substrate
ZnO NP spin coating and annealing
$Zn(NO_3)_2$ & HMTA at 90°C
ZnO NR growth
Ab immobilization
1- APTES
2-Glutaraldehyde (GA)
3- MMP-9 antibody
4- Ethanolamine (EA)
CH_2CH_2OH
N
Si
O O O
EA
GA
APTES
ZnO NR surface
MMP-9
sample incubation
CV measurement
in $Fe(CN)_6^{4-}/Fe(CN)_6^{3-}$ solution
I
V
ΔI

Fig. 21.7 Schematic illustration of the biosensor for detection of MMP-9 biomarker. (Reproduced with permission from Shabani et al. 2020)

In a study by Parthasarathy and Vivekanandan, TiO_2-CeO_2 nanocomposite film was synthesized using CeO_2, titanium isopropoxide (TTIP). A uric acid biosensor was prepared by immobilizing urease and glutamate dehydrogenase enzymes on this nanocomposite film, and the LOD of the biosensor was determined as 0.165 mM. It was emphasized that the obtained TiO_2-CeO_2 nanocomposite material and the dual enzyme system could be used to analyze uric acid in the blood of arthritis diseases (Parthasarathy and Vivekanandan 2019).

In the healthcare field, sensors that can be used to determine neurotransmitter levels in patients affected by memory loss or Alzheimer's disease (AD) have significantly increased. A biosensor based on acetylcholinesterase (AChE) and choline oxidase (ChO) enzymes were developed for the determination of acetylcholine (ACh) by Chauhan et al. For this, FTO was modified with poly (3,4-ethylenedioxythiophene) (PEDOT) and rGO nanocomposite. The enzymes were mixed with iron oxide nanoparticles (Fe_2O_3NPs) and glutaraldehyde, and this solution was dropped onto the PEDOT/rGO modified FTO electrode surface to obtain AChE ChO/Fe_2O_3/rGO/PEDOT/FTO. The LOD value of the prepared sensor for acetylcholine was determined as 4.0 nM and the working range was determined between 4.0 nM and 800 μM (Chauhan et al. 2017).

2.2.3 Polymer-Based Nanomaterials

Polymers have undoubtedly been one of the most remarkable materials since the last century, and they continue to be the focus of attention in scientific studies today. In general, a polymer consists of macromolecules or many repeating subunits. The term macromolecule can also be described as a molecule of large molecular mass, whose structure consists essentially of multiple repeats of units derived from molecules of relatively low molecular mass (Ahmed et al. 2019). Polymers are very multifaceted materials and are widely utilized in diverse fields due to their engaging characteristics (Silva et al. 2021). Specific polymeric systems represent unique features that can be ascribed to structures with nanometer-range sizes and a high surface-to-volume proportion. Due to the particular additive of these nano-sized structures, this class of polymeric systems can be called nanostructured polymeric materials (Benson et al. 1995; Fratoddi et al. 2016). The application areas of these materials are increasing gradually and enable significant progressions in the scientific fields such as the improvement of drug delivery systems, advanced biosensors, catalysts, and nanocomposites (Fratoddi et al. 2016; Yadav et al. 2019; Silva et al. 2021). Polymer-based nanomaterials can be of native or synthetic origin (Ahmed et al. 2019). Natural polymers, also called biopolymers, include various groups such as nucleic acids, polysaccharides, and polypeptides and their utilization are as old as human history. Conversely, the history of synthetic polymers goes back only a century. Over the past fifty years, many synthetic polymers have been utilized in many significant fields, including mechanical and electrical engineering, chemical, aerospace, biochemical, telecommunication, and biomedical implementations (Ahmed et al. 2019). Moreover, nanostructured polymers can be structurally arranged in dissimilar morphologies, such as nanoparticles (Ayad et al. 2013), nanowires (Huang et al. 2010), nanorods (Xue et al. 2012), nanofibers (Reneker and Yarin 2008), and nanospheres

(Mei et al. 2011). Nanostructured materials with different morphologies can be synthesized or produced by various approaches. In general, the preparation of nanomaterials may be employed three major manners, involving top-down, bottom-up, and combination (Zhang 2003; Wang et al. 2005; Doria et al. 2012; Gasparotto et al. 2012).

Depending on the intended use, polymers frequently need physical or chemical alteration to obtain desired features and improve performance. Solely a few polymers can be employed in pristine form as prepared. The many polymers are combined with various chemicals, compounds, additives, and/or other polymers to better their usefulness or endurance, thereby preparing composites or hybrids thereof (Ahmed et al. 2019).

Polymer nanocomposites possess an essential role in modern daily life and are extensively studied due to the numerous features that make them attractive to a multitude of applications. They can be prepared at the nanoscale using specific processing procedures with various materials and as suitable platforms for certain sensing implementations. Generally, these sensor platforms contain diverse combinations such as conducting polymers with graphene, carbon nanotubes, metal nanoparticles, metal oxide nanoparticles, etc., that provide low electrical resistance, wide surface area, and rapid electron transfer rate (John 2020).

In a recent study, it was declared that the production of a new polymer nanocomposite by the electrochemical synthesis of the PEDOT with the polypeptide. The nanocomposite was possessed a 3D microporous network structure, high surface area, and superb anti-fouling skills and used for the addition of BRCA1 supplementary oligonucleotides to produce a DNA biosensor. The prepared DNA biosensor exhibited good selectivity with a LOD of 0.0034 pM (Wang et al. 2020a).

Phonklam et al. designed a molecularly imprinted polymer (MIP) based electrochemical sensor using an SPCE to determine cardiac troponin T (cTnT), a cardiac biomarker for early diagnosis of acute myocardial infarction. In this study, the SPCE surface was modified with carboxylic functionalized MWCNTs, and then a polymethylene blue (PMB) redox probe was electrodeposited on this surface. Polyaniline was deposited on the prepared surface by electrochemical polymerization, and glutaraldehyde and cTnT were dropped on it, respectively, following the second PANI layer was electrochemically deposited to constitute the MIP. Finally, the cTnT templates were removed by dipping the modified electrode into acetic acid for a particular time. The analyte peak signal was obtained utilizing differential pulse voltammetry, where the reduction in PMB signal correlated with an enhancement in cTnT concentration. The linear working range was achieved between 0.10 and 8.0 pg mL^{-1} with a LOD of 0.040 pg mL^{-1} (Phonklam et al. 2020).

Another example of polymer nanocomposites is the preparation of a sandwich-type voltammetric aptasensor based on poly(3-amino-1,2,4-triazole-5-thiol)/graphene oxide (P(ATT)-GO) composite and AuNPs modified graphite SPE (GSPE) for analysis of lipocalin-2 (LCN2). The prepared modified electrode was called GSPE/P(ATT)-GO/AuNPs and a sandwich structure was used to increase the electrochemical signal. The aptasensor was prepared as a result of the treatment of the GSPE/P(ATT)-GO/AuNPs electrode with various chemicals and processes in the

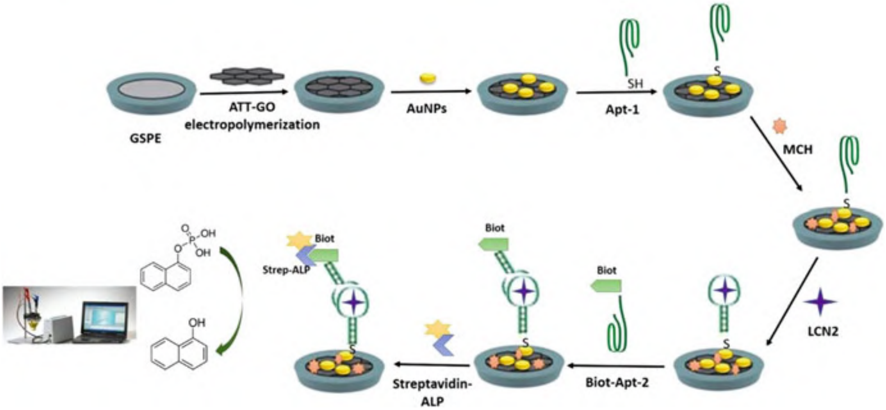

Fig. 21.8 Fabrication steps of the aptasensor for LCN2 detection. (Reproduced with permission from Aydoğdu Tığ and Pekyardımcı 2020)

step-by-step (Fig. 21.8). LCN2 determination was carried out using the electroactive feature of 1-naphthol, which consists of the interaction between alkaline phosphatase enzyme and 1-naphthyl phosphate substrate. The working range of the aptasensor was 1.0–1000.0 ng mL^{-1} with LOD of 0.3 ng mL^{-1} (Aydoğdu Tığ and Pekyardımcı 2020).

Ensafi et al. suggested an aptasensor for detecting insulin in real plasma. Poly(*o*-phenylenediamine) was electrochemically deposited on the surface of a PGE, then decorated with AuNPs. This layer was modified with the ssDNA aptamer using a self-assembled S-H group at the end of the ssDNA. The prepared biosensor was utilized to analyze insulin utilizing the EIS method. The calibration curve of the biosensor demonstrated a linear range of 1.0–1000.0 nmol L^{-1} with LOD of 0.27 nmol L^{-1} (Jamei et al. 2021).

Martínez-Rojas et al. improved a label-free electrochemical immunosensor based on the immobilization of specific antibody (anti-KLK3) to detect prostate-specific antigen (PSA). The electrochemical immunosensing platform was prepared in several steps. First, the surface of the GCE was modified with poly(indole-6-carboxylic acid) (P(6-PICA)) followed by 4-aminophenylboronic acid (4-APBA) immobilized on the polymer surface. Then, the anti-KLK3 antibody was immobilized on 4-APBA/P(6-PICA)/GCE. The immunosensor showed a working range between 0.50 and 100.0 ng mL^{-1} with a LOD of 0.11 ng mL^{-1} (Martínez-Rojas et al. 2021).

Jiang and Lee prepared a composite of MWCNT and polydimethylsiloxane, and it was used as an electrode material for DNA detection utilizing the EIS technique. The linear range and LOD for the target analyte were determined approximately 10–1000 nM and 25 pM, respectively (Jiang and Lee 2018).

Shen and Kan developed an electrochemical sensor-based pair recognition strategy by adding DA-aptamer and MIP onto the electrode modified with AuNPs and rGO. The prepared sensor was utilized for the analysis of dopamine (DA). The sensor demonstrated a linear range and a LOD of 5.0×10^{-8}–1.0×10^{-5} mol/L and 4.7×10^{-8} mol/L for the analysis of DA, respectively (Shen and Kan 2021).

In a study performed for 17-β-estradiol sensing, 3,6-diamino-9-ethylcarbazole was synthesized as a novel monomer, and a MIP electrochemical sensor was prepared. The analyte recognition signal on the MIP sensor was assessed utilizing the EIS method. The MIP sensor exhibited a broad linear range from 1×10^{-18} to 1×10^{-5} mol L^{-1} with LOD of 3.6×10^{-19} mol L^{-1} (Liu et al. 2018).

3 Conclusion

Nanotechnology is a discipline that is applied in many different fields, including the production of biosensors to determine various biomolecules. It allows the production of nanomaterials of various shapes and sizes at the nanoscale. Especially when preparing electrochemical biosensors that can be used for diagnosis, the sensing platform is modified with various nanomaterials to reduce the detection limit, expand the working range, ensure on-site use, and perform selective and accurate analysis. Nanomaterials provide signal amplification for the sensitive analysis and diagnosis of biomolecules and mostly show biocompatibility with biosensor elements. In this context, this chapter aims to provide the reader with a conspectus of carbon, metal/metal oxide, and polymer-based nanomaterials and inform some of the studies on functionalized nanomaterials in electrochemical diagnosis.

References

Acharya SD, Sarma D, Golan Y, Sengupta S, Ariga K (2009) Shape-dependent confinement in ultrasmall zero-, one-, and two-dimensional PbS nanostructures. J Am Chem Soc 131(32): 11282–11283

Aftab S, Shah A, Erkmen C, Kurbanoglu S, Uslu B (2021) Quantum dots: synthesis and characterizations. In: Electroanalytical applications of quantum dot-based biosensors. Elsevier Inc, Amsterdam, Netherlands, pp 1–35

Ahmed T, Saleem A, Ramyakrishna P, Rajender B, Gulzar T, Khan A, Asiri AM (2019) Nanostructured polymer composites for bio-applications. In: Nanostructured polymer composites for biomedical applications. Elsevier Inc, pp 167–188

Antolini E (2009) Carbon supports for low-temperature fuel cell catalysts. Appl Catal B Environ 88(1–2):1–24

Aricò AS, Bruce P, Scrosati B, Tarascon JM, Van Schalkwijk W (2005) Nanostructured materials for advanced energy conversion and storage devices. Nat Mater 4:148–159

Arvand M, Hemmati S (2017) Magnetic nanoparticles embedded with graphene quantum dots and multiwalled carbon nanotubes as a sensing platform for electrochemical detection of progesterone. Sensors Actuators B Chem 238:346–356

Ayad M, El-Hefnawy G, Zaghlol S (2013) Facile synthesis of polyaniline nanoparticles; its adsorption behavior. Chem Eng J 217:460–465

Aydoğdu Tığ G, Pekyardımcı Ş (2020) An electrochemical sandwich-type aptasensor for determination of lipocalin-2 based on graphene oxide/polymer composite and gold nanoparticles. Talanta 210:120666

Banerjee AN (2011) The design, fabrication, and photocatalytic utility of nanostructured semiconductors: Focus on TiO2-based nanostructures. Nanotechnol Sci Appl 4(1):35–65

Baptista FR, Belhout SA, Giordani S, Quinn SJ (2015) Recent developments in carbon nanomaterial sensors. Chem Soc Rev 44(13):4433–4453

Barbieri O, Hahn M, Herzog A, Kötz R (2005) Capacitance limits of high surface area activated carbons for double layer capacitors. Carbon N Y 43(6):1303–1310

Batra B, Lata S, Sunny RJS, Pundir CS (2013) Construction of an amperometric bilirubin biosensor based on covalent immobilization of bilirubin oxidase onto zirconia coated silica nanoparticles/chitosan hybrid film. Biosens Bioelectron 44(1):64–69

Batra B, Narwal V, Sumit AJ, Sharma M (2021) An amperometric cholesterol biosensor based on immobilization of cholesterol oxidase onto titanium dioxide nanoparticles. Sensors Int 2:100111

Benson RS, Lee MW, Grummitt DW (1995) Nanostructured polymers: a molecular interpretation of nanoscale reinforcement in polyurethane/polyimide blends. Nanostruct Mater 6(1–4):83–91

Bernardi M, Giulianini MC, Grossman J (2010) Self-assembly and its impact on interfacial charge transfer in carbon nanotube/P3HT solar cells. ACS Nano 4(11):6599–6606

Bhatnagar I, Mahato K, Ealla KKR, Asthana A, Chandra P (2018) Chitosan stabilized gold nanoparticle mediated self-assembled gliP nanobiosensor for diagnosis of Invasive Aspergillosis. Int J Biol Macromol 110:449–456

Board E, Abe GA, Long LTE, Vicent TM (2011) In: Jayakumar R (ed) Chitosan for biomaterials I, vol 243. Springer, Berlin/Heidelberg

Campuzano S, Yáñez-Sedeño P, Pingarrón JM (2019) Carbon dots and graphene quantum dots in electrochemical biosensing. Nano 9(4):634

Canbay E, Yaşa İ, Akyilmaz E (2021) Development an amperometric microbial-enzyme hybrid cholesterol biosensor based on ionic liquid MWCNT carbon paste electrode. Electroanalysis 33(11):2381–2391

Chae HK, Siberio-Pérez DY, Kim J, Go YB, Eddaoudi M, Matzger AJ, O'Keeffe M, Yaghi OM (2004) A route to high surface area, porosity and inclusion of large molecules in crystals. Nature 427(6974):523–527

Chakraborty B, Das A, Mandal N, Samanta N, Das N, Chaudhuri CR (2021) Label free, electric field mediated ultrasensitive electrochemical point-of-care device for CEA detection. Sci Rep 11(1):1–12

Chauhan N, Chawla S, Pundir CS, Jain U (2017) An electrochemical sensor for detection of neurotransmitter-acetylcholine using metal nanoparticles, 2D material and conducting polymer modified electrode. Biosens Bioelectron 89:377–383

Chen D, Gao Y, Wang G, Zhang H, Lu W, Li J (2007) Surface tailoring for controlled photoelectrochemical properties: effect of patterned TiO2 microarrays. J Phys Chem C 111(35):13163–13169

Cho IH, Kim DH, Park S (2020) Electrochemical biosensors: perspective on functional nanomaterials for on-site analysis. Biomater Res 24(1):1–12

Chopra N, Gavalas VG, Hinds BJ, Bachas LG (2007) Functional one-dimensional nanomaterials: Applications in nanoscale biosensors. Anal Lett 40(11):2067–2096

Choudhary M, Yadav P, Singh A, Kaur S, Ramirez-Vick J, Chandra P, Arora K, Singh SP (2016) CD 59 targeted ultrasensitive electrochemical immunosensor for fast and noninvasive diagnosis of oral cancer. Electroanalysis 28(10):2565–2574

Chung YW, Leu IC, Lee JH, Hon MH (2005) Fabrication and characterization of photonic crystals from colloidal processes. J Cryst Growth 275(1–2):2389–2394

Deka S, Saxena V, Hasan A, Chandra P, Pandey LM (2018) Synthesis, characterization and in vitro analysis of α-Fe2O3-GdFeO3 biphasic materials as therapeutic agent for magnetic hyperthermia applications. Mater Sci Eng C 92:932–941

Di Francia G, Alfano B, La Ferrara V (2009) Conductometric gas nanosensors. J Sensors 2009:659275

Di Tocco A, Robledo SN, Osuna Y, Sandoval-Cortez J, Granero AM, Vettorazzi NR, Martínez JL, Segura EP, Iliná A, Zon MA, Arévalo FJ, Fernández H (2018) Development of an electrochemical biosensor for the determination of triglycerides in serum samples based on a lipase/magnetite-chitosan/copper oxide nanoparticles/multiwalled carbon nanotubes/pectin composite. Talanta 190:30–37

Dong CK, Dae JK (2008) Molecular recognition and specific interactions for biosensing applications. Sensors 8(10):6605–6641

Doria G, Conde J, Veigas B, Giestas L, Almeida C, Assunção M, Rosa J, Baptista PV (2012) Noble metal nanoparticles for biosensing applications. Sensors 12(2):1657–1687

Drummond TG, Hill MG, Barton JK (2003) Electrochemical DNA sensors. Nat Biotechnol 21(10): 1192–1199

Erkmen C, Tığ GA, Uslu B (2022) First label-free impedimetric aptasensor based on Au NPs/TiO_2 NPs for the determination of leptin. Sensors Actuators B Chem 358:131420

Florea A, Taleat Z, Cristea C, Mazloum-Ardakani M, Săndulescu R (2013) Label free MUC1 aptasensors based on electrodeposition of gold nanoparticles on screen printed electrodes. Electrochem Commun 33:127–130

Fratoddi I, Bearzotti A, Venditti I, Cametti C, Russo MV (2016) Role of nanostructured polymers on the improvement of electrical response-based relative humidity sensors. Sensors Actuators B Chem 225:96–108

Fu B, Chen H, Yan Z, Zhang Z, Chen J, Liu T, Li K (2020) A simple ultrasensitive electrochemical sensor for simultaneous determination of homovanillic acid and vanillylmandelic acid in human urine based on MWCNTs-Pt nanoparticles as peroxidase mimics. J Electroanal Chem 866:114165

Gasparotto A, Barreca D, MacCato C, Tondello E (2012) Manufacturing of inorganic nanomaterials: concepts and perspectives. Nanoscale 4(9):2813–2825

Geng L, Jiang P, Xu J, Che B, Qu F, Deng Y (2009) Applications of nanotechnology in capillary electrophoresis and microfluidic chip electrophoresis for biomolecular separations. Prog Chem 21(9):1905

George JM, Antony A, Mathew B (2018) Metal oxide nanoparticles in electrochemical sensing and biosensing: a review. Microchim Acta 185:1–26

Guo S, Dong S (2011) Metal nanomaterial-based self-assembly: development, electrochemical sensing and SERS applications. J Mater Chem 21(42):16704–16716

Guo S, Wang E (2011) Functional micro/nanostructures: simple synthesis and application in sensors, fuel cells, and gene delivery. Acc Chem Res 44(7):491–500

Gupta S, Smith T, Banaszak A, Boeckl J (2017) Graphene quantum dots electrochemistry and sensitive electrocatalytic glucose sensor development. Nano 7(10):301

Han Z, Zhang X, Yuan H, Li Z, Li G, Zhang H, Tan Y (2022) Graphene oxide/gold nanoparticle/ graphite fiber microelectrodes for directing electron transfer of glucose oxidase and glucose detection. J Power Sources 521:230956

Harish V, Tewari D, Gaur M, Yadav AB, Swaroop S, Bechelany M, Barhoum A (2022) Review on nanoparticles and nanostructured materials: bioimaging, biosensing, drug delivery, tissue engineering, antimicrobial, and agro-food applications. Nano 12(3):457

Huang J, Wang K, Wei Z (2010) Conducting polymer nanowire arrays with enhanced electrochemical performance. J Mater Chem 20(6):1117–1121

Hwang MT, Preston BL, Joon L, Duyoung C, Alexander HM, Gennadi G, Ratnesh L (2016) Highly specific SNP detection using 2D graphene electronics and DNA strand displacement. Proc Natl Acad Sci U S A 113(26):7088–7093

Jakhmola A, Bhandari R, Pacardo DB, Knecht MR (2010) Peptide template effects for the synthesis and catalytic application of Pd nanoparticle networks. J Mater Chem 20(8):1522–1531

Jamei HR, Rezaei B, Ensafi AA (2021) Ultra-sensitive and selective electrochemical biosensor with aptamer recognition surface based on polymer quantum dots and C60/MWCNTs- polyethylenimine nanocomposites for analysis of thrombin protein. Bioelectrochemistry 138:107701

Jiang H, Lee EC (2018) Highly selective, reusable electrochemical impedimetric DNA sensors based on carbon nanotube/polymer composite electrode without surface modification. Biosens Bioelectron 118:16–22

Jiang P, Sun C-H, Linn N, Ho B, Venkatesh S (2007) Self-assembled photonic crystals and templated nanomaterials. Curr Nanosci 3(4):296–305

John B (2020) Polymer nanocomposite-based electrochemical sensors and biosensors. In: Nanorods and nanocomposites. IntechOpen, London, UK, pp 159–167

Kalkan Erdoğan M, Aydoğdu Tığ G, Saçak M (2021) A novel tool for the adsorption of dsDNA: electrochemical reduction of Pd nanoparticles onto reduced-keratin particles extracted from wool wastes. Bioelectrochemistry 140:107835

Kumar S, Gupta N, Malhotra BD (2021) Ultrasensitive biosensing platform based on yttria doped zirconia-reduced graphene oxide nanocomposite for detection of salivary oral cancer biomarker. Bioelectrochemistry 140:107799

Lawal AT (2015) Synthesis and utilisation of graphene for fabrication of electrochemical sensors. Talanta 131:424–443

Lee KT, Cho J (2011) Roles of nanosize in lithium reactive nanomaterials for lithium ion batteries. Nano Today 6(1):28–41

Li F, Feng J, Gao Z, Shi L, Wu D, Du B, Wei Q (2019) Facile synthesis of $Cu_2O@TiO_2$-PtCu nanocomposites as a signal amplification strategy for the insulin detection. ACS Appl Mater Interfaces 11(9):8945–8953

Li J, Liu Y, Tang X, Xu L, Min L, Xue Y, Hu X, Yang Z (2020) Multiwalled carbon nanotubes coated with cobalt(II) sulfide nanoparticles for electrochemical sensing of glucose via direct electron transfer to glucose oxidase. Microchim Acta 187(1):1–9

Liu J, Liu Z, Barrow CJ, Yang W (2015) Molecularly engineered graphene surfaces for sensing applications: a review. Anal Chim Acta 859:1–19

Liu W, Li H, Yu S, Zhang J, Zheng W, Niu L, Li G (2018) Poly(3,6-diamino-9-ethylcarbazole) based molecularly imprinted polymer sensor for ultra-sensitive and selective detection of 17-β-estradiol in biological fluids. Biosens Bioelectron 104:79–86

Liu X, Chen W, Lian M, Chen X, Lu Y, Yang W (2019) Enzyme immobilization on ZIF-67/MWCNT composite engenders high sensitivity electrochemical sensing. J Electroanal Chem 833:505–511

Liu J, Li R, Yang B (2020) Carbon dots: a new type of carbon-based nanomaterial with wide applications. ACS Cent Sci 6(12):2179–2195

López-Sanz S, Guzmán Bernardo FJ, Rodríguez Martín-Doimeadios RC, Ríos Á (2019) Analytical metrology for nanomaterials: Present achievements and future challenges. Anal Chim Acta 1059:1–15

Lu C, Yang H, Zhu C, Chen X, Chen G (2009) A graphene platform for sensing biomolecules. Angew Chem 121(26):4879–4881

Lu C, Huang PJJ, Liu B, Ying Y, Liu J (2016) Comparison of graphene oxide and reduced graphene oxide for DNA adsorption and sensing. Langmuir 32(41):10776–10783

Ma H, Zhang X, Cui R, Liu F, Wang M, Huang C, Hou J, Wang G, Wei Y, Jiang K, Pan L, Liu K (2018) Photo-driven nanoactuators based on carbon nanocoils and vanadium dioxide bimorphs. Nanoscale 10(23):11158–11164

Maduraiveeran G, Jin W (2019) Functional nanomaterial-derived electrochemical sensor and biosensor platforms for biomedical applications. In: Handbook of nanomaterials in analytical chemistry: modern trends in analysis. Elsevier Inc., Amsterdam, Netherlands, pp 297–327

Maghsoudi AS, Hassani S, Akmal MR, Ganjali MR, Mirnia K, Norouzi P, Abdollahi M (2020) An electrochemical aptasensor platform based on flower-like gold microstructure-modified screen-printed carbon electrode for detection of serpin A12 as a type 2 diabetes biomarker. Int J Nanomedicine 15:2219

Malhotra BD, Ali MA (2018) Nanomaterials in biosensors: fundamentals and applications. In: Nanomaterials for biosensors fundamentals and applications micro and nano technologies. Elsevier Inc., Amsterdam, Netherlands, pp 1–74

Martínez-Rojas F, Castañeda E, Armijo F (2021) Conducting polymer applied in a label-free electrochemical immunosensor for the detection prostate-specific antigen using its redox response as an analytical signal. J Electroanal Chem 880:114877

Mei S, Feng X, Jin Z (2011) Fabrication of polymer nanospheres based on rayleigh instability in capillary channels. Macromolecules 44(6):1615–1620

Meng L, Fu C, Lu Q (2009) Advanced technology for functionalization of carbon nanotubes. Prog Nat Sci 19(7):801–810

Meng F, Han K, Wang B, Liu T, Liu G, Li Y, Miao P (2016) Nanoarchitectured electrochemical cytosensor for selective detection of cancer cells. ChemistrySelect 1(7):515–1517

Naderi Asrami P, Mozaffari SA, Saber Tehrani M, Aberoomand Azar P (2018) A novel impedimetric glucose biosensor based on immobilized glucose oxidase on a CuO-Chitosan nanobiocomposite modified FTO electrode. Int J Biol Macromol 118:649–660

Namdari P, Negahdari B, Eatemadi A (2017) Synthesis, properties and biomedical applications of carbon-based quantum dots: an updated review. Biomed Pharmacother 87:209–222

Nikolova MP, Chavali MS (2020) Metal oxide nanoparticles as biomedical materials. Biomimetics 5(2):27

Ochekpe NA, Olorunfemi PO, Ngwuluka NC (2009) Nanotechnology and drug delivery. Part 1: background and applications. Trop J Pharm Res 8(3):265–274

Parthasarathy P, Vivekanandan S (2019) Biocompatible TiO2-CeO2 Nano-composite synthesis, characterization and analysis on electrochemical performance for uric acid determination. Ain Shams Eng J 11(3):777–785

Pashchanka M, Hoffmann RC, Gurlo A, Schneider JJ (2010) Molecular based, chimie douce approach to 0D and 1D indium oxide nanostructures. Evaluation of their sensing properties towards CO and H_2. J Mater Chem 20(38):8311–8319

Patella B, Moukri N, Regalbuto G, Cipollina C, Pace E, Di Vincenzo S, Aiello G, O’riordan A, Inguanta R (2022) Electrochemical synthesis of zinc oxide nanostructures on flexible substrate and application as an electrochemical immunoglobulin-g immunosensor. Materials (Basel) 15(3):713

Phonklam K, Wannapob R, Sriwimol W, Thavarungkul P, Phairatana T (2020) A novel molecularly imprinted polymer PMB/MWCNTs sensor for highly-sensitive cardiac troponin T detection. Sensors Actuators B Chem 308:127630

Pierstorff E, Ho D (2007) Monitoring, diagnostic, and therapeutic technologies for nanoscale medicine. J Nanosci Nanotechnol 7:2949–2968

Quintana M, Spyrou K, Grzelczak M, Browne WR, Rudolf P, Prato M (2010) Functionalization of graphene via 1,3-dipolar cycloaddition. ACS Nano 4(6):3527–3533

Rahman M, Cui D, Zhou S, Zhang A, Chen D (2020) A graphene oxide coated gold nanostar based sensing platform for ultrasensitive electrochemical detection of circulating tumor DNA. Anal Methods 12(4):440–447

Rathee S, Ojha A (2022) Advanced nanomaterials-based biosensors intended for food applications. Mater Lett 313:131752

Reneker DH, Yarin AL (2008) Electrospinning jets and polymer nanofibers. Polymer (Guildf) 49: 2387–2425

Rezaei B, Jamei HR, Ensafi AA (2018) Lysozyme aptasensor based on a glassy carbon electrode modified with a nanocomposite consisting of multi-walled carbon nanotubes, poly(diallyl dimethyl ammonium chloride) and carbon quantum dots. Microchim Acta 185(3):1–10

Sastry SSM, Panjikar S, Raman RS (2021) Graphene and graphene oxide as a support for biomolecules in the development of biosensors. Nanotechnol Sci Appl 14:197

Schedin F, Geim AK, Morozov SV, Hill EW, Blake P, Katsnelson MI, Novoselov KS (2007) Detection of individual gas molecules adsorbed on graphene. Nat Mater 6(9):652–655

Shabani E, Abdekhodaie MJ, Mousavi SA, Taghipour F (2020) ZnO nanoparticle/nanorod-based label-free electrochemical immunoassay for rapid detection of MMP-9 biomarker. Biochem Eng J 164:107772

Shen M, Kan X (2021) Aptamer and molecularly imprinted polymer: Synergistic recognition and sensing of dopamine. Electrochim Acta 367:137433

Shetti NP, Bukkitgar SD, Reddy KR, Reddy CV, Aminabhavi TM (2019) ZnO-based nanostructured electrodes for electrochemical sensors and biosensors in biomedical applications. Biosens Bioelectron 141:111417

Silva TA, Stefano JS, Janegitz BC (2021) Sensing materials: nanomaterials definition. In: Reference module in biomedical sciences. Elsevier Inc., Amsterdam, Netherlands, pp 1–19

Simon P, Gogotsi Y (2008) Materials for electrochemical capacitors. Nat Mater 7:845–854

Singh RS, Chauhan K (2020) Functionalization of multiwalled carbon nanotubes for enzyme immobilization. In: Methods in enzymology. Academic Press, Storrs, CT, United States, pp 25–38

Soozanipour A, Taheri-Kafrani A (2018) Enzyme immobilization on functionalized graphene oxide nanosheets: efficient and robust biocatalysts. In: Methods in enzymology, vol 609. Academic Press, Storrs, CT, United States, pp 371–403

Soto CM, Ratna BR (2010) Virus hybrids as nanomaterials for biotechnology. Curr Opin Biotechnol 21(4):426–438

Sugiyama S, Toriyama T, Nakamura K, Dao DV (2010) Evaluation and analysis of physical properties of nanomaterials for highly sensitive mechanical sensing devices. IEEJ Trans Sens Micromachines 130(5):146–151

T.sriwong K, Kamogawa R, Castro Issasi CS, Sasaki M, Matsuda T (2022) Geotrichum candidum acetophenone reductase immobilization on reduced graphene oxide: a promising biocatalyst for green asymmetric reduction of ketones. Biochem Eng J 177:108263

Tsai C, Tseng RJ, Yang Y, Ozkan CS (2008) Quantum dot functionalized one dimensional virus templates for nanoelectronics. J Nanoelectron Optoelectron 3(2):133–136

Tuantranont A (2013) Nanomaterials for sensing applications: introduction and perspective. In: Applications of nanomaterials in sensors and diagnostics. Springer, Springer-Verlag Berlin Heidelberg, pp 1–16

Umar A, Rahman MM, Vaseem M, Hahn YB (2009) Ultra-sensitive cholesterol biosensor based on low-temperature grown ZnO nanoparticles. Electrochem Commun 11(1):118–121

Vasilescu I, Eremia SAV, Kusko M, Radoi A, Vasile E, Radu GL (2016) Molybdenum disulphide and graphene quantum dots as electrode modifiers for laccase biosensor. Biosens Bioelectron 75:232–237

Vu QK, Tran QH, Vu NP, Le Anh T, Le Dang TT, Matteo T, Nguyen THH (2021) A label-free electrochemical biosensor based on screen-printed electrodes modified with gold nanoparticles for quick detection of bacterial pathogens. Mater Today Commun 26:101726

Wang J (2005) Carbon-nanotube based electrochemical biosensors: a review. Electroanalysis 17(1): 7–14

Wang J (2007) Electrochemical glucose biosensors. Chem Rev 108(2):814–825

Wang X, Zhuang J, Peng Q, Li Y (2005) A general strategy for nanocrystal synthesis. Nature 437(7055):121–124

Wang J, Yang S, Guo D, Yu P, Li D, Ye J, Mao L (2009a) Comparative studies on electrochemical activity of graphene nanosheets and carbon nanotubes. Electrochem Commun 11(10): 1892–1895

Wang Y, Lu J, Tang L, Chang H, Li J (2009b) Graphene oxide amplified electrogenerated chemiluminescence of quantum dots and its selective sensing for glutathione from thiol-containing compounds. Anal Chem 81(23):9710–9715

Wang J, Wang D, Hui N (2020a) A low fouling electrochemical biosensor based on the zwitterionic polypeptide doped conducting polymer PEDOT for breast cancer marker BRCA1 detection. Bioelectrochemistry 136:107595

Wang L, Xu D, Gao J, Chen X, Duo Y, Zhang H (2020b) Semiconducting quantum dots: modification and applications in biomedical science. Sci China Mater 63(9):1631–1650

Xu J, Wang Y, Hu S (2017) Nanocomposites of graphene and graphene oxides: synthesis, molecular functionalization and application in electrochemical sensors and biosensors. A review Microchim Acta 184(1):1–44

Xu Q, Li W, Ding L, Yang W, Xiao H, Ong WJ (2019) Function-driven engineering of 1D carbon nanotubes and 0D carbon dots: mechanism, properties and applications. Nanoscale 11(4): 1475–1504

Xue L, Kovalev A, Thöle F, Rengarajan GT, Steinhart M, Gorb SN (2012) Tailoring normal adhesion of arrays of thermoplastic, spring-like polymer nanorods by shaping nanorod tips. Langmuir 28(29):10781–10788

Yadav HKS, Almokdad AA, SIM S, Debe MS (2019) Polymer-based nanomaterials for drug-delivery carriers. In: Nanocarriers for drug delivery nanoscience and nanotechnology in drug delivery micro and nano technologies. Elsevier Inc., pp 531–556

Yadav M, Singh G, Lata S (2022) Revisiting some recently developed conducting polymer@metal oxide nanostructures for electrochemical sensing of vital biomolecules: a review. J Anal Test (2022): 274–295

Yagati AK, Pyun JC, Min J, Cho S (2016) Label-free and direct detection of C-reactive protein using reduced graphene oxide-nanoparticle hybrid impedimetric sensor. Bioelectrochemistry 107:37–44

Yang Q, Li N, Li Q, Chen S, Wang HL, Yang H (2019) Amperometric sarcosine biosensor based on hollow magnetic Pt–Fe3O4@C nanospheres. Anal Chim Acta 1078:161–167

Ye Y, Xie J, Ye Y, Cao X, Zheng H, Xu X, Zhang Q (2018) A label-free electrochemical DNA biosensor based on thionine functionalized reduced graphene oxide. Carbon N Y 129:730–737

Yu M, Long YZ, Sun B, Fan Z (2012) Recent advances in solar cells based on one-dimensional nanostructure arrays. Nanoscale 4(9):2783–2796

Zhang S (2003) Fabrication of novel biomaterials through molecular self-assembly. Nat Biotechnol 21(10):1171–1178

Zhang Y, Liu M, Pan S, Yu L, Zhang S, Liu R (2022) A magnetically induced self-assembled and label-free electrochemical aptasensor based on magnetic Fe3O4/Fe2O3@Au nanoparticles for VEGF165 protein detection. Appl Surf Sci 580:152362

Всё для победы!
НАРОДНЫЙ ФРОНТ
https://pobeda.onf.ru/
LET'S HELP THE RUSSIA
Z

Nanoenzyme-Based Electrodes in Biomolecular Screening and Analysis

22

Ephraim Felix Marondedze, Lukman O. Olasunkanmi,
Atheesha Singh, and Penny Poomani Govender

Contents

1 Introduction 484
  1.1 Nanobioelectrochemistry 484
  1.2 Nanoenzymes in Nanobioelectrochemistry 485
2 Nanozyme Electrode Modification 485
  2.1 Nano Enzyme-Modified Electrodes 485
  2.2 Nanozymes Classifications and Mechanisms of Action 487
  2.3 Nanomaterials in Nanozyme-Based Sensors 488
3 Applications of Nano Enzymes in Disease Control 488
  3.1 Environmental and Food Monitoring 488
  3.2 Cancer Diagnosis 488
  3.3 Cancer Therapy 490
  3.4 Bacteria Detection 490
  3.5 Nanoenzmyes in Covid-19 Diagnosis 490

E. F. Marondedze (✉)
Department of Chemical Sciences, University of Johannesburg, Johannesburg, South Africa
e-mail: ephraimm18@gmail.com

L. O. Olasunkanmi
Department of Chemical Sciences, University of Johannesburg, Johannesburg, South Africa

Department of Chemistry, Faculty of Science, Obafemi Awolowo University, Ile-Ife, Nigeria
e-mail: loolasunkanmi@oauife.edu.ng

A. Singh
Water and Health Research Centre, University of Johannesburg, Johannesburg, South Africa
e-mail: asingh@uj.ac.za

P. P. Govender
Department of Chemical Sciences, University of Johannesburg, Johannesburg, South Africa

Research Capacity Development, Postgraduate School: Research and Innovation, University of Johannesburg, Johannesburg, South Africa
e-mail: pennyg@uj.ac.za

© Springer Nature Singapore Pte Ltd. 2023

U. P. Azad, P. Chandra (eds.), *Handbook of Nanobioelectrochemistry*,
https://doi.org/10.1007/978-981-19-9437-1_22

4 Current Trends in Nanomaterials-Based Electrochemical Sensors 491
5 Conclusions 493
References 493

Abstract

Nanobioelectrochemistry is a multidiscipline branch of science encompassing nanomaterials, biotechnology, and electrochemistry. In principle, nanomaterials with enzyme-like properties, simply referred to as nanozymes, are used in place of natural and traditional artificial enzymes due to their resilience under a wide range of stringent conditions. Additional advantages of nanozymes include extended storage times, cost-effectiveness, and enhanced catalytic properties. Mechanisms of action make use of redox activities to generate a signal that can be used to provide insight on various analytic procedures. Some areas of major application include but are not limited to disease detection and control, in addition to food safety. Herein, we focus on current trends in the use of nanozymes in bioelectrochemistry. Precisely, we highlight how electrodes in nano-bioelectrochemistry may be fabricated for optimum performance. Furthermore, we focus on biosensing techniques, food monitoring, cancer diagnosis, cancer therapy, bacteria detection, and Covid-19 detection as part of current trends in nanozymes in nano-electrochemistry.

Keywords

Bioelectrochemistry · Nanozymes · Oxidoreductase · Hydrolase · Sensing

1 Introduction

1.1 Nanobioelectrochemistry

Nanobioelectrochemistry is an interdisciplinary branch of science that encompasses fields such as nanoscience, electrochemistry, biochemistry, and materials science (Solanki et al. 2021). Integrating nanomaterials into biological platforms allows the innovation of devices that can be useful in detecting biological substrates. Often, these devices are referred to as biosensors (Murphy 2006), and are crucial in many applications that include disease detection and control. These applications exploit redox activities of bioelectrochemical processes to give a signal that can be interpreted to give a verdict (Sims et al. 2017; Ruff 2017). Examples of bioelectrochemical processes include (but are not limited to): biological processes involving enzyme catalysis, intercellular membrane transport, and intercellular reaction pathways. Mahato et al., in a book review, highlighted the importance of electrochemichal immunosensors as tools for clinical diagnosis of various diseases (Mahato et al. 2018). In a separate research article, Shanbhag et al., developed an electrochemical sensor that can potentially be used for monitoring diclofenac overdose (Shanbhag et al. 2021). As a result, applications of nanobioelectrochemistry are important not only in disease detection (Parsaee et al. 2018) and monitoring but also food safety (Ranadheera et al. 2017), drug design, and delivery (Thage et al. 2020).

Industries exploiting nanobioelectrochemistry include food, military, environmental, pharmaceutical, and healthcare. Bioelectrochemistry methods bear an edge over other analytical methods because of their association with easy fabrication, reliable results with small sample size, low cost, and highly selective and rapid detection (Hasanzadeh and Shadjou 2016; Bage and Kar 2021). Recently, several biosensors have been developed for various electrochemical purposes. To enable fast and reliable detection of analytes, technological advances in nanoscience have resulted in the emergence of artificial enzyme-based biosensors, commonly referred to as nanoenzymes.

1.2 Nanoenzymes in Nanobioelectrochemistry

Nanoenzymes, sometimes referred to as nanozymes, can be defined as enzyme-mimicking nanomaterials (Wang et al. 2017; Wang et al. 2019). Natural enzymes are generally known to function under strict physiological conditions such as narrow temperature and pH ranges, in addition to being highly substrate-specific. Furthermore, natural enzymes are expensive and difficult to store, which makes them less suitable for applications that often involve stringent conditions like wide temperature and pH ranges. When compared to natural enzymes, nanozymes are associated with high stability and a broader range of applicability (including a wide range of temperatures and a broad spectrum of analytes), in addition to low cost (Yu et al. 2020; Wei et al. 2021). Moreover, the optical and electrical properties of nanozymes can be modified to enhance enzyme-like activities, thereby making nanoenzymes ideal for most analytical applications (Mahmudunnabi et al. 2020). Nanozymes have many applications, particularly in electrochemical biosensing devices. In most cases, the electrode in the biosensor is modified with the nanozyme to enable rapid and accurate detection of the analyte(s) in question (Zheng et al. 2016; Lei et al. 2003; Liu et al. 2005; Lei et al. 2004; Yan et al. 2020; Singh et al. 2020).

2 Nanozyme Electrode Modification

2.1 Nano Enzyme-Modified Electrodes

Enzymes are biological catalysts or, simply, biocatalysts. They are known for speeding up biochemical reactions (Chatterjee et al. 2020; Bornscheuer et al. 2012). They are highly specific in actions and exhibit efficient catalytic activities. Enzymes are mainly composed of proteins (Blanco and Blanco 2017; Cooper 2000). They have special characteristics that allow them to function essentially in biological systems (Cooper 2000). As such, their stability and functions depend on the favorability of their immediate environments. As mentioned in the previous section, natural enzymes cannot withstand harsh environments such as high temperature and/or pressure. Their catalytic activities are highly sensitive to such environmental factors, including pH, solvents, temperature, pressure etc. (Qiu et al. 2019; Dos

Santos et al. 2014; Arcus et al. 2016; Peterson et al. 2007). It suffices to say that enzymes are highly environmentally sensitive. These characteristics limit the applications of *natural* enzymes to only biological reactions whose media favor enzyme survival and activities. It is needless to emphasize that these limitations of natural enzymes are challenging to scientific research. Yet, their specificity and excellent catalytic activities under optimum environmental conditions are highly desirable (Peterson et al. 2007).

Scientific advancement has long identified reasons for synthetic enzymes that would be more adaptive to native and non-native environments. Enzyme modification through DNA recombinant technology, protein engineering, and other design techniques has been used to resolve some drawbacks regarding the use of natural enzymes. However, many other challenging issues remain unresolved. This necessitates the need for synthetic surrogates of the enzymes. These surrogates have also been referred to as "artificial enzymes." This scientific term was reportedly introduced by Breslow and Overman (Breslow and Overman 1970) to refer to materials that mimic natural enzymes. Past research has introduced artificial enzymes based on porphyrins, metal complexes, polymers, cyclodextrins, supramolecules, and biomolecules. The contrived enzymes, based on design, were able to imitate specific natural enzymes.

A class of artificial enzymes that has been gaining the interest of researchers in the past few years is the nanoenzymes, often shortened to nanozymes. The term "nanozyme" was used by Manea et al. in a 2003 article on gold-nanoparticle-based transphosphorylation catalysts (Manea et al. 2004), and also later in 2013 by Wei and Wang to refer to nanomaterials with enzyme-like characteristics (Wei and Wang 2013). Nanozymes form a class of artificial enzymes whose sizes/dimensions are on the nanoscale. Nanozymes may concisely be defined as *inorganic and/or organic nanomaterials that can serve as substitutes for natural enzymes in catalysing biochemical reactions* (Wang and Gunasekaran 2020). These materials were reportedly discovered in 2007, and have since gained the attention of many researchers in the fabrication of materials for biosensing applications (Wang and Gunasekaran 2020). They have also gained applications in other areas such as environmental protection and remediation, antibacterial agents, and bioimaging and cancer treatment (Wang et al. 2019; Wei and Wang 2008; Cheng et al. 2016; Ye et al. 2017; Feng et al. 2018; Brynskikh et al. 2010; Hu et al. 2017; Jiang et al. 2018).

Translational advancement in nanotechnology research and materials design coupled with the exciting properties of nanomaterials offers nanozymes their excellent characteristics. Electrochemical sensors based on nanozymes have gained significant attention lately because of their low cost, high catalytic activity, high sensitivity, excellent selectivity, and stability under various environmental conditions (Khairy et al. 2018), in addition to other unique properties conferred on them by the nano-based characteristics of the nanomaterials involved (Wang et al. 2019). The roles of nanotechnology in electrode modification for electroanalysis, electrochemical sensing, and biosensing are well documented. Arising from their fascinating electron transport properties, nanomaterials have found wide applications in electrocatalysis. For these reasons, artificial enzymes developed on nano scaffolds are gaining increasing application in biosensing, biomolecular screening, bioanalysis, and diagnostics. A great deal of useful information on the history, definition, characterization, synthesis, functions, and applications of nanozymes can be found in the review article of Wei et al. (Wei and Wang 2013), and several other related publications (Wu et al. 2019; Huang et al. 2019; Jiang et al. 2019; Gao et al. 2020; Sun et al. 2018; Singh 2016; Kuah et al. 2016). This section provides a concise discussion regarding recent developments on the use of nanozymes in electrode modification for biomolecular screening and analysis.

2.2 Nanozymes Classifications and Mechanisms of Action

Nanozymes may be classified based on different criteria. However, a popular criterion for classifying nanozymes is the catalytic reaction mechanism. Nanozymes are classified into two families, namely oxidoreductase and hydrolase (Huang et al. 2019). The former catalyzes oxidation reactions, while the latter catalyzes hydrolysis reactions. Oxidase and peroxidase types of oxidoreductase nanozymes are mostly utilized for electrochemical sensors (Mahmudunnabi et al. 2020). Nanozymes can be further grouped as antioxidants and pro-oxidants, according to their radical scavenging ability (Mahmudunnabi et al. 2020; Singh 2019). In this regard, antioxidant nanozymes scavenge free radicals, while pro-oxidant nanozymes produce free radicals and hence induce oxidative stress (Mahmudunnabi et al. 2020, Singh 2019). Peroxidase and oxidase whose catalytic activities result in the formation of free radicals are considered to be pro-oxidants (Singh 2019). Extended classifications of nanozymes are shown in Fig. 22.1 as extracted from the recent review article by Mahmudunnabi et al. (Mahmudunnabi et al. 2020).

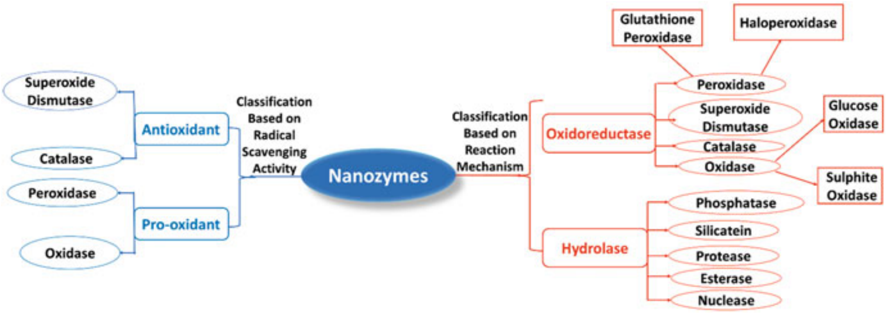
Glutathione Peroxidase
Haloperoxidase
Superoxide Dismutase
Classification Based on Radical Scavenging Activity
Antioxidant
Catalase
Peroxidase
Pro-oxidant
Oxidase
Nanozymes
Classification Based on Reaction Mechanism
Oxidoreductase
Peroxidase
Superoxide Dismutase
Catalase
Oxidase
Glucose Oxidase
Sulphite Oxidase
Hydrolase
Phosphatase
Silicatein
Protease
Esterase
Nuclease

Fig. 22.1 Extensive classification of nanozymes according to reaction mechanism and radical scavenging activity (Huang et al. 2019; Mahmudunnabi et al. 2020; Singh 2019; Rahal et al. 2014)

2.3 Nanomaterials in Nanozyme-Based Sensors

Several nanomaterials have been utilized in the development of nanozyme-based sensors. These include metal oxides such as ZrO_2 [39], NiO (Khairy et al. 2018), and TiO_2 (Qiu et al. 2019). Other nanomaterials previously used for making nanozyme-based biosensors include gold nanoparticles (AuNPs) (Gugoasa et al. 2021), ferromagnetic nanoparticles (Fe_3O_4 NPs) (Gao et al. 2007), and copper nanoclusters (CuNCs) (Goswami et al. 2011). A selected list of nanozymes used for colorimetric detection and quantitative assays of microbes and related analytes in some food samples are presented in Wang and Gunasekaran (2020). Some other nanozymes used in previous studies for the detection of parathion, methyl parathion, isoniazid, acetaminophen, glucose, nifedipine, and atenolol are presented in Table 22.1.

3 Applications of Nano Enzymes in Disease Control

3.1 Environmental and Food Monitoring

Quality control in the food industry is very important for consumer health. Failure to detect either pathogens or certain chemicals may pose a public health risk – in the worst-case scenario, globally. Nanozymes are capable of catalyzing reactions involving chromogenic substrates in trace amounts to yield chromogenic products, which are vital in environmental and food monitoring (Xiang et al. 2021). Xiang et al. fabricated a nanozyme with peroxidase-like enzyme properties using platinum nanoparticles embedded on a silica base (Xiang et al. 2021). In their findings, using 3,3′,5,5′-tetramethylbenzidine (TMB) as a substrate, the nanozyme proved to be highly sensitive to trace amounts of Hg^{2+}, which resulted in the color change of TMB. Quantitative analysis of Hg^{2+} was directly related to the color change of TMB (Xiang et al. 2021). This research can be directly applied to food and environmental monitoring, specifically for the detection and/or monitoring of mercury ions. In another study, Zhang and co-workers (Zhang et al. 2021) synthesized a nanozyme for use in detecting food allergens. Both of these studies are not only important in preventing health hazards but pave the way to identifying other analytes as well.

3.2 Cancer Diagnosis

Diagnosis of cancer in the early stages is of paramount importance to patient treatment. When diagnosed early, most cancers can be treated effectively, and the individual may once again live a cancer-free life. Feng and research group (Feng et al. 2021) fabricated an electrochemical biosensor for Glypican-3 (GPC3), a prominent biomarker for hepatocellular carcinoma (HCC). Their work utilized copper oxide-reduction graphene oxide nanocomposites to obtain a peroxidase-like nanozyme which reacts with the GPC3 aptamer, resulting in a signal. The GPC3 antibody reacts with the probe to form an “antibody-antigen-aptamer,” which

Table 22.1 A list of some selected nanozymes used in previous studies

Nanozyme	Analyte(s)	Analysis technique	Real sample used	Linear range (μM)	LOD (μM)	Ref
NiO/SPE	Parathion	DPV	Urine	0.1–30	0.024	Khairy et al. (2018)
MgO/SPE	Nifedipine Atenolol	DPV	Urine	0.2–104.41 6.66–909.09	0.032 1.76	Khairy et al. (2017)
BiO/SPE	Acetaminophen Isoniazid	DPV	Human serum	0.5–1250 5–1760	30 1.85	Khairy et al. (2017)
CuO/SPE	Glucose	Amperometry	Human blood and urine	50–3000	10	Mahmoud et al. (2016)
ZnO/EGR/GCE	Acetaminophen	SWV	Human serum	10^{-4}–20	3.3×10^{-5}	Jiang et al. (2014)
Fe_3O_4/PDDA/GR/GCE	Acetaminophen	DPV	Urine and blood serum	0.1–100	3.7×10^{-2}	Lu et al. (2012)
AuNP–MWCNT/GCE	Isoniazid	LSSV	Blood serum	0.2–10	0.0003	Wu et al. (2015)
ZrO_2/CPE	Methyl parathion	SWV	Water	0.019–11.40	0.007	Parham and Rahbar (2010)
MWCNT–PAAM/GCE	Methyl parathion	DPV	Water	0.005.0–10	0.002	Zeng et al. (2012)
TiO_2	Parathion	DPV	Cucumber and cabbage	0.05–10	0.01	Li et al. (2006)

catalyzes the reaction between H_2O_2 and $AgNO_3$. Differential Pulse Voltammetry (DPV) is then used to detect and record the signal emanating from this reaction (Feng et al. 2021). This work is very useful in cancer diagnosis and monitoring those undergoing cancer treatment.

3.3 Cancer Therapy

Although nanozymes are important in disease diagnosis, they also play an important role in drug delivery, with cancer being one of the standout diseases where nanozymes are used in therapy. Research presented by Wang and co-workers (Wang et al. 2020) showed a hydrophobic SPIO and IR780 encapsulated in an amphiphilic macromolecule. The resulting theranostic system was a nanoenzyme with phototherapeutic results for triple-negative breast cancer. Of key note was the absence of notable side effects (Wang et al. 2020). In another study (Mei et al. 2020), a nanoenzyme based on natural glucose oxidase integrated on CoFe-layered double hydroxides monolayer nanosheets was fabricated for treating cancer. In the presence of tumor cells, the nanozyme triggers hydroxyl radicals with anti-tumor properties. This research has been proved to be effective both in vitro and in vivo, and paves the way to effective chemotherapy with minimal side effects (Mei et al. 2020).

3.4 Bacteria Detection

Bacteria is one of the most common pathogens. In many instances, glucose metabolism is used to evaluate the presence of bacteria. When exposed to glucose, bacteria can perform glycolysis and the remaining glucose can be used to predict bacterial load. Qiu et al. fabricated glucose oxidase-encapsulated Zn/Co-infinite coordination polymer-based nanozyme (Qiu et al. 2021). The nanozyme was applied for the colorimetric detection of glucose to monitor bacterial viability. Their findings highlighted accurate, rapid detection and usability of the nanozyme across different species of bacteria, both gram-negative and gram-positive (Qiu et al. 2021). In another study (Xue et al. 2021), a biosensor was fabricated for rapid and selective detection of salmonella. MnO2 nanoflowers were used to amplify the signal. For convenience, a smartphone application can be used to determine the concentration of salmonella in a given sample (Xue et al. 2021). This research enables real-time assessment and evaluation of salmonella-related risks.

3.5 Nanoenzmyes in Covid-19 Diagnosis

In early 2020, Covid-19 was declared a global pandemic. Covid-19 is associated with high infection and fatality rates. Rapid detection of SARS-CoV-2 (the virus that causes Covid-19) in various platforms such as work environments and immigration control points has become mandatory. Scientists across the globe have since embarked on a mission to design accurate rapid test kits. For example, Liang et al. (Liang et al. 2021) have since developed a biosensor that utilizes a smartphone-based nanoenzyme for detecting SARS-CoV-2 nucleocapsid protein. Disposable immunochromatography assay and optical sensors are used as the reaction and signal detection devices respectively. This device fabricated by Liang et al. was proved to be very sensitive and accurate in detecting the coronavirus in trace amounts (Liang et al. 2021).

Another study (Liu et al. 2021) fabricated a peroxidase-like nanozyme that enables point of care (POC) antigen tests for screening SARS-CoV-2 infections. Their device exhibited high specificity to SARS-CoV-2 antigen with no cross-reaction with other coronaviruses. When compared to nucleic acid tests, less time was required to give reliable results (Liu et al. 2021). As part of advanced detection methods, Mahapatra et al. emphasizethe use of diagnostic methods such as label-free biosensors, electrical transducer-based detection approaches, and plasmonic biosensing methods, further demonstrating the wide application range and importance of biosensors (Mahapatra et al. 2020). Rapid detection of SARS-CoV-2 can help the entire world to fight the Covid-19 pandemic.

4 Current Trends in Nanomaterials-Based Electrochemical Sensors

The accomplishment of the glucose immunoassay sensor technology has increased the need to develop rapid electrochemical nano-biosensors as diagnostic medical devices that can have extensive impact and application in human disease detection and prevention (Idili et al. 2019; Ligler and Gooding 2019; Jiang et al. 2020; Vermisoglou et al. 2020). According to Das and colleagues (Das et al. 2021), the point of care (POC) diagnostic technique, which follows the World Health Organization's"ASSURED (Affordable, Sensitive, Specific, User-friendly, Rapid and Robust, Equipment-free, Delivered)" criteria, is the gold standard for medical biosensor and bioassay development. The point of care biosensor technology is developed on natural enzyme reusability, efficiency, bioactivity, and portability. However, major limitations in these designs include large expenses, interference, and poor immobilization, causing a lack of stability and activity. Recently, nanotechnology-based modifications have been used to improve the stability of sensing devices (Li et al. 2019; Meng et al. 2020). Advances in the stability of sensor design include the development of wearable, water-resistant, durable, and pliable sensors composed of "rubber-like" complexes, hydrogels, organo-gels, and polymers (Li et al. 2019; Ferrag and Kerman 2020; Meng et al. 2020). Nano-biosensors are based on carbon-, metal oxide-, and metal-based nanomaterials, with gold nanoparticles, graphene, carbon nanotubes, and photonic crystals being the main types of nanomaterials fabricated due to their versatility (Cavalcante et al. 2021; Kuralay 2019). These surfaces are prevalent due to being stable and biocompatible and having effective electron-transfer kinetics (Ferrag and Kerman 2020); however, the basic surfaces lack the specificity (sensitive and selective) for the electrochemical

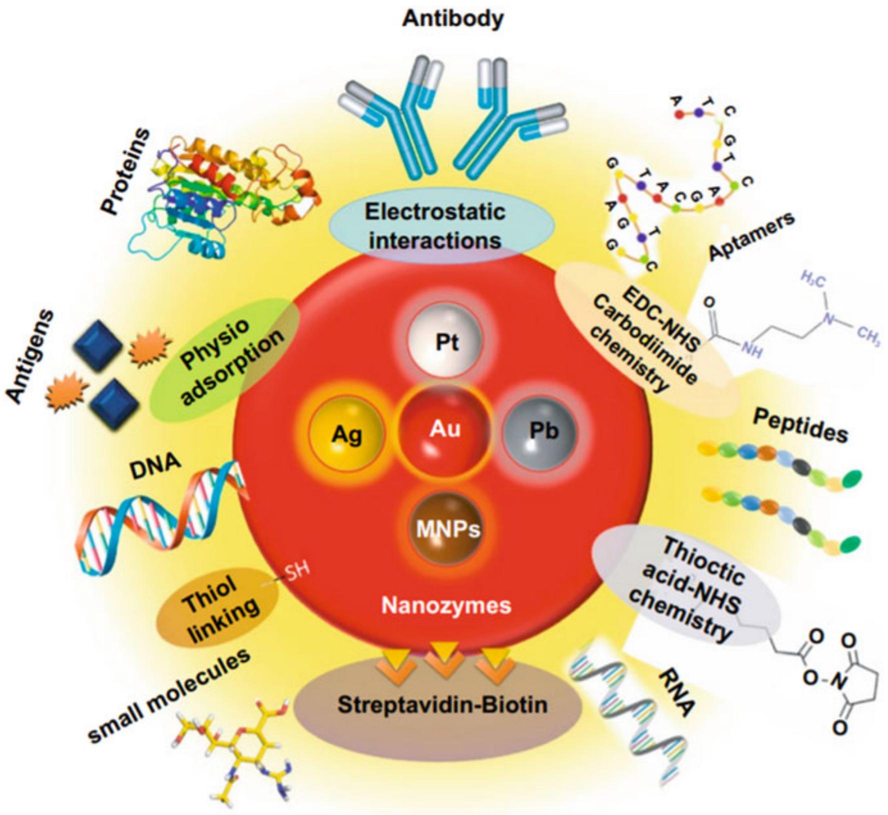
Antibody
Electrostatic interactions
Proteins
Aptamers
EDC-NHS Carbodiimide chemistry
Antigens
Physio adsorption
Pt
Ag
Au
Pb
MNPs
Nanozymes
Peptides
DNA
Thiol linking
SH
Thioctic acid-NHS chemistry
small molecules
Streptavidin-Biotin
RNA

Fig. 22.2 Conjugation chemistry for the surface modification of "nanozymes" (nanoenzymes) with several biorecognition ligands; reprinted with permission from Das et al. (2021)

recognition of trace analytes. Alternatives to overcome these restrictions include the incorporation of specific electro-chemical nano-biosensors into the enzymatic sensing mechanism (Vigneshvar and Senthilkumaran 2018). Biorecognition compounds, such as antibodies (Su et al. 2017; Guo 2004), aptamers, antigens (Vigneshvar and Senthilkumaran 2018), and chemical linkers, are being coupled with nanoenzymes using conjugation chemistry for development (Das et al. 2021) (Fig. 22.2). These nanomaterial sensors are cost-effective and highly sensitive and mimic enzyme function that is dependent on effective electron transfer and good electrical current density (Das et al. 2021). The highly biocompatible matrix of nanoenzymes along with ease of surface modifications with varying biorecognition ligands through conjugation chemistry has provided a cheaper and accessible alternative to biosensors fabrication.

An example of an antibody nanoenzyme-based biosensor is the lateral flow assay for pathogenic *Escherichia coli* detection developed by Han et al. (2018). This fabrication was built on the sandwich immune-assay principle, encompassing a spherical palladium–platinum (Pd–Pt) nanozyme, which was adapted with an anti-*E. coli* monoclonal antibody (mAb) as a detection probe. The conjugated nanozyme–mAb was prepared cost-effectively without using expensive materials and organic linking counterparts. *E. coli* signal amplification occurred through the peroxidase-like activity of Pd–Pt nanoparticles (Han et al. 2018). Similarly, Cheng and colleagues (Cheng et al. 2017) used conjugation chemistry in a dual lateral flow immunoassay (LFIA) combined with a smartphone device to detect pathogenic *Salmonella* and *E. coli* bacteria. This application was based on the signal amplifier of mesoporous core-shell palladium–platinum (Pd–Pt) nanoparticle that elevated peroxidase-like activity and resulted in a highly sensitive dual LFIA device in detecting the pathogens.

Nanoenzyme-based electrochemical sensors are stable under extreme physiological environments and cost-effective in large-scale production, and the large surface to volume ratio enables appropriate surface modifications and conjugations (Das et al. 2021). The application of POC biosensing nanoenzymes has progressed in signal transductions based on the profile, size, and properties, including compatibility, conductivity, and fluorescence.

5 Conclusions

This chapter summarizes various applications of nanozymes in electrochemical devices and other biochemical applications. Emphasis is more central to the use of nanozymes in disease detection and monitoring. Through techniques such as colorimetry, voltammetry, and impedance, nanozymes enable accurate and rapid detection of various substrates which can be interpreted to indicate the presence or absence of the disease in question. Most recently, during the Covid-19 pandemic, nanozymes have been integrated on various electrode types to help fight the pandemic through rapid POC diagnosis. The advantages of nanozymes are their low cost, high sensitivity, wide range of applications, and high stability. In many instances, a single nanozyme can be used to detect multiple analytes, a property which is not available with natural enzymes. This also enables multiple biomarkers to be used where applicable.

Acknowledgements The authors would like to acknowledge funding from the Faculty of Science: University of Johannesburg: Centre for Nanomaterials Science Research, Department of Chemical Sciences, and the National Research Foundation (Grant Number:TTK170405225933) South Africa.

References

Arcus VL, Prentice EJ, Hobbs JK, Mulholland AJ, Van Der Kamp MW, Pudney CR, Parker EJ, Schipper LA (2016) On the temperature dependence of enzyme-catalyzed rates. Biochemistry 55(12):1681–1688

Bage N, Kar P (2021) Ultrasensitive electrochemical sensing of biotin-Avidin interaction on gold electrode bio-conjugated with silver nanoparticles. IEEE Sensors J 21(9):10400–10408

Blanco A, Blanco G (2017) Medical biochemistry. Academic Press

Bornscheuer UT, Huisman G, Kazlauskas R, Lutz S, Moore J, Robins K (2012) Engineering the third wave of biocatalysis. Nature 485(7397):185–194

Breslow R, Overman LE (1970) " artificial enzyme" combining a metal catalytic group and a hydrophobic binding cavity. J Am Chem Soc 92(4):1075–1077

Brynskikh AM, Zhao Y, Mosley RL, Li S, Boska MD, Klyachko NL, Kabanov AV, Gendelman HE, Batrakova EV (2010) Macrophage delivery of therapeutic nanozymes in a murine model of Parkinson's disease. Nanomedicine 5(3):379–396

Cavalcante FTT, de A Falcão IR, da S Souza JE, Rocha TG, De Sousa IG, Cavalcante ALG, De Oliveira ALB, De Sousa MCM, Dos Santos JCS (2021) Designing of nanomaterials-based enzymatic biosensors: synthesis, properties, and applications. Electrochemistry 2(1):149–184

Chatterjee B, Das SJ, Anand A, Sharma TK (2020) Nanozymes and aptamer-based biosensing. Mater Sci Technol 3:127–135

Cheng H, Zhang L, He J, Guo W, Zhou Z, Zhang X, Nie S, Wei H (2016) Integrated nanozymes with nanoscale proximity for in vivo neurochemical monitoring in living brains. Anal Chem 88(10):5489–5497

Cheng N, Song Y, Zeinhom MM, Chang Y-C, Sheng L, Li H, Du D, Li L, Zhu M-J, Luo Y (2017) Nanozyme-mediated dual immunoassay integrated with smartphone for use in simultaneous detection of pathogens. ACS Appl Mater Interfaces 9(46):40671–40680

Cooper GM (2000) The central role of enzymes as biological catalysts. Sinauer Associates

Das B, Franco JL, Logan N, Balasubramanian P, Kim MI, Cao C (2021) Nanozymes in point-of-care diagnosis: an emerging futuristic approach for biosensing. Nano-Micro Lett 13(1):1–51

Dos Santos GP, Da Silva BF, Garrido SS, Mascini M, Yamanaka H (2014) Design, synthesis and characterization of a hexapeptide bio-inspired by acetylcholinesterase and its interaction with pesticide dichlorvos. Analyst 139(1):273–279

Feng L, Dong Z, Liang C, Chen M, Tao D, Cheng L, Yang K, Liu Z (2018) Iridium nanocrystals encapsulated liposomes as near-infrared light controllable nanozymes for enhanced cancer radiotherapy. Biomaterials 181:81–91

Feng H, Bao M, Lian M, Li G (2021. IOP Publishing) Glypican-3 electrochemical aptasensor based on CuO-rGO nanocomposite. J Phys Conf Ser 2009:012071

Ferrag C, Kerman K (2020) Grand challenges in nanomaterial-based electrochemical sensors. Front Sens 1(5):1–4. https://doi.org/10.3389/fsens.2020.583822

Gao L, Zhuang J, Nie L, Zhang J, Zhang Y, Gu N, Wang T, Feng J, Yang D, Perrett S (2007) Intrinsic peroxidase-like activity of ferromagnetic nanoparticles. Nat Nanotechnol 2(9):577–583

Gao L, Fan K, Yan X (2020) Iron oxide nanozyme: a multifunctional enzyme mimetics for biomedical application. Nano:105. https://doi.org/10.1007/978-981-15-1490-6_5

Goswami N, Giri A, Bootharaju M, Xavier PL, Pradeep T, Pal SK (2011) Copper quantum clusters in protein matrix: potential sensor of Pb^{2+} ion. Anal Chem 83(24):9676–9680

Gugoasa LAD, Pogacean F, Kurbanoglu S, Barbu-Tudoran L, Serban A, Kacso I, Pruneanu S (2021) Graphene-gold nanoparticles Nanozyme-based electrochemical sensor with enhanced laccase-like activity for determination of phenolic substrates. J Electrochem Soc 168:067523

Guo LJ (2004) Recent progress in nanoimprint technology and its applications. J Phys D Appl Phys 37(11):R123

Han J, Zhang L, Hu L, Xing K, Lu X, Huang Y, Zhang J, Lai W, Chen T (2018) Nanozyme-based lateral flow assay for the sensitive detection of Escherichia coli O157: H7 in milk. J Dairy Sci 101(7):5770–5779

Hasanzadeh M, Shadjou N (2016) Pharmacogenomic study using bio-and nanobioelectrochemistry: drug–DNA interaction. Mater Sci Eng C 61:1002–1017

Hu M, Korschelt K, Daniel P, Landfester K, Tremel W, Bannwarth MB (2017) Fibrous nanozyme dressings with catalase-like activity for H_2O_2 reduction to promote wound healing. ACS Appl Mater Interfaces 9(43):38024–38031

Huang Y, Ren J, Qu X (2019) Nanozymes: classification, catalytic mechanisms, activity regulation, and applications. Chem Rev 119(6):4357–4412

Idili A, Arroyo-Currás N, Ploense KL, Csordas AT, Kuwahara M, Kippin TE, Plaxco KW (2019) Seconds-resolved pharmacokinetic measurements of the chemotherapeutic irinotecan in situ in the living body. Chem Sci 10(35):8164–8170

Jiang L, Gu S, Ding Y, Jiang F, Zhang Z (2014) Facile and novel electrochemical preparation of a graphene–transition metal oxide nanocomposite for ultrasensitive electrochemical sensing of acetaminophen and phenacetin. Nanoscale 6(1):207–214

Jiang J, He C, Wang S, Jiang H, Li J, Li L (2018) Recyclable ferromagnetic chitosan nanozyme for decomposing phenol. Carbohydr Polym 198:348–353

Jiang D, Ni D, Rosenkrans ZT, Huang P, Yan X, Cai W (2019) Nanozyme: new horizons for responsive biomedical applications. Chem Soc Rev 48(14):3683–3704

Jiang Z, Feng B, Xu J, Qing T, Zhang P, Qing Z (2020) Graphene biosensors for bacterial and viral pathogens. Biosens Bioelectron 166:112471–112471

Khairy M, Khorshed AA, Rashwan FA, Salah GA, Abdel-Wadood HM, Banks CE (2017) Simultaneous voltammetric determination of antihypertensive drugs nifedipine and atenolol utilizing MgO nanoplatelet modified screen-printed electrodes in pharmaceuticals and human fluids. Sensors Actuators B Chem 252:1045–1054

Khairy M, Ayoub HA, Banks CE (2018) Non-enzymatic electrochemical platform for parathion pesticide sensing based on nanometer-sized nickel oxide modified screen-printed electrodes. Food Chem 255:104–111

Kuah E, Toh S, Yee J, Ma Q, Gao Z (2016) Enzyme mimics: advances and applications. Chem Eur J 22(25):8404–8430

Kuralay F (2019) Chapter 12 - nanomaterials-based enzyme biosensors for electrochemical applications: recent trends and future prospects. In: Ozkan SA, Shah A (eds) New developments in nanosensors for pharmaceutical analysis. Academic Press

Lei C-X, Hu S-Q, Shen G-L, Yu R-Q (2003) Immobilization of horseradish peroxidase to a nano-au monolayer modified chitosan-entrapped carbon paste electrode for the detection of hydrogen peroxide. Talanta 59(5):981–988

Lei CX, Wang H, Shen GL, Yu RQ (2004) Immobilization of enzymes on the nano-au film modified glassy carbon electrode for the determination of hydrogen peroxide and glucose. Electroanalysis 16(9):736–740

Li C, Wang C, Wang C, Hu S (2006) Development of a parathion sensor based on molecularly imprinted nano-TiO_2 self-assembled film electrode. Sensors Actuators B Chem 117(1):166–171

Li T, Li Y, Zhang T (2019) Materials, structures, and functions for flexible and stretchable biomimetic sensors. Acc Chem Res 52(2):288–296

Liang C, Liu B, Li J, Lu J, Zhang E, Deng Q, Zhang L, Chen R, Fu Y, Li C (2021) A nanoenzyme linked immunochromatographic sensor for rapid and quantitative detection of SARS-CoV-2 nucleocapsid protein in human blood. Sensors Actuators B Chem 349:130718

Ligler FS, Gooding JJ (2019) Lighting up biosensors: now and the decade to come. Anal Chem 91(14):8732–8738

Liu Z-M, Yang Y, Wang H, Liu Y-L, Shen G-L, Yu R-Q (2005) A hydrogen peroxide biosensor based on nano-au/PAMAM dendrimer/cystamine modified gold electrode. Sensors Actuators B Chem 106(1):394–400

Liu D, Ju C, Han C, Shi R, Chen X, Duan D, Yan J, Yan X (2021) Nanozyme chemiluminescence paper test for rapid and sensitive detection of SARS-CoV-2 antigen. Biosens Bioelectron 173:112817

Lu D, Zhang Y, Wang L, Lin S, Wang C, Chen X (2012) Sensitive detection of acetaminophen based on Fe_3O_4 nanoparticles-coated poly(diallyldimethylammonium chloride)-functionalized graphene nanocomposite film. Talanta 88:181–186

Mahapatra S, Baranwal A, Purohit B, Roy S, Mahto SK, Chandra P (2020) Advanced biosensing methodologies for ultrasensitive detection of human coronaviruses. In: Chandra P, Roy S (eds) Diagnostic strategies for COVID-19 and other coronaviruses. Singapore, Springer Singapore

Mahato K, Kumar S, Srivastava A, Maurya PK, Singh R, Chandra P (2018) Electrochemical immunosensors: fundamentals and applications in clinical diagnostics. In: Handbook of immunoassay technologies. Elsevier

Mahmoud BG, Khairy M, Rashwan FA, Foster CW, Banks CE (2016) Self-assembly of porous copper oxide hierarchical nanostructures for selective determinations of glucose and ascorbic acid. RSC Adv 6(18):14474–14482

Mahmudunnabi RG, Farhana FZ, Kashaninejad N, Firoz SH, Shim Y-B, Shiddiky MJ (2020) Nanozyme-based electrochemical biosensors for disease biomarker detection. Analyst 145(13):4398–4420

Manea F, Houillon FB, Pasquato L, Scrimin P (2004) Nanozymes: gold-nanoparticle-based transphosphorylation catalysts. Angew Chem 116(45):6291–6295

Mei X, Hu T, Wang H, Liang R, Bu W, Wei M (2020) Highly dispersed nano-enzyme triggered intracellular catalytic reaction toward cancer specific therapy. Biomaterials 258:120257

Meng L, Turner AP, Mak WC (2020) Soft and flexible material-based affinity sensors. Biotechnol Adv 39:107398

Murphy L (2006) Biosensors and bioelectrochemistry. Curr Opin Chem Biol 10(2):177–184

Parham H, Rahbar N (2010) Square wave voltammetric determination of methyl parathion using ZrO2-nanoparticles modified carbon paste electrode. J Hazard Mater 177(1–3):1077–1084

Parsaee Z, Karachi N, Abrishamifar SM, Kahkha MRR, Razavi R (2018) Silver-choline chloride modified graphene oxide: novel nano-bioelectrochemical sensor for celecoxib detection and CCD-RSM model. Ultrason Sonochem 45:106–115

Peterson ME, Daniel RM, Danson MJ, Eisenthal R (2007) The dependence of enzyme activity on temperature: determination and validation of parameters. Biochem J 402(2):331–337

Qiu L, Lv P, Zhao C, Feng X, Fang G, Liu J, Wang S (2019) Electrochemical detection of organophosphorus pesticides based on amino acids conjugated nanoenzyme modified electrodes. Sensors Actuators B Chem 286:386–393

Qiu P, Yuan P, Deng Z, Su Z, Bai Y, He J (2021) One-pot facile synthesis of enzyme-encapsulated Zn/co-infinite coordination polymer nanospheres as a biocatalytic cascade platform for colorimetric monitoring of bacteria viability. Microchim Acta 188(10):322

Rahal A, Kumar A, Singh V, Yadav B, Tiwari R, Chakraborty S, Dhama K (2014) Oxidative stress, prooxidants, and antioxidants: the interplay. Biomed Res Int 2014:761264

Ranadheera CS, Prasanna PHP, Vidanarachchi JK, Mcconchie R, Naumovski N, Mellor D (2017) Chapter 12 – Nanotechnology in microbial food safety. In: Oprea AE, Grumezescu AM (eds) Nanotechnology applications in food. Academic Press

Ruff A (2017) Redox polymers in bioelectrochemistry: common playgrounds and novel concepts. Curr Opin Electrochem 5(1):66–73

Shanbhag MM, Ilager D, Mahapatra S, Shetti NP, Chandra P (2021) Amberlite XAD-4 based electrochemical sensor for diclofenac detection in urine and commercial tablets. Mater Chem Phys 273:125044

Sims CM, Hanna SK, Heller DA, Horoszko CP, Johnson ME, Montoro Bustos AR, Reipa V, Riley KR, Nelson BC (2017) Redox-active nanomaterials for nanomedicine applications. *Nanoscale* 9(40):15226–15251

Singh S (2016) Cerium oxide based nanozymes: redox phenomenon at biointerfaces. Biointerphases 11(4):04B202

Singh S (2019) Nanomaterials exhibiting enzyme-like properties (Nanozymes): current advances and future perspectives. Front Chem 7:46

Singh AP, Balayan S, Hooda V, Sarin R, Chauhan N (2020) Nano-interface driven electrochemical sensor for pesticides detection based on the acetylcholinesterase enzyme inhibition. Int J Biol Macromol 164:3943–3952

Solanki S, Pandey CM, Gupta RK, Malhotra BD (2021) Chapter 3 – Nanobioelectrochemistry: fundamentals and biosensor applications. In: Wain AJ, Dickinson EJF (eds) Frontiers of nanoscience. Elsevier

Su H, Li S, Jin Y, Xian Z, Yang D, Zhou W, Mangaran F, Leung F, Sithamparanathan G, Kerman K (2017) Nanomaterial-based biosensors for biological detections. Adv Health Care Technol 3: 19–29

Sun H, Zhou Y, Ren J, Qu X (2018) Carbon nanozymes: enzymatic properties, catalytic mechanism, and applications. Angew Chem Int Ed 57(30):9224–9237

Thage RL, Semegni Y, Naidoo S (2020) Computer-aided: modelled sustainable hybrid catalysts for a Nano-drug delivery system. S Afr J Chem 73:103–110

Vermisoglou E, Panáček D, Jayaramulu K, Pykal M, Frébort I, Kolář M, Hajdúch M, Zbořil R, Otyepka M (2020) Human virus detection with graphene-based materials. Biosens Bioelectron 166:112436

Vigneshvar S, Senthilkumaran B (2018) Current technological trends in biosensors, nanoparticle devices and biolabels: hi-tech network sensing applications. Med Dev Sens 1(2):e10011

Wang W, Gunasekaran S (2020) Nanozymes-based biosensors for food quality and safety. TrAC Trends Anal Chem 126:115841

Wang L, Miao L, Yang H, Yu J, Xie Y, Xu L, Song Y (2017) A novel nanoenzyme based on Fe3O4 nanoparticles@thionine-imprinted polydopamine for electrochemical biosensing. Sensors Actuators B Chem 253:108–114

Wang H, Wan K, Shi X (2019) Recent advances in nanozyme research. Adv Mater 31(45):1805368

Wang S, Mao J, Liu H, Huang S, Cai J, Gui W, Wu J, Xu J, Shen J, Wang Z (2020) pH-sensitive nanotheranostics for dual-modality imaging guided nanoenzyme catalysis therapy and phototherapy. J Mater Chem B 8(22):4859–4869

Wei H, Wang E (2008) Fe_3O_4 magnetic nanoparticles as peroxidase mimetics and their applications in H_2O_2 and glucose detection. Anal Chem 80(6):2250–2254

Wei H, Wang E (2013) Nanomaterials with enzyme-like characteristics (nanozymes): next-generation artificial enzymes. Chem Soc Rev 42(14):6060–6093

Wei H, Gao L, Fan K, Liu J, He J, Qu X, Dong S, Wang E, Yan X (2021) Nanozymes: A clear definition with fuzzy edges. Nano Today 40:101269

Wu B, Hou L, Zhang T, Han Y, Kong C (2015) A molecularly imprinted electrochemical sensor based on a gold nanoparticle/carbon nanotube hybrid material for the sensitive detection of isoniazid. Anal Methods 7(21):9121–9129

Wu J, Wang X, Wang Q, Lou Z, Li S, Zhu Y, Qin L, Wei H (2019) Nanomaterials with enzyme-like characteristics (nanozymes): next-generation artificial enzymes (II). Chem Soc Rev 48(4): 1004–1076

Xiang K, Chen G, Nie A, Wang W, Han H (2021) Silica-based nanoenzymes for rapid and ultrasensitive detection of mercury ions. Sensors Actuators B Chem 330:129304

Xue L, Jin N, Guo R, Wang S, Qi W, Liu Y, Li Y, Lin J (2021) Microfluidic colorimetric biosensors based on MnO_2 nanozymes and convergence – divergence spiral micromixers for rapid and sensitive detection of salmonella. ACS Sens 6(8):2883–2892

Yan Q, Zhi N, Yang L, Xu G, Feng Q, Zhang Q, Sun S (2020) A highly sensitive uric acid electrochemical biosensor based on a nano-cube cuprous oxide/ferrocene/uricase modified glassy carbon electrode. Sci Rep 10(1):1–10

Ye Y, Xiao L, He B, Zhang Q, Nie T, Yang X, Wu D, Cheng H, Li P, Wang Q (2017) Oxygen-tuned nanozyme polymerization for the preparation of hydrogels with printable and antibacterial properties. J Mater Chem B 5(7):1518–1524

Yu Z, Lou R, Pan W, Li N, Tang B (2020) Nanoenzymes in disease diagnosis and therapy. Chem Commun 56:15513

Zeng Y, Yu D, Yu Y, Zhou T, Shi G (2012) Differential pulse voltammetric determination of methyl parathion based on multiwalled carbon nanotubes-poly(acrylamide) nanocomposite film modified electrode. J Hazard Mater 217-218:315–322

Zhang X, Li G, Liu J, Su Z (2021) Bio-inspired Nanoenzyme synthesis and its application in A portable immunoassay for food allergy proteins. J Agric Food Chem 69:14751

Zheng Q, Yu Y, Fan K, Ji F, Wu J, Ying Y (2016) A nano-silver enzyme electrode for organophosphorus pesticide detection. Anal Bioanal Chem 408(21):5819–5827

Engineered Two-Dimensional Materials-Based Smart Biosensors for Point-of-Care Diagnosis

23

Kempahanumakkagaari Surehkumar, K. Manjunath,
Alamelu K. Ramasami, and Thippeswamy Ramakrishnappa

Contents

1 Introduction 500
2 Synthetic Protocols of 2D Materials for Biosensor Applications 502
  2.1 Synthesis of Graphene 502
  2.2 Synthesis of Carboxyl-Functionalized GO Sheets 502
  2.3 Synthesis of GO and GO-AuNP Nanocomposites 503
  2.4 Synthesis of MoS_2 503
  2.5 Synthesis of MoO_3 504
3 Preparation of MXenes 504
  3.1 Preparation of $Ti_3C_2T_x$ MXene 504
  3.2 Preparation of Au/MXene Composite 504
4 Smart-Based Biosensors for Point-of-Care Diagnosis 505
  4.1 Graphene-Based Biosensing Platforms 506
  4.2 MoS_2-Based Biosensing Platforms 507
  4.3 Other 2D Materials as Biosensing Platforms 509
5 Future Prospective 509
References 512

Abstract

After the isolation of freestanding graphene from graphite in 2004, there has been a dramatic craze for two-dimensional (2D) materials among researchers. This may be due to their extensive utilization in various applications, ranging from

---

K. Surehkumar · T. Ramakrishnappa (✉)
Department of Chemistry, BMS Institute of Technology and Management, Bengaluru, Karnataka, India
e-mail: t.ramakrishnappa@bmsit.in

K. Manjunath
Centre for Nano and Soft Matter Sciences (CeNS), Bangalore, Karnataka, India

A. K. Ramasami
Sri Sathya Sai University for Human Excellence, Kalaburagi, Karnataka, India

© Springer Nature Singapore Pte Ltd. 2023

U. P. Azad, P. Chandra (eds.), *Handbook of Nanobioelectrochemistry*,
https://doi.org/10.1007/978-981-19-9437-1_23

protective coatings to biosensors. The layered 2D materials possess tunable optical, electrical, mechanical, and electrochemical properties that enable them to be used in the fabrication of biosensors as well as point-of-care diagnostic tool kits. Furthermore, these 2D materials can be principal sensing elements or can be used as supporting materials during biosensor/point-of-care device/kit fabrication. The present chapter summarizes the methodologies and challenges that come across during the design and synthesis of these 2D materials, as well as studies their various sensing strategies like optical and electrochemical approaches. Furthermore, the use of fabricated biosensors/tool kits for real-time applications has been discussed. Finally, the future prospects of layered 2D materials in biosensor technology have been included.

Keywords

2D materials · Transition metal chalcogenides · Transition metal oxides · Graphene · Biosensors · Point-of-care diagnosis

1 Introduction

Two-dimensional (2D) materials have been extensively used as transducers or substrates of sensing platforms in biosensor systems (Coleman et al. 2011). The 2D materials include graphene and graphene-like structures, graphitic carbon nitrides (g-CNs), transition metal chalcogenides (TMDs), transition metal oxides (TMOs), MXenes, and hexagonal boron nitrides (h-BNs). The properties of the 2D materials are very different from their bulk counterparts, which triggered the scientific community to explore their utility in diverse applications. An interesting feature of 2D materials suited to use in biosensor technology is their larger surface areas with numerous active reaction sites. 2D materials exhibit a broad range of electrical properties, that is, some of them are metallic (graphene), semi-metallic (VS_2 and TaS_2), semiconducting (MoS_2 and WS_2), and insulating in nature (Bolotsky et al. 2019). Similarly, their optical properties are also diversified, like some of them quench fluorescence intensity and highly fluorescent (Balendhran et al. 2013; Chhowalla et al. 2013; Kurapati et al. 2016; Morales-Narváez and Merkoçi 2019). Furthermore, the surface properties of the 2D materials can be tuned through chemical functionalization or defect engineering so that these materials exhibit specific selectivity toward a particular analyte during sensing studies (Shao et al. 2010; Wang et al. 2010). The higher sensitivities exhibited by the 2D materials when used in sensing studies are due to their large surface-to-volume ratios and atomic thickness (Bolotsky et al. 2019). The above-mentioned features of 2D materials yield better surface adsorption properties, which are necessary for both optical and electrochemical sensing operations. The good adsorbent properties of the substrate or sensing material help in concentrating a more significant number of analytes on reacting surface from the bulk solution, resulting in increased sensitivity during electrochemical sensor systems. In addition, higher surface-to-volume ratios of the 2D materials result in a more significant number of analytes surface reactive sites with respect to the volume of the senor material (Varghese et al. 2015). This results in more significant electronic structural changes of the senor material. The modulation in the electronic structures of the sensor material results in enhancing the sensitivity and the limit of detection (LOD) when used in sensor applications (Varghese et al. 2015). Another interesting factor of 2D materials is their excellent surface area per gram (SAPG). The highest theoretical SAPG value of graphene is 2630 m^2/g (Bonaccorso et al. 2015). The SAPG values of 2D materials can be further increased by decreasing the number of layers in their structures through various exfoliation techniques. The SAPG value of h-BN has been increased from 10 to 140 m^2/g and 8.4 to 25,140 m^2/g in the case of the MoS_2 (Liu et al. 2017). The sensor materials with higher SAPG values and lower electrical noise can have lower detection levels in sensing applications.

As a continuation in the research of 2D materials, fascinating composites are reported utilizing defect engineering, doping with hetero atoms or compositing with various nanostructures (Lin et al. 2016; Ren et al. 2017; Zhang et al. 2017). The bandgap of the 2D materials can be modulated by changing their layer numbers, strain, and alloying with other substrates (Bertolazzi et al. 2011). The planar structure of 2D materials make them superior compared to other nanostructures like carbon nanotubes (CNTs) and Si nanowires with respect to compatibility while fabricating sensor systems and devices on a commercial scale using modern techniques (Bolotsky et al. 2019). The CNTs and Si nanowires have some significant differences in their length, diameter, and alignment, making challenging task while fabrication as sensor device using conventional techniques (Bolotsky et al. 2019). The ultrathin 2D materials have remarkable mechanical flexibility, making them to withstand 10% greater strains before rupturing, making them superior to other available best mechanically flexible materials (Bertolazzi et al. 2011). This attractive mechanical flexibility of the 2D materials allows them to fabricate robust sensor systems used in wearable or implantable diagnostic tool kits. The optical biosensors based on TMDs employing plasmonic emissions are found to exhibit 1000 times better response compared to the other methods based on metallic species like Au and Ag (Ouyang et al. 2017). The superior performance of TMDs over metallic elements is due to the longer plasmonic lifetimes of the former materials. Furthermore, the tunable optical properties of the 2D materials can be tuned by functionalization, applying strain or electric field (Ouyang et al. 2017). The optical properties of the materials can be tuned so that the materials can exhibit required absorptions at operational wavelengths (Ouyang et al. 2017). The structural features and related optical and electrical properties of 2D materials discussed in the above sections make them suitable candidates to use in sensor systems for fabricating biosensor devices and miscellaneous diagnostic tool kits. This chapter enumerates the design, synthesis of 2D materials, fabrication of biosensing platforms/diagnostic wearable or implantable test kits using synthesized materials and their applications in disease diagnosis and monitoring.

2 Synthetic Protocols of 2D Materials for Biosensor Applications

A two-dimensional material's synthetic methods play an essential role for various applications, including biosensors, energy storage, catalysis, and so on. Two different ways can obtain the 2D materials: (i) the bottom-up process and (ii) the top-down process, reported in the literature (Rao and Maitra 2015; Xu et al. 2013). Some of the synthetic methods are described here.

2.1 Synthesis of Graphene

To date, several synthetic methods were established to prepare graphene. For example, Geim and his coworkers discovered graphene sheets in 2004 via mechanical exfoliation of pyrolytic graphite using scotch tape, further called as "scotch tape method" (Geim 2009; Novoselov et al. 2004; Park and Ruoff 2009). However, it is still extensively being used in laboratories for the preparation of graphene.

Graphene can also prepare by heating silicon carbide (SiC) single crystals in the presence of a high vacuum or Ar atmosphere (Emtsev et al. 2009; Van Bommel et al. 1975). While heating the SiC, Si sublimates, and C remains on the surface because of the high Si vapor pressure compared to C, which forms graphene (de Heer et al. 2011). The formation of monolayer graphene needs the degradation of at least three layers of SiC (Van Bommel et al. 1975). In 1975, Van Bommel et al. has discovered this technique (Van Bommel et al. 1975). Later, Novoselov et al., and Berger et al. were also reported the preparation of graphene using SiC (Berger et al. 2004; Novoselov et al. 2004). The SiC surface orientation affects the graphene layers thickness; homogeneous, few-layer graphene is formed in Si (0001), but SiC (000$\bar{1}$) yields more disordered graphene layers. It is to be noted that vacuum pressure or temperature may result in different forms of carbon, such as carbon nanotubes (CNTs) and graphite (Cambaz et al. 2008). More recently, Chithaiah et al. developed a large-scale synthesis of rGO nanosheets by green and facile approach via thermal decomposition of glycine and sucrose at 475 °C (Chithaiah et al. 2020). First, reduced graphene oxide (rGO) was prepared by dissolving 2 g of sugar in a 100 mL beaker, then placed in the pre-heated muffle furnace at 475 ± 10 °C, which undergoes decomposition and produces a black foam in just a few min. Finally, the obtained product was used for further analysis.

2.2 Synthesis of Carboxyl-Functionalized GO Sheets

Carbonyl-functionalized GO sheets were prepared by the interaction of chloroacetic acid with graphene sheets in primary conditions. In this reaction, the epoxide(–O–), ester, and hydroxyl(–OH) groups were changed into carboxylic acid groups, forming covalently linked graphene oxide (GO–COOH), which leads to the formation of oxygenated groups in the basal planes and carboxyl groups at the edges (Okhrimenko et al. 2013; Subrahmanyam et al. 2008). Then GO–COOH sheets were subjected to ultrasonication in an aqueous solution (0.275 g/L, 10 mL) which exposed the hydrophilic functional groups, such as –COOH and –OH, on the basal planes of GO sheets shows the chemical structures on GO-COOH sheets.

2.3 Synthesis of GO and GO-AuNP Nanocomposites

During the process, GO (0.5 mg/mL, 20 mL) was subjected to ultrasonication in an aqueous solution for 2 h, then a 100 mL solution of $HAuCl_4 \cdot 3H_2O$ was added. The resultant mixture was stirred for about 30 min to get homogeneous dispersion of Au ions with GO. Next, the solution mixture was heated slowly to 80 °C and added 2 mL of $C_6H_5Na_3O_7 \cdot 2H_2O$ aqueous solution and continued the reaction with constant stirring for 4 h. Finally, centrifuged the resultant material at 6000 RPM for 2 h, and then washed with UPW to remove the excess AuNPs and obtained GO-AuNPs composite. The GO-AuNPs dispersed in UPW and placed in the refrigerator for further analysis (Khalil et al. 2019).

2.4 Synthesis of MoS_2

Several methods are available to prepare 2D MoS_2. Among these, exfoliations of MoS_2 thin layers from bulk 2H MoS_2 and vapor/liquid-phase deposition of MoS_2 on a substrate are familiar. Mechanical exfoliation processes are still being used extensively to prepare 2D MoS_2 using adhesion tapes, which helps develop field-effect biosensors. In addition, several vapor/gas-phase chemical deposition methods were established for the growth of 2D MoS_2 on a wafer scale which yields large dimensional MoS_2 sheets (Balendhran et al. 2012; Liu et al. 2012). The chemical deposition methods initially start with the formation of organic/inorganic precursors of 2D MoS_2 thin films, followed by sulfurization and annealing steps (Balendhran et al. 2012). The materials such as ammonium tetrathiomolybdate and molybdenum oxides have commonly been used as starting precursors (Liu et al. 2012). The sulfurization process is usually carried out at 500 °C or above using sulfur vapor or H_2S gas (Liu et al. 2012). The present scenario is to obtain homogeneous and high-quality wafer-scale 2D MoS_2 sheets for which the substrate crystallinity and other features play a vital role. Sapphire substrates yield good results, but Si/SiO_2 wafers and silica glass substrates have a high demand for developing biosensors (Sarkar et al. 2014; Wang et al. 2014; Zhu et al. 2013). Furthermore, liquid exfoliation techniques are more desirable to obtain 2D MoS_2 suspensions (Benavente et al. 2002; Chrimes et al. 2013). Lithium intercalation techniques are considered for high yield, but it is generally hazardous and needs a longer time (Benavente et al. 2002; Chrimes et al. 2013). Thus, microwave-assisted methods are developed to decrease the reaction time. High power sonication liquid exfoliation methods are also established to enhance the MoS_2 surface adhesion. Colman et al. have developed shear force effect-based liquid exfoliation methods using organic solvents or surfactants that can be readily used to suspend 2D MoS_2 organic solvents, which are compatible with biosensing applications (Coleman et al. 2011; O'Neill et al. 2012; Smith et al. 2011; Voiry et al. 2015).

2.5 Synthesis of MoO_3

The MoO_3 exfoliation method was obtained from the Yao et al. report (Yao et al. 2013). During the experimental process, 1 g of MoO_3 powder ground thoroughly in 1 mL acetonitrile for about 15 min. The homogeneous mixture was subjected to ultrasonication for 2 h in a 1:1 ratio of 40 mL ethanol/water mixture. The exfoliated MoO_3 nanoflakes were obtained by centrifugation of the suspension mixture at 4000 rpm for 30 min (Balendhran et al. 2013). Sreedhara et al. have synthesized ultrathin MoO_3 nanosheets of 1–3 bilayers by oxidation of few-layer MoS_2 nanosheets (Sreedhara et al. 2016).

3 Preparation of MXenes

3.1 Preparation of $Ti_3C_2T_x$ MXene

Titanium carbide sheets were prepared by the mechanical exfoliation of commercially purchased bulk Ti_3AlC_2. Initially, during the process, the bulk Ti_3AlC_2 was dispersed in HF (40%) for 2.5 h, then obtaining suspension was washed several times with distilled water. Later, it is filtered to obtain two-dimensional nanosheets of titanium carbide (MXenes).

3.2 Preparation of Au/MXene Composite

Nanocrystalline Au doped $Ti_3C_2T_x$ MXene nanosheets were obtained by the chemical reduction method (Rakhi et al. 2016). In this method, 0.075 M $HAuCl_4{\cdot}3H_2O$ solution was reduced using 1 M NaOH and 0.1 M $NaBH_4$ with constant stirring and then added 0.05 g of $Ti_3C_2T_x$ to the previous solution mixture. Then the resultant solution sonicated for about 30 min. After the reaction was complete, washed the water a few times and filtered it with cellulose membranes (pore size 0.1 μm). Finally, the purified sample dried at 80 °C for 2 h in a vacuum oven for further analysis.

Mechanical exfoliation techniques have become extensive, very cheap, and simple to prepare several high-quality 2D materials, including graphene, all while producing (Yi and Shen 2015). However, materials obtained by mechanical exfoliation show limitation in size and thickness over a large area; hence, these methods are not desirable for largescale production (Kauling et al. 2018; Li et al. 2016; Novoselov et al. 2004; Wangyang et al. 2016). To overcome these limitations, techniques such as ball milling and three-roll milling attracted significant interest, enhancing the ease of manufacturing and output (Chen et al. 2012; Jeon et al. 2013; Jeon et al. 2012; Ji et al. 2019; Knieke et al. 2010; Zhao et al. 2010). In addition, Liquid-based exfoliation has been considered an alternative exfoliation technique that comprehends both physical methods (sonication-assisted exfoliation) and chemical processes (surfactant-assisted, ion intercalation, ion exchange, and redox-based) (Guardia et al. 2011; Jawaid et al. 2017; Nicolosi et al. 2013; Osada and Sasaki 2009; Radisavljevic et al. 2011). These techniques produce large two-dimensional nanoflakes in solution, but the thickness and lateral dimensions are not controllable (Chen et al. 2012). Furthermore, due to sonication, the liquid exfoliation process leaves chemical impurities from the solvents, leading to a change in the material quality (Novoselov et al. 2004).

The electrochemical deposition technique offers an authentic, economical, and flexible route (via pH, voltage, etc.) to develop 2D materials at low temperatures. This method was used to prepare graphene, reduced graphene oxide (rGO), and several TMDs (Amin et al. 2018; Chakraborty et al. 2013; Chen et al. 2011; Devadasan et al. 2001; Hilder et al. 2011; Hu et al. 2010; Rastogi et al. 2017). Additionally, the solvothermal method offers a cost-effective and straightforward process to synthesize different 2D materials for biosensors with good yield and low environmental effect (Murugesan et al. 2013; Xu et al. 2016; Yan et al. 2016). In contrast to these methods, chemical vapor deposition (CVD) could result in 2D materials on a large surface area with excellent quality films (in terms of uniformity and crystal size) by passing vapor-phase precursors onto the substrates which decompose, resulting in the deposition of a film. Common substrates used in CVD include Si/SiO$_2$, sapphire, and transition metal catalysts (e.g., Cu, Ni) (Fanton et al. 2011; Gui et al. 2014; Hwang et al. 2013; Kim et al. 2009; Li et al. 2009; Reina et al. 2009; Song et al. 2012; Zhan et al. 2012). CVD-grown films can be doped with different elements (Yang et al. 2014; Zhang et al. 2015a). In addition, other methods to prepare 2D materials include molecular beam epitaxy (MBE), colloidal phase methods and Atomic Layer Deposition (ALD) (Dumcenco et al. 2015; Lehtinen et al. 2015; Mahler et al. 2014; Roy et al. 2016; Sreedhara et al. 2018; Sun et al. 2016; Vishwanath et al. 2015; Yan et al. 2010). These techniques provide 2D materials with good uniformity, controllable size, thickness, composition, and material phase. Stacking of 2D materials also possible with these techniques by using different precursors and parameters, which makes promising techniques for biosensing applications.

4 Smart-Based Biosensors for Point-of-Care Diagnosis

The 2D materials have been extensively used in biosensing platforms due to their interesting structural features, as discussed in earlier sections which suited for the fabrication of biosensor platform (James Singh et al. 2021; Lam et al. 2021; Mathew et al. 2021; Mohammadniaei et al. 2019).

4.1 Graphene-Based Biosensing Platforms

Since its introduction as the first 2D material into the material science field, it holds a lion share in the research as well as its usage in various applications. Moreover, its single atomic layer thickness with pure sp^2 hybridization, recent technological advances to produce in bulk quantities in pure form further increased its usage. The below section lists some of the sensing platforms constructed using graphene-based materials.

A non-enzymatic sensor was made using 3D monolithic nanoporous gold scaffold (NPG)-based electrode on supported with graphene paper (GP) was enhanced by an effective and simple ultrasonic electrodeposition technique for compact, ultrasound, and well-dispersed binary platinum-cobalt (PtCo) alloy nanoparticles (Zhao et al. 2016). This sensor evidenced a broad linear range (35 μM–30 mM), sensitivity 7.84 $\mu A\ cm^{-2}\ mM^{-1}$ of glucose sensing and 5 μM limit of detection (LOD) (Lee et al. 2016). The platinum graphite composites-based low-cost, flexible, and non-enzymatic/enzymatic glucose sensor was reported; see Fig. 23.1 (Abellán-Llobregat et al. 2017).

A gold-dried graphene glucose sensor was prepared by CVD using Ag/AgCl as a counterpart electrode that remarkably increased the sensitivity and enabled the sensing of glucose, at a lower concentrations (Liu et al. 2016). Another enzymeless glucose sensor, based on flower-like 2D copper cobaltite ($CuCo_2O_4$) nanosheets

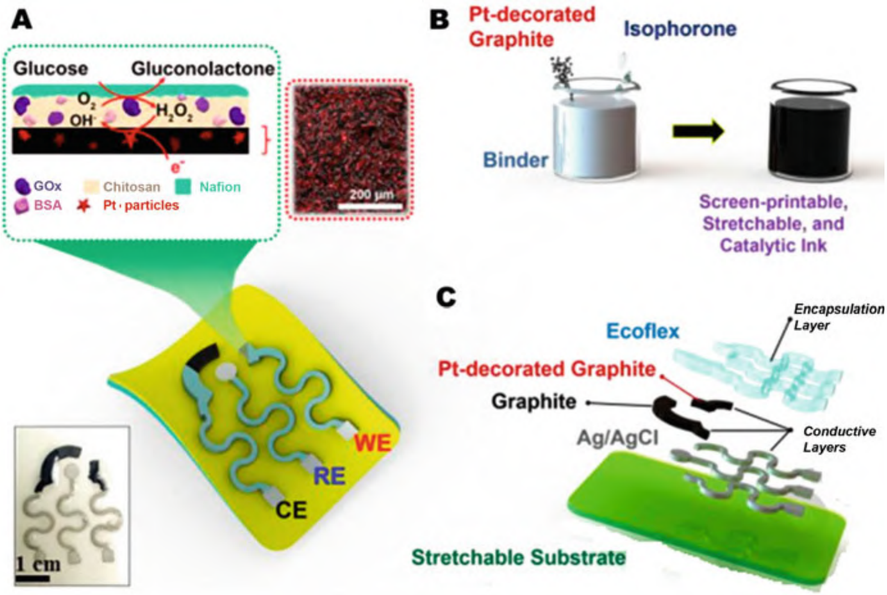
A
Glucose
Gluconolactone
O2
OH-
H2O2
e-
GOx
BSA
Chitosan
Nafion
Pt particles
200 μm
WE
RE
CE
1 cm
B
Pt-decorated Graphite
Isophorone
Binder
Screen-printable, Stretchable, and Catalytic Ink
C
Ecoflex
Encapsulation Layer
Pt-decorated Graphite
Graphite
Ag/AgCl
Conductive Layers
Stretchable Substrate

Fig. 23.1 (**a**) Illustration of the fabricated sensor and sensing mechanism. (**b**) Process involved during fabrication. (**c**) Screen printing process showing a layer of components (Abellán-Llobregat et al. 2017)

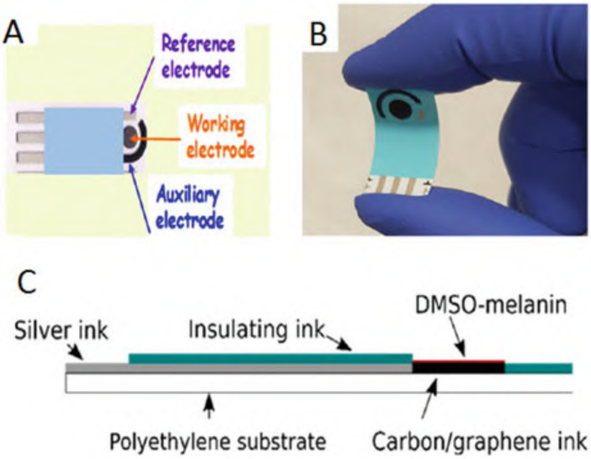

Fig. 23.2 (**a**) The top view of electrode used for pH sensing fabricated by screen printing process. (**b**) Optical image of the electrode. (**c**) Cross section of the electrode (Zhu et al. 2013)

deposited on a flexible graphite paper, was prepared by a simple hydrothermal technique followed by a post-annealing process (Labroo and Cui 2013). The flexible graphene-based sensor was fabricated for lactate sensing, which can be fabricated on different plastic substrates. The authors proved that the sensing response diminishes with increasing the bending angle and number of repetition bandings. However, they demonstrated the sensing abilities under different mechanical bending conditions (Melai et al. 2016).

Another new electrochemical pH sensor was prepared based on melanin pigment functionalized by graphene and dimethyl sulfoxide (DMSO) using a screen printing method is shown in (Fig. 23.2) (Zhu et al. 2013). Graphene oxide (GO)-based pH sensor was developed by drop-casting the GO on the screen-printed electrode substrate to monitor wound healing (Zhu et al. 2013). The sensitivity of the sensor was observed to be ~31.8 mV/pH. The pH was measured using the GO-modified screen-printed electrode by open-circuit potentiometry (Zhu et al. 2013). The selective, sensitive, and versatile laser-induced graphene sensor was fabricated for the detection of human stress hormone cortisol. This sensor is lightweight; microfluidic patch is mechanically stable and can be laminated in accordance with the skin (Fig. 23.3) (Torrente-Rodríguez et al. 2020).

4.2 MoS_2-Based Biosensing Platforms

MoS_2, the 2D layered structure, belongs to the transition metal chalcogenide family, found to be interesting to use in biosensor fabrication because of its excellent photoluminescence properties, tunable bandgap, large surface areas, stability in solution phase, particularly low cytotoxicity, high electron mobility and intercalatable structural features. The electronic, optical, and electrocatalytic properties of these materials are found to be changed with respect to morphology of the MoS_2 structures.

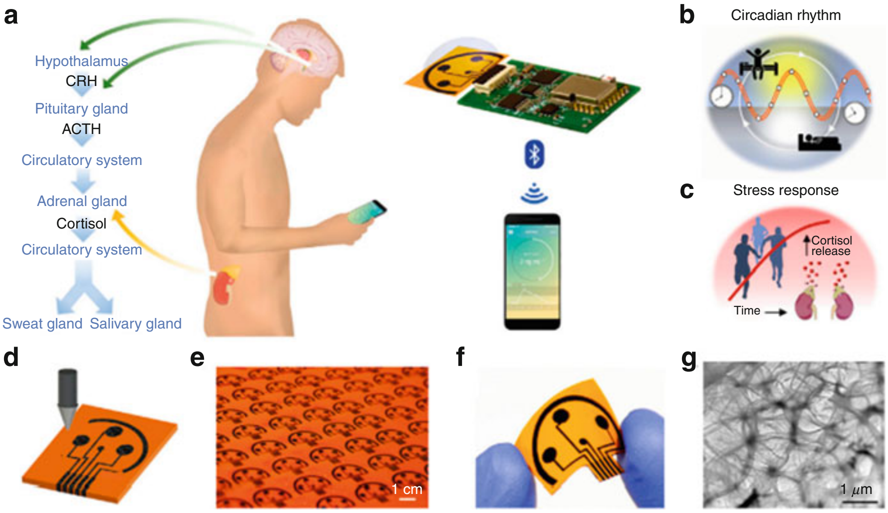

Fig. 23.3 A wireless, integrated graphene-based sweat, stress sensing system (GS4) for (**a**) the analysis of dynamic and non-invasive stress hormone. Schematic representation of the origin of cortisol hormone in sweat and saliva, the use of the GS4 to analyze the cortisol level circulation. Pictorial representation of cortisol dynamics regulated by circadian rhythm (**b**) and triggered by psychological stress (**c**). (**d**) Representation of the laser engraving method of a graphene platform. (**e**) Mass production of graphene sensor arrays on a polyimide substrate. (**f**) Picture of a flexible, disposable graphene sensor array. (**g**) TEM image of the surface of the graphene electrode (Torrente-Rodríguez et al. 2020). **Note**: CRH-corticotropin-releasing hormone; ACTH-adrenocorticotropic hormone

Single-layer MoS_2 nanosheets can quench fluorescence strongly, and their affinity toward ss and dsDNA is different. These two properties of MoS_2 sheets have been used in fabricating the sensor for DNA and other small molecules (Wang et al. 2018). Another MoS-based sensor was developed for small molecules and protein detection based on fluorescence-activated DNA-MoS_2 nanosheets (Kinnamon et al. 2017). The sensor was fabricated by self-assembly of the DNA aptamer on the MoS_2 nanosheets (Kinnamon et al. 2017). The portable biosensor for detecting the usual stress biomarker cortisol was reported based on the label-free MoS_2-integrated porous flexible electrode system (Wang et al. 2018). The specificity of this sensor was achieved by an affinity assay which uses MoS_2 nanosheets and the cortisol antibody as a sensing device. The cortisol was monitored using the fabricated portable sensor system from the perspired human sweat. The electrochemical impedance spectroscopic technique was used for monitoring the cortisol using the fabricated sensor system (Wang et al. 2018). A new sensor category was developed for monitoring analytes of interest in human sweat was reported based on depositing a Cu submicron bud on a freestanding graphene layer deposited with a monolayer of MoS_2 nano crystals (Xi et al. 2014). The fabricated substrate was used as a working electrode system for bifunctional glucose and lactate detection in human sweat by electrochemical amperometric technique (Xi et al. 2014).

4.3 Other 2D Materials as Biosensing Platforms

WS_2 nanosheet fluorescence quenching combined with duplex-specific nuclease signal amplification was found to exhibit preferential affinity toward microRNA (Zhang et al. 2015b). This property has been utilized for differential sensing of mRNA in the presence of ssDNA using the above sensor system (Zhang et al. 2015b). Multiplexed fluorescent detection of DNA was achieved by using a single-layer TaS_2 NS-based nanosensor (Zhou et al. 2018). Black phosphorus nanosheets were effective in sensing and detecting microRNA when used as the fluorescence quenching material, and a good linear response was obtained from 10 nM to 1000 nM using the sensor (Patil et al. 2019). The few-layered thick flakes of ternary copper indium selenide were synthesized, which is a promising platform for atomically layered optoelectronic device development (Tan et al. 2015). Based on their high fluorescence quenching ability, a novel fluorescent sensor for the detection of DNA was developed based on single-layer Ta_2NiS_5 nanosheets (Balendhran et al. 2013). The FET-based biosensor platform using 2D MoO_3 nanoflakes as a conductive channel for bovine serum albumin was reported (Lin et al. 2020). The simple hydrothermal approach was used for direct $NiSe_2$ growth on cellulose paper and used as a disposable glucose sensor (Lin et al. 2020). Recently, a lower concentration sweat lactate sensor that operates on passively expressed eccrine sweat without redox molecules was reported (de Araujo et al. 2017). A three-electrode laser-scribed graphene (LSG) structure on cheap paperboards demonstrated by Araujo et al. Caffeic acid, ascorbic acid, and picric acid can be analyzed using this sensor (Ruecha et al. 2019). Ling et al. came up with a flexible biosensor based on a metal-organic framework (MOF) for the detection of small molecules like L-histidine and ascorbic acid (AA), as well as H_2O_2 (Ruecha et al. 2019). Ruecha et al. recently developed a novel label-free electrochemical impedance immunosensor coupled with a paper-based microfluidic device for the highly sensitive detection of human interferon-γ (IFN-γ), which is a cytokine generated mainly by natural killer cells and T lymphocytes with regard to antigen stimulation; it can be used as a biomarker during tuberculosis diagnosis (Vogt et al. 2012). Semiconducting metal dichalcogenides (e.g., SnS_2 and $SnSe_2$) and buckled graphene analogs (MXenes) have recently emerged as candidate 2D crystals for flexible nanoelectronics (Li et al. 2013, 2014; Song et al. 2013). Table 23.1 summarizes the application of various 2D materials for biosensing applications.

5 Future Prospective

In conclusion, 2D materials have been extensively used as biosensing platforms due to some of their favorable properties. Mainly, two biosensing approaches, electrochemical and fluorescence techniques, were performed using the 2D materials. Among diverse 2D materials, rapheme and its derivatives have been used extensively used to fabricate biosensor platforms. Graphene has been used in the fabrication of electrochemical sensors platforms, whereas its analogs like GO, rGO, GQDs,

Table 23.1 The analytical features of the biosensors fabricated using the 2D materials

Type of 2D substrate	Synthesis route	Modifier	Analyte	Sensing platform	LOD (μg)	Liner range (μg)	References
Single-layer MoS_2	Li intercalation method	NIL	DNA	Fluorescence	0.0005	0–0.015	Sarkar et al. (2014)
MoS_2	Chemical exfoliation	DNA	Proteins	Fluorescence	4 0.0	10–2000	Torrente-Rodríguez et al. (2020)
WS_2	NIL	NIL	MicroRNA	Fluorescence	0.0000003	0–0.1	Wang et al. (2018)
MoS2, TiS_2, TaS_2	Li intercalation method	NIL	DNA	Fluorescence	0.00005	0–0.005	Xi et al. (2014)
Black P NS	Liquid exfoliation	NIL	MicroRNA	Fluorescence	0.00937	0.01–1	Zhang et al. (2015b)
Cu/In/Se	Melting and recrystallization	Ionic Liquid	NIL	Electrical double-layer field-effect transistors	NIL	NIL	Zhou et al. (2018)
Ta_2NiS5 and Ta_2NiSe_5,	Electrochemical Li intercalation and exfoliation	NIL	DNA	Fluorescence	0.00005	0–0.005	Patil et al. (2019)
MoO_3	Mechanical exfoliation	NIL	Bovine serum albumin	FET	NIL	NIL	Torrente-Rodríguez et al. (2020)
Graphene paper + nanoporous gold	Ultrasonic electrodeposition	Pt Co alloy	Glucose	Electrochemical	5 0.0	35–30,000	Torrente-Rodríguez et al. (2020), Sreedhara et al. (2018)
Graphene	CVD	Gold	Biomarkers in sweat	Electrochemical			Zhao et al. (2016)
Pt-decorated graphite	Reduction	NIL	glucose	Electrochemical	6600	33–0.900	Lee et al. (2016)
NiSe2 + cellulose paper	Hydrothermal	NIL	Glucose	Electrochemical	24.8	100–1000	Balendhran et al. (2013)

Cobaltite/ graphite paper	Hydrothermal	NIL	Glucose	Electrochemical	5	0–320	Abellán-Llobregat et al. (2017)
Graphene	CVD	Plastics	Lactate	Electrochemical	0.08	0.08–20	Liu et al. (2016)
Graphene oxide	Ultrasonication	NIL	Human sweat	Electrochemical	1 mM	1000–100,000	Lin et al. (2020)
Graphene paper + MoS2	Hydrothermal and electrodeposition	Cu microbuds	Sweat	Amperometric	0.5	5–1775	Kinnamon et al. (2017)
Paper	Laser scribing	NIL	Picric acid	Electrochemical	NIL	480–2000	Lin et al. (2020)
Cu–MoF	Hydrothermal	NIL	Ascorbic acid, L-histidine, and H_2O_2	Electrochemical	Nil	2.94, 4.1 and 5.3	de Araujo et al. (2017)
G O	Hummer's method	NIL	pH sensor; wound monitoring	Voltage	31.8 mV/pH		Labroo and Cui (2013)
Polyaniline/ graphene /SCE	Wax printing	NIL	Human interferon-gamma	Electrochemical	0.000034	0.05–0.001	Ruecha et al. (2019)
MoS_2	NIL	Cortisol antibodies	Ethyl glucuronide	Electrochemical	0.001	0.001–0.5	Wang et al. (2018)
Graphene sensor patch on polyimide	Laser engraving	NIL	Cortisol	Electrochemical	NA	NA	Zhu et al. (2013)

and carbon dots have been used in the fabrication of fluorescent sensing platforms because of their excellent fluorescence emission properties. The other 2D substrates used in biosensor fabrication includes MoS_2, WS_2, MoO_3, MXenes, MOFs, InS_2, SnS_2 and $SnSe_2$, and so on. Using the aforementioned pristine 2D substrates/2D composites, various portable biosensors, diagnostic tool kits, point-of-care devices, implantable biochips, and so on were fabricated for a variety of medical emergency applications. Numerous portable diagnostic tool kits for specific and accurate sensing of one of the physiologically important analytes, glucose, responsible for deadly diabetes mellitus disease in the human race, have been reported based on 2D substrates. Recently, biosensor platforms for human stress biomarker cortisol were also reported based on the 2D substrates. The 2D biosensor platforms fabricated for cortisol were used to monitor its levels in human sweat and exhibit accurate results. Finally, there are still numerous implications of these materials, with respect to their extensive usage in biosensor fields in order to reach remote places with modest medical facilities due to their portability, cost-effectiveness, and other issues, need to be addressed during the designing, synthesis, and fabrication steps.

References

Abellán-Llobregat A, Jeerapan I, Bandodkar A, Vidal L, Canals A, Wang J, Morallón E (2017) A stretchable and screen-printed electrochemical sensor for glucose determination in human perspiration. Biosens Bioelectron 91:885–891

Amin R, Hossain MA, Zakaria Y (2018) Interfacial kinetics and ionic diffusivity of the electrodeposited MoS2 film. ACS Appl Mater Interfaces 10(16):13509–13518

Balendhran S, Ou JZ, Bhaskaran M, Sriram S, Ippolito S, Vasic Z, Kats E, Bhargava S, Zhuiykov S, Kalantar-zadeh K (2012) Atomically thin layers of MoS_2via a two step thermal evaporation–exfoliation method. Nanoscale 4(2):461–466

Balendhran S, Walia S, Alsaif M, Nguyen EP, Ou JZ, Zhuiykov S, Sriram S, Bhaskaran M, Kalantar-zadeh K (2013) Field effect biosensing platform based on 2D α-MoO_3. ACS Nano 7(11):9753–9760

Benavente E, Santa Ana MA, Mendizábal F, González G (2002) Intercalation chemistry of molybdenum disulfide. Coord Chem Rev 224(1):87–109

Berger C, Song Z, Li T, Li X, Ogbazghi AY, Feng R, Dai Z, Marchenkov AN, Conrad EH, First PN, de Heer WA (2004) Ultrathin epitaxial graphite: 2D electron gas properties and a route toward graphene-based nanoelectronics. J Phys Chem B 108(52):19912–19916

Bertolazzi S, Brivio J, Kis A (2011) Stretching and breaking of ultrathin MoS_2. ACS Nano 5(12): 9703–9709

Bolotsky A, Butler D, Dong C, Gerace K, Glavin NR, Muratore C, Robinson JA, Ebrahimi A (2019) Two-dimensional materials in biosensing and healthcare: from in vitro diagnostics to optogenetics and beyond. ACS Nano 13(9):9781–9810

Bonaccorso F, Colombo L, Yu G, Stoller M, Tozzini V, Ferrari AC, Ruoff RS, Pellegrini V (2015) Graphene, related two-dimensional crystals, and hybrid systems for energy conversion and storage. Science 347(6217):1246501

Cambaz ZG, Yushin G, Osswald S, Mochalin V, Gogotsi Y (2008) Noncatalytic synthesis of carbon nanotubes, graphene and graphite on SiC. Carbon 46(6):841–849

Chakraborty B, Show B, Jana S, Mitra BC, Maji SK, Adhikary B, Mukherjee N, Mondal A (2013) Cathodic and anodic deposition of FeS_2 thin films and their application in electrochemical reduction and amperometric sensing of H_2O_2. Electrochim Acta 94:7–15

Chen L, Tang Y, Wang K, Liu C, Luo S (2011) Direct electrodeposition of reduced graphene oxide on glassy carbon electrode and its electrochemical application. Electrochem Commun 13(2): 133–137

Chen J, Duan M, Chen G (2012) Continuous mechanical exfoliation of graphene sheets via three-roll mill. J Mater Chem 22(37):19625–19628

Chhowalla M, Shin HS, Eda G, Li L-J, Loh KP, Zhang H (2013) The chemistry of two-dimensional layered transition metal dichalcogenide nanosheets. Nat Chem 5(4):263–275

Chithaiah P, Raju MM, Kulkarni GU, Rao CNR (2020) Simple synthesis of nanosheets of rGO and nitrogenated rGO. Beilstein J Nanotechnol 11:68–75

Chrimes AF, Khoshmanesh K, Stoddart PR, Mitchell A, Kalantar-zadeh K (2013) Microfluidics and Raman microscopy: current applications and future challenges. Chem Soc Rev 42(13): 5880–5906

Coleman JN, Lotya M, O'Neill A, Bergin SD, King PJ, Khan U, Young K, Gaucher A, De S, Smith RJ, Shvets IV, Arora SK, Stanton G, Kim H-Y, Lee K, Kim GT, Duesberg GS, Hallam T, Boland JJ, Wang JJ, Donegan JF, Grunlan JC, Moriarty G, Shmeliov A, Nicholls RJ, Perkins JM, Grieveson EM, Theuwissen K, McComb DW, Nellist PD, Nicolosi V (2011) Two-dimensional nanosheets produced by liquid exfoliation of layered materials. Science 331(6017):568–571

de Araujo WR, Frasson CMR, Ameku WA, Silva JR, Angnes L, Paixão TRLC (2017) Single-step reagentless laser scribing fabrication of electrochemical paper-based analytical devices. Angew Chem Int Ed 56(47):15113–15117

de Heer WA, Berger C, Ruan M, Sprinkle M, Li X, Hu Y, Zhang B, Hankinson J, Conrad E (2011) Large area and structured epitaxial graphene produced by confinement controlled sublimation of silicon carbide. Proc Natl Acad Sci 108(41):16900–16905

Devadasan JJ, Sanjeeviraja C, Jayachandran M (2001) Electrodeposition of p-WS2 thin film and characterisation. J Cryst Growth 226(1):67–72

Dumcenco D, Ovchinnikov D, Marinov K, Lazić P, Gibertini M, Marzari N, Sanchez OL, Kung Y-C, Krasnozhon D, Chen M-W, Bertolazzi S, Gillet P, Fontcuberta i Morral, A., Radenovic, A., Kis, A. (2015) Large-area epitaxial monolayer MoS_2. ACS Nano 9(4):4611–4620

Emtsev KV, Bostwick A, Horn K, Jobst J, Kellogg GL, Ley L, McChesney JL, Ohta T, Reshanov SA, Röhrl J, Rotenberg E, Schmid AK, Waldmann D, Weber HB, Seyller T (2009) Towards wafer-size graphene layers by atmospheric pressure graphitization of silicon carbide. Nat Mater 8(3):203–207

Fanton MA, Robinson JA, Puls C, Liu Y, Hollander MJ, Weiland BE, LaBella M, Trumbull K, Kasarda R, Howsare C, Stitt J, Snyder DW (2011) Characterization of graphene films and transistors grown on sapphire by metal-free chemical vapor deposition. ACS Nano 5(10): 8062–8069

Geim AK (2009) Graphene: status and prospects. Science 324(5934):1530–1534

Guardia L, Fernández-Merino MJ, Paredes JI, Solís-Fernández P, Villar-Rodil S, Martínez-Alonso A, Tascón JMD (2011) High-throughput production of pristine graphene in an aqueous dispersion assisted by non-ionic surfactants. Carbon 49(5):1653–1662

Gui Y, Yuan J, Wang W, Zhao J, Tian J, Xie B (2014) Facile solvothermal synthesis and gas sensitivity of graphene/WO_3 nanocomposites. Materials (Basel) 7(6):4587–4600

Hilder M, Winther-Jensen B, Li D, Forsyth M, MacFarlane DR (2011) Direct electro-deposition of graphene from aqueous suspensions. Phys Chem Chem Phys 13(20):9187–9193

Hu Y, Jin J, Wu P, Zhang H, Cai C (2010) Graphene–gold nanostructure composites fabricated by electrodeposition and their electrocatalytic activity toward the oxygen reduction and glucose oxidation. Electrochim Acta 56(1):491–500

Hwang J, Kim M, Campbell D, Alsalman HA, Kwak JY, Shivaraman S, Woll AR, Singh AK, Hennig RG, Gorantla S, Rümmeli MH, Spencer MG (2013) van der Waals epitaxial growth of graphene on sapphire by chemical vapor deposition without a metal catalyst. ACS Nano 7(1): 385–395

James Singh K, Ahmed T, Gautam P, Sadhu AS, Lien D-H, Chen S-C, Chueh Y-L, Kuo H-C (2021) Recent advances in two-dimensional quantum dots and their applications. Nano 11(6):1549

Jawaid A, Che J, Drummy LF, Bultman J, Waite A, Hsiao M-S, Vaia RA (2017) Redox exfoliation of layered transition metal dichalcogenides. ACS Nano 11(1):635–646

Jeon I-Y, Shin Y-R, Sohn G-J, Choi H-J, Bae S-Y, Mahmood J, Jung S-M, Seo J-M, Kim M-J, Chang DW, Dai L, Baek J-B (2012) Edge-carboxylated graphene nanosheets via ball milling. Proc Natl Acad Sci 109(15):5588–5593

Jeon I-Y, Choi H-J, Jung S-M, Seo J-M, Kim M-J, Dai L, Baek J-B (2013) Large-scale production of edge-selectively functionalized graphene nanoplatelets via ball milling and their use as metal-free electrocatalysts for oxygen reduction reaction. J Am Chem Soc 135(4):1386–1393

Ji H, Hu S, Jiang Z, Shi S, Hou W, Yang G (2019) Directly scalable preparation of sandwiched MoS2/graphene nanocomposites via ball-milling with excellent electrochemical energy storage performance. Electrochim Acta 299:143–151

Kauling AP, Seefeldt AT, Pisoni DP, Pradeep RC, Bentini R, Oliveira RVB, Novoselov KS, Castro Neto AH (2018) The worldwide graphene flake production. Adv Mater 30(44):1803784

Khalil I, Yehye WA, Julkapli NM, Rahmati S, Sina AAI, Basirun WJ, Johan MR (2019) Graphene oxide and gold nanoparticle based dual platform with short DNA probe for the PCR free DNA biosensing using surface-enhanced Raman scattering. Biosens Bioelectron 131:214–223

Kim KS, Zhao Y, Jang H, Lee SY, Kim JM, Kim KS, Ahn J-H, Kim P, Choi J-Y, Hong BH (2009) Large-scale pattern growth of graphene films for stretchable transparent electrodes. Nature 457(7230):706–710

Kinnamon D, Ghanta R, Lin K-C, Muthukumar S, Prasad S (2017) Portable biosensor for monitoring cortisol in low-volume perspired human sweat. Sci Rep 7(1):13312

Knieke C, Berger A, Voigt M, Taylor RNK, Röhrl J, Peukert W (2010) Scalable production of graphene sheets by mechanical delamination. Carbon 48(11):3196–3204

Kurapati R, Kostarelos K, Prato M, Bianco A (2016) Biomedical uses for 2D materials beyond graphene: current advances and challenges ahead. Adv Mater 28(29):6052–6074

Labroo P, Cui Y (2013) Flexible graphene bio-nanosensor for lactate. Biosens Bioelectron 41: 852–856

Lam CYK, Zhang Q, Yin B, Huang Y, Wang H, Yang M, Wong SHD (2021) Recent advances in two-dimensional transition metal dichalcogenide nanocomposites biosensors for virus detection before and during COVID-19 outbreak. J Compos Sci 5(7):190

Lee H, Choi TK, Lee YB, Cho HR, Ghaffari R, Wang L, Choi HJ, Chung TD, Lu N, Hyeon T, Choi SH, Kim D-H (2016) A graphene-based electrochemical device with thermoresponsive microneedles for diabetes monitoring and therapy. Nat Nanotechnol 11(6):566–572

Lehtinen O, Komsa H-P, Pulkin A, Whitwick MB, Chen M-W, Lehnert T, Mohn MJ, Yazyev OV, Kis A, Kaiser U, Krasheninnikov AV (2015) Atomic scale microstructure and properties of se-deficient two-dimensional MoSe2. ACS Nano 9(3):3274–3283

Li X, Cai W, An J, Kim S, Nah J, Yang D, Piner R, Velamakanni A, Jung I, Tutuc E, Banerjee SK, Colombo L, Ruoff RS (2009) Large-area synthesis of high-quality and uniform graphene films on copper foils. Science 324(5932):1312–1314

Li X, Mullen JT, Jin Z, Borysenko KM, Buongiorno Nardelli M, Kim KW (2013) Intrinsic electrical transport properties of monolayer silicene and MoS${}_{2}$ from first principles. Phys Rev B 87(11):115418

Li L, Yu Y, Ye GJ, Ge Q, Ou X, Wu H, Feng D, Chen XH, Zhang Y (2014) Black phosphorus field-effect transistors. Nat Nanotechnol 9(5):372–377

Li M-Y, Chen C-H, Shi Y, Li L-J (2016) Heterostructures based on two-dimensional layered materials and their potential applications. Mater Today 19(6):322–335

Lin Z, Carvalho BR, Kahn E, Lv R, Rao R, Terrones H, Pimenta MA, Terrones M (2016) Defect engineering of two-dimensional transition metal dichalcogenides. 2D Mater 3(2):022002

Lin K-C, Muthukumar S, Prasad S (2020) Flex-GO (Flexible graphene oxide) sensor for electrochemical monitoring lactate in low-volume passive perspired human sweat. Talanta 214:120810

Liu K-K, Zhang W, Lee Y-H, Lin Y-C, Chang M-T, Su C-Y, Chang C-S, Li H, Shi Y, Zhang H, Lai C-S, Li L-J (2012) Growth of large-area and highly crystalline mos2 thin layers on insulating substrates. Nano Lett 12(3):1538–1544

Liu S, Hui KS, Hui KN (2016) Flower-like copper cobaltite nanosheets on graphite paper as high-performance supercapacitor electrodes and enzymeless glucose sensors. ACS Appl Mater Interfaces 8(5):3258–3267

Liu G, Robertson AW, Li MM, Kuo WCH, Darby MT, Muhieddine MH, Lin YC, Suenaga K, Stamatakis M, Warner JH, Tsang SCE (2017) MoS_2 monolayer catalyst doped with isolated Co atoms for the hydrodeoxygenation reaction. Nat Chem 9(8):810–816

Mahler B, Hoepfner V, Liao K, Ozin GA (2014) Colloidal synthesis of 1T-WS_2 and 2H-WS_2 nanosheets: applications for photocatalytic hydrogen evolution. J Am Chem Soc 136(40): 14121–14127

Mathew M, Radhakrishnan S, Vaidyanathan A, Chakraborty B, Rout CS (2021) Flexible and wearable electrochemical biosensors based on two-dimensional materials: recent developments. Anal Bioanal Chem 413(3):727–762

Melai B, Salvo P, Calisi N, Moni L, Bonini A, Paoletti C, Lomonaco T, Mollica V, Fuoco R, Di Francesco F (2016) A graphene oxide pH sensor for wound monitoring. Annu Int Conf IEEE Eng Med Biol Soc 2016:1898–1901

Mohammadniaei M, Nguyen HV, Tieu MV, Lee M-H (2019) 2D materials in development of electrochemical point-of-care cancer screening devices. Micromachines 10(10):662

Morales-Narváez E, Merkoçi A (2019) Graphene oxide as an optical biosensing platform: a progress report. Adv Mater 31(6):1805043

Murugesan S, Akkineni A, Chou BP, Glaz MS, Vanden Bout DA, Stevenson KJ (2013) Room temperature electrodeposition of molybdenum sulfide for catalytic and photoluminescence applications. ACS Nano 7(9):8199–8205

Nicolosi V, Chhowalla M, Kanatzidis MG, Strano MS, Coleman JN (2013) Liquid exfoliation of layered materials. Science 340(6139):1226419

Novoselov KS, Geim AK, Morozov SV, Jiang D, Zhang Y, Dubonos SV, Grigorieva IV, Firsov AA (2004) Electric field effect in atomically thin carbon films. Science 306(5696):666–669

O'Neill A, Khan U, Coleman JN (2012) Preparation of High Concentration Dispersions of Exfoliated MoS_2 with Increased Flake Size. Chem Mater 24(12):2414–2421

Okhrimenko DV, Nissenbaum J, Andersson MP, Olsson MHM, Stipp SLS (2013) Energies of the adsorption of functional groups to calcium carbonate polymorphs: the importance of −OH and −COOH groups. Langmuir 29(35):11062–11073

Osada M, Sasaki T (2009) Exfoliated oxide nanosheets: new solution to nanoelectronics. J Mater Chem 19(17):2503–2511

Ouyang Q, Zeng S, Jiang L, Qu J, Dinh X-Q, Qian J, He S, Coquet P, Yong K-T (2017) Two-dimensional transition metal dichalcogenide enhanced phase-sensitive plasmonic biosensors: theoretical insight. J Phys Chem C 121(11):6282–6289

Park S, Ruoff RS (2009) Chemical methods for the production of graphenes. Nat Nanotechnol 4(4): 217–224

Patil PD, Ghosh S, Wasala M, Lei S, Vajtai R, Ajayan PM, Talapatra S (2019) Electric double layer field-effect transistors using two-dimensional (2D) layers of copper indium selenide (CuIn7Se11). Electronics 8(6):645

Radisavljevic B, Radenovic A, Brivio J, Giacometti V, Kis A (2011) Single-layer MoS_2 transistors. Nat Nanotechnol 6(3):147–150

Rakhi RB, Nayak P, Xia C, Alshareef HN (2016) Novel amperometric glucose biosensor based on MXene nanocomposite. Sci Rep 6(1):36422

Rao CNR, Maitra U (2015) Inorganic graphene analogs. Annu Rev Mater Res 45(1):29–62

Rastogi PK, Sarkar S, Mandler D (2017) Ionic strength induced electrodeposition of two-dimensional layered MoS_2 nanosheets. Appl Mater Today 8:44–53

Reina A, Jia X, Ho J, Nezich D, Son H, Bulovic V, Dresselhaus MS, Kong J (2009) Large area, few-layer graphene films on arbitrary substrates by chemical vapor deposition. Nano Lett 9(1): 30–35

Ren X, Ma H, Zhang T, Zhang Y, Yan T, Du B, Wei Q (2017) Sulfur-doped graphene-based immunological biosensing platform for multianalysis of cancer biomarkers. ACS Appl Mater Interfaces 9(43):37637–37644

Roy A, Movva HCP, Satpati B, Kim K, Dey R, Rai A, Pramanik T, Guchhait S, Tutuc E, Banerjee SK (2016) Structural and electrical properties of $MoTe_2$ and $MoSe_2$ grown by molecular beam epitaxy. ACS Appl Mater Interfaces 8(11):7396–7402

Ruecha N, Shin K, Chailapakul O, Rodthongkum N (2019) Label-free paper-based electrochemical impedance immunosensor for human interferon gamma detection. Sensors Actuators B Chem 279:298

Sarkar D, Liu W, Xie X, Anselmo AC, Mitragotri S, Banerjee K (2014) MoS_2 field-effect transistor for next-generation label-free biosensors. ACS Nano 8(4):3992–4003

Shao Y, Wang J, Wu H, Liu J, Aksay IA, Lin Y (2010) Graphene based electrochemical sensors and biosensors: a review. Electroanalysis 22(10):1027–1036

Smith RJ, King PJ, Lotya M, Wirtz C, Khan U, De S, O'Neill A, Duesberg GS, Grunlan JC, Moriarty G, Chen J, Wang J, Minett AI, Nicolosi V, Coleman JN (2011) Large-scale exfoliation of inorganic layered compounds in aqueous surfactant solutions. Adv Mater 23(34):3944–3948

Song HJ, Son M, Park C, Lim H, Levendorf MP, Tsen AW, Park J, Choi HC (2012) Large scale metal-free synthesis of graphene on sapphire and transfer-free device fabrication. Nanoscale 4(10):3050–3054

Song HS, Li SL, Gao L, Xu Y, Ueno K, Tang J, Cheng YB, Tsukagoshi K (2013) High-performance top-gated monolayer SnS2 field-effect transistors and their integrated logic circuits. Nanoscale 5(20):9666–9670

Sreedhara MB, Santhosha AL, Bhattacharyya AJ, Rao CNR (2016) Composite of few-layer MoO_3 nanosheets with graphene as a high performance anode for sodium-ion batteries. J Mater Chem A 4(24):9466–9471

Sreedhara MB, Gope S, Vishal B, Datta R, Bhattacharyya AJ, Rao CNR (2018) Atomic layer deposition of crystalline epitaxial MoS2 nanowall networks exhibiting superior performance in thin-film rechargeable Na-ion batteries. J Mater Chem A 6(5):2302–2310

Subrahmanyam KS, Vivekchand SRC, Govindaraj A, Rao CNR (2008) A study of graphenes prepared by different methods: characterization, properties and solubilization. J Mater Chem 18(13):1517–1523

Sun Y, Wang Y, Sun D, Carvalho BR, Read CG, Lee C-H, Lin Z, Fujisawa K, Robinson JA, Crespi VH, Terrones M, Schaak RE (2016) Low-temperature solution synthesis of few-layer 1T'-MoTe2 nanostructures exhibiting lattice compression. Angew Chem Int Ed 55(8): 2830–2834

Tan C, Yu P, Hu Y, Chen J, Huang Y, Cai Y, Luo Z, Li B, Lu Q, Wang L, Liu Z, Zhang H (2015) High-yield exfoliation of ultrathin two-dimensional ternary chalcogenide nanosheets for highly sensitive and selective fluorescence DNA sensors. J Am Chem Soc 137(32):10430–10436

Torrente-Rodríguez RM, Tu J, Yang Y, Min J, Wang M, Song Y, Yu Y, Xu C, Ye C, IsHak WW, Gao W (2020) Investigation of cortisol dynamics in human sweat using a graphene-based wireless mHealth system. Matter 2(4):921–937

Van Bommel AJ, Crombeen JE, Van Tooren A (1975) LEED and Auger electron observations of the SiC(0001) surface. Surf Sci 48(2):463–472

Varghese SS, Varghese SH, Swaminathan S, Singh KK, Mittal V (2015) Two-dimensional materials for sensing: graphene and beyond. Electronics 4(3):651–687

Vishwanath S, Liu X, Rouvimov S, Mende PC, Azcatl A, McDonnell S, Wallace RM, Feenstra RM, Furdyna JK, Jena D, Grace Xing H (2015) Comprehensive structural and optical characterization of MBE grown $MoSe_2$ on graphite, CaF_2 and graphene. 2D Mater 2(2):024007

Vogt P, De Padova P, Quaresima C, Avila J, Frantzeskakis E, Asensio MC, Resta A, Ealet B, Le Lay G (2012) Silicene: compelling experimental evidence for graphenelike two-dimensional silicon. Phys Rev Lett 108(15):155501

Voiry D, Mohite A, Chhowalla M (2015) Phase engineering of transition metal dichalcogenides. Chem Soc Rev 44(9):2702–2712

Wang Y, Shao Y, Matson DW, Li J, Lin Y (2010) Nitrogen-doped graphene and its application in electrochemical biosensing. ACS Nano 4(4):1790–1798

Wang L, Wang Y, Wong JI, Palacios T, Kong J, Yang HY (2014) Functionalized MoS_2 nanosheet-based field-effect biosensor for label-free sensitive detection of cancer marker proteins in solution. Small 10(6):1101–1105

Wang Z, Dong S, Gui M, Asif M, Wang W, Wang F, Liu H (2018) Graphene paper supported MoS (2) nanocrystals monolayer with Cu submicron-buds: high-performance flexible platform for sensing in sweat. Anal Biochem 543:82–89

Wangyang P, Sun H, Zhu X, Yang D, Gao X (2016) Mechanical exfoliation and Raman spectra of ultrathin PbI2 single crystal. Mater Lett 168:68–71

Xi Q, Zhou D-M, Kan Y-Y, Ge J, Wu Z-K, Yu R-Q, Jiang J-H (2014) Highly sensitive and selective strategy for microRNA detection based on WS_2 nanosheet mediated fluorescence quenching and duplex-specific nuclease signal amplification. Anal Chem 86(3):1361–1365

Xu M, Liang T, Shi M, Chen H (2013) Graphene-like two-dimensional materials. Chem Rev 113(5):3766–3798

Xu Y, Wang Z, Guo Z, Huang H, Xiao Q, Zhang H, Yu X-F (2016) Solvothermal synthesis and ultrafast photonics of black phosphorus quantum dots. Adv Opt Mater 4(8):1223–1229

Yan X, Cui X, Li L-S (2010) Synthesis of large, stable colloidal graphene quantum dots with tunable size. J Am Chem Soc 132(17):5944–5945

Yan J, Chen Z, Ji H, Liu Z, Wang X, Xu Y, She X, Huang L, Xu L, Xu H, Li H (2016) Construction of a 2D graphene-like MoS_2/C_3N_4 heterojunction with enhanced visible-light photocatalytic activity and photoelectrochemical activity. Chemistry 22(14):4764–4773

Yang L, Majumdar K, Liu H, Du Y, Wu H, Hatzistergos M, Hung PY, Tieckelmann R, Tsai W, Hobbs C, Ye PD (2014) Chloride molecular doping technique on 2D materials: WS_2 and MoS_2. Nano Lett 14(11):6275–6280

Yao Y, Tolentino L, Yang Z, Song X, Zhang W, Chen Y, Wong, C.p. (2013) High-concentration aqueous dispersions of MoS_2. Adv Funct Mater 23(28):3577–3583

Yi M, Shen Z (2015) A review on mechanical exfoliation for the scalable production of graphene. J Mater Chem A 3(22):11700–11715

Zhan Y, Liu Z, Najmaei S, Ajayan PM, Lou J (2012) Large-area vapor-phase growth and characterization of MoS_2 atomic layers on a SiO_2 substrate. Small 8(7):966–971

Zhang K, Feng S, Wang J, Azcatl A, Lu N, Addou R, Wang N, Zhou C, Lerach J, Bojan V, Kim MJ, Chen L-Q, Wallace RM, Terrones M, Zhu J, Robinson JA (2015a) Manganese doping of monolayer MoS_2: the substrate is critical. Nano Lett 15(10):6586–6591

Zhang Y, Zheng B, Zhu C, Zhang X, Tan C, Li H, Chen B, Yang J, Chen J, Huang Y, Wang L, Zhang H (2015b) Single-layer transition metal dichalcogenide nanosheet-based nanosensors for rapid, sensitive, and multiplexed detection of DNA. Adv Mater 27(5):935–939

Zhang S, Geryak R, Geldmeier J, Kim S, Tsukruk VV (2017) Synthesis, assembly, and applications of hybrid nanostructures for biosensing. Chem Rev 117(20):12942–13038

Zhao W, Fang M, Wu F, Wu H, Wang L, Chen G (2010) Preparation of graphene by exfoliation of graphite using wet ball milling. J Mater Chem 20(28):5817–5819

Zhao A, Zhang Z, Zhang P, Xiao S, Wang L, Dong Y, Yuan H, Li P, Sun Y, Jiang X, Xiao F (2016) 3D nanoporous gold scaffold supported on graphene paper: freestanding and flexible electrode with high loading of ultrafine PtCo alloy nanoparticles for electrochemical glucose sensing. Anal Chim Acta 938:63–71

Zhou J, Li Z, Ying M, Liu M, Wang X, Wang X, Cao L, Zhang H, Xu G (2018) Black phosphorus nanosheets for rapid microRNA detection. Nanoscale 10(11):5060–5064

Zhu C, Zeng Z, Li H, Li F, Fan C, Zhang H (2013) Single-layer MoS2-based nanoprobes for homogeneous detection of biomolecules. J Am Chem Soc n(16):5998–6001

Nanobiomaterials: Applications in Nanomedicine and Drug Delivery

24

E. Merve Zanbak Çotaoğlu, Cansel Köse Özkan, and Yalçın Özkan

Contents

1 Introduction 520
2 Common Nanobiomaterials for Drug Delivery and Nanomedicine Applications 521
  2.1 Polymeric Biomaterials 522
  2.2 Fibrin 522
  2.3 Silk Fibroin 523
  2.4 Collagen 523
  2.5 Albumin 524
3 Polysaccharide-Based Biomaterials 524
  3.1 Pullulan 524
  3.2 Chitosan 524
  3.3 Alginate 525
  3.4 Cellulose 525
  3.5 Starch 526
  3.6 Self-Assembling Peptides 526
  3.7 Inorganic Nanobiomaterials 527
4 Applications in Nanomedicine and Drug Delivery 528
  4.1 Topical Applications 528
  4.2 Ophthalmic Applications 530
  4.3 Orthopedic Applications 532
  4.4 Dental Applications 534
  4.5 Wound Healing and Tissue Engineering Applications 536
5 Conclusion 537
References 537

Abstract

Nanobiomaterials are used in controlled drug delivery systems, medical devices in the production of prosthetic materials, tissue engineering in the construction of tissue scaffolds, and in the field of nanomedicine. In each of these areas, well-

---

E. M. Zanbak Çotaoğlu · C. Köse Özkan · Y. Özkan (✉)
Department of Pharmaceutical Technology, Gulhane Faculty of Pharmacy, University of Health Sciences, Ankara, Turkey
e-mail: yalcin.ozkan@sbu.edu.tr

© Springer Nature Singapore Pte Ltd. 2023

U. P. Azad, P. Chandra (eds.), *Handbook of Nanobioelectrochemistry*,
https://doi.org/10.1007/978-981-19-9437-1_24

defined polymers classified according to their physicochemical properties and biodegradability are used to provide effective treatments. Fibrin, collagen, albumin, pullulan, chitosan, alginate, cellulose, self-assembling peptides, and hydroxyapatite-based inorganic biomaterial can be given as examples of the main polymers of organic and inorganic origin widely used for drug delivery applications. These polymers have applications in many fields, especially ophthalmology, orthopedics, wound healing, and tissue engineering.

Keywords

Nanobiomaterials · Drug delivery · Application · Nanomedicine · Biodegradable polymer

1 Introduction

Nanotechnology-based drug delivery systems is a multidisciplinary field and provides an advantage by solving challenges such as (i) increasing bioavailability by improving the solubility of hydrophobic drugs, (ii) helping to reach the therapeutic concentration of drugs in a target zone, (iii) reducing toxicity and immunogenic response, (iv) preventing the plasma instability of drugs, and (v) in case of bio-imaging, increasing the contrast of tissue by enhancing permeability with nanoparticles (NPs) (Koutsopoulos 2012; Jacob et al. 2018). Nanotechnology enables targeted delivery of therapeutic agents to the disease site by formulating them in biocompatible nanocarriers such as nanocapsules, micelle systems, and dendrimers. This can be accomplished either by passive targeting of drugs to the site of action or by active targeting of the drug (Parveen et al. 2012). Nano-delivery systems in nanotechnology offer numerous benefits in the treatment of chronic diseases by delivering nano-sized therapeutics to target areas to be treated. In addition, smart drug delivery systems provide significant advances in cancer treatment (Parhi et al. 2012; Patra et al. 2018).

The use of oversized materials in drug delivery poses challenges in terms of in vivo instability, poor bioavailability and poor solubility, poor absorption in the body, target-specific delivery, and potential adverse effects of drugs. Therefore, using nanoscale drug delivery systems to target drugs to specific body parts is considered as an option that can solve these critical problems (Martinho et al. 2011; Jahangirian et al. 2017; Patra et al. 2018). Nanoparticles used in controlled drug delivery and targeted drug delivery systems provide enhanced drug delivery as they can penetrate deeper into tissues, provide increased diffusivity, lack immunogenicity, and have the ability to target specific tissues (Koutsopoulos 2012; Su and Kang 2020). Particle size, zeta potential, cationic surface charge, and solubility of nanoparticles are factors that affect their biocompatibility. These factors influence cytotoxicity, clearance process (kidney or biliary), clearance by the mononuclear phagocyte system/reticuloendothelial system, and enhanced permeability and retention (Parveen et al. 2012; Zamboni et al. 2012). Drug delivery systems are designed

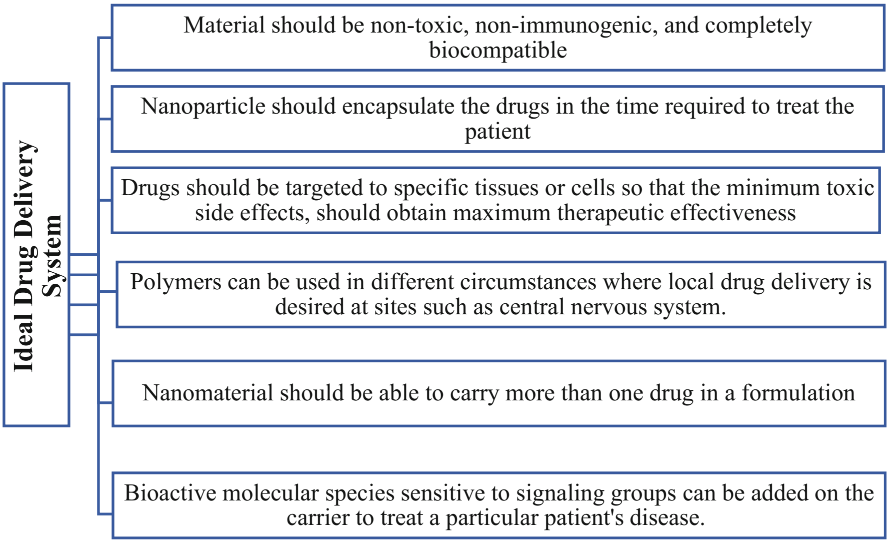
Ideal Drug Delivery System
Material should be non-toxic, non-immunogenic, and completely biocompatible
Nanoparticle should encapsulate the drugs in the time required to treat the patient
Drugs should be targeted to specific tissues or cells so that the minimum toxic side effects, should obtain maximum therapeutic effectiveness
Polymers can be used in different circumstances where local drug delivery is desired at sites such as central nervous system.
Nanomaterial should be able to carry more than one drug in a formulation
Bioactive molecular species sensitive to signaling groups can be added on the carrier to treat a particular patient's disease.

Fig. 24.1 Drug delivery system (2)

to transport a pharmaceutical compound throughout the body and release the therapeutic dose. In these systems, with nano-encapsulation of the active compound, its physicochemical and enzymatic degradation decreases and its bioavailability increases, and its undesirable side effects decrease (Felice et al. 2014; Vega-Vásquez et al. 2020).

The properties of ideal drug delivery systems are given in Fig. 24.1 (Koutsopoulos 2012; Vega-Vásquez et al. 2020).

Nanoscaled materials have chemical, physicochemical, and immunological responsive biological properties. Biodegradable nanomaterials are materials that can naturally degrade in the body under biological conditions (Su and Kang 2020). Biodegradable synthetic polymers are chosen as prosthesis materials for medical device development, scaffolds for tissue engineering, and controlled release medication delivery systems. To provide successful therapies, all of these applications require polymers with well-defined physical, chemical, biological, biomechanical, and degrading properties (Koutsopoulos 2012; Han et al. 2018; Su and Kang 2020).

2 Common Nanobiomaterials for Drug Delivery and Nanomedicine Applications

It is possible to develop controlled release rate, drug targeting, alternative administration methods, and delivery routes with polymer-based nanomaterials. In the future, polymer-based nanomaterials offer a great deal of potential for developing new vaccines and medication systems for vaccination antigens and pharmaceuticals (Han et al. 2018).

In addition, new drug systems involving biomolecules are being developed in the field of nanobiotechnology by utilizing the physical, mechanical, and catalytic properties of nanomaterials. For example, efforts are being made to create nano-bio-conjugates with nanomaterials together with antibodies and enzymes to facilitate drug delivery to the target, for in vivo imaging, and to overcome the challenges associated with modern healthcare applications (Mahato et al. 2020).

Since these systems frequently show similarity in their size and structure to natural carriers such as viruses and serum lipoproteins, they offer specific properties in drug delivery approaches. Furthermore, the multifunctionality with detectable surface groups and specific drug release mechanisms could be followed by additional improved interactions with specific cells and drug concentration in cells. Thus, polymeric systems play an important role in drug and gene delivery (Qiu and Bae 2006; Han et al. 2018).

2.1 Polymeric Biomaterials

As many nano-sized drug delivery systems have been prepared, the importance of polymer structure–property relationships has been increasingly understood and highlighted. Polymer architecture defines the nature of a single polymer molecule, which defines its physicochemical properties. Polymers selected for drug delivery applications are generally classified due to chemical structure, biodegradability, and water solubility. While polymer selection is a major concern, mainly with regard to compatibility with the active substance, the production process needs to be considered as well, since the additives used during polymerization cause drug degradation (Pillai and Panchagnula 2001). Commonly used polymers that have been inspected for drug-delivery applications are given below.

2.2 Fibrin

Fibrin is a type of natural biopolymer involved in blood coagulation steps. Fibrin can be isolated from the patient’s own blood and considered as an effective biomaterial for personalized treatments (Vedakumari et al. 2013).

Fibrin particulates were studied as a drug delivery system for treatment of diseases including cancer as fibrin layers and implantable fibrin gels. Fibrin has outstanding biocompatibility and biodegradable properties and therefore can be used as a matrix for tissue regeneration. Additionally, fibrin has been used as a drug delivery system for controlled release over a prolonged period. Fibrin scaffolds were loaded with platelet-produced growth factors and neurotrophin-3 to stimulate the proliferation and differentiation of embryonic stem cell-derived neural progenitor cells, while fibrin gels with recombinant transforming growth factor beta-1 addition displayed regulated release behavior. Moreover, fibrin sealed implants were studies to treat osteomyelitis. Fibrin nanocarriers provided a suitable system for the controlled release of antibiotics and a convenient method for delivering antibiotics to orthopedic infections. Also, Fibrin nanocarriers have been loaded with chemotherapeutic drugs and have been shown to not cause significant toxicity in vivo. Therefore, fibrin nanocarriers can be used as potential vehicles for drug delivery applications (Vedakumari et al. 2013).

2.3 Silk Fibroin

Silk fibroin is a protein-based biomaterial consisting of amino acid repeats with a repeated sequence of six residues of Gly-Ala-Gly-Ala-Gly-Ser. It is generally used as biomaterial due to its capacity to achieve slow and prolonged drug delivery in the form of films, three-dimensional scaffolds, hydrogels, electrospun fibers, and nanoparticles. Additionally, silk fibroin can be used to deliver genes like other natural proteins. The pH- and temperature- dependent phase behavior of fibroin makes it an exciting system for drug delivery approaches (Kundu et al. 2010; Jacob et al. 2018).

2.4 Collagen

Collagen characterizes the main structural protein that makes up about 30% of all vertebrate body protein. Different types of collagen are required to impart different biological properties to distinct types of body connective tissues. The use of collagen as biomaterial has been enabled by the development of methods for obtaining medical grade animal collagen and, more recently, methods for producing collagen from a patient’s own cells (Purcel et al. 2016).

Collagen has been considered a biocompatible and non-immunogenic polymer. However, it is not clear whether collagen is non-immunogenic or not. Proper cleaning and sterilization with detergents is usually sufficient to reduce the collagen immune response. But xenogeneic collagen can trigger the cross-reactivity of human antibodies targeting animal-derived collagen to human collagen in susceptible humans, resulting in organ damage or autoimmune diseases.

Collagen is the main protein of musculoskeletal and skin tissues, and this is the most abundant protein found in the human body. Collagen is used in drug delivery systems in various shapes and types, with a variety of protein meshes, nanoparticles, films, hydrogels, and rods using protein-based platforms. Drug release from inflated collagen matrices is primarily mediated by diffusion, but enzymatic matrix breakdown and hydrophobic drug–collagen interactions also play a role. Water uptake was inhibited by chemically cross-linked collagen structures, extending drug release (Koutsopoulos 2012).

2.5 Albumin

Albumin is a macromolecular protein that has been presented to be biodegradable and non-toxic with a non-immunogenic profile, and is therefore a perfect candidate for the preparation of nanoparticles.

Encapsulation of drugs into albumin nanoparticles is an important strategy, as various types of drugs can be encapsulated into the particle matrix owing to the diverse drug binding sites present in the albumin molecule. Because of the distinct albumin primary structure and high content of charged amino acids, albumin nanoparticles can permit the electrostatic adsorption of anionic or cationic molecules without the addition of any other chemicals (Elzoghby et al. 2012a). Albumin nanoparticles are used for treating several conditions including burns, surgery or trauma, cardiopulmonary bypass, acute respiratory distress, and hemodialysis. Moreover, the albumin nanoparticle is an acceptable carrier for many chemopreventive drugs and antibiotics, such as ciprofloxacin (Kratz 2008).

3 Polysaccharide-Based Biomaterials

3.1 Pullulan

Pullulan is a linear homopolysaccharide of glucose produced from starch by strains of the fungus *Aureobasidium pullulans*. The unique linkage configuration of pullulan provides the polymer with unique physical characteristics, such as adhesive properties and film formation, which is important for mucosal/transmucosal drug delivery. Furthermore, the structure of pullulan is described as α-(1 → 6) linked maltotriose. It is assumed that pullulan is biodegradable and it is mentioned in studies that pullulan has been used for carrying drugs and genes, mostly using hydrophobic derivatives. Pullulan-based nanoparticles can adhere to the nasal epithelium, which is an important property regarding mucosal administration. Akiyoshi et al. studied pullulan hydrogel nanoparticles (20–30 nm) synthesized to encapsulate and release insulin. Insulin spontaneously and easily formed a stable colloid system by forming complexes with pullulan carrying hydrophobized cholesterol with hydrogel nanoparticles (Akiyoshi et al. 1998).

In another study, Gupta et al. found a methodology for the delivery of encapsulated nucleic acids (~ 50 nm) and genes in pullulan hydrogel nanoparticles. The methodology may be useful in personalized cancer treatments with sequenced genomes and defined targets (Gupta and Gupta 2004).

3.2 Chitosan

Chitosan is the main component of crustaceans such as crabs, shrimps, lobsters, and shrimp in chitin form that can be converted to chitosan by alkaline deacetylation. Chitosan is a highly biodegradable and biocompatible biomaterial, with great potential for use in pharmaceutical applications such as high drug encapsulation, non-toxicity, and bioadhesion.

Chitosan can electrostatically connect to a negatively charged protein or plasmid DNA to produce polymer composites that protect protein and DNA from degradation, making it a good adjuvant or carrier. Chitosan also has strong adsorption, permeability, and moisture retention properties (Kumar 2000).

Chitosan nanoparticles were generally synthesized by ionotropic gelation of chitosan bound to tripolyphosphate. This process involves adding an alkaline tripolyphosphate solution (pH ~ 8) to an acidic chitosan solution. Mixing these solutions results in the direct formation of cationic chitosan nanoparticles (300–400 nm). The drug-loaded chitosan nanoparticles can be prepared by mixing the drug with tripolyphosphate solution and then adding the mixture to the chitosan solution with continuous stirring. The characteristic bioadhesion properties of chitosan allow for greater absorption of the drug from the gut through the epithelial layer.

The blood–brain barrier permeability of drug-loaded chitosan nanoparticles through intranasal administration was also studied and a significant amount of the drug was detected in the CNS. Moreover, delivery of peptide, dopamine, and caspase inhibitors via the blood–brain barrier has been observed following systemic administration by using chitosan nanoparticles. These results suggest that brain cancer patients may benefit from incorporating anti-cancer drugs into chitosan nanoparticles (Bugnicourt and Ladavière 2016).

3.3 Alginate

Alginate-based nanoparticles are another type of nanomaterials. Alginic acid is a negatively charged material consisting of α-l-glucuronic acid and β-d-mannuronic acid. Alginate is a biocompatible and gel-forming agent in the presence of divalent cations such as calcium ions and shows low toxicity, biocompatibility, and relatively low cost. Moreover, alginate nanoparticles can be prepared with sodium alginate in methylcellulose cross-linked with glutaraldehyde (Augst et al. 2006). Gelation under gentle conditions allows encapsulation and release of the sensitive bioactive drug molecule. Research on alginate has been focused on the development and application of alginate particles, which is one of the most commonly used polymers for the formation of hydrogel particles. For instance, various antimicrobial drugs were incorporated in the alginate nanoparticle formulation and showed that the bioavailability of the drugs in alginate nanoparticles was increased in comparison to free drugs (Koutsopoulos 2012; Paques et al. 2014).

3.4 Cellulose

Cellulose is found in wood, plants, marine animals, algae, and bacteria and is the most abundant natural resource on the planet. Acid hydrolysis, enzyme treatment, mechanical disintegration, and chemical reactions can all be used to make cellulose nanoparticles. Moreover, nanoprecipitation methods can be used for the preparation of cellulose nanoparticles (Li et al. 2015). There has been great interest in cellulose nanoparticles for various uses such as in cosmetics, foods, electronics, and drug delivery systems because of their unique properties. Nevertheless, studies on the preparation of cellulose nanoparticles are rare as compared to chitosan, alginate, and dextran nanoparticles. Cellulose nanoparticles can be prepared by hydrolysis of cellulose with concentrated sulfuric acid with a particle size around 100 nm. However, sulfuric acid is a very corrosive reagent, and therefore it is important to use special reactors, which are not suitable for large-scale production of these nanoparticles. Moreover, the size of the particles cannot be precisely controlled by this method (Chin et al. 2018).

3.5 Starch

Starch is a biomaterial with an anhydrous glucose unit that is usually accumulated in the unique and independent granules. Starch nanoparticles can be prepared using acid hydrolysis and enzyme hydrolysis. These nanoparticles show crystalline properties with renewability and biodegradability. Starch has a wide application in drug delivery owing to its distinctive physiochemical and functional properties. This biomaterial can be isolated from natural sources and generally used as a controlled drug delivery system and for bone repair and replacement. The surface area of starch microspheres increases, the adsorption capacity of functional groups increases, the adsorption equilibrium time decreases, and the slow release effect and colloid stability become more obvious (Morán et al. 2013; Kim et al. 2015; Han et al. 2018).

3.6 Self-Assembling Peptides

Self-assembly is universal in nature and defines the spontaneous organization of various distinct units into exact structures. Molecular self-assembly can be explained by association of peptides through non-covalent linkage. Separately, these interactions are weak; however, their enormous amounts will control the structural and conformational behavior of the assembly (Kyle et al. 2009).

Peptide hydrogels are ideal for use in nanomedical applications as they are easy to use, non-toxic, non-immunogenic, non-thrombogenic, biodegradable, and can be applied to localized treatments by injection into a specific tissue. The incorporation of a group of some peptides consisting of hydrophobic and hydrophilic amino acids into electrolyte solution results in the spontaneous formation of 10–20 nm diameter nanofibers. The scaffolds of self-assembling peptide scaffolds are biocompatible, and they can be used for different applications such as tissue engineering applications including bone-cartilage reconstruction, heart tissue regeneration, and angiogenesis due to their coherent molecular design (Rajagopal and Schneider 2004).

These nanofibers combine to form highly hydrated hydrogels with 5–200 nm pore sizes. In addition to their conventional hydrogel properties, peptide hydrogel offers high safety properties as it does not contain toxic chemicals (solvents, cross-linkers) and its degradation products are natural amino acids.

Peptide nanofibers, hydrogels, drug molecules like growth factors, and antibodies can be used for the delivery of proteins with therapeutic properties. This drug delivery is intravenous since transition from gel to liquid occurs during the interaction of peptide solution with biological fluids containing the electrolytes. The release pattern of self-assembling peptides can be changed from days to months depending on the size of the protein or drug compound of any peptide concentration that characterizes the peptide nanofiber density of the hydrogel (Kyle et al. 2009).

3.7 Inorganic Nanobiomaterials

Inorganic materials, as well as metal, silica, and carbon-based materials, have been developed and used in various fields such as energy, technology, and medicine. However, not all inorganic materials can be employed in drug delivery applications since most of them have poor biocompatibility, insufficient drug loading, excessive toxicity, and unpredictable breakdown kinetics. Only silica, carbon, a few metal oxides, metal -organic framework (MOF), and hydroxyapatite have previously been employed as drug delivery methods (Zou et al. 2021).

Inorganic biomaterials are generally used for bone applications, for example, osteomyelitis. Osteomyelitis treatment requires removal of unhealthy bone tissue and application of antibiotics to eliminate any infection caused by bacteria. Intravenous or other drug administration routes may not be effective due to chronic ischemia of necrotic bone and soft tissue. Hence, to achieve the wanted antibacterial effect, it is important to provide a relatively high dose of antibiotics without toxic side effects for a long time. A localized controlled drug delivery device is advantageous because it reduces the systemic toxicity and adverse effects of parenteral antibiotics while also increasing efficiency by delivering higher medication dosages to infected tissue (Zhou and Lee 2011; Koutsopoulos 2012; Alizadeh-Osgouei et al. 2019). The antibacterial activity control of the antibiotic-loaded hydroxyapatite-based drug delivery system prepared for this purpose is shown in Fig. 24.2.

Hydroxyapatite-based drug delivery systems were formulated in order to treat bone diseases, and biomaterial was formulated to suit the size and shape of the diseased bone tissue in specific diseases. Likewise, hydroxyapatite-based drug delivery systems were loaded with several drugs for infections or to increase bone tissue regeneration. The selection of hydroxyapatite for many dental and orthopedic applications was due to this inorganic material being one of the components of bones and teeth, and hydroxyapatite is the most thermodynamically stable phase in a precipitating solution of calcium phosphates (Zhou and Lee 2011; Koutsopoulos 2012; Alizadeh-Osgouei et al. 2019).

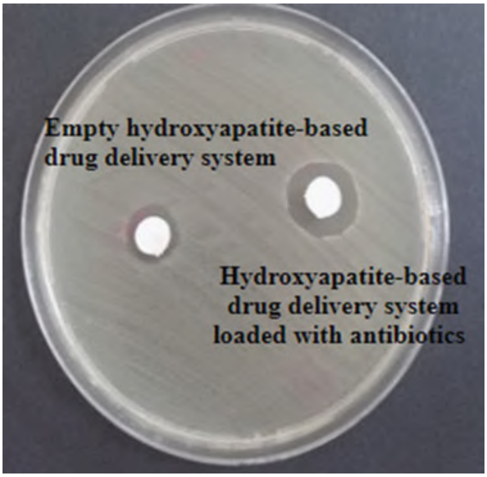
Empty hydroxyapatite-based drug delivery system
Hydroxyapatite-based drug delivery system loaded with antibiotics

Fig. 24.2 Hydroxyapatite-based drug delivery system loaded with antibiotics of antibacterial activity

4 Applications in Nanomedicine and Drug Delivery

Nanobiomaterials are currently in the growth phase in terms of both product variety and number, and in the field of nanomedicine and drug delivery more recently. Most of the patents of these materials in nanomedicine belong to the drug delivery systems. Common applications of nanomaterials are given below.

4.1 Topical Applications

Apart from cosmeceuticals, sunscreens, shampoos, toothpastes, medical diagnostic devices, topical epidermal/transdermal drugs, and parenteral drugs applied under the skin are included in this field. Our knowledge about the safety of nanomaterials released into the environment through these products is limited. In terms of dermatological applications, nanobiotechnological tools can be evaluated in three broad groups: drug delivery systems, diagnostic devices (sensors), and therapeutic devices.

The skin, which is the largest organ of the body, allows many local and parenteral applications. Control of the shape and size of the nanomaterials allows them to be used for human diagnosis and/or therapeutics. For human use (although veterinary practice should not be ignored), it is important to use biologically acceptable materials.

Topical formulations can be used to treat a problem, and to improve treatment, smoothness, softness, stickiness, congestion, and skin hydration. To increase the bioavailability and residence time of the drug, various approaches have been developed to address nanotechnology aspects of absorption or penetration. The main advantages of using and incorporating nanocarriers are related to the capacities of conventional formulations (Elzoghby et al. 2012b).

Encapsulating or incorporating water-soluble molecules, the preservation of drugs results from chemical and physical degradation and provides a controlled release, avoiding repeated administration and providing greater patient compliance (Kamaly et al. 2016).

The most commonly applied nanobiomaterials for topical applications are liposomes, solid lipid nanoparticles, nanoemulsions, polymeric nanoparticles, hydrogels, and microneedles (Severino et al. 2016).

One aim is to use nanosensors at cellular or subcellular level diagnostically (Pelaz et al. 2017). For this purpose, the use of nanotechnological chips has been proposed. These chips can be designed to analyze DNA, proteins, or immunoassays. Nanoparticles (NP) can also be shaped as follower devices beyond being just detectors, by attaching to stem cells, bacteria and viruses, and normal and malignant cells. Such a follow-up may even reveal malignant transformation. The blockade of this activation may allow the development of a new treatment modality.

Due to the nanoscale of the tools used, even single cell behaviors and molecular pathways can be studied in detail, which can allow important developments in basic sciences. Probes used prior to nanotechnology were too large to allow direct observation without significant changes in these chemical processes. An important method that has been used is gold NPs. These particles can be attached to DNA up to 10 nm in size. The easy recognition of gold allows millions of different DNA sequences to be followed at the same time (Hung et al. 2010).

Quantum dots are inorganic fluorides (chemical compounds that reflect light and fluorescence upon excitation), and due to their size, they can enter cells or attach to the surface without affecting normal cellular processes. By attaching CNs to normal and tumoral cells, it is possible to reveal the physiology of both types of cells and to detect the differences in their processes. Quantum dots can also be used for real-time detection of viruses and bacteria (Zhang et al. 2008). This may be of great importance for rapid diagnosis, especially in patients who require immediate treatment selection. Another possible use could be in bioterrorism, where small amounts of toxin need to be detected.

Apart from these uses, NPs can provide precise determination of intracellular and extracellular ions (Na, K, Cl, and Ca), oxygen, OH radicals, and even singlet oxygen level. Various options are available to create NPs of different shapes, sizes, and materials that can affect organic processes. Today, most of the oncological research aims to generate NPs that can bind to cells and specific receptors in specific regions. In most of these initiatives, the main target is the direct transfer of pharmaceutical agents such as chemotherapeutics to the malignant target tissue. The aim is to ensure high efficiency at the targeted point while protecting the surrounding tissue. In addition to malignant cells, premalin cells and abnormal pathways expressing abnormal proteins can also be identified and targeted in this way. Gold NPs can be heated with light energy to create the effect of tumoricidal hyperthermia (Jiménez-Jiménez et al. 2020).

As nanotechnology progresses, nanobots can be made that can display the abnormality, detect it, and then correct it. For this, a feedback line is needed to complete the required treatment process. In terms of the created module, it is possible to eliminate malignancy and infections and develop a regenerative medical process with nano-sized particles. It is a natural result to use NPs as photosensitizers. Photosensitizers used as IV cannot travel very far before the body detects and attaches to them. Binding usually occurs with albumin or low-density lipoprotein. The NP-protein complex is either phagosylated by macrophages or these NP-protein complexes continue their journey in the blood. In most commercial products therapeutics are encapsulated in lipoproteins, primarily very low-density lipoprotein. Since fats and proteins are required for the high metabolic activities of malignant cells and normal cells with rapid turn-over, this encapsulation process is a rational way to target these regions (Senapathy et al. 2020).

4.2 Ophthalmic Applications

The eye is one of the most isolated organs within the body. Numerous barriers such as the cornea, blood–aqueous barrier, blood–retina barrier, and physiological clearance mechanisms such as the blinking reflex and the nasolacrimal drainage system limit the entry of foreign materials into the eye. Nanobiomaterials, especially hydrogels, are used as drug delivery systems to various segments of the eye. Moreover, these systems were formulated to enhance bioavailability of drugs, which is low in many conventional ophthalmic formulations. Invasive methods for ocular drug delivery can increase the bioavailability of drugs; however, intravitreal injection may lead to side effects such as vision loss. To avoid side effects, ophthalmic drug delivery systems should control the drug release to establish an ideal drug concentration over a prolonged period of time and target the drug to a specific tissue and offer patient-friendly applications.

Several polysaccharide nanobiomaterials-based systems have been studied for the treatment of ocular diseases. For instance, cyclosporine A-loaded chitosan nanoparticles have been prepared and it was revealed that the nanoparticles showed promising results in the treatment of dry eye syndrome and conjunctivitis. Chitosan is one of the most suitable polymers for ocular diseases as it is hydrophilic and biodegradable. Moreover, chitosan enhances permeation from the ocular barrier and improves bioavailability.

Because of the small sizes of nanobiomaterial carriers, vitreous barrier permeability of drugs is highly increased, which results in an increase in the rate of drug administration to rear tissues.

Depending upon the bioadhesive characteristics shown by various types of nanoparticles used in nano drug carriers, retention of drug delivery systems in targeted tissues can be significantly prolonged. Nano drug delivery systems developed using nanobiomaterials can be applied as eye drops that require fewer repeated applications because of the greater retention of drugs in the eye, reducing the application cost and improving patient compliance. However, several types of drug delivery systems cannot be applied as ophthalmic delivery systems because the particle size of ocular drug delivery systems must be smaller than 10 μm to prevent scratching of the eye and vision treatment (Zimmer and Kreuter 1995; Liu et al. 2012). Various nanobiomaterial-based ophthalmic drug delivery systems are listed below.

Micellar drug delivery systems are self-assembled nanoparticles from different types of materials which are generally used for the encapsulation of water-insoluble drugs. Micellar drug delivery systems can be produced by the self-assembly method, which includes nanoprecipitation, dialysis, or emulsion.

Micelles have been studied for enhancing the ocular permeability of various drugs and it has been shown that the permeability of drugs was improved compared to drugs in solution form. Studies show that micellar drug delivery systems have potential not only in increasing the stability by encapsulation of drugs, but also in enhancing the drug permeability through different ocular barriers (Liu et al. 2012).

Moreover, biodegradable and biocompatible biomaterials are preferred to avoid adverse effects of the micellar drug carriers on physiological systems. The chitosan-based amphiphilic copolymer synthesized by Qu et al., quaternary ammonium-almitoyl glycol chitosan (GCPQ) micellar nanoparticles, showed up to 20–200 times higher encapsulation of hydrophobic drugs compared to Pluronic block copolymers. Also it was shown that after ocular administration of GCPQ loaded with prednisolone, the bioavailability of prednisolone increased ten-fold compared to an emulsion formulation of prednisolone (Qu et al. 2006). Hydrogel colloids are defined as water-soluble networks protecting 3D structures despite absorbing more than 20% of their weight. As hydrogels can be produced from any hydrophilic material, the chemical and physical characteristics of hydrogels can be tailored by changing the porosity of polymer hydrogel networks in matrices, by changing the cross-link density, or by using external stimulants such as pH or temperature to control the diffusion of drugs within the matrix.

Chitosan was studied for a wide variety of applications because of biocompatible, biodegradable, bioadhesive, and non-toxic characteristics. As a result of sustaining the release of the delivery system in mucin layer and also further increasing the duration of drug activity, the mucoadhesion is essential for ophthalmic drug delivery systems. The release of a drug from the biomaterial-based drug delivery system is dependent on the chitosan content in prepared hydrogels. Moreover, in situ gelling systems were also prepared by addition of different polymers to chitosan gel systems. Subsequently, because of application to the physiological environment, the solution undertakes gelation to form a hydrogel in which the drug is trapped and slowly released through the gel by diffusion. Lipid chitosan complex was also studied for enhancement of cellular uptake in the pre-corneal sections. The higher cellular uptake conjunctiva showed that the prepared nanoparticles primarily trapped by the mucus layer and permeation occur through the conjunctival cells. However, studies showed that precipitate can occur in chitosan particles which is close to physiological pH. A modified version of chitosan can be used to solve the sedimentation problem (Diebold et al. 2007).

An increase in the rate of absorption into the ocular cavity through corneal membranes and therapeutic superiority of topical application of nanomaterial/drug complexes targeting the posterior segments of the eye in comparison with intravitreal or periocular injection has not been proven to date. However, owing to the nature of the eye, it is expected that nanomaterial-based drug delivery systems can be used to overcome the major problems caused by the ocular barriers. Although the biocompatibility and biodegradability of nanobiomaterials studies have shown that the prepared nanoparticles do not show irritation or inflammation in the target zone, the long-term stability and effect of these nanomaterials must be analyzed both in the ocular zone and systemic circulation (Zimmer and Kreuter 1995; Liu et al. 2012).

4.3 Orthopedic Applications

There is a significant interest in orthopedic drug delivery and bone regeneration since these are linked to increased life expectancy. Consequently, studies on bone-related medical treatments and drug delivery systems are increasing. The main purpose of orthopedic research is the selection of the optimum biomaterial which supports cell and tissue growth (Christenson et al. 2007).

Tissue engineering is a promising alternative for regenerating damaged organs, and the success of orthopedic bone implants depends on the biomaterials used. Various synthetic structures were originally prepared to impart bulk properties to the structure, such as sufficient mechanical strength and bearing properties for cell infiltration and tissue organization. While some of these materials closely resemble the characteristics of bone tissue, the structures failed before complete healing occurred. The achievement of successful therapy depends on both the material of the orthopedic implant and the tissue surrounding it. Insufficient tissue regeneration around the biomaterials due to poor surface interaction with tissue causes implantation failure.

Nanoscale protein interactions in natural tissues play a crucial role in controlling cell functions such as proliferation, extracellular matrix production, and migration. Protein adsorption properties depend on the surface properties (roughness, load, chemistry, wettability) of the implanted biomaterials. The particle size of the material affects the relevant protein interactions and surface properties. Studies showed that nanoscaled materials can enhance the adsorption of proteins. In addition, the function of osteoblasts was increased with nanobiomaterials such as fibronectin, vitronectin, laminin, and collagen compared with micron-sized materials.

The extracellular matrix of bone consists of the inorganic biomaterial calcium phosphate, which is similar to hydroxyapatite. As a natural inorganic-based biomaterial, calcium phosphate ceramics show good biocompatibility and they are capable of bonding with the bone. However, their insufficient mechanical properties make them less important for orthopedic use. Hence, calcium phosphate is generally used for coating of metallic implants. Various techniques for preparing calcium phosphate coatings on metals are available, such as plasma sputtering, biomimetic deposition, laser deposition, ion beam deposition, radiofrequency magnetron sputtering deposition, and electrostatic sputtering deposition. However, the most common technique for preparation of calcium phosphate-coated materials for orthopedic and dental use is plasma sputtering. Interestingly, calcium phosphate coatings can be combined with active substances. By using this property, the coating also increases the activity of biomaterial and decreases the infection risk caused by bacteria (Christenson et al. 2007; Szurkowska et al. 2018).

Another coating technique, electrostatic sputtering deposition, helps calcium phosphate to increase the interaction with proteins due to its porous nature. The interaction between proteins and cell receptors increases cell behavior. Moreover, the higher surface area improves the drug delivery potential of calcium phosphate coatings, and the particles can be prepared by electrostatic sputtering deposition.

Other than calcium phosphate, alumina, titania, and hydroxyapatite-based ceramics were also evaluated for their adhesion behaviors. It was revealed that nano-sized particles show higher adhesion with osteoblasts when compared with conventional (micron grain-sized) ceramic formulations. Moreover, enhanced osteoblast functions were found with ceramic particles at sizes below 60 nm (Christenson et al. 2007).

Another design parameter regarding orthopedic nanomaterials is the particle aspect ratio. Combined substrates formulated from nanofibrous alumina (diameter: 2 nm, length >50 nm) showed a significant increase in osteoblast function in vitro compared to similar alumina substrates formulated from nanospheric particles (Price et al. 2003).

Nanophase metals and polymers are another type of nanomaterial which supports the functions of ceramics on bone cells. Additionally, bone cell adhesion can be enhanced using nanophase materials. Research has shown that nanophase materials such as selenium improved the osteoblast functions when compared with traditional biomaterial. Due to selenium having an anti-cancer effect, it was found that the prepared nanophase material can also be used for implants in the treatment of bone cancer.

Along with the hydroxyapatite-collagen biomaterials, nanocomposite bone substitutes can be used for the replacement of bone due to the fact that this biomaterial can mimic natural bone in composition and structure. Hydroxyapatite can facilitate higher osteoconduction and related functions, and these functions can be enhanced using hydroxyapatite in nano-sized rather than conventional material. Nevertheless, hydroxyapatite is a non-osteoinductive material and shows slow biodegradation properties. The disadvantages of hydroxyapatite can be overcome by combining it with collagen. Collagen is a biodegradable biomaterial that can be used to osteoblast cellular systems. The biomaterial can support cellular adhesion and proliferation in prepared nanomaterial systems (Kikuchi et al. 2001).

Nanofiber matrices show incredible potential as tissue engineering scaffolds for bone regeneration. They are mainly suitable to use as bone scaffolds because of their continuous structure. After administration, nanofibers promote a biomimetic environment and the matrix affects the interaction of surrounding cells. Nanofibers also show morphological properties which are similar to the extracellular matrix. It has been shown that nanofiber scaffolds can support the osteogenic differentiation of mesenchymal stem cells (Christenson et al. 2007).

4.4 Dental Applications

The oral cavity is one of the gateways to the biological system. In this region many different bacteria can occur, and the existence of bacteria can lead to various dental diseases. Various biomaterials have been used to treat these diseases; however, treatment efficiency is dependent on the materials used. To improve treatment efficiency, nanoparticles can be used either directly or by incorporating into materials. The unique characteristics of biomaterials such as (i) improved stability in biological environment, (ii) ease of preparation even at large scales, and (iii) controlled release of the active substance of nanoparticles make them an ideal vehicle for dental applications (Elizabeth et al. 2019).

Nanomaterials have been used for carrying drugs in the treatment of dental disorders such as in restoration of tooth decay, remineralization of teeth, and treating infections in the oral cavity. For this purpose, various types of nanomaterials including nanocrystals, nanocomposites, and nanocapsules have been used. For instance, inorganic biomaterial substituted with hydroxyapatite can be used to increase dentin sensitivity and inhibition of tooth decay.

Administration of nanobiomaterials in nanocrystal form is another type of approach in dentistry. Prepared nanoparticles can be formulated as solutions, suspensions, gels, oils, and solid dosage forms. Nanocrystals improve the effect of drugs due to their small sizes, which increases the penetration of drugs into dentinal tubules.

Metal nanoparticles are commonly used as dental material both as pure metal and in a compound form. Silver nanoparticles are used in dental implants, cements, intraoral devices, and drug formulations due to their antimicrobial effects. Metal oxide particles have significant dental effects. Joy et al. reported the antibacterial activity of zinc oxide nano-sized particles added in a resin-based formulation with 10% w/w via the reduction of biofilm growth or accumulation of plaque. The other effects attributed to the metallic nanoparticles are the provision of aesthetically appealing surface appearance, increased power and low polymerization shrinkage, as well as anti-plaque and anti-odor effects.

Silica nanoparticles are widely used in dentistry, especially in toothpastes. Principally, these biomaterials are non-toxic and non-irritating in oral usage. Silica can increase the surface hardness and rheological behavior of formulations. Moreover, the material shows better fixation of dental prostheses in nanoparticle form.

Periodontal diseases are the most common disorders for which nanoparticles are used in dentistry. In these diseases. Periodontal disease is a term describing the pathologic condition which is explained by the degeneration and inflammation of the tissues, periodontal ligament, alveolar bone, and dental cement surrounding and supporting the teeth. The purpose of periodontal disease treatment is to inhibit re-infection of the treatment region by periodontopathic microorganisms, and therefore to remove bacteria or dental plaque on the tooth surface with adequate oral hygiene and mechanical treatment to protect the tooth. Periodontal infections can be managed by local or systemic application of various antibiotics. However, several side effects such as microbial resistance, depression, and tachycardia can be observed, and after systemic drug administration, therapeutic concentrations can be observed for only a short period. Thus, repeated doses are required to extend the therapeutic drug concentration. Conversely, the use of local antibacterial and antimicrobial drugs applied to the infected area can be advantageous in eradicating bacteria, therefore improving the effectiveness of conventional surgical treatment without the unwanted effects of systemically applied drugs. In addition to antimicrobial therapy, a regenerative therapy may be used to restore the damaged structures caused by periodontal diseases. Bone grafts, cements, or tissue regeneration can be used for regenerative therapy. Moreover, fibroblast growth factor, stem cell therapy, and photodynamic therapy can be used both in nanoparticle form and as conventional therapy (Elizabeth et al. 2019; Subramani and Ahmed 2013; Mirsasaani et al. 2012).

Owing to progress in biotechnology, it is possible to use growth factors and other peptide and gene therapies in wound healing and tissue regeneration. Chen et al. concluded that the drug delivery systems loaded with Growth Factors (GFs) should adequately increase the retention time of the drug in the treatment area to provide permission to tissue regenerating cells to emigrate to the injury site and change or eliminate the bioactivity loss. Moreover, characteristics such as easy application, targeted application, controlled release kinetics, and enhancement of cell/tissue permeability are desired (Chen et al. 2009).

Compared to microparticles, nanoparticles have certain benefits such as the penetration ability to the intracellular and extracellular domains, including periodontal pocket areas which are not reached by the other transmission systems due to their small size. Nanoparticle administration to the periodontal region maintains the effective drug release rate by providing an effective accumulation of active agents in the target area for a long time. Moreover, the stability of nanoparticles is better than conventional dosage forms in biological fluids (Elizabeth et al. 2019).

This shows that nanomaterial drug delivery can offer new approaches in preventive drug therapy in dentistry, especially in the treatment of bacterial biofilms and in eliminating tooth decay. A proteinaceous surface coating, a film called pellicle, is formed as a result of the exposure to oral fluids. Bacteria adhere to the pellicle and be colonized the surface of the teeth, then produce dental plaque. Plaque formation is described by bacterial interactions and progressively different bacterial populations. Biofilm formation can be reduced by anti-adhesive surface coatings. Moreover, abrasion-resistant nanocomposite surface coatings were produced and applied to the tooth surface to inhibit the pathogenic consequences of biofilm formation. The fluoro-polymer matrix loaded with inorganic nanoparticles also shows easy-to-clean surface properties which can be used in the protection of biofilm formation (Mirsasaani et al. 2012).

4.5 Wound Healing and Tissue Engineering Applications

Progress in material sciences revealed the use of new nanobiomaterials in wound healing and in special wound care. Soft nanotechnology, including the hydrogel scaffold and drug delivery systems, has been instrumental in wound management, complementing physicobiochemical and mechanical considerations (Singh et al. 2018).

Implantable tissues have been developed that are used in tissue engineering, in humans (e.g., skin and cartilage) or in clinical trials (e.g., bladder and blood vessels). Tissue engineering is based on the principle that cells seeded or harvested on three-dimensional biocompatible scaffolds can reassemble into functional structures resembling natural tissues (Shi et al. 2010).

The dimensional benefits of nanoparticles provide the chance to adapt to systemic circulation and permeation across cell membranes, and they concentrate and accumulate within the cytoplasm. They provide continuous drug release in target areas and can be stored for a longer time in the systemic circulation. The most important feature of nanomaterials for drug delivery originates from the easy and reliable surface modifications for specific tissue/organ targeting (Singh et al. 2018).

One of the most important advantages of nanomaterials is high surface/volume ratio. They can cover a large applied surface area. This feature offers a distinctive opportunity for the surface treatment process where a minimal amount of a drug is needed to cover a large area.

As extracellular matrix formation is the main route in morphogenesis, wound healing, growth, and fibrosis, it is essential to take into consideration extracellular matrix morphology and function when evaluating the design of nanobiomaterials for wound healing and restorative tissue management. Moreover, extracellular matrix-mediated cell signaling aids in the retention of different bioactive molecules such as fibrous proteins, Glycosaminoglycans (GAGs), growth factors, and cytokines, which are essential stages in tissue remodeling at wound sites.

Nano-hydrogels have been developed for wound healing and tissue repair. Nanobiomaterial-based hydrogels are hydrophilic and swallowable materials such as alginate, chitosan, agarose, chitosan, and fibrin. Designed hydrogels require a flexible material simulating the extracellular matrix (ECM). Such hydrated hydrophilic polymer networks often contain pores and void regions between the polymer chains, which can be conducive to improved supply of nutrients and oxygen for the cells. Hydrogels are designed for occlusive dressing, cartilage repair, injectable cellular scaffold, spinal cord injury axonal regeneration, and brain surgery for tissue sealants. The new strategy could be the design of a hydrogel-based bio-scaffold containing fibronectin functional domains and hyaluronan for tissue repair. Fibronectin containing hydrogel matrix helps in situ fibroblast migration, an important step for tissue generation for remodeling damaged tissue, as it is a tremendous environment to promote wound healing by binding with platelet-derived growth factors (Schwall and Banerjee 2009; Shi et al. 2010).

5 Conclusion

Up until now, there have been many studies showing that natural biomaterials are used as drug delivery systems. However, there are still some issues that must be solved. Primarily, a major portion of these studies are only formulation studies, or only in vitro results were evaluated. In addition, organic nanobiomaterials obtained from natural sources were used in many studies and the variation in the origin of the material was ignored. This situation can be overcome by using standardized recombinant nanobiomaterials for the drug delivery system instead of natural origin biomaterials with different variations. Peptide drugs can show low bioavailability and metabolic liability. Moreover, after oral administration, peptides degrade in the gastrointestinal tract. These drawbacks can be overcome by formulating these drugs into nanobiomaterial-based carriers. The prepared biomaterials sustain the drug release, which can be beneficial in several diseases. However, especially in treatments where sudden drug release is required, it is impossible to use these types of drug release systems. Therefore, in future, more studies should look at the suitable manufacture of biopolymers to achieve the desired type of drug release.

References

Akiyoshi K, Kobayashi S, Shichibe S, Mix D, Baudys M, Wan Kim S, Sunamoto J (1998) Self-assembled hydrogel nanoparticle of cholesterol-bearing pullulan as a carrier of protein drugs: complexation and stabilization of insulin. J Control Release 54:313–320

Alizadeh-Osgouei M, Li Y, Wen C (2019) A comprehensive review of biodegradable synthetic polymer-ceramic composites and their manufacture for biomedical applications. Bioact Mater 4: 22–36

Augst AD, Kong HJ, Mooney DJ (2006) Alginate hydrogels as biomaterials. Macromol Biosci 6: 623–633

Bugnicourt L, Ladavière C (2016) Interests of chitosan nanoparticles ionically cross-linked with tripolyphosphate for biomedical applications. Prog Polym Sci 60:1–17

Chen F-M, Shelton RM, Jin Y, Chapple ILC (2009) Localized delivery of growth factors for periodontal tissue regeneration: role, strategies, and perspectives. Med Res Rev 29:472–513

Chin SF, Jimmy FB, Pang SC (2018) Size controlled fabrication of cellulose nanoparticles for drug delivery applications. J Drug Deliv Sci Technol 43:262–266

Christenson EM, Anseth KS, van den Beucken JJP, Chan CK, Ercan B, Jansen JA, Laurencin CT, Li WJ, Murugan R, Nair L, Ramakrishna S, Tuan RS, Webster TJ, Mikos AG (2007) Nanobiomaterial applications in orthopedics. J Orthop Res 25:11–20

Diebold Y, Jarrín M, Sáez V, Carvalho ELS, Orea M, Calonge M, Seijo B, Alonso MJ (2007) Ocular drug delivery by liposome-chitosan nanoparticle complexes (LCS-NP). Biomaterials 28: 1553–1564

Elizabeth P-S, Néstor M-M, David QG (2019) Nanoparticles as dental drug-delivery systems. In: Nanobiomaterials in clinical dentistry. Elsevier, Amsterdam, pp 567–593

Elzoghby AO, Samy WM, Elgindy NA (2012a) Albumin-based nanoparticles as potential controlled release drug delivery systems. J Control Release 157:168–182

Elzoghby AO, Samy WM, Elgindy NA (2012b) Protein-based nanocarriers as promising drug and gene delivery systems. J Control Release 161:38–49

Felice B, Prabhakaran MP, Rodríguez AP, Ramakrishna S (2014) Drug delivery vehicles on a nano-engineering perspective. Mater Sci Eng C 41:178–195

Gupta M, Gupta AK (2004) Hydrogel pullulan nanoparticles encapsulating pBUDLacZ plasmid as an efficient gene delivery carrier. J Control Release 99:157–166

Han J, Zhao D, Li D, Wang X, Jin Z, Zhao K (2018) Polymer-based nanomaterials and applications for vaccines and drugs. Polymers (Basel) 10:1–14

Hung AM, Micheel CM, Bozano LD, Osterbur LW, Wallraff GM, Cha JN (2010) Large-area spatially ordered arrays of gold nanoparticles directed by lithographically confined DNA origami. Nat Nanotechnol 5:121–126

Jacob J, Haponiuk JT, Thomas S, Gopi S (2018) Biopolymer based nanomaterials in drug delivery systems: a review. Mater Today Chem 9:43–55

Jahangirian H, Lemraski EG, Webster TJ, Rafiee-Moghaddam R, Abdollahi Y (2017) A review of drug delivery systems based on nanotechnology and green chemistry: green nanomedicine. Int J Nanomedicine 12:2957–2978

Jiménez-Jiménez C, Manzano M, Vallet-Regí M (2020) Nanoparticles coated with cell membranes for biomedical applications. Biology (Basel) 9:1–17

Kamaly N, Yameen B, Wu J, Farokhzad OC (2016) Degradable controlled-release polymers and polymeric nanoparticles: mechanisms of controlling drug release. Chem Rev 116:2602–2663

Kikuchi M, Itoh S, Ichinose S, Shinomiya K, Tanaka J (2001) Self-organization mechanism in a bone-like hydroxyapatite/collagen nanocomposite synthesized in vitro and its biological reaction in vivo. Biomaterials 22:1705–1711

Kim HY, Park SS, Lim ST (2015) Preparation, characterization and utilization of starch nanoparticles. Colloids Surf B Biointerfaces 126:607–620

Koutsopoulos S (2012) Molecular fabrications of smart nanobiomaterials and applications in personalized medicine. Adv Drug Deliv Rev 64:1459–1476

Kratz F (2008) Albumin as a drug carrier: design of prodrugs, drug conjugates and nanoparticles. J Control Release 132:171–183

Kumar MNVR (2000) A review of chitin and chitosan applications. React Funct Polym 46:1–27

Kundu J, Chung YI, Kim YH, Tae G, Kundu SC (2010) Silk fibroin nanoparticles for cellular uptake and control release. Int J Pharm 388:242–250

Kyle S, Aggeli A, Ingham E, McPherson MJ (2009) Production of self-assembling biomaterials for tissue engineering. Trends Biotechnol 27:423–433

Li MC, Wu Q, Song K, Lee S, Qing Y, Wu Y (2015) Cellulose nanoparticles: structure-morphology-rheology relationship. School of Renewable Natural Resources, Louisiana State University AgCenter, Baton Rouge, Department of Forest Products, Korea Forest Research Institute, Seoul. ACS Sustain Chem Eng 3:821–832

Liu S, Jones L, Gu FX (2012) Nanomaterials for ocular drug delivery. Macromol Biosci 12: 608–620

Mahato K, Kumar A, Purohit B, Mahapatra S, Srivastava A, Chandra P (2020) Nanomaterial functionalization strategies in bio-interface development for modern diagnostic devices. In: Biointerface engineering: prospects in medical diagnostics and drug delivery. Springer, Singapore, pp 195–214

Martinho N, Damgé C, Reis CP (2011) Recent advances in drug delivery systems. J Biomater Nanobiotechnol 02:510–526

Mirsasaani SS, Hemati M, Tavasoli T, Dehkord ES, Yazdi GT, Poshtiri DA (2012) Nanotechnology and nanobiomaterials in dentistry. In: Nanobiomaterials in clinical dentistry. Elsevier, Burlington

Morán JI, Vázquez A, Cyras VP (2013) Bio-nanocomposites based on derivatized potato starch and cellulose, preparation and characterization. J Mater Sci 48:7196–7203

Paques JP, Van Der Linden E, Van Rijn CJM, Sagis LMC (2014) Preparation methods of alginate nanoparticles. Adv Colloid Interf Sci 209:163–171

Parhi P, Mohanty C, Sahoo SK (2012) Nanotechnology-based combinational drug delivery: an emerging approach for cancer therapy. Drug Discov Today 17:1044–1052

Parveen S, Misra R, Sahoo SK (2012) Nanoparticles: a boon to drug delivery, therapeutics, diagnostics and imaging. Nanomed Nanotechnol Biol Med 8:147–166

Patra JK, Das G, Fraceto LF, Campos EVR, Rodriguez-Torres MDP, Acosta-Torres LS, Diaz-Torres LA, Grillo R, Swamy MK, Sharma S, Habtemariam S, Shin HS (2018) Nano based drug delivery systems: recent developments and future prospects. J Nanobiotechnol 16:1–33

Pelaz B, Alexiou C, Alvarez-Puebla RA, Alves F, Andrews AM, Ashraf S, Balogh LP, Ballerini L, Bestetti A, Brendel C, Bosi S, Carril M, Chan WCW, Chen C, Chen X, Chen X, Cheng Z, Cui D, Du J et al (2017) Diverse applications of nanomedicine. ACS Nano 11:2313–2381

Pillai O, Panchagnula R (2001) Polymers in drug delivery Omathanu Pillai and Ramesh Panchagnula. Curr Opin Chem Biol 5:447–451

Price RL, Gutwein LG, Kaledin L, Tepper F, Webster TJ (2003) Osteoblast function on nanophase alumina materials: influence of chemistry, phase, and topography. J Biomed Mater Res – Part A 67:1284–1293

Purcel G, Meliţă D, Andronescu E, Grumezescu AM (2016) Collagen-based nanobiomaterials: challenges in soft tissue engineering. In: Nanobiomaterials in soft tissue engineering: applications of nanobiomaterials. William Andrew is an imprint of Elsevier, Oxford, UK, pp 173–200

Qiu LY, Bae YH (2006) Polymer architecture and drug delivery. Pharm Res 23:1–30

Qu X, Khutoryanskiy VV, Stewart A, Rahman S, Papahadjopoulos-Sternberg B, Dufes C, McCarthy D, Wilson CG, Lyons R, Carter KC, Schätzlein A, Uchegbu IF (2006) Carbohydrate-based micelle clusters which enhance hydrophobic drug bioavailability by up to 1 order of magnitude. Biomacromolecules 7:3452–3459

Rajagopal K, Schneider JP (2004) Self-assembling peptides and proteins for nanotechnological applications. Curr Opin Struct Biol 14:480–486

Schwall CT, Banerjee IA (2009) Micro- and nanoscale hydrogel systems for drug delivery and tissue engineering. Materials (Basel) 2:577

Senapathy GJ, George BP, Abrahamse H (2020) Exploring the role of phytochemicals as potent natural photosensitizers in photodynamic therapy. Anti Cancer Agents Med Chem 20(15): 1831–1844

Severino P, Fangueiro JF, Chaud MV, Cordeiro J, Silva AM, Souto E (2016) Advances in nanobiomaterials for topical administrations: new galenic and cosmetic formulations. In: Nanobiomaterials in galenic formulations and cosmetics. William Andrew, Kidlington, pp 1–23

Shi J, Votruba AR, Farokhzad OC, Langer R (2010) Nanotechnology in drug delivery and tissue engineering: from discovery to applications. Nano Lett 10:3223–3230

Singh AV, Gemmati D, Kanase A, Pandey I, Misra V, Kishore V, Jahnke T, Bill J (2018) Nanobiomaterials for vascular biology and wound management: a review. Veins Lymphat 7:2

Su S, Kang PM (2020) Systemic review of biodegradable nanomaterials in nanomedicine. Nanomaterials 10:656

Subramani K, Ahmed W (2013) Nanobiomaterials in clinical dentistry. William Andrew, Waltham

Szurkowska K, Laskus A, Kolmas J (2018) Hydroxyapatite-based materials for potential use in bone tissue infections. In: Hydroxyapatite – advances in composite nanomaterials, biomedical applications and its technological facets. IntechOpen

Vedakumari WS, Prabu P, Babu SC, Sastry TP (2013) Fibrin nanoparticles as possible vehicles for drug delivery. Biochim Biophys Acta – Gen Subj 1830:4244–4253

Vega-Vásquez P, Mosier NS, Irudayaraj J (2020) Nanoscale drug delivery systems: from medicine to agriculture. Front Bioeng Biotechnol 8:1–16

Zamboni WC, Torchilin V, Patri AK, Hrkach J, Stern S, Lee R, Nel A, Panaro NJ, Grodzinski P (2012) Best practices in cancer nanotechnology: perspective from NCI nanotechnology alliance. Clin Cancer Res 18:3229–3241

Zhang F, Xia Y, Xu L, Gu N (2008) Surface modification and microstructure of single-walled carbon nanotubes for dental resin-based composites. J Biomed Mater Res – Part B Appl Biomater 86:90–97

Zhou H, Lee J (2011) Nanoscale hydroxyapatite particles for bone tissue engineering. Acta Biomater 7:2769–2781

Zimmer A, Kreuter J (1995) Microspheres and nanoparticles used in ocular delivery systems. Adv Drug Deliv Rev 16:61–73

Zou Y, Huang B, Cao L, Deng Y, Su J (2021) Tailored mesoporous inorganic biomaterials: assembly, functionalization, and drug delivery engineering. Adv Mater 33:1–27

Metal Nanoparticles-Based Biomarkers for Clinical Diagnosis

25

Nazlı Şimşek, Niran Öykü Erdoğan, and Gözde Aydoğdu Tığ

Contents

1 Introduction 542
2 Metal Nanoparticles 543
  2.1 Synthesis Methods of Metal Nanoparticles 543
  2.2 Functionalization of Metal Nanoparticles 545
3 Specific Affinity Interaction Between Metal Nanoparticles and Biomolecules 547
  3.1 Electrochemical Detection Principles of Biomarkers Based on Metal Nanoparticles 547
  3.2 Gold Nanoparticles 547
  3.3 Silver 553
  3.4 Other Metal Nanoparticles 559
4 Conclusion 564
References 565

Abstract

The new functional nanomaterials and analytical technologies offer significant advancements for the clinical diagnosis of several biomarkers targeting diseases. Nanostructured metals have superior properties that provide extensive applicability in sensing configurations. Metal nanoparticles exhibit excellent physical and chemical properties by increasing detection sensitivities. Applying these nanoparticles in electrochemical sensing in place of conventional technologies has led to significant developments. Unique properties of metal nanoparticles, such as extremely high electrical conductivity, increased surface area, high electron mobility, small size (sufficient to interact with

---

N. Şimşek · N. Ö. Erdoğan
Ankara University, Graduate School of Natural and Applied Sciences, Department of Chemistry, Ankara, Turkey

G. A. Tığ (✉)
Ankara University, Faculty of Science, Department of Chemistry, Biochemistry Division, Ankara, Turkey
e-mail: gaydogdu@science.ankara.edu.tr

© Springer Nature Singapore Pte Ltd. 2023

U. P. Azad, P. Chandra (eds.), *Handbook of Nanobioelectrochemistry*,
https://doi.org/10.1007/978-981-19-9437-1_25

biological molecules), and stability, make them suitable for detecting biomarkers. Many promising metal nanoparticles, such as gold (Au), silver (Ag), platinum (Pt), palladium (Pd), and copper (Cu) and their bimetallic nanocomposites, have been extensively used for diagnostics purposes and targeted delivery. Electrochemical techniques with a high performance of the metal nanoparticles have an essential role in biomarker detection for accurate sample analysis. The design of a metal nanoparticle decorated electrochemical platform is required to diagnose serious diseases such as cancer, coronary disease, neurological disorders, and obesity. The benefits of the metal nanoparticle modified systems such as cost-effectiveness, simplicity, high selectivity, easy preparation process, real-time monitoring, and simultaneous sensing capability of the critical biomarkers provide a crucial role in fabricating new electrochemical sensing strategies. These strategies include biology, biochemistry, chemistry, electrics-electronics, pharmaceutical sciences, material science, and medicine.

Keywords

Electrochemical · Determination · Biomarker · Gold · Silver · Platinum

1 Introduction

Biomarkers are proteins found in body fluids or tissues that reflect the normal or abnormal activity of the organism (Rezaei et al. 2016). Biomarkers are produced directly by tumor tissue or embryonic tissue. A biomarker is a property that is determined and considered as a result of normal biological processes, pathogenic processes, or a pharmaceutical response to therapeutic intervention, according to the National Institutes of Health (Li et al. 2012). Biomarkers can be a particular molecule or cell, genes, gene products, hormones, or enzymes (Chandra 2013). Biomarkers can be measured in biological media, tissues, cells, or fluids by using different techniques enzyme-linked immunosorbent assay (ELISA) (Arya and Estrela 2018), immunosensors (Mahato et al. 2018), etc. The emergence of biomarkers in body fluids or tissues and changes in their concentrations indicate that they are symptoms of many diseases. For these reasons, measurable biomarkers are a significant advantage in minimizing the screening cost and increasing their usefulness (Li et al. 2012). Nanoscale materials can be classified according to their structures, such as tubes, wires, crystals, rods, thin films, and particles. In recent years, interest in studies using nanomaterials has increased. The remarkable chemical and physical (structural, magnetici optical, and electronic) properties of nanoparticles have gained considerable attention. Structures are nanoscale materials classified according to tubes, wires, crystals, rods, thin films, and particles (Sajid 2022).

Materials with an average diameter of <100 nm are called nanostructures. These structures can be polymers (Shanbhag et al. 2021), particles (Hua et al. 2021), tubes (Onyancha et al. 2021), rods (Ferhan et al. 2021), etc. As a large part of nanotechnology, nanoparticles are widely used in chemistry, biology, physics, and many other areas (Datta et al. 2014). The properties of nanoparticles generally depend on their shape, size, stabilizing chemicals, and controlled preparation conditions. Nanoparticles are the subject of intense research studies as they provide good analytics such as reliability, selectivity, sensitivity, low cost, ease of use, and fabrication (Merkoçi 2013). In addition to these, it is frequently researched due to its imaging, sensing, and optical properties. Nanoparticles have an essential property, such as surface area/volume ratio, which allows them to interact easily with other particles. This high surface area/volume ratio accelerates diffusion in nanoparticles. Metallic nanoparticles have been more interesting in various industrial applications than bulk metals due to their different physical and chemical properties.

2 Metal Nanoparticles

Metals are substances that have a unique shine, have a high tendency to form cations, and are good conductors of heat and electricity. Moreover, metals can be formed into wire and sheets and have high melting and boiling points. Metals combine with oxygen to form basic oxides.

Studies on nanosized materials have made significant progress in recent years to become an important field. Materials are defined as nanosized structures; nanoparticles are divided into different classes such as nanotubes, nanocrystals, nanorods, nanowires, or nano-thin films. The main reason for the studies on this area is that the items show unusual functionality and properties between specific dimensions, unlike their volumetric structures (Merkoçi 2013). Metal nanoparticles have opened up a new field of terminology among nanoparticles in recent years. Many metals are used to synthesize nanoparticles and are called metal nanoparticles. The dimensions of metal nanoparticles are below 100 nm.

Metal nanoparticles have many uses in biomedical applications (Fig. 25.1). Synthesis techniques for most metal nanoparticles are constantly evolving, resulting in improvements in size and shape. Synthesis techniques for most metal nanoparticles are continually changing, resulting in improvements in size and shape. Metal nanoparticles allow direct electron transfer and thus without the need for electron transfer mediators for electrochemical sensing (Liu et al. 2003; Yáñez-Sedeño and Pingarrón 2005).

2.1 Synthesis Methods of Metal Nanoparticles

The synthesis of metal nanoparticles depends on the melting and boiling point of the metal to be used physical and chemical properties such as reactivity with acids,

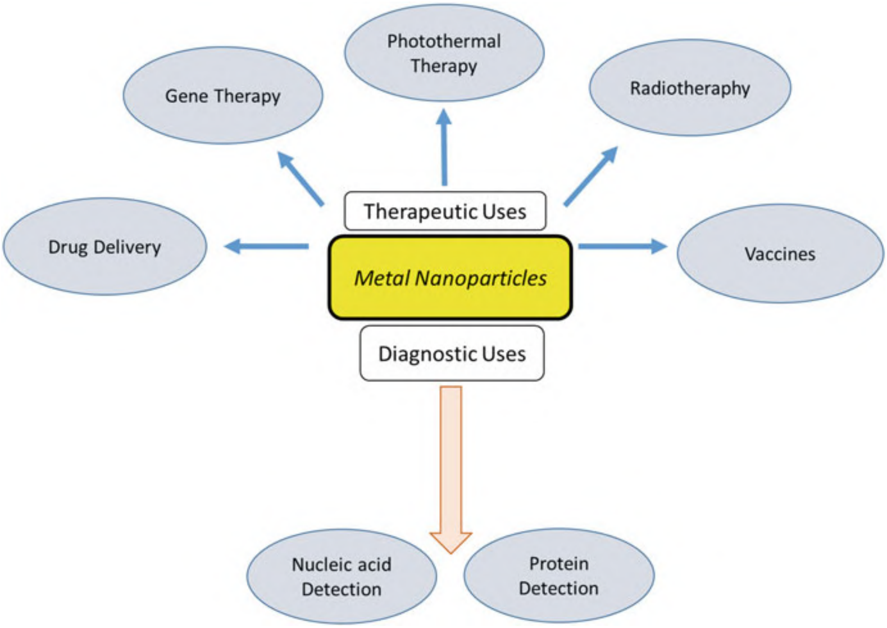
Photothermal Therapy
Gene Therapy
Radiotheraphy
Therapeutic Uses
Drug Delivery
Metal Nanoparticles
Vaccines
Diagnostic Uses
Nucleic acid Detection
Protein Detection

Fig. 25.1 Application areas of metal nanoparticles

bases, and oxygen (Shnoudeh et al. 2019). Many different chemical and physical methods strategies have been proposed for metal nanoparticles in the literature. However, when classified in general, metal nanoparticles can be evaluated into two main classes: bottom-up methods and top-down methods. The main difference between the two methods is the starting material of the metal nanoparticles. Top-down methods use bulk material as starting material, while bottom-up methods use atoms and molecules (Fig. 25.2).

In top-down methods, the bulk material is converted into small nanosized materials. These methods are based on the preparation of metal nanoparticles, reducing the size of the starting material using different chemical and physical processes. Techniques such as mechanical/ball milling, thermal/laser ablation, chemical etching, and sputtering are widely used for preparing nanostructures. Although the top-down methods are easy to implement, it is not suitable for preparing tiny nanoparticles. Changes in nanoparticles' physicochemical and surface chemistry create a significant problem with this method (Meyers et al. 2006).

Bottom-up methods are based on the fact that tiny particles such as atoms and molecules come together to form nanoparticles. In this method, nanostructured building blocks of nanoparticles are formed and ultimately combined to produce the

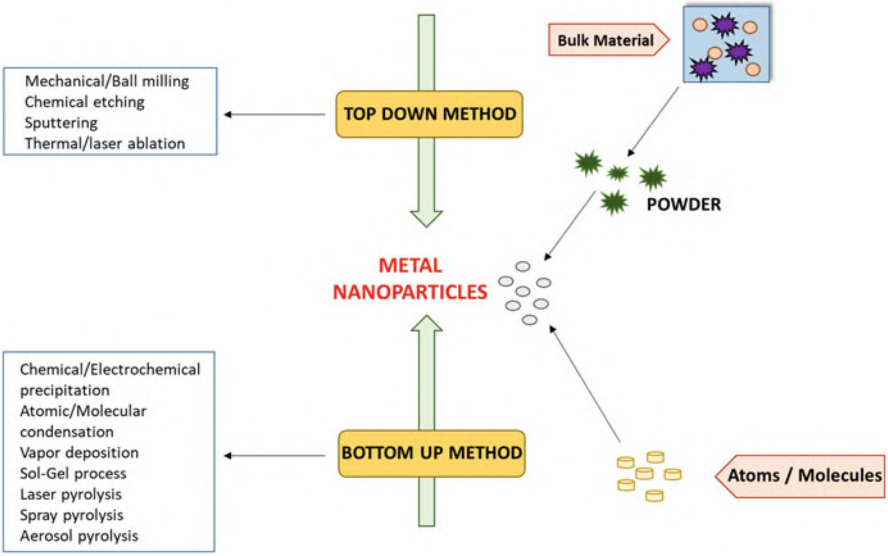
Mechanical/Ball milling
Chemical etching
Sputtering
Thermal/laser ablation
TOP DOWN METHOD
Bulk Material
POWDER
METAL NANOPARTICLES
Chemical/Electrochemical precipitation
Atomic/Molecular condensation
Vapor deposition
Sol-Gel process
Laser pyrolysis
Spray pyrolysis
Aerosol pyrolysis
BOTTOM UP METHOD
Atoms / Molecules

Fig. 25.2 An overview of the top-down and bottom-up methods

nanoparticle. The bottom-up process can be broadly divided into two classes. These are the chemical method and the biological method. Chemical/electrochemical precipitation, atomic/molecular condensation, vapor deposition, sol-gel process, laser, spray, and aerosol pyrolysis methods are used in chemical ways. In biological methods, green synthesis from bacteria, plant extracts, fungus, and algae are mainly selected and applied (Meyers et al. 2006).

After synthesizing metal nanoparticles, the properties (crystal structure, shape, size, maximum absorbance, etc.) are essential. Various spectroscopic and microscopic techniques are used to characterize the obtained particles. These are ultraviolet-visible region spectroscopy (UV-vis), Fourier Transform Infrared Spectroscopy (FT-IR), Scanning Electron Microscope (SEM), Transmission Electron microscopy (TEM), X-ray diffraction analysis (XRD), Thermogravimetric Analysis (TGA)-(Differential Thermal Analysis) DTA, and zeta potential analysis.

2.2 Functionalization of Metal Nanoparticles

Due to the rapid increase in research on metal nanoparticles, many applications are expected. Although some metal particles have superior physical and chemical properties, generally, they do not have a suitable surface for detecting various analytes (Ruckenstein and Li 2005). To increase the selectivity and sensitivity of biosensor, metal nanoparticles should be functionalized to recognize biomolecules and generate higher signals. Processes for the functionalization of metal nanoparticles can be classified as non-covalent interactions such as specific affinity interaction, physical adsorption and retention of biomolecules around nanoparticles, and covalent interaction of biomolecules with functional groups on the nanoparticle surface. Functionalizing the surface stabilizes the nanoparticles against agglomeration and makes them compatible with other phases. For example, when suitable molecules are added to the metal, the metal can become water-soluble (Lei and Ju 2012).

2.2.1 Noncovalent Association of Metal Nanoparticles with Biological Molecules

To increase the sensitivity and specificity of detection, suitable methods must be selected to functionalize metal nanoparticles with biomolecules. By electrostatic attraction, van der Waals, or π–π stacking, biological molecules are immobilized to the metal surface, preventing the destruction of conjugated skeletons and loss of electronic properties of nanoparticles. It is an alternative method for depositing macromolecules such as proteins and enzymes on the metal nanoparticle surface. Another way is to immobilize biocompatible molecules such as nafion solution, chitosan, functional polymers, and oligonucleotides on the nanoparticle surface. These methods can generate many electrons during the electrochemical process to amplify the electrochemical signal and increase the detection sensitivity (Lei and Ju 2012).

2.2.2 Covalent Association of Metal Nanoparticles with Biological Molecules

The binding of functional molecules to metal nanoparticles should be preferred to non-specific physisorption in terms of stability and reparability of surface functionalization. The number of functional groups should be controllable by making appropriate adjustments during functionalization. These can be accomplished by direct chemical reaction, bonding chemical reaction, and click chemistry. In the direct reaction strategy, the functional groups on the nanoparticle surface can be directly attached to the reactive ligands by a reaction facilitated with the help of catalysts (Yu et al. 2006). This method is generally used to bind DNA, aptamer, and antibody-antigen to nanoparticles.

Biochemical functionalization is required in the direct interaction of biomolecules with solid surfaces. A low molar mass is modified to the nanoparticle surface with the help of functional binders. Thus, nanoparticle surfaces are activated with low molar mass binders for direct covalent binding to target molecules. Firstly, the surface is modified with an alkyne or azide; then, this platform is treated with the biomolecule. This reaction is fast and effective, forming water-soluble and biocompatible bonds with moderate reaction conditions (aqueous and neutral media). It offers high selectivity, stability, and robustness than other bonding methods.

3 Specific Affinity Interaction Between Metal Nanoparticles and Biomolecules

Bioconjugation of targeted ligands with nanoparticles is highly effective due to the interaction with affinities, strong complementary and specific recognition interactions such as nucleic acid-DNA, antigen-antibody, streptavidin-biotin, aptamer-protein, lectin-glycan, aptamer-small biomolecule, and hormone. The bond formed is stronger and more stable than any non-covalent interaction (Ding et al. 2008).

3.1 Electrochemical Detection Principles of Biomarkers Based on Metal Nanoparticles

Electrochemistry is one of the sub-branches of chemistry, which studies the electrical behavior of substances by combining studies in electricity and chemistry. For an electrochemical reaction to occur, a solution containing the substance to be analyzed, an electrode system in which the substance is chemically transformed, and a translation system connecting these electrodes are required. The triple electrode system is used in the experiments in the studies. These are the working electrode, counter electrode, and reference electrode. GCE, gold electrodes, screen printed electrodes (SPE), pencil graphite electrodes (PGE) are frequently used as working electrodes. These electrode surfaces are modified with metal nanoparticles (Au, Ag, Pt, Pd, Cu, and similar metals) to be applied to samples with different properties, allowing new production methods and strategies to improve selectivity detection limits.

When electrochemical methods are examined, they have divided into two classes solution and interface methods. In the solution method, the electrical conductivity of the solution is measured. In contrast, the interface methods examine the chemical and physical transformations between the electrode surface and thin solution layers (Fazio et al. 2021).

3.2 Gold Nanoparticles

Nanomaterials provide cost-effectiveness, selectivity, and rapid identification in methods developed for performing clinical diagnoses. AuNPs have stable chemical structures, low toxicity, and high biocompatibility. AuNPs have simple and reproducible synthesis methods. They are known to have the properties to interact with light and resist oxidation. AuNPs increase the selectivity in biosensor applications because they have a high surface/volume ratio that enables the conjugation of biomolecules. It has been observed that AuNPs can label many different cell types, such as closed stem cells and immune cells in chemical diagnosis without harming these types (António et al. 2021; Hammami et al. 2021). Au nanostructures-based biosensors used for the diagnosis of biomolecules have been summarized in Table 25.1.

Table 25.1 Electrochemical biosensors based on Au nanostructures for diagnostic biomolecules

Platform	Biomarker	Method	Linear Range	LOD	Application	References
GCE/AuNPs@MWCNTs-GQDs/EDC-NHS/ab/BSA/PSA	PSA	EIS DPV CV	1–10,000 pg mL^{-1}	0.48 pg mL^{-1}	Human plasma	Ghanavati et al. (2020)
rGO/AuNPs/GCE	PCT	SWV	0.05–100 ng mL^{-1}	0.0001 n mL^{-1}	Human serum	Boonkaew et al. (2021)
Graphene-au NPs	PSA	CV	0–10 ng mL^{-1}	0.59 ng mL^{-1}	Serum samples	Jang et al. (2015)
PGE/AuNPs/P(L-Lys)-GQD	DA and 5-HT	DPV	DA 0.1–80.0 5- HT 0.05–200.0 μM	DA 0.03 μM 5-HT 0.017 μM	FBS	Şimşek and Gözde Aydoğdu (2022)
CNSs@au NPs	PSA, CEA and AFP	SWV	PSA 0.01–100 ng mL^{-1} CEA and AFP 0.01–80 ng mL^{-1}	PSA 3.6 pg mL^{-1} CEA 3.0 pg mL^{-1} AFP 2.6 pg mL^{-1}	Human serum	Li et al. (2021b)
cTnI/anti-cTnI/AuNPs@GQDs/ SPGE	cTnI	EIS CV SWV	Buffer 1–1000 human serum 10–100 pg mL^{-1}	Buffer 0.1 pg mL^{-1} Serum 0.5 pg mL^{-1}	Buffer and human serum	Mansuriya and Altintas (2021)
SPE/AuNPs@rGO/Mb$_{Ab}$	Cardiac biomarker myoglobin	DPV	1–1400 ng.mL^{-1}	0.67 ng.mL^{-1}	Serum samples	Singh et al. (2016)
AuNPs/glycoprofiling	Cancer biomarker prostate	EIS AFM	4 aM–40 nM	4 aM (0.13 fg/mL)	Human serum	Pihíková et al. (2016)
Au@HMPB NPs	Protein biomarker (the soluble α-chain of IL-2 receptor (sCD25))	Amperometric	10 pg mL^{-1}–10 ng mL^{-1}	3 pg mL^{-1}	Human serum	Luo et al. (2019)
Au@cu-MOF nanocapsules	Glutathione (GSH)	DPV	0.01–40 nM and 40 nM–10 μM	2.5 pM 1.044 nM	Serum Tomato Cucumber	Xie et al. (2021)
rGO-GNPs-Cr.6/GCE	L-tryptophan	SWV	0.1–2.5 μM	0.48 μM and 0.61 μM	Diabetic and normal serum	Khoshnevisan et al. (2020)

Abbreviations: *5-HT*: Serotonin, *Ab*: Antibody, *AFM*: atomic force microscopy, *AFP*: α-fetoprotein, *Au*: Gold, *AuNP*: Gold Nanoparticle, *BSA*: Bovine Serum Albumin, *CEA*: carcinoembryonic antigen, *CNS*: Carbon Nanospheres, *Cr.6*: 18-crown-6, *cTnI*: Cardiac Troponin-I, *CV*: Cyclic Voltammetry, *DA*: Dopamine, *DPV*: Differential Pulse Voltammetry, *EDC*: 1-Ethyl-3-(3-dimethyl aminopropyl) carbodiimide, *EIS*: Electrochemical Impedance Spectroscopy, *FBS*: Fetal Bovine Serum, *GCE*: Glassy Carbon Electrode, *GQD*: Graphene Quantum Dots, *GSH*: Glutathione, *HMPB*: Hollow Mesoporous Prussian Blue, *Mb*: Cardiac Myoglobin, *MOF*: Metal Organic Framework, *MWCNT*: Multi-walled Carbon Nanotubes, *NHS*: N-hydroxysuccinimide, *P(L-Lys)*: Poly L-lysine, *PCT*: procalcitonin, *PGE*: Pencil Graphite Electrode, *PSA*: Prostate Specific Antigen, *rGO*: Reduced Graphene Oxide, *sCD25*: Soluble α-chain of interleukin-2 receptor, *SPE*: Screen Printed Electrode, *SPGE*: Screen Printed Gold Electrode, *SWV*: Square Wave Voltammetry

This section gives studies on biosensors developed using AuNP in clinical diagnosis.

Ghavati et al. designed an immunosensor for the detection of prostate cancer biomarkers. The immunosensor platform used for this detection is Au nanoparticles@multiwall carbon nanotubes-graphene quantum dots (AuNPs@MWCNTs-GQDs). This platform features a signal amplifier. It is stated that this platform is coated on a GCE surface. The prostate-specific antigen (PSA) was detected using the AuNPs@MWCNTs-GQDs modified electrode. The designed impedimetric immunosensor was characterized using TEM, EDS, XRD, FTIR, CV, and EIS methods. $[Fe(CN)_6]^{3-/4-}$ was used as a redox probe in the immuno-interactions research using the EIS method. The measurements made for this immunosensor determined that the impedance increase was in a wide range between 1 pg/mL and 10,000 pg/mL. Also, the low detection limit was calculated as 0.48 pg/mL. The ELISA method was selected to analyze the commercial samples to compare the results, and the obtained data were in good agreement. This designed immunosensor can be used for the early diagnosis of prostate cancer (Ghanavati et al. 2020).

L. Li et al. designed an immunosensor with which PSA, carcinoembryonic antigen (CEA), and α-fetoprotein (AFP) can be detected simultaneously. The surface of this immunosensor is coated with GCE. In this immunosensor, Au NPs were efficient and used as signal enhancers. Three different metal ions, Pb^{2+}, Cd^{2+}, and Zn^{2+} were fixed on the surface of the nanocomposites. Since three various analyses have been investigated, the SWV method was used, and the peaks of the analyte signals were determined. Comprehensive measurement linear ranges specified for analytes; PSA is 0.01–100 ng mL^{-1}, CEA and AFP are 0.01–80 ng mL^{-1}. Low detection limits were also found to be PSA 3.6 pg mL^{-1}, CEA 3.0 pg mL^{-1}, and AFP 2.6 pg mL^{-1}, $S/N = 3$. Human serum samples were used to evaluate the designed immunosensor and compared with references. As a result of this comparison, it was observed that there was no difference between the reference and actual samples regarding the early diagnosis of tumors (Li et al. 2021b).

Another study for detecting PSA was done by Talamin et al. (2018). Talamini et al. developed an electrochemical biosensor for PSA detection. This biosensor is based on Liquid crystal (E)-1-decyl-4-[(4-decyloxy-phenyl)diazenyl]pyridinium bromide (BrPy) and is label-free. BrPy, which has a liquid crystal structure, showed redox properties on the surface of the electrode used, and it was also seen that it provided a good film formation. Heparin-stabilized AuNP (AuNP-Hep) and Nafion were also used in this biosensor.

For this reason, it was determined as a redox probe for the developed immunosensor. An incubation period for immunocomplex formation has taken place. This process and immunosensor characterization were performed by CV, SWV, and EIS methods. In this developed immunosensor, PSA concentrations were directly determined by suppressing the BrPy peak used as a redox probe. Accordingly, the range of PSA to which the optimized immunosensor responds is 0.1–50 ng mL^{-1}. The calculated limit of detection for this response is 0.08 ng mL. In this study, in which human blood plasmas were used, reproducibility, selectivity, and accuracy were sufficient (Talamini et al. 2018).

Amyloid-β (Aβ) is a peptide produced in the brain and transported to the blood across the blood-brain barrier, used in the blood-based early diagnosis of Alzheimer's disease (AD). This peptide has several isoforms. In 2020, YK. Yoo, et al. aimed to perform a blood-based Aβ assay using a sandwich-based impedance biosensor. They used gold nanoparticles (AuNP's) and interconnected microelectrodes (IME's). Linear sensitivity and detection limit was determined as 74.84% with 2.87 fold. The blood plasma of a wild mouse (WT) double mutation APP/PS1 transgenic (TG) was used as a sample. Afterward, AB and AD diagnostic abilities were sought in the plasma sample prepared from this blood. As a result, the sandwich assay with AuNP successfully distinguished TG-WT and provided Aβ detection. This result is promising for the early detection of AD (Yoo et al. 2020).

Thirty-three percent of patients with cardiovascular diseases die due to these diseases worldwide. Patients in the risk group should continuously follow-up to prevent these deaths. The strategies require inexpensive and appropriate diagnostic methods. Mansuriya and Altintas developed an ultra-sensitive and enzyme-free nano-immunosensor to diagnose acute myocardial infarction (AMI) early in 2021. The biomarker to diagnose AMI is cardiac troponin-I (cTnI). This developed immunosensor contains Graphene quantum dots (GQDs), AuNPs, and screen-printed gold electrode (SPGE) in its structure. SWV, CV, EIS, and amperometry methods detected cardiac troponin-I levels. These methods allow the evaluation of the biomarker in a wide concentration range. Before using these methods, AuNP synthesis was performed. Then these AuNPs and GQDs were modified to the SPGE. Immobilization of anti-cTnI was provided to carry out the identification. Both buffer and human serum were used as samples in this experiment. The range of investigation ranges for the buffer is 1–1000 pg mL^{-1}, and the calculated detection limit is 0.1 pg mL^{-1}. The human serum's investigation ranges and detection limit values are 10–1000 pg mL^{-1} and 0.5 pg mL^{-1}, respectively. It was observed that the detection time, which varies according to the method used, is in the range of 10.5–13 min. The developed immunosensor gave indistinct responses to some biomolecules but gave a much more pronounced and more pronounced response to cTnI. In addition, the sensitivity and binding affinity of the immunosensor was determined. These values are 6.81 μA cm^{-2} pg mL^{-1} and < 0.89 pM, respectively. CV, SWV, EIS, and atomic force microscopy (AFM) in each sensor development stage. TEM and SEM were used to characterize AuNP, GQD, and nanocomposites. This analysis using four different electrochemical techniques is promising in the early diagnosis of AMI. The sensor's sensitivity, cost, and speed are reasonable (Mansuriya and Altintas 2021).

Simsek and Aydogdu, in a study they conducted in 2021, aimed to determine the neurotransmitters dopamine (DA) and serotonin (5-HT), which are prominent in neurological diseases. The nanocomposite they developed to detect these substances includes AuNP, GQD, and poly(L-lysine). The nanocomposite platform was designated PPGE/AuNPs/P(L-Lys)-GQD. Dopamine and 5-HT to be detected were analyzed by CV and DPV. According to the data obtained from the analysis results, the limit of detection (LOD) values were calculated as 0.03 μM for DA and

0.017 μM for 5-HT. The linear ranges were 0.1–80.0 μM for DA and 0.05–200.0 μM for 5-HT. In this study, fetal bovine serum was used as a sample (Şimşek and Gözde Aydoğdu 2022).

Singh S. et al. developed an immunosensor using cardiac myoglobin as a biomarker. In the first step, a composite consisting of AuNP's and reduced graphene oxide (AuNPs@rGO) was formed. Then, this composite was modified onto a SPE. The methods used to characterize the nanocomposite are TEM, SEM, AFM, FTIR, and EIS. Indium tin oxide-coated glass plates were used to deposit the nanocomposite. The principle of the immunosensor is based on the immobilization of the antibody onto the electrode for the detection of cardiac myoglobin. DPV was used to monitor the immunosensing response. The peak was seen at ~ − 0.5 V against Ag/AgCl. It is known that this peak is due to the decrease in the iron metal of the heme group of myoglobin. In addition, the dynamic linearity range and the LOD value for cardiac myoglobin were 1 ng mL^{-1}–1400 ng mL^{-1} and ~ 0.67 ng mL^{-1}, respectively. These results were eight times better than the results obtained with the ELISA test (Singh et al. 2016).

Luo, J. et al. investigated peroxidase-like activity using an electrochemical probe in 2019. AuNP's functionalized hollow mesoporous Prussian blue nanoparticles (Au@HMPB NPs) were modified to the electrode. The Au@HMPB NPs platform was able to reduce H_2O_2 with high precision. The low detection potential was −0.1 V. The measurements were carried out using the amperometric method. The probe's performance was measured using interleukin-2 (IL-2) protein. The soluble α-chain (sCD25) of this protein served as a biomarker. sCD25s were captured and enriched with magnetic nanospheres functionalized using the antibody. As a result, it was observed that increasing CD25 concentration increased the electrochemical responses to 1 mmol/L H_2O_2 (Luo et al. 2019).

L-tryptophan (L-Trp) is an essential amino acid that can not be synthesized in the human body and needs supplementation in some cases. In L-Trp deficiency, diseases such as anxiety, obesity, and sleep disorders may occur, and in overdose cases, many side effects such as nausea may occur. In 2020, Khoshnevisan K. et al. aimed to detect L-Trp, which was selected as a biomarker in the presence of DA, ascorbic acid (AA), urea, and glucose. For this, a new nanocomposite modified electrode has been developed. This electrode is structurally composed of rGO decorated with 18-crown-6 (Cr.6) and gold nanoparticles (GNPs) on the surface of a GCE. SWV method was used for the activity measurement of this platform. The electrode-modified materials were tested in different combinations, and the electrochemical behavior of L-Trp in these combinations was investigated. Accordingly, the highest oxidation current and potential were observed in the rGO-GNPs-Cr.6/GCE platform, at 40 μA at 0.85 V. Diabetic and normal serums (from female, age 41 volunteers) used as samples were evaluated separately. The low LOD values were determined to be 0.48 μM (for diabetic serum) and 0.61 μM (for normal serum). The linear concentration range in which L-Trp is seen in the SWV method is 0.1–2.5 μM. In the last step, nanocomposite rGO-GNPs-Cr.6 was modified to the GCE, and the obtained platform was applied to the samples. The limit of detection value was extremely low, and the recovery rate was higher than 91.8% (Khoshnevisan et al. 2020).

Cholesterol, an essential component of the mammalian cell membrane, gains the ability to act with multiple immune cell types and is transported to the blood plasma. Thus, it takes part in the production of many molecules. It is a regulator of cancer and some autoimmune conditions (King et al. 2022). Heart diseases are associated with the level of cholesterol in the blood. Huang et al. in 2020, developed an ultra-sensitive biosensor to determine the level of cholesterol in the serum. The biosensor was constructed with electrodeposited AuNPs onto screen-printed carbon electrodes. Cholesterol oxidase (CHOD) and cholesterol esterase (CHER) were immobilized onto Au NPs/SPE surfaces. The use of CHER and CHOD is for the deposition of Ag on the surface. For this purpose, H_2O_2 capable of reducing Ag ions in the solution was produced. Linear Sweep Voltammetry (LSV), CV, and XPS techniques were utilized to characterize the Ag/CHER&CHOD/Au NPs/SPE platform. Anodic stripping voltammetry (ASV) was used to measure the sensitivity of the cholesterol. The anodic stripping peak current of Ag correlates with cholesterol concentration in 5–5000 μg/mL with a regression correlation coefficient of 0.9983. A detection limit was determined as 3.0 μg/mL obtained from the 3σ rule. The developed cholesterol biosensor is a sensitive, reproducible, and successful recovery (Huang et al. 2017).

Thrombin is a serine protease that converts fibrinogen to fibrin. Detection of this type of protease is vital in diseases and abnormalities involving coagulation. This substance is also used to control bleeding in surgeries. Yingjie Li et al. designed a sandwich biosensor for thrombin detection in human serum. Two different thrombin aptamers are used in this sandwich biosensor (TBA1-thrombin-TBA2). The biosensor was developed based on the principle of double signal amplification. First, gold nanoparticles@graphene composite (GNP's@graphene) was obtained by deposition of solution of chloroauric (III) acid tetrahydrate and graphene solutions with CV method. After this modification, thiol-coated TBA1 was immobilized on the GCE surface. TBA2 was anchored to the surface of the GNPs after being modified with $Ru(bpy)_3^{2+}$. Electrochemiluminescence (ECL) and CV methods were used to characterize this biosensor. According to the calculations made according to these methods, the linear range is 0.01–10 nM, and LOD is 6.3 pM. Human serum was used as the sample, and the biosensor's selectivity was checked in the presence of different proteins. The biosensor was found to be sufficiently selective for thrombin in the presence of Bovine Serum Albumin (BSA) and lysozyme (Li et al. 2017).

Choline is a vital nutrient with multiple functions, such as participating in the cell membrane structure, providing signal transmission, and synthesizing essential phospholipids. Since it is also involved in muscle and memory control, it can diagnose AD and Parkinson's diseases early. H.S. Magar et al. designed an amperometric biosensor and aimed to detect choline. Multiwalled carbon nanotubes (MWCNT) and GNPs were used in developing this biosensor. First, MWCNT was modified with Chit, and the carbon nanotubes (CNT) were dispersed. The resulting Chit-MWCNT was then dropped onto the GCE surface, and after this process, GNP was immobilized with choline oxidase (ChOx). The linear range value for the resulting platform (ChOx/(GNP)$_4$/MWCNT/GCE) is 3–120 μM. LOD value was calculated as 0.6 μM. Milk sample was used as an actual sample for this biosensor with a sensitivity of 204 μA cm^{-2} mM^{-1}. In addition, the use of the EIS method was the first for the determination of choline in this study (Magar et al. 2016).

It has been determined that the most common type of cancer that causes the death of women is breast cancer. Again, these statistics show that breast cancer cases make up 29% of other cancer types. A. A. Saeed et al. designed a DNA-based biosensor to detect breast cancer in 2017. In the sandwich-type detection chosen as the detection strategy, two types of DNA were used as biomarkers. These DNAs are ERBB2c and CD24c and were studied in parallel on these two DNAs. AuNP modification and graphene oxide (GO) loading were made to the GCE for the biosensor platform. The platform of the developed biosensor is DNA-c/AuNPs-GO/GCE. The hybridization of the AuNP and GO-bound GCE surface to the target DNA is schematically illustrated in Fig. 25.3. CV and EIS methods were used to characterize developed platforms. Many methods such as Raman spectroscopy, UV–vis spectroscopy, FT-IR, TEM, SEM, and energy-dispersive X-ray spectroscopy have been used to characterize GO. After electrochemical characterization, LOD and sensitivity for both DNAs were calculated separately. LOD value for ERBB2 is 0.16 nM and the sensitivity is 378 nA/nM. When these values were calculated for CD24, the LOD value was 0.23 nM, and the sensitivity was 219 nA/nM. The linear range value is 0.37–10 nM for both DNAs (Saeed et al. 2017).

3.3 Silver

It is seen that nanoparticles have recently played a role in developing modern technologies such as sensors, drugs, and water treatment. AgNPs have started to be preferred more in these applications because they are less costly. Although some problems such as poor stability, oxidation, or agglomeration are encountered in various applications, some solutions have been suggested for AgNPs. Changing particle sizes or creating a synergetic effect are some of these solutions. Several methods for modifying AgNP and other nanoparticles into electrodes: dipping, electrodeposition, spray coating, spin coating, sputtering and electrophoresis, and drop-casting. The use of AgNP at the stage of coating the electrode surface, which is frequently seen in biosensor applications, increases the effect of the surface area and therefore improves the electrocatalytic activity. After AgNP modification, high sensitivity, low detection limit, reproducibility, and fast response were obtained (Abbas and Amin 2022). The performance improvement properties, high conductivity, and catalytic activity of AgNPs in biosensors make it possible to use these nanoparticles to diagnose diseases. In addition, it is known that AgNPs are used as redox mediators during electrochemical biosensor designs since they form

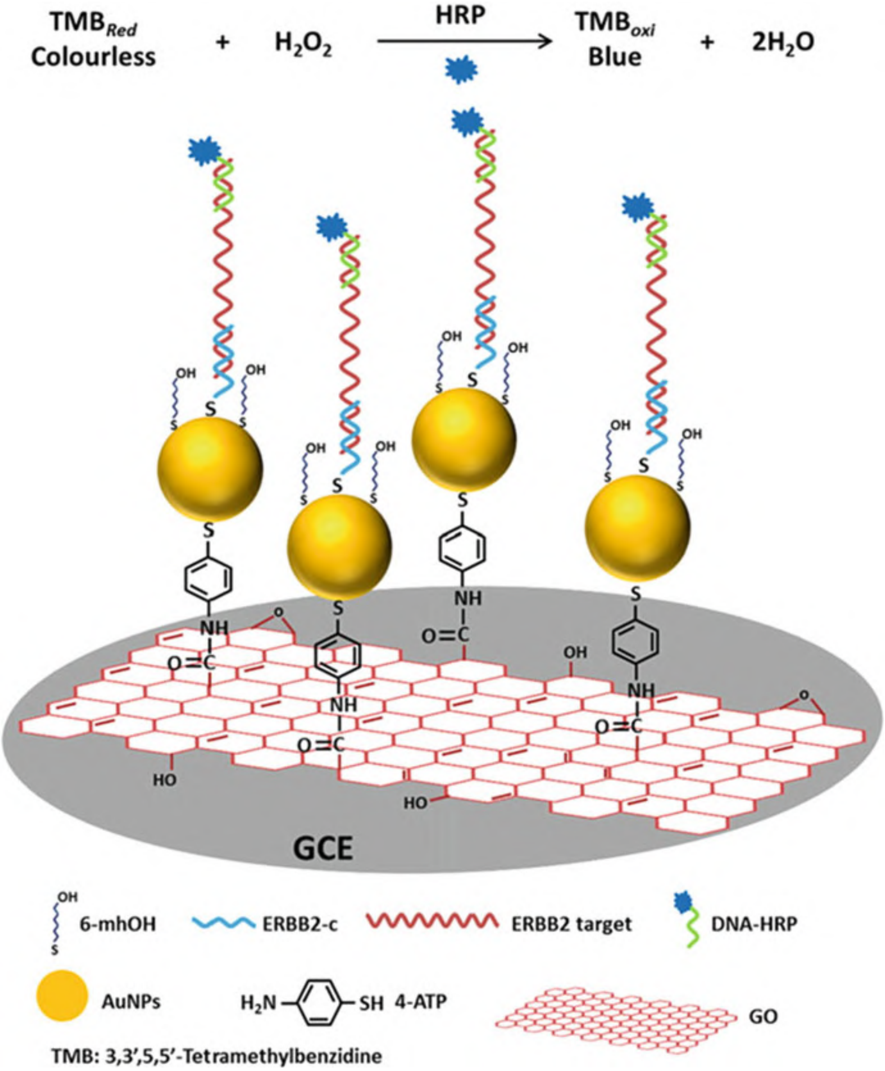
TMB$_{Red}$
Colourless
+
H_2O_2
HRP
TMB$_{oxi}$
Blue
+
$2H_2O$
OH
S
NH
O=C
HO
GCE
6-mhOH
ERBB2-c
ERBB2 target
DNA-HRP
AuNPs
H_2N–⟨⟩–SH 4-ATP
GO
TMB: 3,3′,5,5′-Tetramethylbenzidine

Fig. 25.3 Schematic presentation of the proposed sandwich-type DNA sensor showing the prepared AuNPs-GO/GCE and the hybridization of target DNA with the specific capture probe and HRP-labelled probe. (Reproduced with permission from Saeed et al. 2017)

prominent oxidation peaks in buffer solutions (Miranda et al. 2022). In this section, studies related to the use of AgNPs in the diagnosis of diseases are included.

Recently, Aydogdu Tig aimed to determine the levels of AA, DA, uric acid (UA), and L-Trp simultaneously based on the DPV method. For this purpose, she developed a sensor and used a glassy carbon electrode as an electrode. This electrode used was modified with Ag NP's, GO, and poly(L-arginine) (P(Arg)). The developed sensor showed high electrocatalytic activity against four different substances. CV and EIS methods were used to characterize the electrode and determine its potential against Ag/AgCl. According to the DPV method used to measure AA, DA, UA, and L-Trp levels, the relationship between peak currents and concentration for AA is linear in the range of 4.0–2400.0 μmol L^{-1}. This range is 0.05–50.0 μmol L^{-1} for DP, 0.5–150.0 μmol L^{-1} for UA, and 1.0–150 μmol L^{-1} for L-Trp. Detection limit values were also calculated for these substances. The detection limit value is 0.984 μmol L^{-1} for AA, 0.01 μmol L^{-1} for DA, 0.0142 μmol L^{-1} for UA, and 0.122 μmol L^{-1} for L-Trp. Urine samples were used for the developed sensor. It was determined that it is suitable for detecting various molecules Na^{+}, K^{+}, L-lysine, glucose, L-cysteine, urea, and citric acid in the urine (Tığ 2017).

In 2017, L. Han et al. created a label-free electrochemical immunosensor for detecting PSA. In fabricating this immunosensor, a screen-printed three-electrode system was used, rGO/Ag NP composites were used as support material. Hydrazine hydrate and sodium citrate were used to synthesize rGO/Ag NP. This platform was created by reducing GO to rGO and placing Ag NPs between graphene-structured sheets. Ag NPs inhibited the accumulation of rGO and increased the electrical conductivity. In addition, the conductive path between Ag NP and rGO is because the defects of rGO are covered by AgNP. Characterization was performed at different scan rates and on other platforms with the CV method. In the resulting electrochemical immunosensors, a linear response range of 1.0–1000 ng/mL and a low detection limit value of 0.01 ng/mL were calculated. In addition, the immunosensor is specific, expandable, reproducible, and stable (Han et al. 2017).

Electrochemical immunosensors can also detect diseases caused by viruses (Mahapatra et al. 2020). Awan, M. et al. have developed an immunosensor based on a graphite pencil electrode modified with AgNPs targeting the flavivirus known to cause dengue, one of the viral diseases. This sandwich-type immunosensor was used to detect NS1 biomarker, which has a glycoprotein structure for dengue disease. The development steps of the biosensor and the labeling of the antibody with AgNP are shown schematically in Fig. 25.4. DPV method was selected to characterize the sandwich-based immunosensor. The linear range and detection limit values for detecting the biomarker are 3–300 ng/mL and 0.5 ng/mL, respectively. This immunosensor can be used in broad areas to detect biomarkers against which viral diseases can be seen (Awan et al. 2020).

Human chorionic gonadotropin (hCG) is a type of hormone. Xia, N. et al. used an electrochemical method to detect hCG, but this method did not include antibodies. To determine the applicability of this method, serum and urine samples from pregnant and non-pregnant individuals were used. In this method, peptide/6-mercapto-1-hexanol (peptide/MCH) and AgNP modification were made on gold electrode (AuE) as a platform. LSV method was used for the characterization. Finally, LOD value and concentration range are 0.4 mIU/mL and 1 mIU/mL–0.2 IU/mL, respectively (Xia et al. 2017).

Ortega et al. designed a microfluidic immunosensor in 2015. This immunosensor was designed to detect epithelial cell adhesion molecule (EpCAM), a cancer biomarker. As a platform for the immunosensor, synthesized AgNPs coated with

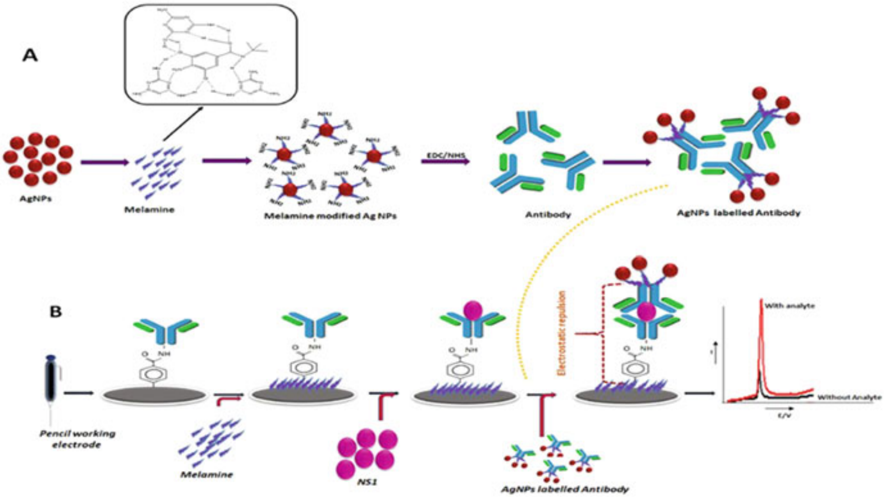

Fig. 25.4 (**a**) Preparation of AgNPs modified antibody (**b**) Construct of electrochemical sandwich immunosensor for diagnosis of dengue biomarker. (Reproduced with permission from Awan et al. 2020)

chitosan were used. Next, this platform was covalently linked to the immunosensor center. Peripheral blood cells were used as samples in this study. Using AgNPs is to immobilize anti-EpCA and identify EpCAM in samples directly. The amount of biomarkers were measured using HRP-conjugated anti-EpCAM-antibody. The detection limits for the developed immunosensor are 2.7 pg mL^{-1}, while for ELISA, this value is 13.9 pg mL^{-1}. As a result, the microfluidic immunosensor is usable, reproducible, and sensitive for detecting epithelial cancer cells. When the test times of the immunosensor developed with the ELISA kit were compared, it was observed that while testing with ELISA took 270 min, it took 34 min with the immunosensor. The chitosan, a natural polymer, has also enabled it to play a stabilizing role (Ortega et al. 2015).

T4 polynucleotide kinase (T4 PNK) is a catalyst belonging to the 50-kinase family. Its task is to transfer and replace the PO_4^{3-} (phosphate) group from ATP to the 50-hydroxyl terminus of polynucleotides. This function repairs the broken ends of DNA or RNA induced by agents and takes part in DNA replication and repair situations. One of the directly or indirectly related diseases is cardiovascular disease groups. It is also known to be associated with Werner and Myelodysplastic syndromes. Yu Jiang et al. developed an electrochemical biosensor to detect T4 PNK in 2019. For this detection method, firstly, a single-stranded DNA probe was immobilized on the surface of the electrode used. Next, the kinase desired to be detected was phosphorylated. The binding of the phosphorylated kinase with the DNA probe with the amino group tag was ensured. The next step aims to reduce the background signals, and for this, DNA probes are released by applying a denaturation process. After the DNA probes were removed, the remaining amino groups remained, and these amino groups were used for the adsorption of AgNPs. LSV, an electrochemical method, was used for characterization, and the linear range detection limit values were calculated. The linear range for this biosensor is 0.1–20 U mL^{-1}, and the detection limit value is 0.01 U mL^{-1} (Jiang et al. 2019).

Estradiol (EST) is an endogenous estrogen steroid. Its structure is 1,3,5 (10)-estratriene-3, 17 β-diol. This steroid acts as a growth hormone for the female reproductive organs. The EST level is significantly lower in postmenopausal women than in women aged 18–35. Caffeine (CAF) is a psychoactive drug with 1,3,7-trimethylxanthine structure and is found in many foods. CAF consumption has many positive and negative functions in women aged 18–35 and in menopausal women. In addition to stimulating the nervous system and cardiovascular systems, it has effects such as causing a lower risk of diabetes, secreting stomach acid, and reducing the risk of Parkinson’s in postmenopausal women. Studies show that there may be a relationship between CAF consumption and the level of EST in the body. Mamta Raj and Rajendra N. Goyal developed a biosensor in 2019 to determine the relationship between CAF and EST levels. Reduced graphene oxide (ErGO), pyrotic graphite, and AgNPs were used for this biosensor. After the modifications, the platform was determined as AgNPs: ErGO/P.G. During the analysis, it was determined that AA, UA, xanthine (XT), and hypoxanthine (HX) in the environment did not pose an obstacle. Serum and urine samples of five women of childbearing age were used throughout the analysis, and EST and CAF characterizations were performed separately. EIS, CV, and SWV methods characterize bare and modified electrodes. The concentration curve range for EST is 0.001–0.175 μM, and the detection limit value is 0.046 nM. The concentration curve range for CAF is 0.001–200 μM, and the detection limit value is 0.54 nM (Raj and Goyal 2019). Ag nanostructures-based biosensors used for the diagnosis of biomolecules have been summarized in Table 25.2.

3.3.1 Platinum

Platinum nanoparticles (PtNP) are widely used in sensing and biosensing applications due to their excellent conductivity, high electrocatalytic activity, and biocompatibility. PtNP immobilized on the electrode surface provides superior conductivity and widens the surface area, enabling sensitive electrochemical determination of molecular and biomolecular analytes (Bakirhan et al. 2018).

In a study by Wang et al. in 2021, cardiac troponin I (cTnl), a suitable marker for diagnosing early AMI, was determined based on a sandwich-type electrochemical aptasensor. After being modified with melamine, Pd@Pt dendritic bimetallic nanoparticles were modified on carbon spheres with a hollow mesoporous structure (Pd@Pt DNs/NH2-HMCS). The unique properties of NH2-HMCS increased the loading capacity and dispersion of Pd@Pt dendritic bimetallic nanoparticles (Pd@Pt DNs), while the affinity interaction between Pd@Pt and the binding stability also improved considerably. The synergistic catalysis effect between NH_2-HMCS and Pd@Pt DNs enhanced the electrocatalytic reduction of H_2O_2 and further strengthened the signal. Under optimum conditions, the prepared aptasensor for detection of cTnI has a wide range of 0.1 pg/mL to 100.0 ng/mL and a low detection limit of

Table 25.2 Electrochemical biosensors based on Ag nanoparticles for diagnostic biomolecules

Platform	Biomarker	Method	Linear range	LOD	Application	References
Ag/TiO_2/rGO/GCE	CA 15–3	Amperometry	0.1–300 UmL^{-1}	0.07 UmL^{-1}	Human serum	Shawky and El-Tohamy (2021)
rGO/ag nanoparticles	PSA	CV	1–1000 ng mL^{-1}	0.01 ng mL^{-1}	Bovine serum albumin	Han et al. (2017)
AgNPs/porous silicon/ GCE	H_2O_2	Amperometry	0.0016–0.5 mM	0.45 × 10–6 M	Hair color oxidant	Ensafi et al. (2016)
GCE/AgNPs/P(Arg)-GO	AA, DA, UA and L-Trp.	DPV	AA 4.0–2400 DA 0.05–50.0 UA 0.5–150.0 L-TRP 1.0–150.0 μmol L^{-1}	AA 0.984 DA 0.01 UA 0.142 L-TRP 0.122 μmol L^{-1}	Human urine samples	Tığ (2017)
AgNPs-Cts	EpCAM	ELISA	10–300 μL min^{-1}	2.7 pg mL^{-1} and 13.9 pg mL^{-1}	Human blood	Ortega et al. (2015)
Ab-ag NP	NS1	DPV	3–300 ng mL^{-1}	0.5 ng mL^{-1}	Human serum	Awan et al. (2020)
GSHOx/AgNPs/c-MWCNT/PANI/au	Glutathione	CV EIS	0.3–3500 uM	0.3 uM	Human erythrocyte	Narang et al. (2012)
rGO/ag NPs/SPCE	PSA	CV	1.0–1000 ng ml^{-1}	0.01 ng ml^{-1}	Serum	Han et al. (2017)
AgNPs/peptide/AuE	Human chorionic gonadotropin (hCG)	LSV	1 mIU/ mL–0.2 IU/mL.	0.4 mIU/mL	Human serum Urine samples	Xia et al. (2017)

Abbreviations: *5-HT*: Serotonin, *Ab*: Antibody, *AFM*: atomic force microscopy, *AFP*: α-fetoprotein, *Au*: Gold, *AuNP*: Gold Nanoparticle, *BSA*: Bovine Serum Albumin, *CEA*: carcinoembryonic antigen, *CNS*: Carbon Nanospheres, *Cr.6*: 18-crown-6, *cTnI*: Cardiac Troponin-I, *CV*: Cyclic Voltammetry, *DA*: Dopamine, *DPV*: Differential Pulse Voltammetry, *EDC*: 1-Ethyl-3-(3-dimethyl aminopropyl) carbodiimide, *EIS*: Electrochemical Impedance Spectroscopy, *FBS*: Fetal Bovine Serum, *GCE*: Glassy Carbon Electrode, *GQD*: Graphene Quantum Dots, *GSH*: Glutathione, *HMPB*: Hollow Mesoporous Prussian Blue, *Mb*: Cardiac Myoglobin, *MOF*: Metal Organic Framework, *MWCNT*: Multi-walled Carbon Nanotubes, *NHS*: N-hydroxysuccinimide, *P(L-Lys)*: Poly L-lysine *PCT*: procalcitonin, *PGE*: Pencil Graphite Electrode, *PSA*: Prostate Specific Antigen, *rGO*: Reduced Graphene Oxide, *sCD25*: Soluble α-chain of interleukin-2 receptor, *SPE*: Screen Printed Electrode, *SPGE*: Screen Printed Gold Electrode, *SWV*: Square Wave Voltammetry

15.4 fg/mL (S/N = 3). With the prepared sensor, human serum samples containing cTnI were analyzed and determined to be suitable for the diagnosis of AMI (Wang et al. 2021).

In a study by Singal et al. in 2018, an impedimetric biosensor was developed to detect the human cardiac biomarker troponin-I (cTnI). PAMAM-Pt was electrochemically deposited on SPCE, and its carboxyl groups were used as binders for site-specific biomolecular immobilization of the protein antibody anti-cTnI. The prepared sensor was characterized by transmission electron microscopy, UV-visible spectroscopy, and electrochemical techniques. Changes in phase angle obtained at an optimized frequency for antigen-antibody interactions were monitored, and an impedance study was performed for biomolecular sensing. A concentration-related increase in the phase angle of the sensor was observed with increasing cTnI concentration in the range of 1 pg mL^{-1} to 100 ng mL^{-1}. The dissociation constant was calculated to be 0.51 pM reflecting high affinity of biosensor toward cTnI analyte arising due to high anti-cTnI loading with a better probe orientation on the 3-dimensional PAMAM-Pt structure (Singal et al. 2018).

In a study conducted by Yola in 2021, a sandwich-based voltammetric immunosensor was designed to determine the breast cancer biomarker human epidermal growth factor receptor 2 (HER2). The sensor was modified with gold nanoparticles and then developed with a copper-organic framework (AuNPs/Cu-MOF) and platinum-doped graphite carbon nitride (g-C_3N_4) with quaternary chalcogenide as the base. Pt-doped g-C_3N_4 composite (Pt/g-C_3N_4) and Cu_2ZnSnS_4 nanoparticle (CZTS NP) quaternary chalcogenide were labeled as CZTS NPs/Pt/g-$_{C3N4.}$ AuNPs functionalized with an amino group, and Cu-MOFs containing carboxylic acid were synthesized. After conjugating primary HER2 antibody and antigen HER2 protein to AuNPs/Cu-MOF as a sensor platform, CZTS NPs/Pt/g-C_3N_4 composite was prepared by hydrothermal method. HER2 immunosensor ready after 30 min of immune reaction, SEM XPS, TEM, XRD method, FTIR, characterized by CV and EIS. The developed sensor showed high sensitivity with a detection limit of 3.00 fg mL^{-1}. In addition, the proposed method has beneficial features such as high selectivity, stability, repeatability, and reusability (Yola 2021).

3.4 Other Metal Nanoparticles

In some studies, biosensor studies have been carried out in which nanoparticles of other metals are used, unlike PtNP, AuNP, and AgNP. In these studies, it is seen that metals are combined singly or bimetallic. As an example of obtaining these metals, the production of chromium particles by electrochemical or chemical reduction methods and the electrochemical deposition of palladium can be given. Other studies on the direct or indirect use of metal nanoparticles in diagnosing diseases are included in this section (Welch and Compton 2006). Hybrid nanostructure-based biosensors used for the diagnosis of biomolecules have been summarized in Table 25.3.

Table 25.3 Electrochemical biosensors based on other/hybrid nanostructures for diagnostic biomolecules

Platform	Biomarker	Method	Linear range	LOD	Application	References
Au-AgNPs/GCE	H_2O_2	Amperometric	0.0005–2 mM	59 × 10–9 M	Human urine Blood serum	Gowthaman et al. (2019)
Au-ag/Co_3O_4NFsc/ GCE	H_2O_2	CV	0.05–5000 μM	0.01 × 10–6	Human breast cancer cells	Zhang et al. (2018)
Nf/Pd@ag/ rGO-NH_2/ GCE	H_2O_2	CV EIS	2–19,500 μM	0.7 μM	Milk samples	Guler et al. (2018)
Ni/ag@C/GCE	H_2O_2	CV	0.03–17 mM	0.01 mM	–	Sheng et al. (2017)
Fe_3O_4@SiO_2-NH2-au@Pd0.30NP	TAAbs	DPV	1–500 ng mL^{-1}	15 pg mL^{-1}	Recombinant protein G Human serum	Adeniyi et al. (2021)
GOD/AuAg HNPs/ ITO	Glucose	ECL	0.0050–1.0 mM	0.40 μM	Saliva Blood	Li et al. (2021a)
Au@Pt/MIL-53(Al)	2019- nCoV-NP.	DPV	0.025–50 ng mL $^{-1}$	8.33 pg mL $^{-1}$	Serum	Tian et al. (2021)
ErGO/AuPdNP	IL-6	EIS	0.1100000 pg mL^{-1}	0.059 pg mL-^{1}	Human serum	Lou et al. (2014)
SPCEs/PEI/NPs A and SPCEs/PEI/NPs B	p53	DPV	1.0–10 × 10^3 pg mL^{-1}	5.0 fg mL^{-1}	Fetal bovine serum (FBS) Saliva Cell lysates of a Saos-2 (p53-null) cell line	Ibáñez-Redín et al. (2020)
Ab2/CA72–4/BSA/ Ab1/rGO-TEPA/GCE	Gastric cancer biomarker CA72–4	EIS	0.001–10 U/mL	0.0003 U/mL	Serum samples	Wu et al. (2015)
Cancer biomarker prostate	Fe_3O_4 NPs/GO sheets	CV SWV	61 fg/mL to 3.9 pg/mL	15 fg/mL	Serum	Sharafeldin et al. (2017)
Ag@au-Fe_3O_4/GCE	Protein biomarker IgG	Amperometric	1 × 10–4–5000 ng mL^{-1}	0.05 pg mL^{-1}	Human serum	Zhang et al. (2016)
CuO-NiO/IL/CPE	Amlodipine (AML)	DPV	0.1–100 μM	0.06 μM	Pharmaceutical formulations human urine Blood plasma samples	Firouzi et al. (2020)
GOx/PVA-Fe_3O_4/Sn	Glucose	CV EIS	5 × 10^{-3}–30 mM	8 uM	Glucose	Sanaeifar et al. (2017)

Abbreviations: *Ab1*: Primary anti-CA72–4 Antibody, *Ab2*: Secondary anti-CA72–4 Antibody, *Ag*: Silver, *AgNP*: Silver Nanoparticle, *AML*: Amlodipine, *Au*: Gold, *AuNP*: Gold Nanoparticle, *BSA*: Bovine Serum Albumin, *CA 72-4*: Gastric Cancer Biomarker, Co_3O_4: Cobalt (II,III) Oxide, *CPE*: Carbon Paste Modified Electrode, *Cuo*: Copper(II) Oxide, *CV*: Cyclic Voltammetry, *DPV*: Differential Pulse Voltammetry, *ECL*: Electrochemiluminescence, *EIS*: Electrochemical Impedance Spectroscopy, *ErGO*: Reduced Graphene Oxide, Fe_3O_4: Iron Oxide, *GCE*: Glassy Carbon Electrode, *GO*: Graphene Oxide, *GOD*: Glucose Oxidase, *GOx*: Glucose Oxidase, H_2O_2: Hydrogen Peroxide, *HNP*: Hollow Nanoparticle, *IgG*: Immunoglobulin G, *IL*: İonic Liquid, *IL-6*: İnterleukin-6, *ITO*: Indium Tin Oxide, *MIL-53(Al)*: Metal Organic Frameworks, *2019-Ncov-NP*: Sarscov-2 Nucleocapsid Protein, *Nf*: Nafion, *Nfs*: Nanofibers, NH_2: Amino Redical, *NiO*: Nickel (II) Oxide, *Pd*: Palladium, *PEI*: Polyethyleneimine, *Pt*: Platinum, *PVA*: Polyvinyl Alcohol, *Rgo*: Reduced Graphene Oxide, SiO_2: Silicon Dioxide, *Sn*: Tin, SPCE: Screen Printed Carbon Electrode, *SWV*: Square Wave Voltammetry, *TAAb*: Tumor-Associated Autoantibodies, *TEPA*: Tetraethylene Pentamine

Different biomarkers can determine the oxidative stress values in our bodies. Gowthaman, N.S.K. et al. designed an electrochemical sensor to detect hydrogen peroxide (HP) level in urine in a study in 2019. HP can be used to determine oxidative stress in the body. Au-AgNPs fabricated carbon cloth, and GCE are used in this designed sensor. $AgNO_3$ and $HAuCl_4$ were used to bind these metal ions to the electrode surface. CV and Differential Pulse Voltammetry (DPV) methods were used to characterize Au-AgNPs modified to the electrode. As a result, the detection limit and range values are, respectively, 59 nM (S/N = 3) and 500 nM–2 mM. This flexible sensor has successfully measured HP (Gowthaman et al. 2019).

In a study by M. Guler et al., H_2O_2, used to detect many diseases, was determined on milk samples. In this work, they developed a sensitive sensor whose platform is Nafion/palladium@silver/reduced graphene oxide/glassy carbon electrode (Nf/Pd@Ag/rGO-NH2/GCE). The rGo-NH2 in the sensor has been developed with other platform layers. FTIR, XRD, and High-resolution transmission electron microscopy (HRTEM) were used to characterize synthesized nanocomposites. In addition, CV and EIS were used for electrochemical characterization. The sensor's success in milk samples indicates that it may also be used for non-enzymatic H_2O_2 determination in other samples. In this study, the linear range of the sensor has a wide range, such as 2–19,500 μM. At the same time, LOD was found to be 0.7 μM. This linear and wide range is due to Pd and Ag nanoparticles (Guler et al. 2018).

H_2O_2 can be detected by developing sensors using nanomaterials. Q. Sheung et al. developed a nanomaterial platform on which H_2O_2 detection was performed in 2017. Next, this platform was modified on a GCE. The Ag@C platform was modified with Nickel (Ni) and supported in this study. Thus, Ni/Ag@C platform was formed. SEM, TEM, energy dispersive X-ray spectroscopy, and FT-IR methods characterize this platform. Then, CV was used to evaluate and electrochemical characterization of H_2O_2 at different concentrations. The calculated linear range of this platform for non-enzymatic H_2O_2 detection is 0.03–17.0 mM. Also, the detection limit value is 0.01 mM (Sheng et al. 2017).

Blood glucose level is data that can be measured in many ways to diagnose diabetes mellitus (DM). It is possible to determine the blood sugar level by a blood draw, but it is a painful and challenging method to follow. In 2021, Li and colleagues developed a sensor for determining glucose levels in saliva and blood. Cluster-like hollow AgAu nanoparticles (AuAg HNP's) were synthesized and modified to the platform. These HNPs are used as glucose detection matrix after characterization by electronic microscopy, UV-Vis spectrometry, IR spectrometry, XRD, XPS, and electrochemical methods. The synthesized AuAg HNPs are modified on indium tin oxide (ITO)-coated glass, part of the biosensor platform. The adhesion of hydrolyzed (3-aminopropyl) trimethoxysilane (APTMS) during AuAg HNP synthesis and modification on ITO, which acts as a basal electrode, increases electrochemiluminescence and provides sensitivity. A glucose sensor was created by adding glucose oxidase to the platform. The resulting GOD/AuAg HNPs/ITO platform was electrochemically characterized by ECL. Figure 25.5 represents the SEM and TEM images of AuAg NPs before and after centrifugation. According to the TEM image, the AuAg alloy has a diameter of 20 nm before centrifugation.

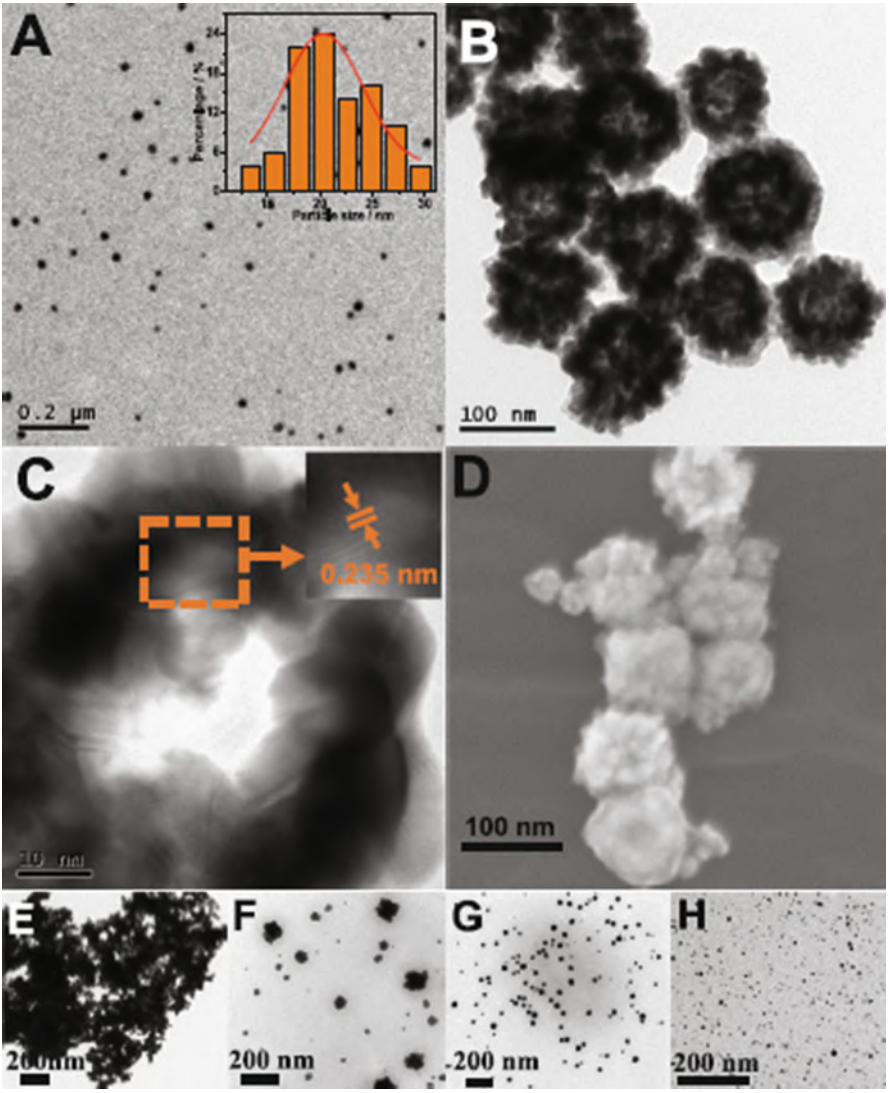
A
Percentage / %
0
6
12
18
24
15
20
25
30
Particle size / nm
0.2 μm
B
100 nm
C
0.235 nm
10 nm
D
100 nm
E
200 nm
F
200 nm
G
200 nm
H
200 nm

Fig. 25.5 The TEM images of (**a**) AuAg NPs before centrifugation and (**b, c**) AuAg HNPs after centrifugation; Inset in (**a**) is the corresponding particle-size distribution histogram, in (**c**) shows the lattice distance of the selected area. (**d**) The SEM image of AuAg HNPs. The TEM images of AuAg NPs obtained without (**e**) and with BSA (F-H). (Reproduced with permission from Li et al. 2021a)

However, it was observed that they tend to form a hollow sphere with a diameter of 100 nm by collecting after centrifugation. The SEM image confirms this claim. As a result, the linear range was determined as 5.0 μM–1.0 mM. In addition, the detection limit value is 0.40 μM. This advanced sensor is suitable for disposable situations. The values obtained from saliva and blood samples were related to each other. (Li et al. 2021a).

In 2019, the world faced a pandemic because of severe acute respiratory syndrome coronavirus 2 (SARS-CoV-2). Due to the significant threat to human health, the diagnostic methods of COVID-19 should be developed by scientists. Some of the techniques used to diagnose COVID-19 to date are real-time reverse-transcriptase polymerase chain reaction (RT-PCR), computed tomography (CT), and serum virus neutralization test (SVNA). In 2021, J. Tian, Z. Liang, O. Hu et al. developed a new biosensor to diagnose this infectious disease where early detection and sensitivity are essential (Tian et al. 2021). This developed biosensor has an electrochemical double aptamer structure. The biomarker used to detect COVID-19 disease is the SARS-CoV-2 nucleocapsid protein (2019-nCoV-NP). First, a gold electrode (GE) was used as the surface, and two different aptamers (thiol modified N48 and N61) were immobilized. Afterward, Au@Pt nanoparticles and horseradish peroxidase (HRP), and G-quadruplex DNAzyme were used to make the necessary detection and increase the sensitivity. The platform of this double aptamer biosensor (Au@Pt/MIL-53(Al)) was characterized by EIS, DPV, and CV methods. Finally, the linear range was found to be 0.025–50 ng $mL^{-1,}$ and LOD was 8.33 pg mL^{-1} (Tian et al. 2021).

It is known that the p53 gene is involved in the growth of cells that suppress tumors. It has been observed that this gene is mutated in many types of cancer. Therefore, detection of protein-structured p53 will be advantageous if used for the early diagnosis of diseases. In 2020, Gisela Ibáñez-Redín and colleagues developed a disposable biosensor based on SPEs to detect the p53 gene. The principle of the aim of this biosensor is to adsorb anti-p53 antibodies to attach to the carboxylated $NiFe_2O_4$ NPs and polyethyleneimine. The platform of this unlabeled biosensor was determined as SPCE/PEI/NPs-Ab B, and the DPV method was used for characterization. The detection limit for the improved disposable immunosensor was calculated as 5.0 fg mL^{-1}. The linear range was extremely wide, 1.0 to 10×10^3 pg mL^{-1}. Negligible errors were observed in high protein fetal bovine serum and cell lysate matrices which shows high selectivity of the immunosensor (Ibáñez-Redín et al. 2020).

Tumor biomarkers are widely used in the diagnosis of cancer diseases. By detecting these markers, it is aimed to obtain information on the extent of the tumor and its preoperative level. In a study by Dan Wu et al. in 2015, a high-sensitivity and non-enzymatic sandwich-type immunosensor was used to detect gastric cancer, the second leading cause of cancer deaths globally. The biomarker used in this study is CA72–4, mucin with a high molecular weight of 220–400 kDa. Pt, Pd, and Fe_3O_4 were used to produce the biosensor, and the synergistic effect of these different nanoparticles was utilized. GCE was used in the immunosensor. First, the primary antibody, anti-CA72–4 (Ab1), was immobilized, and then reduced graphene oxide tetraethylenepentamine (rGO-TEPA) modification was made. The secondary anti-CA72–4 antibody (Ab2) was adsorbed with the nanoparticles. CV was used to characterize bimetallic PtPd NP's and Fe_3O_4 in the presence of PBS. In the DPV studies, the detection limit and linear range were obtained as 0.0003 U/mL and 0.001–10 U/mL, respectively (Wu et al. 2015).

Cardiovascular diseases are a type of disease in which common diseases such as heart attack are also included in the heart and vessels. According to a statistic published by WHO in 2016, 31% of deaths were due to cardiovascular diseases. Mazharul Haque et al. designed a biosensor in 2020 intending to detect nanomolar myoglobin (Mb), a biomarker used to diagnose cardiovascular diseases, at different concentrations. The basis of this biosensor is a gold-plated screen-printed electrode. In addition, Cu-containing ZnO nanoparticles were synthesized and characterized by XRD, Fourier transform infrared spectroscopy methods. Afterward, it was determined that the biomarker Mb was related to the Cu concentration, and CV and EIS methods in the range of 3–15 nM were used for this. As a result of the analysis, the detection limit value was 0.46 nM (Haque et al. 2020).

Polyphenols, an antioxidant, should be abundant in diets to prevent cardiovascular and cancer diseases. Sheetal Chawla et al. designed an amperometric biosensor in 2012 and aimed to determine the total phenolic content in different fruit juices. The AuE was used for this biosensor. First, a composite of carboxylated multiwalled carbon nanotubes (cMWCNTs)/polyaniline (PANI) was decorated. (Lac) was immobilized on this decorated platform, and the resulting platform was modified on the electrode used. SEM, FTIR, CV, and EIS methods were used for the biosensor, which became Lac/NiNPs/cMWCNT/PANI/AuE in the final stage. The Pt wire was chosen for the reference electrode. The detection limit value for the biosensor is 0.05 μM. The linear range was evaluated separately for low and high concentrations. It is 0.1–10 μM for low concentrations and 10–500 μM for high concentrations. Using the electrode 200 times over 4 months shows repeatable results (Chawla et al. 2012).

4 Conclusion

Biomarkers are proteins that reflect the normal or abnormal activity of the organism. It is found in tissues and body fluids. The appearance of biomarkers here and their concentration changes are symptoms of many diseases. Therefore, early diagnosis and diagnosis of biomarkers are crucial. Therefore, rapid, sensitive, and cost-effective analysis methods that can be used in clinical settings are needed to detect biomarkers. Electrochemical sensors for detecting biomarkers have been extensively developed with successful applications. The developed electrochemical sensors are preferred because of their many features, such as high sensitivity and the detection of target biomarkers at low concentrations. To increase the sensitivity of the developed sensor, the sensor surface is modified with functional and conducting molecules. Metal nanoparticles are the most widely used among them. Metal nanoparticles are nanomaterials with an average diameter of less than 100 nm. These metal nanoparticles are often preferred in sensors because they exhibit unusual physical and chemical properties. This way it allows for faster and more precise determination of the substance. To summarize, advances in identifying electrochemical sensors and biomarkers will enable new research areas for ongoing research in this area.

References

Abbas A, Amin HMA (2022) Silver nanoparticles modified electrodes for electroanalysis: an updated review and a perspective. Microchem J 175:107166

Adeniyi O, Sicwetsha S, Adesina A, Mashazi P (2021) Immunoassay detection of tumor-associated autoantibodies using protein G bioconjugated to nanomagnet-silica decorated with Au@Pd nanoparticles. Talanta 226:122127

António M, Vitorino R, Daniel-da-Silva AL (2021) Gold nanoparticles-based assays for biodetection in urine. Talanta 230:122345

Arya SK, Estrela P (2018) Recent advances in enhancement strategies for electrochemical ELISA-based immunoassays for cancer biomarker detection. Sensors (Switzerland) 18(7):2010

Awan M, Rauf S, Abbas A, Nawaz MH, Yang C, Shahid SA, Amin N, Hayat A (2020) A sandwich electrochemical immunosensor based on antibody functionalized-silver nanoparticles (Ab-Ag NPs) for the detection of dengue biomarker protein NS1. J Mol Liq 317:114014

Bakirhan NK, Ozcelikay G, Ozkan SA (2018) Recent progress on the sensitive detection of cardiovascular disease markers by electrochemical-based biosensors. J Pharm Biomed Anal 159:406–424

Boonkaew S, Jang I, Noviana E, Siangproh W, Chailapakul O, Henry CS (2021) Electrochemical paper-based analytical device for multiplexed, point-of-care detection of cardiovascular disease biomarkers. Sensors Actuators B Chem 330:129336

Chandra P (2013) HER2 protein biomarker based sensor systems for breast cancer diagnosis. J Mol Biomark Diagn 05(01):e119

Chawla S, Rawal R, Sharma S, Pundir CS (2012) An amperometric biosensor based on laccase immobilized onto nickel nanoparticles/carboxylated multiwalled carbon nanotubes/polyaniline modified gold electrode for determination of phenolic content in fruit juices. Biochem Eng J 68: 76–84

Datta N, Pal M, Roy U, Mitra R, Pradhan A (2014) World J Pharm Res Inf 13(8):15

Ding L, Cheng W, Wang X, Ding S, Ju H (2008) Carbohydrate monolayer strategy for electrochemical assay of cell surface carbohydrate. J Am Chem Soc 130(23):7224–7225

Ensafi AA, Rezaloo F, Rezaei B (2016) Electrochemical sensor based on porous silicon/silver nanocomposite for the determination of hydrogen peroxide. Sensors Actuators B Chem 231: 239–244

Fazio E, Spadaro S, Corsaro C, Neri G, Leonardi SG, Neri F, Lavanya N, Sekar C, Donato N, Neri G (2021) Metal-oxide based nanomaterials: synthesis, characterization and their applications in electrical and electrochemical sensors. Sensors 21(7):2494

Ferhan AR, Hwang Y, Bin IMS, Anand S, Kim A, Jackman JA, Cho NJ (2021) Ultrahigh surface sensitivity of deposited gold nanorod arrays for nanoplasmonic biosensing. Appl Mater Today 23:101046

Firouzi M, Giahi M, Najafi M, Homami SS, Mousavi SHH (2020) Electrochemical determination of amlodipine using a CuO-NiO nanocomposite/ionic liquid modified carbon paste electrode as an electrochemical sensor. J Nanopart Res 23(4):82

Ghanavati M, Tadayon F, Bagheri H (2020) A novel label-free impedimetric immunosensor for sensitive detection of prostate specific antigen using au nanoparticles/MWCNTs- graphene quantum dots nanocomposite. Microchem J 159:105301

Gowthaman NSK, Arul P, Shim JJ, John SA (2019) Free-standing au-ag nanoparticles on carbon cloth: a non-enzymatic flexible electrochemical sensor for the biomarker of oxidative stress. Appl Surf Sci 495:143550

Guler M, Turkoglu V, Bulut A, Zahmakiran M (2018) Electrochemical sensing of hydrogen peroxide using Pd@ag bimetallic nanoparticles decorated functionalized reduced graphene oxide. Electrochim Acta 263:118–126

Hammami I, Alabdallah NM, Al JA, Kamoun M (2021) Gold nanoparticles: synthesis properties and applications. J King Saud Univ – Sci 33(7):101560

Han L, Liu CM, Dong SL, Du CX, Zhang XY, Li LH, Wei Y (2017) Enhanced conductivity of rGO/Ag NPs composites for electrochemical immunoassay of prostate-specific antigen. Biosens Bioelectron 87:466–472

Haque M, Fouad H, Seo HK, Alothman OY, Ansari ZA (2020) Cu-doped ZnO nanoparticles as an electrochemical sensing electrode for cardiac biomarker myoglobin detection. IEEE Sensors J 20(15):8820–8832

Hua Z, Yu T, Liu D, Xianyu Y (2021) Recent advances in gold nanoparticles-based biosensors for food safety detection. Biosens Bioelectron 179:113076

Huang Y, Cui L, Xue Y, Zhang S, Zhu N, Liang J, Li G (2017) Ultrasensitive cholesterol biosensor based on enzymatic silver deposition on gold nanoparticles modified screen-printed carbon electrode. Mater Sci Eng C 77:1–8

Ibáñez-Redín G, Joshi N, do Nascimento GF, Wilson D, Melendez ME, Carvalho AL, Reis RM, Gonçalves D, Oliveira ON (2020) Determination of p53 biomarker using an electrochemical immunoassay based on layer-by-layer films with $NiFe_2O_4$ nanoparticles. Microchim Acta 187(11):619

Jang HD, Kim SK, Chang H, Choi JW (2015) 3D label-free prostate specific antigen (PSA) immunosensor based on graphene-gold composites. Biosens Bioelectron 63:546–551

Jiang Y, Cui J, Zhang T, Wang M, Zhu G, Miao P (2019) Electrochemical detection of T4 polynucleotide kinase based on target-assisted ligation reaction coupled with silver nanoparticles. Anal Chim Acta 1085:85–90

Khoshnevisan K, Torabi F, Baharifar H, Sajjadi-Jazi SM, Afjeh MS, Faridbod F, Larijani B, Khorramizadeh MR (2020) Determination of the biomarker L-tryptophan level in diabetic and normal human serum based on an electrochemical sensing method using reduced graphene oxide/gold nanoparticles/18-crown-6. Anal Bioanal Chem 412(15):3615–3627

King RJ, Singh PK, Mehla K (2022) The cholesterol pathway: impact on immunity and cancer. Trends in immunology 43(1):78–92

Lei J, Ju H (2012) Signal amplification using functional nanomaterials for biosensing. Chem Soc Rev 41(6):2122–2134

Li J, Li S, Yang CF (2012) Electrochemical biosensors for cancer biomarker detection. Electroanalysis 24(12):2213–2229

Li Y, Li Y, Xu N, Pan J, Chen T, Chen Y, Gao W (2017) Dual-signal amplification strategy for electrochemiluminescence sandwich biosensor for detection of thrombin. Sensors Actuators B Chem 240:742–748

Li D, Tan R, Mi X, Fang C, Tu Y (2021a) An electrochemiluminescent biosensor for noninvasive glucose detection based on cluster-like AuAg hollowed-nanoparticles. Microchem J 167:106271

Li L, Wei Y, Zhang S, Chen X, Shao T, Feng D (2021b) Electrochemical immunosensor based on metal ions functionalized CNSs@au NPs nanocomposites as signal amplifier for simultaneous detection of triple tumor markers. J Electroanal Chem 880:114882

Liu S, Leech D, Ju H (2003) Application of colloidal gold in protein immobilization, electron transfer, and biosensing. Anal Lett 36(1):1–19

Lou Y, He T, Jiang F, Shi JJ, Zhu JJ (2014) A competitive electrochemical immunosensor for the detection of human interleukin-6 based on the electrically heated carbon electrode and silver nanoparticles functionalized labels. Talanta 122:135–139

Luo J, Li T, Yang M (2019) Detection protein biomarker with gold nanoparticles functionalized hollow mesoporous Prussian blue nanoparticles as electrochemical probes. Chin Chem Lett 31(1):202–204

Magar HS, Ghica ME, Abbas MN (December 2016) Brett CMA (2017) a novel sensitive amperometric choline biosensor based on multiwalled carbon nanotubes and gold nanoparticles. Talanta 167:462–469

Mahapatra S, Baranwal A, Purohit B, Roy S, Mahto SK, Chandra P (2020) Diagnostic strategies for COVID-19 and other coronaviruses. Springer Singapore, Singapore, pp 19–36

Mahato K, Kumar S, Srivastava A, Maurya PK, Singh R, Chandra P (2018) Electrochemical immunosensors: fundamentals and applications in clinical diagnostics. In: Handbook of immunoassay technologies. Academic Press, pp 359–414

Mansuriya BD, Altintas Z (2021) Enzyme-free electrochemical nano-immunosensor based on graphene quantum dots and gold nanoparticles for cardiac biomarker determination. Nano 11(3):1–18

Merkoçi A (2013) Nanoparticles based electroanalysis in diagnostics applications. Electroanalysis 25(1):15–27

Meyers MA, Mishra A, Benson DJ (2006) Mechanical properties of nanocrystalline materials. Prog Mater Sci 51(4):427–556

Miranda RR, Sampaio I, Zucolotto V (2022) Exploring silver nanoparticles for cancer therapy and diagnosis. Colloids Surf B Biointerfaces 210:112254

Narang J, Chauhan N, Jain P, Pundir CS (2012) Silver nanoparticles/multiwalled carbon nanotube/polyaniline film for amperometric glutathione biosensor. Int J Biol Macromol 50(3):672–678

Onyancha RB, Ukhurebor KE, Aigbe UO, Osibote OA, Kusuma HS, Darmokoesoemo H, Balogun VA (2021) A systematic review on the detection and monitoring of toxic gases using carbon nanotube-based biosensors. Sens Bio-Sensing Res 34:100463

Ortega FG, Fernández-Baldo MA, Serrano MJ, Messina GA, Lorente JA, Raba J (2015) Epithelial cancer biomarker EpCAM determination in peripheral blood samples using a microfluidic immunosensor based in silver nanoparticles as platform. Sensors Actuators B Chem 221: 248–256

Pihíková D, Belicky KP, Bertok T, Tkac J (2016) Sensitive detection and glycoprofiling of a prostate specific antigen using impedimetric assays. Analyst 141(3):1044–1051

Raj M, Goyal RN (2019) Silver nanoparticles and electrochemically reduced graphene oxide nanocomposite based biosensor for determining the effect of caffeine on estradiol release in women of child-bearing age. Sensors Actuators B Chem 284:759–767

Rezaei B, Ghani M, Shoushtari AM, Rabiee M (2016) Electrochemical biosensors based on nanofibres for cardiac biomarker detection: a comprehensive review. Biosens Bioelectron 78: 513–523

Ruckenstein E, Li ZF (2005) Surface modification and functionalization through the self-assembled monolayer and graft polymerization. Adv Colloid Interf Sci 113(1):43–63

Saeed AA, Sánchez JLA, O'Sullivan CK, Abbas MN (2017) DNA biosensors based on gold nanoparticles-modified graphene oxide for the detection of breast cancer biomarkers for early diagnosis. Bioelectrochemistry 118:91–99

Sajid M (2022) Nanomaterials: types, properties, recent advances, and toxicity concerns. Curr Opin Environ Sci Heal 25:100319

Sanaeifar N, Rabiee M, Abdolrahim M, Tahriri M, Vashaee D, Tayebi L (2017) A novel electrochemical biosensor based on Fe3O4 nanoparticles-polyvinyl alcohol composite for sensitive detection of glucose. Anal Biochem 519:19–26

Shanbhag MM, Ilager D, Mahapatra S, Shetti NP, Chandra P (2021) Amberlite XAD-4 based electrochemical sensor for diclofenac detection in urine and commercial tablets. Mater Chem Phys 273:125044

Sharafeldin M, Bishop GW, Bhakta S, El-Sawy A, Suib SL, Rusling JF (2017) Fe_3O_4 nanoparticles on graphene oxide sheets for isolation and ultrasensitive amperometric detection of cancer biomarker proteins. Biosens Bioelectron 91:359–366

Shawky AM, El-Tohamy M (2021) Signal amplification strategy of label-free ultrasenstive electrochemical immunosensor based ternary ag/TiO_2/rGO nanocomposites for detecting breast cancer biomarker CA 15-3. Mater Chem Phys 272:124983

Sheng Q, Shen Y, Zhang J, Zheng J (2017) Ni doped ag@C core-shell nanomaterials and their application in electrochemical H_2O_2 sensing. Anal Methods 9(1):163–169

Shnoudeh AJ, Hamad I, Abdo RW, Qadumii L, Jaber AY, Surchi HS, Alkelany SZ (2019) Synthesis, characterization, and applications of metal nanoparticles. Elsevier Inc.

Şimşek N, Gözde Aydoğdu TIĞ (2022) Graphene quantum dot-poly(L-lysine)-gold nanoparticles nanocomposite for electrochemical determination of dopamine and serotonin. Electroanalysis 34(1):61–73

Singal S, Srivastava AK, Kotnala RK, Rajesh (2018) Single-frequency impedance analysis of biofunctionalized dendrimer-encapsulated Pt nanoparticles-modified screen-printed electrode for biomolecular detection. J Solid State Electrochem 22(9):2649–2657

Singh S, Tuteja SK, Sillu D, Deep A, Suri CR (2016) Gold nanoparticles-reduced graphene oxide based electrochemical immunosensor for the cardiac biomarker myoglobin. Microchim Acta 183(5):1729–1738

Talamini L, Zanato N, Zapp E, Brondani D, Westphal E, Gallardo H, Vieira IC (2018) Heparin-gold nanoparticles and liquid crystal applied in label-free electrochemical immunosensor for prostate-specific antigen. Electroanalysis 30(2):353–360

Tian J, Liang Z, Hu O, He Q, Sun D, Chen Z (2021) An electrochemical dual-aptamer biosensor based on metal-organic frameworks MIL-53 decorated with au@Pt nanoparticles and enzymes for detection of COVID-19 nucleocapsid protein. Electrochim Acta 387:8

Tığ GA (2017) Development of electrochemical sensor for detection of ascorbic acid, dopamine, uric acid and L-tryptophan based on ag nanoparticles and poly(L-arginine)-graphene oxide composite. J Electroanal Chem 807:19–28

Wang Z, Zhao H, Chen K, Li H, Lan M (2021) Sandwich-type electrochemical aptasensor based on hollow mesoporous carbon spheres loaded with porous dendritic Pd@Pt nanoparticles as signal amplifier for ultrasensitive detection of cardiac troponin I. Anal Chim Acta 1188:339202

Welch CM, Compton RG (2006) The use of nanoparticles in electroanalysis: a review. Anal Bioanal Chem 384(3):601–619

Wu D, Guo Z, Liu Y, Guo A, Lou W, Fan D, Wei Q (2015) Sandwich-type electrochemical immunosensor using dumbbell-like nanoparticles for the determination of gastric cancer biomarker CA72-4. Talanta 134:305–309

Xia N, Chen Z, Liu Y, Ren H, Liu L (2017) Peptide aptamer-based biosensor for the detection of human chorionic gonadotropin by converting silver nanoparticles-based colorimetric assay into sensitive electrochemical analysis. Sensors Actuators B Chem 243:784–791

Xie J, Cheng D, Li P, Xu Z, Zhu X, Zhang Y, Li H, Liu X, Liu M, Yao S (2021) Au/metal–organic framework Nanocapsules for electrochemical determination of glutathione. ACS Appl Nano Mater 4(5):4853–4862

Yáñez-Sedeño P, Pingarrón JM (2005) Gold nanoparticle-based electrochemical biosensors. Anal Bioanal Chem 382(4):884–886

Yola ML (2021) Sensitive sandwich-type voltammetric immunosensor for breast cancer biomarker HER_2 detection based on gold nanoparticles decorated Cu-MOF and Cu_2ZnSnS_4 NPs/Pt/g-C_3N_4 composite. Microchim Acta 188(3):78

Yoo YK, Kim G, Park D, Kim J, Kim YS, Yun Kim H, Yang SH, Lee JH, Hwang KS (2020) Gold nanoparticles assisted sensitivity improvement of interdigitated microelectrodes biosensor for amyloid-β detection in plasma sample. Sensors Actuators B Chem 308:127710

Yu X, Munge B, Patel V, Jensen G, Bhirde A, Gong JD, Kim SN, Gillespie J, Silvio Gutkind J, Papadimitrakopoulos F, Rusling JF (2006) Carbon nanotube amplification strategies for highly sensitive Immunodetection of cancer biomarkers. J Am Chem Soc 128(34):11199–11205

Zhang H, Ma L, Li P, Zheng J (2016) A novel electrochemical immunosensor based on non-enzymatic Ag@Au-Fe_3O_4 nanoelectrocatalyst for protein biomarker detection. Biosens Bioelectron 85:343–350

Zhang Y, Deng D, Zhu X, Liu S, Zhu Y, Han L, Luo L (2018) Electrospun bimetallic Au-Ag/Co_3O_4 nanofibers for sensitive detection of hydrogen peroxide released from human cancer cells. Anal Chim Acta 1042:20–28

Disposable Electrochemical Nanobiosensors for Biomolecular Analysis

26

Gulsah Congur

Contents

1 Introduction 570
2 Disposable Electrode Materials for the Development of an Electrochemical Biosensor ... 572
  2.1 Pencil Graphite Electrodes 572
  2.2 Screen-Printed Electrodes (SPEs) 573
  2.3 Paper-Based Electrodes 574
3 Most Commonly Used Nanomaterials for Construction of Disposable Electrochemical Biosensors 575
  3.1 Nanotubes and Their Use for the Development of Disposable Electrochemical Biosensor Area 576
  3.2 The Applications of Graphene and Its Derivatives 581
4 Concluding Remarks 589
References 590

Abstract

Biosensors are modern analytical tools capable of monitoring diseases, drugs, proteins, environmental pollutants, and bioterrorism agents. They are alternative to the conventional analytical techniques due to the fact that they have practical and miniaturized bodies as well as they have target-specific characteristics. The integration of biosensor technologies into electrochemical analysis methods makes the bioanalytical system more reliable, robust, sensitive, and selective platform that can perform quantitative analysis. The use of nanomaterials and their nanocomposites enhances robustness, sensitivity, and selectivity features of these analytical tools. Herein, nanomaterials-based disposable electrochemical biosensor applications that are frequently used in recent years are presented. Due to distinctive properties of this group of biosensors, high-performance point-of-

---

G. Congur (✉)
Vocational School of Health Services, Department of Pharmacy, Bilecik Seyh Edebali University, Bilecik, Türkiye
e-mail: gulsah.congur@bilecik.edu.tr

© Springer Nature Singapore Pte Ltd. 2023

U. P. Azad, P. Chandra (eds.), *Handbook of Nanobioelectrochemistry*,
https://doi.org/10.1007/978-981-19-9437-1_26

care diagnostics developed by using them are expected to have great global market potential in future.

Keywords

Single use · Electrochemical biosensor · Nanomaterials · Pencil graphite electrode · Screen-printed electrode · Paper-based electrode

1 Introduction

Biosensors are the recognition tools developed for quantitative or semiquantitative monitoring of target molecules by using their target-specific biological recognition (biorecognition) elements (Turner 2013; Wang et al. 2014). Their most common biorecognition elements may be different types of nucleic acids, antibodies, aptamers, enzymes, and cells (Moraskie et al. 2021), and new types of biorecognition elements have been still developing. The interaction between the biorecognition element and the target molecule triggers a biocatalytic reaction that gives a readable signal monitored by a transducer and a digital system (Lakshmipriya and Gopinath 2019). This signal could be observed by different detection techniques such as optical, electrochemical, piezoelectric, colorimetric, etc., and finally, reliable monitoring of the target molecule could be achieved (Pandey and Malhotra 2019).

Since the first biosensor definition introduced by Clark and Lyons (Lakshmipriya and Gopinath 2019; Dowlatshahi and Abdekhodaie 2021) in the field of analytical chemistry, researchers have made great efforts to design ideal biosensor systems adaptable to several areas such as environmental monitoring (Wang et al. 2014; Congur 2021), diagnostic applications for vital diseases (Choudhary et al. 2016; Kamali et al. 2022; Wang 2017), or metabolites related to physical activities (Kim et al. 2019), and development of drugs (Gonçalves et al. 2014). An ideal biosensor system not only must recognize the target molecule -in other words, analyte-selectively and sensitively but also should be robust, cheap, time-saver, portable, and applicable to real-life (Lakshmipriya and Gopinath 2019). Researchers have been taking advantage of nanotechnology science to achieve the desired goals while developing a biosensor structure (Seo et al. 2019; Sharifi et al. 2019; Srivastava et al. 2018). Due to the fact that the modification of the nanomaterials provide large surface area to perform the biocatalytic reaction, an amplified biosensor response, namely a signal, is obtained that results in the sensitive and selective recognition of the analyte. Furthermore, the use of nanomaterials makes biosensors more stable, robust, and miniaturized analytical devices. In the light of these explanations, the term “nanobiosensors” could be defined as the biosensors constructed with at least one type of nanomaterials which are capable of not only precise monitoring of the analyte but also having the properties as fast, stable, and miniaturized.

Selection of the detection method is a paramount feature during the fabrication process of the biosensor systems. The required properties described above are gained in by choosing the right detection strategy. Although there are many types of detection techniques, electrochemical sensing methods take a step forward because they provide to obtain reliable and sensitive quantitative results as well as allow the fabrication of portable devices (Loo and Pui 2020; Thapa et al. 2022). On the other hand, nanomaterials enhance the electron transfer rate resulting signal amplification and providing a larger surface area in the electrochemical biosensor systems (Bhatnagar et al. 2018; Mahato et al. 2019; Mujica et al. 2020; Dowlatshahi and Abdekhodaie 2021). Therefore, there is an increasing number of reports in the literature about the combination of nanotechnology science and the electrochemical biosensors area.

An electrochemical biosensor includes a three-electrode system consisting of a reference electrode, a counter electrode, and a working electrode. The electrochemical measurements are performed in an electrochemical cell that contains the target analyte and/or appropriate measurement solution. The selected nanomaterials are modified at the surface of the working electrode, where the redox reactions related to the biocatalytic reactions occur. Amperometric, potentiometric, voltammetric, or impedimetric responses are obtained as a result of electrochemical measurements. In a voltammetric biosensor, the redox reactions are recognized based on a current value produced by applying a potential at the electrode/electrolyte interface (Batchelor-McAuley et al. 2015). In an impedimetric biosensor, the biosensor response is the impedance value (Dzulkurnain et al. 2021). Voltammetric measurements can be performed with an easy and affordable way, and the biosensor response can be obtained in just few seconds/minutes (Batchelor-McAuley et al. 2015). On the other hand, an impedimetric detection route provides the sensitive analysis of the target molecule by measuring the impedance value after each modification or the interaction step occurring at the surface of the working electrode (Goh et al. 2021; Ahmadi et al. 2022).

The critical factor for the fabrication of disposable electrochemical biosensors is the type of the working electrode. Although several types of working electrodes have been intensively worked to fabricate the electrochemical biosensors, some of them are reusable, such as glassy carbon electrode (GCE), carbon paste electrode (CPE), and metal electrodes. They should be prepared with several mechanical or chemical techniques before their use. These pretreatment techniques are time-consuming, hard to apply for every electrochemical measurement, and require using extra chemical agents (usually acidic solutions). On the other hand, being simple, feasible, and sustainable are the desired features not only for the fabrication of a biosensor system but also for the designing of all new-generation engineered tools. Disposable raw materials help to achieve these features in the structure of an electrochemical biosensor (Killard 2017). Furthermore, they serve stable and appropriate surfaces for modification of the nanomaterials. The principles of the development of a disposable electrochemical biosensor are represented in Fig. 26.1.

In this chapter, disposable electrochemical biosensors developed with different types of nanomaterials for biomolecular analyses are presented. Disposable electrode materials are introduced and how possible to use them as a biosensor is explained in detail. It is aimed to give deep understanding and wide perspective to the audience about nanomaterials-based disposable electrochemical biosensors by giving the modification procedures of nanomaterials in different examples.

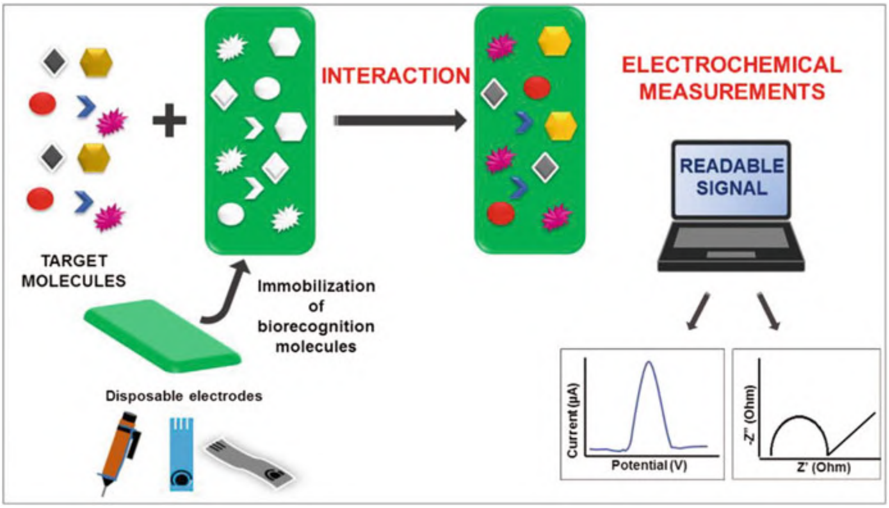
TARGET MOLECULES
INTERACTION
ELECTROCHEMICAL MEASUREMENTS
READABLE SIGNAL
Immobilization of biorecognition molecules
Disposable electrodes
Current (µA)
Potential (V)
-Z" (Ohm)
Z' (Ohm)

Fig. 26.1 Schematic representation of the development of a disposable electrochemical biosensor

2 Disposable Electrode Materials for the Development of an Electrochemical Biosensor

There are different types of single-use materials used for the development of an electrochemical biosensor. However, the potential of their applicability in the electrochemical biosensor area depends on their robustness, affordable, and sustainability structural properties (Killard 2017). Additionally, their easy modification and superior electrical properties make them preferable for the selection of electrode material. In this manner, frequently applied disposable electrode materials are given in this section.

2.1 Pencil Graphite Electrodes

Carbonaceous leads have been widely used for the purpose of writing instead of classical pencils during the last century. Their electrically conductive structure was discovered, and their use as electrode material began. They provide high surface area for modification/immobilization processes as well as provide superior electrochemical properties. Furthermore, they have all the crucial properties that a disposable biosensor should have. However, being cheap and easy to use get them one step forward in implementation of an electrochemical biosensor application.

Pencil leads are produced by mixing the graphite powder with a lump of clay as a binder. Then, this mixture is extruded, and heat treatment is applied (Ishida and Saito 1977). They have different hardness levels ranging from 10H to 10B (Torrinha et al. 2018). The graphite/clay ratio increases from H to B and this ratio also depends on the manufacturer. Therefore, it is important to choose the right hardness level and the manufacturer (Torrinha et al. 2018). There are different reports in the literature to use different hardness levels of the pencil leads as 6B (Down et al. 2016), 8B (Lee et al. 2016), 2B (Lim et al. 2012), 1H (Sha and Badhulika 2019), or HB (Erdem et al. 2009).

Their first use was introduced in the literature by Mašek (1960) as an anode material in the polarographic system. Then, different research groups worked on its usage as an electrode material compared to other classical carbon electrodes (Aoki et al. 1989; Sujaritvanichpong and Aoki 1989; Pishko et al. 1990; Wang et al. 2000). Torrinha et al. (2018) reported that the first PGE-based electrochemical biosensor was introduced by Pishko and coworkers (Pishko et al. 1990). In that study, polycationic redox polymer synthesized with Os complexes was used to modify glucose oxidase enzyme. It was aimed to obtain enhanced redox reactions between the enzyme and its substrate by the modification process. This modified enzyme was immobilized at the graphite lead, and enzyme-substrate reactions were monitored by amperometry.

Joseph Wang and his team performed the electrochemical detection of nucleic acids (transfer RNA, single-stranded DNA, and oligo(dG)$_{20}$) by adsorptive stripping voltammetry technique and PGE (Wang et al. 2000). They compared PGE, CPE, and GCE in terms of biosensor response and showed that the highest guanine oxidation signal could be measured by PGE. They also investigated the effect of the hardness of pencil leads upon the biosensor response and found that HB type gave the best biosensor response. They represented the calibration curves of single-stranded DNA and oligo(dG)$_{20}$ and concluded that PGEs had excellent properties for the detection of trace levels of nucleic acids. This is the first study in the literature for the electrochemical detection of nucleic acids by using PGEs.

There are countless number of PGE-based electrochemical biosensor platform in the literature since 1990s. Some of them are pointed out comprehensively in the third section.

2.2 Screen-Printed Electrodes (SPEs)

Screen-printed electrodes (SPEs) are miniaturized platforms that have the configuration of a printed three-electrode cell system on a robust surface. The printing platform is usually ceramic, but it can also be transparent plastic material or glass (Mincu et al. 2020). The electrical connection is provided between the three-electrode cell and the printed surface. The electrode is directly bound with the potentiostat when an electrochemical measurement is performed. Therefore, practical and time-saving applications could be designed by using these disposable electrodes.

Another important advantage of these electrodes is the requirement of low amount of the sample for electrochemical measurements. In a typical SPE, a 30–40 μL of sample is required for one analysis, but this amount could be diminished by designing personalized SPE systems. As an example, Erdem and her team developed a multichannel screen-printed array which were constructed of 16 working electrodes with 1 reference and 1 counter electrodes (MUX-SPE16) for the electrochemical detection of microRNAs (Erdem et al. 2013; Erdem and Congur 2014). They used just a 3 μL of sample for one electrochemical measurement by this array. In another study of the same research group, 8-channel screen-printed electrochemical array system (MULTI-SPE8) was designed for the detection of activated protein C (Erdem and Congur 2014). This array contained 8 three-electrode systems, and each of them needed a 20 μL of sample for one electrochemical analysis. These array systems allowed performing one-by-one analysis of 16 or 8 different samples. Thus, rapid and multi-screening could be obtained regarding the type of SPEs.

Different carbon- or metal-based working electrodes can be included in an SPE structure. Furthermore, different types of nanomaterials, biomaterials, and polymers are modified easily onto the surface of the SPEs by using different modification techniques such as drop-casting, electropolymerization, and electrodeposition.

2.3 Paper-Based Electrodes

Miniaturization studies of electrochemical biosensors have been performed because of not only the increase in the demand for rapid, reliable, and sensitive monitoring of diseases and the factors threatening environment but also the demand for easily accessible and affordable recognition tools. Cheap and readily available raw materials should be picked out for designing a miniaturized disposable electrochemical biosensor system. At this point, paper is an appropriate candidate due to its eco-friendly, flexible, cheap, biocompatible, and easily shaped structure (Gutiérrez-Capitán et al. 2020). It is an abundant raw material which can be obtained in nature or through recycling process. No external pumping is required due to its porous structure to flow the biofluids through the biosensor surface (Gutiérrez-Capitán et al. 2020; Nilghaz et al. 2016), and capillary action of the fluid happens. Moreover, paper substrates have a high affinity for various types of analytes (Nilghaz et al. 2016; Loo and Pui 2020). Properties such as porosity, flow rate, affinity degree, and thickness vary by paper type. Therefore, choosing the right paper highly affects the selectivity, sensitivity, and other crucial requirements of an electrochemical biosensor platform. Although filter papers and office papers that have different thicknesses are used to design a paper-based electrochemical biosensor, thinner ones are preferable for several printing methods (Loo and Pui 2020). It was reported that the most used one is Whatman grade 1 chromatographic filter paper due to the fact that it has a smooth surface, high alpha-cellulose content, and provides to obtain reproducible and sensitive biosensor response (Silveira et al. 2016). Consequently, this paper type is suitable for biomolecular recognition using electrochemical techniques (Loo and Pui 2020).

One of the significant design features of paper-based biosensor platforms is forming hydrophobic zones. These zones should be defined by hydrophobic walls patterned by using different printing techniques such as photolithography or wax-, inkjet-, screen-, or laser-printing. Forming of hydrophobic zones prevents the unstable flow of the sample solution. Among all printing methods, wax-printing is the most preferable one since desired hydrophobic and hydrophilic zones could be easily and effectively printed onto cellulose matrix (Loo and Pui 2020; Carrilho et al. 2009).

The first paper-based sensor application was designed in a two-dimensional (2D) form. Martinez et al. reported a multiplexed paper-based bioassay for simultaneous detection of different analytes in biological fluids (Martinez et al. 2007). They used chromatography paper and patterned using a photoresist. Three separate zones were formed, two of them were for glucose and bovine serum albumin (BSA) detection, and one of them was the control group. Then, the immobilization of horseradish peroxidase/glucose oxidase or tetrabromophenol blue (TBPB) for the detection of glucose or BSA, respectively. The detection of glucose and BSA at different concentration levels was performed and more sensitive detection of the analytes was achieved compared to commercially available dipsticks. The detection was also tested in artificial urine sample. However, this biosensor platform depended on colorimetric measurements. The first electrochemical application of paper-based biosensors was reported in 2009 by Dungchai et al. (2009). Microfluidic channels were provided by photolithography, and electrodes were placed by screen-printing technique. Thus, three different detection zones constituted with one working electrode, one reference electrode, and one counter electrode were combined in one rigid platform, and this platform was the paper substrate. However, these three zones were interconnected with each other in hydrophilic areas. Each carbon working electrode containing Prussian blue (PB) was modified with glucose oxidase, lactate oxidase, or uricase to detect glucose, lactate, and uric acid in serum samples. PB acted as a redox mediator for the product of the oxidase enzymes and their substrates, H_2O_2. After the interaction between the enzymes and their substrates, direct current chronoamperometry technique was used for electrochemical detection.

As explained in the previous paragraph, it could be possible to see several 2D paper-based electrochemical biosensor applications in the literature. On the other hand, 3D-designed electrochemical biosensors appear as new-generation electrochemical biosensors using paper substrates due to their easy folding and cutting features. In contrast to the ones developed in 2D form, 3D paper-based biosensors have folded structures in a specific configuration. While the working electrode could be in one piece of this folded structure, reference and counter electrodes could be placed in the other parts (Loo and Pui 2020). Thus, sophisticated biosensors can be constructed by using this unique feature of the paper.

3 Most Commonly Used Nanomaterials for Construction of Disposable Electrochemical Biosensors

The world has been changing since the First Industrial Revolution. Manpower has been gradually replaced by machines to increase the productivity and yield of the manufacturing processes. Today, we are living in the time of the Fourth Industrial Revolution defined by Klaus Schwab in 2016 (Min et al. 2019). We have a high-tech world, but we also have environmental disasters, fatal diseases, and a global climate crisis. While some of us are living in prosperity, poverty is still a major problem for others, especially those who live in Africa and the Middle East Region. Our natural resources are running out, but our population is growing. We should fight our problems with sustainable, effective, cheap, and accessible solutions. At this point, nanotechnology science gives us the power to produce a variety of pathways to reach the solutions to our new-generation problems. When a material is produced at the nano level, it generally gains enhanced chemical, physical, mechanical, and thermal properties. Since Richard Feynmann's famous lecture given in 1958, nanotechnology science has been tremendously growing in terms of not only the synthesis of novel nanomaterials but also their applications.

There are several classification types of nanomaterials based on their raw materials, shapes, dimensions, etc. In this chapter, the most commonly used nanomaterials and their applications in the disposable electrochemical biosensor area were stated.

3.1 Nanotubes and Their Use for the Development of Disposable Electrochemical Biosensor Area

"Nanotubes" term was introduced by Iijima in the literature by synthesizing carbon nanotubes (Iijima 1991). Carbon nanotubes consist of sp^2 hybridized carbon atoms oriented in a tubular shape. They are defined as one-dimensional nanomaterials. They are classified as single-walled or multi-walled carbon nanotubes that have hollow inner part since they are formed by rolling up a graphite layer in a honeycomb lattice. They have unique properties such as high electrical and thermal conductivity, providing high surface area for immobilization of biomolecules, being stable and robust surfaces, etc. (Popov 2004; Sawant et al. 2022). Although the "nanotubes" term evokes carbon-based ones, there are other types of nanotubes in the literature. For example, halloysite nanotubes (HNTs) are synthesized using aluminosilicate clay. Their discovery dates back 1800s (Saadat et al. 2020). Mineral sheets are used in their synthesis process; Al, Si, H, and O are the four main elements of them. Their use brings several advantages to the process such as being easily accessible, being sustainable and not harmful, and allowing for modification/immobilization on their surfaces (Saadat et al. 2020; Saif et al. 2018; Goda et al. 2019).

For another nanotube application, lipid bilayer walls are rolled to form an open-ended cylindrical hollow structure. This type of nanotube is called a lipid nanotube (LNT) (Wang et al. 2022). Their formation is based on the membrane form comprised of lipid molecules. Lipid molecules can shape in different orientations based on the physical and chemical properties of the solution that surrounds them. LNTs are one of these orientations of lipid molecules. Their highly oriented structure is a unique feature among other formations. Besides, they provide biomolecule transportation and biomolecular recognition (Wang et al. 2022; Zhou 2008). Another biomolecule-based nanotube form is peptide nanotube (PNT). Protein blocks are formed in a well-developed nanotube structure appropriate for desired modification step (Katouzian and Jafari 2019).

Metal telluride nanotubes are the other nanotube formations comprised of dichalcogenide layers (Hussain and Hussain 2020). Metal chalcogenides are the hybrids of electropositive elements and groups VIA elements (sulfur, selenium and tellurium). They do not form like C atoms in graphite, but they can be rolled to form a tube-like shape. Metal tellurides are a member of chalcogenides family synthesized with tellurium element (Hussain and Hussain 2020). They could have nanotube formation by rolling up the metal telluride layer. Due to the fact that they are the best thermoelectric materials (Ghosh et al. 2021), they are used in photocatalytic and thermocatalytic reactions (Arora et al. 2022). Table 26.1 represents some nanotubes-based disposable electrochemical biosensors. The researches performed since 2015 are represented to give more up-to-date information about this field.

Although some reports about the development of nanotubes-based electrochemical disposable biosensors are represented in Table 26.1, there are countless number of nanotube applications in the electrochemical (bio)sensor area regardless they are disposable or not. Nanotubes evoke the ones synthesized by carbon atoms, namely, carbon nanotubes (CNTs), since most of the applications are performed using them (Devarakonda et al. 2017; Congur et al. 2015b, c; Ensafi et al. 2015; Hernández-Ibáñez et al. 2016; Hu et al. 2018; Kanat et al. 2018; Karimi-Maleh et al. 2015; Lu et al. 2021; Mustafa et al. 2021; Nochit et al. 2021; Sengiz et al. 2015; Taei et al. 2015; Tutunaru et al. 2021; Unal et al. 2017; Viet et al. 2019; Wu et al. 2022; Zhang et al. 2015; Zhou et al. 2016; Zhu et al. 2017). On the other hand, there are some examples in the literature about using different types of nanotubes for the fabrication of disposable electrochemical biosensors (Bolat et al. 2021; Feyzizarnagh et al. 2016; Vural et al. 2018; Yaman et al. 2020). There are some efforts for the designing of HNTs-based electrochemical sensors, but there are few applications for the development of HNTs-based electrochemical biosensors, and there is no report about their usage for the fabrication of disposable ones.

Different types of carbon nanotubes as single-walled (SWCNT) or multi-walled (MWCNT) were synthesized, and several disposable electrochemical biosensor applications were reported. As seen in Table 26.1, PGEs, SPEs, paper substrates, and even chip designs have been used intensively in this area. They can be used by themselves, but they are widely applied by combining different nanomaterials/biomaterials. In one application, PGEs were modified with GOQDs/CMWCNTs to detect the toxicity of metal ions (Cd, Hg, and Pb) and phenols (Zhu et al. 2017). First, GOQDs/CMWCNTs nanocomposite was synthesized and modified at the surface of PGEs by the drop-casting method. The HepG2 cells were grown in a 96-well plate, then, incubated with metal ions or phenolic compounds (pentachlorophenol (PCP), 2,4-dinitrophenol (2,4-DNP), and 2,4,6-trichlorophenol (2,4,6-TCP)) at different concentration levels. The electrochemical detection of the HepG2 cells was investigated by using the CV technique, and well-defined three oxidation peaks were found at +0.67V, +0.94V, and + 1.00 V depending on four purines (guanine/xanthine, adenine, and hypoxanthine, respectively) exist in the cells. The effect of the metals or phenolic compounds was evaluated by monitoring

Table 26.1 Nanotubes-based disposable electrochemical biosensors for the detection of biomolecular recognition

Type of disposable electrode	Type of nanotube/ nanocomposite	Analyte	Biorecognition element	Detection method	LOD	References
PGE	GOQDs/ CMWCNTs	Toxicity of Cd, Hg and Pb, and phenols	HepG2 cells	LSV	–	Zhu et al. (2017)
PGE	SWCNT	p53 gene related DNA sequence	ssDNA probe	DPV	0.88 μM and 0.11 μM	Congur et al. (2015c)
PGE	SWCNT	TPT	dsDNA	DPV	–	Congur et al. (2015b)
PGE	SWCNT	DCB	fsDNA	DPV	–	Kanat et al. (2018)
PGE	SWCNT	6-TG	dsDNA	DPV	–	Unal et al. (2017)
PGE	MWCNT-CHIT	MC	fsDNA	DPV	–	Sengiz et al. (2015)
PGE	MWNTs-Fe_2O_3/ SnO_2^- CHIT	DOX	dsDNA	DPV	–	Taei et al. (2015)
PGE	PP/MWCNTs	6-MP	dsDNA	DPV	0.08 μM	Karimi-Maleh et al. (2015)
PGE	CHIT–MWCNTs	PAP	dsDNA	DPV	0.003 μg/mL	Ensafi et al. (2015)
PGE	AuNP-PNT	miRNA 410	ssDNA probe	EIS	3.90 fM	Yaman et al. (2020)
PGE	PNT-GO	miRNA 192	ssDNA probe	EIS	8 fM	Bolat et al. (2021)
PGE	PANI/AuNP-PNT	PSA	HRP-Ab2	CA	0.68 ng/mL	Vural et al. (2018)
Au-SPE	PNT	H_2O_2	HRP	CA	–	Feyzizarnagh et al. (2016)
SPE	PoAP-CNTs	OA	PP2A	DPV	0.55 μg/L	Zhou et al. (2016)
SPE	SWCNT	hCG	Au-Mab-hCG	DPV	5 pg/mL	Viet et al. (2019)
SPE	WS_2/MWCNTs-OH	2,4,6-TCP, BPAF, PSNPs	CIK	CV	–	Wu et al. (2022)

SPE	CNT-V_2O_5-CS	CIP	DNA aptamer	EIS	0.5 ng/mL	Hu et al. (2018)
SPE	MWCNTs/FcMe/CS	L-lactate	HRP and LOx	CA	22.6 μM	Hernández-Ibáñez et al. (2016)
SPE	MWCNTs/CS	Mitragynine	HRP conjugated antibody	CA	0.018 μg/mL	Mustafa et al. (2021)
Film electrode	Ni–Au composite/CNT/PVA	HIV DNA	ssDNA probe	DPV	0.13 nM	Lu et al. (2021)
Paper	MWCNT	Catechol	Laccase	CA	0.25 μg/mL	Nochit et al. (2021)
Paper	SWCNT/CH	H1N1	Antibody	DPV	10^4 PFU mL^{-1}	Devarakonda et al. (2017)
Au-chip	C-SWCNT:PEDOT	DVSO	AChE	CA, DPV	5.54 ng/mL by CA and 0.447 ng/mL by DPV	Tutunaru et al. (2021)
Pt-chips	PAA/SWNT/CS/GNp	Glucose	GOx	Amperometry	11.1, 5.6 and 16.7 μM	Zhang et al. (2015)

Abbreviations: **Electrodes:** *Au-SPE* screen-printed gold electrode, *SPE* screen-printed carbon electrode, **Type of nanotube/nanocomposite:** *GOQDs/CMWCNTs* graphene oxide quantum dots/carboxylated multi-walled carbon nanotubes, *SWCNT* single-walled carbon nanotubes, *MWCNT-CHIT* multi-walled carbon nanotubes (CNT)-chitosan, *MWNTs-Fe_2O_3/SnO_2^- CHIT* multi-walled carbon nanotubes-Fe_2O_3/SnO_2–chitosan, *PP/MWCNTs* polypyrrole/multi-walled carbon nanotubes, *AuNP-PNT* gold nanoparticle assembled peptide nanotube, *PNT-GO* peptide nanotubes with graphene oxide, *PANI/AuNP-PNT* peptide nanotube, gold nanoparticle, and polyaniline composite, *PoAP-CNTs* poly-o-aminophenol-carbon nanotubes, *WS_2/MWCNTs-OH* tungsten disulfide nanosheets/hydroxylated multi-walled carbon nanotubes, *CNT-V_2O_5-CS* carbon nanotube-V_2O_5-chitosan, *FcMe* ferrocene methanol, *Ni–Au composite/CNT/PVA* nickel metal-organic framework (Ni-MOF) composite/Au nanoparticles/carbon nanotubes/polyvinyl alcohol, *SWCNT/CH* single-walled carbon nanotube/chitosan, *CSWCNT:PEDOT* carboxylic acid functionalized single-walled carbon nanotubes and poly(3,4-ethylenedioxythiophene), *PAA/SWNT/CS/GNp* poly(allylamine)/single-walled carbon nanotube/chitosan/gold nanoparticles, **Analyte:** *DCB* dacarbazine, *6-TG* 6-thioguanine, *6-MP* 6-mercaptopurine, *PAP* phenazopyridine hydrochloride, *miRNA* microRNA, *PSA* prostate-specific antigen, *OA* okadaic acid, *hCG* human chorionic gonadotropin, *2,4,6-TCP* 2,4,6-trichlorophenol, *BPAF* bisphenol AF, *PSNPs* polystyrene nanoplastics, *CIP* ciprofloxacin, *HIV* human immunodeficiency virus, *DVSO* dichlorvos, *Biorecognition elements HepG2 cells* human hepatoma cells, *ssDNA* single-stranded DNA, *dsDNA* double-stranded DNA, *fsDNA* fish sperm double-stranded DNA, *HRP-Ab2* horseradish peroxidase-labeled anti-PSA, *PP2A* protein phosphatase 2A, *Au-Mab-hCG* gold-linked with the second antibody, *CIK* grass carp kidney cell line, *LOx* lactate oxidase, **Detection methods:** *LSV* linear sweep voltammetry, *DPV* differential pulse voltammetry, *EIS* electrochemical impedance spectroscopy, *CA* chronoamperometry the changes at these three signals measured by LSV. IC_{50} levels of these toxic components were determined by this methodology. It was reported that the developed electrochemical biosensor for the detection of toxicity of the selected compounds was more sensitive than the MTT assay which is a conventional method used for the determination of IC_{50} levels.

PGE-based carbon nanotubes modified disposable electrochemical biosensors have been intensively used for the detection of drug-DNA interactions in recent years (Congur et al. 2015b; Ensafi et al. 2015; Kanat et al. 2018; Karimi-Maleh et al. 2015; Sengiz et al. 2015; Taei et al. 2015; Unal et al. 2017). In one of them, MWNTs-Fe_2O_3/SnO_2^- CHIT nanocomposite was synthesized and used for the modification of PGE (Taei et al. 2015). DOX is an anticancer drug that binds dsDNA by intercalation. The electrochemical investigation of the interaction between dsDNA and DOX was performed by using modified PGEs and DPV technique by monitoring the changes in the DOX oxidation signal. MWNTs-Fe_2O_3/SnO_2^- CHIT nanocomposite was modified at the surface of PGE by dipping of PGEs into the nanocomposite solution for 40 min. Then, dsDNA was immobilized at the surface of the modified PGEs by dipping the electrodes in the dsDNA samples in a stirred media for 1 h. DOX samples were transferred into the electrochemical cell, and the interaction of dsDNA and DOX was performed by applying a controlled potential. The interaction was also monitored in human blood and urine samples.

In another study reported by Unal et al. (2017), PGEs were modified with SWCNTs and used for the voltammetric monitoring of dsDNA and 6-TG that is another anticancer drug. The modification of PGEs was characterized by microscopic and electrochemical techniques. dsDNA was immobilized at the surface of SWCNT/PGEs, then the interaction of dsDNA and 6-TG was done at the modified PGE surface. The interaction process was quantitatively detected based on the guanine signals obtained before and after the interaction process. The interaction was performed in the presence of 6-TG at different concentration levels, and the interaction performed during 1, 3, 5, and 7 min was monitored via DPV and EIS techniques. The changes in the biosensor responses obtained by two different techniques were compared.

There are some applications for the modification of PNTs and their nanocomposites at the surface of PGEs (Bolat et al. 2021; Vural et al. 2018; Yaman et al. 2020) and Au-SPE (Feyzizarnagh et al. 2016). Feyzizarnagh et al. (2016) developed HRP encapsulated PNTs modified Au-SPE for amperometric detection of H_2O_2. Encapsulation of the enzyme into the PNTs provided stability and enhanced electron transfer between the electrode and the active site of HRP. They obtained more sensitive results by using PNTs compared to the one obtained by using hydroquinone (HQ).

CNTs and their nanocomposites were widely used for the modification of SPEs (Hernández-Ibáñez et al. 2016; Hu et al. 2018; Mustafa et al. 2021; Viet et al. 2019; Wu et al. 2022; Zhou et al. 2016), papers (Devarakonda et al. 2017; Lu et al. 2021; Nochit et al. 2021), and chip systems (Tutunaru et al. 2021; Zhang et al. 2015). They are miniaturized, easy-to-use, and portable prototypes or devices. A handmade paper-based immunosensor was reported by Devarakonda et al. (2017) for the electrochemical detection of H1N1 virus. First, they applied hydrophobic polydimethylsiloxane (PDMS) modified silica nanoparticles onto the selected part of the Whatman chromatography paper to obtain enhanced hydrophobicity. After the paper dried, they printed the three-electrode system via the stencil-printing technique. Then, they modified at paper-based electrode surface by using chitosan and SWCNTs and immobilized H1N1-specific monoclonal antibody at the modified electrode surface. They used the DPV technique to monitor antibody-antigen interaction, and they found the detection limit as 10^4 PFU mL^{-1} by using the modified paper-based biosensor. They tested the selectivity of the biosensor in the presence of MS2 bacteriophage and influenza B virus.

A micro-fabricated chip system was used for the development of a disposable electrochemical biosensor for the detection of glucose. Micro-fabricated Pt electrodes were prepared by applying the photolithography method onto the surface of the silicon wafer. Then, the layer-by-layer assembly technique was used to construct CS–GNp–glucose oxidase multilayer film onto the SWCNT-modified electrode surface. Enzyme-substrate interaction was monitored quantitatively by amperometry, not only in buffer but also in saliva sample. Reproducible, repeatable, sensitive, and selective results were obtained using the modified paper-based electrochemical biosensor.

3.2 The Applications of Graphene and Its Derivatives

Graphene was discovered by Andre Geim and Kostia Novoselov in 2004 (Geim and Novoselov 2007). Its discovery opened the door for the investigation of 2D nanomaterials, and graphene and its derivatives have been synthesized and used in a great variety of applications such as new-generation batteries, electronic devices, fuel cells, catalysts, and eventually biosensors (Lawal 2018). Graphene has hexagonal-formed sp^2 carbon atoms that have π-π interactions with the binding (bio)molecules (Arshad et al. 2022). It has superior electrochemical, optical, thermal, mechanical, and physical properties (Huo et al. 2018; Pumera 2010; Yu et al. 2021). Exfoliation and oxidation techniques are applied to graphite (Obayomi et al. 2022) to synthesize graphene oxide (GO) which is a versatile form of graphene (Arshad et al. 2022). The oxidation process introduces functional groups into the graphene nanosheets. These functional groups as hydroxyl, carboxyl, epoxide, carbonyl, and phenol groups (Li et al. 2019; Obayomi et al. 2022) act as the binding sites of biomolecules, nanomaterials, and biomaterials (Yu et al. 2021). Therefore, GO forms are more useful for surface modification, immobilization, or the formation of nanocomposites (Joshi et al. 2021; Obayomi et al. 2022). Furthermore, this form has enhanced physical, thermal, and chemical properties (Joshi et al. 2021; Yu et al. 2021).

Graphene and its derivatives are appropriate materials to develop disposable electrochemical biosensors due to their excellent electrical, chemical, and physical properties (Joshi et al. 2021; Yu et al. 2021). Some of the applications reported from 2015 to the present are listed in Table 26.2.

Table 26.2 The use of graphene and its derivatives for the fabrication of disposable electrochemical biosensors

Type of disposable electrode	Type of graphene/ nanocomposite	Analyte	Biorecognition element	Detection method	LOD	References
PGE	GO	miRNA-34a	ssDNA probe	EIS	0.29 μg/mL	Erdem et al. (2017)
PGE	GO	miRNA-34a	ssDNA probe	DPV	1.9 μg/mL	Congur et al. (2015a)
PGE	GO	miRNA-34a	ssDNA probe	EIS	1.84 or 0.5 μg/mL in buffer or serum	Congur et al. (2018)
PGE	GO	miRNA-34a	ssDNA probe	DPV	7.52 μg/mL	Isin et al. (2017)
PGE	CHIT/NRGO	miRNA-660	ssDNA probe	EIS	1.72 or 1.65 μg/mL in buffer or serum	Eksin et al. (2018)
PGE	GQDs	miRNA-541	ssDNA probe	DPV	0.7 fM	Akbarnia et al. (2019)
PGE	rGO	DNR, dsDNA	dsDNA	DPV	2.71 μg/mL for dsDNA	Eksin et al. (2017)
PGE	GKNPs/GPONPs/ GrONPs	Glycerol	GK	Amperometry	0.002 μM	Narwal and Pundir (2019)
PGE	PAMAM/RGO	RTX	dsDNA	DPV	0.56 μM	Hatamluyi and Es'haghi (2018)
PGE	AuNPs/rGO	AFM1	DNA aptamer	EIS	0.3 ng/L	Ahmadi et al. (2022)
PGE	PPy/rGO	DDI	dsDNA	DPV	0.8 nM	Karimi-Maleh et al. (2018)
PGE	rGO/ssDNA-OMC/Ni NPs	L858R	ssDNA	CA	120 nM	Shoja et al. (2018)
PGE	PP/NrG	Epirubicin	dsDNA	DPV	1 nM	Khodadadi et al. (2019)
PGE	LOxNPs/GrONPs	L-lysine	LOxNPs	Amperometry	0.01 μM	Nohwala et al. (2020)
PGE	GNP/RGO	PEN	DNA aptamer	EIS	0.8 fM	Mohammad-Razdari et al. (2019a)
PGE	AuNPs/RGO	SDM	DNA aptamer	EIS	3.7×10^{-16} M	Mohammad-Razdari et al. (2019b)
PGE	Au-Pt BNPs/GO-chit	ZDV	dsDNA	DPV	0.003 pM	Hasanjani and Zarei (2021)

SPE	Au-rGO	*Brettanomyces bruxellensis*	aBAb	Amperometry	8 CFU/mL and 56 CFU/mL in buffer or red wine	Borisova et al. (2017)
SPE	rGO	$A\beta_{1-40}$ and $A\beta_{1-42}$	Antibody	DPV	9.51 and 8.65 fM for $A\beta_{1-40}$ and $A\beta_{1-42}$	Sethi et al. (2021)
SPE	Graphene/rGO	$A\beta_{1-42}$	H31L21 antibody	DPV	2.398 pM	Sethi et al. (2020)
SPE	PEDOT:PSS/ graphene/Nafion	Glucose	*Gluconobacter oxydans*	CA	0.02 M	Plekhanova et al. (2021)
Dual SPE	P3ABA/2D-MoSe2/ GO	CA 15-3 and miRNA-21	Antibody and ssDNA probe	CV	0.14 U/mL and 1.2 fM for CA 15–3 and miRNA-21	Pothipor et al. (2022)
SPE	GNS-PBA	DNA	ssDNA probe	DPV	4.59×10^{-10} μM	Jamaluddin et al. (2020)
SPE	RGO	DNA	ssDNA probe	CV, EIS	–	Chiticaru et al. (2019)
SPE	Graphene	EN2 protein	DNA aptamer	CV	38.5 nM	Settu et al. (2017)
SPE	MnO_2-GNR	Glucose	GOx	CA	0.05 mmol/l	Vukojević et al. (2018)
SPE	agFc-rGO-CS	Glucose	GOx	DPV	0.44 μM	Rabti et al. (2016)
SPE	Au@CGR	HSA	Anti-HSA	MA	1.55 μg/mL	Stanković et al. (2020)
SPE	OerGO	L-lactate	LOD	Amperometry	60 μM	Tu et al. (2016)
SPE	GNPs	LCN-2	DNA aptamer	SWV	0.07 pg/mL	Matassan et al. (2019)
SPE	Graphene acid	DNA	ssDNA	EIS	9% w/w	Flauzino et al. (2022)
SPE	poly(nBA)-rGO	Nitrite	Hb	DPV	0.03 mg/L	Jamaluddin et al. (2018)
SPE	rGO-TEPA@Cu-MOFs@SiO_2@AgNPs	NMP22	Antibody	DPV	33.33 fg/mL	Rong et al. (2021)
SPE	GQD	p24-HIV protein	DNA aptamer	CV	51.7 pg/mL	Gogola et al. (2021)
SPE	2-ABA-functionalized graphene	Parathion	Antibody	EIS	52 pg/L	Mehta et al. (2016)
SPE	NH_2-GO	*Escherichia coli*	Antibody	EIS	2 CFU/mL	Gupta et al. (2019)

(continued)

Table 26.2 (continued)

Type of disposable electrode	Type of graphene/ nanocomposite	Analyte	Biorecognition element	Detection method	LOD	References
SPE	PA-GO	*Saccharomyces cerevisiae*	Antibody	Amperometry	4 CFU/mL	Borisova et al. (2018)
LIG	Graphene	*Salmonella enterica*	Antibody	EIS	13 ± 7 CFU/mL	Soares et al. (2020)
SPE	Graphene	*Vibrio parahaemolyticus*	ssDNA probe (LAMP amplification)	CV	0.15 CFU/mL	Kampeera et al. (2019)
Paper	Graphene	AChE	ATCh	Amperometry	0.1 U/mL	Panraksa et al. (2018)
Paper	GQD	Uric acid and creatinine	Creatininase	SWV	8.4 and 3.7 nmol/L a for uric acid and creatinine	Cincotto et al. (2019)
Paper	Graphene	E2	DNA aptamer	DPV	63.1 fM	Chang et al. (2021)
Paper	Graphene	Insulin	DNA aptamer	DPV	22.7 fM	Liu et al. (2022)
Paper	Graphene	dsDNA	–	CV	0.68 pg/mL	Mohanraj et al. (2020)
Paper	Graphene	NaDH	LDH	CV	0.6 μM	Poletti et al. (2022)
Paper	Graphene and nPt	Glucose and *Escherichia coli*	GOx and RNA aptamer	Amperometry and EIS	0.08 ± 0.02 μM and 4 CFU/mL for glucose and *Escherichia coli*	Burrs et al. (2016)
Paper	Graphene	Kanamycin	DNA aptamer	Potentiometry	30 fg/mL	Yao et al. (2019)
Paper	Graphene and GO	*Escherichia coli*	ConA	EIS	10 CFU/mL	Karuppiah et al. (2021)
Paper	AuNP/rGO/TMC/CN	Glucose	GOx	EIS	0.1 mM	Ahmadi et al. (2021)
Paper	AuNPs/rGO/THI	PSA	DNA aptamer	DPV	10 pg/mL	Wei et al. (2018)

Paper	AuNPs/RGO and AuNPs/MoS_2	miRNA-21 and miRNA-155	ssDNA probe	DPV	12.0 and 25.7 nM by AuNPs/RGO and 51.6 and 59.6 nM by AuNPs/MoS_2 for miRNA-21 and miRNA-155	Torul et al. (2021)
Paper	RGO-TEPA/Au	AFP	Antibody	SWV	0.005 ng/mL	Cao et al. (2017)
Graphene@Ni foam	AuNPs and AgNPs	AFP	Antibody	LSV	2.3 pg/mL	Zhao et al. (2019)
IDEs	Graphene	IFN-γ and IF-10	Antibody	EIS	25 and 46 pg/ml for IFN-γ and IL-10	Parate et al. (2020b)
IDEs	Graphene	Histamine	Antibody	EIS	30.7 μM	Parate et al. (2020a)

Abbreviations: Type of disposable electrode: *LIG* laser-induced graphene electrode, *IDEs* interdigitated electrodes, **Type of graphene/nanocomposite:** *rGO* reduced graphene oxide, *NrG, NRGO* nitrogen-doped reduced graphene oxide, *CHIT, chit, CS* chitosan, *GKNPs/GPONPs/GrONPs* glycerol kinase (GK) and glycerol-3-phosphate oxidase (GPO) nanoparticles (NPs) onto graphene oxide nanoparticles (GrONPs), *PAMAM* poly(amidoamine) dendrimer, *PP, PPy* polypyrrole, *Ni-OTC NPs* Ni(II)-oxytetracycline conducting metallopolymer nanoparticles, *rGO/f-OMC* reduced graphene oxide/carboxyl functionalized ordered mesoporous carbon, *LOxNPs/GrONPs* L-lysine oxidase nanoparticles and graphene oxide nanoparticles, *GQDs* graphene quantum dots, *Au-Pt BNPs* Au-Pt bimetallic nanoparticles, *Au* gold nanoparticles, *PEDOT:PSS* poly(3,4-ethylenedioxythiophene): poly(styrenesulfonate), *PBA* pyrene butyric acid, *GNS* graphene nanospheres, *NH2-GO* amino-functionalized GO, MnO_2*-GNR* manganese dioxide nanoparticles-graphene nanoribbons, *agFc-rGO* ferrocene functionalized rGO, *Au@CGR* gold nanoparticles-carboxylated graphene, *OerGO* graphene by a one-step electrodeposition process, *GNPs* graphene nanoplatelets, *poly(nBA)-rGO* poly(n-butyl acrylate)-rGO, *rGO-TEPA@Cu-MOFs@*SiO_2*@AgNPs* reduced graphene oxide-tetraethylene pentamine@ Cu-based metalorganic frameworks deposited silver nanoparticles, *2-ABA* 2-aminobenzylamine, *PA-GO* propionic acid-functionalized GO, *nPt* platinum nanocauliflower, *AuNPs/rGO/THI* gold nanoparticles/rGO/thionine, *TMC/CN* Trimethyl chitosan/cellulose nanofiber, *RGO-TEPA/Au* RGO-tetraethylene pentamine/Au nanocomposite, **Analytes:** *DNR* daunorubicin, *RTX* rituxan, *AFM1* aflatoxin M1, *DDI* didanosine, *L858R* EGFR exon21 point mutation, *PEN* penicillin G, *SDM* sulfadimethoxine, *ZDV* zidovudine, *EN2 protein* engrailed-2 protein, *LCN-2* lipocalin-2, *NMP22* nuclear matrix protein 22, *AChE* acetylcholinesterase, *E2* 17β-estradiol, *AFP* α-fetoprotein antigen, *IFN-γ* interferon gamma, *IL-10* interleukin 10, *NaDH* nicotinamide adenine dinucleotide, *PSA* prostate-specific antigen, **Biorecognition element:** *GK* glycerol kinase, *aBAb* polyclonal anti-Brett antibody, *LOD* lactate oxidase, *Hb* hemoglobin, *LAMP* loop-mediated isothermal amplification, *ATCh* acetylthiocholine chloride, *LDH* lactate dehydrogenase **Methods:** *MA* multistep amperometry

Due to its appropriate structure for the synthesis of different nanoshaped-materials and the modification, novel graphene-based nanomaterials and their nanocomposites were introduced in the literature. As seen in Table 26.2, GO and rGO are the most applied graphene-based nanomaterials in the disposable electrochemical biosensor area. rGO (or RGO, reduced graphene oxide) is obtained by conversion of GO into rGO through the reduction reaction. The oxygen-contained groups of GO are removed and rGO gains more hydrophobic properties than GO. rGO may have aggregated shape in aqueous solutions, but it has enhanced chemical and electrical properties in comparison to GO (Feng et al. 2020).

miRNAs are short single-stranded RNAs that are indicative nucleic acids for vital diseases such as cancer (Moshiri et al. 2018), neurodegenerative diseases (Congur et al. 2015a), viral infections (Yeung et al. 2005), and diabetes (Assmann et al. 2018). Therefore, the development of miRNA-specific biosensors is an attractive topic, and several electrochemical applications for the fabrication of single-use monitoring tools were reported in the literature (Akbarnia et al. 2019; Congur et al. 2015a, 2018; Eksin et al. 2018; Erdem et al. 2017; Isin et al. 2017; Pothipor et al. 2022; Torul et al. 2021). The prototypes using PGEs, SPEs, and paper-based electrode systems were presented for the fabrication of point-of-care test devices in the future. Briefly, a target miRNA-specific single-stranded DNA probe is used for the sensitive recognition. The nucleic acid hybridization between the DNA probe and its miRNA target is achieved and this hybridization is monitored by using different graphene-based nanomaterial modified electrodes and voltammetric/impedimetric techniques. PGEs serve as cheaper recognition surface than SPEs and paper-based electrodes since no printing costs are required for the development of PGE-based analytical tools. On the other hand, SPE and paper-based ones are relatively close to the device designs.

Graphene quantum dots (GQD, GQDs) are another graphene-based nanomaterial synthesized by introducing a bandgap into the graphene structure (Jin et al. 2015; Kelarakis 2015). They are sustainable alternatives to heavy metal-based quantum dots due to their green synthesis methods and low toxicities (Kelarakis 2015). Their modified physical properties make them good candidates for novel applications in different areas including electrochemical biosensors (Faridbod and Sanati 2019; Thangamuthu et al. 2019). In one of the disposable electrochemical biosensor applications, microRNA-541 which is the biomarker for lung cancer (Lu et al. 2016), diabetes (Han et al. 2012), and cardiovascular diseases (Liu et al. 2014) was monitored by using GQDs modified PGEs (Akbarnia et al. 2019). The nucleic acid hybridization between 5’ NH_2 labeled miRNA-541 specific DNA probe and its RNA target was performed at the surface of covalently activated GQDs-PGE. Then, the electrode was incubated with a restriction enzyme, *Hinf1*, to apply the enzymatic digestion method. Before and after the hybridization, the oxidation signal of guanine base was recorded, and a decrease at this signal was monitored after the hybridization. The enzymatic digestion caused more decreased guanine signal that enhanced the sensitivity of the nanobiosensor. The application of the GQDs-PGE-based electrochemical biosensor was shown in serum samples, and the selectivity of the biosensor was tested against noncomplementary miRNA sequence.

In another GQDs-based disposable electrochemical biosensor design, a microfluidic device was fabricated taking the advantages of GQDs (Cincotto et al. 2019).

The device was constructed by screen printing of two carbon working electrodes onto sheets of polyester. These electrodes were modified with GQDs and used for the electrochemical detection of uric acid and creatinine associated with kidney diseases. Uric acid was directly determined based on its oxidation signal on the working electrode-1 whereas the other one should be treated with creatininase enzyme before creatinine detection. Creatinine was converted to creatine by using the enzyme-substrate reaction, and creatine reacted with an electrochemical mediator, hexaammine-ruthenium (III) chloride. Finally, ruthenium (II) was formed and its oxidation signal was monitored for the detection of creatinine. SWV technique was implemented for both uric acid and creatinine detection and simultaneous detection of both biomarkers could be achieved in human urine samples.

There has been a great effort for electrochemical glucose sensing since the 1960s (Clark and Lyons 1962) through enzymatic and nonenzymatic detection routes. Enzyme-based biomonitoring is preferable to enhance the sensitivity and selectivity of the biosensor system (Vukojević et al. 2018). The enzymatic reaction between glucose oxide and glucose can be monitored by using different electroanalytical techniques (Teymourian et al. 2020). Novel electrochemical glucose biosensors take place in the literature with the applications of graphene-based nanomaterials (Ahmadi et al. 2021; Burrs et al. 2016; Rabti et al. 2016; Vukojević et al. 2018; Plekhanova et al. 2021). Furthermore, graphene-based nanocomposites were used for the fabrication of these biosensors. Vukojević et al. reported an enzymatic glucose biosensor fabricated by using MnO_2 nanoparticles decorated on graphene nanoribbons (GNRs) (Vukojević et al. 2018). They emphasized that although graphene-based nanomaterials were widely used for the construction of electrochemical biosensors, there were limited applications of GNRs that gain a form by a combination of graphene and carbon nanotubes. Their study is the first report in the literature in terms of the use of GNRs decorated with MnO_2 nanoparticles for the development of an electrochemical glucose biosensor. They fabricated SPEs having carbon working electrodes and synthesized the nanocomposite. Then, they prepared MnO_2-GNR/SPE and immobilized GOx onto this modified electrode. The electrochemical and microscopic studies proved the modification of the nanocomposite onto the SPE surface and enhancement at the sensitivity. They monitored glucose via chronoamperometric measurements not only in buffer but also in honey samples.

Table 26.2 represents the examples of antibody-based biosensors, namely immunosensors developed by using graphene-based electrochemical recognition platforms to monitor proteins (Cao et al. 2017; Mehta et al. 2016; Mutić et al. 2020; Parate et al. 2020a, b; Pothipor et al. 2022; Rong et al. 2021; Sethi et al. 2021; Yao et al. 2019) and cells (Borisova et al. 2017, 2018; Gupta et al. 2019; McLamore et al. 2020). A three-dimensional (3D) electrochemical immunosensors was reported by Zhao et al. (2019) for the detection of α-fetoprotein antigen which is a tumor biomarker. For this purpose, graphene@Ni foam was modified with gold nanoparticles (AuNPs) and an AFP-specific antibody (Ab_1) was immobilized. Then, the electrode was incubated with the AFP sample. As a second step, the AFP capture antibody tagged with NH_2 functionalized SiO_2 nanospheres (Ab_2) was immobilized at the surface of the electrode. After the electrodeposition of silver nanoparticles (AgNPs), linear sweep voltammetry (LSV) measurements were performed. It was reported that sensitive and selective detection of the target protein could be achieved by using the developed 3D biosensor system.

Interdigitated electrodes (IDEs) are miniaturized electrode systems that have several advantages (Brosel-Oliu et al. 2019), but the most remarkable property of them is to allow the fabrication of portable and easy-to-use electroanalytical tools. There are some examples of the use of graphene-based nanomaterials for the design of electrochemical biosensors (Parate et al. 2020a, b). Electrochemical histamine immunosensor developed by using IDEs fabricated by aerosol jet printing of graphene ink onto a polyimide substrate was reported by Parate et al. (2020a). The biointeraction between histamine-specific antibody and histamine was monitored by the EIS technique and the charge transfer resistance (R_{ct}) value was recorded before and after each immobilization/interaction step. The changes at the R_{ct} value were evaluated for the detection of histamine and the evaluation of the selectivity. In another study, graphene-based IDEs were developed by using the same technique reported, and used for the fabrication of an impedimetric immunosensor for interferon-gamma (IFN-γ) and interleukin-10 (IL-10) that are the cytokines associated with immune system functions (Conti-Freitas et al. 2012). Similar to the previous study, nyquist diagrams were recorded and the changes at the R_{ct} value were evaluated in terms of the detection of the target molecules.

Selective and sensitive detection of the microorganisms are desirable to monitor the contaminations and microorganisms-related diseases. Thus, there are efforts to develop sensitive and selective recognition platforms for microorganisms by using graphene or its derivatives modified single-use electrochemical biosensors (Borisova et al. 2017, 2018; Gupta et al. 2019; McLamore et al. 2020). *Brettanomyces bruxellensis* (Brett) is a yeast and contaminant factor for wine production. Borisova and coworkers reported an AuNPs-rGO modified SPE fabricated for amperometric detection of Brett (Borisova et al. 2017). After the construction of an AuNPs-rGO/SPE, an antibody that is specific for Brett was immobilized at the electrode surface. Then, antibody-antigen biointeraction occurred and concanavalin A-hydrogen peroxidase conjugate (ConA-HRP) was immobilized at the electrode surface. The redox reaction between ConA-HRP and H_2O_2 was monitored by amperometry. The electrochemical and microscopic characterization of the modified electrode surface was performed, and the sensitivity and selectivity of the developed biosensor system were studied.

Vibrio parahaemolyticus is a foodborne pathogen found in water resources. Its contamination causes diseases in both animals and humans (Kampeera et al. 2019). Kampeera et al. (2019) designed an electrochemical biosensor for sensitive and selective monitoring of *Vibrio parahaemolyticus* in a fast way. The detection principle of that biosensor was the combination of electrochemical detection with loop-mediated isothermal amplification (LAMP) method that enhances the sensitivity and selectivity. They used screen-printed graphene electrode and modified it with graphene nanoparticles. They designed and produced a mini-potentiostat to perform CV and CA measurements. For electrochemical measurements, they mixed the LAMP products with a redox probe containing 2′-(4-hydroxyphenyl) − 5-(4-methyl-1-piperazinyl) − 2,5′-bi(1H-benzimidazole). They measured the oxidation signal of this redox couple after the LAMP amplification of the samples. They performed LAMP reaction with 36 foodborne pathogens and obtained only positive results in the presence of the target pathogen, *Vibrio parahaemolyticus* by using the LAMP-based electrochemical device (LAMP-EC). They found that LAMP-EC gave sensitive and selective results. They could be designed a point-of-care system for the online analysis of a foodborne pathogen.

Aptamers are antibody-like biorecognition molecules that are synthesized through systematic evolution of ligands exponential enrichment (SELEX) methods. They are single-stranded DNA or RNA molecules that have the ability of the specific binding of the target molecules such as drugs, proteins, metals, cells, etc. They are produced *in vitro*, and they are stable, highly sensitive and selective biomolecules that are superior properties in comparison to the antibodies (Famulok et al. 2007). Therefore, numerous applications of aptamers for the development of electrochemical biosensors were reported in the literature (Nooranian et al. 2021; Wen et al. 2017; Iliuk et al. 2011). Some of the graphene-based disposable ones were given in Table 26.2. An SPE modified with graphene nanoplatelets (GNPs) was reported for the voltammetric detection of lipocalin-2 (LCN-2) protein that is associated with different diseases such as kidney disruptions (Viau et al. 2010; Lau et al. 2000) and cancers (Moniaux et al. 2008; Lee et al. 2011; Bauer et al. 2008; Miyamoto et al. 2011). GNP modified SPEs were treated with covalent activation agents, and LCN-2 specific DNA aptamer was immobilized at the modified electrode surface. Bovine serum albumin (BSA) was used as the blocking agent to prevent the unspecific binding of interference factors at the electrode surface. The specific binding of LCN-2 onto the electrode surface was monitored in the presence of a redox couple, $\{Fe(CN)_6\}^{4-/3-}$. The selectivity of the biosensor was tested in the presence of nonspecific DNA aptamer and different proteins under optimum conditions. Spiked LCN-2 in human plasma was also analyzed to prove the applicability of the biosensor in the real-life analysis.

Kanamycin is a veterinary medicine and its common overdose usage cause environmental and agricultural pollution (Song et al. 2011). Due to the importance of monitoring this drug, a paper-based electrochemical aptasensor was designed by Yao et al. (2019). A graphene paper (GNP) was prepared and kanamycin specific DNA aptamer was immobilized at GNP surface. The potentiometric detection of kanamycin was performed in the presence of DNAase I to cleavage the dissociative aptamer and increase the sensitivity. This graphene paper-based potentiometric aptasensor was tested against other antibiotics under optimum experimental conditions. Furthermore, the biosensor response was measured by a smartphone which allowed real-time monitoring of the samples.

4 Concluding Remarks

In this chapter, disposable electrochemical biosensor platforms combined with the most used nanomaterials, nanotubes, and graphene and its derivatives or their nanocomposites were presented. The use of these nanomaterials enhances not only the selectivity and sensitivity but also the robustness of the biorecognition platforms.

The PGE-based electrochemical biosensors are cheap and practical. Therefore, a countless number of electrochemical nanobiosensor were developed by using PGEs. On the other hand, SPEs and paper-based analytical platforms are miniaturized prototypes for devices that are capable of real-time monitoring. Both voltammetric and impedimetric analyses can be implemented with the said single-use electrode types. Several biorecognition elements such as nucleic acids, antibodies, aptamers, and enzymes can be used for the specific detection of the target molecule. However, the right biorecognition element should be chosen to obtain reliable, sensitive, and selective results. Due to the fact that disposable analytical tools have indispensable properties, it is expected that miniaturized and commercialized single-use electrochemical nanobiosensors will have a considerable portion in the field of analytical monitoring in the future.

References

Ahmadi A, Khoshfetrat SM, Kabiri S, Fotouhi L, Dorraji PS, Omidfar K (2021) Impedimetric paper-based enzymatic biosensor using electrospun cellulose acetate nanofiber and reduced graphene oxide for detection of glucose from whole blood. IEEE Sensor J 21:9210–9217

Ahmadi SF, Hojjatoleslamy M, Kiani H, Molavi H (2022) Monitoring of aflatoxin M1 in milk using a novel electrochemical aptasensor based on reduced graphene oxide and gold nanoparticles. Food Chem 73:131321

Akbarnia A, Zarea HR, Moshtaghioun SM, Benvidi A (2019) Highly selective sensing and measurement of microRNA-541 based on its sequence-specific digestion by the restriction enzyme Hinf1. Colloid Surf B 182:110360

Aoki K, Okamoto T, Kaneko H, Nozaki K, Negishi A (1989) Applicability of graphite reinforcement carbon used as the lead of a mechanical pencil to voltammetric electrodes. J Electroanal Chem Int Electrochem 263:323–331

Arora A, Oswal P, Datta A, Kumar A (2022) Complexes of metals with organotellurium compounds and nanosized metal tellurides for catalysis, electrocatalysis and photocatalysis. Coord Chem Rev 459:214406

Arshad F, Nabi F, Iqbal S, Khan RH (2022) Applications of graphene-based electrochemical and optical biosensors in early detection of cancer biomarkers. Colloid Surf B 212:112356

Assmann TS, Recamonde-Mendoza M, Puñales M, Tschiedel B, Canani LH, Crispim D (2018) MicroRNA expression profile in plasma from type 1 diabetic patients: case-control study and bioinformatic analysis. Diabetes Res Clin Pract 141:35–46

Batchelor-McAuley C, Katelhön E, Barnes EO, Compton RG, Laborda E, Molina A (2015) Recent advances in voltammetry. Chem Open 4:224–260

Bauer M, Eickhoff JC, Gould MN, Mundhenke C, Maass N, Friedl A (2008) Neutrophil gelatinase-associated lipocalin (NGAL) is a predictor of poor prognosis in human primary breast cancer. Breast Cancer Res Treat 108:389–397

Bhatnagar I, Mahato K, Ealla KKRA, Asthana A, Chandra P (2018) Chitosan stabilized gold nanoparticle mediated self-assembled gliP nanobiosensor for diagnosis of *Invasive Aspergillosis*. Int J Biol Macromol 110:449–456

Bolat G, Vural OA, Yaman YT, Abaci S (2021) Label-free impedimetric miRNA-192 genosensor platform using graphene oxide decorated peptide nanotubes composite. Microchem J 166:106218

Borisova B, Villalonga ML, Arévalo-Villena M, Boujakhrout A, Sánchez A, Parrado C, Pingarrón JM, Briones-Pérez A, Villalonga R (2017) Disposable electrochemical immunosensor for

Brettanomyces bruxellensis based on nanogold-reduced graphene oxide hybrid nanomaterial. Anal Bioanal Chem 409:5667–5674

Borisova B, Sánchez A, Soto-Rodríguez PED, Boujakhrout A, Arévalo-Villena M, Pingarrón JM, Briones-Pérez A, Parrado C, Villalonga R (2018) Disposable amperometric immunosensor for Saccharomyces cerevisiae based on carboxylated graphene oxide-modified electrodes. Anal Bioanal Chem 410:7901–7907

Brosel-Oliu S, Abramova N, Uria N, Bratov A (2019) Impedimetric transducers based on interdigitated electrode arrays for bacterial detection. Anal Chim Acta 1088:1–19

Burrs SL, Bhargava M, Sidhu R, Kiernan-Lewis J, Gomes C, Claussen JC, McLamore ES (2016) A paper based graphene-nanocauliflower hybrid composite for point of care biosensing. Biosens Bioelectron 85:479–487

Cao L, Fang C, Zeng R, Zhao X, Zhao F, Jiang Y, Chen Z (2017) A disposable paper-based microfluidic immunosensor based onreduced graphene oxide-tetraethylene pentamine/Au nanocompositedecorated carbon screen-printed electrodes. Sens Act B 252:44–54

Carrilho E, Martinez AW, Whitesides GM (2009) Understanding wax printing: a simple micropatterning process for paper-based microfluidics. Anal Chem 81:7091–7095

Chang Z, Zhu B, Liu J, Zhu X, Xu M, Travas-Sejdic J (2021) Electrochemical aptasensor for 17β-estradiol using disposable laser scribed graphene electrodes. Biosens Bioelectron 185:113247

Chiticaru EA, Pilan L, Damian CM, Vasile E, Burns JS, Ioni M (2019) Influence of graphene oxide concentration when fabricating an electrochemical biosensor for DNA detection. Biosensors 9: 113–130

Choudhary M, Yadav P, Singh A, Kaur S, Ramirez-Vick J, Chandra P, Arora K, Singh SP (2016) CD 59 targeted ultrasensitive electrochemical immunosensor for fast and noninvasive diagnosis of oral cancer. Electroanalysis 28:2565–2574

Cincotto FH, Fava EL, Moraesa FC, Fatibello-Filho O, Fariaa RC (2019) A new disposable microfluidic electrochemical paper-based device for the simultaneous determination of clinical biomarkers. Talanta 195:62–68

Clark LC, Lyons C (1962) Electrode systems for continuous monitoring in cardiovascular surgery. Ann N Y Acad Sci 102:29–45

Congur G (2021) An up-to-date review about (bio)sensor systems developed for detection of glyphosate. Int J Env Anal Chem Ahead-of-print, 1–13

Congur G, Eksin E, Erdem A (2015a) Impedimetric detection of microRNA at graphene oxide modified sensors. Electrochim Acta 172:20–27

Congur G, Erdem A, Mese F (2015b) Electrochemical investigation of the interaction between topotecan and DNA at disposable graphite electrodes. Bioelectrochemistry 102:21–28

Congur G, Plucnara M, Erdem A, Fojta M (2015c) Detection of p53 gene by using genomagnetic assay combined with carbon nanotube modified disposable sensor technology. Electroanalysis 27:1579–1586

Congur G, Eksin E, Erdem A (2018) Impedimetric detection of miRNA-34a using graphene oxide modifiedchemically activated graphite electrodes. Sens Act A 279:493–500

Conti-Freitas LC, Foss-Freitas MC, Mamede R, Foss NT (2012) Interferon-gamma and ınterleukin-10 production by mononuclear cells from patients with advanced head and neck cancer. Clinics 67:587–590

Devarakonda S, Singh R, Bhardwaj J, Jang J (2017) Cost-effective and handmade paper-based ımmunosensing device for electrochemical detection of influenza virus sensors. Sensors 17:2597

Dowlatshahi S, Abdekhodaie MJ (2021) Electrochemical prostate-specific antigen biosensors based on electroconductive nanomaterials and polymers. Clin Chim Acta 516:111–135

Down MP, Foster CW, Ji X, Banks CE (2016) Pencil drawn paper based supercapacitors. RSC Adv 6:81130–81141

Dungchai W, Chailapakul O, Henry CS (2009) Electrochemical detection for paper-based microfluidics. Anal Chem 81:5821–5826

Dzulkurnain NA, Mokhtar M, Rashid JIA, Knight VF, Yunus VMZW, Ong KK, Kasim NAM, Noor SAM (2021) A review on ımpedimetric and voltammetric analysis based on polypyrrole conducting polymers for electrochemical sensing applications. Polymers 13:2728

Eksin E, Zor E, Erdem A, Bingol H (2017) Electrochemical monitoring of biointeraction by graphene-based material modified pencil graphite electrode. Biosens Bioelectron 92:207–214

Eksin E, Bikkarolla SK, Erdem A, Papakonstantinou P (2018) Chitosan/nitrogen doped reduced graphene oxide modified biosensor for ımpedimetric detection of microRNA. Electroanalysis 30:551–560

Ensafi AA, Lesani S, Amini M, Rezaei B (2015) Electrochemical ds-DNA-based biosensor decorated with chitosan modified multiwall carbon nanotubes for phenazopyridine biodetection. J Taiwan Inst Chem Eng 54:165–169

Erdem A, Congur G (2014) Label-free voltammetric detection of MicroRNAs at multi-channel screen printed array of electrodes comparison to graphite sensors. Talanta 118:7–13

Erdem A, Karadeniz H, Caliskan A (2009) Single-walled carbon nano-tubes modified graphite electrodes for electrochemical monitoring of nucleic acids and biomolecular interactions. Electroanalysis 21:464–471

Erdem A, Congur G, Eksin E (2013) Multi channel screen printed array of electrodes for enzyme-linked voltammetric detection of MicroRNAs. Sens Act B 188:1089–1095

Erdem A, Eksin E, Isin D, Polat D (2017) Graphene oxide modified chemically activated graphite electrodes for detection of microRNA. Electroanalysis 29:1350–1358

Famulok M, Hartig JS, Mayer G (2007) Functional aptamers and aptazymes in biotechnology, diagnostics, and therapy. Chem Rev 107:3715–3743

Faridbod F, Sanati AL (2019) Graphene quantum dots in electrochemical sensors/biosensors. Curr Anal Chem 15:103–123

Feng J, Ye Y, Xiao M, Wu G, Ke Y (2020) Synthetic routes of the reduced graphene oxide. Chem Paper 74:3767–3783

Feyzizarnagh H, Park BW, Sharma L, Patania MM, Yoon DY, Kim DS (2016) Amperometric mediatorless hydrogen peroxide sensor with horseradish peroxidase encapsulated in peptide nanotubes. Sens Bio-Sens Res 7:38–41

Flauzino JMR, Nguyen EM, Yang Q, Rosati G, Panacek D, Brito-Madurro AG, Madurro JM, Bakandritsos A, Otyepka MC, Merkoçi A (2022) Label-free and reagentless electrochemical genosensor based on graphene acid for meat adulteration detection. Biosens Bioelectron 195:113628

Geim AK, Novoselov KS (2007) The rise of graphene. Nat Mater 6:183–191

Ghosh T, Dutta M, Biswas K (2021) High-performance thermoelectrics based on metal selenides. In: Thermoelectric energy conversion theories and mechanisms, materials, devices, and applications, Woodhead Publishing series in electronic and optical materials, pp 217–246

Goda ES, Gab-Allah MA, Singu BS, Yoon KR (2019) Halloysite nanotubes based electrochemical sensors. Microchem J 147:1083–1096

Gogola JL, Martins G, Gevaerd A, Blanes L, Cardoso J, Marchini FK, Banks CE, Bergamini MF, Marcolino-Junior LH (2021) Label-free aptasensor for p24-HIV protein detection based on graphene quantum dots as an electrochemical signal amplifier. Anal Chim Acta 1166:338548

Goh GL, Tay MF, Lee JM, Ho JS, Sim LN, Yeong WY, Chong TH (2021) Potential of printed electrodes for electrochemical ımpedance spectroscopy (EIS): toward membrane fouling detection. Adv Electron Mater 7:2100043–2100064

Gonçalves AM, Pedro AQ, Santos FM, Martins LM, Maia CJ, Queiroz JA, Passarinha LA (2014) Trends in protein-based biosensor assemblies for drug screening and pharmaceutical kinetic studies. Molecules 19:12461–12485

Gupta A, Bhardwaj SK, Sharma AL, Deep A (2019) A graphene electrode functionalized with aminoterephthalic acid for impedimetric immunosensing of Escherichia coli. Microchim Acta 186:800

Gutiérrez-Capitán M, Baldi A, Fernández-Sánchez C (2020) Electrochemical paper-based biosensor devices for rapid detection of biomarkers. Sensors 20:967

Han B, Shi X, Peng Q, Gao W (2012) Study on genetic variance of miR-541 in type 1 diabetes. ISRN Endocrinol 2012:630861

Hasanjani HRA, Zarei K (2021) DNA/Au-Pt bimetallic nanoparticles/graphene oxide-chitosan composites modified pencil graphite electrode used as an electrochemical biosensor for sub-picomolar detection of anti-HIV drug zidovudine. Microchem J 164:106005

Hatamluyi B, Es'haghi Z (2018) Quantitative biodetection of anticancer drug rituxan with dna biosensor modified pamam dendrimer/reduced graphene oxide nanocomposite. Electroanalysis 30:1659–1668

Hernández-Ibáñez N, García-Cruz L, Montiel V, Foster CW, Banks CE, Iniesta J (2016) Electrochemical lactate biosensor based upon chitosan/carbon nanotubes modified screen-printed graphite electrodes for the determination of lactate in embryonic cell cultures. Biosens Bioelectron 77:1168–1174

Hu X, Gou KY, Kumar VS, Catanante G, Li Z, Zhu Z, Marty JL (2018) Disposable electrochemical aptasensor based on carbon nanotubes-V2O5-chitosan nanocomposite for detection of ciprofloxacin. Sens Act B 268:278–286

Huo PP, Zhao P, Wang Y, Liu B, Yin GC, Dong MD (2018) A roadmap for achieving sustainable energy conversion and storage: graphene-based composites used both as an electrocatalyst for oxygen reduction reactions and an electrode material for a supercapacitor. Energies 11:167–189

Hussain RA, Hussain I (2020) Metal telluride nanotubes: synthesis, and applications. Mat Chem Phys 256:123691

Iijima S (1991) Helical microtubules of graphitic carbon. Nature 354:56–58

Iliuk AB, Hu L, Tao WA (2011) Aptamer in bioanalytical applications. Anal Chem 83:4440–4452

Ishida N, Saito K (1977) Pencil lead and manufacturing method of the same. US Patent No: 4017451

Isin D, Eksin E, Erdem A (2017) Graphene oxide modified single-use electrodes and their application for voltammetric miRNA analysis. Mater Sci Eng C 75:1242–1249

Jamaluddin RZAR, Heng LY, Tan LL, Chong KF (2018) Electrochemical biosensor for nitrite based on polyacrylic-graphene composite film with covalently ımmobilized hemoglobin. Sensors 18: 1343–1359

Jamaluddin RZAR, Tan LL, Chong KF, Heng LY (2020) An electrochemical DNA biosensor fabricated from graphene decorated with graphitic nanospheres. Nanotechnology 31:485501

Jin Z, Owour P, Lei S, Ge L (2015) Graphene, graphene quantum dots and their applications in optoelectronics. Curr Opin Colloid Inter Sci 20:439–453

Joshi DJ, Koduru JR, Malek NI, Hussain CM, Kailasa SK (2021) Surface modifications and analytical applications of graphene oxide. Trend Anal Chem 144:116448

Kamali P, Zandi M, Ghasemzadeh-Moghaddam H, Fani M (2022) Comparison between various biosensor methods for human Tlymphotropic virus1 (HTLV1) detection. Mol Biol Rep 49: 1513–1517

Kampeera J, Pasakon P, Karuwan C, Arunrut N, Sappat A, Sirithammajak S, Dechokiattawan N, Sumranwanich T, Chaivisuthangkura P, Ounjai P, Chankhamhaengdecha S, Wisitsoraat A, Tuantranont A, Kiatpathomchai W (2019) Point-of-care rapid detection of Vibrio parahaemolyticus in seafood using loop-mediated isothermal amplification and graphene-based screen-printed electrochemical sensor. Biosens Bioelectron 132:271–278

Kanat E, Eksin E, Karacicek B, Erac Y, Erdem A (2018) Electrochemical detection of ınteraction between dacarbazine and nucleic acids in comparison to agarose gel electrophoresis. Electroanalysis 30:1566–1574

Karimi-Maleh H, Tahernejad-Javazmi F, Atar N, Yola ML, Gupta VK, Ensafi AA (2015) A novel DNA biosensor based on a pencil graphite electrode modified with polypyrrole/functionalized multiwalled carbon nanotubes for determination of 6-mercaptopurine anticancer drug. Ind Eng Chem Res 54:3634–3639

Karimi-Maleh H, Bananezhad A, Ganjali MR, Norouzi P, Sadrnia A (2018) Surface amplification of pencil graphite electrode with polypyrrole and reduced graphene oxide for fabrication of a guanine/adenine DNA based electrochemical biosensors for determination of didanosine anticancer drug. App Surf Sci 441:55–60

Karuppiah S, Mishra NC, Tsai WC, Liao WS, Chou CF (2021) Ultrasensitive and low-cost paper-based graphene oxide nanobiosensor for monitoring water-borne bacterial contamination. ACS Sens 6:3214–3223

Katouzian I, Jafari SM (2019) Protein nanotubes as state-of-the-art nanocarriers: synthesis methods, simulation and applications. J Control Release 303:302–318

Kelarakis A (2015) Graphene quantum dots: in the crossroad of graphene, quantum dots and carbogenic nanoparticles. Curr Opin Colloid Inter Sci 20:354–361

Khodadadi A, Faghih-Mirzaei A, Karimi-Maleh H, Abbaspourrad A, Agarwalf S, Kumar Gupta V (2019) A new epirubicin biosensor based on amplifying DNA interactions with polypyrrole and nitrogen-doped reduced graphene: experimental and docking theoretical investigations. Sens Act B 284:568–574

Killard AJ (2017) Disposable sensors. Curr Opin Electrochem 3:57–62

Kim J, Campbell AS, BEF Á, Wang J (2019) Wearable biosensors for healthcare monitoring. Nat Biotech 37:389–406

Lakshmipriya T, Gopinath SCB (2019) An introduction to biosensors and biomolecules. In: Nanobiosensors Biomolecular Targeting. Elsevier, pp 1–21

Lau WKO, Blute ML, Weaver AL, Torres VE, Zincke H (2000) Matched comparison of radical nephrectomy vs nephronsparing surgery in patients with unilateral renal cell carcinoma and a normal contralateral kidney. Mayo Clin Proc 75:1236–1242

Lawal AT (2018) Progress in utilisation of graphene for electrochemical biosensors. Biosens Bioelectron 106:149–178

Lee EK, Kim HJ, Lee KJ, Lee HJ, Lee JS, Kim DG, Hong SW, Yoon Y, Kim JS (2011) Inhibition of the proliferation and invasion of hepatocellular carcinoma cells by lipocalin 2 through blockade of JNK and PI3K/Akt signaling. Int J Oncol 38:325–333

Lee SH, Ban YJ, Oh CH, Park HK, Choi S (2016) A solvent-free microbial-activated air cathode battery paper platform made with pencil-traced graphite electrodes. Scientific Reports 6:28588

Li Z, Wang L, Li Y, Feng Y, Feng W (2019) Carbon-based functional nanomaterials: preparation, properties and applications. Compos Sci Technol 179:10–40

Lim J, Ling W, Khan A, Saad B, Ghani SA (2012) Electro polymerized 4-vinyl pyridine on 2B pencil graphite as ionophore for cadmium (II). Talanta 88:477–483

Liu F, Li N, Long B, Fan Y, Liu C, Zhou Q, Murtaza I, Wang K, Li P (2014) Cardiac hypertrophy is negatively regulated by miR-541. Cell Death Dis 5:1171

Liu J, Zhu B, Dong H, Zhang Y, Xu M, Travas-Sejdic J, Chang Z (2022) A novel electrochemical insulin aptasensor: from glassy carbon electrodes to disposable, single-use laser-scribed graphene electrodes. Bioelectrochemistry 143:107995

Loo SW, Pui TS (2020) Cytokine and cancer biomarkers detection: the dawn of electrochemical paper-based biosensor. Sensors 20:1854

Lu YJ, Liu RY, Hu K, Wang Y (2016) MiR-541-3p reverses cancer progression by directly targeting TGIF2 in non-small cell lung cancer. Tumor Immunol 37:12685–12695

Lu Q, Su T, Shang Z, Jin D, Shu Y, Xu Q, Hu X (2021) Flexible paper-based Ni-MOF composite/AuNPs/CNTs film electrode for HIV DNA detection. Biosens Bioelectron 184:113229

Mahato K, Purohit B, Bhardwaj K, Jaiswal A, Chandra P (2019) Novel electrochemical biosensor for serotonin detection based on gold nanorattles decorated reduced graphene oxide in biological fluids and in vitro model. Biosens Bioelectron 142:111502

Martinez AW, Phillips ST, Butte MJ, Whitesides GM (2007) Patterned paper as a platform for inexpensive, low-volume, portable bioassays. Angew Chem Int Ed Engl 46:1318–1320

Mašek J (1960) A simple microcoulometric arrangement for polarographic purposes using the three-electrode system. J Electroanal Chem 1:416–421

Matassan ND, Rizwan M, Mohd-Naim NF, Tlili C, Ahmed MU (2019) Graphene nanoplatelets-based aptamer biochip for the detection of Lipocalin-2. IEEE Sensors J 19:9592–9599

Mehta J, Vinayak P, Tuteja SK, Chhabra VA, Bhardwaj N, Paul AK, Kim KH (2016) Deep A graphene modified screen printed immunosensor for highly sensitive detection of parathion. Biosens Bioelectron 83:339–346

Min J, Kim Y, Lee S, Jang TW, Kim I, Song J (2019) The fourth industrial revolution and its impact on occupational health and safety, worker's compensation and labor conditions. Saf Health Work 10:400–408

Mincu NB, Lazar V, Stan D, Mihailescu CM, Iosu R, Mateescu AL (2020) Screen-printed electrodes (SPE) for in vitro diagnostic purpose. Diagnostics 10:517

Miyamoto T, Kashima H, Suzuki A, Kikuchi N, Konishi D, Seki N, Shiozawa T (2011) Laser-captured microdissection-microarray analysis of the genes involved in endometrial carcinogenesis: stepwise upregulation of lipocalin2 expression in normal and neoplastic endometria and its functional relevance. Hum Pathol 42:1265–1274

Mohammad-Razdari A, Ghasemi-Varnamkhasti M, Izadi Z, Ensafi AA, Rostami S, Siadat M (2019a) An impedimetric aptasensor for ultrasensitive detection of Penicillin G based on the use of reduced graphene oxide and gold nanoparticles. Microchim Acta 186:372

Mohammad-Razdari A, Ghasemi-Varnamkhasti M, Izadi Z, Rostami S, Ensafi AA, Siadat M, Losson E (2019b) Detection of sulfadimethoxine in meat samples using a novel electrochemical biosensor as a rapid analysis method. J Food Comp Anal 82:103252

Mohanraj J, Durgalakshmi D, Rakkesh RA, Balakumar S, Rajendran S, Karimi-Maleh H (2020) Facile synthesis of paper based graphene electrodes for point of care devices: a double stranded DNA (dsDNA) biosensor. J Colloid Inter Sci 566:463–472

Moniaux N, Chakraborty S, Yalniz M, Gonzalez J, Shostrom VK, Standop J, Lele SM, Ouellette M, Pour PM, Sasson AR, Brand RE, Hollingsworth MA, Jain M, Batra SK (2008) Early diagnosis of pancreatic cancer: neutrophil gelatinase-associated lipocalin as a marker of pancreatic intraepithelial neoplasia. Br J Cancer 98:1540–1547

Moraskie M, Roshid HO, O'Connor G, Dikici E, Zingg JM, Deo S, Daunert S (2021) Microbial whole-cell biosensors: current applications, challenges, and future perspectives. Biosens Bioelectron 191:113359

Moshiri F, Salvi A, Gramantieri L, Sangiovanni A, Guerriero P, De Petro G, Bassi C, Lupini L, Sattari A, Cheung D (2018) Circulating miR-106b-3p, miR-101-3p and miR-1246 as diagnostic biomarkers of hepatocellular carcinoma. Oncotarget 9:15350

Mujica ML, Gallaya PA, Perrachionea F, Montemerlo AE, Tamborelli LA, Vaschetti VM, Reartes RM, Bolloc S, Rodríguez MC, Dalmasso PR, Rubianes MD, Rivas GA (2020) New trends in the development of electrochemical biosensors for thequantification of microRNAs. J Pharm Biomed Anal 189:113478

Mustafa RR, Sukor R, Eissa S, Shahrom AN, Saari N, Nor SMM (2021) Sensitive detection of mitragynine from Mitragyna speciosa Korth using an electrochemical immunosensor based on multiwalled carbon nanotubes/chitosan- modified carbon electrode. Sens Act B 345:130356

Narwal V, Pundir CS (2019) Development of glycerol biosensor based on co-immobilization of enzyme nanoparticles onto graphene oxide nanoparticles decorated pencil graphite electrode. Int J Biol Macromol 127:57–65

Nilghaz A, Guan L, Tan W, Shen W (2016) Advances of paper-based microfluidics for diagnostics – the original motivation and current status. ACS Sens 1:1382–1393

Nochit P, Subudom P, Teepoo S (2021) Multiwalled carbon nanotube (MWCNT) based electrochemical paper-based analytical device (ePAD) for the determination of catechol in wastewater. Anal Lett 54:2484–2497

Nohwala B, Chaudharya R, Pundir CS (2020) Amperometric L-lysine determination biosensor amplified with L-lysine oxidase nanoparticles and graphene oxide nanoparticles. Process Biochem 97:57–63

Nooranian S, Mohammadinejad A, Mohajeri T, Aleyaghoo G, Oskuee RK (2021) Biosensors based on aptamer-conjugated gold nanoparticles: a review. Biotechnol Appl Biochem 1–18

Obayomi KS, Lau SY, Danquah M, Chiong T, Takeo M (2022) Advances in graphene oxide based nanobiocatalytic technology for wastewater treatment. Environ Nanotechnol Monit Manag 17:100647

Pandey CM, Malhotra BD (2019) Biosensors: fundamentals and applications, 2nd edn. De Gruyter, Berlin/Boston

Panraksa Y, Siangproh W, Khampieng T, Chailapakul O, Apilux A (2018) Paper-based amperometric sensor for determination of acetylcholinesterase using screen-printed graphene electrode. Talanta 178:1017–1023

Parate K, Pola CC, Rangnekar SV, Mendivelso-Perez DL, Smith EA, Hersam MC, Gomes CL, Claussen JC (2020a) Aerosol-jet-printed graphene electrochemical histamine sensors for food safety monitoring. 2D Mater 7:034002

Parate K, Rangnekar SV, Jing D, Mendivelso-Perez DL, Ding S, Secor EB, Smith EA, Hostetter JM, Hersam MC, Claussen JC (2020b) Aerosol-Jet-printed graphene immunosensor for label-free cytokine monitoring in serum. Appl Mater Interfaces 12:8592–8603

Pishko MV, Katanis I, Lindquist SE, Heller A, Degani Y (1990) Electrical communication between graphite electrodes and glucose oxidase/redox polymer complexes. Mol Cryst Liq Cryst 190: 221–249

Plekhanova Y, Tarasov S, Reshetilov A (2021) Use of PEDOT:PSS/graphene/nafion composite in biosensors based on acetic acid bacteria. Biosensors 11:332–342

Poletti F, Scidà A, Zanfrognini B, Kovtun A, Parkula V, Favaretto L, Melucci M, Palermo V, Treossi E, Zanardi C (2022) Graphene-paper-based electrodes on plastic and textile supports as new platforms for amperometric biosensing. Adv Funct Mater 32:2107941

Popov VN (2004) Carbon nanotubes: properties and application. Mater Sci Eng R 43:61–102

Pothipor C, Bamrungsap S, Jakmune J, Ounnunka K (2022) A gold nanoparticle-dye/poly (3-aminobenzylamine)/two dimensional $MoSe_2$/graphene oxide electrode towards label-free electrochemical biosensor for simultaneous dual-mode detection of cancer antigen 15-3 and microRNA-21. Colloid Surf B 210:112260

Pumera M (2010) Graphene-based nanomaterials and their electrochemistry. Chem Soc Rev 39: 4146–4157

Rabti A, Mayorga-Martinez CC, Baptista-Pires L, Raouafi N, Merkoçi A (2016) Ferrocene-functionalized graphene electrode for biosensing applications. Anal Chim Acta 926:28–35

Rong S, Zou L, Zhu Y, Zhang Z, Liu H, Zhang Y, Zhang H, Gao H, Guan H, Dong J, Guo Y, Liu F, Li X, Pan H, Chang D (2021) 2D/3D material amplification strategy for disposable label-free electrochemical immunosensor based on rGO-TEPA@Cu-MOFs@SiO_2@AgNPs composites for NMP22 detection. Microchem J 168:106410

Saadat S, Pandey G, Tharmavaram M, Braganz V, Rawtani D (2020) Nano-interfacial decoration of Halloysite nanotubes for the development of antimicrobial nanocomposites. Adv Colloid Int Sci 275:102063

Saif MJ, Asif HM, Naveed M (2018) Properties andmodificationmethods of halloysite nanotubes: a state-of-the- art review. Chil Chem Soc 63:4109–4125

Sawant SV, Patwardhan AW, Joshi JB, Dasgupta K (2022) Boron doped carbon nanotubes: synthesis, characterization and emerging applications. Chem Eng J 427:131616

Sengiz C, Congur G, Eksin E, Erdem A (2015) Multiwalled carbon nanotubes-chitosan modified single- use biosensors for electrochemical monitoring of drug- DNA interactions. Electroanalysis 27:1855–1863

Seo SE, Tabei F, Park SJ, Askarian B, Kima KH, Moallem G, Chong JW, Kwon OS (2019) Smartphone with optical, physical, and electrochemical nanobiosensors. J Ind Eng Chem 77:1–11

Sethi J, Bulck MV, Suhail A, Safarzadeh M, Perez-Castillo A, Pan G (2020) A label-free biosensor based on graphene and reduced graphene oxide dual-layer for electrochemical determination of beta-amyloid biomarkers. Microchim Acta 187:288

Sethi J, Suhail A, Safarzadeh M, Sattar A, Wei Y, Pan G (2021) NH_2 linker for femtomolar label-free detection with reduced graphene oxide screen-printed electrodes. Carbon 179:514–522

Settu K, Liu JT, Chen CJ, Tsai JZ (2017) Development of carbongraphene-based aptamer biosensor for EN2 protein detection. Anal Biochem 534:99–107

Sha R, Badhulika S (2019) Few layered MoS_2 grown on pencil graphite: a unique single-step approach to fabricate economical, binder-free electrode for supercapacitor applications. Nanotechnology 30:035402

Sharifi M, Avadi MR, Attar F, Dashtestani F, Ghorchian H, Rezayat SM, Saboury AA, Falahati M (2019) Cancer diagnosis using nanomaterials based electrochemical nanobiosensors. Biosens Bioelectron 126:773–784

Shoja Y, Kermanpur A, Karimzadeh F (2018) Diagnosis of EGFR exon21 L858R point mutation as lung cancer biomarker by electrochemical DNA biosensor based on reduced graphene oxide/ functionalized ordered mesoporous carbon/Ni-oxytetracycline metallopolymer nanoparticles modified pencil graphite electrode. Biosens Bioelectron 113:108–115

Silveira MC, Monteiro T, Almeida GM (2016) Biosensing with paper-based miniaturized printed electrodes–a modern trend. Biosensors 6:51

Soares RRA, Hjort RG, Pola CC, Parate K, Reis EL, Soares NFF, McLamore ES, Claussen JC, Gomes CL (2020) Laser-induced graphene electrochemical immunosensors for rapid and label-free monitoring of salmonella enterica in chicken broth. ACS Sens 5:1900–1911

Song KM, Cho M, Jo H, Min K, Jeon SH, Kim T, Han MS, Ku JK, Ban C (2011) Gold nanoparticle-based colorimetric detection of kanamycin using a DNA aptamer. Anal Biochem 415:175–181

Srivastava AK, Dev A, Karmakar S (2018) Nanosensors and nanobiosensors in food and agriculture. Env Chem Lett 16:161–182

Stanković V, Đurđić S, Ognjanović M, Antić B, Kalcher K, Mutić J, Stanković DM (2020) Anti-human albumin monoclonal antibody immobilized on EDC-NHS functionalized carboxylic graphene/AuNPs composite as promising electrochemical HSA immunosensor. J Electroanal Chem 860:113928

Sujaritvanichpong S, Aoki K (1989) Electrode reactions of 3,4-dihydroxyphenylacetic acid (DOPAC) at glassy carbon, graphite-reinforcement carbon, and carbon fiber electrodes. Electroanalysis 1:397–403

Taei M, Salavati H, Hasanpour F, Shafiei A (2015) Biosensor based on ds-DNA decorated Fe_2O_3/ SnO_2-chitosan modified multiwalled carbon nanotubes for biodetection of doxorubicin. IEEE Sensors J 16:1–1

Teymourian H, Barfidokht A, Wang J (2020) Electrochemical glucose sensors in diabetes management: an updated review (2010–2020). Chem Soc Rev 49:7671–7709

Thangamuthu M, Hsieh KY, Kumar PV, Chen GY (2019) Graphene- and graphene oxide-based nanocomposite platforms for electrochemical biosensing applications. Int J Mol Sci 20:2975

Thapa K, Liu W, Wang R (2022) Nucleic acid-based electrochemical biosensor: recent advances in probe immobilization and signalamplification strategies. WIREs Nanomed Nanobiotechnol 14:1765

Torrinha A, Amorim CG, Montenegro MCBSM, Araújo AN (2018) Biosensing based on pencil graphite electrodes. Talanta 190:235–247

Torul H, Yarali E, Eksin E, Ganguly A, Benson J, Tamer U, Papakonstantinou P, Erdem A (2021) Paper-based electrochemical biosensors for voltammetric detection of miRNA biomarkers using reduced graphene oxide or MOS_2 nanosheets decorated with gold nanoparticle electrodes. Biosensors 11:236–252

Tu D, He Y, Rong Y, Wang Y, Li G (2016) Disposable L-lactate biosensor based on a screen-printed carbon electrode enhanced by graphene. Meas Sci Technol 27:045108–2704514

Turner AFP (2013) Biosensors: sense and sensibility. Chem Soc Rev 42:3184–3196

Tutunaru O, Mihailescu CM, Savin M, Tincu BC, Stoian MC, Muscalu GS, Firtat B, Dinulescu S, Craciun G, Moldovan CA, Ficai A, Ion AC (2021) Acetylcholinesterase entrapment onto carboxyl-modified single-walled carbon nanotubes and poly (3,4-ethylenedioxythiophene) nanocomposite, film electrosynthesis characterization, and sensor application for dichlorvos detection in apple juice. Microchem J 169:106573

Unal DN, Eksin E, Erdem A (2017) Carbon nanotubes modified graphite electrodes for monitoring of biointeraction between 6-thioguanine and DNA. Electroanalysis 29:2292–2299

Viau A, Karoui KE, Laouari D, Burtin M, Nguyen C, Mori K, Pillebout E, Berger T, Mak TW, Knebelmann B, Friedlander G, Barasch J, Terzi F (2010) Lipocalin 2 is essential for chronic kidney disease progression in mice and humans. J Clin Invest 120:4065–4076

Viet NX, Hoan NX, Takamura Y (2019) Development of highly sensitive electrochemical immunosensor based on single-walled carbon nanotube modified screen-printed carbon electrode. Mater Chem Phys 227:123–129

Vukojević V, Djurdjića S, Ognjanović M, Fabián M, Samphaod A, Kalchere K, Stanković DM (2018) Enzymatic glucose biosensor based on manganese dioxide nanoparticles decorated on graphene nanoribbons. J Electroanal Chem 823:610–616

Vural T, Yaman YT, Ozturk S, Abaci S, Denkbas EB (2018) Electrochemical immunoassay for detection of prostate specific antigen based on peptide nanotube-gold nanoparticle-polyaniline immobilized pencil graphite electrode. J Colloid Inter Sci 510:318–326

Wang L (2017) Screening and biosensor-based approaches for lung cancer detection. Sensors 17:2420

Wang J, Kawde AN, Sahlin E (2000) Renewable pencil electrodes for highly sensitive stripping potentiometric measurements of DNA and RNA. Analyst 125:5–7

Wang X, Lu X, Chen J (2014) Development of biosensor technologies for analysis of environmental contaminants. Trend Env Anal Chem 2:25–32

Wang Y, Zhang J, Gao H, Sun Y, Wang L (2022) Lipid nanotubes: formation and applications. Colloid Surf B 212:112362

Wei B, Mao K, Liu N, Zhang M, Yang Z (2018) Graphene nanocomposites modified electrochemical aptamer sensor for rapid and highly sensitive detection of prostate specific antigen. Biosens Bioelectron 121:41–46

Wen L, Qiu L, Wu Y, Hu X, Zhang X (2017) Aptamer-modified semiconductor quantum dots for biosensing applications. Sensors 17:1736

Wu G, Zheng H, Xing Y, Wang C, Yuan X, Zhu X (2022) A sensitive electrochemical sensor for environmental toxicity monitoring based on tungsten disulfide nanosheets/hydroxylated carbon nanotubes nanocomposite. Chemosphere 286:131602

Yaman YT, Vural OA, Bolat G, Abaci S (2020) One-pot synthesized gold nanoparticle-peptide nanotube modified disposable sensor for impedimetric recognition of miRNA 410. Sens Act B 320:128343

Yao Y, Jiang C, Ping J (2019) Flexible freestanding graphene paper-based potentiometric enzymatic aptasensor for ultrasensitive wireless detection of kanamycin. Biosens Bioelectron 123:178–184

Yeung ML, Bennasser Y, Myers TG, Jiang G, Benkirane M, Jeang KT (2005) Changes in microRNA expression profiles in HIV-1-transfected human cells. Retrovirology 2:81

Yu H, Guo W, Lu X, Xu H, Yang Q, Tan J, Zhang W (2021) Reduced graphene oxide nanocomposite based electrochemical biosensors for monitoring foodborne pathogenic bacteria. Food Control 127:108117

Zhang W, Du Y, Wang ML (2015) On-chip highly sensitive saliva glucose sensing using multilayer films composed of single-walled carbon nanotubes, gold nanoparticles, and glucose oxidase. Sens Bio-Sens Res 4:96–102

Zhao C, Li X, An S, Zheng D, Pei S, Zheng X, Liu Y, Yao Q, Yang M, Dai L (2019) Highly sensitive and selective electrochemical immunosensors by substrate-enhanced electroless deposition of metal nanoparticles onto three-dimensional graphene@Ni foams. Sci Bull 64:1272–1279

Zhou Y (2008) Lipid nanotubes: formation, templating nanostructures and drug nanocarriers. Crit Rev Solid State Mater Sci 33:183–196

Zhou J, Qiu X, Su K, Xu G, Wang P (2016) Disposable poly (o-aminophenol)-carbon nanotubes modified screenprint electrode-based enzyme sensor for electrochemical detection ofmarine toxin okadaic acid. Sens Act B 235:170–178

Zhu X, Wu G, Lua N, Yuan X, Li B (2017) A miniaturized electrochemical toxicity biosensor based on graphene oxide quantum dots/carboxylated carbon nanotubes for assessment of priority pollutants. J Hazard Mater 324:272–280

Nanoporous Silica Materials for Electrochemical Sensing and Bioimaging

27

Vinodhini Subramaniyam and Moorthi Pichumani

Contents

1 Introduction 600
  1.1 Preparation of Nanoporous Silica Materials 601
  1.2 Hybridization of Nanoporous Silica to Enhance Opto-electronic Properties for Specific Applications 602
2 Electrochemical Sensing Applications 602
  2.1 Electrochemical Sensing of Metal-Ions and Heavy Metal-Ions 602
  2.2 Electrochemical Sensing of Biomolecules 604
  2.3 Electrochemical Sensing of Gas 605
  2.4 Electrochemical Sensing of Chemical Species 608
  2.5 Electrochemical Sensing of Insecticide, Radiative, Explosive, and Stimulant Drug 608
3 Biosensing and Imaging Applications 609
  3.1 Drug Delivery 609
  3.2 Biomolecules Immobilization/Encapsulation 611
  3.3 Biosensing Through Various Methods 612
  3.4 Bioimaging Applications 613
4 Conclusion and Outlook 614
References 615

Abstract

Silica (SiO_2) is a simple inorganic porous material commonly found on the earth. The homogeneous porosity, hydrothermal firmness, increased surface area, pore size, pore volume, ordered texture, chemical inertness, and biocompatible nature are the iconic and crucial properties of the nanoporous silica. Each specific

---

V. Subramaniyam (✉)
Department of Physics, Karpagam College of Engineering, Coimbatore, India
e-mail: vinonano@srec.ac.in

M. Pichumani
Department of Nanoscience and Technology, Sri Ramakrishna Engineering College, Coimbatore, India
e-mail: mpichumani@srec.ac.in

© Springer Nature Singapore Pte Ltd. 2023

U. P. Azad, P. Chandra (eds.), *Handbook of Nanobioelectrochemistry*,
https://doi.org/10.1007/978-981-19-9437-1_27

properties of the nanoporous silica enables the wide applications into numerous fields. The adaptability of silica is helping in hybridizing with other organic and/or inorganic species. This hybridization with other species enhances the properties of the pristine silica for different applications. Besides, the chemical inertness of the pristine silica is helpful to stabilize the chemical species inside the pores and using in electrochemical sensing of metal/heavy metal ions, biomolecules, gas molecules, insecticide, radiative element, explosive trigger, stimulant drug, and other potential chemical species. The ordered porous structure is used as a backbone in the form of films, coatings, and membranes in electrodes. Additionally, the uniform pore size easing the electrode accessibility by enhancing the diffusivity of charges and ions. The optical property of hybridized silica is greatly utilized in the sensing and imaging applications. Especially, the biocompatibility of the nanoporous silica is playing a predominant role in the bioimaging of cancer cell growth. By the help of drug immobilization, the nanoporous silica can be efficiently utilized in targeting drug delivery in *in vivo* therapeutic applications. The nanoporous silica is the potential material with multitude applications in various fields.

Keyword

Nanoporous silica · Hybridization · Membrane · Electrochemical sensor · Biosensor · Bio-imaging

1 Introduction

Silicon (IV) dioxide (SiO_2) is a common inorganic material is also called Silica. Silica materials can be found as crystalline (quartz) as well as amorphous. The silica, a ceramic material, is composed by one silicon atom and two oxygen atoms coordinated in a linear fashion (O-Si-O). Silica is considered to be a richest mineral present on the earth. The Silica material with its bulk form is used in the production of glasses, concrete, silica foam, MEMS devices, sand casted metallic materials, IC insulators, shale gas and oil hydraulic cracking, additive in food manufacturing, semiconducting materials development, and etc. The chemical inertness and biocompatibility of the silica materials make them as prominent coating material on various electrode materials (Chen et al. 2016). Notably, the porous nature of the silica material is making them as protuberant templates in the preparation of several pristine and hybrid nanoparticles and/or nanostructures. Further, due to the chemical inertness and porous properties, the silica material is used as the ever-classic material in various separation columns (Khoo and Leow 2021).

Porous materials are generally classified into three categories with respect to their pore size such as microporous (0.2 nm < pore diameter < 2 nm), mesoporous (2 nm < pore diameter < 50 nm), and macroporous (50 nm < pore diameter < 1000 nm). Paradoxically, after the development of nanoscience domain, the materials with a pore size of 1 nm < pore diameter < 100 nm, which are either open, closed, and/or interconnected pores, are considered to be nanoporous materials.

Among all, mesoporous materials are coming under the nanoporous materials, as subcategory. Compared with the mesoporous silica, nanoporous silica possess vertical alignment of pores that enhances the surface-to-volume ratio and molecular accessibility.

Nanoporous silica materials including, particles, fibers, membranes, gels, aerogels with large-range order possess outstanding properties such as great surface area, pore size and pore volume, hydrothermal firmness, and homogeneously tailored particle texture (Badiei et al. 2018). Moreover, thermal annealing and ion-irradiation treatments can induce thermal spikes showcasing the improved mechanical stability of nanoporous silica (Kucheyev et al. 2011). Nanoporous silica is broadly used in the form of film in electrodes of the electrochemical sensors. This provides a direct contact toward the surface of the electrode material to the species with solution phase. The nanoporous silica materials are cost effective and being prepared easily than the ideally used carbon black materials for the electrodes used in electrochemical systems. They offer the adaptability with other electroactive and/or conducting additive materials, while formulating the paste for electrode preparation. The nanoporous network ease the charge-electrode accessibility, which results in mass charge transportation. The ordered pore structure with homogeneous size of the nanoporous silica enables the electron and ionic diffusivity (Wei and Hillhouse 2007).

Nanoporous silica materials are also prepared in the form of individual or supported membranes. These membranes are highly required in the broad fields of electrochemistry and molecular separation (Wang et al. 2007; Zhou et al. 2020). Nanoporous silica substrates with protein imprints are utilized in immunoassay sensing (Blinka et al. 2010) and waveguide sensor chips (Horvath et al. 2005) applications. Nanoporous silica are used as supporting stubborn layer, core, or backbone embedded with biological systems like phospholipid bilayers (Kendall et al. 2013; Sun et al. 2015) and cellular level evaluation (Li et al. 2017). Adsorption of metal ions (for example, Be^{+}, Pd^{2+}), sensing of metal ions (for example, Cd^{2+}, Pb^{2+}, Cu^{2+}, Ni^{2+}, Ag^{+}, Hg^{2+}, Fe^{3+}, Cr^{3+}, Ce^{3+}), detection of refractive index (Chen et al. 2016), catalyzation for artificial photosynthesis (Frei 2009), and chemical conversion (Yang and Tang 2019) are also performed using both pristine and functionalized nanoporous silica.

1.1 Preparation of Nanoporous Silica Materials

Nanoporous silica particles are generally synthesized with co-condensation (Fatemeh Silakhori et al. 2020), and stöber method (Di Paolo et al. 2019). Mesoporous silica materials used as a source to the synthesis of nanoporous silica. For example, the nanoporous silica fibers prepared using templated electrospinning method with mesoporous silica, which is primarily synthesized with sol-gel method (Kanehata et al. 2007; Elsherief et al. 2020). Nanoporous silica (amorphous) in large-scale is synthesized from etching the silica sheets. The size and morphology of the resultant silica nanostructures can be easily tuned in this method (Hui et al. 2020). Nanoporous silica structures/films also fabricated on substrates using self-assembly process (Doshi et al. 2005; Bollmann et al. 2007; Canning et al. 2014).

Among all other above-said methods, nanoporous silica synthesis are time-consuming syntheses with high energy and expensive chemicals. But, cost-effective biosynthesis diminishes all the demerits, which presents in the other chemical involved synthetic methods. The nature-gifted photosynthetic microalgae, diatom, possess various micro and nanoporous structures. The diatom with nanoporous silica shells and frustules can be synthesized/cultivated naturally within few days (Gnanamoorthy et al. 2014).

1.2 Hybridization of Nanoporous Silica to Enhance Opto-electronic Properties for Specific Applications

The nanoporous silica itself has photoluminescence property in a long-range from ultraviolet to visible spectrum (Hui et al. 2020) with enhanced surface area and pore size (Elsherief et al. 2020). Further, the luminescence property of the nanoporous silica enhanced by doping (Hayashi et al. 2021) of many materials including Eu (II) (Tagaya et al. 2011), Fe_3O_4–Au core (Zhang et al. 2010), naphthoquinone (Fatemeh Silakhori et al. 2020), spirorhodamineamide (Di Paolo et al. 2019), 9-acridinylamine (Zhad et al. 2011), and diatoms (photosynthetic microorganism, algae) (Yoneda et al. 2016) for fluorescent sensing applications and pH indicator utilizations.

Experiments on synthesis of nanoporous silica aerogels offers enhanced mechanical, thermal, and physiochemical properties (Lee et al. 2006; Hong et al. 2013). Hybridization with magnetic nanoparticles followed by polymer materials functionalization offers the composite a field-dependent magnetization properties with large pores (Liu et al. 2012; Janßen et al. 2018), which enables them to use in many fields such as, drug delivery, adsorption, cellular uptake, bioimaging, etc., Nanoporous silica functionalized with sulfonic acid is used as the nano-reactor in the synthesis of organic materials (Mohammadi Ziarani et al. 2011). Membrane of nanoporous silica-phenyl sulfonic acid with polyvinyl alcohol is applied in the Polymer Electrolyte Membrane (PEM) fuel cells due to their enhanced water retention ability and thermal stability offered by the acidic nature of the nanoporous silica porous structure (Beydaghi et al. 2011). Extensively, the applications of the hybridized nanoporous silica in electrochemical sensing, biosensing, immobilization, drug delivery, and bioimaging are discussed widely in the following sections.

2 Electrochemical Sensing Applications

2.1 Electrochemical Sensing of Metal-Ions and Heavy Metal-Ions

Silica-based materials are globally utilized in the electrochemical sensors to sense metal ions (Yadavi et al. 2013) and heavy metal ions (Rechotnek et al. 2021). Especially, mechanically and thermally stable nanoporous silica materials with homogeneous size, high surface area, and biocompatibility are simple and cost-effective with great sensitivity and selectivity toward metal ion detection. Nanoporous silica modified with 1-(2-pyridylazo)-2-naphthol is used to detect a list of heavy metal ions (Cu^{2+}, Pb^{2+}, Cd^{2+}, and Ni^{2+}) from the samples of water and seafood with a detection limit of 0.4, 0.9, 0.3, and 0.6 ng mL^{-1}. In electrochemical sensing, the adsorption of metal/heavy metal ions into the nanoporous silica, pH is the most crucial parameter. By fixing the pH (offers increased quantitative recovery), the interference of unidentified complex matrices present in real samples could be reduced (Abolhasani and Behbahani 2015). Nanoporous silica in the form of gel, functionalized with dipyridyl (DPSG) used in the electrochemical sensor to sense Ag^+ ions with a detection limit of 1.0×10^{-7} M. The increment in current response, while the Ag^+ ions interact with the electrode is clearly revealed in the Fig. 27.1a. The nanoporous silica offers improved performance, response time, sensitivity, and stability to the electrode (Javanbakht et al. 2007a). Similarly, the Ag^+ ion sensed using nanoporous silica gel are modified with phenylthiourea with a limit of detection, 5 pM L^{-1} (Javanbakht et al. 2009a).

Nanoporous silica is incorporated into polyfurfural, and then coated on a glassy carbon electrode to sense Cd^{2+} and Pb^{2+} ions electrochemically as well as

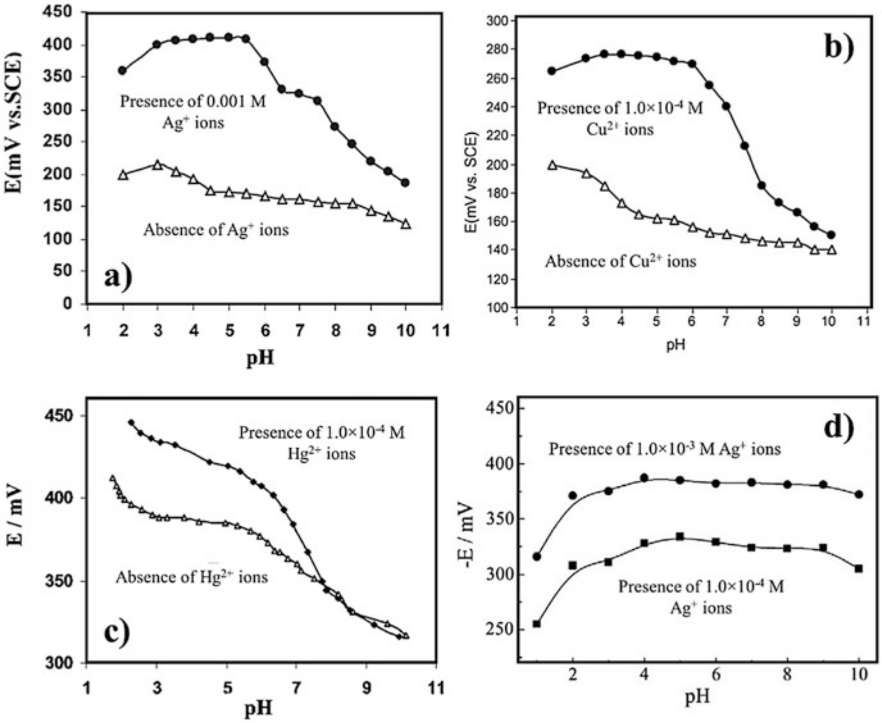

Fig. 27.1 pH response of the freshly prepared electrode vs (**a**) DPSG-based electrode, (**b**) DPNSG-based electrode, (**c**) CPE5-based electrode, and (**d**) DTPSG-based electrode. (Taken from Javanbakht et al. 2007a, b, 2009a, b, c, and Zhang et al. 2012b)

simultaneously with a detection limit of 0.9 ng L^{-1} and 0.02 ng L^{-1}, respectively. The resultant electrode displays improved stability, reliability, selectivity, and sensitivity with a broad linear range (Fang et al. 2019). Dipyridyl group covalently functionalize with nanoporous silica gel (DPNSG) are used to detect the Cu^{2+} heavy metal ions with a limit of detection, 8.0×10^{-8} M. The Fig. 27.1b shows the detection of Cu^{2+} ions with the current hike response. The resultant electrochemical sensor shows enhanced durability and selectivity with quick response time (Javanbakht et al. 2007b). Likewise, the DPNSG modified electrode also tends to detect Ce^{3+} ions with linear response (Javanbakht et al. 2008).

Nanoporous silica gel functionalized with dipyridyl is utilized to determine Hg^{2+} ions with a limit of detection, 8 nM. The electrode possess increased lifetime and stability by limiting the leach of functional groups from the nanoporous silica backbone (Javanbakht et al. 2009c). Detection of Hg^{2+} ions are also performed using nanoporous silica functionalized with thiourea with a limit of detection of 7.0×10^{-8} M dm^{-3}. The hike in current response when the interaction of Hg^{2+} ions with the electrode is shown in Fig. 27.1c. Typically, the electrode exhibits improved performance, sensitivity, and stability (Javanbakht et al. 2009b). Nanoporous silica embedded with glycinyl-urea is used to sense Pb^{2+}, Cu^{2+}, and Hg^{2+} ions with excellent durability by protecting the depletion of the functional ligands (Lin et al. 2004). The nanoporous silica gel modifying with diazo-thiophenol used to sense Ag^{+} ions with a limit of detection, 9.5×10^{-7} M. The electrode responding with high current for the interaction of Ag^{+} ions with the electrode surface is displayed in Fig. 27.1d. This offers quick response time, longer stability, enhanced selectivity, and reproducibility (Zhang et al. 2012a). In the same way, the nanoporous silica gel functionalized with 2-acetylpyridine is used to electrochemically sense Cr^{3+} ions in coffee and tea leaves with a limit of detection, 8.0×10^{-9} M. The quick response time, sensitivity, and stability of the electrode are protected by using nanoporous silica (Zhou et al. 2009).

2.2 Electrochemical Sensing of Biomolecules

The electrochemical sensing method is widely used to detect biomolecules (Liu et al. 2017; Shanbhag et al. 2021). The sensing of the biomolecules are ideally performed by loading the corresponding enzyme into porous electrode materials. Nanoporous materials with high surface area are unique in biomolecule sensing (Zhang et al. 2012b), especially, nanoporous silica (Yu et al. 2006) with chemical inertness and fast charge transfer nature (Dhara and Mahapatra 2020). Specifically, nanoporous silica synthesized from biological source (diatoms) enables surface modifications and diffusivity of the chemical species. Diatomic nanoporous silica membrane with improved rapid sensitivity and greater selectivity, even without the usage of label, is utilized to sense C-reactive protein (Vattipalli et al. 2011). Similarly, diatomic nanoporous silica is used to sense C-reactive protein and myeloperoxidase, inflammatory proteins (Lin et al. 2010) as label-free method.

Transparent nanoporous silica films embedded with triple photoluminescence dopants such as, nitrogen, boron, and carbon quantum dots (CQDs) used to sense glucose with a detection limit ranges from 1.0 mg dL^{-1} to 100 mg dL^{-1} (Kipnusu et al. 2020). Hybridized silica-based immunosensors are in trend now for the immobilization of the antibodies to sense the analytes (Mahato et al. 2018). A Ru-Si@Au nanocomposite-based electrochemical immunosensor (showed in Fig. 27.2), in which the nanoporous silica particles doped with $Ru(bpy)_3^{2+}$ to sense p53 protein. The second part of the Fig. 27.2 clearly shows the nanoporous silica particles, in which the $Ru(bpy)_3^{2}$ embedment followed by labelling. The immunosensor is highly stable and selective toward p53 protein with a detection limit of 22.8 fM in human serum samples (Afsharan et al. 2016). The nanoporous silica is also used as thermal stable coating for the substrates to grow single walled carbon tubes (SWCNTs). The SWCNTs grown on the nanoporous silica substrates are lengthier with interconnections than the uncoated substrate. This interconnection between the SWCNTs increases the electrical conductivity, which results in linear current-voltage (I-V) response. Further, this enhances the signal-to-noise ratio during the prostate-specific antigen (PSA) biomolecule sensing by hydrophobic interaction, π-stacking, and affinity of amino groups (Han et al. 2012).

2.3 Electrochemical Sensing of Gas

The presence of higher specific surface area, pore structure, pore size, pore volume, and defect sites properties in a sensor material plays a vital role in gas sensing applications. For biological-related applications, especially *in vivo*, the sensor material must be biocompatible, chemically stable, mechanically strong, and antifouling in nature. Nanoporous silica are widely used as nanoporous template to synthesize semiconducting sensor materials with required properties. For instance, ZnO nanostructures prepared using nanoporous silica template is offering increased surface roughness with sensitive recognition of hydrogen (H_2) gas (Gupta et al. 2014). For *in vivo* oxygen (O_2) monitoring in living rat brain, vertically oriented nanoporous silica membrane with homogeneous pore size with great porosity is used (Fig. 27.3a). The nanoporous silica is grafted with carbon fiber microelectrode (CFME) sustaining the O_2 analytical sensitivity, compared with the bare CFME. The nanoporous silica coating is protecting the CFME from biofouling and conserving the O_2 permeability. During *in vivo* operation, the electrode displays outstanding current stability with quick response for 2 h. The nanoporous silica makes the CFME capable of monitoring O_2 for a long-term.

Thermally stable nanoporous silica-coated substrates helps to grow longer SWCNTs with interconnected curls and knots from the Fe seed catalyst. This shows a reduced electrical sheet resistance and linear current-voltage (I-V) response, when compared with the uncoated substrates. The interconnected SWCNTs improve the signal-to-noise ratio in large scale sensing of gas molecules with enhanced detection limit. The nanoporous silica-mounted SWCNT is utilized to electrochemically sense the gases ammonia (NH_3) and nitrogen dioxide (NO_2) at room

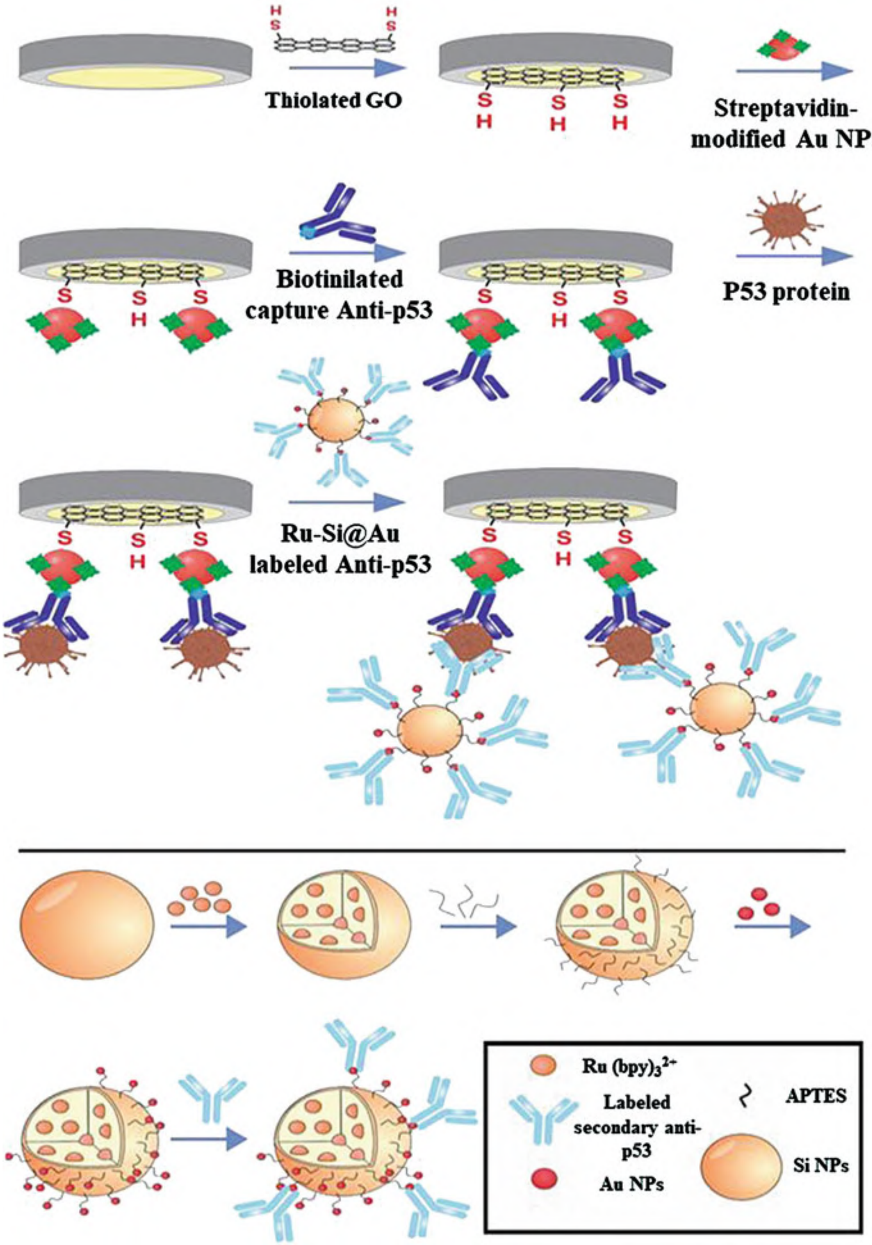
Thiolated GO
Streptavidin-modified Au NPs
Biotinilated capture Anti-p53
P53 protein
Ru-Si@Au labeled Anti-p53
Ru (bpy)$_3^{2+}$
Labeled secondary anti-p53
Au NPs
APTES
Si NPs

Fig. 27.2 Illustration of the preparation of the p53 immuno-electrochemical sensor using Ru-functionalized nanoporous silica@Au nanocomposite. (Taken from Afsharan et al. (2016))

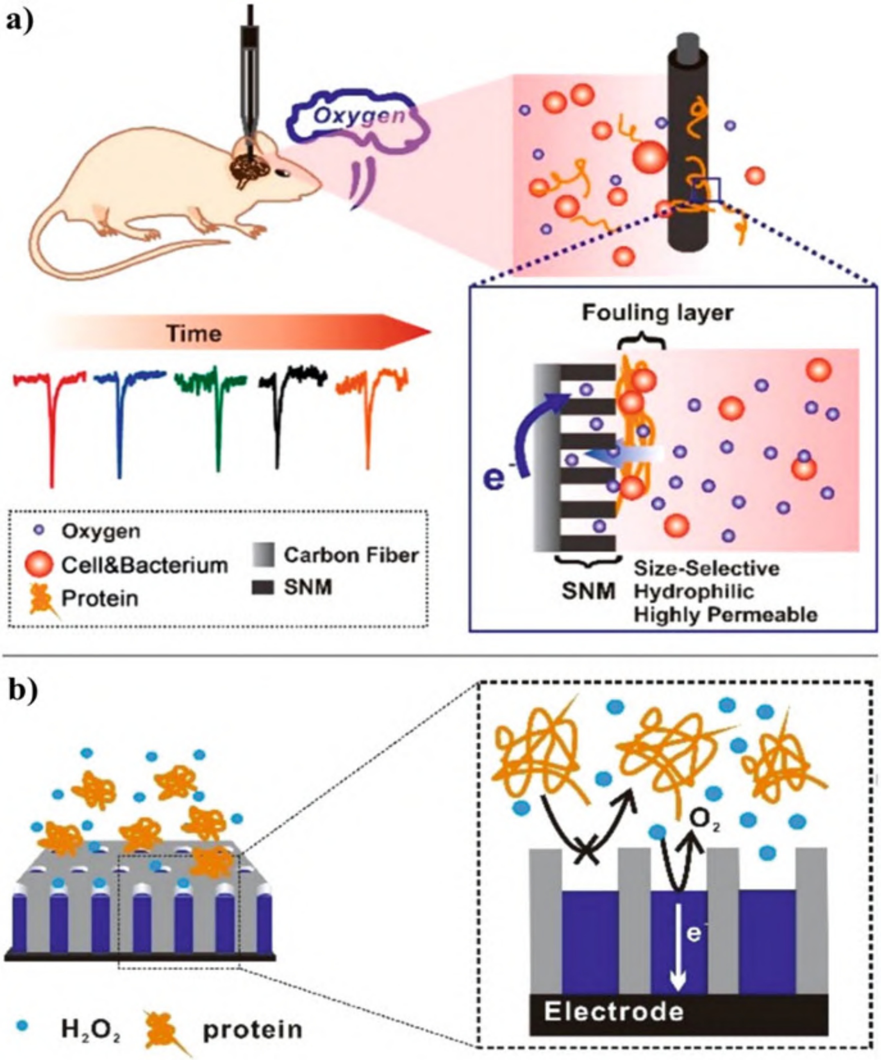
a)
Oxygen
Time
Fouling layer
e-
Oxygen
Cell&Bacterium
Protein
Carbon Fiber
SNM
SNM
Size-Selective
Hydrophilic
Highly Permeable
b)
O_2
e-
Electrode
H_2O_2
protein

Fig. 27.3 (**a**) Continuous O_2 monitoring on living rat brain using nanoporous silica/CFME and (**b**) Detection of H_2O_2 using Pt@nanoporoous silica membrane electrode. (Taken from Zhou et al. (2019) and Li et al. (2020))

temperature. The nanoporous silica substrates offers great diffusion of gas molecules to the sensing electrode. The electrochemical resistance increased for NH_3, since the charge carrier density decreased by the NH_3 molecules (donating electron) and decreased for NO_2, since the charge carrier density increased by the NO_2 molecules (withdrawing electron). This results in great sensitivity and recovery of both the gas molecules (Han et al. 2012).

2.4 Electrochemical Sensing of Chemical Species

The electrochemical sensing is an effective way to determine the organic chemicals. Organic chemicals are often considered to be reactive, hazardous, and can cause several health effects. Nanoporous silica is chemically stable with large sized pores, and is often utilized for sensing applications. Nanoporous silica altered by gold and magnetic microparticles encapsulating enzyme horseradish peroxide is used to sense hydroquinone (HQ) and hydrogen peroxide (H_2O_2). The direct electroreduction of hydroquinone into quinone is performed by the biocatalytic ability of the enzyme. This gives a linear current-voltage response with the limit of detection of 4×10^{-7} M. The response for the detection of hydrogen peroxide is similar to the hydroquinone with linear response and limit of detection, but for different concentration ranges (Elyacoubi et al. 2006).

One more research group also sense the hydrogen peroxide using electrochemical method. Nanoporous silica is etched as microspheres and prepared as electrode by above-mentioned protocol to sense the hydrogen peroxide. The micro-spherical structure enhances the electron transfer to sensitively detect the hydrogen peroxide. Hydrogen peroxide sensing is also achieved by nanoporous silica-based membranes. Nanoporous membrane are embedded with platinum nanostructure catalysts to form the working electrode. As shown in the Fig. 27.3b, the nanoporous silica membrane efficiently hinder the fouling molecules and protect the electrode from fouling and allowing only the interaction of H_2O_2. The fabricated Pt@nanoporous silica membrane/ITO electrode is used in *in vitro* electrochemical detection of hydrogen peroxide from the commercial detergent and *in vivo* electrochemical detection in rat brain for up to 1.5 h.

2.5 Electrochemical Sensing of Insecticide, Radiative, Explosive, and Stimulant Drug

The organic chemicals can be used in constructive manner as well as destructive manner. Many organic chemicals used as pesticides/insecticidescauses soil and water pollutions. The chemicals with radiative nature and exploding nature is used as destructive manner in wars and so on. Also, few of them used as stimulant drugs spoils the life of several youngsters. This creates the urge and necessity to sense the dangerous chemical as shown in Fig. 27.4. Naturally derived nanoporous silica from the diatom (*Phaeodactylum tricornutum*) is hybridized with zirconium dioxide (ZrO_2) to the electrochemical sensing of the insecticide, methyl parathion. The electrode is performed at linear concentration range with low limit of detection, 54.3 pM of methyl parathion. Also, the nanoporous silica/ZrO_2 is very selective toward methyl parathion among all the other highly concentrated interferents (Gannavarapu et al. 2019). Uranium ions are radiative contaminants, which are very unique risk in the contaminated water at very tiny levels. Nanoporous silica modified with acetamide phosphonic acid–coated carbon paste electrode is used to sense the tiny level of uranium ions with ppb (parts per billion) level of limit of detection. The uranium ion forms complex with the ligand in the electrochemical

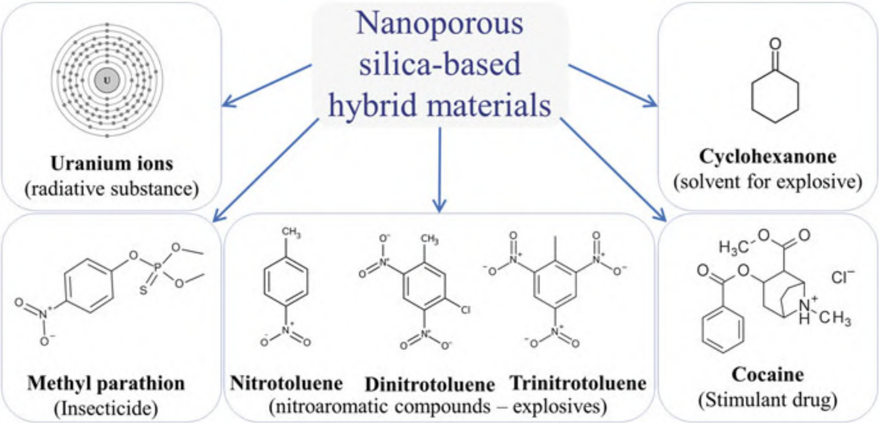
Nanoporous silica-based hybrid materials
Uranium ions
(radiative substance)
Cyclohexanone
(solvent for explosive)
Methyl parathion
(Insecticide)
Nitrotoluene
Dinitrotoluene
Trinitrotoluene
(nitroaromatic compounds – explosives)
Cocaine
(Stimulant drug)

Fig. 27.4 Illustration of the radiative substance, insecticide, nitroaromatic compounds, explosives, and stimulant drug molecules electrochemically sensed by nanoporous silica-based hybrid materials

aqueous solution. This might concentrate the acetamide phosphonic acid ligand from further complex formation. The nanoporous silica prevents this from the concentration of the complex on the electrode surface (Lin et al. 2004).

The nitroaromatic compounds like nitrotoluene, dinitrotoluene, and trinitrotoluene are explosives, which needs to be handled/stored cautiously. Nanoporous silica-based membrane with the electroluminescence label of tris(2,2′-bipyridyl)ruthenium (II)(Ru(bpy)$_3^{2+}$) is used for the effective sensing of nitroaromatic compounds. This electrochemiluminescence response is connected with a smartphone for the ease of detection. Due to the high specific surface area, the nanoporous silica-based membrane electrode is stable with electrochemiluminescence response (Li et al. 2019). Few volatile organic chemicals are not explosives, but can used to turn on the explosives. Cyclohexane is a solvent used to recrystallizes the RDX (1,3,5-trinitro-1,3,5-triazinane) and HMX (1,3,5,7-tetrazocane). The sub-ppm (parts per million) range of cyclohexanone vapor with detection limit of approximately 150 ppb can be sensed using the nanoporous silica-dye microspheres modified electrodes (Li 2018). Further, nanoporous silica membrane is altered with the corresponding aptamer (AGACAAGGAAAATCCTTCAATGAAGTGGGTCG) for the electrochemical sensing of the stimulant drug, cocaine (Abelow et al. 2011).

3 Biosensing and Imaging Applications

3.1 Drug Delivery

The requirement of nanoporous materials arise once a particular target needs the drug when it is necessary. Nanoporous silica with higher surface area, magnetic and luminescent properties make them as prominent material in drug adsorption loading and delivery. Magnetically active nanoporous materials are strongly preferred to ease this targeted localized drug delivery, since they can be simply accessible by using an external magnetic field. For this purpose, the drug carrier material should have enough pore size, good dispersity, biocompatibility, and luminescent to track the particles during transportation. Core-shell type magnetic nanoparticles covered by nanoporous silica can match the requirement of a drug carrier (Janßen et al. 2018). Furthermore, the drug carrier must adsorb the drug molecules and store them efficiently (Liu et al. 2012).

Nanoporous silica is coated on an *in vivo* implant (Bioverit®II prosthetic device) to successfully deliver the ciprofloxacin (antibiotic drug) to the middle ear of the rabbits against the *Pseudomonas aeruginosa* bacterial infections after surgery. The study group rabbits show almost no infection by the bacteria compared with the control group (Lensing et al. 2013). Naturally existing materials also exhibits porous structures, especially, diatoms possess nanoporous silica shells and frustules with inner and outer pore availability. This eases the efficient load and release of the drug molecules. As well as, they are biocompatible to use as drug carriers (Gnanamoorthy et al. 2014). The hydrophilic streptomycin drug loading and in-vitro oral releasing in a diatomic (*Coscinodiscus concinnus*) nanoporous silica is shown in the Fig. 27.5. The drug molecule adsorption into nanopores of the diatomic silica is confirmed by the contraction of pore size after loading and *vice versa*. The nanoporous diatomic silica shows 33.33 ± 2% of drug loading capacity with two-phase release. First phase of drug release occurs in 6 h, which is due to the slack adsorption on the surface. The second phase is occurring as sustainable drug release up to 7 days.

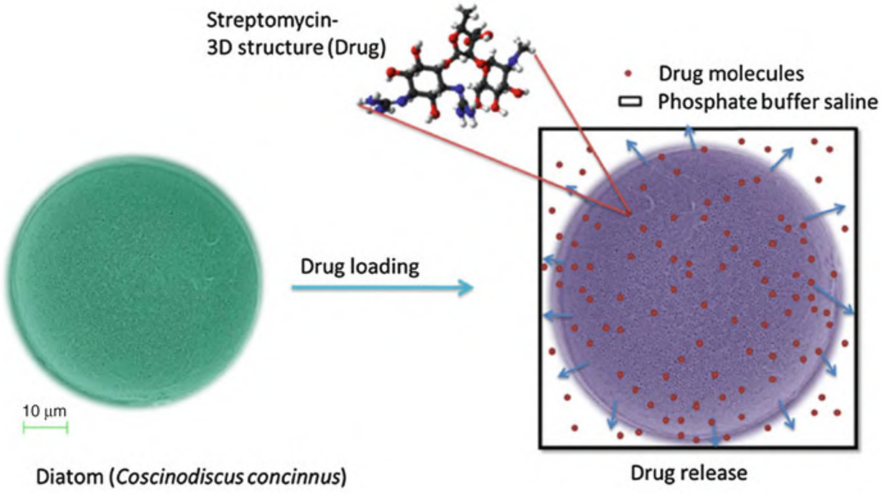

Fig. 27.5 Illustration of streptomycin drug loaded diatomic nanoporous silica during drug release. (Taken from Gnanamoorthy et al. (2014))

3.2 Biomolecules Immobilization/Encapsulation

The nanoporous silica-related materials are always attractive toward the adsorption/encapsulation/immobilization of ions/molecules for various applications, including wastewater treatment, separation, storage, molecular recognition, drug delivery, and sensing. Besides, ionic liquids are immobilized into the nanoporous silica, since the electrochemical devices (for example, fuel cells, batteries, and capacitors) needs electrolytes as well as high surfaced porous electrodes. Nanoporous silica membranes are used to immobilize the ionic liquid (1-hexyl-3-methyl-imidazolium hexafluorophosphate) with enhancement in diffusion co-efficient. This is achieved by the interaction between the ionic liquid and the silanol groups present on surface of the pores. This interaction is clearly seen in the Fig. 27.6a as dark ellipse (Iacob et al. 2010). Likewise, 3-ethynyl-1-methylimidazole ionic liquid is immobilized into the clickable nanoporous silica. This is used to remove H-acid from the wastewater in environmental-related applications (Khaniani et al. 2012).

The nanoporous materials are offering great surface area, stability, reusability, flexibility, and biocompatibility. Especially, in the form of fibers, they offer enhanced enzymatic activity. Nanoporous silica fibers utilized to immobilize the enzymes, namely, horseradish peroxidase, m-AChE, mutant (*Drosophila melanogaster* modified acetylcholinesterase enzyme), and acid phosphatase (ACP) for biosensor and biocatalytic applications (Wei et al. 2001; Sotiropoulou et al. 2005; Patel et al. 2006). Inulinase, a hydrolase enzyme, is immobilized into nanoporous silica modified with octadecyl. This immobilization exhibits 7.89- and 3.73-fold increase in half-life

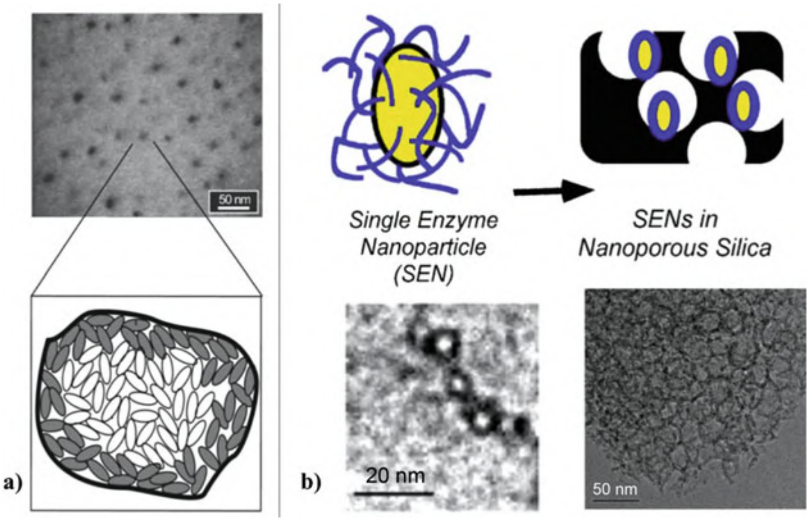

Fig. 27.6 Illustration of (**a**) single nanopore immobilized with ionic liquid elaborated from the Scanning Electron Microscopy (SEM) analysis and (**b**) single enzyme nanoparticle (SEN) immobilized into nanoporous silica. (Taken from Iacob et al. (2010) and Kim et al. (2006))

period of the enzyme. During hydrolysis, the enzyme withstands up to 10 cycles with retained activity (Karimi et al. 2016).

A single enzyme nanoparticle (SEN), α-chymotrypsin is encapsulated inside the positively surface charged silanized nanoporous silica, as shown in the Fig. 27.6b. The SEN interacts with the surface silanol group of the nanoporous silica via covalent bonding, which provides stability to the SENs (Kim et al. 2006). Nanoporous silica is functionalized with alkyl groups to immobilize the enzyme, urease. The immobilization results in storage efficiency and stability (especially, 65-fold greater half-life and 7–13.5-fold activation) (Nabati et al. 2011). Similarly, the silane-functionalized nanoporous silica is also used to immobilize the polysialic acid (polysaccharide, PolySia) (Williams et al. 2015). To developing the bioreactors along with biosensors, the enzymes tyrosine phenol-lyase and tryptophan indole-lyase are immobilized into the nanoporous silica (wet gel). This offers slowly attained steady state and enhanced inhibitors dissociation constant values (Pioselli 2004).

3.3 Biosensing Through Various Methods

Biosensors are the cost-efficient, fast, and simple technique to analyze the biological analytes (Chandra and Roy 2020). The nanoporous silica is used in sensing biomolecules with various methods, other than electrochemical sensing. The nanoporous silica is modified with fluorescein dye and histamine blue to selectively sense the histamine molecule using Fluorescence Resonance Energy Transfer (FRET). As shown in the Fig. 27.7a, the nanoporous silica is acting as solid-state support for the dopants, and the fluorescein dye is indicating the interaction of the histamine molecule with a FRET-ON response (Chaicham et al. 2018). Nanoporous silica film is functionalized with streptavidin and antibody for chemiluminescence immunoassay device to sense carbohydrate antigen 125 (CA 125 protein). The immunosensing device using nanoporous silica, shown in Fig. 27.7b, offers stability, reproducibility, and broad dynamic range with minimal incubation time (Yang et al. 2008). As already discussed, nanoporous silica substrate embedded with antibody of Cy3-troponin and Cy5-protein to sense the troponin I is clearly shown in the Fig. 27.7.c. The nanoporous silica film offers a low limit of detection, 10^{-5} ng mL^{-1} with high reliability (Nampi et al. 2013).

Nanoporous silica is embedded with trypsin (enzyme molecule, proteases) for the rapid label-free optical detection of proteolytic activity. The nanoporous silica offers a greater sensitivity on the interaction of biomacromolecules (Shtenberg et al. 2018). Allantoinase is embedded with nanoporous silica to sense the allantoin (metabolic intermediate) by fluorescence method. The nanoporous silica slightly influence the structure and catalytic activity of the embedded allantoinase. Due to the negligible influence, the device is greatly retaining the activity after several re-uses for quite a lot of months (Marchetti et al. 2020). Other than FRET and fluorescence method, Surface-Enhance Raman Spectroscopy (SERS) is also utilized to sense the biomolecules with nanoporous silica-based methods. Nanoporous silica is imprinted

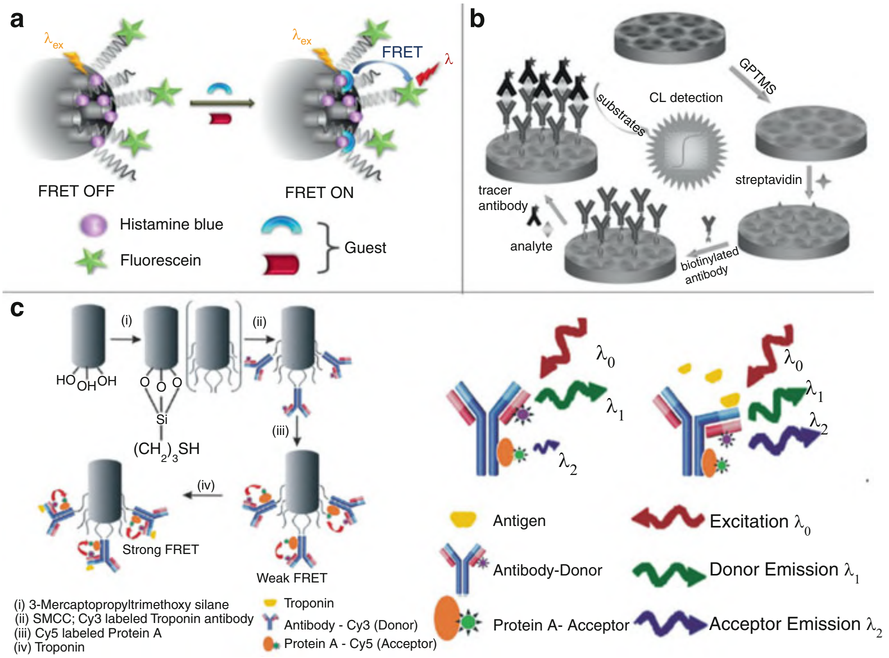
a
λex
λex
FRET
λ
FRET OFF
FRET ON
Histamine blue
Fluorescein
Guest
b
GPTMS
substrates
CL detection
tracer antibody
streptavidin
analyte
biotinylated antibody
c
(i)
(ii)
HO OH OH
O O O
Si
(CH2)3SH
(iii)
(iv)
Strong FRET
Weak FRET
(i) 3-Mercaptopropyltrimethoxy silane
(ii) SMCC; Cy3 labeled Troponin antibody
(iii) Cy5 labeled Protein A
(iv) Troponin
Troponin
Antibody - Cy3 (Donor)
Protein A - Cy5 (Acceptor)
λ0
λ1
λ2
λ0
λ1
λ2
Antigen
Antibody-Donor
Protein A- Acceptor
Excitation λ0
Donor Emission λ1
Acceptor Emission λ2

Fig. 27.7 Illustration of (**a**) Histamine sensing in FRET mechanism using modified nanoporous silica, (**b**) one-step chemiluminescence immunoassay of sensing CA 125, and (**c**) antibody-antigen interaction of Troponin I in FRET phenomenon using nanoporous silica substrate. (Taken from Chaicham et al. (2018), Yang et al. (2008)), and Nampi et al. (2013))

with methacrylate polymer to sense the cholesterol-derived steroid hormone, β-Estradiol in milk. The enhanced surface area of the nanoporous silica is offering a great support for the imprinted polymer to provide active signal augment substrate for SERS sensor. The resultant SERS sensor shows great stability and reusability with a detection limit of 0.073 ng mL^{-1} (Mugo and Lu 2022).

3.4 Bioimaging Applications

Bioimaging using a highly stable material is crucial in detecting the cancer cells (Chandra et al. 2013). The cancer cells are widely imaged using mesoporous silica-based nanoparticles (Rosenholm et al. 2009; Mehravi et al. 2013; Fazaeli et al. 2016). The nanoporous silica featured with large pore and surface area can adsorb and hold enough small to large molecules. Additionally, the non-toxicity, stability biocompatibility, and dispersity enable them to be utilized in many areas including biological and therapeutical applications. Nanoporous silica is doped with Eu^{3+} and folate N-hydroxysuccinimidyl ester (cancer targeting ligand). The N-hydroxysuccinimidyl ester interacts with the cancer cells of HeLa and NIH3T3

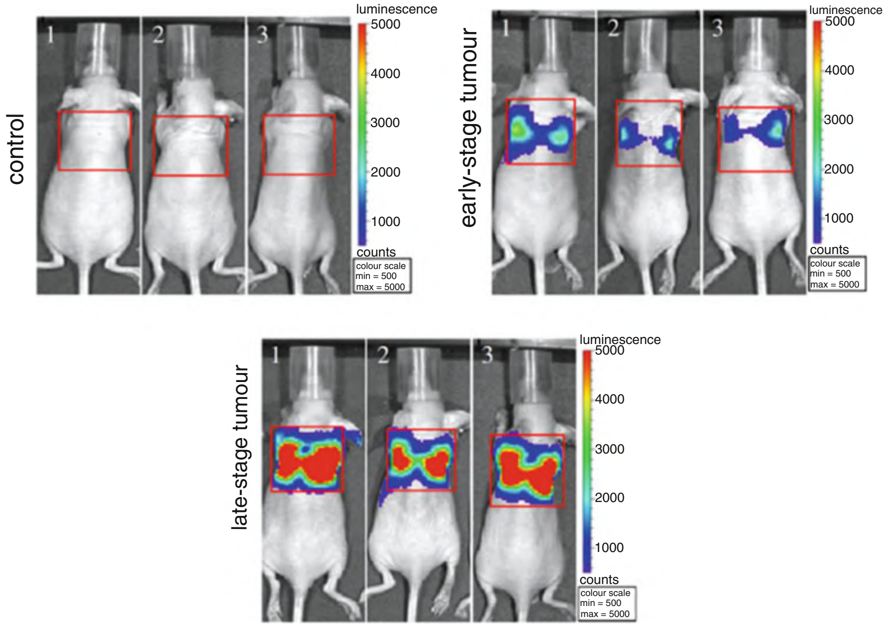
control
1
2
3
luminescence
5000
4000
3000
2000
1000
counts
colour scale
min = 500
max = 5000
early-stage tumour
1
2
3
luminescence
5000
4000
3000
2000
1000
counts
colour scale
min = 500
max = 5000
late-stage tumour
1
2
3
luminescence
5000
4000
3000
2000
1000
counts
colour scale
min = 500
max = 5000

Fig. 27.8 Bioimaging of nude mice lungs with tumour growth of luciferase gene engineered MDA-MB-231 human breast cancer cells. (Taken from Fan et al. (2016))

fibroblasts, the luminescence of Eu^{3+} ions indicating the position of the cells (Tagaya et al. 2013, 2014).

The nanoporous silica is modified with APS (3-aminopropyltriethoxysilane)/ DTPA (diethylenetriamine pentaacetic acid) with Eu^{3+}, Tb^{3+}, and Gd^{3+} separately. This nanoporous silica complex material is used as probe for MRI-optical bioimaging toward mouse macrophage cell line (RAW 264.7). The nanoporous silica is used as carrier to hold the lanthanide ions, which withstands the photobleaching with sharp emission spectrum (Pinho et al. 2012). The highly periodic and homogeneous pore size distribution of nanoporous silica coated chip is utilized to isolate the proteins and peptides of nude mice lungs with tumor growth of luciferase gene engineered MDA-MB-231 human breast cancer cells. The blue to red colored fluorescence response, shown in the Fig. 27.8, implies the growth of the cancer cells. This bioimaging helps in determining the various stages of the growth of breast cancer cells for the targeted and personalized drug supply (Fan et al. 2012).

4 Conclusion and Outlook

Nanoporous silica are the best materials as film or membrane to embed other functional group species, backbone, or substrate to hold chemical/biological species, and matrix to various dopant molecules. The biocompatibility and chemical inertness are playing a crucial role in biological applications. The homogeneous pore size and the vertically aligned distribution is adsorbing the enzymes and drugs kind of biomolecules to encapsulating/immobilizing them into the pores. The surface functional groups of the nanoporous silica-based material are protecting the immobilized molecules from leaching out. This turns the electrode of the biosensor into durable and stable one for a long time. By functionalizing the nanoporous silica with magnetic nanoparticles, the immobilized drug molecules can be delivered at the required area.

Additionally, the optical property of the nanoporous silica is a boon to use them in bioimaging applications. They can be modified with fluorescent materials for the bioimaging, especially for the imaging of the growth of cancer cells. The ordered pore arrangement of the nanoporous silica is easing the diffusivity of ions and charges for the electrochemical sensing of the metal/heavy metal ions (including, Cd^{2+}, Pb^{2+}, Cu^{2+}, Ni^{2+}, Ag^{+}, Hg^{2+}, Fe^{3+}, Cr^{3+}, Ce^{3+}), biomolecules (including, C-reactive protein, myeloperoxidase, glucose, p53 protein, protein-specific antigen), gas molecules (including, hydrogen, oxygen, ammonia, nitrogen dioxide), chemical species (including, hydroquinone, hydrogen peroxide), insecticide (including, methyl parathion), radiative (including, uranium), explosive (including, nitroaromatic compounds, explosive simulant solvents), and simulant drug (including, cocaine) molecules. Besides electrochemical sensing, other efficient methods like FRET, SERS, fluorescence, etc. are utilized to sense biomolecules.

The electrochemical sensing using nanoporous silica-based materials opens up the long-term and simultaneous chemical/biomolecule sensing, health, and environmental monitoring. The efficiency of the nanoporous silica can bring-down the size of the electrode with upholding the sensing capacity. The biocompatibility and non-toxic behavior of the nanoporous silica materials enable them in *in vivo* drug delivery and bioimaging in real-time samples. These real-time biological applications can changeover the medical field with a revolution. On the other hand, nanoporous silica coated templates are used as nano-synthetic reactor to grow CNTs and various nanoparticles. The well-ordered and homogenously sized pore structures can act as better templates for the controlled growth of the nanoparticles in various structures and manners.

References

Abelow AE, White RJ, Plaxco KW, Zharov I (2011) Nanoporous silica colloidal films with molecular transport gated by aptamers responsive to small molecules. Collect Czechoslov Chem Commun 76:683–694

Abolhasani J, Behbahani M (2015) Application of 1-(2-pyridylazo)-2-naphthol-modified nanoporous silica as a technique in simultaneous trace monitoring and removal of toxic heavy metals in food and water samples. Environ Monit Assess 187:4176

Afsharan H, Navaeipour F, Khalilzadeh B, Tajalli H, Mollabashi M, Ahar MJ, Rashidi MR (2016) Highly sensitive electrochemiluminescence detection of p53 protein using functionalized Ru-silica nanoporous@gold nanocomposite. Biosens Bioelectron 80:146–153

Badiei A, Razavi BV, Goldooz H, Mohammadi Ziarani G, Faridbod F, Ganjali MR (2018) A novel fluorescent chemosensor assembled with 2,6-bis(2-benzimidazolyl)pyridine-functionalized nanoporous silica-type SBA-15 for recognition of Hg^{2+} ion in aqueous media. Int J Environ Res 12:109–115

Beydaghi H, Javanbakht M, Salar Amoli H, Badiei A, Khaniani Y, Ganjali MR, Norouzi P, Abdouss M (2011) Synthesis and characterization of new proton conducting hybrid membranes for PEM fuel cells based on poly(vinyl alcohol) and nanoporous silica containing phenyl sulfonic acid. Int J Hydrog Energy 36:13310–13316

Blinka E, Loeffler K, Hu Y, Gopal A, Hoshino K, Lin K, Liu X, Ferrari M, Zhang JXJ (2010) Enhanced microcontact printing of proteins on nanoporous silica surface. Nanotechnology 21:415302

Bollmann L, Urade VN, Hillhouse HW (2007) Controlling interfacial curvature in nanoporous silica films formed by evaporation-induced self-assembly from nonionic surfactants. I. Evolution of nanoscale structures in coating solutions. Langmuir 23:4257–4267

Canning J, Moura L, Lindoy L, Cook K, Crossley MJ, Luo Y, Peng GD, Glavind L, Huyang G, Naqshbandi M, Kristensen M, Martelli C, Town G (2014) Fabricating nanoporous silica structure on D-fibres through room temperature self-assembly. Materials 7:2356–2369

Chaicham A, Kongwutthivech J, Tuntulani T, Tomapatanaget B (2018) Couple of Histamine blue fluorescence chemosensor and surface charge selector of FC-modified silica nanoporous for highly specific histamine detection via FRET-process. Sensors Actuators B Chem 258:621–627

Chandra P, Roy S (2020) Diagnostic strategies for COVID-19 and other coronaviruses, medical virology: from pathogenesis to disease control. https://doi.org/10.1007/978-981-15-6006-4_1

Chandra P, Suman P, Mukherjee M, Kumar P (2013) HER2 protein biomarker based sensor systems for breast cancer diagnosis. J Mol Biomark Diagn 05:1000e119

Chen Y, Li X, Zhou H, Hong X, Geng Y (2016) Refractive index detection range adjustable liquid-core fiber optic sensor based on surface plasmon resonance and a nano-porous silica coating. J Phys D Appl Phys 49:355102

Dhara K, Mahapatra DR (2020) Review on electrochemical sensing strategies for C-reactive protein and cardiac troponin I detection. Microchem J 156:104857

Di Paolo M, Roberti MJ, Bordoni AV, Aramendía PF, Wolosiuk A, Bossi ML (2019) Nanoporous silica nanoparticles functionalized with a fluorescent turn-on spirorhodamineamide as pH indicators. Photochem Photobiol Sci 18:155–165

Doshi DA, Dattelbaum AM, Watkins EB, Brinker CJ, Swanson BI, Shreve AP, Parikh AN, Majewski J (2005) Neutron reflectivity study of lipid membranes assembled on ordered nanocomposite and nanoporous silica thin films. Langmuir 21:2865–2870

Elsherief MA, Morsi RE, Shabaan M, Salem H, Abdel Dayeem S, Elsabee MZ (2020) Tuning of nanoporous silica by electrospinning and sol-gel methods for efficient beryllium uptake. Separat Sci Technol (Philadelphia) 55:35–46

Elyacoubi A, Zayed SIM, Blankert B, Kauffmann JM (2006) Development of an amperometric enzymatic biosensor based on gold modified magnetic nanoporous microparticles. Electroanalysis 18:345–350

Fan J, Deng X, Gallagher JW, Huang H, Huang Y, Wen J, Ferrari M, Shen H, Hu Y (2012) Research article: monitoring the progression of metastatic breast cancer on nanoporous silica chips. Philos Trans R Soc A Math Phys Eng Sci 370:2433–2447

Fan BJ, Deng X, Gallagher JW, Huang H, Huang Y, Wen J, Ferrari M, Shen H, Hu Y (2016) Monitoring the progression of metastatic breast cancer on nanoporous silica chips. Phil Trans R Soc A 370:2433–2447

Fang Y, Cui B, Huang J, Wang L (2019) Ultrasensitive electrochemical sensor for simultaneous determination of cadmium and lead ions based on one-step co-electropolymerization strategy. Sensors Actuators B Chem 284:414–420

Fazaeli Y, Feizi S, Jalilian AR, Hejrani A (2016) Grafting of [64Cu]-TPPF20 porphyrin complex on functionalized nano-porous MCM-41 silica as a potential cancer imaging agent. Appl Radiat Isot 112:13–19

Frei H (2009) Polynuclear photocatalysts in nanoporous silica for artificial photosynthesis. Chimia 63:721–730

Gannavarapu KP, Ganesh V, Thakkar M, Mitra S, Dandamudi RB (2019) Nanostructured diatom-ZrO_2 composite as a selective and highly sensitive enzyme free electrochemical sensor for detection of methyl parathion. Sensors Actuators B Chem 288:611–617

Gnanamoorthy P, Anandhan S, Prabu VA (2014) Natural nanoporous silica frustules from marine diatom as a biocarrier for drug delivery. J Porous Mater 21:789–796

Gupta A, Pandey SS, Nayak M, Maity A, Majumder SB, Bhattacharya S (2014) Hydrogen sensing based on nanoporous silica-embedded ultra dense ZnO nanobundles. RSC Adv 4:7476–7482

Han ZJ, Mehdipour H, Li X, Shen J, Randeniya L, Yang HY, Ostrikov K (Ken) (2012) SWCNT networks on nanoporous silica catalyst support: morphological and connectivity control for nanoelectronic, gas-sensing, and biosensing devices. ACS Nano 6:5809–5819

Hayashi K, Fujimaki Y, Mishiba K, Watanabe H, Imai H (2021) Emergence of practical fluorescence in a confined space of nanoporous silica: significantly enhanced quantum yields of a conjugated molecule. Chem Commun 57:13150–13153

Hong CQ, Han JC, Zhang XH, Du JC (2013) Novel nanoporous silica aerogel impregnated highly porous ceramics with low thermal conductivity and enhanced mechanical properties. Scr Mater 68:599–602

Horvath R, Pedersen HC, Skivesen N, Svanberg C, Larsen NB (2005) Fabrication of reverse symmetry polymer waveguide sensor chips on nanoporous substrates using dip-floating. J Micromech Microeng 15:1260–1264

Hui L, Yongquan H, Lili W, Yanming G, Kaichen H, Xi L, Kexin T, Xiufang L, Hailing Y (2020) Facile synthesis of nanoporous amorphous silica on silicon substrate. J Nanomater 2020:3514764

Iacob C, Sangoro JR, Papadopoulos P, Schubert T, Naumov S, Valiullin R, Kärger J, Kremer F (2010) Charge transport and diffusion of ionic liquids in nanoporous silica membranes. Phys Chem Chem Phys 12:13798–13803

Janßen HC, Warwas DP, Dahlhaus D, Meißner J, Taptimthong P, Kietzmann M, Behrens P, Reifenrath J, Angrisani N (2018) In vitro and in vivo accumulation of magnetic nanoporous silica nanoparticles on implant materials with different magnetic properties. J Nanobiotechnol 16:96

Javanbakht M, Ganjali MR, Norouzi P, Badiei A, Hasheminasab A, Abdouss M (2007a) Carbon paste electrode modified with functionalized nanoporous silica gel as a new sensor for determination of silver ion. Electroanalysis 19:1307–1314

Javanbakht M, Badiei A, Ganjali MR, Norouzi P, Hasheminasab A, Abdouss M (2007b) Use of organofunctionalized nanoporous silica gel to improve the lifetime of carbon paste electrode for determination of copper(II) ions. Anal Chim Acta 601:172–182

Javanbakht M, Khoshsafar H, Ganjali MR, Norouzi P, Badei A, Hasheminasab A (2008) Stripping voltammetry of cerium(III) with a chemically modified carbon paste electrode containing functionalized nanoporous silica gel. Electroanalysis 20:203–206

Javanbakht M, Divsar F, Badiei A, Fatollahi F, Khaniani Y, Ganjali MR, Norouzi P, Chaloosi M, Ziarani GM (2009a) Determination of picomolar silver concentrations by differential pulse anodic stripping voltammetry at a carbon paste electrode modified with phenylthiourea-functionalized high ordered nanoporous silica gel. Electrochim Acta 54:5381–5386

Javanbakht M, Divsar F, Badiei A, Ganjali MR, Norouzi P, Mohammadi Ziarani G, Chaloosi M, Jahangir AA (2009b) Potentiometric detection of mercury(II) ions using a carbon paste electrode modified with substituted thiourea-functionalized highly ordered nanoporous silica. Anal Sci 25:789–794

Javanbakht M, Khoshsafar H, Ganjali M, Badiei A, Norouzi P, Hasheminasab A (2009c) Determination of Nanomolar mercury(II) concentration by anodic-stripping voltammetry at a carbon paste electrode modified with functionalized nanoporous silica gel. Curr Anal Chem 5:35–41

Kanehata M, Ding B, Shiratori S (2007) Nanoporous ultra-high specific surface inorganic fibres. Nanotechnology 18

Karimi M, Habibi-Rezaei M, Rezaei K, Moosavi-Movahedi AA, Kokini J (2016) Immobilization of inulinase from *Aspergillus niger* on octadecyl substituted nanoporous silica: inulin hydrolysis in a continuous mode operation. Biocatal Agric Biotechnol 7:174–180

Kendall EL, Ngassam VN, Gilmore SF, Brinker CJ, Parikh AN (2013) Lithographically defined macroscale modulation of lateral fluidity and phase separation realized via patterned nanoporous silica-supported phospholipid bilayers. J Am Chem Soc 135:15718–15721

Khaniani Y, Badiei A, Ziarani GM (2012) Application of clickable nanoporous silica surface for immobilization of ionic liquids. J Mater Res 27:932–938

Khoo HT, Leow CH (2021) Advancements in the preparation and application of monolithic silica columns for efficient separation in liquid chromatography. Talanta 224:121777

Kim J, Jia H, Lee CW, Chung SW, Kwak JH, Shin Y, Dohnalkova A, Kim BG, Wang P, Grate JW (2006) Single enzyme nanoparticles in nanoporous silica: a hierarchical approach to enzyme stabilization and immobilization. Enzym Microb Technol 39:474–480

Kipnusu WK, Doñate-Buendía C, Fernández-Alonso M, Lancis J, Mínguez-Vega G (2020) Nonlinear optics to glucose sensing: multifunctional nitrogen and boron doped carbon dots with solid-state fluorescence in nanoporous silica films. Part Part Syst Charact 37:2000093

Kucheyev SO, Wang YM, Hamza AV, Worsley MA (2011) Light-ion-irradiation-induced thermal spikes in nanoporous silica. J Phys D Appl Phys 44:085406

Lee SH, Lee EA, Hwang HJ, Moon JW, Han IS, Woo SK (2006) Solvents effects on physicochemical properties of nano-porous silica aerogels prepared by ambient pressure drying method. Mater Sci Forum 510–511:910–913

Lensing R, Bleich A, Smoczek A, Glage S, Ehlert N, Luessenhop T, Behrens P, Müller PP, Kietzmann M, Stieve M (2013) Efficacy of nanoporous silica coatings on middle ear prostheses as a delivery system for antibiotics: an animal study in rabbits. Acta Biomater 9:4815–4825

Li Z (2018) Nanoporous silica-dye microspheres for enhanced colorimetric detection of cyclohexanone. Chemosensors 6:15–18

Li J, Fan N, Wang X, He Z (2017) Cellular level evaluation and lysozyme adsorption regulation of bimodal nanoporous silica. Mater Sci Eng C 76:509–517

Li S, Zhang D, Liu J, Cheng C, Zhu L, Li C, Lu Y, Low SS, Su B, Liu Q (2019) Electrochemiluminescence on smartphone with silica nanopores membrane modified electrodes for nitroaromatic explosives detection. Biosens Bioelectron 129:284–291

Li X, Zhou L, Ding J, Sun L, Su B (2020) Platinized silica nanoporous membrane electrodes for low-fouling hydrogen peroxide detection. ElectroChemChem 7:2081–2086

Lin Y, Yantasee W, Fryxell GE, Conner MM (2004) Electrochemical sensors based on functionalized nanoporous silica for environmental monitoring. Nanosens Mater Dev 5593: 554–560

Lin KC, Kunduru V, Bothara M, Rege K, Prasad S, Ramakrishna BL (2010) Biogenic nanoporous silica-based sensor for enhanced electrochemical detection of cardiovascular biomarkers proteins. Biosens Bioelectron 25:2336–2342

Liu J, Wang B, Budi Hartono S, Liu T, Kantharidis P, Middelberg APJ, Lu GQM, He L, Qiao SZ (2012) Magnetic silica spheres with large nanopores for nucleic acid adsorption and cellular uptake. Biomaterials 33:970–978

Liu J, Cheng H, He D, He X, Wang K, Liu Q, Zhao S, Yang X (2017) Label-free homogeneous electrochemical sensing platform for protein kinase assay based on carboxypeptidase Y-assisted peptide cleavage and vertically ordered mesoporous silica films. Anal Chem 89:9062–9068

Mahato K, Kumar S, Srivastava A, Maurya PK, Singh R, Chandra P (2018) Electrochemical immunosensors: fundamentals and applications in clinical diagnostics. Elsevier Inc

Marchetti M, Ronda L, Percudani R, Bettati S (2020) Immobilization of allantoinase for the development of an optical biosensor of oxidative stress states. Sensors (Switzerland) 20:196

Mehravi B, Ahmadi M, Amanlou M, Mostaar A, Ardestani MS, Ghalandarlaki N (2013) Conjugation of glucosamine with $Gd3+-$based nanoporous silica using a heterobifunctional ANB-NOS crosslinker for imaging of cancer cells. Int J Nanomedicine 8:3383–3394

Mohammadi Ziarani G, Badiei A, Haddadpour M (2011) Application of sulfonic acid functionalized nanoporous silica (SBA-Pr-SO_3H) for one-pot synthesis of quinoxaline derivatives. Int J Chem 3:87–94

Mugo SM, Lu W (2022) Determination of β-Estradiol by Surface-Enhance Raman Spectroscopy (SERS) using a surface imprinted methacrylate polymer on nanoporous biogenic silica. Anal Lett 55:378–387

Nabati F, Habibi-Rezaei M, Amanlou M, Moosavi-Movahedi AA (2011) Dioxane enhanced immobilization of urease on alkyl modified nano-porous silica using reversible denaturation approach. J Mol Catal B Enzym 70:17–22

Nampi PP, Kartha CC, Jose G, Anil AK, Anilkumar T, Varma H (2013) Sol-gel nanoporous silica as substrate for immobilization of conjugated biomolecules for application as fluorescence resonance energy transfer (FRET) based biosensor. Sensors Actuators B Chem 185:252–257

Patel AC, Li S, Yuan JM, Wei Y (2006) In situ encapsulation of horseradish peroxidase in electrospun porous silica fibers for potential biosensor applications. Nano Lett 6:1042–1046

Pinho SLC, Faneca H, Geraldes CFGC, Delville MH, Carlos LD, Rocha J (2012) Lanthanide-DTPA grafted silica nanoparticles as bimodal-imaging contrast agents. Biomaterials 33: 925–935

Pioselli B (2004) Tyrosine phenol-lyase and tryptophan indole-lyase encapsulated in wet nanoporous silica gels: selective stabilization of tertiary conformations. Protein Sci 13:913–924

Rechotnek F, Follmann HDM, Silva R (2021) Mesoporous silica decorated with L-cysteine as active hybrid materials for electrochemical sensing of heavy metals. J Environ Chem Eng 9:106492

Rosenholm JM, Meinander A, Peuhu E, Niemi R, Eriksson JE, Sahlgren C, Lindén M (2009) Targeting of porous hybrid silica nanoparticles to cancer cells. ACS Nano 3:197–206

Shanbhag MM, Ilager D, Mahapatra S, Shetti NP, Chandra P (2021) Amberlite XAD-4 based electrochemical sensor for diclofenac detection in urine and commercial tablets. Mater Chem Phys 273:125044

Shtenberg G, Massad-Ivanir N, Khabibullin A, Zharov I, Segal E (2018) Label-free optical monitoring of proteolytic reaction products using nanoporous silica colloidal assembly. Sensors Actuators B Chem 262:796–800

Silakhori F, Badiei A, Ziarani GM (2020) Naphthoquinone-functionalized nanoporous silica: synthesis, characterization and application for fluorescent sensing of dicromate. J Anal Chem 75:1278–1284

Sotiropoulou S, Vamvakaki V, Chaniotakis NA (2005) Stabilization of enzymes in nanoporous materials for biosensor applications. Biosens Bioelectron 20:1674–1679

Sun J, Jakobsson E, Wang Y, Brinker CJ (2015) Nanoporous silica-based protocells at multiple scales for designs of life and nanomedicine. Life 5:214–229

Tagaya M, Ikoma T, Yoshioka T, Motozuka S, Xu Z, Minami F, Tanaka J (2011) Synthesis and luminescence properties of Eu(III)-doped nanoporous silica spheres. J Colloid Interface Sci 363: 456–464

Tagaya M, Hanagata N, Ikoma T, Kobayashi T, Shiba K, Yoshioka T, Tnaka J (2013) Cytotoxicity and cancer detection ability of the luminescent nanoporous silica spheres immobilized with folic acid derivative. Key Eng Mater 529–530:630–635

Tagaya M, Ikoma T, Xu Z, Tanaka J (2014) Synthesis of luminescent nanoporous silica spheres functionalized with folic acid for targeting to cancer cells. Inorg Chem 53:6817–6827

Vattipalli K, Lin KC, Ramakrishna BL, Prasad S (2011) Enhanced electrochemical detection of cardiovascular biomarker proteins using biogenic nanoporous silica diatoms. Proc IEEE Conf Nanotechnol:237–240

Wang Y, Angelatos AS, Dunstan DE, Caruso F (2007) Infiltration of macromolecules into nanoporous silica particles. Macromolecules 40:7594–7600

Wei TC, Hillhouse HW (2007) Mass transport and electrode accessibility through periodic self-assembled nanoporous silica thin films. Langmuir 23:5689–5699

Wei Y, Xu J, Feng Q, Lin M, Dong H, Zhang WJ, Wang C (2001) A novel method for enzyme immobilization: direct encapsulation of acid phosphatase in nanoporous silica host materials. J Nanosci Nanotechnol 1:83–93

Williams S, Neumann A, Bremer I, Su Y, Dräger G, Kasper C, Behrens P (2015) Nanoporous silica nanoparticles as biomaterials: evaluation of different strategies for the functionalization with polysialic acid by step-by-step cytocompatibility testing. J Mater Sci Mater Med 26:125

Yadavi M, Badiei A, Ziarani GM (2013) A novel Fe^{3+} ions chemosensor by covalent coupling fluorene onto the mono, di- and tri-ammonium functionalized nanoporous silica type SBA-15. Appl Surf Sci 279:121–128

Yang F, Tang J (2019) Catalytic upgrading of renewable levulinic acid to levulinate esters using perchloric acid decorated nanoporous silica gels. ChemistrySelect 4:1403–1409

Yang Z, Xie Z, Liu H, Yan F, Ju H (2008) Streptavidin-functionalized three-dimensional ordered nanoporous silica film for highly efficient chemiluminescent immunosensing. Adv Funct Mater 18:3991–3998

Yoneda S, Ito F, Yamanaka S, Usami H (2016) Optical properties of nanoporous silica frustules of a diatom determined using a 10 μm microfiber probe. Jpn J Appl Phys 55:072001

Yu D, Renedo OD, Blankert B, Sima V, Sandulescu R, Arcos J, Kauffmann JM (2006) A peroxidase-based biosensor supported by nanoporous magnetic silica microparticles for acetaminophen biotransformation and inhibition studies. Electroanalysis 18:1637–1642

Zhad HRLZ, Sadeghi O, Amini MM, Tavassoli N, Banitaba MH, Davarani SSH (2011) Extraction of ultra trace amounts of palladium on 9-acridinylamine functionalized SBA-15 and MCM-41 nanoporous silica sorbents. Sep Sci Technol 46:648–655

Zhang XF, Clime L, Ly HQ, Trudeau M, Veres T (2010) Multifunctional Fe3O4-Au/porous silica@fluorescein core/shell nanoparticles with enhanced fluorescence quantum yield. J Phys Chem C 114:18313–18317

Zhang T, Chai Y, Yuan R, Guo J (2012a) Potentiometric detection of silver (I) ion based on carbon paste electrode modified with diazo-thiophenol-functionalized nanoporous silica gel. Mater Sci Eng C 32:1179–1183

Zhang M, Ge S, Li W, Yan M, Song X, Yu J, Xu W, Huang J (2012b) Ultrasensitive electrochemiluminescence immunoassay for tumor marker detection using functionalized Ru-silica@nanoporous gold composite as labels. Analyst 137:680–685

Zhou W, Chai Y, Yuan R, Guo J, Wu X (2009) Organically nanoporous silica gel based on carbon paste electrode for potentiometric detection of trace Cr(III). Anal Chim Acta 647:210–214

Zhuo L, Hou H, Wei H, Yao L, Sun L, Yu P, Su B, Mao L (2019) In vivo monitoring of oxygen in rat brain by carbon fiber microelectrode modified with antifouling nanoporous membrane. Anal Chem 91:3645–3651

Zhou P, Yao L, Chen K, Su B (2020) Silica nanochannel membranes for electrochemical analysis and molecular sieving: a comprehensive review. Crit Rev Anal Chem 50:424–444

The Affordable Nanomaterial Carbon Black as Nanomodifier for Smart (Bio)Sensors

28

Fabiana Arduini

Contents

1 Introduction 622
2 CB-Based Sensors 624
3 CB-Nanocomposite-Based Sensors 629
4 CB-Based Biosensors 630
5 CB-Nanocomposite-Based Biosensors 632
6 Conclusions 635
References 635

Abstract

The nanomaterials in the recent decades have provided a relevant footprint in the development of smart and sensitive electrochemical (bio)sensors. Since the discovery of carbon nanotubes in 1991, these have largely been used in electrochemical sensors for implementing their analytical features, namely sensitivity, robustness, and storage/working stability. Nowadays, graphene is the carbon-based nanomaterial largely used due to its outstanding features, including large surface area and charge carrier mobility. Among carbon-based nanomaterials, recently carbon black has been re-discovered for the development of electrochemical (bio)sensors, exploiting its outstanding electroanalytical features such as improved electron transfer and resistance to fouling. Furthermore, carbon black can be used as received by suppliers without any chemical and physical treatment. In addition, its cost-effectiveness (approx. 1 €/Kg) and the easiness of obtaining a stable dispersion are added values for the delivery of cheap and reproducible carbon black-based sensors. Herein, I will highlight the multifarious uses of carbon black in the development of smart and cost-effective

---

F. Arduini (✉)
Department of Chemical Science and Technologies, University of Rome “Tor Vergata”, Rome, Italy

SENSE4MED, Rome, Italy
e-mail: fabiana.arduini@uniroma2.it

© Springer Nature Singapore Pte Ltd. 2023

U. P. Azad, P. Chandra (eds.), *Handbook of Nanobioelectrochemistry*,
https://doi.org/10.1007/978-981-19-9437-1_28

electrochemical (bio)sensors by using carbon black alone or combined with other nanomaterials or biocomponents.

Keywords

Carbon-based nanomaterials · Paper-based (bio)sensors · Loading agent · Nanomodifiers

1 Introduction

Carbon black (CB) is a carbon-based nanomaterial constituted of colloidal spheres with a diameter of between 15 and 100 nm which form aggregates with dimensions lower than 1 μm. CB is characterized by the absence of long-range crystalline order, having only small homogeneous domains with some degree of short-range order. The main application of CB in the sensor field is found in the gas sensor sector (Alfè and Gargiulo 2020); indeed, searching in Google Scholar with the words "carbon black," "sensor," and "gas phase," around 21,900 documents were reported. The first application of CB as a nanomaterial for the sensing of analytes in a liquid phase was reported in 2007 by Hočevar and Ogorevc (2007). The authors used CB for the construction of carbon paste micro-electrodes with the aim to evaluate the electrochemical performance toward some analytes such as dopamine, ascorbic acid, Cd^{2+}, and Pb^{2+}. Subsequently, Ogorevc together with Svegl et al. (2008) used CB for its deposition on Indium tin oxide/glass for ascorbic acid, H_2O_2, and copper ions detection. Arduini et al. started to use CB as material for electrode fabrication in the same years with the first publication in 2010. We explored the use of CB in carbon-paste electrode fabrication, testing different analytes and observing a limited improvement in the case of ascorbic acid (Arduini et al. 2010a). In our previous work (Mita et al. 2007), we observed that the use of nanomaterials such as carbon nanotubes hinders the easy obtainment of a reproducible paste to be inserted in the electrode. Thus, we have hypothesized that the main issue in using CB is the high surface area, which is an obstacle in the fabrication of reliable CB-based carbon paste electrodes. With the aim of solving this issue, we have started to prepare a CB-based dispersion for the modification of screen-printed electrodes by drop-casting, observing an outstanding increase of sensitivity in the case of Nicotinamide adenine dinucleotide detection (Arduini et al. 2010b). In addition, we explored the possibility of using CB directly in the ink during the printing process. In this case, we have observed that the maximum amount to add to the ink is 10% wt% because a higher percentage allowed for a high viscosity, which negatively affected the deposition of the inks. By studying the electrochemical response of the CB-based screen-printed electrodes modified in the ink or by drop-casting, we observed that the high amount of CB onto the working electrode surface, observed by using scanning electron microscopy, allowed for the lower peak-to-peak separation and higher intensity of the peaks in the cyclic voltammetry using ferricyanide as redox probe (Arduini et al. 2012). We observed the typical sponge-like appearance of the working electrode surface, due to the presence of carbon black nanoparticles, with the dimension between 17.95 and 32.5 nm in the case of CB N220.

In addition, we observed that the drop-casting procedure is the preferred fabrication method using polyester-based support to prepare a sensitive CB-based electrode, leaving a homogenous film on the working electrode surface. In contrast, in the case of the CB-based screen-printed electrode, in which CB was used in the ink, only limited regions were observed on the working electrode surface.

Another useful issue in the fabrication of effective sensors by drop-casting is the need to use stable dispersion, which is mandatory to obtain reproducible and sensitive drop-cast electrodes. Usually, the concentration selected to prepare a stable dispersion is 1 mg/mL in different solvents, such as dimethylformamide-water (Mazzaracchio et al. 2019) or water with the presence of chitosan (Talarico et al. 2016), cetyltrimethylammonium bromide (Svegl et al. 2008), and dihexadecylphosphate (Silva and Fatibello-Filho 2017). We used acetonitrile in the first study (Arduini et al. 2010b), which is a solvent able to deliver a stable dispersion, leaving a reproducible film on the working electrode surface. However, in the case of the porous insulating layer, the acetonitrile and ethanol-based dispersions are not able to remain well confined on the working electrode surface, and thus a different solvent is used, namely dimethylformamide-water in ratio 1:1 (v/v) (Arduini et al. 2012). Another CB dispersion used is the one which employs chitosan. For instance, we selected the chitosan instead of dimethylformamide-water in ratio 1:1 (v/v) to prepare a dispersion with acetylcholinesterase enzyme, to obtain the most suitable environment for the biomolecules (Talarico et al. 2016). At the same time, the dispersion is also able to affect the electrochemical behavior, as reported by Vicentini et al. (2015). The authors evaluated the electrochemical response of CB-modified glassy carbon electrodes by drop-casting with a few μL of CB dispersion prepared in ultrapure water in the absence and presence of dihexadecylphosphate or in chitosan solution. Cyclic voltammetry as a technique and potassium ferrocyanide as the electrochemical probe obtained the best electrochemical behavior in terms of lower peak-to-peak separation and higher peak intensity using chitosan-based-dispersion, because only the presence of chitosan provided an adherent film on the surface of the working electrode.

In each case of dispersion, the sonication step is required; however, it is important to highlight that after several sonication steps we observed a loss of the electrochemical properties of CB. This behavior can be ascribed to the conversion of CB into a different structure, as reported in the literature. Indeed, Li et al. (2007) demonstrated that after ultrasound irradiation for 44 h, CB N330 was transformed into carbon nanosheets; thus careful attention is recommended in carrying out multiple steps of sonication.

To obtain a stable dispersion, another prerequisite is the type of CB used, indeed the amount of oxygen content and the particle dimension the different CB types allow for delivering dispersions characterized by different stability, as highlighted in Fig. 28.1.

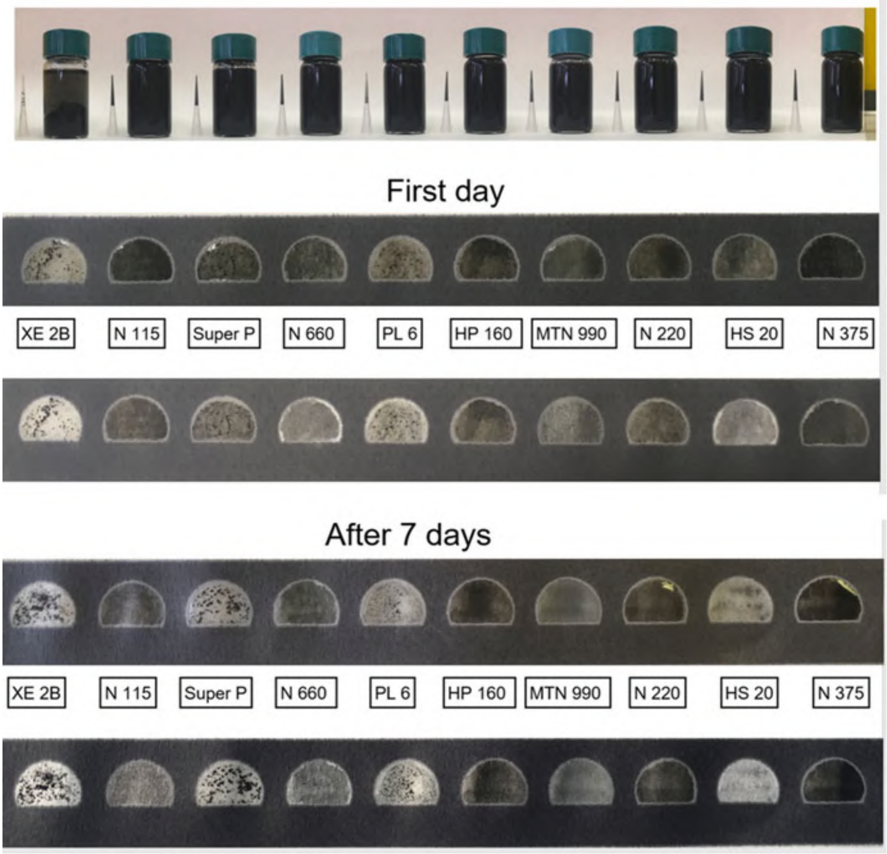
First day
XE 2B
N 115
Super P
N 660
PL 6
HP 160
MTN 990
N 220
HS 20
N 375
After 7 days
XE 2B
N 115
Super P
N 660
PL 6
HP 160
MTN 990
N 220
HS 20
N 375

Fig. 28.1 Dispersion of different types of CB in solution and drop-cast on paper. (Reprinted with permission from Mazzaracchio et al. 2019)

2 CB-Based Sensors

For the design of electrochemical sensors, CB has demonstrated its ability to implement three main figures of the sensors, namely increase of sensitivity, requirement of low applied potential, and resistance to fouling.

Our group demonstrated the outstanding features of CB-based electrochemical sensors in the detection of phenolic compounds, namely catechol, gallic acid, caffeic acid, and tyrosol (Talarico et al. 2015a). Figure 28.2a shows the response using CB-based screen-printed electrodes (black line) and bare electrode (blue line). The results reported in Fig. 28.2a demonstrate the suitability of the CB-based sensors to detect the phenolic compounds tested at the reduced applied potential with a relevant increase of sensitivity and low detection limit, equal to 0.1 μM, 1 μM, 0.8 μM, and 2 μM, respectively, for catechol, gallic acid, caffeic acid, and tyrosol.

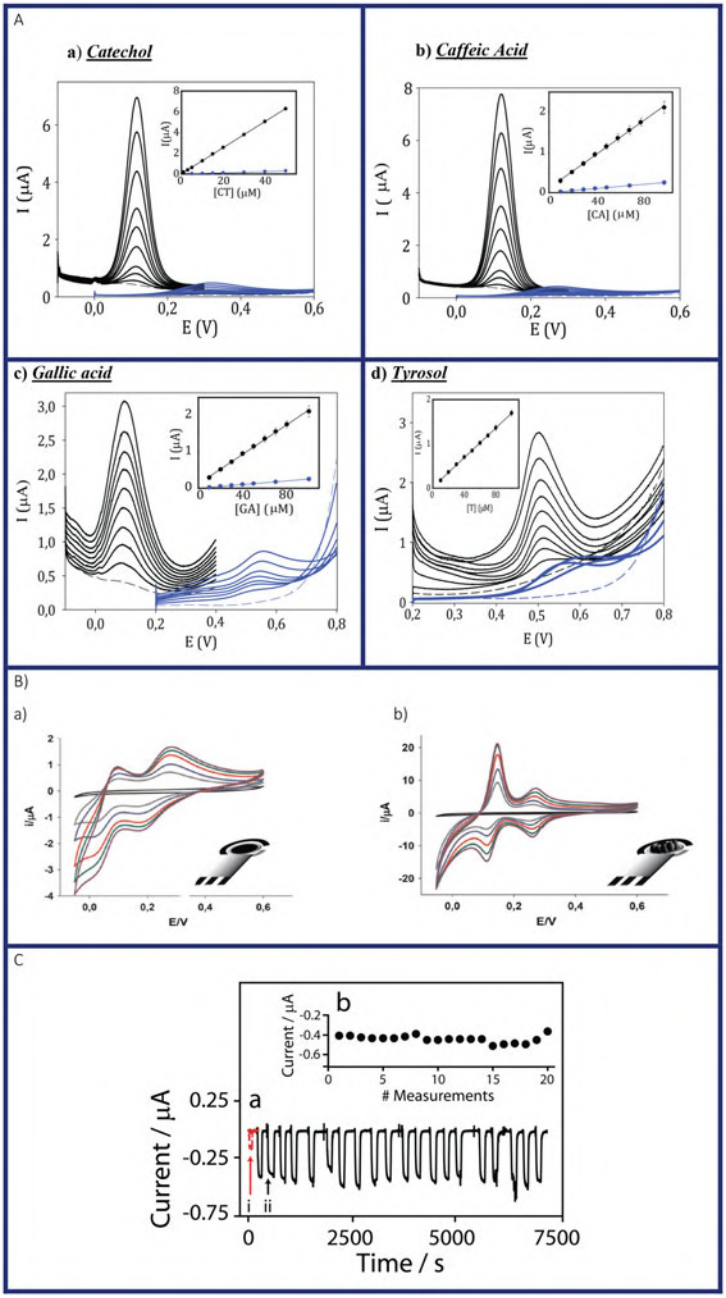

Fig. 28.2 (**a**) Square wave voltammetry using bare screen-printed electrode (blue line) and CB-modified screen-printed electrode (black line) in phosphate buffer solution 0.1 M+ KCl 0.1 M, pH = 7, in absence (dashed line) and in presence of several concentrations (continuous

The capability to detect compounds with increased sensitivity was also highlighted in the case of thiols, namely thiocholine, cysteine, glutathione, and cysteamine (Arduini et al. 2011). In the case of thiocholine and cysteine, a sensitivity of 299 mA $\mathrm{mol}^{-1}\,\mathrm{l\,cm}^{-2}$ and 441 mA $\mathrm{mol}^{-1}\,\mathrm{l\,cm}^{-2}$ was obtained, respectively. The high sensitivity of thiocholine and its ability to bind in ratio 1:1 mercury ions was used to detect mercury. Because the formation of the complex resulted in a no-electroactive complex (thiol–Hg), the decrease of the response is correlated to the concentration of mercury ions, furnishing a quantitative electroanalytical method. By using a selected concentration of thiocholine, a concentration of mercury equal to 5×10^{-9} mol l^{-1} (1 ppb) was detected in standard solution, demonstrating good recovery values in samples of drinking water. The presence of CB on the working electrode surface also demonstrated the capability to detect phosphate ions at low applied potential by reducing the phosphomolybdate complex. In the literature, the possibility to switch the reference colorimetric method with the electrochemical one was reported, replacing the chemical reduction of phosphomolybdate complex with its electrochemical reduction. However, using the classical configuration with an external counter/reference electrode and a microelectrode as working electrode, the second couple of redox peaks were selected with an applied potential of 0.3 V vs Ag/AgCl, even if the first couple of peaks were observed at an applied potential close to 0.1 V, characterized by higher sensitivity (Quintana et al. 2004). Indeed, the authors reported that at the applied potential of +0.1 V vs Ag/AgCl, a drift of signal was observed and this behavior was ascribed to the fouling problem. To overcome this issue, we used a screen-printed electrode modified with CB and observed a well-resolved peak for both the couples of peaks at ca. +0.1 and + 0.3 V together with an increase of sensitivity of ca. 10 times (Talarico et al. 2015b). In addition, we observed the resistance to the fouling problem due to the properties of CB. This sensor was able to detect phosphate in amperometric mode at +125 mV vs Ag/AgCl pseudoreference with linearity up to 100 μM and a detection limit equal to 0.1 μM. The capability of the sensor modified with CB to resist fouling was also demonstrated using this sensor embedded in an automatable flow system for automatically monitoring phosphate (Talarico et al. 2015c). The presence of CB on the surface of the working electrode allowed for the quantification of phosphate by measuring the reduction of phosphomolybdate complex at +125 mV versus Ag/AgCl, without a fouling problem. Indeed, by measuring the phosphate at a concentration of 50 μM 20 times by using the same sensor, the same response was observed within the experimental errors, demonstrating the resistance to fouling in a

Fig. 28.2 (continued) line) of catechol (a), caffeic acid (b), gallic acid (c) and tyrosol (d). Reprinted with permission from Talarico et al. (2015a). (**b**) Cyclic voltammetry using bare screen-printed electrode (a) and CB-modified screen-printed electrode (b) in sulfuric acid solution with molybdate in absence and in presence of increased concentrations of phosphate starting from 0.01 mM up to 0.2 mM. Reprinted with permission from Talarico et al. (2015b). (**c**) CB-modified screen-printed electrode embedded in a flow system to measure 50 μM phosphate (n = 20). Reprinted with permission from Talarico et al. (2015c) flow system using a wall-jet electrochemical cell (Fig. 28.2c). This sensor highlighted the capability to be inserted in a flow system for the online monitoring of phosphate, achieving a detection limit of 6 μM. When tested in different water sources, good recovery percentages were found in the range between 89% and 131.5%.

The automatable systems allow for the monitoring of the analyte in the absence of the operator, thus matching the 11th principle of Green Chemistry with the aim of real-time analysis for pollution prevention. However, the multiple analyses produce a relevant amount of chemicals as waste. To address the issue of reducing the chemicals both as reagents and by-products, we conceived the electrochemical cell in the paper network. We designed a paper-based electrochemical device for the detection of phosphate with the advantage that the paper strip contains all reagents needed for the reaction, allowing for restricted use of chemicals (Cinti et al. 2016a). We loaded into the hydrophilic area all the reagents needed for the measurement, namely molybdate ions, potassium chloride, and sulfuric acid, by adding 10 μL of a solution containing 100 mM molybdate ions, 100 mM potassium chloride, and 100 mM sulfuric acid, followed by solvent evaporation at RT. Indeed, by adding the sample solution (5 μL), solubilization of the reagents entrapped in the cellulosic network occurred, allowing for the measurement of phosphate with a detection limit of 4 μM, using only a few μL of chemicals. In addition, after the measurement, given that the whole electrochemical cell consists of paper, the sensor can be incinerated, further improving the sustainability of this analytical tool. The same approach was also reported by us in the case of bisphenol A detection (Fig. 28.3a). To fabricate a miniaturized and sustainable sensor, we printed the entire electrochemical cell on filter paper and the reagents were loaded into the paper network, to fabricate a reagent-free analytical tool. In this case, the electrochemical cell was printed using ink modified with carbon black for sensitive detection of bisphenol A (Jemmeli et al. 2020). Under optimized conditions, this sensor is able to detect the target analyte by using square wave voltammetry with a detection limit of 0.03 μM. When the sensor was challenged in river and drinking water samples, good recovery values demonstrated its suitability for analyses in water samples by using a reagent-free approach, because the only task required by the operator was to add few μL of the sample onto the working electrode surface.

The electrodes modified with CB were also employed for the simultaneous detection of different compounds. As an example, Raymundo-Pereira et al. (2017) developed a sensor based on a glassy carbon electrode by drop-casting with CB for simultaneous detection of hydroquinone and paracetamol, with the linear range between 80 nM and 230 μM. Deroco et al. (2018a) developed a glassy carbon electrode modified with CB for the detection of amoxicillin and nimesulide by square wave voltammetry with a detection limit of 0.12 and 0.016 μM, respectively. Glassy carbon electrodes modified with CB were also exploited for the detection of dopamine and paracetamol, with a limit of detection of 0.013 and 0.11 μM (Eisele et al. 2019), and for ascorbic acid, dopamine, uric acid, and paracetamol (Vicentini et al. 2016), with detection limits equal to 3.03×10^{-8}, 5.24×10^{-8}, 4.07×10^{-8}, and 4.53×10^{-8} mol L^{-1}, respectively.

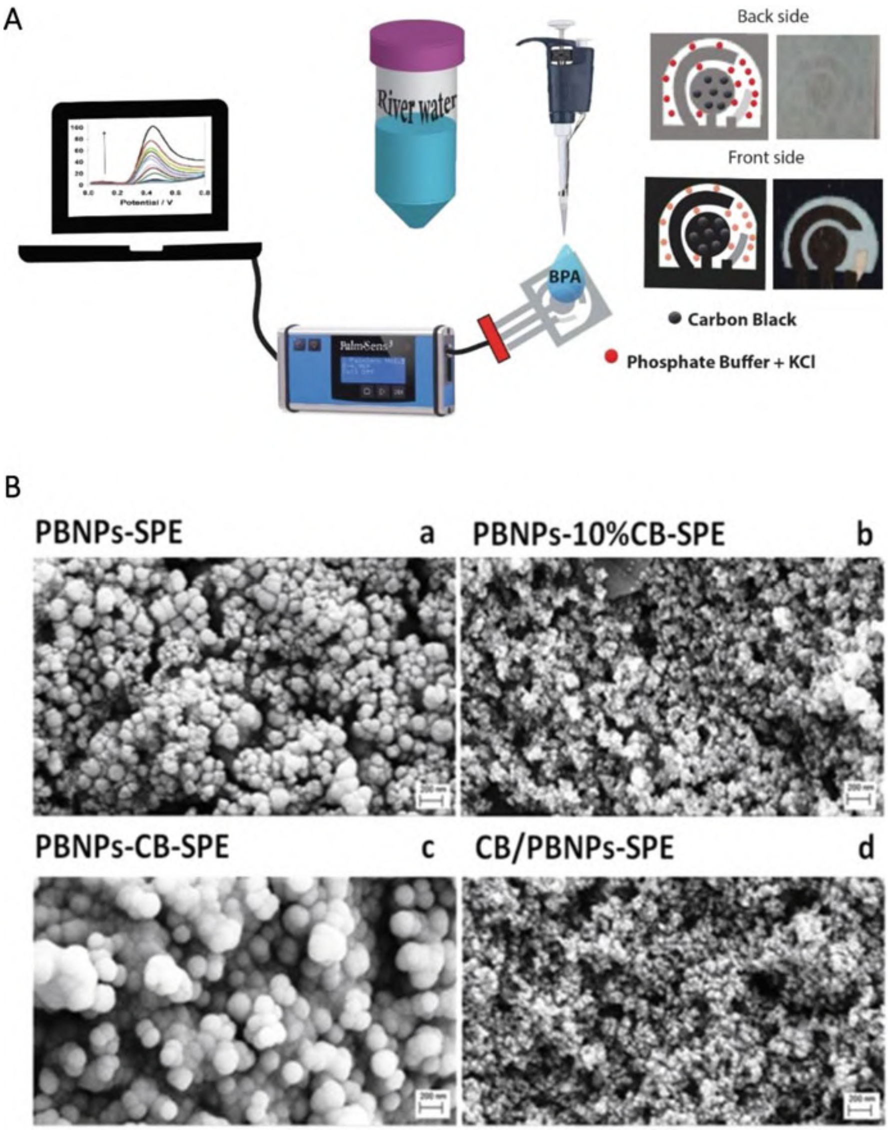
A
Potential / V
River water
BPA
PalmSens3
Back side
Front side
● Carbon Black
● Phosphate Buffer + KCl
B
PBNPs-SPE
a
PBNPs-10%CB-SPE
b
PBNPs-CB-SPE
c
CB/PBNPs-SPE
d
200 nm

Fig. 28.3 (**a**) Paper-based sensor for bisphenol A detection by using screen-printed electrode with graphite ink modified with CB. Reprinted with permission from Jemmeli et al. (2020). (**b**) SEM micrographs of a) bare screen-printed electrode modified with Prussian blue nanoparticles using in situ chemical deposition, b) screen-printed electrode previously modified with CB dispersion and modified with Prussian blue nanoparticles using in situ chemical deposition (bilayer), c) screen-printed electrode previously modified with CB in ink followed by Prussian blue nanoparticles chemical deposition, d) screen-printed electrode modified by drop-casting with a CB/ Prussian blue nanoparticles dispersion. Reprinted with permission from Cinti et al. (2014b)

3 CB-Nanocomposite-Based Sensors

The outstanding features of CB were also exploited in conjunction with other nanomaterials, including metallic nanoparticles such as gold nanoparticles or electrochemical mediators such as Prussian blue nanoparticles. In the case of screen-printed electrodes, the presence of both CB and gold nanoparticles demonstrated superior electrocatalytic performance with respect to only gold nanoparticles or CB. For instance, in the case of H_2O_2 reduction, the electrochemical process was observed at lower negative potentials with the improvement of sensor sensitivity (Arduini et al. 2015a). In the case of stripping analysis of heavy metals, namely As (III) and Hg^{2+}, the presence of CB as a substrate layer before the deposition of gold nanoparticles allowed for improved sensitivity, because the CB layer under the gold nanoparticles layer offers a larger loading area for gold nanoparticles. This configuration encompasses the double layers of CB and the gold nanoparticles exploited for the detection of As(III) trace in drinking water (Cinti et al. 2014a) and mercury ions in river water and soil (Cinti et al. 2016b). Also, Au–Pd core-shell nanoparticles were cast on the glassy electrode surface, exploiting CB as support. In this case, Deroco et al. (2018b) used the modified sensor for hydrazine detection, observing a decrease of applied potential and a low detection limit in respect to bare electrodes. A CB layer as a support layer was also used for the electrodeposition of Prussian blue followed by the deposition of a layer of Nafion to improve the stability of the sensor (Rojas et al. 2018). This platform was employed for hydrogen peroxide at an applied potential of −50 mV (vs. Ag) with linearity between 200 nM and 1 mM, with the final aim to detect hydrogen peroxide in the Neuroblastoma cell line SH-SY5Y. CB was also used to customize the dimension of Prussian blue nanoparticles, tuning the sensitivity of the sensor toward the detection of hydrogen peroxide (Cinti et al. 2014b), by using different modes for the chemical deposition of Prussian blue nanoparticles on CB as follows: (i) in situ Prussian blue nanoparticles chemical deposition on screen-printed electrodes previously modified with CB dispersion (bilayer), (ii) by in situ Prussian blue nanoparticles chemical deposition on screen-printed electrodes prepared with graphite ink containing CB, and (iii) by casting screen-printed electrodes with a CB/ Prussian blue nanoparticles dispersion. The use of CB in different configurations allows for obtaining Prussian blue nanoparticles at different sizes with different electroanalytical features. For instance, screen-printed electrodes modified with CB/Prussian blue nanoparticles dispersion having Prussian blue nanoparticles with an average diameter of 19 ± 3 nm have been characterized by a detection limit of 0.3 μM. CB was also combined with (i) organic electrochemical mediators such as copper-phthalocyanine for the detection of 17β-estradiol by differential pulse voltammetry. The sensor was able to detect the target analyte in river water (S. Paulo State, Brazil) and synthetic urine samples (Wong et al. 2019); (ii) MoS_2 for cocoa catechin determination by differential pulse voltammetry with linearity up to 25 μM and a detection limit of 0.17 μM (Della Pelle et al. 2019); (iii) carbon nanotubes and MoS_2 for bisphenol A detection with a linear range between 0.1 and 130 μM and detection limit equal to 0.08 μM (Thamilselvan et al. 2019), highlighting the suitability of CB to work synergically with other nanomaterials.

4 CB-Based Biosensors

The high surface area of CB and the functional groups present in this nanomaterial such as O-C = O groups confer to CB valuable features for using it in combination with biomolecules, including enzymes, antibodies, and DNA sequences. In 2010, we combined tyrosinase with a CB paste electrode for the fabrication of an amperometric biosensor to detect catechol, reaching a sensitivity of 625 nA/mM and a detection limit of 0.008 mM (Arduini et al. 2010a). The higher sensitivity can be ascribed to the close proximity of the bioreceptor to the nanomaterial, as well as to the capability of CB to load a higher amount of enzyme thanks to its high surface area. CB was also modified by the chemical treatment, which included oxidation with nitric and sulfuric acids 1:1 (v/v) mixture to enhance the oxygenated functional groups for a better immobilization of tyrosinase enzyme in the presence of bovine serum albumin and glutaraldehyde, obtaining a limit of detection of 8.7×10^{-8} mol L^{-1} (Ibáñez-Redín et al. 2018). Nadifiyine et al. (2013) used CB and tyrosinase for carbon paste fabrication for the quantification of phenolic compounds in olive oil, obtaining an agreement with the Folin—Ciocalteu spectrophotometric reference method.

CB-based enzymatic biosensors were also developed using cholinesterase as the biocomponent. As an example, we designed a printed electrode modified by drop-casting with CB to immobilize butyrylcholinesterase enzyme by cross-linking using glutaraldehyde, Nafion, and bovine serum albumin (Fig. 28.4a) (Arduini et al. 2015b). The resistance of CB to the fouling issue was demonstrated in the case of thiocholine detection; indeed, after six successive analyses of the thiocholine, RSD% equal to 3.9 was measured, highlighting the stability of the signal. This biosensor was challenged for the quantification of paraoxon in standard solution with a detection limit of 5 μg L^{-1}, as well as in surface water samples with good recovery values, that is, 96 ± 2%. The suitability of this biosensor in another type of sample, namely olive oil, was also evaluated. Olive oil samples were treated with the QuEChERS method for the extraction of pesticides from the whole fatty matrix and the treated sample was then analyzed using CB-based butyrylcholinesterase biosensor (Arduini et al. 2017). CB was also employed as nanomodifier for the development of smart immunosensors. As an example, Suprun et al. (2012) developed a label-free electrochemical immunosensor by immobilizing the antibody toward cardiac myoglobin immobilized on CB-modified screen-printed electrodes. The peak current variation in square wave voltammetry vs. the logarithm of myoglobin concentration showed a linear range from 5 to 500 μM. Another label-free immunosensor was reported by Aydin et al. using antibodies toward tumor marker p53 as a biocomponent and electrochemical impedance spectroscopy as a technique, reaching a detection limit as low as 3 fg/mL with a wide linear range, that is, 0.01–2 pg/mL (2018). Screen-printed electrodes modified with CB were also

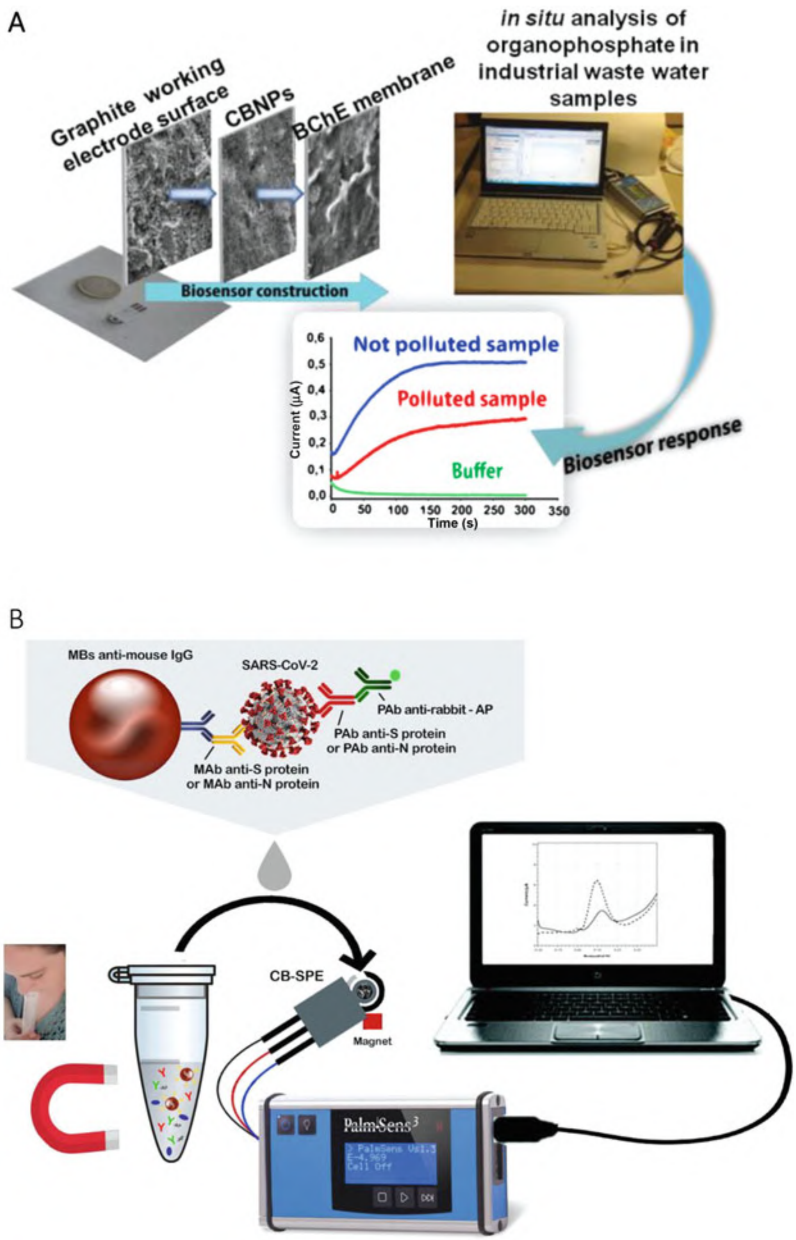
A
Graphite working electrode surface
CBNPs
BChE membrane
Biosensor construction
in situ analysis of organophosphate in industrial waste water samples
Not polluted sample
Polluted sample
Buffer
Biosensor response
Current (μA)
0,0
0,1
0,2
0,3
0,4
0,5
0,6
0
50
100
150
200
250
300
350
Time (s)
B
MBs anti-mouse IgG
SARS-CoV-2
PAb anti-rabbit - AP
PAb anti-S protein
or PAb anti-N protein
MAb anti-S protein
or MAb anti-N protein
CB-SPE
Magnet
PalmSens3

Fig. 28.4 (**a**) CB-based enzymatic biosensor using butyrylcholinesterase as biocomponent to detect organophosphorus pesticides in water samples. Reprinted with permission from Arduini et al. (2015b). (**b**) CB-based immunosensor using magnetic beads to immobilize the immunological chain for SARS-CoV-2 detection in saliva. Reprinted with permission from Fabiani et al. (2021)

recently developed combined with magnetic beads for the immunosensing of SARS-CoV-2 in saliva (Fabiani et al. 2021). Magnetic beads were used as support of immunological chain and secondary antibody with alkaline phosphatase as immunological label for the detection of Spike (S) protein or Nucleocapsid (N) protein, present in the SARS-CoV-2 virus. Screen-printed electrodes modified with CB were used for sensitive detection of 1-naphtol enzymatic by-product (Fig. 28.4b). As conceived, the electrochemical immunoassay was able to detect S and N proteins in untreated saliva with a detection limit equal to 19 ng/mL and 8 ng/mL, respectively. In addition, the data obtained in the case of saliva clinical samples was found to be in agreement with the data obtained using the nasopharyngeal swab specimens and Real-Time PCR reference method, demonstrating the suitability of this cost-effective, non-invasive, and rapid analytical tool. CB was also exploited for the design of a smart DNA sensor, as reported by Yammouri et al. (2017), using pencil graphite modified with CB and DNA probe for microRNA-125a detection. The electrochemical impedance spectroscopy was selected as the electrochemical technique for designing a label-free DNA sensor able to quantify microRNA-125a with a detection limit equal to 10 pM (1 pg/mL). A screen-printed electrode modified with CB was also employed as a platform to design a tailor-made heterogeneous oligonucleotide-antibody biosensor for the quantification of sulfur mustard (Colozza et al. 2021). The immunoassay was fabricated with immobilization process encompassing a primary antibody for the selective recognition of the sulfur mustard-oligonucleotide adduct and an alkaline phosphatase-conjugated anti-mouse anti-IgG as the secondary antibody. The detection was carried out using 1-naphthyl phosphate and measuring the enzymatic by-product in differential pulse voltammetry, obtaining a detection limit equal to 12 μM.

5 CB-Nanocomposite-Based Biosensors

The conjugation of CB with other nanomaterials has established a pillar in the development of smart CB-based electrochemical biosensors by combining CB with other nanomaterials, namely gold nanoparticles, organic and inorganic electrochemical mediators, and several biocomponents to realize a sensitive and reliable bio-device. As an example, we developed a laccase-based biosensor using a thionine/CB-modified screen-printed electrode for the detection of bisphenol A (Portaccio et al. 2013) by entrapping the enzyme on the electrode surface using neutralized aqueous solution of Nafion. In this case, CB was exploited to absorb thionine as an electrochemical mediator to avoid its leakage. Under optimized conditions, the application of this biosensor in a real matrix was evaluated by testing tomato juice samples in metallic cans, obtaining satisfactory recovery values, that is, between 92% and 120%. CB was also combined with Prussian blue for the detection of hydrogen peroxide in the realization of glucose biosensors, as hydrogen peroxide is a glucose oxidase by-product. As an example, Calegari et al. (2017) fabricated a carbon composite electrode based on a mixture of CB, poly(ethylene-co-vinyl acetate), and Prussian blue followed by immobilization of glucose oxidase for glucose detection in tears with a linear range up to 6.95×10^{-4} M. The high surface of CB, as well as its dispersibility, was exploited to load cobalt phthalocyanine (Cinti et al. 2016c). In this way, it was possible to obtain a stable dispersion for production by drop-casting a butyrylcholinesterase-based biosensor able to quantify paraoxon at nM level. Acetylcholinesterase-based biosensors have also been reported by the Evtugyn group (Evtugyn et al. 2014), using CB with thiacalix[4] and Ag nanoparticles, used as reducing and encapsulating agents to avoid nanoparticle aggregation. CB was also exploited to design smart and sensitive enzymatic paper-based biosensors. For instance, we developed a double strip for the detection of butyrylcholinesterase inhibitors, that is, organophosphorus compounds using the working electrode modified in ink, with CB and Prussian blue nanoparticles being able to electrocatalyze the oxidation of enzymatic by-product thiocholine. In the case of paper-based devices, each strip is able to carry out only one measurement because for inhibitive biosensors a dual-strip paper-based device based on lateral flow is conceived (Cinti et al. 2017). This paper-based biosensor consisted of a strip of nitrocellulose loaded with butyrylthiocholine, the enzymatic substrate, an electrochemical cell printed with CB and Prussian blue nanoparticles on the waxed-paper test area, and a test area loaded with a butyrylcholinesterase enzyme loaded using a buffered solution. For the measurement, 10 μL of distilled water was added at the edge of the nitrocellulose strip, on which 10 mM butyrylthiocholine was adsorbed, followed by the measurement of thiocholine enzymatic by-product applying +300 mV (Fig. 28.5a). For the pesticide detection in the sample, the sample was added in the second strip and after 10 min (incubation time), 10 μL of water was added at the edge of the nitrocellulose strip, and was reported for the enzymatic activity measurement in absence of inhibitor. This paper-based device demonstrated a detection limit equal to 3 μg/L. The same CB-based nanocomposite was used for the development of a smart origami system for mustard agent detection, exploiting the capability of CB/Prussian blue nanoparticles to electrocatalyze the reduction of the enzymatic by-product hydrogen peroxide using choline oxidase as biocomponent (Colozza et al. 2019). Because the mustard agents are able to inhibit the choline oxidase, by monitoring the decrease of the response it is possible to quantify the mustard agents in the sample analyzed. The measurements were carried out in the liquid and in the aerosol phases, obtaining a detection limit of 1 mM and 0.019 g/m^3, respectively (Fig. 28.5b).

Elliot’s group evaluated gold nanostars, gold nanospheres, and CB to modify screen-printed electrodes, highlighting the outstanding electrochemical performances of CB-modified screen-printed electrodes and taking into account the low transient current, low capacitance, and good porosity. This platform was used to develop a competitive immunoassay for the detection of shellfish toxin domoic with a detection limit of 0.7 mg kg^{-1} of shellfish (Nelis et al. 2020).

A nanocomposite was synthesized using a two-dimensional tungsten disulfide and acetylene black combined with gold nanoparticles to develop a DNA biosensor (Shuai et al. 2016). The DNA capture probe was immobilized by thiol—gold bonds, followed by hybridization with the target DNA to provide a linearity from 0.001 pM to 100 pM. CB combined with gold nanoparticles was used by Yammouri et al. for

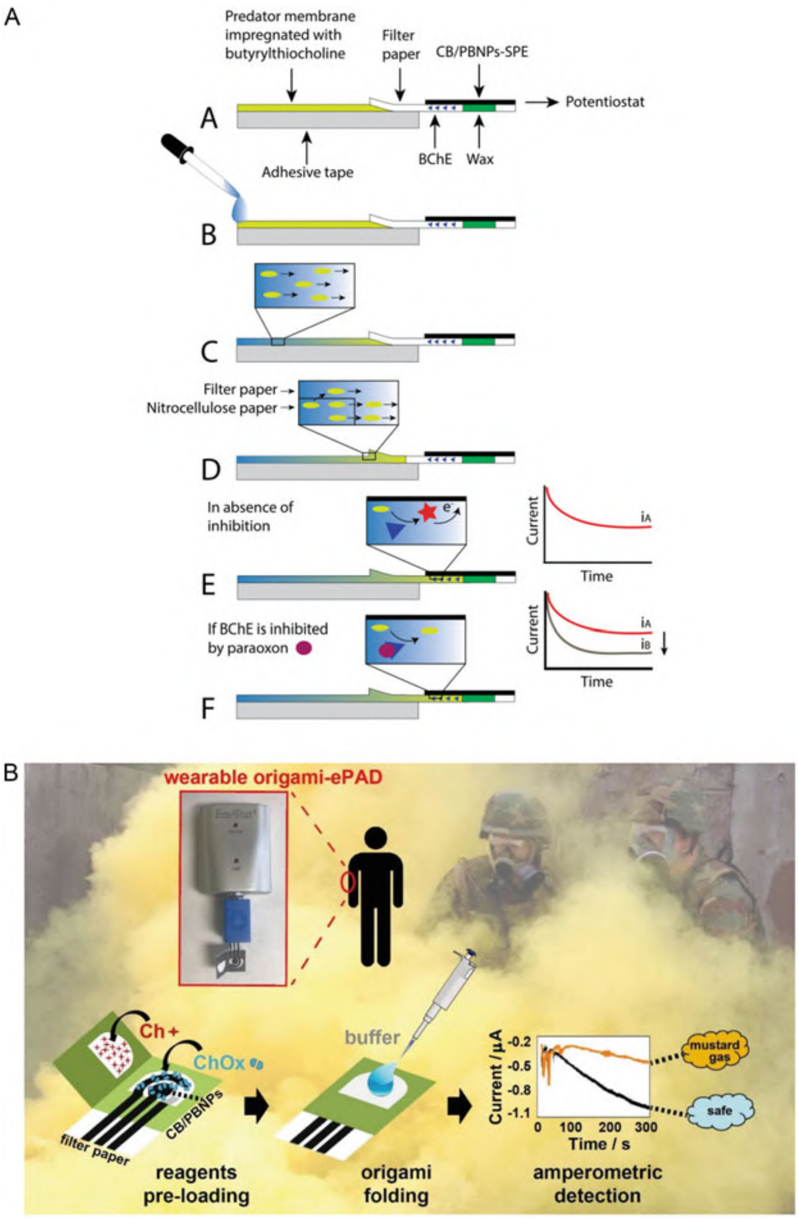
A
Predator membrane impregnated with butyrylthiocholine
Filter paper
CB/PBNPs-SPE
Potentiostat
A
Adhesive tape
BChE
Wax
B
C
Filter paper
Nitrocellulose paper
D
In absence of inhibition
e⁻
Current
iA
Time
E
If BChE is inhibited by paraoxon
Current
iA
iB
Time
F
B
wearable origami-ePAD
Ch +
ChOx
CB/PBNPs
filter paper
buffer
Current / µA
-0.2
-0.5
-0.8
-1.1
0
100
200
300
Time / s
mustard gas
safe
reagents pre-loading
origami folding
amperometric detection

Fig. 28.5 (**a**) Paper-based device using butyrylcholinesterase as biocomponent and CB/Prussian blue nanoparticles as nanocomposite to modify the ink to detect nerve in water samples. Reprinted with permission from Cinti et al. (2017). (**b**) Origami paper-based biosensor for mustard agent detection in gas phase using choline oxidase as biocomponent and CB/Prussian blue nanoparticles as nanocomposite to modify the ink. Reprinted with permission from Colozza et al. (2019)

the realization of an electrochemical biosensor for the detection of microRNA-21, by exploiting the gold nanoparticles to immobilize a thiolated capture probe (complementary sequence of microRNA-21) labeled with methylene blue (Yammouri et al. 2019). After hybridization with the target microRNA-21, a decrease in the methylene blue response was observed, reaching a limit of detection of 1 fM and demonstrating good results in serum.

6 Conclusions

In recent decades, nanomaterials have completely changed the behavior of devices in several fields starting from physical devices, through chemical tools to biological systems. The use of nanomaterials in electrochemical biosensors has established a new route conferring unprecedented features to the nanodevices, including smart configuration, improved sensitivity, and selectivity, combined with an enhancement in terms of working and storage stability (Kour et al. 2020). In the field of carbon-based nanomaterials, the use of carbon nanotubes has opened the route to the use of this type of nanomaterials in the development of newly designed electrochemical (bio)sensors. At present, the position occupied by carbon nanotubes has been replaced by graphene, which has tarnished the use of carbon nanotubes, setting the stage for a new generation of electrochemical biosensors. In this overall scenario, CB is acquiring a relevant role due to its outstanding electrochemical properties combined with its specific features, namely cost-effectiveness and the feasibility to obtain a stable dispersion for the modification of electrodes by drop-casting. Since 2010, increased use of CB in electrochemical (bio)sensors has been observed, demonstrating its re-discovery with a new application as nanomodifier for delivering cost-effective and reliable electrochemical (bio)devices.

References

Alfè M, Gargiulo V (2020) Versatile and scalable approaches to tune carbon black characteristics for boosting adsorption and VOC sensing applications. In: Carbon-based material for environmental protection and remediation, Intechopen, p 65

Arduini F, Giorgio FD, Amine A, Cataldo F, Moscone D, Palleschi G (2010a) Electroanalytical characterization of carbon black nanomaterial paste electrode: development of highly sensitive tyrosinase biosensor for catechol detection. Anal Lett 43(10–11):1688–1702

Arduini F, Amine A, Majorani C, Di Giorgio F, De Felicis D, Cataldo F, Moscone D, Palleschi G (2010b) High performance electrochemical sensor based on modified screen-printed electrodes with cost-effective dispersion of nanostructured carbon black. Electrochem Commun 12(3): 346–350

Arduini F, Majorani C, Amine A, Moscone D, Palleschi G (2011) Hg^{2+} detection by measuring thiol groups with a highly sensitive screen-printed electrode modified with a nanostructured carbon black film. Electrochim Acta 56(11):4209–4215

Arduini F, Di Nardo F, Amine A, Micheli L, Palleschi G, Moscone D (2012) Carbon black-modified screen-printed electrodes as electroanalytical tools. Electroanalysis 24(4):743–751

Arduini F, Zanardi C, Cinti S, Terzi F, Moscone D, Palleschi G, Seeber R (2015a) Effective electrochemical sensor based on screen-printed electrodes modified with a carbon black-Au nanoparticles composite. Sensors Actuators B Chem 212:536–543

Arduini F, Forchielli M, Amine A, Neagu D, Cacciotti I, Nanni F, Moscone D, Palleschi G (2015b) Screen-printed biosensor modified with carbon black nanoparticles for the determination of paraoxon based on the inhibition of butyrylcholinesterase. Microchim Acta 182(3):643–651

Arduini F, Forchielli M, Scognamiglio V, Nikolaevna KA, Moscone D (2017) Organophosphorous pesticide detection in olive oil by using a miniaturized, easy-to-use, and cost-effective biosensor combined with QuEChERS for sample clean-up. Sensors 17(1):34

Aydın EB, Aydın M, Sezgintürk MK (2018) Electrochemical immunosensor based on chitosan/conductive carbon black composite modified disposable ITO electrode: an analytical platform for p53 detection. Biosens Bioelectron 121:80–89

Calegari F, de Souza LP, Barsan MM, Brett CM, Marcolino-Junior LH, Bergamini MF (2017) Construction and evaluation of carbon black and poly (ethylene co-vinyl) acetate (EVA) composite electrodes for development of electrochemical (bio) sensors. Sensors Actuators B Chem 253:10–18

Cinti S, Politi S, Moscone D, Palleschi G, Arduini F (2014a) Stripping analysis of As (III) by means of screen-printed electrodes modified with gold nanoparticles and carbon black nanocomposite. Electroanalysis 26(5):931–939

Cinti S, Arduini F, Vellucci G, Cacciotti I, Nanni F, Moscone D (2014b) Carbon black assisted tailoring of Prussian Blue nanoparticles to tune sensitivity and detection limit towards H_2O_2 by using screen-printed electrode. Electrochem Commun 47:63–66

Cinti S, Santella F, Moscone D, Arduini F (2016a) Hg^{2+} detection using a disposable and miniaturized screen-printed electrode modified with nanocomposite carbon black and gold nanoparticles. Environ Sci Pollut Res 23(9):8192–8199

Cinti S, Talarico D, Palleschi G, Moscone D, Arduini F (2016b) Novel reagentless paper-based screen-printed electrochemical sensor to detect phosphate. Anal Chim Acta 919:78–84

Cinti S, Neagu D, Carbone M, Cacciotti I, Moscone D, Arduini F (2016c) Novel carbon black-cobalt phthalocyanine nanocomposite as sensing platform to detect organophosphorus pollutants at screen-printed electrode. Electrochim Acta 188:574–581

Cinti S, Minotti C, Moscone D, Palleschi G, Arduini F (2017) Fully integrated ready-to-use paper-based electrochemical biosensor to detect nerve agents. Biosens Bioelectron 93:46–51

Colozza N, Kehe K, Dionisi G, Popp T, Tsoutsoulopoulos A, Steinritz D, Moscone D, Arduini F (2019) A wearable origami-like paper-based electrochemical biosensor for sulfur mustard detection. Biosens Bioelectron 129:15–23

Colozza N, Mazzaracchio V, Kehe K, Tsoutsoulopoulos A, Schioppa S, Fabiani L, Steinritz D, Moscone D, Arduini F (2021) Development of novel carbon black-based heterogeneous oligonucleotide-antibody assay for sulfur mustard detection. Sensors Actuators B Chem 328:129054

Della Pelle F, Rojas D, Scroccarello A, Del Carlo M, Ferraro G, Di Mattia C, Martuscelli M, Escarpa A, Compagnone D (2019) High-performance carbon black/molybdenum disulfide nanohybrid sensor for cocoa catechins determination using an extraction-free approach. Sensors Actuators B Chem 296:126651

Deroco PB, Melo IG, Silva LS, Eguiluz KI, Salazar-Banda GR, Fatibello-Filho O (2018a) Carbon black supported Au–Pd core-shell nanoparticles within a dihexadecylphosphate film for the development of hydrazine electrochemical sensor. Sensors Actuators B Chem 256:535–542

Deroco PB, Rocha-Filho RC, Fatibello-Filho O (2018b) A new and simple method for the simultaneous determination of amoxicillin and nimesulide using carbon black within a dihexadecylphosphate film as electrochemical sensor. Talanta 179:115–123

Eisele APP, Valezi CF, Mazziero T, Dekker RF, Barbosa-Dekker AM, Sartori ER (2019) Layering of a film of carboxymethyl-botryosphaeran onto carbon black as a novel sensitive electrochemical platform on glassy carbon electrodes for the improvement in the simultaneous determination of phenolic compounds. Sensors Actuators B Chem 287:18–26

Evtugyn GA, Shamagsumova RV, Padnya PV, Stoikov II, Antipin IS (2014) Cholinesterase sensor based on glassy carbon electrode modified with Ag nanoparticles decorated with macrocyclic ligands. Talanta 127:9–17

Fabiani L, Saroglia M, Galatà G, De Santis R, Fillo S, Luca V, Faggioni G, D'Amore N, Regalbuto E, Salvatori P, Terova G (2021) Magnetic beads combined with carbon black-based screen-printed electrodes for COVID-19: a reliable and miniaturized electrochemical immunosensor for SARS-CoV-2 detection in saliva. Biosens Bioelectron 171:112686

Hočevar SB, Ogorevc B (2007) Preparation and characterization of carbon paste micro-electrode based on carbon nano-particles. Talanta 74(3):405–411

Ibáñez-Redín G, Silva TA, Vicentini FC, Fatibello-Filho O (2018) Effect of carbon black functionalization on the analytical performance of a tyrosinase biosensor based on glassy carbon electrode modified with dihexadecylphosphate film. Enzym Microb Technol 116:41–47

Jemmeli D, Marcoccio E, Moscone D, Dridi C, Arduini F (2020) Highly sensitive paper-based electrochemical sensor for reagent free detection of bisphenol A. Talanta 216:120924

Kour R, Arya S, Young SJ, Gupta V, Bandhoria P, Khosla A (2020) Recent advances in carbon nanomaterials as electrochemical biosensors. J Electrochem Soc 167(3):037555

Li Q, Zhang X, Wu G, Xu S, Wu C (2007) Sonochemical preparation of carbon nanosheet from carbon black. Ultrason Sonochem 14(2):225–228

Mazzaracchio V, Tomei MR, Cacciotti I, Chiodoni A, Novara C, Castellino M, Scordo G, Amine A, Moscone D, Arduini F (2019) Inside the different types of carbon black as nanomodifiers for screen-printed electrodes. Electrochim Acta 317:673–683

Mita DG, Attanasio A, Arduini F, Diano N, Grano V, Bencivenga U, Rossi S, Amine A, Moscone D (2007) Enzymatic determination of BPA by means of tyrosinase immobilized on different carbon carriers. Biosens Bioelectron 23(1):60–65

Nadifiyine S, Haddam M, Mandli J, Chadel S, Blanchard CC, Marty JL, Amine A (2013) Amperometric biosensor based on tyrosinase immobilized on to a carbon black paste electrode for phenol determination in olive oil. Anal Lett 46(17):2705–2726

Nelis JL, Migliorelli D, Jafari S, Generelli S, Lou-Franco J, Salvador JP, Marco MP, Cao C, Elliott CT, Campbell K (2020) The benefits of carbon black, gold and magnetic nanomaterials for point-of-harvest electrochemical quantification of domoic acid. Microchim Acta 187(3):1–11

Portaccio M, Di Tuoro D, Arduini F, Moscone D, Cammarota M, Mita DG, Lepore M (2013) Laccase biosensor based on screen-printed electrode modified with thionine–carbon black nanocomposite, for bisphenol a detection. Electrochim Acta 109:340–347

Quintana JC, Idrissi L, Palleschi G, Albertano P, Amine A, El Rhazi M, Moscone D (2004) Investigation of amperometric detection of phosphate: application in seawater and cyanobacterial biofilm samples. Talanta 63(3):567–574

Raymundo-Pereira PA, Campos AM, Mendonca CD, Calegaro ML, Machado SA, Oliveira ON Jr (2017) Printex 6L carbon nanoballs used in electrochemical sensors for simultaneous detection of emerging pollutants hydroquinone and paracetamol. Sensors Actuators B Chem 252:165–174

Rojas D, Della Pelle F, Del Carlo M, d'Angelo M, Dominguez-Benot R, Cimini A, Escarpa A, Compagnone D (2018) Electrodeposited Prussian Blue on carbon black modified disposable electrodes for direct enzyme-free H2O2 sensing in a Parkinson's disease in vitro model. Sensors Actuators B Chem 275:402–408

Shuai HL, Huang KJ, Chen YX (2016) A layered tungsten disulfide/acetylene black composite based DNA biosensing platform coupled with hybridization chain reaction for signal amplification. J Mater Chem B 4(6):1186–1196

Silva TA, Fatibello-Filho O (2017) Square-wave adsorptive anodic stripping voltammetric determination of ramipril using an electrochemical sensor based on nanostructured carbon black. Anal Methods 9(32):4680–4687

Suprun EV, Arduini F, Moscone D, Palleschi G, Shumyantseva VV, Archakov AI (2012) Direct electrochemistry of heme proteins on electrodes modified with didodecyldimethyl ammonium bromide and carbon black. Electroanalysis 24(10):1923–1931

Svegl IG, Bele M, Ogorevc B (2008) Carbon black nanoparticles film electrode prepared by using substrate-induced deposition approach. Anal Chim Acta 628(2):173–180

Talarico D, Arduini F, Constantino A, Del Carlo M, Compagnone D, Moscone D, Palleschi G (2015a) Carbon black as successful screen-printed electrode modifier for phenolic compound detection. Electrochem Commun 60:78–82

Talarico D, Arduini F, Amine A, Moscone D, Palleschi G (2015b) Screen-printed electrode modified with carbon black nanoparticles for phosphate detection by measuring the electroactive phosphomolybdate complex. Talanta 141:267–272

Talarico D, Cinti S, Arduini F, Amine A, Moscone D, Palleschi G (2015c) Phosphate detection through a cost-effective carbon black nanoparticle-modified screen-printed electrode embedded in a continuous flow system. Environ Sci Technol 49(13):7934–7939

Talarico D, Arduini F, Amine A, Cacciotti I, Moscone D, Palleschi G (2016) Screen-printed electrode modified with carbon black and chitosan: a novel platform for acetylcholinesterase biosensor development. Anal Bioanal Chem 408(26):7299–7309

Thamilselvan A, Rajagopal V, Suryanarayanan V (2019) Highly sensitive and selective amperometric determination of BPA on carbon black/f-MWCNT composite modified GCE. J Alloys Compd 786:698–706

Vicentini FC, Ravanini AE, Figueiredo-Filho LC, Iniesta J, Banks CE, Fatibello-Filho O (2015) Imparting improvements in electrochemical sensors: evaluation of different carbon blacks that give rise to significant improvement in the performance of electroanalytical sensing platforms. Electrochim Acta 157:125–133

Vicentini FC, Raymundo-Pereira PA, Janegitz BC, Machado SA, Fatibello-Filho O (2016) Nanostructured carbon black for simultaneous sensing in biological fluids. Sensors Actuators B Chem 227:610–618

Wong A, Santos AM, Fava EL, Fatibello-Filho O, Sotomayor MDPT (2019) Voltammetric determination of 17β-estradiol in different matrices using a screen-printed sensor modified with CuPc, Printex 6L carbon and Nafion film. Microchem J 147:365–373

Yammouri G, Mandli J, Mohammadi H, Amine A (2017) Development of an electrochemical label-free biosensor for microRNA-125a detection using pencil graphite electrode modified with different carbon nanomaterials. J Electroanal Chem 806:75–81

Yammouri G, Mohammadi H, Amine A (2019) A highly sensitive electrochemical biosensor based on carbon black and gold nanoparticles modified pencil graphite electrode for microRNA-21 detection. Chem Afr 2(2):291–300

Всё для победы!
НАРОДНЫЙ ФРОНТ
https://pobeda.onf.ru/
LET'S HELP THE RUSSIA

Nanobiosensors: Construction and Diagnosis of Disease

29

Cem Erkmen, Bengi Uslu, and Gözde Aydoğdu Tiğ

Contents

1 Introduction 640
2 Concept of Nanobiosensors 641
  2.1 Ideal Features of Nanobiosensors 642
  2.2 Components of Nanobiosensors 642
  2.3 Nanobiosensors for Diagnosis of Disease 643
3 Conclusion 655
References 656

Abstract

Nanobiosensors, which are advancing daily, are of interest to many researchers and enabled developments in this field. Considering the increasing population today, nanobiosensors have become widely used methods for the early diagnosis of many diseases. Compared to traditional analytical methods, nanobiosensors have significant advantages such as high sensitivity and selectivity, shorter analysis time, biocompatibility, and easy miniaturization of used devices for on-site analysis. Like biosensors, nanobiosensors can be classified in various ways, either by biological molecules such as enzymes, antibodies, and

---

C. Erkmen
Faculty of Pharmacy, Department of Analytical Chemistry, Ankara University, Ankara, Turkey

The Graduate School of Health Sciences, Ankara University, Ankara, Turkey

B. Uslu
Faculty of Pharmacy, Department of Analytical Chemistry, Ankara University, Ankara, Turkey

G. A. Tiğ (✉)
Faculty of Science, Department of Chemistry, Ankara University, Ankara, Turkey
e-mail: gaydogdu@science.ankara.edu.tr

© Springer Nature Singapore Pte Ltd. 2023

U. P. Azad, P. Chandra (eds.), *Handbook of Nanobioelectrochemistry*,
https://doi.org/10.1007/978-981-19-9437-1_29

aptamers or by working principles such as optical and electrochemical. This chapter summarizes nanobiosensors designs, characterizations, applications, and advances for detecting various diseases and biomarkers. Current studies of nanobiosensors were given, along with detailed information on nanoparticles' effect, biological molecules, and detection methods. As a result, it can be concluded that the outputs obtained by using nanobiosensor technology will increase the quality of life.

Keywords

Diagnosis · Disease · Electrochemical · Nanobiosensors · Nanomaterials

1 Introduction

Nanotechnology's history dates back to the 1950s and has contributed to the emergence of nanoscale materials with extraordinary properties. In addition, nowadays, developments in nanotechnology have allowed the obtaining of new materials by processing different materials at the atomic level. As the materials approach the nanoscale, they gain many new superior physical and chemical properties. Nano-sized materials exhibit different properties than normal-sized materials due to their surface and quantum effects. Nanomaterials have unique physical, chemical, and mechanical properties with quantum size effects, unique characteristics of surface atoms, size dependence of electronic structure, and high surface/volume ratio. Nanoparticles have found wide applications in many different fields from biomedical, optics, and electronics, and they arouse great interest because they form a bridge between bulk materials and atomic or molecular structures (Asadian et al. 2019; Saleh et al. 2019; Dutta and Das 2021; Shen et al. 2021; Laraib et al. 2022).

Nowadays, the development of sensitive and selective methods for determining and detecting compounds used to diagnose and treat many diseases that threaten human health is possible by integrating nanomaterials into sensors and creating nanosensors. Moreover, biosensors that contain a biological recognition element, such as an enzyme, antibody, or oligonucleotide, and transform the biochemical response resulting from the interaction of this element with the target molecule into a measurable physical signal also enable the development of sensitive and selective analytical methods (Nosrati et al. 2018; Huang et al. 2021a; Tahir et al. 2022; Younis et al. 2022).

To mention the immobilization of nanoparticles on the sensor surfaces, much more sensitive and selective analyses can be performed by expanding the surface area of the biomolecule-modified sensors and increasing their electrical conductivity. This chapter provides recent advancements, salient features, types, and uses of nanobiosensor to determine and detect several diseases.

2 Concept of Nanobiosensors

Sensors are electronic devices that record a physical, chemical, or biological change and convert these changes into a measurable signal. The sensor contains a recognition element that provides a selective response to a particular or group of analytes, thereby minimizing interference from other sample components. Another significant sensor component is the transducer or detector device that generates the signal. It is a signal processor (Balasubramanian and Burghard 2006; Simões and Xavier 2017; Raj and John 2018).

Living organisms have a high sensitivity feature beyond what is known; for example, it has been reported that dogs' sense of smell is 100,000 times more sensitive than humans, eels are sensitive enough to immediately detect a few drops of foreign matter added to tons of water, and algae are very sensitive to toxic substances in the literature (Yonzon et al. 2005; Sekhar and Wignes 2016). All living organisms immediately perceive the changes in their environment and strive to adapt to them to survive. The basis for the in vitro use of biosensors is based on this sensing mechanism.

Combining analysis systems with biological substances that make it possible to detect these stimuli in living things has led to the emergence of biosensors. In this way, while only anion and cation analyzes can be made with classical electrochemical methods, adding biomaterial to the system while preparing the sensor makes it possible to determine many substances (Fatima et al. 1986; Vaz et al. 2022).

While the device that determines and records a physical feature is defined as a sensor, the biosensor is defined as a sensor system that combines a biochemical component with a physicochemical converter. The task of a biosensor is to produce a continuous digital electrical signal proportional to the amount of an analyte. In biosensor systems, changes in physical size are measured by converting them to changes in electrical size. Examples of these changes are current, voltage, and temperature (Chandra 2013; Mahapatra et al. 2020; Nazare et al. 2021).

Generally, nanobiosensors consist of the analyte, bioreceptor, transducer combined with nanomaterials, and finally, detector. The analytes serve as a sample for analysis and/or detection of the respective bioreceptors. Next, a transducer coupled with nanomaterials converts the physiochemical response into an electrical signal. These signals can be measured as different responses such as current, electric potential, conductivity, density, impedance, phase of electromagnetic radiation, mass, temperature, and viscosity. Changes in these responses provide information for quantitative and qualitative determination of the analyte. Nanomaterial used in nanobiosensors act as an interlayer between the transducer and biological agents. The transducer is integrated with nanomaterials to create a nanobiosensor (Sharifi et al. 2020; Sellappan et al. 2022; Thakur and Sankar 2022). The schematic diagram for the basic principle of nanobiosensors is presented in Fig. 29.1.

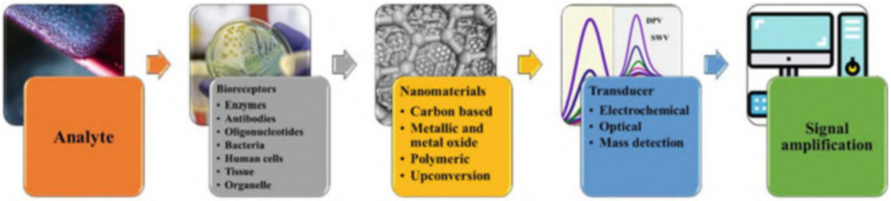

Fig. 29.1 Schematic representation of the nanobiosensors

2.1 Ideal Features of Nanobiosensors

There are main features that an ideal nanobiosensor should have for precise and sensitive determinations. Linearity must be wide enough to detect high analyte concentrations. It should be sufficiently sensitive depending on the analyte concentration exhibiting high selectivity to obtain reliable results. The time to achieve 95% of the total response should be as short as possible. Properties such as biocompatibility, stability at usual storage circumstances, and stabilizability also contribute to the high specificity of nanobiosensors towards the analyte. Nanobiosensors must be distinct and unrestrained of any physical factors such as agitation, pH, etc. In addition, the nanobiosensor designed as a disposable sensing platform is another important feature that attracts users for on-site analysis (Malik et al. 2013; Chamorro-Garcia and Merkoçi 2016; Mahato et al. 2018b).

2.2 Components of Nanobiosensors

Incorporating nanomaterials into biosensors has demonstrated remarkable benefits over conventional sensors and/or last-generation biosensors. These benefits include a relatively higher sensitivity due to a somewhat larger surface area, shorter response time, faster electron transfer capability, high stability, and a long lifetime. Therefore, it is not correct to completely separate the term nanobiosensor or its components from biosensor systems. As with the biosensor, the nanobiosensor has three essential elements: bioreceptor (sensing probe), transducer coupled with nanomaterials, and signal amplification (Parolo and Merkoçi 2013; Srivastava et al. 2018; Gajdosova et al. 2020).

As the first component, bioreceptors are biological components that can capture or interact with the target analyte and respond according to the interaction. Tissues, bacteriophages, proteins, microorganisms, organelles, human cells, nucleic acids, enzymes, and antibodies are the most commonly used biological components to produce nanobiosensors. As the second component, the transducer acts as an interface. It measures external or physical changes, interacts with bioreceptors, and then converts the changes in energy levels into a measurable electrical signal at the detector. Detector elements collect the signals from the transducer and transmit these signals to a microprocessor for analysis.

Moreover, nanobiosensors are a concept that emerged by combining nanomaterials with transducers. Therefore, nanomaterials exhibit a significant role in the current and future advancements of nanobiosensors. Nanomaterials have unique properties such as being more robust, lighter, cheaper, more durable, and sensitive. Common nanomaterials, used in nanobiosensor design, are metallic nanoparticles, carbon nanotubes, magnetic nanoparticles, quantum dots, polymeric nanomaterials, etc. These properties also make nanomaterials attractive in the fabrication of nanobiosensors (Park et al. 2016; Mishra and Rajakumari 2018; Bozal-Palabiyik et al. 2021; Krzyczmonik et al. 2021; Pérez et al. 2021).

Biosensors can be classified according to the types of bioreceptor such as DNA, enzyme or antibody-based, as well as transducer types such as electrochemical, optical, microwave, and mass-based (Chamorro-Garcia and Merkoçi 2016; Thakur and Sankar 2022). Within the scope of this handbook, electrochemical nanobiosensor designs are classified according to bioreceptor type, and information about their structures and their use in the diagnosis of various diseases is presented in this chapter.

2.3 Nanobiosensors for Diagnosis of Disease

In enzyme-based nanobiosensors, enzymes are adsorbed onto electrode surfaces using various immobilization techniques, either by van der Waals force or by chemical bonding. The enzyme and its associated substrate interact on the surface, where the enzyme acts as a biorecognition element with outstanding catalytic properties. The biochemical reactions between enzyme and substrate rely specifically on the biospecificity of enzymes. Monitoring the changes occurring due to the response makes it possible to produce nanobiosensors that offer compassionate, specific, selective, stable, and reproducible results (Yang 2012; Das et al. 2016; Kurbanoglu et al. 2020).

Since the concept of biosensors was introduced by Clark and Lyons in 1962 to measure glucose levels, glucose sensors still maintain their importance today. Because real-time glucose determination in various body fluids is essential to manage the progression of diabetes, one of the most important diseases of our age (Fracchiolla et al. 2013). In their study, Kausaite-Minkstimiene et al. designed a novel amperometric glucose nanobiosensor using a nanobiocomposite consisting of poly(1,10-phenanthroline-5,6-dione) (PPD), poly(pyrrole-2-carboxylic acid) (PPCA), gold nanoparticles (Au NPs), and glucose oxidase (GOx). In this study, firstly, the graphite rod (GR) electrode is a working electrode subjected to the cleaning procedures. Then, PD was dropped to the electrode surface, and electrodeposition using cyclic voltammetry (CV) was performed to obtain PPD/GR electrode. As a second step, Au NPs-entrapped PPCA ((Au NPs)PPCA) layers were created using electrodeposition. To prepare an enzyme-based sensor, (Au NPs)PPCA/PPD/GR electrode was modified with the GOx, and in this study, a mixture of EDC and NHS was used for covalent coupling of GOx to the modified surface. Before amperometric measurements, GOx-(Au NPs)PPCA/PPD/GR electrode was washed and left to dry at room temperature. Choosing electrochemical polymerization and immobilization conditions is one of the most critical steps of enzyme-based sensors to achieve the best analyte response. Because the number of potential scan cycles and the scan rate directly affect the polymeric layer formation and the immobilization of the relevant enzyme on the modified surface. For this study, different ranges were investigated, and the most suitable potential scan cycles were found to be ten and the optimal scan rate to be 100 mV/s. Also, as metallic NPs, Au NPs can improve the analytical signal through their ability to facilitate electron transfer. As a result of the experiments, when 0.15 nM Au NPs concentration was used, the (Au NPs)PPCA layer became more porous and provided a much larger surface area. After optimizing the experimental conditions, the developed enzyme sensor exhibited a wide linear range from 0.20 until 500.0 mM with a relatively low detection limit (LOD) of 0.08 mM for glucose. Furthermore, the designed sensor was highly selectively used for glucose detection in human serum (Kausaite-Minkstimiene et al. 2020).

Nowadays, the great development and commercial success of smartphones, tablets, and smartwatches have brought practical usability in many areas. Moreover, comprehensive digitization also contributes to point-of-care testing (POCT). These trends have the advantage of significantly reducing the extended analysis time compared to traditional analysis methods performed in the laboratory and are an alternative to the complex testing system that delays the ability to the worse conditions of patients (Soni and Jha 2017; Xu et al. 2018). In their work, Jędrzak et al. developed a fast, simple, and mobile smartphone-based nanobiosensor with the potential for glucose measurement in diabetic patients (Fig. 29.2). In this study, $FeCl_3 \cdot 6H_2O$ and $FeCl_2 \cdot 4H_2O$ were used to prepare magnetite nanoparticles via the

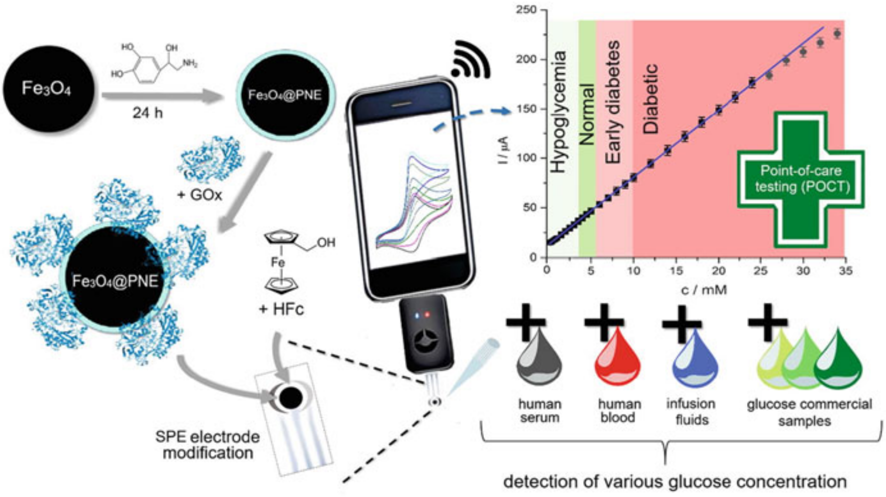
Fe3O4
HO
OH
NH2
HO
24 h
Fe3O4@PNE
+ GOx
Fe3O4@PNE
OH
Fe
+ HFc
SPE electrode modification
250
200
150
100
50
0
I / μA
Hypoglycemia
Normal
Early diabetes
Diabetic
0
5
10
15
20
25
30
35
c / mM
Point-of-care testing (POCT)
human serum
human blood
infusion fluids
glucose commercial samples
detection of various glucose concentration

Fig. 29.2 Schematic illustration of the developed sensor. (Reprinted with permission from Jędrzak et al. (2022))

coprecipitation method. In the second step, magnetite nanoparticles were added to the TRIS buffer solution, and after obtaining a homogeneous mixture, norepinephrine solution was added to this solution. Finally, Fe_3O_4@PNE hybrid material was obtained for surface modification. The optimal amount of Fe_3O_4@PNE and glucose oxidase were mixed in the citric buffer to fabricate the enzyme-based nanosensor. As the next step, 1 μL of the Fe_3O_4@PNE -GOx was deposited on the screen-printed electrode (SPE) surface and dried at room temperature. Quinones or the amino groups in the Fe_3O_4@PNE nanosensor supported the creation of hydrogen bonds between GOx molecules and Fe_3O_4@PNE. Therefore, it can be said that Fe_3O_4@PNE nanoplatform exhibited a higher capability of GOx immobilization on the surface. After completing the electrochemical and surface characterizations, the designed sensor showed a linear concentration range of 0.2–24 mM and a LOD of 6.1 μM. In addition, the developed sensor exhibited long-term stability for 20 weeks. Finally, the developed sensor could be a valuable platform for POCT by a smartphone and potentiostat. Moreover, the developed sensor as a promising POCT biosensor could detect glucose content in human serum and human blood samples (Jędrzak et al. 2022).

In 2020, Eom et al. proposed an enzyme-based electrochemical nanobiosensor for the rapid and accurate detection of cholesterol in saliva samples of hyperlipidemia patients. The flexible electrode was first prepared using polyimide as a working electrode in this study. Platinum nano-cluster (Pt-NC) was electroplated on the surface by potentiostatic mode(−200 mV, 200 s) to modify the electrode surface. The procedure was carried out separately from 1 to 5 times at 100 s intervals. The optimum amount of cholesterol oxidase, cholesterol esterase, and peroxidase were mixed with fabricating an enzyme-based sensor. Subsequently, 15 μL of the enzyme mixture as an optimal amount was dropped on the modified Pt-NC electrode surface. Finally, Nafion was coated on the enzyme-modified surface and dried at ambient temperature to use in the determination of cholesterol. After morphological, topographical, and electrochemical characterization, the proposed sensor showed a more comprehensive concentration range from 2 μM to 486 μM and a LOD of 2 μM. Here, saliva samples were obtained from three hyperlipidemia patients to investigate of the feasibility of an advanced Pt-NC/enzyme/Nafion sensor using amperometric measurements. The received responses showed that a developed sensor can be utilized to determine cholesterol in saliva immediately without pretreating procedures (Eom et al. 2020).

In a study conducted in 2021, Rahimi-Mohseni et al. developed an enzyme-based sensor to detect phenylketonuria (PKU), a congenital disease that occurs in 1 out of every 10,000 newborns. This sensor is based on zinc oxide (ZnO) nanorods, Au NPs, and enzyme phenylalanine hydroxylase (PHA) available in the extract of mosses leaf-like tissue. In this study, firstly, a graphite screen-printed electrode (GSPE) was covered with ZnO nanorods, then this surface was covered by Au NPs. Finally, the moss extract and potassium ferricyanide were coated onto the modified surface. Differential pulse (DP) voltammograms were recorded in phosphate buffer solution (PBS) as supporting electrolytes to perform the electrochemical measurements. When ZnO@Au nanohybrid was covered on the surface of GSPE, the current value was increased, and the ΔE_p value decreased. This phenomenon is due to the electron transfer ability and catalytic activity of ZnO@Au nanohybrid. To investigate surface characterization, field emission scanning electron microscopy (FE-SEM) images of the bare GSPE, ZnO/GSPE, ZnO@Au/GSPE, and ZnO@Au nanohybrid/mosses extract modified GSPE was recorded. Figure 29.3a showed the entire GSPE surface, while Fig. 29.3b showed the presence of ZnO nanorods on the electrode surface. The presence of ZnOs allowed increasing the performance of the developed biosensor due to its small size and high specific surface area. Figure 29.3c showed that Au nanoparticles as shine sphere were dispersed on the ZnO nanorods modified surface.

Moreover, this structure confirmed the successful synthesis of the nanohybrid. Thanks to the changed surface morphology, Fig. 29.3d confirmed the presence of the enzyme layer on the surface of ZnO@Au/GSPE. In addition, the simultaneous presence of Zn, O, and Au on the developed surface was confirmed by energy-dispersive X-ray spectroscopy (EDX) analysis. Under the optimum working conditions, the detection range of 5.0 nM to 100 µM with a LOD of 3.0 nM was obtained.

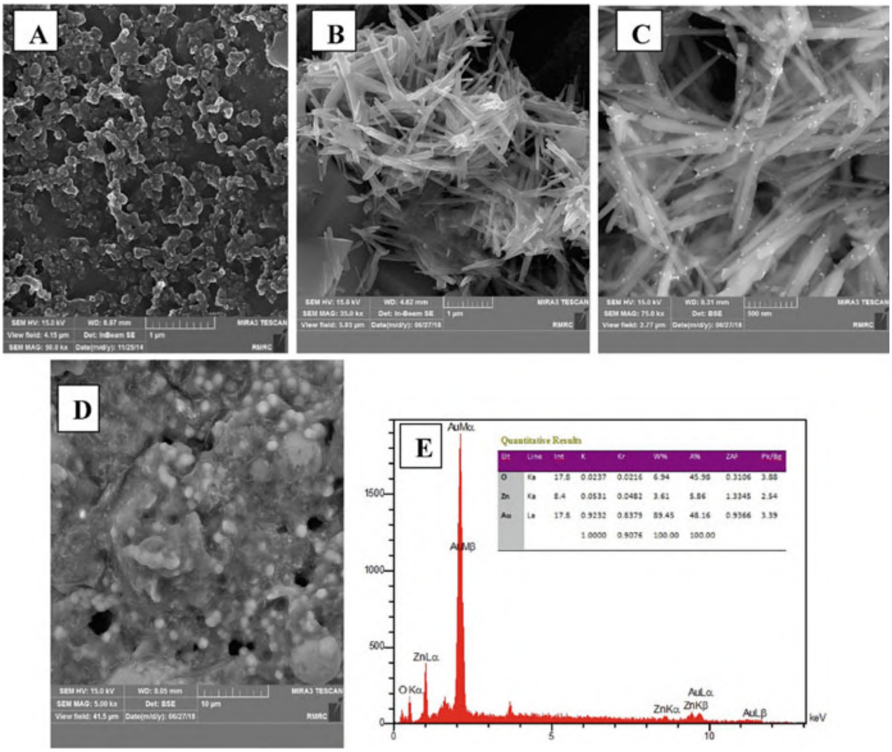

Quantitative Results

Elt	Line	Int	K	Kr	W%	A%	ZAF	Pk/Bg
O	Ka	17.8	0.0237	0.0216	6.94	45.98	0.3106	3.88
Zn	Ka	8.4	0.0531	0.0482	3.61	5.86	1.3348	2.54
Au	La	17.8	0.9232	0.8379	89.45	48.16	0.9366	3.39
			1.0000	0.9076	100.00	100.00		

Fig. 29.3 FE-SEM images of bare GSPE (**a**) ZnO nanorods/GSPE (**b**), ZnO@Au nanohybrid/GSPE (**c**), ZnO@Au nanohybrid/mosses leaf-like extract/GSPE (**d**), and EDX of ZnO@Au nanohybrid (**e**). (Reprinted with permission from Rahimi-Mohseni et al. (2021))

Furthermore, the proposed nanobiosensor was successfully applied to determine phenylalanine in the human blood serum samples (Rahimi-Mohseni et al. 2021).

Deoxyribonucleic acid (DNA)-based biosensors, which serve as oligonucleotides as another biological molecule, can be used to allow a single-chain nucleic acid molecule to define and bind its complementary strand in samples. The interaction mechanism is based on stable hydrogen bonds between the two nucleic acid strands. As seen in many different applications, DNA-based sensors exhibit several advantages. Because synthesis procedures contain simple steps, these sensors allow fast on-site analysis. Moreover, these sensors are simple, quick, and precise, used for surgical, forensic, environmental, and pharmaceutical applications (Oliveira Brett 2005; Abu-Salah et al. 2010, 2015).

In 2021, Pareek et al. suggested a label-free DNA-based nanobiosensor platform to detect human papillomavirus (HPV). Here, the indium tin oxide (ITO) glass electrode was washed with acetic acid and distilled water. Then, chitosan (CHIT) capped Au NPs (ccAu NPs) were electrodeposited on the surface of ITO by the CV method. Further, probe DNA (PDNA) was coated on the ccAu NPs modified ITO electrode, and subsequently, HPV-16 target DNA (TDNA) at different concentrations was immobilized on the probe-modified surface. When the ITO surface was modified with ccAu NPs, due to the conductive properties of ccAu NPs, electron transfer was facilitated, and a suitable surface was obtained for the binding of PDNAs. Under optimal conditions, the linear concentration range from 1 pM to 1 μM and a LOD of 1 pM was found to detect HPV-16. Moreover, the long stability and selectivity of the developed sensor have also shown that it can be a suitable platform for detecting HPV-16 from clinical samples (Pareek et al. 2021).

DNA-based sensors have many advantages in determining disease genes as well as drugs, proteins, or biomarkers. In their study, Zhang et al. developed an electrochemical DNA biosensor using carbon dots (CDs) and graphene oxide (GO) to detect PML/RARα fusion gene. This gene is essential for the early clinical diagnosis of acute promyelocytic leukemia (APL). In this study, the bare glassy carbon electrode (GCE) was rinsed with alumina polishing suspension and distilled water, respectively. Then, the optimal amount of CDs/GO nanocomposites was dropped on the GCE surface and dried at 60 °C. Secondly, the prepared electrode was immersed in PBS containing EDC and NHS. Afterward, the capture probe DNA was incubated on the CDs/GO/GCE at room temperature. At the final step, methylene blue (MB) and complementary sequences of DNA solution were immobilized on the surface to construct a measurement sensor. After the prepared sensor was rinsed with TE buffer, DP voltammograms were recorded to detect PML/RARα fusion gene. Moreover, electrochemical results showed that the excellent conductivity of CDs and the large surface area of GO provided faster electron transfer to enhance the hybridization efficiency of DNA. After experimental conditions such as accumulation time of MB, hybridization time of DNA and hybridization temperature were optimized, the linear detection range from 2.50×10^{-10} M to 2.25×10^{-9} M with a LOD of 83 pM was obtained for use in clinical diagnostic assays (Zhang et al. 2021).

Nowadays, peptides have recently been used as potential antifouling materials due to their unique properties such as easily synthesized processes, cost-effectiveness, biocompatibility, and tunable or modifiable structures. Peptides have the same chemical structures as proteins. However, they have shorter lengths of peptide bonds than proteins. Peptides are also formed by natural or synthetic short polymers of amino acids linked by these bonds. Artificial peptides can be synthesized via standard solid-phase synthesis protocols by screening from the peptide library to provide a specific sequence. In addition, the peptides exhibit many other advantages, including high stability, standard synthetic protocol, easy modification, and outstanding chemical versatility. Therefore, they are ideal molecules as biorecognition elements in biosensors (Liu et al. 2015; Barbosa et al. 2018; Karimzadeh et al. 2018).

In 2020, Hui et al. proposed a novel biosensor based on specifically designed antifouling peptides and a signal amplification strategy to determine prostate-specific antigen (PSA) in human serum samples. As shown in Fig. 29.4, first, the surface of GCE was cleaned. A mixture of poly(ethylene glycol) (PEG) and poly(3,4-ethylene dioxythiophene) (PEDOT) nanocomposites was electrodeposited on the GCE surface by CV. The second step covered the PEG/PEDOT/GCE with the solution, including streptavidin, NHS, and EDC. To develop a peptide-based sensor, self-designed biotin-labeled peptides (Pep1, biotin-PPPPEKEKEKE, and Pep2, biotin-PPPPEKEKEKEHSSKLQC) were synthesized. The mixed solution of the two kinds of peptides was immobilized onto the PEG/PEDOT/GCE surface. This

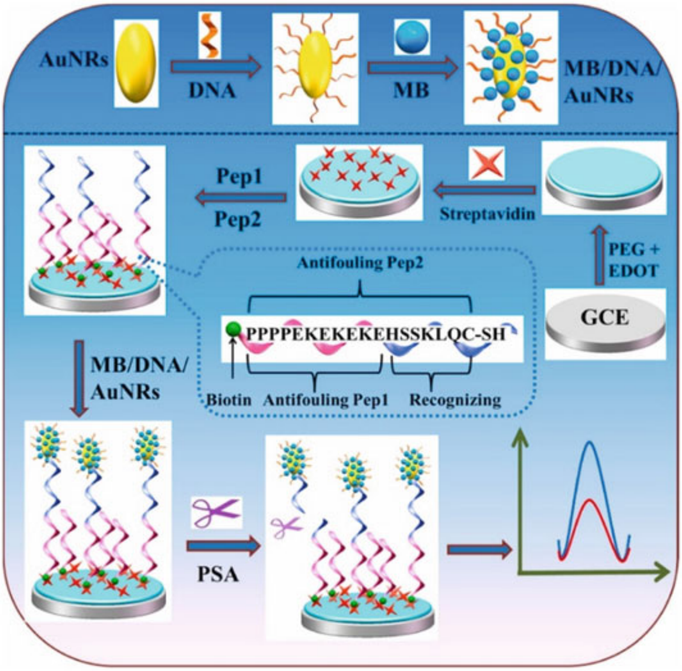

Fig. 29.4 Schematic diagram and working principle of the antifouling electrochemical biosensor. (Reprinted with permission from Hui et al. (2022))

immobilization was based on the strong interaction between biotin and streptavidin. As a signal amplifier, DNA/Au NRs solution was covered onto the Pep/PEG/PEDOT/GCE, and adsorption of MB onto DNA/Au NRs was performed. Before all the electrochemical measurements, the modified surface was immobilized with PSA, and DPV responses were recorded. After the optimum conditions were determined, the developed nanobiosensor showed a wide concentration range from 0.10 pg mL^{-1} to 10.0 ng mL^{-1} with a LOD of 0.035 pg mL^{-1}. Moreover, the developed biosensor was successfully used to determine PSA in human serum samples (Hui et al. 2022).

In their study, Song et al. developed an efficient and simple antifouling biosensor for detecting human immunoglobulin G (IgG) using a Y-shaped peptide constructed with two branches. EKEKEKE and HWRGWVA as peptide sequences were synthesized for antifouling. The bare GCE surface was polished and rinsed before surface modification in this study. To construct modified GCE/PEDOT-citrate surface, electrochemical deposition was performed using a mixed solution consisting of EDOT and sodium citrate. Afterward, GCE/PEDOT-citrate surface was covered with Au NPs by electrodeposition. The PEDOT-citrate/Au NPs modified surface was covered with a Y-shaped peptide solution in the final stage. The developed biosensor was soaked in IgG solutions at room conditions for 90 min; then, measurements were performed. The electrode characterizations showed that unmodified GCE had a higher current value than GCE/PEDOT-citrate. While this indicated the presence of PEDOT-citrate on the GCE surface, it was due to the charge repulsive interaction between negatively charged PEDOT-citrate and negatively $[Fe(CN)_6]^{3-/4-}$ molecules. After the GCE/PEDOT-citrate surface was coated with Au NPs, the excellent electrical conductivity of Au NPs increased the current signal. Under the optimal experimental conditions, it was observed that as the human IgG concentration increased, the DPV current signals decreased. Moreover, reductions in current signals were observed since the redox molecules inhibit electron transfer after the prepared nanosensor was covered with the Y-shaped peptides and unique IgG molecule. The developed sensor exhibited a linear concentration range from 0.1 to 10,000 ng mL^{-1}. The LOD was estimated to be 0.032 ng mL^{-1}. Moreover, the designed sensor was successfully used to detect IgG in clinical human serum samples (Chen et al. 2021).

Very recently, other examples of peptide-based nanobiosensors were proposed to detect trypsin (Lin et al. 2018), epidermal growth factor receptor (EGFR) (Li et al. 2013), human chorionic gonadotropin (hCG) (Xia et al. 2017), human norovirus (Hwang et al. 2017), and miRNA-21 (Kangkamano et al. 2018). The nanomaterials and composites used in these sensors exhibited several advantages: high electrical conductivity, large surface area and mechanical strength, high selectivity, chemical stabilization, and good electron interaction characteristics. These facts led to the evolution of electrochemical nanobiosensors with good sensitivity, a wide linear concentration range, and low LOD values.

Immunosensors are affinity-ligand-based biosensors in which antibodies are used as bio-components, and the antibody-antigen interaction is monitored with a suitable transducer. The main feature of all immunosensors is their specificity resulting from molecular recognition of antigens by antibodies to form a stable complex (Mahato et al. 2018a). Electrochemical immunosensors based on the specificity of antigen-antibody interactions by an electrochemical conversion are the most preferred because of their advantages such as cost, simplicity, sensitivity, miniaturization properties, and rapid analytical response (Pei et al. 2013; Karunakaran et al. 2015; Felix and Angnes 2018). Especially label-free immunosensors are preferred in immunoassay systems due to their potential simplicity and affordability. In 2022, Wu et al. developed a label-free sensor based on multilayer nanocomposite modification of ordered mesoporous carbon (CMK-3), Au NPs, ferrocene carboxylic acid (Fc), magnesium (Mg), aluminum (Al), and layered double hydroxide (LDHs) materials for the detection of cancer antigen 125 (CA125), which is a biomarker for the diagnosis of ovarian cancer. In this study, preparation of a modified sensor was designed by layer-by-layer (LBL) self-assembly by electrostatic attraction, as shown in Fig. 29.5. Firstly, the GCE surface was polished and rinsed with ethanol, hydrochloric acid, and deionized water. Then, 1 mg mL^{-1} of CMK-3 was dropped onto the GCE surface, and Au NPs were coated on the CMK-3 modified electrode. Finally, CMK-3(Au/Fc@MgAl-LDH)n multilayer nanocomposites were obtained using repeating the modification process with Au NPs and Fc@MgAl-LDH with the optimal number of n cycles. To prepare immunosensor, glutaraldehyde (GA) as a crosslinking agent was immobilized on the modified electrode to bind carboxyl (-COOH) of Fc and amino (-NH$_2$) of antibody. Afterward, 1 mg mL^{-1} antibody

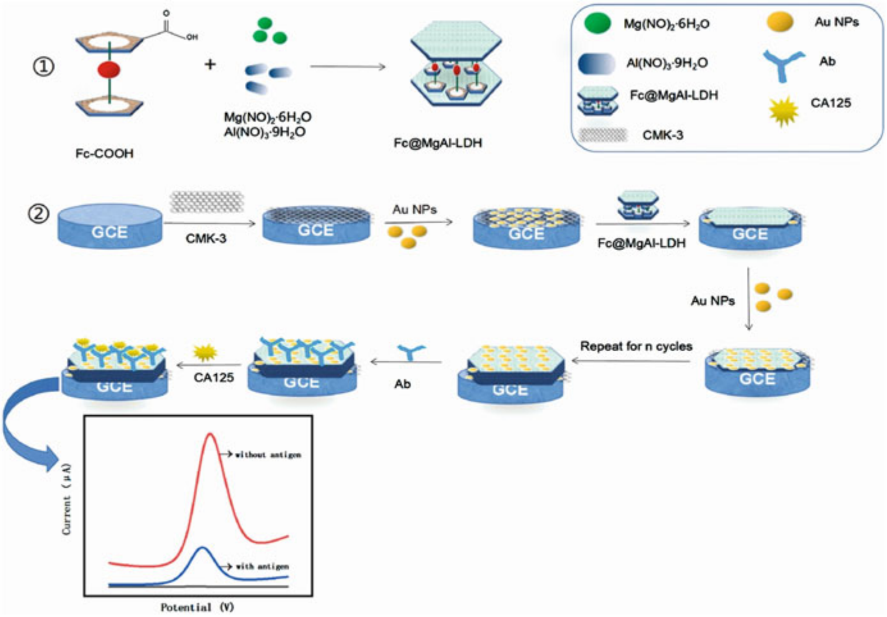
①
Fc-COOH
+
Mg(NO)₂·6H₂O
Al(NO)₃·9H₂O
Fc@MgAl-LDH
Mg(NO)₂·6H₂O
Au NPs
Al(NO)₃·9H₂O
Ab
Fc@MgAl-LDH
CA125
CMK-3
②
GCE
CMK-3
Au NPs
Fc@MgAl-LDH
Repeat for n cycles
Ab
CA125
without antigen
with antigen
Current (μA)
Potential (V)

Fig. 29.5 Schematic of the proposed electrochemical immunosensor. (Reprinted with permission from Wu et al. (2022))

(Ab) solution was dropped onto the modified surface, and the unbound antibody was cleaned with the 0.01 M PBS (pH 7.0) solution. Subsequently, bovine serum albumin (BSA) solution was dropped onto the antibody-modified surface to prevent nonspecific binds. CA125 was immobilized on the modified sensor in the last step to perform DPV measurements. Electrochemical impedance spectroscopy (EIS) was used for the electrochemical characterization of the prepared sensors. The resistance was reduced when the GCE surface was modified with CMK-3(Au/Fc@MgAl-LDH)n nanocomposites. These results provided that the CMK-3(Au/Fc@MgAl-LDH)n were immobilized successfully onto the electrode surface. When the antibody, BSA, and antigen were gradually immobilized on the modified surface, the electrochemical resistance gradually increased due to the rejection of the idioelectric proteins during electronic transfer. These increases demonstrated the successful modification of antibody, BSA, and antigen to the electrode surfaces. In addition, the CV measurements performed also showed the results that nanomaterials and biological samples were surface modified, consistent with the EIS results. Under optimal conditions, the developed immunosensor showed a linear concentration range between 0.01 U mL^{-1} and 1000 U mL^{-1} with a LOD of 0.004 U mL^{-1}. Furthermore, the developed immunosensor, which exhibited long-term stability, provided the utility of accurate detection of CA125 in clinical cancer diagnosis (Wu et al. 2022).

In 2021, a novel label-free electrochemical immunosensor to detect carcinoembryonic antigen (CEA) that serves as a tumor marker using reduced graphene oxide (rGO) was proposed by Jozghorbani et al. In this study, first GCE was rinsed with deionized water, and then rGO was dropped onto the GCE surface and dried at 60 °C. Then, the EDC/NHS solution containing 20 mg mL^{-1} of EDC and 10 mg mL^{-1} of NHS was coated on the rGO/GCE surface. 20 mg mL^{-1} antibody was immobilized on the modified sensor, and this electrode was rinsed with PBS to remove non-covalently bound antibodies. BSA was dropped on the antibody-modified surface to block nonspecific sites, and the electrode surface was rinsed with PBS several times. After optimum parameters, pH, incubation time, and anti-CEA concentration were determined, increasing concentrations of CEA were measured using the developed sensor. The developed immunosensor exhibited a linear concentration-response in the range of 0.1–5 ng mL^{-1} with a LOD of 0.05 ng mL^{-1} for the detection of CEA. The proposed immunosensor was evaluated to detect CEA in the human blood serum samples. Moreover, the obtained results were compared with the standard enzyme-linked immunosorbent assay (ELISA) method (Jozghorbani et al. 2021).

In the case of the nanomaterials and nanocomposites, Au NPs (Carneiro et al. 2017), trimetallic NPs composed of palladium, platinum, and copper (Zhao et al. 2022), metal oxide NPs such as TiO_2 NPs (Shawky and El-Tohamy 2021), and also polymeric materials including polyethyleneimine and chitosan (Li et al. 2021; Shanbhag et al. 2021) supported suitable surfaces to achieve high performance of detection of diseases biomarkers. In particular, the conductivity and biocompatibility of these materials have provided advantages by creating excellent synergetic effects between materials.

In terms of human health, the need for compassionate and specific analysis methods to diagnose a biomarker or related diseases cannot be ignored. Nowadays, sensitive determination of particular analytes in complex samples can be enhanced by using sandwich or labeled methods. In these methods, the analyte binds to the primary antibodies (captured antibodies) followed by labeled secondary antibodies (detection antibodies) (Pei et al. 2013; Ilkhani et al. 2015). In 2020, Zhang et al. proposed a sandwich-type electrochemical immunosensor to detect the N-terminal B-type natriuretic peptide precursor (NT-proBNP) that serves as a diagnostic biomarker of heart failure. In this study, the GCE surface was polished and washed using alumina powder and ultrapure water. Then, Au NPs were electrodeposited onto the GCE using the CV method. Next, optimal amounts of Ab1, BSA, NT-proBNP, and Au@PdPt RTNs-Ab2 were immobilized on the modified electrode surface, respectively. Before each modification, the prepared electrodes were washed with PBS (pH 7.4). To investigate the developed immunosensors, EIS and CV methods were performed. As shown in Fig. 29.6a, when Au NPs were coated on the bare GCE, the diameter of the semicircle of Au NPs modified electrode decreased significantly compared to bare GCE (curves a and b). This decrease was due to the excellent conductivity of Au NPs. In addition, an increasing trend when the Au NPs modified electrode was modified with Ab1, BSA, NT-proBNP, and the Au@PdPt RTNs-Ab2 (curve c-f) layer by layer, respectively, was observed in the diameter of the semicircle. These increases were because the surface's biological materials significantly inhibited interfacial electron transfer efficiency. In Fig. 29.6b, cyclic voltammograms were presented; after the GCE was coated with Au NPs, the peak current of the redox solution increased significantly more. It was recorded that the peak current of the redox solution decreased when the modified surface was coated with Ab1, BSA, NT-proBNP, and Au@PdPt RTNs-Ab2, respectively. All the results observed in CV and EIS showed that each nanoparticle and biological material was influential in detecting NT-proBNP and successfully modified on the electrode

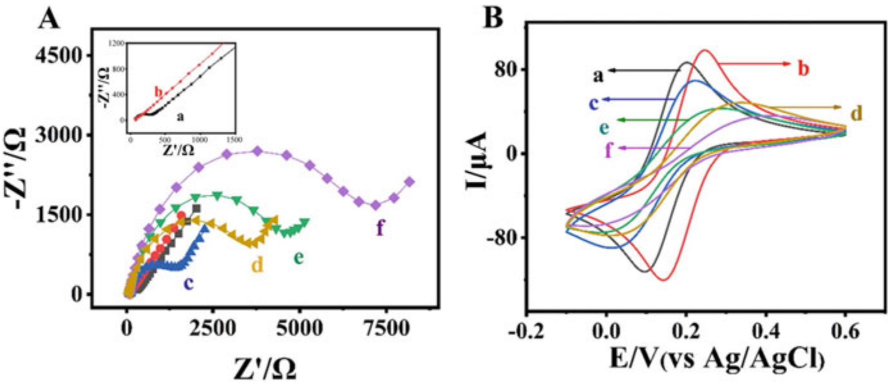

Fig. 29.6 (**a**) EIS and (**b**) CV of bare GCE (**a**), GCE/Au NPs (**b**), GCE/Au NPs/Ab1 (**c**), GCE/Au NPs/Ab1/BSA (**d**), GCE/Au NPs/Ab1/BSA/NT-proBNP (**e**), and GCE/Au NPs/Ab1/BSA/NT-proBNP/Au@PdPt RTNs-Ab2 (**f**). (Reprinted with permission from Zhang et al. (2022))

surfaces. Under optimized experimental conditions, the developed immunosensor showed a wide linear range from 0.1 pg mL^{-1} to 100 ng mL^{-1} and a LOD of 0.046 pg mL^{-1}. Moreover, the use of the developed immunosensor was confirmed by the detection of NT-proBNP in human serum samples (Zhang et al. 2022).

In their work, Yang et al. fabricated a sandwich-type electrochemical immunosensor for the effective detection of hepatitis B surface antigen (HBsAg) based on Au@Pd nanodendrites (NDs) functionalized MoO_2 nanosheets (NSs). Firstly, the GCE surface was polished and rinsed, and Ag NPs were coated on the GCE surface by electrodeposition. Subsequently, Ab1 dispersion was immobilized on the Ag NPs/GCE surface. After immobilization of BSA to the surface to block nonspecific binding sites, HBsAg was coated on this surface. Finally, an Ab2-label solution composed of Au@Pd NDs and amino-functionalized MoO_2 NSs was incubated on the modified surface. Au@Pd NDs/NH_2-MoO_2 NSs could catalyze hydrogen peroxide (H_2O_2) reduction effectively. Therefore, HBsAg analyzes were performed by following the current changes in the reduction of H_2O_2 at different concentrations. The current responses showed that NH_2-MoO_2 had a good catalytic capacity for HBsAg detection. Moreover, increased current responses confirmed that Au@Pd NDs/NH_2-MoO_2 NSs had the greater electrocatalytic performance. Under optimal conditions, the developed immunosensor offered a linear concentration range between 10 fg mL^{-1} and 100 ng mL^{-1} with a LOD of 3.3 fg mL^{-1} to detect of HBsAg. Moreover, the accuracy of the developed immunosensor was satisfactory, which confirmed that the immunosensor possessed an excellent application prospect in clinical samples (Yang et al. 2021).

Following the same trend observed for the nanomaterial-based enzyme, peptide, and label-free sensors, many researchers have reported that the modification of nanomaterials to construct labeled sensors has several advantages. As seen in the kinds of literature in these studies, nanoboxes (Cheng et al. 2021), nanorods (Zhang et al. 2020), metal-organic frameworks (Miao et al. 2019), flower-like NPs (Qian et al. 2019), and also three-dimensional composites (Liu et al. 2021) exhibited superior properties such as a large effective surface area and fast electron transport towards diseases and biomarkers detection.

Aptamers are synthetic strands of DNA or RNA produced by SELEX (systematic evolution of ligands by exponential enrichment). Aptamers can specifically attach to target molecules, cells, and proteins. In recent years, aptamers have provided several advantages such as tolerance to environmental conditions and more excellent stability, easier synthesis route, and more accessible storage than antibodies. Many researchers have suggested aptasensors to detect biomarkers due to the high sensitivity and specificity (Charbgoo et al. 2016; Zhou et al. 2016; Kim et al. 2020).

In their study, Negahdary et al. developed an electrochemical aptasensor to detect amyloid beta (Aβ) based on fern leaves-like Au nanostructure. The detection procedure is based on modifying the thiol-modified RNA aptamer sequence to the electrode surface by Au nanostructures and the binding between the specific aptamer sequence and Aβ. To detect Aβ by the aptasensor, after Aβ binding time was optimized, DP voltammograms were recorded by following redox peaks responses. After optimizing the experimental parameters, the developed aptasensor showed a linear concentration range of 0.002–1.28 ng mL^{-1} and a LOD of 0.4 pg mL^{-1} (88.6 amol L^{-1}). Moreover, the design was successfully used for the determination of Aβ in human blood serum and artificial cerebrospinal fluid samples (Negahdary and Heli 2019).

In another study, Wang et al. designed a sandwich-type aptasensor based on hollow mesoporous carbon spheres loaded with porous dendritic bimetallic Pd@Pt nanoparticles (Pd@Pt DNs) to detect of cardiac troponin I (cTnI). In this work, a screen-printed gold electrode (SPGE) was coated with a thiol-modified aptamer. After washing with MCH, which was used to block non-specific binding sites, cTnI was incubated on the surface to obtain the aptamer-CTnI complex. Then, Pd@Pt DNs/NH_2-HMCS/aptamer (with a different sequence) was dropped on the modified surface, and the developed aptasensor was washed for further use in the analysis. Electrochemical characterization results confirmed that the improvement of the dispersibility of Pt@Pd DNs and the synergistic catalysis between NH_2-HMCS and Pt@Pd DNs provide the more excellent electrocatalytic ability for the ultrasensitive detection of cTnI. To obtain the best performance of the developed aptasensor, the incubation time and concentration of the Pt@Pd DNs/NH_2-HMCS/aptamer label were optimized. Under optimum working conditions, the proposed aptasensor exhibited a linear concentration range from 0.1 pg mL^{-1} to 100.0 ng mL^{-1} and a LOD of 15.4 fg mL^{-1} for cTnI detection. Moreover, the aptasensor was successfully used for cTnI detection in human serum samples (Wang et al. 2021).

Aptamer sequences designed specifically for different molecules such as proteins, biomarkers, and pesticides can also be designed for bacteria. In 2020, a novel aptasensor based on quantum dots and metal oxide NPs was developed by Ghalkhani et al., for the sensitive detection of *Staphylococcus aureus* bacterium (*S. aureus*) that can generate several human infections such as pseudomembranous enteritis, respiratory, and some systemic diseases. In this work, firstly, a nanocomposite composed of silver (Ag) NPs chitosan (Cs), graphene quantum dots (Gr QDs), and nitrogen-doped TiO_2 NPs ($NTiO_2$) was prepared, and then, SPCE surface was modified by this nanocomposite. After the thiol functionalized DNA aptamer was immobilized on the modified electrode, *S. aureus* was immobilized on the aptasensor surface. The experimental conditions were optimized by the pH of the nanocomposite solution and incubation time of bacterium species. According to the obtained DPV responses, the designed aptasensor displayed the linear concentration range of $10–5 \times 10^8$ CFU mL^{-1} with a LOD of 3.3 CFU mL^{-1}. Furthermore, the developed aptasensor was also suitable for human serum samples containing *S. aureus* (Ghalkhani et al. 2022).

In general, the potential for some molecules to bind to aptamers from two different binding sites has been reported; therefore, most sandwich-type sensors have focused on conventionally used antibody-based immunoassays or assay methods using aptamer-antibody pairs to increase sensitivity and selectivity (Huang et al. 2021b; Centane and Nyokong 2022). In their study, Chung et al. designed a magnetic force-assisted sandwich-type sensor for the sensitive detection of thrombin. This study is based on biotinylated thrombin Ab, aptamer with functionalized conducting polymer (poly-(2,2′:5′,5″-terthiophene-3′-p-benzoic acid) (pTBA)), and streptavidin-starch modified magnetic nanoparticle (MNP) combined with toluidine blue O (TBO). The characterization of probe molecules and modified sensor surface was investigated by CV, EIS, X-ray photoelectron spectroscopy (XPS), and UV–VIS spectroscopy. All results indicated that the prepared probe molecules and modified sensors were suitable materials and platforms to detect thrombin. To obtain the best sensor response, the effect of pH, binding times of thrombin and MNP@Ab-TBO, removal time of unbound bioconjugates, and applied potential were investigated. After the optimum conditions were provided, the linear concentration range was found between 1.0 and 500 nM with a LOD of 0.49 nM. Moreover, the recovery experiment results demonstrated that the proposed sensor could detect thrombin in human serum (Chung et al. 2018).

To sum up, when designing the aptamer-based sensors, studies primarily provided quick analysis, higher sensitivity, selectivity, and cost-effectiveness in recent years to detect diseases and biomarkers (Zhang et al. 2019; Erkmen et al. 2022; Farahani et al. 2022; Sun et al. 2022).

3 Conclusion

Integrating nanotechnology into sensor systems and using it in this field offers the chance to improve the performance of nanobiosensors, which are used as sensitive methods, especially in the early diagnosis of diseases. As the most crucial component of nanobiosensors, different nanomaterials such as metallic nanoparticles, carbon-based nanomaterials, polymeric nanostructures, magnetic nanomaterials, quantum dots, nanowire, or nanomembrane structures provide advanced superiority by being integrated into systems for biosensing. These materials facilitate the immobilization of biological materials added to the surfaces due to their large surface-to-volume ratios while at the same time facilitating electron transfer thanks to their conductors; they provide high sensitivity and allow them to be excellent candidates for the nanobiosensors designs. In addition, the affinity between a bioreceptor molecule such as enzyme, peptide, antibody, and aptamer and target analytes such as protein, biomarker, or gene undoubtedly provides extraordinary sensitivity, high specificity, and selectivity. Compared to traditional methods such as chromatographic and spectroscopic methods, which require a time-consuming, large amount of organic solvents, and the use of toxic chemicals, nanobiosensors are quick, sensitive, and selective analytical tools for the diagnosis of several diseases. The different features of nanobiosensors such as accuracy, reproducibility, dynamic capacity change, and sensitivity to environmental changes such as pressure, pH, and temperature make them excellent analytical tools for diagnosing diseases. However, more awareness is needed regarding the advancement of nanobiosensors in commercial applications. In the future, nanobiosensors can be integrated into smart devices and remotely controlled systems with various techniques. Multipurpose use, such as the simultaneous detection of different biomarkers, can be improved with cost-effectively designed biochips. Furthermore, in these developments, self-propelled sensors such as micromotors or microconsoles can contribute to the applications of nanobiosensors.

References

Abu-Salah KM, Ansari AA, Alrokayan SA (2010) DNA-based applications in nanobiotechnology. J Biomed Biotechnol 2010:715295

Abu-Salah KM, Zourob MM, Mouffouk F, Alrokayan SA, Alaamery MA, Ansari AA (2015) DNA-based nanobiosensors as an emerging platform for detection of disease. Sensors (Switzerland) 15(6):14539–14568

Asadian E, Ghalkhani M, Shahrokhian S (2019) Electrochemical sensing based on carbon nanoparticles: a review. Sensors Actuators B Chem 293(April):183–209

Balasubramanian K, Burghard M (2006) Biosensors based on carbon nanotubes. Anal Bioanal Chem 385(3):452–468

Barbosa AJM, Oliveira AR, Roque ACA (2018) Protein- and peptide-based biosensors in artificial olfaction. Trends Biotechnol 36(12):1244–1258

Bozal-Palabiyik B, Kurbanoglu S, Erkmen C, Uslu B (2021) Future prospects and concluding remarks for electroanalytical applications of quantum dots. In: Electroanalytical applications of quantum dot-based biosensors. Elsevier Inc, pp 427–450

Carneiro P, Loureiro J, Delerue-Matos C, Morais S, do Carmo Pereira M (2017) Alzheimer's disease: development of a sensitive label-free electrochemical immunosensor for detection of amyloid beta peptide. Sensors Actuators B Chem 239:157–165

Centane S, Nyokong T (2022) Aptamer versus antibody as probes for the impedimetric biosensor for human epidermal growth factor receptor. J Inorg Biochem 230:111764

Chamorro-Garcia A, Merkoçi A (2016) Nanobiosensors in diagnostics. Nanobiomedicine 3:1–26

Chandra P (2013) HER2 protein biomarker based sensor systems for breast cancer diagnosis. J Mol Biomark Diagn 5(1):1000e119

Charbgoo F, Soltani F, Taghdisi SM, Abnous K, Ramezani M (2016) Nanoparticles application in high sensitive aptasensor design. TrAC – Trends Anal Chem 85:85–97

Chen M, Song Z, Han R, Li Y, Luo X (2021) Low fouling electrochemical biosensors based on designed Y-shaped peptides with antifouling and recognizing branches for the detection of IgG in human serum. Biosens Bioelectron 178:113016

Cheng Q, Feng J, Wu T, Guo Y, Sun X, Ren X, Lee JY, Liu L, Wei Q (2021) Hollow performances quenching label of Au NPs@CoSnO3 nanoboxes-based sandwich photoelectrochemical immunosensor for sensitive CYFRA 21-1 detection. Talanta 233:122552

Chung S, Moon JM, Choi J, Hwang H, Shim YB (2018) Magnetic force assisted electrochemical sensor for the detection of thrombin with aptamer-antibody sandwich formation. Biosens Bioelectron 117:480–486

Das P, Das M, Chinnadayyala SR, Singha IM, Goswami P (2016) Recent advances on developing 3rd generation enzyme electrode for biosensor applications. Biosens Bioelectron 79:386–397

Dutta D, Das BM (2021) Scope of green nanotechnology towards amalgamation of green chemistry for cleaner environment: a review on synthesis and applications of green nanoparticles. Environ Nanotechnol Monit Manag 15:100418

Eom KS, Lee YJ, Seo HW, Kang JY, Shim JS, Lee SH (2020) Sensitive and non-invasive cholesterol determination in saliva: via optimization of enzyme loading and platinum nanocluster composition. Analyst 145:908–916

Erkmen C, Tığ GA, Uslu B (2022) First label-free impedimetric aptasensor based on Au NPs/TiO2 NPs for the determination of leptin. Sensors Actuators B Chem 358:131420

Farahani FA, Alipour E, Mohammadi R, Amini-Fazl MS, Abnous K (2022) Development of novel aptasensor for ultra-sensitive detection of myoglobin via electrochemical signal amplification of methylene blue using poly (styrene)-block-poly (acrylic acid) amphiphilic copolymer. Talanta 237:122950

Fatima T, Bansal S, Husain S, Khanuja M, Islamia JM, Delhi N (1986) Biosensors. IEEE Trans Biomed Eng 33(2):77–268

Felix FS, Angnes L (2018) Electrochemical immunosensors – a powerful tool for analytical applications. Biosens Bioelectron 102:470–478

Fracchiolla NS, Artuso S, Cortelezzi A (2013) Biosensors in clinical practice: focus on oncohematology. Sensors (Switzerland) 13(5):6423–6447

Gajdosova V, Lorencova L, Kasak P, Tkac J (2020) Electrochemical nanobiosensors for detection of breast cancer biomarkers. Sensors (Switzerland) 20(14):1–37

Ghalkhani M, Sohouli E, Khaloo SS, Vaziri MH (2022) Architecting of an aptasensor for the staphylococcus aureus analysis by modification of the screen-printed carbon electrode with aptamer/Ag–Cs-Gr QDs/NTiO2. Chemosphere 293:133597

Huang X, Zhu Y, Kianfar E (2021a) Nano biosensors: properties, applications and electrochemical techniques. J Mater Res Technol 12:1649–1672

Huang Z, Chen H, Ye H, Chen Z, Jaffrezic-Renault N, Guo Z (2021b) An ultrasensitive aptamer-antibody sandwich cortisol sensor for the noninvasive monitoring of stress state. Biosens Bioelectron 190:113451

Hui N, Wang J, Wang D, Wang P, Luo X, Lv S (2022) An ultrasensitive biosensor for prostate specific antigen detection in complex serum based on functional signal amplifier and designed peptides with both antifouling and recognizing capabilities. Biosens Bioelectron 200:113921

Hwang HJ, Ryu MY, Park CY, Ahn J, Park HG, Choi C, Do HS, Park TJ, Park JP (2017) High sensitive and selective electrochemical biosensor: label-free detection of human norovirus using affinity peptide as molecular binder. Biosens Bioelectron 87:164–170

Ilkhani H, Sarparast M, Noori A, Bathaie SZ, Mousavi MF (2015) Electrochemical aptamer/antibody based sandwich immunosensor for the detection of EGFR, a cancer biomarker, using gold nanoparticles as a signaling probe. Biosens Bioelectron 74:491–497

Jędrzak A, Kuznowicz M, Rębiś T, Jesionowski T (2022) Portable glucose biosensor based on polynorepinephrine@magnetite nanomaterial integrated with a smartphone analyzer for point-of-care application. Bioelectrochemistry 145:108071

Jozghorbani M, Fathi M, Kazemi SH, Alinejadian N (2021) Determination of carcinoembryonic antigen as a tumor marker using a novel graphene-based label-free electrochemical immunosensor. Anal Biochem 613:114017

Kangkamano T, Numnuam A, Limbut W, Kanatharana P, Vilaivan T, Thavarungkul P (2018) Pyrrolidinyl PNA polypyrrole/silver nanofoam electrode as a novel label-free electrochemical miRNA-21 biosensor. Biosens Bioelectron 102:217–225

Karimzadeh A, Hasanzadeh M, Shadjou N, de la Guardia M (2018) Peptide based biosensors. TrAC – Trends Anal Chem 107:1–20

Karunakaran C, Pandiaraj M, Santharaman P (2015) Immunosensors. In: Biosensors and bioelectronics. Elsevier Inc, pp 205–245

Kausaite-Minkstimiene A, Glumbokaite L, Ramanaviciene A, Ramanavicius A (2020) Reagent-less amperometric glucose biosensor based on nanobiocomposite consisting of poly(1,10-phenanthroline-5,6-dione), poly(pyrrole-2-carboxylic acid), gold nanoparticles and glucose oxidase. Microchem J 154:104665

Kim SM, Kim J, Noh S, Sohn H, Lee T (2020) Recent development of aptasensor for influenza virus detection. Biochip J 14(4):327–339

Krzyczmonik P, Bozal-Palabiyik B, Skrzypek S, Uslu B (2021) Quantum dots-based sensors using solid electrodes. In: Electroanalytical applications of quantum dot-based biosensors. Elsevier Inc, pp 81–120

Kurbanoglu S, Erkmen C, Uslu B (2020) Frontiers in electrochemical enzyme based biosensors for food and drug analysis. TrAC – Trends Anal Chem 124:115809

Laraib U, Sargazi S, Rahdar A, Khatami M, Pandey S (2022) Nanotechnology-based approaches for effective detection of tumor markers: a comprehensive state-of-the-art review. Int J Biol Macromol 195:356–383

Li R, Huang H, Huang L, Lin Z, Guo L, Qiu B, Chen G (2013) Electrochemical biosensor for epidermal growth factor receptordetection with peptide ligand. Electrochim Acta 109:233–237

Li X, Lin LY, Wang KY, Li J, Feng L, Song L, Liu X, He JH, Sakthivel R, Chung RJ (2021) Streptavidin-functionalized-polyethyleneimine/chitosan/HfO_2-Pr_6O_{11} nanocomposite using label-free electrochemical immunosensor for detecting the hunger hormone ghrelin. Compos Part B Eng 224:109231

Lin Y, Shen R, Liu N, Yi H, Dai H, Lin J (2018) A highly sensitive peptide-based biosensor using $NiCo_2O_4$ nanosheets and g-C_3N_4 nanocomposite to construct amplified strategy for trypsin detection. Anal Chim Acta 1035:175–183

Liu Q, Wang J, Boyd BJ (2015) Peptide-based biosensors. Talanta 136:114–127

Liu Y, Si S, Dong S, Ji B, Li H, Liu S (2021) Ultrasensitive electrochemical immunosensor for ProGRP detection based on 3D-rGO@Au nanocomposite. Microchem J 170:106644

Mahapatra S, Baranwal A, Purohit B, Roy S, Mahto SK, Chandra P (2020) Advanced biosensing methodologies for ultrasensitive detection of human coronaviruses. In: Diagnostic strategies for COVID-19 and other coronaviruses. Springer, pp 19–36

Mahato K, Kumar S, Srivastava A, Maurya PK, Singh R, Chandra P (2018a) Electrochemical immunosensors: fundamentals and applications in clinical diagnostics. In: Handbook of ımmunoassay technologies: approaches, performances, and applications. Academic Press, pp 359–414

Mahato K, Maurya PK, Chandra P (2018b) Fundamentals and commercial aspects of nanobiosensors in point-of-care clinical diagnostics. Biotech 8(3):1–14

Malik P, Katyal V, Malik V, Asatkar A, Inwati G, Mukherjee TK (2013) Nanobiosensors: concepts and variations. ISRN Nanomater 2013:1–9

Miao J, Li X, Li Y, Dong X, Zhao G, Fang J, Wei Q, Cao W (2019) Dual-signal sandwich electrochemical immunosensor for amyloid β-protein detection based on Cu–Al_2O_3-g–C_3N_4–Pd and UiO-66@PANI-MB. Anal Chim Acta 1089:48–55

Mishra RK, Rajakumari R (2018) Nanobiosensors for biomedical application: present and future prospects. Present and future prospects. In: Characterization and biology of nanomaterials for drug delivery. Elsevier Inc, pp 1–23

Nazare A, Pal K, Maji S (2021) 14. Electrochemical biosensors. In: Food, medical, and environmental applications of polysaccharides. Elsevier Inc, pp 403–441

Negahdary M, Heli H (2019) An ultrasensitive electrochemical aptasensor for early diagnosis of Alzheimer's disease, using a fern leaves-like gold nanostructure. Talanta 198:510–517

Nosrati R, Dehghani S, Karimi B, Yousefi M, Taghdisi SM, Abnous K, Alibolandi M, Ramezani M (2018) Siderophore-based biosensors and nanosensors; new approach on the development of diagnostic systems. Biosens Bioelectron 117:1–14

Oliveira Brett AM (2005) Chapter 4 DNA-based biosensors. Compr Anal Chem 44:179–208

Pareek S, Jain U, Bharadwaj M, Chauhan N (2021) Sensing and bio-sensing research A label free nanosensing platform for the detection of cervical cancer through analysis of ultratrace DNA hybridization. Sens Bio-Sensing Res 33:100444

Park CS, Lee C, Kwon OS (2016) Conducting polymer based nanobiosensors. Polymers (Basel) 8(7):1–18

Parolo C, Merkoçi A (2013) Paper-based nanobiosensors for diagnostics. Chem Soc Rev 42(2): 450–457

Pei X, Zhang B, Tang J, Liu B, Lai W, Tang D (2013) Sandwich-type immunosensors and immunoassays exploiting nanostructure labels: a review. Anal Chim Acta 758:1–18

Pérez DJ, Patiño EB, Orozco J (2021) Electrochemical nanobiosensors as point-of-care testing solution to cytokines measurement limitations. Electroanalysis 34(2):184–211

Qian Y, Feng J, Fan D, Zhang Y, Kuang X, Wang H, Wei Q, Ju H (2019) A sandwich-type photoelectrochemical immunosensor for NT-pro BNP detection based on F-Bi_2WO_6 /Ag_2S and GO/PDA for signal amplification. Biosens Bioelectron 131:299–306

Rahimi-Mohseni M, Raoof JB, Aghajanzadeh TA, Ojani R (2021) Phenylketonuria monitoring in human blood serum by mosses extract/ZnO@Au nanoarrays-loaded filter paper as a novel electrochemical biosensor. Microchem J 160:105739

Raj MA, John SA (2018) Graphene-modified electrochemical sensors. In: Graphene-based electrochemical sensors for biomolecules. Elsevier Inc, pp 1–41

Saleh TA, Fadillah G, Saputra OA (2019) Nanoparticles as components of electrochemical sensing platforms for the detection of petroleum pollutants: a review. TrAC – Trends Anal Chem 118: 194–206

Sekhar PK, Wignes F (2016) Trace detection of research department explosive (RDX) using electrochemical gas sensor. Sensors Actuators B Chem 227:185–190

Sellappan L, Manoharan S, Sanmugam A, Anh NT (2022) Role of nanobiosensors and biosensors for plant virus detection. In: Nanosensors for smart agriculture. Elsevier Inc, pp 493–506

Shanbhag MM, Ilager D, Mahapatra S, Shetti NP, Chandra P (2021) Amberlite XAD-4 based electrochemical sensor for diclofenac detection in urine and commercial tablets. Mater Chem Phys 273:125044

Sharifi M, Hasan A, Attar F, Taghizadeh A, Falahati M (2020) Development of point-of-care nanobiosensors for breast cancers diagnosis. Talanta 217:121091

Shawky AM, El-Tohamy M (2021) Signal amplification strategy of label-free ultrasenstive electrochemical immunosensor based ternary Ag/TiO_2/rGO nanocomposites for detecting breast cancer biomarker CA 15-3. Mater Chem Phys 272:124983

Shen Y, Zhang Y, Gao ZF, Ye Y, Wu Q, Chen HY, Xu JJ (2021) Recent advances in nanotechnology for simultaneous detection of multiple pathogenic bacteria. Nano Today 38:101121

Simões FR, Xavier MG (2017) 6 – electrochemical sensors. In: Nanoscience and its applications. Elsevier Inc., pp 155–178

Soni A, Jha SK (2017) Smartphone based non-invasive salivary glucose biosensor. Anal Chim Acta 996:54–63

Srivastava AK, Dev A, Karmakar S (2018) Nanosensors and nanobiosensors in food and agriculture. Environ Chem Lett 16(1):161–182

Sun J, Wang G, Cheng H, Han Y, Li Q, Jiang C (2022) An antifouling electrochemical aptasensor based on hyaluronic acid functionalized polydopamine for thrombin detection in human serum. Bioelectrochemistry 145:108073

Tahir MA, Rafiq A, Dina NE, Amin I, Mansoor S, Zhang L, Mujahid A, Bajwa SZ (2022) Methods for design and fabrication of nanosensors. In: Nanosensors for smart agriculture. Elsevier Inc, pp 53–79

Thakur PS, Sankar M (2022) Nanobiosensors for biomedical, environmental, and food monitoring applications. Mater Lett 311:131540

Vaz R, Frasco MF, Sales MGF (2022) Biosensors: concept and importance in point-of-care disease diagnosis. In: Biosensor based advanced cancer diagnostics. Academic Press, pp 59–84

Wang Z, Zhao H, Chen K, Li H, Lan M (2021) Sandwich-type electrochemical aptasensor based on hollow mesoporous carbon spheres loaded with porous dendritic Pd@Pt nanoparticles as signal amplifier for ultrasensitive detection of cardiac troponin I. Anal Chim Acta 1188:339202

Wu M, Liu S, Qi F, Qiu R, Feng J, Ren X, Rong S, Ma H, Chang D, Pan H (2022) A label-free electrochemical immunosensor for CA125 detection based on CMK-3(Au/Fc@MgAl-LDH)n multilayer nanocomposites modification. Talanta 241:123254

Xia N, Wang X, Yu J, Wu Y, Cheng S, Xing Y, Liu L (2017) Design of electrochemical biosensors with peptide probes as the receptors of targets and the inducers of gold nanoparticles assembly on electrode surface. Sensors Actuators B Chem 239:834–840

Xu D, Huang X, Guo J, Ma X (2018) Automatic smartphone-based microfluidic biosensor system at the point of care. Biosens Bioelectron 110:78–88

Yang H (2012) Enzyme-based ultrasensitive electrochemical biosensors. Curr Opin Chem Biol 16(3–4):422–428

Yang Q, Wang P, Ma E, Yu H, Zhou K, Tang C, Ren J, Li Y, Liu Q, Dong Y (2021) A sandwich-type electrochemical immunosensor based on Au@Pd nanodendrite functionalized MoO2 nanosheet for highly sensitive detection of HBsAg. Bioelectrochemistry 138:107713

Yonzon CR, Stuart DA, Zhang X, McFarland AD, Haynes CL, Van Duyne RP (2005) Towards advanced chemical and biological nanosensors – an overview. Talanta 67(3):438–448

Younis S, Zia R, Tahir N, Bukhari SZ, Khan WS, Bajwa SZ (2022) Nanosensors for animal health monitoring. In: Nanosensors for smart agriculture. Elsevier Inc, pp 509–529

Zhang Y, Figueroa-Miranda G, Lyu Z, Zafiu C, Willbold D, Offenhäusser A, Mayer D (2019) Monitoring amyloid-B proteins aggregation based on label-free aptasensor. Sensors Actuators B Chem 288:535–542

Zhang Y, Zhang Z, Rong S, Yu H, Gao H, Sha Q, Ding P, Pan H, Chang D (2020) A sandwich-type ECL immunosensor based on signal amplification using a ZnO nanorods-L-cysteine-luminol nanocomposite for ultrasensitive detection of prostate specific antigen. Anal Chim Acta 1109: 98–106

Zhang ZY, Huang LX, Xu ZW, Wang P, Lei Y, Liu AL (2021) Efficient determination of pml/rarα fusion gene by the electrochemical dna biosensor based on carbon dots/graphene oxide nanocomposites. Int J Nanomedicine 16:3497–3508

Zhang B, Li F, Han F, Yang H, Jiang C, Tan S, Tu J, Qiao B, Wang X, Wu Q (2022) Bioelectrochemistry A sandwich-type electrochemical immunosensor using trimetallic nanozyme as signal amplification for NT-proBNP sensitive detection. Bioelectrochemistry 145:108075

Zhao H, Cao L, Liu Q, Tang F, Chen L, Wang S, Li Y, Li Y, Li B, Liu H (2022) Label-free electrochemical immunosensor based on PdCuPt/PPY/DCSC as a signal amplification platform for sensitive detection of cardiac troponin I. Sensors Actuators B Chem 351:1–7

Zhou Q, Rahimian A, Son K, Shin DS, Patel T, Revzin A (2016) Development of an aptasensor for electrochemical detection of exosomes. Methods 97:88–93

Metal-Organic Framework for Electrochemical Biosensing Applications

30

Palraj Kalimuthu, Rasu Ramachandran, and Ganesan Anushya

Contents

1 Introduction ... 663
2 Synthesis Methods of MOFs ... 664
  2.1 Solvothermal/Hydrothermal ... 666
  2.2 Slow Evaporation ... 667
  2.3 Mechanochemical ... 667
  2.4 Sonochemical ... 667
  2.5 Microwave Irradiation ... 668
  2.6 Electrochemical ... 668
3 MOFs-Based Electrochemical Sensing of Analytes ... 669
  3.1 Small Biomolecules ... 669
  3.2 Biological Macromolecules ... 677
4 Conclusions ... 681
References ... 682

Abstract

Metal-organic frameworks (MOFs) are a new group of nanoporous materials developed by a typical metal-ligands coordination strategy. MOFs possess a range of unique characteristics, including high porosity, uniform pore structures, ultrahigh active surface area, robust structure, chemical functionality etc. Further, the physicochemical properties of MOFs are tunable based on our requirements, and, therefore, MOFs are afforded to apply in a wide range of applications. Particularly, MOFs have received considerable attention to use as a probe in

---

P. Kalimuthu (✉)
School of Chemistry and Molecular Biosciences, University of Queensland, Brisbane, QLD, Australia
e-mail: p.kalimuthu@uq.edu.au

R. Ramachandran
Department of Chemistry, The Madura College, Madurai, India

G. Anushya
Department of Physics, St. Joseph College of Engineering, Chennai, India

© Springer Nature Singapore Pte Ltd. 2023

U. P. Azad, P. Chandra (eds.), *Handbook of Nanobioelectrochemistry*,
https://doi.org/10.1007/978-981-19-9437-1_30

electrochemical sensor applications. Because, the tunable porosity properties of MOFs offer to detect specific biomolecules as functions similar to enzyme-based sensors. However, the poor conductivity and less stability in aqueous media restrict their usage in many electrochemical applications. In recent years, several nanomaterials have been incorporated into MOFs to improve the conductivity and stability of MOF-based catalysts. This chapter focuses on the recent innovation, development, and improvement of MOFs-based catalysts used for different bioanalytical applications. Further, it described the fundamental electrocatalytic sensing mechanism of the MOF-based probes and summarized the electroanalytical parameters reported for different analytes.

Keywords

Metal-organic framework · Electrocatalysis · Biosensor · Cancer biomarkers · Nucleic acids · Neurotransmitters

Abbreviations

5-hmC	5-hydroxymethylcytosine DNA
ADRB1	Adrenergic receptor gene
AED	Anodic electrodeposition
AgNPs	Silver nanoparticles
Apt	Aptamer
ATP	Adenosine triphosphate
AuNPs	Gold nanoparticles
BSA	Bovine serum albumin
BTC	1,3,5-benzenetricarboxylic acid
CC	Carbon cloth
CEA	Carcinoembryonic antigen
CPE	Convergent paired electrodeposition
Cu(tpa)	Copper terephthalate
CY	Cysteine
DMF	Dimethylformamide
DMSO	Dimethylsulfoxide
DNA	Deoxyribonucleic acid
DPE	Divergent paired electrodeposition
EIS	Electrochemical impedance spectroscopy
ELISA	Enzyme-linked immunosorbent assays
ERG	Electrochemically reduced graphene
GOD	Glucose oxidase
H_3NBB	$4',4''',4''''$- nitrilotris[1,1′-biphenyl]-4-carboxylic acid
HCV	Hepatitis C virus
HER2	Human epidermal growth factor receptor-2
HT	Hexanethiol
MACP	Ni-MOF/AuNPs/CNTs/PDMS
MB	Magnetic bead

miRNAs	microRNAs
MOFs	Metal-organic frameworks
MPF	Metalloporphyrin framework
mRNA	Messenger RNA
N-CNT	N-doped carbon nanotube
NS	Nanosheet (NS)
PANI	Poly(aniline)
PCPs	Porous coordination polymers
PCR	Polymerase chain reaction
PDMS	Poly(dimethylsiloxane)
PGA	Poly(glutamic acid)
PTK7	Tyrosine kinase-7
r-GO	Reduced graphene oxide
RNA	Ribonucleic acid
siRNAs	Small interfering RNAs
snRNAs	Small nuclear RNAs
SPCE	Screen-printed carbon electrode
ssDNA	Single-stranded oligonucleotide
TCPP	Tetra(4-carboxyphenyl)-porphyrin chloride
TDT	Terminal deoxynucleotidyl transferase
tRNA	Transfer RNA

1 Introduction

Biomolecules involve many essential functions in living organisms, including cell functions, energy production and transport, signal processing, building body mass, etc. However, any alteration in the biomolecules concentrations in body fluids can lead to diseases (Polshettiwar et al. 2021). Therefore, accurate detection and quantification of biomolecules are very important to ensure the well-being of the cells and organs. Currently, several analytical methods have been used to detect biomolecules in vivo and in vitro, including enzyme-linked immunosorbent assays (ELISA), polymerase chain reaction (PCR), colorimetric and electrochemical detection, chromatography-mass spectroscopy, vibrational spectroscopy, etc. (Lequin 2005; Laor et al. 1992; Ajay et al. 2017; Kalimuthu et al. 2012; Liu et al. 2001). Among them, electrochemical methods have received tremendous attention due to their facile fabrication strategy, fast response, cost-effectiveness, high sensitivity, easy operation, and portability (Kalimuthu et al. 2013, 2014). Further, a broad range of nanomaterials have been incorporated into the transducer to improve the performance of the electrochemical biosensor (Chen and Chatterjee 2013; Mahato et al. 2018).

Metal-organic frameworks (MOFs), also called as porous coordination polymers (PCPs), have represented a new group of nanoporous materials. MOFs are prepared by a unique metal-ligands coordination strategy. The binding of metal ions to the arms of the linker molecules can produce a cage-like porous structure. The generated porous structure can have a massive internal surface area and active sites (Dhakshinamoorthy et al. 2017; Jiang and Xu 2011). Interestingly, the physicochemical properties of MOFs can be tuned based on our requirement by controlling the metal-ligands coordination process (Czaja et al. 2009). This adaptable structural change of MOFs is more suitable and convenient for different types of functionalization for a wide range of analytes. Further, compared to conventional porous materials (porous oxides and zeolites), MOFs have uniform pore size, ultrahigh active surface area, and a well-connected pore structure. These unique characteristics allow MOFs to utilize numerous applications, including heterogeneous catalysis, biomedical imaging, drug delivery, gas storage, biochemical sensing, etc. (Gulbagca et al. 2019; Keskin and Kizilel 2011; Britt et al. 2008). Considerable works have been published regarding the utilization of MOFs as signal labels in electrochemical sensor applications (Kajal et al. 2022; Zhang et al. 2021). For instance, NiO and Ni nanoparticles embedded MOFs were developed by a facile calcination approach, and the resulting MOFs were successfully applied to quantify glucose concentrations in a human blood sample by an amperometric technique (Shu et al. 2017). Further, Wang et al. developed 2D MOFs nanosheet by a liquid-liquid interfacial reaction approach and the resulting materials were utilized as a probe to sense H_2O_2 in an alkaline medium (Wang et al. 2021). The durability of the fabricated sensor was examined by continuous measuring of H_2O_2 for a prolonged time and found that the catalytic response was almost unaltered up to 20,000 cycles.

However, most MOF-based catalysts lack conductivity and stability in electrolytes, limiting their applications in electrochemical sensors. The leading cause of the poor stability of MOFs in an aqueous medium is attributed to the easily breakable weak metal-ligand coordination bonds by water molecules (Sohail et al. 2018). In addition, ions present in the electrolytes can also be coordinated with the metal nodes, breaking the metal-ligand coordination bonds. Therefore, to improve the conductivity and stability of MOFs, various nanomaterials, including metal nanoparticles and carbon- and graphene-based materials, were integrated into the MOFs (Dhakshinamoorthy et al. 2017; Zhu and Xu 2014). This chapter summarizes the recent development of MOF-based electrocatalysts for biosensing applications. Particularly, the MOF-based biosensors developed for the detection of a range of small biochemical compounds (e.g., H_2O_2, glucose, dopamine, and cysteine), and biological macromolecules (proteins and nucleic acids) are discussed in detail. Further, the sensing mechanism, performance, and electroanalytical parameters of these analytes are outlined in Table 30.1.

2 Synthesis Methods of MOFs

Several approaches are routinely used to develop MOFs, including solvothermal/hydrothermal, slow evaporation, mechanochemical, sonochemical, microwave irradiation, electrochemical, etc. (Zhu and Xu 2014; Stock and Biswas 2012). Among them, the solvothermal/hydrothermal approaches have been extensively used to

Table 30.1 Analytical parameters of MOF-based electrochemical biosensors

Electrode	Analytes	Linear range (M)	Detection limit (M)	References
CC/Co-MOF NS	Glucose	4×10^{-6} – 4.4×10^{-3}	1.2×10^{-6}	Wei et al. (2018)
GC/Ni-MOF/Ni/NiO/C	Glucose	4×10^{-6} – 5.6×10^{-3}	0.8×10^{-6}	Shu et al. (2017)
G/Ni-MOF-74	Glucose	5×10^{-6} – 1.4×10^{-3}	0.4×10^{-6}	Zhang et al. (2018)
GC/CNT-MOF-CoCu	H_2O_2	5×10^{-5}- 2.5×10^{-3}	0.15×10^{-6}	Kim and Muthurasu (2021)
GC/Cu-MOF/MXene	H_2O_2	1×10^{-6}- 6.12×10^{-3}	0.35×10^{-6}	Cheng et al. (2021)
GC/CNT-MOF-CoCu	H_2O_2	5×10^{-5}- 3.5×10^{-3}	0.21×10^{-6}	Kim and Muthurasu (2021)
PtCu@MOFs/C	H_2O_2	1×10^{-5} – 3×10^{-3}	0.2×10^{-6}	Chen et al. (2018)
GC/MPF/PGA	H_2O_2	5×10^{-10} – 1×10^{-3}	30×10^{-9}	Chen et al. (2020)
GC/rGO@Ni-MOF/AuNPs	Dopamine	5×10^{-7} – 1.2×10^{-4}	30×10^{-12}	Yang et al. (2021)
GC/AgPd@Zr-MOF	Dopamine	2×10^{-6} – 42×10^{-6}	0.1×10^{-6}	Hira et al. (2021)
GC/AgNPs@ZIF-67	Dopamine	1×10^{-7}– 2×10^{-4}	50×10^{-9}	Tang et al. (2020)
PDMS/CNTs/Ni-MOF/AuNPs	Dopamine	5×10^{-8}– 1.5×10^{-5}	10×10^{-9}	Shu et al. (2020)
GC/Cu(tpa)/ERG-MOF	Dopamine	1×10^{-6}– 5×10^{-5}	0.21×10^{-6}	Wang et al. (2014)
GC/Au-SH-SiO_2@Cu-MOF	L-Cysteine	2×10^{-8} – 3×10^{-4}	8×10^{-9}	Hosseini et al. (2013)
Au/ Ce-MOF	ATP	1×10^{-8} – 10×10^{-3}	5.6×10^{-9}	Shi et al. (2017)
S1-AuNPs@Cu-MOFs	miRNA-155	1×10^{-12} – 10×10^{-9}	0.35×10^{-12}	Wang et al. (2018)
Ag/Zn@MOF/HCV-RNA probe	HCV-RNA	1×10^{-12} – 100×10^{-9}	0.64×10^{-12}	El-Sheikh et al. (2021)
GC/PtNPs/Hemin@Fe-MIL-88NH_2/Cu^{2+}/CP/HT/DNA Probe	ADRB1	1×10^{-12} – 10×10^{-9}	0.21×10^{-12}	Yuan et al. (2017)
SPCE/MB/5-hmc-DNA	5-hmC-DNA	1×10^{-14} – 1×10^{-9}	9.06×10^{-12}	Cui et al. (2019)

MOF NS MOF nanosheet, *CC* carbon cloth, *PGA* poly(glutamic acid), *MPF* metalloporphyrin framework, *rGO* reduced graphene oxide, *AuNPs* gold nanoparticles, *AgNPs* silver nanoparticles, *Cu(tpa)* copper terephthalate, *ERG* electrochemically reduced graphene, *ADRB1* adrenergic receptor gene, *HT* hexane thiol, *SPCE* screen-printed carbon electrode, *MB* magnetic beads

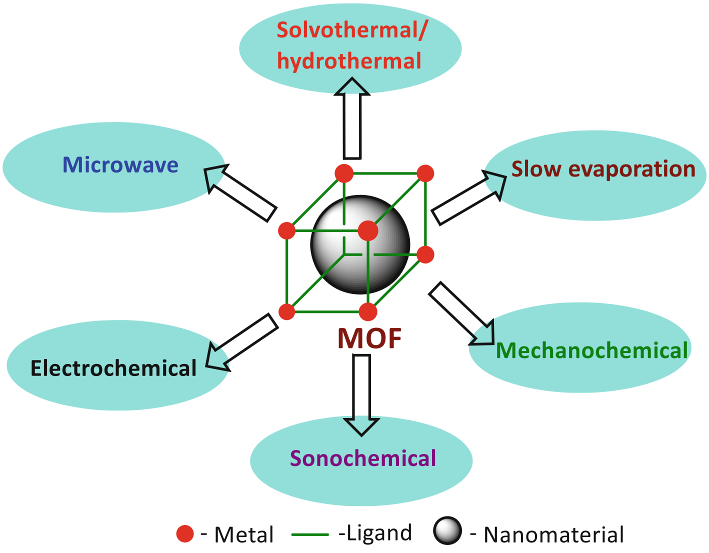

Fig. 30.1 Different synthetic strategies of MOF-based composites

develop MOFs due to their simple protocol. However, the downside of these approaches is required a prolonged time to form MOF crystals. More details of these methods are described below. Figure 30.1 portrays an overview of different synthetic approaches used to construct MOFs in the literature.

2.1 Solvothermal/Hydrothermal

Solvothermal is a facile approach to developing different types of MOFs. In this technique, nonaqueous solvents, including dimethylsulfoxide (DMSO), dimethylformamide (DMF), methanol, ethanol, acetone, etc., are used. However, these solvents are expensive and non-ecofriendly. Therefore, a hydrothermal technique was developed to circumvent this issue where water is the primary solvent in addition to the small quantity of nonaqueous solvents. Further, the reaction is conducted under controlled temperature and pressure by using a closed Teflon container in the hydrothermal method. Usually, the temperature can vary up to 220 °C, and the resulting product is crystalized to get a pure form. This crystallization process can take a few days to weeks. On the other hand, this method affords to obtain a significantly high yield. For example, the Ni-MOF nanosheet was developed by the hydrothermal method by simple mixing p-benzenedicarboxylic acid with $Ni(NO_3)_2$ in DMF (Shu et al. 2017). Then the calcination of the resulting Ni-MOF nanosheet yielded the Ni-MOF/Ni/NiO/C composite and was successfully used as a glucose sensor. In another report, reduced graphene oxide (r-GO)-based Ni-MOF composite was prepared using the solvothermal method (Yang et al. 2021). Firstly, the organic ligand 2-aminoterephthalic acid was dissolved in mixed solvents (ethanol, DMF, and water). Then, $Ni(NO_3)_2$ and rGO were added to the ligand solution and incubated for 2 days at 140 °C to develop the MOF.

2.2 Slow Evaporation

This technique is performed at room temperature without requiring any external energy. Basically, the stable form of metal salts is dissolved in a solvent or mixture of solvents based on their solubility and then leave the resulting mixture for a slow evaporation process to form MOF crystals. Using this strategy, HKUST-1 MOF was prepared by mixing 1,3,5-benzenetricarboxylic acid (BTC) and $Cu(NO_3)_2 3H_2O$ in DMSO (Ameloot et al. 2010). Then the precursor solution was left at 373 K to evaporate the DMSO for more than 24 h and obtained the octahedral-shaped crystal. To speed up the reaction process, Zhuang et al. used methanol to prepare the HKUST-1 MOF at room temperature (Zhuang et al. 2011). The precursor solution was prepared by mixing BTC and $Cu(NO_3)_2 3H_2O$ in DMSO. Then, 200 μL of the precursor was dropped in methanol and stirred for 10 min, and the resulting product was centrifuged.

2.3 Mechanochemical

This method uses a combination of chemical reactions and mechanical forces. The development of MOFs is achieved in three different ways: (i) neat grinding, (ii) liquid-assisted grinding, and (iii) ion- and liquid-assisted grinding. Principally, solvents are unnecessary for the neat grinding approach, whereas a tiny amount of solvent is needed in the liquid-assisted grinding approach and crystallizes the product. On the other hand, the ion- and liquid-assisted grinding approach is almost identical to the liquid-assisted grinding, but a small amount of ionic salt is included in the mixture to speed up the crystallization process. Klimakow et al. used the neat grinding (ball mill) strategy through liquid-assisted grinding of copper acetate and BTC to develop HKUST-1 MOF (Klimakow et al. 2010). Zirconium-based MOFs (UiO-66-NH_2 and UiO-66) were developed through a solvent-free route by a dry milling strategy with the aid of liquid-assisted grinding (Užarević et al. 2016).

2.4 Sonochemical

In this approach, ultrasound waves are used as a heat source to develop MOFs. Basically, the metal salts and organic ligands are dissolved in a particular solvent and sonicated to attain heating for the formation of MOFs. The temperature can be adjusted by controlling the output power of sonication. For instance, the manganese−metalloporphyrin (PCN-222(Mn)) framework was developed by the sonochemical approach (Chen et al. 2020). The mixture of benzoic acid and $ZrOCl_2 \cdot 8H_2O$ were dispersed in DMF under ultrasonic conditions and then heated for 1 h. The resultant mixture was added into Mn-tetra(4-carboxyphenyl)-porphyrin chloride (Mn-TCPP) and sonicated to dissolve. Finally, a blackish green PCN-222 (Mn) composite was obtained. In another report, Wang et al. fabricated the copper terephthalate (Cu(tpa)) doped into electrochemically reduced graphene-MOFs by ultrasonication method (Wang et al. 2014). A homogenous solution of (Cu(tpa)) was prepared by mixing $Cu(NO_3)_2{\cdot}3H_2O$ and terephthalic acid (TPA) in DMF and ethanol by the solvothermal method. Then, the resulting (Cu(tpa)) was doped into GO to form MOF by ultrasonication for 1 h at 100 W.

2.5 Microwave Irradiation

Microwave irradiation is used as a heat source to develop MOFs. Particularly, this method is applied to construct nanosized MOFs. It required significantly less reaction time and achieved highly porous MOFs. Further, the crystallization process is significantly faster than other approaches due to microwave irradiation. Yoo and Jeong developed MOF based on the microwave irradiation strategy (Yoo and Jeong 2008). $Zn(NO_3)_26H_2O$ and benzene-1,4-dicarboxylic acid were solubilized separately in DMF and then mixed together via drop-by-drop addition. The resulting mixture was exposed to microwave irradiation for 5–30 min at 500 W to form a crystal. In another report, ZIF-8 MOF was prepared by mixing sodium formate, zinc chloride, and 2-methylimidazole in methanol under microwave irradiation and then the crystal formation took place after 4 h (Bux et al. 2010).

2.6 Electrochemical

This approach is highly suitable for fabricating a thin MOF film on any conductive electrode materials, and it has several advantages, including this could be performed at room temperature, requires less fabrication time, and controls the reaction and film thickness by an applied potential. Basically, we can achieve a uniform film thickness without any defects. Both oxidation and reduction processes are used to deposit the MOFs on the electrode surface. Different electrochemical techniques are employed and described below. Alizadeh and Nematollah used anodic electrodeposition (AED), convergent paired electrodeposition (CPE), and divergent paired electrodeposition (DPE) for the deposition of MOFs on the electrode surface (Alizadeh and Nematollahi 2019). Sodium nitrate was used as a supporting electrolyte and trimesic acid was employed as an organic ligand, and these chemicals were dissolved in ethanol and coated on an electrode surface by electrochemical deposition. In the CPE method, metal salts are deposited on an anode and cathode by oxidation and reduction processes, respectively. To make the MOF, zinc nitrate and zinc metal were used as two cation sources. During the deposition, zinc nitrate was coated on the cathode by reduction and zinc metal was deposited on the anode by oxidation. In the DPE strategy, the anode and cathode are separated by an H-type electrochemical cell and deposited MOF by an applied potential. Further, HKUST-1 MOF was prepared by electrochemical deposition where copper-coated silicon wafers mesh and copper plate were employed as anode and cathode, respectively (Campagnol et al. 2016). 1,3,5-benzenetricarboxylic acid is the organic linker, and methyltributylammonium methyl sulfate is an electrolyte. Then, electrode potentials were varied from 0–5 V to obtain the different thicknesses of the HKUST-1 MOF.

3 MOFs-Based Electrochemical Sensing of Analytes

Nanomaterials embedded MOFs-based composite materials possess desirable conductivity, biocompatibility, and electroactivity and are highly suitable for sensing several analytes (Zhang et al. 2021; Wang 2017). In addition, the presence of high porosity, homogeneity, and functionalities in the MOFs allow attaching many biocatalysts molecules for designing highly efficient biosensors. The cluster of metal ions nodes present in the MOFs provide redox properties which are highly desirable for electrochemical applications. Further, MOFs act as artificial enzymes due to the specific pore size of MOF, allowing enter the specific size of substrates and blocking all other interfering substances (Nath et al. 2016). The most recent advancements in the development of MOF-based electrochemical biosensors are summarized in this section and discuss the sensing of small and macrobiomolecules.

3.1 Small Biomolecules

3.1.1 Glucose

Glucose is the primary source of fuel for physical activities and body functions. However, the excess accumulation of glucose in human body fluids leads to major complications and this condition is called diabetes. If not treated, it affects most organs, including the nervous system, eyes, kidneys, and cardiovascular system (Petersen et al. 2017; Wojciechowska et al. 2016). In the current state of affairs, researchers (electronics and chemists) have jointly worked to develop a fast and highly sensitive biosensor device to detect and continuously monitor glucose levels in the bloodstream (Johnston et al. 2021). Currently, glucose oxidase (GOD)-based biosensors are available in the market. However, the enzyme-based biosensors have a few drawbacks, such as expensive and inadequate long-term stability due to the denaturation processes. For example, Paul and coworkers developed an enzymatic biosensor for glucose by incorporating GOD and AuNPs into the zeolitic imidazolate framework (ZIF-8) (Paul et al. 2018). The direct electrochemistry of GOD was achieved through the nonturnover response of FAD(−448 mV vs. Ag/AgCl) at the GC/ZIF-8@AuNPs-GOD electrode. Further, the developed composite acts as a bifunctional catalyst, such as it oxidizes glucose and reduces H_2O_2. However, the catalytic responses are very weak and achieved stability for up to 4 months.

On the other hand, a significant interest is made in the development of nonenzymatic-based electrochemical sensors, which are applied to sense a range of biomolecules and emphasize their easy way fabrication process, cost-effectiveness, durability, and long-term stability (Hwang et al. 2018). Among the various electrode materials, gold (Zhong et al. 2015), indium-tin-oxide (Jeon et al. 2015), platinum, nickel, and copper electrodes (Wang et al. 2012) have been widely used in the study of glucose molecules. However, these electrode materials have a few drawbacks, such as high operating potential, poor stability, and low sensitivity, limiting their applications. Therefore, the researchers have continuously focused on developing a highly stable and reliable electrode material for practical applications.

It was found that MOF-based electrode materials exhibited promising electrode materials for the development of glucose biosensors. For instance, Wei et al. prepared a cobalt MOF (Co-MOF) with a 3D nanosheet (NS) array deposited on carbon cloth (CC) using a facile ambient liquid phase method and demonstrated to sense of glucose (Wei et al. 2018). The Co-MOF modified CC exhibited a pronounced catalytic response toward glucose, while unmodified CC failed to show any redox response under identical experimental conditions. Further, the different forms of Co-MOF (powder and nanosheet) were developed and investigated their catalytic response and found that Co-MOF nanosheet delivered a better catalytic response than the powder form of Co-MOF. Further, CC/Co-MOF NS electrode exhibited a linear range and detection limit of 0.004–4.428 mM and 1.2 μM, respectively. Further, highly stable and efficient graphene supported 3D Ni-MOF-74/G composite prepared by in situ technique; Ni-MOF-74 can act as a precursor (Zhang et al. 2018). The graphene is used to enhance the conductivity of the composite and also support the film deposition. The morphology characterization from SEM revealed that Ni-MOF-74 crystal formed like a column-shaped polyhedral structure. The as-prepared composite delivered an excellent catalytic response toward glucose due to the synergistic effect between the graphene and Ni_2P particles. Moreover, the composite electrode achieved a linear range and detection limit of 0.005 to 1.4 mM and 0.44 μM, respectively. In addition, the practical applicability of the optimized electrode was demonstrated by the quantification of glucose in human blood samples.

MOF-based nanocomposite, Ni-MOF/Ni/NiO/C was developed via the calcination process and applied to quantify glucose concentrations in blood serum samples (Shu et al. 2017). The crystal structure of the MOF composite and the electrochemical sensing mechanism are portrayed in Fig. 30.2a. The electrocatalytic activity of the fabricated Ni-MOF/Ni/NiO/C electrode was examined toward the glucose oxidation in 0.1 M NaOH, and the resulting catalytic response was compared with the bare GC and GC/Ni-MOF electrodes in the absence and presence of 400 μM glucose (Fig. 30.2b). As you can see, the bare GC electrode showed a negligible catalytic response for glucose oxidation. In contrast, a higher catalytic oxidation current for glucose was acquired at the GCE/Ni-MOF compared to the bare GC electrode. Interestingly, the catalytic current of glucose was further amplified at GCE/Ni-MOF/Ni/NiO/C compared to GCE/Ni-MOF. Moreover, the catalytic glucose oxidation current was steadily increased upon increasing the glucose concentrations in the range of 0.004–5.6 mM and achieved a detection limit of 0.8 μM. Finally, the optimized sensor was used to quantify glucose concentrations in human serum

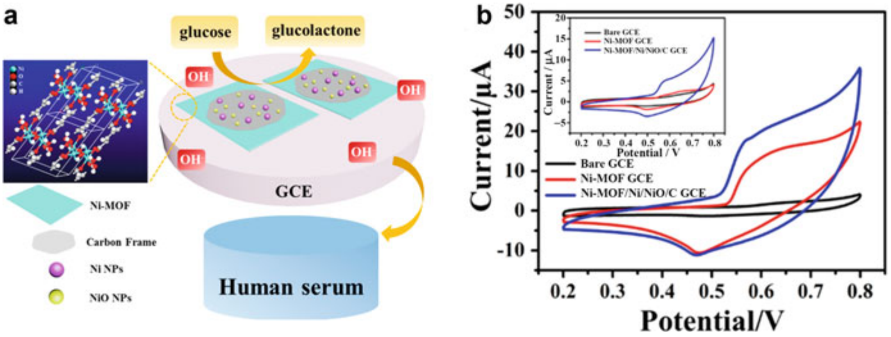

Fig. 30.2 (**a**) Schematic illustration of the Ni-MOF/Ni/NiO/C modified GC electrode used for the detection of glucose in the blood serum sample, and (**b**) cyclic voltammograms (CVs) of different modified electrodes for 400 μM glucose in 0.1 M NaOH at a scan rate of 100 mV s^{-1}. Inset: CVs of modified electrodes in 0.1 M NaOH in the absence of glucose (Shu et al. 2017)

samples, and the obtained values were validated with the enzyme-based spectrophotometry technique.

3.1.2 Hydrogen Peroxide

Hydrogen peroxide (H_2O_2) is an important molecule and involved in various fields like the pharmaceutical industry, waste water treatment, food processing, diagnosis, textile and paper industry, etc. (Chen et al. 2013). Especially, H_2O_2 involves several essential functions in human beings, including gene expression, insulin metabolism, signal transduction, etc. (Di Marzo et al. 2018; Miller et al. 2010). However, excess H_2O_2 concentrations lead to several diseases: Alzheimer's, cancer, inflammation, asthma, and diabetes (Pravda 2020). Therefore, the accurate quantification of H_2O_2 has received enormous interest in biomedical and industrial applications. Particularly, in recent years, MOF-based catalysts have been applied to detect H_2O_2.

Cheng et al. developed a 3D ultrathin flower-like Cu-MOF/MXene composite and deposited it on a GC electrode to detect H_2O_2 (Cheng et al. 2021). The catalyst showed ultrasensitivity to H_2O_2 detection and attained a linear range of 0.001–6.12 mM with a detection limit of 0.35 μM. Further, the GC/Cu-MOF/Mxene electrode reduced H_2O_2 relatively at a higher potential(−0.35 V vs SCE) and, thus, it avoids most of the interfering electrochemically active substances, which are reduced at a very low potential (Ex. O_2). A substantial effort has been made for the fabrication of an N-doped carbon nanotube (N-CNT) anchored with a bimetallic-based MOF (CNT-MOF-CoCu) electrode (Kim and Muthurasu 2021). The FE-SEM revealed that the developed composite appeared as nanocubes with an average size of 450 nm. The as-fabricated CNT-MOF-CoCu nanocomposite displayed remarkable H_2O_2 activity with a linear range of 0.05–3.5 mM and a detection limit of 0.21 μM. Also, the electrode showed catalytic activity toward glucose oxidation. The observed outstanding bifunctional catalytic activity was associated with the synergistic effect between the N-doped CNTs and bimetallic CoCu. Another bimetallic-based nanocomposite (PtCu@MOFs/C) was successfully constructed through a self-sacrificial template (Chen et al. 2018). The PtCu@MOFs/C composite structure is present like a hexagonal star with a size of 40–50 nm. Owing to the synergistic effect between PtCu nanoparticles and MOF shell, the developed catalyst delivered a superior catalytic response for the detection of H_2O_2. Further, an excellent linear range (0.001–3 mM) and detection limit (0.2 μM) were achieved at the optimized composite modified electrode. The interference effect of the PtCu@MOFs/C electrode was examined toward the possible interfering substances such as ascorbic acid, uric acid, and a range of carbohydrates. Interestingly, the sensor exhibited high selectivity for H_2O_2 molecules due to the designed pore size of 0.6 nm, which allows only H_2O_2.

An electrochemical H_2O_2 sensor was constructed based on the manganese (Mn) – metalloporphyrin framework (PCN-222(Mn)) by ultrasonication strategy (Chen et al. 2020). In order to fabricate the sensor, firstly, the as-prepared PCN-222 (Mn) was coated on a GC electrode, and, subsequently, poly-glutamic acid (PGA) was electrochemically polymerized on the PCN-222(Mn) modified electrode to enhance the conductivity of the composite. The conductivity of the resulting composite-polymer modified electrode was examined by electrochemical impedance spectroscopy (EIS) and found that the electrode yielded an R_{CT} value of 211 Ω. This value was almost three times lower than the bare GC electrode (569 Ω). This result clearly indicated that GC/PCN-222(Mn)/PGA composite facilitates better charge transport mobility on the GC electrode. Further, the optimized PGA/PCN-222(Mn) composite was applied to quantify $H_2O_{2,}$ and the sensor delivered a linear sensitivity range of 0.5 μM to 1 mM and the lowest detection limit of 31 nM.

A novel 3D-based cobalt (Co) incorporated zeolite imidazole framework (ZIF-67) was fabricated through a simple plain precipitation reaction under normal conditions (Sun et al. 2020). The developed composite showed poor conductivity, and thus the highly conductive silver nanoparticles (AgNPs) were embedded into the GC/ZIF-67 modified electrode by electrophoretic deposition techniques. Interestingly, the AgNPs combined nanocomposite has achieved a larger surface area and abundant active sites, along with superior conductivity. The optimized composite deposited electrode was applied as a nonenzymatic sensor to detect H_2O_2. Further, the composite ZIF-67 has different morphology depending on the solvent used, as shown in Fig. 30.3a. The composite appeared as a microplate when treated with H_2O (H-ZIF-67) whereas the mixture of solvents such as dimethylformamide and H_2O rendered a 2D ultrathin sheet (D-ZIF-67). Interestingly, the methanol induced the formation of a rhombic dodecahedron structure (M-ZIF-67). The developed different morphologies of composite materials were applied to detect H_2O_2. Among the composites, GC/ZIF-67/Ag and GC/H-ZIF-67/Ag delivered better catalytic responses compared to GC/D-ZIF-67/Ag and GC/M-ZIF-67/Ag. Moreover, to demonstrate the practical applicability of the sensor, the best-performed composite electrode was successfully applied to quantify H_2O_2 in HepG2-type liver cancer cells (Fig. 30.3b).

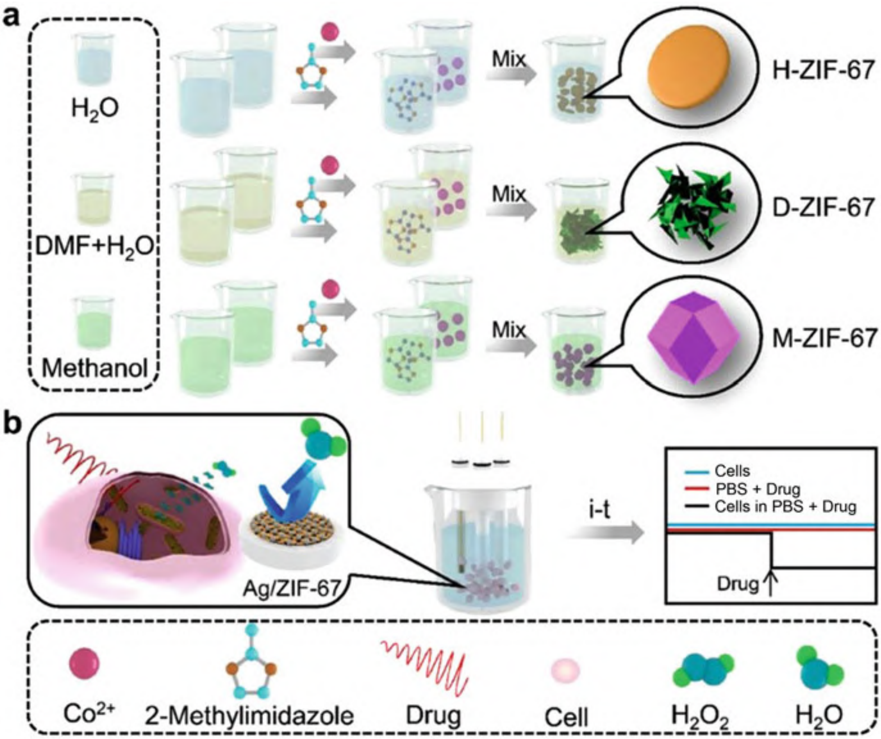

Fig. 30.3 (**a**) Schematic representation for the preparation of H-ZIF-67, D-ZIF-67, and M-ZIF-67; (**b**) Construction and sensing mechanism of the electrochemical sensor to detect H_2O_2 in liver cancer cells (HepG2) (Sun et al. 2020)

3.1.3 Dopamine

Dopamine (DA) is an important neurotransmitter that regulates the biological process in the cardiovascular, hormonal, and central nervous systems (Björklund and Dunnett 2007). In the human body, the excess level of DA content may cause different diseases like Tourette syndrome, depressive disorder, schizophrenia, Parkinson's disease, etc. (Franco et al. 2021). The development of an efficient method for the study of DA molecules up to lower concentration levels is highly desirable for the early diagnosis of illnesses. DA is a highly electroactive molecule, and, thus, electrochemical methods are highly preferable to quantifying it (Kalimuthu and John 2009a, 2010b).

Yang and coworkers developed an electrochemical sensor for DA based on incorporating reduced graphene oxide (rGO) into Ni-based MOF and modified it on the GC electrode. To enhance the conductivity of the composite, AuNPs were electrochemically deposited on the top of the composite modified electrode (Yang et al. 2021). The morphological characterization indicated that rGO on the GC electrode appeared as a curved wrinkled sheet, and it was transformed into a cubic particle upon the integration of Ni-MOF. This implies that MOF structure is retained after mixing these two components. Further, the electrochemically deposited AuNPs are uniformly distributed all over the MOF in the size range of 100–200 nm. The resulting GC/rGO@Ni-MOF/AuNPs electrode was applied to sense DA at pH 6 and obtained a pronounced catalytic response with a linear range of 0.5–120 μM and a detection limit of 0.33 μM.

Bimetallic nanoparticles based MOF (AgPd@Zr-MOF) was designed to use as a sensor for DA detection (Hira et al. 2021). Firstly, Zr-MOF was prepared, and then $AgNO_3$ and $PdCl_2$ were added to it. Followingly, the chemical reductant $NaBH_4$ was added to the mixture to reduce $AgNO_3$ and $PdCl_2$ into bimetallic AgPd nanoparticles. The resulting AgPd@Zr-MOF composite was cast on the GC electrode by drop coating strategy to use for DA detection. The modified electrode exhibited a pronounced catalytic response for the redox reaction of DA at pH 7. Further, an interference study was also conducted with the electroactive DA–related derivatives such as norepinephrine and epinephrine and found that the GC/AgPd@Zr-MOF electrode does not show any significant activities, which indicates that the developed sensor is highly suitable for the selective quantification of DA. Moreover, the sensor achieved a linear range of DA detection from 2–42 μM and a detection limit of 0.1 μM. In addition, the sensor showed long-term stability and retained catalytic response up to 98.1% after 30 days.

Shu and co-workers demonstrated the fabrication of an electrochemical biosensor for real-time monitoring of DA which is released from C6-type cells (Shu et al. 2020). The sensor fabrication strategy and DA sensing mechanism are portrayed in Fig. 30.4. In order to develop the sensor, firstly, poly(dimethylsiloxane) (PDMS) film was coated with a thickness of ~200 nm on a glass slide. Then the PDMS film was incubated in DA solution for 24 h to polymerize DA on the PDMS film. Followingly, CNTs were embedded into the pDA/PDMS film to improve the

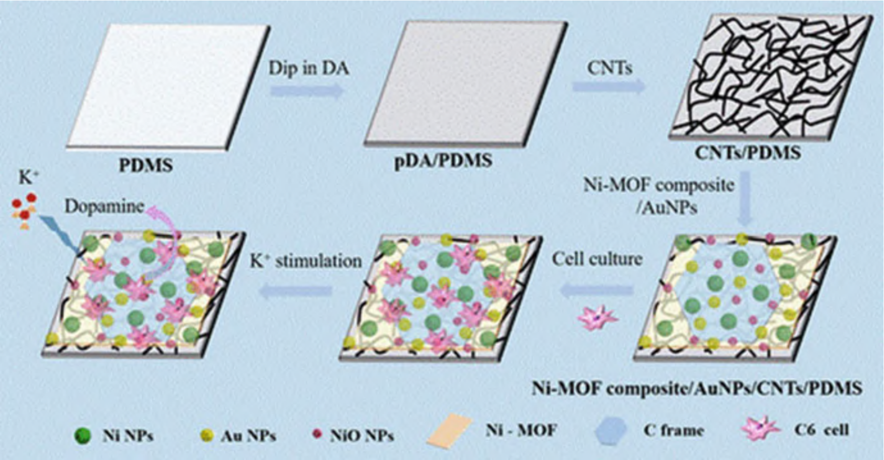

Fig. 30.4 Schematic illustration of the fabrication of NACP film electrode for real-time monitoring of DA released from C6 cells (Shu et al. 2020)

conductivity and structural stability. Finally, Ni-MOF/AuNPs composite was incorporated into pDA/PDMS, and the resulting electrode was referred to Ni-MOF/AuNPs/CNTs/PDMS (NACP). The optimized composite electrode showed outstanding catalytic performance toward the sensing of DA. Further, it was mentioned that the observed catalytic response was associated with the synergistic effect between the AuNPs, CNTs, and Ni-MOF. The nanomaterials AuNPs and CNTs promote heterogeneous and homogeneous electron transfer processes, while Ni and Nio nanoparticles facilitate the catalytic response. Further, the NACP electrode was applied to quantify DA in C6 living cells as part of a practical application. In order to detect the DA from cells, C6 living cells were deposited on NACP film by incubating electrodes in cell culture media for 24 h. SEM image revealed that spindle-shaped cells adsorbed on the electrode surface. DA release from the C6 cell is induced by adding stimulant KCl and the amperometric technique was used to quantify the released DA at an applied potential of 0.3 V vs. Ag/AgCl.

AgNPs-doped ZIF-67 nanopinnas MOF was developed and composite electrochemically deposited on the GC electrode for DA sensing applications (Tang et al. 2020). The size of the AgNPs was estimated to be 15 nm. The optimised electrode was applied for the simultaneous detection of DA with acetaminophen, uric acid, and ascorbic acid. It was found that the sensor exhibited remarkable catalytic responses for all these analytes. Further, the catalytic current steadily increased upon the addition of analytes and achieved a linear range and detection limit of 0.1–100 μM and 0.05 μM, respectively. Copper terephthalate (Cu(tap))-doped MOF was developed via ultrasonication (Wang et al. 2014). It was envisaged that the interaction between Cu(tap) and GO is associated with hydrogen bonding, π−π stacking, and Cu-O coordination. The Cu(tap)-GO was electrochemically reduced to achieve electrochemically reduced graphene (ERG) to improve the conductivity. The composite was optimized with respect to different conditions and used as a sensor for simultaneous detection of DA and acetaminophen. The sensor displayed a pronounced catalytic response for these two analytes and achieved a linear range and detection limit of 1–100 and 1–50 μM and 0.36 and 0.21 μM, respectively, for acetaminophen and DA, respectively.

3.1.4 Cysteine

Cysteine (CY) is a sulfur-containing amino acid and plays a vital role in human biological activities, including metal ion binding, a precursor to the Fe-S cluster and involved in building proteins (Heafield et al. 1990). Further, CY acts as an antioxidizing agent due to potentially trapping reactive oxygen species (Yin et al. 2013). Therefore, the low level of CY in the human body leads to adverse effects such as ischemic stroke, lung and colorectal cancer, cardiovascular diseases, diabetes, and neurological disorders (Rehman et al. 2020). CY is an electrochemically active molecule and highly suitable for electrochemical detection methods (Kalimuthu and John 2009b, 2010a).

For instance, Hosseini et al. constructed an electrochemical sensor for the detection of CY. The sensor fabrication was employed by the doping of Au-SH-SiO_2 into the Cu-MOF (Hosseini et al. 2013). The composite film was optimized by different

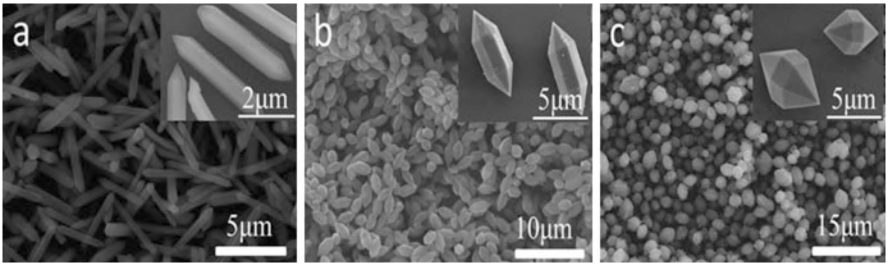

Fig. 30.5 SEM images of MIL-88A crystals with different structures: (**a**) r-MIL-88A, (**b**) s-MIL-88A, and (**c**) d-MIL-88A (Wang et al. 2015)

conditions, and the resulting electrode was used for the detection of CY. The bare GC electrode does not show any catalytic response for CY oxidation. On the other hand, GC/Au-SH-SiO_2@Cu-MOF electrode exhibited a well-defined oxidation current for CY at 0.4 V vs. Ag/AgCl. In contrast, the precursors, Cu-MOFs, showed an oxidation peak for CY at 0.6 V, which indicates that the developed composite has potential catalytic efficiency for CY oxidation. Further, the sensor displayed a linear range and detection limit of 0.02–300 μM and 8 nM, respectively, for CY detection. In another report, the development of a hierarchical Fe_3O_4/carbon-based MOF (Fe_3O_4@C) was demonstrated (Wang et al. 2015). The MIL-88A-based MOF was prepared by linking Fe(III) to the fumaric acid through Fe-O bond. Different morphologies of MIL-88A were developed by changing the concentrations of $FeCl_3 \cdot 6H_2O$ and the nature of the solvent. Figure 30.5 represents that the MIL-88A was prepared under different experimental conditions.

As you can see in Fig. 30.5, the three different shapes (rod, spindle, and diamond) of MIL-88A were obtained based on the experimental conditions. The nucleation rate determines the shape and size of the particles (Torad et al. 2013). Generally, the faster nucleation reaction provides more nuclei, which shortens the particle growth stage, resulting in small-sized particles. On the other hand, the slow nucleation process renders fewer nuclei, allowing to get large-sized particles due to longer reaction time. Further, the solvation also plays a major role in determining particle size. For example, the stronger solvation of Fe^{3+} in DMF leads to slowing down the particle generation speed and causes the formation of large-sized MIL-88A. In contrast, the nucleation process is considered very fast in the water and obtains smaller-sized particles. The equal ratio of $FeCl_3 \cdot 6H_2O$ and fumaric acid (4 mmol) in water provides rod-shaped MIL-88A DMF (r-MIL-88A) with a diameter of 500 μm (Fig. 30.5a) while dissolving in DMF provides diamond-structured MIL-88A (d-MIL-88A) with a diameter of 5 μm (Fig. 30.5c). Nevertheless, spindle-like MIL-88A (s-MIL-88A) with a diameter of 1 μm were obtained while dissolving 2.4 mmol $FeCl_3 \cdot 6H_2O$ and 4.0 mmol fumaric acid in DMF. The as-prepared different shapes of catalysts were used to detect N-acetyl cysteine. Among them, r-MIL-88A showed better electrochemical sensing performances compared to s-MIL-88A and d-MIL-88A. It might be that the smaller size particles possess a higher surface area.

3.2 Biological Macromolecules

Biological macromolecules consist of cellular components involved in numerous vital physiological functions for cell formation and growth. They are classified into four types: proteins, nucleic acid, carbohydrates, and lipids. The precise quantification of these biological macromolecules is biomedically important.

3.2.1 Nucleic Acids

Ribonucleic acid (RNA) is one of the most significant and flexible proteins found in the vast majority of living beings and viruses. As reported, messenger RNA (mRNA) acts as an intermediary carrier of genetic information (Crick 1970), whereas transfer RNA (tRNA) plays as a molecular adaptor that converts the obtained genetic information into a protein sequence (Sharp et al. 1985). Basically, RNA is responsible for converting the instructional genetic information encoded in deoxyribonucleic acid (DNA) into proteins. However, some viruses employ RNA (rather than DNA) to transport genetic information. Further, protein synthesis is carried out by a group of RNA: tRNAs, rRNAs, mRNAs, small nuclear RNAs (snRNAs), microRNAs (miRNAs), and small interfering RNAs (siRNAs) (Gray and Beyer 2020).

The hepatitis C virus (HCV) is widely spread worldwide and causes high mortality and morbidity due to liver cirrhosis and hepatocellular carcinoma (Osman et al. 2017). Therefore, the detection of HCV is performed through the target analyte HCV-RNA. Sheta et al. developed an electrochemical biosensor based on polyaniline (PANI) incorporated Ni-MOF (PANI@Ni-MOF) nanocomposite to quantify HCV-RNA (Sheta et al. 2020). The biosensor was constructed through layer-by-layer immobilization of PANI@Ni-MOF, HCV-RNA probe, and the blocking agent bovine serum albumin (BSA) on the GC electrode. The developed electrode was incubated in target HCV-RNA for the hybridization. EIS was used to investigate the resistivity of the modified electrode. It was found that the R_{ct} value increased while nucleic acid double-strand formation occurred between the target and HCV probe. Further, the R_{ct} value was steadily increased upon increasing concentrations from 1 fM to 100 nM and a detection limit achieved was 0.75 fM.

The same group used a different methodology to detect HCV-RNA. Ag/Zn bimetallic MOF was developed and embedded with the HCV-RNA probe (El-Sheikh et al. 2021). The probe was attached to the MOF by various interactions such as π-π stacking, hydrogen bonding, and electrostatic interaction between the positively charged $-NH_3^+$ present in the MOF and the negatively charged phosphorus backbone of the probe. The formation of nucleic acid double strands between the HCV-RNA probe and the target was examined by glucose oxidation which was catalyzed by the Ag/Zn bimetallic MOF. The glucose oxidation current was linearly increased from 1 fM to 100 nM, and a detection limit was found to be 0.64 fM. Moreover, the practical application of the sensor was demonstrated by the quantification of HCV-RNA in human serum samples.

An electrochemical biosensor was developed to measure miRNA concentration as it is an important biomarker for different types of cancers. The sensor construction was performed by the attachment of probe DNA into AuNPs embedded Cu-MOFs (AuNPs@Cu-MOFs/DNA) (Wang et al. 2018). Then, the target miRNA-155 was attached to the electrode surface. The nucleic acid double-strand formation takes place between probe and target while allowed to interact with them. The probe attached AuNPs@Cu-MOFs is capable of oxidizing glucose molecules. Therefore, the attachment of the target was examined by the increasing glucose oxidation current by differential pulse voltammetry (DPV). The developed sensors yielded extremely high sensitivity for miRNA-155 and achieved the linear range and detection limit of 1.0 fM to 10 nM and 0.35 fM, respectively.

Deoxyribonucleic acid (DNA) is known as the molecule of heredity since it transports genetic information in all living organisms. It is a long deoxyribonucleotide polymer chain, and the length is determined by the amount of nucleotide base pair present. The fundamental roles of DNA are: (i) hold the blueprint for creating proteins and enzymes; (ii) operate as a regulator when there is a lack of the required proteins and enzymes; (iii) carry this information when cell division occurs, and (iv) transfer this information from parental organisms to their offspring (Gait et al. 2006). Basically, genetic information is transferred from DNA to RNA to protein. The primary function of DNA biosensors is to detect complementary DNA sequences or target molecules by attaching a single-stranded oligonucleotide (ssDNA) as a probe to a transducer surface (Hejazi et al. 2009). The probe attached transducer acts as a biosensor that converts the biological event into a detectable signal. Electrochemical DNA biosensors can detect genetic abnormalities, DNA damage, and tiny compounds (e.g., drugs and carcinogens) as well as measure different ions (Thapa et al. 2022).

5-hydroxymethylcytosine (5-hmC) is a pyrimidine nitrogen base in DNA, and it is considered an essential biomarker for the diagnosis of melanoma and leukemia cancers. Cui and coworkers constructed an electrochemical magnetobiosensor to

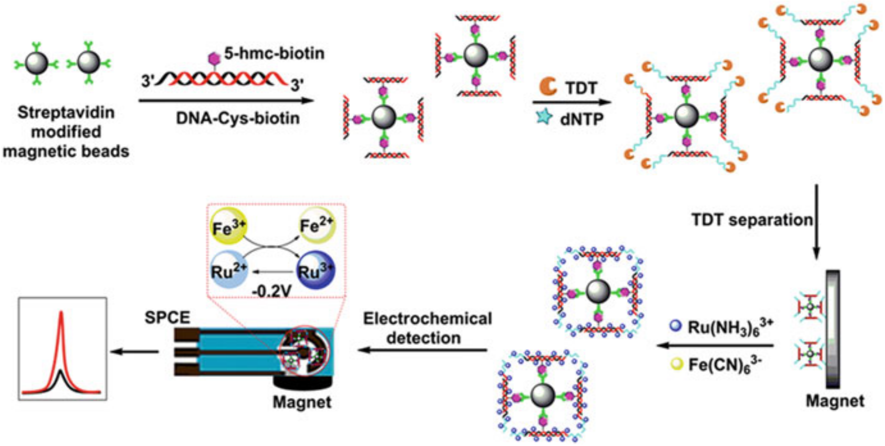

Fig. 30.6 Schematic representation for the development of an electrochemical magnetobiosensor for 5-hmC DNA (Cui et al. 2019)

detect 5-hmC (Cui et al. 2019). The sensor fabrication strategy and sensing mechanism are schematically illustrated in Fig. 30.6. The hybridization between 5-hmC ssDNA and complementary DNA produces the dsDNA. Then the biotin was attached to the 5-hmC of dsDNA. The resulting biotinyl-dsDNAs are attached to the streptavidin-modified magnetic bead (MB) by the specific interaction between biotin and streptavidin. Followingly, terminal deoxynucleotidyl transferase (TDT) is used to expand the length of DNA by the catalytic polymerization reaction where nucleotides are added to the 3′-hydroxy termini of DNA. The redox probes such as $Ru(NH_3)_6^{3+}$ and $Fe(CN)_6^{3-}$ act as primary and secondary electron acceptors, respectively, to facilitate the catalytic reactions. The positively charged primary $Ru(NH_3)_6^{3+}$ electron transfer mediator effectively interacts with the DNA through the negatively charged phosphate backbone. The function of secondary mediator $Fe(CN)_6^{3-}$ is to enhance the electron flow of the redox reaction of primary $Ru(NH_3)_6^{3+}/Ru(NH_3)_6^{2+}$. The binding of biotinylated 5-hmC DNA into streptavidin-modified MB was examined by increasing catalytic current. The observed catalytic current is attributed to the redox response from $Ru(NH_3)_6^{3+}/Ru(NH_3)_6^{2+}$ and not from $Fe(CN)_6^{3-}/Fe(CN)_6^{4-}$ due to the strong repulsion of negatively charged DNA attached to SPCE, which ruled out the false current signal. The catalytic current steadily increased when increasing the loading of 5-hmC DNA on the electrode surface. Further, the optimized sensor showed excellent catalytic performance and achieved the linear range and detection limit of 0.01–1000 pM and 9.06 fM, respectively. Moreover, the developed sensor was applied to detect 5-hmC DNA in cervical and kidney-related cancer cells such as HeLa and HEK 293 T cells, respectively.

An electrochemical DNA biosensor developed for the detection of β1 receptor blocker metoprolol targets the hypertension-carrying adrenergic receptor gene (ADRB1). In order to fabricate the sensor, Hemin and PtNPs are loaded into an amine-modified MOF (Fe-MIL-88-NH_2) (Yuan et al. 2017). The sensing mechanism relies on the H_2O_2 reduction by the Hemin and PtNPs composite. Further, Cu^{2+} was incorporated into the composite to achieve a better electron transfer response. Hexanethiol (HT) was used as a blocking agent to control nonspecific adsorption. It is well known that Hemin is metalloporphyrin and has an excellent peroxidase-like activity. The developed composite PtNPs/Hemin@Fe-MIL-88NH_2/Cu^{2+}/CP/HT was deposited on the GC electrode surface and subsequently attached to the target probe. The catalytic efficiency of the GC/PtNPs/Hemin@Fe-MIL-88NH_2/Cu^{2+}/CP/HT/DNA-probe electrode was examined for the catalytic efficiency of H_2O_2 reduction activity in the presence of various target DNA concentrations. It was found that H_2O_2 reduction decreases upon increasing the analyte concentration due to the hybridization of DNA, which leads to masking the electrode surface and consequently blocking the electron transfer, thereby decreasing the catalytic current.

3.2.2 Detection of Cancer Biomarker Proteins

Increased levels of tumor markers in body fluids are the indicator of tumor development. Therefore, the early diagnosis of the tumor biomarkers is crucial to controlling the cancers. Zhang et al. developed an electrochemical biosensor to quantify carcinoembryonic antigen (CEA) which is responsible for colorectal, breast, colon, and liver cancers. In order to construct a biosensor, Zr-based MOF was incorporated with the CEA-specific aptamer and achieved by a facile de novo synthetic strategy (Zhang et al. 2017). The Zr-MOF was synthesized with a simple mixing of $ZrOCl_2{\cdot}8H_2O$ and $4',4''',4''''$- nitrilotris[1,1′-biphenyl]-4-carboxylic acid (H_3NBB). Then, CEA-specific aptamer is embedded into the Zr-MOF by mixing under sonication for 30 min, and the resulting composite is referred to as the Zr-MOF@Apt_{CEA}. The optimized sensor was used to detect CEA by EIS with a well-known redox couple $[Fe(CN)_6]^{3-/4-}$. The bare Au electrode shows the R_{CT} value of 51.5 ohm, and this value significantly increased to 0.42 kohm while MOF@Apt_{CEA} was coated on the Au surface. The increasing resistance value is associated with the repulsive force between negatively charged phosphate ion in the aptamer and $[Fe(CN)_6]^{3-/4-}$. In addition, the electron blocking effect of aptamer loaded MOF@Apt_{CEA}. Further, R_{CT} was increased to 1.43 kohm when treated with CEA, and it indicates CEA binding with Au/MOF@Apt_{CEA} electrode. Further, the R_{CT} value was systematically increased while increasing the CEA concentration in the analytical solution, and the sensor achieved the linear of 0.001–0.50 ng mL^{-1} and a detection limit of 0.4 pg mL^{-1}.

Adenosine triphosphate (ATP) is responsible for the primary energy source of cells and regulates cellular metabolism. Thus, it acts as an indicator for tumors, cell injury, and many other diseases (Gourine et al. 2005). Shi and coworkers constructed an electrochemical biosensor based on amine-functionalized Ce-MOF for the detection of ATP (Shi et al. 2017). Figure 30.7a portrays the construction of a label-free aptamer embedded Ce-MOF based ATP sensor. Firstly, Ce-MOF was prepared and then coated on the Au electrode via weak covalent and electrostatic interaction. Then, ATP-specific aptamer was embedded into Ce-MOF through hydrogen bonding, as well as electrostatic and π-π interactions. The resulting modified electrode was specifically bound with target analyte ATP and it was analyzed by EIS with a

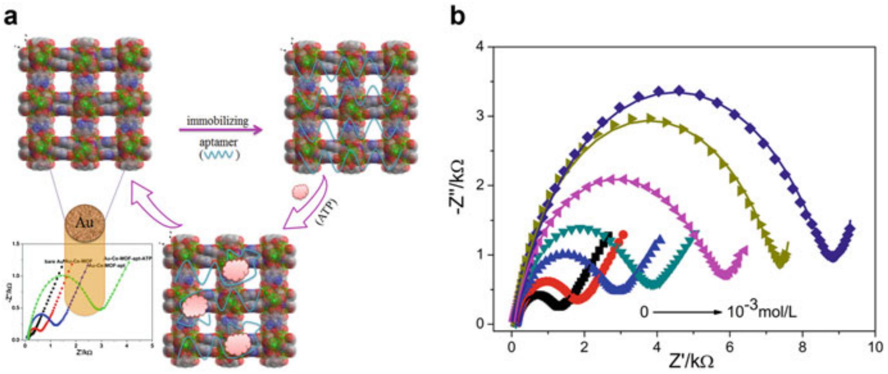

Fig. 30.7 (**a**) Schematic diagram of the development of Ce-MOF-based ATP sensor. (**b**) Nyquist plots for a range of ATP concentrations (0–1 mM) incubated Au/Ce-MOF-apt electrode (Shi et al. 2017)

redox probe $[Fe(CN)_6]^{3-/4-}$. The impedance value was gradually increased upon increasing from 0–10 mM (Fig. 30.7b).

Another impedance-based sensor was developed to detect human epidermal growth factor receptor-2 (HER2). The HER2 is a tumor biomarker protein related to breast cancer. To construct a biosensor, the bimetallic MnFe Prussian blue was amalgamated with AuNPs and coated on the Au electrode surface, and the resulting electrode is referred to as Au/MnFe-PBA@AuNPs (Zhou et al. 2019b). Subsequently, HER2-specific aptamer is attached to the Au/MnFePBA@AuNPs composite. The as-prepared Au/MnFePBA@AuNPs/Apt electrode was used as a sensor probe to detect HER2 by the EIS method with $[Fe(CN)_6]^{3-/4-}$ as a redox probe. The R_{CT} value is significantly increased from 0.35 kohm to 3.02 kohm while increasing the concentrations of HER2 in the range of 0.001–1.0 ng·mL^{-1}. Further, the detection limit was achieved as 0.247 pg·mL^{-1}.

Tyrosine kinase-7 (PTK7) is a primary indicator for leukemias and solid tumors. In order to develop a biosensor for PTK7, Zhou et al. employed the fabrication of bimetallic ZnZr-based MOFs through the MOF-on-MOF method (Zhou et al. 2019a). Two types of MOFs were synthesized, such as Zn-MOF-on-Zr-MOF and Zr-MOF-on-Zn-MOF. SEM images revealed that Zn-MOF-on-Zr-MOF appeared as a hierarchically decussated foliace structure while Zr-MOF-on-Zn-MOF existed as a multilayered nanosheet structure. PTK7-specific aptamer was attached to the developed MOFs and used to detect PTK7 by EIS strategy. The active surface area of the Zn-MOF-on-Zr-MOF and Zr-MOF-on-Zn-MOF was measured by N_2 adsorption-desorption isotherms and found to be 6.01 and 23.8 m^2 g^{-1}. Therefore, Zr-MOF-on-Zn-MOF modified electrode exhibited superior performance for PTK7 sensing.

4 Conclusions

This chapter summarized the recent innovation, development, and electrochemical sensing applications of MOFs-based electrocatalysts. Given the range of ligands and metal clusters, the desirable high active surface area, high porosity, high biomolecules affinity, flexible coordination structures, and different functionalities of MOFs render researchers the opportunity to construct highly efficient, viable biosensors. In addition, MOFs act as artificial enzymes due to their tunable porosity size characteristics. Further, the electrocatalytic activity of MOFs tremendously improved due to the synergistic effect among the biomolecules and multimetal sites and novel organic ligands. Further, it discussed the different synthetic approaches of MOFs and their advantages and disadvantages. Specifically, this chapter discussed the development of MOF-based electrochemical biosensors for small biomolecules (glucose, hydrogen peroxide, dopamine, and cysteine) and biological macromolecules (nucleic acids and cancer biomarker proteins). Moreover, the conductivity and stability of the MOFs dramatically improved when embedded with the range of nanomaterials, but further study is needed to focus on the controllable synthesis of MOFs on the nanoscale with higher conductivity for future perspectives.

References

Ajay PVS, Printo J, Kiruba DSCG, Susithra L, Takatoshi K, Sivakumar M (2017) Colorimetric sensors for rapid detection of various analytes. Mater Sci Eng C 78:1231–1245

Alizadeh S, Nematollahi D (2019) Convergent and divergent paired electrodeposition of metal-organic framework thin films. Sci Rep 9(1):14325

Ameloot R, Gobechiya E, Uji-i H, Martens JA, Hofkens J, Alaerts L, Sels BF, De Vos DE (2010) Direct patterning of oriented metal–organic framework crystals via control over crystallization kinetics in clear precursor solutions. Adv Mater 22(24):2685–2688

Björklund A, Dunnett SB (2007) Fifty years of dopamine research. Trends Neurosci 30(5):185–187

Britt D, Tranchemontagne D, Yaghi OM (2008) Metal organic frameworks with high capacity and selectivity for harmful gases. Proc Natl Acad Sci U S A 105(33):11623–11627

Bux H, Chmelik C, van Baten JM, Krishna R, Caro J (2010) Novel MOF-membrane for molecular sieving predicted by IR-diffusion studies and molecular modeling. Adv Mater 22(42): 4741–4743

Campagnol N, Van Assche TRC, Li M, Stappers L, Dincă M, Denayer JFM, Binnemans K, De Vos DE, Fransaer J (2016) On the electrochemical deposition of metal–organic frameworks. J Mater Chem A 4(10):3914–3925

Chen A, Chatterjee S (2013) Nanomaterials based electrochemical sensors for biomedical applications. Chem Soc Rev 42(12):5425–5438

Chen L, Wang T, Xue Y, Zhou X, Zhou J, Cheng X, Xie Z, Kuang Q, Zheng L (2018) Rationally armoring PtCu alloy with metal-organic frameworks as highly selective nonenzyme electrochemical sensor. Adv Mater Interfaces 5(23):1801168

Chen S, Yuan R, Chai Y, Hu F (2013) Electrochemical sensing of hydrogen peroxide using metal nanoparticles: a review. Microchim Acta 180(1):15–32

Chen Y, Huang W, Wang C, Zhai X, Zhang T, Wang Y, Hu X (2020) Direct growth of poly-glutamic acid film on peroxidase mimicking PCN-222(Mn) for constructing a novel sensitive non-enzymatic electrochemical hydrogen peroxide biosensor. ACS Sustain Chem Eng 8(35): 13226–13235

Cheng D, Li P, Zhu X, Liu M, Zhang Y, Liu Y (2021) Enzyme-free electrochemical detection of hydrogen peroxide based on the three-dimensional flower-like Cu-based metal organic frameworks and MXene nanosheets. Chinese J Chem 8(39):2181–2187

Crick F (1970) Central dogma of molecular biology. Nature 227(5258):561–563

Cui L, Hu J, Wang M, Li C-c, Zhang C-y (2019) Label-free and immobilization-free electrochemical magnetobiosensor for sensitive detection of 5-hydroxymethylcytosine in genomic DNA. Anal Chem 91(2):1232–1236

Czaja AU, Trukhan N, Muller U (2009) Industrial applications of metal-organic frameworks. Chem Soc Rev 38(5):1284–1293

Dhakshinamoorthy A, Asiri AM, Garcia H (2017) Metal organic frameworks as versatile hosts of Au nanoparticles in heterogeneous catalysis. ACS Catal 7(4):2896–2919

Di Marzo N, Chisci E, Giovannoni R (2018) The role of hydrogen peroxide in redox-dependent signaling: homeostatic and pathological responses in mammalian cells. Cell 7(10):156

El-Sheikh SM, Osman DI, Ali OI, Shousha WG, Shoeib MA, Shawky SM, Sheta SM (2021) A novel Ag/Zn bimetallic MOF as a superior sensitive biosensing platform for HCV-RNA electrochemical detection. Appl Surf Sci 562:150202

Franco R, Reyes-Resina I, Navarro G (2021) Dopamine in health and disease: much more than a neurotransmitter. Biomedicine 9(2):109

Gait M, Loakes D, Pyle A, Williams D, Williams N (2006) Nucleic acids in chemistry and biology. Biology 3:13–76

Gourine AV, Llaudet E, Dale N, Spyer KM (2005) ATP is a mediator of chemosensory transduction in the central nervous system. Nature 436(7047):108–111

Gray MW, Beyer AL (2020) Ribonucleic acid (RNA), Mc Graw Hill, Access Science

Gulbagca F, Arikan K, Cellat K, Khan A, Sen F (2019) Metal organic frameworks (MOF's) for biosensing and bioimaging applications. Mater Res Found 58:308–360

Heafield MT, Fearn S, Steventon GB, Waring RH, Williams AC, Sturman SG (1990) Plasma cysteine and sulphate levels in patients with motor neurone, Parkinson's and Alzheimer's disease. Neurosci Lett 110(1–2):216–220

Hejazi M, Raoof JB, Ojani R, Golabi S, Asl E (2009) Brilliant cresyl blue as electroactive indicator in electrochemical DNA oligonucleotide sensors. Bioelectrochemistry (Amsterdam, Netherlands) 78:141–146

Hira SA, Nagappan S, Annas D, Kumar YA, Park KH (2021) NO_2-functionalized metal–organic framework incorporating bimetallic alloy nanoparticles as a sensor for efficient electrochemical detection of dopamine. Electrochem Commun 125:107012

Hosseini H, Ahmar H, Dehghani A, Bagheri A, Tadjarodi A, Fakhari AR (2013) A novel electrochemical sensor based on metal-organic framework for electro-catalytic oxidation of L-cysteine. Biosens Bioelectron 42:426–429

Hwang D-W, Lee S, Seo M, Chung TD (2018) Recent advances in electrochemical non-enzymatic glucose sensors – a review. Anal Chim Acta 1033:1–34

Jeon W-Y, Choi Y-B, Kim H-H (2015) Disposable non-enzymatic glucose sensors using screen-printed nickel/carbon composites on indium tin oxide electrodes. Sensors 15(12):31083–31091

Jiang H-L, Xu Q (2011) Porous metal-organic frameworks as platforms for functional applications. Chem Commun (Cambridge, U K) 47(12):3351–3370

Johnston L, Wang G, Hu K, Qian C, Liu G (2021) Advances in biosensors for continuous glucose monitoring towards wearables. Front Bioeng Biotechnol 9:733810

Kajal N, Singh V, Gupta R, Gautam S (2022) Metal organic frameworks for electrochemical sensor applications: a review. Environ Res 204:112320

Kalimuthu P, Fischer-Schrader K, Schwarz G, Bernhardt PV (2013) Mediated electrochemistry of nitrate reductase from arabidopsis thaliana. J Phys Chem B 117(25):7569–7577

Kalimuthu P, John SA (2009a) Electropolymerized film of functionalized thiadiazole on glassy carbon electrode for the simultaneous determination of ascorbic acid, dopamine and uric acid. Bioelectrochemistry 77(1):13–18

Kalimuthu P, John SA (2009b) Nanostructured electropolymerized film of 5-amino-2-mercapto-1,3,4-thiadiazole on glassy carbon electrode for the selective determination of l-cysteine. Electrochem Commun 11(2):367–370

Kalimuthu P, John SA (2010a) Selective determination of homocysteine at physiological pH using nanostructured film of aminothiadiazole modified electrode. Bioelectrochemistry 79(2): 168–172

Kalimuthu P, John SA (2010b) Simultaneous determination of ascorbic acid, dopamine, uric acid and xanthine using a nanostructured polymer film modified electrode. Talanta 80(5):1686–1691

Kalimuthu P, Kappler U, Bernhardt PV (2014) Catalytic voltammetry of the molybdoenzyme sulfite dehydrogenase from sinorhizobium meliloti. J Phys Chem B 118(25):7091–7099

Kalimuthu P, Leimkühler S, Bernhardt PV (2012) Catalytic electrochemistry of xanthine dehydrogenase. J Phys Chem B 116(38):11600–11607

Keskin S, Kizilel S (2011) Biomedical applications of metal organic frameworks. Ind Eng Chem Res 50(4):1799–1812

Kim S e, Muthurasu A (2021) Highly oriented nitrogen-doped carbon nanotube integrated bimetallic cobalt copper organic framework for non-enzymatic electrochemical glucose and hydrogen peroxide sensor. Electroanalysis 33(5):1333–1345

Klimakow M, Klobes P, Thünemann AF, Rademann K, Emmerling F (2010) Mechanochemical synthesis of metal−organic frameworks: a fast and facile approach toward quantitative yields and high specific surface areas. Chem Mater 22(18):5216–5221

Laor O, Torgersen H, Yadin H, Becker Y (1992) Detection of FMDV RNA amplified by the polymerase chain reaction (PCR). J Virol Methods 36(3):197–207

Lequin RM (2005) Enzyme immunoassay (EIA)/enzyme-linked immunosorbent assay (ELISA). Clin Chem (Washington, DC, U S) 51(12):2415–2418

Liu Z, Short J, Rose A, Ren S, Contel N, Grossman S, Unger S (2001) The simultaneous determination of diazepam and its three metabolites in dog plasma by high-performance liquid chromatography with mass spectroscopy detection. J Pharm Biomed Anal 26(2):321–330

Mahato K, Kumar S, Srivastava A, Maurya PK, Singh R, Chandra P (2018) Chapter 14 - Electrochemical Immunosensors: fundamentals and applications in clinical diagnostics. In: Vashist SK, Luong JHT (eds) Handbook of immunoassay technologies. Academic, pp 359–414

Miller EW, Dickinson BC, Chang CJ (2010) Aquaporin-3 mediates hydrogen peroxide uptake to regulate downstream intracellular signaling. Proc Natl Acad Sci 107(36):15681–15686

Nath I, Chakraborty J, Verpoort F (2016) Metal organic frameworks mimicking natural enzymes: a structural and functional analogy. Chem Soc Rev 45(15):4127–4170

Osman D, Ali O, Obada M, El-Mezayen H, El-Said H (2017) Chromatographic determination of some biomarkers of liver cirrhosis and hepatocellular carcinoma in Egyptian patients. Biomed Chromatogr 31(6):e3893

Paul A, Vyas G, Paul P, Srivastava DN (2018) Gold-nanoparticle-encapsulated ZIF-8 for a mediator-free enzymatic glucose sensor by amperometry. ACS Appl Nano Mater 1(7): 3600–3607

Petersen MC, Vatner DF, Shulman GI (2017) Regulation of hepatic glucose metabolism in health and disease. Nat Rev Endocrinol 13(10):572–587

Polshettiwar SA, Deshmukh CD, Baheti AM, Wani MS, Bompilwar E, Jambhekar D, Choudhari S, Tagalpallewar A (2021) Recent trends on biosensors in healthcare and pharmaceuticals: an overview. Int J Pharm Invest 11(2):131–136

Pravda J (2020) Hydrogen peroxide and disease: towards a unified system of pathogenesis and therapeutics. Mol Med (Cambridge, Mass) 26(1):41–41

Rehman T, Shabbir MA, Inam-Ur-Raheem M, Manzoor MF, Ahmad N, Liu Z-W, Ahmad MH, Siddeeg A, Abid M, Aadil RM (2020) Cysteine and homocysteine as biomarker of various diseases. Food Sci Nutr 8(9):4696–4707

Sharp SJ, Schaack J, Cooley L, Burke DJ, Söll D (1985) Structure and transcription of eukaryotic tRNA genes. CRC Crit Rev Biochem 19(2):107–144

Sheta SM, El-Sheikh SM, Osman DI, Salem AM, Ali OI, Harraz FA, Shousha WG, Shoeib MA, Shawky SM, Dionysiou DD (2020) A novel HCV electrochemical biosensor based on a polyaniline@Ni-MOF nanocomposite. Dalton Trans 49(26):8918–8926

Shi P, Zhang Y, Yu Z, Zhang S (2017) Label-free electrochemical detection of ATP based on amino-functionalized metal-organic framework. Sci Rep 7(1):6500

Shu Y, Lu Q, Yuan F, Tao Q, Jin D, Yao H, Xu Q, Hu X (2020) Stretchable electrochemical biosensing platform based on Ni-MOF composite/Au nanoparticle-coated carbon nanotubes for real-time monitoring of dopamine released from living cells. ACS Appl Mater Interfaces 12(44): 49480–49488

Shu Y, Yan Y, Chen J, Xu Q, Pang H, Hu X (2017) Ni and NiO nanoparticles decorated metal–organic framework Nanosheets: facile synthesis and high-performance nonenzymatic glucose detection in human serum. ACS Appl Mater Interfaces 9(27):22342–22349

Sohail M, Altaf M, Baig N, Jamil R, Sher M, Fazal A (2018) A new water stable zinc metal organic framework as an electrode material for hydrazine sensing. New J Chem 42(15):12486–12491

Stock N, Biswas S (2012) Synthesis of metal-organic frameworks (MOFs): routes to various MOF topologies, morphologies, and composites. Chem Rev 112(2):933–969

Sun D, Yang D, Wei P, Liu B, Chen Z, Zhang L, Lu J (2020) One-step electrodeposition of silver nanostructures on 2D/3D metal–organic framework ZIF-67: comparison and application in electrochemical detection of hydrogen peroxide. ACS Appl Mater Interfaces 12(37): 41960–41968

Tang J, Liu Y, Hu J, Zheng S, Wang X, Zhou H, Jin B (2020) Co-based metal-organic framework nanopinnas composite doped with Ag nanoparticles: a sensitive electrochemical sensing platform for simultaneous determination of dopamine and acetaminophen. Microchem J 155:104759

Thapa K, Liu W, Wang R (2022) Nucleic acid-based electrochemical biosensor: recent advances in probe immobilization and signal amplification strategies. WIREs Nanomed Nanobiotechnol 14(1):e1765

Torad NL, Hu M, Kamachi Y, Takai K, Imura M, Naito M, Yamauchi Y (2013) Facile synthesis of nanoporous carbons with controlled particle sizes by direct carbonization of monodispersed ZIF-8 crystals. Chem Commun 49(25):2521–2523

Užarević K, Wang TC, Moon S-Y, Fidelli AM, Hupp JT, Farha OK, Friščić T (2016) Mechanochemical and solvent-free assembly of zirconium-based metal–organic frameworks. Chem Commun 52(10):2133–2136

Wang G, He X, Wang L, Gu A, Huang Y, Fang B, Geng B, Zhang X (2012) Non-enzymatic electrochemical sensing of glucose. Microchim Acta (186):161–186

Wang H-S (2017) Metal-organic frameworks for biosensing and bioimaging applications. Coord Chem Rev 349:139–155

Wang H, Jian Y, Kong Q, Liu H, Lan F, Liang L, Ge S, Yu J (2018) Ultrasensitive electrochemical paper-based biosensor for microRNA via strand displacement reaction and metal-organic frameworks. Sens Actuators B 257:561–569

Wang L, Zhang Y, Li X, Xie Y, He J, Yu J, Song Y (2015) The MIL-88A-derived Fe_3O_4-carbon hierarchical nanocomposites for electrochemical sensing. Sci Rep 5(1):14341

Wang M, Dong X, Meng Z, Hu Z, Lin Y-G, Peng C-K, Wang H, Pao C-W, Ding S, Li Y, Shao Q, Huang X (2021) An efficient interfacial synthesis of two-dimensional metal–organic framework Nanosheets for electrochemical hydrogen peroxide production. Angew Chem Int Ed 60(20): 11190–11195

Wang X, Wang Q, Wang Q, Gao F, Gao F, Yang Y, Guo H (2014) Highly dispersible and stable copper terephthalate metal–organic framework–graphene oxide nanocomposite for an electrochemical sensing application. ACS Appl Mater Interfaces 6(14):11573–11580

Wei Z, Zhu W, Li Y, Ma Y, Wang J, Hu N, Suo Y, Wang J (2018) Conductive Leaflike cobalt metal–organic framework nanoarray on carbon cloth as a flexible and versatile anode toward both electrocatalytic glucose and water oxidation. Inorg Chem 57(14):8422–8428

Wojciechowska J, Krajewski W, Bolanowski M, Krecicki T, Zatonski T (2016) Diabetes and cancer: a review of current knowledge. Exp Clin Endocrinol Diabetes 124(5):263–275

Yang S, Zhang J, Bai C, Deng K (2021) Gold nanoparticle decorated rGO-encapsulated metal-organic framework composite sensor for the detection of dopamine. Can J Chem 99(5):465–473

Yin C, Huo F, Zhang J, Martínez-Máñez R, Yang Y, Lv H, Li S (2013) Thiol-addition reactions and their applications in thiol recognition. Chem Soc Rev 42(14):6032–6059

Yoo Y, Jeong H-K (2008) Rapid fabrication of metal organic framework thin films using microwave-induced thermal deposition. Chem Commun 21:2441–2443

Yuan G, Wang L, Mao D, Wang F, Zhang J (2017) Voltammetric hybridization assay for the β1-adrenergic receptor gene (ADRB1), a marker for hypertension, by using a metal organic framework (Fe-MIL-88NH2) with immobilized copper(II) ions. Microchim Acta 184(9): 3121–3130

Zhang S, Rong F, Guo C, Duan F, He L, Wang M, Zhang Z, Kang M, Du M (2021) Metal–organic frameworks (MOFs) based electrochemical biosensors for early cancer diagnosis in vitro. Coord Chem Rev 439:213948

Zhang Y, Xu J, Xia J, Zhang F, Wang Z (2018) MOF-derived porous Ni_2P/graphene composites with enhanced electrochemical properties for sensitive nonenzymatic glucose sensing. ACS Appl Mater Interfaces 10(45):39151–39160

Zhang Z-H, Duan F-H, Tian J-Y, He J-Y, Yang L-Y, Zhao H, Zhang S, Liu C-S, He L-H, Chen M, Chen D-M, Du M (2017) Aptamer-embedded zirconium-based metal–organic framework composites prepared by de novo bio-inspired approach with enhanced biosensing for detecting trace analytes. ACS Sensors 2(7):982–989

Zhong G-X, Zhang W-X, Sun Y-M, Wei Y-Q, Lei Y, Peng H-P, Liu A-L, Chen Y-Z, Lin X-H (2015) A nonenzymatic amperometric glucose sensor based on three dimensional nanostructure gold electrode. Sens Actuators B 212:72–77

Zhou N, Su F, Guo C, He L, Jia Z, Wang M, Jia Q, Zhang Z, Lu S (2019a) Two-dimensional oriented growth of Zn-MOF-on-Zr-MOF architecture: a highly sensitive and selective platform for detecting cancer markers. Biosens Bioelectron 123:51–58

Zhou N, Su F, Li Z, Yan X, Zhang C, Hu B, He L, Wang M, Zhang Z (2019b) Gold nanoparticles conjugated to bimetallic manganese(II) and iron(II) Prussian blue analogues for aptamer-based impedimetric determination of the human epidermal growth factor receptor-2 and living MCF-7 cells. Microchim Acta 186(2):75

Zhu Q-L, Xu Q (2014) Metal-organic framework composites. Chem Soc Rev 43(16):5468–5512

Zhuang J-L, Ceglarek D, Pethuraj S, Terfort A (2011) Rapid room-temperature synthesis of metal–organic framework HKUST-1 crystals in bulk and as oriented and patterned thin films. Adv Funct Mater 21(8):1442–1447

Engineered Nanobiomarkers for Point-of-Care Analysis of Biomolecules

31

Md Abdus Subhan and Tahrima Subhan

Contents

1 Introduction 688
2 Point-of-Care Testing Technologies for Biomolecular Diagnostics 690
3 Nanobiomarker for the Development of Biosensors and POCT Devices 692
4 Conclusion and Future Outlook 696
References 697

Abstract

Nanobiomarkers are interesting in POCT because they improve analytical performance and make the detection process quick and easy. POCT used nanotechnology to identify illness biomarkers such as infections, cancer cells, enzymes, proteins, and small-molecule metabolites. Nanobiomarkers are used at many points in the disease detection, monitoring, and prevention processes. Biomolecules are evaluated using a variety of parts, readout systems, and biosensors made from synthetic nanomaterials. The use of POCT sensing devices is emerging as a crucial technique for the early diagnosis of pathogenic microorganisms or biomolecules. In terms of use, greater user accessibility, timely detection, accuracy, and sensitivity, POCT is quite advantageous. Innovative strategies are used in the most recent research developments for POCT-based SARS-CoV-2 recognition techniques.

M. A. Subhan (✉)
Department of Chemistry, ShahJalal University of Science and Technology, Sylhet, Bangladesh
e-mail: subhan-che@sust.edu

T. Subhan
Khajanchibari International School and College, Sylhet, Bangladesh

Department of Social Work, ShahJalal University of Science and Technology, Sylhet, Bangladesh

© Springer Nature Singapore Pte Ltd. 2023

U. P. Azad, P. Chandra (eds.), *Handbook of Nanobioelectrochemistry*,
https://doi.org/10.1007/978-981-19-9437-1_31

Keywords

Point-of-care testing · Nanobiomarker · Biomolecules · Nanozymes · POCT regulations

1 Introduction

A biomarker can provide an unique pharmacological response to a treatment and can be extremely important in a variety of biological and pathological processes. Finding biomarkers in human diseased tissue or cells is clinically extremely important, particularly for individualized treatment, illness diagnosis, and prognosis. Point-of-care testing (POCT) devices are increasingly using nanobiomarkers to boost detection performance. They serve as labels for signal production, transduction, and amplification or as carriers for immobilizing biorecognition components. POCT are used to identify illness biomarkers, such as pathogens, cancer cells, tiny molecules, metabolites, enzymes, proteins, and nucleic acids. Recent developments in microfluidics-based devices, printable electrochemical biosensors, and lateral flow tests are well known (Mattiuzzi et al. 2012; Song et al. 2014).

Biomarkers are utilized in different stages of disease detection, monitoring, and protection (Fig. 31.1). Engineered nanomaterial-based biosensors may evaluate biomolecules using a variety of parts and readout configurations (Table 31.1) (Wang et al. 2020). For instance, there is now a lot of interest in the creation of biosensors that can detect biomarkers and biomolecules as well as immunological checkpoints that may be used in liquid biopsies to detect and evaluate cancer (Jayanthi et al. 2017; Mummareddy et al. 2021).

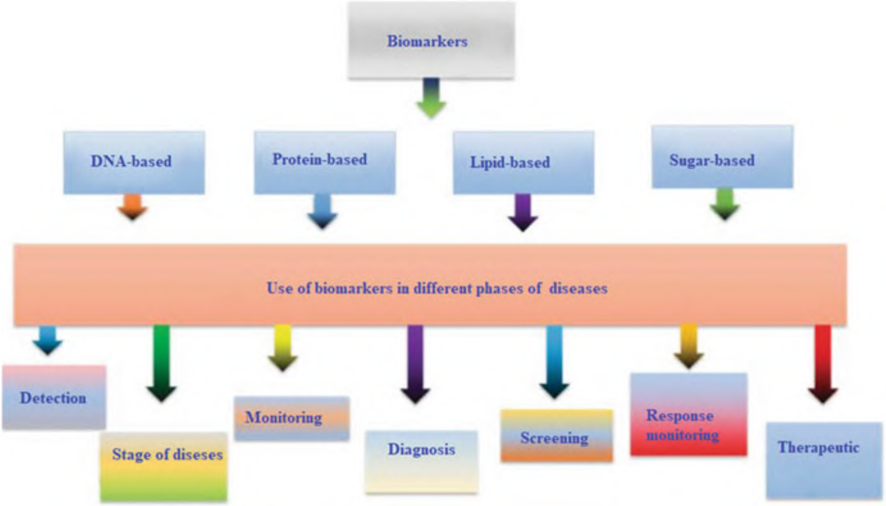
Biomarkers
DNA-based
Protein-based
Lipid-based
Sugar-based
Use of biomarkers in different phases of diseases
Detection
Stage of diseses
Monitoring
Diagnosis
Screening
Response monitoring
Therapeutic

Fig. 31.1 Application of biomarkers at various illness phases

Table 31.1 Biosensors for biomolecules based on nanomaterials: component and readout setups (Wang et al. 2020)

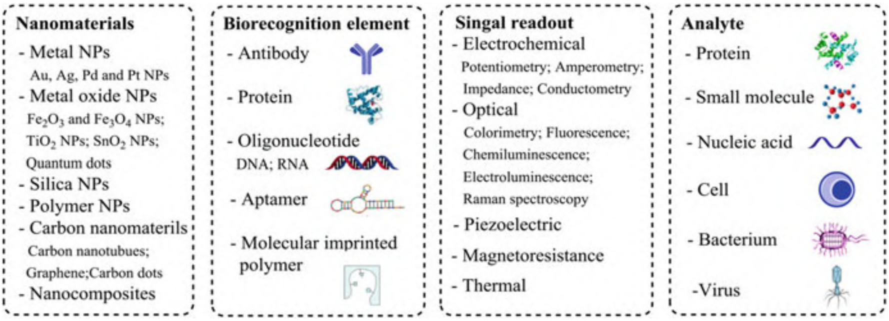

Nanomaterials
- Metal NPs
  Au, Ag, Pd and Pt NPs
- Metal oxide NPs
  Fe_2O_3 and Fe_3O_4 NPs; TiO_2 NPs; SnO_2 NPs; Quantum dots
- Silica NPs
- Polymer NPs
- Carbon nanomaterils
  Carbon nanotubues; Graphene;Carbon dots
- Nanocomposites

Biorecognition element
- Antibody
- Protein
- Oligonucleotide
  DNA; RNA
- Aptamer
- Molecular imprinted polymer

Singal readout
- Electrochemical
  Potentiometry; Amperometry; Impedance; Conductometry
- Optical
  Colorimetry; Fluorescence; Chemiluminescence; Electroluminescence; Raman spectroscopy
- Piezoelectric
- Magnetoresistance
- Thermal

Analyte
- Protein
- Small molecule
- Nucleic acid
- Cell
- Bacterium
-Virus

Table 31.2 Different types of cancer biomarkers

Biomarker	Cancer type
AFP	Liver cancer, hepatocellular carcinoma (HCC)
BCR-ABL	Chronic myeloid leukemia
ApoA1, CA125, CA19-9, CEA, ApoA2, and TTR	Pancreatic cancer, pancreatic ductal adenocarcinoma (PDAC)
CEA	Colorectal cancer
EGFR	Non-small-cell lung carcinoma, breast cancer
HER-2, ER, PR	Breast cancer
BRCA1/BRCA2	Breast/Ovarian cancer
KLK6/7, GSTT1, PRSS8, FOLR1, ALDH1, and miRNAs	Ovarian cancer
BRAF V600E S100	Melanoma/Colorectal cancer Melanoma
KIT	Gastrointestinal stromal tumor
PSA	Prostate cancer

The advancement in the discovery of disease biomarkers has brought to light important issues with the implementation and management of oncology and other diseases. It is beneficial in regulatory problems, future outlooks, the analysis of data, and the careful choice of medicines. The discovery of promising biomarkers is helpful for detection of several forms of human malignancies in blood serum, including prostate, breast, lung, and ovary (Table 31.2). The US-FDA has approved numerous cancer biomarkers for use in the diagnosis and prognosis of various illnesses. Due to the complex structure and low specificity, sensitivity, and reproducibility of biomarkers, statistical analysis and nanotechnologies are integrated to provide far more effective ways for identifying and approving new biomarkers for various diseases (Taj et al. 2020).

In comparison to tissue biopsies, the detection of promising cancer indicators from blood is reasonably quick (Table 31.2). Traditional immunohistochemistry calls for intrusive methods, specialized equipment, and tissue samples. Furthermore, IHC assays typically take longer time. On-demand assays based on biosensors have been created for doctors to help them get beyond these obstacles. Investigations are being done into quick, accurate, and highly sensitive methods of detecting biomarkers. Immune checkpoints have additionally made it possible to quickly assess the prognosis of malignancy from liquid biopsies. These tools combined various detector classes with digital outputs to evaluate soluble cancer or immunological checkpoint markers in liquid biopsy samples. Two main essential features of these sensing devices include: (a) they only need a small amount of the patient's blood, and (b) they are useful in quickly choosing and identifying the best therapy regimen for the patients, such as ICB therapy.

2 Point-of-Care Testing Technologies for Biomolecular Diagnostics

For identification, treatment and prevention of diseases molecular diagnostics play a significant role. Conventional techniques and devices for such applications are limited to laboratory use only that uses blood samples. They are expensive, labor- and time-intensive, dependent on sophisticated equipment, and call for experienced operators. They also rely on sample purification. Contrarily, the benefits of point-of-care diagnostics include the ability to receive data from a finger prick using a drop of blood, such as with the V-chip detection of protein biomarkers (Fig. 31.2). These emerging technologies, such as nanotechnology, microfluidics, and biotechnology,

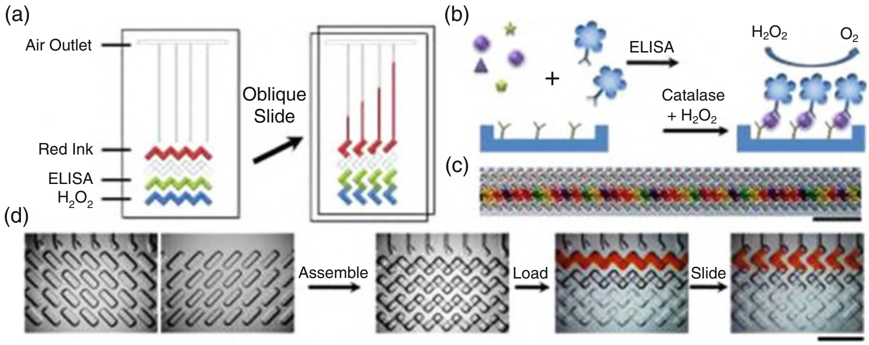

Fig. 31.2 Protein biomarker detection with a V-chip (Mattiuzzi et al. 2012; Song et al. 2014). (**a**) The V-schematic chip's design. (**b**) The ELISA response and the oxygen production process. (**c**) Fifty different antibodies can be put onto the V-chip utilizing swab tips. (**d**) Microscopically magnified photos of normal operational procedures in a 50-plex V-chip. (Adapted from Yujun et al. 2014 with permission)

have the potential to enable more rapid, precise, and affordable illness diagnosis (Mattiuzzi et al. 2012; Song et al. 2014).

Saliva, sweat, tears, and urine can be used to quickly obtain analytical capabilities and trustworthy diagnostic results at or close to the patient's location thanks to recent developments in POCT and in vitro diagnostic medical tools (Park et al. 2022). Prior to receiving on-site medical treatment and rendering clinical judgments, consistent diagnosis encounters still play a big role in actual clinical trials. Precise diagnostic methods that can detect biomarkers in biofluids including blood, sweat, tears, saliva, or urine are referred to as innovative classes of POCT devices (Fig. 31.3). One of the early candidates to improve the analytical efficiency and stability under difficult conditions is the use of a new molecularly imprinted polymer (MPI) system as a synthetic bioreceptor for POCT devices. It is essential to have MIP-based biorecognition systems available as receptors for particular compounds with high specificity and selectivity. Therefore, the development of better MIP technology is essential for biomolecule identification. Wearable technology will promote POCT-based diagnostic systems for high expandability to MIP-based periodontal diagnosis and the future recommendations of MIP-based biosensors (Park et al. 2022).

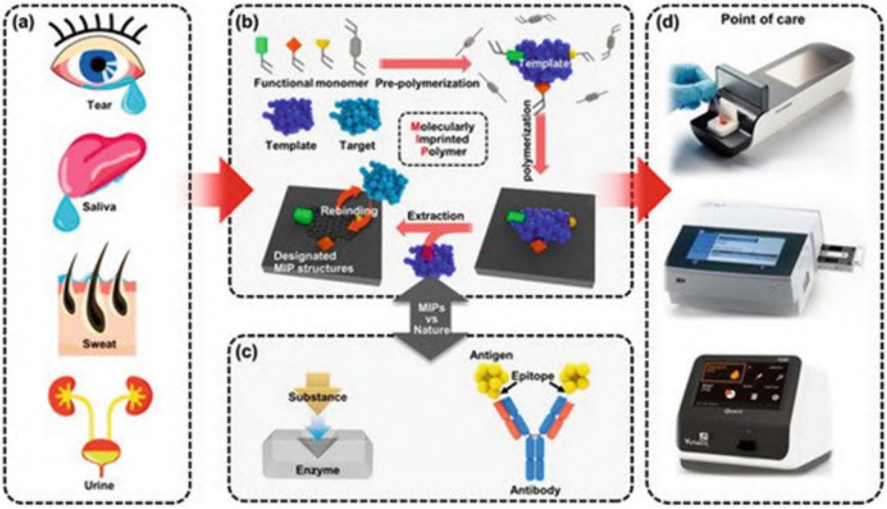
(a)
Tear
Saliva
Sweat
Urine
(b)
Functional monomer
Pre-polymerization
Template
Template
Target
Molecularly Imprinted Polymer
polymerization
Rebinding
Extraction
Designated MIP structures
MIPs vs Nature
(c)
Substance
Enzyme
Antigen
Epitope
Antibody
(d)
Point of care

Fig. 31.3 A MIP-based-biosensors use a benchtop-scale POCT device to find biomarkers in biofluids (Park et al. 2022). (**a**) Tears, saliva, sweat, and urine are examples of biofluids that reflect human health conditions. (**b**) Manufacturing molecularly imprinted systems that contain biorecognition sites, (**c**) using natural biorecognition systems like the enzyme-substrate complex (left) and antigen-antibody reaction (right), and (**d**) using benchtop-scale POCT devices based on immunoassays

3 Nanobiomarker for the Development of Biosensors and POCT Devices

In modern health care system, low-price, highly sensitive, and reliable, deliverable identification strategies are essential (Ahmed et al. 2016). In order to achieve the desired outcome in biosensor and bioassay, POCT, an emerging detection method, has received considerable attention. The advantages of nanomaterials that mimic enzymes include resilience with high stability in physiological settings, affordability, long-term storage, and abundance of manufacture on a wide scale (Wei and Wang et al. 2013). Nanozymes are suitable for surface modification, bioconjugation, and have a large surface area to volume ratio. Additionally, nanozyme's clever response to external stimuli, capacity for self-assembly, and enzyme-mimicking activities make them suitable for a variety of applications, including in vitro sensing of biomolecules like glucose, nucleic acid, proteins, and biomarkers of cancer, as well as in vivo sensing, bio-imaging, tissue engineering, therapeutics, and others (Wei and Wang et al. 2013; Wu et al. 2019; Wang et al. 2016). However, new uses of nanozymes in biosensing are exceptional because of their capacity to transmit signals based on features such as size, shape, fluorescence, biocompatibility, as well as magnetic, electrical, and thermal conductivity. As a result, biosensor development and POCT bioassay are among the most significant applications of nanozymes (Wu et al. 2019; Quesada-González and Merkoçi 2018). Nanozyme-based POCT devices have been advanced in recent time for ultrasensitive and fast detection of biomolecules, contaminants, pathogens, and environmental as well as health-care-related toxins (Kim et al. 2015). These nanozyme-based POCT bioassay devices are only suitable for on-site isolated areas with few resources because of the complex operations and equipment requirements. To solve the issue, the WHO is pushing for the creation of new POCTs based on nanozymes while adhering to its ASSURED requirements (Smith et al. 2018). ASSURED criteria represent three main characteristics: accuracy, accessibility, and affordability. Recent improvements in POCT devices that use the right nanozymes as a crucial part of the sensing process are undoubtedly a promising strategy.

POCT devices must be quick, sensitive, and reliable in order to identify biomarkers, environmental toxins, pathogens, and other substances early and quickly. They ought to be reasonably priced and economically viable for use on-site. The most promising POCT devices for identifying and measuring analytes in various samples include paper-based microfluidics, lateral flow strips (LFS), lateral flow assays (LFA), and electrochemical and calorimetric biosensors. Paper-based materials for biosensing platform design greatly decreases fabrication cost. Conjugation of the sample analytes, detection, and signal amplification are the fundamental components of paper-based bioassays. For increased sensitivity, numerous metal oxide NPs with high enzyme-mimetic function have been employed as signal amplifiers and identification probes in low-cost POCT devices (Wang et al. 2018; Gao et al. 2020). In addition to the cheap production method of inexpensive POCT biosensors, a number of characteristics of enzyme-mimicking NPs play a key role in affordable low-cost detection (Wu et al. 2019; Quesada-González and Merkoçi

2018). The benefit of employing nanozymes is simple synthesis without the need for expensive chemicals and equipment, which considerably reduces the cost of manufacturing. This makes it possible to use a variety of metals, metal oxides, and MOF nanozymes for the convenient construction of biosensors. Duan and colleagues developed Fe_3O_4 nanozyme-based immunochromatographic strips that were substantially more sensitive than colloidal gold strips in detecting the glycoprotein of the Ebola virus (EBOV-GP) at 1 ng mL^{-1} (2 Duan et al. 2015).

Fe_3O_4 magnetic NPs are the first enzyme-mimicking nanoparticles synthesized by simple process with low-cost starting materials, which exhibits peroxidase-like property (Gao et al. 2007). Herein, the Fe_3O_4 nanozyme was prepared by facile hydrothermal process. In addition, the Fe_3O_4 nanozyme coupled with Abs was made utilizing a straightforward EDC/NHS carbodiimide cross-linking procedure (1-ethyl-3-(3-dimethylaminopropyl)carbodiimide/N-Hydroxysuccinimide). Abs processes typically increase the cost of manufacturing biosensors. However, the cost of fabrication increases with complexity when compared to traditional ELISA, which involves an additional step and uses HRP-conjugated Ab as a colorimetric signal amplifier (Duan et al. 2015). Additionally, compared to ELISA, the signal amplification was 100 times higher due to intrinsic peroxidase-like activity of Fe_3O_4 toward 3,3′-diaminobenzidine (DAB) (Duan et al. 2015). Li et al. reported a straightforward and inexpensive photoelectrochemical (PEC) immunoassay (Li et al. 2019). Following the Ab (specific to prostate-specific antigen, PSA) conjugations, histidine-modified Fe_3O_4 was produced using microwave assistance. The price of making biosensors can be reduced by using inexpensive Fe_3O_4 in place of native enzymes (like HRP). Reusing POCT devices and nanozyme-based biosensors is essential for low-cost POCT applications since it lowers the cost. There are numerous studies on the creation of less expensive, refillable paper-based bioassays for identifying disease biomarkers or biomolecules using designed nanoprobes that mimic enzymes (Bradbury et al. 2019; Mahmudunnabi et al. 2020; Ornatska et al. 2011).

The fabrication of biosensors has become more affordable and cost-effective because of biocompatible nanozymes, a wealth of surface tunability with many biorecognition ligands, and simple conjugation procedures as opposed to complex organic counterparts. Numerous biorecognition components, including as aptamers, antigens, and chemical linkers, have been coupled with nanozymes utilizing a straightforward conjugation approach to create low-cost biosensors (Cheng et al. 2017; Han et al. 2018; Zhang and Li 2016; Zhang et al. 2018; Su et al. 2013) (Fig. 31.4). Han et al. developed a lateral flow assay based on nanozymes for the detection of *Escherichia coli* O157:H7 in milk (Fig. 31.5) (Han et al. 2018). The sandwich immunoassay concept, which used Pd-Pt NPs enhanced with an anti-*Escherichia coli* O157:H7 mAb as a recognition probe, served as the basis for the invention of the LFA. Pd-Pt and mAb were combined at a basic pH to create the nanozyme@mAb conjugates (8.2–8.5). The LFA preparation is less expensive thanks to this simple conjugation method without expensive reagents and organic connecting equivalents. Instead of using costly reagents and organic linkers, which would have affected the active sites, to prepare natural enzyme-Ab conjugates for

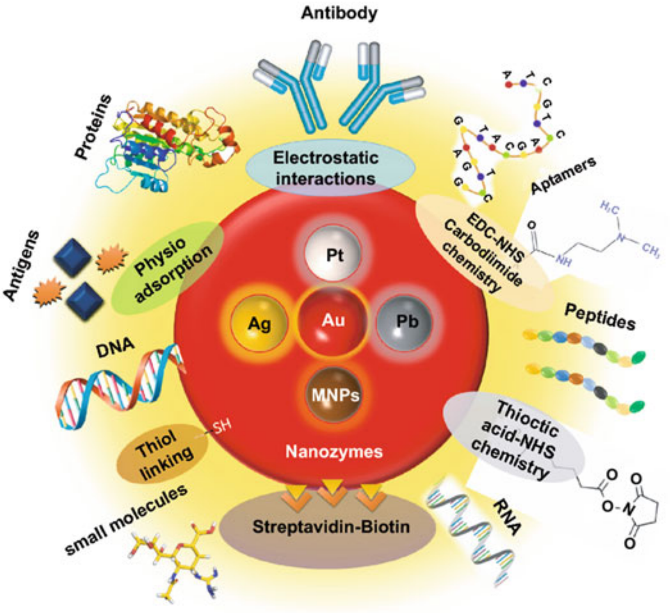
Antibody
Proteins
Electrostatic interactions
Aptamers
EDC-NHS Carbodiimide chemistry
Antigens
Physio adsorption
Pt
Ag
Au
Pb
MNPs
Peptides
DNA
Thiol linking
SH
Nanozymes
Thioctic acid-NHS chemistry
small molecules
Streptavidin-Biotin
RNA

Fig. 31.4 Numerous biorecognition ligands and several conjugation mechanisms for surface-modifying nanozymes (Das et al. 2021)

conventional immunoassay, this makes the process complex and costly (Jeanson et al. 1988). The Pd-Pt NPs' excellent peroxidase-like activity, which catalyzed the oxidation of TMB (3,3′,5,5′-tetramethylbenzidine) in the presence of H_2O_2, provided the basis for the signal amplification in the detection of *Escherichia coli* O157: H7 (Cheng et al. 2017). For the detection of *Salmonella enteritidis* and *Escherichia coli* O157:H7, Cheng and coworkers demonstrated the use of Pd@Pt NPs as a signal amplifier in a dual lateral flow immunoassay connected with a smartphone (Ornatska et al. 2011). They employed a conjugation strategy based on the physisorption of mouse anti-*E. coli* O157:H7 and mouse anti-*S. enteritidis* mAbs (1 mg mL-1) on Pd@Pt surfaces. The dual LFIA device's sensitivity to target pathogens was strengthened by the improved peroxidase-like activity of Pd@Pt, with predictable recoveries (Ornatska et al. 2011). Aptamers are a target-specific detecting ligand that are utilized in the same way as Abs in the construction of biosensors. You can purchase aptamers straight from the business (Xie et al. 2020; Ou et al. 2019). Improved cross-linking procedures using straightforward chemical linkers or the use of modified aptamers for simple conjugations also helped to lower the overall cost of producing biosensors. Aptamers used in nanozyme-based biosensors could therefore be a suitable contender in terms of price under the ASSURED requirements. For instance, Yang and his team have demonstrated the creation of colorimetric

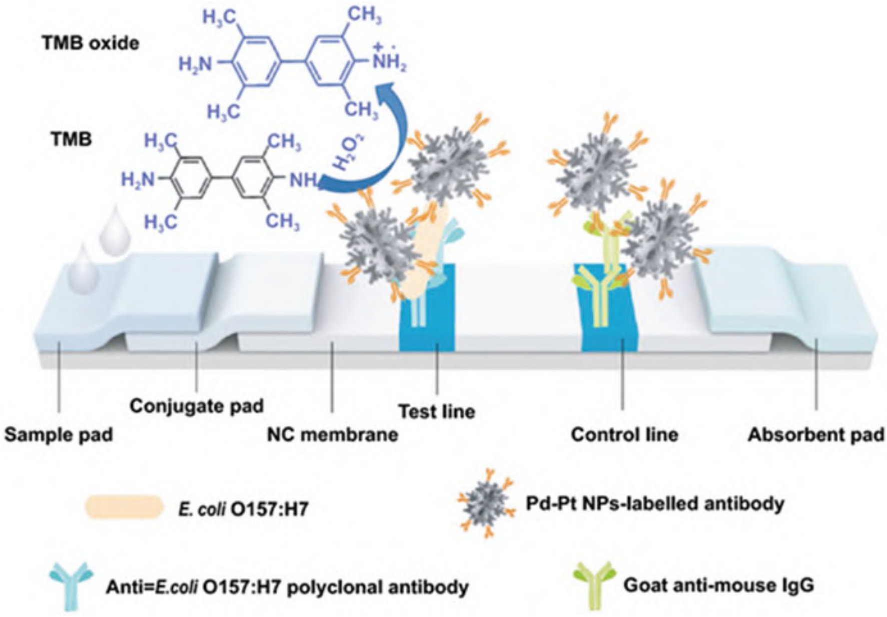

Fig. 31.5 *Escherichia coli* O157 detection using a Pd-Pt nanozyme-based LFA: H7: nitrocellulose (Das et al. 2021)

aptasensors connected to Fe_3O_4 nanozymes for the detection of thrombin with an extremely low LOD of 1 nM (Zhang et al. 2010).

For use in the early identification of infections or biomarkers, POCT sensing devices are essential instruments. These tools are crucial for specialist or doctor clinical diagnoses, as well as for everyday household or outdoor use in distant places with little resources. An innovative system has been used in the development of POCT devices that meet the ASSURED standards. Here, the instrument or biosensing system needs to be reasonably priced, low maintenance, and highly sensitive to detect analytes at lower concentrations.

POCT uses fast diagnostic tests. The results are accomplished or interpreted by expert operator in a variety of settings. Quick tests used in POCT are applicable for many purposes including NAAT, antigen, or Ab tests, and COVID-19, which has high transmissibility. At the moment, reverse transcription-polymerase chain reaction is the main method of diagnosing COVID-19 (RT-PCR). There are many other detection techniques in use, including electrochemical sensors, immunochromatography, CRISPR, isothermal nucleic acid amplification, and immunochromatography. However, the majority of current testing is done in large hospitals and other health care facilities. With increased user accessibility, quick detection, accuracy, and sensitivity in an epidemic situation, POCT is very useful and lessens the testing burden on hospitals. Thus, POCT is advantageous for daily epidemic control, quick identification, and immediate treatment. Modern research advancements in POCT-based SARS-CoV-2 detection methods present opportunities for POCT-based

SARS-CoV-2 detection to advance quickly, at cheap cost, and in a shorter amount of time (Song et al. 2021).

4 Conclusion and Future Outlook

Nanobiomarkers are striking in POCT to improve the analytical performance. The POCT makes the detection process facile and fast. The identification of disease biomarkers, such as pathogens, cancer cells, enzymes, proteins, and small-molecule metabolites, depends on POCT. In many stages of illness detection, monitoring, and prevention, nanobiomarkers are employed. Different NPs-based biosensor components and readout configurations analyze biomolecules. The use of POCT sensing devices is essential for the early detection of infections and disease biomarkers/ biomolecules. In terms of practice, user accessibility, prompt detection, accuracy, and sensitivity, POCT is promising. Modern research and advancements in POCT-based SARS-CoV-2 detection techniques are forward-looking strategies at the moment.

For promising application and advancement of POCT, proper regulatory concerns are essential for monitoring point-of-care testing compliance. In general, POCT regulatory strategy requirements concentrate on two areas: (1) training and proficiency of those performing the testing and (2) ensuring that each test is conducted strictly in accordance with the manufacturer's instructions (https://www.aacc.org/cln/articles/2016/february/monitoring-point-of-care-testing-compliance).

By restructuring laboratory services, POCT began to depart from conventional clinical laboratory medicine in the 1980s. Laboratory management faced difficulties due to the widespread deployment of POCT devices. Especially in ensuring that these technologies are used correctly. Today, POCT regulators use a variety of techniques to maintain control over several devices and check the compliance of numerous operators across various health care programs.

The first POCT techniques were usually manual. They had poor data management skills and little to no quality control. Modern POCT technology has substantially improved and changed. Recording the information required to prove agreement, however, still requires a lot of work. Furthermore, despite the quick development of POCT devices and their increased usage, POCT operators usually lack a sufficient awareness of the legal requirements for training, documentation, and licensure. Because of this, nurses and other health care professionals frequently view POCT coordinators as law enforcement organizations who indiscriminately enforce legislation. Experts in laboratory medicine, who are well-trained to support excellent patient care and efficient use of POCT-based resources, find themselves in an uncomfortable situation. As a result, regulatory difficulties relating to POCT are important in hospital and other health care facility settings, and there are likely solutions to meet the criteria.

References

Ahmed SR, Kim J, Suzuki T, Lee J, Park EY (2016) Enhanced catalytic activity of gold nanoparticle-carbon nanotube hybrids for infuenza virus detection. Biosens Bioelectron 85: 503–508. https://doi.org/10.1016/j.bios.2016.05.050

Bradbury DW, Azimi M, Diaz AJ, Pan AA, Falktoft CH et al (2019) Automation of biomarker preconcentration, capture, and nanozyme signal enhancement on paper-based devices. Anal Chem 91(18):12046–12054. https://doi.org/10.1021/acs.analchem.9b03105

Cheng N, Song Y, Zeinhom MMA, Chang YC, Sheng L et al (2017) Nanozyme-mediated dual immunoassay integrated with smartphone for use in simultaneous detection of pathogens. ACS Appl Mater Interfaces 9(46):40671–40680. https://doi.org/10.1021/acsami.7b12734

Das B, Franco JL, Logan N, Balasubramanian P, Kim MI, Cao C (2021) Nanozymes in point-of-care diagnosis: an emerging futuristic approach for biosensing. Nanomicro Lett 13:193

Duan D, Fan K, Zhang D, Tan S, Liang M et al (2015) Nanozyme-strip for rapid local diagnosis of Ebola. Biosens Bioelectron 74:134–141. https://doi.org/10.1016/j.bios.2015.05.025

Gao L, Zhuang J, Nie L, Zhang J, Zhang Y et al (2007) Intrinsic peroxidase-like activity of ferromagnetic nanoparticles. Nat Nanotechnol 2(9):577–583. https://doi.org/10.1038/nnano.2007.260

Gao Y, Zhou Y, Chandrawati R (2020) Metal and metal oxide nanoparticles to enhance the performance of enzyme-linked immunosorbent assay (ELISA). ACS Appl Nano Mater 3(1): 1–21. https://doi.org/10.1021/acsanm.9b02003

Han J, Zhang L, Hu L, Xing K, Lu X et al (2018) Nanozymebased lateral flow assay for the sensitive detection of Escherichia coli O157:H7 in milk. J Dairy Sci 101(7):5770–5779. https://doi.org/10.3168/jds.2018-14429

Jayanthi VSPKSA, Das AB, Urmila S (2017) Recent advances in biosensor development for the detection of cancer biomarkers. Biosens Bioelectron 5:91. https://doi.org/10.1016/j.bios.2016.12.014

Jeanson A, Cloes JM, Bouchet M, Rentier B (1988) Comparison of conjugation procedures for the preparation of monoclonal antibody-enzyme conjugates. J Immunol Methods 111(2):261–270. https://doi.org/10.1016/0022-1759(88)90135-4

Kim M, Kim MS, Kweon SH, Jeong S, Kang MH et al (2015) Simple and sensitive point-of-care bioassay system based on hierarchically structured enzyme-mimetic nanoparticles. Adv Healthc Mater 4(9):1311–1316. https://doi.org/10.1002/adhm.201500173

Li W, Fan GC, Gao F, Cui Y, Wang W et al (2019) High-activity Fe_3O_4 nanozyme as signal amplifer: a simple, low-cost but efficient strategy for ultrasensitive photoelectrochemical immunoassay. Biosens Bioelectron 127:64–71. https://doi.org/10.1016/j.bios.2018.11.043

Mahmudunnabi RG, Farhana FZ, Kashaninejad N, Firoz SH, Shim YB et al (2020) Nanozyme-based electrochemical biosensors for disease biomarker detection. Analyst 145(13):4398–4420. https://doi.org/10.1039/d0an00558d

Mattiuzzi A, Jabin I, Mangeney C et al (2012) Electrografting of calix[4]arenediazonium salts to form versatile robust platforms for spatially controlled surface functionalization. Nat Commun 3:1283

Mummareddy S, Pradhan S, Narasimhan AK, Natarajan A (2021) On demand biosensors for early diagnosis of cancer and immune checkpoints blockade therapy monitoring from liquid biopsy. Biosensors 11:500. https://doi.org/10.3390/bios11120500

Ornatska M, Sharpe E, Andreescu D, Andreescu S (2011) Paper bioassay based on ceria nanoparticles as colorimetric probes. Anal Chem 83(11):4273–4280. https://doi.org/10.1021/ac200697y

Ou D, Sun D, Lin X, Liang Z, Zhong Y et al (2019) A dualaptamer-based biosensor for specific detection of breast cancer biomarker HER2 via flower-like nanozymes and DNA nanostructures. J Mater Chem B 7(23):3661–3669. https://doi.org/10.1039/c9tb00472f

Park R, Jeon S, Jeong J, Park SY, Han DW, Hong SW (2022) Biosensors 12:136

Quesada-González D, Merkoçi A (2018) Nanomaterial-based devices for point-of-care diagnostic applications. Chem Soc Rev 47(13):4697–4709. https://doi.org/10.1039/c7cs00837f

Smith S, Korvink JG, Mager D, Land K (2018) The potential of paper-based diagnostics to meet the ASSURED criteria. RSC Adv 8(59):34012–34034. https://doi.org/10.1039/C8RA06132G

Song Y, Huang YY, Liu X, Zhang X, Ferrari M, Qin L (2014) Point-of-care technologies for molecular diagnostics using a drop of blood. Trends Biotechnol 32(3):132–139

Song Q, Sun X, Dai Z et al (2021) Point-of-care testing detection methods for COVID-19. Lab Chip 21:1634–1660

Su H, Zhao H, Qiao F, Chen L, Duan R et al (2013) Colorimetric detection of Escherichia coli O157:H7 using functionalized Au@Pt nanoparticles as peroxidase mimetics. Analyst 138(10): 3026–3031. https://doi.org/10.1039/c3an00026e

Taj A, Gondal AR, Sadia Bajwa Z (2020) Biomarkers and their role in detection of biomolecules. In Nanobiosensors. https://doi.org/10.1002/9783527345137.ch4

Wang X, Hu Y, Wei H (2016) Nanozymes in bionanotechnology: from sensing to therapeutics and beyond. Inorg Chem Front 3(1):41–60. https://doi.org/10.1039/c5qi00240k

Wang Q, Wei H, Zhang Z, Wang E, Dong S (2018) Nanozyme: an emerging alternative to natural enzyme for biosensing and immunoassay. TrAC – Trends Anal Chem 105:218–224. https://doi.org/10.1016/j.trac.2018.05.012

Wang X, Li F, Guo Y (2020) Recent trends in nanomaterial-based biosensors for point-of-care testing. Front Chem 8:586702

Wei H, Wang E (2013) ChemInform abstract: nanomaterials with enzyme-like characteristics (Nanozymes): next-generation artifcial enzymes. ChemInform 44(38). https://doi.org/10.1002/chin.201338273

Wu J, Wang X, Wang Q, Lou Z, Li S et al (2019) Nanomaterials with enzyme-like characteristics (nanozymes): next generation artifcial enzymes (II). Chem Soc Rev 48(4):1004–1076. https://doi.org/10.1039/c8cs00457a

Xie J, Tang MQ, Chen J, Zhu YH, Lei CB et al (2020) A sandwich ELISA-like detection of C-reactive protein in blood by citicoline-bovine serum albumin conjugate and aptamer-functionalized gold nanoparticles nanozyme. Talanta 217:121070. https://doi.org/10.1016/j.talanta.2020.121070

Zhang L, Li L (2016) Colorimetric thrombin assay using aptamer functionalized gold nanoparticles acting as a peroxidase mimetic. Microchim Acta 183(1):485–490. https://doi.org/10.1007/s00604-015-1674-6

Zhang Z, Wang Z, Wang X, Yang X (2010) Magnetic nanoparticle-linked colorimetric aptasensor for the detection of thrombin. Sens Actuators B Chem 147(2):428–433. https://doi.org/10.1016/j.snb.2010.02.013

Zhang T, Tian F, Long L, Liu J, Wu X (2018) Diagnosis-ofrubella-virus-using-antigenconjugated-aupt-nanorods-asnanozyme-probe. Int J Nanomedicine 13:4795. https://doi.org/10.2147/IJN.S171429

Nanodendrite a Promising Material for Bioanalytical Application

32

Alexander Pinky Steffi, Ramachandran Balaji, Ying-Chih Liao, and Narendhar Chandrasekar

Contents

1 Introduction 700
2 Gold Nanodendrites for Cancer Therapy Bioanalytical Application (Monometallic NDs) 703
3 Pt Nanodendrites for Bioanalytical Applications 705
4 Pt Nanodendrites with ZnO Nanorods Electrode (Bimetallic Nanodendrites) 707
5 Rare Earth Material-Based Nanodendrites 709
6 Graphene Loaded Bimetallic Nanodendrites 712
7 Conclusion 714
References 714

Abstract

Multidisciplinary initiatives in the area of nanomedicine for biological applications have made significant progress toward overcoming typical constraints of conventional drug delivery, which including poor biomagnification, wettability, and non-specific bioavailability and targeting. For better bioanalytical performance, a novel class of metal nanostructures with a distinctive dendritic-shaped morphology has been developed. Because of their specific physicochemical, refractive, and electrical features, branched metal nanoparticles or metal nanodendrites are thought to have intriguing qualities for biological applications.

A. P. Steffi
Department of Nanoscience and Technology, Sri Ramakrishna Engineering College, Coimbatore, India

R. Balaji
Department of Electronics and communication Engineering, Koneru Lakshmaiah Education Foundation, Andhra Pradesh, India

Y.-C. Liao
Department of Chemical Engineering, National Taiwan University, Taipei, Taiwan

N. Chandrasekar (✉)
Department of BioNano Technology, Gachon University, Seongnam-si, Republic of Korea

© Springer Nature Singapore Pte Ltd. 2023

U. P. Azad, P. Chandra (eds.), *Handbook of Nanobioelectrochemistry*,
https://doi.org/10.1007/978-981-19-9437-1_32

Owing to their three-dimensional (3D) large surface area, nanodendrites may improve the loading efficiency of bioactive chemicals and can selectively transport their cargo to tumor cells utilizing their stimuli-responsive capabilities. Nanodendrites may evade detection and removal by bioimages because to their propensity to concentrate enough inside cells. Furthermore, active targeting ligands like antibodies and proteins may be added to these therapeutic nanodendrites to improve tumor targeting, resulting in a multipurpose nanoplatform with customizable methods. Nanodendrites are especially exceptional and extremely interesting in their architectural layout between metal nanoparticles with additional structural morphologies including such nanoplates, nanorods, nanocages, nanoprisms, nanostars, nanodumbbells, etc., due to their own three-dimensional (3D) morphology to numerous dense clusters of branches of highly permeable surface features. This chapter contains a concentrated examination of metallic nanodendrites for potential bioanalytical uses. In consideration of their production techniques, we have emphasized the different kinds and characteristics of metallic nanodendrites. Following that, current developments in the production of dendritic-shaped nanoparticles with significant photothermal and stimuli-responsive medicinal functions are reviewed in depth. Finally, we present exciting potential for improving bioanalytical applications in particular for cancer treatment by developing metallic nanodendrites.

Keywords

Nanodendrites · Metallic nanoparticles · Bioanalytical applications · Therapeutic drug delivery

1 Introduction

Classical bioanalytical and cancer therapies have been shown to be restricted in terms of treatment results during the previous several decades, not-withstanding their effectiveness. Because most cancer therapy and bioanalysis medications can’t differentiate between normal and malignant cells, they have various negative side effects. Furthermore, inadequate and/or poor drug deposition at target areas, as well as the threat of antibiotic resistance in cancer therapy regimens, remain significant challenges. These obstacles have limited the use of traditional treatment, necessitating the development of new ways to enhance treatment outcomes (Kadian et al. 2021).

The development of nanoparticles-based delivery systems as a novel approach to established medicines has been able to alleviate the issues that chemo-drugs are known to cause. Nanomaterials therapeutic techniques have mostly focused on the exact release and accumulation of medicines in specific cells, tissues, and organs. By using active or passive targeting, nanomaterials may increase intracellular medication delivery to cancer cells and avoiding acute damage to normal cells. Drug-loaded nanoparticles, on the other hand, should cross a number of very complicated cellular obstacles to approach its target. Despite the fact that nanomaterials have enhanced drug delivery methods significantly, several problems like tumor targeting, inadequate systemic circulation, inadequate drug encapsulation, inconsistency, and toxicity always need significant interventions for enhanced and efficient treatment. Nanodendrites are extremely unusual and intriguing in its architectural design because of their three-dimensional (3D) shape with many dense arrays of branches of porous surface structure. When compared to smooth surface nanocrystals, the high density of flaws on the surface may lead to a much enhanced surface region to volume ratio. These flaws may give several binding sites on a single branch of a nanodendrite with numerous linked sub-branches, allowing for outstanding multivariant characteristics in applications like catalysis (Kannan et al. 2014).

In the disciplines of biomedicine, bioanalysis, and clinical medicine, however, demand for these materials is rising. Because of its multifunctional structure, superior biocompatibility, and nontoxicity, nanodendrites have piqued attention as potential substances for biomedical and bioanalytical technologies. Nanodendrites with the combinations of various metals including carbon materials, such as graphene oxides (GOs)-based biosensors & drug delivery systems, along with carbon nanotubes (CNTs)-based bioimaging reagents, have worked their way into numerous biomedical investigation domains after several years of study. Nanodendrites offer greater biocompatibility over inorganic quantum dots when compared to certain other nanomaterials that have been thoroughly examined. Figure 32.1 shows the The SEM and TEM images of Pt dendrites (Lu et al. 2016).

Monometallic, bimetallic, and then in a few instances trimetallic nanodendrites exhibiting outstanding adjustable shape-dependent characteristics have previously been described to construct diverse assemblages. High selectivity and sensitivity, higher catalytic activity, increased antibacterial activity, increased drug loading capacity, and outstanding durability and biocompatibility are only a few of the advantages of noble metal-based methods. Furthermore, the inclusion of a few metals in the structure have allowed for a variety of metallic nanodendrite morphological topologies and alignments, including core–shell, alloy, hybrid nanostructures, and sub-clusters. The promising physicochemically produced features are owing to the synergistic or multifunctional effect caused by the combination of two different separate metals, which has been extensively studied.

Metallic nanodendrites (NDs) have been demonstrated to have a wide range of potential uses in a variety of fields, and they remain to excite researchers' curiosity. When compared to smooth surfaced nanocrystals, dendritic/branched nanostructures having porous and irregular surfaces give an extraordinarily wide surface area with high-density active sites. When comparing to nanorods, nanostars, and nanoshells, complex morphologies like nanodendrites may significantly increase photo-absorption (Khan et al. 2018), for example, found that 3D Pt-on-Au bimetallic nanodendrites with a rough surface had a wide extinction region that red-shifted to the NIR region, leading in much better electrocatalytic activity than core/shell Au@PtNPs having a smooth surface (Patra et al. 2016).

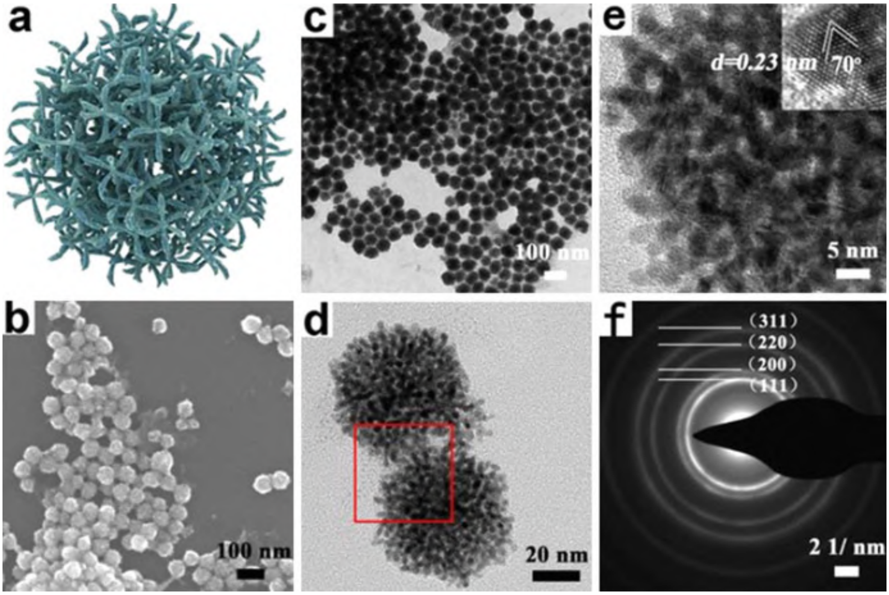

Fig. 32.1 SEM and TEM images of individual porous Pt nanodendrites. The model of the porous Pt nanodendrite (**a**). SEM image (**b**). TEM image (**c**). The higher magnification image of Pt dendrite (**d**). High-resolution TEM of Pt nanodendrite for the selected portion (**e**). SEAD pattern (**f**). (Reproduced with permission (Lu et al. 2016))

Nanodendrites are an appealing material for a variety of applications, including catalysis, hydrogen storage and sensing, pollution reduction in automobiles, and so on. Nanodendrites have been widely regarded as a superior alternative material for catalytic oxidation of formic acid and oxygen reduction in a proton-exchange membrane (PEM) fuel cell. Nanoparticles of different forms, including nanobars, nanorods, nanocubes, octahedra, icosahedra, nanowires, and nanoplates, have attracted a lot of attention. Surfactants and polymers, as well as extreme temperature interactions in organic environments, were used to create anisotropic Pd-based dendritic-like architectures. Researchers, for example, reported highly branched Pd nanostructures for the rapid catalytic conversion of nitrobenzene to aniline, despite the fact that it was synthesized in a non-aqueous medium. $PdCl_2$ was used to make branching Pd dendritic nanoparticles (Fig. 32.2) in a combination of oleylamine and oleic acid (Kannan et al. 2014). Since various crystalline interfaces have varied surface atom concentrations and electrical structures, tweaking the shape rather than the size may produce remarkable improvements in certain aspects. As a result, the characteristics of nanostructures with odd forms may vary significantly from those of spherical dimensions. Anisotropic nanomaterials like this have a lot of promise in signal processing in bioanalysis and biodiagnosis. Apart from size, particle morphology has been acknowledged as an essential characteristic trait that may be altered for drug delivery applications. Due to the strong electric field formed on metal nanoparticles upon light illumination and the production of hot spots, metallic

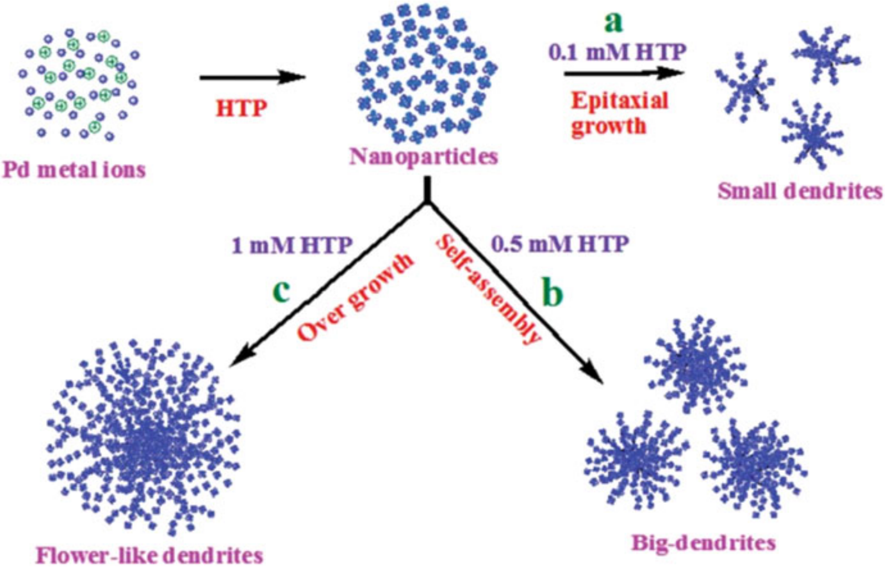

Fig. 32.2 Schematic presentation for the growth mechanism for Pd dendritic nanostructures. (Reproduced with permission (Kannan et al. 2014))

nanostructures are also particularly helpful in different spectroscopic methods, particularly surface enhanced Raman scattering (SERS). Bringing two or more metal nanoparticles together may further modify and improve these features. The huge increase in the SERS signal at nanoparticle junctions, which permits the identification of individual atoms, is an outstanding example. When nanoparticles aggregate, the intensity of far-field scattering increases significantly. As a result, the capacity to arrange metal nanoparticles into assemblies is critical for fulfilling metallic nanoparticles' maximum potential (Lee et al. 2010).

2 Gold Nanodendrites for Cancer Therapy Bioanalytical Application (Monometallic NDs)

Nanodendrites (NDs) represent a kind of nanoparticles with distinctive hyperbranched morphologies. NDs have lately gained a lot of research interest because of their exceptionally high surface area, which may considerably improve catalytic, electrochemical, and drug transport capabilities. NDs of metal and bimetals, such as Pt, Pd, Au, AuePd, AuePt, PdePt, PdeCo, PdeNi, and PteCu, have recently been synthesized using a variety of methods. The degree of bifurcation (DB) is a critical quantity in polymer research because it impacts the chemical, physical, and mechanical properties of dendritic polymers. Many features of inorganic dendritic nanoparticles (NPs), including such optical attenuation and catalysis, may also be

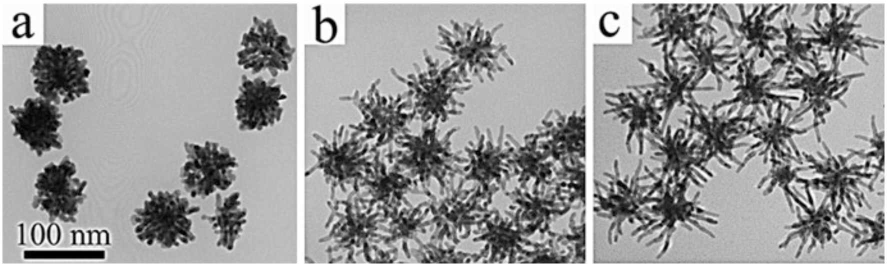

Fig. 32.3 TEM images of Au nanodendrites for cancer therapy with high (**a**), medium (**b**), and low (**c**) degree of branching. (Reproduced with permission (Qiu et al. 2016))

influenced by the Nanodendrites. While varied degree of branching gold nanodendrites (Fig. 32.3) have been reported (Qiu et al. 2016).

In order to carry out a synthesis, 20 mL of 60 mM $HAuCl_4$ in ethanol, different amounts of seeds, and 15 mL of 0.4 M ascorbic acid in methanol have all been introduced to the reaction vial after 4 mL of 0.1 M ethanolic solution of amines (butylamine, octylamine, dodecylamine, hexadecylamine, octa A rocker shaker was then used to stir the solutions violently in a short seconds before they were left for 30 min to facilitate the creation of AuNanodendrites. They were then centrifuged and re-dispersed into 2 mL of THF after being cleaned with chloroform and ethanol once and the same amount of each precursor was utilized in chloroform synthesis, also with sole change in solvent.

Among all optical spectrum of metallic NPs with basic shapes, including such nanospheres, nanorods, and nanocubes, there is frequently a strong, narrow localized surface plasmon resonance (LSPR) band. The Au nanodendrites, on the other hand, possess intricate branching architectures, which indicates their extinction bands are much wider. The Au nanodendrites of strong, medium, and weak dendrites are referred to as S-NDs, M-NDs, and W-NDs, respectively. The attenuation band for S-NDs is concentrated about 700 nm; however, M-NDs and L-NDs have lower peak intensities in this range, but absorb more light beyond 1000 nm. The structural difference of Au nanodendrites should be blamed for their nanodendrites-dependent optical spectrum. Higher dendrites, for example, are mostly made up of shorter rod-like branches that absorb heavily in the shorter wavelength area. This finding backs up a previous finding that stronger gold nanorods caused optical attenuation to migrate to higher wavelength (Lv et al. 2015).

Despite several studies on nanodendrites of different metals and bimetals have indeed been published, researchers are the first to show that the nanodendrites in principle, and Au nanodendrites in specific, may be modified by utilizing long chain basic amines as structurally guiding agents. This study also demonstrates a unique and straightforward way for making high-quality Au nanodendrites using readily accessible ingredients. We were able to explore how the disease are affected the different features of Au nanodendrites owing to this finding. Researchers discovered that the easily manipulated enabled us to tune the optical characteristics of Au nanodendrites throughout a large near-infrared range, allowing us to investigate

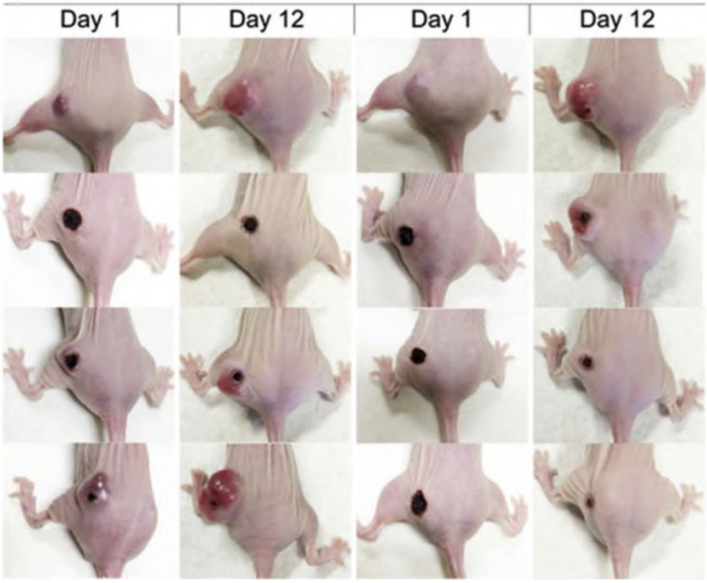

Fig. 32.4 Photothermal treatment of MCF-7 tumors by using AuNDs of different degree of branching. Days 1 and 12 posttreatment of Au nanodendrites photos of a representative mouse within every group. (Reproduced with permission (Qiu et al. 2016))

the wavelength-dependent photo-thermal features of Au nanodendrites in vitro and in vivo. Given that the physiochemical characteristics of nanoparticles have shown to have a significant impact on their biological destiny, it is highly probable that the nanodendrites could have an impact on the interaction of Au NPs with cells (in vitro) and tumors (in vivo), potentially affecting their internalization and bio-distribution (Fig. 32.4) (Yang et al. 2013).

3 Pt Nanodendrites for Bioanalytical Applications

During 2008–2016, Au NDs accounted for 62.5% of articles addressing nanoparticle use for radiosensitization effect, trailed by gadolinium (11%), then silver nanoparticle (6%), according to Yang et al. (2013). Only a few studies have used platinum nanomaterials (Pt NDs) as a radiosensitizer, particularly when using therapeutically effective radiation beams. Platinum combinations like cisplatin and carboplatin are well-known chemotherapeutic medicines used to treat cancer. Cisplatin has been shown to produce radiosensitization by inhibiting DNA repairs (Ye et al. 2012). Researchers found that Pt NDs-loaded DNA had a factor of 2.1 enhanced DNA double-strand break (DSB), suggesting that PtNDs cause more fatal damage when exposed to carbon ions. Pt NDs effectively boosted gamma radiation impact on radioresistant cells by more than 40%, according to a recent discovery by Wang et al. (2017).

Researchers investigated the innovative platinum nanodendrites (PtNDs) as radiosensitizer for therapeutic megavoltage photon energy to see whether they might be used in clinical applications. PtNDs of various sizes were synthesized and characterized for use in radiotherapy. Using clinical megavoltage photon sources, the cytotoxicity profile and radiosensitization capacities of PtNDs of various sizes was experimentally assessed.

Researchers stated that PtNDs was manufactured utilizing a chemical reduction process. To begin, mix 5.19, 10.38, 15.57, and 25.94 mg of potassium tetrachloroplatinate (II) (K_2PtCl_4) powder with 2.5 mL deionized water to make aqueous mixtures with four distinct levels of K_2PtCl_4. Subsequently, in a centrifuge machine, 2 mL of every concentration of K_2PtCl_4 aqueous mixture were combined with 20 mg of PluronicF-127 and 2 mL of 88% formic acid for a moment. After being sonicated for 12 min in an ultrasonicator, the solutions became black, suggesting the production of PtND particles. To eliminate the residual, the Pt NDs concentrations were centrifuged and rinsed thrice with DI water. For characterization, certain Pt NDs specimens were immersed in DI water. For antitumor activity and radiosensitization investigations, the PtNDs suspensions was dissolved in cell culture medium (Jiao et al. 2013).

Muhammad Afiq and his co-workers have prepared Pt NDs of various core sizes (Fig. 32.5) and used them in radiotherapy (Muhammad Afiq et al. 2018).The

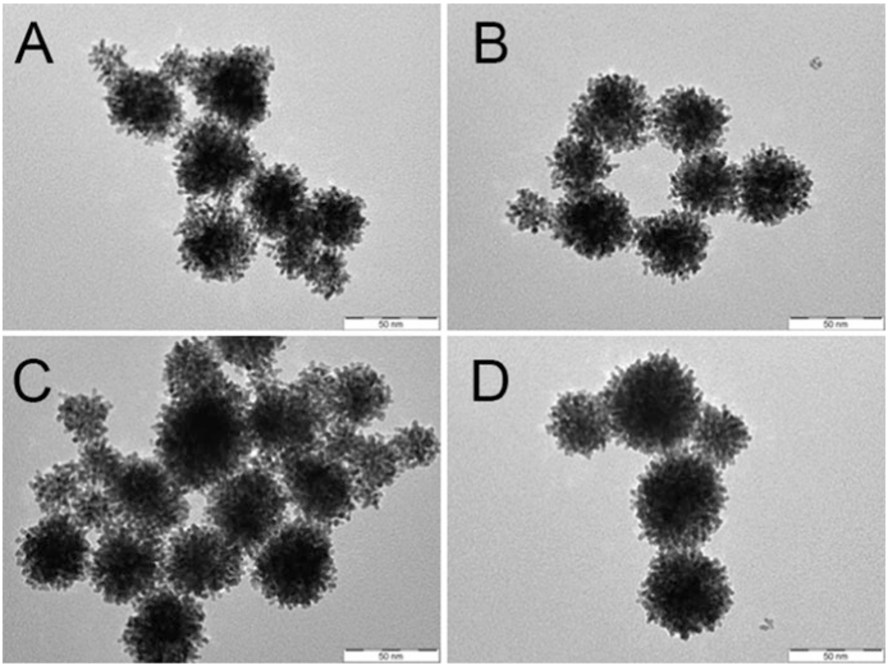

Fig. 32.5 TEM images of Pt Nanodendrites with various core sizes. (**a**) 29 nm, (**b**) 36 nm, (**c**) 42 nm, and (**d**) 52 nm. (Reproduced with permission (Muhammad Afiq et al. 2018))

research shows that Pt NDs may be used as a radiosensitizer in megavoltage photon radiation emitted. Following irradiation with a 6 MV photon energy, PtNDs exhibits strong radiosensitization effects against HeLa cell lines, with up to a twofold augmentation. PtNDs with a SER of 2.31, 2.27, 1.96, and 1.77 created the most radiosensitization, followed by 42, 29, and 52 nm.

As a result, it s possible that characteristics like Pt ND size and morphology are to blame for the increased radiosensitization consequences. The appropriate PtNDs size must be chosen in order to increase radiation contact potential and thus achieve a favorable radiosensitization result. Additional research explores the possibilities of investigation. To show and evaluate the use of platinum-based nanoparticles for a radiosensitizer in radiotherapy, this research provided the first evidence (Sun et al. 2017).

4 Pt Nanodendrites with ZnO Nanorods Electrode (Bimetallic Nanodendrites)

Nanodendrites to assist the traditional biochemical electrochemical measurement of glucose is the most prevalent use of nanotechnology for diabetes detection devices. Expanded surface area, higher effective electron transport from enzymes to electrodes, and additional production to insert extra catalytic processes are all benefits of incorporating nanoparticles into these sensors. Even though modifiers, labelling factors, or immobilizer agents, metal nanoparticles such as Au, Pt, Ag, Fe, Zn, Cu, Pd, and Ir are inserted onto the electrode layer of glucose sensors. A glucose sensor device has been implanted with metallic Au or Pt nanoparticles (PtNPs). In comparison to other nanoparticles, Au does have a greater work function of 5.1 eV and is much more chemically durable. Pt, on the other hand, has a greater sweep current and work function (5.65 eV) than Au (5.1 eV). As a result, PtNPs should have greater chemical durability and persistence. PtNPs also have strong analytical efficiency, with a uniformity range of 1 - 0.1 mM and a high selectivity of 0.20 M for the produced glucose sensor. Although PtNPs have superior electrical characteristics and a greater work potential than conventional nanoparticles, they are projected to increase and enhance the productivity of glucose sensors (Muhammad Afiq et al. 2018).

While using Pt NDs as a glucose biosensor, the form of the particles should be addressed. Distinct forms of nanoparticles exhibit different behaviors. Due to the obvious presence of a significant number of edges, sharp ends, and vertices on their branching, PtNPs with a dendritic architecture have sparked special interest among nanoparticles owing they may give a reasonably high-specific surface area and a high-specific activity. Sharp points in platinum nanodendrites (PtNDs) possess a significant potential to increase electric fields and cause substantial local electromagnetic field amplification.

Using chemical reduction to change the precursor K_2PtCl_4 concentrations, different sizes of PtNDs were produced. Depending on Pt ND size, glucose percentage in 0.01 M PBS, and Nafion quantity incorporated to the nanocomposite, the

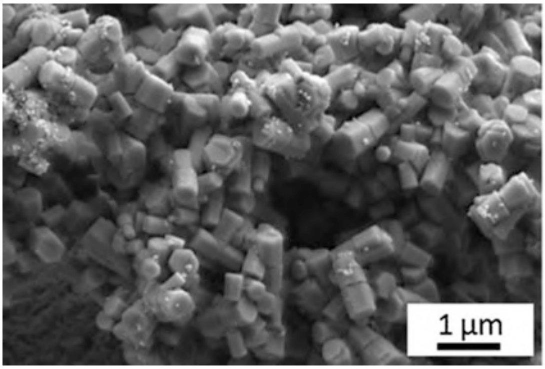

Element	Wt%	At%
O K	11.14	38.03
ZnL	66.73	55.77
PtM	22.13	06.20

Fig. 32.6 EDX of Pt nanodendrites and ZnO nanorods. (Reproduced with permission (Razak et al. 2016))

topological, structural, and glucose-sensing behavior of Pt NDs was investigated. The discovered qualities were addressed in detail.

Chemical reduction technique was used to manufacture Pt NDs. To make different sizes of PtNDs, numerous amounts of K_2PtCl_4 solution were synthesized in water: 5, 10, 15, 20, and 25 mM. Pluronic F127 (20 mg) then was applied to the K_2PtCl_4 that had been made. Following that, 2 mL of 88% formic acid was quickly added. The mixture and stirred constantly to insure that all ingredients were dissolved and mixed well. For 12 min, the combined solution was submerged in an ultrasonic bath. The PtND suspension was thoroughly rinsed with DI water after the reaction was finished. The residue was removed by centrifugation for 20 min at 9000 rpm. Following that, 4 mL DI water was introduced to individual sample, and the colloidal Pt NDs specimen was kept at room temperature. To synthesize Pt NDs with ZnO NRs, various Pt ND sizes were spin deposited at 5000 rpm for 50 s on over of the synthesized ZnO NRs/ITO. The procedure was carried out several times. The samples subsequently cured for 1 h at 160 °C to remove organic contaminants and ensure adequate adherence to the surface. EDX images of Pt dendrites and ZnO nanorods have been given in Fig. 32.6 (Razak et al. 2016).

Figure 32.7 shows the cyclic Voltammetry curves of the Nafion/GOx/42 nm PtNDs/ZnONRs/ITO electrode in 0.01 M PBS electrolytes with varied amounts of glucose (0.1–20 mM) at a potential scan rate of 50 mVs^{-1}. The resulting calculated values revealed the redox peak associated with H_2O_2 production as well as a satisfactory response to different glucose doses. The anodic and cathodic peak currents rose progressively with advancing glucose content, as seen in Fig. 32.7. The results demonstrated that GO immobilized on a PtND/ZnONRs electrode has good electrocatalytic activity and sensing ability of biomaterials.

Different sizes of PtNDs were effectively created in this study by varying the quantity of K_2PtCl_4, with 5, 10, 15, 20, and 25 mM K_2PtCl_4 yielding 29, 36, 42, 52, and 62 PtNDs, accordingly. The GOx subsequently immobilized on the prepared film after the PtNDs were spin deposited onto ZnO NRs. PtNDs on the ZnO NRs

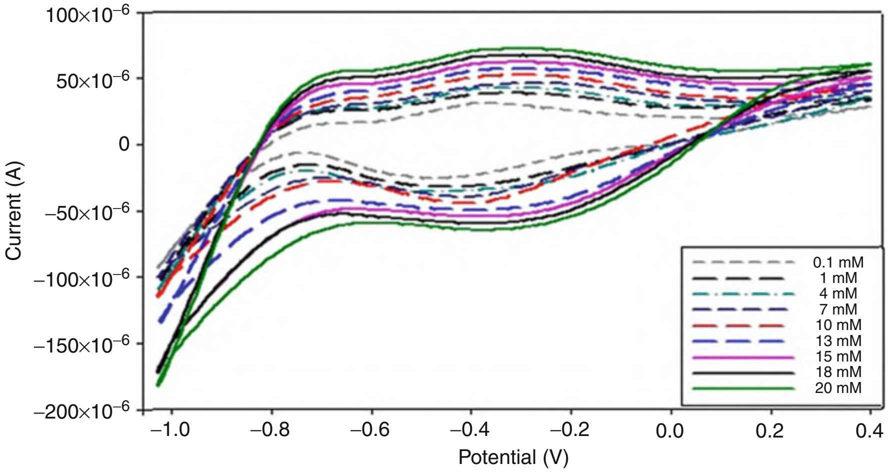

Fig. 32.7 CV graph of various concentration of glucose at Pt-nanodendrites-ZnO nanorods-ITO electrode. (Reproduced with permission (Razak et al. 2016))

surface improved the catalytic activity for glucose oxidation as well as the electron transport among glucose and also the electrode substrate. The glucose detecting characteristics of ZnONRs adorned using 42 nm PtNDs were the best. The electrocatalytic performance of Nafion/GOx/42 nm PtNDs/ZnONRs/ITO was greater than that of GOx/42 nm PtNDs/ZnONRs/ITO, demonstrating the role of Nafion in biosensing. The intensity of the electrochemical reaction grew in the following process at various electrodes: Nafion/GOx/42 nm PtNDs/ZnONRs/ITO > Nafion/GOx/ZnONRs/ITO > Nafion/GOx/42 nm PtNDs/ITO > Nafion/GOx/ZnONRs/ITO > Nafion/GOx/. In comparison to various Pt ND sizes, Nafion/GOx/42 nm PtNDs/ZnONRs/ITO demonstrated glucose sensitivity at 5.85 A/mM, a linear range of 1–18 mM, and a LOD of 1.56 mM. These findings suggest the PtND/ZnONRs electrode with immobilized GOx in biodegradable Nafion might be used as a glucose sensing element (Razak et al. 2016).

5 Rare Earth Material-Based Nanodendrites

Lower phonon frequencies, inadequate auto-fluorescence interference, long penetration durations, exceptional brightness, outstanding stabilities, and nonblinking emission make rare-earth Yb^{3+} and Er^{3+}-doped $NaYF_4$-based upconversion nanoparticles (UCNPs) very attractive in bioimaging applications. The size, shape, and mixture of $NaYF_4$: Yb^{3+}/Er^{3+} UCNPs influence their benefits. The Upconversion luminencence emission (UCLE) strength of NaYF4: $Yb^{3+/}Er^{3+}Tm^{3+}$ nanoplates, for instance, was much higher than that of nanospheres, nanoellipses, and nanoprisms. By lowering the size of the particles of Y_2O_3: 1% Er^{3+}/4% Yb^{3+} UCNPs, varied wavelengths of blue, red, and green UCLEs appear. The multicolored UCLE released by $NaYF_4$:

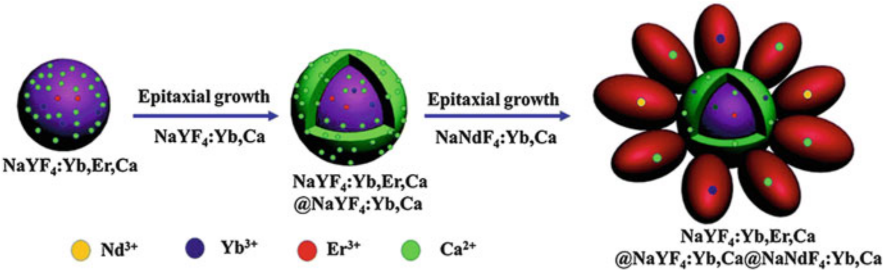

Fig. 32.8 Schematic diagram of fabrication of nanodendrites. (Reproduced with permission (Abualrejal et al. 2019))

Yb/Er core-shell UCNPs varied from visible region to near infrared (NIR). Consequently, as compared to -NaYF$_4$: Yb^{3+}/Er^{3+}UCNPs, BaGdF5: Yb^{3+}/Er^{3+} core-shell UCNPs increased the UCLE by four times (Abualrejal et al. 2019).

Figure 32.8 shows the thermal degradation method was used to create a novel type of three-dimensional core multiple shell upconversion nanodendrites (UCNDs) consisting of a core (NaYF$_4$: Yb, Er, Ca), transition zone (NaYF$_4$: Yb, Ca), and external surface (NaNdF4: Yb, Ca) (Abualrejal et al. 2019). As predicted, the UCNDs self-assemble into a unique spatial nano architectonic configuration with many arms encircling a shortened middle core and spherical inner core. In comparison to regular UCNPs, the uniquely developed UCNDs have a number of advantages. UCNDs, in specific, incorporate elements of core-double shells (e.g., high UCLE, lower radioactive decay loss, multicolor emissions, and low phonon energies) with the incomparable advantages of nanodendrites (e.g., elevated accessible contact area, low density, great consistency, and various surface edges). The Yb^{3+}-enriched transition layer allows for effective excitation energy transfer between Nd^{3+} and Er^{3+} while also avoiding unnecessary quenching impacts produced by Nd^{3+} trapped in the outer shell with a high concentration. The UCLE of UCNDs and UCND@SiO$_2$-COOH was compared to core UCNPs and core-shell UCNPs as a result of their excellent characteristics. The in vitro and in vivo UCL bioimaging characteristics of UCND@SiO$_2$-COOH were also thoroughly explored in order to demonstrate the use of UCNDs in biological investigation (Liang et al. 2020).

Ten milligram per kilogram of bodyweight UCND@SiO$_2$-COOH in 0.9% NaCl solution were infused into mouse via the tail vein for in vivo bioimaging. Using 980 nm laser stimulation, significant green UCL signals was efficiently produced from the liver location at 0.5 h after injection this can be seen in the Fig. 32.4. The largest increase in UCLE signals was attained after 8 h, following by a minor drop at 24 h (Fig. 32.4). Those findings show that UCND@SiO$_2$-COOH's powerful UCLE can readily penetrate deep tissue and has a lot of promise for in vivo imaging techniques. The mice were euthanized 8 h after injection to assess the biodistribution

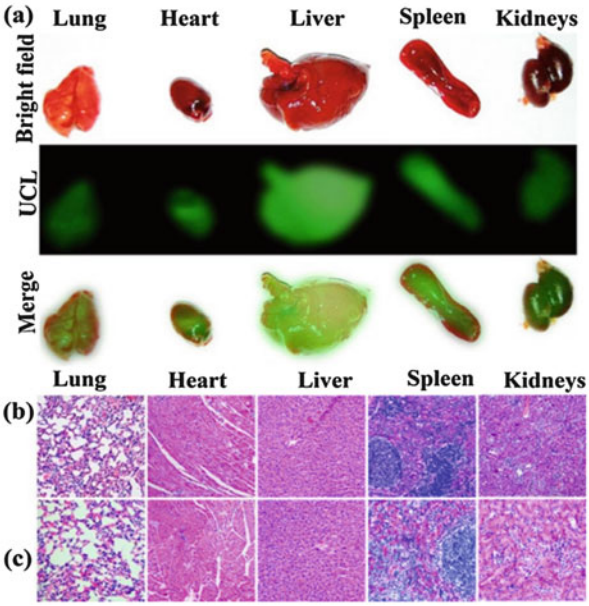

Fig. 32.9 Ex-vivo UCL images of several organs taken from mice implanted with UCND@SiO_2-COOH (**a**). Investigation of tissues taken from the organs of (**b**) untreated and (**c**) treated mice. (Reproduced with permission (Abualrejal et al. 2019))

of UCND@SiO_2-COOH. The liver, lung, heart, kidney, and spleen were all collected and scanned using a 980 nm laser excitation. Those organs UCL image depicts apparent green emission at varying frequencies, Fig. 32.4. The liver and spleen have substantially greater UCL signal strength than the remaining tissues. Inductively coupled plasma spectrometry was used to investigate the concentrations of UCND@SiO_2-COOH in various organs (ICP-MS). The liver and spleen had much greater levels of UCND@SiO_2-COOH than the other organs. This finding indicates that UCND@SiO_2-COOH accumulates mostly in the liver and spleen. The occurrence coincides with earlier observations (Zeng et al. 2020).

Researchers created a core-double shells with numerous branching arms for spatially UCNDs. The outer shell's slightly elevated Nd^{3+} boosts absorption energy, whereas the inner layer works as a protective barrier, avoiding the quenching interface among Er^{3+} and $Nd^{3+.}$ Furthermore, Yb^{3+} in the intermediate layer ensures that Nd^{3+} and Er^{3+} exchange excitation energy efficiently. At 980 nm, those structural and elemental advantages increased the UCLE of UCNDs by 5 and 15 times, correspondingly, as comparing to core-shell UCNPs and core UCNPs. Without considerable toxicity, carboxy-terminated silica shells encapsulated UCNDs (UCND@SiO_2-COOH) were effectively used as luminescence probes (Fig. 32.9) for in vitro and in vivo bioimaging (Abualrejal et al. 2019). This research might pave the path for the development of customized luminous markers for bioimaging techniques.

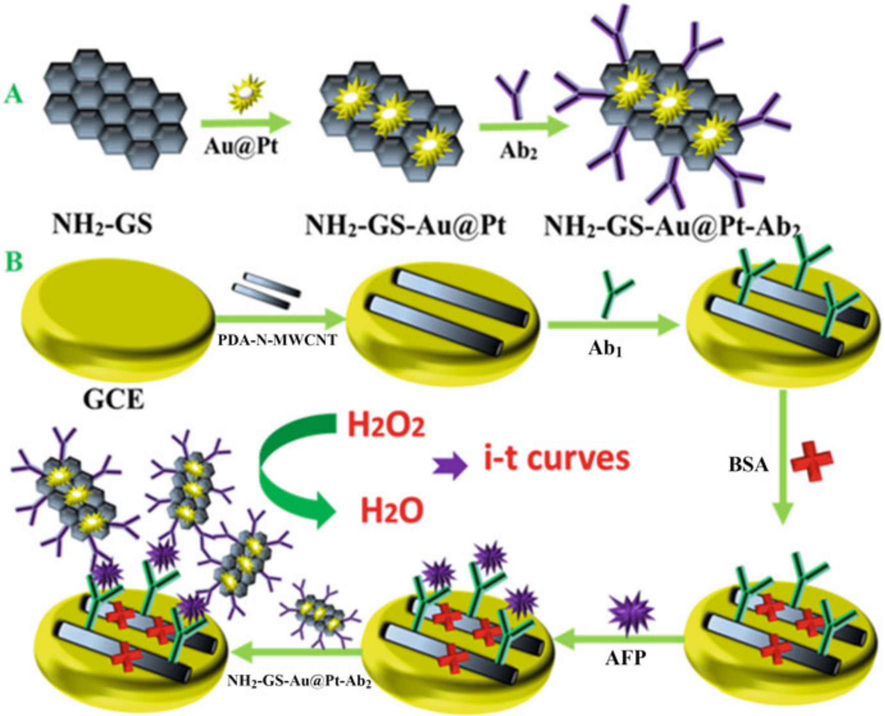

Fig. 32.10 Schematic of NH_2-GS/Au@Pt/Ab_2 (**a**) and the fabrication procedure of the immunosensor (**b**). (Reproduced with permission (Jiao et al. 2016))

6 Graphene Loaded Bimetallic Nanodendrites

Protein biomarkers identification that is ultrasensitive and specific is critical in medical diagnostics and drug research. The clinical examination of cancer biomarkers, in particular, is critical for early cancer detection. The tumor marker alpha fetoprotein (AFP) is used to identify malignancies of the liver, reproductive organs, As a result, developing a reliable approach for identifying AFP that is both sensitive and discriminating is quite desirable. Electrochemiluminescent assays and enzyme-linked immunosorption assays are two examples of analytical techniques.

Figure 32.10 shows a sandwich-type electrochemical immunosensor with amino ring designed and synthesized graphene (NH_2-GS) packed mesoporous Au@Pt nanodendrites (NH_2-GS/Au@Pt) and poly-dopamine nanostructured N-doped multi-walled carbon nanotubes for AFP identification (PDA-N-MWCNT) (Jiao et al. 2016). To the best of our knowledge, PDA-N-MWCNT, could provide a hydrophilic functionality for the appropriate immobilization of predominant antibody (Ab1) by the poly-dopamine film from the out exterior of N-doped multi-

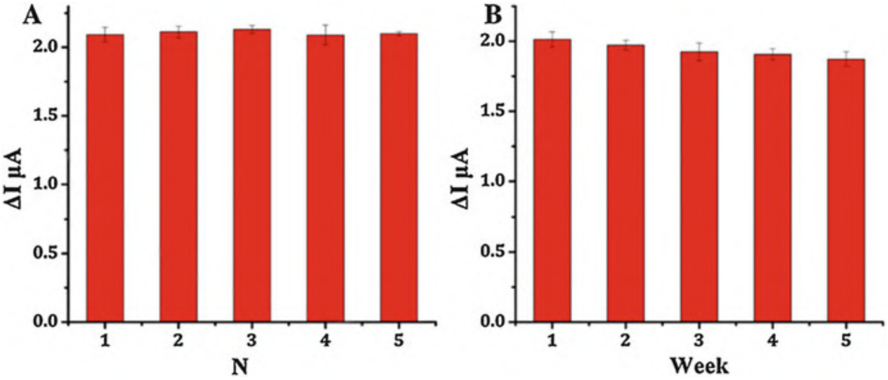

Fig. 32.11 (**a**) Existing immunosensor fluctuations toward five distinct electrodes in the same manner; (**b**) the AFP immunosensor stabilization study. (Reproduced with permission (Jiao et al. 2016))

walled carbon nanotube (N-MWCNT), while retaining the superior electron transfer capacity of N-MWCNT, which favors improved sensitivity. Because there are so many electroactive sites in the mesoporous architecture, biometallic Au@Pt nanodendrites have outstanding electrocatalytic efficiency. Since it incorporates all created indications by the inserted massive Au@Pt nanodendrites, NH_2-GS/Au@Pt nanomaterials may be manufactured as an appropriate signal label. As a consequence, all of these materials' properties contributed to the created electrochemical immunosensor's exceptional effectiveness (Jiao et al. 2016).

The electrochemical impedance spectrum (EIS) is a useful tool for characterizing immunosensor assembling procedures. EIS had a semicircle component at higher frequency and a linear part at lower frequency, this was recognized. The electron-transferring barrier was connected with high frequencies, whereas the dispersion stage of the entire process was correlated with lower frequencies. Whenever the electrode was changed with PDA-N-MWCNT (curve b) (Jiao et al. 2016), it had a low resistance and was substantially smaller than the GCE electrode (curve a) (Jiao et al. 2016). The explanation for this is because PDA-NMWCNT may help with electron transport. Because Ab1, BSA, and AFP may obstruct electron transmission, the impedance of this electrode was visibly enhanced when they were immobilized one after the other (curves c–e) (Jiao et al. 2016). After longer incubation of NH_2-GS/Au@Pt/Ab_2 (curve f) (Jiao et al. 2016), the semicircular remained bigger, indicating that Ab2 may also inhibit electron transport. The developed immunosensor shows very good stability and reproducibility (Fig. 32.11) was clearly formed effectively (Jiao et al. 2016; Zheng et al. 2013).

The excellent fabrication of immunosensor PDA-N-MWCNT provided a hydrophilic surface to immobilize antibodies for biomedical applications surface for immobilizing Ab (1); (2) PDA-N-MWCNT customized electrode equipped more electrochemical energetic area, which could also efficiently enhance the immunosensor's responsivity; (3) GS might load a large number of high semiconducting and high electrocatalytic energetic Au@Pt nanodendrites for signal multiplication (Sahu et al. 2013).

7 Conclusion

We have discussed the preparation and application of numerous nanodendrites and their potential application for the treatment of cancer and other electroanalytical applications.

References

Abualrejal MMA, Eid K, Tian R, Liu L, Chen H, Abdullah AM, Wang Z (2019) Rational synthesis of three-dimensional core-double shell upconversion nanodendrites with ultrabright luminescence for bioimaging application. Chem Sci 10(32):7591–7599

Jiao L, Zhang L, Du W, Li H, Yang D, Zhu C (2013) Au@Pt nanodendrites enhanced multimodal enzyme-linked immunosorbent assay. Nanoscale 11(18):8798–8802

Jiao L, Mu Z, Zhu C, Wei Q, Li H, Du D, Lin Y (2016) Graphene loaded bimetallic Au@Pt nanodendrites enhancing ultrasensitive electrochemical immunoassay of AFP. Sensors Actuators B Chem 231:513–519

Kadian S, Sethi SK, Manik G (2021) Recent advancements in synthesis and property control of graphene quantum dots for biomedical and optoelectronic applications. Mater Chem Front 5(2): 627–658

Kannan P, Dolinska J, Maiyalagan T, Opallo M (2014) Facile and rapid synthesis of Pd nanodendrites for electrocatalysis and surface-enhanced Raman scattering applications. Nanoscale 6(19):11169–11176. https://doi.org/10.1039/C4NR02896A

Khan MS, Naqvi SA, Nisar N, Nawab F (2018) Medical students perspective about adverse effects of caffeine consumption. Rawal Med J 43(1):156–160

Lee YW, Kim M, Kim Y, Kang SW, Lee J-H, Han SW (2010) Synthesis and electrocatalytic activity of Au-Pd alloy nanodendrites for ethanol oxidation. J Phys Chem C 114(17):7689–7693

Liang S, Wang H, Li Y, Qin H, Luo Z, Huang B, Zhao X, Zhao C, Chen L (2020) Rare-Earth based nanomaterials and their composites as electrode materials for high performance supercapacitors: a review. Sustain Energy Fuels 4(8):3825–3847

Lu S, Eid K, Li W, Cao X, Pan Y, Guo J, Wang L, Wang H, Gu H (2016) Gaseous NH_3 confers porous Pt nanodendrites assisted by halides. Sci Rep 6:26196

Lv J-J, Wang A-J, Ma X, Xiang R-Y, Chen J-R, Feng J-J (2015) One-pot synthesis of porous Pt-Au nanodendrites supported on reduced graphene oxide nanosheets toward catalytic reduction of 4-nitrophenol. J Mater Chem A 3(1):290–296. https://doi.org/10.1039/C4TA05034G

Muhammad Afiq KA, Ab Rashid R, Lazim RM, Dollah N, Razak KA, Rahman WN (2018) Evaluation of radiosensitization effects by platinum nanodendrites for 6 MV photon beam radiotherapy. Radiat Phys Chem 150:40–45. https://doi.org/10.1016/j.radphyschem.2018.04.018

Patra S, Roy E, Madhuri R, Sharma PK (2016) Nanocomposite of bimetallic nanodendrite and reduced graphene oxide as a novel platform for molecular imprinting technology. Anal Chim Acta 918:77–88. https://doi.org/10.1016/j.aca.2016.02.046

Qiu P, Yang M, Qu X, Huai Y, Zhu Y, Mao C (2016) Tuning photothermal properties of gold nanodendrites for in vivo cancer therapy within a wide near infrared range by simply controlling their degree of branching. Biomaterials 104:138–144. https://doi.org/10.1016/j.biomaterials.2016.06.033

Razak KA, Neoh SH, Ridhuan NS, Nor NM (2016) Effect of platinum-nanodendrite modification on the glucose-sensing properties of a zinc-oxide-nanorod electrode. Appl Surf Sci 380:32–39

Sahu SC, Samantara AK, Dash A, Juluri RR, Sahu RK, Mishra BK, Jena BK (2013) Graphene-induced Pd nanodendrites: a high performance hybrid nanoelectrocatalyst. Nano Res 6(9): 635–643

Sun Y, Zhang J, Li J, Zhao M, Liu Y (2017) Preparation of protein imprinted polymers: via protein-catalyzed EATRP on 3D gold nanodendrites and their application in biosensors. RSC Adv 7(45):28461–28468. https://doi.org/10.1039/C7RA03772D

Wang S, Wu Y, Yang G, Li T, Luo H, Li L-H, Bai Y, Li L, Liu L, Cao Y, Ding H, Zhang T (2017) Wearable sweatband sensor platform based on gold nanodendrite array as efficient solid contact of ion-selective electrode. Anal Chem 89(19):10224–10231

Yang F, Cheng K, Wu T, Zhang Y, Yin J, Wang G, Cao D (2013) Preparation of Au nanodendrites supported on carbon fiber cloth and its catalytic performance to H_2O_2 electroreduction and electrooxidation. RSC Adv 3(16):5483–5490

Ye K-H, Liu Z-Q, Li N, Xiao K, Wang J, Su Y-Z (2012) 3D Sn-based alloy nanodendrites: electrodeposition as a superior route for synthesizing complex dendritic nanostructures. J Electrochem Soc 159(12):D737–D741

Zeng Z, Xu Y, Zhang Z, Gao Z, Luo M, Yin Z, Zhang C, Xu J, Huang B, Luo F, Du Y, Yan C (2020) Rare-Earth-containing perovskite nanomaterials: design, synthesis, properties and applications. Chemical Society Reviews 49(4):1109–1143

Zheng L, Li LXY, Xu J, Kang X, Zou Z, Yang S, Xia J (2013) Facile preparation of polydopamine-reduced graphene oxide nanocomposite and its electrochemical application in simultaneous determination of hydroquinone and catechol. Sensors Actuators B Chem 177:344–349. https://doi.org/10.1016/j.snb.2012.11.006

Всё для победы!
НАРОДНЫЙ ФРОНТ
https://pobeda.onf.ru/
LET'S HELP THE RUSSIA

Nanobiopolymers-Based Electrodes in Biomolecular Screening and Analysis

33

Palraj Kalimuthu

Contents

1 Introduction 719
2 Type of Biopolymers 722
3 Strategies for Immobilization of Biocatalysts into Biopolymers 723
  3.1 Adsorption 723
  3.2 Covalent Attachment 724
  3.3 Cross-Linking 724
  3.4 Encapsulation 724
  3.5 Entrapment 725
4 Applications 725
  4.1 Chitosan-Based Nanocomposite Electrodes 725
  4.2 Cellulose-Based Nanocomposite Electrodes 730
  4.3 Alginate-Based Nanocomposite Electrodes 732
  4.4 Collagen-Based Nanocomposite Electrodes 735
5 Conclusions 736
References 737

Abstract

Biopolymers possess diverse functional groups and excellent biocompatibility toward a wide range of biomolecules, and these characteristics are highly regarded for the construction of highly stable and reliable biosensors. Among the various biosensors, electrochemical biosensors are most widely applied in various applications owing to their outstanding sensing performances, cost-effectiveness, and facile fabrication strategy. Further, with the recent advancements in electronic instruments, the electrochemical sensor devices can be miniaturized into portable devices, which promote them to apply practical applications such as real-time health monitoring and on-site analysis.

P. Kalimuthu (✉)
School of Chemistry and Molecular Biosciences, University of Queensland, Brisbane,
QLD, Australia
e-mail: p.kalimuthu@uq.edu.au

© Springer Nature Singapore Pte Ltd. 2023

U. P. Azad, P. Chandra (eds.), *Handbook of Nanobioelectrochemistry*,
https://doi.org/10.1007/978-981-19-9437-1_33

Furthermore, a range of nanomaterials can be integrated into the biopolymers to enhance sensor performances such as high sensitivity, low detection limit, and fast response. This chapter starts by describing the types of biopolymers and their different immobilization strategies for attaching biocatalysts to electrode surfaces. Then, the recent advancements of biopolymers embedded nanocomposite materials for the construction of electrochemical biosensors, immunosensors, and aptasensors to detect a range of biomolecules such as proteins, cancer biomarkers, nucleic acids, vitamins, sugars, neurotransmitters, and pharmaceutical drugs. Further, the fundamental sensing mechanism of the biopolymers-based electrochemical biosensors is discussed. Moreover, the reported analytical parameters for these analytes are summarized.

Keywords

Nanobiopolymers · Biocatalyst immobilization · Electrocatalysis · Biosensors · Nanocomposite

Abbreviations

3D-HPC	Three-dimensional hierarchically porous carbon
AA	Ascorbic acid
ABT	4-aminobenzenethiol
AGP	Alpha-1-acid glycoprotein
AuNCs	Gold nanocubes
AuNPs	Gold nanoparticles
CAP	Chloramphenicol
CC	Catechol
CD	Carbon dots
CDI	1,4-carbonyldiimidazole
CHIT	Chitosan
CHIT-Fc-co-BPEI-Fc	Chitosan-co-grafted-branched polyethylenimine redox conjugates
CMC	Carboxymethyl cellulose
CNC	Cellulose nanocrystals
CNCC	Nanocrystalline cellulose
COL	Collagen
DA-Apt	Dopamine binding aptamer
DOPA	3,4-dihydroxyphenylalanine
DPV	Differential pulse voltammetry
EP	Epinephrine
EPA	Environmental Protection Agency
ERGO	Electrochemically reduced graphene oxide
GC	Glassy carbon
GCSC	Grass carp skin collagen
GF	Graphene foam
GO	Graphene oxide

GOD	Glucose oxidase
GR	Graphite
Hb	Hemoglobin
HEC	Hydroxyethyl cellulose
HQ	Hydroquinone
HRP	Horseradish peroxidase
HVA	Homovanillic acid
ITO	Indium tin oxide
LIG	Laser-induced graphene
LO	Lactate oxidase
LSCM	Laser scanning confocal microscopy
Mb	Myoglobin
MNs	Magnetic nanoparticles
MWCNTs	Multiwalled carbon nanotubes
NC	Nanocrystal
NDEA	N-nitrosodiethanolamine
NDMA	N-nitrosodimethylamine
NF	Norfloxacin (NF)
N-GQDs	Nitrogen-doped graphene quantum dots
NSE	Neuron-specific enolase
PANI	Polyaniline
PDH	Phenylalanine dehydrogenase
PEDOT	Poly(3,4-ethylenedioxythiophene)
PEI	Polyethylenimine
PG	Progesterone
PSA	Prostate-specific antigen
PtNPs	Platinum nanoparticles
PU	Polyurethane
RC	Resorcinol
ROS	Reactive oxygen species
SA	Sodium alginate
SPCE	Screen-printed carbon electrode
SWCNH	Single-walled carbon nanohorns
SWCNTs	Single-walled carbon nanotubes
TA	Tyramine
TEMED	Tetramethylenediamine

1 Introduction

An electrochemical biosensor contains recognition elements, including enzymes, antibodies, nucleic acid, proteins, cells, etc. These biorecognition elements specifically interact with a particular analyte and produce a measurable electrical signal. The intensity of the electrical signal corresponds to the concentration of the analyte present in the analytical medium (Ronkainen et al. 2010). In addition, another essential component is the transducer (electrode) which plays a crucial role in electrochemical biosensors that support immobilizing the bioreceptors and also transducing the biochemical events (for example, enzyme-substrate reaction) into electrical signals in the form of voltage, current, and impedance (Kalimuthu et al. 2014, 2015a).

Most biosensors suffer from stability because the bioreceptor molecules tend to lose their activity once removed from their natural environment. Importantly, biocatalysts are relatively expensive compared to nanomaterials-based catalysts. Therefore, it is crucial to construct a reusable biosensor to reduce the cost of the analysis. Effective immobilization of the bioreceptor on the transducer affords the construction of a highly stable and reusable electrochemical biosensor. Consequently, the development of immobilization strategies has received significant attention in the biotechnology and biomedical fields. Among the support matrices explored in the literature, biopolymers have gained significant attention due to their facile fabrication approach, cost-effectiveness, biocompatibility, and presence of active functional groups (COOH, NH_2, and OH), which allow attaching bioreceptors through covalent, hydrogen bonding, and electrostatic interactions (Kalimuthu et al. 2017b, c).

However, the natural biopolymers are nonconductive, and it is beneficial for constructing impedance-based biosensors (Roquero et al. 2020; Zhao et al. 2019), but it restricts their usage in most other electrochemical applications that need conductivity. This issue is easily resolved when biopolymers are embedded in highly conductive nanomaterials. The biopolymers integrated nanomaterials endow higher biocompatibility with enhanced electrical communication for immobilized biological recognition elements and achieve viable biosensors.

A range of nanomaterials, including metal nanoparticles, graphene-based materials, carbon nanotubes, and carbon quantum dots, have been combined with various biopolymers to fabricate the biopolymer-nanocomposite materials (Krishnan et al. 2017; Singh et al. 2013; Zhang et al. 2018; Wei et al. 2021; Wan et al. 2010; Mahato et al. 2019). The resulting materials achieve plenty of attractive properties, including biodegradability, biocompatibility, nontoxicity, excellent mechanical flexibility, and durability. For instance, Krishnan et al. demonstrated direct voltammetry of glucose oxidase (GOD) at chitosan (CHIT) embedded Pd@Pt nanocubes modified glassy carbon (GC) electrode (Krishnan et al. 2017). GOD is attached to the CHIT by covalent attachment through an amide bond with the aid of bifunctional cross-linker glutaraldehyde (GTA). In another report, the direct electrochemistry of hemoglobin was achieved at collagen incorporated multiwalled carbon nanotubes modified GC electrode and successfully applied to detect H_2O_2 (Zong et al. 2007a).

This chapter presents the recent development of nanobiopolymers-based electrochemical biosensors for a range of biomolecules detection and quantification. The sensor fabrication strategies, biopolymer's role in the sensor, and basic sensing mechanisms are described. Particularly, this chapter covers the biopolymers (i.e., chitosan, cellulose, alginate, and collagen) due to their widespread applications in sensor development. In addition, the reported analytical parameters for these analytes are summarized in Table 33.1. Also, this chapter encourages the readers

Table 33.1 Analytical parameters of biopolymer-based electrochemical biosensors

Electrode	Analyte	Linear range (µM)	Detection limit (nM)	References
CP/CHIT-GQDs	Epinephrine	0.36–380	0.3	Tashkhourian et al. (2018)
SPCE/CHIT-MNs-GR-PU	Epinephrine	0.1–0.6	14	Mattioli et al. (2020)
ITO/CH-nY_2O_3/anti-FQ/BSA	Norfloxacin	0.000001–10	0.00387	Yadav et al. (2020)
GC/COL-MWNTs/Hb	H_2O_2	0.6–30	130	Zong et al. (2007a)
GC/GCSC-GO/DA-aptamer	Dopamine	0.001–1	0.75	Wei et al. (2019)
GC/ZrO_2-COL/Mb	H_2O_2	1–85	63	Zong et al. (2007b)
SPCE/N-GQDs/CHIT	Dopamine	1–200	145	Ben Aoun (2017)
GC/MWCNT-CHIT-ZrO_2	Serotonin	0.8–5	0.6	Devnani et al. (2015)
SPCE/CMC-$Mn_3(PO_4)_2$	$O_2^{-\cdot}$	0.057–2.95	8.47	Yun et al. (2022)
GC/ERGO-CHIT/Au/HRP	H_2O_2	10–6310	400	Devaraj et al. (2020)
GC/3D-HPC/SA	Catechol	0.05–150	30	Wei et al. (2021)
LIG/CMC@TiO_2/Ag	Chloramphenicol	0.01–100	7	Chang et al. (2022)
Au/PANI-*c*-(CHIT-CNTs)-GOD	Glucose	1000–20,000	100,000	Wan et al. (2010)
GC/PEDOT/AuNPs/CNCC	Ascorbic acid	0.88–15,000	290	Fan et al. (2018)
Au/GO-CHIT/PDH	Phenylalanine	0.5–15,000	416	Naghib et al. (2014)
GC/CHIT-CDs/DNA	N-nitrosodiethanolamine	0.0096–0.4	9.6	Majumdar et al. (2020)
SPCE/CHIT-Fc-co-BPEI-Fc	Lactate	50–1500	172,000	Gan et al. (2021)
GC/CHIT/Pd@Pt-NC/GOD	Glucose	1000–6000	200	Krishnan et al. (2017)

SPCE screen-printed carbon electrode, *MNs* magnetic nanoparticles, *CHIT* chitosan, *GR* graphite, *PU* polyurethane, *GC* glassy carbon, *COL* collagen, *Mb* myoglobin, *N-GQDs* nitrogen-doped graphene quantum dots, *MWCNTs* multiwalled carbon nanotubes, *CMC* carboxymethyl cellulose, *ERGO* electrochemically reduced graphene oxide, *HRP* horseradish peroxidase, *3D-HPC* three-dimensional hierarchically porous carbon, *SA* sodium alginate, *LIG* laser-induced graphene, *GOD* glucose oxidase, *PANI* polyaniline, *PEDOT* poly(3,4-ethylenedioxythiophene), *AuNPs* gold nanoparticles, *CNCC* nanocrystalline cellulose, *PDH* phenylalanine dehydrogenase, *GO* graphene oxide, *CD* carbon dots, *CHIT-Fc-co-BPEI-Fc* chitosan-cografted-branched polyethylenimine redox conjugates, *NC* nanocrystal to understand the importance of biopolymers in sensor devices and how to develop and improve the sensors matrices to achieve higher sensing performances.

2 Type of Biopolymers

In general, biopolymers can be divided into three categories based on their origins: plant-based biopolymers, animal-based biopolymers, and microbial-based biopolymers. A list of biopolymers derived from different sources is given in Chart 33.1. Plant-based biopolymers are categorized into proteins or polysaccharides and reported to be multifunctional, nontoxic, abundant in nature, and low cost. On the other hand, animals can produce a broad range of biopolymers as a substantial part of their cellular and morphological related metabolic activities. Basically, the biopolymers are produced from different parts of the cells (cytoplasm, cell wall, and organelles) by enzymatic processes. The generated biopolymers are primarily involved in the life cycle and support essential cellular and metabolic activities. Further, microbes can produce a range of biopolymers (polyamides, polysaccharides, polyphosphates, and polyesters) similar to animals to protect themselves from the unfavorable environment.

Among the biopolymers listed in Chart 33.1, chitosan, cellulose, alginate, and collagen have been extensively used to fabricate various electrochemical sensors, and, thus, this chapter mainly focuses on them. The chemical structure of the targeted polymers is given in the following Fig. 33.1. The polymers contain various active functional groups such as OH, NH_2, COOH, and C=O and are beneficial for attaching to biocatalysts or electrode materials via electrostatic, covalent, and hydrogen bonding interactions.

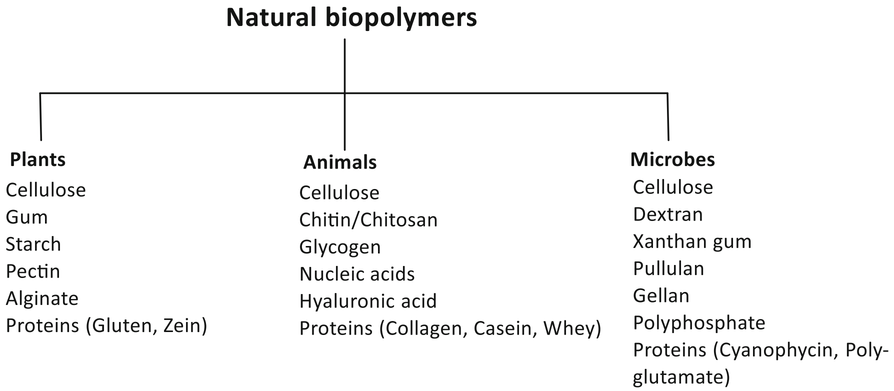

Natural biopolymers

Plants	Animals	Microbes
Cellulose	Cellulose	Cellulose
Gum	Chitin/Chitosan	Dextran
Starch	Glycogen	Xanthan gum
Pectin	Nucleic acids	Pullulan
Alginate	Hyaluronic acid	Gellan
Proteins (Gluten, Zein)	Proteins (Collagen, Casein, Whey)	Polyphosphate
		Proteins (Cyanophycin, Poly-glutamate)

Chart 33.1 The categorization of biopolymers is based on their origin

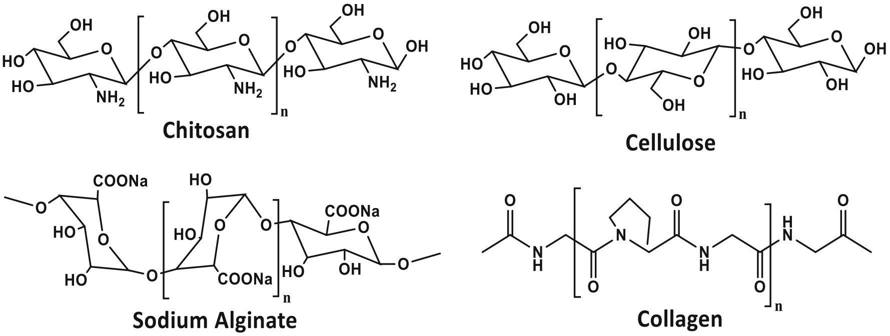

Fig. 33.1 Chemical structure of biopolymers

3 Strategies for Immobilization of Biocatalysts into Biopolymers

As mentioned before, the biocatalysts immobilization methods are very important to constructing a stable, sensitive, and efficient electrochemical biosensor. Because, the immobilized biocatalysts are readily available to the substrate for the catalytic reaction and achieve a higher turnover in a short period of time compared to the biocatalysts solubilized in an aqueous medium. In addition, the immobilized biocatalysts offer to reuse in a large scale processing which minimizes the production costs. Basically, the biopolymers have several active functional groups and, thus, once modified on the electrode surface, they deliver different forces such as binding, bonding, and attraction to immobilize the biocatalysts. So far, several methods have been reported in the literature and briefly summarized below. The choice of the immobilization method primarily depends upon the nature of the biocatalyst.

3.1 Adsorption

It is a facile approach to attaching the biocatalyst to an electrode surface by weak adsorption forces such as hydrogen bonding, van der Waals interaction, as well as ionic and hydrophobic interactions (Kalimuthu et al. 2016b). For instance, the nitrate reductase was successfully adsorbed on the biopolymer chitosan modified glassy carbon electrode (Kalimuthu et al. 2021b). The enzyme modified electrode showed a pronounced catalytic response and retained 80% catalytic response after 3 months. Nevertheless, sometimes, these weak interactions result in a high possibility of leaking biocatalyst from the electrode surface. The desorption of biocatalysts is associated with several factors such as electrolyte composition, pH, and ionic strength of the analytical medium.

3.2 Covalent Attachment

Covalent attachment of biocatalyst to the polymer modified electrode is a popular method to construct a biosensor. Because, a strong bond formation takes place between the biocatalyst and biopolymer which restricts the catalyst leak from the electrode surface. Usually, the biocatalysts contain a range of amino acids (lysine, arginine, histidine, and aspartic acid). The presence of NH_2 or COOH group in the amino acids are used to attach to the electrode surface. To initiate the attachment, first, the COOH group is activated by multifunctional reagents such as carbodiimide, N-hydroxy succinimide, etc. (Novick and Rozzell 2008), and then the COOH activated biocatalyst is coupled to the NH_2 group modified electrode through an amide bond.

3.3 Cross-Linking

Similar to covalent attachment, cross-linking is also an efficient method to immobilize the biocatalyst. Several cross-linking agents are used to immobilize enzymes, including genipin, glutaraldehyde (GTA), ethylene glycol–based diglycidyl ethers, epichlorohydrin, bisisocyanate, and bis-diazobenzidine (Kalimuthu et al. 2022; Wong and Wong 1992). These cross-linkers contain active functional groups such as hydroxy, methoxy, and aldehyde, and they covalently attach to the enzyme via the amine group present in the amino acids. Among them, GTA has been extensively used to immobilize several enzymes due to its low cost and effective cross-linking efficiency. However, GTA is unsuitable for some enzymes (e.g., nitrilases) as a result of its toxic effect (Sheldon 2007).

3.4 Encapsulation

It is one of the effective methods used to fabricate the enzyme-based biosensor. In this strategy, the enzyme is covered and controlled from leaking by polymer membrane walls, but the enzyme is allowed to move freely inside the membrane. Basically, the membrane is semipermeable which allows the substrate and mediator to enter the membrane to reach the enzyme for catalysis (Kalimuthu et al. 2015b, 2016a). In addition, there is no requirement for chemical activation of the electrode surface to immobilize the enzyme and thus, enzyme activity remains unchanged. Further, this method is highly suitable for immobilizing larger biocatalysts, cells, and microorganisms. It is crucial to select the proper pore size of the membrane to achieve an effective encapsulation. The routinely used biopolymer-based membranes are chitosan, cellulose, alginate, and maltodextrin (Kalimuthu et al. 2021b).

3.5 Entrapment

In this method, a cross-linker, monomer, and enzyme are mixed together and cast on an electrode surface (Sharma and Singh 2020). The resulting polymer or gel network captures the enzyme and allows the substrate to pass through the membrane to react with the enzyme. It leads to biosensors with good sensitivity and durability. The only disadvantage of this method is that the cross-linking agent also cross-linked the enzyme, thus affecting the enzyme activity by limiting the diffusion. Also, the loading of the biocatalyst was reduced as a consequence of cross-linking.

4 Applications

4.1 Chitosan-Based Nanocomposite Electrodes

Chitosan (CHIT) is a versatile biopolymer used for many applications owing to its active NH_2 and OH functional groups, abundant nature, cost-effectiveness, good mechanical stability, doping feasibility, good permeability, hydrophilicity, biodegradability, and nonimmunogenic properties (Kou et al. 2021). The molecular weight of the CHIT determines its solubility. For instance, below 9 kDa is easily soluble while $>$22 kDa is sparingly soluble in an aqueous medium. However, more than 30 kDa is required to dissolve in an acidic medium (Ilyina et al. 2000). In addition to solubility, all other physicochemical properties are varied while changing the molecular weight of the CHIT. In terms of electrochemical sensor applications, CHIT is effectively used as a binding agent for immobilizing receptors (enzymes, antibodies, DNA, etc.) and nanomaterials (carbon- and metal-based nanomaterials) due to its strong adhesion properties on a wide range of electrode surfaces (Kalimuthu et al. 2017a, 2020, 2021a, b; Samadi Pakchin et al. 2018; Singh et al. 2013; Bhatnagar et al. 2018). The presence of NH_2 and OH groups endows the opportunity for attaching bioreceptors through electrostatics, covalent, and physical interactions. Several cross-linking agents have been used for the covalent attachment of bioreceptors on electrode surfaces, such as GTA, carbodiimides, glyoxal, N-hydroxy succinimide, cyanuric chloride, and epichlorohydrin. However, these agents are sometimes harmful to bioreceptors. On the other hand, the electrostatic and physical entrapment techniques are most favorable due to there is no harmful chemical modification of the bioreceptors. This section describes the fabrication of CHIT embedded electrochemical biosensors.

Epinephrine (EP) is one of the vital neurotransmitters in the central nervous system, and its abnormal concentrations cause adverse health effects on human beings. For instance, a low level of EP leads to Parkinson's disease, whereas a high level affects the human body metabolism, immune system, and blood pressure. Tashkhourian and coworkers used chitosan as a binding agent to immobilize the graphene quantum dots (GQDs) on carbon paste electrodes to detect EP (Tashkhourian et al. 2018). The GQDs were strongly adsorbed on the electrode surface due to effective electrostatic interaction between the positively charged NH_3^+ at the chitosan polymer and negatively charged COO^- at GQDs based on the pH. The as-prepared electrode delivered an excellent analytical performance to EP detection and achieved a linear range of 0.36–380 μM and a detection limit of 0.3 nM. The practical applicability of the optimized electrode examined the detection of EP in blood serum and EP containing injection samples. Another group reported the construction of a disposable electrochemical sensor for EP based on CHIT-coated magnetite (Fe_3O_4) nanoparticles modified graphite-polyurethane composites (CHIT-MNPs-GR-PU) (Mattioli et al. 2020). The constructed CHIT-MNPs-GR-PU modified SPCE showed a better catalytic performance than the CHIT-free composite. The CHIT coating on MNPs is expected to protect MNPs from aerobic and electrochemical oxidation at the operating potentials and achieve a better catalytic response. Further, the composite modified electrode showed a linear range and detection limit of 0.3–0.6 μM and 14 nM, respectively. Furthermore, the practical application of the sensor was demonstrated to detect EP in synthetic cerebrospinal fluids and synthetic urine samples. Also, the sensor exhibited long-term stability and found that only 4% catalytic response declined after 5 months of storage. In contrast, the catalytic response was decreased by 23% in the same period of time at CHIT-free composite electrode and it indicates the CHIT provides significant stability for the composite film.

Carcinoembryonic antigen (CEA) is considered one of the critical clinical tumor markers, and, therefore, the detection of CEA plays a vital role in clinical and biomedical research. In order to detect the CEA, Li et al. constructed an electrochemical immunosensor using a composite prepared with thiol functionalized CHIT (T-CHIT), thiol functionalized graphene (T-Gr), and AuNPs at the GC electrode (Li et al. 2015). The presence of thiol groups at graphene and CHIT endow to form a very stable film with AuNPs through the Au-S covalent bond. Then the GC/T-CHIT-AuNPs-T-Gr electrode was incubated in anti-CEA for 6 h at 4 °C. To avoid any nonspecific adsorption, bovine serum albumin (BSA) was added to the GC/T-CHIT-AuNPs-T-Gr/anti-CEA electrode to block any free active sites. The morphology of the composite film was examined by SEM, and it revealed that the composite appeared to be a 3D structure with a porous surface which is highly suitable for biomacromolecules adsorption. The optimized sensor yielded two linear ranges, such as 0.3–8.0 ng mL^{-1} and 8.0–100 ng mL^{-1} and a detection limit of 0.03 ng mL^{-1}. The longevity of the immunosensor was investigated and found that the sensor response decreased by 5.4% after 30 days. In another report, CHIT was used to immobilize the glucose oxidase (GOD) at graphene aerogel (GA), and Prussian blue (PB) modified SPCE (Hu et al. 2022). The developed electrode was successfully applied to detect glucose concentrations in the range of 0.5–6.0 mmol L^{-1} with a detection limit of 0.15 mmol L^{-1}. In terms of practical applicability, the optimized sensor was demonstrated to quantify glucose in blood serum samples.

Progesterone (PG) is a steroid hormone that regulates reproductive systems in humans, and its detection is crucially essential (Filicori 2015). An aptasensor was constructed to detect the PG with gold nanocubes (AuNCs), CHIT, hydroxyethyl cellulose (HEC), and **DNA aptamer** (Velayudham et al. 2021). The construction of the aptasensor is as follows. Firstly, the CHIT and HEC were blended as a gel by a free radical polymerization reaction. Then, the PG-specific aptamer (PG_{Apt}) was functionalized with –SH group and attached to AuNCs surface, and the resulting PG_{Apt}-AuNCs were combined with CHIT-HEC gel and coated on an Au electrode. The aptamer modified sensor delivered excellent activity toward the detection of PG. Moreover, prostate cancer is a life-threatening disease for men. Therefore, the early diagnosis of prostate cancer is very important. Soares et al. developed an impedance-based electrochemical biosensor for prostate cancer by detecting PCA3 biomarkers (Soares et al. 2019). In order to fabricate the biosensor, an amine-terminated prostate-specific PCA3-containing single-stranded DNA probe (TTTTTTCCCAGGGATCTCTGTGCTTCC) was loaded on the interdigitated Au electrode surface by a layer-by-layer approach with CHIT and MWCNT. The developed sensor delivered an excellent sensing performance toward PCA3 biomarkers.

N-nitrosamines are potential carcinogenic substances. Therefore, Majumdar and coworkers developed an electrochemical biosensor for N-nitrosodimethylamine (NDMA) and N-nitrosodiethanolamine (NDEA) based on DNA-carbon dots (Majumdar et al. 2020). The sensor fabrication protocol is given in Fig. 33.2. Firstly, the CHIT-carbon dot composite was prepared and then coated on the GC electrode by the drop coating method. Subsequently, the DNA probe was coated on the GC/CHIT-carbon dot electrode. Finally, the target analytes (NDMA or NDEA) were attached to the DNA probe, and the resulting electrode was examined by differential

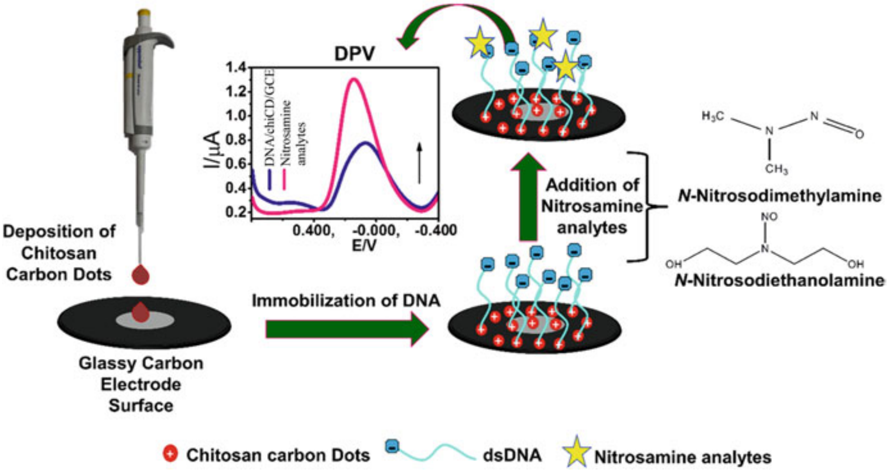
DPV
1.4
1.2
1.0
0.8
0.6
0.4
0.2
I/μA
DNA/chiCD/GCE
Nitrosamine analytes
0.400, -0.000, -0.400
E/V
Deposition of Chitosan Carbon Dots
Glassy Carbon Electrode Surface
Immobilization of DNA
Addition of Nitrosamine analytes
H_3C
N
N
O
CH_3
N-Nitrosodimethylamine
NO
N
OH
OH
N-Nitrosodiethanolamine
Chitosan carbon Dots
dsDNA
Nitrosamine analytes

Fig. 33.2 Fabrication of GC/CHIT-carbon dots-DNA electrode for N-nitrosamines detection (Majumdar et al. 2020)

pulse voltammetry (DPV). The oxidation current responses were substantially increased upon increasing substrate concentrations.

Further, Gan et al. developed a mediated enzymatic biosensor based on ferrocene attached CHIT (CHIT-Fc) modified electrode (Gan et al. 2021). It was found that the developed CHIT-Fc is soluble at lower pH (2.5–3.5). But this pH is not suitable for enzyme catalytic reactions, because most of the enzyme catalytic reactions occur at neutral pH. To resolve this issue, ferrocene integrated branched polyethyleneimine (BPEI-Fc) was prepared, which is soluble at higher pH (8.0–9.0). Then the BPEI-Fc was co-grafted with CHIT-Fc. The resulting co-grafted redox couple (CHIT-Fc-co-BPEI-Fc) is soluble at neutral pH. These co-grafted redox couples have amine groups and are thus attached with amine residues of target enzymes through GTA cross-linkage. Authors used this technique to develop glucose and lactose biosensors with GOD and lactate oxidase (LO) as catalysts. The optimized enzymatic sensors exhibited a detection limit of 0.047 and 0.172 mM for glucose and lactose, respectively.

1-ethyl-6-fluoro-1,4-dihydro-4-oxo-7-(piperazine-1-yl) quinolone-3-carboxylic acid is also known as norfloxacin (NF) and is used as an antibiotic to treat various bacterial related infections. However, the extensive use of NF causes several side effects such as heartburn, rectal pain, stomach cramps, etc. A rare earth metal oxide, yttrium oxide (Y_2O)-based immunosensor was reported to quantify NF (Yadav et al. 2020). In order to construct a sensor, a nanostructured Y_2O (nY_2O) was developed by a one-step hydrothermal strategy. Then, the CHIT was added to the nY_2O to improve biocompatibility. Followingly, the fluoroquinolones antibodies (anti-FQ) were attached to the CHIT-nY_2O composite via EDC + NHS covalent coupling. For the attachment, the COOH groups of anti-FQ were activated by EDC + NHS reaction and then attached to $–NH_2$ groups of CHIT through an amide bond. The developed composite was immobilized on an indium tin oxide (ITO) electrode and used as an electrochemical immunosensor. Further, BSA was included on the electrode surface to avoid any nonspecific binding. The optimized sensor showed remarkable sensing performance toward NF and achieved a linear range of 1 pM–10 μM and a detection limit of 3.87 pM.

A hydrogel-based enzymatic glucose biosensor was reported, and the hydrogel was developed by the combination of CHIT and CeO_2/MnO_2 hollow nanosphere. These materials were linked via a covalent linkage through the formation of an amide bond between the amine group of CHIT and COOH groups of CeO_2/MnO_2 (Liang et al. 2020). Then, GOD was attached to the composite through the strong electrostatic interaction with the CeO_2/MnO_2. The optimized sensor showed outstanding performance in glucose detection and attained a broad linear range (1–111 mM) and higher sensitivity (176 μA mM) with the continuous working ability for more than 30 days. Further, a bimetallic (Pd@Pt)-based enzymatic biosensor was reported for glucose detection. The GOD was attached with CHIT through a covalent linkage and then incorporated into the Pd@Pt nanocube (Krishnan et al. 2017). It is envisaged that the CHIT renders biocompatibility and

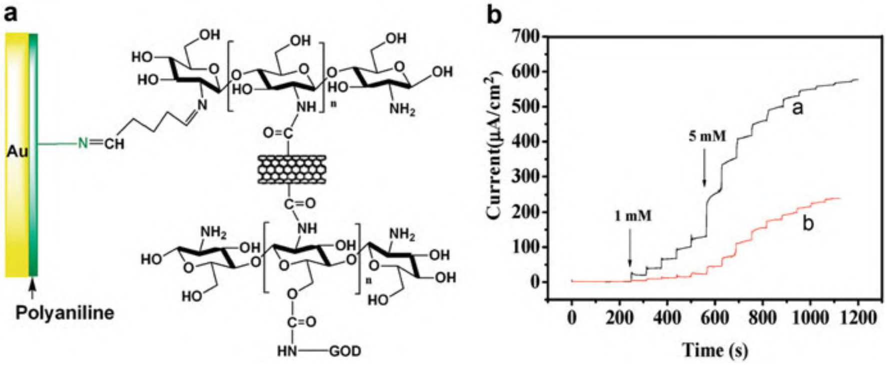

Fig. 33.3 (**a**) Schematic diagram for the construction of the Au/ABT/PANI-CNTs-CHIT-GOD electrode and (**b**) amperometric *i*/*t* curves of the (*a*) Au/ABT/PANI-CNTs-CHIT-GOD and (*b*) Au/ABT/CNTs-CHIT-GOD electrodes (Wan et al. 2010)

improves the stability of GOD, whereas Pd@Pt facilitates an electron transfer reaction. Interestingly, the direct electron transfer of GOD was achieved at the CHIT-Pd@Pt composite modified GC electrode. The fabricated sensor exhibited a linear range and sensitivity of 1–6 mM and 6.82 μA cm^{-2} mM^{-1}, respectively, for glucose detection. Further, no significant response to interfering substances such as ascorbic acid (AA), citric acid, and lactic acid was observed.

An amperometric biosensor for glucose was reported based on PANI and CHIT-coupled carbon nanotubes (CHIT-CNTs) modified Au electrode (Wan et al. 2010). The fabrication of the GOD-based glucose sensor was schematically shown in Fig. 33.3a. Firstly, the CHIT-CNTs were prepared by attaching CHIT with CNTs. Subsequently, the self-assembled monolayer of 4-aminobenzenethiol (ABT) was fabricated on the Au electrode surface, and then PANI coated on Au/ABT by a chemical oxidative graft polymerization strategy using an oxidizer $(NH_4)_2S_2O_8$. Followingly, the CHIT-CNTs were attached to Au/ABT/PANI electrode by GTA bifunctional cross-linker via an amide bond formation between free amine groups of polymers (PANI and CHIT) and aldehyde group of GTA. Finally, GOD was attached to the Au/ABT/PANI-CNTs-CHIT electrode by 1,4-carbonyldiimidazole (CDI) through covalent attachment. The as-prepared GOD modified polymer composite electrode was applied to detect glucose by the amperometric technique. Figure 33.3b represents the amperometric *i*/*t* curves for the increment of glucose concentration by an applied potential of 0.5 V vs. Ag/AgCl. As you can see, the PANI attached sensor electrode delivered a better catalytic response compared to the PANI-free sensor electrode. Further, the optimized composite sensor electrode (Au/ABT/PANI-CNTs-CHIT-GOD) yielded a linear range and sensitivity of 1–20 mM and 21 μA/(mM cm^2), respectively, toward glucose detection and retained the catalytic response of more than 80% after 2 months.

4.2 Cellulose-Based Nanocomposite Electrodes

Cellulose is a polysaccharide found in the cell wall of green plants, and the polymer chain is connected with β-D-glucose units. Cellulose is converted into nanocelluloses (NCs) via acid hydrolysis to improve the physicochemical properties. The converted NCs exhibit remarkable characteristics, including excellent biodegradability, high surface area, high porosity and strength, good mechanical properties, low density, and no toxicity (Kamel and Khattab 2020). Further, the presence of hydroxyl groups are advantageous for attaching NCs to various biocatalysts at different electrode surfaces.

NCs are classified into three types such as cellulose nanocrystals (CNC), cellulose nanofibrils, and bacterial cellulose, according to their morphology (Thomas et al. 2018; Tan et al. 2019). Further, the CNC contains four different polymorphs (crystalline structure) denoted as cellulose I, cellulose II, cellulose III, and cellulose IV based on their cellulose chain orientations (Gong et al. 2018). Each one has different properties and behavior due to different physical and chemical structures. To examine the crystalline structure–based catalytic behavior of CNC, Dortez and coworkers constructed the electrochemical biosensors with cellulose I (CNC-I) and cellulose II (CNC-II) and compared their catalytic behaviors (Dortez et al. 2022). In order to develop the biosensors, CNCs were incorporated into single-walled carbon nanotubes (SWCNTs) and coated on SPCE. The morphology characterization techniques revealed that CNC-I has appeared as a sharp and straight needle with a mesoporous structure, while CNC-2 existed as a shorter and twisted rod with a macroporous structure. Further, CNCs modified electrodes were characterized by electrochemical methods. SPCE/SWCNTs-CNC-I (177 mV) showed marginally better reversibility toward $Fe(CN)_6^{4-}/Fe(CN)_6^{3-}$ redox couple compared to SPCE/SWCNTs-CNC-II (184 mV). However, SPCE/SWCNTs-CNC-II (0.177 cm^2) has exhibited a higher active surface area than SPCE/SWCNTs-CNC-II (0.163 cm^2).

The constructed electrodes were applied to detect the crucial metabolites simultaneously, such as uric acid, dopamine, and tyrosine. The SPCE/SWCNTs-CNC-II has yielded a slightly better catalytic response than SPCE/SWCNTs-CNC-I. Further, the sensors were used to detect inflammatory disease biomarker protein, alpha-1-acid glycoprotein (AGP), and it was tagged with electroactive redox compound Os(VI) $O_2(OH)_2$-TEMED (potassium osmate [VI] dihydrate, *N*,*N*,*N*′,*N*′-tetramethylenediamine). It was found that the SPCE/SWCNTs-CNC-II showed a significantly better catalytic response than SPCE/SWCNTs-CNC-I. The observed higher catalytic response at SPCE/SWCNTs-CNC-II indicated the macroporous nature of CNC-II allows loading of a higher amount of macromolecules AGP, whereas the mesoporous structure of CNC-I limits the loading of AGP.

Reactive oxygen species (ROS) such as superoxide anion $O_2^{\cdot-}$, hydroxyl radical (OH·), hydroxyl ion (OH^-), hydroxyl radical (·OH), and hydrogen peroxide (H_2O_2) are produced during aerobic metabolism and cause damage to proteins, lipids, and DNA (Schieber and Chandel 2014). On the other hand, they also act as signaling molecules to regulate some important physiological processes (Finkel 2011). However, these highly active species possess a very short half-life which restricts their monitoring in real time. An electrochemical sensor was developed to quantify the ROS released from the cells. In order to develop the electrochemical sensor, $Mn_3(PO_4)_2$ was utilized as a catalyst and showed an efficient catalytic response to the dismutation of $O_2^{\cdot -}$ (Yun et al. 2022). Further, the biocompatible carboxymethyl cellulose (CMC) is incorporated into the $Mn_3(PO_4)_2$ due to favor the attachment of living cells. To induce the release of ROS from the living cells, the nonsteroid mycotoxin, Zearalenone (ZEA) was employed. The CMC-$Mn_3(PO_4)_2$ composite slurry was prepared by simple mixing and coated on an SPCE, and cured at room temperature. The resulting electrode was characterized by cyclic voltammetry and found that the electrode shows a well-defined redox peak around 0.5 V, regarded as the redox reaction of Mn^{2+}/Mn^{3+}. Upon introduction of $O_2^{\cdot -}$, both oxidation and reduction peaks current amplified as a result of oxidation and reduction reaction of $O_2^{\cdot -}$. It is expected that during the oxidation process, MnO_2 and H_2O_2 are generated by the oxidation of Mn^{2+} by $O_2^{\cdot -}$ while Mn^{2+} and O_2 are produced by the reduction of MnO_2 by $O_2^{\cdot -}$ (Luo et al. 2009). The electrode performance toward the oxidation of $O_2^{\cdot -}$ was examined by chronoamperometric technique. The catalytic current steadily increased from 57.50 nM to 2.95 μM toward $O_2^{\cdot -}$ concentrations and achieved a detection limit of 8.47 nM. To demonstrate the practical applicability of the developed sensor, $O_2^{\cdot -}$ was detected from IPEC-J2 cells. The $O_2^{\cdot -}$ catalytic oxidation current increased substantially upon the addition of ZEA into the testing buffer solution due to the ZEA-triggered release of $O_2^{\cdot -}$ from the IPEC-J2 cells.

Chloramphenicol (CAP) is a potent antibiotic substance and is used for food processing and aquaculture production (Dong et al. 2020). However, the consumption of CAP causes serious illnesses such as grey baby syndrome, leukemia, and aplastic anemia in humans and animals (Duan et al. 2017). Chang et al. constructed an electrochemical sensor to quantify CAP by the integration of semiconductor TiO_2 nanoparticles (TiO_2 NPs), CMC, and silver nanoparticles (AgNPs) on laser-induced graphene (LIG) (Chang et al. 2022). The sensor fabrication process is schematically illustrated in Fig. 33.4. Firstly, AgNPs were prepared under 60 °C, and then CMC-TiO_2 composite was developed by simple mixing of CMC and TiO_2 NPs. Then, the resulting CMC-TiO_2 composite was coated on LIG surface and dried under an infrared lamp, and, subsequently, AgNPs dispersed on LIG/CMC-TiO_2 to improve the conductivity. The authors mentioned that the presence of –OH and –COOH functional groups in CMC facilitate the adsorption of TiO_2, AgNPs, and CAP. The optimized sensor was applied to detect CAP, and it showed a quasi-reversible redox wave at 12 mV vs. Ag/AgCl in addition to the irreversible reduction wave at −67 mV for CAP. Further, a linear range and detection limit of 0.01–100 μM and 0.007 μM, respectively, were achieved at the LIG/CMC-TiO_2/AgNPs electrode. Moreover, the developed electrode was demonstrated to quantify CAP in natural water samples.

The detection of DNA bases such as adenine, thymine, guanine, and cytosine is most important for clinical and medical applications because genetic information is encoded through these bases by DNA (Wei et al. 2010). Ortolani et al. designed an electrochemical biosensor to quantify adenine and guanine by the combination of single-walled carbon nanohorns (SWCNH) and nanocellulose (NC) (Ortolani et al.

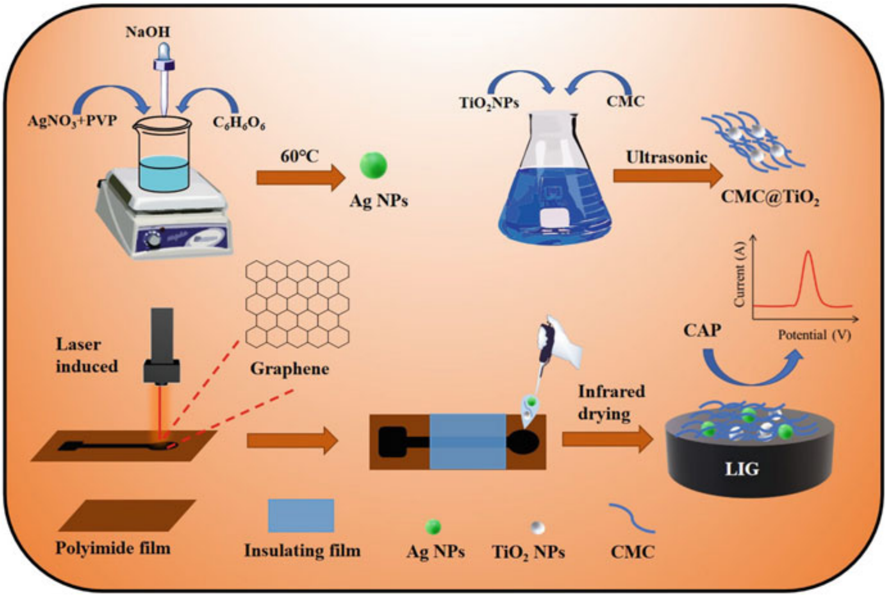
NaOH
AgNO$_3$+PVP
C$_6$H$_6$O$_6$
60°C
Ag NPs
TiO$_2$NPs
CMC
Ultrasonic
CMC@TiO$_2$
Current (A)
Potential (V)
CAP
Laser induced
Graphene
Infrared drying
LIG
Polyimide film
Insulating film
Ag NPs
TiO$_2$ NPs
CMC

Fig. 33.4 Schematic illustration for the fabrication of LIG/CMC@TiO$_2$/AgNPs electrode (Chang et al. 2022)

2019). The NC was derived from sugarcane bagasse. The fabricated sensor showed an excellent catalytic response toward the detection of adenine and guanine. The linear range was found to be 7.4×10^{-7}–6.4×10^{-6} mol L^{-1} and from 7.4×10^{-6} to 2.1×10^{-4} mol L^{-1} with a detection limit of 1.7×10^{-7} mol L^{-1} and 1.4×10^{-6} mol L^{-1}, for guanine and adenine, respectively.

4.3 Alginate-Based Nanocomposite Electrodes

Alginate is a linear polyanionic polysaccharide obtained naturally from brown marine algae and bacteria. The chemical structure of alginate consists of L-guluronic acid and β-1,4-linked D-mannuronic acid units and includes four carboxylic and hydroxy groups (Fig. 33.1). These active functional groups afford to construct different types of bioactive and electrochemically active nanomaterials (Teng et al. 2021). The formation and stability of alginate gel are highly sensitive to the binding efficiency of the metal ions and other materials, and it endows opportunities to apply in many applications.

An electrochemical immunosensor was reported to detect a tumor biomarker, neuron-specific enolase (NSE), and the sensor probe was designed by combining alginate hydrogel, silica oxide nanoparticles (SiO$_2$-NPs), GOD, MWCNTs, and NSE-specific antibody (NSE-Ab) on the GC electrode surface (Yin and Ma 2019).

The incorporation of MWCNTs in the probe can facilitate the electrical conductivity of the composite. For the sensor fabrication, firstly, MWCNTs were coated on the GC electrode and on top of that Fe^{3+}-alginate hydrogel was deposited. Then, the positively charged Fe^{3+} ion is electrostatically attached to the alginate hydrogel through the negatively charged COOH group of alginate. The sensing strategy is designed based on the stability of Fe^{3+}-alginate hydrogel. It was found that trivalent Fe^{3+} is strongly attached to alginate compared to divalent Fe^{2+}. Therefore, the conversion of Fe^{3+} to Fe^{2+} is triggered while reacting with H_2O_2, which is produced by the enzymatic conversion of glucose into gluconic acid and H_2O_2. It leads to destroy the hydrogel due to weak interaction between Fe^{2+} and alginate. Basically, the Fe^{3+}-hydrogel is nonconductive and thus hydrogel-coated GC electrode shows high resistance. However, in contrast, once the hydrogel is destroyed, then the resistivity of the electrode decreases. The resistivity changes were examined by the redox activities of a well-known redox probe $[Fe(CN)_6]^{3-/4-}$. The destruction of Fe^{3+}-alginate hydrogel can be controlled by the addition of NSE, and, therefore, the accurate quantification of NSE is possible by this immunosensor. The same methodology was used to construct an electrochemical sensor to release the DNA, but a GOD-mimicking nanozyme was employed instead of GOD (Roquero et al. 2020). The sensor electrode fabrication and sensing mechanism are schematically shown in Fig. 33.5. DNA was labeled with a fluorescent dye (DNA-FAM) to detect the DNA release from Fe^{3+}-alginate hydrogel. The film fabrication was attained by the electrochemical deposition of DNA-FAM attached Fe^{3+}-alginate hydrogel on a graphite electrode. The hydrogel film was protected by polyethylenimine (PEI) where alginate was covalently attached to PEI through an amide bond formed between the NH_2 group of PEI and the COOH group of alginate by carbodiimide coupling reactant EDC.

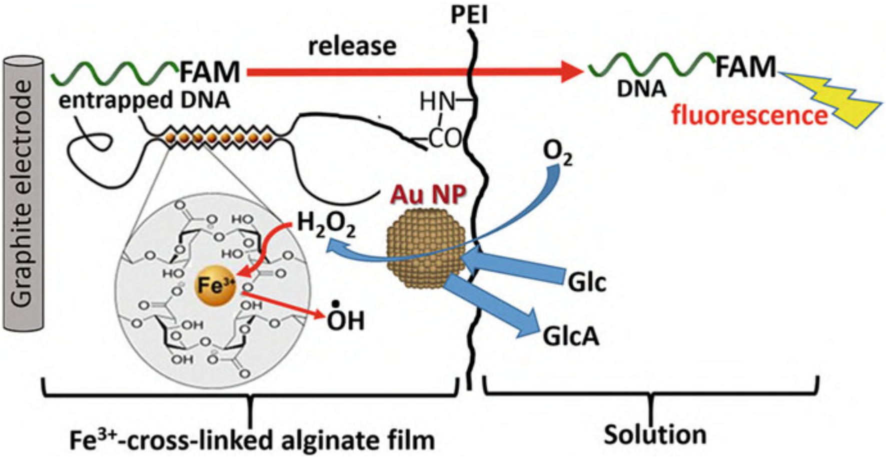

Fig. 33.5 Schematic illustration for the enzyme triggered release of DNA-FD from the Fe^{3+}cross-linked alginate hydrogel (Roquero et al. 2020)

In another report, alginate hydrogel was developed with Ca^{2+} to detect the tumor biomarker prostate-specific antigen (PSA) by impedimetric immunosensors (Zhao et al. 2019). The sensor fabrication strategy is shown in Fig. 33.6. The sensor construction starts with the electrochemical deposition of AuNPs on the GC electrode and, followingly, PSA-specific antibodies (PS-Ab1) attached to AuNPs. Then the immuno-probe $CaCO_3$ microspheres with a size of 900 nm to 1 μm were incorporated into the AuNPs modified electrode. The conductivity of the modified electrodes was examined with a redox probe $[Fe(CN)_6]^{3-/4-}$ and found that AuNPs deposited electrode showed a higher conductivity as expected. The electrode resistivity was increased upon coating of aptamer-1 (Ab_1), aptamer-2 (Ab_2), BSA, and $CaCO_3$. The resistivity of the electrode further significantly increased while incubating into the SA buffer due to the formation of a hydrogel. It was mentioned that the $CaCO_3$ dissolved under an acidic environment and released the Ca^{2+}, which coordinated with negatively charged alginate and formed insoluble hydrogel on the electrode surface and thereby reducing the electrode conductivity.

The isomers of dihydroxybenzene, such as catechol (CC), hydroquinone (HQ), and resorcinol (RC), are used in the preparation of antioxidants, cosmetics, and pesticides (Suresh et al. 2012). However, the US Environmental Protection Agency (EPA) is considered them as environmental pollutants due to their toxicological

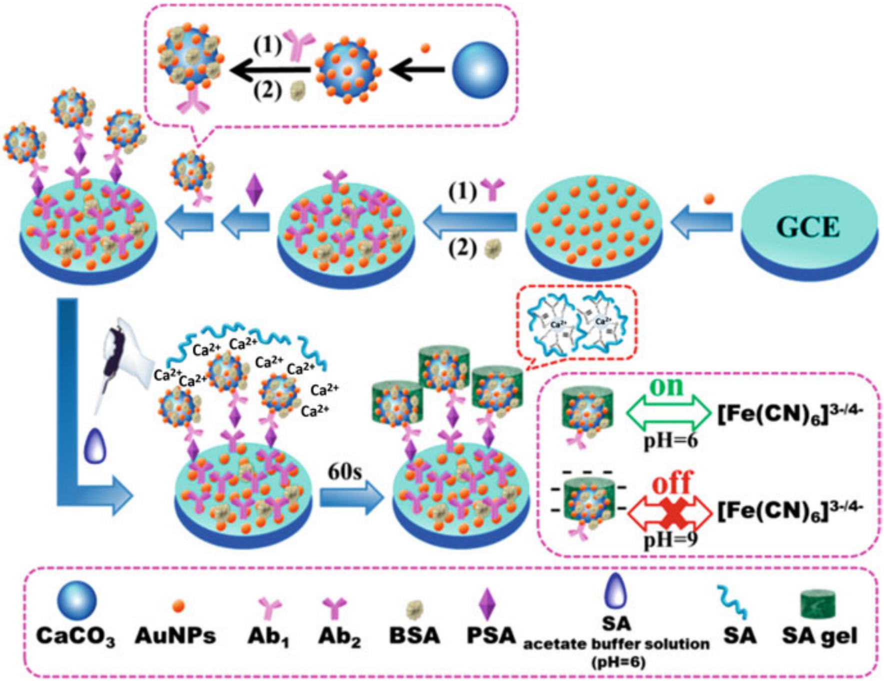

Fig. 33.6 Fabrication of Ca^{2+}-triggered pH response sodium alginate hydrogel to develop sandwich-type impedimetric immunosensor of PSA (Zhao et al. 2019)

effect. Wei et al. developed an electrochemical sensor based on 3D hierarchically porous carbon derived from sodium alginate (referred to as SA-900) to detect them (Wei et al. 2021). The porous carbon was prepared by a facile carbonization strategy. During the process, sodium alginate converts into sodium carbonate at 500–650 °C. Further, the sodium carbonate decomposed into different products such as Na_2CO_3, Na_2O, and CO_2. The CO_2 further reacts with C to form CO ($CO_2 + C = 2CO$), thereby producing a porous structure. In order to develop an electrochemical sensor, the resulting porous carbon was coated on the GC electrode by the drop coating method. The GC/SA-900 electrode exhibited a well-pronounced catalytic response toward CC, HQ, and RC, and the oxidation peaks are well distinguished upon addition together. On the other hand, the bare GC electrode showed a weak oxidation response for them and also failed to separate CC and HQ oxidation peaks. The authors mentioned the observed outstanding catalytic performances due to the high conductivity, large active surface area, and porous structure of SA-900. These results imply that the GC/SA-900 electrode is suitable for the simultaneous determination of CC, HQ, and RC. The practical applicability of the GC/SA-900 electrode was also demonstrated to detect them in natural water samples.

4.4 Collagen-Based Nanocomposite Electrodes

Collagen (COL) is a type of protein composed of amino acids: proline, glycine, and hydroxyproline, and possesses a triple-helix structure (Zhao et al. 2021). COL is found in the bone and skin tissues and plays many cellular processes. COL is extensively used to make composite biomaterial due to its biocompatibility and low antigenicity (Izu et al. 2021). Further, COL is used to immobilize various proteins for different applications due to its favorable hydrophilicity and biocompatibility. For instance, grafted collagen (COL) was used to immobilize the hemoglobin (Hb) on the GC electrode surface (Zong et al. 2007a). To improve the conductivity of the COL modified electrode, MWCNTs were incorporated into the matrix. The resulting COL-MWCNTs-Hb electrode exhibited a pronounced electrochemical response for Hb and found a well-defined redox peak at −360 mV vs SCE for Hb containing heme redox couple ($Fe^{III/II}$). The scan rate–dependent experiment revealed that Hb strongly adsorbed on the COL-MWNTs matrix. Further, the heme one-electron redox process was confirmed from the pH dependence experiments, and it shows −52.1 mV/pH. The optimized electrode was successfully used to reduce H_2O_2 at physiological pH. Further, the electrode retained its stability up to 80% after 2 weeks.

Very recently, Hu et al. reported the 3D electrochemical biosensor to monitor reactive oxygen species (ROS) which were released from microglia cells (Hu et al. 2021). For the fabrication of the sensor, COL hydrogel was integrated into the platinum nanoparticles (PtNPs) modified graphene foam (GF). To improve the sensor stability, poly(3,4-ethylenedioxythiophene) (PEDOT) coated on GF/PtNPs electrode. The overall sensor fabrication process is given in Fig. 33.7. The PtNPs were electrochemically deposited on GF. BV2 cells were used to develop a model

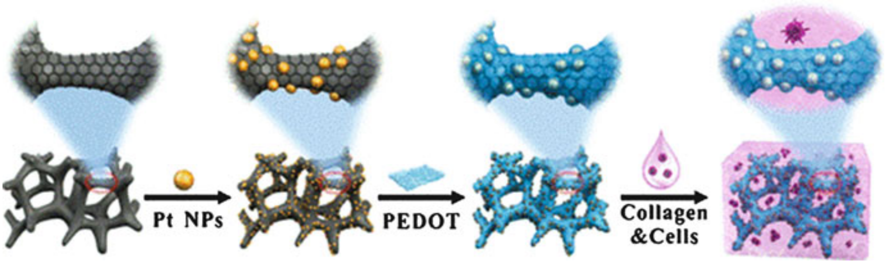

Fig. 33.7 Fabrication of the collagen hydrogel integrated 3D GF/PtNPs/PEDOT sensor (Hu et al. 2021)

system. To achieve cells proliferation, BV2 cells were dispersed in COL solution and coated on GF/PtNPs/PEDOT electrode. The BV2 cells modified electrode incubated for 84 h to acquire cell growth. A laser scanning confocal microscopy (LSCM) study revealed that cell growth was distributed all over the interspace of the COL polymer. Further, the release of ROS was examined by chronoamperometric technique and found that the current spike was apparent at different time intervals due to the consumption of the diffused ROS species from the 3D collagen network. However, no such current spike was noted while avoiding the BV2 cells in the matrix. Based on the calibration curve, the concentration of ROS was estimated to be 90 nM.

The use of COL from mammalian sources (pig and calf) is questionable due to the possibility of transmitting avian influenza and bovine spongiform encephalopathy (Zeng et al. 2009). However, according to biosafety protocol, the COL derived from fish sources is safe. Therefore, Wei et al. used a grass carp skin COL (GCSC) for the development of an aptasensor for neurotransmitter detection. The GCSC integrated graphene oxide (GO) composite was used to attach an aptamer to detect dopamine (DA) (Wei et al. 2019). Firstly, the GCSC was mixed with GO by ultrasonication, and then DA-aptamer (5′-GTCTCTGTG TGCGCCAGAGAACACTGGGGCAGATATGGGCCAGCACAGAATGAGGCCC-3′) was attached with COL through a simple drop coating strategy. The DA-aptamer is strongly adsorbed to the triple-helical structure of GCSC by possible π-π stacking and hydrogen bonding interactions. The optimized sensor showed a remarkable catalytic response to DA quantification and achieved a linear range and detection limit of 1–1000 nM and 0.75 nM, respectively. The selectivity of the sensor was examined with the potential interferences such as ascorbic acid (AA), tyramine (TA), homovanillic acid (HVA), and 3,4-dihydroxyphenylalanine (DOPA) and the electrode shows negligible catalytic response for them.

5 Conclusions

This chapter presents an overview of the various strategies employed for developing biopolymers-based electrochemical biosensors. It is evidenced that biopolymers have contributed tremendously to the construction of electrochemical biosensors for a broad range of biomedical applications. The biopolymers-based nanocomposite electrode materials act as the best substitute for traditional nonbiodegradable sensing materials due to their biocompatibility, biodegradability, long-term stability, sensitivity, selectivity, and cost-effectiveness. Importantly, the biopolymers containing functional groups (NH_2, COOH, OH, and CO) are readily modified based on our requirements and used to attach biocatalyst or electrode materials through covalent, electrostatic, and hydrogen bonding interactions to construct reliable biosensors. Among the biopolymers, here electrochemical sensing applications of chitosan, cellulose, alginate, and collagen due to their widespread usage in sensor fabrication are described. Further, it outlines the utilization of the physicochemical behavior of biopolymers for sensing applications and corresponding fundamental sensing mechanisms. Overall, cyclic voltammetry and amperometric techniques were used for enzyme-based sensors, whereas electrochemical impedance spectroscopy was employed for immunosensors. Mostly, the biocatalyst is attached to biopolymers by covalent and cross-linking strategies, but entrapment and adsorption are also often employed. This appeals biopolymers are considered promising materials for the development of various biosensors.

References

Ben Aoun S (2017) Nanostructured carbon electrode modified with N-doped graphene quantum-chitosan nanocomposite: a sensitive electrochemical dopamine sensor. R Soc Open Sci 4(11):171199

Bhatnagar I, Mahato K, Ealla KKR, Asthana A, Chandra P (2018) Chitosan stabilized gold nanoparticle mediated self-assembled gliP nanobiosensor for diagnosis of invasive Aspergillosis. Int J Biol Macromol 110:449–456

Chang C, Wang Q, Xue Q, Liu F, Hou L, Pu S (2022) Highly efficient detection of chloramphenicol in water using Ag and TiO_2 nanoparticles modified laser-induced graphene electrode. Microchem J 173:107037

Devaraj M, Rajendran S, Jebaranjitham JN, Ranjithkumar D, Sathiyaraj M, Manokaran J, Sundaravadivel E, Santhanalakshmi J, Ponce LC (2020) Horseradish peroxidase-immobilized graphene oxide-chitosan gold nanocomposites as highly sensitive electrochemical biosensor for detection of hydrogen peroxide. J Electrochem Soc 167(14):147517

Devnani H, Satsangee S, Jain R (2015) MWCNT-chitosan-ZrO_2 nanocomposite modified sensor for sensitive and selective electrochemical determination of serotonin. Int J Innov Res Sci Eng Technol 4:406–416

Dong X, Yan X, Li M, Liu H, Li J, Wang L, Wang K, Lu X, Wang S, He B (2020) Ultrasensitive detection of chloramphenicol using electrochemical aptamer sensor: a mini review. Electrochem Commun 120:106835

Dortez S, Sierra T, Alvarez-Sanchez MA, Gonzalez-Dominguez JM, Benito AM, Maser WK, Crevillen AG, Escarpa A (2022) Effect of nanocellulose polymorphism on electrochemical analytical performance in hybrid nanocomposites with non-oxidized single-walled carbon nanotubes. Microchim Acta 189(2):62

Duan Y, Wang L, Gao Z, Wang H, Zhang H, Li H (2017) An aptamer-based effective method for highly sensitive detection of chloramphenicol residues in animal-sourced food using real-time fluorescent quantitative PCR. Talanta 165:671–676

Fan J, Liang S, Zhang M, Xu G (2018) Fabrication of nanocomposite electrochemical sensors with poly(3,4-ethylenedioxythiophene) conductive polymer and Au nanoparticles adsorbed on carboxylated nanocrystalline cellulose. J Bioresour Bioprod 3(1):30

Filicori M (2015) Clinical roles and applications of progesterone in reproductive medicine: an overview. Acta Obstet Gynecol Scand 94(S161):3–7

Finkel T (2011) Signal transduction by reactive oxygen species. J Cell Biol 194(1):7–15

Gan L, Loke FWL, Cheong WC, Ng JSH, Tan NC, Zhu Z (2021) Design and development of ferrocene-containing chitosan-cografted-branched polyethylenimine redox conjugates for monitoring free flap failure after reconstructive surgery. Biosens Bioelectron 186:113283

Gong J, Mo L, Li J (2018) A comparative study on the preparation and characterization of cellulose nanocrystals with various polymorphs. Carbohydr Polym 195:18–28

Hu X-B, Qin Y, Fan W-T, Liu Y-L, Huang W-H (2021) A three-dimensional electrochemical biosensor integrated with hydrogel enables real-time monitoring of cells under their in vivo-like microenvironment. Anal Chem 93(22):7917–7924

Hu T, Wang D, Xu J, Chen K, Li X, Yi H, Ni Z (2022) Glucose sensing on screen-printed electrochemical electrodes based on porous graphene aerogel@prussian blue. Biomed Microdevices 24(1):14

Ilyina AV, Tikhonov VE, Albulov AI, Varlamov VP (2000) Enzymic preparation of acid-free-water-soluble chitosan. Process Biochem 35(6):563–568

Izu Y, Adams SM, Connizzo BK, Beason DP, Soslowsky LJ, Koch M, Birk DE (2021) Collagen XII mediated cellular and extracellular mechanisms regulate establishment of tendon structure and function. Matrix Biol 95:52–67

Kalimuthu P, Heath MD, Santini JM, Kappler U, Bernhardt PV (2014) Electrochemically driven catalysis of *Rhizobium* sp. NT-26 arsenite oxidase with its native electron acceptor cytochrome c552. Biochim Biophys Acta Bioenerg 1837(1):112–120

Kalimuthu P, Fischer-Schrader K, Schwarz G, Bernhardt PV (2015a) A sensitive and stable amperometric nitrate biosensor employing *Arabidopsis thaliana* nitrate reductase. J Biol Inorg Chem 20(2):385–393

Kalimuthu P, Heider J, Knack D, Bernhardt PV (2015b) Electrocatalytic hydrocarbon hydroxylation by ethylbenzene dehydrogenase from *Aromatoleum aromaticum*. J Phys Chem B 119(8): 3456–3463

Kalimuthu P, Belaidi AA, Schwarz G, Bernhardt PV (2016a) Low potential catalytic voltammetry of human sulfite oxidase. Electrochim Acta 199:280–289

Kalimuthu P, Ringel P, Kruse T, Bernhardt PV (2016b) Direct electrochemistry of nitrate reductase from the fungus *Neurospora crassa*. Biochim Biophys Acta Bioenerg 1857(9):1506–1513

Kalimuthu P, Belaidi AA, Schwarz G, Bernhardt PV (2017a) Chitosan-promoted direct electrochemistry of human sulfite oxidase. J Phys Chem B 121(39):9149–9159

Kalimuthu P, Havemeyer A, Clement B, Kubitza C, Scheidig AJ, Bernhardt PV (2017b) Human mitochondrial amidoxime reducing component (mARC): an electrochemical method for identifying new substrates and inhibitors. Electrochem Commun 84:90–93

Kalimuthu P, Hsiao J-C, Nair RP, Kappler U, Bernhardt PV (2017c) Bioelectrocatalysis of sulfite dehydrogenase from *Sinorhizobium meliloti* with its physiological cytochrome electron partner. ChemElectroChem 4(12):3163–3170

Kalimuthu P, Petitgenet M, Niks D, Dingwall S, Harmer JR, Hille R, Bernhardt PV (2020) The oxidation-reduction and electrocatalytic properties of CO dehydrogenase from *Oligotropha carboxidovorans*. Biochim Biophys Acta Bioenerg 1861(1):148118

Kalimuthu P, Kruse T, Bernhardt PV (2021a) Deconstructing the electron transfer chain in a complex molybdoenzyme: assimilatory nitrate reductase from *Neurospora crassa*. Biochim Biophys Acta Bioenerg 1862(3):148358

Kalimuthu P, Kruse T, Bernhardt PV (2021b) A highly sensitive and stable electrochemical nitrate biosensor. Electrochim Acta 386:138480

Kalimuthu P, Harmer JR, Baldauf M, Hassan AH, Kruse T, Bernhardt PV (2022) Electrochemically driven catalysis of the bacterial molybdenum enzyme YiiM. Biochim Biophys Acta Bioenerg 1863(3):148523

Kamel S, Khattab TA (2020) Recent advances in cellulose-based biosensors for medical diagnosis. Biosensors 10(6):67

Kou S, Peters LM, Mucalo MR (2021) Chitosan: a review of sources and preparation methods. Int J Biol Macromol 169:85–94

Krishnan SK, Prokhorov E, Bahena D, Esparza R, Meyyappan M (2017) Chitosan-covered Pd@Pt core–shell nanocubes for direct electron transfer in electrochemical enzymatic glucose biosensor. ACS Omega 2(5):1896–1904

Li G, Xue Q, Feng J, Sui W (2015) Electrochemical biosensor based on nanocomposites film of thiol graphene-thiol chitosan/nano gold for the detection of carcinoembryonic antigen. Electroanalysis 27(5):1245–1252

Liang Z, Zhang J, Wu C, Hu X, Lu Y, Wang G, Yu F, Zhang X, Wang Y (2020) Flexible and self-healing electrochemical hydrogel sensor with high efficiency toward glucose monitoring. Biosens Bioelectron 155:112105

Luo Y, Tian Y, Rui Q (2009) Electrochemical assay of superoxide based on biomimetic enzyme at highly conductive TiO_2 nanoneedles: from principle to applications in living cells. Chem Commun 21:3014–3016

Mahato K, Purohit B, Bhardwaj K, Jaiswal A, Chandra P (2019) Novel electrochemical biosensor for serotonin detection based on gold nanorattles decorated reduced graphene oxide in biological fluids and in vitro model. Biosens Bioelectron 142:111502

Majumdar S, Thakur D, Chowdhury D (2020) DNA carbon-nanodots based electrochemical biosensor for detection of mutagenic nitrosamines. ACS Appl Bio Mater 3(3):1796–1803

Mattioli IA, Cervini P, Cavalheiro ETG (2020) Screen-printed disposable electrodes using graphite-polyurethane composites modified with magnetite and chitosan-coated magnetite nanoparticles for voltammetric epinephrine sensing: a comparative study. Microchim Acta 187(6):318

Naghib SM, Rabiee M, Omidinia E (2014) Electrochemical biosensor for L-phenylalanine based on a gold electrode modified with graphene oxide nanosheets and chitosan. Int J Electrochem Sci 9: 2341–2353

Novick S, Rozzell D (2008) Immobilization of enzymes by covalent attachment, Microbial Enzymes and Biotransformations, Humana Press, New Jersey pp 247–271

Ortolani TS, Pereira TS, Assumpção MHMT, Vicentini FC, Gabriel de Oliveira G, Janegitz BC (2019) Electrochemical sensing of purines guanine and adenine using single-walled carbon nanohorns and nanocellulose. Electrochim Acta 298:893–900

Ronkainen NJ, Halsall HB, Heineman WR (2010) Electrochemical biosensors. Chem Soc Rev 39(5):1747–1763

Roquero DM, Bollella P, Melman A, Katz E (2020) Nanozyme-triggered DNA release from alginate films. ACS Appl Bio Mater 3(6):3741–3750

Samadi Pakchin P, Ghanbari H, Saber R, Omidi Y (2018) Electrochemical immunosensor based on chitosan-gold nanoparticle/carbon nanotube as a platform and lactate oxidase as a label for detection of CA125 on comarker. Biosens Bioelectron 122:68–74

Schieber M, Chandel NS (2014) ROS function in redox signaling and oxidative stress. Curr Biol 24(10):R453–R462

Sharma M, Singh SP (2020) Chapter 11. Enzyme entrapment approaches and their applications. In: Singh SP, Pandey A, Singhania RR, Larroche C, Li Z (eds) Biomass, biofuels, biochemicals. Elsevier, Dordrecht, pp 191–216

Sheldon RA (2007) Cross-linked enzyme aggregates (CLEAs): stable and recyclable biocatalysts. Biochem Soc Trans 35(Pt 6):1583–1587

Singh A, Sinsinbar G, Choudhary M, Kumar V, Pasricha R, Verma HN, Singh SP, Arora K (2013) Graphene oxide-chitosan nanocomposite based electrochemical DNA biosensor for detection of typhoid. Sensors Actuators B Chem 185:675–684

Soares JC, Soares AC, Rodrigues VC, Melendez ME, Santos AC, Faria EF, Reis RM, Carvalho AL, Oliveira ON (2019) Detection of the prostate cancer biomarker PCA3 with electrochemical and impedance-based biosensors. ACS Appl Mater Interfaces 11(50):46645–46650

Suresh S, Srivastava VC, Mishra IM (2012) Adsorption of catechol, resorcinol, hydroquinone, and their derivatives: a review. Int J Energy Environ Eng 3(1):32

Tan K, Heo S, Foo M, Chew IM, Yoo C (2019) An insight into nanocellulose as soft condensed matter: challenge and future prospective toward environmental sustainability. Sci Total Environ 650:1309–1326

Tashkhourian J, Nami-Ana SF, Shamsipur M (2018) Designing a modified electrode based on graphene quantum dot-chitosan application to electrochemical detection of epinephrine. J Mol Liq 266:548–556

Teng K, An Q, Chen Y, Zhang Y, Zhao Y (2021) Recent development of alginate-based materials and their versatile functions in biomedicine, flexible electronics, and environmental uses. ACS Biomater Sci Eng 7(4):1302–1337

Thomas B, Raj MC, Athira KB, Rubiyah MH, Joy J, Moores A, Drisko GL, Sanchez C (2018) Nanocellulose, a versatile green platform: from biosources to materials and their applications. Chem Rev 118(24):11575–11625

Velayudham J, Magudeeswaran V, Paramasivam SS, Karruppaya G, Manickam P (2021) Hydrogel-aptamer nanocomposite based electrochemical sensor for the detection of progesterone. Mater Lett 305:130801

Wan D, Yuan S, Li GL, Neoh KG, Kang ET (2010) Glucose biosensor from covalent immobilization of chitosan-coupled carbon nanotubes on polyaniline-modified gold electrode. ACS Appl Mater Interfaces 2(11):3083–3091

Wei F, Lillehoj PB, Ho C-M (2010) DNA diagnostics: nanotechnology-enhanced electrochemical detection of nucleic acids. Pediatr Res 67(5):458–468

Wei B, Zhong H, Wang L, Liu Y, Xu Y, Zhang J, Xu C, He L, Wang H (2019) Facile preparation of a collagen-graphene oxide composite: a sensitive and robust electrochemical aptasensor for determining dopamine in biological samples. Int J Biol Macromol 135:400–406

Wei L, Huang X, Zhang X, Yang X, Yang J, Yan F, Ya Y (2021) High-performance electrochemical sensing platform based on sodium alginate-derived 3D hierarchically porous carbon for simultaneous determination of dihydroxybenzene isomers. Anal Methods 13(9):1110–1120

Wong SS, Wong L-JC (1992) Chemical crosslinking and the stabilization of proteins and enzymes. Enzym Microb Technol 14(11):866–874

Yadav AK, Dhiman TK, Lakshmi GBVS, Berlina AN, Solanki PR (2020) A highly sensitive label-free amperometric biosensor for norfloxacin detection based on chitosan-yttria nanocomposite. Int J Biol Macromol 151:566–575

Yin S, Ma Z (2019) “Smart” sensing interface for the improvement of electrochemical immunosensor based on enzyme-Fenton reaction triggered destruction of Fe^{3+} cross-linked alginate hydrogel. Sensors Actuators B Chem 281:857–863

Yun Y, Lu Z, Jiao X, Xue P, Sun W, Qiao Y, Liu Y (2022) Involvement of $O_2^{\cdot -}$ release in zearalenone-induced hormesis of intestinal porcine enterocytes: an electrochemical sensor-based analysis. Bioelectrochemistry 144:108049

Zeng S-k, Zhang C-h, Lin H, Yang P, Hong P-z, Jiang Z (2009) Isolation and characterisation of acid-solubilised collagen from the skin of Nile tilapia (*Oreochromis niloticus*). Food Chem 116(4):879–883

Zhang Q, Qing Y, Huang X, Li C, Xue J (2018) Synthesis of single-walled carbon nanotubes–chitosan nanocomposites for the development of an electrochemical biosensor for serum leptin detection. Mater Lett 211:348–351

Zhao L, Yin S, Ma Z (2019) Ca^{2+}-triggered pH-response sodium alginate hydrogel precipitation for amplified sandwich-type impedimetric immunosensor of tumor marker. ACS Sensors 4(2): 450–455

Zhao C, Xiao Y, Ling S, Pei Y, Ren J (2021) Structure of collagen. Methods Mol Biol 2347:17–25

Zong S, Cao Y, Ju H (2007a) Direct electron transfer of hemoglobin immobilized in multiwalled carbon nanotubes enhanced grafted collagen matrix for electrocatalytic detection of hydrogen peroxide. Electroanalysis 19(7-8):841–846

Zong S, Cao Y, Zhou Y, Ju H (2007b) Reagentless biosensor for hydrogen peroxide based on immobilization of protein in zirconia nanoparticles enhanced grafted collagen matrix. Biosens Bioelectron 22(8):1776–1782

Future Perspective of Nanobiomaterials in Human Health Care

34

Chandan Hunsur Ravikumar, Paskorn Muangphrom,
Pat Pataranutaporn, and Werasak Surareungchai

Contents

1 Introduction 742
2 Types of Nanobiomaterials 743
  2.1 Present Nanobiomaterials 743
  2.2 Future Materials 744
  2.3 Nanobiomaterials Applications in Human Health Care 747

C. Hunsur Ravikumar (✉)
Sensor Technology Laboratory, Pilot Plant Development and Training Institute, King Mongkut's University of Technology Thonburi, Bangkok, Thailand

Centre for Nano and Material Sciences, Jain Global Campus, Jain (Deemed-to-be-University), Bengaluru, India

P. Muangphrom
Sensor Technology Laboratory, Pilot Plant Development and Training Institute, King Mongkut's University of Technology Thonburi, Bangkok, Thailand

Nanoscience and Nanotechnology Graduate Program, Faculty of Science, King Mongkut's University of Technology Thonburi, Bangkok, Thailand

P. Pataranutaporn
MIT Media Lab, Massachusetts Institute of Technology, Cambridge, MA, USA

W. Surareungchai (✉)
Sensor Technology Laboratory, Pilot Plant Development and Training Institute, King Mongkut's University of Technology Thonburi, Bangkok, Thailand

Nanoscience and Nanotechnology Graduate Program, Faculty of Science, King Mongkut's University of Technology Thonburi, Bangkok, Thailand

School of Bioresources and Technology, King Mongkut's University of Technology Thonburi, Bangkok, Thailand
e-mail: wersak.sur@kmutt.ac.th

© Springer Nature Singapore Pte Ltd. 2023

U. P. Azad, P. Chandra (eds.), *Handbook of Nanobioelectrochemistry*,
https://doi.org/10.1007/978-981-19-9437-1_34

2.4 Diagnostics 748
2.5 Wearable Sensors 750
3 Future Perspective and Conclusion 753
References 755

Abstract

Nanobiomaterials have been dramatically involved in human health care since the past decades. The development of these nanobiomaterials has enabled researchers to monitor the progression of newly emerged diseases in highly complex human systems through several biomarkers, electrolytes, and metabolites in human secretions. In this chapter, recent development in this field including the importance of some bionanomaterials for human health care has been summarized. Our speculation for the future perspective of using nanobiomaterials for human healthcare has also been discussed.

Keywords

Carbon nanomaterials · Metallic nanomaterials · Lab-on-a-chip · Lipoproteins · Nanobiomaterials · Oligonucleotide-based nanobiomaterials · Peptide nanoparticles · Perovskite quantum dots · Quantum dots · Silica nanomaterials · Wearable sensors

1 Introduction

Medical technologies regarding human health care have been developed dramatically over the past decades aiming for both acceptable quality and affordable cost. However, due to the complexity of human systems as well as the newly emerged diseases, health care becomes more complicated in the present. Thus, new approaches to specifically target the roots of each disease and to develop new drugs including other medical devices are required.

The scale of health care therapies is now reducing to nanoscale as this technology provides many promising opportunities based on its unique physicochemical properties (Daima and Bansal 2015; El Haj 2020). In particular, nanobiomaterials can be easily modified to mimic biological environmental properties of human systems leading to high biocompatibility with varieties of applications. Examples of such are drug delivery, biosensors, real-time disease monitoring, bioimaging, and tissue engineering (Di Marzio et al. 2020; Ni et al. 2020; Puttaswamy et al. 2020; Raveendran et al. 2020; Sha et al. 2020; Shah et al. 2020; Wang et al. 2017, 2020b; Witika et al. 2020; Zuo et al. 2020).

In this chapter, several types of nanobiomaterials are introduced. We also describe recent advances of nanobiomaterials to elevate human's quality of life, which include Lab-on-a-chip, diagnostics, and wearable sensors. At the end of this chapter, the advantages and disadvantages including the future perspective of using bionanomaterials in human health care are discussed.

2 Types of Nanobiomaterials

Nanotechnology has diversified applications in almost every sector of science. With the emergence of the use of nanomaterials in biology, several terms emerged. Includes, nanobiotechnology, bionanotechnology, and nanobiology terms used to express the use of nano-sized materials in biological applications. For better understanding, this section has been divided into two main sections describing Present and Future nanobiomaterials highlighting the status of the different materials applied to end application in human health care.

2.1 Present Nanobiomaterials

2.1.1 Metallic Nanomaterials

Metallic nanoparticles (NPs) are the first kind to be used for sensing and diagnostic applications. Au, Ag, and Pt are extensively used for developing sensor and their applications. As metallic NPs can be molded into shapes such as spherical, rods, shells, and cages emitting their unique properties (Huang and El-Sayed 2010). This holds the advantage with several techniques to sense many biomaterials. Several noble metallic NPs have been reported. Their promising properties relies on their tunable optical properties, which include Surface Plasmon absorption and scattering as well as fluorescence. All of these achieved by tuning size, shape, and composition of the metallic NPs (Jain et al. 2006; Lee and El-Sayed 2005). Among the reported noble metallic NPs, AuNPs were the first NPs and are extensively used in lateral flow immunoassays (LFA) (Blanco-Covián et al. 2017). They have been widely used in biomedical applications as they can be synthesized easily and have good biocompatibility. One example of AuNPs with unique and interesting properties is gold nanoshell, which can improve a contrast in optical coherence tomography (OCT). Thereby, a previous report attempted to utilize this gold nanoshell in combination with near IR (NIR) photothermal ablation for both tumor diagnostic and therapy dual application (Gobin et al. 2007).

2.1.2 Silica Nanomaterials

Silica NPs are one of the most used probes, mainly used in fluorescence-related assays. The shape can contribute to their photophysical properties. Different types of silica-based NPs are synthesized such as monoliths, fibers, rod-like particles, tubes, solid and hollow nanospheres, and mesoporous NPs (Jafelicci et al. 1999; Miyaji et al. 1999; Lai et al. 2011; Jafari et al. 2019). Silica is a versatile nontoxic material. Unlike other NPs, these are extensively used to phase transfer the material from non-aqueous to aqueous by silica polymers even at the expenditure of the size of the particle. The physicochemical property of the material can be changed. The development of silica NPs coated with Fe_2O_3, CdSe quantum dots (QDs), and AuNPs have been previously reported with their use in novel MRI and optical image contrasting agents for living cell imaging (Gerion et al. 2001; Selvan et al. 2007; Bottini et al. 2007). Applications related to the materials have been discussed in the following section.

2.1.3 Quantum Dots

Colloidal QDs possess highlighted photophysical properties for biosensing and diagnostic applications beyond many other NPs. QDs become beneficial as compared to bulk particles due to their quantum confinement effects from material compositions and dimensionality (Chandan et al. 2018). Size-tunable photophysical and optical properties with broad absorption and narrow emission makes it a wonder material (Chandan and Geetha 2013; Chandan et al. 2014). This is evident in its use in photovoltaics, biosensors, and light-emitting diodes (LEDs) (Kusuma et al. 2019; Ravikumar et al. 2019, 2020). They are mainly composed of chalcogenides such as CdS, CdSe, CdTe, ZnS, ZnSe, etc. The property and stability can be enhanced by encapsulating with a thin layer of inorganic shell with a wider bandgap. Such encapsulation tends to increase the electron carrier mobility with stability and photoluminescence quantum yields (PLQY), which are more suitable for biosensors and bioimaging applications. The surface phenomenon plays a major role. The surface can be covalently or electrostatically modified with biochemical analogs and biomaterials making specific and selective probes. The emission range of QDs varies from UV region to NIR region depending on the type of the QDs. The only drawback that held back this material is its stability in various environments. They tend to agglomerate at higher pH making them susceptible to use in vivo, where various pH conditions are present. Still, contribution by this material is huge in different end applications.

2.2 Future Materials

2.2.1 Carbon Nanomaterials

Even though carbon material has been used much earlier to metallic NPs, this section of material cannot be considered present or future. Carbon nanomaterials will still be used, and it is a past, present, and future wonder material in biosensing and electronic application. Carbon was the first material to be used in electrochemical sensors after metallic NPs. With continuous progress in nanotechnology, carbon materials have reached from bulk macroscopic size to nanoscale. Different types of nanoscale allotropes of carbon have been discovered which varied from zero- to three-Dimensional structures and been applied in different to almost all fields such as electronics(Baughman et al. 2002), energy storage, conversion (Kusuma et al. 2018), display (Liu et al. 2012), and biological and chemical sensor (Ravikumar et al. 2019). Various allotropes include graphene oxide, graphene, carbon nanotubes, Buckyballs, and nano-ribbons (Kusuma et al. 2018). Graphene and its related allotropes have been extensively used in biosensing applications due to their unique electro-optical and physicochemical properties. Electrical conductivity is high as metal, with uninterrupted electron mobility makes them suitable for electrochemical and biochemical sensors. When carbon materials are further cut below 10 nm, their characteristic changes. Sub 5 nm-sized carbon particles tend to mimic quantum dots. Unlike sp^3 hybridized carbon materials, they are sp^2 hybridized. Even though there are bare fluorescent carbon QDs and graphene QDs, which without any functional group on the surface, fluorescent carbon nanodots with an irregular shape, containing functional groups on the surface, and highly water-soluble are also reported (Liu et al. 2019).

The important property of the carbon nanomaterial is their nontoxicity and stability in various environments. The synthesis source can be varied from the CO_2 from the air to food waste and plant residue, which are a rich source of carbon. Synthesis of these materials was rather easy with the use of an autoclave, chemical vapor deposition (CVD), and so on. The only disadvantage is it requires an inert condition to synthesize few allotropes of carbons such as graphene and nano-carbons at high temperature. Carbon allotropes such as graphene and graphene oxide can readily adsorb DNA, and other biomolecules, due to π-π interaction. This is advantageous in designing biosensors and diagnostics.

2.2.2 Biological Nanoparticles

NPs can be made using biological materials such as proteins and peptides. Some cell organelles may recognize the NPs even though they are not toxic and making mimicking NPs are too difficult. Lipoproteins (LPs) and peptide-based NPs are some of the important classes of biological NPs. LPs are micelle-like spherical NPs forming from the arrangement or assembly of lipids and proteins. The structure of LPs contains two major components, both of which aid the transportation of water-soluble lipids in the blood. The first component of LPs is an apolar core containing triglycerides and cholesteryl esters. The second component surrounding the apolar core is a phospholipid monolayer shell of unesterified cholesterol and apolipoprotein. Owing to these two components, LPs-based NPs have great biodegradability, biocompatibility, and stability in vivo.

Based on LPs density, they can be divided into five different types, (1) high-density LPs (HDL, 5–15 nm), (2) low-density LPs (18–28 nm), (3) intermediate-density LPs (25–50 nm), (4) very-low-density LPs (30–80 nm), and (5) chylomicrons (100–1000 nm). Such example of the utilization of LPs-based NPs include the incorporation of the hydrophobic core of the plasma-derived low-density LPs with lipophilic drugs for drug delivery into the receptor of tumor sites (Rensen et al. 2001). NIR dye functionalized low density LPs NPs can also be used for in vivo imaging of cancer in live animals by exposing them to NIR radiation, thus, opening the more avenue of LP NPs usage (Chen et al. 2007).

Peptide NPs are the small sequence of peptides that can be developed into the desired shape through self-assembly or by binding with other types of NPs to show desired biophysical characteristics. Such self-assembled peptides lead to various types of structures, such as oligomeric coiled α-coil helix and icosahedron (Raman et al. 2006; Yang et al. 2018). Peptide NPs can also be modified using targeting moieties. Previous study found that the core of peptide NPs with 6–10 nm in diameter is suitable for encapsulating QDs for their use as contrast agents in bioimaging with a variety of probes for MRI, such as gadolinium, fluorescence, and iron oxide NPs. Trimeric coiled structures of peptide NPs allow the binding with some specific oligonucleotides that can be effective in gene delivery and therapy. Peptides NPs have better cell permeability and can be exploited for targeting and imaging tumor cells and also in MRI (Koch et al. 2005).

2.2.3 Inorganic Hybrid Nanomaterials

As discussed in the earlier section of QDs, which is also a type of inorganic nanomaterial, this section briefs about perovskite quantum dots (PQDs), a new class of QDs. PQDs are tri-halide perovskites that generally have the structural formula of AMX_3, where $A = CH_3NH_3$, $(C_2H_5)NH_3{}^+$, $HC(NH_2)_2{}^+$; M = Pb, Sn, and Ge; and X = Cl, Br, and I. This formula represents the organic-inorganic lead halide PQDs. However, these PQDs suffer a huge issue related to stability (Halali et al. 2020). Organic Pb halide PQDs tend to be oxidized and lose their property in the open air. This lead to the development of all inorganic Pb halide PQDs, where organic moieties were replaced with metal cations such as Cs (Zhang et al. 2020a). All inorganic Pb halide PQDs improved the stability, but stability for long is still a difficult task. PQDs are more dominant than chalcogenide QDs such as CdSe, CdS, and CdTe. The PLQY can reach as high as 90%, which is most suitable for biosensing and bioimaging applications. But unlike chalcogenide QDs, PQDs tend to decompose in aqueous media (Zhang et al. 2018). Apart from these, many reaches reported about replacing toxic Pb with other cations, such as Sn, Bi, etc. (Leng et al. 2016; Li et al. 2019b). This reduced the toxicity comparably to Pb. Typically, PQDs are synthesized through the hot injection method at the inert condition with the presence of oleyl amine and oleic acid. Cs-oleate is injected into the hot mixture of $PbBr_2$, and soon after 10–20 s, it was quenched in ice-cold water. The precipitate is purified and stored in air-tight containers. Typically, with a change in halide ions, the color of the PQDs changes from blue to red (Zhang et al. 2018).

Many research has been shown to use them as optical sensors for toxic chemicals (Huang et al. 2020), gas sensors (Kakavelakis et al. 2018; Natkaeo et al. 2018), and also metal ions sensors (Aamir et al. 2016). The material modified with other materials showed tremendous improvement in sensing applications. Toxic metal ions such as Pb, Cd, Cu, and Hg have been sensed by cation exchange reaction by quenching the PL intensity of the PQDs (Aamir et al. 2016; Lu et al. 2017; Zhang et al. 2018). This material has been included in “FUTURE” material based on unique and robust photophysical properties. If the stability barrier is to be breached and make them most stable, it can be used in almost every field of photovoltaics, sensors, and displays. This can be an excellent choice for bioimaging, if it can be brought to an aqueous medium. Even though many approaches have been demonstrated, it is not up to the mark of commercialization.

2.3 Nanobiomaterials Applications in Human Health Care

As old proverb "health is wealth" is an industry with never-ending gold mine. The present generation of people are more cautious of their health, and it can be seen with the exponential growth of health-related device sales and research. Now, every person wants the result at the fingertip, which encourages the researchers to develop new ideas and nanomaterials for health-related techniques that can be used in advanced miniaturized devices that can fit in and onto the body. Scientific techniques are better understood, and sometimes, it is simplified to make laymen understand. Based on this concept, the use of nanobiomaterial in human health care has been divided into four different subsections. This section gives an insight into the possible futuristic ideas that can monitor human health using different nanobiomaterials. Such of these monitors include Lab-on-a-chip, diagnostics, and wearable sensors.

2.3.1 Lab-on-a-Chip

Lab-on-a-chip (LOC) platform been a very significant tool for target analysis, and treatment with interest for biologicals such as DNA, proteins, and cells-related studies or other types of diagnostics (Baranwal et al. 2018). This is because of the benefit imparted due to the reduced or smaller sample size/volume, with low cost and abundant possibilities to build integrated devices, where the analytical device can be made into conventional ones. With the development of nanotechnology, the platform has become smaller and more accessible. Several improvements for desired properties of LOC can also be achieved by using a wide variety of tunable nanomaterials. Such example of the utilization of nanomaterials as a key building block is the development of LOC platform for environmental monitoring systems including the detection and analysis of heavy metals (Aragay et al. 2011). With the advantage of nanomaterial size, it is also possible to design a biosensing system with much efficacy and smaller size enabling the visualization of stronger interaction between nanobiomaterials and LOCs platforms.

Many nanomaterials with LOCs platforms have been reported for sensing- and biosensing-related applications. Electrochemical and optical detection are predominant methods used in LOCs for various biochemical, biological, and metal ion sensing. Among the nanomaterials, carbon nanotubes have received the highest attention as they provide excellent thermal stability and conductivity. It can be deposited onto different substrate surfaces easily either through chemical vapor deposition (CVD) or plasma-enhanced CVD. Carbon nanotubes (CNTs) modified transducers can increase current density due to their large surface area, thus allowing more biomolecular attachment and can increase the selectivity of the probe. Okuno et al. demonstrated the developing of a label-free immunosensor by printing an array of Pt microelectrodes modified with CNTs using CVD to enhance the total prostate-specific antigen detection (Okuno et al. 2007). This method allows better electron transfer with an improved limit of detection (LOD) reaching 0.25 ng/mL (Morton et al. 2009). CNTs are also commonly used in field-effect transistors (FET). Javey et al. demonstrated that a combination of the ohmic metal with CNTs and high electric constant as gate film insulators and electrostatically doped CNTs segments on the source or drain electrode (Javey et al. 2004). This approach can provide the "ON-OFF" role to CNTs that is similar to the metal oxide-based semiconductor field-effect transistor. Lee et al. selectively assembled layers of Indium oxide and silica NPs onto the multisite channel area of resistors by layer by layer. Later, they immobilized the glucose oxidase on these layers and used conductimetry to detect a glucose content. Current (A) dependence on glucose concentrations with sensitivity directly depends on the fabricated channel and the resistor dimension showed glucose detection sensitivity at 4–12 nA/mM (Lee et al. 2011).

Another important application gaining tremendous attention of LOC is cancer detection. Several changes to the LOC microfluidic device such as changing the geometry of the device, capturing using NPs, and using biophysical markers to detect circulating tumor cells (CTCs) have been previously reported (Yu et al. 2011). The FDA-approved cell search platform uses ferrofluids that are loaded with epithelial cell adhesion molecule (EpCAM) modified/coated particles to capture CTCs (Yu et al. 2011). Hoshino et al. developed in context with microfluidics, where immunomagnetic CTC detection was used to capture cancer cells inside wide microchannels that were modified with high-intensity magnetic field efficiently. Microfluidic systems were geometrically enhanced microstructures to sort CTC cells (Hoshino et al. 2011). Nagrath et al. developed silicon micropots coated with EpCAM from whole blood (Nagrath et al. 2007). Kirby et al. also demonstrated the new type of geometrically enhanced differential immunocapture (GEDI) chip, specifically improved the collision frequency between the target cells and that of the antibody-coated micropots. This process enhances CTC enrichment (Kirby et al. 2012). The detection is not limited to cancer detection but also many other markers were used to detect different diseases. There is a tremendous amount of research going on in this field, making the device as small as possible and reducing the analyte size to microliter level. It may be possible in less than a decade that multirole devices can be attached to continuous monitoring of human health. Figure 34.1 gives a brief idea of microfluidic for CTCs capture and detection.

2.4 Diagnostics

Early diagnosis and disease monitoring are crucial for human health care. The development of nanomaterials-based diagnostic devices has focused on the reliability, high sensitivity, and rapid detection of the diseases (Purohit et al. 2020; Syedmoradi et al. 2017). In general, nanomaterials are designed based on the binding capability of nanomaterials to disease-related targets, so-called disease biomarkers. Then signals from the nanomaterial-biomarker binding complex are observed by which the limit of detection could be lower than the nM scale in some reports (Sha et al. 2020; Sim et al. 2021; Wang et al. 2020a; Zuo et al. 2020; Quesada-González and Merkoçi 2018). In addition to common nanoparticles, e.g., gold and silver nanoparticles, recent studies showed that nanohybrid such as fullerenes-metal organic framework and nanoporous anodic alumina-oligonucleotide also exhibited accurate and rapid diagnostic capability within 1–2 h for the detection of miR-3675-3p and *Candida auris* fungus, respectively (Pla et al. 2020; Zuo et al. 2020).

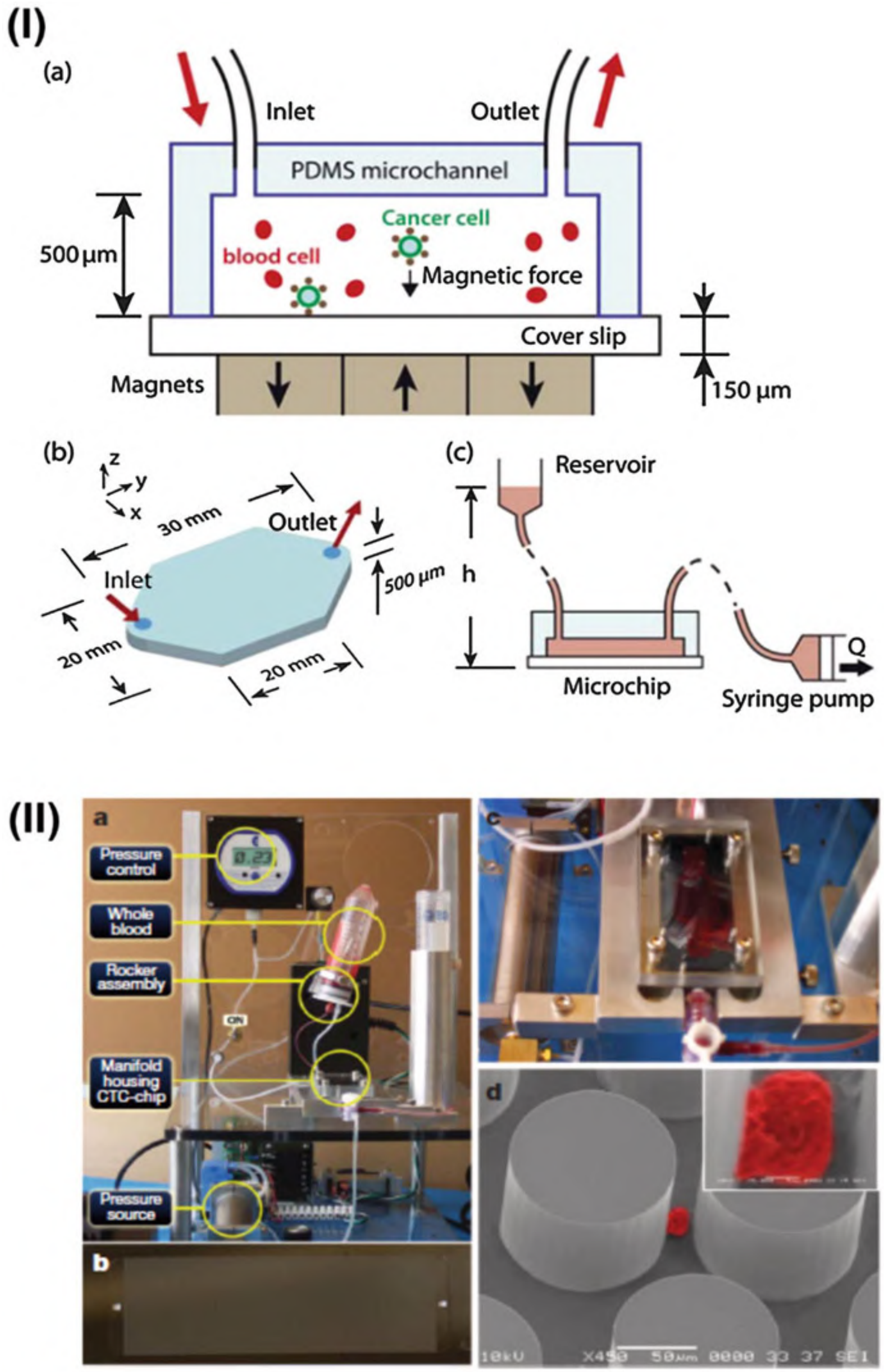
(I)
(a)
Inlet
Outlet
PDMS microchannel
500 μm
Cancer cell
blood cell
Magnetic force
Cover slip
Magnets
150 μm
(b)
z
y
x
30 mm
Outlet
Inlet
500 μm
20 mm
20 mm
(c)
Reservoir
h
Microchip
Syringe pump
Q
(II)
a
Pressure control
Whole blood
Rocker assembly
Manifold housing CTC-chip
Pressure source
b
c
d
10kU X450 50μm 0000 33 37 SEI

Fig. 34.1 (**I**) Schematic of a microfluidic device to isolate CTCs from whole blood. (Reprinted with permission from Hoshino et al. (2011)). (**II**) The design of immunomagnetic cancer cells detection microchip. (Reprinted with permission from Nagrath et al. (2007))

Using oligonucleotide nanobiomaterials as disease diagnostic tools has been paid more attention lately due to their self-assembling ability, programmability, high biocompatibility, and small size (Chen et al. 2018a). Among these, aptamers exhibited high binding affinity against several antibodies with on par or even lower limit of detection than ELISA technique giving a possibility to be used as an aptasensor for super sensitive immunoassay (Citartan and Tang 2019; He et al. 2021; Lin et al. 2020; Sim et al. 2021). Recent study showed that Zn^{2+}-dependent DNAzyme could be used as a nondestructive analyzer for tumor-associated membrane protein imaging (Chen et al. 2018b). Several attempts to improve the binding affinity as well as the signal readout have also been paid. This led to the self-assembly of DNA into a packed shape like tetrahedral nanotweezers or nanoflowers. Having a packing structure aids DNA toward the resistance of intrinsic interferences in biological matrices, such as nuclease digestion and thermodynamic fluctuations, and can avoid the generation of false-positive signals (He et al. 2017; Lv et al. 2020). Figure 34.2 shows some of the examples for the development of diagnosis.

CRISPR/Cas also showed its applicability in disease diagnosis. A high variety of Cas endonucleases together with the easily modifiable sgRNA provide a great potential of disease-related nucleic acid detection in human biological materials (Bonini et al. 2021; Dai et al. 2020; Li et al. 2019a; van Dongen et al. 2020; Wu et al. 2021; Zhang 2019). The utilization of either Cas9 or dCas9 to modulate the electrical signal from the binding with its target based on the sequence of sgRNA showed its rapid detection of dsDNA target within 15 min and the target concentration could reach the fM scale (Hajian et al. 2019; Xu et al. 2020). The discovery of Cas12, Cas13, and Cas14 families further aid the detection of their targeted nucleic acid. The utilization of these proteins in disease diagnostic is based on their collateral cleavage ability to nearby reporter ssDNA (Cas12 and Cas14) and ssRNA (Cas13) molecules once the proteins bind with the targets, thus releasing the detectable signal (Abudayyeh et al. 2016; Aman et al. 2020; Bruch et al. 2019; Harrington et al. 2018; Li et al. 2018; Shan et al. 2019; Sun et al. 2020; Zhang 2019). Using dual Cas, so-called casCRISPR, for the detection of miRNAs was also recently reported (Sha et al. 2020).

2.5 Wearable Sensors

World Economic Forum reported that the nature of the disease will be unsettled by the introduction of technology by 2030. The fourth industrial revolution will make sure that humans can get longevity and become healthier. In the future, the hospital may be like a garage where individuals go to hospitals to be patched up and tracked, thus revolutionizing health care. Health status can be monitored while physicians traveling anywhere in the world or even AI can come up (Arduini 2021). Thereby, real-time monitoring of physiological parameters is important for both hospital settings and daily activities. In response to this, wearable sensors are a key role in Internet of Things (IoTs) in health care as they can provide not only new avenues to monitor individuals continuously, but also vital information regarding their health. The present available commercial wearable sensors are aimed at physical sensing

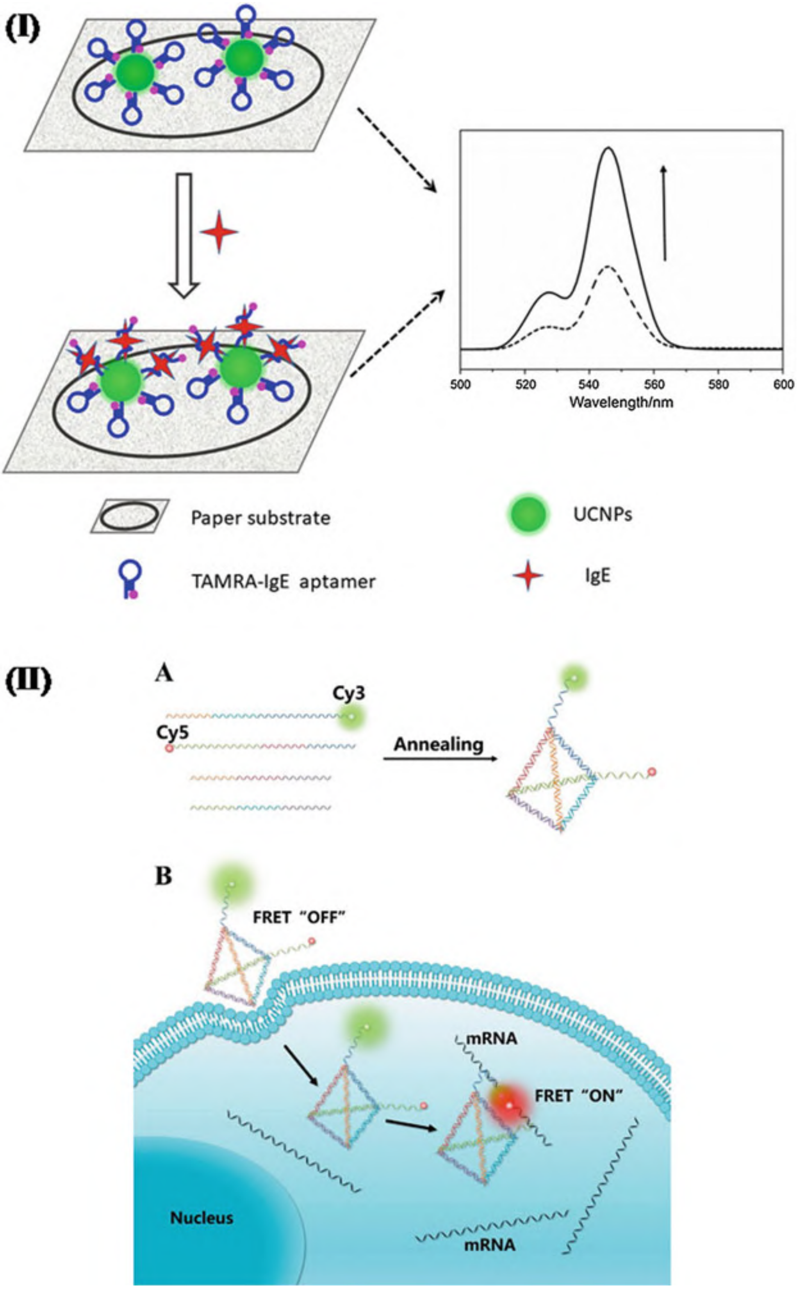
(I)
500
520
540
560
580
600
Wavelength/nm
Paper substrate
UCNPs
TAMRA-IgE aptamer
IgE
(II)
A
Cy3
Cy5
Annealing
B
FRET "OFF"
mRNA
FRET "ON"
Nucleus
mRNA

Fig. 34.2 Examples of some oligonucleotide-based nanobiomaterials for diagnosis. (**I**) Paper-based UC-LRET aptasensor for IgE detection. (Reprinted with permission from He et al. (2021)). (**II**) Synthesis (*A*) and mechanism (*B*) of the DNA tetrahedron nanotweezer (DTNT) nanoprobe for tumor-related mRNA detection in living cells. (Reprinted with permission from He et al. (2017))

without any information at molecular level. Such information includes a change in blood color, heartbeat, and temperature. Joseph Wang is pioneered such wearable sensors to detect the target at the molecular level. Wang's group works on developing batteryless wearable sensors. They also pioneered the analysis of sweat and urine samples. Sweat and urine are some of the important analyte samples excreted; by assessing them analytically, one can find the monitor and the health status of an individual. Sempionatto et al. demonstrated the wearable electrochemical sensors for monitoring vitamin C in sweat. They immobilized the ascorbate oxidase on the flexible screen-printed electrode (SPE) and used simulated sweat as their sample. The oxidation of ascorbic acid directly proportional to the concentration of vitamin C was measured by the amperometer (Sempionatto et al. 2020). Glucose wearable sensor has been classic of all the wearable sensors as it can be monitored through tears (Chu et al. 2011), sweat (Yang et al. 2020), and also urine (Nyein et al. 2016). Yao et al. from Parviz's group developed a contact-lens based amperometeric glucose sensor, which can monitor and send the data through wireless data transmission (Yao et al. 2011). This technology is now taken up by Google and they are further developing it. Kagie et al. also reported the laterally rolled screen-printed contact lens-based sensor, which can monitor the fluids in tear. It can monitor the dynamic change in norepinephrine and glucose (Kagie et al. 2008).

Apart from these mentioned molecular sensors, another important use of wearable sensors is in the detection of nerve agents. Colozzo et al., reported the development of an origami paper-based wearable sensors. The electrodes were modified with choline oxidase enzyme with conductive ink. Exploiting the absorption property of paper, it was preloaded with choline esterase. Later, the paper was exposed to sulphur mustard nerve gas, which can oxidize the choline esterase. Hence, change in current was monitored which they reported the LOD of 1 mM and 0.019 g/min/m^3 for liquid and gas phase (Colozza et al. 2019). Wang's group developed for the first time the skin and textile wearable sensor to detect and monitor nerve agents in vapor phase. They used organophosphate hydrolase modified using elastomeric inks to aid more flexibility to the device. The functionality of electronic interface was also maintained even under imparted mechanical stress due to bending and twisting of the textile and able to transfer the data by wireless data transmission. The enzymatic by-product nitrophenol was detected using square wave voltammetry. The fabricated epidermal tattoo and textile sensors showed a LOD of 12 mg/mL (Mishra et al. 2018b).

Tattoos will be the next big thing in biosensing platform. The temporary tattoos which can be put on skin when needed and can be erased is an art with a specific function. They can also be used like a smart jewelry (Jin et al. 2017). Wang's group previously reported the tattoo-based glucose sensing platform. This tattoo-based epidermal diagnostic device works on the principle of reverse ionophoretic extraction of glucose and enzyme-based ampherometric biosensor. It can be used to monitor the variation of glycemic level during food intake (Bandodkar et al. 2015). This sensor is a non-invasive type of glucose sensor, which can be used for efficient monitoring of diabetes. Mishra et al. used a pH-sensitive polyaniline sensor in combination with organophosphate hydrolase to develop a potentiometric tattoo-based biosensor for real-time on-body quantification of simulant for G-type nerve agent. Using nebulizer solution of nerve agent simulant, di-isopropyl fluorophosphate, the developed tattoo sensor demonstrated linearity over the range of 20–120 mM with LOD of 10 mM (Mishra et al. 2018a). Kim et al. developed the tattoo-based alcohol sensor. Transdermal delivery of pilocarpine drug inducing sweat was enabled by this prototype via iontophoresis. From the generated sweat, ethanol was detected amperometrically. They fabricated the alcohol oxidase enzyme and Prussian blue electrode transducers to detect ethanol in sweat before and after alcohol consumption (Kim et al. 2016).

The above section discussed the non-invasive type of sensors. Still some data has to be collected invasively to compare and to monitor more accurately. Microneedles (MNs), a type of needle with a height not more than 1 mm, can penetrate the dermal layer infusing minimal invasive and minimal pain. It was first reported use for drug delivery. Later, due to minimal invasive property adapted for human health monitoring. It took a trend, and it has been applied for glucose monitoring (Zhang et al. 2020b; Caliò et al. 2016), lactate (Caliò et al. 2016; Bollella et al. 2019), alcohol (Mohan et al. 2017), and uric acid (Gao et al. 2019). Goa et al. demonstrated the Au/Ti coated flexible microarray MNs for electrochemical detection of glucose, uric acid, and cholesterol. The Au/Ti coated microarrays were again modified with glucose oxidase, uricase, and cholesterol oxidase. Cholesterol needs to be studied from the invasive body fluid; hence, MNs approach is most suitable (Gao et al. 2019). MNs were also used to detect nerve agents, methyl paraoxon, morphine, and norfentanyl. Mishra et al. demonstrated real time monitoring on the body studies to detect and monitor the opioids nerve agents such as methyl paraxons, morphine, and norfentanyl on a single platform of MNs (Mishra et al. 2020). Such monitoring and sensing are not limited to above-mentioned analyte, but also can be extended to other toxic substances owing to importance to human welfare. Figure 34.3 depicts different types of wearable sensors including label type, tattoo type, microneedle, and contact lens for different analyte analyses.

3 Future Perspective and Conclusion

In this review, we have explored the state-of-the-arts nanobiomaterials for medical and health care applications in various integrative platforms ranging from lab-on-chip to wearable biosensors. The nanobiomaterials have enabled researchers to capture the insights of human health conditions through novel sensing capabilities of disease biomarkers, metabolites, and electrolytes in human biofluids such as blood, sweat, and saliva (Heikenfeld et al. 2019). Despite global efforts and progress in nanobiomaterials, the most recent works in the field remain in the lab as proof-of-concept biosensing platforms, and only small steps can be taken toward clinical and commercialize applications in the field (Kim et al. 2019). We believe that for the research in nanobiomaterials to have translational impacts in the real world, researchers must overcome the following three challenges:

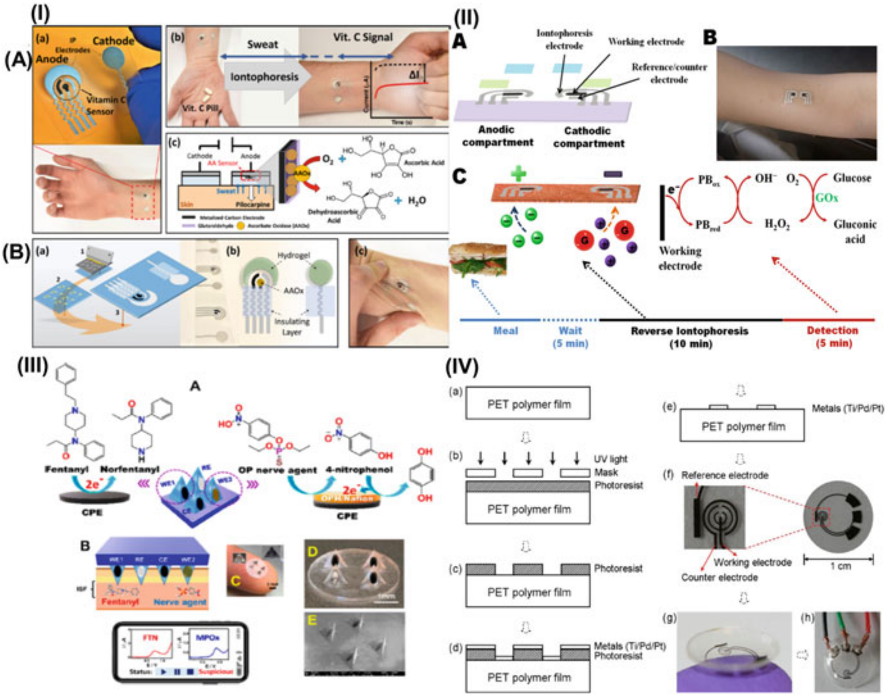
(I)
(A)
(a)
Cathode
Anode
Electrodes
Vitamin C Sensor
(b)
Sweat
Vit. C Signal
Iontophoresis
ΔI
Vit. C Pill
(c)
Cathode
Anode
AA Sensor
Skin
Sweat
Pilocarpine
Ascorbic Acid
O₂
AAOx
H₂O
Dehydroascorbic Acid
(B)
(a)
(b)
Hydrogel
AAOx
Insulating Layer
(c)
(II)
A
Iontophoresis electrode
Working electrode
Reference/counter electrode
Anodic compartment
Cathodic compartment
B
C
PB_ox
PB_red
OH⁻
O₂
H₂O₂
Glucose
GOx
Gluconic acid
Working electrode
Meal
Wait (5 min)
Reverse Iontophoresis (10 min)
Detection (5 min)
(III)
A
Fentanyl
Norfentanyl
CPE
OP nerve agent
4-nitrophenol
OPH-Nafion
CPE
B
C
D
E
Fentanyl
Nerve agent
FTN
MPOx
(IV)
(a) PET polymer film
(b) UV light Mask Photoresist PET polymer film
(c) Photoresist PET polymer film
(d) Metals (Ti/Pd/Pt) Photoresist PET polymer film
(e) Metals (Ti/Pd/Pt) PET polymer film
(f) Reference electrode
Working electrode
Counter electrode
1 cm
(g)
(h)

Fig. 34.3 Examples of some wearable sensors. (**I**) Wearable sensor for ascorbic acid (vitamin C) determination using stimulated sweat as a target of detection (Reprinted with permission from Sempionatto et al. 2020). (**II**) Noninvasive glucose sensing using a Tattoo-based platform. (Reprinted with permission from Bandodkar et al. (2015)). (**III**) Microneedle sensor array for detecting opioids and nerve agents. (Reprinted with permission from Mishra et al. (2020)). (**IV**) Overall fabrication of wearable sensor. (Reprinted with permission from Yao et al. (2011))

1) **Reusability:** Most of the sensing techniques developed using nanobiomaterials, except the enzymatic reaction approach, are non-reusable, and are only a one-off solution. However, for the nanobiomaterials to be integrated into the future healthcare system such as medical facilities enabling at-home usage, researchers must come up with a solution that allows for repeated and continuous use of nanobiomaterials in human biofluid samples. A solution could be either creating an extremely low-cost disposable part and a mechanism to automatically replacing the used sensor with the new one (Pataranutaporn et al. 2019) or developing a regenerative approach that replenishes the chemicals used on the sensing platform or washing mechanism to reset the sensor.
2) **Integration:** For nanobiomaterials to have a translational impact, researchers must come up with a robust sensing and easily deployable sensing platform by improving the device assembling methods to support the scale of the manufacturing facility, enhancing biofluid sampling protocol, advancing the flexible property of the materials for comfortable use on the human body, and finally multiplexing various sensors into a single compact platform.

3) **Data processing:** Once the nanobiomaterials device can be optimized, produced in large-scale manufacturing, and in the hands of patients and physicians, the final challenge for the researcher is to distinguish between noise and signals captured from the device transforming the data into actionable insight for medical interventions. Until this point, most of the researches in nanobiomaterials have used the sensor to separately detect changes in specific biomarkers, metabolites, and electrolytes in a controlled environmental setting with minimal interference. However, in the real world those biomarkers, metabolites, and electrolytes interact with one another in non-linear/stochastic ways and are being influenced by the patient’s behavioral and environmental factors resulting in complex patterns. Thus, simply looking at the mere changes of the biomarkers without understanding the context such as the patient’s current behavior, time, and location could lead to a misinterpretation of the signals. To overcome this, future nanobiomaterials must integrate with other physiological sensors to obtain data such as heart rate, EEG, EMG, as well as contextual information including time, GPS location, and accelerometer data to holistically understand the patient conditions.

These technological challenges are critical for maximizing the impact of nanobiomaterials out of the lab to real-world impact and widespread adoption of the platform. Some of these challenges are specific to the sensing techniques or target molecules of interest whereas others are shared by all biosensing systems. Nonetheless, nanobiomaterials present an exciting opportunity toward the future of personalized healthcare, where patients can collect temporal and high-resolution data from their body for individualized and preventative medical intervention using the sensors on, around, and inside their bodies.

References

Aamir M, Sher M, Malik MA, Akhtar J, Revaprasadu N (2016) A chemodosimetric approach for the selective detection of Pb^{2+} ions using a cesium based perovskite. New J Chem 40: 9719–9724

Abudayyeh OO, Gootenberg JS, Konermann S, Joung J, Slaymaker IM, Cox DB, Shmakov S, Makarova KS, Semenova E, Minakhin L, Severinov K, Regev A, Lander ES, Koonin EV, Zhang F (2016) C2c2 is a single-component programmable RNA-guided RNA-targeting CRISPR effector. Science 353:aaf5573

Aman R, Mahas A, Mahfouz M (2020) Nucleic acid detection using CRISPR/Cas biosensing technologies. ACS Synth Biol 9:1226–1233

Aragay G, Pons J, Merkoçi A (2011) Recent trends in macro-, micro-, and nanomaterial-based tools and strategies for heavy-metal detection. Chem Rev 111:3433–3458

Arduini F (2021) Nanomaterials and cross-cutting technologies for fostering smart electrochemical biosensors in the detection of chemical warfare agents. Appl Sci 11:720

Bandodkar AJ, Jia W, Yardımcı C, Wang X, Ramirez J, Wang J (2015) Tattoo-based noninvasive glucose monitoring: a proof-of-concept study. Anal Chem 87:394–398

Baranwal A, Srivastava A, Kumar P, Bajpai VK, Maurya PK, Chandra P (2018) Prospects of nanostructure materials and their composites as antimicrobial agents. Front Microbiol 9:422

Baughman RH, Zakhidov AA, De Heer WA (2002) Carbon nanotubes – the route toward applications. Science 297:787–792

Blanco-Covián L, Montes-García V, Alexandre Girard M, Fernández-Abedul T, Pérez-Juste J, Pastoriza-Santos I, Faulds K, Graham D, Blanco-López MC (2017) Au@Ag SERRS tags coupled to a lateral flow immunoassay for the sensitive detection of pneumolysin. Nanoscale 9:2051–2058

Bollella P, Sharma S, Cass AEG, Antiochia R (2019) Microneedle-based biosensor for minimally-invasive lactate detection. Biosens Bioelectron 123:152–159

Bonini A, Poma N, Vivaldi F, Kirchhain A, Salvo P, Bottai D, Tavanti A, Di Francesco F (2021) Advances in biosensing: the CRISPR/Cas system as a new powerful tool for the detection of nucleic acids. J Pharm Biomed Anal 192:113645

Bottini M, D'Annibale F, Magrini A, Cerignoli F, Arimura Y, Dawson MI, Bergamaschi E, Rosato N, Bergamaschi A, Mustelin T (2007) Quantum dot-doped silica nanoparticles as probes for targeting of T-lymphocytes. Int J Nanomed 2:227

Bruch R, Baaske J, Chatelle C, Meirich M, Madlener S, Weber W, Dincer C, Urban GA (2019) CRISPR/Cas13a-powered electrochemical microfluidic biosensor for nucleic acid amplification-free miRNA diagnostics. Adv Mater 31:e1905311

Caliò A, Dardano P, Di Palma V, Bevilacqua MF, Di Matteo A, Iuele H, De Stefano L (2016) Polymeric microneedles based enzymatic electrodes for electrochemical biosensing of glucose and lactic acid. Sensors Actuators B Chem 236:343–349

Chandan HR, Geetha BR (2013) Study on precipitation efficiency of solvents in postpreparative treatment of nanocrystals. J Mater Res 28:3003–3009

Chandan HR, Saravanan V, Pai RK, Geetha Balakrishna R (2014) Synergistic effect of binary ligands on nucleation and growth/size effect of nanocrystals: studies on reusability of the solvent. J Mater Res 29:1556–1564

Chandan HR, Schiffman JD, Geetha Balakrishna R (2018) Quantum dots as fluorescent probes: synthesis, surface chemistry, energy transfer mechanisms, and applications. Sensors Actuators B Chem 258:1191–1214

Chen J, Corbin IR, Li H, Cao W, Glickson JD, Zheng G (2007) Ligand conjugated low-density lipoprotein nanoparticles for enhanced optical cancer imaging in vivo. J Am Chem Soc 129: 5798–5799

Chen T, Ren L, Liu X, Zhou M, Li L, Xu J, Zhu X (2018a) DNA nanotechnology for cancer diagnosis and therapy. Int J Mol Sci 19:1671

Chen X, Zhao J, Chen T, Gao T, Zhu X, Li G (2018b) Nondestructive analysis of tumor-associated membrane protein integrating imaging and amplified detection in situ based on dual-labeled DNAzyme. Theranostics 8:1075–1083

Chu MX, Shirai T, Takahashi D, Arakawa T, Kudo H, Sano K, Sawada S-i, Yano K, Iwasaki Y, Akiyoshi K (2011) Biomedical soft contact-lens sensor for in situ ocular biomonitoring of tear contents. Biomed Microdevices 13:603–611

Citartan M, Tang TH (2019) Recent developments of aptasensors expedient for point-of-care (POC) diagnostics. Talanta 199:556–566

Colozza N, Kehe K, Dionisi G, Popp T, Tsoutsoulopoulos A, Steinritz D, Moscone D, Arduini F (2019) A wearable origami-like paper-based electrochemical biosensor for sulfur mustard detection. Biosens Bioelectron 129:15–23

Dai Y, Wu Y, Liu G, Gooding JJ (2020) CRISPR mediated biosensing toward understanding cellular biology and point-of-care diagnosis. Angew Chem Int Ed Engl 59:20754–20766

Daima HK, Bansal V (2015) Influence of physicochemical properties of nanomaterials on their antibacterial applications. In: Nanotechnology in diagnosis, treatment and prophylaxis of infectious diseases, Academic Press, 151–166, ISBN 9780128013175

Di Marzio N, Eglin D, Serra T, Moroni L (2020) Bio-fabrication: convergence of 3D bioprinting and nano-biomaterials in tissue engineering and regenerative medicine. Front Bioeng Biotechnol 8:326

El Haj J (2020) The grand challenges of medical technology. Front Med Technol 2:1

Gao J, Huang W, Chen Z, Yi C, Jiang L (2019) Simultaneous detection of glucose, uric acid and cholesterol using flexible microneedle electrode array-based biosensor and multi-channel portable electrochemical analyzer. Sensors Actuators B Chem 287:102–110

Gerion D, Pinaud F, Williams SC, Parak WJ, Zanchet D, Weiss S, Alivisatos AP (2001) Synthesis and properties of biocompatible water-soluble silica-coated CdSe/ZnS semiconductor quantum dots. J Phys Chem B 105:8861–8871

Gobin AM, Lee MH, Halas NJ, James WD, Drezek RA, West JL (2007) Near-infrared resonant nanoshells for combined optical imaging and photothermal cancer therapy. Nano Lett 7: 1929–1934

Hajian R, Balderston S, Tran T, deBoer T, Etienne J, Sandhu M, Wauford NA, Chung JY, Nokes J, Athaiya M, Paredes J, Peytavi R, Goldsmith B, Murthy N, Conboy IM, Aran K (2019) Detection of unamplified target genes via CRISPR-Cas9 immobilized on a graphene field-effect transistor. Nat Biomed Eng 3:427–437

Halali VV, Sanjayan CG, Suvina V, Sakar M, Geetha Balakrishna R (2020) Perovskite nanomaterials as optical and electrochemical sensors. Inorg Chem Front 7:2702–2725

Harrington LB, Burstein D, Chen JS, Paez-Espino D, Ma E, Witte IP, Cofsky JC, Kyrpides NC, Banfield JF, Doudna JA (2018) Programmed DNA destruction by miniature CRISPR-Cas14 enzymes. Science 362:839–842

He L, Lu DQ, Liang H, Xie S, Luo C, Hu M, Xu L, Zhang X, Tan W (2017) Fluorescence resonance energy transfer-based DNA tetrahedron nanotweezer for highly reliable detection of tumor-related mRNA in living cells. ACS Nano 11:4060–4066

He M, Shang N, Zhu Q, Xu J (2021) Paper-based upconversion fluorescence aptasensor for the quantitative detection of immunoglobulin E in human serum. Anal Chim Acta 1143:93–100

Heikenfeld J, Jajack A, Feldman B, Granger SW, Gaitonde S, Begtrup G, Katchman BA (2019) Accessing analytes in biofluids for peripheral biochemical monitoring. Nat Biotechnol 37: 407–419

Hoshino K, Huang Y-Y, Lane N, Huebschman M, Uhr JW, Frenkel EP, Zhang X (2011) Microchip-based immunomagnetic detection of circulating tumor cells. Lab Chip 11:3449–3457

Huang X, El-Sayed MA (2010) Gold nanoparticles: optical properties and implementations in cancer diagnosis and photothermal therapy. J Adv Res 1:13–28

Huang H, Hao M, Song Y, Dang S, Liu X, Dong Q (2020) Dynamic passivation in perovskite quantum dots for specific ammonia detection at room temperature. Small 16:1904462

Jafari S, Derakhshankhah H, Alaei L, Fattahi A, Varnamkhasti BS, Saboury AA (2019) Mesoporous silica nanoparticles for therapeutic/diagnostic applications. Biomed Pharmacother 109: 1100–1111

Jafelicci M Jr, Rosaly Davolos M, José dos Santos F, José de Andrade S (1999) Hollow silica particles from microemulsion. J Non-Cryst Solids 247:98–102

Jain PK, Lee KS, El-Sayed IH, El-Sayed MA (2006) Calculated absorption and scattering properties of gold nanoparticles of different size, shape, and composition: applications in biological imaging and biomedicine. J Phys Chem B 110:7238–7248

Javey A, Guo J, Farmer DB, Wang Q, Yenilmez E, Gordon RG, Lundstrom M, Dai H (2004) Self-aligned ballistic molecular transistors and electrically parallel nanotube arrays. Nano Lett 4: 1319–1322

Jin H, Abu-Raya YS, Haick H (2017) Advanced materials for health monitoring with skin-based wearable devices. Adv Healthc Mater 6:1700024

Kagie A, Bishop DK, Burdick J, La Belle JT, Dymond R, Felder R, Wang J (2008) Flexible rolled thick-film miniaturized flow-cell for minimally invasive amperometric sensing. Electroanalysis 20:1610–1614

Kakavelakis G, Gagaoudakis E, Petridis K, Petromichelaki V, Binas V, Kiriakidis G, Kymakis E (2018) Solution processed $CH_3NH_3PbI_3$–x Cl x perovskite based self-powered ozone sensing element operated at room temperature. ACS Sensors 3:135–142

Kim J, Jeerapan I, Imani S, Cho TN, Bandodkar A, Cinti S, Mercier PP, Wang J (2016) Noninvasive alcohol monitoring using a wearable tattoo-based iontophoretic-biosensing system. ACS Sensors 1:1011–1019

Kim J, Campbell AS, de Ávila BE, Wang J (2019) Wearable biosensors for healthcare monitoring. Nat Biotechnol 37:389–406

Kirby BJ, Jodari M, Loftus MS, Gakhar G, Pratt ED, Chanel-Vos C, Gleghorn JP, Santana SM, Liu H, Smith JP (2012) Functional characterization of circulating tumor cells with a prostate-cancer-specific microfluidic device. PLoS One 7:e35976

Koch AM, Reynolds F, Merkle HP, Weissleder R, Josephson L (2005) Transport of surface-modified nanoparticles through cell monolayers. Chembiochem 6:337–345

Kusuma J, Geetha Balakrishna R, Patil S, Jyothi MS, Chandan HR, Shwetharani R (2018) Exploration of graphene oxide nanoribbons as excellent electron conducting network for third generation solar cells. Sol Energy Mater Sol Cells 183:211–219

Kusuma J, Chandan HR, Geetha Balakrishna R (2019) Conjugated molecular bridges: a new direction to escalate linker assisted QDSSC performance. Sol Energy 194:74–78

Lai G, Wu J, Leng C, Ju H, Yan F (2011) Disposable immunosensor array for ultrasensitive detection of tumor markers using glucose oxidase-functionalized silica nanosphere tags. Biosens Bioelectron 26:3782–3787

Lee K-S, El-Sayed MA (2005) Dependence of the enhanced optical scattering efficiency relative to that of absorption for gold metal nanorods on aspect ratio, size, end-cap shape, and medium refractive index. J Phys Chem B 109:20331–20338

Lee D, Ondrake J, Cui T (2011) A conductometric indium oxide semiconducting nanoparticle enzymatic biosensor array. Sensors 11:9300–9312

Leng M, Chen Z, Yang Y, Li Z, Zeng K, Li K, Niu G, He Y, Zhou Q, Tang J (2016) Lead-free, blue emitting bismuth halide perovskite quantum dots. Angew Chem Int Ed 55:15012–15016

Li SY, Cheng QX, Wang JM, Li XY, Zhang ZL, Gao S, Cao RB, Zhao GP, Wang J (2018) CRISPR-Cas12a-assisted nucleic acid detection. Cell Discov 4:20

Li Y, Li S, Wang J, Liu G (2019a) CRISPR/Cas systems towards next-generation biosensing. Trends Biotechnol 37:730–743

Li D, Xu W, Zhou D, Ma X, Chen X, Pan G, Zhu J, Ji Y, Ding N, Song H (2019b) Cesium tin halide perovskite quantum dots as an organic photoluminescence probe for lead ion. J Lumin 216:116711

Lin B, Tian T, Lu Y, Liu D, Huang M, Zhu L, Zhu Z, Song Y, Yang C (2020) Tracing tumor-derived exosomal PD-L1 by dual-aptamer activated proximity-induced droplet digital PCR. Angew Chem Int Ed Engl 60(14):7582–7586

Liu P, Wei Y, Liu K, Liu L, Jiang K, Fan S (2012) New-type planar field emission display with superaligned carbon nanotube yarn emitter. Nano Lett 12:2391–2396

Liu ML, Chen BB, Li CM, Huang CZ (2019) Carbon dots: synthesis, formation mechanism, fluorescence origin and sensing applications. Green Chem 21:449–471

Lu L-Q, Tan T, Tian X-K, Li Y, Deng P (2017) Visual and sensitive fluorescent sensing for ultratrace mercury ions by perovskite quantum dots. Anal Chim Acta 986:109–114

Lv J, Dong Y, Gu Z, Yang D (2020) Programmable DNA nanoflowers for biosensing, bioimaging, and therapeutics. Chemistry 26:14512–14524

Mishra RK, Barfidokht A, Karajic A, Sempionatto JR, Wang J, Wang J (2018a) Wearable potentiometric tattoo biosensor for on-body detection of G-type nerve agents simulants. Sensors Actuators B Chem 273:966–972

Mishra RK, Martin A, Nakagawa T, Barfidokht A, Lu X, Sempionatto JR, Lyu KM, Karajic A, Musameh MM, Kyratzis IL (2018b) Detection of vapor-phase organophosphate threats using wearable conformable integrated epidermal and textile wireless biosensor systems. Biosens Bioelectron 101:227–234

Mishra RK, Yugender Goud K, Li Z, Moonla C, Mohamed MA, Tehrani F, Teymourian H, Wang J (2020) Continuous opioid monitoring along with nerve agents on a wearable microneedle sensor array. J Am Chem Soc 142:5991–5995

Miyaji F, Davis SA, Charmant JPH, Mann S (1999) Organic crystal templating of hollow silica fibers. Chem Mater 11:3021–3024

Mohan AMV, Windmiller JR, Mishra RK, Wang J (2017) Continuous minimally-invasive alcohol monitoring using microneedle sensor arrays. Biosens Bioelectron 91:574–579

Morton J, Havens N, Mugweru A, Wanekaya AK (2009) Detection of trace heavy metal ions using carbon nanotube-modified electrodes. Electroanalysis 21:1597–1603

Nagrath S, Sequist LV, Maheswaran S, Bell DW, Irimia D, Ulkus L, Smith MR, Kwak EL, Digumarthy S, Muzikansky A (2007) Isolation of rare circulating tumour cells in cancer patients by microchip technology. Nature 450:1235–1239

Natkaeo A, Phokharatkul D, Hodak JH, Wisitsoraat A, Hodak SK (2018) Highly selective sub–10 ppm H_2S gas sensors based on Ag-doped $CaCu_3Ti_4O_{12}$ films. Sensors Actuators B Chem 260:571–580

Ni JS, Li Y, Yue W, Liu B, Li K (2020) Nanoparticle-based cell trackers for biomedical applications. Theranostics 10:1923–1947

Nyein HY, Yin WG, Shahpar Z, Emaminejad S, Challa S, Chen K, Fahad HM, Tai L-C, Ota H, Davis RW (2016) A wearable electrochemical platform for noninvasive simultaneous monitoring of Ca^{2+} and pH. ACS Nano 10:7216–7224

Okuno J, Maehashi K, Kerman K, Takamura Y, Matsumoto K, Tamiya E (2007) Label-free immunosensor for prostate-specific antigen based on single-walled carbon nanotube array-modified microelectrodes. Biosens Bioelectron 22:2377–2381

Pataranutaporn P, Jain A, Johnson CM, Shah P, Maes P (2019) Wearable lab on body: combining sensing of biochemical and digital markers in a wearable device. In: 2019 41st annual international conference of the IEEE Engineering in Medicine and Biology Society (EMBC), pp 3327–3332

Pla L, Tormo-Mas MA, Ruiz-Gaitan A, Peman J, Valentin E, Sancenon F, Aznar E, Martinez-Manez R, Santiago-Felipe S (2020) Oligonucleotide-capped nanoporous anodic alumina biosensor as diagnostic tool for rapid and accurate detection of *Candida auris* in clinical samples. Emerg Microbes Infect 10:407–415

Purohit B, Vernekar PR, Shetti NP, Chandra P (2020) Biosensor nanoengineering: design, operation, and implementation for biomolecular analysis. Sensors Int 1:100040

Puttaswamy SV, Lubarsky GV, Kelsey C, Zhang X, Finlay D, McLaughlin JA, Bhalla N (2020) Nanophotonic-carbohydrate lab-on-a-microneedle for rapid detection of human cystatin C in finger-prick blood. ACS Nano 14:11939–11949

Quesada-González D, Merkoçi A (2018) Nanomaterial-based devices for point-of-care diagnostic applications. Chem Soc Rev 47:4697–4709

Raman S, Machaidze G, Lustig A, Aebi U, Burkhard P (2006) Structure-based design of peptides that self-assemble into regular polyhedral nanoparticles. Nanomed Nanotechnol Biol Med 2: 95–102

Raveendran M, Lee AJ, Sharma R, Walti C, Actis P (2020) Rational design of DNA nanostructures for single molecule biosensing. Nat Commun 11:4384

Ravikumar CH, Gowda MI, Geetha Balakrishna R (2019) An “OFF–ON” quantum dot–graphene oxide bioprobe for sensitive detection of micrococcal nuclease of *Staphylococcus aureus*. Analyst 144:e116

Ravikumar CH, Shwetharani R, Geetha Balakrishna R (2020) Surface modified glass substrate for sensing *E. coli* using highly stable and luminescent CdSe/CdS core shell quantum dots. J Photochem Photobiol B 204:111799

Rensen PCN, de Vrueh RLA, Kuiper J, Bijsterbosch MK, Biessen EAL, van Berkel TJC (2001) Recombinant lipoproteins: lipoprotein-like lipid particles for drug targeting. Adv Drug Deliv Rev 47:251–276

Selvan ST, Patra PK, Ang CY, Ying JY (2007) Synthesis of silica-coated semiconductor and magnetic quantum dots and their use in the imaging of live cells. Angew Chem 119:2500–2504

Sempionatto JR, Khorshed AA, Ahmed A, De Loyola e Silva AN, Barfidokht A, Yin L, Goud KY, Mohamed MA, Bailey E, May J, Aebischer C, Chatelle C, Wang J (2020) Epidermal enzymatic biosensors for sweat vitamin c: toward personalized nutrition. ACS Sensors 5: 1804–1813

Sha Y, Huang R, Huang M, Yue H, Shan Y, Hu J, Xing D (2020) Cascade CRISPR/cas enables amplification-free microRNA sensing with fM-sensitivity and single-base-specificity. Chem Commun 57:893–905

Shah JV, Gonda A, Pemmaraju R, Subash A, Bobadilla Mendez C, Berger M, Zhao X, He S, Riman RE, Tan MC, Pierce MC, Moghe PV, Ganapathy V (2020) Shortwave infrared-emitting theranostics for breast cancer therapy response monitoring. Front Mol Biosci 7:569415

Shan Y, Zhou X, Huang R, Xing D (2019) High-fidelity and rapid quantification of miRNA combining crRNA programmability and CRISPR/Cas13a trans-cleavage activity. Anal Chem 91:5278–5285

Sim J, Baek MS, Lee KH, Kim DM, Byun JY, Shin YB (2021) A highly sensitive and versatile transcription immunoassay using a DNA-encoding tandem repetitive light-up aptamer. Talanta 224:121921

Sun HH, He F, Wang T, Yin BC, Ye BC (2020) A Cas12a-mediated cascade amplification method for microRNA detection. Analyst 145:5547–5552

Syedmoradi L, Daneshpour M, Alvandipour M, Gomez FA, Hajghassem H, Omidfar K (2017) Point of care testing: the impact of nanotechnology. Biosens Bioelectron 87:373–387

van Dongen JE, Berendsen JTW, Steenbergen RDM, Wolthuis RMF, Eijkel JCT, Segerink LI (2020) Point-of-care CRISPR/Cas nucleic acid detection: recent advances, challenges and opportunities. Biosens Bioelectron 166:112445

Wang R, Zhou L, Wang W, Li X, Zhang F (2017) In vivo gastrointestinal drug-release monitoring through second near-infrared window fluorescent bioimaging with orally delivered microcarriers. Nat Commun 8:14702

Wang H, Wu T, Li M, Tao Y (2020a) Recent advances in nanomaterials for colorimetric cancer detection. J Mater Chem B 9:e163

Wang X, Xie Y, Jiang N, Wang J, Liang H, Liu D, Yang N, Sang X, Feng Y, Chen R, Chen Q (2020b) Enhanced antimalarial efficacy obtained by targeted delivery of artemisinin in heparin-coated magnetic hollow mesoporous nanoparticles. ACS Appl Mater Interfaces 13:e70

Witika BA, Makoni PA, Mweetwa LL, Ntemi PV, Chikukwa MTR, Matafwali SK, Mwila C, Mudenda S, Katandula J, Walker RB (2020) Nano-biomimetic drug delivery vehicles: potential approaches for COVID-19 treatment. Molecules 25:5952

Wu H, Chen X, Zhang M, Wang X, Chen Y, Qian C, Wu J, Xu J (2021) Versatile detection with CRISPR/Cas system from applications to challenges. TrAC Trends Anal Chem 135:116150

Xu W, Jin T, Dai Y, Liu CC (2020) Surpassing the detection limit and accuracy of the electrochemical DNA sensor through the application of CRISPR Cas systems. Biosens Bioelectron 155:112100

Yang C, Wu T, Qi Y, Zhang Z (2018) Recent advances in the application of vitamin E TPGS for drug delivery. Theranostics 8:464

Yang Y, Song Y, Bo X, Min J, Pak OS, Zhu L, Wang M, Tu J, Kogan A, Zhang H (2020) A laser-engraved wearable sensor for sensitive detection of uric acid and tyrosine in sweat. Nat Biotechnol 38:217–224

Yao H, Shum AJ, Cowan M, Lähdesmäki I, Parviz BA (2011) A contact lens with embedded sensor for monitoring tear glucose level. Biosens Bioelectron 26:3290–3296

Yu M, Stott S, Toner M, Maheswaran S, Haber DA (2011) Circulating tumor cells: approaches to isolation and characterization. J Cell Biol 192:373–382

Zhang F (2019) Development of CRISPR-Cas systems for genome editing and beyond. Q Rev Biophys 52:112

Zhang D, Xu Y, Liu Q, Xia Z (2018) Encapsulation of $CH_3NH_3PbBr_3$ perovskite quantum dots in MOF-5 microcrystals as a stable platform for temperature and aqueous heavy metal ion detection. Inorg Chem 57:4613–4619

Zhang X, Wu X, Liu X, Chen G, Wang Y, Bao J, Xu X, Liu X, Zhang Q, Yu K (2020a) Heterostructural CsPbX3-PbS (X = Cl, Br, I) quantum dots with tunable Vis–NIR dual emission. J Am Chem Soc 142:4464–4471

Zhang BL, Yang Y, Zhao ZQ, Guo XD (2020b) A gold nanoparticles deposited polymer microneedle enzymatic biosensor for glucose sensing. Electrochim Acta 358:136917

Zuo J, Yuan Y, Zhao M, Wang J, Chen Y, Zhu Q, Bai L (2020) An efficient electrochemical assay for miR-3675-3p in human serum based on the nanohybrid of functionalized fullerene and metal-organic framework. Anal Chim Acta 1140:78–88

35 Carbon Nanodots-Based Electrodes in Biomolecular Screening and Analysis

Venkataraman Dharuman

Contents

1 Introduction 764
2 Glucose Sensing at Carbon Quantum Dots 766
3 CND-Based DNA Sensors 771
4 Neurotransmitter Analysis Using CND-Based Transducer 775
5 CND Biosensors in Food 778
6 CND Biosensors in Environmental Applications 778
7 Future Perspectives 779
References 780

Abstract

Development of highly sensitive and rapid sensor devices is the current requirement for early diagnosis of communicable and non-communicable diseases, and discretion of edible food consumption and environmental pollutants to safeguard the healthy society. Advanced nanomaterials offer a viable solution to improve the sensitivity of biosensing. Zero-dimensional carbon (CND) and graphene (GND) nanodots are intensively explored recently in the fields of electronics, materials, capacitors, and sensors as electrode material due to their fluorescence, tuneable electronic characteristics, natural abundance, biocompatibility, presence of oxy functional groups, and less toxicity. This chapter presents recent developments and applications, with special interest as an electrode material for chemical and biochemical sensing.

Keywords

Carbon dot · Electrode · Bioanalysis · Glucose · Neurotransmitters · Food · Environmental

V. Dharuman (✉)
Department of Bioelectronics and Biosensors, Alagappa University, Karaikudi, India
e-mail: dharumanudhay@yahoo.com

© Springer Nature Singapore Pte Ltd. 2023

U. P. Azad, P. Chandra (eds.), *Handbook of Nanobioelectrochemistry*,
https://doi.org/10.1007/978-981-19-9437-1_35

1 Introduction

Electrochemistry plays pivotal role in developing modern bio-screening and analytical instruments for applications in medical, environmental, transportation, and agricultural fields due to its simple operation, easy instrumentation, portability, reduced sample volume in micro or nanolitre scale, direct data correlation with electronic signal, fast analysis, and cost-effectiveness. The electrochemical sensor measures changes in either current or resistance of the working electrode upon its interaction with recognition layer or target present in the analyte solution. Carbon with atomic number 6 and mass 12, a natural ubiquitous material, has been exploited heavily in batteries, capacitors, energy storage devices, and transducers in electrocatalysis and biosensors from eighteenth century following its application in chloroalkali industries. This is due to its high corrosion resistance, wide potential range, and tuneable surface properties with like hydroxyl, keto, and carboxyl groups. Both graphite and glassy carbon became workhorses in the development of electroanalytical science. These low cost materials are regularly employed in development of sensors for various bioanalytes sensing, including toxic gases. Compared to these electrodes, invention of carbon nano derivatives like fullerene, carbon nano tubes, graphene, carbon dots with extended basic sp^2 carbon network, aromatic structure with enhanced surface-to-volume ratio, distinct optical and electronic properties provide new dimensions of applications in sensing science and technology (Campuzano et al. 2019; Ji et al. 2019). In the carbon nano family, zero-dimensional CND and GND have attracted considerable interests as an electrode material for sensing applications (Ngo et al. 2020; Ji et al. 2020; Hassanvand et al. 2020; Molaei 2020).

Origin of CND invention is dated back to the pioneering work of carbon nanotube (CNT) synthesis by arc discharge method and electrophoretic purification by Xu et al. (2004). During this process, black-colored CND having size below 10 nm with fluorescent activity was obtained (Sun et al. 2006; Ji et al. 2020). Strong photoluminscent nature resulting from quantum confinement of sp^2 aromatic carbon and tunable size, shape and edge effects (Tang et al. 2019). On the other side, its good aqueous solubility, biocompatibility with less toxicity enables its application in imaging, drug delivery, and sensing. It is amorphous spherical material consisting of sp^2 (graphitic) containing –OH, COOH, NH_2 groups (Hu et al. 2019; Hoang et al. 2019a, b), which are used to anchor for chemical and biological molecules, doping with phosphorous, sulfur, and boron to form respective derivatives. CNDs are prepared by both chemical (hydrothermal, electrochemical, ultrasonication, microwave) and physical (laser ablation, arc discharge, plasma treatment) methods (Sweetman et al. 2019; Iravani and Varma 2020; Huang et al. 2019; Zhao et al. 2020; Liu et al. 2020; Tajik et al. 2020) and detailed in recent reviews (Ngo et al. 2020; Ji et al. 2020; Hassanvand et al. 2020; Molaei 2020). Bottom-up method utilizes citric acid, glucose, polyethylene glycol, urea, ionic liquids, and so on, as precursors in the synthetic routes like pyrolysis-solvothermal, hydrothermal carbonization, and microwave/ultrasonication (Hoang et al. 2019a, b). Similar to the enhanced photoluminescence observed for CND due to the presence of edge functional groups, CND exhibits higher electrochemical heterogeneous electron transfer rate than the GND (Ratinac et al. 2011). GND obtained from graphene through top-down method has lateral size below 100 nm with sp^2 and sp^3 carbons arranged in sheet like structure, whereas CND contains sp^2 conjugated carbon network with carboxyl and aldehyde functional groups and edges (Ponomarenko et al. 2008; Lu et al. 2019a, b). Electronic and electrochemical properties of CND and GND are quite similar to graphene, graphite, GCE, and boron-doped diamond electrodes, which exhibit potential window of ca. –2.0 to 2.0 V in 0.1 M PBS and lower charge transfer resistance for electroactive ferro/ferricayanide and ruthenium hexamine redox couples (Faridbod and Sanati 2019; Hassan et al. 2014). For comparison, the GND was prepared using top-down method, while CND was prepared via bottom-up method by pyrolysis of lauryl gallate at 270 °C. These QDs modified the basal plan pyrolytic graphite (BPPG) electrode by drop casting method (1 mg mL^{-1} in 50 mM phosphate buffer solution, pH 7.2). Cyclic voltammetric studies using CND and GND transducer indicate an oxidation peak at ~0.4 V (vs. Ag/AgCl) for the presence of quinine functionality in CND, whereas the GND shows no peak in the potential window ~+ 1.1 V and − 1.0 V confirming absence of quinine functionality. This study again confirms higher heterogeneous electron transfer rate for CND than the GND and BPPG (Tian et al. 2021; Martínez-Periñán et al. 2019). Studies further confirmed that (Lim et al. 2015) the electrochemical properties of NDs are influenced by preparation method, number of edge planes, oxy functional groups, size, and shape (Li et al. 2019a, b, c; Fajardo et al. 2019). These differential properties of CND and GND drive them as electrode material for sensitive sensing of bioanalytes (Fig. 35.1). Medical, food, and environmental importance of glucose, neurotransmitters, DNA, antigen, metal ions, organic pollutants and their presence in ultralow concentrations in sample matrices invited high

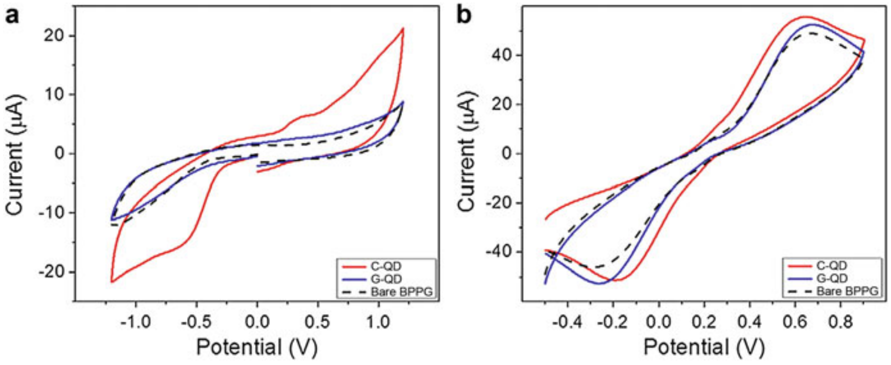

Fig. 35.1 Cyclic voltammograms of GND and CND compared against bare BPPG in (**a**) 50 mM phosphate buffer (pH 7.2) and (**b**) 10 mM potassium ferro/ferricyanide. Scan rate: 100 mV s^{-1} (Lim et al. 2015), reproduced with copyright permission from Elsevier

interest for their quantification using sensitive electrode materials like CND and GND.

2 Glucose Sensing at Carbon Quantum Dots

Diabetes, a chronic disease, occurs due to high accumulation of unutilized glucose in blood leading impairment or malfunctioning of human organs like heart, kidney, liver failures, blindness and stroke and increases the mortality rate. Worldwide prevalence of diabetes is predicted to be 10.9% in 2045 (Teymourian et al. 2020) and impacts economic development by increasing medical expense. Normal range of glucose in body fluid ranges from 80 mg/dL to 140 mg/dL (4.4–7.7 mM/dL) for healthy person compared to diabetes person having glucose concentration more than 140 mg/dL. Early detection of this chronic disease by quantifying small incremental change in blood glucose concentration level from the 140 mg/dL will prevent patient from organ failure and enhances lifespan of diabetes with proper medication and change in lifestyle. This drives development of cost-effective sensors for glucose estimation by both invasive and non-invasive methods. In the research and development, the important parameters of sensor investigated are linearity range (output signal varies linearly with concentration), limit of detection (LOD, lowest concentration at which sensor gives inferable output signal), accuracy, signal stability and reproducibility. Carbon dot (GND, CND, NCND) and its composite with metal or polymer are used in both fluorescence and electrochemical glucose sensing (Ngo et al. 2020; Ji et al. 2020; Hassanvand et al. 2020; Molaei 2020). Fluoresce emission property of nanomaterial (absorbing shorter wavelength light and emiting higher wavelength light) is widely utilized for biosensing. Because enzyme proteins interact strongly with graphene dots through hydrophobic and π-electron characters, peroxidase-like activity of CND and N-doped CND were to quantify H_2O_2 and glucose (Zheng et al. 2013)-based horseradish peroxidise and 3,5,5-tetramethylbenzidine (TMB). Compared to graphene and graphene oxide which quenches fluorescence, the inherent fluorescence by GND and CND lead developments of "turn-off" and "turn-on" glucose sensors. In the turn-on fluorescence, decoration metal ion on CND or GND quenches inherent fluorescence of NDs and removal of the metal by chemical reaction will turn on the fluorescence. For example, AgNP decoration on CND's surface quenches fluorescence. In the next step, H_2O_2 generated from the GOD and glucose reaction etches away the AgNP on CND surface and restores fluorescence of CND (Ma et al. 2017a, b). GND was modified with boronic acid using 3-aminobenzeneboronic acid, (APBA-GND) CND in "turn-off" mode non-enzymatic fluorescence glucose sensing (Qu et al. 2013; Shen and Xia 2014). High-affinity interaction of boronic acid with glucose leads aggregation of CND and quenching of fluorescence with blue shifting the fluorescence peak. Fluorescence intensity decreases with increasing glucose concentration in a linear range from 0 to 10 mM with LOD 5.0 μM. The sensor showed high selectivity in presence of other saccharides, for example, D-fructose, mannose, galactose, sucrose, lactose, and maltose. Similarly, the APBA-CND sensor showed a lower linear range 9–900 μM and higher LOD 1.5 μM. These parameters are 10–250 and 3–200 times lower than other boronic acid-based fluorescent nano sensing systems (Sun and Lei 2017; Wei et al. 2014; Mello et al. 2019). Linear range of glucose detection, suitable for clinical analysis, is extended by CND incorporated and glucose-imprinted poly(*N*-isopropylacrylamide-acrylamide-vinylphenylboronic acid) [poly(NIPAM-AAm-VPBA)] copolymer microgels in developing "turn-off" glucose sensing by Wang et al (Wang et al. 2015). The "turn-off" glucose sensing was developed in presence of Fe^{2+} ions, CND, GOD. Reaction between Fe^{2+} and H_2O_2 (Fenton's reaction) produces hydroxyl radicals and quenches CND fluorescence (Mello et al. 2019); see Fig. 35.2. A "turn-on" fluorescence glucose sensing was reported by utilizing CND and MnO_2. Following the reaction between GOD and glucose to produce 151 H_2O_2 and the removal of MnO_2 metal nanoparticles from the CND surface, a fluorescence 150 signal was visible at 510 nm. The linear range of this sensor is 2 to 130 M with a LOD of 50 nM. (Ma et al. 2017a, b).

Compared to the fluorescence method, electrochemical technique that measures changes in current or resistance of the electrode before and after target analyte reaction is attracting very high interest owing to its simple experimental designs, direct data correlation, portable, and user-friendly instrumental operations. In this method, GOD enzyme was immobilized onto a Platinum electrode using semipermeable selective polymers (poly carbomate and cellulose acetate) and its reaction with blood glucose produces gluconic acid and H_2O_2. The latter is detected amperometrically at 0.6 V (Ag/AgCl). Output current is directly proportional to the glucose concentration, Eqs. 35.1, 35.2 and 35.3. This principle was proposed in 1962 by Leland C. Clark at New York Academy of sciences symposium (Heller and Feldman 2008; Pohanka and Skladal 2008):

$$\mathrm{GOD(FAD)} + \mathrm{Glucose} \rightarrow \mathrm{Glucolactone} + \mathrm{FADH_2} - \mathrm{GOD} \tag{35.1}$$

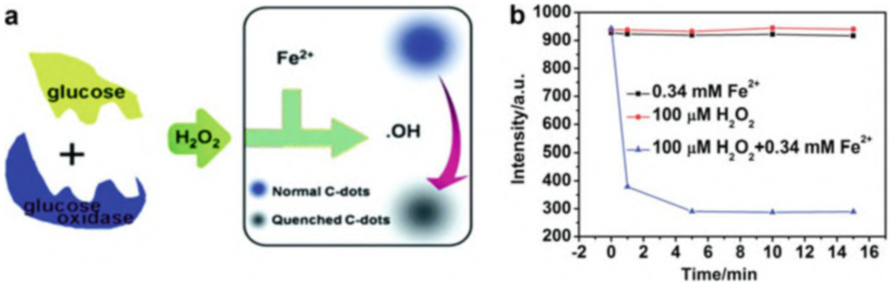

Fig. 35.2 (**a**) Scheme of glucose sensing in presence of Fe^{2+} and H_2O_2 using CND (available in journal online version). (**b**) Time-dependent fluorescence changes of C-dots at 410 nm in the presence of Fe^{2+} and H_2O_2, respectively; time-dependent fluorescence changes of C-dots in the presence of Fe^{2+} and H_2O_2 simultaneously (Wei et al. 2014), reproduced with copyright permission from the Royal Society of Chemistry

$$\mathrm{FADH_2 - GOD + O_2 \rightarrow FAD - GOD + H_2O_2} \tag{35.2}$$

$$\mathrm{H_2O_2\ Pt\ (0.6\ V\ Ag/AgCl) \rightarrow ½\ O_2 + 2H_2O} \tag{35.3}$$

Because the redox active $FADH_2$ in the GOD is embedded in the protein shell, direct charge transfer (DET) from $FADH_2$ to transducer is too slow and limits glucose sensing. DET enhancing strategies lead development of three different generations of glucose sensors. In the first generation, GOD was immobilized onto a Pt surface and glucose sensing was made by measuring H_2O_2 oxidation current at 0.2–0.8 V (SCE) and oxygen mediates glucose oxidation. However, higher oxidation potential of H_2O_2 co-oxidizes potential interferents like ascorbic and uric acid. In addition, poor solubility of O_2 in biological fluids leads signal instability. Interferences signal was eliminated using cation exchange or perm selective polymer membranes (poly carbomate and cellulose acetate) (Newman and Turner 2005). Second-generation sensor replaced the oxygen mediator using non-physiological metal complex such as ferrocene, quinone, ruthenium complexes, ferricyanide, phenoxazine and/or organic conducting salts, which are coimmobilized with GOD using binder and conducting carbon paste and /or polymer. Use of these mediators reduced glucose sensing over potentials below 0.7 V by enhancing the DET. The major drawback of this is leaching of aqueous soluble mediator from the immobilization matrix affecting data accuracy and DET rate. This is alleviated in the third-generation sensors, where GOD is wired with conducting nanomaterials or polymers to mediate directly the glucose oxidation. Close proximity between the enzyme and electrode increases DET signaling process and sensitivity. Infusion of advanced nanomaterials and nanoelectronics in the design and development of sensor technology produces innovative glucose monitoring devices for both in-vitro and in-vivo quantification. Nano metals, metal oxides, carbons (graphite, CNTs, graphene, and carbon dot) are utilized in developing all three generations of glucose sensors. The sensing properties such as selectivity, sensitivity, reproducibility, stability, and linear range depend highly on the nature of electrode material and enzyme immobilization methods (Teymourian et al. 2020). GOD is attached on the CND, GND, and N, S-doped CND by two different methods. In the first method, surface groups are used for covalent linking of GOD enzyme on the carbon surface. In the second method, CND surface is decorated nano metal, metal oxide or polymer followed by GOD immobilization. Apart from these two methods, entrapment of GOD enzyme in ionic liquid having low vapour pressure and tunable chemical properties increases the stability, conductivity, and detection sensitivity. Therefore, the first-generation glucose sensor was fabricated using CND, amino-terminated IL (1-butyl-3-methylimidazolium tetrafluoroborate [apmim][BF_4]) and GOD. Graphite rod was electrochemically exfoliated in presence of ionic liquid ([apmim][BF4] to form CND-[apmim][BF_4] composite (Li et al. 2014). The composite is then mixed with GOD in nafion polymer and modified the GCE. The sensor showed an O_2 reduction peak at −0.3 V to produce H_2O_2 and the reduction peak current varies linearly form 0 μM to 2 mM with LOD 7 μM. The sensor is validated to quantify blood glucose in 4 mL of 0.1 M PBS (pH 7.4). The measured concentration of 6.4 mM is nearly equal to the value (6.7 mM) of commercial glucometer. Similarly, NCND-chitosan-GOD (Ji et al. 2016)-modified GCE detects glucose at lower negative potential −0.47 V in human serum sample in the range from 1 to 12 mM (R = 0.99). For this, NCND was prepared from polyacrylamide material by hydrothermal method and mixed with chitosan polymer and GOD. This sensor exhibits good stability; reproducibility and selectivity in presence of potential interferences uric acid, ascorbic acid, dopamine, tryptophan, tyrosine, and cysteine. Since covalent linkage provides high stability to the reaction layer, the CND-AuNP GOD (Buk and Pemble 2019) layer is tethered on cysteamine monolayer functionalized gold microarray using carbodiimide coupling and glucose sensing was made in the linear range 0.16–4.32 mM at −0.6 V in air saturated PBS (pH 7.4) and wine. The data reliability was verified using commercial meter and spectrometric method; see Fig. 35.3. Self reduction property of CND prepared from citric acid is used to deposit Ag from $AgNO_3$ to form CND-Ag and dispersed in chitosan polymer to form Chitosan-AgNPs@GNDs (Tran et al. 2019). This composite exhibits H_2O_2 reduction current at −0.5 V selectively in presence of 0.1 μA lactose in range from 0.1 to 2 mM. Differences in linear ranges and LODs, may arise from different experimental conditions, immobilization chemistry and sample matrices used for glucose analysis. Similar to glucose analysis, lactate metabolite analysis was reported using CND-Lactase oxidase in human serum in alkaline condition (Bravo et al. 2019). Thermal carbonization method was used to prepare CND from ethylene glycol bis-(2-aminoethyl ether)-N,N,N,N-tetraacetic acid (EGTA), and tris(hydroxymethyl)amino methane. Lactate oxidase, glucose oxidase, and uricase enzymes were used to prepare biosensors and analytical parameters from CND-lactase biosensor were; linear range from 3.0 to 500 μM with sensitivity $4.98 \times 10^{-3} \mu A \mu M^{-1}$ and LOD 0.9 μM.

Although enzyme-based glucose sensor is accurate and reliable, it suffers from long term stability at elevated temperature and pH, requires complex immobilization procedure (Du Toit and Di Lorenzo 2014; Adeel et al. 2020). Therefore, non-enzymatic glucose attracts greater interest in recent times in the context of low cost sensor fabrication for regular diabetes monitoring. Hence, direct glucose sensing at metal (Pt, Au, Ag, Pd, Cu, Ni, etc.) and metal oxide (CuO, RuO_2, NiO, CoO, MnO_2, Co_3O_4, etc.) surface is a fascinating research area. These materials are reactive in pH $\geq$ 7, where higher oxidation state of metal ion mediates the glucose oxidation (Zhu et al. 2016; Shankara Narayanan et al. 2013; Dharuman and Chandrasekara Pillai 2006) to CO, H_2O, and O_2. However, electrode fouling from CO adsorption on electrode surface, poor selectivity, signal instability and fabrication cost are limiting their practical applications. Carbon nanomaterials are used as support to anchor these metal or metal oxides to enhance surface area and sensing. Hydrothermally prepared $NiCo_2O_4$ is attached on NH_2-GND surface on carbon cloth to form $NiCo_2O_4$/GNDs carbon cloth (Wu et al. 2020). This senses glucose at +0.6 V in 0.1 M NaOH in the range from 1 to 159×10^{-6} M and obtained LOD 0.27×10^{-6} M (S/N = 3). In another work, the $NiCo_2O_4$ is electrodeposited on CND-MWCNT-1-butyl-3-methyl-imidazolium bromide (MWCNTs/IL/GND) to get CND-MWCNT-$NiCo_2O_4$ (Nasr-Esfahani et al. 2019a, b). Glucose is detected at +0.45 V in linear ranges from 1.0 to190.0 and 190.0 to 4910 mM with LOD

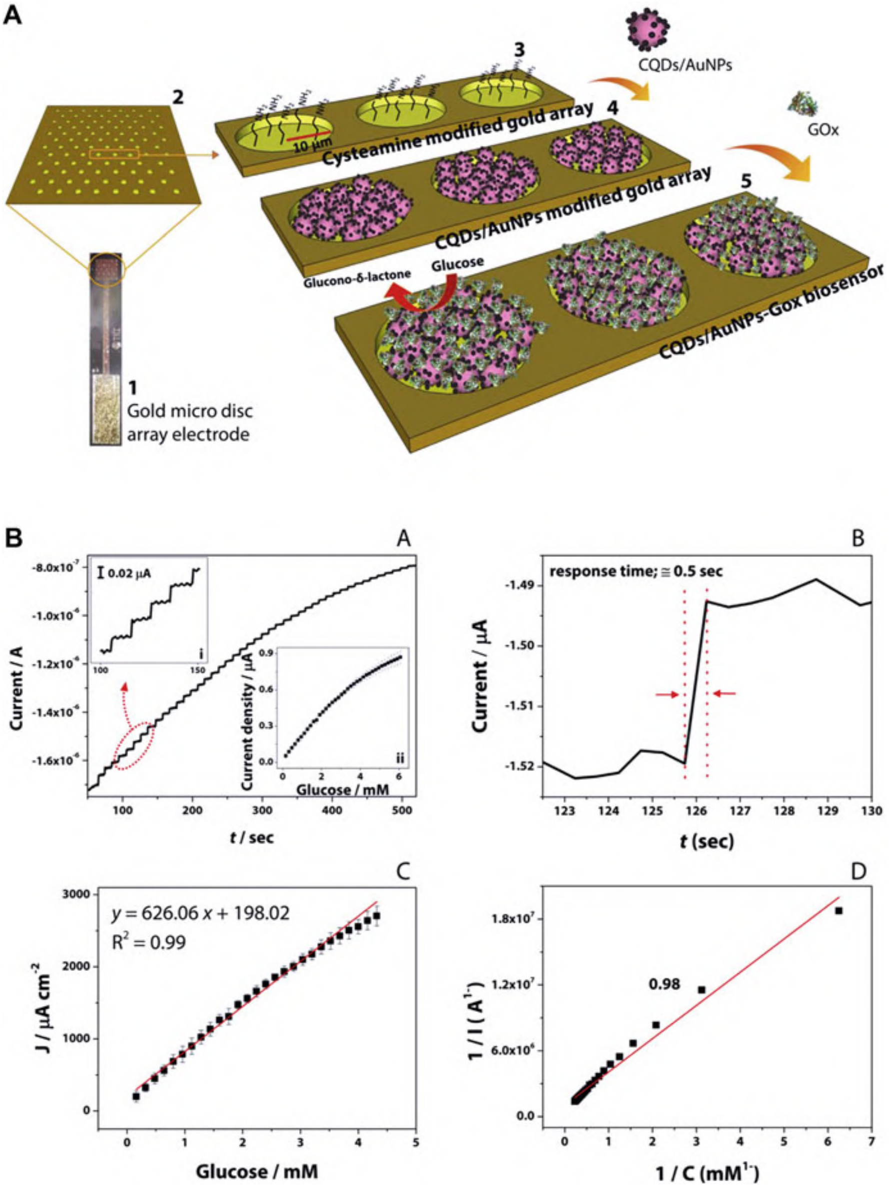

Fig. 35.3 (**a**) Schematic diagram of the biosensor preparation process; (1) the bare individual disk array electrode, (2) magnified surface of array, (3) amine-functionalized gold surface after cysteamine modification, (4) CNDs/AuNPs attached surface, (5) GOx enzyme immobilized overall CNDs/AuNPs-GOx biosensor. Note that the size of the electrodes, nanomaterials, and biomolecule shown are not drawn to scale. (B) A. Chronoamperometric response of the CNDs/AuNPs-GOx micro disk array biosensor to the serial addition of 20 mL of 40 mM glucose in O_2-saturated 0.01 M PBS (pH 7.4) at a working potential of 0.6 V (inset i; detailed presentation of serial addition steps

0.3 mM. Glucose Concentration in human blood serum estimated using this sensor is comparable with hospital values. Electrochemically synthesized CND is used to anchor CuO by sonication to form CND-CuO composite and modified GCE to sense glucose at +0.5 V in the linear ranges from 0.5 to 5 mM selectively in presence of potential interferences viz., ascorbic acid, uric acid, dopamine, sucrose, and lactose. Sensor is validated in human blood serum samples (data not given) (Sridara et al. 2020). Hydrothermally derived GND was modified using CoNiAl synthesized by co-precipitation method. Carbon paste was prepared by mixing it with graphite, CND-CoNiAl, and paraffin oil. Glucose sensing was made in 0.1 M NaOH at 0.0 V in a range 0.01–14.0 mM with LOD 6 μM (S/N = 3) and sensitivity 48.717 μAmM^{-1} (Samuei et al. 2017). Practical applicability is demonstrated by measuring glucose in pre-treated orange and mango juices. Other than glucose sensing application, direct sensing of other metabolites H_2O_2, lactate using both CND and GND transducers. H_2O_2 is a potentially important oxidant and disinfectant in medical industry and its quantification of H_2O_2 is very important. In electrochemical method, conventionally enzymes like hemoglobin, myoglobin, and horseradish peroxidase have been used. PtNP-CND/ILGO composite was prepared using Hydrothermally derived CND-PtNP and mixed with [(apmin(BF_4)] and GO. H_2O_2 is sensed in PBS in the potential window +0.6 to −0.6 V by observing a reduction peak. Calibration curve was constructed by measurement of H_2O_2 reduction current at −0.08 V in the linear range from 0.5 to 10 mM selectively in presence of interferences UA, AA, and DA (Chen et al. 2018) GNDs-chitosan (GNDs-CS)-methylene composite film was reported for H_2O_2 sensing (Mollarasouli et al. 2017). GND/ZnO nanofibers (NFs) was used to sensing of intracellular release of H_2O_2 from cancerous and non-cancerous cells after anticancer drugs were administered with good selectivity and sensitivity (Yang et al. 2015). CNDs/octahedral-cuprous oxide (Cu_2O) composite was reported by Li et al., for detecting H_2O_2 at +0.6 V in the linear range from 0.02 to 4.3 mM with LOD 8.4 mM. Cu_2O/Nafion film electrode prepared without showed lower linear range from 0.3 to 4.1 mM and LOD 128 mM (Li et al. 2015).

3 CND-Based DNA Sensors

Gene sequence and antigen sensing based on sequence-specific affinity interaction provide deeper insight into basic understanding of disease development, detection, and prevention at early stage. Because the sequence-specific analysis or screening of DNA based on Watson-Crick base pairing principle is an easy and sensitive method

◀

Fig. 35.3 (continued) and inset ii; corresponding calibration curve of the biosensor). (**b**) The response time for the biosensor to reach the steady-state current. (**c**) Corresponding linear range of the biosensor. (**d**) The Lineweaver-Burk plot of the micro disk array biosensor (Buk and Pemble 2019), reproduced with copyright permission from Elsevier for the diagnosis of inherited diseases at early stage, fluorescence, electrical/electrochemical, mass, and thermal-based techniques are developed. Conventionally, a capture or target recognition layer is immobilized on a solid transducer to detect target DNA. In electrochemical method changes in the current, resistance, and capacitance of the transducer before and after its modification with capture probe (DNA, antibody, aptamer, cell, or tissue) and its sequential interaction with the target DNA are compared. Metals, metal oxides, polymers, graphite, carbon nanomaterials (single and multiwalled CNTs), graphene, carbon dots have been utilized as the transducers for developing DNA and immunosensors, envisaging the influence of transducer material in improving the sensitivity and selectivity. In addition to the conducting nature of transducer, immobilization method of recognition layer and other experimental conditions influence selectivity and sensitivity of target sensing. The recognition layer is immobilized using physical adsorption, covalent linking, entrapment, and encapsulation methods (Boon et al. 2000; Ferapontova 2018). Pyrolytic graphite electrode was modified with GND and single-stranded DNA (ssDNA) was physically adsorbed. Electrochemical behavior of this modified electrode was measured in presence of ferri/ferrro cyanide redox probe and observed decreased peak current for two reasons. (i) The ssDNA block the CND surface where ferri/ferrro cyanide redox probe reaction occurs. (ii) Electrostatic repulsion between the negatively charged ssDNA and ferri/ferrro cyanide redox probe may decrease direct reaction. Following this, the surface is hybridized with complementary target DNA and re-measured the electrochemical behavior and compared. The formation of dsDNA on CND surface removes the ssDNA and increases ferri/ferrro cyanide redox probe and hence increase in peak current was observed (Zhao et al. 2011).

Aptamers are short chain single-stranded nucleic acids (oligo nucleotides) or peptide molecules, synthesized by Systematic Evolution of Ligands by Exponential Enrichment (SELEX) method. These strands bind strongly with high affinity and specificity with targets and induce conformational changes. CND is used as the immobilization matrix for aptamer for sensing of DNA, antibody, or antigen (Blind and Blank 2015). Endocrine disrupting chemicals (EDC) interaction with endocrine receptors causes range of health hazards, including cancer, thyroid, obesity, and cardiovascular diseases. Conventionally chromatography and capillary electrophoresis methods are used for the detection of EDCs. But they are time consuming and expensive. Citrate derived CND is electrochemically deposited on a screen-printed electrode by potential cycling method. The surface is further functionalized with glutaraldehyde to covalently attach amine-functionalized aptamer for the detection of 17β-Estradiol (E2) in presence of progesterone, estriol (E3) and bisphenol A (Mat Zaid et al. 2020) using EIS technique in the presence of ferri/ferrocyanide redox probe. Differences between the charge transfer resistances (R_{CT}) obtained before and after E2 binding with aptamer (ΔRct %) was taken as the indicator of reaction between the probe and target. Decrease in the R_{CT} was noticed due to electrostatic repulsion between the immobilized aptamer and negatively charged ferri/ferrro cyanide redox. Binding of target antigen further increases the negative charge density and molecular crowding at the electrode/electrolytes interface and R_{CT}. ΔRct % varies linearly with concentration from 1.0×10^{-7} to 1.0×10^{-12} M with LOD 0.5×10^{-12} M. River water sample is spiked with known concentrations of E2 and signal recovery of 92.3% and 101.2% and RSD ($n = 3$) were observed. Insulin is a peptide hormone controlling the carbohydrate metabolism and its dysfunction lead diabetes and other physical impairments. Although insulin is quantified using nanomaterial-modified electrodes, use of high-affinity aptamer as recognition layer for detection of this peptide hormone is more specific and selective. For this, CND-chitosan polymer blend-modified GCE is functionalized glutaraldehyde and immobilized with aptamer (Abazar and Noorbakhsh 2019). Selective binding of insulin with aptamer is interrogated by EIS in range from 500 pM to 10 nM and observed LOD 106.8 pM (S/N = 3) and sensitivity 80.07 Ω nM^{-1}, respectively. D-penicillamine (DAP)-modified CND was decorated with AgNP to form composite DPA-CND-AuNP and modified with citrate capped and cysteamine-functionalized AuNP. Thiolated DNA was immobilized on this surface using gold thiol chemistry for the detection of *Haemophilus influenza* genome target in presence of double stranded intercalator toluidine blue. The sensor indicates presence of point mutation (one-, two-, and three-base mismatch mutations) in genome sequence and complementary target DNA (Saadati et al. 2020). This sensor exhibits a linear range from pM to 1 zM and LOD 1 zM. NiO-AuNFs prepared by electrospinning process was deposited on CND-MWCNT and modified a carbon screen-printed electrode. After blocking the unmodified surface using bovine serum albumin, NH_2-aptamer is covalently linked using EDC/NHS coupling. Aptamer Au-NiO-CND–MWCNT-SPCE detected target progesterone (Samie and Arvand 2020) in the range 0.01–1000 nM with LOD and LLQ 1.86 pM and 6.21 pM, respectively. CND/GCE was applied for direct quantification of Inosine (INO) which consists hypoxanthine and D-ribose (Karthikeyan et al. 2019). Interstitial concentrations of INO greater than 1 mM lead sepsis, morbidity, and mortality. Oxidation current of INO increases linearly with concentration in the range from 50×10^{-9} to 20×10^{-6} M and LOD 8.3×10^{-9} M (S/N = 3). Layer-by-layer construction method was used for fabrication of immune sensor for detecting IL-13R alpha 2. In the first step, diazonium-modified SPCE is immobilized with streptavidine using 1-ethyl-3-[3-dimethylaminopropyl] carbodiimide (EDC)/ e, N-hydroxysulfosuccinimide (Sulfo-NHS) (EDC/NHS) coupling. Biotin-labeled capture goat antihuman IL-13sRα2 antibody (BCAb) and IL-13sR alpha 2 were immobilized in a sequential step. In a parallel step, GND-MWCNT is functionalized HRP using EDC/NHS and antihuman IL-13sRα2 antibody detector antibody (Dab). Now these two are brought together for sensing step wherein IL-13Rα2 in colorectal cell lysates is reacted with DAb in presence of Hydroquinone in the range from 2.7 to 100 ng mL^{-1} IL-13sR alpha 2, with LOD value of 0.8 ng mL^{-1}(Serafin et al. 2019); see Fig. 35.4**.** Sandwich immunosensor was constructed on GND-Fe_3O_4@Ag core-shell nanostructure for the detection of Mycobacterium tuberculosis antigen (Tufa et al. 2018). NGND@SiO_2–Ru-PtNPs aptamer for thrombin (Du et al. 2019) and NGND-AuNP-NG CEA-binding aptamer (Shekari et al. 2019) were also reported. Sandwich hybridization miRNA detection is reported using acid-functionalized GND. Enzyme label HRP present on reporter DNA generated H_2O_2 and detected in the range from 1 fM to 100 pM and LOD 0.14 fM (Hu et al. 2016). The sensor was

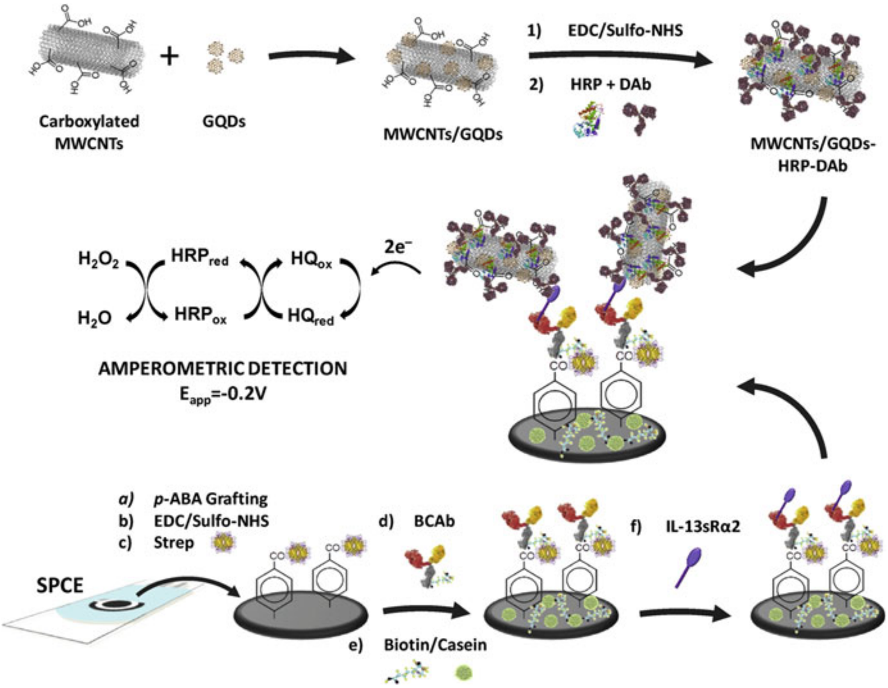
Carboxylated MWCNTs
+
GQDs
MWCNTs/GQDs
1) EDC/Sulfo-NHS
2) HRP + DAb
MWCNTs/GQDs-HRP-DAb
H_2O_2
H_2O
HRP_{red}
HRP_{ox}
HQ_{ox}
HQ_{red}
2e⁻
AMPEROMETRIC DETECTION
E_{app}=-0.2V
CO
a) p-ABA Grafting
b) EDC/Sulfo-NHS
c) Strep
SPCE
d) BCAb
e) Biotin/Casein
f) IL-13sRα2

Fig. 35.4 Schematic display of the different steps involved in the construction of the sandwich amperometric immunosensor for IL13sRα2 based on the immobilization of BCAb onto Strep/p-ABA/SPCE and the use of MWCNTs/GNDs-HRP-DAb nanocarriers (Serafín et al. 2019), reproduced with copyright permission from Elsevier

applied for detection of M.SssI MTase and restriction endonuclease HpaII in the linear range 1–40 unit mL^{-1} with LOD 0.3 unit mL^{-1}. Real application was demonstrated by monitoring M.SssI MTase activity inhibitor screening of procaine and epicatechin (Peng et al. 2017). Tyrosine kinase in human serum was quantified using disposable immunosensing platform prepared by immobilization of the specific anti-AXL antibody on GND on SPCE in presence of ferri/ferrocyanide redox probe in the linear range from 1.7 to 1000 pg mL^{-1} and LOD 0.5 pg mL^{-1}. Human serum samples collected from 5 different patients were spiked with target protein having concentrations from 25 to 250 pg mL^{-1} and observed good recovery of electrochemical signal (Mollarasouli et al. 2018). rGO/MWCNT/CS/CND was functionalized using glutaraldehyde and anti-lysozyme aptamer was immobilized. The bioelectrode was utilized for the detection of lysosome in the concentration range from 20 fM to 10 nM with LOD 1.9 fM. Practical application was demonstrated by estimating lysosome in egg white, which was diluted in human serum, urine, and blood (Rezaei et al. 2018). Wang group reported (Wang et al. 2013) ultrasensitive detection of Avian leucosis viruses using Fe_3O_4/GND, apoferritin-encapsulated Cu and secondary antibody. Conjugation of primary antibody with avian leucosis viruses antigen and secondary antibody releases Cu^{2+} from the apoferritin and detected electrochemically. Cu^{2+} current is proportionally increases in the linear range $10^{2.08}$ to $10^{4.50}$ TCID 50/mL with LOD 115 $TCID_{50}$/mL (S/N = 3). Metal-organic framework consisting both metal and organic ligand attracts good attention in improving electrochemical sensing activities. In this context, bimetallic metal–organic framework based on zirconium and hafnium (ZrHf-MOF)-modified CND (CNDs@ZrHf-MOF) was reported for human epidermal growth factor receptor-2 (HER2) detection in MCF-7 cells (Gu et al. 2019).

Detection of DNA drug interaction was demonstrated using daunorubicin (Eksin et al. 2020), topotecan (Mahmoudi-Moghaddam et al. 2019) $[Ru(bpy)_3]^{2+}$ (Liu et al. 2019a, b), and antimalarial drug quinacrine (Kucherenko et al. 2019) on CND-based electrodes. Methyldopa in pharmaceutical and biological samples were detected using DNA-modified CND electrodes in a dynamic linear range 0.04–750.0 μM with LOD 0.01 μM (Pathak et al. 2019). GNDs-PANI/ZnO composite was utilized for simultaneous sensing of Irinotecan (CPT-11), and 5-Fluorouracil (5-FU) in the linear ranges 0.1–25.0 and 0.1–50.0 μM and LODs 0.011 and 0.023 μM, respectively, in the pharmaceutical and biological samples (Sanati and Faridbod 2017). Applications of GND/CND-based modified electrodes for estimating pharmaceutical drugs is reviewed by Zahra Hassanvand et al. (Hatamluyi et al. 2019). Liposome anchored CND-AgNPs has detected for DNA in the linear range 10^{-16} to 10^{-11} M. (Oliveira et al. 2019). NGND-Au/Ag reported for detecting hydroxyl urea (Divya et al. 2019). Biological macromolecules such as proteins and peptides are formed using 20 basic amino acids. Amino acids are used for recycling, transamination, or energy production in body. Oxy functional groups on GND films attached to GCE were reduced electrochemically followed by AuNP deposition. MIB was then self assembled to form MIB/Au/ERGND/GCE composite for simultaneous detections of glutathione, UA, and tryptophan. Linear ranges of 0.03–40.0 μM and 40.0–1300.0 μM and LOD of 9 nM were observed for GSH (Mazloum-Ardakani et al. 2015). L-cysteine was quantified using PPy/GNDs@PB/GF-modified GCE (Wang et al. 2016).

4 Neurotransmitter Analysis Using CND-Based Transducer

Neurotransmitter (NT) is a signaling molecule existing at synaptic region between two excitable neuronal cells and involves in cell-cell communication in controlling central nervous system functions relating to physiological and human behavior. Detection and understanding role of each neuro chemical are essential to identify different neurological disease diagnoses and therapeutic applications. Concentrations of these chemicals are in the order of nano to femto mole per litter. Abnormal changes in the concentration level lead several diseases, notably Parkinson, Huntington, Alzheimer disease, strokes, hypertension, and so on, requiring control and quantification of these chemicals (Tavakolian-Ardakani et al. 2019). Electrochemical method became simple and important technique in neuro disease diagnosis. Carbon-based micro electrodes were already being used in medical applications for recording brain and neural connectivity. Still development of highly sensitive electrode or sensors is essential for the early diagnosis. High activity of neuro transmitters at carbon surfaces like graphite, glassy carbon electrode and their composites with metal, metal oxide, polymer were reported for the detection of biologically important neuro transmitters (dopamine, uric acid, serotonin, epinephrine, norepinephrine) in biological fluids. Surfactant stabilized CND/ZnO was implemented for simultaneous detections of Paracetamol and Ciprofloxacin. The sensor showed linear ranges 0.05–30.0 μM and 0.01–30.0 μM, with LODs 2.47 nM and 1.97 nM, respectively for Paracetamol and Ciprofloxacin (Hatamluyi et al. 2020). CND /MWCNT was reported for detection of dopamine and spiked dopamine, over a dynamic linear range 0.25–250 μM, with LODs 95 nM and 110 nM (S/N = 3), respectively (Kunpatee et al. 2020). GND /chitosan composite was used for simultaneous sensing triclosan and methyl paraben in cosmetics at +0.60 V (triclosan) and + 0.81 V (vs. Ag/AgCl). While triclosan exhibits linear range 0.10–10.0 μM with LODs 0.03, the methylparaben showed LOD 0.04 μM (Kumar Arumugasamy et al. 2020). 3-Aminopropyl-triethoxysilane-modified carbon nano dot (CDs-APTES) is biofunctionalized with acetylcholine esterase and choline oxidase using glutaraldehyde linker for the determination of acetylcholine indirectly by measuring H_2O_2 oxidation current at +0.4 V (Santana and Spinelli 2020**)**. A N-CND@Co_3O_4/MWCNT composite simultaneously determines Flutamide (FLU) and Nitrofurantoin (NF). The sensor exhibits linear ranges from 0.05 to 590 μM and 0.05 to 1220 μM and LOD 0.0169 μM and 0.044 μM, respectively (Bodur et al. 2020**)**. New robust nano-hybrid microelectrode was designed using BCND /ZnO nanorod for analysis of hydroquinone (HQ). Its higher activity compared to other similar reported work is attributed to vertically aligned ZnO nanorod on BCND. Linear response observed is 0.1 to 100 μM with LOD 0.03 μ M (Muthusankar et al. 2020). GND-MWCNT composite detects dopamine (DA) in linear range from 0.005 to 100 μM with LOD 0.87 nM (3S/N). Practical utility is demonstrated for sensing in DA in human serum and DA secreted from live PC12 cells (Hang and Bai 2020). Simultaneous analysis of norepinephrine and acetylcholine was made at GNDs/IL/CPE fabricated with CND and ionic liquid. It showed a linear range 0.2–400.0 μ M for norepinephrine (LOD 0.06 μM) (Huang et al. 2020). Polyethylene glycol-modified CND (PEG-CND) is electropolymerized on GCE for ascorbic acid detection. Two linear ranges of 0.01–3 mM and 4–12 mM were obtained with LOD 10 μM selectively in presence of potential interferents dopamine and uric acid (Jahani et al. 2020). CNDs prepared via a nitric acid oxidation of porous organic polymer (POP) and mechanochemical Friedel-Crafts alkylation is decorated with chitosan polymer and graphene on GCE for DA sensing by electrochemiluminescence (ECL) method with ammonium persulfate as a coreactant. Linear range observed is from 0.06 to 1.6 μM with LOD of 0.028 μ M (S/N = 3) in presence of interferences (Wei et al. 2019). Ag_2O-modified N,S-doped CND (Ag_2O/Ag@NS-CND), developed via hydrothermal method using p-iminobenzenesulfonic acid, senses amperometrically catechol at 0.25 V in linear response from 0.2 to 180 μ M with LOD 13 nM (S/N = 3) in water (Xu et al. 2019). Au-GNDs-Nafion (Zhan et al. 2019) senses DA in human urine and showed a linear range from 2 μM to 50 μM with LOD 0.84 μM. SnO_2/PANI/N-GND nanocomposite detects DA in the concentration range from 5×10^{-7} to 2×10^{-4} M with LOD 2.2×10^{-7} M (S/N = 3) (Jang et al. 2019). Lac-F,N-CDs GCE shows a LOD of 0.014 μM and sensitivity 219.17 μ A cm^{-2} mM^{-1} for catechol detection in tap water (Hsu and Wu 2019). CND-Fe_3O_4 NPs exhibited ultrafast electron transfer kinetics for uric acid oxidation (Liu et al. 2019a, b). CND detected adrenaline in presence of serotonin and ascorbic acid (Abbas et al. 2019). GCE/GNDs/AuNPs was developed for norepinephrine determination in a linear range 0.5 and 7.5 μM, with LOD 0.15 μM (Shankar et al. 2019). Sonochemically developed N-CND/SnO_2 utilized for riboflavin detection with sensitivity 2.496 μ A μM^{-1} cm $^{-2}$ in a linear range from 0.05 to 306 μM and LOD 8 nM (Fajardo et al. 2019). CND-AuNP reported for selective sensing of dopamine in presence of ascorbic acid and uric acid in a linear range from 10 to 600 μM and LOD 0.7 ± 0.18 μM. Blood serum and urine samples were employed for validating the sensor performance (Muthusankar et al. 2019a, b). GND-chitosan showed excellent electrosensing activity for epinephrine in a concentration range from 0.36 to 380 μM with LOD 0.3 nM (Kumar et al. 2018). CuO-His-GND detects hydroquinone in linear range 0.001–40 μ M and LOD 0.31 nM at S/N 3 in natural water samples (Tashkhourian et al. 2018). GND/SPE is used for simultaneous sensing of dopamine and tyrosine in the linear range from 0.1–1000 and 1.0–900 μM (Chen et al. 2019). GNDs/GCE was simultaneously detected hydroquinone and catechol and exhibits a peak separation of 113 mV between them. The sensor showed a linear range from 0.5 to 100 μM with LOD 0.08 μM (S/N = 3) (Beitollahi et al. 2018).

Molecularly imprinted polymers (MIPs), reported in 1930 Polyakov, synthesized using polymer template in presence of target molecules to sense structurally identical molecules via host-guest interaction. These materials exhibit high stability in rugged and horse environment and selectivity in sensing applications. Although different polymer templates were reported continuously, it possesses drawbacks of degradation, tedious synthetic procedure and stability. Electrochemical MIPs utilize the conductive substrates like carbon nano tubes, graphene, graphene oxide, gold nanoparticles and carbon dots in addition to polymer matrix to enhance the detection sensitivity (Walcarius and Sibottier 2005; Tang et al. 2018). Dopamine and chlorpromazine template Nicotinamide polymer CND-NiS_2 was reported for the detection of DA and CPZ in the linear ranges from 0.05–8 μ M and 8–40 μM and 0.005 to 2 μM with LODs 2.8 nM and 0.25 nM (S/N = 3) (Bel Bruno 2019). Amine-functionalized GND decorated with MnO_2 employed for vitamin B-2 and dopamine detection in linear ranges from 0.1 to 100 μM and LODs 0.04 μ M (V-B2) and 0.05 μ M (dopamine) (Lu et al. 2020). NCND-C_3N_4 –polypyrrole MIP was used for sensing of epinephrine in a linear range from 1.0×10^{-12} to 1.0×10^{-9} M and observed LOD 3.0×10^{-13} M (Lu et al. 2019a, b). N,S@GND-AuNP polymerized P-aminothiophenol MIP is used for detection of antiviral drug sofosbuvir (SOF) in a linear range 1–400 nM (Yola and Atar 2019).

5 CND Biosensors in Food

Increasing the consumption, production, and storage of food grains requires sensitive and selective sensors to ascertain the food quality. Recently both optical and electrochemical sensors were developed for monitoring temperature, humidity, pH, gases, pesticides, and pathogens (Mahmoud et al. 2019). CND-AuNP is used to quantify ractopamine (Rac) in the concentration range from 0.01 to 32.5 mgL^{-1} with LOD 1.2 μgL^{-1}, which is lower than previous report (1.5 μg/L) (Mustafa and Andreescu 2018). CTAB stabilized CND –chitosan composite is used for the analysis of food preservative mesalzine between the concentration range from 0.1 to 10 μM with LOD 0.05 μM (Song et al. 2020). GND-ZrO_2-BSA detects Ochratoxin A in coffee with detection range (1–20 ng mL^{-1}), sensitivity (5.62 μA mL ng^{-1} cm^{-2}), LOD (0.38 ng/mL), and signal recovery (95%) (Jalalia et al. 2020). N-CND/HP-Cu_2O/MWCNT hybrid composite detects caffeic acid at LOD 0.004 μ M with sensitivity 31.85 μA μ M^{-1} cm^{-2} (Gupta et al. 2020). NS-CND simultaneously determine paracetamol and p-aminophenol with peak potential difference is 0.24 V in linear ranges from 0.1 to 220 μM with LOD 26 nM (paramacetamol) and from 1.0 to 300 μM with LOD 38 nM (at S/N = 3) (PAP). Accuracy of detection is compared with HPLC method (Muthusankar et al. 2019a, b). GNDs/IL/MWCNTs-PANI senses imidacloprid in a linear range from 0.03 to 12.0 μ M L^{-1} with LOD 9 nM L^{-1}. Practical utility was demonstrated by quantification in vegetable samples (Wang et al. 2019). DNA-based sensing of *S. typhimurium* was made using MOF fabricated using grapheme –UiO-67 –AuNP using HRP labelled aptamer in a linear range from 2×10^1 to 2×10^8 CFU mL^{-1} with LOD 5 CFU mL^{-1} (S/N = 3) (Nasr-Esfahani et al. 2019a, b).

6 CND Biosensors in Environmental Applications

Environmental Sensors are essential for understanding the influence of environmental toxic gas pollutants volatile organic compounds, carbon dioxide, carbon monoxide, nitrogen and sulphur oxides (Dai et al. 2019). CND/ZrO_2 composite is applied for detection methyl parathion in rice in linear range from 0.2 ng mL^{-1} to 48 ng mL^{-1}, with LOD 0.056 ng mL^{-1} (Hanrahan et al. 2004). GND detects 10-Hydroxycamptothecin in the linear ranges from 1.5×10^{-8} M L^{-1} to 5.0×10^{-7} M L^{-1} and 5.0×10^{-7} M L^{-1} to 3.0×10^{-6} ML^{-1} with LOD 1.5×10^{-8} ML^{-1} and signal recoveries of 94.2–104% (Reddy et al. 2019). GNDs/PEDOT/GCE was used for rutin detection in the linear range 0.05 μ M and 10 μ M with LOD 11 nM (Li et al. 2019a, b, c). p-aminobenzenesulfonic acid CND-modified pencil graphite sensed folic acid selectively and sensitively in pharmaceutical and urine samples (Meng et al. 2019). Observed linear range was 2.2–30.8 ng mL^{-1} and LOD 2.02 ng mL^{-1}. N,S,P CNDs-AuNP-aptamer detects bisphenol in the concentration range 0.01 μM–120 μM, with LOD 5.273×10^{-10} M (Guney 2019). Similarly, bisphenol S was detected using B, N, F-CND-AgNP between concentration range from 1×10^{-8} M to 5×10^{-5} M with LOD 1.12×10^{-8} M in environmental and biological samples (Yao et al. 2019). A nanopore sensor was developed using SAuNPE-Prussian Blue on polypyrrole CND for hydrazine sensing at 0.3 V in a linear range 0.5–80 M and LOD 0.18 M (S/N = 3) in human urine (Yao et al. 2019). GND-modified SPE was utilized for the sensing of diethylstilbestrol in the linear range 0.05 to 7.5 μM L^{-1} with LOD 8.8 nM L^{-1} and 29.0 nM L^{-1}, respectively (Chen et al. 2019) in water. NGND derived from polyaniline was applied for the sensitive detection of 2,4,6-trinitrophenolwith LOD 0.2 ppb (similar to 200 ng/1 or 1 nM), (Gevaerd et al. 2019). GNDs/GNPs/GCE was developed for the determination of luteolin in pH 5.0. The sensor exhibits a wide linear range from 1×10^{-8} to 1×10^{-8} M with LOD 1.0 nM (S/N = 3) and signal recovery between 98.8% and 101.4% in peanut hull (Ramachandran et al. 2019). GND-CuO was reported for histidine detection (Tang et al. 2019). GND modified with mesoporous carbon ceramic electrode (DMCCE-GNDs) was used detection and determination of zolpidem (Zip) with LOD 0.061 μM Zlp (S/N = 3) (Hua et al. 2019). Nitrite detection at 3D flower-like beta-Ni(OH)$_2$@CDs in the linear range from 2.5×10^{-6} to 1.2×10^{-3} M with LOD 0.03 mM(S/N = 3) and detection sensitivity 647.8 mA mM^{-1} cm^{-2} (Dehgan-Reyhan and Najafi 2019). Michael addition is introduced into an AChE-based electrochemical sensing platform to enrich intermediate TCh on N-MAL-CD surface to detections of methyl parathion and paraoxon in the linear ranges 3.8×10^{-15}-3.8×10^{-10} M (methyl parathion) and 1.8×10^{-14}-3.6×10^{-10} M (paraoxon) with LODs 1.4×10^{-15} M and 4.8×10^{-15} M. (Mollarasouli et al. 2018). GND/ITO-based immunosensor is used to detect aflatoxin B-1 (AFB(1) in maize with sensitivity 213.88 $(ngmL^{-1})^{-1}$ cm^{-2} and LOD 0.03 $ngmL^{-1}$ and 0.05 ngg^{-1}, respectively, (Xu et al. 2018). CDs/Fe3O4 composite-modified g-C3N4 was reported for the detection of thiocyanate (SCN^{-}) in linearity range (0.001–0.900 μ M) and LOD 0.23 μ M (S/N = 3) (Bhardwaj et al. 2018). Review of NGND in biosensing and biomedical fields (Ponnaiah et al. 2018) was recently presented. Nafion/Hb/GOD/CILE was applied for quantifications of trichloroacetic acid, (6.0 similar to 100.0 mM.L^{-1}), $NaNO_2$ (2.0 similar to 12.0 mM.L^{-1}) and H_2O_2 (6.0 similar to 30.0 mM^{-1}) with good stability (Li et al. 2019a, b, c). Various environmental pollutions were detected Apt/AgNPs/thiol-GND/GCE (Karimzadeh et al. 2018) for TNT, GNDs/AgNP/GCE for TBHQ (Li et al. 2020), PEDOT-CNDs/GCE (Jiao et al. 2018) and NGNDs @ NCNFs/GCE (Li et al. 2017) for NO_2^{-}, Pt/NCNDs-MWCNT/GCE (Zhang et al. 2016), β-CD-GNDs-GCE (Zhang et al. 2015) for CH_3OH, NH2GNDs/CoPc/GCE (Centane et al. 2018), PPy/CDs/PB/SAuNPE for N_2H_2 (Chen et al. 2019a) were registered in literature.

7 Future Perspectives

Carbon dots prepared by different bottom-up methods are being reported as they provide new insights into their physical and chemical properties. These properties invite new challenges in their application. Although studies are rigorously focused on their utility in the development of different sensors in research laboratories for bioanalysis and screening, application as a smart device which could sense, quantify, and screen the diseased biosamples on field is still a challenging research area.

Differences in the linearity, sensitivity, and selectivity arose from different synthesis methods and routes adopted in literature indicated strong influence of synthesis methods on the sensing properties. Most of the researches confined to fabricate thin film electrode using drop casting method. Along with influence of synthesis method, the thin film fabrication using ink-jet, screen printing or chemical vapor deposition methods have to be adopted for fabrication of CND/GND sensor devices with controlled activity for practical and on-field applications.

Acknowledgment Author acknowledges financial supports from University Grants Commission (UGC) STRIDE (AU: SO (P&D) STRIDE Comp.I projects 2020: 21.12.2020) scheme, Alagappa University, Karaikudi, India.

References

Abazar F, Noorbakhsh A (2019) Chitosan-carbon quantum dots as a new platform for highly sensitive insulin impedimetric aptasensor. Sensors Actuators B Chem 304:127281

Abbas MW, Soomro RA, Kalwar NH, Zahoor M, Avci A, Pehlivan E, Hallam KR, Willander M (2019) Carbon quantum dot coated Fe_3O_4 hybrid composites for sensitive electrochemical detection of uric acid. Microchem J 146:517–524

Adeel M, Rahman MM, Caligiuri I, Canzonieri V, Rizzolio F, Daniele S (2020) Recent advances of electrochemical and optical enzyme-free glucose sensors operating at physiological conditions. Biosens Bioelectron 165:112331

Beitollahi H, Dourandish Z, Ganjali MR, Shakeri S (2018) Voltammetric determination of dopamine in the presence of tyrosine using graphite screen-printed electrode modified with graphene quantum dots. Ionics 24:4023–4031

Bel Bruno JJ (2019) Molecularly imprinted polymers. Chem Rev 119:94–119

Bhardwaj H, Singh C, Kotnala RK, Sumana G (2018) Graphene quantum dots-based nano-biointerface platform for food toxin detection. Anal Bioanal Chem 410:7313–7323

Blind M, Blank M (2015) Aptamers selection technology and recent advances. Mol TherNucl Acids 4:e223

Bodur OC, Dinc S, Ozmen M, Arslan FA (2020) Sensitive amperometric detection of neurotransmitter acetylcholine using carbon dot-modified carbon paste electrode. Biotechnol Appl Biochem 68:1886

Boon EM, Ceres DM, Drumond TG, Hill MG, Barton JK (2000) Mutation detection by electrocatalysis at DNA-modified electrodes. Nat Biotechnol 18:1096–1100

Bravo I, Gutierrez-Sanchez C, Garcia-Mendiola T, Revenga-Parra M, Pariente F, Lorenzo E (2019) Enhanced performance of reagent-less carbon nanodots based enzyme electrochemical biosensors. Sensors 19:5576

Buk V, Pemble MF (2019) A highly sensitive glucose biosensor based on a micro disk array electrode design modified with carbon quantum dots and gold nanoparticles. Electrochim Acta 298:97–105

Campuzano S, Yanez-Sedeno P, Pingarron JM (2019) Carbon dots and graphene quantum dots in electrochemical biosensing. Nano 9:634–651

Centane S, Sekhosana EK, Matshitse R, Nyokong T (2018) Electrocatalytic activity of a push-pull phthalocyanine in the presence of reduced and amino functionalized graphene quantum dots towards the electrooxidation of hydrazine. J Electroanal Chem 820:146–160

Chen D, Zhuanga X, Zhai J, Zhenga Y, Lua H, Chena L (2018) Preparation of highly sensitive Pt nanoparticles-carbon quantum dots/ionic liquid functionalized graphene oxide nanocomposites and application for H_2O_2 detection. Sensors Actuators B Chem 255:1500–1506

Chen W, Li RY, Li ZJ, Yang YQ, Zhu HY, Liu JK (2019) Promising copper oxide-histidine functionalized graphene quantum dots hybrid for electrochemical detection of hydroquinone. J Alloys Compd 777:1001–1009

Chen W, Wang H, Tang H, Yang C, Guan X, Li Y (2019a) Amperometric sensing of hydrazine by using single gold nanopore electrodes filled with Prussian Blue and coated with polypyrrole and carbon dots. Microchim Acta 186:350–357

Dai G, Li Z, Luo FF, Ai SY, Chen B, Wang QJ (2019) Electrochemical determination of Salmonella typhimurium by using aptamer-loaded gold nanoparticles and a composite prepared from a metal-organic framework (type UiO-67) and graphene. Microchim Acta 186:620

Dehgan-Reyhan S, Najafi M (2019) Defective mesoporous carbon ceramic electrode modified graphene quantum dots as a novel surface-renewable electrode: the application to determination of zolpidem. J Electroanal Chem 832:241–246

Dharuman V, Chandrasekara Pillai K (2006) RuO_2 electrode surface effects in electrocatalytic oxidation of glucose. J Solid State Electrochem 10:967–979

Divya KP, Karthikeyan R, Sinduja B, Grace AA, John SA, Hahn JH, Dharuman V (2019) Carbon dots stabilized silver-lipid nano hybrids for sensitive label free DNA detection. Biosens Bioelectron 133:48–54

Du Toit H, Di Lorenzo M (2014) Glucose oxidase directly immobilized onto highly porous gold electrodes for sensing and fuel cell applications. Electrochim Acta 138:86–92

Du FK, Zhang H, Tan XC, Ai CH, Li MR, Yan J, Liu M, Wu YY, Feng DF, Liu SG, Han HY (2019) Nitrogen-doped graphene quantum dots doped silica nanoparticles as enhancers for electrochemiluminescence thrombin aptasensors based on 3D graphene. J Solid State Electrochem 23(2019):2579–2588

Eksin E, Senturk H, Zor E, Bingol H, Erdem A (2020) Carbon quantum dot modified electrodes developed for electrochemical monitoring of Daunorubicin-DNA interaction. J Electroanal Chem 862:114011

Fajardo A, Tapia D, Pizarro J, Segura R, Jara P (2019) Determination of norepinephrine using a glassy carbon electrode modified with graphene quantum dots and gold nanoparticles by square wave stripping voltammetry. J Appl Electrochem 49:423–432

Faridbod F, Sanati AL (2019) Graphene quantum dots in electrochemical sensors/biosensors. Curr Anal Chem 15:103–123

Ferapontova EE (2018) DNA electrochemistry and electrochemical sensors for nucleic acids. Annu Rev Anal Chem 11:197–218

Gevaerd A, Banks CE, Bergamini MF, Marcolino LH (2019) Graphene quantum dots modified screen-printed electrodes as electroanalytical sensing platform for diethylstilbestrol. Electroanalysis 31:838–843

Gu C, Guo C, Li Z, Wang M, Zhou N, He L, Zhang Z, Du M (2019) Bimetallic ZrHf-based metal-organic framework embedded with carbon dots: ultra-sensitive platform for early diagnosis of HER2 and HER2-overexpressed living cancer cells. Biosens Bioelectron 134:8–15

Guney S (2019) Electrochemical synthesis of molecularly imprinted poly(p-aminobenzene sulphonic acid) on carbon nanodots coated pencil graphite electrode for selective determination of folic acid. J Electroanal Chem 845:113518

Gupta PK, Chauhan D, Khan ZH, Solanki PR (2020) ZrO_2 Nanoflowers decorated with graphene quantum dots for electrochemical immunosensing. ACS Appl Nano Mater 3:2506–2516

Hang Y, Bai X (2020) Flexible microsensor made of boron doped graphene quantum dots/ZnO nanorod for voltammetric sensing of hydroquinone. J Electrochem Soc 167:027541

Hanrahan G, Patil DG, Wang J (2004) Electrochemical sensors for environmental monitoring: design, development and applications. J Environ Monit 6:657–664

Hassan M, Haque E, Reddy KR, Minett AI, Chen J, Gomes VG (2014) Edge-enriched graphene quantum dots forenhanced photo-luminescence and supercapacitance. Nanoscale 6: 11988–11994

Hassanvand Z, Jalali F, Nazari M, Parnianchi F, Santoro C (2020) Carbon nano-dots in electrochemical sensors and biosensors: a review. ChemElectroChem 22:15–35

Hatamluyi B, Es'haghi Z, Modarres Zahed F, Darroudi M (2019) A novel electrochemical sensor based on GQDs-PANI/ZnO-NCs modified glassy carbon electrode for simultaneous determination of Irinotecan and 5-Fluorouracil in biological samples. Sensor Actuat B-Chem 286:540

Hatamluyi B, Zahed FM, Es'haghi Z, Darroudi M (2020) Carbon quantum dots co-catalyzed with ZnO nanoflowers and poly (CTAB) nanosensor for simultaneous sensitive detection of paracetamol and ciprofloxacin in biological samples. Electroanalysis 32:1818–1827

Heller A, Feldman B (2008) Electrochemical glucose sensors and their applications in diabetes management. Chem Rev 108:2482–2505

Hoang VC, Dave K, Gomes VG (2019a) Iodine doped composite with biomass carbon dots and reduced graphene oxide: a versatile bifunctional electrode for energy storage and oxygen reduction reaction. J Mater Chem A 7:22650–22662

Hoang VC, Dave K, Gomes VG (2019b) Carbon quantum dot-based composites for energy storage and electrocatalysis: mechanism, applications and future prospects. Nano Energy 66: 104093–104110

Hsu WF, Wu TM (2019) Electrochemical sensor based on conductive polyaniline coated hollow tin oxide nanoparticles and nitrogen doped graphene quantum dots for sensitively detecting dopamine. J Mater Sci Mater Electron 30:8449–8456

Hu T, Zhang L, Wen W, Zhang X, Wang S (2016) Enzyme catalytic amplification of miRNA-155 detection with graphene quantum dot-based electrochemical biosensor. Biosens Bioelectron 77: 451–456

Hu C, Li M, Qiu J, Sun YP (2019) Design and fabrication of carbon dots for energy conversion and storage. Chem Soc Rev 48:2315–2337

Hua Y, Li S, Cai YY, Liu H, Wan YQ, Yin MY, Wang FX, Wang H (2019) A sensitive and selective electroanalysis strategy for histidine using the wettable well electrodes modified with graphene quantum dot-scaffolded melamine and copper nanocomposites. Nanoscale 11:2126–2130

Huang D, Zhou H, Wu Y, Wang T, Sun L, Gao P, Sun Y, Huang H, Zhou G, Hu J (2019) Bottom-up synthesis and structural design strategy for graphene quantum dots with tunable emission to the near infrared region. Carbon 142:673–684

Huang QT, Lin XF, Tong LL, Tong QX (2020) Graphene quantum dots/multiwalled carbon nanotubes composite based electrochemical sensor for detecting dopamine release from living cells. ACS Sustain Chem Eng 8:1644–1650

Iravani S, Varma RS (2020) Green synthesis, biomedical and biotechnological applications of carbon and graphene quantum dots, a review. Environ Chem Lett 18:703–727

Jahani PM, Jafari M, Gupta VK, Agarwal S (2020) Graphene quantum dots/ionic liquid modified carbon paste electrode-based sensor for simultaneous voltammetric determination of norepinephrine and acetylcholine. Int J Electrochem Sci 15:947–958

Jalalia F, Hassanvanda Z, Baratia A (2020) Electrochemical sensor based on a nanocomposite of carbon dots, hexadecyltrimethylammonium bromide and chitosan for mesalazine determination. J Anal Chem 75:544–552

Jang HS, Kim D, Lee C, Yan B, Qin X, Piao Y (2019) Nafion coated Au nanoparticle-graphene quantum dot nanocomposite modified working electrode for voltammetric determination of dopamine. Inorg Chem Commun 105:174–181

Ji H, Zhou F, Gu J, Shu CX, Jia K, X. (2016) Nitrogen-doped carbon dots as a new substrate for sensitive glucose determination. Sensors 16:630

Ji Z, Dervishi E, Doorn SK, Sykora M (2019) Size dependent electronic properties of uniform ensembles of strongly confined graphene quantum dots. J Phys Chem Lett 10:953–959

Ji C, Zhou Y, Leblanc RM, Peng Z (2020) Recent developments of carbon dots in biosensing: a review. ACS Sens 5:2724–2741

Jiao M, Li Z, Li Y, Cui M, Luo X (2018) Poly(3,4-ethylenedioxythiophene) doped with engineered carbon quantum dots for enhanced amperometric detection of nitrite. Microchim Acta 185:249

Karimzadeh A, Hasanzadeh M, De Shadjou N, la Guardia M (2018) Optical bio (sensing) using nitrogen doped graphene quantum dots: recent advances and future challenges. TrAC Trends Anal Chem 108:110–121

Karthikeyan R, Nelson DJ, John SA (2019) Non-enzymatic determination of purine nucleotides using a carbon dot modified glassy carbon electrode. Anal Methods 11:3866–3873

Kucherenko IS, Soldatkin OO, Kucherenko DY, Soldatkina OV, Dzyadevych SV (2019) Advances in nanomaterial application in enzyme-based electrochemical biosensors: a review. Nanoscale Adv 1:4560–4577

Kumar Arumugasamy S, Govindaraju S, Yun K (2020) Electrochemical sensor for detecting dopamine using graphene quantum dots incorporated with multiwall carbon nanotubes. Appl Surf Sci 508:145294

Kumar PS, Megarajan S, Reddy GRK, Anbazhagan V (2018) Facile synthesis of gold nanoparticles using carbon dots for electrochemical detection of neurotransmitter, dopamine in human serum and as a chemocatalyst for nitroaromatic reduction. IET Nanoniotechnol 12:909–914

Kunpatee K, Traipop S, Chailapakul O, Chuanuwatanakul S (2020) Simultaneous determination of ascorbic acid, dopamine, and uric acid using graphene quantum dots/ionic liquid modified screen-printed carbon electrode, Sens. Actuat. B: Chem 314:128059

Li H, Chen L, Wu H, He H, Jin Y (2014) Ionic liquid-functionalized fluorescent carbon nanodots and their applications in electrocatalysis, biosensing, and cell imaging. Langmuir 30:15016–15021

Li Y, Zhonga Y, Zhanga Y, Weng W, Li S (2015) Carbon quantum dots/octahedral Cu_2O nanocomposites for non-enzymatic glucose and hydrogen peroxide amperometric sensor. Sensors Actuators B Chem 206:735–743

Li L, Liu D, Wang K, Mao H, You T (2017) Quantitative detection of nitrite with N-doped graphene quantum dots decorated N-doped carbon nanofibers composite-based electrochemical sensor. Sensor Actuat B-Chem 252:17–23

Li M, Chen T, Gooding JJ, Liu J (2019a) Review of carbon and graphene quantum dots for sensing. ACS Sensors 4:1732–1748

Li K, Li YF, Wang L, Yang LX, Ye BX (2019b) Study the voltammetric behavior of 10-Hydroxycamptothecin and its sensitive determination at electrochemically reduced graphene oxide modified glassy carbon electrode. Arab J Chem 12:2732–2739

Li KX, Xu JQ, Arsalan M, Cheng N, Sheng QL, Zheng JB, Cao W, Yue TL (2019c) Nitrogen doped carbon dots derived from natural seeds and their application for electrochemical sensing. J Electrochem Soc 166:B56–B62

Li XY, Xie H, Luo GL, Niu YY, Li XB, Xi YR, Xiong Y, Chen Y, Sun W (2020) Electrochemistry and electrocatalysis of hemoglobin based on graphene quantum dots modified electrode. Curr Anal Chem 16:308–315

Lim CS, Hola K, Ambrosi A, Zboril R, Pumer M (2015) Graphene and carbon quantum dots electrochemistry. Electrochem Commun 52:75–79

Liu L, Anwar S, Ding HZ, Xu MS, Yin Q, Xiao YZ, Yang XY, Yan MQ, Bi H (2019a) Electrochemical sensor based on F,N-doped carbon dots decorated laccase for detection of catechol. J Electroanal Chem 840:84–92

Liu C, Guo LQ, Zhang B, Lu LP (2019b) Graphene quantum dots mediated electron transfer in DNA base pairs. RSC Adv 9:31636–31644

Liu W, Li M, Jiang G, Li G, Zhu J, Xiao M, Zhu Y, Gao R, Yu A, Feng M, Chen Z (2020) Graphene quantum dots-based advanced electrode materials: design, synthesis and their applications in electrochemical energy storage and electrocatalysis. Adv Energy Mater 10: 2001275–2001323

Lu JJ, Kou Y, Jiang X, Wang MJ, Xue YY, Tian BW, Tan L (2019a) One-step preparation of poly (glyoxal-bis(2-hydroxyanil))-amino-functionalized graphene quantum dots-MnO_2 composite on electrode surface for simultaneous determination of vitamin B-2 and dopamine. Colloids Surf Physicochem Eng Aspects 580:123652

Lu D, Tao R, Wang Z (2019b) Carbon-based materials for photodynamic therapy: a mini-review. Front Chem Sci Eng 13:310–323

Lu ZW, Li YZ, Liu T, Wang GT, Sun MM, Jiang YY, He H, Wang YY, Zou P, Wang XX, Zhao QB, Rao HB (2020) A dual-template imprinted polymer electrochemical sensor based on AuNPsm and nitrogen-doped graphene oxide quantum dots coated on NiS_2/biomass carbon for simultaneous determination of dopamine and chlorpromazine. Chem Eng J 389:124417

Ma H, Liu X, Wang X, Li X, Yang C, Iqbal A, Liu W, Li J, Qin W (2017a) Sensitive fluorescent light-up probe for enzymatic determination of glucose using carbon dots modified with MnO_2 nanosheets. Microchim Acta 184:177–185

Ma J-L, Yin B-C, Wu X, Ye, B.-Ce. (2017b) Simple and cost-effective glucose detection based on carbon nanodots supported on silver nanoparticles. Anal Chem 89:1323–1328

Mahmoud AM, El-Wekil MM, Mahnashi MH, Ali MFB, Alkahtan SA (2019) Modification of N,S co-doped graphene quantum dots with p-aminothiophenol-functionalized gold nanoparticles for molecular imprint-based voltammetric determination of the antiviral drug sofosbuvir. Microchim Acta 186:617

Mahmoudi-Moghaddam H, Tajik S, Beitollahi H (2019) A new electrochemical DNA biosensor based on modified carbon paste electrode using graphene quantum dots and ionic liquid for determination of topotecan. Microchem J 150:104085

Martínez-Periñán E, Bravo I, Rowley-Neale SJ, Lorenzo E, Banks CE (2019) Carbon nanodots as electrocatalysts towards the oxygen reduction reaction. Electroanalysis 30:436–444

Mat Zaid MH, Abdullah J, Rozi N, Mohamad Rozlan AA, Abu Hanifah S (2020) A sensitive impedimetric aptasensor based on carbon nanodots modified electrode for detection of 17ß-estradiol. Nano 10:1346

Mazloum-Ardakani M, Aghaei R, Abdollahi-Alibeik M, Moaddeli A (2015) Fabrication of modified glassy carbon electrode using graphene quantum dot, gold nanoparticles and 4-(((4-mercaptophenyl) imino)methyl) benzene-1,2-diol by self-assembly method and investigation of their electrocatalytic activities. J Electroanal Chem 738:113–122

Mello GPC, Simoes EFC, Crista DMA, Leito JMM, Pinto da Silva JCG, Esteves da Silva L (2019) Glucose sensing by fluorescent nanomaterials. Crit Rev Anal Chem 49:542–552

Meng RQ, Li QL, Zhang SJ, Tang JK, Ma CL, Jin RY (2019) GNDs/PEDOT bilayer films modified electrode as a novel electrochemical sensing platform for rutin detection. Int J Electrochem Sci 14:11000–11011

Molaei MJ (2020) Principles, mechanisms, and application of carbon quantum dots in sensors: a review. Anal Methods 12:1266–1287

Mollarasouli F, Asadpour-Zeynali K, Campuzano S, Yanez-Sedeno P, Pingarronm JM (2017) Non-enzymatic hydrogen peroxide sensor based on graphene quantum dots-chitosan/methylene blue hybrid nanostructures. Electrochim Acta 246:303–314

Mollarasouli F, Majidi MR, Asadpour-Zeynali K (2018) Amperometric sensor based on carbon dots decorated self-assembled 3D flower-like beta-$Ni(OH)_2$ nanosheet arrays for the determination of nitrite. Electrochim Acta 291:132–141

Mustafa F, Andreescu S (2018) Chemical and biological sensors for food-quality monitoring and smart packaging. Foods 7:168–190

Muthusankar G, Rajkumar C, Chen SM, Karkuzhali R, Gopu G, Sangili A, Sengottuvelan N, Sankar R (2019a) Electrochemical functionalization of polypyrrole nanowires for the development of ultrasensitive biosensors for detecting microRNA. Sensors Actuat B-Chem 281: 478–485

Muthusankar G, Sethupathi M, Chen SM, Devi RK, Vinoth R, Gopu G, Anandhan N, Sengottuvelan N (2019b) N-doped carbon quantum dots@hexagonal porous copper oxide decorated multiwall carbon nanotubes: a hybrid composite material for an efficient ultrasensitive determination of caffeic acid. Compos Part B 174:106973

Muthusankar G, Devi RK, Gopu G (2020) Nitrogen-doped carbon quantum dots embedded Co_3O_4 with multiwall carbon nanotubes: an efficient probe for the simultaneous determination of anticancer and antibiotic drugs. Biosens Bioelectron 150:111947

Nasr-Esfahani P, Ensafi AA, Rezaei B (2019a) Fabrication of a highly sensitive and selective modified electrode for imidacloprid determination based on designed nanocomposite graphene quantum dots/ionic liquid/multiwall carbon nanotubes/polyaniline. Sensors Actuat B-Chem 296:126682

Nasr-Esfahani P, Ensafi AA, Rezaei B (2019b) MWCNTs/ionic liquid/graphene quantum dots nanocomposite coated with nickel-cobalt bimetallic catalyst as a highly selective non-enzymatic sensor for determination of glucose. Electroanalysis 31:40–49

Newman JD, Turner APF (2005) Home blood glucose biosensors: a commercial perspective. Biosens Bioelectron 20:2435–2453

Ngo Y-LT, Jana J, Chung JS, Hur SH (2020) Electrochemical biosensors based on nanocomposites of carbon-based dots. Korean Chem Eng Res 58:499–513

Oliveira R, Amaro F, Azevedo M, Vale N, Goncalves H, Antunes C, Rego R (2019) New voltammetric and spectroscopic studies to quinacrine-DNA-Cdots interaction. Electrochim Acta 306:122–131

Pathak K, Kumar A, Prasad BB (2019) Functionalized nitrogen doped graphene quantum dots and bimetallic Au/Ag core-shell decorated imprinted polymer for electrochemical sensing of anti-cancerous hydroxyurea. Biosens Bioelectron 127:10–18

Peng X, Hu T, Bao T, Zhao L, Zeng X, Wen W, Zhang X, Wang S (2017) A label-free electrochemical biosensor for methyltransferase activity detection and inhibitor screening based on graphene quantum dot and enzyme-catalyzed reaction. J Electroanal Chem 799:327–333

Pohanka M, Skladal P (2008) Electrochemical biosensors – principles and applications. J Appl Biomed 6:57–64

Ponnaiah SK, Periakaruppan P, Vellaichamy B, Paulmony T, Selvanathan R (2018) Picomolar-level electrochemical detection of thiocyanate in the saliva samples of smokers and non-smokers of tobacco using carbon dots doped Fe3O4 nanocomposite embedded on g-C_3N_4 nanosheets. Electrochim Acta 283:914–921

Ponomarenko LA, Schedin F, Katsnelson MI, Yang R, Hill EW, Novoselov KS, Geim AK (2008) Chaotic dirac billiard in graphene quantum dots. Science 320:356–358

Qu Z-B, Zhou X, Gu L, Lan R, Sun D, Yu D, Shi G (2013) Boronic acid functionalized graphene quantum dots as a fluorescent probe for selective and sensitive glucose determination in microdialysate. Chem Commun 49:9830–9832

Ramachandran A, Nair JSA, Yesodha SK (2019) Polyaniline derived nitrogen-doped graphene quantum dots for the ultratrace level electrochemical detection of trinitrophenol and the Eefective differentiation of nitroaromatics: structure matters. ACS Sustain Chem Eng 7: 6732–6743

Ratinac KR, Yang W, Gooding JJ, Thordarson P, Braet F (2011) Graphene and related materials in electrochemical sensing. Electroanalysis 23:803–826

Reddy PP, Naidoo EB, Sreedhar NY (2019) Electrochemical preparation of a novel type of C-dots/ZrO_2 nanocomposite onto glassy carbon electrode for detection of organophosphorus pesticide. Arab J Chem 12:2300–2309

Rezaei B, Jamei HR, Ensafi AA (2018) An ultrasensitive and selective electrochemical aptasensor based on rGO-MWCNTs/Chitosan/carbon quantum dot for the detection of lysozyme. Biosens Bioelectron 115(2018):37–44

Saadati A, Hassanpour S, Hasanzadeh M, Shadjou N (2020) Binding of pDNA with cDNA using hybridization strategy towards monitoring of Haemophilus influenza genome in human plasma samples. Int J Biol Macromol 150:218–227

Samie HA, Arvand M (2020) Label-free electrochemical aptasensor for progesterone detection in biological fluids. Bioelectrochemistry 133:107489

Samuei S, Fakkar J, Rezvani Z, Shomali A, Habibi B (2017) Synthesis and characterization of graphene quantum dots/CoNiAl-layered doublehydroxide nanocomposite: application as a glucose sensor. Anal Biochem 521:31–39

Sanati AL, Faridbod F (2017) Electrochemical determination of methyldopa by graphene quantum dot/1-butyl-3-methylimidazolium hexafluoro phosphate nanocomposite electrode. Int J Electrochem Sci 12(2017):7997–8005

Santana ER, Spinelli A (2020) Electrode modified with graphene quantum dots supported in chitosan for electrochemical methods and non-linear deconvolution of spectra for spectrometric methods: approaches for simultaneous determination of triclosan and methylparaben. Microchim Acta 187:1436–5073

Serafin V, Valverde A, Martinez-Garcia G, Martinez-Periñán E, Comba F, Garranzo-Asensio M, Barderas R, Yanez-Sedeno P, Campuzano S, Pingarron JM (2019) Graphene quantum dots-functionalized multi-walled carbon nanotubes as nanocarriers in electrochemical immunosensing. Determination of IL-13 receptor alpha 2 in colorectal cells and tumor tissues with different metastatic potential. Sensors Actuators B Chem 284:711–722

Shankar SS, Shereema RM, Ramachandran V, Sruthi TV, Kumar VBS, Rakhi RB (2019) Carbon quantum dot-modified carbon paste electrode-based sensor for selective and sensitive determination of adrenaline. ACS Omega 4:7903–7910

Shankara Narayanan J, Anjalidevi C, Dharuman V (2013) Nonenzymatic glucose sensing at ruthenium dioxide–poly(vinyl chloride)–nafion composite electrode. J Solid State Electrochem 17:937–947

Shekari Z, Zare HR, Falahati A (2019) Electrochemical sandwich aptasensor for the carcinoembryonic antigen using graphene quantum dots, gold nanoparticles and nitrogen doped graphene modified electrode and exploiting the peroxidase-mimicking activity of a G-quadruplex DNAzyme. Microchim Acta 186:530

Shen P, Xia Y (2014) Synthesis-modification integration: one-step fabrication of boronic acid functionalized carbon dots for fluorescent blood sugar sensing. Anal Chem 86:5323–5329

Song C, Wei Q, Li H, Gao H, An J, Qi B (2020) Highly sensitive electrochemical sensor based on carbon dots reduced gold nanoparticles for ractopamine detection in pork meat. Int J Electrochem Sci 15:3495–3503

Sridara T, Upan J, Saianand G, Tuantranont A, Karuwan C, Jakmunee J (2020) Non-enzymatic amperometric glucose sensor based on carbon nanodots and copper oxide nanocomposites electrode. Sensors 20:808

Sun X, Lei Y (2017) Fluorescent carbon dots and their sensing applications. Trends Anal Chem 89: 163–180

Sun YP, Zhou B, Lin Y, Wang W, Fernando KAS, Pathak P, Meziani MJ, Harruff BA, Wang X, Wang HF, Luo PJG, Yang H, Kose ME, Chen BL, Veca LM, Xie SYJ (2006) Quantum-sized carbon dots for bright and colorful photoluminescence. J Am Chem Soc 128:7756–7757

Sweetman MJ, Hickey SM, Brooks DA, Hayball JD, Plush SE (2019) A practical guide to prepare and synthetically modify graphene quantum dots. Adv Funct Mater 29:1808740–1808757

Tajik S, Dourandish Z, Zhang K, Van Beitollahi H, Le Q, Jang HW, Shokouhimehr M (2020) Carbon and graphene quantum dots: a review on syntheses, characterization, biological and sensing applications for neurotransmitter determination. RSC Adv 10:15406–15429

Tang J, Ma XQ, Liu J, Zheng SB, Wang JF (2018) Simultaneous determination of hydroquinone and catechol using carbon glass electrode modified with graphene quantum dots. Int J Electrochem Sci 13:11250–11262

Tang J, Huang R, Zheng SB, Jiang SX, Yu H, Li ZR, Wang JF (2019) A sensitive and selective electrochemical sensor based on graphene quantum dots/gold nanoparticles nanocomposite modified electrode for the determination of luteolin in peanut hulls. Microchem J 145:899–907

Tashkhourian J, Nami-Ana SF, Shamsipur M (2018) Designing a modified electrode based on graphene quantum dot-chitosan application to electrochemical detection of epinephrine. J Mol Liq 266:548–556

Tavakolian-Ardakani Z, Hosu O, Cristea C, Mazloum-Ardakani M, Marrazza G (2019) Latest trends in electrochemical sensors for neurotransmitters: a review. Sensors 19:2037

Teymourian H, Barfidokht A, Wang J (2020) Electrochemical glucose sensors in diabetes management: an updated review (2010–2020). Chem Soc Rev 49:7671–7709

Tian L, Li Z, Wang P, Zhai X, Wang X, Li T (2021) Carbon quantum dots for advanced electrocatalysis. J Energ Chem 55:279–294

Tran HV, Le TA, Giang BL, Piro B, Tran LD (2019) Silver nanoparticles on graphene quantum dots as nanozyme for efficient H_2O_2 reduction in a glucose biosensor. Mater Res Express 6:115403

Tufa LT, Oh S, Tran VT, Kim J, Jeong KJ, Park TJ, Kim HJ, Lee J (2018) Electrochemical immunosensor using nanotriplex of graphene quantum dots, Fe_3O_4, and Ag nanoparticles for tuberculosis. Electrochim Acta 290:369–377

Walcarius A, Sibottier E (2005) Electrochemically-induced deposition of amine-functionalized silica films on gold electrodes and application to Cu(II) detection in (hydro)alcoholic medium. Electroanalysis 17:1716–1726

Wang X, Chen L, Su X, Ai S (2013) Electrochemical immunosensor with graphene quantum dots and apoferritin-encapsulated Cu nanoparticles double-assisted signal amplification for detection of avian leukosis virus subgroup J. Biosens Bioelectron 47:171–177

Wang H, Yi J, Velado D, Yu Y, Zhou S (2015) Immobilization of carbon dots in molecularly imprinted microgels for optical sensing of glucose at physiological pH. ACS Appl Mater Interfaces 7:15735–15745

Wang L, Tricard S, Yue P, Zhao J, Fang J, Shen W (2016) Polypyrrole and graphene quantum dots Prussian Blue hybrid film on graphite felt electrodes: application for amperometric determination of L-cysteine. Biosens Bioelectron 77:1112–1118

Wang JJ, Zhang H, Zhao JH, Zhang RY, Zhao N, Ren HL, Li YC (2019) Simultaneous determination of paracetamol and p-aminophenol using glassy carbon electrode modified with nitrogen- and sulfur- co-doped carbon dots. Microchim Acta 186:733

Wei J, Qiang L, Ren J, Ren X, Tang F, Meng X (2014) Fluorescence turn-off detection of hydrogen peroxide and glucose directly using carbon nanodots as probes. Anal Methods 6:1922–1927

Wei YY, Zhang D, Fang YX, Wang H, Liu YY, Xu ZF, Wang SJ, Guo Y (2019) Detection of ascorbic acid using green synthesized carbon quantum dots. J Sensors 2019:9869682

Wu MY, Zhu JW, Ren YF, Yang N, Hong Y, Wang WJ, Huang W, Si WL, Dong XC (2020) NH_2-GNDs-doped Nickel-Cobalt oxide deposited on carbon cloth for non-enzymatic detection of glucose. Adv Mater Interfaces 7:1901578

Xu X, Ray R, Gu Y, Ploehn HJ, Gearheart L, Raker K, Scrivens WA (2004) Electrophoretic analysis and purification of fluorescent single-walled carbon nanotube fragments. J Am Chem Soc 126: 12736–12737

Xu JJ, Yu CF, Feng T, Liu MY, Li FT, Wang Y, Xu JJ (2018) N-Carbamoylmaleimide-treated carbon dots: stabilizing the electrochemical intermediate and extending it for the ultrasensitive detection of organophosphate pesticides. Nanoscale 10:19390–19398

Xu ZL, Deng SE, Zhang FL, Li H, Cheng YZ, Wei LY, Wang JY, Zhou BL (2019) A mechanochemically synthesized porous organic polymer derived CND/chitosan-graphene composite film electrode for electrochemiluminescence determination of dopamine. RSC Adv 9: 39332–39337

Yang C, Hu L-W, Zhu H-Y, Ling Y, Tao J-H, Xu C-X (2015) rGO quantum dots/ZnO hybrid nanofibers fabricated using electrospun polymer templates and applications in drug screening involving an intracellular H_2O_2 sensor. J Mater Chem B 3:2651–2659

Yao J, Chen M, Li NN, Liu CH, Yang M (2019) Experimental and theoretical studies of a novel electrochemical sensor-based on molecularly imprinted polymer and B, N, F-CNDs/AgNPs for enhanced specific identification and dual signal amplification in highly selective and ultra-trace bisphenol S determination in plastic products. Anal Chim Acta 1066:36–48

Yola ML, Atar N (2019) Development of molecular imprinted sensor including graphitic carbon nitride/N-doped carbon dots composite for novel recognition of epinephrine. Compos Part B Eng 175:107113

Zhan TR, Ding GY, Cao W, Li JM, She XL, Teng HN (2019) Amperometric sensing of catechol by using a nanocomposite prepared from Ag/Ag_2O nanoparticles and N,S-doped carbon quantum dots. Microchim Acta 186:743

Zhang J-J, Wang Z-B, Li C, Zhao L, Liu J, Zhang L-M, Gu D-M (2015) Multiwall-carbon nanotube modified by N-doped carbon quantum dots as Pt catalyst support for methanol electrooxidation. J Power Sources 289:63–70

Zhang J-J, Sui X-L, Zhao L, Zhang L-M, Gu D-M, Wang ZB (2016) Effect of N-doped carbon quantum dots/multiwall-carbon nanotube composite support on Pt catalytic performance for methanol electrooxidation. RSC Adv 6:67096–67101

Zhao J, Chen G, Zhu L, Li G (2011) Graphene quantum dots-based platform for the fabrication of electrochemical biosensors. Electrochem Commun 13:31–33

Zhao C, Song X, Liu Y, Fu Y, Ye L, Wang N, Wang F, Li L, Mohammadniaei M, Zhang M, Zhang Q, Liu J (2020) Synthesis of graphene quantum dots and their applications in drug delivery. J Nanobiotechnol 18(2020):142–1731

Zheng A-X, Cong Z-X, Wang J-R, Li J, Yang H-H, Chen G-N (2013) Highly-efficient peroxidase-like catalytic activity of graphene dots for biosensing. Biosens Bioelectron 49:519–524

Zhu H, Li L, Zhou W, Shao Z, Chen X (2016) Advances in non-enzymatic glucose biosensors based on metal oxides. J Mater Chem B 4(2016):7333–7349

Всё для победы!
НАРОДНЫЙ ФРОНТ
https://pobeda.onf.ru/
LET'S HELP THE RUSSIA

Engineered Nanopaper Electrode Array Fabrication and Biomedical Applications

36

Tingfan Wu and Haiyun Liu

Contents

1 Introduction 790
2 Fabrication of Electrodes on Paper 790
  2.1 Printing 791
  2.2 Pencil Drawing 795
  2.3 Conductive Tape Pasting 797
  2.4 Chemical Deposition 797
  2.5 Magnetron Sputtering 798
3 Biomedical Applications 798
  3.1 Proteins 798
  3.2 DNA 799
  3.3 Dopamine 801
  3.4 Glucose/Lactate/Uric Acid/Ascorbic Acid 801
  3.5 Cholesterol 803
  3.6 Cancer Cells/Markers 803
4 Challenge and Future 805
References 805

Abstract

Point of care testing (POC) has been increasingly crucial for disease diagnoses and monitoring. However, the existing conventional methods need large-scale instruments, complex procedures, and skilled operators. By comparison, nanopaper electrode array provides simplicity, portability, reproducibility, low cost, and high selectivity and sensitivity for analytical measurements in a variety of applications ranging from clinical diagnostics to disease monitoring. In this review, fabrication and application of nanopaper electrode array have been elaborated with various examples. Finally, challenges and the future of nanopaper electrode array have also been discussed.

T. Wu · H. Liu (✉)
Institute for Advanced Interdisciplinary Research, University of Jinan, Jinan, Shandong, China
e-mail: chm_liuhy@ujn.edu.cn

© Springer Nature Singapore Pte Ltd. 2023

U. P. Azad, P. Chandra (eds.), *Handbook of Nanobioelectrochemistry*,
https://doi.org/10.1007/978-981-19-9437-1_36

Keywords

Point of care testing · Disease diagnoses · Nanopaper electrode array · Simplicity

1 Introduction

For the past few years, millions of deaths have been recorded due to inadequate or even shortage of health services (Mahato et al. 2020). Current traditional approaches of disease diagnosis and monitoring are generally based on molecular biology microbial culture techniques (Mahato et al. 2021). These diagnostic processes require the use of multiple methods and a variety of advanced and sophisticated instruments, and these analysers are large, complex, and require specialist personnel to operate (Ammu et al. 2012; Cunningham et al. 2014). These characteristics significantly increase the economic and time cost of diagnosis.

Various improved diagnostics have been produced thus far, with consistent reports of equivalent analytical results in smaller settings. Among these options, the paper-based (PB) electrode has received a lot of attention. Paper substrates have been employed in such diagnostic devices because of its sufficient quantity, low cost, and flexibility for detecting procedures.

Nanopaper is a renewable and ecologically beneficial substance. It is formed of the same material as regular paper, but its fiberdiameter is significantly smaller than ordinary paper's. Furthermore, as compared to plastic substrates, nanopaper has significantly higher thermal stability. Because of the benefits listed above, nanopaper can house a wide range of devices (Apilux et al. 2010; Barandun et al. 2019; Dossi et al. 2014; Jia Huang et al. 2013). Formalized paraphrase based on paper substrates have piqued the interest of many researchers and businesses, since paper is used as the substrate, the technology offers significant advantages in terms of flexibility, cost effectiveness, and environmental friendliness (Mahato et al. 2017, 2021).

2 Fabrication of Electrodes on Paper

Recently, cellulose paper appears as a flexible, low-cost, readily available, and environmentally friendly material in flexible electronic devices such as supercapacitors, nanogenerators, sensors, and so on.

Due to the characteristics of rough paper surface, in addition to the electrode printing and magnetron sputtering technology suitable for various substrates, but also include pencil drawing, conductive tape paste, and other technologies, which also realizes the preparation method of PBsensor electrode is simple, low cost, no solvent.

In general, electrodes are required for PBsensors. PB electrodes can be fabricated in various ways, such as printing, magnetron sputtering, conductive tape paste, and pencil drawing.

2.1 Printing

Printing technology is a well-established and broadly used technique for manufacturing electrodes for biochemical sensors. The development of portable, low-cost, and fast sensors is imperative in the sensing field. Printed electrodes offer not only the economic advantages of inexpensive, ease of manufacture and versatility, but also the electrochemical properties of high sensitivity and reproducibility (Metters et al. 2011).

2.1.1 Screen-Printing

Dungchai and his co-workers (Dungchai et al. 2009) put forward the first electrochemical PB analytical devices (ePAD), which fabricated carbon electrodes by screen-printing technique. Compared with the traditional colorimetric method, the electrochemical method can well improve the performance of microfluidic PB analytical devices, such as sensitivity and selectivity, which are of concern. The geometry of screen-printed electrodes can be drawn utilizing drawing software such as Corel Draw, Adobe Illustrator or Adobe Freehand, and different geometries have different effects on the performance of the electrode. For instance, in Dungchai's work, the electrodes were screen-printed on paper. The working and counting electrodes were made from Prussian blue carbon ink and the reference electrodes was made by Ag/AgCl ink. Among them, Prussian blue was used as redox medium to enhance the selectivity of H_2O_2.The current resistance in the circuit is minimized by designing the counter electrode's geometry to be bigger compared to the working and reference electrodes. In addition, all electrodes' conductive pads coated with Ag/AgCl ink can better lower resistance. This device is used for simultaneous determination of critical health markers in undiluted serum samples.

Apilux et al. presented a device using colorimetric detection to detect of multiple metal in wastewater samples. Three screen-printed electrodes were integrated to a paper device's hydrophilic area. Among them, carbon was used as working and counter electrodes, and Ag/AgCl ink was used as a reference electrode and each electrode's conductive pads (Apilux et al. 2010). This system had ability to detect Au and Fe at the same time in wastewater samples.

For ePAD measurements, commercial screen-printed electrodes (SPEs) were used. For trace metal measurement, a novel approach was developed that a paper substrate coupled with commercial SPEs (Tan et al. 2010). To increase measurement precision, a standard was set on the paper substrate and used. A commercial glucometer was combined with ePADs (Fig. 36.1). This approach not only becomes commercial availability, but also tests the health critical health markers in the blood (Nie et al. 2010). For a variety of tests, utilizing portable glucometers in conjunction with ePADs provides a handy and rapid way of detection.

During this time, SPEs have evolved into 3D and multi-dimensional ePAD device by Wang and his co-workers (Wang et al. 2012) constructed 3D ePAD, which consists of two layers of paper and dual working electrodes, which share a counter and a reference electrode. The first layer was made up of a hydrophilic circular center area linked to two circular working areas on the bottom layer, which loads the

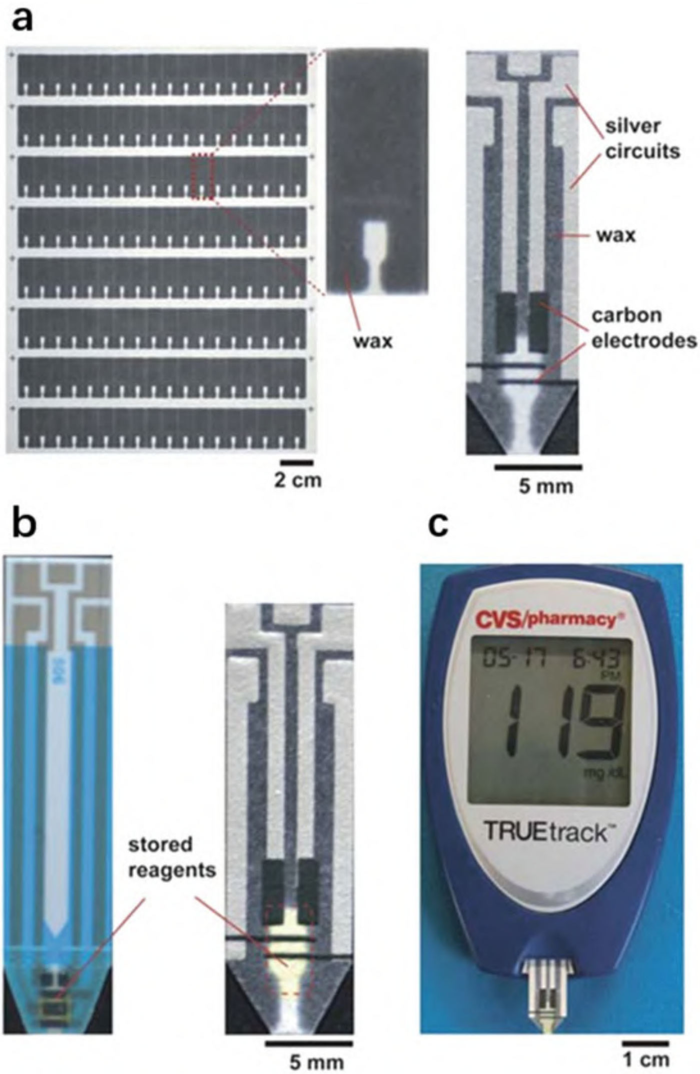
a
silver
circuits
wax
carbon
electrodes
wax
2 cm
5 mm
b
c
stored
reagents
5 mm
CVS/pharmacy
05-17 6:43
PM
119
mg/dL
TRUEtrack
1 cm

Fig. 36.1 A Commercial Glucometer (Nie et al. 2010). (**a**) On the left is an array of microfluidic paper channels and a channel enlarged view made on chromatographic paper, and on the right is a representative microfluidic paper device of electrodes made using screen printing. (**b**) On the left is a commercial strip made of plastic, on the right is an ePAD made of a layer of paper; dry chemical reagents are stored in the test area in the dashed square. (**c**) The glucometer is used as a reader. (Copyright (2010) Royal Society of Chemistry)

Screen-Printed Carbon Electrodes (SPCEs). The working electrodes were modified with the multi-walled carbon nanotubes/chitosan combination and were brought into alignment with the center of the circular area including the reference and counter electrodes. The multi-walled carbon nanotubes/chitosan coating made the device become more sensitive and can determine multiple tumor markers in blood samples at the same time. Furthermore, further work employed a variant of above system to create eight working electrodes on same layer that shared a counter and a reference electrode (Zang et al. 2012). With this enhanced design, rapid detection of high throughput detection diversity is realized. Moreover, a 3D ePAD conductive carbon ink was integrated into a self-powered origami PAD, which used aptamers as the sensing probe and using a digital multimeter as a simple electrochemical signal reader (Liu et al. 2012). Because the capacitor provided a large instantaneous current, which was effectively amplified current, the signal amplification from direct current measurement was 17-fold.

2.1.2 Stencil-Printing

In a similar way to screen printing, stencil-printing utilizes an open mask or stencil to create the electrodes. Solid films, such as adhesive tape and transparent film, are easily made from stencils by craft or laser cutters. The strong point of this method is that the masks can be generated quickly and at low cost.

Dungchai et al. reported a stencil-printed electrodes that the solution flow across to produce convection and enhance signal (Dungchai et al. 2011). The working electrode, counter electrode, and reference electrode are all stencil printed onto the same piece of paper and a hydrophilic channel is made using photolithography on another piece of paper. Two pieces of paper are bonded with double-sided adhesive tape so that there is angular contact between paper channel and electrode. Glucose in urine and Pb^{2+}in an aqueous solution can be selective detected.

The usage of stencil printing was further investigated. A carbon electrode is printed onto a wax-printed paper and merged with the polymer layer to construct a flow channel on the PB electrodes (Godino et al. 2012). Carbon nanotubes also been employed in the coating of cellulose fibers as conductive material. Carbon nanotube inks are used to produce conductive paper into which a special ion-selective film is then dropped using a stencil (Novell et al. 2012). The conductive paper was employed as an ion-selective electrode for K^+, NH_4^+, and so on measurements. Carbon nanotubes were also employed to construct pH sensing electrodes by sucking a mixture of carbon nanotubes into the paper through a metal stencil. Another conductive material, polypyrrole, is combined with cellulose fibres to produce PB polypyrrole electrodes (Olsson et al. 2012), which can be utilized as an alternative to paper electrodes. The paper is first soaked in a pyrrole solution and then polymerized on the paper fibers by the action of a chemical oxidizing agent. The electrochemical properties of the resulting electrode show that the charging capacity is increased, so the system can be used for energy storage.

2.1.3 Inkjet-Printing

A commercial inkjet printer can be used to fabricate electrodes utilizing inkjet-printing. As a new PB electrochemical for oxygen sensing, Chengguo and his co-workers constructed gold electrode arrays composed of gold nanoparticles (GNPs) on flexible and porous substrates like paper substrate by inkjet-printing (Fig. 36.2a, b) (Hu et al. 2012). GNPs were first printed on substrate by inkjet-

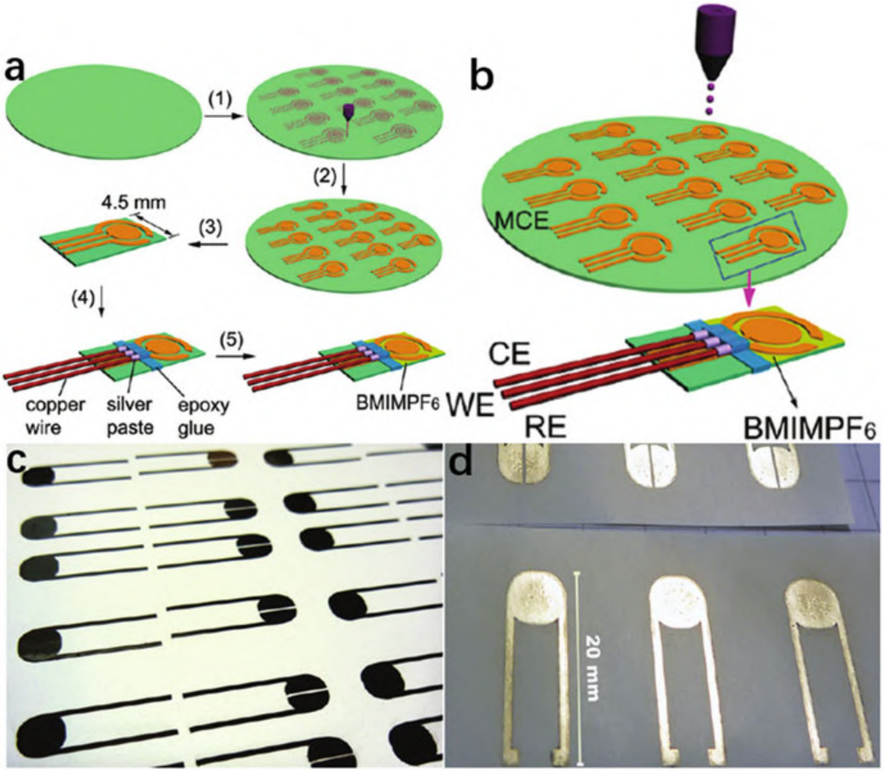

Fig. 36.2 Inkjet-printing (**a**) (1) Inkjet-printing of GNP patterns, (2) GNP pattern expansion into gold electrode arrays, (3) PB gold electrode arrays (PGEAs) are cut from their ensembles. (4) Links to sections on the PGEA and (5) BMIMPF$_6$ is added to form a complete prepared oxygen sensor. (**b**) PGEAs. (Hu et al. 2012) Copyright (2012) American Chemical Society. (**c**) Unsintered Au electrodes and (**d**) IR-sintered inkjet-printed Au electrodes (Maattanen et al. 2012). (Copyright (2012) Ameri can Chemical Society)

printing, then sintered by infrared to form more stable electrodes, oxidation-resistant, and acid-resistant (Maattanen et al. 2012). Self-assembled octade-canethiol monolayers were used to further functionalize the electrodes. The functionalized electrodes might be used for printing diagnosis of molecular recognition and detection. Furthermore, electrodes for a bioelectric sensor were fabricated using silver nanoparticle ink-jet printing (Yang et al. 2012) (Fig. 36.2c, d). The electrode resistance obtained by this method was reduced to a more desirable level.

In addition, Liu's group created a sensor by employing the inkjet-printing technique to print photosensitive conductive ink on a paper substrate (Yuan et al. 2016). This ink is a photosensitive alternating copolymer P (VM-Alt-MA) (PVMA), which is prepared by copolymerization of 7-(4-vinylbenzyloxy) -4-methylcoumarin (VM) with maleic anhydride (MA). PVMA provides a soft template for the oxidative polymerization of poly (3,4-ethylenedioxythiophene). This template is called

PEDOT for short. A steady PEDOT: PVMA photosensitive aqueous was obtained. Then, using this aqueous dispersion as inks, they employed inkjet-printing technique to make a sensor. After photo-dimerization of coumarin groups, the printed photosensitive conductive film PEDOT: PVMA may be cross-linked. The inkjet printing approach was used by Manohar's group to create a Chemiresistor (Ammu et al. 2012). It is a thin film made of single-walled carbon nanotubes (CNT) bunched onto cellulose that can sensitively detect low concentrations of oxidizing gases, such as NO_2 and Cl_2, at room temperature and without the need for vapor concentration. Compare to the films impregnated on a plastic substrate, the CNT films printed inkjet on acid-free paper are more durable.

2.1.4 Other Printing Techniques

Whitesides' group printed a high-accuracy electrical respiration sensor using specific proportional concentration of ink. For the ink, to achieve the desired printing consistency, the graphite ink was diluted with Ercon ET160in a 55:45 weight ratio and the solvent was mixed using an ultrasonicator to obtain a homogeneous dispersion. The graphite ink (Ercon Graphite Ink 3456) was then digitally printed on paper by using a ballpoint pen and a process cutter/printer (Graphtec Craft Robo Pro) to form a PB sensor.

Guder and his co-workers have described a completely new type of printed electrical gas sensor (Barandun et al. 2019). This technology takes advantage of the inherent hygroscopic characteristics of cellulose fibers on the paper; it may appear dry on the surface, but the paper contains a lot of water that has been adsorbed from the environment, allowing sensing using wet chemical methods without the need to manually add water to the substrate. This device is very sensitive to water-soluble gases and respond quickly and reversibly. At a fraction of the cost, the sensors function as well as or better than most commercial ammonia sensors. The suggested sensors may be put into food packaging to check freshness to operate as wireless, battery-free gas sensors, which can be probed with cellphones.

2.2 Pencil Drawing

Pencil is the stationery we use every day, its core is mainly composed of conductive graphite that allows it to be used to make PB electrical devices. Dossi and his groupet presented a primary ePAD composed of graphite electrodes by pencil-drawn (Dossi et al. 2013). The system was used to electrochemically detect ascorbic acid (AA) and sunset yellow dye. In addition, Dossi and his coworkers have demonstrated a similar device also using a dual working electrode system to detect different substances in the mixture at distinct working electrode potentials (Dossi et al. 2013a). Kubota and his group demonstrated the usage of graphite pencils as electrodes in combination with μPADs for glucose detection (Santhiago and Kubota 2013). Thus it can be seen, the application of pencil drawing to make electrodes has been widely researched

(Kurra and Kulkarni 2013). Even though pencil drawing has the benefits of simple to manufacture, stability, and low cost, the moisture in the paper can have an effect on the electrical properties of pencil drawing.

Kano and his coworkers developed a PB humidity biosensor using an HB pencil, which had a very high sheet resistance of the kΩ level and did not detect humidity effectively (Kano and Fujii 2018). In addition, they made PB pressure sensors with electrodes drawn on paper using an 8B pencil, which had a much lower sheet resistance of 800 Ω sq^{-1}. There is a distinction in the resistance of the electrodes made by different kinds of pencils as a result of the varying graphite composition of the pencil lead, as demonstrated by the samples above. As a result, the sheet resistance of different PB electrodes drawn from various pencil (1B-12B). This results indicated that the sheet resistance of PB electrodes drawn by pencil cores (1B-5B) was greater than 2100 Ω sq^{-1}, but the sheet resistance of PB electrodes drawn by pencil cores (6B-12B) was lower than 700 Ω sq^{-1}, so that pencil cores (6B-12B) were a better choice for PB electrodes. Although PB pencil electrodes offer the benefits of being easy to prepare, inexpensive, and environmentally benign, their electrochemical characteristics are influenced by too many factors, such as pencil type, drawing process. As a result, the researchers looked into alternative simple methods for making electrodes on a paper substrate. Koga and his group created a one-time molecular sensor device out of paper from paper for the detection of NO_2 (Koga et al. 2019). A two-step paper making and pencil-draw were used to combine a cellulose nanofiber paper substrate, a ZnO nanowire sensor, and a graphite electrode. The device can effectively detect nitrogen dioxide and has the advantages of cut-and-paste use and simple disposal. Zhang's group has produced a PB sensor device for NO_2 measurement at room-temperature (Zhang et al. 2015). The printed Ag interdigitated electrodes provide low resistance, as it is also possible to assemble AgNPs onto peeled graphene sheets for use as PB NO_2 gas sensors. The pencil-drawn sensor's benefits combined with the Zigbee wireless module make it an ideal platform for low-cost and portability. Because just an affordable, commercially available pencil lead is required, incorporating pencil lead into ePADs is possibly the easiest and simplest technique to produce electrodes for ePADs. Fei and his group discussed the invention of a type of complete carbon-based humidity sensor that is handwritten on a paper substrate (Fig. 36.3) (Zhao et al. 2017). Commercial pencils were used to write the electrodes, and an oxidized multi-walled carbon nanotubes (o-MWCNTs) ink marker was utilized to draw the sensitive layer. The resulting devices are highly reproducible, stable, and sensitive. Carbon is currently employed mostly in biology and medicine as nanostructures of carbon nanotubes (Liu et al. 2017).

Dossi and his group devised a novel method to produce handmade pencils cores. In this method, pencil cores are made by mixing the modifier with the conductive material toner, binder, and hardener in different proportions, which has the advantages of good reproducibility, simple fabrication, and low cost (Dossi et al. 2014). Moreover, the electrodes made by doping different substances exhibit different properties, such as reversible electrochemical behavior of some and good

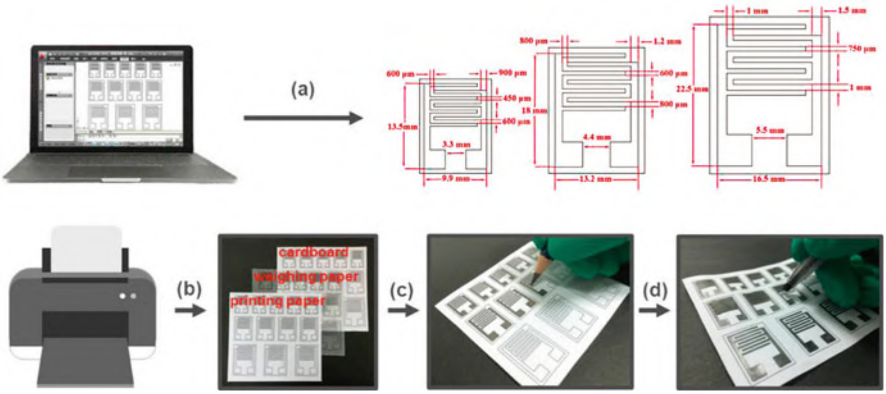

Fig. 36.3 Schematic diagram of fabrication a PB sensor using pencil drawing. (**a**) Structure design by AutoCAD, (**b**) printing outline, (**c**) handwriting electrodes, and (**d**) drawing sensitive layer by o-MWCNTs-ink markers (Zhao et al. 2017). (Copyright (2017) American Chemical Society)

electrocatalytic activity of others. The synthesized pencil cores are expected to be well automated when mounted on a computer-controlled plotter.

2.3 Conductive Tape Pasting

The copper foil adhesive tapes have been employed as electrodes for PB sensors in the past. Nonetheless, the adhesive copper foil tape electrodes are unable to withstand the constant bending, which results in poor wearability and fragile sensors. With the advancement of the manufacturing sector, flexible polyester conductive adhesive tape has been developed, which aids in the resolution of the compatibility issue between rigid electrodes and paper. Tai Group has produced a simple and versatile PB humidity sensor in which they have a conductive tape pasting technology for creating a PB humidity sensor (Duan et al. 2019). It is made in two easy steps: Firstly, two aluminum wires are taped to the surface of the paper using two polyester conductive tapes to form two electrodes. Then, the sensor is encapsulated with an insulating PI adhesive tape. In this study, the flexible polyester conductive adhesive tape ensures excellent compatibility and stability between the electrodes and the paper. A good insulating PI tape to improve its mechanical bendability.

2.4 Chemical Deposition

Noviana’s thermoplastic electrode (TPE) production method was derived from a simple solvent-assisted electrode manufacturing method (Fig. 36.4). A 160 μm wide TPE tape was prepared by replacing PMMA with a cyclic olefin copolymer as the binder. The electrode arrays were easily made and had a lower electrode dimensions and gap than the traditional screen-printing process (Noviana et al. 2019).

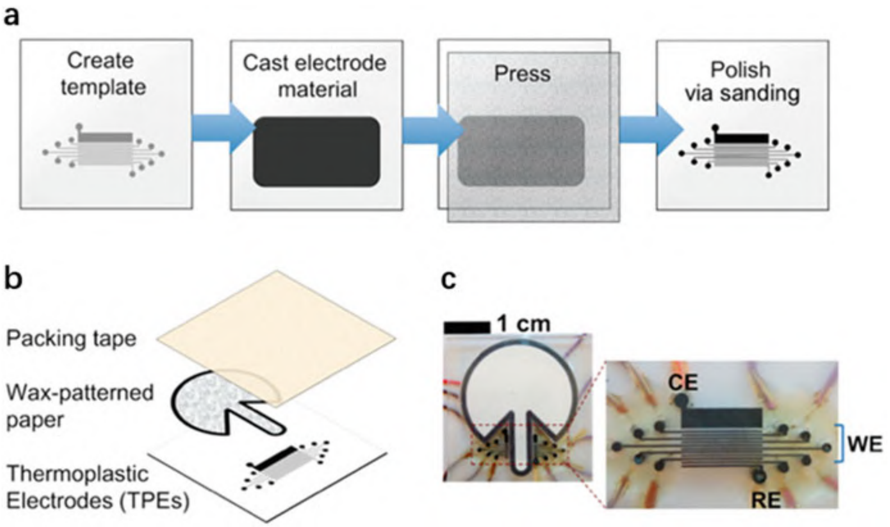

Fig. 36.4 Chemical Deposition. (**a**) Schematic diagram of TPE fabrication. (**b**) assembly into an electrochemical PAD. (**c**) TPE (Noviana et al. 2019). (Copyright (2019) American Chemical Society)

2.5 Magnetron Sputtering

For the first time, Tang and his coworkers have demonstrated a PB substrate colloidal quantum dot (PbS CQD), which was used to detect NO_2 by bonding NO_2 to the PbS CQD surface (Liu et al. 2014). The interdigital gold electrodes were printed on the substrate using radio frequency magnetron sputtering technique, then layer-by-layer spin coating of PbS CQDs with $NaNO_2$processing in an air environment at room temperature. This sensor exhibits high performance to detect of NO_2 at room temperature, due to its very large surface area and solution treatment, like fast response, high sensitivity, great reversibility, and outstanding flexibility ability and stability.

3 Biomedical Applications

3.1 Proteins

In recent years, enzyme-linked immunosorbent assays (ELISAs) have a growing range of applications in the biomedical field. Yu and his group developed the first ELISA-based ePAD that is able to identify several targets from practical samples (Zang et al. 2012). Using a multiplexed format, the sensor identified numerous cancer biomarkers. The study incorporates two types of ELISA models: indirect immunoassays and sandwich immunoassays. Whitesides and his group used an indirect immunoassay that required first placing the desired antigen modified directly on paper, then a blocker, and then a primary enzyme-conjugated antibody (Cheng et al. 2010). The more the antigen binds to the antibody, the stronger the signal will be. The role of the blocker is to keep the antibody from non-specifically attaching to the paper in the absence of the antigen, resulting in a false positive. The template for the sandwich ELISA is an antibody in the first layer, a blocking agent in the second layer, and an antigen and enzyme bound secondary antibody in the third layer. In order to remove unbound substrates, BS solution containing Tween 20 is always used between each stage of the ELISA procedure. Alkaline phosphatase and horseradish peroxidase are two common enzymes coupled as tags.

Lots of researches have improve some new methods to modify the paper and electrodes to strengthen the performance of the ELISA since it was incorporated onto paper, examples include modification of the paper with chitosan or graphene and modification of the electrode with a self-assembled monolayer of succinimidyl propionate. Chitosan is modified onto the paper and then removed by a washing process to remove non-specific binding proteins, resulting in a device that can detect proteins at the ng level (Fig. 36.5a) (Liu et al. 2015).

Methods for detecting proteins without immunoassay have been developed. Crooks and his group put forward a biosensor using a conformational switching experiment to detect of DNA and thrombin (Fig. 36.5b) (Cunningham et al. 2014). This sensor generates a signal that is dependent on the target-induced “open”or “off” of an oligonucleotide probe on the electrode. One end of this probe is attached to the gold electrode by a sulfhydryl group, and the other end of the probe has a redox reporter, usually methylene blue or ferrocene. The probe undergoes a conformational change with the presence or absence of the target, thereby changing the position of the redox reporter relative to the electrode. When there is no target, the redox reporter can be close to the electrode, producing a large signal. In contrast, when the target is present, the redox reporter is away from the electrode and the current signal is greatly reduced. The sensor can detect both DNA and protein, also has the strong points of good stability, low sample consumption, and high reproducibility. Another sensor was made by Vallée-Bélisle, which was based on DNA utilizing steric hindrance effects (Mahshid et al. 2015). The system is composed of a DNA capture probe and a DNA signal probe with a small recognition element and a redox label. When the target protein is not present, the DNA capture probe and the DNA signal probe bind by base complementary pairing, resulting in a large current signal. When the target protein is present, the spatial site block prevents the binding of the DNA signal probe, resulting in a reduced current signal. With this device, we can detect low nanomolar levels of proteins in whole blood samples in a very short time.

3.2 DNA

Immobilizing the appropriate probe on the electrode surface can make DNA detection more sensitive, specific, accurate, and stable. Yu and his coworkers pioneered the use of AuNP/graphene modified screen-printed electrodes SPCEs in a 3D folding

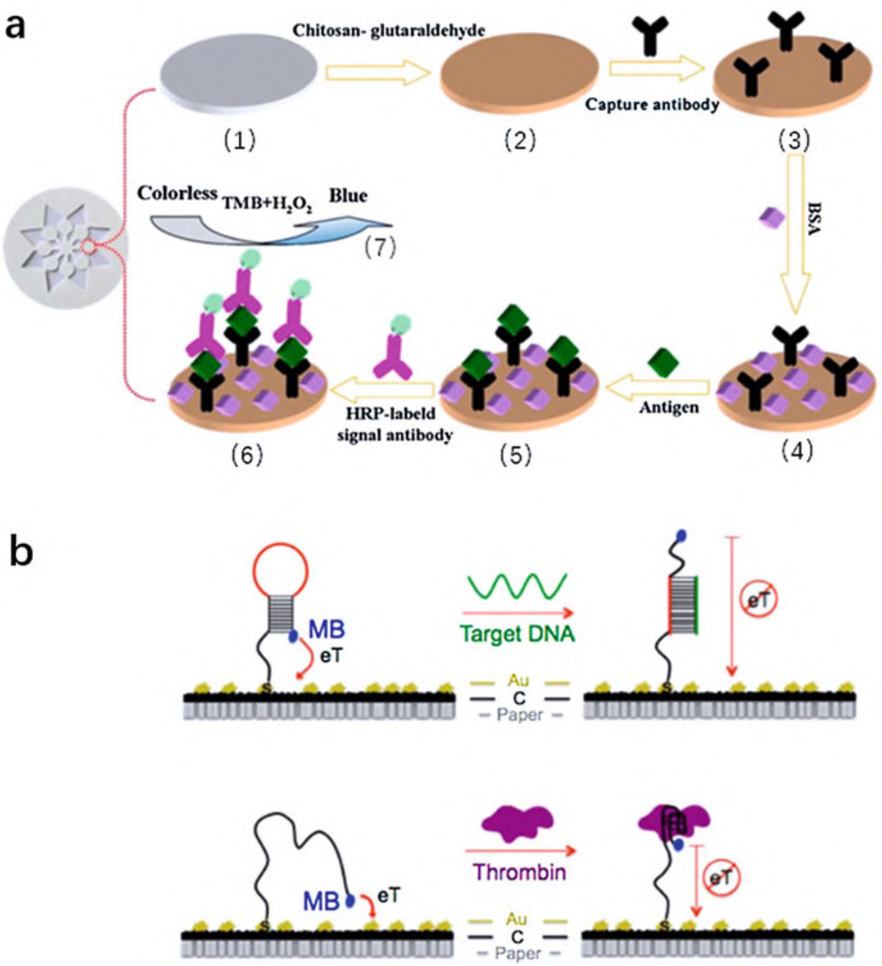
a
Chitosan- glutaraldehyde
Capture antibody
(1)
(2)
(3)
BSA
Colorless TMB+H_2O_2 Blue
(7)
HRP-labeld signal antibody
Antigen
(6)
(5)
(4)
b
MB
eT
Target DNA
Au
C
Paper
eT
MB
eT
Thrombin
Au
C
Paper
eT

Fig. 36.5 (**a**) A schematic of a typical sandwich ELISA based on paper (Liu et al. 2015). (Copyright (2015) American Chemical Society). (**b**) An "off" biosensor for DNA and thrombin detection based on paper (Cunningham et al. 2014). (Copyright (2014) American Chemical Society)

ePAD device for DNA measurement (Lu et al. 2012). Thionine was bound to double-stranded DNA to form a compound. The compound acted as a signal tag and bound to complementary ssDNA modified on nanopore gold to form a biocouple, the resulting biocouple was an excellent amplification label. As a consequence, the amplification is very well performed and can detect target DNA down to 2 nM. To detect Hepatitis B virus, Crooks and his coworkers developed a sliding origami device with magnetic microbeads (MBs) and AgNP-modified electrodes (Li et al. 2015). AgNP labels provide nearly 250,000-fold magnification, and magnetic micro-beads are loaded with DNA capture probes, which are integrated into the detection electrode to provide great magnification. As a result, the device has excellent electrochemical performance and can detect HBV up to 85 pM.

3.3 Dopamine

The discovery of analytical approaches to reliably identify neurotransmitters is important for brain research and the diagnosis of certain illnesses. Henry and his group produced a multilayer ePAD for the detection of dopamine (DA) (Rattanarat et al. 2012). The device is composed of three layers. In the first layer, a hydrophilic sample spot is used to concentrate the sample. The second layer contains two holes, the first hole is for collecting the concentrated sample, the second hole is modified with sodium dodecyl sulfate (SDS) for transferring the sample. The third layer is printed with a carbon electrode using screen-printed for electrochemical measurement of the signal. The preferential electrostatic interaction of the analyte with the SDS allows for signal enhancement for the quantitative detection of DA in serum. The device has the advantages of simplicity and portability. This device can detect both DA and paracetamol with high sensitivity and without the need for a separation step to complete. Feng et al. present a disposable PB integrated device that can be used to detect dopamine in rat (Feng et al. 2015). The device consists of a carbon tape electrode attached to a glass sheet that is modified with carbon nanotubes and Nafion and treated with oxygen plasma. The device exhibits excellent electrochemical performance. The addition of Nafion to carbon tape electrodes enhanced selectivity for DA determination by preventing AA from reaching the electrode surface. Additionally, because Nafion has negative charges that facilitate DA adsorption which can amplify electrochemical signals of DA. This device for detecting DA not only uses less sample, but also has a high sensitivity.

3.4 Glucose/Lactate/Uric Acid/Ascorbic Acid

Henry and his coworkers showed the electrochemical detection using PB microfluidic devices. The microfluidic channels were fabricated on paper by photolithography, and electrodes were manufactured on PB microfluidic devices by screen printing technology (Dungchai et al. 2009). The oxidase reacts with the target to produce H_2O_2, and the selectivity of the working electrode is enhanced by utilizing Prussian blue as a redox medium to determine health markers. Compared to conventional measurement methods, this method shows little error in values. The device gives a low-cost and portable platform to detect for health markers. The polyvinylpyrrolidone (PANI) was also employed to adapt SPCEs for AA detection utilizing an inkjet printing process to increase the analytical performance of ePADs (Kit-Anan et al. 2012). Because of the strong electrochemical catalysis of AA by polyaniline, the analytical property is greatly improved by printing a polyaniline layer on the working electrode. This PANI modified sensor has a LOD as low

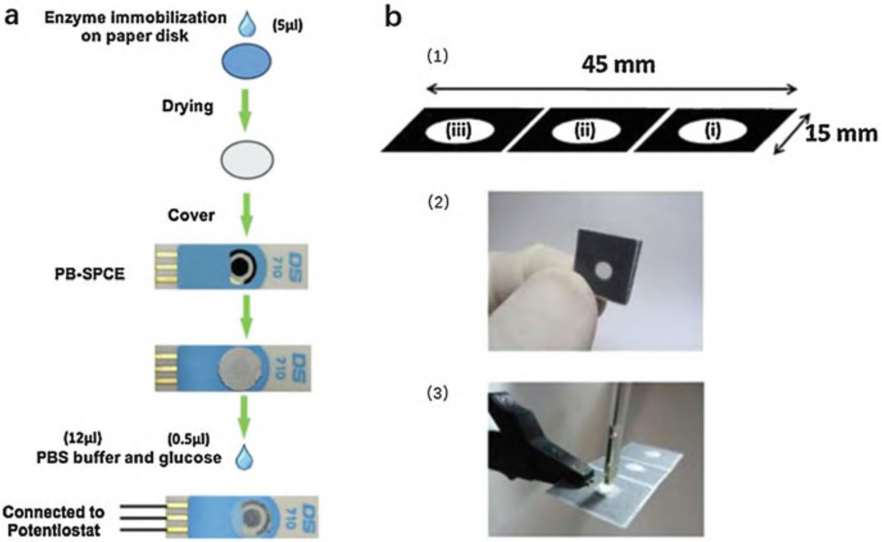

Fig. 36.6 (**a**) A GOx-immobilized PB-SPE for detection glucose (Chandra Sekar et al. 2014). (Copyright (2014) Elsevier). (**b**) An ePAD glucose sensor (Santhiago and Kubota 2013). (Copyright (2013) Elsevier)

as 30 µMof AA under ideal circumstances utilizing 5 layers of printed PANI with no interference from Uric Acid (UA).

Glucose has been an important target in ePAD research. As a result, novel strategies for improving the performance of ePADs for glucose measurement have been devised. Additionally, a dumbbell-shaped ePAD design was developed for determining glucose levels in whole blood (Noiphung et al. 2013). The device is not only simple, fast and portable, but also can detect a variety of health markers in the blood. A similar study developed an amperometric glucose sensor with a PB substrate (Chandra Sekar et al. 2014) (Fig. 36.6a). Immobilization of glucose oxidase (GOx) by simple physical adsorption, which avoids complex immobilization methods using multiple chemicals, thus ensuring that the original enzyme structure is not affected and optimal activity is achieved. The sensor is simple to prepare, low cost, portable and with good sensitivity and selectivity, making it a powerful and convenient platform with promising applications in resource-limited settings. Another advantage of a paper device is the possibility to integrate layers with various functions. As a result, Kubota and his group created an ePAD for glucose detection (Santhiago and Kubota 2013). Three hydrophilic zones contained on a wax-patterned device (Fig. 36.6b). This ePAD consisted of three layers for various tasks such as filtering, GOxreaction, and following redox mediator reaction inside a detecting zone. Two electrodes made of silver ink and graphite pencil were also present in the detecting zone.

A commercial equipment was also coupled with ePADs to improve their analytical performance for glucose detection. Whitesides and his group demonstrated the usage of a glucometer for ePAD devices for the detection of a lot of compounds relevant to human health in blood, saliva, and urine (Nie et al. 2010). Based on existing blood glucose meters, this study enables point-of-care diagnosis of health markers other than blood glucose through ePADs. A microelectrochemical sensing platform with integrated power supply is reported by Liu and Crooks (2012). The platform reads the signal through the electrochromic reading of Prussian blue dots, and no external power supply is required during the whole process. The sensor is easy to fabricate, inexpensive, and ideally sensitive for point-of-care sensing.

3.5 Cholesterol

The other one important physical fitness measure is cholesterol index, which has been effectively included into ePADs. A method of cholesterol detection is use polyvinylpyrrolidone (PVP), electrospray nanocomposite graphene (G), and PANI upon the material named SPCE can increase the area of electrode surface and increase the sensitivity of detection (Ruecha et al. 2014). The anionic sodium dodecyl sulfate coating is used to reduce AA interference by its electrostatic repulsion on the working electrode modified by the PVP/G/PANI. According to the result of Siangproh and his coworkers, the limit of detection (LOD) for cholesterol was about 1 μM and the current signal is four times the unmodified electrode (Nantaphol et al. 2015). The cholesterol analysis performance of ePADs can be enhanced by using the AgNP/boron-doped diamond (BDD) electrode. The BDD electrode has superior electrochemical features that can be summarized as low background current and high stability. These features can improve the repeatability and sensitivity of the detection by boosting Signal to Noise Ratio. The electrode was modified using AgNPs to catalyze the reduction reaction of H_2O_2. Compared to the unmodified electrode, not only was the chemical signal improved, but also the detection potential was reduced. Cholesterol oxidase was immediately dropped onto the hydrophilic surface of the ePAD, and the generated H_2O_2 was measured by reduction, removing any potential influence from the oxidizable components in test samples. These components including but not limited to UA and AA.

3.6 Cancer Cells/Markers

Early cancer detection is critical to improving patients' chances of survival while also delivering effective and successful therapy. As a result, rapid, accurate, and sensitive methods for cancer cells detection and identification of carcinogenic biomarkers have always been the main research direction of ePADs development. Yu and his coworkers in 2014 proposed a 3D ePAD that can detect cancer cells. There are four working electrodes on this device, each with its own counter and reference electrode (Su et al. 2014). To act as a working electrode, an excellently designated paper area was changed for providing the macroporous AuNP coated cellulose fiber with high specific surface area. The cancer cell type uses human acute promyelocytic leukemia cells (HL-60), which are fixed on the working paper electrode by targeting aptamer (KH1C12), then use the electrode for its detection. Furthermore, the team recently disclosed a method to detected K-562 cells which is based on Au nanoparticles in the ePAD platform (Li et al. 2015a). The K-562 cells are indicators for the diagnosis of early human chronic myeloid leukemia; at the same time, this method has excellent sensitivity and stability because of the Au@PdPtNPs. This Au@PdPtNPs had similar activity to peroxidase, it could enhance the signal by catalyzing H_2O_2 reduction. The system showed more robust catalytic activity, compared with the previously published enzymatic peroxidase system.

In addition to detecting cancer cells, the ePAD techniques for cancer biomarker detection have also been largely enhanced according to Song and his group (Li et al. 2013), who put forward a 3D origami composite electrochemical immune device used for detection of carcinoembryonic antigen (CEA) and alpha-fetoprotein with porous Ag nanomaterial working electrode. Furthermore, a unique rectangular silvermodified paper electrode was developed to detect cancer antigen 125 (CA125) and cancer antigen 199 (CA199) (Li et al. 2014). The paperworking electrode was tagged with nanoporous porous silver-chitosan coated with metal ions to enhance signal amplification. The LOD of CA199 or CA125 are both below 0.1 million of units per milliliter. In addition, Yan and his group in 2015 reported an immunodevice based on a 3D origami platform (Ma et al. 2015). The device is based on the paper electrode modified by gold nanorods and Au/BSA nanospheres coated by metal ion which act as tracking markers to detected CEA or CA125 synchronously. On the one hand, the addition of AuNRs-PWE provided a biocompatible matrix for antibody fixation, on the other hand, it increased the electrochemical signal of metal ions, such as Pb^{2+} and Cd^{2+}. The Au/BSA-metal ion tracer is produced by Au/BSA transport. This approach has an excellent sensitivity, whose LOD for CEA is less than or equal to 0.08 $pg \cdot mL^{-1}$ and the LOD of CA125 is 0.06 $mU \cdot mL^{-1}$. Furthermore, a sensor for detecting prostate protein antigen (PSA) was developed (Li et al. 2014a). In this system, PSA is acting as a biomaker of prostatic cancer and the sensor requires an AuNP on the screen-printed PWE surface modification, and then electrodeposited MnO_2 on the Au PWE to generate 3D nanowires. The enzymatic label redox cycling immunoassay served as the foundation for this immunoassay. GOx, 3, 3′, 5, 5′-tetramethylbenzidine, and glucose, in that order, served as enzyme tags, redox terminator, and substrates. The LOD of the proposed immunosensor is 0.0012 $ng \cdot ml^{-1}$, which performs well in PSA measurement.

In order to solve the complexity of enzyme purity, denaturation, and immobilization, a simple and convenient method for detecting cancer markers without enzyme immunosensor was established. On publication, Yan and his group in 2015 described an enzyme-free electrochemical immune sensor (Sun et al. 2015). In this strategy, an electrochemical biosensor was established by using hydrothermal method to modify ZnO nanorods on the rGOpaper electrode to reach highly sensitive and specific detection of human chorionic gonadotropin, carcinoembryonic antigen and prostate-specific antigen. rGO helps improve the conductivity of the sensing platform and ZnO nanorods provide a great number of binding sites for antibody capture. In addition, the current generated by hydrogen peroxide reduction serves as a signal output system, which amplifies the current signal under the high catalytic activity of silver nanoparticles stabilized by bovine serum protein. The construction of the enzyme-free immune sensing platform provides a simple, convenient, economical, and efficient application strategy, showing a broad application prospect in the field of clinical diagnosis. Following that, the group also proposed an enzyme-free electrochemical immune device with a paper electrode sensor platform modified with gold nanorods (Sun et al. 2015a). In this paper, we modified the signal antibody on porous zinc oxide and silver nanoparticles, and successfully realized the double specific capture of prostate specific antigen by the high selectivity of the capture antibodyand signal antibody. Under the high catalytic activity of silver nanoparticles, hydrogen peroxide was reduced, and the generated current response was used as a signal reporting system to realize the highly sensitive electrochemical detection of prostate specific antigen without enzyme.

4 Challenge and Future

Nanopaper electrode arrays have been widely employed in the biomedical field and have made significant advances in biochemical sensing. This chapter provides a summary of the available techniques for fabricating nanopaper electrode arrays and their application to biosensing. Particularly noteworthy is the production of electrode arrays, which plays a critical role in electrochemical behavior and functioning and has a significant influence on electrode performance. As a result, electrode production processes, materials, and geometries have been explored and improved to achieve the maximum degree of electrode performance. For the application of nanopaper electrode arrays in biosensing, the range of detection objects will be more diverse, the functionality of the sensors more integrated, and there are good prospects for low-cost, environmentally friendly, portable, and point-of-care diagnostics.

References

Ammu S, Dua V, Agnihotra SR, Surwade SP, Phulgirkar A, Patel S, Manohar SK (2012) Flexible, all-organic chemiresistor for detecting chemically aggressive vapors. J Am Chem Soc 134(10): 4553–4556

Apilux A, Dungchai W, Siangproh W, Praphairaksit N, Henry CS, Chailapakul O (2010) Lab-on-paper with dual electrochemical/colorimetric detection for simultaneous determination of gold and iron. Anal Chem 82:1727–1732

Barandun G, Soprani M, Naficy S, Grell M, Kasimatis M, Chiu KL, Ponzoni A, Guder F (2019) Cellulose fibers enable near-zero-cost electrical sensing of water-soluble gases. ACS Sensors 4(6):1662–1669

Chandra Sekar N, Mousavi Shaegh SA, Ng SH, Ge L, Tan SN (2014) A paper-based amperometric glucose biosensor developed with Prussian Blue-modified screen-printed electrodes. Sensors Actuators B Chem 204:414–420

Cheng CM, Martinez AW, Gong J, Mace CR, Phillips ST, Carrilho E, Mirica KA, Whitesides GM (2010) Paper-based ELISA. Angew Chem Int Ed Engl 122(28):4881–4884

Cunningham JC, Brenes NJ, Crooks RM (2014) Paper electrochemical device for detection of DNA and thrombin by target-induced conformational switching. Anal Chem 86(12):6166–6170

Dossi N, Toniolo R, Pizzariello A, Impellizzieri F, Piccin E, Bontempelli G (2013) Pencil-drawn paper supported electrodes as simple electrochemical detectors for paper-based fluidic devices. Electrophoresis 34(14):2085–2091

Dossi N, Toniolo R, Piccin E, Susmel S, Pizzariello A, Bontempelli G (2013a) Pencil-drawn dual electrode detectors to discriminate between analytes comigrating on paper-based fluidic devices but undergoing electrochemical processes with different reversibility. Electroanalysis 25(11): 2515–2522

Dossi N, Toniolo R, Impellizzieri F, Bontempelli G (2014) Doped pencil leads for drawing modified electrodes on paper-based electrochemical devices. J Electroanal Chem 722–723:90–94

Duan Z, Jiang Y, Yan M, Wang S, Yuan Z, Zhao Q, Sun P, Xie G, Du X, Tai H (2019) Facile, flexible, cost-saving, and environment-friendly paper-based humidity sensor for multifunctional applications. ACS Appl Mater Interfaces 11(24):21840–21849

Dungchai W, Chailapakul O, Henry CS (2009) Electrochemical detection for paper-based microfluidics. Anal Chem 81:5821–5826

Dungchai W, Chailapakul O, Henry CS (2011) A low-cost, simple, and rapid fabrication method for paper-based microfluidics using wax screen-printing. Analyst 136:77–82

Feng Q-M, Cai M, Shi C-G, Bao N, Gu H-Y (2015) Integrated paper-based electroanalytical devices for determination of dopamine extracted from striatum of rat. Sensors Actuators B Chem 209:870–876

Godino N, Gorkin R 3rd, Bourke K, Ducree J (2012) Fabricating electrodes for amperometric detection in hybrid paper/polymer lab-on-a-chip devices. Lab Chip 12(18):3281–3284

Hu C, Bai X, Wang Y, Jin W, Zhang X, Hu S (2012) Inkjet printing of nanoporous gold electrode arrays on cellulose membranes for high-sensitive paper-like electrochemical oxygen sensors using ionic liquid electrolytes. Anal Chem 84(8):3745–3750

Jia Huang HZ, Chen Y, Preston C, Rohrbach K, Cumings J, Liangbing H (2013) Highly transparent and flexible nanopaper transistors. ACS Nano 7(3):2106–2113

Kano S, Fujii M (2018) All-painting process to produce respiration sensor using humidity-sensitive nanoparticle film and graphite trace. ACS Sustain Chem Eng 6(9):12217–12223

Kit-Anan W, Olarnwanich A, Sriprachuabwong C, Karuwan C, Tuantranont A, Wisitsoraat A, Srituravanich W, Pimpin A (2012) Disposable paper-based electrochemical sensor utilizing inkjet-printed Polyanilin. J Electroanal Chem 685:72–78

Koga H, Nagashima K, Huang Y, Zhang G, Wang C, Takahashi T, Inoue A, Yan H, Kanai M, He Y, Uetani K, Nogi M, Yanagida T (2019) Paper-based disposable molecular sensor constructed from oxide nanowires, cellulose nanofibers, and pencil-drawn electrodes. ACS Appl Mater Interfaces 11(16):15044–15050

Kurra N, Kulkarni GU (2013) Pencil-on-paper: electronic devices. Lab Chip 13(15):2866–2873

Li W, Li L, Li M, Yu J, Ge S, Yan M, Song X (2013) Development of a 3D origami multiplex electrochemical immunodevice using a nanoporous silver-paper electrode and metal ion functionalized nanoporous gold-chitosan. Chem Commun (Camb) 49(83):9540–9542

Li W, Li L, Ge S, Song X, Ge L, Yan M, Yu J (2014) Multiplex electrochemical origami immunodevice based on cuboid silver-paper electrode and metal ions tagged nanoporous silver-chitosan. Biosens Bioelectron 56:167–173

Li L, Xu J, Zheng X, Ma C, Song X, Ge S, Yu J, Yan M (2014a) Growth of gold-manganese oxide nanostructures on a 3D origami device for glucose-oxidase label based electrochemical immunosensor. Biosens Bioelectron 61:76–82

Li X, Scida K, Crooks RM (2015) Detection of hepatitis B virus DNA with a paper electrochemical sensor. Anal Chem 87(17):9009–9015

Li Y, Yu J, Ding B (2015a) Facile and ultrasensitive sensors based on electrospinning-netting nanofibers/nets. In: Electrospinning for high performance sensors. Springer, Cham, pp 1–34

Liu H, Crooks RM (2012) Paper-based electrochemical sensing platform with integral battery and electrochromic read-out. Anal Chem 84(5):2528–2532

Liu H, Xiang Y, Lu Y, Crooks RM (2012) Aptamer-based origami paper analytical device for electrochemical detection of adenosine. Angew Chem Int Ed Engl 124(28):6925–6928

Liu H, Li M, Voznyy O, Hu L, Fu Q, Zhou D, Xia Z, Sargent EH, Tang J (2014) Physically flexible, rapid-response gas sensor based on colloidal quantum dot solids. Adv Mater 26:2718–2724

Liu W, Guo Y, Zhao M, Li H, Zhang Z (2015) Ring-oven washing technique integrated paper-based immunodevice for sensitive detection of cancer biomarker. Anal Chem 87(15):7951–7957

Liu H, Zhang L, Yan M, Yu J (2017) Carbon nanostructures in biology and medicine. J Mater Chem B 5(32):6437–6450

Lu J, Ge S, Ge L, Yan M, Yu J (2012) Electrochemical DNA sensor based on three-dimensional folding paper device for specific and sensitive point-of-care testing. Electrochim Acta 80: 334–341

Ma C, Li W, Kong Q, Yang H, Bian Z, Song X, Yu J, Yan M (2015) 3D origami electrochemical immunodevice for sensitive point-of-care testing based on dual-signal amplification strategy. Biosens Bioelectron 63:7–13

Maattanen A, Ihalainen P, Pulkkinen P, Wang S, Tenhu H, Peltonen J (2012) Inkjet-printed gold electrodes on paper: characterization and functionalization. ACS Appl Mater Interfaces 4(2): 955–964

Mahato K, Srivastava A, Chandra P (2017) Paper based diagnostics for personalized health care: emerging technologies and commercial aspects. Biosens Bioelectron 96:246–259

Mahato K, Purohit B, Kumar A, Chandra P (2020) Paper-based biosensors for clinical and biomedical applications: emerging engineering concepts and challenges. In: Paper based sensors. Elsevier, Amsterdam, pp 163–188

Mahato K, Purohit B, Kumar A, Srivastava A, Chandra P (2021) Next-generation immunosensing technologies based on nano-bio-engineered paper matrices. In: Immunodiagnostic technologies from laboratory to point-of-care testing. Springer, Singapore, pp 93–110

Mahshid SS, Camire S, Ricci F, Vallee-Belisle A (2015) A highly selective electrochemical DNA-based sensor that employs steric hindrance effects to detect proteins directly in whole blood. J Am Chem Soc 137(50):15596–15599

Metters JP, Kadara RO, Banks CE (2011) New directions in screen printed electroanalytical sensors: an overview of recent developments. Analyst 136(6):1067–1076

Nantaphol S, Chailapakul O, Siangproh W (2015) Sensitive and selective electrochemical sensor using silver nanoparticles modified glassy carbon electrode for determination of cholesterol in bovine serum. Sensors Actuators B Chem 207:193–198

Nie Z, Deiss F, Liu X, Akbulut O, Whitesides GM (2010) Integration of paper-based microfluidic devices with commercial electrochemical readers. Lab Chip 10(22):3163–3169

Noiphung J, Songjaroen T, Dungchai W, Henry CS, Chailapakul O, Laiwattanapaisal W (2013) Electrochemical detection of glucose from whole blood using paper-based microfluidic devices. Anal Chim Acta 788:39–45

Novell M, Parrilla M, Crespo GA, Rius FX, Andrade FJ (2012) Paper-based ion-selective potentiometric sensors. Anal Chem 84(11):4695–4702

Noviana E, Klunder KJ, Channon RB, Henry CS (2019) Thermoplastic electrode arrays in electrochemical paper-based analytical devices. Anal Chem 91(3):2431–2438

Olsson H, Carlsson DO, Nyström G, Sjödin M, Nyholm L, Strømme M (2012) Influence of the cellulose substrate on the electrochemical properties of paper-based polypyrrole electrode materials. J Mater Sci 47:5317–5325

Rattanarat P, Dungchai W, Siangproh W, Chailapakul O, Henry CS (2012) Sodium dodecyl sulfate-modified electrochemical paper-based analytical device for determination of dopamine levels in biological samples. Anal Chim Acta 744:1–7

Ruecha N, Rangkupan R, Rodthongkum N, Chailapakul O (2014) Novel paper-based cholesterol biosensor using graphene/polyvinylpyrrolidone/polyaniline nanocomposite. Biosens Bioelectron 52:13–19

Santhiago M, Kubota LT (2013) A new approach for paper-based analytical devices with electrochemical detection based on graphite pencil electrodes. Sensors Actuators B Chem 177: 224–230

Su M, Ge L, Ge S, Li N, Yu J, Yan M, Huang J (2014) Paper-based electrochemical cyto-device for sensitive detection of cancer cells and in situ anticancer drug screening. Anal Chim Acta 847: 1–9

Sun G, Zhang L, Zhang Y, Yang H, Ma C, Ge S, Yan M, Yu J, Song X (2015) Multiplexed enzyme-free electrochemical immunosensor based on ZnO nanorods modified reduced graphene oxide-paper electrode and silver deposition-induced signal amplification strategy. Biosens Bioelectron 71:30–36

Sun G, Liu H, Zhang Y, Yu J, Yan M, Song X, He W (2015a) Gold nanorods-paper electrode-based enzyme-free electrochemical immunoassay for prostate specific antigen using porous zinc oxide spheres–silver nanoparticles nanocomposites as labels. New J Chem 39(8):6062–6067

Tan SN, Ge L, Wang W (2010) Paper disk on screen printed electrode for one-step sensing with an internal standard. Anal Chem 82:8844–8847

Wang Y, Liu N, Ning B, Liu M, Lv Z, Sun Z, Peng Y, Chen C, Li J, Gao Z (2012) Simultaneous and rapid detection of six different mycotoxins using an immunochip. Biosens Bioelectron 34(1): 44–50

Yang G, Xie L, Mantysalo M, Chen J, Tenhunen H, Zheng LR (2012) Bio-patch design and implementation based on a low-power system-on-chip and paper-based inkjet printing technology. IEEE Trans Inf Technol Biomed 16(6):1043–1050

Yuan Y, Zhang Y, Liu R, Liu J, Li Z, Liu X (2016) Humidity sensor fabricated by inkjet-printing photosensitive conductive inks PEDOT:PVMA on a paper substrate. RSC Adv 6(53): 47498–47508

Zang D, Ge L, Yan M, Song X, Yu J (2012) Electrochemical immunoassay on a 3D microfluidic paper-based device. Chem Commun (Camb) 48(39):4683–4685

Zhang J, Huang L, Lin Y, Chen L, Zeng Z, Shen L, Chen Q, Shi W (2015) Pencil-trace on printed silver interdigitated electrodes for paper-based NO_2 gas sensors. Appl Phys Lett 106(14):143101

Zhao H, Zhang T, Qi R, Dai J, Liu S, Fei T (2017) Drawn on paper: a reproducible humidity sensitive device by handwriting. ACS Appl Mater Interfaces 9(33):28002–28009

Electrochemical Sensors Based on Nanostructured Materials for Point-of-Care Diagnostics

37

Duygu Harmanci, Simge Balaban Hanoglu, and Duygu Beduk

Contents

1 Introduction 810
2 Nanomaterials 811
3 Classification of Nanomaterials Based on the Dimension 811
4 Zero-Dimensional (0D) Nanomaterials 811
5 One-Dimensional (1D) Nanomaterials 812
6 Two-Dimensional (2D) Nanomaterials 813
7 Three-Dimensional (3D) Nanomaterials 814
8 Nanomaterials in Diagnostics 814
9 What Is “Point of Care”? 815
10 Electrochemical Sensors as PoC Tests 816
11 Classification of Nanomaterial-Based Electrochemical Sensors 816
12 Enzyme-Based Electrochemical Sensor 817
13 Non-enzymatic Electrochemical Sensor 818
14 Electrochemical Immunosensors 821
15 Nucleic Acid-Based Sensors (Genosensors and Aptasensors) 822
16 Other Electrochemical Sensors 823
17 Conclusion 823
References 824

Abstract

As analytical devices, electrochemical biosensors convert interactions of biochemical events into electrical signals. The most important factor in these systems is analytical performance. For this reason, nanomaterials with unique properties are often used in their development. Nowadays, these nanomaterials also contribute to the miniaturization of the developed electrochemical systems in a

---

D. Harmanci (✉)
Central Research Test and Analysis Laboratory Application and Research Center, Ege University, Izmir, Turkey

S. Balaban Hanoglu · D. Beduk
Department of Biotechnology, Graduate School of Natural and Applied Sciences, Ege University, Izmir, Turkey

© Springer Nature Singapore Pte Ltd. 2023

U. P. Azad, P. Chandra (eds.), *Handbook of Nanobioelectrochemistry*,
https://doi.org/10.1007/978-981-19-9437-1_37

format called “point of care” (PoC) to perform on-site measurements in applications such as diagnostics and monitoring, especially in the health and environmental fields. In this chapter, nanomaterials and their use in electrochemical sensing systems are discussed. The importance of electrochemical systems and their evolution into “point-of-care” devices (PoCD) is highlighted.

Keywords

Nanomaterial · Diagnostics · Electrochemical sensors · Point of care · PoC

1 Introduction

The working principle of electrochemical sensors is based on the generation of an electrical signal proportional to the concentration of the analyte of interest. A simple electrochemical system has three electrodes: working, reference, and counter electrode. Different sensors can be developed using the most appropriate electrochemical sensing technique for the analyte being measured (Hammond et al. 2016; Mahapatra et al. 2020).

Electrochemical sensors enable rapid measurements with small sample volumes. They are also widely used as low-cost, easy-to-use systems, particularly in biomedical and environmental applications. The best-known example of such a system is glucose meters. It is typically the most popular system still used for healthcare monitoring. Since the day it was developed by Clark, it has been updated in various ways and has evolved into a “point-of-care” device (PoCD) suitable for bedside use (Cho et al. 2020).

In recent years, the development of miniaturized systems that allow bedside or on-site measurement, such as blood glucose meters, has become very topical. This is because, despite the developments in healthcare that accompany the increase in the world's population, there are always interruptions in processes such as the diagnosis, follow-up, and treatment of diseases (Quesada-González and Merkoçi 2018). The growing population not only in health care demands but also has brought an increasing demand for food, which has led to various measures for sustainable agriculture. Given the problems in both areas, portable, user-friendly devices are being developed to enable the measurement of various parameters. Today, these tests, which allow for on-site or bedside measurement, are referred to as “point-of-care” (PoC) tests. These tests can be optical or electrochemical, depending on the measurement method. Here, the focus will be on electrochemical PoC devices (Wang et al. 2020a).

Whether optical or electrochemical, the analytical performance of PoC devices is critical. These devices should be specifically designed for the analyte of interest and either not react at all or react only slightly to other similar molecules. Sensitivity and stability are other important factors (Quesada-González and Merkoçi 2018). Even if a system is developed electrochemically, it must have high reproducibility and sensitivity when used in a PoCD. Advances in nanotechnology and the unique properties of nanomaterials are being extensively used in the development of this innovative and powerful system (Hammond et al. 2016; Quesada-González and Merkoçi 2018). Nanomaterials, usually used as electrodes or auxiliary matrices, contribute to the enhancement of the signal to be generated for the analyte of interest. For this purpose, they sometimes have additional electrocatalytic properties and sometimes work in perfect biocompatibility with their exceptional electron mobility and capture biomolecules (Cho et al. 2020).

Therefore, in this chapter, nanomaterials are first discussed and then electrochemical sensors, which are also used as PoC systems, are explained with examples.

2 Nanomaterials

Nanomaterials are unique structures in the range of 1–100 nm with at least one dimension in the submicron or nanoscale (Baig et al. 2021). Nanomaterials exhibit innovative and amazing properties not observed in bulk materials. Nanostructures with different physical and physicochemical properties can be created by modifying the chemical composition, atomic structure, dimension, design, and synthesis processes of nanomaterials (Kebede and Imae 2019). Therefore, the aforementioned nanostructure materials are receiving much attention due to their potential to improve current and future technologies.

3 Classification of Nanomaterials Based on the Dimension

Nanomaterials occur in a range of morphologies, including tubular, spherical, and irregular, and they can be found in single, aggregated, or fused forms (Rafiei-Sarmazdeh et al. 2019). Dimensionality is the most important characteristic that categorizes the different forms of nanostructures because the properties of nanomaterials can vary depending on their size and morphology. Nanomaterials are classified into four types based on their dimensionality: zero, one, two, and three as shown in Fig. 37.1.

4 Zero-Dimensional (0D) Nanomaterials

In zero-dimensional nanomaterials, all dimensions are limited to the nanoscale. They are spherical or quasi-spherical nanoparticles with a diameter of less than 100 nm and are also referred to as point-like particles (Wang et al. 2020b). They include quantum dots, polymer dots, fullerenes, nanospheres, magnetic nanoparticles, and noble metal nanoparticles such as gold, palladium, platinum, and silver (Tuantranont 2013). Nanomaterials with 0D structures exhibit a variety of physical and chemical properties, including high surface-to-volume ratio, optical stability, wavelength-dependent photoluminescence, chemical stability, cellular permeability, biocompatibility, and the high binding ability for biomolecules. Carbon-based nanomaterials are among the most studied 0D nanomaterials in the field of nanotechnology because they can be produced at low cost, have low inherent toxicity, and possess

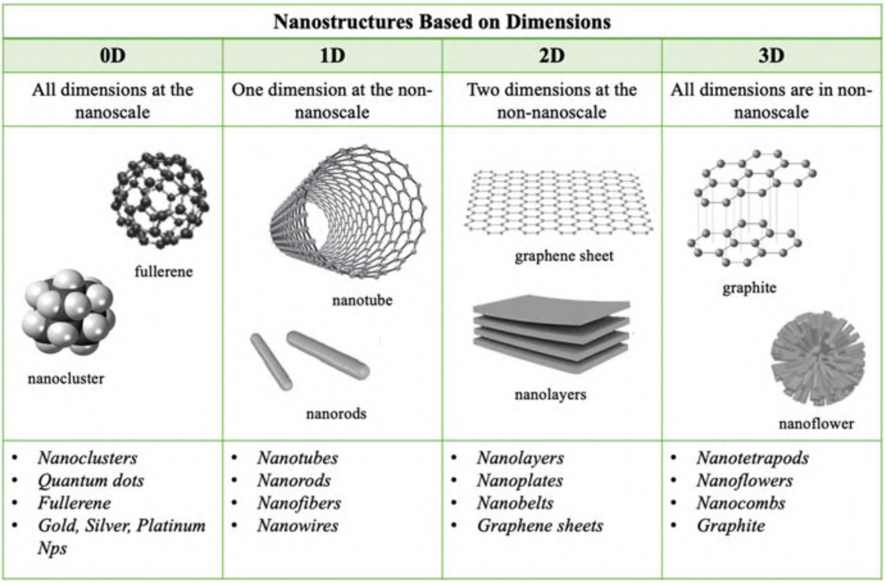

Nanostructures Based on Dimensions			
0D	**1D**	**2D**	**3D**
All dimensions at the nanoscale	One dimension at the non-nanoscale	Two dimensions at the non-nanoscale	All dimensions are in non-nanoscale
fullerene nanocluster	nanotube nanorods	graphene sheet nanolayers	graphite nanoflower
- *Nanoclusters* - *Quantum dots* - *Fullerene* - *Gold, Silver, Platinum Nps*	- *Nanotubes* - *Nanorods* - *Nanofibers* - *Nanowires*	- *Nanolayers* - *Nanoplates* - *Nanobelts* - *Graphene sheets*	- *Nanotetrapods* - *Nanoflowers* - *Nanocombs* - *Graphite*

Fig. 37.1 Nanostructures based on dimensions with examples

multifunctional surface functionality (Wang et al. 2020b). Due to the inherent structural properties of 0D nanomaterials, such as ultra-small size and high surface-to-volume ratio, they have more active edge regions per unit mass. By resizing nanomaterials and transforming them into zero-dimensional structures, one can impart new properties to the newly fabricated structure that are different from those of higher-dimensional materials (Malhotra and Ali 2018).

0D nanomaterials have high affinity for biomolecules and can be considered as powerful sensing materials for enzymes, antibodies, proteins, nucleic acids, and a variety of other clinically important substances. They enable the development of various biosensor platforms with high conductivity, specific optical properties, and low power consumption (Wang et al. 2020b). They can be used as an important probe to improve the sensitivity of biosensors to enhance their analytical performance, disease diagnosis, and pathogen detection. For this reason, 0D nanomaterials have triggered numerous studies in the field of biosensing in recent years. They have great potential for biomedical applications such as nanomedicine, cosmetics, bioelectronics, biosensors, and biochips (J. Wang et al. 2013b).

5 One-Dimensional (1D) Nanomaterials

One-dimensional nanomaterials can be defined as materials that have one dimension at the nanoscale, while the other two dimensions are at the macroscale (Tuantranont 2013; Welch et al. 2021). Their thickness can be one nanometer, but their length can be millions of times larger, ranging from hundreds to thousands of micrometers. The diameters of these nanoscale materials can be in both the x and y directions and their growth is linear in one dimension (Malhotra and Ali 2018). The length and diameter of these nanomaterials affect their absorption wavelengths, and their shape has significant effects on their applicability. Their length and thickness provide mechanical strength, which is advantageous in the development of larger nanostructured materials. Well-aligned 1D nanostructures could exhibit superior properties compared to their disordered equivalents (Su et al. 2012). The systematic arrangement of these nanoparticles into functional assemblies remains a challenge for the integration of 1D nanostructures into technological applications. For this reason, the fabrication of 1D nanomaterials is not straightforward and often requires rigorous synthetic processes to control their homogeneity (Tuantranont 2013).

1D nanostructures include nanorods, nanotubes, nanofibers, nanopillars, and nanowires (Kebede and Imae 2019). Due to their relative simplicity, they can be integrated into microelectronic processes, nanoscale wires, and/or tubes to fabricate active devices such as biochips through the use of novel nanobiotechnology. Therefore, one-dimensional structures such as nanowires and nanotubes are considered to be better primary transducers in biosensors (Patolsky et al. 2006).

6 Two-Dimensional (2D) Nanomaterials

Two-dimensional (2D) nanomaterials can consist of single-layered atoms or an ultrathin layer of a few atoms extending in both x and y dimensions. Two dimensions of these materials are at the nanoscale and one dimension is at the macroscale (Tuantranont 2013). They can have a surface area of several square micrometres while their thickness is in the nanoscale (Malhotra and Ali 2018). Due to their thickness and dimensions at both macro and nanoscales, they are considered the thinnest nanomaterials (Rafiei-Sarmazdeh et al. 2019). Ultrathin 2D nanomaterials are a new type of nanomaterials with sheet-like structures and transverse dimensions greater than 100 nm but generally less than 5 nm thick. The best-known examples of the class of 2D nanomaterials include nanolayers, nanoplates, nanobelts, nanodiscs, graphene, nanofilms, and nanocoatings. Graphene, one of the most widely used and fundamental 2D materials, has unique properties that make it valuable for a wide range of applications (Rafiei-Sarmazdeh et al. 2019). The electrical, optical, and mechanical characteristics of 2D materials can depend on the number of layers. They have large surface areas and anisotropic physical/chemical properties due to their unusual structures (Chimene et al. 2015). 2D nanomaterials are attracting growing interest from a variety of scientific disciplines. With their particular geometries, they exhibit unique shape-dependent features, high anisotropy, and chemical properties allowing them to be used as key components for nanodevices in functional electronics, catalysis, supercapacitors, and batteries (Tuantranont 2013). 2D nanomaterials are widely used for drug and gene delivery, biosensing, multimodal imaging, antimicrobial agents, tissue engineering, and cancer therapy due to their excellent biocompatibility and degradability. They have the largest specific surface area of any known material, which means they contain huge reservoirs and anchoring sites for successful uptake and delivery of therapeutic agents (Cai and Yang 2020).

7 Three-Dimensional (3D) Nanomaterials

Three-dimensional nanomaterials (3D) are materials with all dimensions at the macroscale and are not limited to the nanoscale in any dimension (Malhotra and Ali 2018). 3D nanomaterials include multi-nanolayers, nanorod or nanowire bundles, ordered aggregates of nanoparticles, and nanocrystals with nanoscale features such as nanotetrapods, nanoflowers, nanocombs, and nanotubes (Kebede and Imae 2019). Non-spherical nanoparticles have quite similar properties to 0D nanomaterials; nevertheless, variations in shape often lead to changes in absorption (Quesada-González and Merkoçi 2018). These materials have three-dimensional porosity that can enhance molecular movement. 3D nanostructures are an important material because of their many uses in catalysis, as magnetic materials, and as battery electrode materials. There are many different types of 3D materials, each with its own size and shape, leading to unique applications in sensing. Recently, the synthesis of 3D nanostructures with controllable structure and composition, larger surface area, and sufficient absorption sites for all relevant compounds in a small space has attracted great research interest.

8 Nanomaterials in Diagnostics

Due to their unique properties in the nanoscale size range, nanostructured materials have proven to be a powerful and effective tool for new technologies and have been used in the development of clinical diagnostic applications. In healthcare, there is a growing demand for more sensitive, less expensive and faster diagnostic tests. Infections and diseases need to be detected at an early stage to improve the prognosis of the disease and enable rapid and effective treatment. The combined use of various nanostructured materials will enable the creation of innovative multifunctional nanomedical platforms for multimodal imaging, diagnosis, and treatment (Kim et al. 2009).

Medicine and biomedical engineering are one of the most promising and challenging disciplines using nanostructured materials. Nanoparticle-based diagnostics have the advantage of being able to target a wide range of molecules. Nanostructures have the unique ability to detect small changes in biomolecules because their size is close to that of many target analytes, such as nucleic acids and proteins. They can be combined with analytical tests performed on samples from the human body, such as blood, saliva, and tissue. These tests are used to detect disease and track a person's health status. Parameters such as the identification of disease biomarkers at low concentrations, the time required to perform a test, the stability of components within the test, the cost of analysis, and the availability of analytical measurements are major factors in diagnostics today. Nanomaterials can be easily functionalized with different types of markers or labels to create nanoparticle-based diagnostic tools for a specific disease. Size, structure, surface area, chemical activity, and porosity can be changed to make them more suitable for different purposes. By modifying existing nanostructured materials, it is possible to predictably control and alter modify the characteristics of current nanostructured materials and endow them with biological properties and functions to better integrate them into biomedical systems. Modified nanostructured materials offer new and unique properties of nanomaterials, such as their optical, fluorescent, and magnetic properties, which have been used to develop new devices for disease diagnostics. Currently, nanotechnology is being used to develop cheaper, faster, more sensitive and more accurate tests and devices such as microchips, biosensors, nanorobots, microelectromechanical systems, and nanoelectronics for medical diagnostic applications (Jackson et al. 2017; Malhotra and Ali 2018).

Biosensors based on nanomaterials have revealed many opportunities for early detection and diagnosis of disease-related biomarkers. A number of nanostructured materials and composites have been developed for various sensing applications on different sensing platforms using a variety of preparation techniques (Tuantranont 2013). Selectivity, sensitivity, and specificity of biosensors are achieved by simple conjugation of ligands to a certain target molecule on the surface of nanomaterials. The unique characteristics of nanomaterials have paved the way for the development of a wide range of electrochemical sensors with enhanced analytical capabilities (Chen and Chatterjee 2013; Anik 2017). To increase the performance of biosensors, a variety of nanostructured materials with strong electrochemical activity, biocompatibility, high electrical conductivity, and large specific areas have been used as electron transfer mediators (Cho et al. 2020). The special properties of nanostructured metal nanoparticles such as gold, silver, and nickel, and semiconductor materials such as ZnO, TiO_2, CeO_2, and SnO_2 have been used to construct biosensors (Shetti et al. 2019).

With this information in mind, we will explore the innovative, low-cost, and user-friendly miniaturized systems using nanomaterials under the following headings.

9 What Is “Point of Care”?

As mentioned earlier, point-of-care tests (PoCT), especially in the biomedical field, means that the test is performed on-site, nearby. They are mainly used for diagnostic purposes, but in recent years they are also preferred for control purposes. PoC devices are mostly devices that have evolved from biosensors. The best known are pregnancy and ovulation tests, which were developed within the framework of optical biosensors, while blood glucose meters are of electrochemical origin. In particular, smartphones, which almost everyone owns, have led to various developments in the use of these devices. The measurement results can be analyzed by integrating them into smartphones (Quesada-González and Merkoçi 2018; Wang et al. 2020a). Here we discuss the potential of using electrochemical biosensors as PoC devices. Thanks to the advantages of nanomaterials, we will also mention the properties of surface area, biocompatibility, and increased sensitivity. In these devices, we can talk about a combination of biomaterials and nanomaterials. These biomaterials include enzymes, proteins, nucleic acids, antibodies, and so on, which are used in biosensors. They can also be easily conjugated with various biological labeling elements.

Of course, it should not be forgotten that all these systems should be tested for analytical performance during and after development and confirmed with comparative results for parameters determined by conventional methods (Misra et al. 2017). Much time must be spent in the laboratory to develop and deploy these devices.

In the next section, electrochemical biosensors are discussed in detail as PoC devices.

10 Electrochemical Sensors as PoC Tests

Sensors are described as small, fast, portable, and inexpensive devices for selective analysis (Goode et al. 2015). In addition, the use of electrochemistry in these devices has led to the development of more sensitive, practical, and cost-effective systems (Mahato et al. 2018). Today, electrochemical sensor systems can meet the need for portable, sensitive, practical, and accurate PoC testing (Anik 2017). From this perspective, this Part discusses the classification of nanomaterial-based electrochemical sensing systems and their potential as PoC tests.

11 Classification of Nanomaterial-Based Electrochemical Sensors

Electrochemical sensors are defined as devices that use an electrochemical transducer to measure the change in electrical potential that occurs as a result of the chemical reaction between biological recognition molecules and target analytes (Antuña-Jiménez et al. 2012). Electrochemical measurements mainly use three-electrode systems: the reference electrode, the counter electrode, and the working electrode. Briefly, the reference electrode is used to stabilize the potential of the working electrode, while the counter electrode (auxiliary electrode) closes the circuit and provides the electric current flow in the electrochemical cell (Honeychurch 2012). In addition to these electrodes, the other electrode is the working electrode where oxidation and reduction reactions between the biological recognition molecules and the target analytes are performed (Skoog et al. 2017). Ag/AgCl and platinum electrodes are used as reference and counter electrodes, respectively. Electrode types such as gold, carbon, graphene, and so on can be used as working electrodes, and the working electrodes can be designed with nanostructures as desired (Grieshaber et al. 2008). Recently, the development of electrochemical sensors based on nanomaterials has become popular because they increase the selectivity and sensitivity of the electrochemical sensor (Zhu et al. 2015). Electrochemical sensors based on nanomaterials can be classified as non-enzymatic, enzymatic, genosensors, immunosensors, cytosensors, and other electrochemical sensors (Fig. 37.2).

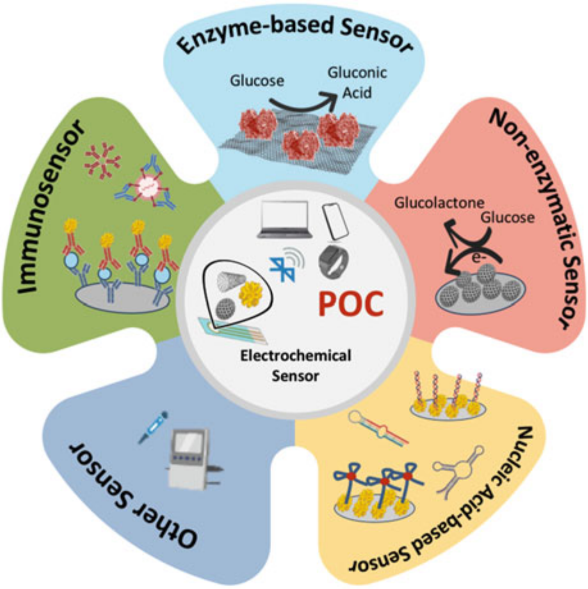

Fig. 37.2 Classification of electrochemical biosensors based on nanostructures

12 Enzyme-Based Electrochemical Sensor

Enzymes can be defined as protein-based biological catalysts (Anik 2017). In enzyme-based electrochemical sensors, highly specific enzymes are combined with sensitive electrochemical transducers. In these sensor systems, the enzymes are immobilized on the surface of the working electrode. The immobilization step is one of the most important steps as it affects the selectivity of the sensor system (Zhu et al. 2015). For enzyme electrodes, the electrical interaction between the electrode surface and the active site of the enzyme is another very important requirement. This is because the active site of some enzymes is isolated by a protein shell. This shell inhibits oxidation or reduction at any potential (Wang 2005). The target molecules can easily interact with the active site of the enzyme if the electrode surface is equipped with nanostructured materials (Çubukçu et al. 2007).

Glucose sensors are one of the most commonly developed enzyme-based sensing systems. The vital importance of glucose measurement, especially for diabetics, has increased the need for this type of PoC sensor system. The most important parameter in the systems developed for this need is durability, that is, the stability problem. This problem was overcome with the enzyme-based biosensor system developed with nickel nanoparticles by the work of Bandodkar et al. (2018). They were able to obtain reproducible results that remained stable for up to 8 months. In this system, the prepared enzyme pellets are attached to the surface of the SPE electrode using the magnetic effect of nickel nanoparticles, and the amount of glucose in mg/dL can be quantified within seconds using an android-based smartphone application. With the rapid development of PoC technology in recent years, the detection of glucose from sweat samples with wearable sensors has become possible (Zheng et al. 2021). The surface of the fabric-based 3D chip was functionalized with multi-walled carbon nanotubes (MWCNTs) and Prussian blue (PB) and then coated with glucose oxidase and chitosan. This device can chronoamperometrically monitor the amount of glucose in the sweat sample for 9 h, allowing continuous monitoring of the health status of the individual.

Enzymatic-electrochemical sensor systems are not limited to glucose; PoC devices have been developed to monitor many molecules important to human health, such as urea and amylase. A PoC system to determine the amount of phosphate in saliva using one's smartphone was developed by Bai et al (2021). First, the surface of screen-printed carbon electrodes (SPCE) is covered with an enzyme layer containing pyruvate oxide and MWCNTs, followed by a glutaraldehyde and Nafion layer. Phosphate was determined chronoamperometrically from saliva samples using an android-based smartphone application, and a response was obtained in less than 10 s (see Table 37.1 for examples described here and more).

13 Non-enzymatic Electrochemical Sensor

In non-enzymatic sensor systems, the measurement is based on the direct reduction/oxidation of target molecules such as glucose without the enzyme (Hassan et al. 2021). These sensors were developed as an alternative to the problems caused by temperature, humidity, and pH changes in enzymatic sensors. They have advantages such as low cost, high stability, fast and low detection limits and good sensitivity and are now widely studied and used (Park et al. 2006). Nanomaterials form a hybrid with metals used in the development of non-enzymatic sensors and lead to innovative ideas due to their effective surface area, mass transfer, and ability to increase sensor performance (Tee et al. 2017). Similar to enzymatic sensor systems, glucose sensors have taken the lead in non-enzymatic sensor systems (G. Wang et al. 2013a).

Nanomaterial-based non-enzymatic glucose sensing systems have been developed and can be used as PoC due to their advantageous properties. Today, non-enzymatic measurement of glucose, $[Na^+]$, and $[K^+]$ is possible with sensor systems designed as portable devices. In the system, Cr and Au nanometals were deposited on the substrate PET by electron beam evaporation and the surface was then coated with an insulating Al_2O_3 insulating layer for the electrode. When preparing the electrode system for glucose measurement, a chitosan/$NiCo_2O_4$ solution was dropped onto the Au electrode surface. For the preparation of $[Na^+]$ and $[K^+]$ sensor systems, the Au electrode surface was coated with Na^+ membrane (Na ionophore X, Na-TFPB, PVC, DOS, and tetrahydrofuran) and K^+ membrane (valinomycin, NaTPB, PVC, DOS, and cyclohexanone). The obtained sensors were integrated with micro-supercapacitors and used for the detection of glucose, $[Na^+]$ and $[K^+]$ from sweat samples. The sensitivities of the sensors were calculated to be 0.5 μA/μM for glucose, 0.031 nF/mM for $[Na^+]$, and 0.056 nF/mM for $[K^+]$ (Lu et al. 2019). The glucose sensor integrated into a

Table 37.1 Studies regarding potential electrochemical based

	Target analyte	Sensor classification	Nanomaterial/s	Ref
1	Phosphate in saliva	Enzymatic sensor	MWCNTs	(Bai et al. 2021)
2	Sweat glucose	Enzymatic sensor	MWCNTs	(Zheng et al. 2021)
3	Urea	Enzymatic sensor	AuNP	(Roy et al. 2021)
4	Uric acid	Enzymatic sensor	CNTs	(Yang et al. 2021)
5	α-amylase	Enzymatic sensor	AuNP	(Mandal et al. 2019)
6	Glucose	Enzymatic sensor	Nickel nanoparticle/ graphite	(Bandodkar et al. 2018)
7	Lactate	Enzymatic sensor (wearable tattoo sensor)	Carbon electrode/CNT	(Jia et al. 2013)
8	BchE	Paper-based enzymatic sensor	PBNPs	(Scordo et al. 2018)
9	Physostigmine, Rivastigmine, and Donepezil	Enzymatic sensor	PBNPs	(Caratelli et al. 2020)
10	Glucose	Enzymatic sensor	VACNTs	(Azimi et al. 2021)
11	Glucose	Non-enzymatic sensor	rGO	(Ji et al. 2017)
12	Carcinoembryonic antigen (CEA)	Immunosensor	PtNPs	(Yu et al. 2019)
13	COVID-19 spike antigen	Immunosensor	FTO/AuNP	(Mahari et al. 2020)
14	COVID-19	Immunosensor	AuNP	(Beduk et al. 2021)
15	*Plasmodium vivax* (Pv)-infected malaria	Immunosensor	Au-rGO	(Singh et al. 2021)
16	Blood protein biomarker NT-proBNP	Immunosensor	AuNP or AgNP	(Beck et al. 2022)
17	CP4-EPSPS	Immunosensor	AuNP	(Gao et al. 2019)
18	Microalbuminuria	Immunosensor	AuNC/PS	(Shaikh et al. 2019)
19	PSA	Immunosensor	Ag-nano ink	(Farshchi et al. 2021)
20	COVID-19	Genosensor	GNP/AuNP	(Alafeef et al. 2020)
21	*Mycobacterium tuberculosis*	Genosensor	SPGE/GPNP	(Jaroenram et al. 2020)

(continued)

Table 37.1 (continued)

	Target analyte	Sensor classification	Nanomaterial/s	Ref
22	Breast cancer biomarkers	Aptamer-based sensor	LSG/AuNP	(Rauf et al. 2021)
23	CEA	Aptamer-based sensor	Graphene	(Chakraborty et al. 2021)
24	NGAL	Aptamer-based sensor	AgNP ink	(Rosati et al. 2022)
25	Ammonia	Other	IDE	(Brannelly and Killard 2017)
26	Tyrosine	Other	SPE/CB nanomaterial	(Fiore et al. 2022)
27	Ascorbic acid, dopamine, and uric acid	Other	SPE/GO-AuNP	(Ji et al. 2018)
28	Methyl xanthine drug (caffeine)	Other	Carbon electrode/CNT	(Tai et al. 2018)
29	Glucose, Na^+, Ca^{2+}, K^+, and pH	Other	CNT fiber	(Wang et al. 2018)
30	AgNP	Other	Carbon ink/AgNP	(Cunningham et al. 2016)
31	HER2	Other	Near-infrared quantum dots and iron nanoparticles	(Loo et al. 2011; R Mas 2013)
32	Diclofenac	Other	Amberlite XAD-4	(Shanbhag et al. 2021)

Ag silver, *AgNPs* silver nanoparticles, *Ag ink* silver conductive ink, *Au* gold, *AuNC* gold nanocrystal, *AuNP* gold nanoparticle, *BChE* butyrylcholinesterase, *CEA* carcinoembryonic antigen, *CB* carbon black, *CNT* carbon nanotube, *CP4 EPSPS* 5-enol-pyruvylshikimate-3-phosphate synthase from *Agrobacterium* sp. CP4, *FTO* fluorine-doped tin oxide electrode, *GNP* graphene nanoplatelets, *GPNP* graphene nanoparticle powder, *GO* graphite oxide, *IDE* silver screen-printed interdigitated electrode, *LSG* laser-scribed graphene, *MWCNTs* multi-walled carbon nanotubes, *NGAL* neutrophil gelatinase-associated lipocalin, *NT-proBNP* N-terminal pro-brain type natriuretic peptide, *PBNPs* Prussian blue-nitrogen-doped graphene nanocomposite, *PSA* prostate-specific antigen, *PtNPs* platinum nanoparticles, *rGO* reduced graphene oxide, *SPE* screen-printed electrode, *SPGE* screen-printed graphene electrode, *VACNTs* vertically aligned carbon nanotube

smartphone developed by Ji et al. (2017) can be cited as another example. In this study, the surface of the screen-printed electrode (SPE) was coated with graphene oxide nanosheets and then a 3-aminophenyl boronic acid (APBA) nanocomposite was dropped onto the surface. The developed sensor platform was connected to a smartphone via an application and performed measurements. The system can determine glucose in blood serum with a detection limit of 0.026 mM (see Table 37.1 for examples described here and more).

Nanomaterial-based non-enzymatic sensors are currently available in the literature, although their design and integration as PoC are very limited. To facilitate the use of these systems, which are very useful for glucose systems, by making them user-friendly, it would be much better to develop them as PoC in the future.

14 Electrochemical Immunosensors

Electrochemical immunosensors are a type of sensor that use antibodies as detection agents. Electrochemical signals are generated in the sensor systems as a result of antibody recognition of the target analyte (Cho et al. 2018). The detection limit (LOD) is one of the most important analytical parameters for immunosensor systems and the sensitivity of the systems is low due to the small number of markers detected per biological recognition event. In order to decrease LOD, the use of nanomaterials has been the main goal in the development of platforms (Lim and Ahmed 2016). In addition, nanomaterials are widely used in immunosensing systems due to their surface area to volume ratio, conformational freedom for antibodies, surface reaction activity, and acceleration of electron transfer at the electrode surface (Wan et al. 2013). Nanomaterials-based electrochemical immunosensors are suitable systems for PoC because they offer advantages over other sensing technologies, such as high sensitivity, ease of manipulation, and ease of integration with other analytical devices (Quesada-González and Merkoçi 2018).

Nanomaterials-based electrochemical immunosensors have been developed for COVID-19 impacting the world today. However, one of the most important parameters here is that the developed sensor system can be used without an expert and the results can be transmitted to medical personnel without contact. In this regard, the design of the system developed for COVID-19 as a PoC and its integration into a device is very important. An electrochemical sensor system for the detection of COVID-19 in serum samples using a laser-scribed graphene electrode (LSG) modified with gold nanoparticles (AuNP) and specific antibodies was developed by Beduk et al (2021). The sensor system, which achieves a detection limit of 2.9 ng/ml, was miniaturized by integrating it into a PoC device so that the results can be accessed via smartphones. As another electrochemical immunosensor system, fluorine-doped tin oxide (FTO) electrodes were similarly modified with AuNP and nCovid-19 monoclonal antibodies (Mahari et al. 2020). Their device called eCovSens, which can measure COVID from saliva samples has a detection limit of 90 fM.

Electrochemical immunosensors are being developed for testing diseases and pathogens, which may be important not only for COVID-19 but also for humans and the environment. One of the best examples is the immunosensor system developed for the 5-enolpyruvilshikimate-3-phosphate synthase protein isolated from the CP4 protein (CP4-EPSPS) of the Agrobacterium species strain (Gao et al. 2019). In this study, a sandwich immunosensor system is developed. To increase the sensitivity, AuNPs were first functionalized with streptavidin-horseradish peroxidase (HRP) and the monoclonal antibody of CP4-EPSPS. Then, chitosan, AuNPs, and polyclonal antibodies for CP4-EPSPS (pAb) were immobilized on the SPCE surface. After genetically modified crop samples were applied to the electrode surface, functionalized AuNP nanoprobes were placed on the surface and measurements were performed. The LOD value of the system that can be used as PoC was calculated to be 0.05 ng/mL (see Table 37.1 for examples described here and more).

15 Nucleic Acid-Based Sensors (Genosensors and Aptasensors)

Genosensors and aptasensors are types of sensors that use nucleic acids to recognize the target analyte. In genosensors, a hybridization reaction occurs between recognition molecules such as DNA, and RNA and the target molecule such as ssDNA, and detection occurs accordingly. In contrast, in the aptasensor method, DNA or RNA aptamers that can bind to the target molecule with high affinity and specificity are immobilized in the sensor system as recognition molecules (Paniel et al. 2013).

A genosensor was developed and integrated into the PoC that can be used for rapid diagnosis of the present disease, COVID -19. An easy-to-use, paper-based electrochemical genosensor with a response time of fewer than 5 min was presented by Alafeef et al (2020). Graphene nanopellets were coated on the surface of the filter paper and the gold electrode was prepared by micro-Au deposition. Highly specific antisense oligonucleotides (ssDNA) conjugated with AuNP were deposited on the electrode surface, and detection was performed with SARS-CoV-2 RNAs isolated from Vero cells. Electrochemical results were obtained using a homemade circuit, and LOD was determined to be 6.9 copies/μL. Another genosensor to detect and measure COVID -19 using a smartphone was developed by Zhao et al (2021). First, a nanocomposite structure containing Au and Fe_3O_4, which was named premix A, and a graphene functional p-sulfocalix [8]arene (SCX8-RGO) enriched in toluidine blue (TB) and functionalized with Au, a structure named premix B, were synthesized. Subsequently, premix A and then premix B were incubated with the viral RNA determined as the target and SPCE was immobilized on the electrode surface and electrochemical measurements were performed using a smartphone.

Aptasensors are also widely used in cancer research as they can be used for screening and diagnosis of cancer biomarkers. Among the available studies, an aptasensor system developed by Rauf et al. (2021) stands out for the detection of Her-2, a biomarker for breast cancer. Moreover, this system is integrated with a PoC device that allows measurement with a smartphone so that diagnosis can be made without the help of an expert. In this system, LSG electrodes modified with gold nanoparticles were modified with DNA aptamers, and the LOD value for Her-2 was found to be 0.008 ng/mL. An aptasensor system was developed for the detection of carcinoembryonic antigen (CEA), a marker for cancers such as breast, ovarian, lung, and pancreas (Chakraborty et al. 2021). In this study, a working electrode was printed with carbon ink on a PET substrate and an SPE electrode was designed. After deposition of graphene on the working electrode, the surface was coated with ZnO nanorods and the aptamer was immobilized. The detection limit of the aptasensor system in human serum was determined to be 1 fg/mL (see Table 37.1 for examples described here and more).

16 Other Electrochemical Sensors

There are also other types of sensors called nanomaterial-based that do not use substances such as aptamers, antibodies, and enzymes as detection materials. Systems designed as wearables are the types of sensors that have attracted attention as PoC in recent years. Wearable sensors, which are widely used in health imaging applications such as drug analysis, allow the analysis of sweat, unlike other sensors. Fiore et al. (2022) designed an electrochemical sensor system to detect tyrosine using carbon black as an intelligent nano modifier. A wearable electrochemical fabric was developed that allows the analysis of glucose, Na^+, K^+, Ca^{2+}, and pH in a single sensor system (Wang et al. 2018). For this purpose, CNT fibers are coated with active materials that identify the target analytes. For the detection of glucose, CNT fibers are coated with chitosan, the enzyme glucose oxidase, and Prussian blue, while the other target analytes are coated with appropriate membranes. For the detection of Na^+, K^+, Ca^{2+}, the CNT surfaces Na-TFPB, PVC, DOS, and tetrahydrofuran remained constant, while the ionophores used (sodium, calcium, potassium) were varied. With the developed wearable fiber sensor based on nanomaterials, sweat measurements can be made in real-time via a smartphone connection. Doping controls and drug use monitoring can be performed with wearable sensors. The electrochemical wearable sensor that enables the analysis of the methylxanthine drug caffeine from sweat was developed by Tai et al (2018). The surface of PET was modified with CNT and Nafion after being coated with carbon as a working electrode. The sensor system is sweat-powered. The cholinergic agonist hydrogel technique was used for iontophoresis (sweat-driven technique), and caffeine measurement was successfully performed by computer via Bluetooth connection (see Table 37.1 for examples described here and more).

17 Conclusion

Advances in nanotechnology have reached an amazing level thanks to the contributions of scientists. The increase in knowledge about nanotechnology and the widespread use of nanomaterials have both paved the way for the development of new technologies and contributed to the development and improvement of existing technologies. The glucose sensor developed by Clark is the best example of this development and change. With the diversification of nanomaterials, their use in electrochemical systems will be one of the most popular topics not only today but also in the future.

The widely used PoC devices have now reached a level that can be described as a revolution in the health field. The use of nanomaterials in devices specifically designed for the analytes we are dealing with today has simplified the complex systems and improved the parameters of analytical performance. Some studies showing that the use of nanomaterials as electrodes or electrocatalysts in electrochemical sensing systems has resulted in higher sensitivity and lower detection limits are summarized in Table 37.1.

We can list the reasons why nanomaterials, which offer different advantages depending on their size, are preferred in electrochemical systems as follows:

- Gold, magnetic, and silver nanoparticles, known as OD, are easy to synthesize, small, can be easily conjugated, and can easily interact with other nanomaterials.
- Carbon nanotubes and nanowires, known as 1D, are among the most attractive classes of electrochemical sensing systems thanks to their high conductivity, directivity, and structural durability. This can be exploited to increase the selectivity of PoC devices. However, the fact that they must meet interface requirements to be integrated into these systems indicates that further study is needed in this area.
- Graphene, known as 2D, can be used in electrochemical systems because it is easily modified and flexible.
- They can be specified as non-spherical 3D nanoparticles and photonic crystals. They can cooperate with other nanoparticles.

It is possible that the newly explored forms of electrochemical sensing systems based on these nanomaterials, which offer various advantages, can be supported by advanced studies and transferred to routine practice after proving their functionality in real samples. PoC devices derived from electrochemical systems based on nanomaterials will occupy a larger place in our lives in the future.

References

Alafeef M et al (2020) Rapid, ultrasensitive, and quantitative detection of SARS-CoV-2 using antisense oligonucleotides directed electrochemical biosensor chip. ACS Nano 14(12): 17028–17045. https://doi.org/10.1021/acsnano.0c06392

Anik Ü (2017) 12 - Electrochemical medical biosensors for POC applications. In: Narayan RJ (ed) Medical biosensors for Point of Care (POC) applications. Woodhead Publishing, pp 275–292. https://doi.org/10.1016/B978-0-08-100072-4.00012-5

Antuña-Jiménez D et al (2012) Chapter 1 – Molecularly imprinted electrochemical sensors: past, present, and future. In: Li S et al (eds) Molecularly imprinted sensors. Elsevier, Amsterdam, pp 1–34. https://doi.org/10.1016/B978-0-444-56331-6.00001-3

Azimi S et al (2021) Developing an integrated microfluidic and miniaturized electrochemical biosensor for point of care determination of glucose in human plasma samples. Anal Bioanal Chem 413(5):1441–1452. https://doi.org/10.1007/s00216-020-03108-3

Bai Y et al (2021) An inkjet-printed smartphone-supported electrochemical biosensor system for reagentless point-of-care analyte detection. Sensors Actuators B Chem 346:130447. https://doi.org/10.1016/j.snb.2021.130447

Baig N, Kammakakam I, Falath W (2021) Nanomaterials: a review of synthesis methods, properties, recent progress, and challenges. Mater Adv 2(6):1821–1871. https://doi.org/10.1039/D0MA00807A

Bandodkar AJ et al (2018) Re-usable electrochemical glucose sensors integrated into a smartphone platform. Biosens Bioelectron 101:181–187. https://doi.org/10.1016/j.bios.2017.10.019

Beck F, Horn C, Baeumner AJ (2022) Ag nanoparticles outperform Au nanoparticles for the use as label in electrochemical point-of-care sensors. Anal Bioanal Chem 414(1):475–483. https://doi.org/10.1007/s00216-021-03288-6

Beduk T et al (2021) Rapid point-of-care COVID-19 diagnosis with a gold-nanoarchitecture-assisted laser-scribed graphene biosensor. Anal Chem 93(24):8585–8594. https://doi.org/10.1021/acs.analchem.1c01444

Brannelly NT, Killard AJ (2017) An electrochemical sensor device for measuring blood ammonia at the point of care. Talanta 167:296–301. https://doi.org/10.1016/j.talanta.2017.02.025

Cai S, Yang R (2020) Two-dimensional nanomaterials with enzyme-like properties for biomedical applications. Front Chem 8. https://www.frontiersin.org/article/10.3389/fchem.2020.565940. Accessed 26 Apr 2022

Caratelli V et al (2020) Precision medicine in Alzheimer's disease: an origami paper-based electrochemical device for cholinesterase inhibitors. Biosens Bioelectron 165:112411. https://doi.org/10.1016/j.bios.2020.112411

Chakraborty B et al (2021) Label free, electric field mediated ultrasensitive electrochemical point-of-care device for CEA detection. Sci Rep 11(1):2962. https://doi.org/10.1038/s41598-021-82580-y

Chen A, Chatterjee S (2013) Nanomaterials based electrochemical sensors for biomedical applications. Chem Soc Rev 42(12):5425–5438. https://doi.org/10.1039/C3CS35518G

Chimene D, Alge DL, Gaharwar AK (2015) Two-dimensional nanomaterials for biomedical applications: emerging trends and future prospects. Adv Mater 27(45):7261–7284. https://doi.org/10.1002/adma.201502422

Cho I-H et al (2018) Current technologies of electrochemical immunosensors: perspective on signal amplification. Sensors 18(1):207. https://doi.org/10.3390/s18010207

Cho I-H, Kim DH, Park S (2020) Electrochemical biosensors: perspective on functional nanomaterials for on-site analysis. Biomater Res 24(1):6. https://doi.org/10.1186/s40824-019-0181-y

Çubukçu M, Timur S, Anik Ü (2007) Examination of performance of glassy carbon paste electrode modified with gold nanoparticle and xanthine oxidase for xanthine and hypoxanthine detection. Talanta 74(3):434–439. https://doi.org/10.1016/j.talanta.2007.07.039

Cunningham JC et al (2016) Paper-based sensor for electrochemical detection of silver nanoparticle labels by galvanic exchange. ACS Sensors 1(1):40–47. https://doi.org/10.1021/acssensors.5b00051

Farshchi F et al (2021) An innovative immunoanalysis strategy towards sensitive recognition of PSA biomarker in human plasma samples using flexible and portable paper based biosensor: a new platform towards POC detection of cancer biomarkers using integration of pen-on paper technology with immunoassays methods. ImmunoAnalysis 1(1):6–6. https://doi.org/10.34172/ia.2021.06

Fiore L et al (2022) Smartphone-assisted electrochemical sensor for reliable detection of tyrosine in serum. Talanta 237:122869. https://doi.org/10.1016/j.talanta.2021.122869

Gao H et al (2019) A portable electrochemical immunosensor for highly sensitive point-of-care testing of genetically modified crops. Biosens Bioelectron 142:111504. https://doi.org/10.1016/j.bios.2019.111504

Goode JA, Rushworth JVH, Millner PA (2015) Biosensor regeneration: a review of common techniques and outcomes. Langmuir ACS J Surf Colloids 31(23):6267–6276. https://doi.org/10.1021/la503533g

Grieshaber D et al (2008) Electrochemical biosensors – sensor principles and architectures. Sensors 8(3):1400–1458. https://doi.org/10.3390/s80314000

Hammond JL et al (2016) Electrochemical biosensors and nanobiosensors. Essays Biochem. Edited by P. Estrela 60(1):69–80. https://doi.org/10.1042/EBC20150008

Hassan MH et al (2021) Recent advances in enzymatic and non-enzymatic electrochemical glucose sensing. Sensors 21(14):4672. https://doi.org/10.3390/s21144672

Honeychurch KC (2012) 13 – Printed thick-film biosensors. In: Prudenziati M, Hormadaly J (eds) Printed films. Woodhead Publishing series in electronic and optical materials. Woodhead Publishing, pp 366–409. https://doi.org/10.1533/9780857096210.2.366

Jackson TC, Patani BO, Ekpa DE (2017) Nanotechnology in diagnosis: a review. Adv Nanopart 6(3):93–102. https://doi.org/10.4236/anp.2017.63008

Jaroenram W et al (2020) Graphene-based electrochemical genosensor incorporated loop-mediated isothermal amplification for rapid on-site detection of Mycobacterium tuberculosis. J Pharm Biomed Anal 186:113333. https://doi.org/10.1016/j.jpba.2020.113333

Ji D et al (2017) Smartphone-based cyclic voltammetry system with graphene modified screen printed electrodes for glucose detection. Biosens Bioelectron 98:449–456. https://doi.org/10.1016/j.bios.2017.07.027

Ji D et al (2018) Smartphone-based integrated voltammetry system for simultaneous detection of ascorbic acid, dopamine, and uric acid with graphene and gold nanoparticles modified screen-printed electrodes. Biosens Bioelectron 119:55–62. https://doi.org/10.1016/j.bios.2018.07.074

Jia W et al (2013) Electrochemical tattoo biosensors for real-time noninvasive lactate monitoring in human perspiration. Anal Chem 85(14):6553–6560. https://doi.org/10.1021/ac401573r

Kebede MA, Imae T (2019) Chapter 1.1 – Low-dimensional nanomaterials. In: Ariga K, Aono M (eds) Advanced supramolecular nanoarchitectonics. William Andrew Publishing (Micro and Nano Technologies), pp 3–16. https://doi.org/10.1016/B978-0-12-813341-5.00001-2

Kim J, Piao Y, Hyeon T (2009) Multifunctional nanostructured materials for multimodal imaging, and simultaneous imaging and therapy. Chem Soc Rev 38(2):372–390. https://doi.org/10.1039/B709883A

Lim SA, Ahmed MU (2016) Electrochemical immunosensors and their recent nanomaterial-based signal amplification strategies: a review. RSC Adv 6(30):24995–25014. https://doi.org/10.1039/C6RA00333H

Loo L et al (2011) Highly sensitive detection of HER2 extracellular domain in the serum of breast cancer patients by piezoelectric microcantilevers. Anal Chem 83(9):3392–3397. https://doi.org/10.1021/ac103301r

Lu Y et al (2019) Wearable sweat monitoring system with integrated micro-supercapacitors. Nano Energy 58:624–632. https://doi.org/10.1016/j.nanoen.2019.01.084

Mahapatra S et al (2020) Advanced biosensing methodologies for ultrasensitive detection of human coronaviruses. In: Chandra P, Roy S (eds) Diagnostic strategies for COVID-19 and other coronaviruses. Medical virology: from pathogenesis to disease control. Springer, Singapore, pp 19–36. https://doi.org/10.1007/978-981-15-6006-4_2

Mahari S et al (2020) eCovSens-ultrasensitive novel in-house built printed circuit board based electrochemical device for rapid detection of nCovid-19 antigen, a spike protein domain 1 of SARS-CoV-2. bioRxiv, p. 2020.04.24.059204. https://doi.org/10.1101/2020.04.24.059204

Mahato K et al (2018) Chapter 14 – Electrochemical immunosensors: fundamentals and applications in clinical diagnostics. In: Vashist SK, Luong JHT (eds) Handbook of immunoassay technologies. Academic, pp 359–414. https://doi.org/10.1016/B978-0-12-811762-0.00014-1

Malhotra BD, Ali MA (2018) Chapter 1 – Nanomaterials in biosensors: fundamentals and applications. In: Malhotra BD, Ali MA (eds) Nanomaterials for biosensors. William Andrew Publishing (Micro and Nano Technologies), pp 1–74. https://doi.org/10.1016/B978-0-323-44923-6.00001-7

Mandal N et al (2019) Point-of-care-testing of α-amylase activity in human blood serum. Biosens Bioelectron 124–125:75–81. https://doi.org/10.1016/j.bios.2018.09.097

Mas RV (2013) Biomarker discovery and validation in kidney transplantation. J Mol Biomarkers Diagn 04(01). https://doi.org/10.4172/2155-9929.1000e115

Misra S et al (2017) 2 - Validation and regulation of point of care devices for medical applications. In: Narayan RJ (ed) Medical biosensors for point of care (POC) applications. Woodhead Publishing, pp 27–44. https://doi.org/10.1016/B978-0-08-100072-4.00002-2

Paniel N et al (2013) Aptasensor and genosensor methods for detection of microbes in real world samples. Methods 64(3):229–240. https://doi.org/10.1016/j.ymeth.2013.07.001

Park S, Boo H, Chung TD (2006) Electrochemical non-enzymatic glucose sensors. Anal Chim Acta 556(1):46–57. https://doi.org/10.1016/j.aca.2005.05.080

Patolsky F, Zheng G, Lieber CM (2006) Nanowire-based biosensors. Anal Chem 78(13): 4260–4269. https://doi.org/10.1021/ac069419j

Quesada-González D, Merkoçi A (2018) Nanomaterial-based devices for point-of-care diagnostic applications. Chem Soc Rev 47(13):4697–4709. https://doi.org/10.1039/C7CS00837F

Rafiei-Sarmazdeh Z, Zahedi-Dizaji SM, Kang AK (2019) Two-dimensional nanomaterials, nanostructures. IntechOpen. https://doi.org/10.5772/intechopen.85263

Rauf S et al (2021) Gold nanostructured laser-scribed graphene: a new electrochemical biosensing platform for potential point-of-care testing of disease biomarkers. Biosens Bioelectron 180: 113116. https://doi.org/10.1016/j.bios.2021.113116

Rosati G et al (2022) A plug, print & play inkjet printing and impedance-based biosensing technology operating through a smartphone for clinical diagnostics. Biosens Bioelectron 196: 113737. https://doi.org/10.1016/j.bios.2021.113737

Roy D et al (2021) 3-D printed electrode integrated sensing chip and a PoC device for enzyme free electrochemical detection of blood urea. Bioelectrochemistry (Amsterdam, Netherlands) 142: 107893. https://doi.org/10.1016/j.bioelechem.2021.107893

Scordo G et al (2018) A reagent-free paper-based sensor embedded in a 3D printing device for cholinesterase activity measurement in serum. Sensors Actuators B Chem 258:1015–1021. https://doi.org/10.1016/j.snb.2017.11.134

Shaikh MO et al (2019) Electrochemical immunosensor utilizing electrodeposited Au nanocrystals and dielectrophoretically trapped PS/Ag/ab-HSA nanoprobes for detection of microalbuminuria at point of care. Biosens Bioelectron 126:572–580. https://doi.org/10.1016/j.bios.2018.11.035

Shanbhag MM et al (2021) Amberlite XAD-4 based electrochemical sensor for diclofenac detection in urine and commercial tablets. Mater Chem Phys 273:125044. https://doi.org/10.1016/j.matchemphys.2021.125044

Shetti NP et al (2019) Nanostructured titanium oxide hybrids-based electrochemical biosensors for healthcare applications. Colloids Surf B Biointerfaces 178:385–394. https://doi.org/10.1016/j.colsurfb.2019.03.013

Singh P et al (2021) Design of a point-of-care device for electrochemical detection of *P. vivax* infected-malaria using antibody functionalized rGO-gold nanocomposite. Sensors Actuators B Chem 327:128860. https://doi.org/10.1016/j.snb.2020.128860

Skoog DA, Holler FJ, Crouch SR (2017) Principles of instrumental analysis. Cengage Learning, Mason

Su B, Wu Y, Jiang L (2012) The art of aligning one-dimensional (1D) nanostructures. Chem Soc Rev 41(23):7832–7856. https://doi.org/10.1039/C2CS35187K

Tai L-C et al (2018) Methylxanthine drug monitoring with wearable sweat sensors. Adv Mater 30(23):1707442. https://doi.org/10.1002/adma.201707442

Tee SY, Teng CP, Ye E (2017) Metal nanostructures for non-enzymatic glucose sensing. Mater Sci Eng C Mater Biol Appl 70(Pt 2):1018–1030. https://doi.org/10.1016/j.msec.2016.04.009

Tuantranont A (2013) Nanomaterials for sensing applications: introduction and perspective. In: Tuantranont A (ed) Applications of nanomaterials in sensors and diagnostics. Springer, Berlin/Heidelberg, pp 1–16. https://doi.org/10.1007/5346_2012_41

Wan Y et al (2013) Development of electrochemical immunosensors towards point of care diagnostics. Biosens Bioelectron 47:1–11. https://doi.org/10.1016/j.bios.2013.02.045

Wang J (2005) Nanomaterial-based electrochemical biosensors. Analyst 130(4):421–426. https://doi.org/10.1039/B414248A

Wang G et al (2013a) Non-enzymatic electrochemical sensing of glucose. Microchim Acta 180(3): 161–186. https://doi.org/10.1007/s00604-012-0923-1

Wang J et al (2013b) Advances in nano-scaled biosensors for biomedical applications. Analyst 138(16):4427–4435. https://doi.org/10.1039/C3AN00438D

Wang L et al (2018) Weaving sensing fibers into electrochemical fabric for real-time health monitoring. Adv Funct Mater 28(42):1804456. https://doi.org/10.1002/adfm.201804456

Wang X, Li F, Guo Y (2020a) Recent trends in nanomaterial-based biosensors for point-of-care testing. Front Chem 8.

Wang Z et al (2020b) Application of zero-dimensional nanomaterials in biosensing. Front Chem 8. https://www.frontiersin.org/article/10.3389/fchem.2020.00320. Accessed 26 Apr 2022

Welch EC et al (2021) Advances in biosensors and diagnostic technologies using nanostructures and nanomaterials. Adv Funct Mater 31(44):2104126. https://doi.org/10.1002/adfm.202104126

Yang M et al (2021) A 3D electrochemical biosensor based on Super-Aligned Carbon NanoTube array for point-of-care uric acid monitoring. Biosens Bioelectron 179:113082. https://doi.org/10.1016/j.bios.2021.113082

Yu Z et al (2019) Saw-toothed microstructure-based flexible pressure sensor as the signal readout for point-of-care immunoassay. ACS Sensors 4(9):2272–2276. https://doi.org/10.1021/acssensors.9b01168

Zhao H et al (2021) Ultrasensitive supersandwich-type electrochemical sensor for SARS-CoV-2 from the infected COVID-19 patients using a smartphone. Sensors Actuators B Chem 327:128899. https://doi.org/10.1016/j.snb.2020.128899

Zheng L, Liu Y, Zhang C (2021) A sample-to-answer, wearable cloth-based electrochemical sensor (WCECS) for point-of-care detection of glucose in sweat. Sensors Actuators B Chem 343:130131. https://doi.org/10.1016/j.snb.2021.130131

Zhu C et al (2015) Electrochemical sensors and biosensors based on nanomaterials and nanostructures. Anal Chem 87(1):230–249. https://doi.org/10.1021/ac5039863

Всё для победы!
НАРОДНЫЙ ФРОНТ
https://pobeda.onf.ru/
LET'S HELP THE RUSSIA

Nanobiosensors: Designing Approach and Diagnosis

38

Masoud Negahdary and Lúcio Angnes

Contents

1 Introduction 830
2 Applications of the Electrochemical Nano Immunosensors in the Early Diagnosis of Diseases 831
3 Applications of the Electrochemical Nano and Peptide-Based Biosensors in the Early Diagnosis of Diseases 836
4 Applications of the Electrochemical Nanoaptasensors in the Early Diagnosis of Diseases 843
5 A Summary and a Viewpoint About Electrochemical Nanobiosensors: Construction and Diagnosis of Diseases 847
6 Final Remarks 852
References 853

Abstract

In this chapter, we evaluated electrochemical biosensors designed to diagnose various diseases. The biorecognition elements in these biosensors consisted of antibodies, aptamers, and peptides. The studied biosensors used different nanomaterials (nanoparticles, nanostructures, nanocomposites, and other nano-based materials) to amplify the output signals and increase the diagnostic sensitivity. Here, all efforts were made to review and introduce the latest related research. The classification of the included biosensors was based on the type of biorecognition element and the type of analyte related to each type of disease, where a number of them were evaluated and reviewed in detail. Other designed biosensors related to each defined section have also been presented in several tables. Complete details of each biosensor have been offered in the tables. The final sections of this chapter provide a brief overview of the importance, prospects, and future of these biosensors.

M. Negahdary · L. Angnes (✉)
Department of Fundamental Chemistry, Institute of Chemistry, University of São Paulo, São Paulo, Brazil
e-mail: luangnes@iq.usp.br

© Springer Nature Singapore Pte Ltd. 2023

U. P. Azad, P. Chandra (eds.), *Handbook of Nanobioelectrochemistry*,
https://doi.org/10.1007/978-981-19-9437-1_38

Keywords

Nanomaterial-based biosensors · Immunosensors · Aptasensors · Peptide-based biosensors · Macromolecules · Electrochemical detection · Bioanalysis

1 Introduction

The use of new technologies is an important achievement in the rapid and accurate diagnosis of various diseases (Choudhary et al. 2016; Mahapatra et al. 2020). *Biosensors* are devices that respond to the presence of a particular substance (analyte) in an environment and produce measurable signals (Felix and Angnes 2018; Negahdary 2020a, b; Negahdary et al. 2020). A biosensor is composed of (at least) three parts: a biorecognition element, a signal transducer, and a detector. The analyte recognized by a biosensor comprises a wide range of chemical or biological substances, such as small organic molecules, peptides, proteins, nucleic acids, carbohydrates, tissue, or whole cells (Bakshi et al. 2021; Rong et al. 2021; Zhao et al. 2021; Yang et al. 2021; Zhang et al. 2021b; Abrego-Martinez et al. 2022; Bhatnagar et al. 2018; Shanbhag et al. 2021). The most selective biorecognition elements more recently introduced for biosensors include antibodies, aptamers, and peptide sequences. Ideally, this component should have a high affinity (low limit of detection (LOD)), high selectivity (minimum interference effect), wide dynamic range, and short response time (Negahdary and Heli 2019a; Heiat and Negahdary 2019; Negahdary et al. 2019a; Negahdary and Heli 2019b; Taheri et al. 2018; Chandra et al. 2012). A signal transducer can convert a molecular recognition event into a measurable signal such as fluorescence, chemiluminescence, colorimetric, or electrochemical/electrical outputs (Öndeş et al. 2021b; Song et al. 2021; Amouzadeh Tabrizi et al. 2021). The selection of signal transducer depends on other considered biosensor components and the type of detection technique(s).

In this chapter, our emphasis is on diagnosing diseases using electrochemical techniques. Biosensors equipped with various nanomaterials have recently provided efficient diagnoses for many acute and chronic diseases (Negahdary and Heli 2018; Negahdary 2020a, b; Mahato et al. 2018). The combination of biorecognition elements with nanomaterials, or the modification of the surface of the signal transducers with nanomaterials, has created biosensors with higher sensitivity and specificity (Pumera et al. 2007; Mahato et al. 2019). The purpose of designing and using nanobiosensors to diagnose various diseases is to reach a faster diagnosis, higher sensitivity, more accessible (portable), and less expensive application.

The available detection methods to diagnose various diseases often have several challenges to be overcome, such as lowering their cost, decreasing the time for each analysis, simplifying complicated diagnostic procedures, improving their specificity, and minimizing the effect of interfering agents (Gooding 2006; Morales and Halpern 2018).

One of the long-term goals of nanobiosensors design is to provide sensitive, selective, and portable diagnostic tools that will offer early diagnosis and subsequently accelerate therapeutic procedures. Nanobiosensors have great potential for important applications to diagnose many diseases, among them myocardial infarction (MI), cancers, and so on, that can save the lives of thousands of patients each year and significantly reduce the treatment costs (Negahdary and Heli 2019a, b; Heiat and Negahdary 2019; Negahdary et al. 2019a; Taheri et al. 2018). Because it is clear that rapid diagnosis of diseases increases the likelihood of treatment and rescue of patients, the rapid diagnosis of diseases in the early stages can also reduce treatment costs. Nanobiosensors can also be used to diagnose and monitor the status of diseases such as cancers (Heiat and Negahdary 2019).

In this chapter, we investigated the application of electrochemical nanobiosensors in the diagnosis of various diseases. It should be noted that three essential biorecognition elements used to build nanobiosensors (antibodies, aptamers, and peptides) and also analytes have been applied for the classification. This chapter covers the recent primary efforts to design electrochemical nanobiosensors (immunosensors, aptasensors, and peptide-based biosensors) to diagnose various diseases, all the articles being discussed here, whereas the most of included researches was published in 2020–2021. It is hoped that our presentation in this chapter can be used as guiding content for the design of new electrochemical nanobiosensors.

2 Applications of the Electrochemical Nano Immunosensors in the Early Diagnosis of Diseases

The most decisive laboratory test for diagnosing MI and myocardial injury is the accurate measurement of troponin (Chapman et al. 2020). Troponin contains a set of three protein subunits (Troponin T (TnT), Troponin I (TnI), and Troponin C (TnC)). Assays of TnI and TnT are considered the gold standard of MI diagnosis when patients with clinical signs are referred to the emergency units (Reichlin et al. 2009). Figure 38.1 shows the three-dimensional structure of the troponin complex (Shave et al. 2010). The subunits of this protein form a complex that regulates the interaction between actin and myosin, which plays an essential role in the contractions of various muscles, including the heart muscle. In the muscle contraction/relaxation process, the three subunits – the calcium-binding component (TnC), the inhibitory component (TnI), and the tropomyosin-binding component (TnT) – perform complementary roles (Katrukha 2013).

The European society of cardiology (ESC) and the American college of cardiology (ACC) have also considered minor myocardial ischemia as MI. In fact, due to the high diagnostic specificity of the troponin biomarker in the first days after a MI, as well as the direct relationship between the amount of troponin released from myocardial muscle and necrotic area into the circulation and the high stability of this biomarker in the blood (8–14 days), this biomarker is considered as the best preferred-biomarker for diagnosis of MI (Mair et al. 2018; Chapman et al. 2020; Negahdary et al. 2017, 2018, 2019a, b; Negahdary 2020a; Negahdary and Heli 2019a).

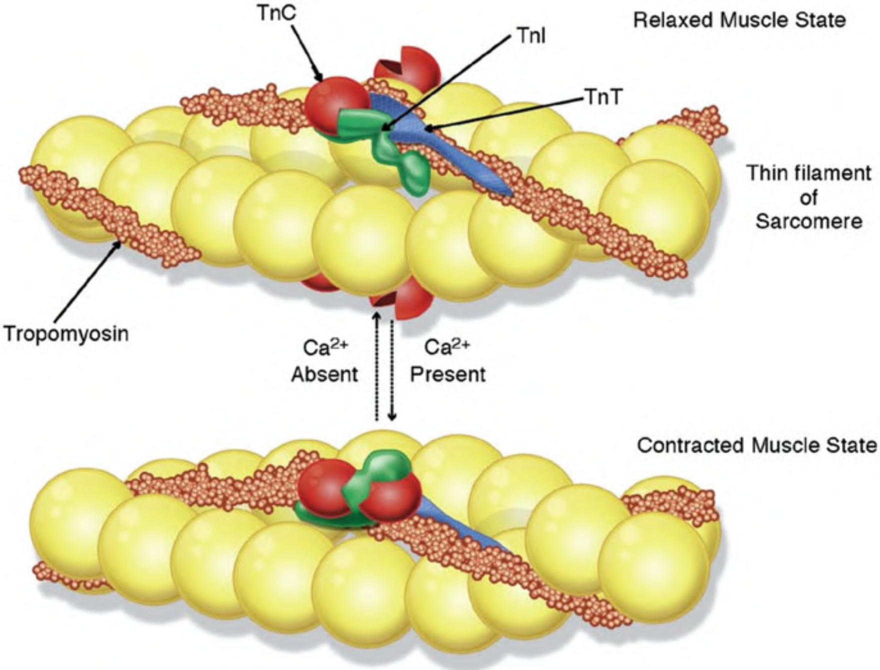

Fig. 38.1 Three-dimensional structure of the troponin complex in the process of muscle relaxation and contraction. (Reproduced with permission from Shave et al. (2010))

In a research, an immunosensor was designed for detection of TnI using a modified glassy carbon electrode (GCE) with AuPtPd porous fluffy-like nanodendrites (AuPtPd FNDs) (Cen et al. 2021). Here, as one of the initial procedures, AuPtPd FNDs were synthesized. First, 50 mmol L^{-1} thymine was dissolved in water, and then by using 1 M NaOH, the pH of this solution was increased to 10. Afterward, the temperature of the mentioned solution was elevated to 60 °C, and then 24.3 mmol L^{-1} $HAuCl_4$, 38.6 mmol L^{-1} H_2PtCl_6, and 100 mmol L^{-1} H_2PdCl_4 were added. This mixture was kept at the mentioned temperature for 20 min (Fig. 38.2). At the next step, 100 mmol L^{-1} L-ascorbic acid (AA) was added and stirred, and the achieved mixture was kept at room temperature for 12 h. Finally, the product was centrifuged and dried at 60 °C. In order to design an immunosensing platform, a defined amount of AuPtPd FNDs was dissolved in the deionized water, and a drop of this suspension was transferred to the GCE surface (the signal transducer). The suspension on the surface of GCE was dried at room temperature naturally. At the next step, a defined concentration of TnI antibody as the biorecognition element was immobilized on the surface of GCE-AuPtPd FNDs, and the unwanted binding sites of antibody molecules were blocked by bovine serum albumin (BSA) (Fig. 38.2). Finally, the prepared biosensor was immersed in the various concentrations of TnI as the analyte. The electrochemical assays were

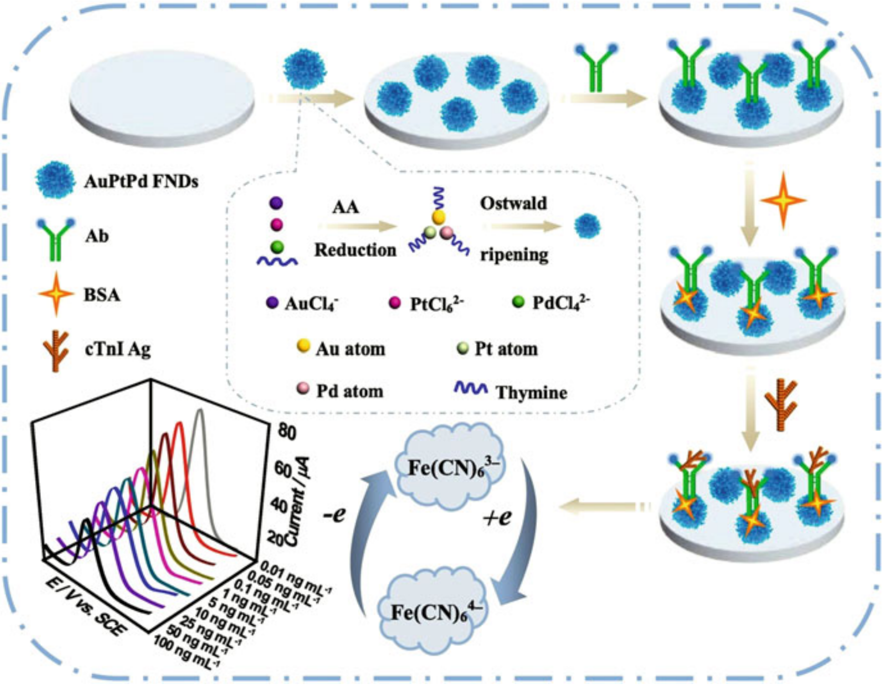
AuPtPd FNDs
Ab
BSA
cTnI Ag
AA
Reduction
Ostwald
ripening
AuCl4-
PtCl6 2-
PdCl4 2-
Au atom
Pt atom
Pd atom
Thymine
80
60
40
20
Current / µA
E/V vs. SCE
0.01 ng mL-1
0.05 ng mL-1
0.1 ng mL-1
1 ng mL-1
5 ng mL-1
10 ng mL-1
25 ng mL-1
50 ng mL-1
100 ng mL-1
-e
+e
Fe(CN)6 3-
Fe(CN)6 4-

Fig. 38.2 An immunosensor designed to diagnose TnI using a modified GCE with AuPtPd FNDs. (Reproduced with permission from Cen et al. (2021))

followed using differential pulse voltammetry (DPV) in the presence of $[Fe(CN)_6]^{3-}$ as the redox marker while the counter and references electrodes were platinum and saturated calomel, respectively. The presence of TnI led to the decrease of DPVs peak current. At this condition, the signal decrease was related to the electrode surface's reduced free area and the increment of analyte concentrations. This signal-off immunosensor could detect TnI in a linear range from 0.01 to 100.0 ng mL^{-1}, and the reported LOD was about 3 pg mL^{-1}.

Carcinoembryonic Antigen (CEA) is a glycoprotein tumor marker produced in the fetal gastrointestinal tract. Its levels before birth reach maximum but decline immediately after birth. In the early 1960s, it was discovered that CEA was present in the blood of adults with colorectal tumors and was initially thought the CEA to be specific for colorectal cancer (Tang et al. 2020; Pishvaian et al. 2016; Xiang et al. 2013). It was then discovered that this tumor marker is present in patients with a variety of carcinomas (cancers related to liver, bile duct, breast, and pancreas), sarcomas, and even many benign diseases (colitis, diverticulitis, and cholecystitis) and especially liver diseases such as cirrhosis and hepatitis is also present with high levels (Al-Kazzaz and Dr 2015; Al-Mudhaffar and Dr 2017). This tumor marker is used to determine the severity and prognosis of several types of cancers, as well as to control and monitor several diseases. Smokers also have high levels of CEA. In general, its levels should generally be less than 5 ng mL^{-1} (Sajid et al. 2007; Tang et al. 2007); otherwise, its level is abnormal. This tumor marker has the highest possible level in metastasis and also in failed treatment of liver and bone cancers. By measuring the level of this antigen, the patients can be informed about several possible cancers in various stages.

In a study, an immunosensor was developed for early detection of CEA using a modified GCE with $ZnMn_2O_4$@rGO nanocomposite and Au NPs (Fan et al. 2021). As the first step, $ZnMn_2O_4$@rGO nanocomposite was synthesized by the following procedure: The GO solution was mixed with ethylene glycol and then ultrasonicated. Afterward, the obtained suspension was mixed with the defined concentrations of urea, $MnCl_2 \cdot 4H_2O$, and $ZnCl_2$ and then inserted in an oil bath and kept at 200 °C for 24 h. Then, the filtration was performed, and the mixture was kept at 60 °C for 12 h. Finally, the material was calcined at 600 °C for 2 h under N_2 atmosphere, and the $ZnMn_2O_4$@rGO nanocomposite was achieved. In order to set up the CEA immunosensing platform, a GCE was applied as the signal transducer and modified with the prepared 15 mg mL^{-1} $ZnMn_2O_4$@rGO nanocomposite by immersing the working electrode in the related nanostructure solution. At the next step, the GCE-$ZnMn_2O_4$@rGO nanocomposite was modified with Au NPs through an electrodeposition procedure (V: −0.2 V, time: 30 s). The Au NPs synthesis solution consisted of 5 mmol L^{-1} $HAuCl_4$ and 0.01 M Na_2SO_4. Subsequently, a CEA-specific antibody as the biorecognition element was immobilized on the surface of the modified GCE with $ZnMn_2O_4$@rGO nanocomposite and Au NPs. Then, the unwanted binding sites of the antibody on the surface of GCE were blocked by using the BSA solution. Finally, the prepared immunosensor was evaluated in the presence of various concentrations of the analyte. All the electrochemical measurements were followed using a three-electrode system; the mentioned GCE was the working, and platinum and Ag/AgCl electrodes were applied as the counter and reference, respectively. The electrochemical assays were followed by the DPV as the detection technique and supported by $[Fe(CN)_6]^{3-/4-}$ as the redox marker. This electrochemical immunosensor could detect CEA in a linear range from 0.01 to 50 ng mL^{-1}, and the reported LOD was equal to 1.93 pg mL^{-1}.

Prostate-specific antigen (PSA) is a protein produced primarily by prostate cells (Wu et al. 2001). The prostate is a small gland that produces part of the seminal fluid. Most of the PSA produced is excreted through the seminal fluid, and some other amounts enter the bloodstream. PSA is present in the blood in two forms, free and complex (bound with a protein) (Nordström et al. 2018). Usually, all men have a small amount of PSA in their blood. Elevated PSA levels may be a sign of a prostate problem. In more than 80% of men with prostate cancer, PSA levels are higher than 4 ng mL^{-1} (Raouafi et al. 2019). However, levels above 4 ng mL^{-1} are not always associated with cancer. The PSA assay may be used as a promising tumor marker to screen and monitor prostate cancer. The goal of screening is to diagnose prostate cancer until the cancer cells are still in the prostate and have not spread (metastasis) to other organs (Romesser et al. 2018; Spratt et al. 2018). High increases in PSA levels in the blood are usually associated with prostate cancer but may also be associated with prostatitis and benign prostatic hyperplasia (BPH) (Fadila et al.

2020; Logozzi et al. 2019). It was also observed that, with age, PSA levels in all men usually increase.

With age, the weight of the prostate increases, and this enhanced size mostly leads to BPH or prostate cancer. As an outcome, the risk of prostate cancer increases with age (Boeri et al. 2021; Butler et al. 2020). If prostate cancer is diagnosed in the early stages (when still limited), generally it is not fatal, and with surgery or radiotherapy, the patients will have about 95% survival rate. However, in the late stages, when metastasis has occurred and other organs such as lymph nodes, bones, liver, and lungs are also affected, the life span after hormone therapy is only about 2 years (Hassanipour et al. 2020; de Crevoisier et al. 2018; Smith et al. 2018). Therefore, the initial diagnosis of prostate cancer is essential. Today, electrochemical biosensors have been used as valuable tools in the early detection of PSA (Sattarahmady et al. 2017; Negahdary et al. 2020; Rahi et al. 2016; Yazdani et al. 2019; Felix and Angnes 2018).

A very effective immunosensor was built on a fluorine-doped tin oxide (FTO) electrode modified with Au nanorods (NRs)-reduced-graphene oxide (rGO) nanocomposite as the signal transducer and was used to determine many concentrations of PSA (Chen et al. 2021c). First, Au NRs were synthesized. A solution of 1 mmol L^{-1} $HAuCl_4$ was prepared and then reduced by 0.01 mol L^{-1} $NaBH_4$. In this way, the seed solution of Au was obtained. Then, 0.1 mol L^{-1} cetyltrimethylammonium bromide (CTAB) and 1 mmol L^{-1} $HAuCl_4$ were mixed and then heated at 60 °C for 30 min; afterward, 2 M HCl and 10 mmol L^{-1} $AgNO_3$ were added to the prepared mixture and stirred for 2 min. Finally, the prepared seed solution of Au was added to the mixture, and after 300 min, Au NRs were achieved. In another procedure, GO was produced based on the Hummers method by applying graphite powder. Then, a defined concentration (2 mg mL^{-1}) of the produced rGO mixed with 0.2 mg mL^{-1} Au NRs and led to producing Au NRs-rGO nanocomposite. In order to develop the immunosensing platform, an FTO electrode was considered as the working electrode and modified with Au NRs-rGO nanocomposite (Fig. 38.3). Afterward, FTO-Au NRs-rGO was modified with chitosan to enhance the

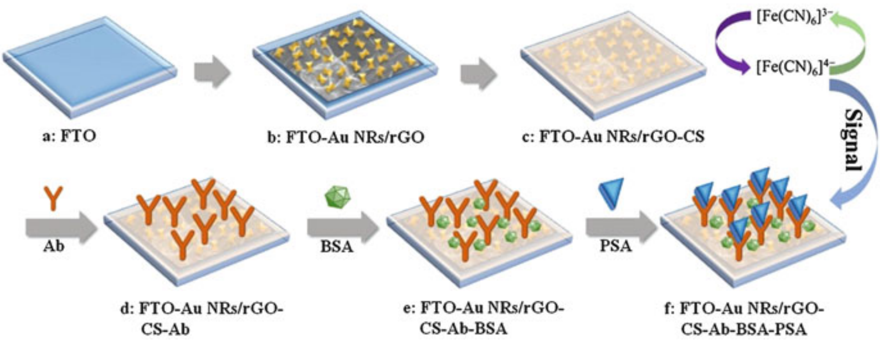

Fig. 38.3 An immunosensor for detection of PSA by applying a modified FTO electrode with Au NRs-rGO nanocomposite. (Reproduced with permission from Chen et al. (2021c))

biocompatibility and stability of the used nanocomposite on the surface of the FTO electrode. At the next step, a considered PSA antibody as the biorecognition element was dropped on the surface of the working electrode, and then the unspecified binding sites of the immobilized antibody were blocked by BSA. Finally, the prepared immunosensor was applied to detect the various concentrations of PSA (Fig. 38.3). The electrochemical assays were followed using the DPV technique and via a three-electrode system where the modified FTO, platinum, and saturated calomel electrodes were applied as the working, counter, and reference, respectively. The principle of detection was based on the changes found between the electron transfer rates. In the absence of PSA, the electron transfer rate was at the maximum value, but in the presence of the analyte, the bound status between the antibody and analyte led to blocking the electron transfer rate along with the increment of PSA concentrations. So, the lowest DPV peak current was found at the highest concentration of the analyte. This signal-off immunosensor detected PSA in a range from 0.1 to 150 ng mL^{-1}, and the reported LOD was equal to 0.016 ng mL^{-1}.

In Table 38.1, comprehensive details for nanoimmunosensors designed to diagnose various diseases have been provided.

3 Applications of the Electrochemical Nano and Peptide-Based Biosensors in the Early Diagnosis of Diseases

A peptide-based biosensor was developed for early detection of TnI by applying a mercury film-modified screen-printed electrode as the transducer (Xie et al. 2021). For this electrochemical biosensor, the peptide-oligonucleotide conjugate (POC)-templated quantum dots (QDs) (POC@QDs) were first synthesized. In order to synthesize this nanocomposite, the sodium hydrogen telluride (NaHTe) solution was prepared. Afterward, another solution containing 100 μmol L^{-1} POC, 1.25 mmol L^{-1} $CdCl_2$, and 1.05 mmol L^{-1} glutathione was prepared and mixed with the NaHTe solution. The pH of the obtained mixture was adjusted to 9, and then the temperature was increased to 100 °C for 5 min and then cooled slowly. Finally, the precipitation occurred after centrifuging, and the phosphate buffer solution (PBS) was applied to provide a resuspended POC@QDs nanocomposite when needed. In order to setup this biosensor, 4 mg mL^{-1} magnetic beads were functionalized with streptavidin and were mixed with a PBS solution containing 2 μmol L^{-1} of a peptide sequence (FYSHSFHENWPS) as the biorecognition element and incubated at room temperature for 120 min. Then, the purification of peptide-functionalized magnetic beads (Pep@MBs) nanocomposite was followed and then resuspended in the PBS solution. At the next step, a mixture containing a defined concentration of TnI (analyte), POC@QDs, and Pep@MBs was prepared and incubated at 37 °C for 45 min to produce the biosensing structure as a sandwich form (QDs@cTnI@MBs). Before the electrochemical measurements, MBs molecules were removed, and the remaining solution was mixed with 0.5 M nitric acid to release Cd^{2+} and subsequently mixed with 0.2 M HAc-NaAc buffer (pH 5.2). In order to present the biosensing principle of this electrochemical peptide-based biosensor, it should be

Table 38.1 The features and details about applied components in recent developed electrochemical nanoimmunosensors for diagnosis of diseases

Analyte	Transducer	Nanomaterial (s)	Redox marker	Detection technique (s)	Detection range	LOD	Ref.
Epithelial growth factor receptor (EGFR)	GE	Gold nanostructure	$[Fe(CN)_6]^{3-/4-}$	DPV	10 pg mL^{-1}–100 ng mL^{-1}	6.9 pg mL^{-1}	Bakshi et al. (2021)
PSA	FTO electrode	Au NRs-rGO composite	$[Fe(CN)_6]^{3-/4-}$	DPV	0.1–150 ng mL^{-1}	0.016 ng mL^{-1}	Chen et al. (2021c)
Alpha-fetoprotein (AFP)	Screen-printed electrode (SPE)	Ordered mesoporous carbon (OMC)@Au NPs	$[Fe(CN)_6]^{3-/4-}$	DPV	10 fg mL^{-1}–100 ng mL^{-1}	3.33 fg mL^{-1}	Rong et al. (2021)
Carbohydrate antigen 19-9 (CA19-9)	GCE	Multiwalled carbon nanotube and magnetite nanoparticle (MWCNT-Fe_3O_4)	$[Fe(CN)_6]^{3-/4-}$	SWV	1.0 pg mL^{-1}–100 ng mL^{-1}	0.163 pg mL^{-1}	Kalyani et al. (2021)
Interleukin-6	ITO	Acetylene black (AB)	$[Fe(CN)_6]^{3-/4-}$	EIS	0.01–50 pg mL^{-1}	3.2 fg mL^{-1}	Aydin et al. (2021b)
SARS-CoV-2	SPE	Magnetic beads (MBs)	N,N-dimethylformamide	DPV	S protein: 0.04–10 μg mL^{-1} N protein: 0.01–0.6 μg mL^{-1}	S protein: 19 ng mL^{-1} N protein: 8 ng mL^{-1}	Fabiani et al. (2021)
TnI/C-reactive protein (CRP)/ procalcitonin (PCT)	Transparency film screen-printed-based electrode	GO	$[Fe(CN)_6]^{3-/4-}$	SWV	TnI: 0.001–250 ng mL^{-1} CRP: 1–1000 ng mL^{-1} PCT: 0.0005–250 ng mL^{-1}	TnI: 0.16 pg mL^{-1} CRP: 0.38 ng mL^{-1} PCT: 0.27 pg mL^{-1}	Boonkaew et al. (2021)

(continued)

Table 38.1 (continued)

Analyte	Transducer	Nanomaterial (s)	Redox marker	Detection technique (s)	Detection range	LOD	Ref.
Human parathyroid hormone (PTH)	Screen-printed carbon electrode (SPCE)	Multiwalled carbon nanotube (MWCNT)/Au NPs	$[Fe(CN)_6]^{4-}$	DPV/SWV	DPV: 10^3–3×10^5 fg mL^{-1} SWV: 10^3–3×10^5 fg mL^{-1}	DPV: 0.886 pg mL^{-1} SWV: 0.065 pg mL^{-1}	Chen et al. (2021a)
Hunger hormone ghrelin (GHRL)	SPE	HfO_2-Pr_6O_{11} nanomaterials	$[Fe(CN)_6]^{3-/4-}$	DPV	0.01 pg mL^{-1}–50 ng mL^{-1}	0.006 pg mL^{-1}	Sun et al. (2021)
CCR4 antigen	ITO	Acid-substituted poly (pyrrole) polymer	$[Fe(CN)_6]^{3-/4-}$	EIS	0.02–8 pg mL^{-1}	6.4 fg mL^{-1}	Aydin et al. (2021a)
Procalcitonin (PCT)	GCE	PtCoIr nanowires/ SiO_2@Ag NPs	$[Fe(CN)_6]^{3-/4-}$	DPV	0.001–100 ng mL^{-1}	0.46 pg mL^{-1}	Wang et al. (2021d)
PSA	SPE	Sulfur-doped graphene QDs@gold nanostar (S-GQDs@Au NS)	$[Fe(CN)_6]^{3-/4-}$	LSV	10 fg mL^{-1}–50 ng mL^{-1}	0.29 fg mL^{-1}	Tran et al. (2021)
Cancer antigen 125 (CA125)	SPE	Boron nitride (BN) nanosheets	$[Fe(CN)_6]^{3-/4-}$	DPV	5–100 U	1.18 U mL^{-1}	Öndeş et al. (2021a)
IgG	SPCE	Graphene-TiO_2	$[Fe(CN)_6]^{3-}$	EIS	62.5–2000 ng mL^{-1}	2.81 ng mL^{-1}	Siew et al. (2021)
Hepatitis B surface antigen (HBsAg)	ITO	Fe_3O_4 NFs	$[Fe(CN)_6]^{3-/4-}$	DPV	0.5 pg mL^{-1}–0.25 ng mL^{-1}	0.16 pg mL^{-1}	Wang et al. (2021b)

TnI	GCE	AuPtPd porous fluffy-like nanodendrites (AuPtPd FNDs)	$[Fe(CN)_6]^{3-}$	DPV	0.01–100 ng mL^{-1}	3 pg mL^{-1}	Cen et al. (2021)
CEA	GCE	Silica coated nickel/carbon (Ni/C@SiO_2) nanocomposites/gold nanoparticle-coated PANI microsphere (CPS@PANI@Au NPs)	$[Fe(CN)_6]^{3-/4-}$	DPV	0.006–12 ng mL^{-1}	1.56 pg mL^{-1}	Tian et al. (2021a)
PSA	GCE	Poly(indole-6-carboxylic acid) (PICA) nanowire	6-PICA	SWV	0.5–100 ng mL^{-1}	0.11 ng mL^{-1}	Martínez-Rojas et al. (2021)
Carbohydrate antigen 15-3 (CA15-3)	GCE	PtCo alloyed nanodendrites (PtCo NDs)	$[Fe(CN)_6]^{3-/4-}$	DPV	0.1–200 U mL^{-1}	0.0114 U mL^{-1}	Ge et al. (2021)
PSA	GCE	MWCNT-Fe_3O_4 nanocomposite	$[Fe(CN)_6]^{3-/4-}$	DPV	2.5 pg mL^{-1}–100 ng mL^{-1}	0.39 pg mL^{-1}	Shamsazar et al. (2021)
CEA	GCE	$ZnMn_2O_4$@rGO/Au NPs	$[Fe(CN)_6]^{3-/4-}$	DPV	0.01–50 ng mL^{-1}	1.93 pg mL^{-1}	Fan et al. (2021)

noted that POC and analyte contained trypsin substrate in their sequences and in the sandwich structure of QDs@cTnI@MBs when trypsin was applied, QDs molecules were released through a proteolysis process. The release of QDs led to producing more Cd^{2+} molecules and enhancement of the output electrochemical DPVs. The releasing amount of QDs from the sandwich structure had a direct relationship with the concentration of TnI. This signal-on peptide-based biosensor detected TnI in a linear range from 0.001 to 100 ng mL^{-1} while the reported LOD was about 0.42 pg mL^{-1}.

In another research, a PSA biosensor was developed based on an antibody-peptide sandwich platform by applying a modified GCE with Au@PDA@BCN nanocomposite as the signal transducer (Zheng et al. 2021). Initially, boron-doped carbon nitride (BCN) nanosheets were synthesized by the one-step calcination procedure. Here, 5 g 4-pyridylboronic acid was transferred to a corundum boat and heated at 800 °C for 180 min. Afterward, a core-shell substrate (polydopamine (PDA)@BCN) was produced by mixing BCN and dopamine in a 100 mmol L^{-1} Tris-HCl buffer. This mixture was then sonicated (30 min), stirred, and centrifuged to produce PDA@BCN nanocomposite. At the next step, to produce Au@PDA@BCN nanocomposite, Au NPs were synthesized from $HAuCl_4$ by applying the sodium citrate reduction procedure. Then, a defined concentration of PDA@BCN and Au NPs were mixed and stirred at 4 °C for 4 h and subsequently centrifuged and washed with deionized water. Finally, the required amount of the synthesized Au@PDA@BCN nanocomposite was dispersed in the deionized water and kept in the refrigerator for future use.

In other synthesizing procedures, covalent organic framework (COF), MnO_2@COF, and AuPt@MnO_2@COF were synthesized. The solvothermal method was applied for synthesizing the COF by mixing 1,2,4,5-Tetrakis-(4-formylphenyl) benzene (TFPB) and 1,4-diaminobenzene (PPDA). This mixture was ultrasonicated, and then 6 M acetic acid was added and filled in an oil bath to follow the required reactions at 120 °C for 3 days. The product was washed with tetrahydrofuran and acetone, and the COF was achieved. At the next step, to synthesize MnO_2@COF, required amounts of solid COF and $HClO_4$ were added in the deionized water and sonicated for 10 min. Afterward, the temperature of the mixture was adjusted at 30 °C, and then a defined amount of $KMnO_4$ was added. This mixture was then stirred, sonicated, and centrifuged, respectively. The final product was washed with deionized water, and the MnO_2@COF as a powder was obtained using freeze-drying.

AuPt@MnO_2@COF nanocomposite was produced by the $NaBH_4$ reduction method. In this synthesizing method, MnO_2@COF was mixed with ethanol and then sonicated. At the next step, $HAuCl_4$ and H_2PtCl_6 were added to the above mixture and sonicated for 60 min. Finally, the $NaBH_4$ was added to the mixture and then was sonicated and centrifuged. The AuPt@MnO_2@COF was attained and, based on the required concentration, was resuspended in PBS solution. Subsequently, a bioconjugated structure (peptide/methylene blue/AuPt@MnO_2@COF) was produced. First, 2.5 mg mL^{-1} MB and 2 mg mL^{-1} AuPt@MnO_2@COF nanocomposite solutions were prepared, then mixed, and kept under stirring for

12 h. Afterward, the mixture was centrifuged and then washed with deionized water to remove extra methylene blue. At this moment, methylene blue/ AuPt@MnO_2@COF nanocomposite was obtained and dispersed into the PBS solution. Finally, 1 mg mL^{-1} PSA peptide (CGGGGMERCPIKMFYNLGSPYMNI) was added to the final mixture and stirred at 4 °C for 12 h. The centrifuge and washing with PBS solution provide the peptide/methylene blue/AuPt@ MnO_2@COF bioconjugated structure.

In order to set up the biosensing platform, a GCE was applied as the working electrode and then modified with Au@PDA@BCN nanocomposite. Afterward, the PSA antibody as one part of the biorecognition element was added on the surface of the GCE-Au@PDA@BCN nanocomposite, and then the unwanted and unspecified antibody binding sites were blocked by BSA. Subsequently, the considered concentrations of analyte were prepared and dropped on the surface of the signal transducer. Finally, the prepared bioconjugated structure (peptide/methylene blue/ AuPt@MnO_2@COF) was added. So, the analyte was located in a sandwich structure between the antibody and peptide (antibody-analyte-peptide). The electrochemical assays were followed by the DPV technique while the applied methylene blue molecules in the bioconjugated structure contributed as the redox marker. The electrochemical behavior of this biosensor confirmed that after modification of the surface of GCE with Au@PDA@BCN nanocomposite due to the increased active surface area, the DPV peak current was increased. After immobilization of the PSA antibody and PSA, the DPVs peak currents were reduced regularly based on the blocking of the electron transfer rate. However, after immobilization of the bioconjugated structure on the surface of the signal transducer, the DPV peak current increased again due to the high conductivity of AuPt NPs. This antibody-peptide sandwich-based PSA signal-on biosensor could detect this cancer biomarker in a linear range from 0.00005 to 10 ng mL^{-1}, and the found LOD was about 16.7 fg mL^{-1}.

In another research, a CEA biosensor was developed by applying a modified ITO electrode with polyaniline (PANI) and Au NPs (Hao et al. 2020). First, CdS QDs nanostructure was synthesized. 20 mmol L^{-1} $CdCl_2$ and 20 mmol L^{-1} MPA were mixed, and the pH of the solution was adjusted to 11 using 1 mol L^{-1} NaOH. Afterward, 20 mmol L^{-1} thioacetamide was added, and the mixture was stirred for 30 min at room temperature; in sequence, the temperature was enhanced to 80 °C and kept for 10 h. Finally, the purification of CdS QDs nanostructure was followed by applying deionized water for 12 h at room temperature. In another procedure, Au-luminol-DNA2 Probe was produced. Initially, Au-luminol solution was prepared and then mixed with a thiol-functionalized aptamer sequence (DNA 2: 5′-Cy5-TATCCAGCTTATTCAATTTTTTTT–$(CH_2)_6$-SH-3′). After 12 h, Au-S covalent bond was established between the Au and thiol molecules, and a conjugated structure of Au-luminol-DNA2 Probe was achieved. In order to design the electrochemical biosensing platform, an ITO electrode was used as the signal transducer and modified with PANI via an electropolymerization procedure(−0.2 V to +0.8 V at 100 mV s^{-1}). At the next step, the ITO-PANI was modified with Au NP colloid (Fig. 38.4). Subsequently, a peptide sequence (DKDKDKDPPPPC) was

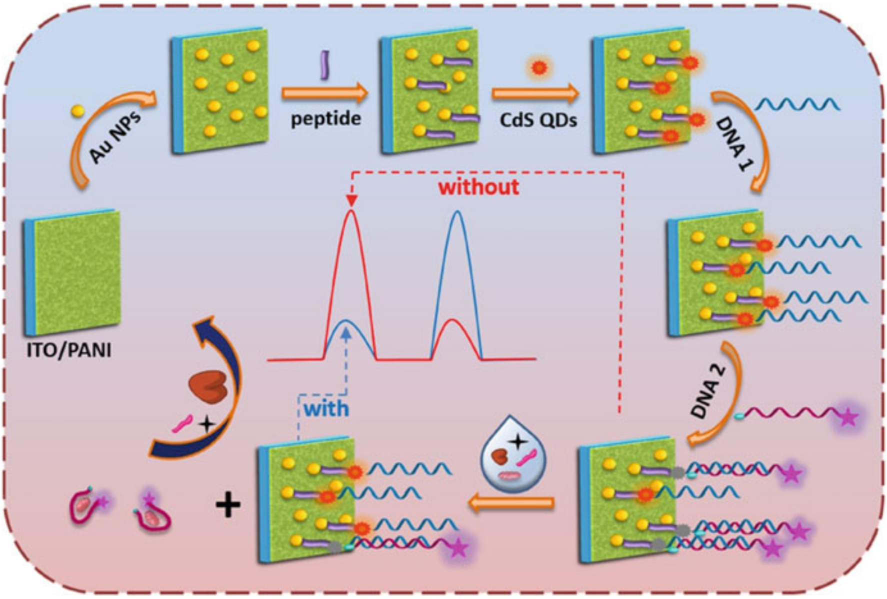

Fig. 38.4 An ECL peptide-aptamer biosensor for detection of CEA by applying the modified ITO electrode with PANI and Au NPs. (Reproduced with permission from Hao et al. (2020))

immobilized on the surface of ITO-PANI-Au NPs. The interaction between the peptide sequence and ITO-PANI-Au NPs occurred through the Au-S covalent bond. At the next step, the carboxyl group of the prepared CdS QDs nanostructure was activated by EDC/NHS, and then this nanostructure was coated on the surface of ITO-PANI-Au NPs-peptide (Fig. 38.4). At this point, an amine-functionalized aptamer sequence (DNA1: 5′-AATTGAATAAGCACCCCCTTTTTT-$(CH_2)_6$-NH_2-3′) was immobilized on the surface of ITO-PANI-Au NPs-peptide-CdS QDs nanostructure and could create the amide bond with CdS QDs nanostructure molecules. As the final step, enough amount of the prepared Au-luminol-DNA2 Probe was dropped on the surface of the signal transducer, and hybridization could be established between DNA1 and DNA2 strands. The prepared biosensor was applied for the determination of the various concentrations of CEA. In the designed biosensor, the CdS QDs nanostructure was applied as the cathode ECL emitter, and the Au-luminol-DNA2 Probe (containing Cy5 as the fluorophore agent) was as the anode ECL emitter. In the absence of the analyte, the negative potential related to the ECL signal of CdS QDs nanostructure was quenched, and the positive potential related to the ECL signal of the Au-luminol-DNA2 probe remained. However, in the presence of the analyte, the affinity between the DNA1 and CEA was intense to break the hybridization between DNA1 and DNA2. This event led to the decrement in the positive potential of the Au-luminol-DNA2 probe and an enhancement in negative potential related to the ECL signal of CdS QDs nanostructure. The ratio between ECL output responses provided a quantitative method for the detection of this cancer biomarker. This biosensor could detect CEA in a linear range up to 100 ng mL^{-1} and with an LOD of about 0.13 pg mL^{-1}.

In Table 38.2, comprehensive details for nano and peptide-based biosensors designed to diagnose various diseases have been provided.

4 Applications of the Electrochemical Nanoaptasensors in the Early Diagnosis of Diseases

An aptasensor based on electrochemiluminescence (ECL) was developed to determine various concentrations of TnI by using a modified GCE with CdS QDs (Kitte et al. 2021). In this research, two nanostructures were applied. First, CdS QDs (medium size: 5 nm) were synthesized from a mixture of 0.017 mol L^{-1} Cd $(NO_3)_2{\cdot}4H_2O$ and 0.082 mol L^{-1} $Na_2S{\cdot}9H_2O$. In the second procedure, Au nanoparticles (Au NPs) (medium size: 5 nm) were synthesized by mixing 0.1 mol L^{-1} $NaBH_4$ and 0.25 mmol L^{-1} $HAuCl_4$ in a solution containing HCl/HNO_3 (3:1). A conjugated structure was obtained at the next step by mixing a defined concentration of (5′-CGCATGCCAAACGTTGCCTCATAGTTCCCTCCCCGTGTCC-3′)-a thiol-functionalized aptamer-and Au NPs. In order to design this aptasensing platform, a GCE was chosen as the signal transducer, and its surface was modified with CdS QDs nanostructure. Subsequently, to establish the carboxyl groups on the surface of this signal transducer, a solution containing 3-mercaptopropionic acid (MPA), 0.1 mol L^{-1} NaCl, and 0.1 mol L^{-1} PBS (pH 7.4) was used. Then, the obtained carboxyl groups were activated by immersing the electrode in 25 mmol L^{-1} 1-ethyl-3-(3-dimethylaminopropyl)-carbodiimide hydrochloride/N-hydroxy-succinimide (EDC/NHS) (1:1) solution. Afterward, (5′-CGTGCAGTACGCCAACCTTTCT CATGCGCTGCCCCTCTTA-3′) an amine-functionalized aptamer was immobilized on the surface of the prepared GCE, and nonspecific binding sites were blocked by mercaptohexanol (MCH). Then TnI as the analyte was added on the surface of the signal-transducer. Finally, the conjugated aptamer-Au NPs were added, and consequently, a sandwich structure was established (Au NPs-aptamer/TnI/aptamer/CdS QDs nanostructure/GCE). The electrochemical measurements were followed in a solution containing $[Fe(CN)_6]^{3-/4-}$ as the redox signal marker and in a three-electrode system, whereas the modified GCE, platinum, and Ag/AgCl electrodes were applied as the working, counter, and reference, respectively. The ECL assays were performed in the presence of 0.05 M ${S_2O_8}^{2-}$ as the coreactant agent. The presence of TnI as the analyte was led to develop the sandwich structure based on the found affinity between aptamers strands and analyte molecules, while the used nanostructures created an optimum electron transfer rate. This event provided ECL signals at the maximum value, and this event had a direct relation along with enhancement of the concentrations of the analyte. According to the authors, the linear detection range for this TnI aptasensor was situated between 1 fg mL^{-1} to 10 ng mL^{-1}, and the obtained LOD was 0.75 fg mL^{-1}.

Table 38.2 The features and details about applied components in recent developed electrochemical nano and peptide-based biosensors for diagnosis of diseases

Analyte	Transducer	Peptide	Functional group interacted with the peptide sequence	Nanomaterial(s)	Redox marker	Detection technique	Detection range	LOD	Ref.
Botulinum neurotoxin serotype A and C	Paper-based electrode	CLYRIDEANQRATLM	Thiol	Au NPs	$[Fe(CN)_6]^{3-/4-}$	SWV	Up to 1 nmol L^{-1}	10 pmol L^{-1}	Caratelli et al. (2021)
Candida yeasts (*C. krusei*, *C. glabrata*, *C. albicans*, and *C. tropicalis*)	GE	Clavanin A: VFQFLGKIIHHVGNFVHGFSHVF	Nonpolar amino acid residues (FLPII)	TiO_2 NPs	$[Fe(CN)_6]^{3-}$	EIS	10^1–10^6 CFU mL^{-1}	2–3 CFU mL^{-1}	Ribeiro et al. (2021)
E. coli O157:H7	SPCE	QKVNIDELGNAIPSGVLKDD	Thiol	Au NPs	$[Fe(CN)_6]^{3-/4-}$	EIS	Up to 500 CFU mL^{-1}	2 CFU mL^{-1}	Ropero-Vega et al. (2021)
AFP	GCE	CPPPPEKEKEKEK	NH_2	PANI	$[Fe(CN)_6]^{3-/4-}$	DPV	0.1 fg mL^{-1}–1 ng mL^{-1}	0.03 fg mL^{-1}	Zhao et al. (2021)
miRNA-192	Pencil graphite electrode (PGE)	FF	–[a]	GO	$[Fe(CN)_6]^{3-/4-}$	EIS	10 fmol L^{-1}–1 n mol L^{-1}	8 fmol L^{-1}	Bolat et al. (2021)
PSA	GCE	CGGGGMERCPIKMFYNLGSPYMNI	–[a]	Au@PDA@BCN nanocomposite/ AuPt@MnO_2@COF nanocomposite	$[Fe(CN)_6]^{3-/4-}$	DPV	0.00005–10 ng mL^{-1}	16.7 fg mL^{-1}	Zheng et al. (2021)
Matrix metalloproteinase 2 (MMP-2)	GE	FGPLGVRGKGGC/ FGGGASLWWSEKL	Cucurbit[8]uril (CB[8])	Ag NPs	$[Fe(CN)_6]^{3-/4-}$	SWV	0.5 pg mL^{-1}–50 ng mL^{-1}	0.12 pg mL^{-1}	Cheng et al. (2021)
Tumor exosomes	GCE	FNFRLKAGAKIRFGRGC	Thiol	Au NFs/Au NPs@g-C_3N_4 nanocomposite	$[Fe(CN)_6]^{3-/4-}$	ECL	1×10^2–1×10^7 particles μL^{-1}	39 particles μL^{-1}	Liu et al. (2021)

Dopamine	GCE	FEKF	Fluorene methoxycarbonyl (Fmoc)	Au NPs	Fluorine methoxycarbonyl (Fmoc)	DPV	0.1–10 μmol L^{-1}	21 nmol L^{-1}	Wang et al. (2021c)
Human chorionic gonadotrophin (hCG)	ITO	PPLRINRHILTR/ EKEKEKEPPPPC	NH_2	Au NPs	$[Fe(CN)_6]^{3-/4-}$	PEC	0.5–1000 mIU mL^{-1}	0.19 mIU mL^{-1}	Gu et al. (2021)
TnI	Mercury film modified screen-printed electrode	FYSHSFHENWPS/ GGGAFYSHSFHENWPSK	Biotin	QDs/magnetic beads	–[b]	DPV	0.001–100 ng mL^{-1}	0.42 pg mL^{-1}	Han et al. (2021a)
Trypsin	GCE	HWRGWVC	–[a]	Au NPs/Ag@CeO_2 NPs	$S_2O_8^{2-}/SO_4^{\cdot -}$	ECL	10 fg mL^{-1}–100 ng mL^{-1}	3.46 fg mL^{-1}	Song et al. (2021)
Protein kinase A	ITO	LRRASLGGGGC	Thiol	Au NPs/ZrO_2-CdS octahedral nanocomposite	$[Fe(CN)_6]^{3-/4-}$	PEC	0.001–100 U mL^{-1}	0.00035 U mL^{-1}	Xiao et al. (2021)
Rituximab	GE	CGSGSGSWPRWLEN	–[a]	Au NPs	$[Fe(CN)_6]^{3-/4-}$	EIS	0.1–50 μg mL^{-1}	35.26 ng mL^{-1}	Huang et al. (2021)
Immunoglobulin G (IgG)	GCE	CPPPPEK(HWRGWVA) EKEKE/CPPPPEK EKEKE HWRGWVA	Thiol	Au NPs	$[Fe(CN)_6]^{3-/4-}$	DPV	100 pg mL^{-1}–10 μg mL^{-1}	32 pg mL^{-1}	Chen et al. (2021b)
Antibody of rheumatoid arthritis	Screen-printed polycarbonate electrode	Inter-alpha-trypsin inhibitor-3 $(ITIH3)^{542-556}$	Thiol	Au NPs	$[Fe(CN)_6]^{3-/4-}$	EIS	0.25–1 mmol L^{-1}	–[c]	Lin et al. (2022)
Human epidermal growth factor receptor 2 (HER2)	GCE	FEKF	Fluorine methoxycarbonyl group (Fmoc)	Nanofibrous network structure	Fmoc/$[Fe(CN)_6]^{3-/4-}$	DPV	0.1 ng mL^{-1}–1 μg mL^{-1}	45 pg mL^{-1}	Tao et al. (2021a)
CEA	ITO	DKDKDKDPPPPC	Thiol	CdS QDs/Au NPs	$[Fe(CN)_6]^{3-/4-}$	ECL	Up to 100 ng mL^{-1}	0.13 pg mL^{-1}	Hao et al. (2020)

[a] The functional group interacted with the peptide sequence not reported
[b] The redox marker not reported
[c] The LOD not reported

In another investigation, a photoelectrochemical (PEC) aptasensor was developed for early detection of PSA by applying ZnO NA-CdS nanocomposite and iodide-doped bismuth oxychloride flower-array ($I_{0.2}$:$BiOCI_{0.8}$) as the photocathode agent (Feng et al. 2021). The zinc oxide nanorod array (ZnO NA) was initially synthesized by preparing a mixture containing 0.02 mol L^{-1} $Zn(NO_3)_2{\cdot}6H_2O$, 0.03 mol L^{-1} NaOH, and methanol. This mixture was heated several times at 60 °C to dry on the reference/counter microelectrodes. Afterward, to do the calcination process, the temperature of the mixture was reached to 350 °C and kept for 30 min. Then, the obtained ZnO seed was mixed with a solution containing 0.05 mol L^{-1} $Zn(NO_3)_2{\cdot}6H_2O$ and 0.05 mol L^{-1} hexamethylenetetramine, and the obtained mixture was kept at 90 °C for 6 h. Finally, the CdS QDs were added (drop by drop), producing ZnO NA-CdS nanocomposite. This nanocomposite was used as the photoanode. The indium tin oxide (ITO) equipped with poly (dimethylsiloxane) (PDMS) microelectrode channels was applied as the working electrode, and then $I_{0.2}$:$BiOCI_{0.8}$ as a photocathode was synthesized on its surface with the following procedure. A mixture of NaCI and KI was prepared and dissolved in the deionized water (solution 1), and $Bi(NO_3)_3{\cdot}5H_2O$ was dissolved in glycol (solution 2). Afterward, solution 1 and solution 2 were added on the surface of the working electrode in sequence. Then, the chitosan solution containing acetic acid and glutaraldehyde was added on the surface of the modified working electrode with $I_{0.2}$:$BiOCI_{0.8}$ to provide the immobilization capability of the biorecognition element. At the next step, an amine-functionalized aptamer sequence (5′-NH_2-C_6-AATTAAAGCTCGCCAT-CAAATAGC-3′) as the biorecognition element was added on the surface of the signal transducer, and the BSA solution was also applied to prevent unwanted immobilization of the aptamer strands. Finally, the prepared aptasensor was used for the detection of various concentrations of PSA based on the variations of the cathodic photocurrents in the presence of luminol as the chemiluminescence agent. This aptasensor reported a linear detection range for PSA from 50 fg mL^{-1} to 50 ng mL^{-1}, and the reported LOD was about 25.8 fg mL^{-1}.

In another research, a CEA aptasensor was developed by modifying a GCE with polydopamine (PDA)@graphene (Gr) (Zhang et al. 2021a). Initially, PDA@Gr nanocomposite was synthesized; GO was first synthesized from graphite powder based on the Hummers' method. Then, 100 μL ammonia was mixed with 1 mg mL^{-1} GO and stirred. Afterward, 1 mg mL^{-1} dopamine, hydrazine hydrate, and deionized water were also added to the GO mixture. The obtained mixture was finally stirred at room temperature for 20 min and subsequently was kept at 60 °C for 4 h to achieve the final PDA@Gr nanocomposite. In another procedure, PDA@Gr-Pd-Pt nanodendrites (NDs) nanostructure was synthesized; first, the concentration of 0.50 mg mL^{-1} PDA@Gr nanocomposite was prepared and then mixed with a defined amount of PDDA and 10 mg mL^{-1} K_2PdCl_4. Afterward, 20 mmol L^{-1} $NaBH_4$ was added to the above mixture and stirred while it was kept at 25 °C for 30 min. At this step, PDA@Gr-PdNPs nanostructure was attained. Finally, to synthesize PDA@Gr-Pd-PtNDs nanostructure, a considered amount of PDDA and ascorbic acid was added to PDA@Gr-PdNPs nanostructure and then stirred. The temperature was raised and fixed when attained at 90 °C. At this moment, H_2PtCl_6

was added to the final mixture, and after 180 min, PDA@Gr-Pd-PtNDs, the desired nanostructure, was obtained. In another procedure, an amine-functionalized aptamer sequence (aptamer 2: 5′-AGGGGGTGAAGGGATACCC-3′) was applied and mixed with PDA@Gr-Pd-PtNDs nanostructure, and the conjugation (covalent binding: Pd-NH and Pt-NH) process was followed by stirring for 180 min. Finally, 0.50 mg mL^{-1} hemin was added to the final mixture, and the product was stirred for 60 min at 4 °C; in sequence, the aptamer 2-hemin-PDA@Gr/Pd-PtNDs structure was obtained. In order to provide the aptasensing structure, a GCE was elected as the working electrode and modified with PDA@Gr nanocomposite. Afterward, an aptamer sequence (aptamer 1: 5′-ATACCAGCTTATTCAATT-3′) as a part of the biorecognition element was immobilized on the surface of GCE-PDA@Gr. Subsequently, the analyte was dropped on the surface of GCE-PDA@Gr-aptamer 1 and could be bound with the aptamer 1 from one side. In addition, the conjugated aptamer 2 with PDA@Gr/Pd-PtNDs nanostructure was immobilized on the surface of the electrode and created a sandwich platform where the analyte was located between two aptamer sequences (GCE-PDA@Gr-aptamer 1-CEA-aptamer 2-PDA@Gr/Pd-PtNDs). The electrochemical assays were followed by DPV techniques and in the presence of hydroquinone (HQ) as the redox marker and in a three-electrode system (GCE: working; platinum: counter; saturated calomel electrode: reference). During the electrochemical assays, the maximum electron transfer rate was found in the absence of the analyte. In the presence of the analyte, due to the existing affinity between the aptamer strands (aptamer 1 and aptamer 2) and the analyte (CEA), the creation sandwich structure (aptamer 1-CEA-aptamer 2) reduced the electron transfer rate proportionally. The reduction of DPVs peak currents depended on concentrations of CEA. The higher concentration of the analyte created the bigger accumulation of bound aptamers-analyte units resulting in greater obstruction for electron transfer. This signal-off aptasensor detected the CEA in a linear range from 50 pg mL^{-1} to 1 μg mL^{-1}, and the reported LOD was about 6.3 pg mL^{-1}. In Table 38.3, details for electrochemical nanoaptasensors designed to diagnose various diseases have been provided.

5 A Summary and a Viewpoint About Electrochemical Nanobiosensors: Construction and Diagnosis of Diseases

In previous sections, the different kinds of electrochemical nanobiosensors applied for different diseases were examined. Details of these sensors are presented in Tables 38.1, 38.2, and 38.3 including information about the nanomaterials used. The biorecognition elements used in the structure of biosensors: antibodies, aptamers, and peptides, were considered to build Tables 38.1, 38.2, and 38.3. The performance of this kind of electrode is determined by the influence of various factors such as the type of nanostructure used to modify the electrode surface, the technique used in electrochemical assays, the type of redox marker, and the type of analyte. Indeed, when calibrating the biosensor platform, the optimal signal transducer should be selected. Different signal transducers such as GCE, gold electrode

Table 38.3 The features and details about applied components in recent developed electrochemical nanoaptasensors for diagnosis of diseases

Analyte	Transducer	Aptamer sequence	Functional group interacted with aptamer	Nanomaterial (s)	Redox marker	Detection technique (s)	Detection range	LOD	Ref.
Amyloid beta (Aβ)	ITO	5′-GCCTGTGTTGGGGCGGGTGCG-3′	NH_2	MoS_2 QDs@Cu NWs/CuO/g-C_3N_4 nanosheets	4-chloro-1-naphthol (4-CN)	PEC	10 fmol L^{-1}–0.5 μmol L^{-1}	5.79 fmol L^{-1}	Zhang et al. (2021b)
Tau-381 protein	CPE	5′-GCGGAGCGTGGCAGG-3′	Thiol	Au NPs-$MoSe_2$ NSs nanocomposite	$[Fe(CN)_6]^{3-/4-}$	PEC	0.5 fM–1.0 nmol L^{-1}	0.3 fmol L^{-1}	Hun and Kong (2021)
Dopamine	GCE	5′-GTCTCTGTGTGCGCCAGAGAACACTGGGGCAGATATGGGCCAGCACAGA-ATGAGGCCC-3′	Thiol	rGO/Au NPs	$[Fe(CN)_6]^{3-/4-}$	DPV	5×10^{-8}–1×10^{-5} mol L^{-1}	4.7×10^{-8} mol L^{-1}	Shen and Kan (2021)
Glycated albumin	SPCE	5′-TGCGGTTCGTGCGGTTGTAGTAC-3′	Biotin	GO-Pb nanocomposite	$[Fe(CN)_6]^{3-/4-}$	SWV	0.005–10 μg mL^{-1}	0.77 ng mL^{-1}	Putnin et al. (2021)
Adenosine triphosphate (ATP)	GCE	5′-TGGAAGGAGGCGTTATGAGGGGGTCCA-3′	NH_2	Mesoporous Fe_3O_4@Cu@Cu_2O	$[Ru(bpy)_2(dppz)]^{2+}$	ECL	0.5–2500 nmol L^{-1}	0.17 nmol L^{-1}	Qing et al. (2021)
Thrombin	ITO	5′-GGTTGGTGTGGTTGG-3′/5′-AGTCCGTGGTAGGGCAGGTTGGGGTGACT-3′	Thiol/NH_2	Silver nanowires (Ag NWs)-particles (PCs)/Pt-zinc ferrite ($ZnFe_2O_4$)	$[Fe(CN)_6]^{3-/4-}$	Chronoamperometry (CA)	0.05 pmol L^{-1}–35 nmol L^{-1}	0.016 pmol L^{-1}	Zhang et al. (2021c)
α-synuclein	GCE	5′-TTTTTGGTGGCTGGAGGGGGCGCGAACG-3′	NH_2	Au nanostars (Au NSs)	$[Fe(CN)_6]^{3-/4-}$	EIS	0.10 amol L^{-1}–10 fmol L^{-1}	0.07 amol L^{-1}	Tao et al. (2021b)
TnI	SPCE	5′-NH_2-$(CH_2)_6$-CGTGCAGTACGCCAACCTTTCTCATGCGCTGCCCCTCTTA-3′	NH_2	GO	HQ	Amperometry	1 pg mL^{-1}–1 μg mL^{-1}	0.6 pg mL^{-1}	Villalonga et al. (2021)

p24-HIV protein	SPE	p24 ssDNA aptamer	NH_2	Graphene QDs	$[Fe(CN)_6]^{3-/4-}$	CV	0.93 ng mL^{-1}–93 µg mL^{-1}	51.7 pg mL^{-1}	Gogola et al. (2021)
SARS-CoV-2 S-protein	SPCE	5′-CAGCACCGACCTTGTGCTTTGGGAGTGCTGGTCCAAGGGCGTTAATGGACA-3′	Thiol	Au NPs	$[Fe(CN)_6]^{3-/4-}$	EIS	10 pmol L^{-1}–25 nmol L^{-1}	1.30 pmol L^{-1}	Abrego-Martinez et al. (2022)
17β-Estradiol (E2)	GCE/laser-scribed graphene electrode (LSGE)	5′-NH_2-AAGGGATGCCGTTTGGG-3′/5′-CCCAAGTTCGGCATAGTG-SH-3′/5′-AAGCTTGGGCCATGCCCAGGAAGGACCCAAACGG-3′/5′-CCGTTTGGGTCCTTCCTGGGCATGGCCCAAGCTT-3′	NH_2/thiol	Graphene/Au NPs	$[Fe(CN)_6]^{3-/4-}$	DPV	1×10^{-13}–1×10^{-9} mol L^{-1}	63.1 fmol L^{-1}	Chang et al. (2021)
TnI	GCE	5′-CGTGCAGTACGCCAACCTTTCTCATGCGCTGCCCCTCTTA-3′/5′-CGCATGCCAAACGTTGCCTCATAGTTCCCTCCCCGTGTCC-3′	Carboxyl/thiol	CdS QDs/Au NPs	$[Fe(CN)_6]^{3-/4-}$	ECL	1 fg mL^{-1}–10 ng mL^{-1}	0.75 fg mL^{-1}	Kitte et al. (2021)
TnI	GE	5′-CGTGCAGTACGCCAACCTTTCTCATGCGCTGCCCCTCTTA-3′	–[a]	Nanodiamonds (NDs) and hydrogen-substituted graphdiyne (HsGDY) HsGDY@NDs	$[Fe(CN)_6]^{3-/4-}$	EIS	0.00001–100 ng mL^{-1}	6.29 fg mL^{-1}	Wang et al. (2021a)
SARS-CoV-2 nucleocapsid protein (2019-nCoV-NP)	GE	5′-GCTGGATGTCGCTTACGACAATATTCCTTAGGGGCACCGCTACATTGACACATCCAGC-3′/5′-GCTGGATGTTGACC	Thiol	MOFs NH_2–MIL-53 NPs/Au@Pt NPs	HQ	DPV	0.025–50 ng mL^{-1}	8.33 pg mL^{-1}	Tian et al. (2021b)

(continued)

Table 38.3 (continued)

Analyte	Transducer	Aptamer sequence	Functional group interacted with aptamer	Nanomaterial (s)	Redox marker	Detection technique (s)	Detection range	LOD	Ref.
		TTTACAGATCGGATTCTGTGGGGCGTTAAACTGACACATCCAGC-3′							
MCF-7 cancer cells	GCE	5′-NH_2-TTTGGTGGTGGTGGTTGTGGTGGTGGTGG-3′	NH_2	rGO-chitosan-Au NPs nanocomposite	$[Fe(CN)_6]^{3-/4-}$	EIS	1×10^1–1×10^6 cells mL^{-1}	4 cells mL^{-1}	Shafiei et al. (2021)
Her-2	Laser-scribed graphene (LSG)-based electrodes	5′-AACCGCCCAAATCCCTAAGAGTCTGCACTTGTCATTTTGTATATGTATTTGGTTTTTGGCTCTCACAGACACACTACACACGCACA-3′	Thiol	Au NPs	$[Fe(CN)_6]^{3-/4-}$	SWV	0.1–200 ng mL^{-1}	0.008 ng mL^{-1}	Rauf et al. (2021a)
TnI	LSG-based electrodes	5′-CGTGCAGTACGCCAACCT TTCTCATGCG CTGCCCCTCTTA-3′	Thiol	Zinc ferrite NPs ($ZnFe_2O_4$ NPs)	$[Fe(CN)_6]^{3-/4-}$	SWV	0.001–200 ng mL^{-1}	0.001 ng mL^{-1}	Rauf et al. (2021b)
TnI	GCE	5′-CGTGCAGTACGCCAACCTTTCTCATGCGCTGCCCCTCTTA-3′	–[a]	Cu NWs/MoS_2/rGO nanocomposite	$[Fe(CN)_6]^{3-/4-}$	DPV	5×10^{-13}–1×10^{-10} g mL^{-1}	1×10^{-13} g mL^{-1}	Han et al. (2021b)
SARS-Cov-2 receptor-binding domain (RBD)	ITO	5′-NH_2-$(CH_2)_6$-CAGCACCGACCTTGTGCTTTGGGAGTGCTGGTCCAAGGGCGTTAATGGACA-3′	NH_2	gC_3N_4 CdS QDs	$[Fe(CN)_6]^{3-/4-}$	PEC	0.5–32 nmol L^{-1}	0.12 nmol L^{-1}	Amouzadeh Tabrizi et al. (2021)

CEA	GCE	5′-ATACCAGCTTATTCAATT-3′/5′-AGGGGGTGAAGGGATACCC-3′	NH_2	PDA@Gr/Pd-Pt NDs	HQ/$[Fe(CN)_6]^{3-/4-}$	DPV	50 pg mL^{-1}–1 μg mL^{-1}	6.3 pg mL^{-1}	Zhang et al. (2021a)
MUC1	GCE	5′-NH_2-TTTTTGCAGTTGATCCTTTGGATACCCTGG-3′	NH_2	$Ru(bpy)_3^{2+}$@SiO_2 NPs	$[Fe(CN)_6]^{3-/4-}$	ECL	7.53–753 μg mL^{-1}	0.83 μg mL^{-1}	Hu et al. (2021)
Tumor necrosis factor α (TNF-α)	GE	5′-biotin-GCGGCCGATAAGGTCTTTCCAAGCGAACGAATTGAACCGC-3′	Biotin	CeO_2@Au NRs	$[Fe(CN)_6]^{3-/4-}$	DPV	2–2 × 10^6 pg mL^{-1}	0.6 pg mL^{-1}	Ding et al. (2021)
Epithelial sodium channel (ENaC)	SPCE	5′-CGGTGAGGGTCGGGTCCAGTAGGCCTACTGTTGAGTAGTGGGCTCC-3′	NH_2	CeO_2 NPs	$[Fe(CN)_6]^{3-/4-}$	DPV	0.05–3.0 ng mL^{-1}	0.012 ng mL^{-1}	Hartati et al. (2021)
PSA	ITO	5′-AATTAAAGCTCGCCATCAAATAGC-3′	NH_2	CdS/ZnO NA	$[Fe(CN)_6]^{3-/4-}$	PEC	50 fg mL^{-1}–50 ng mL^{-1}	25.8 fg mL^{-1}	Feng et al. (2021)

[a] The functional group interacted with the aptamer sequence not reported

(GE), ITO, screen-printed electrodes, and so on were applied in the sensors gathered in Tables 38.1, 38.2, and 38.3. Each of these biomolecules has advantages and disadvantages, the priorities of which have varied according to the goals of the researchers. One of the essential points that should be considered in using the biorecognition elements is considering the functional groups used in interaction with these biomolecules. These functional groups are used to adapt successful interactions with the target surfaces. The stability and compatibility of these functional groups with the biorecognition elements play an important role in the sensitivity, stability, reproducibility, and regeneration of biosensors. The most important functional groups used in the biorecognition elements structure were thiol and amine. Usually, the thiol group is important to establish successful interactions with gold. The amine functional group is more suitable for interaction with carbon-based surfaces. The biorecognition elements are immobilized on surfaces in two general ways. In the first case, these biomolecules are fixed directly on the surface of the signal transducer (bare or modified surface with nanostructures). In the second case, several types of biorecognition elements are used in the structure of biosensors. In this case, the simultaneous use of antibody-aptamer, antibody-peptide, aptamer-peptide, antibody-antibody, peptide-peptide, and aptamer-aptamer can be mentioned. In some cases, one of the mentioned units, including antibodies, aptamers, or peptides, is not immobilized on the surface of the signal transducer directly and interacts with the other components of the biorecognition element. The analytes considered in the investigated electrochemical nanobiosensors in most cases include markers of diseases with high importance in the early diagnosis such as cancers, MI, etc., which early diagnosis can prevent severe mortality and also pave the way for successful and low-cost treatments. Various diagnostic techniques were used in the studied electrochemical nanobiosensors, the most important of which include DPV, EIS, SWV, ECL, and PEC. Other important information of the studied biosensors such as detection range, LOD, and redox markers used has also been included in Tables 38.1, 38.2, and 38.3.

6 Final Remarks

Nanobiosensors have opened new roads for optimal disease diagnosis. In this chapter, we evaluated the application of electrochemical nanobiosensors in the diagnosis of several critical diseases. The purpose of using nanomaterials in the structure of biosensors is to provide more reliable diagnoses. In fact, the nanomaterials used have improved the reactivity and sensitivity of biosensors due to their increased surface-to-volume ratio. In addition, the nanostructures used as the biosensor components have created more stable bonds between the various biosensor components due to their specific morphologies. Nanomaterials used in the structure of electrochemical biosensors have been used both individually and in combination as nanocomposite structures.

Acknowledgments This chapter was supported by São Paulo State Foundation for Research – FAPESP (Fellowship 2019/27021-4 and projects 2014/50867-3 and 2017/13137-5) and the National Council for Research – CNPq (process 311847-2018-8).

References

Abrego-Martinez JC, Jafari M, Chergui S, Pavel C, Che D, Siaj M (2022) Aptamer-based electrochemical biosensor for rapid detection of SARS-CoV-2: nanoscale electrode-aptamer-SARS-CoV-2 imaging by photo-induced force microscopy. Biosens Bioelectron 195:113595

Al-Kazzaz FF, Dr SAM (2015) Molecular characterization of carcinoembryonic antigen (CEA) in some colorectal tumors. CreateSpace Independent Publishing Platform, Scotts Valley

Al-Mudhaffar SA, Dr SAM (2017) Protein engineering of of carcinoembryonic antigen and their receptors: protein engineering. CreateSpace Independent Publishing Platform, Scotts Valley

Amouzadeh Tabrizi M, Nazari L, Acedo P (2021) A photo-electrochemical aptasensor for the determination of severe acute respiratory syndrome coronavirus 2 receptor-binding domain by using graphitic carbon nitride-cadmium sulfide quantum dots nanocomposite. Sensors Actuators B Chem 345:130377

Aydin EB, Aydin M, Sezgintürk MK (2021a) Fabrication of electrochemical immunosensor based on acid-substituted poly(pyrrole) polymer modified disposable ITO electrode for sensitive detection of CCR4 cancer biomarker in human serum. Talanta 222:121487

Aydin EB, Aydin M, Sezgintürk MK (2021b) A novel electrochemical immunosensor based on acetylene black/epoxy-substituted-polypyrrole polymer composite for the highly sensitive and selective detection of interleukin 6. Talanta 222:121596

Bakshi S, Mehta S, Kumeria T, Shiddiky MJ, Popat A, Choudhury S, Bose S, Nayak R (2021) Rapid fabrication of homogeneously distributed hyper-branched gold nanostructured electrode based electrochemical immunosensor for detection of protein biomarkers. Sensors Actuators B Chem 326:128803

Bhatnagar I, Mahato K, Ealla KKR, Asthana A, Chandra P (2018) Chitosan stabilized gold nanoparticle mediated self-assembled gliP nanobiosensor for diagnosis of invasive Aspergillosis. Int J Biol Macromol 110:449–456

Boeri L, Capogrosso P, Cazzaniga W, Ventimiglia E, Pozzi E, Belladelli F, Schifano N, Candela L, Alfano M, Pederzoli F (2021) Infertile men have higher prostate-specific antigen values than fertile individuals of comparable age. Eur Urol 79:234–240

Bolat G, Akbal Vural O, Tugce Yaman Y, Abaci S (2021) Label-free impedimetric miRNA-192 genosensor platform using graphene oxide decorated peptide nanotubes composite. Microchem J 166:106218

Boonkaew S, Jang I, Noviana E, Siangproh W, Chailapakul O, Henry CS (2021) Electrochemical paper-based analytical device for multiplexed, point-of-care detection of cardiovascular disease biomarkers. Sensors Actuators B Chem 330:129336

Butler SS, Muralidhar V, Zhao SG, Sanford NN, Franco I, Fullerton ZH, Chavez J, D'Amico AV, Feng FY, Rebbeck TR (2020) Prostate cancer incidence across stage, NCCN risk groups, and age before and after USPSTF Grade D recommendations against prostate-specific antigen screening in 2012. Cancer 126:717–724

Caratelli V, Fillo S, D'Amore N, Rossetto O, Pirazzini M, Moccia M, Avitabile C, Moscone D, Lista F, Arduini F (2021) Paper-based electrochemical peptide sensor for on-site detection of botulinum neurotoxin serotype A and C. Biosens Bioelectron 183:113210

Cen S-Y, Ge X-Y, Chen Y, Wang A-J, Feng J-J (2021) Label-free electrochemical immunosensor for ultrasensitive determination of cardiac troponin I based on porous fluffy-like AuPtPd trimetallic alloyed nanodendrites. Microchem J 169:106568

Chandra P, Koh WCA, Noh H-B, Shim Y-B (2012) In vitro monitoring of i-NOS concentrations with an immunosensor: the inhibitory effect of endocrine disruptors on i-NOS release. Biosens Bioelectron 32:278–282

Chang Z, Zhu B, Liu J, Zhu X, Xu M, Travas-Sejdic J (2021) Electrochemical aptasensor for 17β-estradiol using disposable laser scribed graphene electrodes. Biosens Bioelectron 185:113247

Chapman AR, Adamson PD, Shah AS, Anand A, Strachan FE, Ferry AV, Ken Lee K, Berry C, Findlay I, Cruikshank A (2020) High-sensitivity cardiac troponin and the universal definition of myocardial infarction. Circulation 141:161–171

Chen G-C, Liu C-H, Wu W-C (2021a) Electrochemical immunosensor for serum parathyroid hormone using voltammetric techniques and a portable simulator. Anal Chim Acta 1143:84–92

Chen M, Song Z, Han R, Li Y, Luo X (2021b) Low fouling electrochemical biosensors based on designed Y-shaped peptides with antifouling and recognizing branches for the detection of IgG in human serum. Biosens Bioelectron 178:113016

Chen S, Xu L, Sheng K, Zhou Q, Dong B, Bai X, Lu G, Song H (2021c) A label-free electrochemical immunosensor based on facet-controlled Au nanorods/reduced graphene oxide composites for prostate specific antigen detection. Sensors Actuators B Chem 336:129748

Cheng W, Ma J, Kong D, Zhang Z, Khan A, Yi C, Hu K, Yi Y, Li J (2021) One step electrochemical detection for matrix metalloproteinase 2 based on anodic stripping of silver nanoparticles mediated by host-guest interactions. Sensors Actuators B Chem 330:129379

Choudhary M, Yadav P, Singh A, Kaur S, Ramirez-Vick J, Chandra P, Arora K, Singh SP (2016) CD59 targeted ultrasensitive electrochemical immunosensor for fast and noninvasive diagnosis of oral cancer. Electroanalysis 28:2565–2574

de Crevoisier R, Bayar MA, Pommier P, Muracciole X, Pêne F, Dudouet P, Latorzeff I, Beckendorf V, Bachaud J-M, Laplanche A (2018) Daily versus weekly prostate cancer image guided radiation therapy: phase 3 multicenter randomized trial. Int J Radiat Oncol Biol Phys 102:1420–1429

Ding Y, Zhang M, Li C, Xie B, Zhao G, Sun Y (2021) A reusable aptasensor based on the dual signal amplification of Ce@AuNRs-PAMAM-Fc and DNA walker for ultrasensitive detection of TNF-α. J Solid State Electrochem 26(1):e8

Fabiani L, Saroglia M, Galatà G, de Santis R, Fillo S, Luca V, Faggioni G, D’Amore N, Regalbuto E, Salvatori P, Terova G, Moscone D, Lista F, Arduini F (2021) Magnetic beads combined with carbon black-based screen-printed electrodes for COVID-19: a reliable and miniaturized electrochemical immunosensor for SARS-CoV-2 detection in saliva. Biosens Bioelectron 171:112686

Fadila AN, Rahaju AS, Tarmono T (2020) Relationship of prostate-specific antigen (PSA) and prostate volume in patients with biopsy proven benign prostatic hyperplasia (BPH). Qanun Med 4:171–177

Fan X, Deng D, Chen Z, Qi J, Li Y, Han B, Huan K, Luo L (2021) A sensitive amperometric immunosensor for the detection of carcinoembryonic antigen using $ZnMn_2O_4$@reduced graphene oxide composites as signal amplifier. Sensors Actuators B Chem 339:129852

Felix FS, Angnes L (2018) Electrochemical immunosensors – a powerful tool for analytical applications. Biosens Bioelectron 102:470–478

Feng J, Dai L, Ren X, Ma H, Wang X, Fan D, Wei Q, Wu R (2021) Self-powered cathodic photoelectrochemical aptasensor comprising a photocathode and a photoanode in microfluidic analysis systems. Anal Chem 93:7125–7132

Ge X-Y, Feng Y-G, Cen S-Y, Wang A-J, Mei L-P, Luo X, Feng J-J (2021) A label-free electrochemical immnunosensor based on signal magnification of oxygen reduction reaction catalyzed by uniform PtCo nanodendrites for highly sensitive detection of carbohydrate antigen 15-3. Anal Chim Acta 1176:338750

Gogola JL, Martins G, Gevaerd A, Blanes L, Cardoso J, Marchini FK, Banks CE, Bergamini MF, Marcolino-Junior LH (2021) Label-free aptasensor for p24-HIV protein detection based on graphene quantum dots as an electrochemical signal amplifier. Anal Chim Acta 1166:338548

Gooding JJ (2006) Nanoscale biosensors: significant advantages over larger devices? Small 2: 313–315

Gu S, Shi X-M, Zhang D, Fan G-C, Luo X (2021) Peptide-based photocathodic biosensors: integrating a recognition peptide with an antifouling peptide. Anal Chem 93:2706–2712

Han K, Li G, Tian L, Li L, Shi Y, Huang T, Li Y, Xu Q (2021a) Multifunctional peptide-oligonucleotide conjugate promoted sensitive electrochemical biosensing of cardiac troponin I. Biochem Eng J 174:108104

Han Y, Su X, Fan L, Liu Z, Guo Y (2021b) Electrochemical aptasensor for sensitive detection of cardiac troponin I based on CuNWs/MoS_2/rGO nanocomposite. Microchem J 169:106598

Hao Q, Wang L, Niu S, Ding C, Luo X (2020) Ratiometric electrogenerated chemiluminescence sensor based on a designed anti-fouling peptide for the detection of carcinoembryonic antigen. Anal Chim Acta 1136:134–140

Hartati YW, Komala DR, Hendrati D, Gaffar S, Hardianto A, Sofiatin Y, Bahti HH (2021) An aptasensor using ceria electrodeposited-screen-printed carbon electrode for detection of epithelial sodium channel protein as a hypertension biomarker. R Soc Open Sci 8:202040

Hassanipour S, Delam H, Arab-Zozani M, Abdzadeh E, Hosseini SA, Nikbakht H-A, Malakoutikhah M, Ashoobi MT, Fathalipour M, Salehiniya H (2020) Survival rate of prostate cancer in Asian countries: a systematic review and meta-analysis. Ann Glob Health 86:2

Heiat M, Negahdary M (2019) Sensitive diagnosis of alpha-fetoprotein by a label free nano-aptasensor designed by modified Au electrode with spindle-shaped gold nanostructure. Microchem J 148:456–466

Hu Z, Zhao B, Miao P, Hou X, Xing F, Chen Y, Feng L (2021) Three-way junction DNA based electrochemical biosensor for microRNAs detection with distinguishable locked nucleic acid recognition and redox cycling signal amplification. J Electroanal Chem 880:114861

Huang S, Tang R, Zhang T, Zhao J, Jiang Z, Wang Q (2021) Anti-fouling poly adenine coating combined with highly specific CD20 epitope mimetic peptide for rituximab detection in clinical patients' plasma. Biosens Bioelectron 171:112678

Hun X, Kong X (2021) An enzyme linked aptamer photoelectrochemical biosensor for Tau-381 protein using AuNPs/$MoSe_2$ as sensing material. J Pharm Biomed Anal 192:113666

Kalyani T, Sangili A, Nanda A, Prakash S, Kaushik A, Kumar Jana S (2021) Bio-nanocomposite based highly sensitive and label-free electrochemical immunosensor for endometriosis diagnostics application. Bioelectrochemistry 139:107740

Katrukha I (2013) Human cardiac troponin complex. Structure and functions. Biochemistry 78: 1447–1465

Kitte SA, Tafese T, Xu C, Saqib M, Li H, Jin Y (2021) Plasmon-enhanced quantum dots electrochemiluminescence aptasensor for selective and sensitive detection of cardiac troponin I. Talanta 221:121674

Lin C-Y, Nhat Nguyen UT, Hsieh H-Y, Tahara H, Chang Y-S, Wang B-Y, Gu B-C, Dai Y-H, Wu C-C, Tsai IJ, Fan Y-J (2022) Peptide-based electrochemical sensor with nanogold enhancement for detecting rheumatoid arthritis. Talanta 236:122886

Liu X, Wang Q, Chen J, Chen X, Yang W (2021) Ultrasensitive electrochemiluminescence biosensor for the detection of tumor exosomes based on peptide recognition and luminol-AuNPs@g-C_3N_4 nanoprobe signal amplification. Talanta 221:121379

Logozzi M, Angelini DF, Giuliani A, Mizzoni D, Di Raimo R, Maggi M, Gentilucci A, Marzio V, Salciccia S, Borsellino G (2019) Increased plasmatic levels of PSA-expressing exosomes distinguish prostate cancer patients from benign prostatic hyperplasia: a prospective study. Cancers 11:1449

Mahapatra S, Baranwal A, Purohit B, Roy S, Mahto SK, Chandra P (2020) Advanced biosensing methodologies for ultrasensitive detection of human coronaviruses. In: Diagnostic strategies for COVID-19 and other coronaviruses. Springer, Singapore

Mahato K, Kumar S, Srivastava A, Maurya PK, Singh R, Chandra P (2018) Chapter 14. Electrochemical immunosensors: fundamentals and applications in clinical diagnostics. In: Vashist SK, Luong JHT (eds) Handbook of immunoassay technologies. Academic Press, Cambridge, MA

Mahato K, Purohit B, Bhardwaj K, Jaiswal A, Chandra P (2019) Novel electrochemical biosensor for serotonin detection based on gold nanorattles decorated reduced graphene oxide in biological fluids and in vitro model. Biosens Bioelectron 142:111502

Mair J, Lindahl B, Hammarsten O, Müller C, Giannitsis E, Huber K, Möckel M, Plebani M, Thygesen K, Jaffe AS (2018) How is cardiac troponin released from injured myocardium? Eur Heart J Acute Cardiovasc Care 7:553–560

Martínez-Rojas F, Castañeda E, Armijo F (2021) Conducting polymer applied in a label-free electrochemical immunosensor for the detection prostate-specific antigen using its redox response as an analytical signal. J Electroanal Chem 880:114877

Morales MA, Halpern JM (2018) Guide to selecting a biorecognition element for biosensors. Bioconjug Chem 29:3231–3239

Negahdary M (2020a) Aptamers in nanostructure-based electrochemical biosensors for cardiac biomarkers and cancer biomarkers: a review. Biosens Bioelectron 152:112018

Negahdary M (2020b) Electrochemical aptasensors based on the gold nanostructures. Talanta 216:120999

Negahdary M, Heli H (2018) Applications of nanoflowers in biomedicine. Recent Pat Nanotechnol 12:22–33

Negahdary M, Heli H (2019a) An electrochemical troponin I peptisensor using a triangular icicle-like gold nanostructure. Biochem Eng J 151:107326

Negahdary M, Heli H (2019b) An ultrasensitive electrochemical aptasensor for early diagnosis of Alzheimer's disease, using a fern leaves-like gold nanostructure. Talanta 198:510–517

Negahdary M, Behjati-Ardakani M, Sattarahmady N, Yadegari H, Heli H (2017) Electrochemical aptasensing of human cardiac troponin I based on an array of gold nanodumbbells-applied to early detection of myocardial infarction. Sensors Actuators B Chem 252:62–71

Negahdary M, Behjati-Ardakani M, Sattarahmady N, Heli H (2018) An aptamer-based biosensor for troponin I detection in diagnosis of myocardial infarction. J Biomed Phys Eng 8:167–178

Negahdary M, Behjati-Ardakani M, Heli H (2019a) An electrochemical troponin T aptasensor based on the use of a macroporous gold nanostructure. Microchim Acta 186:377

Negahdary M, Behjati-Ardakani M, Heli H, Sattarahmady N (2019b) A cardiac troponin T biosensor based on aptamer self-assembling on gold. Int J Mol Cell Med 8:271–283

Negahdary M, Sattarahmady N, Heli H (2020) Advances in prostate specific antigen biosensors-impact of nanotechnology. Clin Chim Acta 504:43–55

Nordström T, Akre O, Aly M, Grönberg H, Eklund M (2018) Prostate-specific antigen (PSA) density in the diagnostic algorithm of prostate cancer. Prostate Cancer Prostatic Dis 21:57–63

Öndeş B, Evli S, Uygun M, Aktaş Uygun D (2021a) Boron nitride nanosheet modified label-free electrochemical immunosensor for cancer antigen 125 detection. Biosens Bioelectron 191:113454

Öndeş B, Sinem E, Uygun M, Uygun DA (2021b) Boron nitride nanosheet modified label-free electrochemical immunosensor for cancer antigen 125 detection. Biosens Bioelectron 2021:113454

Pishvaian M, Morse MA, McDevitt J, Norton JD, Ren S, Robbie GJ, Ryan PC, Soukharev S, Bao H, Denlinger CS (2016) Phase 1 dose escalation study of MEDI-565, a bispecific T-cell engager that targets human carcinoembryonic antigen, in patients with advanced gastrointestinal adenocarcinomas. Clin Colorectal Cancer 15:345–351

Pumera M, Sanchez S, Ichinose I, Tang J (2007) Electrochemical nanobiosensors. Sensors Actuators B Chem 123:1195–1205

Putnin T, Waiwinya W, Pimalai D, Chawjiraphan W, Sathirapongsasuti N, Japrung D (2021) Dual sensitive and rapid detection of glycated human serum albumin using a versatile lead/graphene nanocomposite probe as a fluorescence–electrochemical aptasensor. Analyst 146:4357–4364

Qing M, Chen SL, Sun Z, Fan Y, Luo HQ, Li NB (2021) Universal and programmable rolling circle amplification-CRISPR/Cas12a-mediated immobilization-free electrochemical biosensor. Anal Chem 93:7499–7507

Rahi A, Sattarahmady N, Heli H (2016) Label-free electrochemical aptasensing of the human prostate-specific antigen using gold nanospears. Talanta 156–157:218–224

Raouafi A, Sánchez A, Raouafi N, Villalonga R (2019) Electrochemical aptamer-based bioplatform for ultrasensitive detection of prostate specific antigen. Sensors Actuators B Chem 297:126762

Rauf S, Lahcen AA, Aljedaibi A, Beduk T, Ilton de Oliveira Filho J, Salama KN (2021a) Gold nanostructured laser-scribed graphene: a new electrochemical biosensing platform for potential point-of-care testing of disease biomarkers. Biosens Bioelectron 180:113116

Rauf S, Mani V, Lahcen AA, Yuvaraja S, Beduk T, Salama KN (2021b) Binary transition metal oxide modified laser-scribed graphene electrochemical aptasensor for the accurate and sensitive screening of acute myocardial infarction. Electrochim Acta 386:138489

Reichlin T, Hochholzer W, Bassetti S, Steuer S, Stelzig C, Hartwiger S, Biedert S, Schaub N, Buerge C, Potocki M (2009) Early diagnosis of myocardial infarction with sensitive cardiac troponin assays. N Engl J Med 361:858–867

Ribeiro KL, Frías IAM, Silva AG, Lima-Neto RG, Sá SR, Franco OL, Oliveira MDL, Andrade CAS (2021) Impedimetric CLAVMO peptide-based sensor differentiates ploidy of *Candida* species. Biochem Eng J 167:107918

Romesser PB, Pei X, Shi W, Zhang Z, Kollmeier M, McBride SM, Zelefsky MJ (2018) Prostate-specific antigen (PSA) bounce after dose-escalated external beam radiation therapy is an independent predictor of PSA recurrence, metastasis, and survival in prostate adenocarcinoma patients. Int J Radiat Oncol Biol Phys 100:59–67

Rong S, Zou L, Li Y, Guan Y, Guan H, Zhang Z, Zhang Y, Gao H, Yu H, Zhao F, Pan H, Chang D (2021) An ultrasensitive disposable sandwich-configuration electrochemical immunosensor based on OMC@AuNPs composites and AuPt-MB for alpha-fetoprotein detection. Bioelectrochemistry 141:107846

Ropero-Vega JL, Redondo-Ortega JF, Galvis-Curubo YJ, Rondón-Villarreal P, Flórez-Castillo JM (2021) A bioinspired peptide in TIR protein as recognition molecule on electrochemical biosensors for the detection of *E. coli* O157:H7 in an aqueous matrix. Molecules 26:2559

Sajid KM, Parveen R, Sabih D, Chaouachi K, Naeem A, Mahmood R, Shamim R (2007) Carcinoembryonic antigen (CEA) levels in hookah smokers, cigarette smokers and non-smokers. J Pak Med Assoc 57:595

Sattarahmady N, Rahi A, Heli H (2017) A signal-on built in-marker electrochemical aptasensor for human prostate-specific antigen based on a hairbrush-like gold nanostructure. Sci Rep 7:1–8

Shafiei F, Saberi RS, Mehrgardi MA (2021) A label-free electrochemical aptasensor for breast cancer cell detection based on a reduced graphene oxide-chitosan-gold nanoparticle composite. Bioelectrochemistry 140:107807

Shamsazar A, Asadi A, Seifzadeh D, Mahdavi M (2021) A novel and highly sensitive sandwich-type immunosensor for prostate-specific antigen detection based on MWCNTs-Fe_3O_4 nanocomposite. Sensors Actuators B Chem 346:130459

Shanbhag MM, Ilager D, Mahapatra S, Shetti NP, Chandra P (2021) Amberlite XAD-4 based electrochemical sensor for diclofenac detection in urine and commercial tablets. Mater Chem Phys 273:125044

Shave R, Baggish A, George K, Wood M, Scharhag J, Whyte G, Gaze D, Thompson PD (2010) Exercise-induced cardiac troponin elevation: evidence, mechanisms, and implications. J Am Coll Cardiol 56:169–176

Shen M, Kan X (2021) Aptamer and molecularly imprinted polymer: synergistic recognition and sensing of dopamine. Electrochim Acta 367:137433

Siew QY, Pang EL, Loh H-S, Tan MTT (2021) Highly sensitive and specific graphene/TiO_2 impedimetric immunosensor based on plant-derived tetravalent envelope glycoprotein domain III (EDIII) probe antigen for dengue diagnosis. Biosens Bioelectron 176:112895

Smith DP, Calopedos R, Bang A, Yu XQ, Egger S, Chambers S, O'Connell DL (2018) Increased risk of suicide in New South Wales men with prostate cancer: analysis of linked population-wide data. PLoS One 13:e0198679

Song X, Zhao L, Luo C, Ren X, Yang L, Wei Q (2021) Peptide-based biosensor with a luminescent copper-based metal–organic framework as an electrochemiluminescence emitter for trypsin assay. Anal Chem 93:9704–9710

Spratt DE, Dai DL, Den RB, Troncoso P, Yousefi K, Ross AE, Schaeffer EM, Haddad Z, Davicioni E, Mehra R (2018) Performance of a prostate cancer genomic classifier in predicting metastasis in men with prostate-specific antigen persistence postprostatectomy. Eur Urol 74: 107–114

Sun Y, Fang L, Zhang Z, Yi Y, Liu S, Chen Q, Zhang J, Zhang C, He L, Zhang K (2021) A multitargeted electrochemiluminescent biosensor coupling DNAzyme with cascading amplification for analyzing myocardial miRNAs. Anal Chem 93:7516–7522

Taheri RA, Eskandari K, Negahdary M (2018) An electrochemical dopamine aptasensor using the modified Au electrode with spindle-shaped gold nanostructure. Microchem J 143:243–251

Tang H, Chen J, Nie L, Kuang Y, Yao S (2007) A label-free electrochemical immunoassay for carcinoembryonic antigen (CEA) based on gold nanoparticles (AuNPs) and nonconductive polymer film. Biosens Bioelectron 22:1061–1067

Tang H, Wang H, Yang C, Zhao D, Qian Y, Li Y (2020) Nanopore-based strategy for selective detection of single carcinoembryonic antigen (CEA) molecules. Anal Chem 92:3042–3049

Tao D, Wang J, Song S, Cai K, Jiang M, Cheng J, Hu L, Jaffrezic-Renault N, Guo Z, Pan H (2021a) Polythionine and gold nanostar-based impedimetric aptasensor for label-free detection of α-synuclein oligomers. J Appl Electrochem 51:1523–1533

Tao D, Wang J, Song S, Cai K, Jiang M, Cheng J, Hu L, Jaffrezic-Renault N, Guo Z, Pan H (2021b) Polythionine and gold nanostar-based impedimetric aptasensor for label-free detection of α-synuclein oligomers. J Appl Electrochem 51:e3

Tian J-K, Zhao M-L, Song Y-M, Zhong X, Yuan R, Zhuo Y (2021a) MicroRNA-triggered deconstruction of field-free spherical nucleic acid as an electrochemiluminescence biosensing switch. Anal Chem 93:13928–13934

Tian J, Liang Z, Hu O, He Q, Sun D, Chen Z (2021b) An electrochemical dual-aptamer biosensor based on metal-organic frameworks MIL-53 decorated with Au@Pt nanoparticles and enzymes for detection of COVID-19 nucleocapsid protein. Electrochim Acta 387:138553

Tran HL, Darmanto W, Doong R-A (2021) Electrochemical immunosensor for ultra-sensitive detection of attomolar prostate specific antigen with sulfur-doped graphene quantum dot@gold nanostar as the probe. Electrochim Acta 389:138700

Villalonga A, Estabiel I, Pérez-Calabuig AM, Mayol B, Parrado C, Villalonga R (2021) Amperometric aptasensor with sandwich-type architecture for troponin I based on carboxyethylsilanetriol-modified graphene oxide coated electrodes. Biosens Bioelectron 183:113203

Wang C, Li J, Kang M, Huang X, Liu Y, Zhou N, Zhang Z (2021a) Nanodiamonds and hydrogen-substituted graphdiyne heteronanostructure for the sensitive impedimetric aptasensing of myocardial infarction and cardiac troponin I. Anal Chim Acta 1141:110–119

Wang J-M, Yao L-Y, Huang W, Yang Y, Liang W-B, Yuan R, Xiao D-R (2021b) Overcoming aggregation-induced quenching by metal−organic framework for electrochemiluminescence (ECL) enhancement: Zn-PTC as a new ECL emitter for ultrasensitive microRNAs detection. ACS Appl Mater Interfaces 13:44079–44085

Wang W, Han R, Tang K, Zhao S, Ding C, Luo X (2021c) Biocompatible peptide hydrogels with excellent antibacterial and catalytic properties for electrochemical sensing application. Anal Chim Acta 1154:338295

Wang X-Y, Feng Y-G, Wang A-J, Mei L-P, Luo X, Xue Y, Feng J-J (2021d) Facile construction of ratiometric electrochemical immunosensor using hierarchical PtCoIr nanowires and porous SiO_2@Ag nanoparticles for accurate detection of septicemia biomarker. Bioelectrochemistry 140:107802

Wu G, Datar RH, Hansen KM, Thundat T, Cote RJ, Majumdar A (2001) Bioassay of prostate-specific antigen (PSA) using microcantilevers. Nat Biotechnol 19:856–860

Xiang B, Snook AE, Magee MS, Waldman SA (2013) Colorectal cancer immunotherapy. Discov Med 15:301

Xiao K, Meng L, Du C, Zhang Q, Yu Q, Zhang X, Chen J (2021) A label-free photoelectrochemical biosensor with near-zero-background noise for protein kinase A activity assay based on porous ZrO_2/CdS octahedra. Sensors Actuators B Chem 328:129096

Xie X, Wang Z, Zhou M, Xing Y, Chen Y, Huang J, Cai K, Zhang J (2021) Redox host–guest nanosensors installed with DNA gatekeepers for immobilization-free and ratiometric electrochemical detection of miRNA. Small Methods 5:2101072

Yang L, Wang J, Lü H, Hui N (2021) Electrochemical sensor based on Prussian blue/multi-walled carbon nanotubes functionalized polypyrrole nanowire arrays for hydrogen peroxide and microRNA detection. Microchim Acta 188:25

Yazdani Z, Yadegari H, Heli H (2019) A molecularly imprinted electrochemical nanobiosensor for prostate specific antigen determination. Anal Biochem 566:116–125

Zhang F, Liu Z, Han Y, Fan L, Guo Y (2021a) Sandwich electrochemical carcinoembryonic antigen aptasensor based on signal amplification of polydopamine functionalized graphene conjugate Pd-Pt nanodendrites. Bioelectrochemistry 142:107947

Zhang J, Zhang X, Gao Y, Yan J, Song W (2021b) Integrating CuO/g-C_3N_4 p-n heterojunctioned photocathode with MoS_2 QDs@Cu NWs multifunctional signal amplifier for ultrasensitive detection of AβO. Biosens Bioelectron 176:112945

Zhang Q, Li W, Zhao F, Xu C, Fan G, Liu Q, Zhang X, Zhang X (2021c) Electrochemical sandwich-type thrombin aptasensor based on silver nanowires & particles decorated electrode and the signal amplifier of Pt loaded hollow zinc ferrite. Colloids Surf A Physicochem Eng Asp 611:125804

Zhao S, Liu N, Wang W, Xu Z, Wu Y, Luo X (2021) An electrochemical biosensor for alpha-fetoprotein detection in human serum based on peptides containing isomer D-amino acids with enhanced stability and antifouling property. Biosens Bioelectron 190:113466

Zheng J, Zhao H, Ning G, Sun W, Wang L, Liang H, Xu H, He C, Zhao H, Li C-P (2021) A novel affinity peptide–antibody sandwich electrochemical biosensor for PSA based on the signal amplification of MnO_2-functionalized covalent organic framework. Talanta 233:122520

Development of Nanoparticle-Modified Ultramicroelectrodes and Their Electroanalytical Application

39

Burcin Bozal-Palabiyik, Ozge Selcuk, and Bengi Uslu

Contents

1 Introduction 862
2 Definition, Classification, Fabrication, Characterization, and Advantages of Ultramicroelectrodes 863
3 Nanoparticle Usage for Fabrication of Ultramicroelectrodes and Applications 866
4 Conclusion 876
References 876

Abstract

An ultramicroelectrode is an electrode whose characteristic dimensions are smaller than 25 μm. They have been used in electrochemistry for the last 30 years and can be used in studying extremely small sample volumes. Due to these advantages, ultramicroelectrodes have revolutionized electrochemical applications and methodologies. They have also transformed the time/space accessibility of experimentation. Nanomaterials are materials whose dimensions are at the nanometer scale (1–100 nm) or assembled at this range. When compared to conventional materials the structure and properties of nanomaterials are essentially changed. They show chemical, physical, and electronic properties that are not seen in other materials or even materials from which the nanoparticles were prepared. Nanomaterials are used for electrode modification, also including ultramicroelectrodes at electrochemical sensing systems; among these nanomaterials, one can count carbon nanoparticles, noble metal nanoparticles, metal oxide nanoparticles, and bimetallic nanoparticles. This chapter examines the role of nanoparticles in designing ultramicroelectrodes and their applications. The

---

B. Bozal-Palabiyik · B. Uslu (✉)
Department of Analytical Chemistry, Faculty of Pharmacy, Ankara University, Ankara, Turkey
e-mail: buslu@pharmacy.ankara.edu.tr

O. Selcuk
Mersin University, Mersin, Turkey

© Springer Nature Singapore Pte Ltd. 2023

U. P. Azad, P. Chandra (eds.), *Handbook of Nanobioelectrochemistry*,
https://doi.org/10.1007/978-981-19-9437-1_39

concepts, geometries, fabrication, and advantages of ultramicroelectrodes are defined and discussed. Finally, the applications of nanoparticle-modified electrodes are presented in such a way as to display the advantages of modification as well as the ultra-small size of the electrodes.

Keywords

Ultramicroelectrode · Nanoparticles · Electrochemistry · Modification

1 Introduction

Electrochemistry is all about chemical phenomena concerning separation of charge, which results in a homogenous transfer of charge in solution or heterogeneous charge transfer on the surface of electrodes. During electrochemical measurements, electron transfers occur at the interface between the solution and the working electrode (Brett and Oliveira-Brett 1994). The working electrode is the most significant element of an electrochemical cell, and deciding on working electrode materials is critically important for the success of experimental procedures. This material has to demonstrate a positive redox behavior with the analyte as well as rapid and reproducible electron transfer without fouling of the electrode. Moreover, the cost of the material, its toxicity, its versatility in transforming into useful geometries, and facile renewal of its surface after measurement are the basic factors in terms of choosing the right electrode material (Anon 2020).

Solid electrodes that are employed in voltammetric measurements are generally produced by encapsulation of electrode material with an insulating glass cover or polymeric materials such as Teflon, polychlorotrifluoroethylene, or polyetheretherketone. The most widely preferred electrodes are the disc electrodes; generally, the diameters chosen are 1.0, 3.0, and 10.0 mm. Electrodes with these sizes produce currents measured between μA and lower mA for analytes whose concentration is close to 1 mM under transient (time-dependent) conditions (Bond 1994; Anon 2020).

Bard and colleagues define four categories of electrodes in terms of their sizes: (1) normal, conventional, or macroelectrodes (dimensions of millimeters, centimeters, or meters), (2) microelectrodes (MEs) (dimensions between 25 μm and 1 mm), (3) ultramicroelectrodes (UMEs) (dimensions between 10 nm and 25 μm), and finally nanoelectrodes or nanodes (dimensions smaller than 10 nm) (Bard et al. 2012). These numbers might refer to different dimensions of electrodes in line with their shapes. For instance, they might refer to a radius for round-shaped electrodes, such as disk, sphere, hemisphere, or cylinder forms, or width for a band or ring UME (Zoski 2002). Although there are different lengths mentioned to define UMEs, generally, 20 μm or 25 μm is determined (Xie et al. 2005).

Different electrodes made of different materials are miniaturized into many geometric shapes. Their common characteristic is that the electrode size is considerably smaller than the diffusion layer at their surface. Microelectrodes are far better than conventional electrodes in terms of signal to background characteristics thanks to their decreased double-layer capacitance related to their small surface and radial diffusion to their edges. Their geometry and lower current density gives them the capacity to work with ionic conductive polymers, lubricants, and solutions without supporting electrolytes at lower temperatures, in high-resistant environments including low dielectric solvents, or at gas phase (Stradiotto et al. 2003).

Miniaturization of electrochemical systems has significant applications. For instance, miniaturized biofuel cells are successfully prepared, and at present nanoelectrodes are prepared as sensors (Szamocki et al. 2007). Wightman offered working electrode miniaturization for the first time to determine neurotransmitters both within and outside of living organisms. Moreover, researchers apply microelectrodes for searching microscopic spaces, detection at micro-fluid systems, analysis of samples with very small volumes, and time-resolved probing of processes at single cells (Stradiotto et al. 2003). Miniaturization allows microelectrodes to achieve significant versatility in studying electrochemical processes. They can be used at highly resistant media and in very small samples at shorter response times (Amatore et al. 2010).

A UME is an electrode whose characteristic dimensions are smaller than 25 μm (Wang et al. 2021; Goodwin et al. 2021). They have been used in electrochemistry for the last 30 years. They can be used to study extremely small sample volumes (Lupu et al. 2008). Thanks to these advantages, UMEs have revolutionized electrochemical applications and methodologies. They have also transformed the time/space accessibility of experimentation (Kottke et al. 2008).

Nanomaterials or nanostructured materials are materials whose dimensions are at the nanometer scale (1–100 nm) or assembled at this range. When compared to conventional materials the structure and properties of nanomaterials are essentially changed (Zhang et al. 2019). Their physical, chemical, and electronic properties are not observable when other materials or even materials from which the nanoparticles have been prepared are employed in their place. Nanomaterials are used for electrode modification also including UMEs at electrochemical sensing systems. There are different types of nanomaterials produced from carbon, noble metals such as Au or Pt nanoparticles, metal oxides, or bimetals (Kempahanumakkagari et al. 2017).

This chapter examines the role of nanoparticles in designing UMEs and their applications. First, the concepts of MEs and UMEs are defined in such a way as to understand the differences between them. Second, the geometries, fabrication, and advantages of UMEs are analyzed. Finally, the chapter discusses how these nanoparticle-modified electrodes are employed in electrochemical measurements, and displays the advantages of modification as well as the ultra-small size of the electrodes.

2 Definition, Classification, Fabrication, Characterization, and Advantages of Ultramicroelectrodes

There are various arguments regarding differentiating the definitions of ME and UME. Instead of engaging in differentiation, previous studies tend to use these two concepts interchangeably. For instance, according to Pletcher, MEs are also commonly called UMEs (Pletcher 1991). Some researchers, on the other hand, do not prefer to use the concept of UME, and for the sake of a more consistent terminology, they prefer to adopt the concept of ME (Štulík et al. 2000). Amatore and colleagues draw attention to the ambiguity of this differentiation. According to them, such definitions based on size may appear useless because size matters only for the users of the electrodes. They argue that electroanalytical chemists or molecular electrochemists prefer to use different definitions. Instead of categorization based on size, they offer a classification based on particular properties of electrodes. Still, for practical purposes, different definitions based on the size of the electrodes seem to be useful. Therefore, more recent studies differentiate between ME and UME principally based on their sizes (Amatore et al. 2010).

To summarize, in order for an electrode to be defined as a UME, one dimension of the electrode should be smaller than the diffusion layer that emerges during a standard electroanalytical experiment, and this dimension is generally smaller than 25 μm, as mentioned above (Holt 2011). What distinguishes a UME from a macroelectrode is that the UME can achieve diffusion layers larger than their characteristic dimension (Bard et al. 2012). In other words, smaller size increases the effectiveness of mass transport and thereby differentiates UMEs from conventional macroelectrodes, where diffusion is directly related to the electrode surface (Kaifer and Gómez-Kaifer 1999).

According to Aoki, who has published one of the earliest reviews on UMEs, there are three types of UMEs in terms of their shape. These are (1) point electrodes, which are concentrated and distributed in the solution in a spherical form; (2) line electrodes, which generally take cylinder form in concentration and distribution; and (3) plane electrodes, which are composed of point and line electrodes on a planar insulator, specifically taking a disk form (Aoki 1993).

Zoski made a similar shape-based classification: (1) disk UMEs, (2) hemispherical and spherical UMEs, (3) inlaid ring UMEs, (4) ring-disk UMEs, and (5) finite conical (etched) UMEs (Zoski 2002). On the other hand, Kaifer and Gómez-Kaifer's classification was more comprehensive: (1) disk UMEs, (2) sphere UMEs, (3) wire UMEs, (4) ring UMEs, (5) band UMEs, (6) array UMEs, and (7) interdigitated array UMEs (Kaifer and Gómez-Kaifer 1999).

There are numerous methods for fabricating UMEs. The most frequently applied methods are glass encapsulation sealing metal wires or carbon fibers into glass. However, there are other coating materials and techniques such as electropolymerization, electrophoretic deposition, tip-dipping in a varnish or molten paraffin, tip-transformation by various materials, or using Teflon-like materials as insulators (Liu et al. 2005).

After fabrication, the characterization of UMEs is generally performed via employing scanning electron microscopy (SEM), scanning electrochemical microscopy (SECM), or steady-state voltammetry. SEM-based characterization tries to determine whether the metal/fiber and insulator at the tip of the UME have been sealed properly, while in steady-state voltammetry studies, the radius of the UME can be estimated to determine whether electrode response follows the UME theory. More recently, SECM has been utilized to evaluate the size and shape of the designed UMEs by bringing the UME tip closer to electrically insulating or conductive substrates. This is the diffusion-limited current that has been measured by using a redox mediator at the surface of the tip of the UME which has a distance from the substrate (Zoski 2002).

The extra-small size of UMEs confers significant advantages on UMEs. The first advantage is that the smaller the currents, the smaller the ohmic drops, meaning that errors of residual cell resistance values are minimal. Second, the smaller the electrode surface, the smaller the electrode capacitance values, leading to shorter electrode time constants, which allows the measurement of faradaic currents relieved of charging currents at shorter times. Third, mass transport mechanisms of the UMEs are more efficient in that they facilitate the emergence of steady-state currents. Fourth, the size advantage is also present in probing regions covering very small spaces such as synapses of nerves (Kaifer and Gómez-Kaifer 1999; González-García et al. 2007; Chang and Zen 2007; Wang et al. 2021). Fifth, these electrodes can be employed in highly resistive environments to detect very small amounts of material of concern at shorter times with improved sensor sensitivity (Amatore et al. 2010; Lotfi Zadeh Zhad and Lai 2015). Sixth, the UMEs can be used for in vivo electrochemical measurements. For instance, they are employed for measuring neurotransmitters and relevant compounds in the brain. The usage of UMEs without any sample alteration, thanks to their small size leading to small currents, also contributes to their employment in in vivo measurements (Lupu et al. 2008). Jones and colleagues coated conductive polymer on 2 μm 3D UMEs which were produced to examine neural networks. The 3D structure of developed electrodes increased surface area while preserving its minimum side dimension and its coating by poly (3,4-ethylenedioxythiophene): polystyrene sulfonate (PEDOT:PSS) resulted in reaching acceptable thermal noise levels through decreasing electrochemical impedance. They concluded that the UMEs provided more perspectives in increasing the quality of microelectrode array recordings and ameliorating the neuron–electrode interface, and therefore they were promising devices for studying neuronal networks (Jones et al. 2020). In sum, improved sensitive measurement, high mass transport, significant temporal resolution, lower charging currents, higher signal-to-noise ratio, and the capacity to measure in very small environments and sample volumes are the basic advantages of UMEs compared to conventional electrodes (Coutinho et al. 2008).

Besides these advantages, the UMEs have the disadvantage of lack of sensitivity. Arrays of UMEs (UMEAs) have been designed to overcome this limitation (González-García et al. 2007). UMEAs are devices formed by assembling several identical UMEs, which amplifies the current in line with the number of UMEs. Loosely packed arrays result in the expected current signal in parallel to the number of UMEs, whereas closely packed arrays behave like a macroelectrode with a current proportion to the total surface area of the UMEs in the array (Orozco et al. 2010). Various micro/nanoelectrode series adapted to different measurement conditions were designed and produced to meet the sensing requirement. Bottom-up fabrication techniques used to prepare micro/nanoelectrode arrays involved electrode material (metal, carbon, ceramic, etc.) layer deposition or growth on the top, bottom, or formation in-between sandwich structure related to the templates or substrates (silicon, glass, polymer, ceramic, etc.). Another significant method used to manufacture microelectrode arrays is photolithography, in which photoresists and illumination sources exposure resulted in insulation of the surface and drilling of micron holes based on parts of thin film or the bulk of a substrate removal selectively. There are other processes for fabricating microelectrode arrays such as screen printing, deposition, membrane formation, and firing. More recently, ink-jet and 3D printing technologies have been found to be significant alternatives for high-resolution microstructures enabling complex electrode patterns at micro scale (Liu et al. 2020). After fabricating the UMEs, it is important to evaluate their sealing quality because the current transient curves of gases (H_2, O_2, and N_2, etc.) might evolve catalytic reactions leading to misleading quantitative results (Bodappa 2020).

Miniaturization and microfabrication techniques producing UMEs allow these electrodes to have reproducible and controllable dimensions which enable researchers to reliably measure very low electrochemical currents at nanoampere levels (Wahl et al. 2014). These advantages of UMEs allow them to be used in numerous fields. For example, array-type UMEs were used as effective tools for analytical detection of heavy metals in natural waters (Feeney and Kounaves 2000), disk UMEs were employed to investigate battery materials to assess their cycle lifetime (Guilminot et al. 2007), a UME was developed at the tip of a micropipette to detect enzymes leading to a miniaturized electrochemical biosensor (Zhang et al. 2013), a UME-nanopipette probe was designed for SECM and scanning ion conductance microscopy for imaging the surface topography without contacting it (Comstock et al. 2010), a Pt-UME was developed as a pH microsensor by employing anodic electrodeposition of iridium oxide films (Zhu et al. 2018), and a carbon-fiber platinized UME was fabricated as an artificial synapse to produce data on the oxidative bursts occurring at human fibroblasts (Amatore et al. 2000). In other words, UMEs are applied in medical, energy, environmental, scanning, and sensing fields, as well as pH measurements (Monteiro and Koper 2021).

Overall, UMEs have revolutionized electrochemical applications by extending the boundaries of electrochemistry into small sizes, nanosecond timescales, hydrodynamic applications, resistant environments, and single biological cells that are almost impossible to achieve by conventional electrodes. Usability in unusual media other than highly ionic conducting solutions and measurement of extremely small values in picoliter scales enable the researchers to interrogate single cells. These are unique characteristics of UMEs that open new possibilities and enlighten otherwise unknown parts of microenvironments (Forster and Keyes 2007).

3 Nanoparticle Usage for Fabrication of Ultramicroelectrodes and Applications

The use of nanoparticles (NPs) in electrochemistry for electrode modification has been increasing over the years. The reasons for this increasing usage stem from their unique physical and chemical characteristics, which their bulk forms do not display.

Nanomaterials, which have a controlled morphology and better surface functionality, provide researchers with very sensitive and selective surfaces that allow the electrodes to better detect the analytes of concern. Despite their advantages in electrochemical detection, it is very difficult to immobilize them properly on the electrode surface and functionalize them with desired pieces. The more efficiently these steps are accomplished, the better the electrode performance. Electrodeposition, polymerization, chemical binding, and physical adsorption are the major methods used for electrode modification with nanomaterials (Baig et al. 2019). NPs have four main advantages in electroanalysis, namely enhanced mass transport, more effective surface area, improved control over electrode microenvironment, and high surface-to-volume ratio, that make them a preferable catalyst (Welch and Compton 2006).

In this section of the chapter, selected literature studies, which used nanoparticles to fabricate UMEs and to modify UMEs, will be discussed. Table 39.1 is a summary of studies in the literature demonstrating the applications of nanoparticle-modified UMEs.

The use of metal nanoparticles decreases excess potentials of electroanalytical reactions and preserves the reversibility of redox reactions at the same time. Moreover, it is easy to electrodepose noble nanoparticles on the working electrode. The most frequently used metal nanoparticles are Au and Pt NPs for their facile electrodeposition on the surface of almost all types of electrodes to develop general surface properties (Kempahanumakkagari et al. 2017). They offer high sensitivity through immobilizing biomolecules, biocatalytic activities, facile preparation, significant biocompatibility, larger surface-to-volume ratio, and fast electron transfer (Rajapaksha et al. 2021).

The first example of metal nanoparticle-modified UMEs was made of AuNPs. Demaille and coworkers prepared spherical UMEs with a diameter of 1–30 μm. The AuNPs and 1,9-nonanditiol molecules are self-assembled at the glass micropipette tip via colloid chemistry approach. The technique applied here was confinement of the dithiol linking agent to the micropipette tip and subsequent immersion of the tip into a solution containing AuNPs. The result was the growth of spheres with a good shape and gold metallic brightness. Before the preparation of the self-assembled electrode, the inner wall of the micropipette was coated with a conductive carbon; therefore, micro-spheres could be electrically contacted. Finally, for electricity connection the pipette was filled with liquid Ga/In eutectic and a thin Ni wire was placed (Fig. 39.1) (Demaille et al. 1997).

With this method used for UME preparation, unlike all other methods employed for producing UMEs with comparable sizes, electrode geometry could be perfectly controlled, and reproducible results could be obtained; moreover, preparing such a UME was quite simple. According to the obtained results, the electrode assumed the electrochemical properties of Au and behaved as an ideal microelectrode both in aqueous and acetonitrile electrolyte solutions. Moreover, it was concluded that these UMEs could be employed as tips of SECM providing experimental approach curves perfectly associated with the conductive substrate theory (Demaille et al. 1997).

PtNPs were preferred by Wu and colleagues to modify carbon fiber UMEs (PtNPs/CFUME) to design an amperometric biosensor. PtNPs accumulated

Table 39.1 Summary of selected literature studies for NPs-modified UME applications

Analyte	Electrode	Method	Nanoparticle	Nanoparticle modification method	Linear range /detection limit	Application	Reference
H_2O_2	HRP/PtNPs/ CFUMEs	Amperometry	PtNPs	Electrodeposition	0.64 μM–3.6 mM/0.35 μM	–	(Wu et al. 2006)
Copper (II)	AuNPs/UMEA	Anodic stripping voltammetry	AuNPs	Electrodeposition	0–10 μM/ 0.30 μM	Soil samples	(Orozco et al. 2008)
CO	Nafion/PtNPs/ SPUME	Amperometry	PtNPs	Electrodeposition	Up to 1000 ppm	–	(Chou et al. 2009)
Catechol	HRP/AuNPs/ AuUME array	Amperometry	AuNPs	Electrodeposition	0.1–0.4 mM/0.05 mM	–	(Orozco et al. 2009)
BOD	PdNPs/COOH-rGN/UMEA	Cyclic voltammetry	PdNPs/ COOH-rGN	For COOH-GN: self-assembled and electroreduced; For PdNPs: electrodeposited	1–30 mg L^{-1}	–	(Wang et al. 2014)
		Amperometry	PdNPs/ COOH-rGN		2–15 mg L^{-1}	Spiked water samples	(Wang et al. 2017)
Dissolved oxygen	PdNPs/COOH-rGN/UMEA	Chronoamperometry	PdNPs/rGN-COOH		0.9–7.2 mg mL^{-1}	–	(Wang et al. 2015)
Glycerol	PtRu/SPUME	Chronoamperometry	PtRu NPs	Electrodeposition	0.92–92 mg L^{-1}/ 0.51 mg L^{-1}	Commercial B100 biodiesel samples	(Chen et al. 2015)

NO	Chitosan/ AuNPs/ Transparent carbon UMEA	Square wave voltammetry	AuNPs	Electrodeposition	5–100 μM/ 0.2 ± 0.1 μM	–	(Elliott et al. 2017)
Arsenic	AuNPs/CFUME	Differential pulse anodic stripping voltammetry	AuNPs	Electrodeposition	5–60 μg L^{-1}/ 0.9 μg L^{-1}	Tap and well waters	(Carrera et al. 2017)
H_2O_2	HRP-AuNCs/ MWCNTs/ CFUME	Amperometry	MWCNTs	By dipping CFUME in the black suspension	2–24 μM/ 443 nM	Calf serum samples	(Ren et al. 2020)

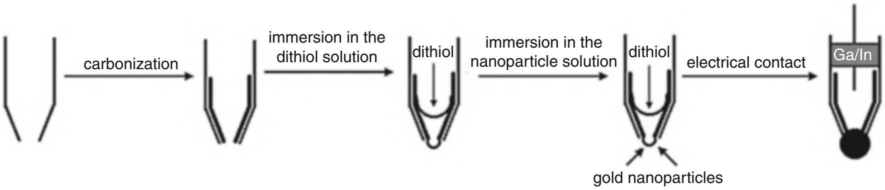
carbonization
immersion in the dithiol solution
dithiol
immersion in the nanoparticle solution
dithiol
electrical contact
Ga/In
gold nanoparticles

Fig. 39.1 Schematic representation of self-assembled Au-UME preparation. (Reprinted with permission from Demaille et al. (1997))

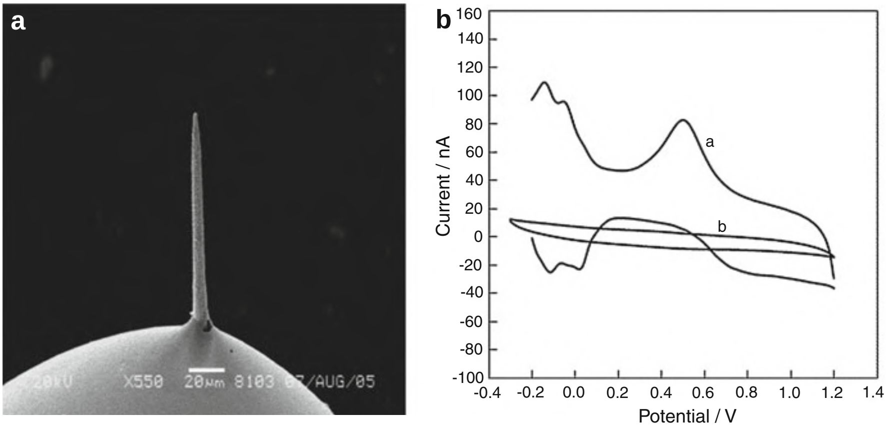

Fig. 39.2 SEM image of the PtNPs/CFUME (**a**) and cyclic voltammograms of PtNPs/CFUME (a) and bare CFUME (b) in 0.5 M H_2SO_4 solution at 100 mV s^{-1} (**b**). (Reprinted with permission from Wu et al. (2006). Copyright (2021) Elsevier)

electrochemically on UMEs increased surface areas tremendously by the electron transfer properties between UMEs and electroactive centers of recognizing elements of enzymes of the biosensor. Figure 39.2 shows the SEM image of PtNPs/CFUME and the cyclic voltammetric responses of bare CFUME and PtNPs/CFUME in 0.5 M H_2SO_4. It can be understood from Fig. 39.2b that increased signal verifies the deposition of PtNPs onto the CFUME surface. Horseradish peroxidase (HRP) enzyme was preferred as a recognition element of the biosensor to detect H_2O_2 using an amperometric method, which did not include a mediator. Wu and colleagues obtained a linear response vis-à-vis H_2O_2 concentration between 0.64 µM and 3.6 mM and a detection limit of 0.35 µM (Wu et al. 2006).

Another example where PtNPs are preferred is the screen-printed edge band UME (SPUME) gas sensor for detecting CO, produced by Chou and coworkers. The study presented results concerning electrodeposits of PtNPs on the SPUME (width: 20 µm) and used as an amperometric CO gas sensor. PtNPs were preferred for their catalytic effects against CO oxidation and their chemical stability. In designing the sensor, Nafion was used for the transmission of protons thanks to its hygroscopic nature and for the penetration of gases into electrodes. According to this study, the edge diffusion effect at the UME resulted in depositing homogenous sizes and allowed the PtNPs to be distributed without protective or capped agents. This method has the advantage of simplicity in producing a conventional three-electrode configuration compared to other CO gas sensors. The designed gas sensor obtained good linearity up to 1000 ppm and a sensitivity of 3.76 nA/(ppm·cm^2). There was no need for a supporting – in other words internal – electrolyte in the scheme of the sensor, and this was the most obvious advantage of this UME system (Chou et al. 2009).

Miniaturization is quite useful for designing a light, small, and multi-array sensor. Such sensors respond rapidly, consuming few materials and solvents; therefore, they gave the advantage of having been used as a bio-device with improved portability or a bio-artificial micro-appliance with enhanced implantability (Huang et al. 2007). A gold UME array (UMEA) modified by gold nanoparticles (AuNPs) was employed for a biosensor design with HRP as a model-recognizing element (Orozco et al. 2009). AuNPs are favored for their good biocompatibility, excellent conductivity abilities, and high surface-to-volume ratios (Guo and Wang 2007). The gold ME and UME series used in this study were produced by using Si/SiO$_2$/metal structures via standard photolithographic techniques. The surface area of MEs was 1.62×10^{-2} cm^2. A UMEA with three different geometries was used for experimentation. The first series included 100 disk-shaped microelectrodes (diameter = 10 μm) with a total surface area of 7×10^{-2} cm^2. The second series included 400 disks, while the third series included 1600 disks with a diameter of 5 μm. When the sensitivities of these electrodes with different geometries were compared, the highest sensitivity was obtained with the array of 400 disks with a diameter of 5 μm. AuNPs were electrodeposited at the surface of UMEA, and therefore the active surface increased up to 100-fold while natural electrolytic properties remained unchanged. HRP was immobilized by covalent bonding over the three transducer platforms via a thiol self-assembled monolayer. The biosensor designed was employed for detecting catechol amperometrically. What is more significant in this study was the performance comparison of bare and AuNPs-modified UMEAs with microelectrodes. Using UMEAs modified with AuNPs enhanced the biosensor sensitivity threefold compared to bare UMEA and 80-fold compared to microelectrode-based biosensors. Moreover, the designed biosensor showed a linear response to catechol with a concentration range of 0.1 mM to 0.4 mM and with a detection limit of 0.05 mM (Orozco et al. 2009).

In another work conducted by Orozco and colleagues, the formation of a self-assembled monolayer (SAM) was analyzed at Au-UMEAs modified with AuNPs. Thus, a basis for bioreceptors was provided to bind to transducers for biosensor design. The two thiol derivatives selected for SAM in the study were 3.3′-dithiodipropionic acid di (N-hydroxysuccinimide) ester and 11-mercaptoundecanoic acid molecules. Accordingly, the AuNPs deposited electrochemically on the electrode surface seemed to be vital for arranging thiolated probes and electron transfer processes at the interface between the electrode and the solution. Orozco and colleagues compared the electrochemical performance of the developed SAM/AuNPs/Au-UMEA with SAM/bare UMEA and SAM/bare ME. Comparative studies with bare electrodes have proven that as the SAM layer was mounted on the AuNPs modified UMEA surface, the electron transfer became more efficient. As a result of this study, it has been observed that the advantageous properties of AuNPs, together with the higher sensitivities obtained with UMEA-based devices, resulted in a significant improvement of the limit of detection values of biosensors (Orozco et al. 2012).

AuNPs-modified UMEA was also used to determine copper (II) from soil samples by Orozco et al. AuNPs were electrodeposited from AuNPs solution including 20 nm particles on the UMEA under the 1.6 V potential for 20 min. This procedure increased the surface area and there was no loss of analytical performance. The performance of AuNPs-modified UMEA compared to bare UMEA and the modified one showed a sensitivity of 25.9 ± 1.3 $\text{nC}\cdot\mu\text{M}^{-1}$ while the bare one showed 7.5 ± 0.6 $\text{nC } \mu\text{M}^{-1}$ sensitivity. Modified and bare UMEAs also differentiated according to their linear ranges. Modified UMEA gave a broader range (0–10 μM) than the bare one (0–2 μM) (Orozco et al. 2008).

Elliott and colleagues produced AuNPs-modified transparent carbon UMEA with an easy-to-manufacture method for selective determination of nitric oxide (NO). Chitosan/AuNPs solution was electrodeposited on the electrode surface via chronoamperometry by applying a potential at -1.00 V for 60 s. The effect of chitosan and AuNPs modification in NO determination was measured by square wave voltammetry, indicating that the modification significantly enhanced the electrochemical oxidation of NO. The limit of detection value was reported as 0.2 ± 0.1 μM. This shows that these electrodes can be used in in situ mechanical and kinetic characterization of electrochemical reactions, and demonstrated a significant sensitivity (Elliott et al. 2017).

Carrera and colleagues also preferred AuNPs as modifiers for sensor design in determining arsenic in natural waters. The AuNPs were deposited potentiostatically at -0.90 V for 15 s to modify on CFUME. Cyclic voltammetry and electrochemical impedance spectroscopy were studied for electrochemical characterization, and an SEM connected to an X-ray microanalysis system was employed to observe the presence of AuNPs on CFUME. The anodic stripping voltammetry method was preferred for the determination of arsenic. Carrera and colleagues concluded that compared to standard carbon electrodes, the developed modified electrode has a fast response for the determination of arsenic with advanced analytical properties such as improved reproducibility, enhanced selectivity, lower detection limit values (0.9 $\mu\text{g L}^{-1}$), and a significant sensitivity (0.0176 $\text{nA } \mu\text{g L}^{-1}$) compared to standard carbon electrodes (Carrera et al. 2017).

Lee and colleagues developed a simple method to prepare nanoporous gold-modified UMEs. These electrodes were produced by a single potential sweep from 0.7 V to 1.35 V in phosphate buffer solution (pH 8.0) that contained 1 M KCl. Well-defined nanoporous gold structures were constructed on Au surfaces with a single potential scan within 100 s. The formation of nanoporous gold was demonstrated by taking SEM images. While this method is employed on small-sized Au surfaces without relating it to electrode geometry, it cannot be applied to conventional macroelectrodes. The impact of the size of the electrode as well as scan rates on nanoporous gold formation was thoroughly examined. This modified electrode was utilized for detecting glucose amperometrically with 20-μL sample volumes (Lee and Kim 2021).

Chen and colleagues have developed a non-enzymatic method for glycerol quantitation in biodiesel using a SPUME modified with PtRu NPs. Oxidation of glycerol with periodate resulted in the formation of the formic acid and formaldehyde whose detection was performed by the designed electrochemical sensor at the gas phase. Thus, the two steps of the procedure, namely sample preparation and determination, were combined as one single step. Moreover, this eliminated solution-phase interferences and therefore enhanced selectivity in analyzing glycerol. PtRu deposited on SPUME first at -0.6 V for 10 s in 150 ppm $HAuCl_4$ and at -0.6 V at a potential of 25 s in 50 ppm $RuCl_3$ and 150 ppm H_2PtCl_6. Au NPs were first deposited to decrease PtRu's particle size. 3 μL Nafion solution was dripped onto PtRu-SPUME for its hygroscopicity to conduct protons and allow gases to penetrate the electrode. In UME, the edge diffusion effect increased in mass transfer rate and resulted in a more homogeneous size with NPs' distribution regardless of preservatives. Characterization was made by SEM, X-ray photoelectron spectroscopy, and X-ray energy dispersive spectroscopy to verify the structure and molecular composition of PtRu NPs. The limit of detection value was found as 0.51 mg L^{-1} and the concentration range was 0.92–92 mg L^{-1} in the assay of glycerol. Especially in biodiesel to monitor free glycerol, extraction was no longer required to eliminate organic interferences (Chen et al. 2015).

Graphene (GN) has many advantages including large surface area, high conductivity, and fast electron transfer. Pd is of great interest due to similar productions for oxygen reaction in electrocatalysts. Pd has attracted the attention of researchers conducting electrocatalytic studies of oxygen reaction due to its Pt-like properties, being more abundant and cheaper than Pt. The GN/Pd NPs composite-based sensors combine the advantageous properties of GN and Pd, which were applied in the electrocatalysis of oxygen or other species. Wang and colleagues investigated reduced carboxylic GN/PdNPs (COOH-rGN/PdNPs)-modified UMEA and employed this electrode in determining biochemical oxygen demand (BOD) electrochemically. The micro-electro-mechanical system technique was used to fabricate the UMEAs. To fabricate COOH-rGN/PdNPs-sensitive film, first COOH-GN was self-assembled and then electroreduced, and finally electrodeposited the PdNPs on UMEA. Drop-casting, which is a common method of modifying GN, is improper for UMEA modification because this method makes UMEA's insulating layer conductive, causing UMEA to lose its unique properties. For this reason, self-assembling was preferred for GN modification. When the sensitive film of COOH-GN, COOH-rGN, and PdNPs was compared to the sensitive film of COOH-rGN/PdNPs, it was observed that the latter demonstrated a satisfiable electroreduction performance toward dissolved oxygen. Based on the COOH-rGN/PdNPs-modified UMEA, a BOD microsensor was designed through electrodeposition of 1 mM palladium nitrate in the solution of 0.1 M H_2SO_4 at the potential of -0.3 V for 5 s. The linear range was obtained from 1 to 30 mg L^{-1} for BOD determination (Wang et al. 2014).

Wang and colleagues used the modification of COOH-rGN/PdNPs in another work for the amperometric determination of BOD and immobilized magnetite-functionalized *Bacillus subtilis* to the UMEA surface. Although this microsensor has satisfactory features, it has some disadvantages such as long response time due to slow mass transfer. Wang and colleagues produced a new sensor to improve that sensor. To do so, they used *Bacillus subtilis*, which functionalized using Fe_3O_4 to enhance mass transfer which was immobilized by using a permanent magnet. Modified UMEA was used in detecting different concentrations of dissolved oxygen after the respiration of micro-organisms. Due to the rapid mass transfer of magnetite-functional microbes on the electrode surface, it could be carried out in 5 min. The best-achieved calibration plot at -0.4 V potential was linear in the concentration range 2–15 mg L^{-1} of BOD. It has been successfully applied in spiked water samples (Wang et al. 2017).

In another study, Wang and colleagues compared the performance of NH_2-GN and COOH-GN NPs for dissolved oxygen determination. UMEAs were manufactured with a micro-electromechanical system technique and each UME had a radius of 10 μm. When NH_2-GN-modified UMEA and the COOH-GN-modified UMEA were compared, it was observed that the latter demonstrated a superior electrochemical reduction to dissolved oxygen, as it was dispersed better and had more active sites. Electroreduction of the COOH-GN on UMEA was used to obtain reduced COOH-GN (COOH-rGN). This process not only increased the conductivity but also enhanced the catalysis performance. Eventually, the PdNPs/rGN-COOH composite was included in the microsensor. Dissolved oxygen microsensor was applied by the chronoamperometry method in the linear range of 0.9–7.2 mg mL^{-1} at a potential of -0.4 V (Wang et al. 2015).

Carbon nanotubes (CNTs) are cylindrical tube-shaped and one-dimensional constructs made up of sp^2 hybrid carbon atoms. They have a nanometer fraction and a diameter of tens of nanometers, while they can reach a few centimeters in length. In line with the cylindrical graphene layer numbers, they can be categorized as single-walled carbon nanotubes (SWCNTs), dual-walled carbon nanotubes, and multi-walled carbon nanotubes (MWCNTs). While SWCNTs consist of a single graphene sheet rolled into a tube-like structure, MWCNTs are composed of several graphene layers with a radius of 2–100 nm and a distance around 0.34 nm between layers. CNTs are preferred for their unique properties such as good mechanical, electrical, and tensile strength, superior surface area, and good thermal conductivity (Luo et al. 2006; Baig et al. 2019; Aralekallu and Sannegowda 2021).

Dumitrescu and colleagues developed a simple and reproducible method for designing disk-shaped SWCNT-UMEs. Such a properly characterized electrode geometry allowed the researchers to investigate the major electrochemical properties of the SWCNTs. In this study factors like redox mediator potential, concentration, and the impact of background electrolyte were examined. The researchers were able to grow ultra-pure SWCNTs via chemical vapor deposition, during which FeNPs were used as catalyzer at the insulating surface of SiO_2. Figure 39.3 represents a scheme for the electrode preparation steps. What is significant is that even if the surface coverage of SWCNT was <% 1, with <mM concentrations of redox species,

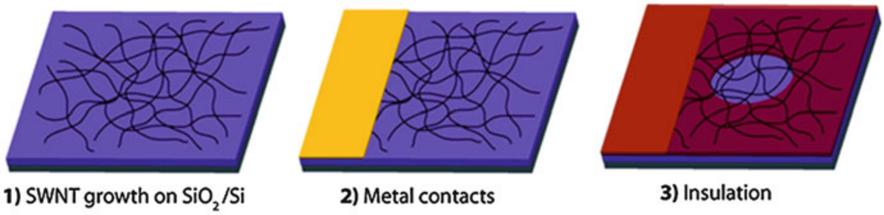

Fig. 39.3 Schematic of the lithographic procedure for fabricating SWNT disk UMEs. (Reprinted with permission from Dumitrescu et al. (2008). Copyright (2021) ACS)

an SWCNT-modified UME behaved like a solid UME. However, it showed considerable advantages such as unequaled rapid response times, low background currents, and high mass transfer rate toward active parts of the electrode surface (Dumitrescu et al. 2008).

Su and colleagues fabricated SWCNT ensembles-modified UMEs as a probe for SEM. In doing so, pristine SWNTs were self-assembled onto Au-UMEs by employing 1-(1-Pyrenyl)-1-methanethiol (PyMT) as an adhesion molecule. Then methylene blue (MB) was immobilized on the sensor. To study the electrochemistry of this sensor, cyclic voltammetry was used. For modifying the SWCNT, the PyMT/Au-UMEs were soaked in an SWCNTs dispersion in dimethylformamide (1.0 mg/mL) and left for 3 h at room temperature. For MB modification, the SWCNTs/PyMT/Au-UMEs were immersed in 5 mM MB prepared in acetonitrile for 30 min. The fabricated SWCNTs/UMEs combined the steady-state diffusion current of UMEs and the ability for MB immobilization of the SWCNTs (Su et al. 2012).

Joshi and colleagues developed an electrophoretic method to prepare and modify the UMEs. Loading the UMEs with the desired catalyst-composite material is important for performing fast-scan cyclic voltammetry measurements. MWCNTs have been used for modification. The study illuminated the CO adsorption rate on the selected catalysts. The peaks resulting from the adsorption of the CO were explained as a function of screening rates. The area below the peak correlated with the CO adsorption rate on these catalysts. The average rate of CO adsorption in methanol oxidation at Pt-MWCNTs/UME was evaluated as 13.5×10^{-8} mol cm^{-2} s^{-1}. The proposed method can be generalized toward any electrocatalyst of interest (Joshi et al. 2018).

Ren and colleagues preferred both Au nanoclusters (AuNCs) and MWCNTs for CFUME modification to develop an enzyme-based biosensor for detecting hydrogen peroxide (H_2O_2) amperometrically. Modified electrodes were produced using HRP and biomineralized fluorescent AuNCs. The immobilization of HRP-AuNCs on CFUMEs coated with MWCNTs produced this significant biosensor. Adjoining HRP with AuNCs resulted in maintenance of biological activity for the catalytic reaction of H_2O_2. The CFUME was immersed into the black suspension (0.5 mL) and the solution was placed in an 80 °C oven until drying. HRP-AuNCs were produced on the electrode by soaking MWCNTs/CFUMEs in HRP-AuNC solutions.

The detection limit of the H_2O_2 biosensor is found as approximately 443 nM. Long-term stability and good reproducibility emerged as the two significant advantages of the designed biosensor. MWCNTs can effectively remove biomacromolecule contamination of the electrode surface; moreover, the researchers were able to increase sensitivity via expanding the surface area through modification. The developed sensor was employed to measure H_2O_2 in serum solution and attained high selectivity and sensitivity (Ren et al. 2020).

4 Conclusion

It is the aim of this study to review the development of NPs-modified UMEs and their electroanalytical applications. UMEs are preferred for their advantages vis-à-vis conventional electrodes such as improved sensitivity, lower charging currents, smaller ohmic drops, higher mass transports, and signal-to-noise ratio. Moreover, they can be employed for measurements at microenvironments and very small sample volumes. These advantages make them attractive devices used in various fields including medicine, energy, environment, scanning, and sensing.

In addition to these advantages, UMEs achieve additional benefits after being modified with nanoparticles. First, NPs increased the surface area of the electrodes which enhances their sensitivity. Second, NPs modification resulted in lower background currents, even higher mass transfer rate, and rapid response times. Third, conductivity and catalytic performance are improved through modification.

It is observed that carbon-based NPs and metal NPs are mostly preferred for UME modification. Among metal nanoparticles, Au and Pt NPs are widely chosen for their facile electrodeposition on the surface of the electrode together with their higher sensitivity, ease of preparation, and significant biocompatibility. Overall, the UMEs can be considered as a promising electrode type allowing researchers to examine microenvironments and detect analytes at very small sample volumes especially in in vivo applications.

References

Amatore C, Arbault S, Bruce D, De Oliveira P, Erard M, Vuillaume M (2000) Analysis of individual biochemical events based on artificial synapses using ultramicroelectrodes: cellular oxidative burst. Faraday Discuss 116:319–333

Amatore C, Cile Pebay C, Thouin L, Wang A, Warkocz J-S (2010) Difference between ultra-microelectrodes and microelectrodes: influence of natural convection. Anal Chem 82: 6933–6939

Anon (2020) C. Working Electrodes. https://chem.libretexts.org/@go/page/61543. Accessed 30 Apr 2021

Aoki K (1993) Theory of ultramicroelectrodes. Electroanalysis 5:627–639

Aralekallu S, Sannegowda LK (2021) Metal nanoparticles for electrochemical sensing applications. In: Mustansar Hussai C, Kumar Kailasa S (eds) Handbook of nanomaterials for sensing applications. Elsevier, Amsterdam, pp 589–629

Baig N, Sajid M, Saleh TA (2019) Recent trends in nanomaterial-modified electrodes for electroanalytical applications. TrAC – Trends Anal Chem 111:47–61

Bard AJ, Inzelt G, Scholz F (eds) (2012) Electrochemical dictionary, 2nd Revised edn. Springer Berlin Heidelberg, New York

Bodappa N (2020) Rapid assessment of platinum disk ultramicroelectrodes' sealing quality by a cyclic voltammetry approach. Anal Methods 12(27):3545–3550

Bond AM (1994) Past, present and future contributions of microelectrodes to analytical studies employing voltammetric detection. A review. Analyst 119(11):1–21

Brett CMA, Oliveira-Brett AM (1994) Electrochemistry: principles, methods, and applications. Oxford University Press, Oxford

Carrera P, Espinoza-Montero PJ, Fernández L, Romero H, Alvarado J (2017) Electrochemical determination of arsenic in natural waters using carbon fiber ultra-microelectrodes modified with gold nanoparticles. Talanta 166:198–206

Chang JL, Zen JM (2007) A poly(dimethylsiloxane)-based electrochemical cell coupled with disposable screen printed edge band ultramicroelectrodes for use in flow injection analysis. Electrochem Commun 9(12):2744–2750

Chen WC, Li PY, Chou CH, Chang JL, Zen JM (2015) A nonenzymatic approach for selective and sensitive determination of glycerol in biodiesel based on a PtRu-modified screen-printed edge band ultramicroelectrode. Electrochim Acta 153:295–299

Chou C-H, Chang J-L, Zen J-M (2009) Homogeneous platinum-deposited screen-printed edge band ultramicroelectrodes for amperometric sensing of carbon monoxide. Electroanalysis 21(2): 206–209

Comstock DJ, Elam JW, Pellin MJ, Hersam MC (2010) Integrated ultramicroelectrode-nanopipet probe for concurrent scanning electrochemical microscopy and scanning ion conductance microscopy. Anal Chem 82(4):1270–1276

Coutinho CFB, Coutinho LFM, Lanças FM, Câmara CAP, Nixdorf SL, Mazo LH (2008) Development of instrumentation for amperometric and coulometric detection using ultramicroelectrodes. J Braz Chem Soc 19(1):131–139

Demaille C, Brust M, Tsionsky M, Bard AJ (1997) Fabrication and characterization of self-assembled spherical gold ultramicroelectrodes. Anal Chem 69(13):2323–2328

Dumitrescu I, Unwind PR, Wilson NR, Macpherson JV (2008) Single-walled carbon nanotube network ultramicroelectrodes. Anal Chem 80(10):3598–3605

Elliott J, Duay J, Simoska O, Shear JB, Stevenson KJ (2017) Gold nanoparticle modified transparent carbon ultramicroelectrode arrays for the selective and sensitive electroanalytical detection of nitric oxide. Anal Chem 89(2):1267–1274

Feeney R, Kounaves SP (2000) Microfabricated ultramicroelectrode arrays: developments, advances, and applications in environmental analysis. Electroanalysis 12(9):677–684

Forster RJ, Keyes TE (2007) Ultramicroelectrodes. In: Zoski CG (ed) Handbook of electrochemistry. Elsevier, Amsterdam, pp 155–171

González-García O, Ariño C, Díaz-Cruz JM, Esteban M (2007) Chronoamperometric and voltammetric characterization of gold ultramicroelectrode arrays. Electroanalysis 19(4): 429–435

Goodwin S, Coldrick Z, Heeg S, Grieve B, Vijayaraghavan A, Hill EW (2021) Fabrication and electrochemical response of pristine graphene ultramicroelectrodes. Carbon N Y 177:207–215

Guilminot E, Corcella A, Chatenet M, Maillard F (2007) Comparing the thin-film rotating disk electrode and the ultramicroelectrode with cavity techniques to study carbon-supported platinum for proton exchange membrane fuel cell applications. J Electroanal Chem 599(1):111–120

Guo S, Wang E (2007) Synthesis and electrochemical applications of gold nanoparticles. Anal Chim Acta 598(2):181–192

Holt KB (2011) Diamond ultramicroelectrodes and nanostructured electrodes. In: Brillas E, Martinez-Huitle CA (eds) Synthetic diamond films: preparation, electrochemistry, characterization, and applications. Wiley, Hoboken, pp 133–152

Huang HC, Huang SY, Lin CI, Der LY (2007) A multi-array sensor via the integration of acrylic molecularly imprinted photoresists and ultramicroelectrodes on a glass chip. Anal Chim Acta 582(1):137–146

Jones PD, Moskalyuk A, Barthold C, Gutöhrlein K, Heusel G, Schröppel B, Samba R, Giugliano M (2020) Low-impedance 3D PEDOT:PSS ultramicroelectrodes. Front Neurosci 14:405

Joshi VS, Poudyal DC, Satpati AK, Patil KR, Haram SK (2018) Methanol oxidation reaction on Pt based electrocatalysts modified ultramicroelectrode (UME): novel electrochemical method for monitoring rate of CO adsorption. Electrochim Acta 286:287–295

Kaifer A, Gómez-Kaifer M (1999) Ultramicroelectrodes and their applications. In: Kaifer A, Gómez-Kaifer M (eds) Supramolecular electrochemistry. Wiley-VCH, Weinheim, pp 45–54

Kempahanumakkagari S, Deep A, Kim KH, Kumar Kailasa S, Yoon HO (2017) Nanomaterial-based electrochemical sensors for arsenic – a review. Biosens Bioelectron 95:106–116

Kottke PA, Kranz C, Kwon YK, Masson JF, Mizaikoff B, Fedorov AG (2008) Theory of polymer entrapped enzyme ultramicroelectrodes: fundamentals. J Electroanal Chem 612(2):208–218

Lee S, Kim J (2021) Single potential scan methods for nanoporous gold formation on ultramicroelectrode surfaces. Electroanalysis 33:1–7

Liu B, Rolland JP, DeSimone JM, Bard AJ (2005) Fabrication of ultramicroelectrodes using a "teflon-like" coating material. Anal Chem 77(9):3013–3017

Liu Y, Li X, Chen J, Yuan C (2020) Micro/nano electrode array sensors: advances in fabrication and emerging applications in bioanalysis. Front Chem 8:573865

Lotfi Zadeh Zhad HR, Lai RY (2015) Comparison of nanostructured silver-modified silver and carbon ultramicroelectrodes for electrochemical detection of nitrate. Anal Chim Acta 892: 153–159

Luo X, Morrin A, Killard AJ, Smyth MR (2006) Application of nanoparticles in electrochemical sensors and biosensors. Electroanalysis 18(4):319–326

Lupu S, Lete C, Marin M, Totir N (2008) Electrochemistry of metal hexacyanoferrates and conducting polymers bilayer structures deposited on conventional size electrodes and ultramicroelectrodes. II. Modified ultramicroelectrodes. Rev Roum Chim 53(7):547–552

Monteiro MCO, Koper MTM (2021) Measuring local pH in electrochemistry. Curr Opin Electrochem 25:100649

Orozco J, Fernández-Sánchez C, Jiménez-Jorquera C (2008) Underpotential deposition−anodic stripping voltammetric detection of copper at gold nanoparticle-modified ultramicroelectrode arrays. Environ Sci Technol 42(13):4877–4882

Orozco J, Jiménez-Jorquera C, Fernández-Sánchez C (2009) Gold nanoparticle-modified ultramicroelectrode arrays for biosensing: a comparative assessment. Bioelectrochemistry 75(2): 176–181

Orozco J, Fernández-Sánchez C, Jiménez-Jorquera C (2010) Ultramicroelectrode array based sensors: a promising analytical tool for environmental monitoring. Sensors 10(1):475–490

Orozco J, Jiménez-Jorquera C, Fernández-Sánchez C (2012) Electrochemical performance of self-assembled monolayer gold nanoparticle-modified ultramicroelectrode array architectures. Electroanalysis 24(3):635–642

Pletcher D (1991) Why microelectrodes? In: Montenegro MI, Queiros MA, Daschbach JL (eds) Microelectrodes: theory and applications. Springer Science and Business Media, B.V., Alvo, pp 3–16

Rajapaksha RDAA, Hashim U, Gopinath SCB, Parmin NA, Fernando CAN (2021) Nanoparticles in electrochemical bioanalytical analysis. In: Gopinath SCB, Gang F (eds) Nanoparticles in analytical and medical devices. Elsevier, Amsterdam, pp 83–112

Ren Q-Q, Yang F, Ren W, Wang C, Jiang W-S, Zhao Z-Y, Chen J, Lu X-Y, Yu Y (2020) Amperometric biosensor based on coimmobilization of multiwalled carbon nanotubes and horseradish peroxidase-gold nanocluster bioconjugates for detecting H2O2. J Nanomater 2020:9627697

Stradiotto NR, Yamanaka H, Valnice M, Zanoni B (2003) Electrochemical sensors: a powerful tool in analytical chemistry. J Braz Chem Soc 14(2):159–173

Štulík K, Amatore C, Holub K, Mareček V, Kutner W (2000) Microelectrodes. Definitions, characterization, and applications (Technical report). Pure Appl Chem 72(8):1483–1492

Su L, Tong Y, Shu T, Gong W, Zhang X (2012) Single-walled carbon nanotube ensembles modified gold ultramicroelectrodes prepared by self-assembly deposition method with 1-(1-pyrenyl)-1-methanethiol monolayer as an adhesion layer. Electrochem Commun 20(1):163–166

Szamocki R, Velichko A, Holzapfel C, Mücklich F, Ravaine S, Garrigue P, Sojic N, Hempelmann R, Kuhn A (2007) Macroporous ultramicroelectrodes for improved electroanalytical measurements. Anal Chem 79(2):533–539

Wahl A, Barry S, Dawson K, MacHale J, Quinn AJ, O'Riordan A (2014) Electroanalysis at ultramicro and nanoscale electrodes: a comparative study. J Electrochem Soc 161(2): B3055–B3060

Wang J, Bian C, Tong J, Sun J, Hong W, Xia S (2014) Reduced carboxylic graphene/palladium nanoparticles composite modified ultramicroelectrode array and its application in biochemical oxygen demand microsensor. Electrochim Acta 145:64–70

Wang J, Bian C, Tong J, Sun J, Li Y, Hong W, Xia S (2015) Modification of graphene on ultramicroelectrode array and its application in detection of dissolved oxygen. Sensors 15(1): 382–393

Wang J, Li Y, Bian C, Tong J, Fang Y, Xia S (2017) Ultramicroelectrode array modified with magnetically labeled Bacillus subtilis, palladium nanoparticles and reduced carboxy graphene for amperometric determination of biochemical oxygen demand. Microchim Acta 184(3): 763–771

Wang M, Liu J, Liang X, Gao R, Zhou Y, Nie X, Shao Y, Guan Y, Fu L, Zhang J, Shao Y (2021) Electrochemiluminescence based on a dual carbon ultramicroelectrode with confined steady-state annihilation. Anal Chem 93(10):4528–4535

Welch CM, Compton RG (2006) The use of nanoparticles in electroanalysis: a review. Anal Bioanal Chem 384(3):601–619

Wu Z, Chen L, Shen G, Yu R (2006) Platinum nanoparticle-modified carbon fiber ultramicroelectrodes for mediator-free biosensing. Sensors Actuators B Chem 119(1):295–301

Xie X, Stueben D, Berner Z (2005) The application of microelectrodes for the measurements of trace metals in water. Anal Lett 38(14):2281–2300

Zhang D-W, Liu JX, Nie J, Zhou YL, Zhang XX (2013) Micropipet tip-based miniaturized electrochemical device combined with ultramicroelectrode and its application in immobilization-free enzyme biosensor. Anal Chem 85(4):2032–2036

Zhang Z, Cong Y, Huang Y, Du X (2019) Nanomaterials-based electrochemical immunosensors. Micromachines 10(6):1–19

Zhu Z, Liu X, Ye Z, Zhang J, Cao F, Zhang J (2018) A fabrication of iridium oxide film pH microsensor on Pt ultramicroelectrode and its application on in-situ pH distribution of 316L stainless steel corrosion at open circuit potential. Sensors Actuators B Chem 255:1974–1982

Zoski CG (2002) Ultramicroelectrodes: design , fabrication, and characterization. Electroanalysis 15–16:1041–1051

Всё для победы!
НАРОДНЫЙ ФРОНТ
https://pobeda.onf.ru/
LET'S HELP THE RUSSIA

Bimetallic Nanocatalysts Used in Bioelectrochemical Detection and Diagnosis

40

Ruchika Chauhan, Zondi Nate, Atal Gill, and
Rajshekhar Karpoormath

Contents

1 Introduction 882
  1.1 What Are Bimetallic Nanocatalysts 882
  1.2 Types of Bimetallic or Orientation of Bimetallic Nanomaterials 883
2 Properties and Synthesis of Bimetallic Nanocatalyst 884
  2.1 Properties 884
  2.2 Chemical and Electrochemical Reduction 885
  2.3 Micro-emulsion and Thermal Decomposition Methods 886
3 Application of Bimetallic Nanocatalyst in Bioelectrochemical Detection and Diagnosis 886
  3.1 Biosensors Based on Target Analyte 887
4 Conclusion and Future Perspectives 893
References 893

Abstract

Bimetallic nanocatalysts are emerging entities due to their advanced properties, which are mainly driven by the synergistic effects of two metals. For bioelectrochemical detection, bimetallic nanocatalysts act as an electronic chain to enhance the electron transport between redox moiety present in biomolecules (proteins, enzymes, peptides, etc.) and electrode surface, and it may also enhance the electrochemical reaction rate. It has been observed that the electrocatalytic bimetals enhance the selectivity and sensitivity of biosensors. Structural configurations like composition, size, and shape influence the electrocatalytic behavior of bimetallic nanomaterials. This chapter discussed the recent advances in the

---

R. Chauhan · Z. Nate · A. Gill · R. Karpoormath (✉)
Department of Pharmaceutical Chemistry, College of Health Sciences, University of KwaZulu-Natal, Durban, South Africa
e-mail: karpoormath@ukzn.ac.za

© Springer Nature Singapore Pte Ltd. 2023

U. P. Azad, P. Chandra (eds.), *Handbook of Nanobioelectrochemistry*,
https://doi.org/10.1007/978-981-19-9437-1_40

synthesis and characterization of bimetallic nanocatalysts and their applications in electrochemical biosensing and the future perspectives of bimetallic nanocatalysts for bioelectrochemical detection.

Keywords

Bimetallic nanocatalyst · Electrochemical sensors · Biosensors · Immunosensors · Bimetals alloy

1 Introduction

1.1 What Are Bimetallic Nanocatalysts

Metal nanoparticles have unique catalytic properties due to their intrinsic electronic tendencies (Schmid 2011). The aggregation of the nanoparticles is a significant concern, which may lead to changes in their structure and nanoscale catalyst properties (An and Somorjai 2015; Picone et al. 2016). Bimetallic nanoparticles have distinctive physicochemical properties because of the synergistic effect of electronic alteration between two metals (Notar Francesco et al. 2014; Peng et al. 2015; Zhu et al. 2015). In bimetallic nanoparticles, two different metals combine and show some enhanced functionalities like stability, selectivity, and catalytic activity over their monometallic nanoparticles (Yu et al. 2011b). Recently bimetallic nanoparticles have received attention because of their enhanced electrocatalyst characteristic (Chen et al. 2012b) compared to monometallic nanoparticles. Sinfelt et al. introduced bimetallic catalyst firstly, with the combination of transition metals (Ru-Cu, Ni-Cu, and Os-Cu) to reduce undesired C-C activation for hydrogenolysis (Sinfelt 1977). Nantaphol et.al have described bimetallic catalysts property in Pt/Au nanocatalyst. It was synthesized by sequentially electrodeposition of Au and Pt at boron-doped diamond electrode (BDD). The developed Pt/Au/BDD electrode exhibited higher catalytic property than the individual metal electrodes (Nantaphol et al. 2017). This study accelerated bimetallic catalysts in several reactions of dehydrogenation, oxidation, and hydrogenolysis (Alonso et al. 2012; Zaera 2013; Gilroy et al. 2016).

The inherent electrocatalysis properties of bimetallic nanoparticles have been used to construct various sensors and biosensors (Sun et al. 2012; Hossain and Park 2014; Li et al. 2015c; Cho et al. 2020). The ligand and geometry play a significant role in bimetallic nanocatalyst; the d-band of transition metal shifts to lower energies, reducing the adsorbate-metal bond strength, which may change its selectivity (Nørskov et al. 2009). The synthesis of bimetallic nanocatalyst emphasizes morphology, dispersion, and atom distribution in complex and characterization techniques, which confirm all these parameters. These bimetallic nanostructures are in different forms like core-shell structures, alloys, and hybrids of monometallic nanoparticles (Chen et al. 2012a; Li et al. 2021).

1.2 Types of Bimetallic or Orientation of Bimetallic Nanomaterials

The assembling pattern of bimetals during synthesis makes them multiple-dimension shapes. Therefore, they are categorized into three categories: alloy, core-shell, and heterostructure, as shown in Fig. 40.1a–c. Each category is discussed in the next section.

1.2.1 Bimetallic Nanoparticles (Alloys)

Alloys are a homogeneous mixture of bimetals and are subdivided into ordered alloy and random alloy. The alloys have arbitrary atomic orders, and metal-metal bonds are the leading moiety of the whole structure. The mixing of two metals is driven by forces that regulate crystal morphology; higher the interaction force promotes high bond strength, intimate mixing of metals, and charge transfer (Ferrando et al. 2008). In general, for the chemical synthesis of bimetallic alloy nanocatalyst, strong reducing agents have been utilized at the controlled condition to conduct the simultaneous reduction of both metals (Mariscal et al. 2011). Researchers have reported a range of bimetallic alloy of Pt with different noble or transition metals, the catalytic property and stability of bimetal alloy dependent on their structure and composition (Chantry et al. 2013). Pt-Fe alloy synthesized under controlled temperature and obtained well-ordered intermetallic stacking of both metals, which improved catalytic property in fct-FePt compared to the fcc-FePt (Kim et al. 2010). Xu et al. have reported a facile one-step room-temperature procedure for Pt_3Ni bimetallic alloy with unique electrocatalytic properties (Xu et al. 2012).

1.2.2 Bimetallic Nanoparticles (Core-Shell)

In core-shell bimetallic nanoparticles, the first inner core is nucleated with one metal which followed by the formation of the shell using another metal, it forms a thin homogenous layer. Noble or transition metals are dimensionally stable therefore commonly used for core in the bimetallic catalyst. Core-shell bimetals retain control morphology and composition (Liu et al. 2012). Bimetallic nanomaterials with core-

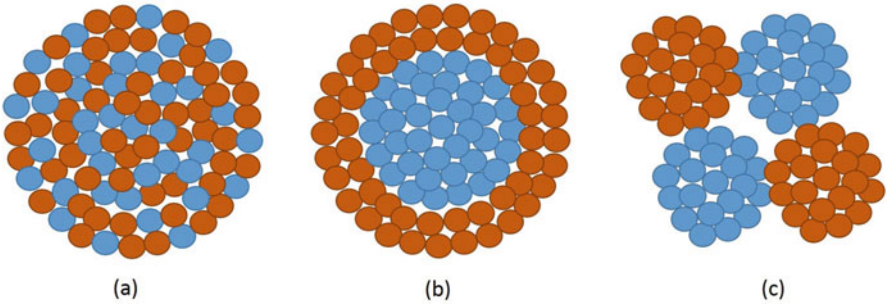

Fig. 40.1 Bimetallic nanoparticles structures: (**a**) alloyed, (**b**) core-shelled, and (**c**) heterogeneous

shell structure are electrocatalysts in nature; researchers use noble metals with cheap other materials.

Recently, the redox-transmetalation method has been used widely for the synthesis of core–shell-type bimetallic nanomaterials (Park et al. 2004). For this, the first core is synthesized by reducing metal ions then the second metal precursor is added to form a shell. Redox transmetalation is the process where metal salt comes in contact with the core surface and gets reduced via the surface atom of the core metal.

1.2.3 Bimetallic Nanoparticles (Heterostructured)

In heterostructured bimetallic nanocatalysts, both metals create nuclei and grow separately at the mixed interface; individual nucleation happens because of the unique reduction potential of each metal. Figure 40.1c depicted a seed-mediated route for the formation of heterostructured bimetallic nanocatalysts. The morphology of heterostructured bimetallic nanocatalysts determined by the growth of the second metal would be either island or layered. Various factors, including associated constant, matching, or mismatching of lattice structures surface-interface energy correlations affect the morphology of heterostructured bimetal (Zeng et al. 2012).

2 Properties and Synthesis of Bimetallic Nanocatalyst

2.1 Properties

The combination of two different metals to form bimetallic nanoparticles is gaining interest in various applications compared to monometallic nanoparticles. This is because of their unique size and shape-dependent catalytic, thermal, electronic, and optical effects (Sharma et al. 2019; Rajeev et al. 2021). In biosensing applications, the most common advantage of bimetallic over monometallic nanoparticles includes: enhanced sensitivity, specificity, stability, and biocompatibility (Fig. 40.2). The properties of bimetallic nanoparticles are mostly influenced by the size, shape, composition, and degree of agglomeration. These factors can be controlled by the method of synthesis. During the synthesis of bimetallic nanoparticles, the mixing of the two metal ions results in the introduction of an extra degree of freedom (Sharma et al. 2019; Rajeev et al. 2021). This leads to the formation of a

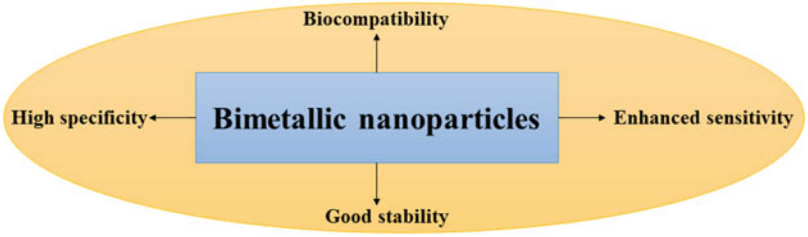

Fig. 40.2 Advantages of bimetallic nanoparticles in diagnostic tools

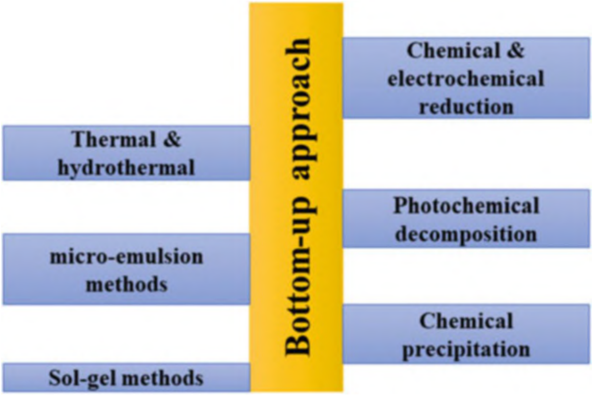

Fig. 40.3 Common methods for synthesis of bimetallic nanoparticles using bottom-up approach

new metal-metal bond length. Nanoparticles can be synthesized by both the top-down approach (physical methods) and the bottom-up approach (chemical approach). The top-down approach revolves around the breaking down of bulk material to required sizes (Loza et al. 2020). This is normally done by lithographic processes such as grinding, sputtering, laser ablation, and dealloying (Park et al. 2017; Loza et al. 2020; Stephanie et al. 2021). One of the main advantages of this method is the absence of solvent contamination in the prepared nanoparticles. The top-down approach is not frequently used because of some disadvantages such as the high level of contamination and challenges with controlling the morphology and size of the nanoparticles. In the bottom-up approach, the required structures are formed molecule by molecule or atom by atom through supermolecular or covalent interactions (Iqbal et al. 2012). The frequently used methods for the synthesis of bimetallic nanoparticles include; chemical and electrochemical reduction, hydrothermal, thermal, and photochemical decomposition, sol-gel, chemical precipitation, and micro-emulsion methods (Sharma et al. 2019; Loza et al. 2020; Scaria et al. 2020). Some of these methods are explained in Fig. 40.3.

2.2 Chemical and Electrochemical Reduction

This method involves the reduction of metal ions with various reducing agents to form zero-valent state monometallic or bimetallic nanoparticles. This method is cost-effective, easy to set up, and allows for the toiling of nanoparticles to the desired morphology (Wang et al. 2011; An and Somorjai 2015). The size and shape of the nanoparticles can be controlled by changing various experimental parameters such as the concentration of the reducing and capping agent, temperature, and time. The main disadvantages of this method is the formation of aggregated nanoparticles. This normally occurs when lower reduction metals and light transition metal precursors are used (Rajeev et al. 2021). To solve this challenge, capping molecules such as glucose and ascorbic acid are used during the synthesis process. Although significant progress has been made in improving this method, controlling the experimental parameters for the desired morphology remains a challenge.

In electrochemical reduction, the metal ions are reduced on the surface of the electrode using electricity. This method is cost-effective and produces nanoparticles with high purity. Capping molecules are used to stabilize the nanoparticles. The size, shape, density, and composition of the bimetallic nanoparticles can be controlled by varying several experimental parameters such as current, potential, electrolyte, electrode material, and precursor concentration.

2.3 Micro-emulsion and Thermal Decomposition Methods

Micro-emulsion is a solution that is made up of at least three different components (polar component, non-polar component, and surfactants). The polar and non-polar components in the solution are separated by a layer that is formed by the surfactants. Although this method offers some advantages such as the ability to control the size by varying the oil-water ratio. It is not commonly used because of the complexity involved in the reaction. The thermal decomposition method for the preparation of bimetallic nanoparticles can be defined as an endothermic reaction that involves the use of high temperatures to break and form new bonds. In this method, the size and morphology of bimetallic nanoparticles are influenced by several factors such as capping agent concentration, temperature, metal precursor ratio, and reaction time.

3 Application of Bimetallic Nanocatalyst in Bioelectrochemical Detection and Diagnosis

Biosensors are conventionally fabricated by employing various types of recognition elements such as nucleic acids, receptors, microbes, organelles, tissues, cells, organisms, enzymes, and membranes. These sensors are modified to obtain desired properties to achieve high precision to detect the target analyte by using the natural affinity of recognition element toward the analyte, for example, monoclonal antibodies (Sharma et al. 2016; Morales and Halpern 2018).

The involvement of an electrocatalyst in the biosensors helps in the facilitation of the electron transfer between the reactants and the electrode surface. Further, the electrocatalyst may also aid in the chemical reaction occurring between the electrode-analyte, resulting in an increase or decrease in the rate of electrochemical reaction. Electrocatalyst can be coated over the electrode surface or can itself be the electrode surface. These can be homogenous or heterogeneous such as an enzyme or composite nanoparticles.

The evolution of the design of the biosensor can be divided into three generations (Putzbach and Ronkainen 2013). The first generation involved the use of enzymes catalyzed reaction to achieve a chemical reaction at the electrode surface, which would trigger an electron transfer. The biosensors of the second generation involved mostly single-use testing systems. These used an additional electron mediator, which produced an improved output response. This generation uses the rate of flow of electrons toward the electrode surface from the analyte. These improve the performance of the sensor by removing the dependence of an additional reaction occurring in First-generation biosensors at the electrode surface. The third generation attempts to immobilize both enzyme and mediator on the electrode surface, which makes the biorecognition element an essential part of the biosensor structure. This method directly joins the enzyme and electrode removing the need for mediator or diffusion involvement, further, the incorporation of catalytic structures increases the electron transfer rate. This leads to improved sensing response and work is being done for the commercialization of these devices.

3.1 Biosensors Based on Target Analyte

3.1.1 Hydrogen Peroxide Sensing: Combined H_2O_2 and Glucose Sensing

Detection of H_2O_2 has become essential due to its wide range of applications in industrial, healthcare, and anti-terror activities. H_2O_2 holds high importance in the clinical field to determine various important metabolites like uric acid and glucose. Due to the production of H_2O_2 from the enzymatic decomposition of urea or glucose, it needed to be addressed and it cannot be detected via fluorescence. Hence, the development of a sensitive approach for the detection of H_2O_2 without any interference of external electroactive agents is still a challenge. Here we focus on sensors for H_2O_2 using bimetallic catalysts, Table 40.1 shows the bimetallic structures used for sensing of H_2O_2 with their respective sensitivities and limit of detections.

The work carried out by the researchers consisted of the various bimetallic element as an active catalytic element. A schematic representation of sensors and biosensors based on bimetallic catalyst shown in Fig. 40.4. Initial works were mostly based on gold (Au) being used in combination with other elements like silver (Ag) and platinum (Pt). Yu et al. and Che et al. synthesized Au/Pt bimetallic catalyst supported on alloyed nanoparticles and DNA-L-cysteine-polypyrrole on modified glassy carbon electrode respectively (Che et al. 2009; Yu et al. 2011b). These studies concluded that the intrinsic catalytic active nature of Au/Pt nanoparticles facilitated electron transfer and a facile method for the fabrication of a highly effective biosensor. Finally, non-enzymatic and mediator-free sensors have been fabricated using the same approach using Pt and carbon in different forms to produce the catalytic material for the effective detection of H_2O_2 (Chen et al. 2012b; Janyasupab et al. 2013; Lu et al. 2013; Chang et al. 2014; Kung et al. 2014; Li et al. 2015b).

3.1.2 Glucose Sensing: Combined H_2O_2 and Glucose Sensing

Diabetes is an increasingly concerning problem around the world. Due to which the effective and rapid detection of blood glucose levels has become necessary. Various glucose sensors have been fabricated using numerous methods involving enzymatic and catalytic routes. Here we will cover the methods utilizing bimetallic

Table 40.1 Bimetals and their composites with other materials used for H_2O_2 sensing

S. No.	Bimetals	Composites	Limit of Detection (LOD)	Reference
1	Pt/Au	Pt/Au bimetals nanoparticles with graphene-carbon nanotube (PtAu/G-CNTs) hybrid	–	(Lu et al. 2013)
2	Pt/Ru	Pt/Ru @ three-dimensional graphene foam (PtRu/3D GF)	0.04 μM	(Kung et al. 2014)
3	Au/Pt	Bimetals (Au/Pt) on chitosan-room temperature ionic liquid (Chi/RTIL) layer	60 nM	(Yu et al. 2011b)
4	Au/Pt	Au@Pt@Au core-shell on graphene oxide sheets	0.02 μM	(Li et al. 2015b)
5	Au/Pt	Au/Pt @ polypyrrole-L-cysteine	1.3 μM	(Che et al. 2009)
6	Pt/Ir	Composite with carbon black (VulcanXC-72R)	–	(Chang et al. 2014)
7	Au/Ag	AuAg@ nafion film (1-butyl-3-methylimidazoliumte trifluoroborate)	–	(Tsai et al. 2010)
8	Pt/Pd	PtPd /MWCNT bimetal nanocatalyst	1.2 μM	(Chen et al. 2012b)
9	Pt/Cu Pt/Ni Pt/Pd Pt/Rh	Bimetal nanoparticles composites with carbon black VulcanXC-72R	PtCu/C = 12.2 μM, PtNi/C = 31.5 μM, PtPd/C = 114.0 μM, PtRh/C = 34.8 μM.	(Janyasupab et al. 2013)

nanoparticles for the fabrication of glucose sensors. Various bimetallic nanocomposites have been employed to detect glucose listed in Table 40.2.

Yang et al. (2011) have reported facile method with rapid and environmental-friendly approach to electrochemically deposit graphene oxide/gold-palladium nanoparticles on the working electrode in a controlled environment and reduce the novel composite via potentiostatic route. Electrodeposition was carried out by ultrasonicator to make a non-enzymatic sensor using alloyed nanoparticles like PtRu, PtPd, and PtAu on MWCNTs ionic liquids (Xiao et al. 2009). These non-enzymatic electrochemical sensors provided highly selective detection without any interference from major interfering species. MWCNTs lead to higher sensitivity toward the analyte by providing high peak currents. The bimetallic nanoparticles with Pt are the once which are exploited the most but recent advances have used other combinations of metals as well. The literature on the sensor research does provide the details construction and analytical data in details but however lacks the reason for the choice of nanomaterial for detection of a particular analyte.

Additionally, another non-enzymatic glucose sensor using peroxide via amperometric response employed Pt-Pd composite (Niu et al. 2012). This nanocomposite

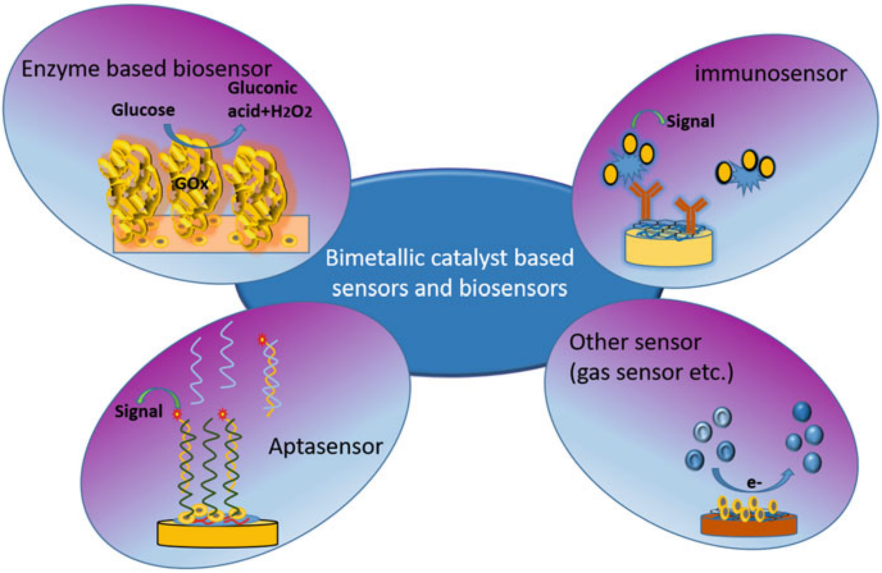
Enzyme based biosensor
Glucose
Gluconic acid+H2O2
GOx
immunosensor
Signal
Bimetallic catalyst based sensors and biosensors
Signal
Aptasensor
Other sensor (gas sensor etc.)
e-

Fig. 40.4 Schematic illustration of bimetallic catalyst-based biosensors

deposited easily reduced peroxide in neutral pH and also increased electrocatalytic activity as compared to individual metal nanoparticles.

3.1.3 Uric Acid and Cholesterol Sensing

Yan et al. (2013) employed a Pt/Pd-reduced graphene oxide nanocomposite which were reduced via electrochemical route and deposited on the electrode. This provided a sensing platform to simultaneously detect AA, dopamine, and UA via differential pulse voltammetry method. Finally, the practical applicability of the sensor was tested in by carrying out the quantitative analysis in serum and urine samples.

TGPHs (TiO_2-graphene-Pt-Pd hybrid nanocomposites) led to better electron transport to the transducer element which increasing the effective surface area of the sensor (Cao et al. 2013b). Further, gold nanoparticles and cholesterol oxidase were deposited over the TGPHs to carry out cholesterol sensor. The sensor was tested with meat, fish oil, and eggs and provided an effective tool for detection of cholesterol in food products. Finally, Table 40.3 provides the bimetallic nanoparticles employed for cholesterol and uric acid sensing.

3.1.4 Carcinoembryonic Antigen (CEA)

CEA helps in adhesions of cells and hold them together. It is a type of glycoprotein found in gastrointestinal tissue when the fetus is developing inside the uterus. This stop once the baby is fully formed and about to be born.

Table 40.2 Bimetals and their composites with other materials used for glucose sensing

S. No.	Metals	Composites	Limit of Detection (LOD)	Reference
1	Pt/Au	Bimetallic nanoparticles @ single-stranded DNA-graphene nanocomposites	0.3 μM	(Leng et al. 2014)
2	Cu/Ag	Cu/Ag nanocomposite at three-dimensional Ni foam	0.08 μM	(Li et al. 2015a)
3	Au/Ag	Bimetallic Au-Ag heterogeneous nanorods	25 μM	(Han et al. 2015a)
4	Au/Pd	Au/Pd (1:1) @ reduced graphene nanosheet	6.9 μM	(Yang et al. 2011)
5	Pt/Te	Pt electrode–Te microtubes (Pt/Te-MTs)	0.1 mM	(Guascito et al. 2012)
6	Cu/Au	Cu/Au nanotubes	2 μM	(Tee et al. 2015)
7	Au/Cu	Bimetal intermetallic Au/Cu nanowire.	–	(Kim et al. 2015)
8	Pt/Ni	Pt/NiNP chemically reduced GO nanocomposites	35 mM	(Gao et al. 2011)
9	Pt/Pd	Bimetals Pt/Pd @ multi-walled carbon nanotubes (MWCNTs)	0.031 mM	(Chen et al. 2012a)
10	Ag/Ni	Bimetallic Ag/Ni alloys @ GCE	0.49 μM	(Miao et al. 2013)
11	Pd/Pt	Pd/PtNPs decorated @ reduced graphene oxide	–	(Hossain and Park 2015)
12	Pt/M Where M = Ru, Sn	Pt-M@PVP-MWCNT	0.7 mM and 0.3 mM respectively	(Kwon et al. 2012)
13	Pt/Pd	Mesoporous carbon vesicles	0.12 mM	(Bo et al. 2011)
14	Au/Pt	Inorganic-organic hybrid nanocomposite of Au/Pt-Ni (II)–pyromellitic acid @ CNTs	55 nM	(Gholivand and Azadbakht 2012)
15	Cu/Au	Copper atom @ AuNps	50 nM	(Shi et al. 2011)
16	Cu/Au	Cu/Au bimetal	0.8 pM	(Casella et al. 1997)
17	Cu/Ni	Dendritic Cu-Ni bimetallic composite self-assembled @titanate film.	0.35 μM	(Tong et al. 2010)
18	Pt/Pd	Nanocluster of Pt-Pd-like snowflake @ gold screen-printed electrode (Au-SPE)	10 mM	(Niu et al. 2012)
19	Au/Pd	3D flower-shaped Au-Pd core-shell nanoparticles @ionic liquid	1.0 nM	(Chen et al. 2010)
20	Au/Ag	Au@Ag heterogeneous nanorods	39 μM	(Han et al. 2015b)
21	Pt/Ru, Pt/Pd, Pt/Au	Bimetallic nano Pt composite decorated on MWCNT ionic liquid composite layer	0.05 mM	(Xiao et al. 2009)

Table 40.3 Bimetals and their composites used to detect uric acid and cholesterol

S. no.	Analyte detected	Bimetals	Bimetals and composites	Limit of Detection (LOD)	Reference
1	Cholesterol	Pt/Pd	Pt-Pd/chitosan/GO nanocomposite	0.75 μM	(Cao et al. 2013)
2	Uric acid	Pd/Pt	Pd-Pt poly (diallyldimethylammonium chloride)-reduced GO	0.10 μM	(Yan et al. 2013)
3	Cholesterol	Pt/Pd	Pt-Pd/TiO_2–graphene nanocomposite	0.017 μM	(Cao et al. 2013)
4	Uric acid	Pt/Au	Pt-Au nanoparticles on nafion with functionalized MWCNTs	–	(Umasankar et al. 2007)
5	Cholesterol	Au/Pt	AuPt/chitosan/ionic liquid nanocomposite	10 μM	(Safavi and Farjami 2011)

Table 40.4 Bimetals and their composites used for carcinoembryonic antigen (CEA) detection

S. No.	Bimetals	composites	Limit of detection (LOD)	Reference
1	Au/Pt	Au/Pt nanochains	0.11 pg/ mL	(Cao et al. 2013c)
2	Au/Ag	Au/Ag core-shell nanoparticles @ 4 mercaptobenzoic acid	5 pg/mL	(Chen et al. 2013)

The first sensor (Cao et al. 2013c) employed bimetallic nanostructures for sandwich type of electrochemical sensing platform. This opened up a next-generation immunosensing platforms for making next generation of sensors using different methods. Table 40.4 summarizes the different bimetallic nanoparticles used for CEA.

3.1.5 Long Non-coding RNA, Human Tissue Polypeptide Antigen, Cancer Antigen 125, CCRF-CEM Cells, Carbohydrate Antigen 19-9, Cardiac Troponin I

These diseases use immune complexation method to carry out detection of the respective biomarkers. However, they employ bimetallic nanoparticles to enhance the output response of the system. Researchers have employed different nanoparticles like Re-Au, Au-Pd, and Pd-Pt to achieve the desired results (Yang et al. 2015; Wang et al. 2014; Cai et al. 2011).

For example, Pd-Pt nanoparticles were used by (Liu et al. 2015) to carry out detection of hepatocellular carcinoma by attaching relevant RNA sequence to the nanoparticles. Another approach involved bimetallic Cu-Au functionalized with highly selective aptamers to carry out detection of CCRT-CEM cells (Ye et al. 2015).

Another nanosensor employed Pt-Pd to detect long non-coding RNA which is known to regulate the levels of HCC (hepatocellular carcinoma) in body was detected by Liu et al. Another approach by Ye et al. utilized a bimetallic nanoparticle system consisting of Au for the detection of malignant disease. This was done to make an iodide-responsive colorimetric platform with nanomaterials, which compromised Cu-Au nanoparticle probe functionalized with aptamers probe to detect CCRF-CEM cells for human leukemia. Finally, Table 40.5 covers the bimetallic nanoparticles that have been employed to carry out the detection of various diseases mentioned above.

3.1.6 Glutamate and Dopamine

Yu et al. (2011a) have focused toward glutamate sensor using ionic liquid based substrate with electrochemically deposited Au-Pt nanoparticles. This was utilized to measure glutamate using glutamate oxidase as the biorecognition element immobilized on the bimetallic nanoparticles. Finally, the prepared electrode performed very well with high sensitivity and reproducible results toward glutamate detection at ~200 mV.

In case of dopamine detection Huang et al. (2014) employed Pt-Ag bimetallic nanocomposite which are decorated over nanoporous carbon fibers over GCE. The

Table 40.5 Bimetals and their composites for miscellaneous analytes detection

S. No.	Analyte detected	Bimetals	Composites	Limit of detection (LOD)	Reference
1	Dopamine	Ag/Pt	Ag/Pt decorated on electrospun nanoporous carbon fiber (pCNF)	0.11 μM	(Huang et al. 2014)
2	Glutamate (Glu)	Au/Pt	Au/Pt @ hydroxyl functionalized ionic liquid $[C_3(OH)_2$ mim] $[BF_4]$ -Nafion composite	0.17 μM	(Yu et al. 2011a)
3	Highly upregulated liver cancer non-coding RNA	Pt/Pd	Pt-Pd nanodendrites/GO/Au	0.247 $fMmL^{-1}$	(Liu et al. 2015)
4	Cancer antigen (CA)-125	Re/Au	Re/Au nanoparticle-CA125Ab-immunocomplex catalysis with Te(VI)-Sn(II)	0.02 mU/ml	(Cai et al. 2011)
5	Cardiac troponin I (CTnI)	Pt/Au	Pt/Au nanoparticles @ AuNP-modified Ru $(phen)_3^{2+}$-doped SiO_2 nanoparticles	3.3 $pg.mL^{-1}$	(Xiao et al. 2014)
6	Human tissue polypeptide antigen (hTPA)	Pd/Pt	Pd/Pt bimetal nanocatalyst used as label for secondary antibody	1.2 pg/mL	(Wang et al. 2014)
7	Human acute lymphoblastic leukemia (T cell line)	Cu/Au	Cu-Au bimetals iodide catalyst composite	5 cells/100 μL buffer	(Ye et al. 2015)
8	CA19-9 (carbohydrate antigen)	Au/Pd	Au/Pd core-shell-GO composite @Au-porous graphene	0.006 U/ml	(Yang et al. 2015)

prepared electrode was highly sensitive toward dopamine as the analyte, even in presence of ascorbic acid and uric acid.

4 Conclusion and Future Perspectives

The application of bimetallic nanoparticles in diagnostic tools such as electrochemical biosensors and chemical sensors is increasing. This is due to the unique properties such as size and morphology-dependent catalytic, thermal, electronic, and optical effects. Bimetallic nanoparticles enhance the sensitivity, selectivity, stability, and reproducibility of electrochemical sensors compared to monometallic nanoparticles. In this chapter, the properties of bimetallic and various synthesis methods were covered, in addition to their applications in chemical and biosensors. More work still needs to be done to synthesize different bimetallic nanoparticles; this will increase their application scope.

References

Alonso DM, Wettstein SG, Dumesic JA (2012) Bimetallic catalysts for upgrading of biomass to fuels and chemicals. Chem Soc Rev 41(24):8075–8098

An K, Somorjai GA (2015) Nanocatalysis I: synthesis of metal and bimetallic nanoparticles and porous oxides and their catalytic reaction studies. Catal Lett 145(1):233–248

Bo X, Bai J, Yang L, Guo L (2011) The nanocomposite of PtPd nanoparticles/onion-like mesoporous carbon vesicle for nonenzymatic amperometric sensing of glucose. Sensors Actuators B Chem 157(2):662–668

Cai W, Liang A, Liu Q, Liao X, Jiang Z, Shang G (2011) Catalytic effect of ReAu nanoalloy on the Te particle reaction and its application to resonance scattering spectral assay of CA125. Luminescence 26(5):305–312

Cao S, Zhang L, Chai Y, Yuan R (2013a) Electrochemistry of cholesterol biosensor based on a novel Pt-Pd bimetallic nanoparticle decorated graphene catalyst. Talanta 109:167–172

Cao S, Zhang L, Chai Y, Yuan R (2013b) An integrated sensing system for detection of cholesterol based on TiO_2-graphene-Pt-Pd hybrid nanocomposites. Biosens Bioelectron 42:532–538

Cao X, Wang N, Jia S, Guo L, Li K (2013c) Bimetallic AuPt nanochains: synthesis and their application in electrochemical immunosensor for the detection of carcinoembryonic antigen. Biosens Bioelectron 39(1):226–230

Casella IG, Gatta M, Guascito MR, Cataldi TRI (1997) Highly-dispersed copper microparticles on the active gold substrate as an amperometric sensor for glucose. Anal Chim Acta 357(1):63–71

Chang S-H, Yeh M-H, Rick J, Su W-N, Liu D-G, Lee J-F, Liu C-C, Hwang B-J (2014) Bimetallic catalyst of PtIr nanoparticles with high electrocatalytic ability for hydrogen peroxide oxidation. Sensors Actuators B Chem 190:55–60

Chantry RL, Atanasov I, Siriwatcharapiboon W, Khanal BP, Zubarev ER, Horswell SL, Johnston RL, Li ZY (2013) An atomistic view of the interfacial structures of AuRh and AuPd nanorods. Nanoscale 5(16):7452–7457

Che X, Yuan R, Chai Y, Ma L, Li W, Li J (2009) Hydrogen peroxide sensor based on horseradish peroxidase immobilized on an electrode modified with DNA-L-cysteine-gold-platinum nanoparticles in polypyrrole film. Microchim Acta 167(3-4):159–165

Chen X, Pan H, Liu H, Du M (2010) Nonenzymatic glucose sensor based on flower-shaped Au@Pd core–shell nanoparticles–ionic liquids composite film modified glassy carbon electrodes. Electrochim Acta 56(2):636–643

Chen K-J, Lee C-F, Rick J, Wang S-H, Liu C-C, Hwang B-J (2012a) Fabrication and application of amperometric glucose biosensor based on a novel PtPd bimetallic nanoparticle decorated multi-walled carbon nanotube catalyst. Biosens Bioelectron 33(1):75–81

Chen KJ, Chandrasekara Pillai K, Rick J, Pan CJ, Wang SH, Liu CC, Hwang BJ (2012b) Bimetallic PtM (M=Pd, Ir) nanoparticle decorated multi-walled carbon nanotube enzyme-free, mediator-less amperometric sensor for H_2O_2. Biosens Bioelectron 33(1):120–127

Chen G, Chen Y, Zheng X, He C, Lu J, Feng S, Chen R, Zeng H (2013) Surface-enhanced Raman scattering study of carcinoembryonic antigen in serum from patients with colorectal cancers. Appl Phys B 113(4):597–602

Cho I-H, Kim DH, Park S (2020) Electrochemical biosensors: perspective on functional nanomaterials for on-site analysis. Biomater Res 24(1):6

Ferrando R, Jellinek J, Johnston RL (2008) Nanoalloys: from theory to applications of alloy clusters and nanoparticles. Chem Rev 108(3):845–910

Gao H, Xiao F, Ching CB, Duan H (2011) One-step electrochemical synthesis of PtNi nanoparticle-graphene nanocomposites for nonenzymatic amperometric glucose detection. ACS Appl Mater Interfaces 3(8):3049–3057

Gholivand MB, Azadbakht A (2012) Fabrication of a highly sensitive glucose electrochemical sensor based on immobilization of Ni(II)–pyromellitic acid and bimetallic Au–Pt inorganic–organic hybrid nanocomposite onto carbon nanotube modified glassy carbon electrode. Electrochim Acta 76:300–311

Gilroy KD, Ruditskiy A, Peng H-C, Qin D, Xia Y (2016) Bimetallic nanocrystals: syntheses, properties, and applications. Chem Rev 116(18):10414–10472

Guascito MR, Chirizzi D, Malitesta C, Siciliano M, Siciliano T, Tepore A (2012) Amperometric non-enzymatic bimetallic glucose sensor based on platinum tellurium microtubes modified electrode. Electrochem Commun 22:45–48

Han L, Li C, Zhang T, Lang Q, Liu A (2015a) Au@Ag heterogeneous nanorods as nanozyme interfaces with peroxidase-like activity and their application for one-pot analysis of glucose at nearly neutral pH. ACS Appl Mater Interfaces 7(26):14463–14470

Han T, Zhang Y, Xu J, Dong J, Liu C-C (2015b) Monodisperse AuM (M=Pd, Rh, Pt) bimetallic nanocrystals for enhanced electrochemical detection of H_2O_2. Sensors Actuators B Chem 207: 404–412

Hossain MF, Park JY (2014) Amperometric glucose biosensor based on Pt-Pd nanoparticles supported by reduced graphene oxide and integrated with glucose oxidase. Electroanalysis 26(5):940–951

Hossain MF, Park JY (2015) An enzymatic hybrid electrode platform based on chemically modified reduced graphene oxide decorated with palladium and platinum alloy nanoparticles for biosensing applications. J Electrochem Soc 162(7):B185–B192

Huang Y, Miao YE, Ji S, Tjiu WW, Liu T (2014) Electrospun carbon nanofibers decorated with Ag-Pt bimetallic nanoparticles for selective detection of dopamine. ACS Appl Mater Interfaces 6(15):12449–12456

Iqbal P, Preece JA, Mendes PM (2012) Nanotechnology: the “top-down” and “bottom-up” approaches. In: Supramolecular chemistry. Wiley, Chichester

Janyasupab M, Liu C-W, Zhang Y, Wang K-W, Liu C-C (2013) Bimetallic Pt–M (M=Cu, Ni, Pd, and Rh) nanoporous for H_2O_2 based amperometric biosensors. Sensors Actuators B Chem 179: 209–214

Kim J, Lee Y, Sun S (2010) Structurally ordered FePt nanoparticles and their enhanced catalysis for oxygen reduction reaction. J Am Chem Soc 132(14):4996–4997

Kim S-I, Eom G, Kang M, Kang T, Lee H, Hwang A, Yang H, Kim B (2015) Composition-selective fabrication of ordered intermetallic Au-Cu nanowires and their application to nano-size electrochemical glucose detection. Nanotechnology 26(24):245702

Kung C-C, Lin P-Y, Buse FJ, Xue Y, Yu X, Dai L, Liu C-C (2014) Preparation and characterization of three dimensional graphene foam supported platinum-ruthenium bimetallic nanocatalysts for hydrogen peroxide based electrochemical biosensors. Biosens Bioelectron 52:1–7

Kwon S-Y, Kwen H-D, Choi S-H (2012) Fabrication of nonenzymatic glucose sensors based on multiwalled carbon nanotubes with bimetallic Pt-M (M = Ru and Sn) catalysts by radiolytic deposition. J Sensors 2012:784167

Leng J, Wang W-M, Lu L-M, Bai L, Qiu X-L (2014) DNA-templated synthesis of PtAu bimetallic nanoparticle/graphene nanocomposites and their application in glucose biosensor. Nanoscale Res Lett 9(1):99

Li H, Guo CY, Xu CL (2015a) A highly sensitive non-enzymatic glucose sensor based on bimetallic Cu-Ag superstructures. Biosens Bioelectron 63:339–346

Li X, Liu Y, Hemminger JC, Penner RM (2015b) Catalytically activated Palladium@Platinum nanowires for accelerated hydrogen gas detection. ACS Nano 9(3):3215–3225

Li X-R, Xu M-C, Chen H-Y, Xu J-J (2015c) Bimetallic Au@Pt@Au core–shell nanoparticles on graphene oxide nanosheets for high-performance H2O2 bi-directional sensing. J Mater Chem B 3(21):4355–4362

Li G, Zhang W, Luo N, Xue Z, Hu Q, Zeng W, Xu J (2021) Bimetallic nanocrystals: structure, controllable synthesis and applications in catalysis, energy and sensing. Nanomaterials 11(8):1926

Liu X, Wang D, Li Y (2012) Synthesis and catalytic properties of bimetallic nanomaterials with various architectures. Nano Today 7(5):448–466

Liu F, Xiang G, Jiang D, Zhang L, Chen X, Liu L, Luo F, Li Y, Liu C, Pu X (2015) Ultrasensitive strategy based on PtPd nanodendrite/nano-flower-like@GO signal amplification for the detection of long non-coding RNA. Biosens Bioelectron 74:214–221

Loza K, Heggen M, Epple M (2020) Synthesis, structure, properties, and applications of bimetallic nanoparticles of noble metals. Adv Funct Mater 30(21):1909260

Lu D, Zhang Y, Lin S, Wang L, Wang C (2013) Synthesis of PtAu bimetallic nanoparticles on graphene-carbon nanotube hybrid nanomaterials for nonenzymatic hydrogen peroxide sensor. Talanta 112:111–116

Mariscal MM, Mayoral A, Olmos-Asar JA, Magen C, Mejía-Rosales S, Pérez-Tijerina E, José-Yacamán M (2011) Nanoalloying in real time. A high resolution STEM and computer simulation study. Nanoscale 3(12):5013–5019

Miao Y, Wu J, Zhou S, Yang Z, Ouyang R (2013) Synergistic effect of bimetallic Ag and Ni alloys on each other's electrocatalysis to glucose oxidation. J Electrochem Soc 160(4):B47–B53

Morales MA, Halpern JM (2018) Guide to selecting a biorecognition element for biosensors. Bioconjug Chem 29(10):3231–3239

Nantaphol S, Watanabe T, Nomura N, Siangproh W, Chailapakul O, Einaga Y (2017) Bimetallic Pt–Au nanocatalysts electrochemically deposited on boron-doped diamond electrodes for non-enzymatic glucose detection. Biosens Bioelectron 98:76–82

Niu X, Chen C, Zhao H, Chai Y, Lan M (2012) Novel snowflake-like Pt-Pd bimetallic clusters on screen-printed gold nanofilm electrode for H_2O_2 and glucose sensing. Biosens Bioelectron 36(1):262–266

Nørskov JK, Bligaard T, Rossmeisl J, Christensen CH (2009) Towards the computational design of solid catalysts. Nat Chem 1(1):37–46

Notar Francesco I, Fontaine-Vive F, Antoniotti S (2014) Synergy in the catalytic activity of bimetallic nanoparticles and new synthetic methods for the preparation of fine chemicals. ChemCatChem 6(10):2784–2791

Park J-I, Kim MG, Jun Y-W, Lee JS, Lee W-R, Cheon J (2004) Characterization of superparamagnetic "Core−Shell" nanoparticles and monitoring their anisotropic phase transition to ferromagnetic "solid solution" nanoalloys. J Am Chem Soc 126(29):9072–9078

Park H, Reddy DA, Kim Y, Lee S, Ma R, Lim M, Kim TK (2017) Hydrogenation of 4-nitrophenol to 4-aminophenol at room temperature: boosting palladium nanocrystals efficiency by coupling with copper via liquid phase pulsed laser ablation. Appl Surf Sci 401:314–322

Peng L, Ringe E, Van Duyne RP, Marks LD (2015) Segregation in bimetallic nanoparticles. Phys Chem Chem Phys 17(42):27940–27951

Picone A, Riva M, Brambilla A, Calloni A, Bussetti G, Finazzi M, Ciccacci F, Duo L (2016) Reactive metal–oxide interfaces: a microscopic view. Surf Sci Rep 71(1):32–76

Putzbach W, Ronkainen NJ (2013) Immobilization techniques in the fabrication of nanomaterial-based electrochemical biosensors: a review. Sensors (Basel) 13(4):4811–4840

Rajeev R, Datta R, Varghese A, Sudhakar YN, George L (2021) Recent advances in bimetallic based nanostructures: synthesis and electrochemical sensing applications. Microchem J 163:105910

Safavi A, Farjami F (2011) Electrodeposition of gold-platinum alloy nanoparticles on ionic liquid-chitosan composite film and its application in fabricating an amperometric cholesterol biosensor. Biosens Bioelectron 26(5):2547–2552

Scaria J, Nidheesh PV, Kumar MS (2020) Synthesis and applications of various bimetallic nanomaterials in water and wastewater treatment. J Environ Manag 259:110011

Schmid G (2011) Nanoparticles: from theory to application. Wiley, Strauss GmbH, Morlenbach, Germany

Sharma S, Byrne H, O'Kennedy RJ (2016) Antibodies and antibody-derived analytical biosensors. Essays Biochem 60(1):9–18

Sharma G, Kumar A, Sharma S, Naushad M, Prakash Dwivedi R, Alothman ZA, Mola GT (2019) Novel development of nanoparticles to bimetallic nanoparticles and their composites: a review. J King Saud Univ – Sci 31(2):257–269

Shi H, Zhang Z, Wang Y, Zhu Q, Song W (2011) Bimetallic nano-structured glucose sensing electrode composed of copper atoms deposited on gold nanoparticles. Microchim Acta 173: 85–94

Sinfelt JH (1977) Heterogeneous catalysis: some recent developments. Science 195(4279):641–646

Stephanie R, Kim MW, Kim SH, Kim J-K, Park CY, Park TJ (2021) Recent advances of bimetallic nanomaterials and its nanocomposites for biosensing applications. TrAC Trends Anal Chem 135:116159

Sun X, Guo S, Liu Y, Sun S (2012) Dumbbell-like PtPd-Fe_3O_4 nanoparticles for enhanced electrochemical detection of H_2O_2. Nano Lett 12(9):4859–4863

Tee SY, Ye E, Pan PH, Lee CJJ, Hui HK, Zhang S-Y, Koh LD, Dong Z, Han M-Y (2015) Fabrication of bimetallic Cu/Au nanotubes and their sensitive, selective, reproducible and reusable electrochemical sensing of glucose. Nanoscale 7(25):11190–11198

Tong S, Xu Y, Zhang Z, Song W (2010) Dendritic bimetallic nanostructures supported on self-assembled titanate films for sensor application. J Phys Chem C 114(49):20925–20931

Tsai T, Thiagarajan S, Chen S (2010) Green synthesized Au Ag bimetallic nanoparticles modified electrodes for the amperometric detection of hydrogen peroxide. J Appl Electrochem 40: 2071–2076

Umasankar Y, Thiagarajan S, Chen SM (2007) Nanocomposite of functionalized multiwall carbon nanotubes with nafion, nano platinum, and nano gold biosensing film for simultaneous determination of ascorbic acid, epinephrine, and uric acid. Anal Biochem 365(1):122–131

Wang L, Nemoto Y, Yamauchi Y (2011) Direct synthesis of spatially-controlled Pt-on-Pd bimetallic nanodendrites with superior electrocatalytic activity. J Am Chem Soc 133(25):9674–9677

Wang Y, Wei Q, Zhang Y, Wu D, Ma H, Guo A, Du B (2014) A sandwich-type immunosensor using Pd-Pt nanocrystals as labels for sensitive detection of human tissue polypeptide antigen. Nanotechnology 25(5):055102

Xiao F, Zhao F, Mei D, Mo Z, Zeng B (2009) Nonenzymatic glucose sensor based on ultrasonic-electrodeposition of bimetallic PtM (M=Ru, Pd and Au) nanoparticles on carbon nanotubes-ionic liquid composite film. Biosens Bioelectron 24(12):3481–3486

Xiao L, Chai Y, Wang H, Yuan R (2014) Electrochemiluminescence immunosensor using poly (l-histidine)-protected glucose dehydrogenase on Pt/Au bimetallic nanoparticles to generate an in situ co-reactant. Analyst 139(16):4044–4050

Xu Y, Hou S, Liu Y, Zhang Y, Wang H, Zhang B (2012) Facile one-step room-temperature synthesis of Pt3Ni nanoparticle networks with improved electro-catalytic properties. Chem Commun 48(21):2665–2667

Yan J, Liu S, Zhang Z, He G, Zhou P, Liang H, Tian L, Zhou X, Jiang H (2013) Simultaneous electrochemical detection of ascorbic acid, dopamine and uric acid based on graphene anchored with Pd-Pt nanoparticles. Colloids Surf B Biointerfaces 111:392–397

Yang J, Deng S, Lei J, Ju H, Gunasekaran S (2011) Electrochemical synthesis of reduced graphene sheet-AuPd alloy nanoparticle composites for enzymatic biosensing. Biosens Bioelectron 29(1): 159–166

Yang F, Yang Z, Zhuo Y, Chai Y, Yuan R (2015) Ultrasensitive electrochemical immunosensor for carbohydrate antigen 19-9 using Au/porous graphene nanocomposites as platform and Au@Pd core/shell bimetallic functionalized graphene nanocomposites as signal enhancers. Biosens Bioelectron 66:356–362

Ye X, Shi H, He X, Wang K, He D, Yan L, Xu F, Lei Y, Tang J, Yu Y (2015) Iodide-responsive cu-au nanoparticle-based colorimetric platform for ultrasensitive detection of target cancer cells. Anal Chem 87(14):7141–7147

Yu Y, Liu X, Jiang D, Sun Q, Zhou T, Zhu M, Jin L, Shi G (2011a) [$C_3(OH)_2$mim][BF_4]-Au/Pt biosensor for glutamate sensing in vivo integrated with on-line microdialysis system. Biosens Bioelectron 26(7):3227–3232

Yu Y, Sun Q, Liu X, Wu H, Zhou T, Shi G (2011b) Size-controllable gold-platinum alloy nanoparticles on nine functionalized ionic-liquid surfaces and their application as electrocatalysts for hydrogen peroxide reduction. Chem Eur J 17(40):11314–11323

Zaera F (2013) Nanostructured materials for applications in heterogeneous catalysis. Chem Soc Rev 42(7):2746–2762

Zeng J, Zhu C, Tao J, Jin M, Zhang H, Li ZY, Zhu Y, Xia Y (2012) Controlling the nucleation and growth of silver on palladium nanocubes by manipulating the reaction kinetics. Angew Chem Int Ed Engl 51(10):2354–2358

Zhu C, Yang G, Li H, Du D, Lin Y (2015) Electrochemical sensors and biosensors based on nanomaterials and nanostructures. Anal Chem 87(1):230–249

Всё для победы!
НАРОДНЫЙ
ФРОНТ
https://pobeda.onf.ru/
LET'S HELP THE RUSSIA

Nano-Perovskites Derived Modified Electrodes in Biomolecular Detection

41

Jasmine Thomas and Nygil Thomas

Contents

1 Introduction 900
2 Basic Principles of Electrochemical Biomolecular Detection 901
  2.1 Conventionally Used Electrodes in Sensor Study 901
  2.2 Fundamentals of Electrode Reactions 902
  2.3 Different Techniques Used for Biosensing Study 903
  2.4 Types and Kinetics of Electron Transfer 903
  2.5 Practical Sensing Procedure 904
3 Recent Advances in Sensing of Biomolecules Using Perovskites 905
  3.1 Neurotransmitter (Dopamine) Sensing 905
  3.2 Dopamine and Uric Acid Sensing 910
  3.3 Hydroquinone Sensing 911
  3.4 Glucose Sensing 912
  3.5 Nitrofurantoin Sensing 913
  3.6 Lornoxicam 913
  3.7 Acetaminophen 914
4 Conclusions 914
References 916

Abstract

Metals, metal oxides, spinels, perovskites, carbon based materials, and organic compounds were explored widely for the electrochemical identification and quantification of biomolecules. Over the last few years, perovskite oxides (ABO_3) modified electrodes have picked up momentum due to their excellent catalytic activity, electronic conductivity, and low cost. This chapter discusses the basic principles of electrochemical sensing, electrode reaction, different tech-

---

J. Thomas
St. Joseph's HSS Vayattuparamba, Kannur, Kerala, India

N. Thomas (✉)
Department of Chemistry, Nirmalagiri College, Kannur, Kerala, India

© Springer Nature Singapore Pte Ltd. 2023

U. P. Azad, P. Chandra (eds.), *Handbook of Nanobioelectrochemistry*,
https://doi.org/10.1007/978-981-19-9437-1_41

niques used in sensing study, kinetics of electron transfer, along with sensing of different biomolecules and their limit of detection values using perovskite-modified electrodes. The mechanism and the reaction behind the electrochemical sensing of biomolecules have been discussed in detail. The different perovskites used for sensing of different biomolecules and their limit of detection values are also summarized in table.

Keywords

Perovskite · Biomolecules · Electrodes · Electrochemical sensing

1 Introduction

Electrochemical biomolecule detection has been investigated widely because of their great importance in the early diagnosis of important diseases. The electrochemical responses from the biomolecule during the application of current or potential can be measured and quantified exactly by electrochemical techniques such as cyclic voltametery (CV), differential pulse voltammetry (DPV), square wave voltammetry (SWV), chronoamperometry, etc. Nowadays the development in the device fabrication made electrochemical sensing techniques a popular one. In electrochemical sensor, the recognition element that is the electrocatalyst-coated electrode catalyzes the elecrtrochemical oxidation and reduction of the biomolecule and the output device amplifies and quantifies the signal.

Among the different available sensor materials, perovskite materials are quite new materials in sensor applications. It is a material that has the same crystal structure as the mineral calcium titanium oxide ($CaTiO_3$) (Sasaki et al. 1987). The general notation of such material is ABX_3, here A and B represent cations and X is an anion that forms an octahedron around B ions. In perovskite oxides (ABO_3), B represents the trivalent first row transition element having small radius, A is a trivalent lanthanide or alkaline earth metal having large radius, and O represents the oxygen atom. Here A, B, and O are in the ratio of 1:1:3. In the cubic form, the atoms A, B, and oxygen are located at the body center, cube corner, and face center positions, respectively. Depending upon the A and B site elements and the preparation method some distortions or deformation may happen in the cubic structure and results in rhombohedral, orthorhombic, tetragonal, and hexagonal forms. Three dimensional octahedral corner sharing atomic arrangements are present in perovskite materials, whereas in layered perovskites, the atomic arrangements are observed in such a way that the two-dimensional layers of corner sharing octahedra are separated by cation layers. In perovskite, the charges of A and B atoms should be in the form of $A^{3+}B^{3+}O_3$, $A^{4+}B^{2+}O_3$, and $A^{1+}B^{5+}O_3$ (Atta et al. 2016).

Perovskites have properties like superconductivity, ferroelectricity, ionic conductivity, mixed electronic and ionic conductivity. They also have significant catalytic activity toward different chemical reactions (Deka et al. 2018). The perovskites with Cu in the B site exhibit high temperature superconductivity and is associated with oxygen nonstoichiometry. At the same time, some perovskites ($LaCoO_3$ and $LaMnO_3$) exhibit excellent electronic conductivity comparable to that of metals and it can be improved by A-site doping with different cations. Here, the electronic conductivity is related to the number of mobile charge carriers created during doping. Because of the excellent catalytic activity and stability due to the oxygen activation from oxygen vacancies and high surface activity to oxygen reduction ratio, perovskites are considered as an oxidation-activated catalyst. In addition, perovskites have excellent potential as electrodes material. The existence of different structures due to phase transitions is also one of the reasons for these properties. Among different perovskites, some of them contain localized electrons, delocalized energy-band states, and a transition between these two behaviors. This can be achieved by the incorporation of A or B site ions of various charge and size. Depending upon the size and charge of the A and B site metal ions in perovskites, the electronic properties of these materials become altered. The fine particles of nano-perovskite having large surface-to-volume ratio (Sa/vol) and nano size can be used to fabricate electrodes and thereby reduce the amount of catalyst to minimum (Thomas et al. 2021c).

2 Basic Principles of Electrochemical Biomolecular Detection

The electrochemical sensors consist of the transducer, signal processing, and display unit. Here the transducer is the electrode system and the processing unit is the potentiostat. The analyte we are interested is taken in a specially designed compartment. The working electrode (WE), reference electrode (RE), and counter electrodes (CE) were placed in that compartment. A reaction such as oxidation or reduction happens at the interface of the electrode surface and the bulk analyte. The processing unit converts the information from this reaction into an electrical signal. The potentiostat and the processing unit intensify the signal. The WE is modified with materials that have some special interaction with the analyte molecules. The nano material enhances the electro catalytic activity. The CE is connected to the control amplifier output, which forces current to flow through the electrodes. The potential difference of the WE and the RE and the current between the CE and the WE are monitored using potentiostat. The current is measured using the Higher CR (shunt) or Low CF (current follower) for high and low currents, respectively. The Diffamp (differential amplifier) measures the potential difference between the RE and WE. The input of the control amplifier, E_{in} (digital to analog converter) set the waveform and the corresponding signal is introduced into the summation point (Σ) (Murari et al. 2004).

2.1 Conventionally Used Electrodes in Sensor Study

The conventionally used electrodes in this study are RE, CE, and WEs. The electrode which measures the potential of the WE without the flow of current through it is referred to as RE, and it completes the electrochemical cell. The commonly used REs are standard calomel electrode (SCE), Ag/AgCl electrode, Hg/HgO electrode, etc. The RE should be electrochemically reversible and its potential is determined with the help of Nernst equation. The potential of this electrode should be constant regardless of the small current that flows through it. The counter reactions of the reactions occurring at the WE are taking place at the CE. This reaction balances the total charge accumulated due to the WE reaction. The CE should be inert and have large surface area. Electrochemical changes/reactions of our interest are taking place at the WE. The common WE are glassy carbon electrode, carbon paste electrode, Au, Ag, Pt, graphite, boron-doped diamond electrode, etc. The electrode surface should be physical defect free for obtaining consistent result. It should be chemically polarized, electro chemically and chemically inert. It should possess wide potential window. The area of the WE should be small enough to get better current density (Bard et al. 2001).

2.2 Fundamentals of Electrode Reactions

In an electrochemical reaction, charge transfer occurs among an electrode surface and the analyte molecules. The different steps involved in the electrode reaction are movement of the analyte in to an interface (mass transport), electron transfer between the analytes present at the vicinity of the electrode material and the electrode, movement of the oxidized or reduced analyte from electrode surface to the bulk and electrode surface renewal for the accommodation of new analyte. The schematical representations are shown in Fig. 41.1.

Consider an electrode reaction $O + ne^{-} \leftrightarrow R$, the current corresponding to the electrochemical reaction has linear relationship with reaction rate. The other factors that influence the current response are the electrode surface area and surface concentration of the analyte molecule. The theoretical studies show that rate of reaction depends upon the applied voltage and the mass transport during the electrode reaction. Based on the applied voltage, the activation energy for the oxidation and reduction reaction of the species will change in a linear fashion. The movement of

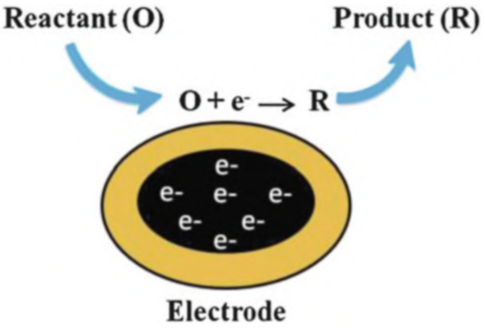

Fig. 41.1 Reaction in the electrode surface

the reactant from the bulk to the interface (mass transport) occurs through three different modes such as diffusion, migration, and convection. Diffusion is the movement of the species which arises from local uneven concentrated species. So this makes a concentration gradient in the solution close to the WE and the bulk. Migration is the movement of charged ions that arise due to the potential gradient. This movement is influenced by electrostatic force of attraction and repulsion. This can be minimized by adding supporting electrolytes like KCl. The third type of mass transport is the convection. It is the movement of species due to the action of force. The factors that influence the rate and kinetics of electrode reactions are applied voltage, reactivity of an analyte, features of the electrode surface, and the nature of the interface between an electrode and the solution (electron transfer occurring region). During the sensing mechanism, an electrical energy is supplied to the electrode. It changes the energy of an electron within the electrode material. Based on the applied voltage, the Fermi level (place of highest energy electron) of the electrode material gets altered. From this level, electron moves to the analyte and the oxidation reduction reactions occur. The current corresponding to this oxidation and reduction reaction is related to the electron transfer rate and the movement of analyte toward and away from the interface of the electrode (Bard et al. 2001).

2.3 Different Techniques Used for Biosensing Study

CV is the widely employed technique in electrochemical studies (Choudhary et al. 2016). It is used to study the thermodynamics and kinetics of electrochemical redox process. The excitation signal used in this technique is the E-t triangular waveform. Here the potential scan is from initial potential (E_i) to the final potential (E_f) and then from E_f to E_i. The current versus potential graph is obtained during the cyclic voltammetric experiment. The thermodynamic and kinetic information of the electrochemical reaction can be calculated by using cyclic voltammetric data. In differential pulse voltammetry (DPV), potential pulse is applied in a linear or staircase potential ramp and the current is measured. The peak shaped current versus potential plot is known as differential pulse voltammogram (Bhatnagar et al. 2018). This technique has enhanced sensitivity compared to other methods. An electrochemical impedance spectrum gives information regarding the resistance associated with the flow of current through the circuit. Here the potential and the current are reported in the sinusoidal form. In chronoamperometry, working electrode potential is fixed to a constant at which electrochemical reaction happens. Potential excitation signal is used and the current versus time plot is obtained. This plot is called chronoamperogram (Bard et al. 2001).

2.4 Types and Kinetics of Electron Transfer

There are three types of electron transfer reactions present depending upon the nature of the reactant species. The reversible, quasi reversible, and irreversible reactions are common in electro analysis. In reversible electron transfer reaction, the rate of mass transport is slower than electron transfer kinetics. In this system, oxidized and reduced analytes are in equilibrium and follow Nernstian behavior. The electrochemical reaction kinetics depends on the electrical double layer structure and the electrode material. The value of heterogeneous rate constant and the charge transfer coefficient defines the kinetics feasibility and the energy used to lower the activation energy of the reaction. The electrochemical reaction with higher heterogeneous rate constant defines the easiness of the reaction between the reactant and the material of the electrode. In quasi reversible electron transfer reaction, the mass transport and electron transfer rates are comparable and do not follow Nernstian behavior. In this case both oxidation and reduction reaction give characteristics peaks in CV. In irreversible electron transfer reaction, the rate of mass transport is fast compared to electron transfer kinetics. Here only oxidation or reduction reaction is taking place and do not follow Nernstian behavior (Mahato et al. 2019).

2.5 Practical Sensing Procedure

The experimental setup (Fig. 41.2) of electrochemical sensors involves three electrodes (as RE, CE, and WE) in contact with the analyzing analyte solution. The driving force for the sensing of the electrochemical sensor is a direct current. In the experimental setup, the two electrodes such as WE and RE are placed very close to avoid the IR drop. Here the focus is on the WE. The oxidation or reduction current of

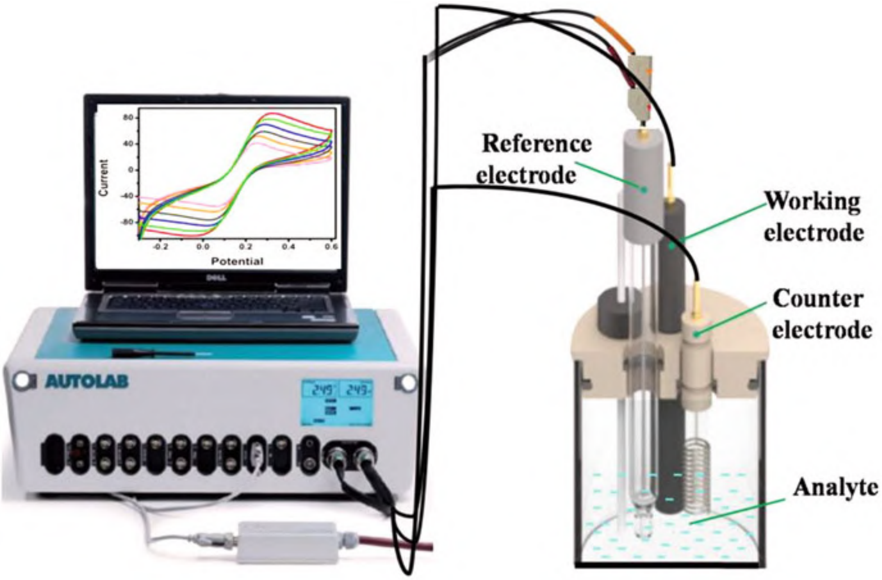

Fig. 41.2 Standard electrochemical sensing setup

the analyte is enhanced by coating the WE with electro catalytically active materials. The potential is applied in between RE and the WE and the current is measured in between the CE and the WE.

Here the solution and the electrodes are in static condition. The central point of the sensor is the working electrode. The materials or the electro catalyst used for the application as a sensor should have high conductivity, wide potential window, low cost, abundance, corrosion resistance, and enhanced physical and chemical stability. The conductivity of the material can be improved by the addition of appropriate amount of different types of carbon materials. The modifier material should catalyze the oxidation or reduction of the analyte.

3 Recent Advances in Sensing of Biomolecules Using Perovskites

ABO_3 type perovskite materials were widely synthesized by precipitation, solution combustion, and hydrothermal methods. Based on the synthesis method, these materials show different morphology and surface characteristics. The surface area, surface metal ion, and the defects have a direct correlation with the catalytic and electrical properties of these materials. Because of the thermal stability of these materials, it is widely used as a catalyst in catalytic applications. In the past few years, researchers used this perovskite as an electrode modifier for the detection of alcohols, glucose, amino acids, H_2O_2, and neurotransmitters (Fig. 41.3).

3.1 Neurotransmitter (Dopamine) Sensing

Dopamine (DA) is an essential catecholamine neurotransmitter that exists in the mammalian central nervous system. It is produced from tyrosine. DA is vital for the exact functioning of cardiovascular, hormonal, and central nervous systems. The usual DA level in brain fluids and blood is approximately 25–50 nM. The abnormal level of DA influences our emotions, motivation, etc. The quantification of DA in body fluid has an essential role in the detection of Parkinson's disease and psychiatric disorders (Wightman et al. 1988).

Carbon paste electrode (CPE) and $SrPdO_3$-based CPE (CPE/$SrPdO_3$) is one of the electrochemical DA sensor. This electrode showed the limit of detection (LOD) of 9.3 nM. Along with this advantage, it allows the simultaneous detection of DA, ascorbic acid (AA), and uric acid (UA) (Atta et al. 2014).

By simple precipitation method, $BaZrO_3$ (BZO) was synthesized and used as a modifier for DA sensing. Because of the proton conducting nature of the barium zirconate, BZO/CPE showed better activity than CPE. The same trend was observed in the case of charge transfer and electrochemically active surface area. In barium zirconate, Zr can show variable oxidation state. So oxygen vacancies are created in $BaZrO_3$ and which enhances the oxidation of DA. Depending up on the pH of the medium and the scan rate, the oxidation rate of the analyte was changed. It indicates

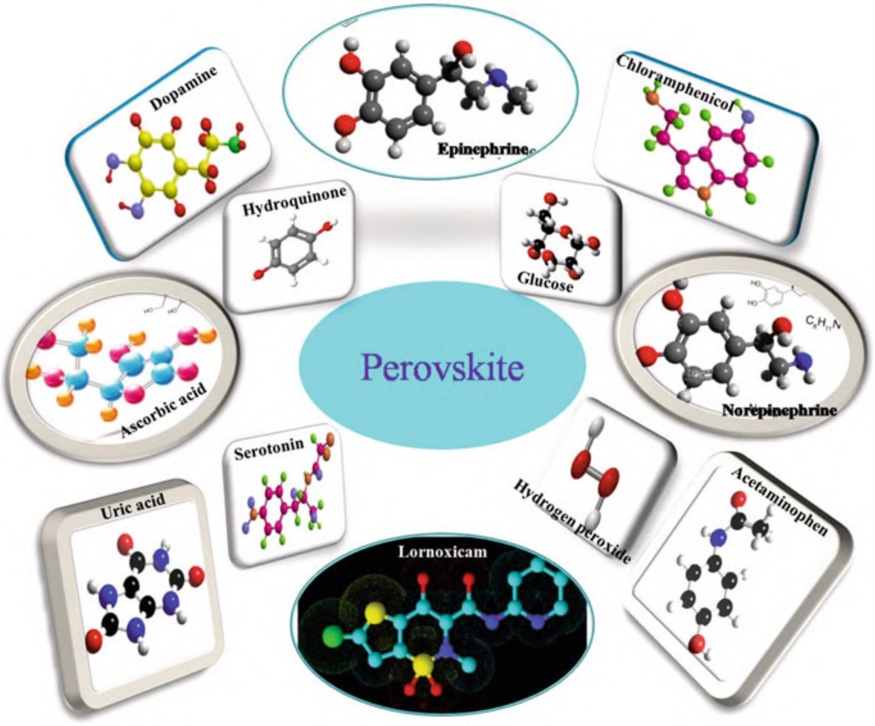
Perovskite
Dopamine
Epinephrine
Chloramphenicol
Hydroquinone
Glucose
Ascorbic acid
Norepinephrine
Serotonin
Hydrogen peroxide
Uric acid
Lornoxicam
Acetaminophen

Fig. 41.3 Different biomolecules detected electrochemically using perovskite materials

the proton coupled electron transfer mechanism of DA oxidation. Here the LOD of the DA was 5 pM (Thomas et al. 2021b).

The $LaFeO_3$/Glassy carbon electrode ($LaFeO_3$/GCE) was used to detect DA. Here $LaFeO_3$/GCE showed tenfold increase in DA oxidation peak compared to GCE. In $LaFeO_3$/GCE, the DA oxidation peaks were observed at ~0.30 V (vs. Ag/AgCl) whereas its reduction potential was ~0.24 V (vs. Ag/AgCl). The crystal field theory/crystal field stabilization energy suggests that the cation present in the octahedral position is responsible for the catalytic activity. The enhancement in current response may due to the B site Fe in the modifier. The inter conversion of Fe^{III} to Fe^{IV} and Fe^{IV} to Fe^{III} occurring in the surface of the electrode influence the oxidation and reduction reaction. The mechanism corresponding to the conversion of DA to dopamine quinone can be given below,

$$\mathrm{LaFeO_3 - Fe^{III} + OH^- \rightarrow LaFeO_3(OH^-) - Fe^{IV} + e^-}$$

$$\mathrm{LaFeO_3(OH^-) - Fe^{IV} + Dopamine \rightarrow LaFeO_3 - Fe^{III} + DQ}$$

The influence of pH (4 to 9) on the current and potential for DA oxidation was investigated. The results exhibit a maximum current at pH 8 and a negative shift in peak potential on varying pH from 4 to 9. The electron transfer kinetic study shows that there is a direct correlation between the peak current and scan rate. Normally the dopamine oxidation follows a quasi-reversible nature. The DA detection using DPV suggest that two linear range are present and is usual for adsorption controlled reaction. Normally the current response depends on the number of adsorbed analyte molecules on the electrode. At lower concentrations, monolayer is formed close to the electrode surface, whereas at higher concentration it forms multilayer. This leads to a split in the linear dynamic range. In $LaFeO_3$/GCE, the LOD of DA is 10 nM. The excellent selectivity toward DA detection in presence of AA and UA was also investigated in this study (Vijayaraghavan et al. 2017).

Wang et al. synthesized $LaFeO_3$ by citrate method followed by calcination. The electrode modification was carried out by drop casting various amounts of a suspension of 100 mg $LaFeO_3$ in 10 ml alcohol solution and the optimal catalyst loading was 10 μL. Any change in the peak current or the overpotential is the direct indication of the electro catalytic activity of any catalyst. Here, peak current was increased and overpotential was decreased on modification. In terms of the mechanistic point of view, under the electrochemical condition, $LaFeO_3$ may interact with the H- atom of the –OH group of DA, and weaken the energy of O-H bond and increase the electron transfer rate. Here the improved surface area of the $LaFeO_3$ modified electrode compared to bare electrode helps to enhance the contact area of DA and electrode. This also helps the fast electron transfer and reaction rate of DA oxidation. The pH studies reveal that neutral pH is the optimum condition for further study. LOD of DA using modified electrode was 3.0×10^{-8} M (Wang et al. 2009).

P K Gopi et al. synthesized graphene oxide decorated strontium titanate modified GCE for DA sensing. Here $SrTiO_3$ and graphite oxide (GO) were synthesized separately and during the electrode fabrication, a suspension of 1.0 mg of $SrTiO_3$ and 2.0 mg of GO were prepared in 1.0 mL of water. Because of the excellent electrical properties of $SrTiO_3$/GO, the charge transfer resistance is reduced dramatically. The electrochemically active surface area of $SrTiO_3$/GO/GCE becomes higher than the other electrodes. This is the reason for the higher rate of electron transfer between the $SrTiO_3$/GO/GCE and the $K_3[Fe(CN)_6]$. This helps the increased electrochemical oxidation of DA. In comparison to other electrodes in this work, the $SrTiO_3$/GO/GCE showed better catalytic activity toward DA sensing and is due to the Π - to -Π interaction between GO and $SrTiO_3$ along with other factors. The LOD of DA was calculated to be 0.01 μM (Gopi et al. 2020).

A series of perovskite $LaFeO_3$, $LaCoO_3$, $LaNiO_3$ were prepared by solution combustion method by Jasmine et al. The electrode modification was carried out by bulk modification method. Here DA, serotonin, acetaminophen, and tyrosine was used as the analyte molecule. Among three perovskites $LaNiO_3$/CPE showed better activity in comparison to $LaFeO_3$/CPE and $LaCoO_3$/CPE. The greater conductivity, smaller charge transfer resistance, higher active surface area, oxygen deficiency in $LaNiO_3$ and Ni rich surface sites may be the reason for the better activity of $LaNiO_3$ modified electrode than other electrodes. In all the three perovskites, the B site atoms Co, Fe, and Ni are in octahedral coordination and exist as Co^{3+} (high spin state and low spin state), Fe^{3+} (high spin sate), and Ni^{3+} (low spin state). In Fe^{3+}, Co^{3+}, and

Ni^{3+}, the number of outer shell electrons are 5, 6, and 7. These systems are expected to have weak, no, and strong Jahn Teller effect. So the t_{2g} orbitals become filled and e_g orbitals become unevenly occupied. In electrochemical studies, the input potential induces variation in the energy of the electrode material. The 3d electron energy order here is $Ni^{3+} > Co^{3+} > Fe^{3+}$. This variation causes an enhancement in the DA oxidation in $LaNiO_3$/CPE than other electrodes. The pH and scan rate also influence the reaction rate. The modified electrode showed better activity at pH 7 and 8. The sensitivity studies showed that the LOD of DA was 9 nM (Thomas et al. 2021d).

The $LaCoO_3$ nanoparticles were found to possess sensing activity. S. Priyatharshni et al. synthesized $LaCoO_3$ via hydrothermal method using urea, citric acid, and Cetyltrimethylammonium Bromide (CTAB) as surface modifier. In the sensing study, $LaCoO_3$ synthesized by urea surfactant exhibits the higher current response compared to those obtained via CTAB and citric acid. This higher current response is due to its porous morphology and higher surface area. Because of the effective charge transfer among electrode and DA, the current intensity of DA oxidation increases linearly with its concentration. The increase in the oxidation/reduction of DA with increase in scan rate implies that the electron transfer reaction present in this case is diffusion controlled one. At the same time, DA oxidation and reduction potential shifted toward positive and negative directions, respectively. The positive shift of the oxidation and reduction potential with decreasing pH depends on the electrostatic repulsive force among the electrode and the cationic DA. In acidic pH, positive ions are accumulated on the electrode surface and therefore oxidation current response decreases with decreasing pH. Whereas in basic pH, the negative ions are accumulated on the electrode surface and it attracts the DA toward the electrode and enhance the current response. The studies suggest that this redox reaction is a two-electron/proton transfer process. The concentration dependent studies suggest that while using $LaCoO_3$/GCE, the LOD of DA was determined to be 3.53 μM (Priyatharshni et al. 2017).

S. Priyatharshni et al. synthesized $LaMnO_3$ in presence of varying concentrations of ethylene glycol via hydrothermal method. While using $LaMnO_3$/GC, the DA oxidation current rises with rise in its concentration. The reason behind this phenomenon may be the effective charge transport between the molecular orbital and conduction band of DA. In order to evaluate the electron transfer mechanism of this electrochemical reaction, the scan rate variation studies were carried out and it shows that diffusion controlled mechanism is happening here. From this experiment, they found that the electrode conductivity increases with increase in electron charge transfer. The blue shift and red shift of anodic and cathodic potential is related to the potential consumption for electron transfer with respect to reaction time. Depending upon the decrease in pH of the medium, the red-shift in potential also happens. Exactly like $LaCoO_3$, the oxidation current of DA rises with rise in pH. Here the LOD of DA was 6.22 μM (Priyatharshni et al. 2016).

Priyatharshni et al. synthesized $LaNiO_3$ using citric acid, urea, and CTAB as surfactant via hydrothermal method. Among different $LaNiO_3$ electrocatalysts, the

$LaNiO_3$ prepared using urea showed better electrocatalytic activity compared to other $LaNiO_3$ catalysts. This is due to the spherical shape and higher surface area of $LaNiO_3$ prepared using urea. This improves the adsorption rate of DA. The LOD of dopamine using this electrode becomes 4.07 μM (Priyatharshni et al. 2021).

Nada F. Atta synthesized $SrPdO_3$ via solution combustion method and optimized the composition of $SrPdO_3$ in $SrPdO_3$/CPE. The $SrPdO_3$ synthesized using different fuels like glycine, urea and citric acid. The glycine-nitrate mixture shows better electrocatalytic activity toward DA oxidation. The reason for this result is the tiny size, greater surface area and better porosity of $SrPdO_3$ synthesized using glycine compared to urea and citric acid. While using $SrPdO_3$ modifier, the peak current of DA oxidation and reduction increased by 73% and 99% compared to CPE. In addition to that the peak potentials moved to lower values and the peak separation became 98 mV after modification. This is due to the oxygen vacancies and catalytic property of Pd^{4+} in the perovskite structure which enhance the DA oxidation. Along with this, the assumption behind the charge transfer mechanism is that the electrode surface should be active and promote DA adsorption, proton and electron transfer. In the oxidation of DA the oxygen adsorption energy or the moderate bond formation between the oxygen atom and the transition element of the perovskite also influence the reaction rate. The pH-dependent DA oxidation study reveals that the oxidation current increased upto pH 7.4 and then decreasing. The concentration-dependent study reveals that the detection limit of DA is 9.3 nM with sensitivity of 0.88066 A/$molL^{-1}$ (Atta et al. 2014).

Jasmine et al. synthesized $LaNi_{0.2}Co_{0.8}O_3$, $LaNi_{0.4}Co_{0.6}O_3$, $LaNi_{0.6}Co_{0.4}O_3$, and $LaNi_{0.8}Co_{0.2}O_3$ via solution combustion method and used as modifier for CPE. The DA oxidation studies reveal that the incorporation of Co in the B site of $LaNi_XCo_{1-X}O_3$ by replacing particular amount of Ni decreases the DA oxidation rate. Here the better sensitivity was shown by $LaNi_{0.8}Co_{0.2}O_3$ and therefore potential and current responses of DA oxidation were improved by 0.023 V and 1.5 fold. In $LaNi_{0.8}Co_{0.2}O_3$, the Ni^{3+} exists in the low spin state (LS) and Co^{3+} in the LS and high spin state (HS). Based on the percentage composition of cobalt in $LaNi_xCo_{1-x}O_3$, the percentage of LS and HS Co^{3+} are different. Due to this difference in the spin state of Co^{3+} in different samples, DA oxidation current varies. Normally DA exists in the neutral form (DA) (in acidic medium), protonated form (DAH+) (in neutral medium), and zwitter ionic form (DA±)(in basic medium). In electrochemical DA oxidation, the basic pH improves the oxidation (lower potential) compared to acidic medium. At the same time, the DA oxidation becomes reversible in acidic and quasi reversible in basic buffer. This is the direct indication of the involvement of the proton coupled electron transfer mechanism of DA oxidation. The pKa and the oxidation potential also have direct relationship, i.e., the increase in pKa increases the $2e^-/2H^+$ reaction. The protons present at the vicinity of the electrode become high at acidic pH and hence it reduces the DA oxidation and enhances the oxidized DA reduction. The oxidation current of DA is lower at acidic pH and higher at basic pH. The kinetic studies suggest the diffusion controlled mechanism in DA oxidation. The LOD of DA is also calculated by this electrode and the value becomes 3 nM (Thomas et al. 2021c).

Roselin et al. synthesized $MgTiO_3$, $La_{0.5}Mg_{0.5}TiO_3$, and studied the DA sensing. In comparison with bare GCE, $MgTiO_3$/GCE, and $La_{0.5}Mg_{0.5}TiO_3$ /GCE, the higher DA oxidation current density and lower peak potential were shown by La-doped $MgTiO_3$/GCE. The reason behind this observation is the higher electrical conductivity and specific surface area of La-doped $MgTiO_3$/GCE compared to others. The stability, mechanism and concentration dependent DA oxidation was studied with varying scan rate. LOD of DA was investigated by chronoamperometric study and is equal to 1.32 μM (Ranjitha et al. 2021).

Z. Anajafi synthesized $NdFeO_3$ by a thermal treatment method and used it as a modifier for screen printed carbon electrode. In comparison to bare screen printed electrode, the $NdFeO_3$ modified screen printed electrode showed better current response. The improvement in the surface area and the electrocatalytic activity is the reason for this activity. Here the perovskite act as a center for electrostatic interaction between the WE and the analyte. This opens up the electron transfer path and enhances the electron transfer. Here the LOD of DA is 270 nM and is determined by square-wave voltammetry (Anajafi et al. 2019).

Jasmine et al. synthesized $BaMnO_3$ nanostructures via simple precipitation followed by calcinations step. A suspension of catalyst ink was prepared by sonicating $BaMnO_3$ and super P carbon black in a 1:3 isopropyl alcohol water mixture. Here 5 μL of nafion was acting as the binder. Because of the conductivity of the super P carbon black (SP) and the catalytic activity of $BaMnO_3$, the modification of the electrode by these two components made the new electrode a favorable one for the sensitive quantification of DA. The pico molar level (50 pM) sensing of DA was obtained by using $BaMnO_3$ + SP modified carbon paste electrode (Thomas et al. 2021a).

Yogendra Kumar et al. prepared $LaFeO_3$ via combustion reaction using sugar and ethanolamine as fuel and then used it for electrochemical sensing of DA. The electrochemical properties of the semiconducting materials are normally influenced by its particle size, band gap, surface defects, capping ligand, and composition. The value of peak potential separation is the direct indication of electrons transfer rate. In order to understand all these effects, a careful analysis was carried out and it suggested that $LaFeO_3$/Graphite (GP) showed better activity compared to GP. pH 6 buffer solution was used for the all analysis (Kumar et al. 2020).

3.2 Dopamine and Uric Acid Sensing

Aparna et al. synthesized $FeTiO_3$ via hydrothermal method and studied the DA and UA sensing. For this study, the glassy carbon electrode was modified with 10 μL solution of 1 mg $FeTiO_3$ dispersed in 1 mL ethanol. The better surface area, oxygen vacancy, and (Fe,Ti) redox states are the reason for the improved catalytic activity toward DA and UA detection. Here DA adsorbed on $FeTiO_3$ through the electrostatic force of attraction. The oxygen vacancies present in the perovskite help the adsorption of DA into the perovskite site. Later DA oxidation occurs with respect to the applied potential and is a $2H^+/2e^-$ transfer process. The LOD of DA was determined to be 1.3 nM and that of uric acid was 30 nM (Aparna and Sivasubramanian 2019).

Lignesh Durai et al. synthesized $ZnSnO_3$ by hydrothermal methods and used it as a modifier. In order to study the better composition of electrode material, they varied the weight % of $ZnSnO_3$ from 0.1, 0.3, 0.5, to 0.7 and analyzed the peak to peak separation and half-cell potential of 5 mM $Fe(CN)_6{}^{3-/4-}$. From these results, weight % of $ZnSnO_3$ showed better activity compared to others. The reason is the better effective surface area and optimum diffusion layer thickness at the interface of electrode and electrolyte. At higher weight % of $ZnSO_3$, the diffusion layer thickness was not adequate for the proper transfer of electrons between the analyte and the electrode. The optimum pH for this study was obtained to be 7. This observation is due to the optimum interaction of H^+/OH^- in between the electrode and electrolyte. During the electrochemical reaction of DA and UA, well-defined oxidation peaks are present due to the inter conversion of Sn^{2+} to Sn^{4+} in the SnO_6 octahedron of the perovskite. Here the LOD of UA is 0.55 μM and that of DA was 2.65 nM (Durai and Badhulika 2020b).

Lignesh Durai et al. synthesized β-$NaFeO_2$ via one-step solid-state reaction and used it for the detection of DA, UA, Xanthine (Xn), and Hypoxanthine (Hxn). The optimization of electrode fabrication study reveals that 0.5 wt% NFO/GCE is better for this sensing study. The diffusion controlled electrochemical oxidation of the analytes were confirmed by scan rate variation study. The electrochemically active surface area study reveals that 72% increase in surface area was observed during modification in comparison to GCE. Here the oxy functional groups of β-$NaFeO_2$ allow the immediate electron transfer. The influence of scan rate study reveals the diffusion controlled mechanism and the charge transfer coefficient (α) and apparent charge transfer rate constant (ks) were calculated using Laviron's model. Here the value of α_a and α_c is 0.2967 and 0.3871 and k_s was calculated as 0.4593 cms^{-1}. The concentration-dependent studies of all the four analytes reveals that the LOD of UA, DA, Hxn, and Xn were 158 nM, 2.12 nM, 95 nM, and 129 nM, respectively (Durai and Badhulika 2020a).

3.3 Hydroquinone Sensing

Khursheed Ahmad synthesized nitrogen-doped reduced graphene oxide (N-rGO) and strontium zirconate ($SrZrO_3$) composite by precipitation followed by reflection method in presence of urea. The electrode modification was carried out by drop casting 8 μL of the N-rGO/$SrZrO_3$ composite. The high surface area and the synergistic interaction between $SrZrO_3$ and N-rGO may be the reason for the improvement in electrocatalytic oxidation of hydroquinone. The electrochemically active surface area analysis and electrochemical impedance spectra analysis also agree with the enhanced activity of the composite material. The pH study support the neutral pH condition for all analysis. The linearly increased current scan rate relation reveals the diffusion controlled process. The highly sensitive square wave voltammetry was used for LOD calculation and here the value becomes 0.61 μM (Ahmad et al. 2020).

3.4 Glucose Sensing

Umamaheswari et al. synthesized cerium aluminate embedded on carbon nitride modified GCE (CAO/CN/GCE) for the sensitive detection of glucose. The optimization amount of 8 μL CAO/CN on GCE showed better activity. The electrode reaction kinetic studies via scan rate variation suggest that the glucose oxidation is a diffusion controlled process. The shift toward positive potential with increasing scan rate indicates the feasibility of the reaction. The amperometric sensing of glucose using CAO/CN/ GCE gave LOD of 0.86 nM (Rajaji et al. 2021).

F Jia et al. synthesized perovskite $LaTiO_3$ with silver (Ag). The Ag content (0.08, 0.1, 0.2, and 0.6) was varied via sol gel method and used for glucose sensing. Among different perovskites doped with Ag, the $LaTiO_3$-Ag 0.1 showed better non-enzymatic electrochemiluminescence (ECL) behavior. Luminol show ECL behavior and the addition of glucose the ECL intensity increases. The small size and porous structure of $LaTiO_3$-Ag0.1 particle along with active area of the electrode may be the reason for fast electron-transfer rate. The pH-dependent study reveals that pH value of 7.4 shows maximum ECL intensity. This is due to the accelerated conversion of luminol to form 3-aminophthalate anions. The LOD values of glucose is calculated to be 2.50×10^{-9} M using CV (Jia et al. 2015).

Ekram et al. synthesized $SrPdO_3$ via solution combustion method and then constructed modified graphite/$SrPdO_3$/M_{nano} (M = Ag, Pt and Pd) electrode for the detection of glucose. The metal nanoparticle deposition is carried out by applying suitable potential window. The modification using graphite/$SrPdO_3$/Au_{nano} showed 39.6 times greater current response compared to bare electrode. Due to the proper synergism between gold nanoparticle and $SrPdO_3$, modified electrode showed promising results. Here presence of $SrPdO_3$ and Au complement the charge transfer property and catalytic activity. In $SrPdO_3$, Palladium is in the +4 oxidation state. The uniform distribution of the Pd^{4+} and the presence of oxygen vacancy help glucose oxidation. The number of electrons present in the d orbital of the B site ion also influences the partial bond formation with the analyte. In this modifier material, gold acts as an electron channel among the electrode and the analyte. The other characteristics of gold nanoparticles were high effective surface area, electrocatalytic activity, high conductivity, and enhanced sensitivity. The LOD toward glucose detection become 9.3 nM (El-Ads et al. 2015).

Zhen Zhang et al. synthesized $Co_{0.4}Fe_{0.6}LaO_3$ nanoparticles via sol–gel method for glucose and hydrogen peroxide sensing. Here the electrode modification was carried out by drop casting 10 μL of 3 mg $Co_{0.4}Fe_{0.6}LaO_3$ in 1 ml suspension. During the electrochemical reaction of glucose, the $Co_{0.4}Fe_{0.6}LaO_3$/CPE showed better current response than bare CPE. This is due to the electro-catalytic property of this perovskite toward the oxidation of glucose. Here the sensor has a LOD of 10 nM for glucose (Zhang et al. 2013).

3.5 Nitrofurantoin Sensing

Vinitha et al. synthesized gadolinium orthoferrite/RGO nanocomposite by hydrothermal route and the catalyst ($GdFeO_3$/RGO) loading into GC electrode was analyzed by CV experiment. Here the optimum catalyst loading was 6 mL of $GdFeO_3$/RGO catalyst. The negative potential shift after modification is related to the higher surface area, numerous active sites ($GdFeO_3$), the influence of layered RGO, and conductivity. Along with all these properties, electrical contacts, synergistic effects, and interfacial interactions between $GdFeO_3$ and RGO create new functionalities and enhance the activity. The other important thing is that during the composite formation between $GdFeO_3$ and RGO, the van der Waals interaction among graphene sheets reduces and the surface area of the product becomes higher. The kinetics of this reaction was studied, and the results indicate that this is an adsorption-controlled process. The pH-dependent nitrofurantoin (NFT) reduction study indicates the irreversible nature of NFT reduction and the better current response was observed at pH 7. The NFT sensing property was analyzed by using DPV technique and the obtained LOD was 0.0153 mM while using $GdFeO_3$/RGO/GCE (Mariyappan et al. 2021).

3.6 Lornoxicam

Mona et al. synthesized $BaNb_2O_6$ nanofiber and used it for the sensing of Lornoxicam and Paracetamol. The buffer solution used in this study was Britton–Robinson buffer solution. The electrochemical studies reveal that $BaNb_2O_6$/CPE shows better activity and are due to the electrical conductivity and the synergistic effect. The influence of the pH study on electrochemical reaction reveals the protonation-deprotonation process. Here the highest current response was observed at pH 7 indicating that neutral pH is optimum for this study. Here the LOD was determined to be 0.6 nM (Mohamed et al. 2018).

3.7 Acetaminophen

Arockiajawahar et al. synthesized $GdTiO_3$ via sol-gel GTO(S) and hydrothermal GTO(H) methods, then allowed to encapsulate layered graphene (Gr) during catalyst solution preparation by sonicating appropriate amount of graphene and $GdTiO_3$. Among the bare, native oxides and composites, GTO(S)-Gr composite shows better activity. The hike in the oxidation current of acetaminophen using GTO(S)-Gr may be due to the enhanced π-interactions between graphene and perovskite, oxygen, and cation vacancies. During the electrochemical reaction, acetaminophen moves toward the electrode and interacts with the holes in the $GdTiO_3$ surface. Then it allows electron transfer and results in higher current response for electro-oxidation of acetaminophen. The GTO(S)-Gr/GCE could give a LOD of 58.85 nM for acetaminophen detection (Grace et al. 2021).

Daixin Ye et al. synthesized $LaNi_{0.5}Ti_{0.5}O_3/CoFe_2O_4$ (LNT-NFO) through the combination of ceramic, wet chemical, and sol-gel methods in order to detect paracetamol molecule. Here 5 μL of LNT–NFO suspension in water was used for electrode modification. After modification, there is a decrease in overvoltage and increase in the faradic current, which indicate the feasibility of paracetamol oxidation. In this case, the partially filled d orbital of the transition metal in the perovskite acts as an active site for paracetamol oxidation. Here the LOD of paracetamol is 0.19 μM (Ye et al. 2012). Table 41.1 summarizes the electroanalytical application of nano-perovskites modified electrodes for biomolecular detection.

4 Conclusions

Nano-Perovskites Derived Modified Electrodes are being looked upon as the ideal candidates for meeting the demands of an excellent sensor. Highly stable structural characteristics and versatile functionalities of the perovskites make them ideal for the sensor applications. Nano-perovskites are explored for designing better sensors as they possess high specific surface area, faster kinetics, more electroactive sites, etc. Biologically important molecules like Dopamine, Uric acid, Hydroquinone, Glucose, Nitrofurantoin, Lornoxicam, Acetaminophen, and Nucleic acid could be detected and quantified using perovskite modified electrodes. Researchers continue their efforts to address the issues related to stability, sensitivity, resolution by engineering perovskite materials by doping, morphology control and compositing with other materials, etc. Design, development and optimization of efficient, sensitive, and low cost sensor systems are vital for the affordable early-stage diagnosis of many diseases.

Table 41.1 Comparison of perovskite modified electrodes for biomolecule detection

Electrodes	Analyte	Linear Range	LOD	Reference
LaMnO$_3$/GCE	DA	1–100 μM	6220 nM	(Priyatharshni et al. 2016)
LaCoO$_3$/GCE	DA	1–100 μM	3530 nM	(Priyatharshni et al. 2017)
LaNiO$_3$/CPE	DA ST AAP	0.08–20 μM 0.1–6.7 6.7–80 μM 0.3–27 μM	9 nM 14 nM 35 nM	(Thomas et al. 2021d)
LaNiO$_3$ /GCE	DA	5–50 μM	4.07 μM	(Priyatharshni et al. 2021)
LaNi$_{0.8}$Co$_{0.2}$O$_3$/CPE	DA UA AAP	0.08 mM–80 nM 0.08 mM–50 nM 0.1–0.01 mM 0.01 mM–1 μM	3 nM 5 nM 100 nM	(Thomas et al. 2021c)
LaFeO$_3$/GCE	DA	1–6	10	(Vijayaraghavan et al. 2017)
LaFeO$_3$/GCE	AA DA UA	500–3000 μM 1–6 μM 100–600 μM	3×10^{-8} M	(Wang et al. 2009)
LaFeO$_3$/GCE	AA DA UA	0.02–1.6 μM	0.059 μM	(Kumar et al. 2020)
FeTiO$_3$/GCE	AA DA UA	1–90 μM 110–350 μM 1–150 μM 200–500 μM	30 nM 0.0013 μM	(Aparna and Sivasubramanian 2019)
La$_x$Mg$_{1-x}$TiO$_3$/GCE	DA	5–50 μM	1.32 μM	(Ranjitha et al. 2021)
SrTiO$_3$ –GO/GCE	DA	0.005–531 μM	0.01 μM	(Gopi et al. 2020)
SrPdO$_3$/CPE	AA DA UA	7–70 μM	0.0093 μM	(Atta et al. 2014)
BZO-2/CPE	AA DA UA	0.17 mM–5 μM 0.05 mM–0.05 nM 1 μM–5 nM	0.5 μM 5 pM 0.5 nM	(Thomas et al. 2021b)
BaMnO$_3$ + SP/GCE	DA, ST	300–0.1 nM 10–2300 nM	50 pM 5 nM	(Thomas et al. 2021a)
NdFeO$_3$/Screen printed Carbon electrode	DA	0.5–100 μM 150–400 μM	270 nM	(Anajafi et al. 2019)
ZnSnO$_3$/GCE	DA UA	0.01–5 1–5000 μM	2.65 nM 0.55 μM	(Durai and Badhulika 2020b)
β-NaFeO$_2$/GCE	DA UA	0.010–4,10–40 μM 0.5–20 μM	2.12 nM 158 nM	(Durai and Badhulika 2020a)
N-rGO/SrZrO$_3$/GCE	Hydroquinone	25–2500 μM	0.61 μM	(Ahmad et al. 2020)

(continued)

Table 41.1 (continued)

Electrodes	Analyte	Linear Range	LOD	Reference
CAO/CN/GCE	Glucose	0.01–1034.5 μM	0.86 nM	(Rajaji et al. 2021)
$LaTiO_3$-Ag 0.1	Glucose		2.50 nM	(Jia et al. 2015)
Graphite/$SrPdO_3$/M_{nano} (M = Ag, Pt and Pd) electrode	Glucose	7–70 μM	9.3 nM	(El-Ads et al. 2015)
$Co_{0.4}Fe_{0.6}LaO_3$/CPE	Glucose	0.05–5, 5–500 μM	10 nM	(Zhang et al. 2013)
$GdFeO_3$/RGO/GCE	Nitrofurantoin	0.001–249 μM	0.0153 mM	(Mariyappan et al. 2021)
$BaNb_2O_6$/CPE	Lornoxicam	4.0 nM–1.0 μ M, 1.0 μM–2.5 × 10^{-4} M	0.6 nM	(Mohamed et al. 2018)
GTO(S)-Gr/GCE	Acetaminophen	50–95 nM, 100–700 nM, 900–1500 nM	58.85 nM	(Grace et al. 2021)
$LaNi_{0.5}Ti_{0.5}O_3$/$CoFe_2O_4$	Acetaminophen	0.5–901 μM	0.19 μM	(Ye et al. 2012)

References

Ahmad K, Kumar P, Mobin SM (2020) A highly sensitive and selective hydroquinone sensor based on a newly designed N-rGO/$SrZrO_3$ composite. Nanoscale Adv 2:502–511

Anajafi Z, Naseri M, Marini S, Espro C, Iannazzo D, Leonardi SG, Neri G (2019) $NdFeO_3$ as a new electrocatalytic material for the electrochemical monitoring of dopamine. Anal Bioanal Chem 411:7681–7688

Aparna TK, Sivasubramanian R (2019) $FeTiO_3$ nanohexagons based electrochemical sensor for the detection of dopamine in presence of uric acid. Mater Chem Phys 233:319–328

Atta NF, Ali SM, El-ads EH, Galal A (2014) Nano-perovskite carbon paste composite electrode for the simultaneous determination of dopamine, ascorbic acid and uric acid. Electrochim Acta 128: 16–24

Atta NF, Galal A, El-Ads EH (2016) Perovskite nanomaterials – synthesis, characterization, and applications. IntechOpen, Croatia, pp 107–151

Bard AJ, Faulkner LR, Swain E, Robey C (2001) Fundamentals and applications, 2nd edn. Wiley, New York

Bhatnagar I, Mahato K, Ealla KKR, Asthana A, Chandra P (2018) Chitosan stabilized gold nanoparticle mediated self-assembled gliP nanobiosensor for diagnosis of Invasive Aspergillosis. Int J Biol Macromol 110:449–456

Choudhary M, Yadav P, Singh A, Kaur S, Ramirez-Vick J, Chandra P, Arora K, Singh SP (2016) CD 59 targeted ultrasensitive electrochemical immunosensor for fast and noninvasive diagnosis of oral cancer. Electroanalysis 28:2565–2574

Deka S, Saxena V, Hasan A, Chandra P, Pandey LM (2018) Synthesis, characterization and in vitro analysis of α-Fe_2O_3-$GdFeO_3$ biphasic materials as therapeutic agent for magnetic hyperthermia applications. Mater Sci Eng C 92:932–941

Durai L, Badhulika S (2020a) Facile synthesis of large area pebble-like β-$NaFeO_2$ perovskite for simultaneous sensing of dopamine, uric acid, xanthine and hypoxanthine in human blood. Mater Sci Eng C 109:110631

Durai L, Badhulika S (2020b) One pot hydrothermal synthesis of large area nano cube like $ZnSnO_3$ perovskite for simultaneous sensing of uric acid and dopamine using differential pulse voltammetry. IEEE Sensors J 20:13212–13219

El-Ads EH, Galal A, Atta NF (2015) Electrochemistry of glucose at gold nanoparticles modified graphite/$SrPdO_3$ electrode – towards a novel non-enzymatic glucose sensor. J Electroanal Chem 749:42–52

Gopi PK, Muthukutty B, Chen S (2020) Platelet-structured strontium titanate perovskite decorated on graphene oxide as a nanocatalyst for electrochemical determination of neurotransmitter dopamine. New J Chem 44:18431–18441

Grace AA, Dharuman V, Hahn JH (2021) $GdTiO_3$ perovskite modified graphene composite for electrochemical simultaneous sensing of acetaminophen and dopamine. J Alloys Compd 886:161256

Jia F, Zhong H, Zhang W, Li X, Wang G, Song J, Cheng Z, Yin J, Guo L (2015) A novel nonenzymatic ECL glucose sensor based on perovskite. Sensors Actuators B Chem 212: 174–182

Kumar Y, Pramanik S, Das DK (2020) Lanthanum ortho-ferrite ($LaFeO_3$) nano-particles based electrochemical sensor for the detection of dopamine. Biointerface Res Appl Chem 10: 6182–6188

Mahato K, Purohit B, Bhardwaj K, Jaiswal A, Chandra P (2019) Novel electrochemical biosensor for serotonin detection based on gold nanorattles decorated reduced graphene oxide in biological fluids and in vitro model. Biosens Bioelectron 142:111502

Mariyappan V, Keerthi M, Chen S, Jeyapragasam T (2021) Nanostructured perovskite type gadolinium orthoferrite decorated RGO nanocomposite for the detection of nitrofurantoin in human urine and river water samples. J Colloid Interface Sci 600:537–549

Mohamed MA, Hasan MM, Abdullah IH, Abdellah AM, Yehia AM, Ahmed N, Abbas W, Allam NK (2018) Smart bi-metallic perovskite nano fibers as selective and reusable sensors of nano-level concentrations of non-steroidal anti-inflammatory drugs. Talanta 185:344–351

Murari K, Stanaćević M, Cauwenberghs G, Thakor NV (2004) Integrated potentiostat for neurotransmitter sensing: a high sensitivity, wide range VLSI design and chip. IEEE Eng Med Biol Mag 24:23–29

Priyatharshni S, Divagar M, Viswanathan C, Mangalaraj D, Ponpandian N (2016) Electrochemical simultaneous detection of dopamine, ascorbic acid and uric acid using $LaMnO_3$ nanostructures. J Electrochem Soc 163:460–465

Priyatharshni S, Tamilselvan A, Viswanathan C, Ponpandian N (2017) $LaCoO_3$ nanostructures modified glassy carbon electrode for simultaneous electrochemical detection of dopamine, ascorbic acid and uric acid. J Electrochem Soc 164:152–158

Priyatharshni S, Navadeepthy D, Srividhya G, Viswanathan C, Ponpandian N (2021) Physicochemical and engineering aspects highly stable and selective $LaNiO_3$ nanostructures modified glassy carbon electrode for simultaneous electrochemical detection of neurotransmitting compounds. Colloids Surf A Physicochem Eng Aspects 618:126387

Rajaji U, Ganesh P, Chen S, Govindasamy M, Kim S, Alshgari RA, Shimoga G (2021) Deep eutectic solvents synthesis of perovskite type cerium aluminate embedded carbon nitride catalyst: high-sensitive amperometric platform for sensing of glucose in biological fluids. J Ind Eng Chem 102:312–320

Ranjitha R, Manikandan A, Baby JN, Panneerselvam K, Subashchandrabose R, George M, Slimani Y, Almessiere A, Baykal A (2021) Hexagonal basalt-like ceramics Lax Mg_{1-x} TiO_3 ($x = 0$ and 0.5) contrived via deep eutectic solvent for selective electrochemical detection of dopamine. Phys B Condens Matter 615:413068

Sasaki S, Prewitt CT, Bass JD, Schulze WA (1987) Orthorhombic perovskite CaTiO3 and $CdTiO_3$: structure and space group. Acta Crystallogr Sect C Cryst Struct Commun 43:1668–1674

Thomas J, Anitha PK, Thomas T, Thomas N (2021a) Pico molar sensing of dopamine in presence of serotonin using $BaMnO_3$/carbon nanostructures. J Electrochem Soc 168:077513

Thomas J, Anitha PK, Thomas T, Thomas N (2021b) $BaZrO_3$ based non enzymatic single component single step ceramic electrochemical sensor for the picomolar detection of dopamine. Ceram Int 48:7168–7182

Thomas J, Anitha PK, Thomas T, Thomas N (2021c) Electrocatalytic sensing of dopamine: how the Co content in porous $LaNi_xCo_xO_3$ perovskite influences sensitivity? Microchem J 168:106443

Thomas J, Anitha PK, Thomas T, Thomas N (2021d) The influence of B-site cation in $LaBO_3$ (B = Fe, Co, Ni) perovskites on the nanomolar sensing of neurotransmitters. Sensors Actuators B Chem 332:129362

Vijayaraghavan T, Sivasubramanian R, Hussain S (2017) A facile synthesis of $LaFeO_3$ -based perovskites and their application towards sensing of neurotransmitters. ChemistrySelect 2: 5570–5577

Wang G, Sun J, Zhang W (2009) Simultaneous determination of dopamine, uric acid and ascorbic acid with $LaFeO_3$ nanoparticles modified electrode. Microchim Acta 164:357–362

Wightman RM, May LJ, Michael AC (1988) Detection of dopamine. Anal Chem 60:769–779

Ye D, Xu Y, Luo L, Ding Y, Wang Y, Liu X (2012) $LaNi_{0.5}Ti_{0.5}O_3/CoFe_2O_4$-based sensor for sensitive determination of paracetamol. J Solid State Electrochem 16:1635–1642

Zhang Z, Gu S, Ding Y, Zhang F, Jin J (2013) Determination of hydrogen peroxide and glucose using a novel sensor platform based on $Co_{0.4}Fe_{0.6}LaO_3$ nanoparticles. Microchim Acta 180: 1043–1049

Всё для победы!
НАРОДНЫЙ ФРОНТ
https://pobeda.onf.ru/
LET'S HELP THE RUSSIA

Electrochemical Impedance Spectroscopy (EIS) Principles and Biosensing Applications

42

Hilmiye Deniz Ertuğrul Uygun and Zihni Onur Uygun

Contents

1 Introduction 920
2 Biosensor Surface Circuit Models and Expected Data 923
3 Setting Impedance Parameters for Biosensing Applications 926
4 Impedance for Biosensor Applications 926
5 Conclusions 930
References 930

Abstract

Electrochemical impedance spectroscopy (EIS) used in biosensor systems is a label-free measurement method used in the measurement of electrochemical reactions. With this method, electrode surface characteristics, surface kinetics, and mass transport transfer can be measured. All these measurements can be performed with a single method. With EIS, the electrochemical circuit diagram of the surface can be drawn by scanning starting from a certain frequency. With this circuit diagram, the surface of the electrode can be seen electrochemically. In addition to the electrochemical measurement, it is actually possible to obtain strong mathematical data. All of this mathematical data can be verified by experimental measurements and provides opportunities to verify experimental results. In this way, there are both modifications in the development of biosensors and the possibility of quantitative measurement. This makes the system one step ahead of other methods in biosensor applications. The use of time as a function of this measurement made with alternating current also increases the sensitivity of

---

H. D. Ertuğrul Uygun
Center for Fabrication and Application of Electronic Materials, Dokuz Eylül University, İzmir, Turkey

Z. O. Uygun (✉)
Faculty of Medicine Medical Biochemistry Department, Kafkas University, Kars, Turkey

Center of Translational Medicine Research Center, Koç University, İstanbul, Turkey

© Springer Nature Singapore Pte Ltd. 2023

U. P. Azad, P. Chandra (eds.), *Handbook of Nanobioelectrochemistry*,
https://doi.org/10.1007/978-981-19-9437-1_42

the measurement. In this frequency measurement, the resistance of the electrode surface is measured as impedance and more suitable results are obtained. In biosensor applications, since the resistance of the electrode surface is measured in ohms, it is also important to process the data obtained afterward, to find the appropriate circuit model optimize the non-faradaic measurements, and how the measurement is optimized within the redox probe. For this reason, this measurement system, which is seen as a simple surface resistance measurement, is actually seen as a very complex and knowledge-based method. Therefore, the advantages are extremely numerous. Among the most important advantages of EIS are its fast electrode kinetics, the detection of non-electroactive species, and its power to perform measurements without the need for microscopic surface imaging techniques. In this book chapter, the application of EIS in biosensors, calculation methods, and different sub-applications are evaluated.

Keywords

Biosensor · Electrochemical impedance spectroscopy · Chronoimpedance · Affinity biosensors

1 Introduction

Engineers have used electrochemical impedance spectroscopy to determine the electrical circuit model. Because of the progressive development of electrical circuit models, terms such as impedance, capacitance, stationary phase element, and Warburg impedance have been introduced (Vivier and Orazem 2022). After the development of electrochemical research studies, it started to be used for electrochemical analysis. In particular, the monitoring of redox reactions and the examination of the electrode-electrolyte interface using impedance, the examination of the properties of the electrode surface and its applications were carried out with EIS and the process of the redox reaction according to the surface characteristics that determine the double layer capacitance of the electrode, adsorption, and mass transfers are measured. In addition, the physical properties of the surface, the resistance of the liquid measured in the electrochemical cell, the surface charges, and the geometric structure of biosensor surface structures can also be seen.

Electrochemical impedance spectroscopy is a method in which electrical circuit components of the electrode surface can be determined. These circuit components are also derivatized from Ohm's law. The most important point in this measurement system, in which frequency scanning is performed spectroscopically, is that the applied potential contains alternating current (AC) character. As it is known, Ohm's law is that the product of current and resistance gives voltage, that is, potential. It is important to define these elements according to biosensor systems. Although mathematically it is appropriate to look at the electrical circuit model over non-biosensor applications of impedance, it would be more accurate to evaluate impedance according to biosensor systems (Magar et al. 2021). Figure 42.1 shows

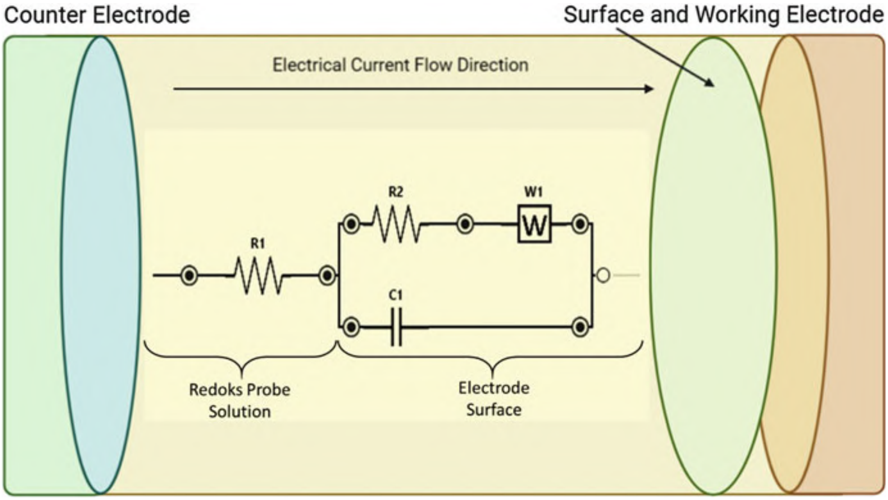

Fig. 42.1 General electrical circuit model of biosensor systems

the surface of an electrode by EIS. The electrode composed of three electrode systems. These are working electrode, counter electrode, and reference electrode. The circuit model between these two electrodes is completed by the current flowing through the measured solution. Depending on the character of this liquid, circuit elements can also be shaped and their measurements can change. When the data are examined, the elements called solution resistance, biosensor surface resistance (electron transfer resistance), Warburg impedance, capacitance, and stationary phase element are seen (Ertuğrul and Uygun 2013).

The current can pass over these elements, but is stored in the capacitively derived elements (C1). Laplace Transforms, Complex Numbers, and Fourier Transforms are used to explain impedance mathematically (Griffiths 1978; He and Fu 2001; Oshana 2006; Råde and Westergren 2004). The explanation of these transforms for how impedance can be measured is, briefly, that the potential and current, which vary with time, can change in a frequency measurement. In other words, using Ohm's law as a function of time in the calculation of resistance is called impedance. It is known that the electrical wave character changes when alternative current is used, that is, it has an imaginary part and a real part when evaluated with complex numbers in impedance measurement with frequency generation. Moreover, there should be phase angle to add this equation. In biosensor systems, on the other hand, since the impedance of the actual measured electrode, that is, the working electrode, is the impedance, there are graphic styles shaped according to the required measurement. Although there are basically two different diagrams, the most frequently used ones are Nyquist plots and Bode plots. The difference between these two graphs is that Nyquist plots form a three-axis graph showing imaginary impedance and real impedance (Figure 42.2a), and Bode plots show impedance versus frequency and phase angle versus frequency (Figure 42.2b). In the creation of the circuit model

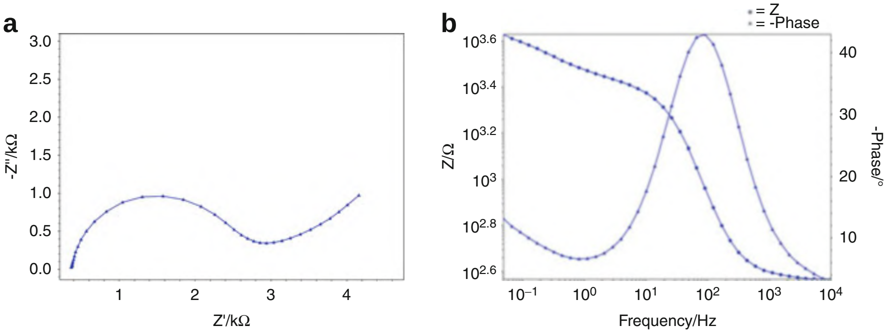

Fig. 42.2 (**a**) Schematic representation of Nyquist plot, (**b**) schematic representation of Bode plot (PSTrace 5.9)

used in the calculation of impedance, these two diagrams should be evaluated together. The impedance presents a semicircle; when the frequency goes to infinity, the impedance goes to zero because the impedance of the capacitor becomes zero and when the frequency goes to zero the impedance becomes real Z = R because a constant DC can flow through the circuit. In order to calculate these circuit elements, a mathematical circuit model should be created first and circuit elements can be calculated using programs according to this circuit model (Uygun and Ertuğrul Uygun 2014).

$$Z_0 = \frac{E}{i} = \frac{\mathrm{Sin}(\omega t)}{\mathrm{Sin}\ (\omega t + \theta)}\ \text{Definition of the Impedance}$$

Direct impedance measurement can be seen with Nyquist plots. A characteristic impedance measurement can be seen in Fig 42.2a. Here, as the impedance frequency decreases, the electron transfer resistance shows a sinusoidal character. The linear part shows the Warburg impedance, that is, the mass transport resistance. The angle that the Warburg impedance makes with the x-axis shows the phase angle. In biosensor systems, the dominance of impedance and Warburg impedance are proportional, while the phase angle changes, according to the properties of the surface. While the biosensor surface changes with the load of the measured liquid, it also shows the change in surface resistance because of modifications. Accordingly, the Warburg impedance shows the transfer of the mass in the measured solution to the biosensor surface.

It is extremely advantageous to measure impedance over a circuit model using alternative current rather than simple resistance measurement. Among these advantages, besides fast analysis, wide frequency scanning, sensitive measurement, there are also disadvantages of high cost device. Moreover, the biggest point to be considered in alternating current is that it causes the surface to deteriorate when measuring biological molecules. Particularly, nanomaterials with pointed sharp ends and corners can create arcs when applying high frequency and voltage, which causes the surface to deteriorate (Li et al. 2014). For this reason, measurements can be performed at potentials of 10 mV and below. However, DC is used especially in measurements involving redox probes to be used in faradaic measurements (Lasia 2011). The creation of a redox reaction at this potential and the monitoring of this reaction on the electrode constitute the main purpose of the measurement. In measurements involving a redox probe, the impedance is called the electron transfer resistance (R2, Rct). This impedance represents the resistance encountered by the electron emitted from the redox probe as it passes the electrode surface. Otherwise, Warburg impedance shows that linear diffusion of the redox probe to surface. Two elements are affected by electrode surface charges that repel or attract of redox probe by biosensor surface. The rate of conversion of the redox probe is also important in the formation of the semicircle in Nyquist plots. While the semi-circle character is dominant in fast reactions, linear impedance is observed in slow reactions (Sluyters and Oomen 1960). Especially in impedance measurements used in biosensors, it is important to define the circuit models and calculate the impedance curve obtained.

2 Biosensor Surface Circuit Models and Expected Data

While stationary phase measurements are carried out with solid electrode types used in biosensor systems, different circuit models are determined according to the plot obtained from the measurement result. Using the Nyquist plot (Fig. 42.3) obtained in

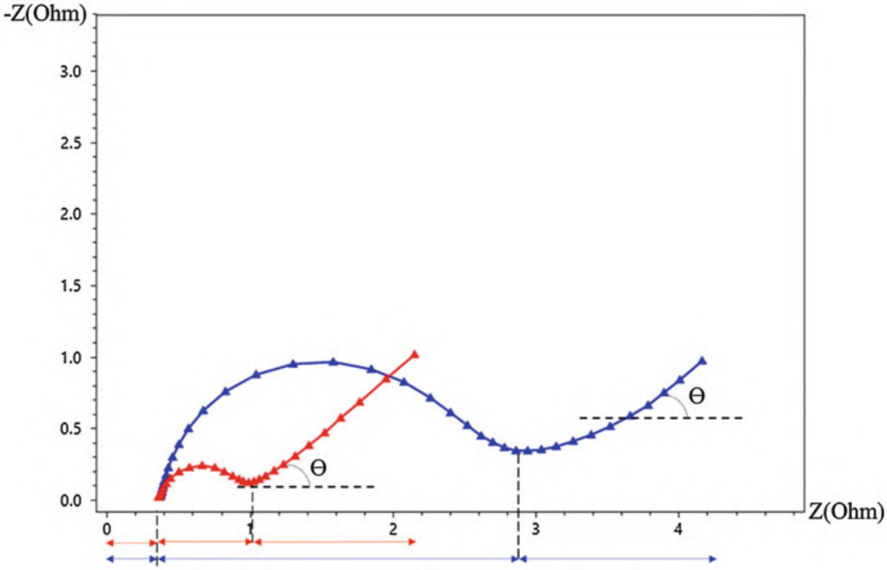

Fig. 42.3 EIS measurement in Ferri/Ferro cyanide redox probe of gold (red) and carbon (blue) electrodes impedances in redox probe solution (PSTrace 5.9)

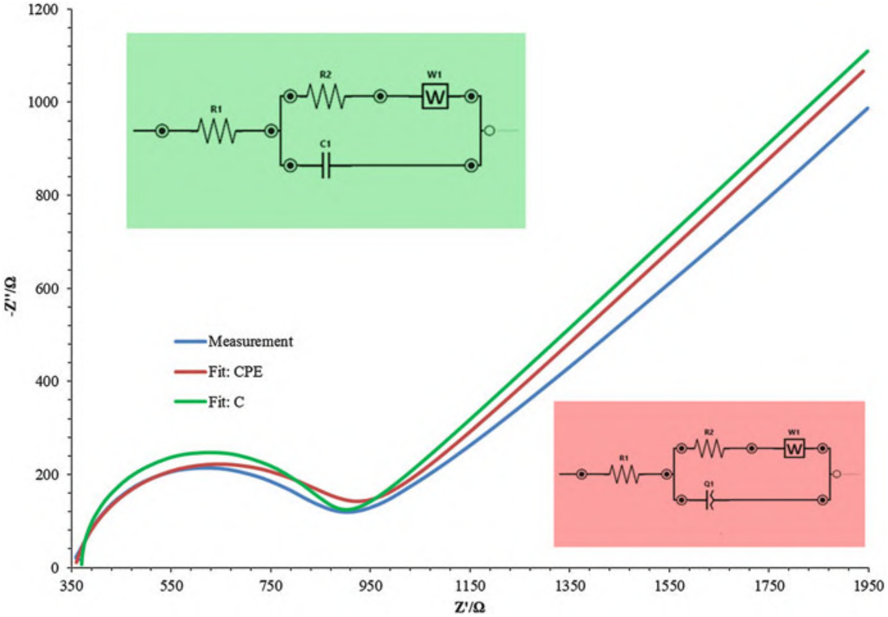

Fig. 42.4 EIS fitting on individual circuit models, blue EIS is obtained data, red and green EIS are the fitting of the blue EIS (showed in Excel)

impedance measurement, it is used in calculation and surface characterization in biosensor systems is explained through data.

Figure 42.3 shows a Nyquist plot and marked points at different points on this plot. Now, let us examine these data and consider the evaluation of the data through the biosensor system. The beginning point is not zero when looking at both impedance curves. The reason for this is that the current coming out of the counter electrode first passes the redox probe. That is, the layer at the top of the biosensor is the redox probe and this impedance shows the solution resistance (Rs or R1 in figure). The Rs value is inversely proportional to the concentration of the redox probe solution ingredients. Biosensor surface is represented by Rct or R2 in Fig. 42.4. As can be seen in the Fig. 42.4, the rapid transformation of the redox reaction through the layer is seen at the reaction rate on the surface, and it can be seen that the conductivity of the gold electrode is better than that of carbon (Red EIS). The part from the beginning point of the impedance curves to the end of the semicircle shows the surface impedance of the biosensor. Along with this impedance is a double layer capacitance (Wu 2022) not seen in the Nyquist plot. The most common situation in impedance curves is the fitting problem after the appropriate circuit diagram is created after the data. This is due to insufficient observation. In some cases, the apex of the semicircle becomes flattened toward the x-axis, that is, the apex of the imaginary impedance, which mathematically, is lower. The basis of this situation is the slowdown of the conversion rate of the redox probe on the surface formed because of the biosensor modification of the modified surface. For this reason, the double layer capacitance, which is included in the circuit model as a capacitance (C), should be shown as a constant phase element (CPE) (Fig. 42.4). The EIS shown in blue in Fig. 42.4 is experimentally obtained, while the other red and green ones are the curves fitted according to different circuit models. As a result of not evaluating the surface diffusion control properly, if the semi-circle is treated as ideal and a capacitor is placed in the circuit diagram, the EIS fitting data, which is seen in green, is obtained. In this case, although the margin of error in the calculation increases, the EIS calculation is made incorrectly, because the surface is not homogeneous as expected. On the other hand, the fit curve shown in red is close to the experimental data. Therefore, the margin of error is lower. The next step in the evaluation of EIS data is mass transport transfer, that is, the diffusion of the redox probe moving toward the biosensor surface or a different substance if the measurement is taken in a different liquid. This is represented by the Warburg impedance and the angle it makes with the x-axis is shown as the phase angle (ϴ). This linear part changes inversely with the semicircle. As the impedance decreases on a conductive surface, the Warburg impedance becomes dominant. There is also a situation that should be considered exceptional. This is the interaction between the surface charges of the biosensor and the charge of the redox probe. There is an electrostatic attraction between the surface-redox probe with different charge, that is, the redox probe moves electrostatically with diffusion to the surface and the mass transport transfer resistance (W) increases. In this case, more redox probes are transformed by diffusion than they should be on the surface. In this case, more electron flow than observed by diffusion reduces the electron transfer resistance by shadowing it. Therefore, impedance is a very powerful measurement method in biosensor development. In some studies, when the protein immobilized to the surface is positively charged, it attracts the redox probe and lowers the impedance (Uygun et al. 2020). This situation, which suggests that the immobilization procedure is faulty under normal conditions, is an indication that the surface loads should also be examined.

With this information, a suitable circuit model should be created to calculate the EIS. If the surface is homogeneously immobilized and layers are successfully formed, a single semi-circle character is seen. However, when different surfaces such as more than one layer, pore structure, micro-channels are seen on the surface, more than one half-circle character is normal. In this case, follow-up models are created by following the Nyquist plot curves obtained in the circuit diagram. Information on this can be obtained from a study in which impedance circuit models are described (Uygun and Ertuğrul Uygun 2014).

3 Setting Impedance Parameters for Biosensing Applications

Adjustment of measurement parameters in impedance-based biosensors is related to observance of experimental conditions, electrode type, and presence of redox probe. In impedimetric measurements, the potential of the redox probe is primarily found. Among these impedance parameters is the DC parameter, and it is obtained from measurements performed inside the redox probe by cyclic voltammetry. This parameter is used in the electrochemical conversion of the redox probe in faradaic measurements and is the parameter that creates the electron transfer resistance. On the other hand, voltammetric measurements can be performed by specifying the potential scan with Open Circuit Potential (OCP) versus the reference electrode. Potentials are featured with the OCP; the open circuit potential must be determined before the EIS performance. Another parameter is the polarization of the surface and the AC value in charge of sending the current with frequency. The actual amplitude must be small enough to prevent a current response with considerable higher harmonics of the applied ac frequency. Another parameter is frequency. While the magnitude of the frequency is related to the electrode, faradaic measurements are preferred when it is desired to take measurements under 0.1 Hz at small frequencies. At high frequencies, if the sinusoidal character is not seen, the measurement should start from the frequency at the point showing the sinusoidal character (Uygun et al. 2020). Measurements can be carried out with frequency scanning (EIS), as well as systems that measure the interaction of matter to the surface over time. A single frequency is used in these measurements. There are studies in the form of single frequency impedance or chronoimpedance as it is known in some studies (Ertuğrul Uygun et al. 2020; Uygun et al. 2021; Uygun and Girgin Sağin 2021). When these data are used in impedimetric measurements, the surface electron transfer resistance can be plotted according to the appropriate Nyquist plot curve.

4 Impedance for Biosensor Applications

Electrochemical impedance spectroscopy, which is used in biosensors, can be used as a quantitative method for both monitoring biosensor development stages and measurement. While developing the biosensor, a suitable immobilization layer should be prepared on the electrode surface (Fig. 42.5). The choice of this immobilization layer is completely related to the measurement method and the biorecognition receptor. Whether the measurement method is stationary or moving, measurement affects the immobilization material. Impedimetric biosensors are usually performed with static measurements. Apart from this, it is very important that there is no leakage from the surface, as the measurement is carried out entirely for the measurement of surface substances. In order to prevent this, covalent immobilization methods are generally preferred. These methods create a covalent bond between the immobilization material and the biorecognition receptor by using cross-linkers (EDEC/NHS, glutaraldehyde, etc.). Biosensor systems are suitable for label-free

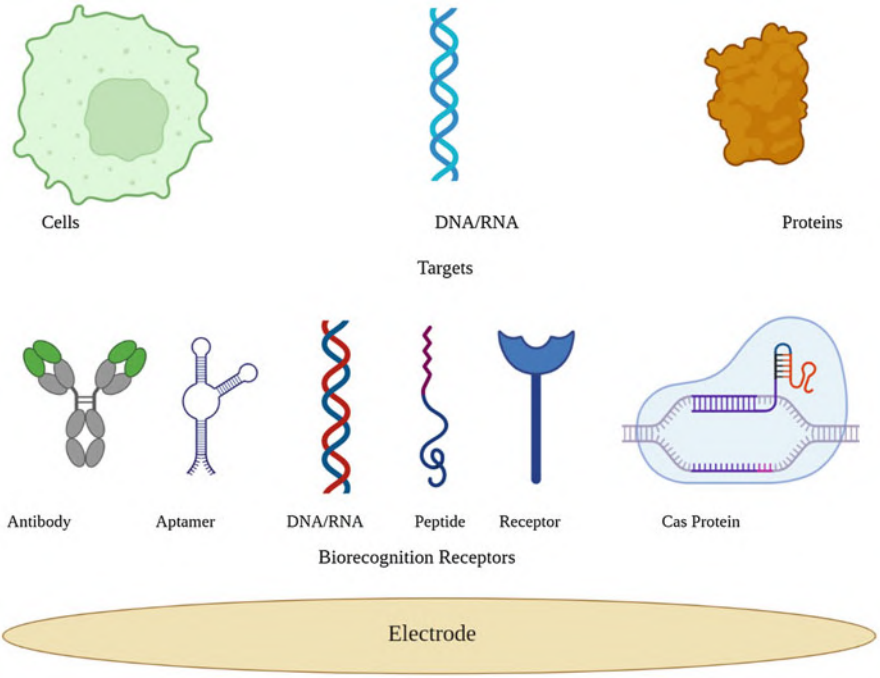

Fig. 42.5 Schematic representation of biorecognition elements and targets

measurements as they do not require an electrochemical reaction on the electrode surface. Therefore, the biorecognition receptor does not need to generate an electroactive signal. Binding of the target molecule is sufficient for measurement in the biosensor. This binding state can also be monitored by electrochemical impedance spectroscopy. Here, the general immobilization methods used in biosensor systems are valid. The point to be considered is that when materials with pointed ends such as graphene are immobilized to the surface, if an alternative current of 10 mV or more is applied, no arc should be formed on the surface of the biosensor. In this case, organic molecules can be electrically affected. This causes inaccurate measurements while the signal is being received. Especially in label-free methods, this information is important since the source of the signal is not known whether it is due to interaction between biomolecules or adsorption. Although this is a disadvantage, signal optimization steps are required. The first point to be applied in label-free methods is the optimization of the binding time of the biorecognition receptor and the analyte. However, in stationary measurements such as EIS, this can be found as a result of the repetitive incubation-measurement process. Considering that biomolecules can respond within milli seconds, this optimization is not very possible in the laboratory environment. Therefore, surface characterization methods that measure time-dependent binding label-free should be tried. Here, method development should continue by measuring the precise coupling time with single frequency impedance measurement, that is, chronoimpedance, which is a subtype of EIS. The biggest advantage of chronoimpedance is that it increases the selectivity of the biorecognition receptor with time-dependent measurement (Fedacı et al. 2022; Mumcu et al. 2022; Uygun and Atay 2021).

As a result, in impedimetric biosensors, it is important to know beforehand the sharp relationship between the biorecognition receptor and the analyte. Moreover, the total charge of the immobilization material, electrode, and analyte after binding needs to be evaluated. Electrode, analyte, biorecognition receptor, and immobilization layer should be considered as complementary while developing an impedimetric biosensor in this way.

The measurement of cells with biosensors is extremely complex. Since cells contain highly heterogeneous structures, selectivity becomes a big problem as different cell types show similarity to each other. In cases where the cell loses its vitality or its structure is damaged, mechanisms that can create false signals emerge. In cell assays, cell determination is mostly made by selecting cell surface antigens. In this case, biosensor systems are developed by using molecules such as antibodies, aptamers, peptides, etc.

Escherichia coli O157:H7 determination was performed with the help of nanoporous membranes in a biosensor system developed for whole cell assay (Joung et al. 2013). Due to the antibody-pathogen interactions, the ionic impedance of the electrolytes was measured with the impedance spectra through the nanopores. In this study, they performed label-free determination of *E. coli* in milk samples with a detection limit as low as 83.7 CFU/mL. In another study (Mantzila et al. 2008), polyclonal anti-Salmonella antibodies were used to determine Salmonella types. For immobilization, the SAM layer was formed and covalently bound with glutaraldehyde. Again, high sensitivity bacteria determination was carried out in milk.

Apart from studies using antibodies, single-chain synthetic nucleic acids called aptamers have also been used. Aptamer technology works like an antibody and the target molecule can be bound. In this way, it can be designed for a desired molecule. Since they can show affinity for a molecule, measurement can be performed by targeting cell surface antigens in biosensors used in cell determination. For example, in a study in which prostate cancer cells (LNCaP) were performed impedimetrically using prostate-specific membrane antigens (PSMA), sensitivity up to 1 cell was achieved (Uygun and Sağin 2021). In the study, a biosensor system was developed using gold nanoparticle electrodes. The aptamer sequences obtained as activated with thiol were modified on the biosensor surface and measurement was performed impedimetrically. Since a label-free measurement was made in this study, the measurement time was determined as chronoimpedimetric. Again, in a different study, SARS-COV2 determination was performed impedimetrically in measurements performed with aptamer technology (Tabrizi and Acedo 2022). Carbon fiber nanomaterials were modified with gold nanoparticles and used for aptamer immobilization on the carbon electrode surface. The SARS-CoV-2 receptor-binding domain was targeted for measurement in this study and analysis was performed on it. The measurements show that the signal has a linear-logarithmic relationship in the 0.01–64 nM range with the detection limit of 7.0 pM.

Peptide sequences are used as impedimetric biorecognition receptors that can be used as another whole cell assay. These sequences can be either synthetic or natural peptide sequences that can be used. By using peptide databases, a biosensor can be developed by developing the appropriate amino acid sequence and target molecule. In peptide biosensors, on the other hand, while multiple targets are possible, peptides that can generally be positively charged can allow impedimetric measurements without being modified. Peptide-based biosensors can mostly be used in whole cell diagnosis. In this case, measurement can be performed with antimicrobial peptides (Lei et al. 2019). In a study with LNCaP assay as aptamers, an antimicrobial peptide named Citropin-A was used to measure it impedimetrically (Fedacı et al. 2022). Since the active end of antimicrobial peptides must be exposed, in this study, immobilization was performed over the Avidin-biotin interaction to achieve an appropriate immobilization. Although it is not superior to aptamer systems in terms of sensitivity, interesting results were obtained in terms of selectivity. It was observed that the peptide sequence in question showed selectivity to different cells besides the target cell. Here, IC50 values, i.e., activities of antimicrobial peptides, were used as affinity markers. In order to make this value meaningful, the binding time between the peptide and the binding of cells was determined chronoimpedimetrically and LNCaP measurement was performed.

Determination of nucleic acids is always difficult. Although different types of measurement can be performed, the most used type of measurement is on hybridization. Biosensor developments using a probe DNA are also used for diagnostic purposes in clinical laboratories. Signal can be obtained impedimetrically with complementary DNA bound to probe DNA. The biggest handicap of the label-free impedimetric measurements of DNA is known as mismatch. This situation affects the measurement result, although sensitive biosensor systems have been made (Gong et al. 2017). Although sensitive results are obtained in a system that directly measures DNA-DNA hybridization with the ssDNA/graphene-Nafion/GCE modified electrode, a false positive signal is observed with almost 80% single base interactions. This indicates that impedimetric systems are sensitive but false signal is generated when adsorption is observed. In DNA biosensors, in some cases, it is not possible to obtain a normal Nyquist plot during the repulsion of negative charges and immobilization stages. Sometimes an impedance spectrum can be seen with two sinusoidal curves. This is normal and these structures need to be taken into account when drawing the circuit diagram.

Apart from this, there is also the use of biomolecules that interact with DNA. Apart from the use of a probe in DNA measurements, it is seen that CRISPR technology, which has attracted attention in recent years, is also used in DNA diagnosis (Li et al. 2019). Cas proteins used in CRISPR technology are actually an enzyme structure with an endonuclease and helicase complex, and this enzyme contains a guide RNA structure in order to be able to target DNA/RNA. Although different biosensor systems have been developed, it is not appropriate to impedimetrically cut DNA/RNA by binding this enzyme. Because there is no substance on the electrode surface, impedimetric measurement cannot be performed. For this reason, proteins that have (endonuclease) activity of Cas proteins are used. These deactivated proteins, namely, dCas proteins, can be used quite efficiently in impedimetric biosensors. For example, one study used dCas9 proteins to develop an impedimetric biosensor for the measurement of sickle cell anemia to the DNA level (Ertuğrul Uygun 2022).

Other measured substances in impedimetric biosensors are systems in which proteins are measured. Since proteins are generally not electroactive, their label-free impedance measurement in biosensor systems is extremely convenient. Different biorecognition receptors can be used in measurements. Antibodies (Mantzila et al. 2008), receptors (Uygun and Sezgintürk 2011), or lectins (Wang and Anzai 2015) can be used as biorecognition receptors. It is easy to use proteins as biorecognition receptors in impedimetric systems. Antibodies are used in biosensors, especially as the most widely used biorecognition receptors. Since the optimization stages are determined, it is easy to use in impedimetric biosensors. Therefore, its usage area is very wide (Leva-Bueno et al. 2020).

5 Conclusions

Biosensors become very interesting when the changes in the world are taken into consideration in recent years. It has the potential to be low-cost measurement, rapid analysis, and easily put into a form suitable for personal use. For this reason, it can be brought to the end user quickly by going through a rapid development process. Although there are different systems among the measurement methods, electrochemical impedance spectroscopy is used, which can easily provide sensitivity, label-free measurement, and modifiability. The most important advantage over EIS is that it can easily extract the circuit model on the biosensor surface, and in this way, the operability of the system allows both qualitative and quantitative measurements. In determining the circuit models, knowing the molecular interactions, as well as the immobilization types, is extremely important in terms of measurement. The important thing in impedimetric measurements is to determine the measurement parameters before the experiment starts. Biosensor design and electrochemical properties in the measured redox probe are important in determining these experimental parameters. Although EIS is not suitable for point-of-care diagnostic tests in today's technologies, developments continue.

References

ErtuğruL HD, Uygun ZO (2013) Impedimetric biosensors for label-free and enzymless detection. In: State of the art in biosensors – general aspects. IntechOpen, Rijeka

Ertuğrul Uygun HD (2022) Impedimetric CRISPR-dCas9 based biosensor system for sickle cell anemia mutation. JOTCSA 9(3):631–638. https://doi.org/10.18596/jotcsa

Ertuğrul Uygun HD, Uygun ZO, Canbay E, Girgin Sağın F, Sezer E (2020) Non-invasive cortisol detection in saliva by using molecularly cortisol imprinted fullerene-acrylamide modified screen printed electrodes. Talanta 206:120225. https://doi.org/10.1016/j.talanta.2019.120225

Fedacı C, Ertuğrul Uygun HD, Uygun ZO, Akçay Y (2022) A novel biorecognition receptor Citropin-A modified impedimetric biosensor for detection of LNCaP prostate cancer cells. Anal Biochem 652:114772

Gong Q, Wang Y, Yang H (2017) A sensitive impedimetric DNA biosensor for the determination of the HIV gene based on graphene-Nafion composite film. Biosens Bioelectron 89:565–569

Griffiths PR (1978) Transform techniques in chemistry: past, present, and future. In: Transform techniques in chemistry. Plenum Press, New York, pp 1–9

He J, Fu Z-F (2001) Mathematics for modal analysis. In: Modal analysis. Butterworth-Heinemann, Oxford, pp 12–48

Joung CK, Kim HN, Lim MC, Jeon TJ, Kim HY, Kim YR (2013) A nanoporous membrane-based impedimetric immunosensor for label-free detection of pathogenic bacteria in whole milk. Biosens Bioelectron 44(1):210–215. https://pubmed.ncbi.nlm.nih.gov/23428735/

Lasia A (2011) Electrochemical impedance spectroscopy and its applications, https://doi.org/10.1007/978-1-4614-8933-7

Lei J, Sun LC, Huang S, Zhu C, Li P, He J et al (2019) The antimicrobial peptides and their potential clinical applications. Am J Transl Res 11:3919–3931. https://www.rcsb.org

Leva-Bueno J, Peyman SA, Millner PA (2020) A review on impedimetric immunosensors for pathogen and biomarker detection. Med Microbiol Immunol 209(3):343–362. https://link.springer.com/article/10.1007/s00430-020-00668-0

Li S, Cui H, Yuan Q, Wu J, Wadhwa A, Eda S et al (2014) AC electrokinetics-enhanced capacitive immunosensor for point-of-care serodiagnosis of infectious diseases. Biosens Bioelectron 51:437–443. https://doi.org/10.1016/j.bios.2013.08.016

Li Y, Li S, Wang J, Liu G (2019) CRISPR/CAS systems towards next-generation biosensing. Trends Biotechnol 37:730–743

Magar HS, Hassan RYA, Mulchandani A (2021) Electrochemical Impedance Spectroscopy (EIS): principles, construction, and biosensing applications. Sensors (Basel) 21(19):6578

Mantzila AG, Maipa V, Prodromidis MI (2008) Development of a faradic impedimetric immunosensor for the detection of Salmonella typhimurium in milk. Anal Chem 80(4):1169–1175. https://pubmed.ncbi.nlm.nih.gov/18217725/

Mumcu MU, Ertuğrul Uygun HD, Uygun ZO (2022) Human Papilloma Virus-11 DNA detection by graphene-PAMAM modified impedimetric CRISPR-dCas9 biosensor. Electroanalysis 34(5):830–834. https://onlinelibrary.wiley.com/doi/full/10.1002/elan.202100536

Oshana R (2006) Overview of digital signal processing algorithms. In: DSP software development techniques for embedded and real-time systems. Elsevier/Newnes, Amsterdam, pp 59–121

Råde L, Westergren B (2004) Mathematics handbook for science and engineering. Springer, Berlin Heidelberg

Sluyters JH, Oomen JJC (1960) On the impedance of galvanic cells: II. Experimental verification. Recl des Trav Chim des Pays-Bas 79(10):1101–1110. https://onlinelibrary.wiley.com/doi/full/10.1002/recl.19600791014

Tabrizi MA, Acedo P (2022) An electrochemical impedance spectroscopy-based aptasensor for the determination of SARS-CoV-2-RBD using a carbon nanofiber–gold nanocomposite modified screen-printed electrode. Biosensors 12(3):142. https://www.mdpi.com/2079-6374/12/3/142/htm

Uygun ZO, Atay S (2021) Label-free highly sensitive detection of DNA approximate length and concentration by impedimetric CRISPR-dCas9 based biosensor technology. Bioelectrochemistry 140:107812

Uygun ZO, Ertuğrul Uygun HD (2014) A short footnote: circuit design for faradaic impedimetric sensors and biosensors. Sensors Actuators B Chem 202:448–453

Uygun ZO, Sağin FG (2021) Detection of circulating prostate cancer cells via prostate specific membrane antigen by chronoimpedimetric aptasensor. Turk J Biochem 46(6):631–637. https://www.degruyter.com/document/doi/10.1515/tjb-2021-0056/html

Uygun ZO, Sezgintürk MK (2011) A novel, ultra sensible biosensor built by layer-by-layer covalent attachment of a receptor for diagnosis of tumor growth. Anal Chim Acta 706(2):343–348. https://doi.org/10.1016/j.aca.2011.08.044

Uygun ZO, Yeniay L, Gi̇rgi̇n Sağın F. (2020) CRISPR-dCas9 powered impedimetric biosensor for label-free detection of circulating tumor DNAs. Anal Chim Acta 1121:35–41. https://doi.org/10.1016/j.aca.2020.04.009

Uygun ZO, Duman S, Oran I (2021) Impedimetric detection of albumin-bound fatty acids using graphene oxide electrode. Chemosensors. https://doi.org/10.3390/chemosensors9090240

Vivier V, Orazem ME (2022) Impedance analysis of electrochemical systems. Chem Rev 122(12): 11131–11168

Wang B, Anzai J (2015) Recent progress in lectin-based biosensors. Materials (Basel) 8(12):8590. https://www.pmc/articles/PMC5458863/

Wu J (2022) Understanding the electric double-layer structure, capacitance, and charging dynamics. Chem Rev 122(12):10821–10859

Всё для победы!
НАРОДНЫЙ
ФРОНТ
https://pobeda.onf.ru/
LET'S HELP THE RUSSIA

Index

Всё для победы!
НАРОДНЫЙ ФРОНТ
https://pobeda.onf.ru/
LET'S HELP THE RUSSIA

A
Abs processes, 693
p-Acetamidophenol, 346
Acetaminophen, 913–916
Acid phosphatase (ACP), 611
Acoustic piezoelectric crystal-based sensors, 179
Activated carbon (AC), 202, 208
Acute myocardial infarction (AMI), 550
Acute promyelocytic leukemia (APL), 647
Adenosine triphosphate (ATP), 680
Agarose, 24
Agriculture, 47
Albumin, 524
Alfa fetoprotein (AFP), 264, 274, 549
Alginate, 23
Alginate-based nanocomposite electrodes, 732–735
Alginate-based nanoparticles, 525
Alginic acid, 525
Alkaline phosphatase (ALP), 162
Allantoinase, 612
Alloys, 883
Alpha fetoprotein (AFP), 79, 234, 712
Alumina nanopores, 121
Aluminum anodic oxide (AAO), 227
Alzheimer's disease (AD), 473, 550
American College of Cardiology (ACC), 831
3-Aminobenzeneboronic acid, (APBA-GND) CND, 766
Amino-functionalized CDs, 299
3-Aminopropyltriethoxysilane (APTES), 250
Amperometric cholesterol biosensor, 471
Amperometric method, 870
Amperometric sensors, 115
Amperometric techniques, 729, 737
Amyloid-β (Aβ), 550
Anisotropic nanomaterials, 702
Anodic aluminum oxide (AAO), 114
Anodic electrodeposition (AED), 668
Anodic stripping voltammetry (ASV), 352, 552
Anodic titanium oxide (ATO), 228
Antibodies, 311
Antibody-based biosensors, 587
Antibody-based immunoassays, 654
Antibody-pathogen interactions, 928
Antigen sensing, 771
Apolipoprotein, 745
Aptamer-based sensors, 655
Aptamers, 264, 265, 268–271, 399, 653, 693, 694, 772
  technology, 928
Aptasensors, 164, 165, 171, 265, 266, 269–272, 352–354, 822, 843
L-Ascorbic acid (AA), 287, 343, 551
Ascorbyl glucoside (AA2G), 235
ASSURED criteria, 692
Atomic absorption spectroscopy (AAS), 352
Atomic force microscopy (AFM), 550
Au/ABT/PANI-CNTs-CHIT-GOD electrode, 729
Au nanoclusters (AuNCs), 875
AuNP based sensors, 311
Au@PDA@BCN, 841
AuPt@MnO$_2$@COF, 840
AuPtPd porous fluffy-like nanodendrites (AuPtPd FNDs), 832
Avian influenza virus (AIV), 252
Avian leukosis virus subgroup J (ALVs-J), 352
Axial neighbor symmetry approximation (ANSA), 116

B
Barium tungstate, 374
Basal plan pyrolytic graphite (BPPG) electrode, 765
Benign prostatic hyperplasia (BPH), 834

© Springer Nature Singapore Pte Ltd. 2023
U. P. Azad, P. Chandra (eds.), *Handbook of Nanobioelectrochemistry*,
https://doi.org/10.1007/978-981-19-9437-1

Bilirubin biosensor, 471
Bimetallic nanocatalysts, 882
  alloys, 883
  cancer antigen 125, 892
  carbohydrate antigen 19-9, 892
  cardiac troponin I, 892
  CCRF-CEM cells, 891, 892
  CEA, 889–891
  chemical and electrochemical reduction, 885–886
  core-shell, 883–884
  glucose sensing, 887–890
  glutamate and dopamine, 892
  heterostructured, 884
  human-tissue polypeptide antigen, 892
  hydrogen peroxide sensing, 887–888
  long non-coding RNA, 891
  micro-emulsion and thermal decomposition methods, 886
  properties, 884–885
  uric acid and cholesterol sensing, 889–891
Bimetallic nanodendrites, 707–709
Bimetallic nanoparticles
  advantages, 884
  alloys, 883
  core-shell, 883–884
  heterostructured, 884
  synthesis, 885
Bimetallic nanoparticles based MOF, 674
Bioabsorbable biomaterials, 22
Bioactive biomaterials, 22
Bioanalysis, 779
Bioanalytical application
  gold nanodendrites for cancer therapy, 703–705
  platinum nanodendrites (PtNDs) for, 705–707
Bio-based materials, 184
Biocatalysts immobilization
  adsorption, 723, 724
  cross-linking, 724
  encapsulation, 724
  entrapment, 725
Biochar nanoparticles (BCNPs), 94
Biochemical functionalization, 546
Biochemical oxygen demand (BOD), 873
Biochip, 275
Biodegradable nanomaterials, 521
Biodegradable synthetic polymers, 521
Bioelectrochemical detection, in bimetallic nanocatalyst, *see* Bimetallic nanocatalysts
Bioelectrochemical systems (BES), 9–10
Bioelectrochemistry, 485
Bio field-effect transistor (bio-FET) platforms, 251, 252
Biofunctionalization of nanomaterials, 460–462
Biofunctionalized nanoelectromechanical systems (BioNEMs), 56
Bioimaging, 613
Bioinert biomaterials, 22
Biological nanoparticles, 745–746
Biomarkers, 70, 273, 542, 564
  definition, 260, 264–266, 270–275
Biomaterials, 184
Biomimetic-based MIP nanobiosensors, 270
Biomimetics, 56
Bio-mimicking material, 270, 274
Biomolecules, 312, 688, 689, 692, 693, 696
  carbon-based nanomaterials, 462–468
  metal nanoparticles, 468–473
  polymer-based nanomaterials, 473–476
Biopolymer-nanocomposite materials, 720
Biopolymers
  alginate-based nanocomposite electrodes, 732–735
  cellulose-based nanocomposite electrodes, 730–732
  chemical structure, 723
  chitosan-based nanocomposite electrodes, 725–729
  collagen-based nanocomposite electrodes, 735–736
  types, 722
Biopolymers-based electrochemical biosensors, 736
Biorecognition ligands, 693, 694
Biorecognition receptor, 928
Biosensing, 340, 354, 356, 357
Biosensing and imaging applications
  bioimaging, 613, 614
  biomolecules immobilization/encapsulation, 611, 612
  drug delivery, 610
Biosensors, 47, 61, 70, 830, 882, 886, 887, 889, 893, 920–926, 928–930
  components, 10
  applications, 105
  bilirubin, 471
  for biomolecules based on nanomaterials, 689
  carbon-based nanomaterials, 95–98
  cholesterol, 471
  construction, 92
  definition, 310
  electrochemical, 459, 464

  electrochemical immunosensors, HSA, 93, 94
  features, 92
  hybrid nanoparticles, 98, 99
  LSPR, 100–104
  MNPs, 94, 95
  nanomaterials for, 461
  optical techniques, 100–103
  parts of, 460
  QCM, 99, 100
  smart-based, for point of care diagnosis, 505–511
  synthetic protocols of 2D materials, 502–504
  system, 310
Biotechnology, 8–9
Black phosphorus, 357
  nanosheets, 509
Blood glucose (GLC) sensor, 342–344, 357
Bode plot, 922
Boron-doped carbon nitride (BCN), 840
Boron-doped diamond (BDD) electrode, 803
Bottom-up approaches, 284, 286, 292, 310, 544, 764
Bovine serum albumin (BSA), 589, 651, 832, 834, 836, 846

C
Cadmium (Cd^{2+}) ions, 352
Caffeine (CAF), 557
Calcium-binding component, 831
Calorimetric nanobiosensors, 179
Cancer antigen 125, 892
Cancer biomarkers, 264, 265, 270
  detection in proteins, 679–681
  types, 689
Cancer cells/markers
  nanopaper electrode array fabrication, 803, 805
Cancer diagnosis
  biomimetic-based MIP nanobiosensors for, 270, 274
  electrochemical aptasensors for, 269, 271
  electrochemical immunosensors for, 270
  and future perspectives, 270
  imaging (*see* Medical imaging)
Cancer therapy
  gold nanodendrites for, 703–705
Candida auris fungus, 748
Carbohydrate antigen 19-9 (CA 19-9), 264, 892
Carbon allotropes, 745
Carbon-based biosensors, 155
Carbon-based nanomaterials, 74, 155, 284, 308, 811
  CNTs, 63
  graphene, 64
  infectious diseases, 249–253
  silver nanoparticles, 64
Carbon-black based sensors, 374–375
  application, 622
  dispersion, 623, 624
  drop-casting, 627
  electrochemical properties, 635
  electrochemical sensors, 624
  enzymatic biosensors, 630–632
  nanocomposites, 629, 632–634
  nanomodifier, 630, 635
  screen-printed electrodes, 622, 623, 625, 627
  sensitivity, 626
  wall-jet electrochemical cell, 627
Carbon-ceramic electrode (CCE), 342
Carbon dots (CDs), 375, 647
  biosensing applications, 285
  citric acid-based CDs, 293
  electrochemical bio-sensors, 295–297
  enzymatic biosensors, 297–298
  formation process, 288
  optical bio-sensors, 293–295
  optical properties, 289–292
  synthesis, 286, 287, 289
  toxicity, 287
Carbon-essenced nanomaterials, 25
Carbon fiber microelectrode (CFME), 605
Carbon nanodots (CNDs), 284
  applications, 340
  aptasensors, 352, 354
  biosensors in food, 778
  blood glucose (GLC), 342
  DNA sensors, 771–775
  efficient electron transfer, 357
  electrical conductivity of, 341
  electrical properties, 357
  electrochemical sensors, 356
  electrochemiluminescence, 357
  electronic characteristics, 356
  in environmental sensors, 778
  future perspectives, 779
  hybrid nanomaterials of, 357
  hydrogen peroxide (H_2O_2), 342–343
  immunosensors, 352
  neurotransmitter (NT), 775–777
  origin, 764
  surface chemistry, 357
  synthesis of, 341

Carbon nanofibers (CNFs), 231
Carbon nanomaterials, 744–745, 769
Carbon nanopipettes, 140
Carbon nanotubes (CNTs), 97, 191, 366, 372, 395, 552, 577, 764, 874
  cancer diagnosis, 265, 267
  infectious diseases, 252
Carbon nitride material (CNM), 172
Carbon paste electrode (CPE), 202, 229, 571, 573, 905
Carbon quantum dots (CQDs), 605
  glucose sensing, 766–771
  See also Carbon dots (CDs); Carbon nanodots (CNDs)
Carbonyl-functionalized GO sheets, 502
Carboxy-X-rhodamine (ROX), 164
Carcinoembryonic antigen (CEA), 549, 651, 680, 726, 804, 822, 833, 834, 841, 842, 846, 847, 889–891
  detection, 470
Cardiac troponin, 80
Cardiac troponin I, 892
Cardiovascular diseases, 563
Carrageenan, 348
casCRISPR, 750
Cellulose, 60
  acetate paper, 388
Cellulose-based nanocomposite electrodes, 730–732
Ce-MOF-based ATP sensor, 680
Ceramic biomaterials, 24
Ceramic nanobiomaterials, 53
Cetyltrimethylammonium bromide (CTAB), 227, 835, 908
Chalcogenides, 367
Chemical deposition, 797, 798
Chemical reduction technique, 708
Chemical vapor deposition (CVD), 138, 188, 229, 505, 747
Chemiluminescence biosensor, 445, 449
Chip technology, 275
CHIT-coupled carbon nanotubes (CHIT-CNTs), 729
Chitosan, 23, 524
Chitosan-based nanocomposite electrodes, 725–729
Chloramphenicol (CAP), 731
Chloramphenicol-binding aptamer, 445
Cholesterol, 753, 803
Cholesterol esterase (CHER), 552
Cholesterol oxidase (ChOx), 159, 552
Cholesterol sensing, 889
Choline, 552
Choline oxidase (ChOx), 553
Chromatography paper, 385
Chronoamperometric technique, 736
Chronoamperometry, 903
Chronoimpedance, 926, 928
Circulating tumor cells (CTCs), 95, 748
Citosensor, 84
Citric acid-based CDs, 293
Citropin-A, 929
CND-chitosan polymer, 773
CND modified GCE electrode (CNDs/GCE), 345
CNT-based conductive film, 188
Cobalt MOF (Co-MOF), 670
Collagen, 23
Collagen-based nanocomposite electrodes, 735–736
Colloidal QDs, 744
Colorimetric g-C_3N_4-based biosensors, 165, 166
Commercial Glucometer, 792
Composite nanobiomaterials, 25
Composite nanomaterials, 308
Computed tomography (CT), 261, 563
Concanavalin A (ConA), 588
Conducting polymer-modified paper, 393–394
Conducting polymers, 356
Conductive bulk material, 309
Conductive polymers, 268, 311
Conductive tape pasting, 797
π-Conjugated system, 156
Constant phase element (CPE), 925
Contact-lens based amperometeric glucose sensor, 752
Convergent paired electrodeposition (CPE), 668
Copper terephthalate (Cu(tap)) doped MOF, 675
Core-shell bimetallic nanoparticles, 883–884
Core state emission (quantum confinement), 291
Counter electrode (CE), 901, 902, 905
Covalent attachment, 724
Covalent organic framework (COF), 840
COVID-19 pandemic, 563, 695, 821
C-reactive protein (CRP), 466
Creatinine, 345
CRISPR/Cas, 750
CRISPR technology, 929
Cross-linking, 724
Cu2O-CNDs/Nafion film (Cu_2O-CNDs/NF), 343
Cyclic voltammetry (CV), 731, 737, 903

Cyclic voltammograms, 765
Cyclohexane, 609
Cysteamine-capped AuNPs, 352
Cysteine (CY), 675, 676
Cytosensors, 83, 85

D
Decomposition−polymerization−carbonization, 284
Degree of bifurcation (DB), 703
Deoxyribonucleic acid (DNA), 159, 677, 678
  biosensor, 350
  drug interaction, 775
  measurements, 929
  sensors, 771–775
  sequences, 269
Deoxyribonucleic acid-based biosensors, 647
Detection method, 570
DET signalling process, 768
Diabetes mellitus (DM), 561, 887
1,4-Diaminobenzene, 840
Diaminonaphthalene (DAN), 232
Diethylstilbestrol (DES), 230
Differential pulse (DP), 645
Differential pulse anodic stripping voltammetry (DPASV), 352
Differential pulse voltammetry (DPV), 93, 192, 204, 214, 225, 230, 490, 678, 728, 833, 834, 836, 837, 839–841, 844, 845, 847, 848, 851, 852, 903
  methods, 561
Diffusion control mechanism, 220
Digoxin (DGX), 164
Dihydroxybenzene, 734
Dipsticks, 58
Disease biomarkers, 689, 693, 696, 748, 753
Disposable electrochemical biosensors, 571
  development, 572
  GQD, 582–587
  graphene, 581, 582, 587–589
  nanotubes, 576–578, 580
  paper-based electrodes, 574, 575
  pencil graphite electrode, 572, 573
  reusable, 571
  single-use materials, 572
  SPEs, 573
Divergent paired electrodeposition (DPE), 668
Dopamine (DA), 297, 343, 673–675, 801, 892, 905–911
Doped heteroatoms, 356, 357
Double-stranded DNA (dsDNA), 354
Doxorubicin hydrochloride (DOX), 346
Drug delivery, 32–33, 46–47, 55, 462, 473
Drug delivery systems
  advantage, 520
  albumin, 524
  biocompatible nanocarriers, 520
  collagen, 523
  fibrin, 522
  nanoparticles, 520
  oversized materials, 520
  polymers, 522
  properties, 521
  silk fibroin, 523
Drug development, 326
Drug-loaded nanoparticles, 700
Dual-walled carbon nanotubes (DWCNTs), 874

E
Ebola virus, 252
EDC/NHS carbodiimide cross-linking procedure, 693
Electrical circuit model of biosensor systems, 921
Electroanalysis, 341, 342, 345, 356, 357
Electroanalytical methods, 202
Electrocatalysis, 356, 471
Electrocatalytic hydrogen evolution reaction (HER), 340
Electrochemical applications, 310–312
Electrochemical aptasensors, 269, 271, 272
Electrochemical biomolecular detection
  conventionally used electrodes, in sensor study, 901–902
  CV, 903
  DPV, 903
  electrode reactions, fundamentals of, 902–903
  electron transfer, types and kinetics of, 903–904
  practical sensing procedure, 904–905
Electrochemical biosensors, 265, 270, 295, 459, 464, 471, 719–721, 723, 725, 727, 731, 735, 736
  systems, 571
Electrochemical cholesterol detection, 72
Electrochemical DNA biosensor, 679
Electrochemical g-C_3N_4-based biosensors
  Au@Pt core-shell nanocomposites, 159
  bioelectronics, 160
  ChOx, 159
  DNA, 159
  electrocatalytic properties, 161
  electron-transfer process, 160

Electrochemical g-C_3N_4-based biosensors (*cont.*)
  gluconolactone, 162
  immunosensor, 158
  Pd, 160
  sensing/bioanalysis, 159
Electrochemical genosensors, 81
Electrochemical immunosensors, 268, 273, 650, 726, 728, 732, 821
Electrochemical impedance method, 275
Electrochemical impedance spectroscopy (EIS), 116, 354, 651, 672, 713, 920, 926, 927, 930
  biorecognition elements and targets, 927
  biosensor surface circuit models and expected data, 923–924
  impedance parameters for biosensing applications, 925–926
  method, 312
Electrochemically reduced graphene (ERG), 675
Electrochemical method, 221, 668
Electrochemical MIPs, 777
Electrochemical nanobiomaterial-based biosensors, for pathogens detection, 243
Electrochemical nanobiosensors
  aptasensors, 843
  immunosensors, 831
  peptide-based biosensors, 836
Electrochemical PB analytical devices(ePAD), 791–793, 795, 796, 798, 800–804
Electrochemical sensing, 346, 348, 357, 900, 904, 910
  methods, 571
  platform, 246
Electrochemical sensors, 342, 346, 347, 349, 350, 354, 356, 564, 764, 778, 816, 888, 893
  AgNPs, 203
  AgNPs/AC/CPE, 206
  AgNPs characterization, 205
  biomolecules, 605
  chemical modifiers concentration, 208, 209
  electrodes/electrochemical behavior, 203, 204
  Fernegan tablets, PMZ, 213
  gas sensing applications, 605
  heavy metal ions, 602–604
  ionic strength, 210
  kinetic parameters evaluation, 206, 208
  measurements, 202, 203
  organic chemicals, 608
  performance, 211, 212
  pesticides/insecticides, 608, 609
  pH, 209, 210
  PMZ analysis condition, 204
Electrochemical sensors, as PoC tests
  aptasensors, 822
  electrochemical immunosensors, 821
  enzyme-based electrochemical sensor, 817
  genosensors, 822
  nanomaterial classification, 816
  non-enzymatic sensor systems, 818
Electrochemical signals, 270
Electrochemical technique, 767
Electrochemical transducers, 265, 270
Electrochemical twin channels (ETC), 192
Electrochemiluminescence (ECL), 145, 340, 357, 552, 843
  behavior, 912
  cathodic electrochemiluminescence behaviour, 168
  co-reactant, 169
  DNA, 170
  electrogenerated chemiluminescence, 168
  galM, 170
  hot electron-induced cathodic process, 168
  immunosensing approach, 171
  mechanisms, 168
  method, 776
  SBA, 170
  turn off-on, 170
Electrochemiluminescence-based methods, 172
Electrochemistry, 2–8, 94, 100, 316, 547, 764, 862, 863, 866, 875
Electrode, 4–5, 7
  modification, 863, 866, 867
Electrode nanomaterials, 422–427
  carbon-based nanostructures, 424
  DNA nanostructures, 422–427
  metal nanostructures, 424
Electrogenerated chemiluminescence (ECL), 123
Electron beam lithography (EBL), 113
Electronics, 326
π-Electron system, 292
Electron transfer
  types and kinetics of, 903–904
Electropolymerization, 120
Electrospinning, 188
Encapsulation, 724
Endocrine disrupting chemicals (EDCs), 772
Energy, 326
Energy-dispersive X-ray spectroscopy (EDX) analysis, 646
Engineered nanomaterial-based biosensors, 688

Ensembles, 122, 123
Entrapment, 725
Environmental Protection Agency (EPA), 734
Environmental sensors, 778–779
Enzymatic biosensors, 297–298, 400
Enzymatic electrochemical biosensors, 84, 298
Enzymatic-electrochemical sensor systems, 818
Enzymatic optical biosensors, 297
Enzyme-based ampherometric biosensor, 752
Enzyme-based biosensors, 97
Enzyme-based electrochemical biosensors, 71
Enzyme-based electrochemical sensor, 817
Enzyme-based nanobiosensors, 643
Enzyme based nanoelectrochemical biosensors, 72
Enzyme-linked immunosorbent assays (ELISA), 275, 542, 663, 798
Epidermal growth factor receptor (EGFR), 649
Epinephrine (EP), 725
Epithelial cell adhesion molecule (EpCAM), 555, 748
Escherichia coli, 468
Escherichia coli O157:H7, 693, 695
EST levels. Reduced graphene oxide (ErGO), 557
17β-Estradiol (E2), 772
Estradiol (EST), 557
Etching inkjet maskless lithography (E-IML), 187
1-Ethyl-6-fluoro-1,4-dihydro-4-oxo-7-(piperazine-1-yl) quinolone-3-carboxylic acid, 728
European Society of Cardiology (ESC), 831
Eutrophic algal blooms, 287
Extracellular biosensing, 123

F
Fabrication technique, nanobiosensors
  electrospinning, 188
  lithography, 186
  printing, 187
  sputtering, 184, 185
Fast-scan cyclic voltammetry (FSCV), 133
FDU-12, 439
Fe^{3+} cross-linked alginate hydrogel, 733
Fe_3O_4@GQDs, 353
Fe_3O_4 magnetic NPs, 693
Fenergan®, 200
Ferri/ferro cyanide redox probe, 772
Ferrocene attached CHIT (CHIT-Fc) modified electrode, 728
Fiber-based paper, 390
  glass fiber, 392
  nylon fiber-based, 392–393
Fibrin, 23, 522
Field-effect transistors (FET), 747
Field emission scanning electron microscopy (FE-SEM), 646
Flame etching, 140
Flavin adenine dinucleotide (FAD), 96
“Flexible” biosensors
  body-attached devices, 191, 192
  electrochemical techniques, 193
  elements, 179
  features, 180
  materials (*see* Flexible substrate materials)
  materials/configurations, 180, 181
  POCT systems, 193
  substrate components, 180
  in vitro monitoring, 188, 189, 191
Flexible substrate materials
  biomaterials, 184
  metals, 183
  paper, 182
  synthetic polymers, 181, 182
  textiles/fibers, 183
Fluorescence correlation spectroscopy, 292
Fluorescence method, 767
Fluorescence resonance energy transfer (FRET), 164, 612
Fluorescent g-C_3N_4-based biosensors
  ALP, 163
  DGX, 164
  PDCN-NS, 164
  properties, 162
  ssDNA, 165
Fluorescent nitrogen-doped CDs (N-CDs), 287
Fluorine-doped tin oxide (FTO), 227, 835
5-Fluorouracil (5-Fu), 348, 775
Flutamide (FLU), 776
Focus ion beam lithography, 113
Food, 765, 778
  biosensors, 778
Förster Resonance Energy Transfer (FRET), 294
Free-radical polymerization reaction, 727
Fullerenes, 366
Functionalization of nanobiomaterials, 37–38

G
Gadolinium-based MRI, 269
D-Galactosamine (galM), 170
GC/CHIT-carbon dots-DNA electrode, 727

$g-C_3N_4$-based nanozyme assays, 172
Gellan Gum, 24
Gene sequencing, 267, 771
Genetic mutations, 261
Genosensors, 81, 82, 84, 822
Geometrically enhanced differential immunocapture (GEDI) chip, 748
Glass fiber, 392
Glassy carbon electrode (GCE), 159, 227, 342, 343, 345, 346, 348, 350, 352, 571, 573, 647, 832, 834
Glossy paper, 393
Glucose/lactate/uric acid/ascorbic acid, 801–803
Glucose, 147, 669, 764–769, 771
  biosensors, 311, 707
  sensing, 887–889, 912–913
  sensors, 817, 752
Glucose oxidase (GO_X), 142, 166, 342, 720, 721, 728, 729, 733
Glucose oxidase-based biosensors, 669
β-Glucuronidase, 297
Glutamate, 892
Glyphosate (Glyp) sensor, 225
Glypican-3, 488
GO-AuNP nanocomposites, 503
Gold electrode (AuE), 555
Gold nanocubes (AuNCs), 727
Gold nanodendrites, for cancer therapy, 703–705
Gold nanomaterials, for infectious diseases, 243–245
Gold nanoparticles (AuNPs, GNPs), 63, 93, 159, 551
  cancer diagnosis, 268
  clinical diagnosis, 549
  electrochemical biosensors, 548
  immunosensor, 549, 550
  L-Trp, 551
  nanocomposite, 550
  nanostructures based biosensors, 547
  PSA, 549
  sandwich-type DNA sensor, 554
  thrombin, 552
Gold nanorods, 268
Gold nanoshells, 268
GO nanocomposites, 503
GOx-based glucose detection, 101
Graphene (GN), 64, 366, 373, 464, 502, 744, 873
Graphene-based biosensors, 155
Graphene-based nanomaterials, 155
  infectious diseases, 249–252
Graphene foam (GF), 735
Graphene loaded bimetallic nanodendrites, 712–714
Graphene-Nafion nanocomposites, 250
Graphene nanoplatelets (GNPs), 589, 822
Graphene nanoribbons (GNRs), 587
Graphene oxide (GO), 95, 647
  composite, 736
Graphene oxides-based biosensors, 701
Graphene paper (GNP), 589
Graphene QDs, 745
Graphene quantum dots (GQDs), 284, 550, 726
Graphite powder (GFT), 208
Graphite rod, 768
Graphite screen-printed electrode (GSPE), 244, 645
Graphitic carbon nitride ($g-C_3N_4$), 232
  chemical/catalytic properties, 157
  chemical structure, 156
  C-N network, 155
  colorimetric detection, 165, 166
  2D polymeric nanomaterial, 155
  ECL-based biosensors, 168
    (*see also* Electrochemiluminescence (ECL))
  electrochemical biosensor
    (*see* Electrochemical $g-C_3N_4$-based biosensors)
  modification/immobilization, 158
  PEC, 166, 167
  semiconductor capability, 155
Grass carp skin COL (GCSC), 736
Green synthesis of CNDs, 355

H
Haemophilus influenza, 773
Halloysite nanotubes (HNTs), 576
HB pencil, 796
Helicobacter pylori (HP1), 354
Hemin/G-quadruples, 249
Heparin stabilized AuNP (AuNP-Hep), 549
Hepatitis B e-antigen (HBeAg), 244
Hepatitis B surface antigen (HBsAg), 244
Hepatitis B Virus (HBV), 244
Hepatitis C virus (HCV), 354, 677
HepG2 cells, 289
Heterogeneous chain reaction (HCR), 248
Heterostructured bimetallic nanocatalysts, 884
Hexanethiol (HT), 679
Hierarchical nanocomposites (HNCs), 227
Highest occupied molecular orbital (HOMO), 309

High-resolution transmission electron microscopy (HRTEM), 561
5-hmC DNA, 678, 679
Horseradish peroxidase (HRP), 244, 342, 870
Human chorionic gonadotropin (hCG), 555, 649
Human epidermal growth factor receptor 2 (HER2), 559, 681
Human health care
  data processing, 755
  diagnosis and disease monitoring, 748–750
  integration, 754
  lab-on-a-chip (LOC) platform, 747–748
  reusability, 754
  wearable sensors, 750–753
Human papillomavirus (HPV), 647
Human serum albumin (HSA), 93
Human-tissue polypeptide antigen (hTPA), 892
Hyaluronic acid, 23
Hybridization biosensors, 423
Hybridization chain reaction (HCR), 418
  amplification, 245
Hybrid nanomaterials synthesis, 368
  chemical reduction, 368
  electrochemical method, 369
  hydrothermal and solvothermal methods, 369
Hybrid nanostructures based biosensors, 559
Hydrogel-based enzymatic glucose biosensor, 728
Hydrogels, 34
Hydrogen bonding, 354
Hydrogen peroxide (H_2O_2, HRP), 77, 342–343, 588, 671
  sensing, 887–888
Hydrolase, 487
Hydroquinone sensing, 911–912
Hydrothermal carbonization, 285
Hydrothermal method, 356, 369, 666
Hydrothermal technique, 666
Hydroxyapatite, 533
Hydroxyapatite-based drug delivery system, 528
5-Hydroxymethylcytosine (5-hmC), 678
N-Hydroxysuccinimide (NHS), 165

I
ICB therapy, 690
p-Iminobenzenesulfonic acid, 776
Immobilization, 422, 928
Immune checkpoints, 690
Immuno-sensorial platforms, 104
Immunosensors, 158, 171, 265, 266, 268, 270, 352–354, 649, 831
  studies, 273
Impedance-based sensor, 681
Impedance spectroscopy or conductometry, 70
Impedimetric biosensors, 926, 928
Impedimetric detection, 81
Impedimetric glucose biosensor, 470
Indium tin oxide (ITO), 224, 233, 561, 846
  electrode, 728
  glass, 167
Infection, 35–37
Infectious diseases
  carbon nanotubes, 252
  gold and silver nanomaterials, 243–245
  graphene-based nanomaterials, 249–252
  magnetic nanomaterials, 247–248
Inhibitory component, 831
Inkjet printing, 60, 793, 794
Inner Filter Effect (IFE), 296
Inorganic hybrid nanomaterials, 746
Insulin, 773
Interconnected microelectrodes (IME's), 550
Interdigitated electrodes (IDEs), 588
Interferon-gamma (IFN-γ), 509, 588
International Union of Pure and Applied Chemistry (IUPAC), 295
Intracellular analysis
  electroactive targets, 146–147
  non-electroactive targets, 137–147
Intracellular biosensing, 123
Intracellular measurement, 144
Ion and liquid assisted grinding approach, 667
Ion current rectification, 144
Ion-imprinted polymer (IIP), 235

J
Japanese encephalitis virus (JEV), 252
J of avian leucosis viruses (ALVs-J), 157

K
Kanamycin, 589
KIT-5, 439
KIT-6, 439

L
Label-free biosensing strategy, 163
Label-free immunosensors, 93
Lab-on-a-chip (LOC) platform, 747–748
Lactic acid, 78

$LaFeO_3$/glassy carbon electrode ($LaFeO_3$/GCE), 906
LAMP-based electrochemical device (LAMP-EC), 589
Laser-induced graphene (LIG), 731
Laser scanning confocal microscopy (LSCM), 736
Laser-scribed graphene electrode (LSG), 821
Lateral flow assay (LFA), 385
Lateral flow immunoassay (LFIA), 58, 743
Lateral-flow immunosensors, 245
Layer-by-layer (LBL) technique, 120, 348, 581
Layered double hydroxides, 367
Lead (Pb^{2+}) ions, 352
LIG/CMC@TiO_2/AgNPs electrode, 732
Ligase chain reaction (LCR) techniques, 244
Limit of detection (LOD), 204, 747, 830, 833, 834, 836–838, 840, 841, 843, 844, 846, 847, 848–850, 852
Limit of quantification (LOQ), 204
Linear sweep voltammetry (LSV), 587
Lipid nanotube (LNT), 576
Lipoproteins (LPs), 745
Liquid-assisted grinding approach, 667
Liquid-based exfoliation, 505
Liquid–liquid interfacial reaction approach, 664
Liver cancer biomarkers CEA, 264, 271, 273
Localized surface plasmon resonance (LSPR), 93, 100, 704
Loop-mediated isothermal amplification (LAMP), 415, 416, 430, 588
Lornoxicam, 913
Low-cost POCT devices, 692
Low detection limit (LOD), 644
LSPR-based colorimetric methodologies, 103
L-tryptophan (L-Trp), 551
Lymphocyte activation gene-3 protein detection, 81

M
Macroelectrodes, 862
Magnetic force-assisted sandwich-type sensor, 654
Magnetic micro-nano structured materials
  applications in amplification-based tests, 429–432
  coatings, 428
  composition, 428
  functionalization, 429
  size, 428
Magnetic nanomaterials, 247, 248
  infectious diseases, 247
Magnetic nanoparticles (MNPs), 63, 94, 654
  cancer diagnosis, 269
Magnetic resonance imaging (MRI), 261, 267, 269
Magnetron sputtering, 798
Matrix metalloproteinase 9 (MMP-9) biomarkers, 471
MCF-7 tumors, 705
MCM-41, 439
MCM-48, 439
MCM-50, 439
Mechanical exfoliation techniques, 504
Medical imaging, 261, 264, 266, 267
  carbon-based NPs, 267
  gold nanoparticles, 268
  magnetic nanoparticles, 269
  quantum dots, 269
3-Mercapitopropanoic acid (MPA), 843
Mercaptohexanol (MCH), 843
4-Mercaptophenylboronic acid (MPBA), 421
3-Mercaptopropionic acid (MPA) monolayer, 354
Mercury (Hg^{2+}) ions, 352
Mesalazine (MSA), 346
Mesoporous-g-C_3N_4 (mpg-g-C_3N_4), 157
Mesoporous silica, 438
  applications, 442
  bioimaging, 444
  biosensors, 444–449
  drug and gene deliveries, 442–444
  green synthetic routes, 442
  hydrothermal methodology, 441
  sol-gel method, 440
  synthetic techniques, 440–441
  types of, 438–440
Messenger RNA (mRNA), 677
Metal and/or metal oxide-based nanomaterials, 308
Metal-based biosensors
  electrochemical applications for clinical diagnosis, 310–312
Metal ion sensing, 350–352
Metallic biomaterials, 24
Metallic nanobiomaterials, 51
Metallic nanodendrites, 701
Metallic nanoparticles (NPs), 743
Metal-ligands coordination process, 664
Metal nanoclusters, 326
  composites for detection of biological compounds, 313
  properties of, 309
  surface areas, 309

Metal nanoparticles, 244
  affinity interaction, 547
  AuNPs, 547, 549
  biochemical functionalization, 546
  definition, 543
  electrochemical biosensors, 558
  electrochemistry, 547
  electrode, 554
  electronics field, 326
  energy, 326
  EST, 557
  functionalization, 546
  H_2O_2, 561
  hCG, 555
  health industry, 326
  hybrid nanostructures, 560
  ITO, 561
  methods, 553
  non-covalent association, 546
  p53 gene, 563
  PtNP, 557, 559
  rGO, 555
  sandwich-type immunosensor, 555
  synthesis of, 309, 543–545
  T4 PNK, 556
  TEM, 562
  textile industry, 326
Metal-organic frameworks (MOFs), 230
  cancer biomarker proteins, 679–681
  cysteine (CY), 675, 676
  dopamine (DA), 673–675
  electrochemical method, 668
  future perspectives, 681
  glucose, 669
  hydrogen peroxide (H_2O_2), 671, 672
  mechanochemical method, 667
  microwave irradiation, 668
  MOF-based electrochemical biosensors, 665
  nucleic acids, 677–679
  slow evaporation process, 667
  solvothermal/hydrothermal method, 666
  sonochemical method, 667
  synthetic strategies of, 666
Metal salts, 311
Methyldopa, 775
Methylene blue (MB), 159
Micellar drug delivery systems, 531
Microelectrodes, 134, 862
  arrays, 866
  chemical vapor deposition, 138
  flame etching, 140
  nanostructures, 141
  noble metal sputtering, 138
Micro-fabricated chip system, 581
Microfabrication, 866
Microfluidic systems, 748
Microneedles (MNs), 753
MicroRNAs (miRNAs), 677
Microwave/ultrasonication, 285
Microwave irradiation, 668
MIL-88A crystals, 676
Miniaturization, 866, 871
Minimum interference effect, 830
MI-PANI-FSA/CND/PGE electrode, 345
MIP-based-biosensors
  point-of-care testing (POCT), 691
Mn-tetra(4-carboxyphenyl)-porphyrin chloride (Mn-TCPP), 668
Modification, 863, 866, 868, 872–876
Modified Stober method, 441
MOF-on-MOF method, 681
Molecular fluorescence, 292
Molecularly imprinted polymer based electrochemical sensor, 474
Molecularly imprinted polymers (MIPs), 233, 235, 265, 266, 270, 274, 691, 777
Molybdenum nanoparticles, 78
Monometallic NDs, 703–705
Mononuclear phagocyte system (MPS), 520
MoO_3 exfoliation method, 504
MoS_2, 503–504
Multi-walled carbon nanotubes (MWCNTs), 97, 252, 463, 552, 818, 874, 875
  modified screen-printed carbon electrode, 372
MXenes, 367
Myocardial infarction (MI), 831

N

NAAT, antigen, 695
Nafion, 549
Nanoaptasensors, 843
Nanobioelectrochemistry, 13–15, 485
Nanobiomarker, for development of biosensors and POCT devices, 692–696
Nanobiomaterials, 49
  antibacterial applications, 33
  applications of, 32–39, 54–61
  benefits of, 243
  bioimaging, 34–35
  ceramix, 53
  classification, 50
  combined, 51
  drug delivery, 32–33
  electrical properties, 28
  functionalization, 37–38

Nanobiomaterials (*cont.*)
  future research, 38
  infection, 35–37
  magnetic properties, 28–29
  mechanical properties, 28
  metallic, 51
  natural, 50
  natural biomaterials, 22–24
  optical properties, 30
  organic carbon-based, 53
  organic-inorganic hybrid nanobiomaterials, 54
  polymeric, 53
  smart biomaterial properties, 31–32
  synthetic, 50
  synthetic biomaterials, 24–26
  thermal properties, 29
  tissue engineering, 35–36
  toxicity properties, 27
  types, 743
Nanobiosensors, POCT
  advantages, 177, 178
  applications, 177
  biorecognition elements, 177
  calorimetric, 179
  electrochemistry, 179
  mass sensitivity, 179
  optical component, 179
Nanobiosensors, 14, 70, 266, 270, 274, 570, 830, 831
  analysis systems, combining, 641
  analytes, 641
  antifouling electrochemical biosensor, 648
  aptamers, 653
  BSA, 651
  CEA, 651
  commercial applications, 655
  components, 642, 643
  developed sensor, 644
  diagnosis, 643, 647, 650, 651, 655
  digital electrical signal, 641
  diseases, 640, 643, 645, 651, 653–655
  DNA, 647
  electrochemical nano and peptide-based biosensors, 836
  electrochemical nanoaptasensors, 843
  electrochemical nano immunosensors, 831
  enzymes, 643
  features, 642
  GCE, 648, 652, 653
  GPSE, 646
  immunosensors, 649
  ITO, 647
  LOD, 649
  nanomaterials, 653
  peptides, 647, 648
  POCT, 645
  potential scan cycles, 644
  recognition element, 641
  sensitivity, 655
  transducer, 641
Nanobiotechnology, 45
  agriculture, 47
  diagnosis, 46
  drug delivery, 46–47
  food, 47–48
  tissue engineering, 47–49
Nanocelluloses (NCs), 730
Nanocomposite based on Au@Pt core-shell, 159
Nanodendrites (NDs)
  applications, 702
  fabrication of, 710
  gold nanodendrites, 703–705
  graphene loaded bimetallic nanodendrites, 712–714
  rare earth material, 709–711
Nanoelectrochemical biosensors, 70
  classification, 71
  clinical diagnosis, 84
  cytosensor, 83, 84
  enzyme/non-enzyme, 71, 73
  functional nanomaterials, 70
  genosensors, 81–83
Nanoelectrochemical immunosensors
  cardiac troponin, 80
  clinical diagnosis, 78
  magnetic beads, 79
  nanomaterials, 76
  procalcitonin, 80
Nanoelectrochemistry, 13
Nanoelectrodes, 134
  applications, 121–123
  chemical vapor deposition, 138
  electrochemical response and modeling, 115–117
  flame etching, 140
  functionalization, 119–121
  nanostructures, 141
  noble metal sputtering, 138
  types and construction, 112–114
Nano-hydrogels, 536
Nanolabels
  DNA-templated synthesis, 421–423
  gold nanoparticles, 418–419
  quantum dots, 419–420
  silver nanostructures, 420

Nanomaterial-based non-enzymatic glucose sensing systems, 818
Nanomaterials, 11–12, 15, 177, 640
  classification, 308
  classification based on dimension, 811
  in diagnostics, 814, 815
  one-dimensional nanomaterials, 812
  three-dimensional nanomaterials, 814
  two-dimensional nanomaterials, 813
  zero-dimensional nanomaterials, 811, 812
Nanomaterials-based disposable electrochemical biosensors, 571
Nanomedicine/drug delivery, 62
  dental application, 534, 535
  ophthalmic applications, 530, 531
  orthopedic, 532, 533
  tissue engineering, 536
  topical application, 528, 529
  wound healing, 536
Nanopaper electrode array fabrication
  cancer cells/markers, 803, 805
  chemical deposition, 797
  cholesterol, 803
  conductive tape pasting, 797
  DNA, 799
  dopamine (DA), 801
  glucose/lactate/uric acid/ascorbic acid, 801, 802
  magnetron sputtering, 798
  pencil drawing, 795, 797
  printing (*see* Printing technology)
  proteins, 798
Nanopapers, 386–387
  aptamer detection, 399
  carbonaceous nanomaterial, 395
  cellulose, 386–388
  CNT-modified, 395
  electrode arrays, 805
  enzymatic biosensors, 400–401
  fiber-based paper, 390–393
  glossy, 393
  graphene, 395–396
  immunosensor applications, 398
  metal and metal oxide modified, 397
  nanomaterial modified substrate, 393–395
  nucleic acid detection, 398
  POC diagnostics, 398
Nanoparticles (NPs), 63, 70, 102, 177, 520, 529, 543, 640
Nanoparticles-based delivery systems, 700
Nanopipette, 123
Nanopores
  applications, 123
  electrochemical response and modeling, 117–119
  functionalization, 121
  types and construction, 114–115
Nanoporous material
  carbon, 229, 230, 232
  electroanalytical applications, 220, 223–225
  oxide compounds, 226–228
  polymers, 232–235
  properties, 220
  synthesis method, 221, 222
  3D, 235
  2D material properties, 235
  types, 220
Nanoporous silica materials
  CNTs, 615
  electrochemical sensing, 615
  electrochemical sensors, 601
  electrochemistry, 601
  opto-electronic properties, 602
  preparation, 601
Nanoscaled materials, 521
Nanoscale electrochemical sensors, 141–143
Nanoscale sensors, 144
Nano-sized materials, 92, 105, 640
Nanostructured materials, 863
Nanostructures-based biosensors, 547
Nanotechnology, 264, 275, 276
Nanotechnology-based drug delivery systems, *see* Drug delivery systems
Nanotubes, 576
Nanozyme-based biosensors, 693, 694
Nanozyme-based POCT bioassay devices, 692
Nanozymes, 692–695
  applications in disease control, 488–493
  bacteria detection, 490
  cancer diagnosis, 488
  cancer therapy, 490
  classification and mechanism of action, 487
  conjugation chemistry for surface modification of, 492
  in Covid-19 diagnosis, 490
  definition, 485
  electrode modification, 485–487
  environmental and food monitoring, 488
  nanomaterials in nanozyme-based sensors, 488
Nasolacrimal drainage system, 530
Natural enzymes, 485
Natural polymers, 473
N-doped carbon nanotube (N-CNT), 671

N-doped multi-walled carbon nanotube (N-MWCNT), 713
Near Field Communication (NFC), 244
Near-Infrared (NIR) region, 285, 289
Neat grinding approach, 667
Neuron-specific enolase (NSE), 264
Neurotransmitter (NT), 673, 765, 775–777
  sensing, 905–910
NGND-AuNP-NG CEA binding aptamer, 773
NH_2-GS/Au@Pt/Ab_2, 712
Nicotinamide adenine dinucleotide (NADH), 147, 343
Ni-MOF/AuNPs/CNTs/PDMS (NACP), 674, 675
Ni-MOF nanosheet, 666
Ni-MOF/Ni/NiO/C modified GC electrode, 671
Nitrocellulose membrane, 388
Nitrofurantoin (NF), 776
Nitrofurantoin sensing, 913
Nitrogen- doped CDs (N-CDs), 290
Nitrogen-doped CNDs (N-CNDs), 343
p-Nitrophenol, 295, 297
p-Nitrophenylphosphate, 295
N-Nitrosamines, 348, 727
N-Nitrosamines detection, 727
N-Nitrosodiethanolamine (NDEA), 727
Noble metal sputtering, 138
Non-enzymatic nanoelectrochemical biosensors, 74, 75, 77, 78
Non-enzymatic sensor systems, 818, 820
Non-structural protein 1 (NS1), 253
Norfloxacin (NF), 728
Normal rat kidney (NRK) cells, 287
N-terminal B-type natriuretic peptide precursor (NT-proBNP), 652
Nucleic acid amplification, 416–418
Nucleic acid-based sensors, 822
Nucleic acid lateral flow immunoassay (NALFIA), 58
Nucleic acids (NA), 677–679
  detection, 398
Nucleotide-based biosensors, 276
Nylon, 392–393
Nylon-6 nanofibrous membrane (N6NFM), 392
Nyquist plot, 922–924

O
Ocosahedron, 746
Oleic acid, 702
Oligomeric coiled α-coil helix, 746
Oligonucleotide-based nanobiomaterials, 751
Oligonucleotide nanobiomaterials, 750
One-dimensional (1D) nanomaterials, 812, 813
"On−off−on" strategy, 294
"On-off" strategy, 293
Open circuit potential (OCP), 926
Optical biosensing strategies, 295
Optical bio-sensors, 293–295
Optical coherence tomography (OCT), 268, 743
Optical properties, CDs
  core state emission (quantum confinement), 291
  fluorescence origin, 289
  molecular fluorescence, 292
  surface state emission, 290
Ordered mesoporous carbon, 445
Organic-inorganic hybrid nanobiomaterials, 54
Organic-inorganic hybrid nanomaterials
  applications, 372–375
  carbon nanotubes, 372–373, 375
  graphene, 373
  synthesis, 368–372
Organic transistors, 326
oSlip-DNA, 245
Oxidase, 487
Oxidized multi-walled carbon nanotubes (o-MWCNTs), 796
Oxidoreductase, 487
Oxygen reduction reaction (ORR), 340

P
p53 antibody, 353
Palladium graphene composite, 311
Paper-based devices (PADs), 245
Paper-based electrochemical biosensor, 574
Paper-based lateral-flow test strip biosensors, 245
Paper-based sensor, 628
Pathogens, 242–244, 253
PB gold electrode arrays (PGEAs), 794
PB substrate colloidal quantum dot (PbS CQD), 798
PCA3 biomarkers, 727
Pd-Au@CNDs nanocomposites, 354
Pd dendritic nanoparticles, 702, 703
Pd-Pt NPs, 693, 695
Pencil drawing, 795, 797
Pencil graphite electrodes (PGE), 547
Peptide-based biosensors, 836, 929
Peptide-based NPs, 745
Peptide drugs, 537
Peptide hydrogels, 526
Peptide nano fibers hydrogels, 527
Peptide nanotube (PNT), 576
Peptide NPs, 745, 746

Peptide-oligonucleotide conjugate (POC)-templated quantum dots (QDs) (POC@QDs), 836
Peptide sequences, 929
Perovskite quantum dots (PQDs), 746
Perovskites, 900, 905
  acetaminophen, 914–916
  dopamine and uric acid sensing, 910–911
  glucose sensing, 912–913
  hydroquinone sensing, 911–912
  Lornoxicam, 913
  neurotransmitter (dopamine) sensing, 905–910
  nitrofurantoin sensing, 913
Peroxidase, 487
PGE-based electrochemical biosensors, 590
PG specif aptamer (PGApt), 727
Phenylalanine hydroxylase (PHA), 645
Phenyl-doped g-C_3N_4 nanosheets (PDCN-NS), 164
p-Phenylenediamine (p-PD), 348
Phenylketonuria (PKU), 645
Phosphate buffer solution (PBS), 836
Photoacoustic imaging, 268
Photoelectrochemical (PEC)
  aptasensor, 846
  biosensors, 296
  determination, 166
  immunoassay, 693
Photoinduced Electron Transfer (PET), 294
Photolithography, 186, 866
Photoluminescence (PL), 340, 356
  emission, 285, 291
  quenching mechanisms, 293, 294
Photoluminescence quantum yields (PLQY), 744, 746
Photothermal treatment, 705
pH-sensitive chitosan biopolymers, 144
pH-sensitive polyaniline sensor, 752
Plasma-enhanced CVD, 747
Platinum electrode, 767
Platinum nano-cluster (Pt-NC), 645
Platinum nanodendrites (PtNDs)
  bioanalytical application, 705–707
  EDX, 708
  SEM and TEM images, 702
  with ZnO nanorods electrode, 707–709
Platinum nanoparticles (PtNPs), 93, 557
Point-of-care (PoC)
  biosensor, 491
  electrochemical sensors
    (*see* Electrochemical sensors, as PoC tests)
Point-of-care devices (PoCD, POC), 242, 810
Point-of-care diagnosis
  graphene-based biosensing platforms, 506–508
  laser scribed graphene structure, 509
  MoS_2 based biosensing platforms, 507–508
Point-of-care (POC) diagnostics, 57–59
  assay based on nanomaterials, 62–64
  assay based on printed electrodes, 61–62
Point-of-care testing (POCT), 176, 310, 644, 815
  applications, 688
  biorecognition ligands, 694
  diagnostic tests, 695
  Escherichia coli O157:H7, 694
  fabrication of biosensors, 693
  Fe_3O_4 nanozyme, 693
  laboratory services, 696
  MIP-based-biosensors, 691
  paper-based materials for biosensing, 692
  protein biomarker detection, 690
Poly 3,4-ethylene dioxythiophene (PEDOT), 233
Polyacrylonitrile (PAN) nanofibers, 188
Polyaniline (PANI), 232, 841
Polyaniline incorporated Ni-MOF (PANI@Ni-MOF) nanocomposite, 677
Poly(dimethylsiloxane) (PDMS), 182, 581, 674, 846
Poly-dopamine nanostructured N-doped multi-walled carbon nanotubes (PDA-N-MWCNT), 712, 713
Polyethylene glycol (PEG), 285
Polyethylene glycol modified CND (PEG-CND), 776
Polyethyleneimine (PEI), 191
Polyethylene naphthalate (PEN), 181
Polyethylene terephthalate (PET), 181
Polyhydroxyalkanoates (PHAs), 184
Polyimides (PI), 181
Poly-L-cysteine (P-Cys), 353
Polymerase chain reaction analysis (PCR), 103
Polymer-based nanomaterials, 521
Polymeric biomaterials, 25
Polymerize chain reactions (PCR), 242, 244, 245
Poly(methyl methacrylate) (PMMA), 192
Polyphenols, 564
Polypyrrole (PPy), 232, 345
Polysaccharide-based biomaterials
  alginate, 525
  cellulose, 525, 526
  chitosan, 524, 525

Polysaccharide-based biomaterials (*cont.*)
  inorganic materials, 527
  pullulan, 524
  self-assembling peptides, 526
  starch, 526
Poly(sodium 4-styrene sulfonate) (PSS), 234
Polyvinylpyrrolidone, 801
Porous coordination polymers (PCPs), *see* Metal-organic frameworks (MOFs)
Porous graphene oxide (PrGO), 96
Porous materials, 600
Porous organic polymer (POP), 776
Positron emission tomography (PET), 261
Precipitation method, 905
Printed electrical gas sensor, 795
Printing technology, 187
  inkjet printer, 793
  screen-printing, 791–793
  stencil-printing, 793
Procalcitonin, 80
Progesterone (PG), 727
Promethazine hydrochloride (PMZ)
  antiallergic, 200
  non-official methods, 201
  structure, 201
Prostate cancer, 470, 835
Prostate-specific antigen (PSA), 549, 648, 734, 834–836, 840, 846
  biomolecule sensing, 605
Prostate-specific membrane antigens (PSMA), 928
Protein-based biosensors, 96
Protein biomarker detection, 690
Protein essenced natural biomaterials, 23
Proteins, 798
Prussian blue (PB), 818
  film, 142
Pullulan, 524
Pullulan-based nanoparticles, 524
Pyrolysis-solvothermal method, 285
Pyrophosphate (PPi), 162

Q

Quantum confinement, 291, 292
Quantum dots, 30, 56, 98, 264, 267, 269, 366, 419–420, 744
  cancer diagnosis, 264, 265, 267, 269, 270
Quartz crystal microbalance (QCM), 99
Quaternary ammonium-almitoyl glycol chitosan (GCPQ), 531
Quercetin (QU) detection, 224

R

Raman spectroscopy, 268
Rare earth material based nanodendrites, 709
Reactive oxygen species (ROS), 730
Real-Time PCR reference method, 632
Reduced graphene oxide quantum dots (rGO QDs), 342
Reduced graphene oxide (rGO), 96
  nanopapers, 396
Reduced graphene oxide-based Ni-MOF composite, 666
Reduced graphene oxide tetraethylenepentamine (rGO-TEPA), 563
Reference electrode (RE), 901, 902, 904
Resistive-pulse sensing (RPS), 114
Reticuloendothelial system (RES), 520
Reverse-transcriptase polymerase chain reaction (RT-PCR), 563
RhPt nanodendrites, 80
Ribo Nucleic Acid (RNA), 677
  sequences, 269
Rolling circle amplification, 416

S

Salt impregnated inkjet maskless lithography (SIIML), 187
Sandwich-based voltammetric immunosensor, 559
Sandwich-type immunosensor, 555
SARS-CoV-2 detection, 696
SARS-CoV-2 receptor-binding domain, 928
SBA-15, 439
Scanning electrochemical microscopy (SECM), 864
Scanning electron microscopy (SEM), 864
Screen-printed carbon electrodes (SPCEs), 818, 792
Screen-printed edge band UME (SPUME), 870, 873
Screen printed electrodes (SPEs), 61, 547, 573, 645, 752, 820
Screen-printed gold electrode (SPGE), 550, 654
Screen printing, 181, 791–793
Selective modification, 119
Self-assembled monolayer (SAM), 871
Semiconductor single-walled carbon nanotubes (SWNTs), 267
Semipermeable selective polymers, 767
Sensitive immunoassays, 275
Serum virus neutralization test (SVNA), 563
Signal amplification approach, 448

Signal transducer, 830
Silica nanoparticles, 534, 743
Silk, 23
  fibroin, 523
Silver nanomaterials, for infectious diseases, 243–245
Silver nanoparticles (AgNPs), 64, 202, 203
Silver nanowire/reduced graphene oxide (AgNW/rGO), 311
Single-chain synthetic nucleic acids, 928
Single enzyme nanoparticle (SEN), 612
Single-photon emission computed tomography (SPECT), 261
Single-stranded DNA (ssDNA), 465, 772
Single-stranded nucleic acid (ssDNA), 164
Single-stranded oligonucleotide (ssDNA), 678
Single-walled carbon nanotubes (SWCNTs), 82, 97, 252, 605, 730, 874, 875
Slow evaporation process, 667
Small interfering RNAs (siRNAs), 677
Small nuclear RNAs (snRNAs), 677
Smart biomaterials, 31–32
Sodium dodecyl sulfate (SDS), 801
Sodium hydrogen telluride, 836
Sodium nitrate, 668
Solar energy, 326
Solid electrodes, 862
Solvothermal method, 369, 505, 666
Sonochemical method, 667
Soybean agglutinin (SBA), 170
Spectrophotometric method, 201
Spent battery carbon dots, 352
Sputtering, 184, 189
Sputtering indium oxide (In_2O_3), 185
Squamous-cell carcinoma (SCC), 264
π-π Stacking interaction, 354
Staphylococcus aureus (*Staph. aureus*) bacteria, 245
Stober synthesis, 440
Strand displacement reactions (SDRs), 417
Strip-based tests
  advancements of capillary flow assays, 60–61
  dipstick, 58
  lateral flow assays, 58
Sulfur-doped GQDs (S-GQDs), 287
Surface enhanced Raman scattering (SERS), 100, 703
Surface-Enhance Raman Spectroscopy (SERS), 612
Surface-modifying nanozymes, 694
Surface plasmon absorption, 743
Surface Plasmon Resonance (SPR) spectroscopy, 101
Surface state emission, 290
Surgical hypothermia, 29
Synthetic hydrothermal methodology, 441
Syringol/catechol, 160
Systematic evolution of ligands by exponential enrichment (SELEX), 265, 270, 589, 772

T
Tattoos, 752
  tattoo-style wearable biosensors, 192
Template-free method, 221
Temporary tattoos, 752
Teonex®, 181
Terminal deoxynucleotidyl transferase (TDT), 679
Tetrabromophenol blue (TBPB), 575
Tetraethyl orthosilicate (TEOS), 227
1,2,4,5-Tetrakis-(4-formylphenyl) benzene (TFPB), 840
3,3′,5,5′-Tetramethylbenzidine (TMB), 488
Textile-based carbon electrodes (TCEs), 183
Textile industry, 326
T4 polynucleotide kinase (T4 PNK), 556
Thermal decomposition method, 155, 886
Thermoplastic electrode (TPE) production method, 797
Thiol functionalized CHIT (T-CHIT), 726
Thiol functionalized graphene (T-Gr), 726
Thiol group, 852
Thionine, 157
3D biosensor system, 588
3D collagen network, 736
3D GF/PtNPs/PEDOT sensor, 736
3D graphene-based macro-mesoporous nanomaterials (GF-MC), 231
3D graphene electrodes, 75
3D graphene network (3DGN), 230
Three-dimensional nanomaterials (3D), 814
3D nanowires, 804
Three-electrode systems, 187
Thrombin, 552
Time-resolved electron paramagnetic resonance spectroscopy, 292
TiO_2-CeO_2 nanocomposite film, 473
Tissue engineering, 35, 55, 532
Titania nanotube arrays, 311
Titanium carbide sheets, 504–505
Toehold mediated strand displacement reactions (TMSDRs), 417
Toluidine blue O (TBO), 655
Top-down approach, 284, 310, 544
Traditional immuno-histochemistry, 689

Transducers, 265, 270, 310, 764, 765, 768, 771, 772
Transfer RNA (tRNA), 677
Transition metal chalcogenides, 507
Transition metal oxides (TMOs), 500
Transmission electron microscopic (TEM) imaging, 163
Transparent nanoporous silica films, 605
2,4,6-Trinitrotoluene (TNT), 348
Tropomyosin-binding component, 831
Troponin, 831, 832
Tryptophan (TRP) isomers, 346
Tumor biomarkers, 563
Tumor necrosis factor-alpha (TNFα), 100, 189
Tungstic anhydride (WO3), 345
"Turning off' Raman signal, 101
"Turn off' fluorescence biosensors, 165
2D graphene nanosheets, 462
Two-dimensional (2D) materials
  analytical features of the biosensors fabricated using, 510
  for biosensor applications, 502–504
  carbonyl-functionalized GO sheets, 502
  copper cobaltite nanosheets, 506
  future research, 509
  GO and GO-AuNP nanocomposites, 503
  graphene, 502
  MoO_3, 504
  MoS_2, 508
  MXenes, 504–505
Two-dimensional (2D) nanomaterials, 813
Tyrosine kinase-7 (PTK7), 681

U
Ultramicroelectrodes (UMEs), 133, 862, 863, 876
  definition, classification, fabrication, characterization and advantages of, 863–866
  disadvantage, 865
  nanoparticle usage for fabrication and applications, 866–869
  UMEAs, 865
Ultraviolet absorption spectrophotometry, 201
UME array (UMEA), 865, 871–873
Upconversion luminencence emission (UCLE), 709
Upconversion nanodendrites (UCNDs), 710, 711
Uric acid (UA), 343
  sensing, 889, 910

V
V-Chip, 690
Vertically configured nanostructures, 122
Vesicle impact electrochemical cytometry (VIEC), 139
Vibrio parahaemolyticus, 588
Vitamin D_2, 346
Vitamin D_2 antibody (Ab-VD2), 346

W
Warburg impedance, 922, 923, 925
Wax printing, 60
Wearable electrochemical fabric, 823
Wearable sensors, 750–753, 754, 823
Wearable technology, 691
Whatman paper, 386–387
Working electrode (WE), 901–904

Y
Yttria-doped zirconia-rGO nanocomposite, 471

Z
Zearalenone (ZEA), 731
Zeolite imidazole framework (ZIF-67), 672
Zero-dimensional nanomaterials, 811
Zika DNA, 245
Zirconium based MOFs, 667
ZnO nanorods, 804
  electrode, 707–709